BJR

THE BRITISH JOURNAL OF RADIOLOGY

Volume 65 Number 778 October 1992

CUK-H06085-30-P25864

30

-ray Diagnosis • Ultrasound • Interventional Radiology
Radiotherapy • Oncology • Hyperthermia
Nuclear Medicine • Nuclear Magnetic Resonance
adiation Physics • Radiobiology • Radiation Protection

BJR is published by The British Institute of Radiology BIR

"IS THERE A WAY TO VERIFY PATIENT DOSAGE DELIVERED DURING RADIATION THERAPY...ACCURATELY, RELIABLY AND INSTANTANEOUSLY?"

THERE IS WHEN YOU USE THE NUCLEAR ASSOCIATES' RAINBOW PATIENT DOSE VERIFICATION SYSTEM.

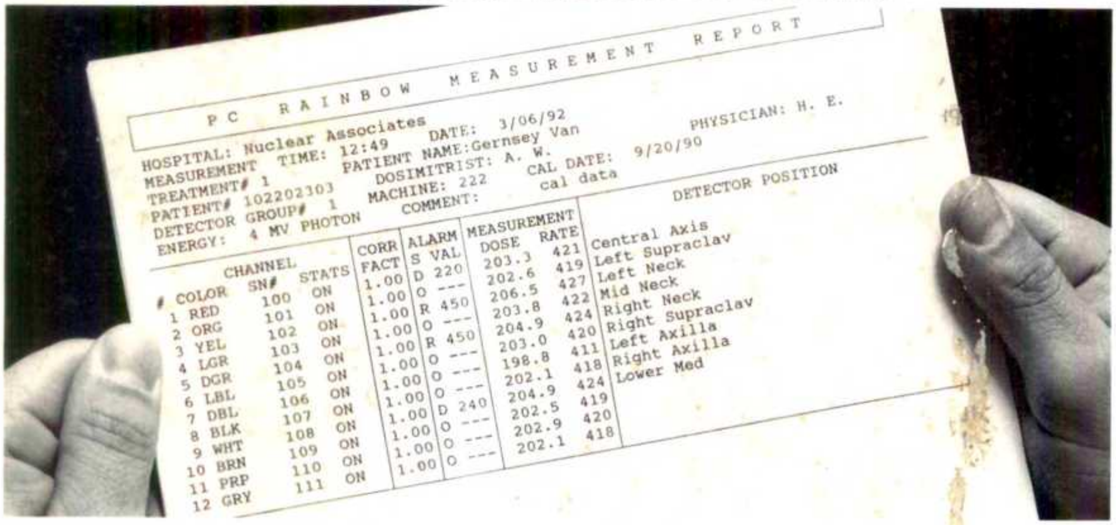

```
P C   R A I N B O W   M E A S U R E M E N T   R E P O R T

HOSPITAL: Nuclear Associates      DATE:  3/06/92                  PHYSICIAN: H. E.
MEASUREMENT  TIME: 12:49   PATIENT NAME:Gernsey Van
TREATMENT# 1                DOSIMITRIST: A. W.    CAL DATE:  9/20/90
PATIENT# 102202303          MACHINE: 222            cal data
DETECTOR GROUP#  1              COMMENT:
ENERGY:   4 MV PHOTON
                            CORR|ALARM|MEASUREMENT|       DETECTOR POSITION
       CHANNEL              FACT|S VAL| DOSE  RATE|
# COLOR  SN#   STATS        1.00|D 220| 203.3  421|Central Axis
 1 RED   100    ON          1.00|O ---| 202.6  419|Left Supraclav
 2 ORG   101    ON          1.00|R 450| 206.5  427|Left Neck
 3 YEL   102    ON          1.00|O ---| 203.8  422|Mid Neck
 4 LGR   103    ON          1.00|R 450| 204.9  424|Right Neck
 5 DGR   104    ON          1.00|O ---| 203.0  420|Right Supraclav
 6 LBL   105    ON          1.00|O ---| 198.8  411|Left Axilla
 7 DBL   106    ON          1.00|O ---| 202.1  418|Right Axilla
 8 BLK   107    ON          1.00|D 240| 204.9  424|Lower Med
 9 WHT   108    ON          1.00|O ---| 202.5  419|
10 BRN   109    ON          1.00|O ---| 202.9  420|
11 PRP   110    ON          1.00|O ---| 202.1  418|
12 GRY   111    ON
```

We call it the PC-RAINBOW. You'll call it great! The PC-RAINBOW System uses an IBM™ PC computer (or equivalent) and ties it to the proven strengths of Nuclear Associates' diode dosimetry systems. Results: Patient dose monitoring and QC beam analysis in radiation therapy, performed easily, accurately and reliably — across a wide range of treatment modalities — with up to 12 detector channels.

PC-RAINBOW consist of a high-speed, microprocessor-controlled electrometer mounted on a "goes anywhere" mobile stand. Controller software for an IBM PC compatible computer and a 30-meter interface cable complete the system. And when it comes to the features, PC-RAINBOW:

- Provides up to 12 detector channels plus a trigger channel for maximum measurement verification.
- Alerts the operator to possible dose misadministration.
- Provides for storage of calibration factors for up to 20 sets of 12 diodes.
- Lets you apply individual correction factors to any or all diodes at the time of measurement.
- Is suitable for whole body treatment at dose rates below 5 rads/min.
- Has user-selectable alarms for any combination or number of channels.
- Allows you to store patient exposure data on floppy disk, or print out on any PC-compatible printer.

PC RAINBOW
TRIGGER

So when you're looking for the way to verify patient dosage accurately, and reliably, look to the PC-RAINBOW System from Nuclear Associates.

IBM™, International Business Machines, Inc.

And for more information, request Bulletin 4451-14

NUCLEAR ASSOCIATES

VICTOREEN

Division of VICTOREEN, INC.
100 VOICE ROAD • P.O. BOX 349
CARLE PLACE, NY 11514-0349 U.S.A.
(516) 741-6360
FAX (516) 741-5414

P 55854

4-65

BJR THE BRITISH JOURNAL OF RADIOLOGY

Established 1896

The Editorial Board

Honorary Editors
D. M. King, MB, BS, FRCR, DMRD
F. A. Duck, BSc, MSc, PhD

Diagnostic Radiology
Deputy Editor: G. H. Whitehouse, MB, BS, FRCP, FRCR, DMRD

Associate Editors
J. B. Bingham, MA, MRCP, MSc, FRCR
A. M. Davies, MB, ChB, DMRD, FRCR
P. Dawson, BSc, PhD, MB, BS, MRCP, MInstP, FRCR
A. H. Freeman, MB, BS, FRCR
P. R. Goddard, BSc, MB, BS, MD, DMRD, FRCR
H. C. Irving, MB, BS, DMRD, FRCR
J. B. Karani, FRCR
J. Pemberton, BSc, MB, BS, MRCP, LRCS, FFR, FRCR, DMRD
A. M. Peters, BSc, MSc, MB, ChB, MD, MRCPath
D. W. Pilling, MB, ChB, DCH, DMRD, FRCR
J. F. Reidy MB, BS, FRCP, FRCR
M. B. Rubens, MB, BS, LRCP, MRCS, DMR, FRCR
P. J. Shorvon, MB, BS, MRCP, FRCR
A. R. Valentine, MB, BS, MRCS, LRCP, FRCR, DMRD
J. Virjee, MB, ChB, FRCR

Physics and Technology
Deputy Editor: C. K. Bomford, BSc, MPhil, FInstP

Associate Editors
D. R. Dance, MA, PhD, FIPSM
P. C. Jackson, BSc, PhD, FInstP, CPhys, FIPSM
R. A. Shields, PhD

Radiotherapy and Oncology
Deputy Editor: D. M. Tait, MB, ChB, MRCP, FRCR

Associate Editors
R. Beaney, BSc, MB, ChB, MD, MRCP, FRCR
P. R. Blake, MD, MB, BS, BSc, FRCR
D. J. Cole, MB, BS, MRCP, FRCR
J. Glaholm, BSc, MRCP, FRCR

Radiobiology
Deputy Editor: J. W. Hopewell, BSc, PhD

Associate Editors
D. Hirst, BSc, PhD
A. J. Mill, BSc, ARCS, PhD
T. E. Wheldon, BSc, PhD, FInstP

Associate Editors Overseas
S. G. A. Chenery, PhD, FCCPM (North America)
B. J. Cremin, MD, FRCR, FRACR (South Africa)
R. Fox, DPhil (Australia)
M. Takahashi, MD (Japan)

The British Journal of Radiology is published monthly by the British Institute of Radiology, 36 Portland Place, London W1N 4AT. Telephone 071-580 4189 (editorial); Facsimile 071-255 3209. Editorial communications should be addressed to the Honorary Editors in accordance with the Instructions to Authors published in the January issue each year, copies of which may be obtained from the Managing Editor upon request.

Subscriptions. The monthly fulfilment is carried out by BJR Subscriptions, PO Box 500, Leicester LE99 0AA, UK. Telephone 0858 410510; Facsimile 0858 434190. The 1992 annual subscription is £152 for EEC (incl. UK) readers and £167 for readers in the rest of the world. These prices include delivery by sea mail; airmail rates are £10 extra for Europe and £30 extra for the rest of the world, effective from March 1992. Copies of this journal sent to subscribers in Bangladesh, Canada, India, Japan, Pakistan, Sri Lanka and USA are air-speeded for quicker delivery at no extra cost. Subscriptions are on a calendar year basis only.

Managing Editor: T. R. Hogan, BSc, PhD
Sales and Promotions Manager: H. D. Smith
Production Editor: J. Becker, BA
Publications Secretary: J. Rodd, BA

Advertisements. Enquiries should be addressed to the Sales and Promotions Manager at the above address.
Tel: 071-631 1168.

US mailing agents
Mercury Airfreight Internations Ltd Inc. Second class postage paid at Rahway, NJ, USA. Postmaster: send address corrections to the BJR, c/o Mercury Airfreight International Ltd Inc., 2323 Randolph Avenue, Avenel, NJ 07001, USA.

Back issues prior to the current volume can be ordered from the BIR at the above address.

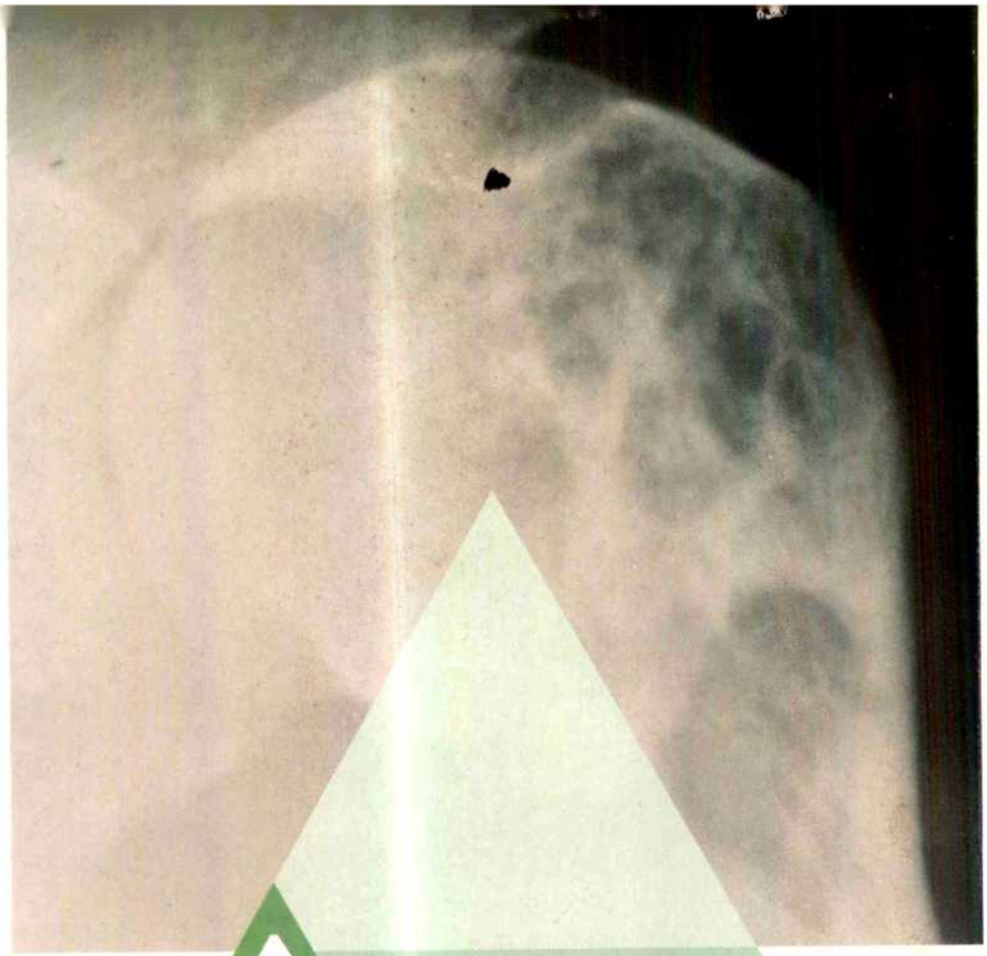

Aredia®

pamidronate disodium

for the treatment of tumour-induced hypercalcaemia

- **Reliable response**
  "Calcium concentration fell in all patients [n=30] and was restored to normal in all but two"[1]
- **Sustained effectiveness**
  Normocalcaemia maintained for an average of 3 weeks[1]
- **Well tolerated**
  Reported side-effects not of clinical relevance[1,2]
- **Effective as a single infusion**

Ciba

Prescribing Notes Aredia® (pamidronate disodium) **Presentation** Ampoules of 5ml aqueous injectable concentrate containing 15mg pamidronate disodium (calculated as the anhydrous form) for intravenous infusion. **Indication** Tumour-induced hypercalcaemia. **Dosage** Adults and elderly : Depending on the initial calcium plasma level, 15-90mg by slow intravenous infusion in sodium chloride 0.9%. Infusion rate should not exceed 30mg/2hrs, and concentration should not exceed 30mg/250ml. Total dose can be given either as a single i.v. infusion or divided over 2-4 consecutive days. Rehydration with normal saline before treatment is recommended. Not recommended for children. See full prescribing information. **Contraindications** Known hypersensitivity to pamidronate disodium or other bisphosphonates. **Precautions** Monitor clinical and biochemical effects. Do not administer as a bolus injection. Do not co-administer with other bisphosphonates, plicamycin (mithramycin) or calcium containing infusion solutions. Caution in patients with severe renal insufficiency (multiple dosing recommended); haemodialysis; pregnancy. Theoretical interference with bone scintigraphy examinations. **Side-effects** Asymptomatic hypocalcaemia and transient pyrexia. Occasionally transient lymphocytopenia and hypomagnesaemia. Less frequently reactions at infusion sites and gastrointestinal effects. For further information see full prescribing information. **Packs** Ampoules 15mg/5ml (PL0001/0138) in packs of 4, basic NHS price £96.62. ® denotes registered trademark. Full prescribing information is available on request from Ciba Laboratories, Horsham, West Sussex RH12 4AB. **References :** 1. Morton AR, et al. Single Dose Versus Daily Intravenous Aminohydroxypropylidene Bisphosphonate (ADP) for the Hypercalcaemia of Malignancy. Br Med J 1988; 296: 811-814. 2. Ralston SH, et al. Treatment of Cancer Associated Hypercalcaemia with Combined Aminohydroxypropylidene Diphosphonate and Calcitonin. Br Med J 1986; 292: 1549-1550.

VOL 65 NO 778 OCTOBER 1992

The British Journal of Radiology
Contents

Page

Papers

Appearances of choroidal osteomas with diagnostic imaging 845
P. A. Bloom, J. D. Ferris, A. Laidlaw and P. R. Goddard

The role of hysterosalpingography in modern gynaecological practice 849
R. Rajah, J. M. McHugo and M. Obhrai

Portable chest radiography in intensive care: a comparison of computed and conventional radiography 852
P. Jennings, S. P. G. Padley and D. M. Hansell

Doppler ultrasound scanning in the detection of renal artery stenosis in hypertensive patients 857
C. T. Postma, J. van Aalen, T. de Boo, G. Rosenbusch and T. Thien

Can serum prostate-specific antigen replace bone scintigraphy in the follow-up of metastatic prostatic cancer? 861
G. R. J. Sissons, R. Clements, W. B. Peeling and M. D. Penney

Localized loss of the infrabronchial descending aortic interface as a normal variant 865
W. F. C. van Gelderen

Pelvic phleboliths: is there an association with diverticulitis? 868
E. H. de Vries, A. Z. Ginai, S. G. F. Robben and W. C. J. Hop

Staging of hilar cholangiocarcinoma by ultrasound and duplex sonography: a comparison with angiography and operative findings 871
C. Looser, S. C. Stain, H. U. Baer, J. Triller and L. H. Blumgart

A figure of merit for the assessment of image intensifier systems 878
D. W. McRobbie, A. P. Hancock and I. A. Castellano

Radial diffusion coefficient mapping 885
A. Madden and M. O. Leach

Impact of hydration status on body composition as measured by dual energy X-ray absorptiometry in normal volunteers and patients on haemodialysis 895
F. F. Horber, F. Thomi, J. P. Casez, J. Fonteille and Ph. Jaeger

Single- versus dual-energy quantitative computed tomography for spinal densitometry in patients with rheumatoid arthritis 901
R. F. J. M. Laan, L. J. Th. o. van Erning, J. A. M. Lemmens, L. B. A. van de Putte, S. H. J. Ruijs and P. L. C. M. van Riel

Efficacy of low-dose iodine-131 ablation of post-operative thyroid remnants: a study of 69 cases 905
S. F. Leung, M. W. M. Law and S. K. W. Ho

Functional changes in the pig kidney following irradiation with fractionated doses of fast neutrons (42 $\mathrm{MeV}_{d\rightarrow Be}$) 910
M. E. C. Robbins, D. W. H. Barnes, J. W. Hopewell, J. F. Knowles, M. Rezvani and J. M. Sansom

Retrospective analysis of nasopharyngeal carcinoma treated during 1976–1985: late complications following megavoltage irradiation 918
A. W. M. Lee, S. C. K. Law, S. H. Ng, D. K. K. Chan, Y. F. Poon, W. Foo, S. K. O, S. Y. Tung, F. K. Cheung and J. H. C. Ho

Technical notes

Localization of impalpable breast lesions using the Hawkins needle 929
T. M. Walker and H. B. Ross

Single energy quantitative computed tomography: the effects of phantom calibration material and kVp on QCT bone densitometry 931
R. W. Whitehouse and J. E. Adams

Case reports

Second malignant neoplasm following treatment of Hodgkin's disease: a case report 935
V. S. N. Rao, K. A. Dinshaw, S. K. Shrivastava, M. A. Muckaden, S. Susnerwala, S. H. Advani, J. J. Vyas and N. M. Kavarana

Extradural paraganglioma with multiple skeletal metastases 938
R. Jindel, A. K. Gupta, A. K. Mahapatra, C. S. Bal and R. M. Singhal

Intrathoracic lymphadenopathy and HIV infection 940
N. C. Cowan, J. R. Salisbury and J. Moxham

Basal cell carcinomas do metastasize 943
E. J. Junor, I. Campbell and R. P. Symonds

Case of the month

A curious case of pelvic calcification 945
D. J. Grier and G. N. A. Sibley

Short communication

Visualization of the axillary vein during $^{99}Tc^{m}$ methoxy-isobutyl-isonitrile (MIBI) myocardial imaging 947
P. W. P. Bearcroft and E. P. Wraight

Correspondence

Radiation protection associated with well woman screening 949
E. J. Roebuck

Radiation protection associated with well woman breast cancer screening 949
J. Patnick

Standards of radiation protection in mammographic screening 950
P. C. Shrimpton and B. F. Wall

Radiation protection associated with well women breast cancer screening 950
J. Law, D. R. Dance, K. Faulkner, M. C. Fitzgerald, M. L. Ramsdale and A. Robinson

Authors' reply 952
B. M. Moores and E. T. Henshaw

Book review

The Physics and Radiobiology of Fast Neutron Beams. *D. K. Bewley* 954

BIR Bulletin *facing page* 954

BIR THE BRITISH INSTITUTE OF RADIOLOGY

Founded 1897
Incorporated by Royal Charter
Partron: Her Majesty The Queen

The British Institute of Radiology is an association of persons interested in radiology and allied subjects. Meetings are held monthly from October until May. Particulars of membership and other information may be obtained on application to the General Secretary at the Institute, 36 Portland Place, London W1N 4AT. Telephone: 071-580 4085 and 071-580 4189. Fax: 071-255 3209.

President
W. Hateley, MB, ChB, FRCPEd, FRCR, DMRD

Honorary Secretaries:
N. W. Garvie, MAMB, BChir, MRCP, DMRD, FRCR, MSc
J. Law, BSc, PhD, FInstP, CPhys

Honorary Treasurer
D. S. McIntosh, BSc, PhD, MRPharmS, MRSC, MIMC

General Secretary
Mary-Anne Piggott, BSc, MBA, MBIM

© 1992 The British Institute of Radiology. This publication is copyright under the Berne Convention and the Universal Copyright Convention. All rights reserved, apart from any relaxations permitted under national copyright laws, no part of this publication may be reproduced, stored in a retrieval system or transmitted in any form or by any means without the prior permission of the copyright owners. Permission is not, however, required to copy abstracts of papers or of articles on condition that a full reference to the source is shown. Multiple copying of the contents of the publication without permission is always illegal.

Published by The British Institute of Radiology, 36 Portland Place, London W1N 4AT. Origination by BPCC Whitefriars Ltd, Tunbridge Wells, and printed and bound in Great Britain by BPCC Wheatons Ltd, Exeter.
ISSN 0007 1285

VOL 65 NO 779 NOVEMBER 1992

The British Journal of Radiology

Contents

Page

Papers

Direct coronal computed tomography of the temporomandibular joint in patients with rheumatoid arthritis 955
P. Goupille, B. Fouquet, P. Cotty, D. Goga and J.-P. Valat

Vasoconstriction by angiographic contrast media in isolated canine arteries 961
N. Gomi

Percutaneous drainage of splenic abscesses: an effective and safe procedure 968
I. Hadas-Halpren, N. Hiller and M. Dolberg

One-view *versus* two-view mammography in baseline screening for breast cancer: a review 971
J. A. A. M. van Dijck, A. L. M. Verbeek, J. H. C. L. Hendriks and R. Holland

Sonography in thyroid carcinoma in children 977
C. J. Garcia, A. Daneman, K. McHugh, H. Chan and D. Daneman

Enlarged mediastinal lymph nodes in the fibrosing alveolitis of systemic sclerosis 983
S. J. Garber, A. U. Wells, R. M. duBois and D. M. Hansell

Prediction of birthweight by fetal ultrasound biometry 987
D. A. Nzeh, S. Rimmer, W. M. O. Moore and L. Hunt

The effect of thin K-edge filters on radiation dose in dental radiography 990
D. S. MacDonald-Jankowski and C. P. Lawinski

The distribution of medical X-ray doses amongst individuals in the British population 996
D. Hart and J. C. Le Heron

Efficiency of a lead-containing tie for radiation protection of the thyroid gland 1003
H.-M. Klein and A. Stargardt

Measuring radiation exposure during percutaneous drainages: can shoulder dosemeters be used to estimate finger doses? 1007
T. Vehmas and H. Tikkanen

Effect of diatrizoate on the function of the isolated perfused rat kidney 1011
P. Brown, J. Haylor, S. K. Morcos, G. H. Cope and A. M. El Nahas

Stage IB cervical carcinoma: a clinical audit 1018
M. N. Gaze, C. G. Kelly, P. R. C. Dunlop, A. T. Redpath, G. R. Kerr and V. J. Cowie

Calcium antagonists protect mice against lethal doses of ionizing radiation 1025
G. L. Floersheim

Technical notes

Phantoms for evaluating the performance characteristics of bone densitometers 1030
G. J. Royle and R. D. Speller

Case reports

Segmental reversal of intrahepatic portal flow due to a liver metastasis 1035
R. Kishimoto, K. Choji, T. F. Massoud, S. Matsuoka, M. Chen, N. Fujita and G. Irie

Intrarenal varices mimicking hydronephrosis 1038
W. Kincaid and R. Edwards

Transitional cell carcinoma of the bladder associated with Crohn's disease: case report and review of the literature 1040
Y. Fujimura, T. Kihara, J. Uchida, K. Hoshika, I. Sato, T. Eimoto, Y. Furukawa, A. Sone and K. Ohashi

The Swiss cheese brain 1042
A. Jackson, M. J. Dobson and P. N. Cooper

Demonstration by computed tomography of a case of internal small bowel herniation 1045
J. C. Hoeffel, J. Zimberger, B. Pocard and C. Hoeffel

Caecal herniation through the foramen of Winslow: diagnosis by computed tomography 1047
M. R. Schuster, R. K. Tu and K. A. Scanlan

Case of the month

Dense bones 1049
S. Vinnicombe, C. Heron and M. Wansbrough-Jones

Short communication

Correlations between α/β and $T_{\frac{1}{2}}$: implications for clinical biological modelling 1051
D. J. Brenner

Correspondence

The role of ^{99}Tc^{m}-HMPAO white cell imaging in suspected orthopaedic infection 1055
D. Wilson

Authors' reply 1055
C. Copping, S. M. Dalgleish, N. J. Dudley, P. A. Griffiths, M. Harrington, R. Potter and B. D. Smith

Coil embolization using a saline flush technique 1055
P. G. Tarazov, E. M. Gapchenko, I. A. Dmitrieva and V. K. Ryzhkov

Imaging of organ function 1056
K. A. Miles

Fluid levels in a spinal aneurysmal bone cyst following biopsy 1056
D. Kessel

Proceedings

Proceedings of the Scottish Radiological Society 1058
Radiodiagnosis programme, 9 November 1991
Radiodiagnosis programme, 14 March 1992

Book reviews 1064

Meetings and courses 1068

BIR THE BRITISH INSTITUTE OF RADIOLOGY

Founded 1897
Incorporated by Royal Charter
Partron: Her Majesty The Queen

The British Institute of Radiology is an association of persons interested in radiology and allied subjects. Meetings are held monthly from October until May. Particulars of membership and other information may be obtained on application to the General Secretary at the Institute, 36 Portland Place, London W1N 4AT.
Telephone: 071-580 4085 and 071-580 4189.
Fax: 071-255 3209.

President
W. Hately, MB, ChB, FRCPEd, FRCR, DMRD

Honorary Secretaries:
N. W. Garvie, MAMB, BChir, MRCP, DMRD, FRCR, MSc
J. Law, BSc, PhD, FInstP, CPhys

Honorary Treasurer
D. S. McIntosh, BSc, PhD, MRPharmS, MRSC, MIMC

General Secretary
Mary-Anne Piggott, BSc, MBA, MBIM

© 1992 The British Institute of Radiology. This publication is copyright under the Berne Convention and the Universal Copyright Convention. All rights reserved, apart from any relaxations permitted under national copyright laws, no part of this publication may be reproduced, stored in a retrieval system or transmitted in any form or by any means without the prior permission of the copyright owners. Permission is not, however, required to copy abstracts of papers or of articles on condition that a full reference to the source is shown. Multiple copying of the contents of the publication without permission is always illegal. Published by The British Institute of Radiology, 36 Portland Place, London W1N 4AT. Origination by BPCC Whitefriars Ltd, Tunbridge Wells, and printed and bound in Great Britain by BPCC Wheatons Ltd, Exeter.
ISSN 0007 1285

VOL 65 NO 780 DECEMBER 1992

The British Journal of Radiology

Contents

Page

Papers

The assessment of carotid and vertebral arteries; a comparison of CFM duplex ultrasound with intravenous digital subtraction angiography 1069
I. Colquhoun, C. P. Oates, K. Martin, K. Hall and T. A. Whittingham

^{99}Tc^{m}-Technegas and krypton-81m ventilation scintigraphy: a comparison in known respiratory disease 1075
J. M. James, J. J. Lloyd, B. C. Leahy, S. Church, C. C. Hardy, R. A. Shields, M. C. Prescott and H. J. Testa

Comparison of a subjective and a quantitative assessment of the neonatal chest radiograph 1083
B. Yuksel, A. Greenough and J. Karani

Myocardial damage following coronary bypass surgery: assessment with antimyosin antibody uptake 1086
J. Jiménez-Heffernan, J. M. Latre, M. Concha, M. Torres, M. Martínez-Paredes, J. M. Llamas-Elvira, F. M. González, A. Valverde and A. Mateo

Computed tomographic appearances of the pelvis following hindquarter amputation 1093
J. Fowler, A. M. Davies, S. R. Carter, R. J. Grimer and R. S. Sneath

Assessment of mammographic film processor performance in a hospital and mobile screening unit 1097
J. G. Murray, D. J. Dowsett, O. Laird and J. T. Ennis

The influence of needle size on post-myelography headache: a controlled trial 1102
G. M. McGann, F. V. Gleeson, I. Kelly, A. R. Valentine, A. Platts, P. Butler and B. J. Crump

Does Myodil introduced for ventriculography lead to symptomatic lumbar arachnoiditis? 1105
C. A. Rowland Hill, J. V. Hunter, I. F. Moseley and B. E. Kendall

Clearance of iopamidol, a non-ionic contrast medium, by CAPD in patients with end-stage renal failure 1108
P. K. Donnelly, N. Burwell, A. McBurney, J. W. Ward, J. Walls and E. M. Watkin

Late follow-up of lung function after whole lung irradiation for Wilms' tumour 1114
S. P. Attard-Montalto, J. E. Kingston, O. B. Eden and P. N. Plowman

Influence of radiologist grade on fluoroscopic patient dose 1119
P. R. Hoskins and J. R. Williams

Comparison of the effect of different reference data on Lunar DPX and Hologic QDR-1000 dual-energy X-ray absorptiometers 1124
M. A. Laskey, A. J. Crisp, T. J. Cole and J. E. Compston

Technical note

Sialography using a paediatric intravenous cannula 1130
G. D. Walker

Case reports

Primary leiomyosarcoma of the superior vena cava with massive thrombosis treated by local fibrinolysis 1131
M. Marini, E. Tovar, Mª F. López-Fernández, F. Pombo and E. Rodríguez

Hodgkin's disease—a very late recurrence 1133
I. J. M. Johnson and R. Pillai

Dural venous sinus thrombosis following myelography: demonstration by magnetic resonance imaging 1134
R. W. J. Hartley, A. Jackson and R. S. Cooke

Lethal micromelic facial bones sclerosis dysplasia 1137
D. Müller, K. Kozlowski and D. Sillence

Non-endoscopic per oral biliary stent insertion 1140
J. Singanayagam, H. K. Chow and D. J. West

Yolk sac tumour of the testis in childhood 1142
V. Thava, N. Cooper and J. A. Egginton

Case of the Month

Fit and . . . well 1145
R. D. Thomas and A. J. Gould

Correspondence

Fluid levels in a spinal aneurysmal bone cyst following biopsy 1147
A. M. Davies

Cranial stereotactic multiple arc radiotherapy 1147
D. Jones

Authors' reply 1147
E. S. Thomson and D. Doughty

Acronyms in bone densitometry 1148
H. K. Genant, C. C. Gluer, K. G. Faulkner, S. Majumdar, S. T. Harris, K. Engelke and C. van Kuijk

Latent image fading and mean glandular dose in mobile mammographic screening 1148
K. J. Robson, C. J. Kotre and K. Faulkner

Book reviews 1150

Meetings and courses 1154

Index to Vol. 65 1155

BIR THE BRITISH INSTITUTE OF RADIOLOGY

Founded 1897
Incorporated by Royal Charter
Partron: Her Majesty The Queen

The British Institute of Radiology is an association of persons interested in radiology and allied subjects. Meetings are held monthly from October until May. Particulars of membership and other information may be obtained on application to the General Secretary at the Institute, 36 Portland Place, London W1N 4AT. Telephone: 071-580 4085 and 071-580 4189. Fax: 071-255 3209.

President
W. Hately, MB, ChB, FRCPEd, FRCR, DMRD

Honorary Secretaries:
N. W. Garvie, MAMB, BChir, MRCP, DMRD, FRCR, MSc
J. Law, BSc, PhD, FInstP, CPhys

Honorary Treasurer
D. S. McIntosh, BSc, PhD, MRPharmS, MRSC, MIMC

General Secretary
Mary-Anne Piggott, BSc, MBA, MBIM

© 1992 The British Institute of Radiology. This publication is copyright under the Berne Convention and the Universal Copyright Convention. All rights reserved, apart from any relaxations permitted under national copyright laws, no part of this publication may be reproduced, stored in a retrieval system or transmitted in any form or by any means without the prior permission of the copyright owners. Permission is not, however, required to copy abstracts of papers or of articles on condition that a full reference to the source is shown. Multiple copying of the contents of the publication without permission is always illegal. Published by The British Institute of Radiology, 36 Portland Place, London W1N 4AT. Origination by BPCC Whitefriars Ltd, Tunbridge Wells, and printed and bound in Great Britain by BPCC Wheatons Ltd, Exeter.

ISSN 0007 1285

1992, *The British Journal of Radiology*, 65, 845–848

VOLUME 65 NUMBER 778 OCTOBER 1992

The British Journal of Radiology

Appearances of choroidal osteomas with diagnostic imaging

By Philip A. Bloom, FRCS(Ed), FCOphth, John D. Ferris, MB, ChB, Alistair Laidlaw, FRCS (Glas), FCOphth and *Paul R. Goddard, MD, FRCR

Department of Ophthalmology, Bristol Eye Hospital, and *Bristol MRI Centre, Frenchay Hospital, Bristol, UK

(*Received 13 October 1991 and in revised form 18 February 1992, accepted 12 March 1992*)

Keywords: Choroidal osteoma, Computed tomography, Fluorescein angiography, Magnetic resonance imaging, Ultrasound

Abstract. The diagnostic imaging appearances of three choroidal osteomas (osseous choristomas) are presented. This rare, benign choroidal tumour is being recognized with increasing frequency, and is important to remember in the differential diagnosis of any unusual mass in the ocular fundus lest it be mistaken for a more sinister lesion. All three osteomas were demonstrated by ocular ultrasound (US), fluorescein angiography (FA) and computed tomography (CT) but none by plain radiography. None of the lesions was visible on magnetic resonance imaging (MRI); the reason for this is probably the bony nature of the tumours. The appearances of choroidal osteomas on US, FA, plain radiography and CT are discussed. To our knowledge this is the first report of a series of choroidal osteomas investigated by MR.

Choroidal osteoma was first described 14 years ago (Gass et al, 1978) and in the same year the alternative term osseous choristoma was suggested (Joffe et al, 1978). It was originally described as exceedingly rare but it is now clear that choroidal osteoma is more common than was thought previously. Choroidal osteomas may be found in one or both eyes and are more common in young women, and at the posterior pole of the fundus. They follow a benign clinical course (Shields et al, 1988), and the main difficulty in their management relates to their similarity to other choroidal lesions on fundoscopy. It is important to differentiate these tumours from other more sinister masses such as amelanotic malignant melanomas. Although the history and serial examination may be helpful in this regard, the radiological appearances of the tumour are highly suggestive of its nature and so it is important that these are recognized.

Patients and methods

Three patients with choroidal osteoma were identified retrospectively using a registry of interesting cases at Bristol Eye Hospital. Their case records were reviewed, together with their previous radiological investigations. Orbital magnetic resonance (MR) imaging was then performed on all three, with informed consent, to investigate the appearances of these tumours with MR. There was no clinical doubt as to the diagnoses.

Case reports and results

Case 1

A man aged 29 years was investigated for low visual acuity and central visual field defects (scotomata) in both eyes. He was found to have bilateral choroidal osteomas (Fig. 1). Ultrasound (US) (Figs 2 and 3), fluorescein angiography (FA) and computed tomography (CT) (Fig. 4) were performed and showed a mass with the radiographic density of bone arising from the choroid at the posterior pole of each eye. Neither plain radiography nor MR demonstrated the lesion in either eye.

Case 2

A woman aged 36 years was being followed up for a choroidal mass in the left eye, unchanged over 10 years. She complained of distortion of vision and an enlarged blind spot. US showed a highly reflective choroidal mass and FA a mottled, hyperfluorescent mass elevating the retina around and below the optic disc (Fig. 5). Orbital CT demonstrated a bony mass arising from the posterior pole of the right eye (Fig. 6) but plain radiography did not show the lesion. MR (Fig. 7) did not definitely demonstrate the lesion; although there was an area of low signal around the optic disc, this was of similar signal to the surrounding choroid.

Case 3

A man aged 32 years was investigated for poor visual acuity in the right eye, which was found to be due to a choroidal mass at the posterior pole. This was shown to

---

Address correspondence to Philip A. Bloom, Moorfields Eye Hospital, City Road, London EC1V 2PD, UK.

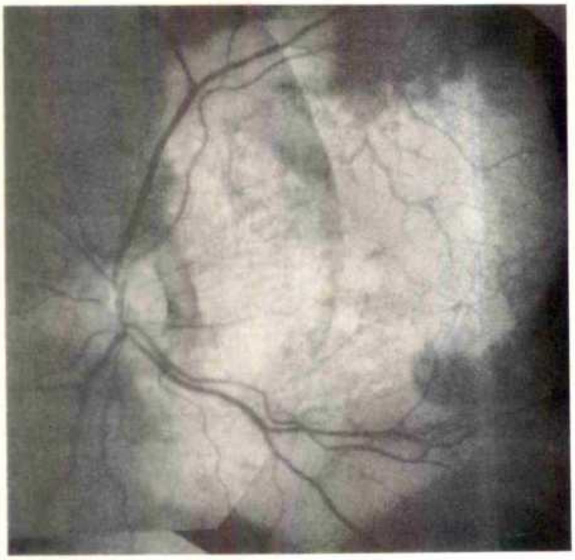

Figure. 1. Posterior pole montage photograph of the left eye of patient 1. The choroidal osteoma can be seen as a pale, discoid mass temporal to the optic disc.

be a choroidal osteoma by its characteristic US, FA and CT (Fig. 8) appearances. Plain radiography and MR failed to show the lesion.

Discussion

These are the only cases of choroidal osteoma known to have been seen at this hospital over the last 10 years, which gives a rough prevalence of 1 per 200 000 new ophthalmic cases. However, this figure is probably an underestimate because the diagnosis has not been recognized until recently.

A choristoma is defined as a non-neoplastic tumour-like mass of developmental origin in which tissues foreign to the site of the lesion are found. The pathogenesis of choroidal osteomas is unknown, but histologically they are composed of mature bone (Gass et al, 1978).

Characteristic appearances

The fundoscopic picture is of a pale, irregularly edged and elevated, discoid choroidal mass at the posterior pole of the fundus (Fig. 1), usually positioned around the macula or optic disc. When depressed by a scleral depressor, a choroidal osteoma may be seen to move "en masse" (Gass et al, 1978).

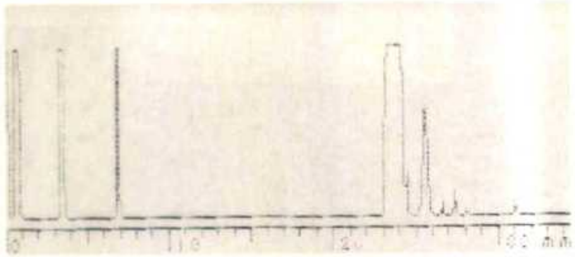

Figure 2. US (A-scan) of the left eye of patient 1, showing the choroidal osteoma as a sharp peak of reflectivity. The echoes of diminishing intensity behind the lesion are caused by internal reflection within the osteoma.

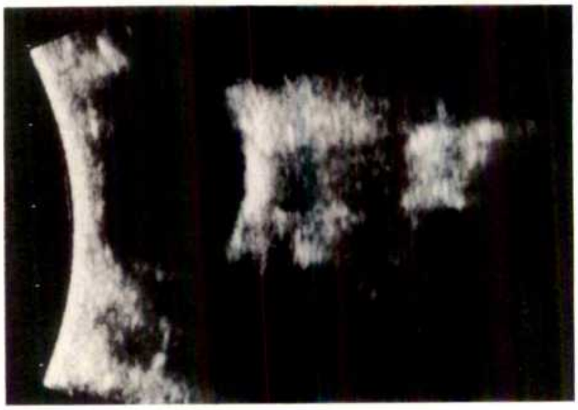

Figure 3. US (B-scan) of the left eye of patient 1, showing the choroidal osteoma as a highly reflective choroidal mass, with an acoustic shadow behind it.

Because they are composed of bone, choroidal osteomas are highly reflective on US, and this reflectivity often persists even when the US gain is greatly reduced (Gass et al, 1978). This is a useful feature that helps differentiate them from malignant melanomas. However, choroidal haemangiomas and some other tumours may calcify (Gass et al, 1978; Brant-Zawadzki and Enzmann, 1979; Hedges et al, 1982), with a consequent increase in ultrasound signal that may make their differentiation from choroidal osteoma more difficult. A-scan shows the choroidal osteoma as a sharp peak of reflectivity masking the normal orbital US pattern, with echoes of rapidly diminishing intensity behind the lesion caused by internal reflection within the osteoma. B-scan shows a dense, reflective choroidal mass, with an acoustic shadow behind it.

Fluorescein angiography characteristically shows

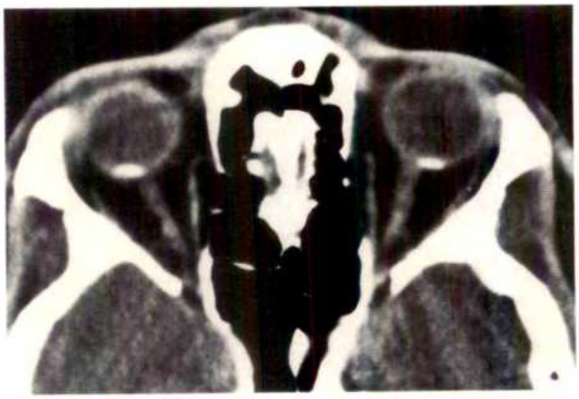

Figure 4. CT of the orbits of patient 1, showing bilateral choroidal osteomas as choroidal masses with the radiographic density of bone.

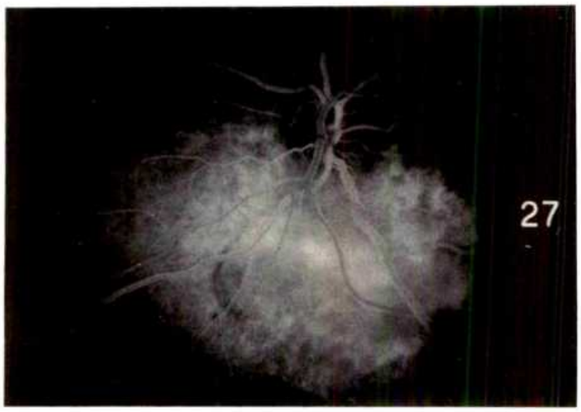

Figure 5. Fluorescein angiogram of the choroidal osteoma in the left eye of patient 2, showing the hyperfluorescent osteoma elevating the retina around and below the optic disc.

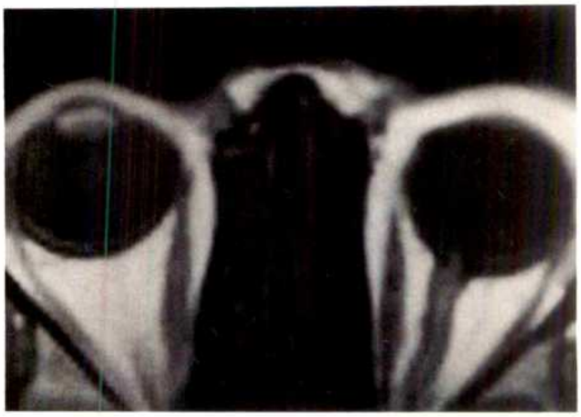

Figure 7. T_1-weighted MR image of the orbits of patient 2, which fails to demonstrate the lesion in the left eye. An area of low signal around the optic disc could not be definitely distinguished from the surrounding choroid.

mottled hyperfluorescence of the choroid on early transit films and more generalized late hyperfluorescence (Gass et al, 1978; Bryan et al, 1983). These FA appearances may differentiate choroidal osteomas from other simulating lesions, so FA is indicated despite the occasional morbidity and mortality associated with the use of fluorescein and other intravenous contrast media.

On CT and occasionally on plain radiographs, choroidal osteomas have the appearances of mature bone (Gass et al, 1978; Bryan et al, 1983). A posterior choroidal mass with the radiological density of bone, shown on CT not to be confined to the optic nerve head, is suggestive of choroidal osteoma (Turner et al, 1983).

Posterior ocular calcification may also occur in retinoblastoma, vascular tumours such as haemangiomas, optic disc drusen, the phakomatoses (retinal hamartomas), optic nerve head tumours, hypercalcaemic states, phthisis bulbi (shrunken globe, the end stage of many post traumatic or chronic inflammatory conditions), dystrophic calcification and other less clinically important conditions (Zeiter, 1962; Frisen et al, 1978; Brant-Zawadzki & Enzmann, 1979; Goldstein & Miller, 1982; Hedges et al, 1982; Bryan et al, 1983; Turner et al, 1983; Char et al, 1990). Bone formation may supervene when the blood supply to the area is abundant (Zeiter, 1962; Gass et al, 1978).

To our knowledge, this is the first reported series of choroidal osteomas investigated by MR. There is one other report in the literature of the use of MR in attempting, but failing, to demonstrate a presumed choroidal osteoma (Santoni et al, 1988). This was, however, in an abnormal microphthalmic eye in which the authors did not exclude phthisis as the cause of the calcification.

Because osteomas are composed of bone, MR appears to be of little use in their diagnosis. Dense bone results in little or no signal on MR imaging and MR is a poor method of demonstrating calcification. The signal characteristics of the choroidal osteomas described

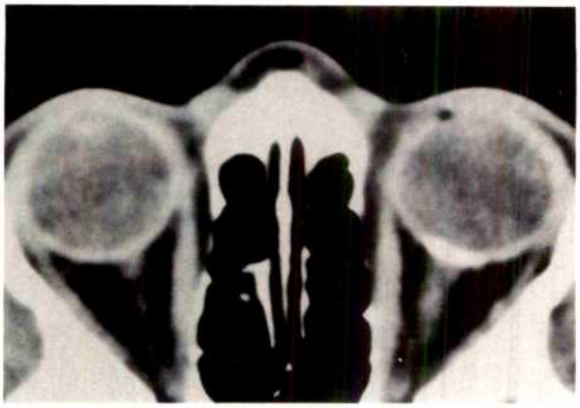

Figure 6. CT of the orbits of patient 2, showing the choroidal osteoma in the left eye as a mass with the radiographic density of bone.

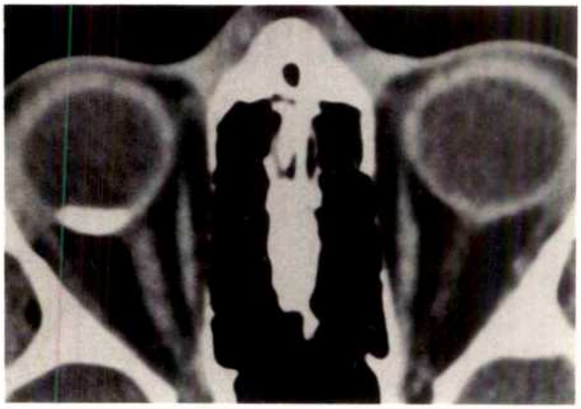

Figure 8. CT of the orbits of patient 3, showing the choroidal osteoma in the right eye as a mass with the radiographic density of bone.

above were not different from those of the adjacent normal choroid and consequently, despite their large size, the osteomas were not visualized on MR. This negative finding may be of clinical use, however, because MR reliably demonstrates uveal malignant melanomas in most cases, although there is some controversy about their precise signal characteristics (Marx et al, 1990).

The importance of diagnosis

From a combination of history, clinical examination and diagnostic imaging, it should be possible to differentiate choroidal osteomas from other choroidal lesions. The most important differential diagnosis is from malignant tumours of the uveal tract that may require treatment in the form of enucleation of the eye, local resection of the tumour or radiotherapy. It is well recognized that enucleation of the eye may be performed in error for tumours thought to be malignant melanomas when subsequent histological examination reveals a benign lesion (Kirk & Petty, 1956; Robertson & Campbell, 1979; COMS Group, 1990). Choroidal osteoma was first described following similar mistakes (Gass et al, 1978; Williams et al, 1978).

Although choroidal osteomas show characteristic appearances with US, FA and CT, none of these investigations is 100% sensitive and specific when used alone. Routine evaluation of choroidal masses should therefore involve all of these tests. If all potential differential diagnoses are considered and complete examination is performed as described, errors should not occur. In this study, MR has not been shown to be useful in the investigation of choroidal osteomas. Further studies may show whether MR helps to exclude the diagnosis by positively identifying a lesion, in the uncommon event that diagnostic doubt exists despite performing all other investigations.

Acknowledgments

The authors are grateful to Mr J. C. Dean Hart for his help in reading the manuscript, and to Mr R. H. B. Grey for making the diagnoses and for his permission to report the cases.

References

BRANT-ZAWADZKI, M. & ENZMANN, D. R., 1979. Orbital computed tomography: calcific densities of the posterior globe. *Journal of Computer Assisted Tomography*, *3*(4), 503–505.

BRYAN, R. N., LOUIS, R. A. & MILLER, S. L., 1983. Choroidal osteoma. *AJNR*, *4*, 491–494.

CHAR, D. H., UNSOLD, R., SOBEL, D. F., SALVOLINI, U. & NEWTON, T. H., 1990. Computed tomography: ocular and orbital pathology. In: *Modern Neuroradiology*, Vol. 4. *Radiology of the Eye and Orbit*, ed. by T. H. Newton and L. A. Bilaniuk (Raven Press, New York), pp. 9.1–9.64.

THE COMS (COLLABORATIVE OCULAR MELANOMA STUDY) GROUP, 1990. Accuracy of diagnosis of choroidal melanomas in the collaborative ocular melanoma study. *Archives of Ophthalmology*, *108*, 1268–1273.

FRISEN, L., SCHOLDSTROM, G. & SVENDSEN, P., 1978. Drusen in the optic nerve head: verification by computerised tomography. *Archives of Ophthalmology*, *96*, 1611–1614.

GASS, J. D. M., GUERRY, R. K., JACK, R. L. & HARRIS, G., 1978. Choroidal osteoma. *Archives of Ophthalmology*, *96*, 428–435.

GOLDSTEIN, B. G. & MILLER, J., 1982. Metastatic calcification of the choroid in a patient with primary hyperparathyroidism. *Retina*, *2*, 76–79.

HEDGES T. R., III, POZZI-MUCELLI, R., CHAR, D. H. & NEWTON, T. H., 1982. Computed tomographic demonstration of ocular calcification: correlations with clinical and pathological findings. *Neuroradiology*, *23*, 15–21.

JOFFE, L., SHIELDS, J. A. & FITZGERALD, J. R., 1978. Osseous choristoma of the choroid. *Archives of Ophthalmology*, *96*, 1809–1812.

KIRK, H. Q. & PETTY, R. W., 1956. Malignant melanoma of the choroid. *Archives of Ophthalmology*, *56*, 843–860.

MARX, H. F., COLETTI, P. M., RAVAL, J. K., BOSWELL, W. D. & ZEE, C. S., 1990. Magnetic resonance imaging features in melanoma. *Magnetic Resonance Imaging*, *8*, 683–689.

ROBERTSON, D. M. & CAMPBELL, R. J., 1979. Errors in the diagnosis of malignant melanoma of the choroid. *American Journal of Ophthalmology*, *87*, 269–275.

SANTONI, G., RICCI, A. L., LUPIDI, G., CIORBA, E. & FIORE, C., 1988. Choristome osseux de la choroïde bilatéral et microphtalmie asymétrique. *Journal Français d'Ophtalmologie*, *11*(4), 363–367.

SHIELDS, C. L., SHIELDS, J. A. & AUCHSBERGER, J. J., 1988. Review: choroidal osteoma. *Survey of Ophthalmology*, *33*, 17–27.

TURNER, R. M., GUTMAN, I., HILAL, S. K., BEHRENS, M. & ODEL, J., 1983. CT of drusen bodies and other calcific lesions of the optic nerve: case report and differential diagnosis. *AJNR*, *4*, 175–178.

WILLIAMS, A. T., FONT, R. L., VAN DYK, H. J. L. & RIEKHOF, F. T., 1978. Osseous choristoma of the choroid simulating a choroidal melanoma. *Archives of Ophthalmology*, *96*, 1874–1877.

ZEITER, H. J., 1962. Calcification and ossification in ocular tissue. *American Journal of Ophthalmology*, *53*, 265–274.

1992, *The British Journal of Radiology*, *65*, 849–851

The role of hysterosalpingography in modern gynaecological practice

By R. Rajah, FRCS, FRCR, J. M. McHugo, MRCP, FRCR and *M. Obhrai, MD, MRCOG

Departments of Radiology and *Gynaecology, Women's Hospital, Showell Green Lane, Sparkhill, Birmingham B11 4HL, UK

(*Received 5 September 1991 and in final form 23 March 1992, accepted 6 May 1992*)

Keywords: Hysterosalpingogram, Infertility, Laparoscopy

Abstract. A retrospective review of hysterosalpingography (HSG) in a major gynaecological centre was carried out. 324 patients attended (95%) for HSG out of 341 patients referred for this investigation. 189 examinations (58.3%) were abnormal. The requests and radiological findings were reviewed and the results compared with laparoscopy. HSG remains an integral part of gynaecological investigation and its value has not diminished in modern practice.

The aim of the study was to assess the role and efficacy of hysterosalpingography (HSG) in general gynaecological practice.

HSG has been performed for over 70 years, the first 3000 cases being reported in 1930. Modifications to the technique have taken place over the years, and non-ionic contrast agents have recently been introduced. With the increasing use of laparoscopy, the use of HSG in the investigation of infertility has diminished. Laparoscopic examination provides accurate information about extrinsic tubal pathology, but is poor in diagnosing intrinsic tubal pathology. Some researchers (Cumming & Taylor, 1979) believe that this may be overcome by the development of tuboscopy, but HSG still remains a more accurate and efficient method for the diagnosis of intrinsic tubal disease.

This retrospective review was performed to assess the role of HSG in the investigation and treatment of infertility.

Patients

Requests for HSG were reviewed over 18 months (January 1989 to June 1990). 17 patients either declined the investigation or became pregnant before the investigation. The mean age was 31 years (range 20–40 years).

Methods

324 examinations were performed out of 341 requests, the examination being performed either by a consultant radiologist (J.M.) or a post-FRCR senior registrar. An initial explanation of the procedure was given by the radiographer immediately prior to the procedure by the radiologist.

A supine control radiograph was obtained. Thereafter, the patient was placed in lithotomy position on the fluoroscopic table close to the lower end. The vulva was cleansed with 1% chlorhexidine and a digital examination undertaken to locate the cervix. The cervix was localized with a Cuscoe's speculum. Following cleaning, the anterior lip of the cervix was stabilized with a simple tenaculum and a metallic cannula with an acorn (varying in size depending on the size of the external os) was placed in the cervical os. The tenaculum was hooked onto the spine of the metallic cannula, maintaining a pressure to prevent leakage of contrast medium (Ioxaglate 320). Following injection, radiographs were obtained to show uterine and tubal anatomy and peritoneal spillage.

If no free spillage on either side was seen, a relaxant (hyoscine butylbromide or glucagon) was given intravenously to eliminate tubal spasm (Gerlock & Hooser, 1976). Further contrast medium was introduced and radiographs taken. If the distal ends of the fallopian tubes were dilated and no spillage occurred, an immediate prone radiograph was taken on removal of the instruments. The results were then explained to the patient.

Results

The majority of HSG examinations were performed for infertility (Table I), primary (35%) or secondary (21%). The examination was performed prior to, or following, tubal surgery in 58 patients (19%). In 18 cases, HSG was requested for the investigation of congenital uterine anomalies, fibroids or in the follow-up of Asherman's syndrome.

Table I. Clinical problems requiring investigation

	No. (%)
Primary infertility	114 (35.2%)
Secondary infertility	96 (20.6%)
Post-tubal surgery for primary infertility	35 (10.8%)
Post-tubal surgery for secondary infertility	16 (4.9%)
Post-sterilization check	7 (2.2%)
To check patency following reversal of sterilization	12 (3.7%)
Prior to reversal of sterilization	5 (1.5%)
Others	19 (5.5%)

Address correspondence to Dr J. M. McHugo.

Table II. Radiological findings at HSG

Findings	*n*
Uterus	
Normal	275 (84.8%)
Congenital abnormalities	19 (5.8%)
Bicornuate	6
Unicornuate	6
Arcuate	4
Septate	1
Uterus didelphys	2
Acquired abnormalities	27 (8.3%)
Fibroid	18
Polyps	5
Asherman's syndrome	3
Post-Caesarean scar	1
Tubes	
Normal	167 (51.5%)
Unilateral	4
Bilateral	163

The results are shown in Table II and III. The investigations were abnormal in 58% of patients and a uterine abnormality was demonstrated in 46 patients (14%). All these abnormalities were either not apparent at laparoscopy or were not seen. These results indicate that HSG defines uterine anatomy and is the investigation of choice in congenital uterine abnormality.

Tubal occlusion was apparent in 123 patients; the majority of these were detected at laparoscopy, but the site of occlusion was more accurately demonstrated on HSG (Table III). Salpingitis isthmica nosdosa was seen in 15 patients.

In our series, laparoscopy failed to demonstrate tubal patency in 20 patients where no pelvic pathology (6.8%) was found. HSG confirmed bilateral patency in 13 of these patients. In the other seven patients, HSG failed to demonstrate bilateral patency (in some, unilateral patency was established). This high failure rate may be related to the fact that antispasmodics are not given routinely during laparoscopy.

Table III. Site of occlusion as demonstrated at HSG

	n
Blockage (37.9%)	
Cornual	
Bilateral	9
Unilateral	30
Isthmic	
Bilateral	18
Unilateral	37
Fimbrial	
Bilateral	4
Unilateral	25
Tube abnormalities (20.6%)	
Bilateral hydrosalpinges, no spill	16
Unilateral hydrosalpinx, no spill	21
Bilateral hydrosalpinges, localised spill	5
Unilateral hydrosalpinx, localised spill	10
SIN, bilateral	5
SIN, unilateral	10

SIN, salpingitis isthmica nodosa.

Discussion

HSG demonstrated accurately the uterine cavity and tubal lumen. Several investigators (Taylor, 1977; Cumming & Taylor, 1979) have advocated the combined use of laparoscopy and hysteroscopy for evaluation of the fallopian tubes and uterine cavity, replacing HSG. Some workers (Snowden et al, 1984) believe laparoscopy alone is inaccurate in predicting tubal disease, with high false positive (16%) and high false negative (13%) rates. The false positive rate rises further to 31% for uterine abnormalities. Hence, these workers advocate both laparoscopy and HSG. HSG, however, remains superior for assessing intrinsic tubal disease.

In this series, HSG failed to demonstrate unilateral tubal patency once, whereas laparoscopy failed to demonstrate tubal patency either unilaterally or bilaterally in 6% of patients. HSG and laparoscopic findings were similar in 94% of our patients. This result is greater than previous reports (76%; Keirse & Vandervellen, 1973). The exact reason for this difference is unclear, but the use of a water-soluble (low osmolar) contrast agent and the expertise of the person performing the procedure are possible factors. 58% of our examinations were performed by a consultant radiologist (J.M.) with a particular interest in gynaecology, the remainder by an experienced senior registrar in radiology.

HSG is inaccurate in assessing extrinsic tubal adhesions (Duff et al, 1983). Delayed views may be helpful here, but this is not our experience. In our series, laparoscopy failed totally in one patient to visualize the uterus and the tubes because of dense adhesions. In this case, HSG was able to demonstrate a normal uterus with bilateral spillage.

Congenital and acquired lesions of the uterus are well demonstrated by HSG (Foda et al, 1962); however, minor congenital abnormalities of the uterus can be easily missed at laparoscopy (Craig, 1973). Furthermore, ultrasound failed to detect major congenital abnormalities in our series, and this limitation must be kept in mind. HSG remains the examination of choice for the investigation of congenital uterine anomalies.

Histological prediction of acquired uterine lesions by HSG is poor; it is impossible to distinguish fibromyomata from polyps radiologically. In our practice the majority of HSG examinations are performed for infertility (55%) or for tubal surgery (19.4%). With the advent of catheter dilatation of the occluded proximal tube, HSG may play an increasingly important role (Thurmond, 1991).

In conclusion, we feel strongly that HSG provides additional information to laparoscopy and both investigations should be performed in the investigation of infertility. Laparoscopy remains superior in assessing extratubular pathology and HSG is superior in demonstrating uterine and intraluminal tubular pathology. Both investigations are equally effective in the assessment of the patient following tubal surgery; HSG, however, is considerably less invasive.

References

CUMMING, D. C. & TAYLOR, P. J., 1979. Historical predictability of abnormal laparoscopic finding in the infertile woman. *Journal of Reproductive Medicine*, *23*, 295–298.

CRAIG, C. S. J., 1973. Congenital abnormalities of the uterus and fetal wastage. *South African Medical Journal*, *47*, 2000–2005.

DUFF, D. E., FRIED, A. M., WILSON, E. A. & HAACK, D. G., 1983. Hysterosalpingography and laparoscopy: A comparative study. *American Journal of Roentgenology*, *141*, 761–763.

FODA, M. S., YOUSSEF, A. F., SHAFEEK, M. A. & KASSEM, K. A., 1962. Hysterography in diagnosis of abnormalities of uterus. *British Journal of Radiology*, *35*, 115–121, 783–792, 836–842.

GERLOCK, A. J. & HOOSER, C. W., 1976. Oviduct response to glucagon during hysterosalpingography. *Radiology*, *119*, 727–728.

KEIRSE, M. J. N. C. & VANDERVELLEN, R., 1973. A comparison of hysterosalpingography and laparoscopy in the investigation of inferility. *Obstetrics and Gynaecology*, *41*, 685–688.

SNOWDEN, E. U., JARRETT, J. C., II & DAWOOD, M. Y., 1984. Comparison of diagnostic accuracy of laparoscopy, hysteroscopy and hysterosalpingography in evaluation of female infertility. *Fertility and Sterility*, *41*, 709–713.

TAYLOR, P. J., 1977. Correlations in infertility: symptomatology, hysterosaplingography, laparoscopy and hysteroscopy. *Journal of Reproductive Medicine*, *18*, 339–442.

THURMOND, A. M., 1991. Selective salpingography and fallopian tube recanalization. *American Journal of Roentgenology*, *156*, 33–38.

1992, *The British Journal of Radiology*, *65*, 852–856

Portable chest radiography in intensive care: a comparison of computed and conventional radiography

By *Paul Jennings, MRCP, FRCR, *Simon P. G. Padley, MRCP, FRCR and David M. Hansell, MRCP, FRCR

Department of Radiology, Royal Brompton National Heart and Lung Hospital, Sydney Street,
London SW3 6NP, UK

(*Received 8 November 1991 and in revised form 9 March 1992, accepted 6 May 1992*)

Keywords: Digital radiography, Chest radiography

Abstract. A prospective study was performed comparing computed and conventional radiography for the detection and visibility of cardiovascular devices in intensive care unit patients. Computed images were obtained using a commercially available 2K × 2K, 12-bit storage phosphor plate system. Image sets from 50 patients were assessed independently by three observers. A significant difference between the types of image was found for the detection of mediastinal drainage tubes and prosthetic valves. Computed images allowed greater confidence in the identification of courses and tips of lines. This advantage was most marked with edge-enhanced computed images.

Consistent high-quality portable chest radiographs are difficult to obtain. Computed radiography employing reusable photostimulable phosphor plates has several advantages: the wide dynamic range of these imaging plates ensures that retakes due to incorrect exposure are rarely necessary. In addition, a reduction in radiation dose to the patient, whilst obtaining high-quality images, can be achieved (Cohen et al, 1989). Digital aquisition of the image enables post-processing such as contrast manipulation and edge enhancement. A theoretical disadvantage of computed radiographic systems is their reduced spatial resolution. Conventional screen/film combinations have a resolution of greater than 10 line pairs/mm whilst computed systems achieve at best 5 line pairs/mm in adult chest radiography.

In most centres, portable chest radiography is most frequently requested on the intensive care unit and in this context the evaluation of drains, catheters and other cardiovascular devices is of prime importance. These devices also lend themselves to detection studies as their presence or absence can be verified with certainty. We undertook a prospective study to compare objectively the performance of a computed radiographic system, the first of its kind in clinical operation in the UK, with conventional film/screen radiography in this setting. The degree to which post-processing of the digital image improved the detection of cardiovascular devices was also investigated.

Materials and methods

A Fuji FCR AC-1 computed radiographic system (Fuji Photo Film UK Ltd) was in clinical operation on the adult intensive care unit for 3 months before the study was started. This system uses a reusable photostimulable phosphor plate (europium-doped barium fluoride bromide) housed in a cassette which is exposed in the same manner as a conventional film cassette. The imaging plate is scanned by a helium-neon laser which stimulates luminescence from the latent image; this signal is detected by a photomultiplier and subseqently digitized with a pixel matrix of 1760 × 2140 (pixel size 0.2 mm × 0.2 mm). The digital information is processed and recorded by laser printer on to film (Sonada et al, 1983). This system is configured to give the option of a single image on 24 cm × 30 cm film or a pair of smaller images, one of which is processed to resemble a conventional radiograph with a non-linear gradient curve and minimal spatial frequency enhancement; the second image of the pair has a wide latitude linear gradient and spatial frequency enhancement six times normal, generated by unsharp masking, which produces an edge-enhanced effect (Fig. 1). For this study all images were produced in the paired format.

Approval for this study was given by the Hospital Ethics Committee. Consent for two radiographs to be taken, conventional film/screen and computed, was obtained from 50 consecutive adult patients undergoing major cardiopulmonary surgery. The sets of radiographs were obtained at the same time during the first or second post-operative day on the intensive care unit. The film/screen combination was Kodak XL with Regular calcium tungstate screens. Both computed and conventional images were obtained at 80 kVp and 3 mAs using Picker Explorer mobile units.

The computed image pairs were separated and each of the three images (conventional, computed and

---

Address correspondence to Dr D. M. Hansell, Department of Radiology, Royal Brompton National Heart and Lung Hospital, Sydney Street, London SW3 6NP, UK.

*Present addresses: Dr P. Jennings, Department of Imaging, The Ipswich Hospital, Heath Road, Ipswich, Suffolk, and Dr S. Padley, Department of Radiology, Vancouver General Hospital, 10th Avenue and Heather Street, Vancouver, BC, Canada.

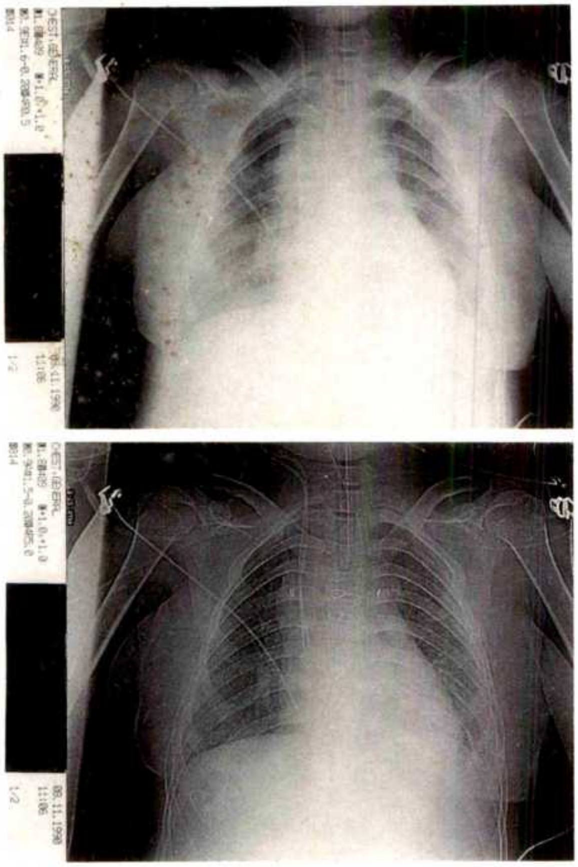

Figure 1. Format of laser printed hard copy pair. Lower image with wide latitude linear gradient and high spatial frequency enhancement.

computed enhanced) were assessed independently on separate occasions by three radiologists who were accustomed to interpreting computed radiographs. A questionnaire was completed for each image, in which the observers recorded their identification of individual cardiovascular devices. Each patient had at least one device *in situ* when the radiographs were obtained. The numbers of each type of device detected were summed for the three observers to produce detection scores. The visibility of the course and tip of all lines including central venous catheters and intercostal tubes were scored on a five point scale: 5, definitely identified; 4, probably identified; 3, indeterminate; 2, probably not identified; 1, definitely not identified.

The significance of any difference in visibility of devices in the three types of image was measured using McNemars' test. Confidence levels for course and tip visibility were compared using the Wilcoxon matched pairs signed ranks test and binomial two-tailed p-values obtained (Armitage & Berry, 1971).

Results

A total of 159 devices were present in the 50 patients, consisting of central venous catheters, Swan-Ganz catheters, endotracheal tubes, prosthetic valves, permanent pacing wires, intercostal and mediastinal drainage tubes. Detection scores for the different devices are shown in Table I.

All Swan-Ganz catheters, endotracheal tubes and pacing wires were detected on each of the three types of radiograph. Other devices were most frequently detected on the computed radiography images with highest detection scores for enhanced images: the most marked differences in detection scores were found for prosthetic valves and mediastinal drains. For the latter, 44% were detected on conventional film and 76% on enhanced computed images ($p < 0.025$).

No statistically significant differences were found in the detection scores for central catheters; however, significant differences were found in the confidence levels for the evaluation of the courses and tips of these devices, with the highest levels of confidence recorded for computed radiographs with enhancement ($p < 0.0001$). Similar results were obtained for mediastinal drains ($p < 0.001$).

Subsequent review of the films alongside each other confirmed that the reason for missed or inadequately visualized devices was due to relative underexposure of the mediastinum, chest wall or upper abdomen. This was most obvious on conventional film/screen radiographs (Fig. 2).

Discussion

In conventional radiography the film has three tasks, namely the capture, display and storage of the image.

Table I. Detection scores for each device summed for the three observers

Device (n)	Detection scores (%)		
	Conventional	Standard computed	Enhanced computed
Central venous catheters (102)	290 (95)	302 (99)	295 (96)
Mediastinal drains (15)	20 (44)	25 (56)	34 (76)
Endotracheal tubes (15)	45 (100)	45 (100)	45 (100)
Intercostal tubes (13)	38 (97)	38 (97)	39 (100)
Prosthetic valves (9)	14 (52)	21 (78)	25 (93)
Pacing wires (3)	9 (100)	9 (100)	9 (100)

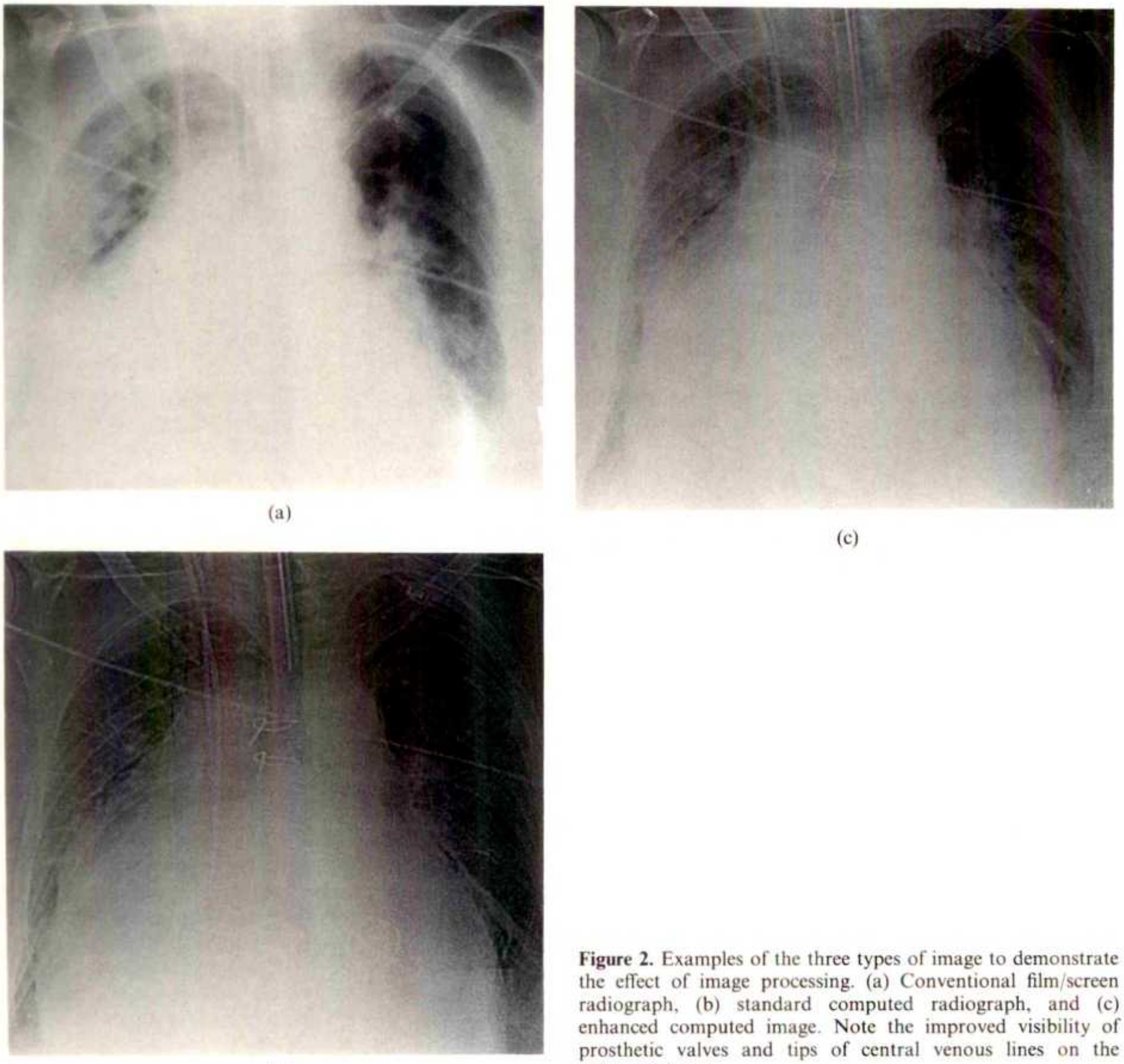
(a)

(c)

(b)

Figure 2. Examples of the three types of image to demonstrate the effect of image processing. (a) Conventional film/screen radiograph, (b) standard computed radiograph, and (c) enhanced computed image. Note the improved visibility of prosthetic valves and tips of central venous lines on the enhanced image.

For the function of image display and storage, film is excellent. As a receptor, however, film is far from ideal. The spatial resolution of film/screen combinations is more than adequate but the requirements of wide latitude and high speed tend to be mutually exclusive in terms of good contrast and low image noise (Merritt et al, 1985). A compromise is usually made between wide latitude to encompass a necessary wide exposure range (*e.g.* lung through to mediastinum) and sufficient contrast for the visibility of low-contrast detail. These drawbacks are compounded in portable bedside radiography by the difficulties of patient positioning, a short film–focus distance, poor control of scattered radiation and a lack of automatic exposure devices. As a result many chest radiographs obtained with portable equipment are of suboptimal diagnostic quality.

Computed radiographic systems offer the advantages of images that have been optimized for a wide range of exposure conditions (Fraser et al, 1989). The photoluminescence/dose response is almost two orders of magnitude greater than a conventional film/screen combination and this may also allow a lower patient radiation dose to be used. The minimum dose is limited in practice by an increase in quantum noise in the image as the exposure is decreased. Comparative studies have addressed the potential problem of lower spatial resolution in digital systems, particularly in their application to chest imaging (Goodman et al, 1986, 1988; Lams & Cocklin, 1986). These investigators concluded that a pixel size less than 0.4 mm is required for the accurate detection of subtle abnormalities such as pneumothoraces and septal lines.

Most of these studies used digitized images taken from conventional chest radiographs but more recently comparisons of conventional and computed radiographic systems using photostimulable phosphors have been published. These range from the subjective perceptions of diagnostic quality, which proved favourable (Fuhrman et al, 1988), to carefully designed observer performance studies of the detection of pneumothorax (Fajardo et al, 1989; Kehler et al, 1990), mediastinal lesions and pulmonary nodules (Morioka et al, 1988; Schaefer et al, 1990).

There have been some discordant results but in general, for these, tasks computed radiography has been equivalent or superior to conventional radiography. Post-processing of the digital image using techniques such as spatial frequency "edge" enhancement by unsharp masking theoretically offers the potential for increased visibility of features such as pneumothoraces and low-contrast structures (Ishida, 1987). This was confirmed by Goodman et al (1988) but the authors noted that for abnormalities other than pneumothorax, the edge enhanced images were significantly worse. Several studies have raised doubts about the accuracy of digital radiography in the detection of interstitial lung disease with, under certain circumstances, inferior performance compared with conventional radiographs (McMahon et al, 1985; Foley et al, 1987; Goodman et al, 1988; Schaefer et al, 1991). Post-processing inevitably changes the characteristics of normal lung features such as vessels and may certainly cause difficulties in interpretation for those unfamiliar with the appearances. The degree and type of image post-processing have a profound effect on the visibility of different structures within the chest. One elegant study has demonstrated that with high-frequency edge enhancement, computed radiographs can be equal in performance to film/screen radiography for the detection of interstitial lung disease (Schaefer et al, 1991). Post-processing needs to be tailored. As in other digital techniques such as computed tomography it is likely that no single image display will be sufficient for all tasks.

Most clinical users of computed radiographic systems routinely obtain a pair of images as described above (Fig. 1), one configured to match closely a conventional chest radiograph, the other post-processed to enhance certain features. To date there has been only one study of the supposed advantage of this dual format and of the relative value of the two images (Saito et al, 1988). This paper assessed a wide range of features including unverified lung pathology. Images were assessed by only one observer and statistical evaluation was not attempted. Another study that looked specifically at the detection of cardiovascular devices relied on images taken with the two techniques several hours apart and assessed the standard and enhanced computed images concurrently and compared these with conventional radiography (Thompson et al, 1989).

Our results confirm that there is an objective improvement in the detection of cardiovascular devices using computed radiography rather than conventional radiography for portable chest radiographs. Furthermore, this advantage is increased by post-processing of the digital image using a wide latitude, linear dose/density gradient and edge enhancement. The potential problems of an unfamiliar appearance of the lungs and reduced visibility of interstitial disease can be overcome by the simultaneous display of an unenhanced "analogue look-alike" image with the enhanced image.

References

Armitage, P. & Berry, G., 1971. *Statistical Methods in Medical Research* (Blackwell Scientific Publications, Oxford).

Cohen, M. D., Long, B., Cory, D. A., Broderick, N. J. & Smith, J. A., 1989. Digital imaging of the newborn chest. *Clinical Radiology, 40,* 365–368.

Fajardo, L. L., Hillman, B. J., Pond, G. D., Carmody, R. F., Johnson, J. E. & Ferrell, W. R., 1989. Detection of pneumothorax: comparison of digital and conventional imaging. *American Journal of Roentgenology, 152,* 475–480.

Foley, W. D., Goodman, L. R. & Wilson, C. R., 1987. The effect of varying pixel size and image processing on the detection of interstitial lung disease. In *Proceedings of the Chest Imaging Conference,* Madison, Wisconsin (Medical Physics Publishing Corp), pp. 113–123.

Fraser, R. G., Sanders, C., Barnes, G. T., McMahon, H., Giger, M. L., Doi, K., Templeton, A. W., Cox, G. C., Dwyer, S. J., Merritt, C. R. B. & Jones, J. P., 1989. Digital imaging of the chest. *Radiology, 171,* 297–307.

Fuhrman, C. R., Gur, D., Good, B., Rockette, H., Cooperstein, L. A. & Feist, J. H., 1988. Storage phosphor radiographs versus conventional films: interpreters perceptions of diagnostic quality. *American Journal of Roentgenology, 150,* 1011–1014.

Goodman, L. R., Foley, W. D., Wilson, C. R., Rimm, A. A. & Lawson, T. L., 1986. Digital and conventional chest images: observer performance with film digital radiography system. *Radiology, 158,* 27–33.

Goodman, L. R., Foley, W. D., Wilson, C. R., Tikofsky, R. S. & Hoffman, R. G., 1988. Pneumothorax and other lung diseases: effect of altered resolution and edge enhancement on diagnosis with digitised radiographs. *Radiology, 167,* 83–88.

Ishida, M., 1987. Image processing. In *Computed Radiography,* ed. by Y. Tateno, T. Iinuma and M. Takano (Springer-Verlag, Tokyo), pp. 25–30.

Kehler, M., Albrechtsson, U., Andresdottir, A., Larusdottir, H. & Lundin, A., 1990. Accuracy of digital radiography using stimulable phosphor for diagnosis of pneumothorax. *Acta Radiologica, 31,* 47–53.

Lams, P. M. & Cocklin, M. L., 1986. Spatial resolution requirements for digital chest radiographs: an ROC study of observer performance in selected cases. *Radiology, 158,* 11–19.

McMahon, H., Vyborny, C. J., Sabeti, V., Metz, C. E. & Doi, K., 1985. The effect of digital unsharp masking on the detectability of interstitial infiltrates and pneumothoraces. *Proceedings of SPIE, 555,* 246–252.

Merritt, C. R. B., Mathews, M. D., Scheinhorn, D. & Balter, S., 1985. Digital imaging of the chest. *Journal of Thoracic Imaging, 1*(1), 1–13.

Morioka, C., Brown, K., Balter, S., Milos, M. J., Huang, H. K., Kangarloo, H., Boechat, I. M. & Batra, P., 1988. Receiver operator characteristic analysis of chest radiographs with computed radiography and conventional analogue films. *Radiology, 169,* 349.

SAITO, H., KURASHINA, T., ISHIBASHI, I., SHIMANUKI, Y. & SAKAMOTO, K., 1988. Digital radiography in an intensive care unit. *Clinical Radiology, 39*, 127–130.

SCHAEFER, C. M., GREENE, R., OESTMANN, J. W., HALL, D. A., LLEWELLYN, H. J., McCARTHY, K. A., PILE-SPELLMAN, E. R. & RUBENS, J. R., 1990. Digital storage phosphor imaging versus conventional film radiography in CT-documented chest disease. *Radiology, 174*, 207–210.

SCHAEFER, C. M., GREENE, R., OESTMANN, J. W., LLEWELLYN, H. J., MROSE, H. E., PILE-SPELLMAN, E. R., RUBENS, J. R. & LINDEMANN, S. R., 1991. Interstitial lung disease: impact of postprocessing in digital storage phosphor imaging. *Radiology, 178*, 733–738.

SONADA, M., TAKANO, M., MIYAHARA, J. & KATO, H., 1983. Computed radiography utilizing scanner laser stimulated luminescence. *Radiology, 148*, 833–838.

THOMPSON, M. J., KUBICKA, R. A. & SMITH, C., 1989. Evaluation of cardiovascular devices on chest radiographs: digital vs analogue radiographs. *American Journal of Roentgenology, 153*, 1165–1168.

1992, *The British Journal of Radiology*, *65*, 857–860

Doppler ultrasound scanning in the detection of renal artery stenosis in hypertensive patients

By Cornelis T. Postma, MD, Joost van Aalen, MD, *Theo de Boo, MSc, †Gerd Rosenbusch, MD, PhD and Theo Thien, MD, PhD

Department of Medicine, Division of General Internal Medicine, and Departments of *Medical Satistics and †Diagnostic Radiology, University Hospital, Postbox 9101, 6500 HB Nijmegen, The Netherlands

(*Received 4 November 1991 and in revised form 6 April 1992, accepted 28 April 1992*)

Keywords: Doppler ultrasound scanning, Renal artery stenosis, Hypertension

Abstract. The diagnostic accuracy of Doppler ultrasound in the detection of renal arterial disease has been assessed in a prospective study of 61 hypertensive patients. The findings of Doppler ultrasound were compared with the results of renal angiography. In 15 patients (24.5%) no accurate Doppler signs could be obtained and the Doppler ultrasound examination was considered a technical failure. Of the remaining 46 patients, 24 had renal artery stenosis. Nine of the stenoses were not detected by Doppler ultrasound and in three patients a false positive diagnosis of renal artery stenosis was made. The sensitivity of Doppler ultrasound was 62.5%, the specificity 86.4% and the overall diagnostic acccuracy was 73.9%. By comparing the 15 patients in whom Doppler ultrasound failed with the 46 in whom it was successful, age appeared to be higher and creatinine clearance lower in the failure group. By comparing the 34 patients with true positive and true negative results with the 12 patients with false results, no significant differences were found. In a multivariate analysis, higher age showed a significant relation to failure of Doppler ultrasound. Doppler ultrasound has limited value in the screening of hypertensive patients for renal artery stenosis.

Renal artery stenosis is a frequent cause of secondary hypertension. Its prevalence among hypertensive patients varies between 0.5 and 10%, depending on the age of those studied and the institution where the study is undertaken (Anderson et al, 1988). The detection of renal artery stenosis is important since hypertension may be cured or improved after relief of the stenosis (Novick et al, 1981; Sos et al, 1988). Non-invasive procedures to detect renal arterial disease are not sensitive enough to use as screening procedures (Postma et al, 1990; McCarthy & Weber, 1990). Invasive tests also have a limited value in screening for this condition (Svetkey et al, 1989; Postma et al, 1991; Mann et al, 1991; Roubidoux et al, 1991). Renal angiography is still the most reliable procedure to detect renal artery stenosis, but a more practical non-invasive test remains preferable. With the development of Doppler ultrasound it became possible to examine abdominal vessels, including the renal arteries. By this technique stenosed renal arteries could be identified (Greene et al, 1981). Initial studies with various Doppler criteria reported sensitivities and specificities that ranged from 89 to 100% and 73 to 93%, respectively (Avasthi et al, 1984; Handa et al, 1988).

Because of the non-invasive nature of this technique we considered it an important and promising screening procedure for renal artery stenosis and initiated a prospective study to determine the value of renal artery Doppler ultrasound in the detection of renal artery stenosis. We also analysed which clinical characteristics contributed to success or failure of the procedure.

Patients and methods

The Doppler ultrasound technique was studied prospectively in 61 hypertensive patients of whom 122 kidneys were depicted. A diagnosis of hypertension was made if at three outclinic visits, the patients had a supine diastolic blood pressure above 90 mmHg. Baseline blood pressure was the mean of three readings in a period when antihypertensive medication had been withheld for at least 2 weeks. Renal angiography was performed in all patients. The only criterion for inclusion in this study was that in the evaluation of a hypertensive patient, renal arteriography was indicated.

The arteriograms were all read by an experienced radiologist who was unaware of the results of the ultrasound study. Hypertensive patients underwent renal angiography on clinical indications: age, severity of hypertension, difficulties with effective treatment, and sudden changes in blood pressure level. The interval between angiography and the ultrasound examination was always less than 6 months; the examinations were usually within 1 week. Antihypertensive medication was stopped at least 2 weeks before the examinations. If one renal artery was insufficiently visualized to obtain Doppler signals, the procedure was considered a failure in that patient. A diagnosis of occlusion was made if the renal artery could be clearly seen but no Doppler signal could be obtained. Patients with multiple renal arteries were included in the study and not considered technical failures if at least one renal artery, on each side, had been identified. On this basis the study group was divided into two subgroups: patients in whom Doppler

P 25864

ultrasound failed, and those in whom both renal arteries could be visualized and studied by Doppler ultrasound.

These two groups were then compared to see if any clinical characteristic was related to the failure of the Doppler ultrasound. Another subdivision was made of patients in whom ultrasound was technically successful. A comparison between true positive and true negative versus false positive and false negative was made among these subjects. The clinical characteristics compared among the various groups were: age, sex, blood pressure at the time of examination, Quetelet index (body mass index) (kg/m^2), renal function (estimated creatinine clearance (ECC), Cockroft & Gault, 1976), kidney size, pathology of the renal artery stenosis as determined by radiological criteria and degree of the stenosis expressed as a percentage of luminal diameter. The stenoses were divided into five categories: less than 50%, 50–75%, 75–90%, greater than 90% and complete occlusion. Stenoses of less than 50% were considered haemodynamically insignificant.

Statistics

Differences between two (sub)groups were tested with Wilcoxon's two-sample test. To identify clinical characteristics possibly related to the occurrence of technical failure, a stepwise logistic regression analysis was used. The same method was used in terms of true (positive or negative) or false within the group of patients with a technically accurate result. Results were regarded statistically significant if $p < 0.05$, two sided.

Doppler ultrasound examination procedure

Examinations were performed by technicians experienced in Doppler techniques, with supervision by radiologists. The patients were examined in the morning, in the fasting state, to avoid bowel gas. A colour duplex real-time system was used with a 3.5 MHz sector transducer for imaging and 3.0 MHz for Doppler (Sonolayer phased array scanner SSA-270 A, Toshiba, Tokyo). The patients were examined in the supine position. When necessary the patients were placed in left lateral decubitus for the right kidney and in right lateral decubitus for the left kidney. Colour Doppler was used to identify the renal arteries. When optimally audible and visible, the Doppler spectra (angle of less than 60° and greater than 30° between transducer and vessel) from the aorta, the main renal artery proximally and distally, the midzone and the arcuate arteries were recorded. The examination lasted between 45 and 60 min for both sides. The sample size was ±2 mm. According to Dubbins (1986) and Robertson et al (1988), increased peak frequency ($\geqslant 4$ kHz) and broadening of the normal spectrum were taken as evidence of a significant, *i.e.* a more than 50%, luminal stenosis. An assessment of the severity of the stenoses was not attempted.

Table I. Clinical characteristics of all patients ($n = 61$) and of patients with technical success ($n = 46$) *versus* technical failure ($n = 15$)

	All patients	Technical success	Technical failure
Gender M/F	39/22	26/20	13/2
Age (years)	50.9 (15.1)	48.4 (16.2)[a]	58.7 (7.5)
Quetelet index (kg/m^2)	25.5 (4.92)	24.9 (4.5)	27.2 (5.8)
Creatinine serum (μmol/dm^3)	142.5 (118.5)	131.2 (115.3)	177.0 (125.4)
Creatinine clearance (ml/min)	70.8 (29.5)	75.3 (29.6)[a]	57.0 (25.1)
Baseline blood pressure			
Systolic (mmHg)	179.2 (24.6)	177.1 (24.0)	185.7 (26.0)
Diastolic (mmHg)	105.7 (13.5)	105.0 (13.9)	107.8 (12.2)

Between brackets one standard deviation.
[a] $p < 0.05$.

Results

The study included 39 male and 22 female patients. The mean age was 50.9 (15.1, ±1 SD) years (Table I). The mean baseline systolic blood pressure was 179.2 (±24.6) mmHg, and the mean diastolic blood pressure was 105.7 (±13.5) mmHg (Table I). The arterial blood supply of 122 kidneys was visualized by renal arteriography. In 15 patients (24.5%), including 11 with a stenosis, no accurate Doppler signals could be obtained and these studies were considered technical failures (Table I). In the remaining 46 patients the results of the Doppler ultrasound were technically satisfactory and the outcome could be compared with the results of renal angiography. 13 kidneys had two renal arteries and one had three. With Doppler ultrasound none of the accessory renal arteries was identified. A renal artery stenosis was present in 24 of the 46 patients. There were eight stenoses of 50–75%, six of 75–90% and four > 90%; six renal arteries were totally occluded. Included were five bilateral stenoses, of which the more severe stenosis was used for the classification. Of the 24 patients with renal artery stenosis, 15 were identified by Doppler ultrasound as having a stenosis (Table II). Nine stenoses were not accurately detected. Of these nine patients, three had bilateral stenoses that were recognized as unilateral stenoses by Doppler ultrasound, including one patient in whom a diagnosis of unilateral renal

Table II. Doppler ultrasound in the detection of renal artery stenosis in hypertensive patients: results of Doppler ultrasound in comparison with renal angiography

		Arteriography	
		+	–
Doppler ultrasound	+	15	3
	–	9	19

Sensitivity, 62.5%. Positive predictive value, 83.3%.
Specificity, 86.4%. Negative predictive value, 67.9%.
Accuracy, 73.9%. Prevalence of RAS, 52%.

Table III. Patients with technical success of Doppler ultrasound subdivided in two groups, agreement with arteriography (N = 34) or not (N = 12)

	Agreement	No agreement
Gender MF	21/13	7/5
Age (years)	48.2 (16.5)	48.9 (15.8)
Quetelet index (kg.m^2)	25.1 (4.8)	24.4 (3.8)
Creatinine serum (μmol/Ldm^3)	116.5 (94.2)	172.9 (158.8)
Creatinine clearance (ml/min)	80.4 (28.1)	60.6 (30.0)
Renal artery stenosis (number of patients)	15	9
Baseline blood pressure		
Systolic (mmHg)	174.9 (24.9)	183.5 (20.9)
Diastolic (mmHg)	103.5 (14.9)	109.4 (10.0)

Between brackets one standard deviation (1SD), unless indicated otherwise.
Between the two groups no significant differences were noted.

artery stenosis was made contralateral to the arteriographically demonstrated stenosis. Of the 22 patients without a stenosis, 19 were correctly identified as such by Doppler ultrasound. Three were falsely identified as renal artery stenosis. This resulted in a sensitivity of 62.5% and a specificity of 86.4%. The overall diagnostic accuracy was 73.9% (Table II).

To identify factors adversely influencing the Doppler ultrasound examination, we compared the clinical characteristics of the 46 patients in whom Doppler ultrasound was successful and the 15 in whom no adequate Doppler ultrasound examination could be obtained. Age was significantly lower in successful examinations: 48.4 (±16.2) *vs.* 58.7 (±7.5) years $p < 0.05$ (Table I). Creatinine clearance was significantly lower in the patients in whom Doppler ultrasound was unsuccessful, namely 57.0 (±25.1) *vs.* 75.3 (±29.6) ml/min, $p < 0.05$ (Table I). The other clinical characteristics showed no significant differences between the two groups.

In the group of 46 patients in whom a successful Doppler ultrasound examination was performed, the data of 34 patients with a true positive or true negative result were compared with the data of the 12 patients with a false positive or false negative result. No differences in clinical characteristics were found between these two groups (Table III). The pathology of the stenosis, *i.e.* atherosclerosis, fibromuscular dysplasia or other, the degree of the stenosis and kidney size were not significantly different. In a stepwise logistic regression procedure, in which all the aforementioned clinical data of all patients were included, a significant positive relation was found between higher age and technical failure of Doppler ultrasound ($p < 0.05$). The same procedure used in the 46 patients with successful examinations showed no relation between any of the mentioned clinical and stenosis characteristics and true or false outcome of Doppler ultrasound.

Discussion

Methods of screening hypertensive patients for renal artery disease are the subject of continuing research because the most adequate procedure has, as yet, not been found. The optimal procedure should be simple, non-invasive, easy to perform and inexpensive. Non-invasive screening methods are not accurate enough to be implemented as reliable screening tests (Postma et al, 1990). With the development, and initially very promising results, of Doppler ultrasound a step forward seemed to have been made (Avasthi et al, 1984; Handa et al, 1988). More recent studies, however, have reported less favourable results of Doppler ultrasound with sensitivities of 0% and a highest specificity of 37% (Berland et al, 1990; Desberg et al, 1990). In these studies, the main renal artery was identified in only 51–58% of kidneys (Berland et al, 1990; Desberg et al, 1990). In one of the studies a time limitation was set for the Doppler ultrasound procedure and was probably one of the main reasons for the high technical failure rate (Desberg et al, 1990). In our study, without time limitations, we still found 24.5% technical failures in our patients. In the present study, 11% of kidneys had multiple renal arterial supply. As others have found (Berland et al, 1990; Desberg et al, 1990), in our study multiple renal arterial supply was not identified by Doppler ultrasound. Because of the possibility of stenoses in any of the involved arteries, the identification of one patent main renal artery does not exclude stenosis elsewhere in the arterial supply of a kidney.

In our population with a prevalence of renal artery stenosis of 52%, the resulting positive predictive value

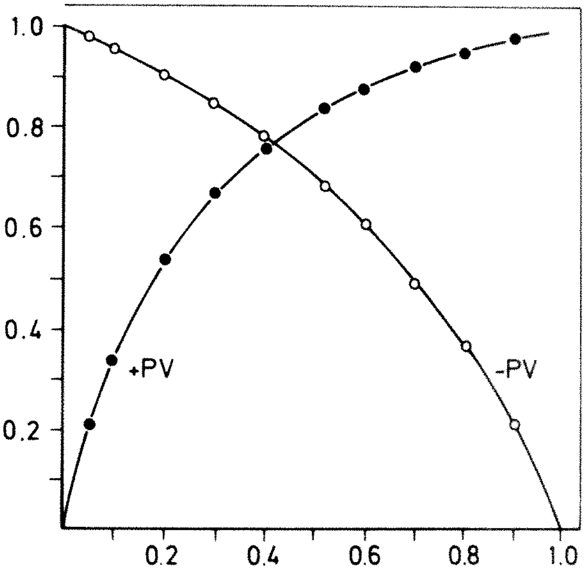

Figure 1. Receiver operated characteristic curve of the Doppler ultrasound technique in the detection of renal artery stenosis. Prevalence is indicated on the x-axis. Positive and negative predictive values are shown by the lines on the graph and their values are indicated on the y-axis.

of Doppler ultrasound was 83.3% and the negative predictive value 67.9% (Fig. 1). For a prevalence of renal artery stenosis of 5%, which is more probable in the general hypertensive population, the positive predictive value would be 19.5% and the negative predictive value 97.8% (Fig. 1). Thus with a 5% prevalence, the probability that renal artery stenosis is present in the case of a positive Doppler ultrasound would rise from 5% to 19.5% and the probability that stenosis is absent in the case of a negative Doppler ultrasound would rise from 95 to 97.8%.

We analysed if (and which) clinical characteristics could indicate technical failure or false negative and false positive results. Univariate analysis showed a significant difference in age and creatinine clearance between patients who had successful examinations and those for whom it failed. In a multivariate analysis of the patients of these two groups, only age showed an independent and significant relation to technical failure. Multivariate analysis in the groups with true positive and true negative results versus those with false positive and false negative results, showed no clinical criteria significantly related to a false result of Doppler ultrasound. The suggested relation between body structure, *i.e.* more obese subjects and technical failure (Handa et al, 1988) could not be established in our study. The relation between technical failure and age could point to a diminished flow as a cause. Another possibility is that older patients cannot lie still for the longer periods necessary for Doppler ultrasound or that they have more bowel gas preventing an adequate examination.

In conclusion, although the specificity of Doppler ultrasound in the screening of renal arterial disease in hypertensive patients is acceptable, its low sensitivity makes it unsatisfactory as a screening procedure for renal artery stenosis in unselected hypertensive patients.

Acknowledgments

We thank the Doppler ultrasound technicians, Mrs D. Jansen-Bell, Mrs M. Eykmans-Winterink and Mrs C. Wouters, for their excellent technical assistance.

References

Anderson, G. H., Jr, Blakeman, N. & Streeten, D. H. P., 1988. Prediction of renovascular hypertension. Comparison of clinical diagnostic indices. *American Journal of Hypertension, 1,* 301–304.

Avasthi, P. S., Voyles, W. F. & Greene, E. R., 1984. Noninvasive diagnosis of renal artery stenosis by echo-Doppler velocimetry. *Kidney International, 25,* 824–829.

Berland, L. L. Koslin, D. B., Routh, W. D. & Keller, F. S., 1990. Renal artery stenosis: prospective evaluation of diagnosis with color duplex US compared with angiography. *Radiology, 174,* 421–423.

Cockroft, D. W. & Gault, M. H., 1976. Prediction of creatinine clearance from serum creatinine. *Nephron, 16,* 31–41.

Desberg, A. I., Paushter, D. M., Lammert, G. K., Hale, J. C., Troy, R. B., Novick, A. C., Nally, J. V. Jr & Weltevreden, A. M., 1990. Renal artery stenosis: evaluation with colour Doppler flow imaging. *Radiology, 177,* 749–753.

Dubbins, P. A., 1986. Renal artery stenosis: duplex doppler evaluation. *British Journal of Radiology, 59,* 225–229.

Greene, E. R., Venters, M. D., Avasthi, P. S., Conn, R. L. & Jahnke, R. W., 1981. Noninvasive characterisation of renal artery blood flow. *Kidney International 20,* 523–529.

Handa, N., Fukanaga, R., Ogawa, S., Matsumoto, M., Kimura, K. & Kamada, T., 1988. A new accurate and non-invasive screening method for renovascular hypertension: the renal artery Doppler technique. *Journal of Hypertension, 6* (Suppl. 4), S458–S460.

Mann, S. J., Pickering, T. G., Sos, T. A., Uzzo, R. G., Sarkar, S., Friend, K., Rackson, M. E. & Laragh, J. H., 1991. Captopril renography in the diagnosis of renal artery stensosis: accuracy and limitations. *American Journal of Medicine, 90,* 30–40.

McCarthy, J. E. & Weber, A. B., 1990. The captopril test and renovascular hypertension: a cautionary tale. *Archives of Internal Medicine, 150,* 493–495.

Novick, A. C., Straffen, R. A., Stewart, B. H., Gifford, R. W. & Vidt, D. de, 1981. Diminished operative morbidity and mortality in renal revascularisation. *Journal of the American Medical Association, 246,* 749–753.

Postma C. T., Steen, P. H. M. van der, Hoefnagels, W. H. L., Boo, Th. de & Thien, Th., 1990. The captopril test in the detection of renovascular disease in hypertensive patients. *Archives of Internal Medicine, 150,* 625–628.

Postma, C. T., Oijen, A. van, Barentsz, J. O., Boo, Th. de, Hoefnagels, W. H. L., Corstens, F. H. M. & Thien, Th., 1991. The value of tests predicting renovascular hypertension in patients with renal artery stenosis treated by angioplasty. *Archives of Internal Medicine, 151,* 1531–1535.

Robertson, R., Murphy A. & Dubbins, P. A., 1988. Renal artery stenosis: the use of duplex ultrasound as a screening technique. *British Journal of Radiology, 61,* 196–201.

Roubidoux, M. A., Reed Dunnick, N., Klotman, P. E., Newman, G. E., Cohan, R. H., Kadir, S. & Svetkey, L. P., 1991. Renal vein renins: inability to predict response to revascularisation in patients with hypertension. *Radiology, 178,* 819–822.

Sos, T. A., Pickering, T. G., Sniderman, K., Saddekni, S., Case, D. B., Silane, M. F., Vaughan, D. E. Jr. & Laragh, J. H., 1983. Percutaneous transluminal renal angioplasty in renovascular hypertension due to atheroma or fibromuscular dysplasia. *New England Journal of Medicine, 309,* 274–279.

Svetkey, L. P., Himmelstein, S. I., Dunnick, N. R., Wilkinson, R. H. Jr., Bollinger, R., McCann, R. L., Beytas, E. M. & Klotman P. E., 1989. Prospective analysis of strategies for diagnosing renovascular hypertension. *Hypertension, 14,* 247–257.

1992, *The British Journal of Radiology*, *65*, 861–864

Can serum prostate-specific antigen replace bone scintigraphy in the follow-up of metastatic prostatic cancer?

By G. R. J. Sissons, MRCP, FRCR, R. Clements, MA, FRCS, FRCR, *W. B. Peeling, MA, FRCS and †M. D. Penney, MD, MRCPath

Departments of Radiology, *Urology and †Chemical Pathology, Royal Gwent Hospital, Newport, Gwent NP9 2UB, UK

(*Received 21 November 1991 and in revised form 16 April 1992, accepted 28 April 1992*)

Keywords: Prostate cancer, Scintigraphy, Prostate-specific antigen

Abstract. Bone scintigraphy is the most sensitive imaging technique for the initial detection of bone metastases and is widely used in the staging of prostatic cancer. This study was performed to assess whether the development of further bone metastases can be detected by serial measurements of the serum glycoprotein prostate-specific antigen (PSA) as an alternative to follow-up scintigraphy. The bone scintigrams and PSA levels of 101 patients with metastatic prostate cancer entered into two therapeutic trials have been reviewed. Serial results of both investigations were available in 59 cases. In three cases new bone deposits were observed without a corresponding rise in PSA. In two other cases the scintigrams were considered to be suspicious of progression with no change in PSA levels; however, further follow-up indicated that these changes were not due to metastases. In 13 cases PSA levels were rising in advance of new deposits on the scintigrams. In the remaining 41 cases the PSA levels and scintigraphic findings paralleled each other. We conclude that serial estimation of PSA levels is a simpler marker for disease progression than bone scintigraphy in metastatic prostatic cancer, but that neither technique in isolation gives complete accuracy.

Prostatic cancer is the third most common cause of male cancer death in the UK. There is a spectrum of disease activity (George, 1988) with many tumours found incidentally at post-mortem examination (Scott et al, 1969). It has been appreciated recently that many tumours are multifocal within the prostate, and that tumours may be found within the transition and central zones as well as the more common location in the peripheral zone (McNeil et al, 1988).

The most important prognostic indicator at initial diagnosis is the presence or absence of bone metastases. The demonstration of widespread disease has a major bearing on management as there is no prospect of cure. However, hormonal manipulation of various types can produce useful palliation.

The most sensitive technique for detecting bone metastases is bone scintigraphy (O'Donoghue et al, 1978) and this remains an established technique in the initial staging of prostatic cancer. In clinical trials, many patients with bone metastases are subsequently monitored with serial scintigrams to assess disease progression.

Prostate-specific antigen (PSA) is a serum glycoprotein first described by Wang et al in 1979. It is highly specific for prostatic epithelium and serum levels are usually raised in advanced prostatic cancer (98% of patients with stage D_2 disease described by Ercole et al, 1987). Comparative studies indicate that it is more frequently elevated in disease than acid phosphatase or alkaline phosphatase measurements in both locally advanced and metastatic prostatic cancer (Emtage et al, 1987). The cost of each assay is considerably less than that of scintigraphy and avoids the use of ionizing radiation. Thus the use of a serum assay as opposed to an isotope bone scan in the follow-up of such patients would offer several advantages. This study was performed to determine whether the progression of bone metastases can be detected by serial measurements of PSA as an alternative to routine follow-up bone scans. Scintigraphy could then be reserved to localize the extent and distribution of disease when progression is suspected.

Patients and methods

The bone scintigrams and serum PSA levels of 101 patients with advanced prostatic cancer have been reviewed retrospectively. Each patient had been entered into one of two therapeutic trials of different regimens of hormonal manipulation. Patients were recruited into the first study (goserelin *vs.* orchidectomy) in 1984–86 and into the second (cyproterone acetate *vs.* goserelin *vs.* cyproterone acetate + goserelin). Each patient had histologically proven prostatic carcinoma and was considered to have one or more bone metastases on a staging bone scintigram.

Scintigrams were performed at entry and then at 6-monthly intervals. Images were obtained 2–4 h after injection of 500 MBq of technetium-99 m methylene diphosphonate using a General Electric 400T gamma camera with a general-purpose collimator. The scintigrams were reviewed by a single radiologist noting any change in the number of deposits, and compared with the original report. If there was any discrepancy, the

---

Address correspondence to Dr R. Clements.

scintigrams were reviewed by a third radiologist and a consensus view obtained.

PSA levels were measured using the Hybritech Tandem PSA-R assay starting in 1986. These were performed at 0, 1, 2, 3, 6, 9 and 12 months and then at 6-monthly intervals. In 17 cases entered in late 1985 no results were available for up to the first 6 months of treatment but the remaining sequence was available for review.

In 21 cases the PSA sequence was not adequate for meaningful analysis (mainly patients entered in 1984/5). In a further 21 cases no bone scan sequence was available. This was because patients were withdrawn from the study or died before scintigraphic follow-up, or the images could not be traced. Serial results of both investigations were available in 59 cases.

Results

Analysis was confined to the 59 patients in whom a meaningful sequence of PSA and scintigraphy results were obtained.

PSA levels were elevated (> 4 ng/ml) in all 42 patients where an initial pre-treatment value had been performed. In one case the result of 6.7 ng/ml was below the level of 10 ng/ml commonly taken as being the threshold for suspicion of significant prostatic cancer.

Following treatment, PSA levels were recorded at less than 10 ng/ml in 38 out of the 59 cases, mostly within 6 months after the start of therapy. The PSA levels and bone scintigrams were reviewed to assess subsequent disease progresson and the main findings are summarized in Table I.

Patients have been divided into four groups according to the relationship of PSA values to the scintigraphic appearances.

Group A

In 19 patients, following an initial fall, the PSA levels remained at a stable level with no associated progression on the bone scintigram during the period of follow-up.

Group B

In this group of 22 patients, the PSA level increased during the period of observation and this increase corresponded with disease progression on the scintigram. The PSA level increase was a minimum of 25% above the initial PSA level.

Table I. PSA and scintigraphy in 59 patients with hormonally treated prostate cancer

	Scintigrams	
	Stable	Suggests progression
PSA levels		
Stable	19	5
Suggests progression	13	22

Group C

In 13 patients the PSA level increased (as defined in Group B) in advance of progression on the bone scintigram.

Group D

In five cases the bone scintigram appeared to be progressing whilst the PSA level was unchanged. Details of these five patients are outlined below.

Case 1. This 66-year-old man with a poorly differentiated tumour had an initial PSA of 62 ng/ml and a solitary deposit on the initial bone scintigram. He was treated with goserelin, and at 6 months the PSA was 3.7 ng/ml whilst the bone scan demonstrated 10 deposits. In the same period the prostatic acid phosphatase fell from 53 U/l to 5 U/l whilst the alkaline phosphatase increased slightly from 113 IU/l to 125 IU/l. The patient had no symptoms of bone metastases at this time. Such symptoms were reported 3 months later, and the patient died after a further 6 weeks. The PSA level became elevated during the last month of life to 14.4 ng/ml.

Case 2. This 74-year-old man sustained a pathological fracture of his femur, and biopsy of the fracture site revealed prostatic adenocarcinoma. Clinical examination revealed a T_3 carcinoma of prostate and he was treated with goserelin and cyproterone acetate. The initial PSA level was 1610 ng/ml and with treatment this fell to below 10 ng/ml. Bone scintigraphy revealed additional deposits in the thoracic and lumbar spine. These persisted during treatment, and new metastases appeared in the right ribs after 2 years treatment, whilst the PSA level remained below 2 ng/ml and the alkaline phosphatase remained stable at about 125 IU/l. The patient has no symptoms of bone metastases 18 months after the new areas of bone activity were seen on the scintigram.

Case 3. A 60-year-old man presented with a T_3 prostatic tumour. Initial PSA level was 22 ng/ml and a bone scan demonstrated increased activity at D11. Treatment started with goserelin and the PSA level fell to, and subsequently stayed in, the normal range within 2 months. A 6-month follow-up bone scintigram showed metastatic involvement of the skull vault. In the same period the alkaline phosphatase changed from 73 IU/l to 91 IU/l, and the prostatic acid phosphatase increased from 0.4 to 1.7 U/l. The patient had no symptoms of bone metastases.

Case 4. An 83-year-old patient with a T_3 prostatic tumour and bone metastases had an initial PSA level of 164 ng/ml. Following treatment with cyproterone acetate and goserelin, the PSA level fell progressively, to 5 ng/ml at 6 months and to the normal range by 18 months. It has subsequently remained in the normal range. The initial scintigram showed sternal metastases and at 18 months increased tracer activity was noted in the lower ribs. This was interpreted as further bone metastases. This abnormal activity disappeared at 24 months and the scan subsequently appeared normal.

Table II. Scintigraphy in the monitoring of progression of bone metastases

	Presence of disease progression	
	Yes	No
Prediction of disease progression by scintigraphy		
Yes	25	2
No	13	19

Table III. Serum PSA measurements in the monitoring of progression of bone metastases

	Presence of disease progression	
	Yes	No
Prediction of disease progression by PSA		
Yes	35	0
No	3	21

The serum alkaline phosphatase remained in the normal range throughout the period.

Case 5. This 70-year-old man with a moderately differentiated carcinoma had an initial PSA measurement of 35 ng/ml, and the initial scintigram revealed multiple areas of activity in the ribs, lumbar and thoracic spine. After treatment with cyproterone acetate, the PSA level fell over 5 months to the normal range and has subsequently remained in the normal range. The bone scintigram reverted to normal, but at 2 years increased activity was noted in the lumbar spine. The PSA level remained normal, and radiographs of the lumbar spine demonstrated degenerative change only. The alkaline phosphatase was initially 154 IU/l and during the period of treatment remained stable at about 120 IU/l.

A combination of serum PSA measurements and scintigraphy may be used to achieve a more accurate assessment of progressive bone metastases, and the results may be regrouped as in Tables II and III to permit calculation of the predictive values of scintigraphy and serum PSA measurements in the monitoring of disease progression. In the 13 Group C patients, it is impossible to be certain that the rise in serum PSA level that occurred prior to the progression noted by scintigraphy reflects prior progression of bone metastases and not progression of soft-tissue disease at that time; the predictive value of PSA for detecting progressive bone disease should be viewed with this caveat. The predictive value of positive scintigraphy is 92.5%, whilst that of negative scintigraphy is 59.4%, *i.e.* four out of 10 patients will not show disease progression by scintigraphy when it is considered that true progression is occurring. The predictive value of positive serum PSA levels for disease progression is 100%, whilst that of a negative PSA result is 87.5%, *i.e.* approximately one in 10 patients will not show disease progression by PSA when it is considered true progression is occurring.

Discussion

Serum PSA levels are now widely used in the diagnosis of prostatic cancer patients. Their role in the initial staging of the disease has been investigated by Stamey and Kabalin (1989): in 230 men, PSA was directly proportional to advancing clinical stage, but it statistically failed to distinguish between consecutive stages B_2 and B_3 and between stages C and D_1. We have recently investigated the relative roles of isotope bone scanning and serum PSA measurements in the initial assessment of newly diagnosed patients with prostatic cancer and it may be that isotope scintigraphy is not justified in the initial staging assessment of patients with newly diagnosed cancer if the PSA level is below 20 ng/ml. The findings of Chybowski et al (1991) would support this view. 521 randomly chosen patients with newly diagnosed untreated prostatic cancer were retrospectively reviewed. The median serum PSA concentration in patients with a positive bone scan was 158 ng/ml, whereas men with a negative bone scan had a median serum PSA level of 11.3 ng/ml. The 99.7% negative predictive value of a low serum PSA concentration for bone scan findings was particularly noted. In 306 men with a serum PSA level of 20 ng/ml or less, only one patient (PSA 18.2 ng/ml) had a positive bone scan, and these authors concluded that staging bone scintigraphy in a previously untreated prostatic cancer patient with a low PSA may not be necessary.

Serum PSA levels are also widely used in the follow-up of prostatic cancer patients after radical prostatectomy and radiotherapy to detect recurrent disease. The use of PSA levels in patients treated with hormonal manipulation has also been investigated by several authors. In 45 patients investigated by Stamey et al (1989) 9% had undetectable PSA levels and 22% of PSA levels were within the normal range within 2 years of treatment. The majority of patients demonstrated an initial, often dramatic, decrease of PSA levels during the first 6 months treatment, but after 6 months 72% of patients had increasing PSA levels. This suggested that the PSA level at 6 months after starting treatment could distinguish patients with a favourable response to treatment from those in whom a limited response to treatment would be expected. Leo et al (1991) evaluated 81 patients with advanced prostate cancer who were subdivided into two groups depending on whether they had received no prior treatment or previous treatment with orchidectomy or diethylstilboestrol. The median serum PSA concentration was 96 ng/ml in the untreated group and 16.5 ng/ml in the previously treated group, despite the groups having similar symptoms and widespread metastatic disease on bone scintigraphy. The findings demonstrate that the serum PSA may have a different significance in patients who have been treated hormonally.

In the present study there was no clear response to treatment in 16 out of 59 cases (27%). Median survival in this group is approximately 6 months (Schmidt, 1983). Of the 16 patients in whom the PSA values did not decrease to below 10 ng/ml, only one survived beyond 2 years from entry. If a response is achieved then PSA levels often fall to below this level. A subsequent rise is highly suspicious of disease progression. In two cases this rise was from a level of less than 5 ng/ml to 5–10 ng/ml. These rather subtle fluctuations in PSA response were more likely to be observed at the beginning of the study, when samples were drawn at more frequent intervals, than later on when the test was performed 6-monthly. By comparison, scintigraphy alone is a less reliable index of disease response.

In 13 cases a rise in PSA pre-dated progression on bone scintigraphy. In two cases this was due to PSA results being performed between scintigrams early in the trial. In the 11 other patients this earlier rise was detected even when the paired 6-monthly results were assessed. It is difficult to be certain whether this is related to an imperceptible change in the activity of the bone metastases on scintigraphy or alternatively related to progression of soft-tissue disease. Assessment of lymph node status by pelvic computed tomography or of more distant disease in the abdomen and chest was not routinely performed in the patients under study.

In this study PSA failed to predict disease progression confirmed on scintigraphy in three out of 59 cases (Cases 1–3). A similar observation has been made in one patient described by Goldrath and Messing (1989). They offer several possible explanations for this finding, including laboratory error, autoantibodies to PSA, tumour heterogeneity or hypogonadism. Of these, tumour heterogeneity, with only some areas of the tumour sensitive to goserelin, appears to be most likely.

The present survey has not attempted to evaluate the question of whether routine laboratory and scintigraphy investigations of patients are justified in the follow-up of prostatic bone metastases. It does, however, demonstrate that the interpretation of such investigations may not be straightforward, and that neither technique can in isolation give complete accuracy. Optimal scintigraphic interpretation will only occur if full clinical details are available together with the PSA level. In view of the higher efficiency of PSA in monitoring disease progression, the most appropriate policy may be to use PSA as the routine investigation and reserve scintigraphy for the symptomatic patient or the patient in whom a change of management is contemplated.

Acknowledgments

The authors thank Mrs B. Pritchard for expert secretarial assistance.

References

CHYBOWSKI, F. M., LARSON KELLER, J. J., BERGSTRALH, E. J. & OESTERLING, J. E., 1991. Predicting radionuclide bone scan findings in patients with newly diagnosed, untreated prostate cancer: prostate specific antigen is superior to all other, clinical parameters. *Journal of Urology*, *145*, 313–318.

EMTAGE, L. A., LEWIS, P. W. & BLACKLEDGE, G. R. P., 1987. The role of prostate specific antigen in the baseline assessment of patients undergoing hormone therapy for advanced prostatic cancer. *British Journal of Urology*, *60*, 572–577.

ERCOLE, C. J., LANGE, P. H., MATHISEN, M., CHIOU, R. K., REDDY, P. K. & VESSELLA, R. L., 1987. Prostate specific antigen and prostatic acid phosphatase in the monitoring and staging of patients with prostatic cancer. *Journal of Urology*, *138*, 1181–1184.

GEORGE, N. J. R., 1988. Natural history of localised prostatic cancer managed by conservative therapy alone. *Lancet*, *1*, 494–497.

GOLDRATH, D. E. & MESSING, E. M., 1989. Prostate specific antigen: not detectable despite tumour progression after radial prostatectomy. *Journal of Urology*, *142*, 1082–1084.

LEO, M. E., BILHARTZ, D. L., BERGSTRAHL, E. J. & OESTERLING, J. E., 1991. Prostate specific antigen in hormonally treated stage D_2 prostate cancer: is it always an accurate indicator of disease status? *Journal of Urology*, *145*, 802–806.

MCNEIL, J. E. REDWINE, E. A., FREIHA, E. S. & STAMEY, T. A., 1988. Zonal distribution of prostatic adenocarcinoma. Correlation with histologic pattern and distribution of spread. *American Journal of Surgical Pathology*, *12*, 897–906.

O'DONOGHUE, E. P. N., CONSTABLE, E. R., SHERWOOD, T., STEVENSON, J. J. & CHISHOLM, G. D. 1978. Bone scanning and plasma phosphatases in carcinoma of the prostate. *British Journal of Urology*, *50*, 172–177.

SCHMIDT, J. D., 1983. The patient, disease status and treatment options for prostate cancer: stages D1 and D2. *Prostate*, *4*, 493–502.

SCOTT, R., MUTCHNIK, D. L., LASKOWSKI, T. Z. & SCHMALHORST, W. R., 1969. Carcinoma of the prostate in elderly men: incidence, growth characteristics and clinical significance. *Journal of Urology*, *101*, 602–607.

STAMEY, T. A. & KABALIN, J. N., 1989. Prostate specific antigen in the diagnosis and treatment of adrenocarcinoma of the prostate. I. Untreated patients. *Journal of Urology*, *141*, 1070–1075.

STAMEY, T. A., KABALIN, J. N., FERRARI, M. & YANG, M., 1989. Prostate specific antigen in the diagnosis and treatment of adenocarcinoma of the prostate. IV. Anti-androgen treated patients. *Journal of Urology*, *141*, 1088–1090.

WANG, M. C., VALENZUELA, L. D., MURPHY, G. P. & CHU, T. M., 1979. Purification of a human prostate specific antigen. *Investigative Urology*, *17*, 159–163.

1992, *The British Journal of Radiology*, 65, 865–867

Localized loss of the infrabronchial descending aortic interface as a normal variant

By W. F. C. van Gelderen

Department of Radiology, Tygerberg Hospital, Tygerberg 7505, Cape Town, South Africa

(Received 20 September 1991 and in revised form 1 April 1992, accepted 6 May 1992)

Keywords: Silhouette sign, Thoracic descending aorta

Abstract. Localized loss of the aortic interface may occur as a normal variant or may be due to an adjacent mass or opacification. The former category is divided into four types depending on position and length of loss of interface. The findings on conventional chest radiographs are correlated with computed tomographic findings.

In a study of 45 000 chest radiographs, specific attention was given to the infrabronchial descending aorta, and in 18 cases a localized loss of interface was encountered. These cases were further evaluated by other radiological techniques including computed tomography (CT).

In the absence of an associated adjacent soft-tissue lesion being responsible for the localized loss of the silhouette sign, these findings were all shown to be variations of normal.

Methods and results

Over a 12-year period approximately 45 000 chest radiographs were examined giving special attention to the area behind the cardiac shadow, as seen on frontal radiographs. Specific attention was given to the outline of the descending aorta, where this was visible and was not overlying the thoracic spine.

The descending aorta takes a gradual sweep from the arch to its hiatus in the diaphragm, and its left border usually forms a clearly defined uninterrupted interface. In rare instances, the outline of the infrabronchial descending aorta showed a localized loss of interface, variable in position and extent. As a normal variation, this was encountered in only 18 of the approximately 45 000 frontal chest radiographs examined. More frequently loss of the interface was due to adjacent mediastinal or pulmonary disease, but these cases are not included in the present study.

Four different varieties of loss of interface were encountered:

Group I: Short high-segment loss (three patients).
Group II: Short mid-segment loss (three patients).
Group III: Short low-segment loss (five patients).
Group IV: Long mid-segment loss (seven patients).

Six out of 18 patients (33%) examined were male. All patients were between 17 and 45 years of age, except for two patients who were 61 and 68 years old. The majority of patients presented either after trauma or for routine radiographs. All chest radiographs were normal with the exception of one patient in Group II (pneumonia right middle lobe) and two ptients in Group IV (one patient with a right-sided pleural effusion and another with mitral valve disease). No abnormality was noted on lateral radiographs, which were available for most patients. At least one patient in each group also had a radiograph in the supine position and the localized loss of interface was still visible in all these patients in the supine position.

In all patients the localized loss of interface was visible on follow-up radiographs, where these were done, except in two patients in Group III. In one patient it was identified on only one radiograph, and in another patient, following a stabwound in the chest without a pneumothorax or a haemothorax, the anomaly was visible on the expiration radiograph, but not on the inspiration radiograph.

Fluoroscopy in erect and supine positions was performed in two patients from Group I, one patient from Group II, two patients from Group III and three patients from Group IV. The interface was restored in its entirely in every patient with an obliquity of 5–30° (right anterior oblique position). In Groups I–III the interface was re-established with a lower obliquity, whereas Group IV required a greater degree of rotation before the aortic interface became uninterrupted.

Contrast-medium enhanced CT of the mediastinum was carried out in two patients from Group III and one patient from Group IV. In all these patients the descending aorta was clearly delineated and no adjacent mass or vascular structure could be identified. Contrast-medium-enhanced CT of one patient from Group I (Fig. 1) demonstrated that a pulmonary vein adjacent to the descending aorta and situated in the aortic-pulmonary artery angle was responsible for the localized loss of interface of a short segment of infrabronchial descending aorta on the chest radiograph (Fig. 2). Unfortunately, CT could not be performed in other patients from Group I, as these patients were lost to follow-up, as with patients from Group II.

The length of loss of interface varied considerably between the different groups: Group I, 3.4, 4.0 and 5.5 cm; Group II, 2.2, 2.6 and 2.8 cm; Group III,

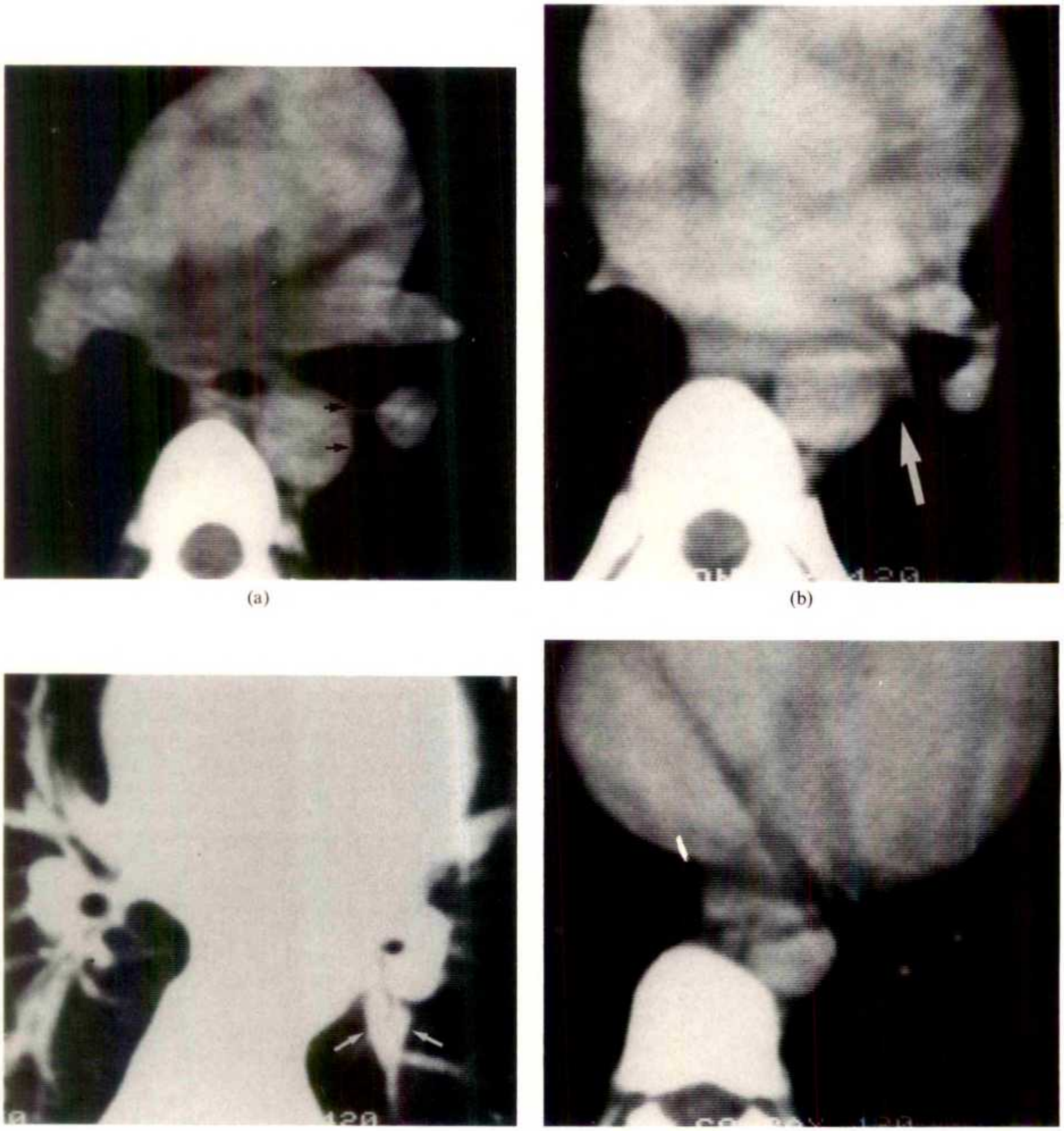

(a)

(b)

(c)

(d)

Figure 1. *Case 1.* Contrast-medium-enhanced CT scans confirm that the localized loss of interface, which is seen on the chest radiograph, is due to the inferior pulmonary veins filling the aortic–pulmonary artery angle (arrow on mediastinal window of (b) and arrows on lung window of (c) at same level). More veins were visible on four contiguous 8 mm sections immediately below this level. Figures (a) and (d) are sections above and below the level of localized loss of silhouette. The segment between small arrows (a) demonstrates the lateral aspect of the aorta normally seen at a tangent, producing a normal interface on chest radiographs. In (b) no such tangent is present, resulting in loss of interface.

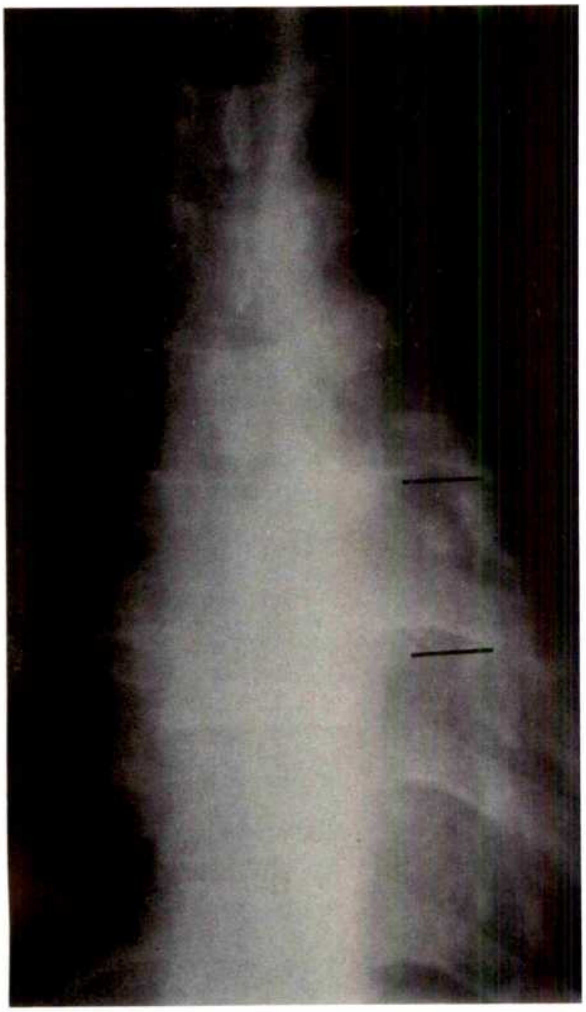

Figure 2. *Case 1.* Frontal chest radiograph demonstrates loss of a 4.0 cm segment of immediate infrabronchial descending aortic silhouette (between bars). No associated adjacent mass was noted.

2.1–4.4 cm (five patients, mean length of 3.4 cm); Group IV, 7.2–8.9 cm (seven patients, mean length of 7.9 cm).

Only patients with a very definite segmental loss of interface were included in the study. There were many examples of a localized loss of clarity of outline, where the outline was still partly visible or became visible by angling the lower half of the radiograph or viewing the radiograph in different positions (*e.g.* decubitus position). These cases are not included in this study.

Discussion

The well-known silhouette sign (Felson, 1973) can indicate an intrathoracic lesion adjacent to the heart, aorta or diaphragm. The sign applies equally well to the descending aorta, where adjacent consolidation, pleural fluid collection, mediastinal bleeding or neoplasm may be responsible (Figley, 1969). Pulmonary ligament nodes have also been implicated as a cause (Berne, et al, 1969).

Effacement of the entire descending aortic interface is not uncommonly due to adjacent disease. The loss of a short segment of interface may also be due to adjacent consolidation or lymph nodes. The loss of interface as a normal variant, with no demonstrable vascular or other structure, as seen in Group II–IV patients, is, however, most unusual. The cause of this appearance remains obscure but it was suggested (Genereux, 1983) that the posterior mediastinal reflections, including the paraspinal and para-aortic lines, do not depict, strictly anatomical structures but instead represent optical phenomena (Mach bands) formed as a result of the particular anatomical shape, rather than tissue composition, of the lung–mediastinal interface.

In one patient from Group I, contrast-medium-enhanced CT demonstrated a vascular aetiology. An inferior pulmonary vein effaced the angle formed between the aorta and pulmonary artery over a 4 cm distance corresponding with the exact position of the loss of silhouette on the chest radiograph.

In all cases detailed here, there was only a localized loss of silhouette and no associated lung or mediastinal lesion was present. In the absence of adjacent opacification no further investigation is required. Localized loss of interface may be ascribed to a normal variant or optical phenomenon.

References

BERNE, A. S., GERLE, R. D. & MICHELL, G. E., 1969. The mediastinum: normal roentgen anatomy and radiologic techniques. *Seminars in Roentgenology*, *4*, 1–21.

FELSON, B., 1973. Localization of intrathoracic lesions. In *Chest Roentgenology* (W. B. Saunders, Philadelphia), pp. 22–60.

FIGLEY, M. M., 1969. Mediastinal minutiae. *Seminars in Roentgenology*, *4*, 22–32.

GENEREUX, G. P., 1983. The posterior pleural reflections. *American Journal of Roentgenology*, *141*, 141–148.

1992, *The British Journal of Radiology*, *65*, 868–870

Pelvic phleboliths: is there an association with diverticulitis?

By E. H. de Vries, MD, A. Z. Ginai, MD, PhD, S. G. F. Robben, MD and *W. C. J. Hop, MSc

Departments of Radiology and *Epidemiology and Biostatistics, University Hospital Dijkzigt and Erasmus University Rotterdam, The Netherlands

(*Received 2 January 1992 and accepted 6 May 1992*)

Keywords: Pelvic phleboliths, Diverticulitis, Diverticulosis

Abstract. Pelvic phleboliths are familiar structures to radiologists although their pathogenesis is not fully understood. The literature suggests a relationship between the prevalence of phleboliths and diverticular disease, and with a low-fibre diet. Phleboliths are said to be seen more frequently in women and on the left side in the pelvis. Their number seems to increase with advancing age. We have attempted to establish relations of phleboliths with diverticulitis, diverticulosis, sex, age and pelvic location. In this study the only statistically significant relation was an increase of the number of phleboliths with advancing age.

Pelvic phleboliths, which represent calcified thrombi in pelvic veins, are by no means rare and are a common finding on plain abdominal radiographs. Phleboliths are not normally found in other parts of the body, except when associated with arteriovenous malformations and certain other vascular lesions. Very little is known about the aetiology of pelvic phleboliths, or why phleboliths are present in some people and not in others.

It has been suggested that some relationship exists between a low-fibre diet, diverticulosis and phleboliths (Hunter et al, 1984). The reason for a higher prevalence of thrombosis of pelvic veins in the case of diverticulosis is thought to be due to thrombosis at the site of damaged intima as a result of excessive straining at stools. Another cause for thombosis in general is slow blood flow. Decrease of venous flow may result from many causes, one of which is venous compression in oedematous inflammed tissues such as in peri-diverticulitis. To investigate the possible role of diverticulitis in the causation of phleboliths it was decided to define the number, location and prevalence of phleboliths in a group of patients with proven diverticulitis. The findings in this group were compared with two randomly selected groups of patients: one with diverticulosis (without any history of diverticulitis) and another group without any colon abnormality on barium enema examination.

Materials and methods

The plain abdominal radiographs from barium enemas of patients with a proven diagnosis of diverticulitis (Group I) were studied for the prevalence, number and location of pelvic phleboliths.

For comparison, two groups were randomly chosen from barium enema examinations, one with diverticulosis but without any history of diverticulitis (Group II) and another group with no abnormality in the colon (Group III).

The three groups of patients studied were:

Group I (diverticulitis): 89 patients, 48 male, 41 female, mean age 65 years (range 27–86 years).
Group II (diverticulosis): 58 patients, 28 male, 30 female, mean age 66 years (range 33–88 years).
Group III (normal colon): 71 patients, 31 male, 40 female, mean age 54 years (range 18–86 years).

The plain abdominal radiographs were independently scored for the number and location (R, L) of pelvic phleboliths by three radiologists. Two of the radiologists were unaware of the barium enema results at the time of scoring. In a small number of cases where differences existed in the scoring for the number of phleboliths, a consensus was reached by examining the abdominal radiographs together.

Statistical methods

Numbers of phleboliths on the left and right side were compared using Wilcoxon's test. The prevalence of phleboliths on both sides was compared using McNemar's test. Differences in numbers of phleboliths between groups were evaluated using the Kruskal–Wallis test. Correlation coefficients given are Spearman's; *P*-values given are two-sided; 0.05 was considered to be the limit of significance.

Results

The percentages of patients with phleboliths present for the diverticulitis, diverticulosis and control groups were, respectively, 66% (59/89), 76% (44/58) and 52% (37/71). The prevalence of phleboliths appeared to be greater on the left side compared with the right side in diverticulitis and controls (Table I).

The number of phleboliths was also statistically significantly larger on the left side for the latter groups. The differences, however, were generally small. In each group there was a significant correlation between the numbers of phleboliths on the left and right side of patients (controls: $r = 0.63$, $p < 0.001$); diverticulosis: $r = 0.55$, $p < 0.001$; diverticulitis: $r = 0.59$, $p < 0.001$).

---

*Address correspondence to E. H. de Vries, MD, Department of Radiology, University Hospital Rotterdam–Dijkzigt, Dr Molewaterplein 40, 3015 GD Rotterdam, The Netherlands.

Table I. Percentages of cases with phleboliths present according to patient group

Side	Controls	Diverticulosis	Diverticulitis
Left	48% (34/71)*	64% (37/58)	57% (51/89)**
Right	30% (21/71)*	57% (33/58)	44% (39/89)**

*$p < 0.005$, **$p < 0.05$.

Table II. Number of phleboliths according to patient group by age. Data given are median (range); n denotes the number of patients

Group	Age subgroup (years)		
	$\leqslant 45$	46–65	> 65
Controls	0 (0–6) $n = 26$	1 (0–12) $n = 23$	1 (0–28) $n = 22$
Diverticulosis	0 (0–1) $n = 3$	3 (0–22) $n = 20$	3 (0–27) $n = 35$
Diverticulitis	0 (0–17) $n = 6$	1 (0–14) $n = 36$	2 (0–23) $n = 47$

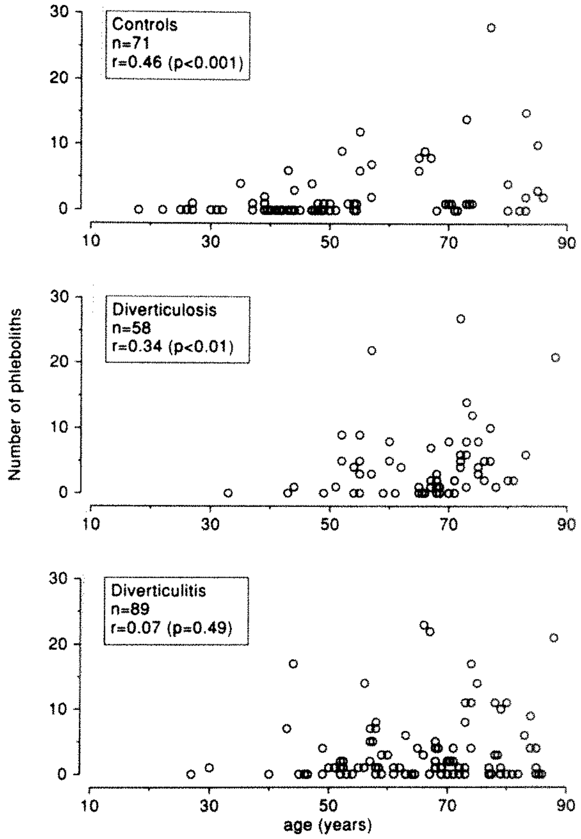

Figure 1. Number of phleboliths against the age of the patients (see text).

Figure 1 shows the number of phleboliths (total of the left and right side) and the age of patients for the various groups. The number of phleboliths increased significantly with advancing age for controls ($r = 0.46$; $p < 0.001$) and for diverticulosis ($r = 0.34$; $p < 0.01$). No significant increase was found for diverticulitis ($r = 0.07$; $p = 0.49$). Similar correlations were found for the left and right side separately.

In view of the increasing numbers of phleboliths with advancing age, and because controls tended to be younger, comparisons between the three groups were made within age ranges.

Table II gives the median number of phleboliths according to age range ($\leqslant 45$, 46–65, > 65 years). No significant differences between the three patient groups were present for any age range. The same applied when the left and right side were analysed separately.

Although females tended to have more phleboliths than males, the differences were not significant.

Discussion

Pelvic phleboliths are calcified thrombi in pelvic veins (Shemilt, 1972). Their cause, and pathological and clinical significance are obscure. Rokitansky described one anatomically in 1856 (cited in Culligan, 1926), and Wydler in 1911 concluded, on microscopical grounds, that they were due to calcification of non-organized thrombi (Culligan, 1926). The radiological features of phleboliths were not recognized until 1908 by Clark (cited in Culligan, 1926).

Phleboliths originate as thrombi in the pelvic veins and are the result of injury to the vein wall. Although in children the pelvic veins and venous plexuses may be protected by valves, these have mostly disappeared in adult life. These unprotected veins are subjected to large and abrupt rises in pressure (up to 400 mmHg) during normal acts of coughing and straining (Shemilt, 1972). The veins, which are thin-walled and surrounded by loose connective tissue, become distended by the high intraluminal pressure, which may damage the intima with the formation of a protective thrombus.

Why the thrombi in the pelvic veins become calcified has never been explained. Clots in this situation apparently remain localized and exhibit dystrophic calcification. Of the many theories for dystrophic calcification, that of a locally high concentration of phosphatase in the perivascular soft tissues would best explain the formation of phleboliths (Robison, 1923).

Several studies by Burkitt show that phleboliths and diverticular disease are very rare in developing countries (Burkitt et al, 1977, 1985). They are virtually never seen in Black Africans. As pelvic phleboliths are as common in black Americans as in white Americans, they are probably related to environmental rather than genetic causes.

Burkitt's studies suggest there is a relation between a low-fibre diet and the prevalence of diverticular disease and pelvic phleboliths. Pelvic phleboliths are thought to originate as a result of injured vein walls, caused by raised intra-abdominal pressure during evacuation of firm stools, and an increased clotting tendency, as seen with low-fibre diets (Burkitt et al, 1985). Besides these possible aetiological factors, decreased venous blood flow is likely to be important in the pathogenesis of thrombosis in pelvic veins, with phleboliths as a consequence. Venous blood flow decreases as intra-abdominal pressure rises during evacuation of a low-bulk stool. Another reason for decrease of venous blood flow is venous compression in inflammed, oedematous peri-diverticular tissue in peri-diverticulitis. As diverticulitis is usually on the left, a study was performed to investigate if phleboliths existed more frequently on the left in patients who had a history of diverticulitis on the left.

An attempt was also made to define if age and sex have any influence on the number and prevalence of pelvic phleboliths (Burkitt et al, 1977; Marquis, 1977; Dubrisay et al, 1978; Mattson, 1980).

Our study showed that there were more phleboliths on the left side than on the right in the diverticulitis group and in the control group, but not in the diverticulosis group. No specific correlation of phleboliths with diverticular disease has been shown. There were also no statistically significant difference in the number of phleboliths between males and females in all three groups.

However, the relationship between the amount of phleboliths and age is interesting. There is an increasing number of phleboliths with advancing age in all groups except in the diverticulitis group. To gain a better understanding of the relationship with age, each group was arbitrarily divided into three subgroups, *i.e.* $\leqslant 45$, 46–65, > 65 years. This showed no significant differences between the three patient groups for all three age ranges. The same applied when the left and right side were analysed separately.

Conclusion

In this study, we could not establish a significant relationship between the prevalence of phleboliths and diverticulosis/itis. This does not necessarily rule out diverticular disease as an aetiological factor.

This study shows no relation to sex or preference for the increased prevalence of left-sided phleboliths. An increase in the number of pelvic phleboliths with advancing age has been shown.

Other factors such as straining at stools due to causes other than diverticular disease and conditions that give rise to persistent or repeated increase in intra-abdominal pressure may be considered as aetiological factors. Inflammatory conditions in the pelvis other than diverticulitis may play a role. The pathogenesis of pelvic phleboliths is multifactorial and complex.

References

BURKITT, D. P., LATTO, C., JANVRIN, S. B., MAYOU, B., 1977. Pelvic phleboliths. Epidemiology and postulated etiology. *Medical Intelligence, 296*, 1387–1389.

BURKITT, D. P., CLEMENTS, J. R. & EATON, S. B., 1985. Prevalence of diverticular disease, hiatus hernia and pelvic phleboliths in black and white Americans. *Lancet, 19*, 880–881.

CULLIGAN, J. M., 1926. Phleboliths. *Journal of Urology, 15*, 175–188.

DUBRISAY, J., DANAN, G. & PATRI, B., 1978. Association diverticulose colique et phlebolithes pelviens. *La Nouvelle Presse Medicale, 7*, 3049.

HUNTER, T. B., MERKLEY, R. & PITT, M. J., 1984. Relation between pelvic phleboliths and diverticular disease of the colon. *American Journal of Roentgenology, 143*, 105–107.

MARQUIS, J. R., 1977. The incidence of pelvic phleboliths in pediatric patients. *Pediatric Radiology, 5*, 211–212.

MATTSON, T., 1980. Frequency and location of pelvic phleboliths. *Clinical Radiology, 31*, 115–118.

ROBINSON, F., 1923. The possible significance of Hexosephosphoric esters in ossification. *Biochemical Journal, 17*, 286.

SHEMILT, P., 1972. The origin of phleboliths. *British Journal of Surgery, 59*, 695–700.

1992, *The British Journal of Radiology*, 65, 871–877

Staging of hilar cholangiocarcinoma by ultrasound and duplex sonography: a comparison with angiography and operative findings

By *Christian Looser, MD, †‡Steven C. Stain, MD, †Hans U. Baer, MD, *Jürgen Triller, MD and †§Leslie H. Blumgart, MD

*Institute for Diagnostic Radiology and †Clinic for Visceral and Transplantation Surgery, Inselspital, University of Berne, CH-3010 Berne, Switzerland

(Received 6 January 1992 and accepted 6 May 1992)

Keywords: Proximal bile duct tumours, Cholangiocarcinoma, Klatskin tumours, Staging, Ultrasound, Angiography, Duplex sonography

Abstract. The pre-operative radiological assessment of proximal bile duct tumours is clinically important as resection may be limited by tumour extension along the bile ducts, into hepatic parenchyma or the adjacent vascular structures. Demonstration of the extent of biliary and vascular involvement can direct additional investigations and definitive treatment. 22 patients with hilar cholangiocarcinoma were studied pre-operatively by conventional ultrasound (US) and duplex sonography (DS). The extent of tumour infiltration and vascular involvement was compared with arteriography and operative findings. Bile duct dilatation and the level of obstruction was documented by US in 22 (100%), and the tumour was shown by US in 19 (86%). In these 19 patients, the extent of extraductal extension compared with operative findings was correct in 13, underestimated in two, and in four infiltration was massed. Vascular patency or involvement was correctly determined by DS in 19 (86%), and by arteriography in 18 (82%). In two of the three incorrect DS interpretations, lobar atrophy and contralateral hypertrophy distorted the hilar anatomy. US with DS is valuable in the pre-operative staging of proximal bile duct tumours in predicting ductal and vascular involvement.

Adenocarcinomas of the proximal bile ducts are rare tumours first reported by Altemeier et al in 1957, and have been associated with the eponym Klatskin tumours (Klatskin, 1965). In the United States, it is estimated that hepatobiliary tumours comprise 5% of newly diagnosed tumours in the gastrointestinal tract (Kreger et al, 1991). The autopsy incidence of proximal cholangiocarcinomas is 0.01–0.46% (Kirschbaum & Kosoll, 1941; Kuwayti et al, 1957; Sako et al, 1975). Typically, hilar cholangiocarcinomas are small with diameters of 1–3 cm. The extent and exact location within the hilum may be difficult to determine at operation, therefore it is important to have pre-operative staging (Voyles et al, 1983). Modern operative techniques combined with newer methods of imaging have permitted resection in up to 40% of patients in specialized hepatobiliary centres (Baer et al, unpublished data).

This study was performed to assess the value of ultrasound (US) and duplex sonography (DS) in the pre-operative staging of proximal hilar cholangiocarcinoma. While US has been reported useful in the staging of proximal bile duct tumours, the use of DS to determine vascular involvement has not been extensively studied.

Materials and methods

Between 1986 and 1989, 22 patients (13 male, 9 female) with hilar cholangiocarcinoma were assessed pre-operatively by abdominal US with DS. The mean age was 61 years (range 41–75 years). The sonographic staging was performed with the Toshiba SSH 100 and Acuson 128 ultrasound machines, both of which had a pulsed duplex unit, and were equipped with sector and curved array sonographic heads of 3.5 MHz and 5.0 MHz. DS identified the hepatic artery, portal vein and their primary intrahepatic branches in all patients.

In all patients, a selective arteriogram of the superior mesenteric artery and coeliac trunk was performed. The examinations were initially performed with conventional techniques using a 5.5 F Cobra catheter and non-ionic contrast medium (Omnipaque 350). If necessary, digital subtraction angiography was used. With the conventional technique, 60 ml of contrast medium was injected with a flow of 5–7 ml/s. The contrast medium was diluted 1 : 1 with normal saline for digital subtraction.

Percutaneous transhepatic cholangiography was performed in 10 of the 22 patients. Arteriography was performed after the other pre-operative investigations (US, DS, computed tomography (CT), percutaneous transhepatic cholangiography (PTC), endoscopic retrograde cholangiopancreatography (ERCP)) and the angiographer was blind to the US and DS results. All

---

Address correspondence to Jürgen Triller, MD.

‡Present address: Department of Surgery, Rm 9900, LAC-USC Med. Center, 1200 N. State Street, Los Angeles, CA 90033, USA.

§Present address: Department of Surgery, Memorial Sloan-Kettering Cancer Center, 1275 York Avenue, New York, NY 10021, USA.

patients were operated on shortly after the radiological investigations (within 7 and 10 days). The US and DS results were correlated with the arteriographic and operative findings.

Results

Ultrasound

Dilated bile ducts and the level of obstruction were identified by US in all 22 patients. 20 tumours involved the hepatic confluence, and two were located in the common hepatic duct. US identified a tumour mass in 19 of the 22 patients (86%). The tumour was not identified by US in three patients. In one of these patients, the tumour was intramural in a circular fashion, which did not produce a discrete mass. The second patient had perihepatic adhesions from a previous cholecystectomy, which caused a poor sonographic signal, and the final patient had excessive artefact from a previously placed biliary stent. Eight of the 19 sonographically identified tumours were isoechoic (42%) in comparison to the liver parenchyma. Eight were hyperechoic (42%), and three were hypoechoic (16%). The mean tumour diameter was 3 cm (0.5–6 cm). The patients were classified by operative findings.

Group 1: Tumour growth confined to the bile duct wall or endolumen ($n = 10$).

The sonographic criteria of the endoluminal tumours were proof of an intraductal mass lesion with clear demarcation of outline distinct from the bile duct wall. The US result was accurate in eight patients (80%) (Figs 1, 2). The tumour mass was not identified in one patient. In an additional patient the tumour was visualized, but the extent of diffuse intramural growth was not seen. In this patient, US identified hepatic metastases, which allowed pre-operative planning of a palliative procedure.

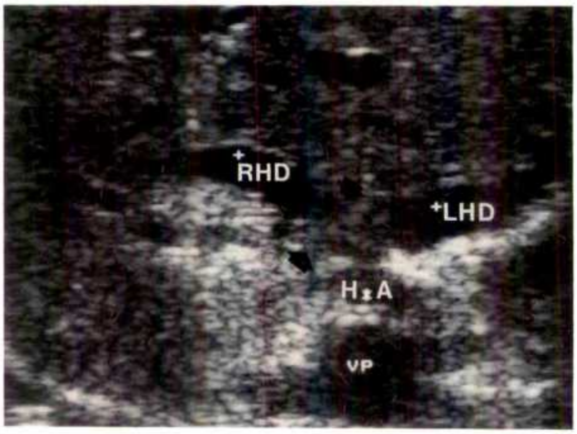

Figure 2. Endoluminal tumour (arrows) at the confluence of the right hepatic duct (RHD) and left hepatic duct (LHD). The hepatic artery (HA) and portal vein (VP) are not involved.

Group 2: Extraductal infiltration into the surrounding tissue ($n = 12$). This group was further divided into tumour growth that extended into the hepatic parenchyma ($n = 9$) or into the hepatoduodenal ligament ($n = 3$).

Identification of extraductal tissue was regarded as tumour. Criteria of the extraductal tumour infiltration were heterogeneity of the normal bile duct wall structure with spreading of isoechogenic tumour mass contiguous with the periportal fat tissue adjacent to the liver parenchyma. Loss of demarcation of the extraductal tumour tissue of the liver parenchyma was regarded as a direct infiltration and not as tumour-related mass effect.

The infiltration of the liver tissue was correctly described in four of nine patients (45%) (Fig. 3). The depth of invasion was underestimated in two (22%) and

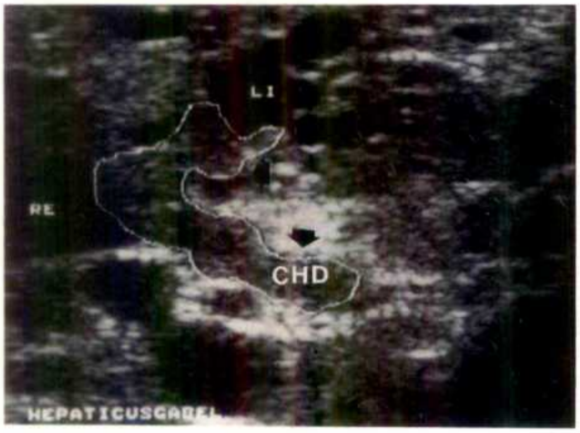

Figure 1. Proximal cholangiocarcinoma (arrows) with only endoluminal extension into the left hepatic duct (LI). The right hepatic duct is free of tumour (RE). No evidence of transmural extension at the level of the common hepatic duct (CHD).

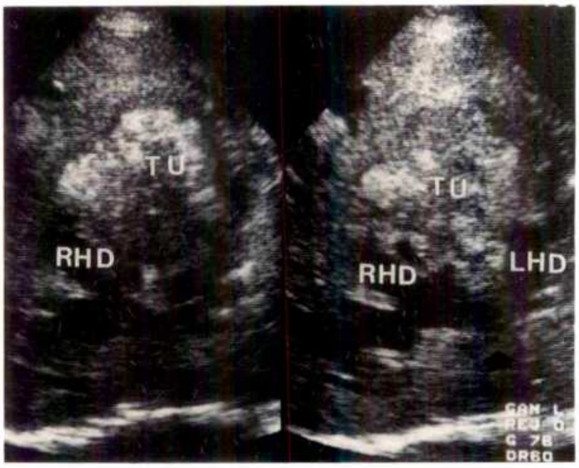

Figure 3. Large cholangiocarcinoma (TU) extending into segment IV with infiltration along the bile ducts beyond the bifurcation (arrow) of the right hepatic ducts (RHD) and left hepatic duct (LHD).

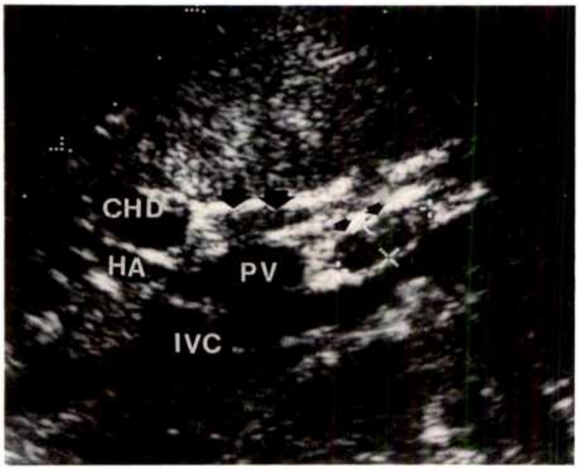

Figure 4. Intraluminal tumour (large arrows) is seen in the common hepatic duct (CHD) located anterior to the portal vein (PV) and hepatic artery (HA). Enlarged regional lymph node (small arrows) anterior to the inferior vena cava (IVC); histology showed reactive hyperplasia.

missed in three (33%). In two of the latter patients, the tumour was not shown. The sonographic criteria for invasion of the hepatoduodenal ligament was an isoechogenic structure extending from the tumour or longitudinal spread along the confines of the hepatoduodenal ligament with obliteration of the ligamentous fat stripe. Invasion of the hepatoduodenal ligament was accurately visualized in one of three patients (33%) (Fig. 4); the tumour extension was missed in the other two (67%).

In summary, US correctly identified the depth of local tumour extension in 13 of 22 patients (59%) and in 13 of 19 patients in whom the tumour was seen (68%). By inclusion of the additional two patients in whom parenchymal infiltration was identified but underestimated, the positive predictive value of tumour infiltration if the tumour can be visualized was 77% (15 of 19 patients). There were no US demonstrations of parenchymal or hepatoduodenal ligament infiltration not confirmed at operation. Only one patient had liver metastases identified at operation. These had been identified preoperatively by US.

Irregular nodular structure of an enlarged lymph node was regarded as representing tumour. Seven patients had enlarged hilar lymph nodes at operation. Three of these nodes showed reactive hyperplasia, and four were proven histologically to be metastatic. US visualized two of the seven as being enlarged (Fig. 4).

In 16 out of 22 patients (72%) the extent of intraluminal tumour spread into the right or left hepatic duct was judged correctly. Contiguous infiltration into subsegmental ducts was not assessed sonographically, as unilateral intrahepatic parenchymal infiltration was an operative indication for an extended hepatic resection.

Duplex sonography

DS was generally performed in the lateral position for longitudinal examination of the hepatic and portal vessels. All 22 patients also had hepatic arteriography and late-phase portography.

For extrahepatic tumours, vascular stenosis increased the median flowspeed (jet stream phenomenon) by comparison with the pre-stenotic areas. Post-stenotic turbulences were identified. The medium velocities in the segmental branches of the portal vein within intrahepatic tumours were significantly lowered by comparison with the segmental branches not involved with tumour.

Post-stenotic turbulence or jet stream phenomenon at the level of the stenosis cannot be seen intrahepatically because venous blood flow in the segmental branches of the portal vein is too low. Intrahepatic portal vein occlusion can be identified because of the missing blood

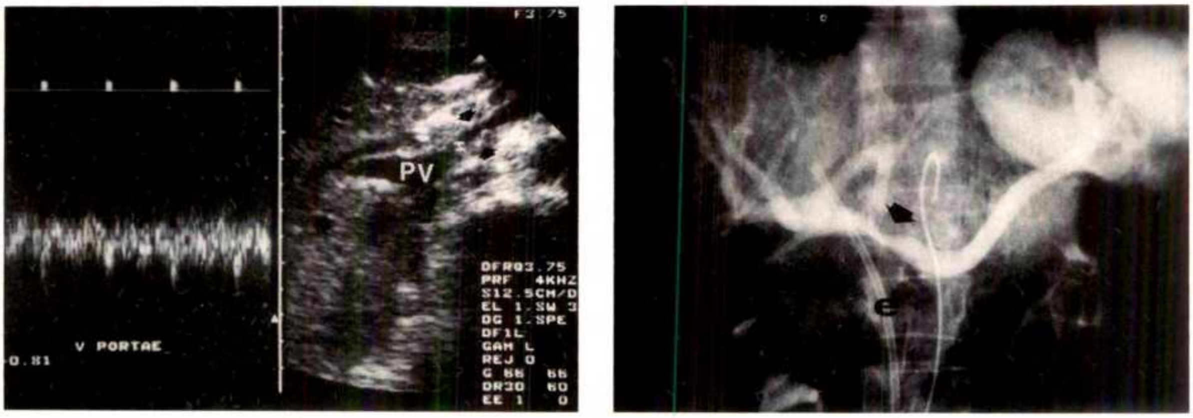

(a)

(b)

Figure 5. Proximal cholangiocarcinoma with stenosis and encasement of the portal vein. (a) DS shows jet phenomenon at the level of the stenosis with turbulence and increased central hepatopedal flow, and elevated median venous flow velocity. High-grade stenosis (arrows) of the portal vein (PV). (b) Portal venography after coeliac trunk injection reveals stenosis (arrow) of the main portal vein below the hilum. A biliary endoprosthesis is in place (e).

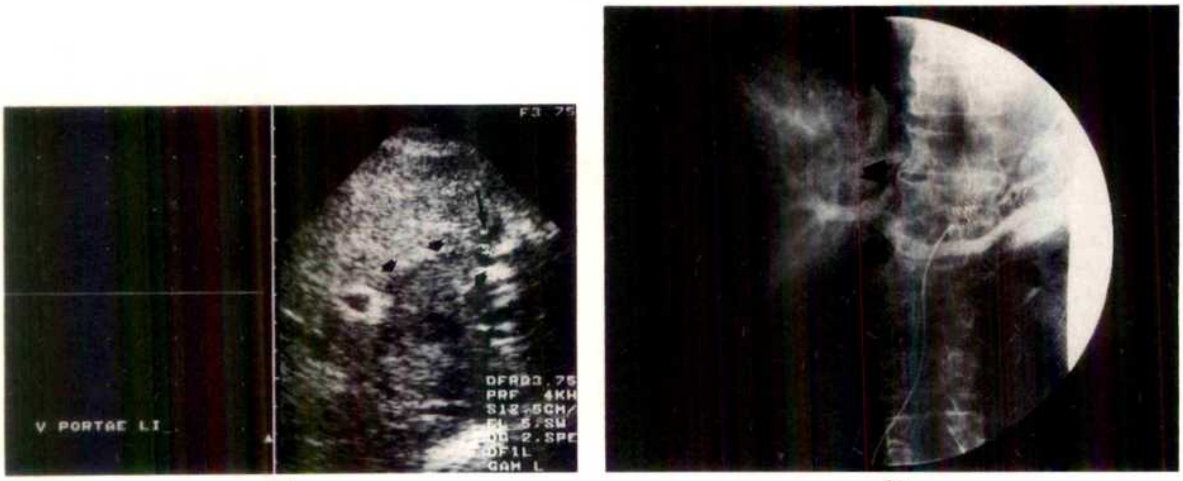

(a) (b)

Figure 6. Left portal vein occlusion due to tumour infiltration with subsequent left lobar atrophy. (a) DS demonstrates absent flow in the left portal vein (large arrow) due to tumour infiltration (small arrows). (b) Portal venography after coeliac trunk injection shows occlusion just beyond the origin of the left portal vein (arrow).

flow signal distal to the tumour with a Doppler angle of less than 60°.

In 13 patients, there was no tumour involvement by DS. Arteriography and portography were also normal. These patients had no vascular involvement at operation.

Nine patients had vascular involvement confirmed by operation; duplex accurately described six of these. In two of the six, there was extrahepatic portal vein stenosis, also identified by portal venography (Fig. 5). DS identified two patients with unilateral portal vein occlusion also identified at portography and confirmed at operation (Fig. 6). DS correctly identified two stenoses of a unilateral intrahepatic portal vein branch confirmed at operation. One was missed by angiography, and was misinterpreted as an occlusion.

The duplex findings were incorrect in three patients.

Patient 1. DS of the hepatic artery and the portal vein were thought to be normal. Hepatic arteriography revealed hepatic artery encasement. Portal venography was interpreted as normal. At operation, localized tumour encasement of the portal vein and proper hepatic artery caudal to the hilar plate was found.

Patient 2. DS showed a normal hepatic artery and a stenosis of the left branch of the portal vein. Arteriography and portal venography were normal. At operation, the apparent compression was due to right lobe atrophy with compensatory left lobar hypertrophy.

Patient 3. DS visualized a normal hepatic artery and what was thought to be a normal portal vein. The hepatic arteriogram and portal venography were also normal. There was marked left lobar atrophy which distorted the hilum. The bile duct could not be dissected free from the involved portal vein and a palliative biliary enteric bypass was performed.

Vascular involvement was accurately predicted by DS

Table I. Results of duplex sonography

Duplex sonography	Arteriography	Operative findings
HA and PV normal (13)	HA and PV normal (13)	HA and PV normal (13)
PV stenosis (2)	PV stenosis (2)	PV stenosis (2)
PV branch occlusion (2)	PV branch occlusion (2)	PV branch occlusion (2)
PV branch stenosis (2)	*Missed by angiography (1) *Occlusion (1)	PV branch stenosis (2)
*HA normal; *PV normal (1)	*PV normal; HA encasement (1)	HA and PV encasement
*Left PV stenosis; HA normal (1)	HA and PV normal (1)	HA and PV normal
*PV normal; HA normal (1)	*PV normal; HA normal (1)	HA normal; PV involved

Columns refer to radiological or operative findings. HA, hepatic artery; PV, portal vein.
*Incorrect radiological diagnosis of either the hepatic artery or portal vein. Numbers in parentheses refer to numbers of patients.

in 19 patients (86%), and by arteriography in 18 of the 22 patients (82%) (Table I). In two of the three failures by DS, the atrophy with hypertrophy produced hilar distortion, which prevented accurate delineation of the anatomy.

11 of the 22 patients (50%) underwent local tumour excision (Voyles et al, 1983) or hepatic resection (Kirshbaum & Kosoll, 1941). Palliative biliary enteric bypass decompression was performed in 11 (50%).

Discussion

In the early 1980s, PTC, hepatic arteriography and portal venography were regarded as the gold standards of imaging proximal bile duct tumours (Gibbons et al, 1983; Voyles et al, 1983; Beazley et al, 1984). US was used to demonstrate dilated intrahepatic ducts, and is still the first radiological investigation employed in the assessment of obstructive jaundice (Thomas et al, 1982; Scharschmidt et al, 1983; Saint Marc Girardin et al, 1985). In the clinical staging of bile duct tumours, US will demonstrate dilated intra- and extrahepatic bile ducts, as well the level of obstruction. In the current series, this was possible in 100% of the cases. The diagnosis of a bile duct lesion or a hilar mass as the cause of obstruction was made in 86% of our patients. Gibson et al (1986) and Yeung et al (1988) reported similar accuracies of 88% and 86%, respectively. The high sensitivity is possible due to the high resolution of modern ultrasound equipment.

Tumours localized to the bile ducts were found intraoperatively in 10 patients. US identified tumour limited to endoluminal or mural bile duct involvement in eight patients (80%) (Figs 1, 2). These tumours, if confined to the hilar area, are more likely to be resectable by local hilar resection. Sclerosing tumours that infiltrate into the surrounding tissue or along the bile ducts are more difficult to assess sonographically and to remove surgically.

Tumours growing extraductally can infiltrate into the hepatoduodenal ligament or into the liver parenchyma. Infiltration of the hepatoduodenal ligament was identified by US in only one of three patients. If a small part of the tumour lies extramurally, this often cannot be distinguished from hilar lymph nodes which may or may not be enlarged. The slow-growing nature of the lesions may not produce a hypoechoic rim of surrounding oedema, which can discern tumour infiltration from the surrounding structures. The identification of spread into the peritumoral inflammatory reaction is not sonographically possible.

Infiltration into the liver parenchyma was identified in six of nine patients, although underestimated in two. This finding may be due to the echogenicity of the tumours. Nearly half of the tumours were isoechoic, but sonomorphological structure was different compared with the surrounding liver tissue, and the delineation of the parenchymal invasion of an isoechoic tumour is difficult if a hypoechoic rim of oedema is not present. If the tumour is large, the primary site of origin and depth of infiltration into the surrounding tissue is difficult to recognize sonographically (Fig. 3). The differential diagnosis should include hepatic metastases, or primary hepatocellular carcinoma invading the hilum.

We attribute little clinical significance to sonographically identified lymph nodes. US is poor in this regard, as only two of seven enlarged nodes were seen by US (Fig. 4). Even at operation, only four of seven actually contained metastatic tumour. Haematogenous metastases from cholangiocarcinoma are unusual (Kirshbaum & Kosoll, 1941; Kuwayti et al, 1952). Only one patient was found to have liver metastases, which were documented by US, allowing planning of a palliative procedure.

Conventional US can provide an accurate demonstration of bile duct dilatation and of the level of obstruction (Baron et al, 1982; Machan et al, 1986; Karstrup, 1988). The sensitivity of tumour identification is also reasonably high, but the accuracy of US in visualization of the ductal extension of tumour or extraductal infiltration is less clear. US has been used to predict the proximal tumour extent by involvement of ducts above the secondary bifurcations. Gibson et al (1986) found US to be more accurate than CT in this regard (32% versus 0%), but both modalities were poor by comparison with PTC. Here, US correctly predicted the extent of intrahepatic ductal spread in only 70% of patients. We therefore believe direct cholangiography is usually necessary to identify proximal tumour extent.

In the absence of metastases, another obstacle to successful resection is vascular involvement. Modern operative techniques have permitted major hepatic resection for hilar tumours with low morbidity and mortality (Langer et al, 1985; Bengmark et al, 1988; Pinson & Rossi, 1988). Vascular reconstruction may be employed in selected cases (Tsuzuki et al, 1983; Blumgart et al, 1984; Sakaguchi & Nakamura, 1986). Our one perioperative death occurred after ligation of the hepatic artery and subsequent necrosis. Arterial ligation is poorly tolerated by the jaundiced liver, and we now would recommend arterial reconstruction if such a resection is undertaken (Thomas et al, 1990). If ductal infiltration is unilateral, the limits of resectability depend on the state of the hepatic and protal vasculature. Our criteria for unresectability are:

1. Occlusion of the main portal vein or hepatic artery (except in unusual circumstances).
2. Bilateral involvement or primary hepatic arterial or portal venous branches.
3. Combination of unilateral vascular involvement with cholangiographic evidence of extensive contralateral spread.
4. Hepatic or nodal metastases.

The sonographic accuracy of predicting resectability was 60%. If DS can reliably predict unresectability based on the involvement of the hepatic and portal vessels, arteriography would not be necessary in the clearly unresectable patients. In our initial experience in proximal bile duct tumours, we believe DS to be fairly accurate (86%), and comparable to arteriography in the assessment of hilar vessels (Figs 5, 6). It is difficult by angiography or at operation to distinguish compression from actual tumour extension, which will not permit dissection from the adjacent vessels. In the two patients in whom vascular involvement was missed by DS, arteriography was also incorrect. The one false positive duplex sonogram of portal vein stenosis was due to compression, but from the contralateral hypertrophied lobe and not from tumour extension. In vascular encasement by tumour without stenosis, DS does have an advantage over the grey-scale scan, as there is no visible change of the flow velocity or flow profile. Close to the vessel wall, inhomogeneity of flow is to be expected, caused by the loss of elasticity of the vessel wall adjacent to the tumour. It is possible that colour-flow Doppler sonography may be more accurate.

Two of the three incorrect diagnoses were made when lobar atrophy and contralateral hypertrophy was present. The atrophy–hypertrophy complex is most often caused by long-standing unilateral bile duct or portal vein obstruction (Longmire & Tompkins, 1975; Czerniak et al, 1986). In Klatskin tumours, the latter is more common. The compensatory hypertrophy causes an axial rotation of the portal triad, which makes radiological imaging and operative resection difficult. The presence of an atrophy/hypertrophy complex indicates a marked progression of the local tumour growth (Hadjis et al, 1989), and careful evaluation of the affected portal venous structures with both DS and angiography is necessary.

DS is important in the demonstration of intrahepatic branches of the portal vein as distinct from dilated bile ducts, which may be difficult with grey-scale imaging alone. DS gives information about relevant perfusion of the two liver lobes independently of tumour spread.

Conclusions

In the staging of proximal cholangiocarcinomas, the advantages of US and Doppler US are as follows.

The level of the biliary obstruction can clearly be determined. Ductal tumour spread is underestimated in 30% of cases. Direct cholangiography is still necessary. Peritumoral infiltration is seen, but may be underestimated, especially extrahepatic extension along the hepatoduodenal ligament. Recognition of enlarged local lymph nodes is meaningless, since tumour cannot be distinguished from hyperplasia. Final assessment of resectability should be performed intraoperatively, if criteria for unresectability are not clearly identified pre-operatively.

The addition of DS to conventional US is valuable. DS is equal to angiography in the identification of vascular involvement. DS may assist in the selection of patients for potential resection and, more importantly, non-invasively identify those patients clearly unresectable who might be considered as candidates for non-operative palliation (Carrasco et al, 1985; Irving, 1989; Neuhaus et al, 1991).

References

ALTEMEIER, W. A., GALL, E. A., ZINNINGER, M. M. & HOXWORTH, P. I., 1957. Sclerosing carcinoma of the major intrahepatic ducts. *Archives of Surgery, 75*, 450–460.

BARON, R. L., STANLEY, R. J., LEE, J. K. T., KOEHLER, R. E., MELSON, G. L., BALFE, D. M. & WEYMAN, P. J., 1982. A prospective comparison of the evaluation of biliary obstruction using computed tomography and ultrasonography. *Radiology, 145*, 91–98.

BEAZLEY, R. M., HADJIS, N., BENJAMIN, I. S. & BLUMGART, L. H., 1984. Idiopathological aspects of high bile duct cancer. Experience with resection and bypass surgical treatments. *Annals of Surgery, 199*, 623–636.

BENGMARK, S., ECKBERG, H., EVANDER, A., KLOFVER-STAHL, B. & TRANBERG, K. G., 1988. Major liver resection for hilar cholangiocarcinoma. *Annals of Surgery, 207*, 120–125.

BLUMGART, L. H., BENJAMIN, I. S., HADJIS, N. S. & BEAZLEY, R. T., 1984. Surgical approaches to cholangiocarcinoma at the confluence of the hepatic ducts. *Lancet, i*, 66–70.

CARRASCO, C. H., WALLACE, S., CHARNSANGAVEL, C., RICHLI, W., WRIGHT, K. C., FANNING, T. & GIANTURCO, C., 1985. Expandable biliary endoprosthesis: an experimental study. *American Journal of Roentgenology, 145*, 1279–1281.

CZERNIAK, A., SOREIDE, O., GIBSON, R. N., HADJIS, N. S., KELLEY, C. J., BENJAMIN, I. S. & BLUMGART, L. H., 1986. Liver atrophy complicating benign bile duct strictures. Surgical and interventional radiologic approaches. *American Journal of Surgery, 152*, 294–300.

GIBBONS, C. P., GRIFFITHS, G. J. & CORMACK, A., 1983. The role of percutaneous transhepatic cholangiography and grey-scale ultrasound in the investigation and treatment of bile duct obstruction. *British Journal of Surgery, 70*, 404–496.

GIBSON, R. N., YEUNG, E., THOMPSON, J. N., CARR, D. H., HEMINGWAY, A. P., BRADPIECE, H. A., BENJAMIN, I. S., BLUMGART, L. H. & ALLISON, D. H., 1986. Bile duct obstruction: radiologic evaluation of the level, cause and tumor resectability. *Radiology, 160*, 43–47.

HADJIS, N. S., ADAM, A. A., GIBSON, R., BLENKHARN, J. I., BENJAMIN, I. S. & BLUMGART, L. H., 1989. Nonoperative approach to hilar cancer determined by the atrophy–hypertrophy complex. *American Journal of Surgery, 157*, 395–399.

IRVING, J. D., ADAM, A. A., DICK, R., DONDELINGER, R. F., LUNDERQUIST, A. & ROCHE, A., 1989. Gianturco expandable metallic biliary stents: results of a European clinical trial. *Radiology, 172*, 321–326.

KARSTRUP, S., 1988. Ultrasound diagnosis of cholangiocarcinoma at the confluence of the hepatic ducts (Klatskin tumours). *British Journal of Radiology, 61*, 987–990.

KIRSHBAUM, J. D. & KOSOLL, D. D., 1941. Carcinoma of the gallbladder and extrahepatic bile ducts. *Surgery, Gynecology and Obstetrics, 93*, 740–754.

KLATSKIN, G., 1965. Adenocarcinoma of the hepatic ducts at its bifurcation within the porta hepatis. *American Journal of Medicine, 38*, 241–256.

KREGER, B. E., SPLANSKY, G. L. & SCHATZKIN, A., 1991. The cancer experience in the Framingham Heart Study Cohort. *Cancer, 67*, 1–6.

KUWAYTI, K., BAGENSTOSS, A. H., STAUFFER, M. H. & PRIESTLEY, J. T., 1957. Carcinoma of the major intrahepatic and the extrahepatic bile ducts exclusive of the papilla of Vater. *Surgery, Gynecology and Obstetrics, 104*, 357–366.

LANGER, J. C., LANGER, B., TAYLOR, B. R., ZELDIN, R. & CUMMINGS, B., 1985. Carcinoma of the extrahepatic bile ducts: results of an aggressive surgical approach. *Surgery, 98*, 752–759.

LONGMIRE, W. P. JR & TOMPKINS, R. K., 1975. Lesions of the segmental and lobar hepatic ducts. *Annals of Surgery*, *182*, 478–495.

Machan, L., Muller, L. & Cooperberg, P. L., 1986. Sonographic diagnosis of Klatskin tumors. *American Journal of Roentgenology*, *147*, 509–512.

Neuhaus, H., Hagenmuller, E., Griebel, M. & Classen, M., 1991. Percutaneous cholangioscopic or transpapillary insertion of self-expanding biliary metal stents. *Gastrointestinal Endoscopy*, *37*, 31–37.

Pinson, C. W. & Rossi, R. L., 1988. Extended right hepatic lobectomy, left hepatic lobectomy, and skeletonization resection for proximal bile duct cancer. *World Journal of Surgery*, *12*, 52–59.

Saint Marc Girardin, M. F., Leminor, M., Alperovitch, A., Roudot-Thoroval, F., Metreau, J. M. & Dhumeaux, D., 1985. Computer-aided selection of diagnostic tests in jaundiced patients. *Gut*, *26*, 961–967.

Sakaguchi, S. & Nakamura, N., 1986. Surgery of the portal vein in resection of cancer of the hepatic hilus. *Surgery*, *99*, 344–349.

Sako, S., Seitzinger, G. L. & Garside, E., 1957. Carcinoma of the extrahepatic bile ducts: review of the literature and report of six cases. *Surgery*, *41*, 416–437.

Scharschmidt, B. F., Goldberg, H. I. & Schmid, R., 1983. Approach to the patient with cholestatic jaundice. *New England Journal of Medicine*, *308*, 1515–1519.

Thomas, M. J., Pellegrini, C. A. & Way, L. W., 1982. Usefulness of diagnostic tests for biliary obstruction. *American Journal of Surgery*, *144*, 102–108.

Thomas, P. G., Baer, H. U., Matthews, J. B., Gertsch, P. & Blumgart, L. H., 1990. Post-operative hepatic necrosis due to reduction in arterial flow during surgery for chronic biliary obstruction. *Digestive Surgery*, *7*, 31–35.

Tsuzuki, T., Ogata, Y., Iida, S., Nakanishi, T., Takenaka, Y. & Yoshii, H., 1983. Carcinoma of the bifurcation of the hepatic ducts. *Archives of Surgery*, *118*, 1147–1151.

Voyles, C. R., Bowley, N. J., Allison, D. J., Benjamin, I. S. & Blumgart, L. H., 1983. Carcinoma of the extrahepatic biliary tree. Radiologic assessment and therapeutic alternatives. *Annals of Surgery*, *197*, 188–194.

Yeung, E. Y. C., McCarthy, P., Gompertz, R. H., Benjamin, I. S., Gibson, R. N. & Dawson, P., 1988. The radiologic appearance of hilar cholangiocarcinoma (Klatskin tumours). *British Journal of Radiology*, *61*, 991–995.

1992, *The British Journal of Radiology*, *65*, 878–884

A figure of merit for the assessment of image intensifier systems

By D. W. McRobbie, MSc, A. P. Hancock, MSc and *I. A. Castellano, MSc

Riverside District Department of Medical Physics, Charing Cross Hospital, Fulham Palace Road,
London W6 8RF, and *Clinical Physics Department, St Mary's Hospital, Praed Street, London W2 1NY, UK

(*Received 10 June 1991 and in revised form 25 September 1991, accepted 1 February 1992*)

Keywords: Image intensifiers, Quality assurance

Abstract. A dimensionless figure of merit (F), which combines key aspects of the performance of image intensifier systems, is derived. This figure is ideally independent of input air kerma rate and field size and relates to the fundamental characteristics of the image reception chain. In practice it is calculated from measurements of the threshold contrast (noise) and limiting resolution using the Leeds test objects and the input air kerma rate. Several practical examples illustrate its usefulness in simple performance assessment and quality assurance procedures. A comparison is made with the use of detection index diagrams.

Following the recent publication on patient dose reduction in diagnostic radiology (Royal College of Radiologists/National Radiological Protection Board (RCR/NRPB), 1990), there is an increased awareness of the requirement for quality assurance (QA) and performance assessment for diagnostic X-ray systems. Techniques for both full and rapid assessment of image intensifier systems (the "Leeds test objects") have been in existence for some time and are well established (Hay et al, 1985; Grant et al, 1987). These techniques depend on the subjective assessment of test patterns by experienced observers under consistent and reproducible X-ray beam quality conditions (the "calibrated beam"). In particular, parameters that may be measured include the limiting resolution of the whole system (high-frequency response), the field size, the noise and contrast loss (low-frequency response).

A measure of the overall subjective image quality is obtained from the curves of threshold contrast detail detectability or detection index (defined as the reciprocal of the product of threshold contrast and detail diameter). This enables the observer to assess the visibility of different sized objects over a range of X-ray contrast. Typical examples of measured detection index diagrams are illustrated in Figs 4 and 5. Ideally, the detection index has a constant value but, in practice, technical deficiencies (*e.g.* unsharpness) result in a dependence on detail size (Cowen et al, 1987).

Whilst such diagrams can provide a useful impression of the overall image quality, their interpretation is complicated by their non-linear nature and, in addition, one must also consider the input air kerma rate with which they were generated. They also do not especially relate to the field size or magnification used.

The purpose of this paper is to derive from simple theoretical considerations a figure of merit that takes into account the main image quality parameters with respect to input air kerma rate and field size. The usefulness of this quantity is illustrated with some practical examples. Ideally, a fluoroscopy system will yield a single figure of merit for all field sizes and air kerma rates, thus facilitating serial measurements for QA purposes and performance assessment.

Theory

This section gives a brief and semi-empirical derivation of the figure of merit. A more detailed analysis is presented in the Appendix.

Image signal and noise

The final image signal is limited by the number of X-ray photons N_X absorbed and converted in the input surface of the image intensifier per unit time. This is given by:

$$N_X = k_1 Q \dot{K}_{air} d^2 \qquad (1)$$

where d is the diameter of the input aperture of the intensifier, $\dot{K}_{air}$ is the input air kerma rate measured at the intensifier surface, Q is the detective quantum efficiency of the input phosphor, and the constant k_1 includes a conversion from air kerma to photon flux density and geometric factors ($\pi/4$). In general, neither k_1 nor Q are constant in relation to the X-ray kilovoltage and beam quality. However, the use of a "calibrated beam" at 70 kVp with 1 mm additional copper filtration (as specified for the Leeds test objects) effectively ensures that both these factors are rendered constant for all measurements.

The two principal sources of noise are the quantum noise (*i.e.* that associated with the incident X-ray photon statistics) and the electronic or system noise from the TV camera and associated electronics. Under normal operating conditions, the quantum noise will be the dominant component.

The quantum noise results from random fluctuations within the useful (*i.e.* absorbed) X-ray photon distribution, given by the standard deviation of the number of photons which, according to Poisson statistics for N_X such photons per unit time is:

$$n_q = N_X^{\frac{1}{2}} \tag{2}$$

and to a first approximation the signal-to-noise ratio (SNR) is given by:

$$\mathrm{SNR} = N_X^{\frac{1}{2}} \tag{3}$$

As our measurements depend on the subjective perception of a test object (in particular Leeds TO N3), the "noise" measured will be dependent on a psychophysical factor, which we can formalize as a function f_P in addition to the physical origins of the noise. Also, as we are dealing with standard 1 V video signals and generally using automatic brightness control (ABC), we can assign a nominal value of 1 for the signal; hence, the perceived "noise" (or threshold contrast) for a given detail size, for the case when quantum noise is dominant, is given by:

$$n = f_P/N_X^{\frac{1}{2}} \tag{4}$$

where f_P is, in the most general case, a function of the detail size relative to the observer's visual field. Using the Leeds test objects TO N3 or TOR(TVF), we are considering the large detail limit for which f_P should be effectively constant. From Equation 1:

$$n = \frac{f_P}{(k_1 Q \dot{K}_{air})^{\frac{1}{2}} d} \tag{5}$$

Equation 5 applies in the limit of dominant quantum noise arising from the initial absorption and conversion of X-ray photons.

Resolution

In the assessment of spatial resolution, the Leeds test objects only permit measurement of the limiting resolution of the system. The value of the limiting resolution depends on the noise and the shape of the overall system modulation transfer function (MTF). The shape of the MTF may not be obtained using the Leeds test objects. A general approach is outlined in the Appendix as the following argument is illustrative but empirical.

In general, for a modern intensifier, the overall limiting resolution will be determined primarily by the characteristics of the TV camera (Moores, 1984). The improved limiting resolution at higher magnifications arises primarily as a consequence of improved spatial sampling by the video system, resulting from the presentation of a zoomed field of view to the camera aperture. Thus, along the direction of the TV lines the absolute limiting resolution (line pairs/mm) is:

$$R = \frac{\text{video system bandwidth}}{\text{frame rate} \times \text{lines/frame} \times 2d} \tag{6}$$

To a first approximation (the validity of which is discussed in the Appendix) the limiting resolution, as measured according to the Leeds technique and for a given system, is inversely proportional to the field diameter.

Combining Equations 5 and 6 we have:

$$R/n\dot{K}_{air}^{\frac{1}{2}} = k_2 Q^{\frac{1}{2}}/f_P \tag{7}$$

where k_2 encompasses both k_1 and the constant video characteristics from Equation 6. The left-hand side of this equation constitutes the three measurable parameters. Assuming consistent perception criteria (which is a basic requirement in the Leeds system), the right-hand side is ideally invariant for a given system, depending on the fundamental features of the imaging system. This dependence is explored at greater length in the Appendix.

We thus define the figure of merit as:

$$\mathrm{F} = kR/n\dot{K}_{air}^{\frac{1}{2}} \tag{8}$$

where k is an appropriately chosen constant (with the units of mm $\mathrm{Gy}^{\frac{1}{2}}/\mathrm{s}^{\frac{1}{2}}$) which renders F dimensionless. This is a simple indicator of the fundamental quality of the imaging system. This quantity, moreover, is independent of air kerma rate and selected field size, ideally being invariant for a given intensifier system over a range of operating conditions.

Experimental method

A number of image intensifier systems of various types (six mobile C-arms, 13 fixed units) and ages located in Riverside and Parkside Districts were evaluated using the Leeds test objects (Cowen et al, 1987) as part of an annual QA programme for X-ray equipment. In particular, the Huttner line-pair object and objects N3 and TO10 were used. For subjective evaluations two observers participated. The tests were carried out for a calibrated X-ray beam of 70 kV using 1 mm copper additional filtration plus extra low atomic number material where necessary; the air kerma rates on the input face of the intensifier were measured using a Radcal flat ion chamber and electrometer. Measurements were also performed using TO10 to assess the overall image quality in terms of the detection index for comparison with the derived values of figure of merit. For the measurement of limiting resolution, the additional 1 mm copper was removed and a low kV employed in accordance with standard practice.

Where possible, different field sizes were assessed. On two of the fixed systems the input air kerma rate was varied over the range 0.17–0.87 μGy/s for the normal field of view. One of these (system 5) had continuous control of the input air kerma rate under automatic brightness control, whilst the other (system 2) was operated under manual control by changing the mA, which necessitated altering the monitor brightness for each air kerma rate. The limiting resolution was measured in the normal way at low kV under automatic brightness control.

The constant k in Equation 8 was chosen such that an intensifier operating at 0.35 μGy/s air kerma with a noise value (threshold contrast) of 3% at 70 kV and a limiting resolution of 1.2 lp/mm resulted in a value of unity for F. This gave a numerical value for k of 1.48.

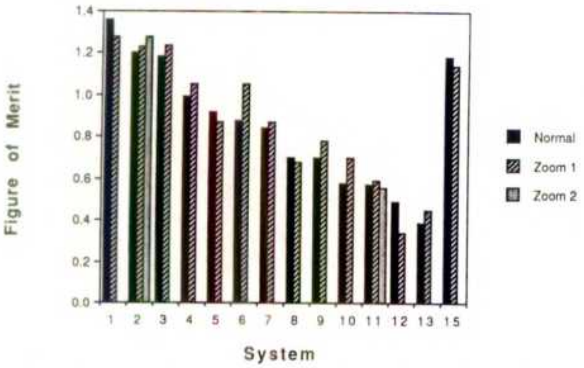

Figure 1. Figures of merit for image intensifiers with a choice of magnifications.

Results

Dependence on field size

Figure 1 shows the calculated figures of merit for all the fluoroscopy systems in this study that had zoom facilities (all fixed plus one mobile). To within experimental uncertainty (discussed below), the figures of merit are invariant on the field size for all the systems.

Dependence on input air kerma rate

Figure 2 shows the effect of continuously varying the input air kerma rate for systems 2 (manual) and 5 (auto). The figure of merit can be seen to remain fairly constant over this range as predicted, with possibly a hint of a fall-off for high air kerma rates for system 2. This is consistent with the relative magnitude of electronic noise increasing with respect to the decreasing quantum noise. For system 2 the figure of merit had a mean of 0.85 and standard deviation of 0.06, and for system B a mean of 0.87 and standard deviation of 0.06. It is noted that the performance of system 2 under manual operation appeared inferior to its normal functioning under automatic control.

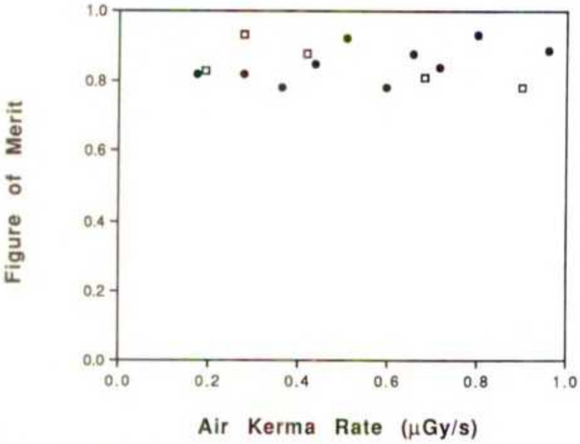

Figure 2. Figure of merit *vs.* input air kerma rate for two fluoroscopic systems (●, system 5 auto; □, system 2 manual).

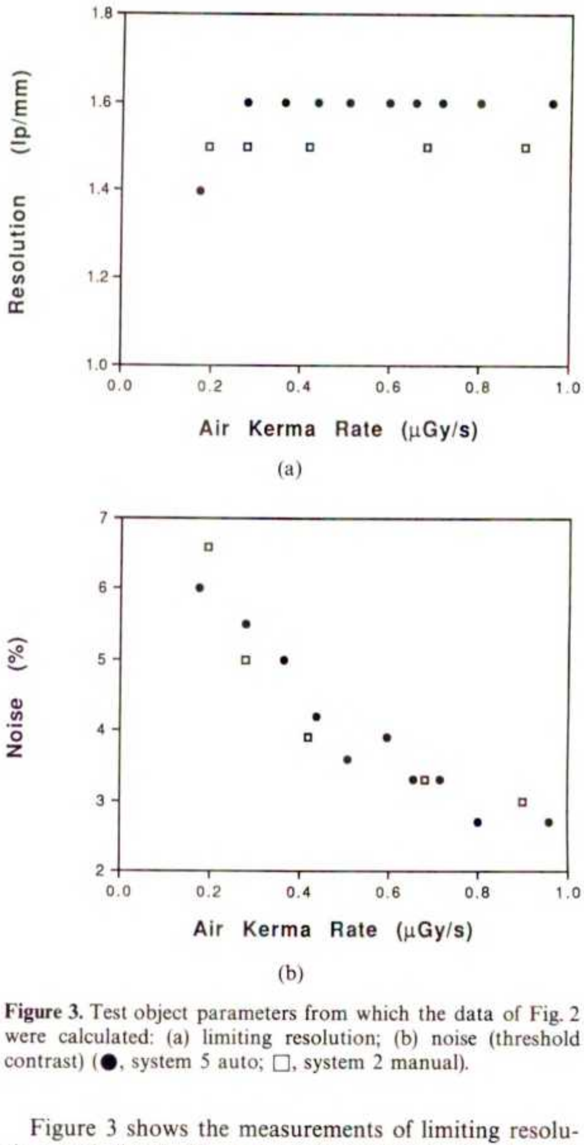

(a)

(b)

Figure 3. Test object parameters from which the data of Fig. 2 were calculated: (a) limiting resolution; (b) noise (threshold contrast) (●, system 5 auto; □, system 2 manual).

Figure 3 shows the measurements of limiting resolution and threshold contrast from which the data in Fig. 2 were calculated. Only for very low input air kerma rates was there a problem with the measurement of limiting resolution. Other evidence of the independence of F from input air kerma rate is presented below.

Comparison with detection index diagrams

The detection index diagram gives a graphical representation of the overall image quality as perceived from a TV monitor. Figure 4(a) shows resultant detection index diagrams for TO10 for field sizes of 33.5, 22 and 15 cm measured for system 11. These were obtained with input air kerma rates of 0.75, 0.99 and 1.59 μGy/s. Thus, the nature of image information perceived by the observer has been properly altered by the use of magnification. However, the underlying performance of the system is constant, as revealed by the figure of merit (Fig. 1).

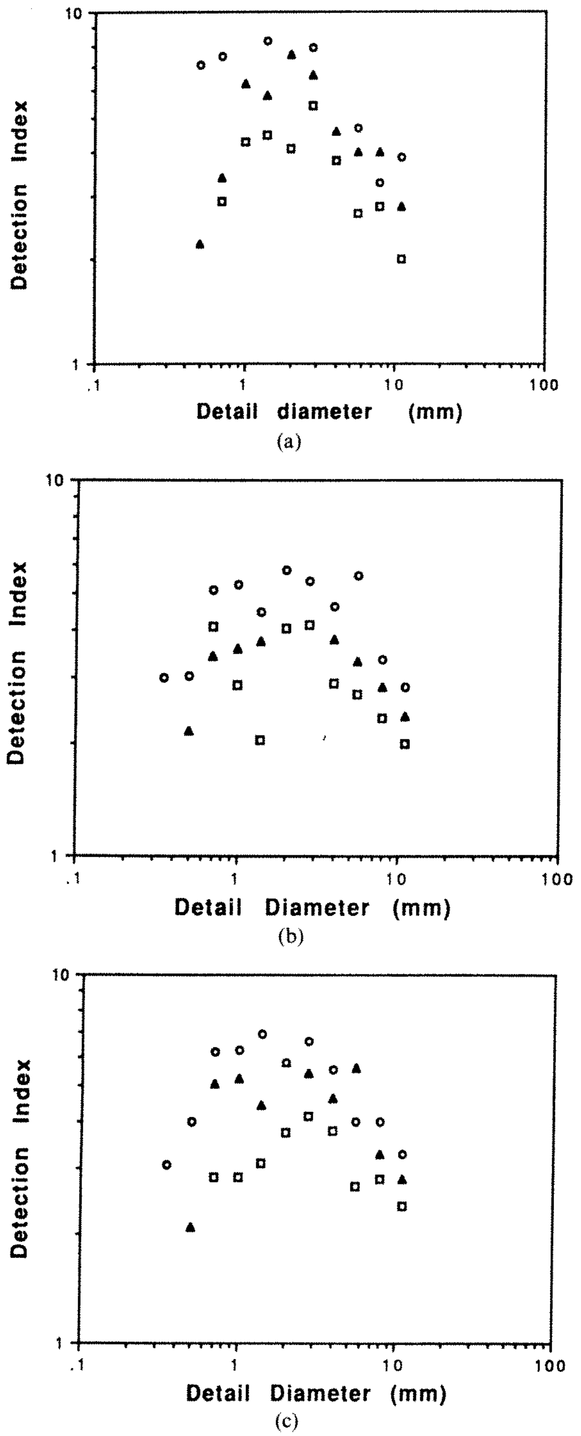

(a)

(b)

(c)

Figure 4. Detection index diagrams for various image intensifiers. (a) System 11 with three field sizes (□, normal; ▲, zoom 1; ○, zoom 2); (b) system 2, normal, three input air kerma rates, 0.16 (□), 0.22 (▲) and 0.33 (○) μGy/s; (c) example of good (○) (system 8), average (▲) (system 2) and poor (□) (system 10) detection index diagrams. Detection index is measured in units of mm^{-1}.

Figure 4(b) shows results for system 2 operated at three different input air kerma rates (0.16, 0.22 and 0.33 μGy/s) on normal field size under automatic brightness control. For each of these the detection index curves are different, reflecting what is actually seen on the TV monitor as a consequence of increased air kerma rate. The calculations of the figure of merit are 1.11, 1.23 and 1.20, respectively, indicating the underlying constant performance of the image reception chain in a manner not immediately apparent from the detection index diagrams. The lowest air kerma rate resulted in a degraded measurement of limiting resolution as the effect of quantum noise was not sufficiently suppressed, hence giving the slightly lower value of F.

Table I shows the figure of merit and related measured parameters for the normal fields (9 in) for the 13 fixed fluoroscopic units. Detection index curves were classified crudely into three main classes: good, average and poor (illustrated in Fig. 4(c)). For those in the average category an indication is given as to whether the measurements generally fell above (+) or below (−) the average.

It is noticeable that the two systems for which the detection index curves were deemed particularly good gave figures of merit below the average, mainly on account of their high dose rates. The best figures of merit correspond to systems displaying a combination of features, but particularly low dose rates. Several of the worst systems are very old and overdue for replacement, which has led to a downward bias for the mean values shown at the foot of Table I. Table II shows the results for the six mobile systems. Of these, numbers 14, 16, 17, 18 and 19 were of similar type and age.

Detection index curves are generally interpreted by comparing them visually against "standard" detection index diagrams. It is thus necessary to consider both the field size and the dose rates in order to assess the performance in a meaningful manner. The comparison standard normally used (Cowen et al, 1987) is for an input air kerma rate of 0.26 μGy/s. For a proper comparison of performance, this dose rate should be used, which is often inconvenient to achieve. Moreover, the system may not be optimized for operation at this rate. The figure of merit provides a simple and convenient yardstick of relative performance which can be used at the system's usual automatic dose rate. In addition, the quality of data in detection index diagrams is often poor (as in Fig. 4). This can further complicate their interpretation.

Serial quality assurance measurements

The use of the figure of merit in serial QA measurements is illustrated in a retrospective study on system 10. Figure 5(a) shows a series of detection index curves plotted over a time scale of 5 years during which the input air kerma rate has been re-set. Whilst a deterioration in image quality is apparent from these curves, it is not clear to what extent this deterioration was due to the changes in air kerma rates encountered. The figure of merit (Fig. 5(b)) takes account of these changes, but

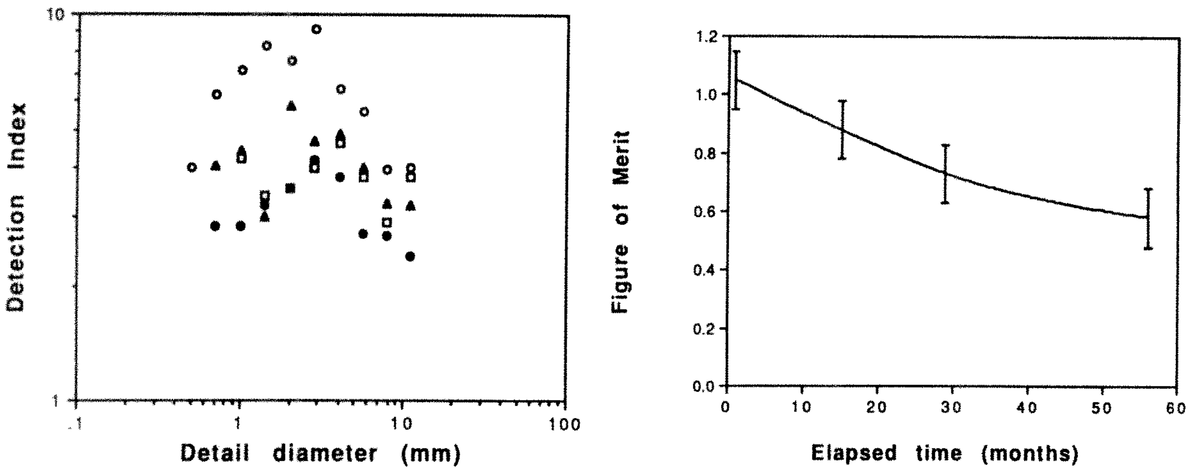

(a) (b)

Figure 5. Long-term assessment of image quality: (a) detection index diagrams for four assessments with different input air kerma rates set (○, 0 months, 0.87 μGy/s; ▲, 15 months, 0.24 μGy/s; □, 29 months, 0.24 μGy/s; ●, 56 months, 0.20 μGy/s); (b) figures of merit for the same tests showing underlying deterioration in imaging performance.

Table I. Comparison of figure of merit, input air kerma rates and detection index curves for 13 fixed fluoroscopic systems (9 in FOV)

System	Age (years)	Input air kerma rate ($\dot{K}_{air}$) (μGy/s)	Threshold contrast "noise" (n) (%)	Limiting resolution (R) (lp/mm)	Figure of merit (F)	Detection index curve
1	5	0.28	3.3	1.6	1.4	Average +
2	0	0.33	3.0	1.4	1.2	Average
3	12	0.33	2.3	1.06	1.2	Average
4	4	0.39	2.7	1.12	1.0	Average +
5	8	0.51	3.6	1.6	0.9	Average −
6	4	0.50	2.7	1.12	0.9	Average −
7	6	0.41	2.7	1.25	0.8	Poor
8	5	1.12	2.5	1.25	0.7	Good
9	3	0.60	2.7	1.0	0.7	Good
10	17	0.20	3.6	0.63	0.6	Poor
11	2	0.75	2.0	0.67	0.6	Poor
12	17	0.26	3.3	0.56	0.5	Poor
13	17	0.24	5.5	0.71	0.4	Poor
Mean		0.46	3.07	1.07	0.84	

Table II. Comparison of figure of merit, input air kerma rates and detection index curves for six mobile fluoroscopic systems (6 in FOV)

System	Age (years)	Input air kerma rate ($\dot{K}_{air}$) (μGy/s)	Threshold contrast "noise" (n) (%)	Limiting resolution (R) (lp/mm)	Figure of merit (F)
14	5	0.37	2.3	1.6	1.6
15	6	0.45	3.0	1.5	1.2
16	7	0.39	3.0	1.5	1.2
17	3	0.44	3.3	1.4	0.9
18	7	0.52	3.6	1.4	0.8
19	11	0.57	3.3	1.3	0.8
Mean		0.46	3.08	1.45	1.08

also shows an underlying trend of deteriorating imaging performance consistent with the age and condition of the equipment. This was confirmed by invasive measurements of the intensifier conversion factor carried out by the manufacturer. The error bars represent an experimental uncertainty of 10%.

Experimental uncertainties

In all these results the uncertainties in the figure of merit result mainly from uncertainties in the determination of threshold contrast ("noise"). Using two observers, the number of details seen in object N3 never varied by more than one-half (corresponding to a 0.3% contrast variation in a mean of 3.0% contrast) with no variation in the number of bar patterns seen in the resolution test. From this we determine the uncertainty in the figure of merit as 10% or, if we attribute a nominal uncertainty in the limiting resolution of 0.07/1.2 lp/mm (corresponding to one-quarter bar pattern), a combined uncertainty of 12%.

Discussion

The results show that our proposed figure of merit may be used to compare the performance of fluoroscopic imaging systems with different field sizes and air kerma rates in a manner not readily achievable using detection index diagrams alone. For most systems the performance of the system at various magnifications will result in a single value of F.

The figure of merit is essentially independent of input air kerma rate over the normal range encountered. At very high air kerma rates we expect the figure of merit to decrease as the other noise sources become significant compared with the quantum noise. Also, at very low air kerma rates under automatic brightness control, there may be a contribution from quantum noise in the determination of the limiting resolution, leading to reduced value of F. This would not normally occur and can be avoided if there is manual mA control.

The independence from input air kerma rate means that the figure of merit reflects the imaging capability of the equipment rather than the photon statistics of the X-ray beam. This is useful for detecting any real deterioration in the image reception chain, or for re-setting inappropriate dose rates.

It is important to understand the relationship between the figure of merit and the input air kerma rate. A figure of merit of unity or above does not necessarily mean that the dose rates set are appropriate for clinical use. It does, however, mean that the image reception aspects of the equipment are functioning adequately, and enables the user to predict the image quality achievable with reduced dose rates.

Other image quality parameters not considered here (*e.g.* field uniformity, distortion, temporal resolution) are also important. It is thought that some of these could be incorporated into a more sophisticated figure of merit.

Conclusions

A simple figure of merit, which describes the performance of image intensifier systems in a quantitative way, can be derived from first principles. The result is ideally independent of the magnification and dose rate employed. With care it can be used as an indicator of comparative performance of systems. It can be calculated from the standard measurements obtainable from the Leeds QA test object TOR(TVF). We have found it to be useful in our QA programmes.

Acknowledgments

R. Nicholson and A. Marvin (Westminster Hospital) participated in the measurements on system 5. The authors are grateful to Dr R. G. Dale for encouragement, support and helpful comments concerning the manuscript.

Appendix

Signal-to-noise ratio

For a full discussion of the signal-to-noise ratio (SNR) we need to consider the system noise (principally from the camera) n_s in addition to the X-ray quantum noise. In the video signal these components add in quadrature. From Equations 1, 2 and 3:

$$\mathrm{SNR} = \frac{k_1 Q \dot{K}_{\mathrm{air}} d^2 \mathrm{GOVA}}{(k_1 Q \dot{K}_{\mathrm{air}} d^2 (\mathrm{GOVA})^2 + (A n_s)^2)^{\frac{1}{2}}} \qquad \text{(A1)}$$

where O is the optical transmittance of the lens system, V is the detection efficiency of the camera, A is the video gain and G is the gain of the intensifier, such that:

$$\text{Conversion factor C} = k_1 Q\mathrm{G}(4/\pi) \qquad \text{(A2)}$$

Rearranging Equation A1:

$$\mathrm{SNR} = \frac{(k_1 Q \dot{K}_{\mathrm{air}} d^2)^{\frac{1}{2}}}{(1 + (A n_s/\mathrm{GOVA} n_q)^2)^{\frac{1}{2}}} \qquad \text{(A3)}$$

Thus:

$$\mathrm{SNR} = \frac{(k_1 Q \dot{K}_{\mathrm{air}} d^2)^{\frac{1}{2}}}{(1 + (v_{\mathrm{dc}}/v_{\mathrm{q}})^2)^{\frac{1}{2}}} \qquad \text{(A4)}$$

where v_{dc} and v_{q} denote the video noise signals produced by the camera dark current and general electronic noise and X-ray quantum noise, respectively. The magnitude of such noise voltages can be determined from examining the video signal resulting from the use of the Leeds test object TO E1. Provided the quantum noise is dominant, the simple Equations 2–5 will be valid. Clearly, if this condition were not applicable (*e.g.* if the conversion factor of the intensifier was poor), then the calculated figure of merit would be further reduced and would be indicative of some system fault.

This analysis has not considered specifically the multiplicative aspects of the noise statistics (Chesters, 1982). Such an analysis leads to the appearance of an additional term in the denominator of Equation 3 which would normally be relatively small and can be absorbed into the system noise. It should also be noted that the results obtained from the Leeds TO N3 also depend to an extent on the low spatial frequency response (contrast loss) of the system. Thus, both the low and high spatial frequency response influence the figure of merit in a manner consistent with the general image quality.

Resolution

The total MTF of the imaging system can be written as the product of MTFs of the constituent elements:

$$\mathrm{MTF}_{\mathrm{total}}(f) = \mathrm{MTF}_{\mathrm{int}}(f) \times \mathrm{MTF}_{\mathrm{opt}}(f) \times \mathrm{MTF}_{\mathrm{TV}}(f) \quad \text{(A5)}$$

where the right-hand side denotes the product of the MTFs for the intensifier, the optical coupling and the television system, respectively. We can consider the MTF of the lens system to be approximately unity over the relevant range of spatial frequencies.

The definition of limiting resolution R is given as being the argument of the MTF for which the following applies (Cowen et al, 1987):

$$\mathrm{MTF}_{\mathrm{total}}(R) = k_{\mathrm{P}}\sigma \quad \text{(A6)}$$

where k_{P} is a psychophysical constant (usually assumed to be equal to 2) and σ is the power of the noise. The measurement is such that quantum noise is suppressed so that σ is the power of the electronic noise.

The use of magnification m means that, effectively, the TV camera sees a modified spatial frequency $f' = f/m$, as does the output screen of the intensifier, and hence the combined MTF under magnification is:

$$\mathrm{MTF}_{\mathrm{total}}(f) = \mathrm{MTF}_{\mathrm{in}}(f) \times \mathrm{MTF}_{\mathrm{out}}(f/m) \times \mathrm{MTF}_{\mathrm{TV}}(f/\mathrm{m}) \quad \text{(A7)}$$

where $\mathrm{MTF}_{\mathrm{in}}$ denotes the response for the input screen and $\mathrm{MTF}_{\mathrm{out}}$ the response of the output screen (including the electron focusing).

In this way we define the cases for limiting resolution for a normal (r) and magnified (R) image as:

$$\begin{aligned} \mathrm{MTF}_{\mathrm{in}}(r) \times \mathrm{MTF}_{\mathrm{out}}(r) \times \mathrm{MTF}_{\mathrm{TV}}(r) &= k_{\mathrm{P}}\sigma \\ \mathrm{MTF}_{\mathrm{in}}(R) \times \mathrm{MTF}_{\mathrm{out}}(R/m) \times \mathrm{MTF}_{\mathrm{TV}}(R/m) &= k_{\mathrm{P}}\sigma \end{aligned} \quad \text{(A8)}$$

where, under automatic brightness control, the system noise power will be essentially the same in both instances.

If the intensifier input screen MTF is constant over the spatial frequency range r to R, then by definition:

$$R = mr \quad \text{(A9)}$$

where the magnification m is proportional to $1/d$. The validity of this result depends on the extent to which the input response can be considered constant over the given spatial frequency range. In practice, this relationship holds reasonably well within the limitations of the measurement technique. Any additional degradation resulting from poor focusing or distortion will be reflected in a further reduction of the figure of merit.

References

Chesters, M. S., 1982. Perception and evaluation of images. In *Scientific Basis of Medical Imaging*, ed. by P. N. T. Wells (Churchill Livingstone, Edinburgh), pp. 237–280.

Cowen, A. R., Clarke, O. F., Coleman, N. J., Craven, D. M., McArdle, S. & Hay, G. A., 1987. *Leeds Test Objects Instruction Manual.*

Grant, A. M., Kehoe, T. M. & Law, J., 1987. Use of a simple Leeds test object for rapid assessment of image intensifiers. *British Journal of Radiology, 60,* 1019–1021.

Hay, G. A., Clarke, O. F., Coleman, B. A. & Cowen, A. R., 1985. A set of X-ray test objects for quality control in television fluoroscopy. *British Journal of Radiology, 58,* 335–344.

Moores, B. M., 1984. Physical aspects of digital fluorography. In *Digital Radiology—Physical and Clinical Aspects*, ed. by R. M. Harrison and I. Isherwood (Institute of Physical Sciences in Medicine, London), pp. 45–58.

RCR/NRPB, 1990. Patient dose reduction in diagnostic radiology. *Documents of the NRPB, vol. 1,* no. 3.

1992, *The British Journal of Radiology*, 65, 885–894

Radial diffusion coefficient mapping

By Anthoula Madden, PhD and Martin O. Leach, PhD

CRC Clinical Magnetic Resonance Research Group and Joint Department of Physics, Institute of Cancer Research and Royal Marsden Hospital, Sutton, Surrey SM2 5PT, UK

(Received 4 February 1991 and in final form 27 February 1992, accepted 26 March 1992)

Keywords: Diffusion, Nuclear magnetic resonance, IVIM, *In vivo* diffusion

Abstract. The two-dimensional mapping of the effective diffusion coefficient of water in tissues may provide a useful method of tissue characterization to complement T_1 and T_2 relaxation time studies for diagnostic purposes. Current diffusion techniques rely on the application of large gradient strengths and long echo times to achieve the required sensitivity. This, in turn, limits the applicability of the technique to tissues having long T_2s with rapid water diffusion. In addition, the inherent directionality of these methods results in only the partial encoding of diffusion information. A modified diffusion sequence is presented, radial diffusion mapping (RAD), which provides enhanced sensitivity diffusion maps by employing gradient sensitization in three orthogonal directions. Results in both phantoms and volunteers are presented, together with an investigation of the effects of T_2 on the measurement accuracy. Using RAD, a two- to five-fold improvement in sensitivity was achieved, thus significantly enhancing the dynamic range of the method and allowing more accurate *in vivo* diffusion measurements to be carried out.

The molecular diffusion coefficient (D) is a measure of the average rate of translational motion of a molecule per unit time due to thermal agitation (Kärger et al, 1988). The random character of this phenomenon results in spin dephasing and, consequently, signal attenuation, the effect being proportional to the diffusion coefficient of the material under study. *In vivo* the degree of molecular mobility of intracellular or extracellular water is governed by tissue properties, including viscosity, temperature and the restrictive nature of cell barriers, resulting in an *effective* diffusion coefficient D_e. Pathological environments, such as oedema or malignancy, are reflected through changes in D_e as a result of alterations in the intracellular structure of tissues (Hazelwood et al, 1974; Taylor & Bushell, 1985; Le Bihan et al, 1988). The measurement of the diffusive properties of tissues may, therefore, constitute an additional tissue characterization method, since the information encoded in these maps differs from that provided by T_1 and T_2 studies. Diffusion maps only reflect translational motion over distances of a few micrometres, whilst the T_1 and T_2 processes reflect both translational and rotational motions over less than 1 nm.

The effective diffusion coefficient (D_e) of tissues is between 10% and 50% that of pure water at room temperature ($D_{\mathrm{tissue}} = 0{\cdot}2\text{–}1{\cdot}16 \times 10^{-3}$ mm^2/s, $D_{\mathrm{free}} = 2{\cdot}25 \times 10^{-3}$mm^2/s; Beall et al, 1984). Several hypotheses have been evoked to explain this difference, including water–protein interactions, low cell–membrane permeability or the presence of obstructions, such as proteins and other macromolecules, that restrict the motion of water molecules. D_e will also be affected by the presence of blood perfusion through the imaging region; however, the blood fraction is typically only 1–5% of the volume being imaged, so its effects would be proportionally small. Elevated diffusion coefficients in regions of oedema or malignancy are believed to be due to the breakdown of molecular binding mechanisms and the removal of cell barriers (Hazlewood et al, 1974; Le Bihan et al, 1988). These changes are usually accompanied by an increase in the T_1 and T_2 of the tissue under study.

The main shortcoming of the two-dimensional diffusion mapping techniques employed to date (Le Bihan & Breton, 1985; Taylor & Bushell, 1985) is their limited sensitivity and dependence on large gradient strengths and long echo times. Furthermore, diffusion is treated as a *directional* phenomenon, which is assumed to be isotropic, since diffusion along only one orthogonal axis is encoded, namely that of the applied gradient. Anisotropic diffusion regimes, arising from restrictive physiological structures such as the myelin fibres in white matter (Moseley et al, 1989), would thus fail to be detected if sensitizing gradients parallel to the long axis of the fibres were not applied. Furthermore, even if the diffusion process were isotropic, only part of the available sensitivity would be used in the production of the diffusion map.

In order to overcome these limitations, a modified diffusion measuring sequence was developed, employing gradient sensitization in three orthogonal directions (Avraamidou & Leach, 1988; Madden, 1990). This radial diffusion mapping (RAD) technique results in an enhancement in diffusion sensitivity because of the larger net diffusion gradient applied, which encodes spin motion in the x, y and z directions. Consequently, diffusion maps with accentuated diffusion effects are produced, and this is achieved without any increase in

---

Address correspondence to Dr M. O. Leach, Joint Department of Physics, Institute of Cancer Research and Royal Marsden Hospital, Downs Road, Sutton, Surrey SM2 5PT, UK.

echo time, thus reducing the need for gradients with higher technical specifications or longer interpulse intervals.

Theoretical basis of the method

Consider the echo amplitude, $S(\mathrm{TE})$, formed at time TE following a spin-echo experiment (Stejskal & Tanner, 1965):

$$S(\mathrm{TE}) = S_0 . \exp\left(\frac{\mathrm{TE}}{T_2}\right) . \exp\left[-b . D\right] \tag{1}$$

where

$$b = -\gamma^2 . G^2 . d^2 . \left(\frac{2d}{3} + I\right) \tag{2}$$

where S_0 is the spin density in the image, including T_1 effects, TE is the echo time, γ is the gyromagnetic ratio, and D is the diffusion coefficient of the material. The diffusion coefficient is described by $\mathbf{I} . \mathbf{V}/6$, where $\mathbf{V}$ is the mean molecular speed in any direction and $\mathbf{I}$ is the distance travelled in that direction. d and I are the gradient timing parameters as defined in Fig. 1 (bold-faced notation denotes vector quantities). b is the gradient factor, including gradient duration effects (Le Bihan et al, 1986).

At any infinitesimal point in time, a snapshot of the diffusing molecules would show their velocity vectors at some angle relative to the applied gradient. If the angle between the instantaneous velocity vector, $\mathbf{V}$, of a diffusing molecule and the applied pulsed gradient, $\mathbf{G}$, is denoted by θ, the only velocity vector component that contributes to the signal attenuation in a conventional diffusion map is that along the direction of the applied gradient:

$$\mathbf{G} . \mathbf{V} = |\mathbf{G}||\mathbf{V}| \cos\theta \tag{3}$$

If, however, three pulsed diffusion gradients are applied along each of the three orthogonal directions, as shown in Fig. 1, then the instantaneous velocity vector components of a molecule in any direction will experience a gradient according to:

$$\mathbf{G} . \mathbf{V} = \mathbf{G}_x . \mathbf{V}_x + \mathbf{G}_y . \mathbf{V}_y + \mathbf{G}_z . \mathbf{V}_z \tag{4}$$

where $\mathbf{G}_x$, $\mathbf{G}_y$ and $\mathbf{G}_z$ are the gradients along the three orthogonal axes, x, y and z. The resulting signal attenuation observed in an image would, therefore, be the integral over time of the sum of the effects of each of these three gradient components on the random molecular motions.

If the three orthogonal gradients each have magnitude $\mathbf{G}$, the resultant maximum gradient field ($\mathbf{T}$) will be given by:

$$\mathbf{T} = \hat{\mathbf{i}} G_x + \hat{\mathbf{j}} G_y + \hat{\mathbf{k}} G_z \tag{5}$$

where $\hat{\mathbf{i}}$, $\hat{\mathbf{j}}$ and $\hat{\mathbf{k}}$ are unit vectors along the three orthogonal axes. The resultant gradient magnitude is, therefore, given by:

$$|\mathbf{T}| = \sqrt{G_x^2 + G_y^2 + G_z^2} = \sqrt{3} . G \tag{6}$$

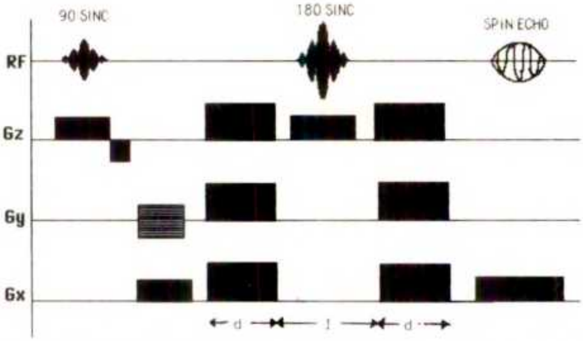

Figure 1. The RAD pulse sequence. Motion-encoding gradient lobes are applied along x, y and z on either side of the 180° pulse, resulting in improved sensitivity over the IVIM sequence (Le Bihan et al, 1986).

assuming the three gradients are of equal magnitude (*i.e.* $G_x = G_y = G_z = G$). Furthermore, since the resulting signal attenuation is proportional to the square of the applied gradient (Equation 1), a three-fold improvement in sensitivity would be expected on this basis. This represents a *maximum* improvement that could be achieved in the absence of anisotropies. Anisotropic diffusion regimes would result in reduced enhancement depending on the geometry of the anisotropy.

The resultant gradient field lies at an angle determined by the vector sum of the three gradient components. The spin-echo image obtained represents the average over time of the general probability distribution of a molecule for lateral displacement along the gradient direction, *i.e.* from position r_0 to r after a time t (Kärger et al, 1988):

$$P(r, r_0, t) = (4\pi Dt)^{-\frac{1}{2}} . \exp\left[\frac{-(r-r_0)^2}{4Dt}\right] \tag{7}$$

Since this process is random, and each molecule within the imaging volume follows a random path during the imaging time, the image amplitude represents the average over time of the molecular displacements of the diffusing molecules, given by the integral of Equation 7.

Materials and methods

In order to investigate the sensitivity improvement achieved when using pulsed gradients along all three orthogonal directions, diffusion measurements were carried out using both the intravoxel incoherent motion technique (IVIM) (Le Bihan & Breton, 1985) and a RAD sequence, and the results were compared.

The IVIM/RAD pulse sequences

Images were taken on a 1.5 T Siemens Magnetom using the following imaging parameters: echo time (TE) = 118 ms, repetition time (TR) = 1 s, slice thickness (SL) = 10 mm, two acquisitions and matrix size of 256 × 256, whilst the sequence timing parameters were: $d = 40$ ms and $I = 15$ ms (Fig. 1). Pulsed gradients of 0, 3 or 6 mT/m were applied along the readout direction in the IVIM sequence or along all three directions in the RAD sequence. The three sequences will be referred to as IVIM0, IVIM3 and IVIM6 or RAD0, RAD3 and RAD6, depending on the applied gradient strength. These gradient strengths corresponded to b values in the range 0.77–174 s/mm^2 for IVIM and 0.77–517 s/mm^2 for RAD. The resultant gradient magnitudes were 0, 3 or 6 mT/m for the IVIM sequence and 0, 5.2 or 10.4 mT/m for the RAD sequence.

The diffusion phantom

A circular phantom, filled with gadolinium-doped water and incorporating samples of distilled water, acetone, dimethyl-sulphoxide (DMSO) or cyclohexane from Aldrich (Dorset, UK) was used to verify the method. The samples were enclosed in 60 ml capacity polypropylene tubes and kept at room temperature. They were chosen to cover a diffusion range from 0.014 to 4.8×10^{-3} mm^2/s in order to encompass the physiological range. Three spin-echo data sets were acquired using either the IVIM or RAD sequences, so that two-dimensional maps of the diffusion coefficients within the imaging slice could be computed.

Anisotropic diffusion measurements

In order to investigate the extent to which the presence of restrictive barriers will be reflected in the calculated value of D_e, a series of studies using celery were carried out. Celery was chosen as a suitable phantom since it consists of elongated fibres which exhibit dimensional anisotropies along their short and long axis. One would, therefore, expect fast diffusion *along* the fibres, where there are no restrictions, but slow diffusion *across* the fibres. Spin-echo images were acquired with the diffusion gradient direction selected along the z or x axis, which was respectively either parallel or at right angles to the fibres. The diffusion coefficient was calculated from the three spin-echo data sets and compared with that obtained using the RAD method, where gradients are applied in all three orthogonal directions. The RAD technique may improve the sensitivity of the technique to diffusion effects; however, directional diffusion information related to possible structural anisotropies, as in the case of muscle fibres, will be lost because of averaging. There may, therefore, be a need for directional as well as RAD measurements.

Dependence of measurement accuracy on T$_2$ *and SNR*

To examine the extent to which T_2 effects have influenced the phantom measurements, the T_2 of each sample was measured using a standard multiecho sequence with the following measurement parameters: 32 echoes, TE = 28–648 ms, TR = 4 s, matrix size = 256 × 256, SL = 10 mm, one acquisition. The range of echo times used was chosen to ensure it included the T_2 of all samples and to obtain as many points as possible for the exponential fit. The T_2 of each sample was then calculated from an exponential fit to the 32 spin-echo data sets, which are free of diffusion effects owing to the low gradient strengths applied.

In vivo *diffusion measurements*

The diffusion enhancement obtained using the RAD method was also investigated *in vivo* in order to assess the extent to which diffusion weighting was introduced, depending on the direction of the applied gradient. The following examination protocol was used. Sagittal scout scans were first acquired using a spin-echo sequence (TR = 0.4 s, TE = 28 ms, matrix size = 256 × 256, SL = 10 mm, one acquisition) in order to position correctly the axial slices to be used in the diffusion examination. Slices were selected both above and through the ventricles, and also through the ventricles and the eyes. A standard transmit/receive head coil was used and all studies were ECG-gated in order to minimize motion artefacts. The three spin-echo data sets were then used to generate diffusion maps and to calculate D_e.

Calculation of two-dimensional diffusion maps

The signal intensity in each of the three spin-echo data sets is given by Equation 1. The greater the value of b, the more pronounced the effects of diffusion on the echo amplitude. The signal dependence on S_0 and T_2 may be eliminated by dividing two images having identical timing but different gradient strengths and hence b values. From the division of the two data sets, a diffusion-weighted image may be obtained by taking the logarithm of the intensity ratio, as shown below (Wesbey et al, 1984; Le Bihan & Breton, 1985):

$$\ln\left[\frac{S_1(x,y,z)}{S_2(x,y,z)}\right] = -D(x,y,z).(b_2-b_1) \qquad (8)$$

The diffusion coefficient may then be calculated on a voxel-by-voxel basis provided the two b values are known and a suitable reference sample, such as water, is also used:

$$D(x,y,z) = \ln\left[\frac{S_1(x,y,z)}{S_2(x,y,z)}\right]/(b_2-b_1) \qquad (9)$$

A plot of $\ln[S_1(x,y,z)/S_2(x,y,z)]$ versus (b_2-b_1) gives a straight line, the slope of which is equal to the diffusion coefficient of the material under study. Intensity measurements averaged over the cross-sectional area of each sample within the phantom were used to plot straight lines for gradient values of 0, 1, 2, 3, 4, 5, and 6 mT/m. A least-squares fit program gave the slope of each curve and, hence, the diffusion coefficient of each material. Neeman et al (1990) have recently reported that the Stejskal and Tanner equation breaks down when using large imaging gradients owing to the presence of cross-terms between the diffusion and parallel imaging gradients, which may be particularly important in microscopy experiments. The imaging gradients used in our experiments were 1.566×10^{-3} T/m, thus the diffusion gradient effect was a factor of 7 greater than the cross-terms in the case of the 3 mT/m gradient, and a factor of 14 greater in the case of the 6 mT/m gradient. The cross-terms were, therefore, ignored in the following calculations.

The accuracy, δD, with which D can be determined may be calculated by simple propagation of errors of the quantities of Equation 9 (Hazlewood et al, 1974):

$$\delta D = \frac{1}{(b_2-b_1)} \cdot \frac{1}{\mathrm{SNR}_1} \cdot \sqrt{1+\left(\frac{S_2}{S_1}\right)^2} \qquad (10)$$

where SNR_1 is the signal-to-noise ratio in the IVIM3/RAD3 data set. Diffusion accuracy may, therefore, be improved by maximizing the SNR as well as the difference between the b values of the two pulse sequences. The *minimum* D that can be imaged using a spin-echo sequence is limited by the T_2 of the material under study, as this determines the signal-to-noise ratio as well as the maximum diffusion-encoding gradient and hence b value on a given imaging system.

Results and discussion

Comparison of the IVIM and RAD phantom results

The diffusion coefficient of each sample in the phantom was calculated as outlined above, and the results are tabulated in Table I, together with published values included for comparison. The regression coefficients of the plots for acetone, water, cyclohexane and DMSO were, respectively, 0.99, 0.98, 0.91 and 0.18. The poorer fit for DMSO results from its smaller diffusion coefficient. The IVIM and RAD uncertainties are calculated from the standard deviation of the mean value in the region of interest by error propagation using Equation 10. Table II indicates the percentage improvement in sensitivity

$$\{[\delta(S_1 \div S_2)_{\mathrm{RAD}}/\delta(S_1 \div S_2)_{\mathrm{IVIM}}] \times 100\%\}$$

achieved with the application of orthogonal gradient fields and the corresponding T_2 of each sample. The intensity ratio $\delta(S_1 \div S_2)_{\mathrm{RAD}}$ represents the enhancement in image intensities between the RAD3 and RAD6 spin-echo images, while $\delta(S_1 \div S_2)_{\mathrm{IVIM}}$ represents the enhancement in image intensities between the IVIM3 and IVIM6 spin-echo images. Since these spin-echo data sets ultimately determine the level of contrast in the calculated diffusion map, any increase in sensitivity achieved by the RAD sequence would be reflected by an increased ratio between the S_1 and S_2 image intensities. Uncertainty in Tables II and III is the standard error of the mean of the region of interest from eight measurements.

Table II. Percentage improvement in diffusion sensitivity using the RAD technique compared with IVIM and T_2 measurements of samples

Sample	% Sensitivity improvement (Mean ± SEM, $n=8$)	T_2 of sample (ms)
Acetone	500 ± 60	345 ± 22
Distilled water	330 ± 10	270 ± 20
Cyclohexane	260 ± 30	177 ± 11
DMSO	185 ± 4	218 ± 18

It is apparent from Table I that the results obtained using the IVIM sequence are in good agreement with other published work. The RAD results are similar for the acetone sample; however, the errors become increasingly large as T_2 decreases (see Table II). The shorter the T_2 of a material, the less accurate the measurement, and although RAD has resulted in greater diffusion sensitivity (Table III), the calculated uncertainty values are generally greater than those of IVIM.

Factors affecting diffusion measurement accuracy. Although application of the RAD sequence resulted in increased diffusion sensitivity, as predicted on p. 886, the calculated diffusion values have greater uncertainty than those determined by the IVIM method. This may be a consequence of a number of factors. Switching three magnetic field gradients during TE leads to more severe eddy current effects in the RAD images, which cause signal reduction, thus resulting in a greater signal difference between the diffusion-sensitized and the normal

Table I. Comparison of the calculated diffusion coefficients using the IVIM and RAD method

Sample	IVIM diffusion coefficient[a]	RAD diffusion coefficient[a]	Published values[a]	Reference
Acetone	4.9 ± 0.1	5.0 ± 0.2	4.5–4.8	Cantor & Jonas (1977)
			4.97 ± 0.2	Le Bihan et al (1988)
Distilled water	2.6 ± 0.1	3.3 ± 0.2	2.31	Cantor & Jonas (1977)
			2.21 ± 0.1	Le Bihan et al (1988)
			2.34 ± 0.08	Stejskal & Tanner (1965)
			2.25–2.51	James & McDonald (1973)
Cyclohexane	1.6 ± 0.1	2.3 ± 0.3	1.47	Wesbey et al (1984)
			1.58	Cantor & Jonas (1977)
DMSO	0.7 ± 0.3	1.7 ± 0.3	0.84	Ahn et al (1986)

[a] Diffusion coefficients are quoted in units of 10^{-3} mm^2/s. All measurements were conducted at room temperature.

Table III. Diffusion sensitivity enhancement relative to water using the RAD method[a]

Sample name	Signal enhancement relative to water	Diffusion coefficient relative to water
Acetone	1.5 ± 0.2	1.5 ± 0.1
Distilled water	1.0 ± 0.0	1.0 ± 0.0
Cyclohexane	0.8 ± 0.1	0.8 ± 0.1
DMSO	0.6 ± 0.0	0.4 ± 0.0

[a] The results are expressed relative to the signal intensity of water (mean ± SEM, $n = 8$). They are also compared with the ratio of the diffusion coefficient of each material relative to water.

spin-echo image. This would lead to overestimation of the value of D, which is, indeed, what is observed in Table I.

In our imaging system, the largest eddy currents were associated with the y-gradient (Gowland, 1990), which was only applied during RAD data acquisition. This may account for the greater uncertainty associated with these measurements. For the IVIM images the diffusion-encoding gradient was always applied along the readout direction (x).

It is also evident from Table II that the diffusion enhancement achieved is not a simple factor of 3, as predicted by the theoretical considerations on p. 886, but rather a more complicated effect. This discrepancy was attributed to changes in the T_2^* of each sample owing to the presence of the additional gradients, which can cause degradation of the field homogeneity as a result of eddy currents. The effect was particularly pronounced in the case of samples with a high diffusion rate owing to the rapid loss of signal. Eddy current compensation techniques or the application of shielded gradient fields may minimize such effects, thus allowing the more accurate determination of D using the RAD technique.

The effect of T_2 *on diffusion measurement accuracy.* Both diffusion and T_2 relaxation result in signal attenuation, and it is not always straightforward to isolate their individual effects. Diffusion modifies the observed T_2, $(T_2)_{\text{obs}}$, according to Wesbey et al (1984):

$$\frac{1}{(T_2)_{\text{obs}}} = \frac{1}{T_2} + \frac{\gamma^2 . G^2 . D . \text{TE}^2}{12} \tag{11}$$

Increasing the gradient strength would, therefore, significantly reduce $(T_2)_{\text{obs}}$ and, hence, the SNR in the two data sets. The shorter the T_2 of a material and the higher its D, the more pronounced the attenuation effect in the image. Since large gradient lobes are required to measure D, which in turn increases the time interval prior to signal acquisition (and hence TE), the longer the T_2, the more accurate will be the diffusion measurement. If the T_2 of a material is comparable to or smaller than TE, it is not possible to carry out diffusion measurements accurately.

In the presence of large gradient fields, the second term will dominate the T_2 effect for high diffusion samples such as acetone. One would, therefore, expect acetone to show a marked reduction in $(T_2)_{\text{obs}}$ compared with DMSO or cyclohexane, which would be reflected by a much faster drop in signal, but not quite so dramatic as occurs with water. This is consistent with the results of Table II (p. 887). The lower D materials also tend to have shorter T_2s, hence, the percentage effect of the gradient on signal attenuation is proportionally smaller owing to the more rapid relaxation effects. The sensitivity of the method will, therefore, depend on both the T_2 of a material and its diffusion coefficient.

The observed signal enhancement in each sample relative to water when using RAD is summarized in Table III, where it is also compared with the diffusion coefficient of each material relative to water. The results of Table III indicate that there is a strong correlation between the achievable signal enhancement and the diffusion coefficient of a material, indicating a proportionality relation as expected from Equation 8. The higher resultant gradient field in the RAD sequence has, therefore, ensured that the observed reduction in signal in the diffusion maps is dominated by diffusion rather than T_2 effects.

Dependence of measurement accuracy on SNR

The sensitivity of the RAD technique was also investigated and compared with that of IVIM for a range of slice thicknesses, in order to assess the effect of SNR on the measurement accuracy. The SNR will be proportional to the slice thickness as predicted by the relation derived by Hoult and Lauterbur (1979):

$$\text{SNR} \propto \frac{V_s}{\sqrt{\Delta f}} \tag{12}$$

where V_s is the sample volume and Δf is the measurement bandwidth. The sample volume is proportional to the slice thickness, SL, therefore, Equation 12 may be modified to:

$$\text{SNR} \propto \frac{\text{SL}}{\sqrt{\Delta f}} \tag{13}$$

so that the SNR is proportional to the slice thickness. This is, indeed, what was found experimentally. The results for the water sample are shown in Fig. 2, while those for DMSO are shown in Fig. 3. Similar curves were also obtained for acetone and cyclohexane.

It is evident from the figures that the slope of the curve is dependent on the gradient strengths applied. This is in agreement with the theoretical results as can be seen by substituting for the image bandwidth, Δf using the Larmor relation:

$$\Delta f = \gamma . (G_x . X + G_y . Y + G_z . Z) \tag{14}$$

These figures confirm that, for this range of diffusion coefficients (0.84–$4.6 \times 10^{-3}\,\text{mm}^2/\text{s}$), the RAD method offers a two- to five-fold improvement in sensitivity, thus

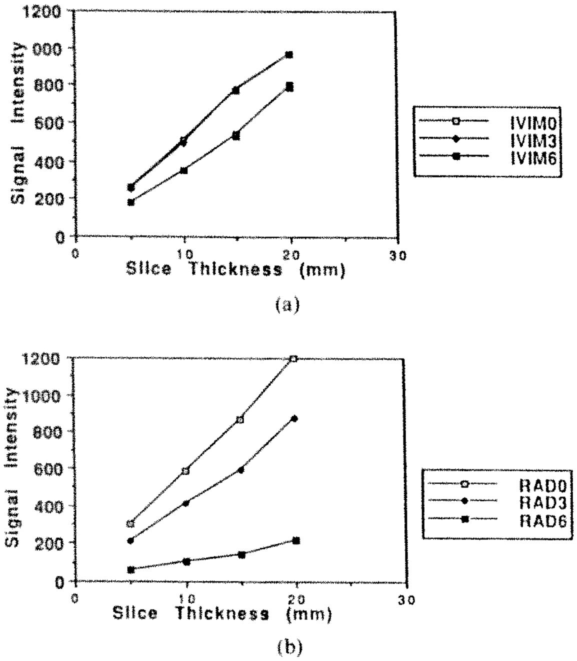

Figure 2. The variation in signal intensity with slice thickness using (a) the IVIM and (b) the RAD pulse sequence for the water sample. To compensate for the lower signal obtained with the RAD6 sequence, a higher amplification factor was used for the RAD sequences than that used for the IVIM sequences. The 3mT/m gradients do not significantly sensitize the IVIM3 sequence to diffusion effects, compared with the IVIM0 sequence.

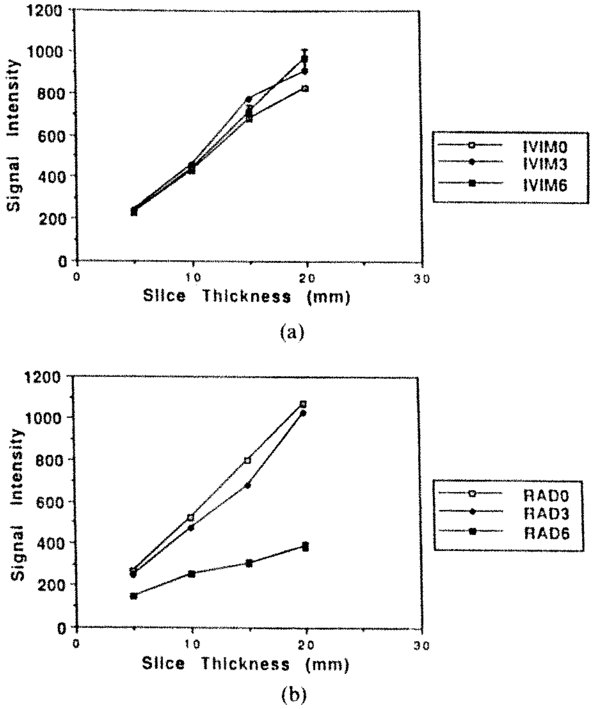

Figure 3. The variation in signal intensity with slice thickness using (a) the IVIM and (b) the RAD pulse sequence for the DMS0 sample. To compensate for the lower signal obtained with the RAD6 sequence, a higher amplification factor was used for the RAD sequences than that used for the IVIM sequences.

significantly enhancing the dynamic range of the method and, thus, allowing the more accurate determination of diffusion coefficients. Access to lower D values would be particularly valuable for the slower diffusion materials as well as for *in vivo* studies. As seen in the two figures, the greater the slice thickness, the better the SNR and, hence, the more pronounced the enhancement in the RAD sequence, as one would expect. However, when conducting *in vivo* studies this improvement in sensitivity must be weighted against the presence of partial volume effects, as large-scale averaging may obscure clinically important features.

Diffusion anisotropies in the presence of restrictions

The higher uncertainty associated with calculated D values at short T_2 may be particularly important in *in vivo* measurements, since the diffusion coefficient of intracellular water is about half that of free water. Furthermore, the presence of restrictions, such as cell membrane barriers, may further reduce this value (Hazlewood et al, 1974). The measurement accuracy can only be increased by the use of larger b values; however, these are not available on our imaging system.

The detection of *restricted diffusion* regimes is dependent on the time available for diffusion between the two gradient lobes in the IVIM sequence, $(d+I)$. If this time is long compared with that required for a molecule to encounter a barrier, restricted diffusion effects will become visible. A rough estimate of the restrictive dimensions that can be detected may be obtained from the Einstein equation: since $\langle r^2 \rangle = 2.D.t$ for diffusion along one gradient direction, a diffusion time of 55 ms allows a distance $r \approx 10\ \mu m$ to be traversed. If barriers are present at distances shorter than $10\ \mu m$, the observed diffusion coefficient will be lower than expected. However, if barriers are present at distances greater than $10\ \mu m$, restricted diffusion effects will *not* be detectable, as molecules do not, on average, encounter a barrier during $(d+I)$.

The effective molecular diffusion coefficient (D_e) of celery was found to be $3.2 \pm 1.5 \times 10^{-3}$ mm^2/s along the fibres (z), whilst only $2.2 \pm 1.5 \times 10^{-3}$ mm^2/s across the fibres (x), and $2.3 \pm 0.5 \times 10^{-3}$mm^2/s when gradients are applied along x, y and z. The calculated diffusion maps are shown in Fig. 4. The T_2 of celery was in the range 250–350 ms using a multi-point imaging measurement (Gowland, 1990). Despite the large uncertainty associated with these calculations because of the low SNR of images, the results show a similar trend to those reported by Moseley et al (1989), and imply that the presence of restrictions will cause diffusion coefficient modifications. The calculated values will, therefore,

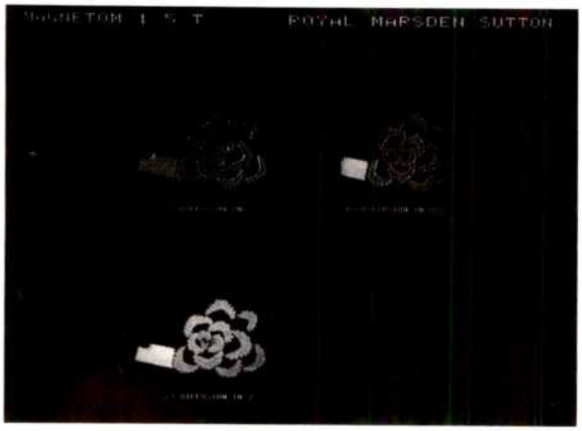
MAGNETOM 1.5 T
ROYAL MARSDEN SUTTON

Figure 4. The calculated diffusion maps for celery using (a) IVIM along its short axis, (b) RAD and (c) IVIM along its long axis. Notice that diffusion is slower in case (a), maximum in case (c) and has an intermediate value in case (b), as expected.

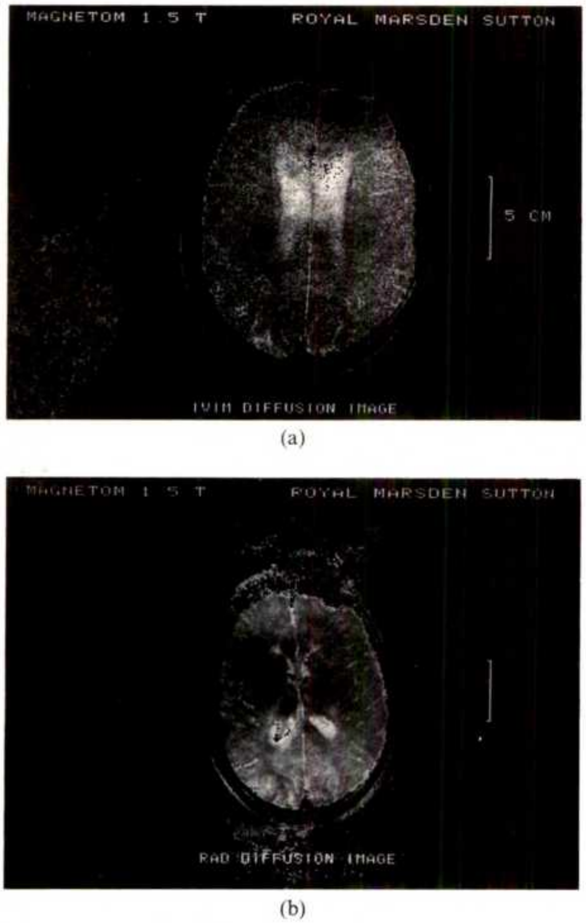
MAGNETOM 1.5 T
ROYAL MARSDEN SUTTON
5 CM
IVIM DIFFUSION IMAGE
RAD DIFFUSION IMAGE

(a)

(b)

Figure 5. The calculated diffusion maps with (a) IVIM and (b) RAD in a volunteer, using 3mT/m gradients and ECG gating.

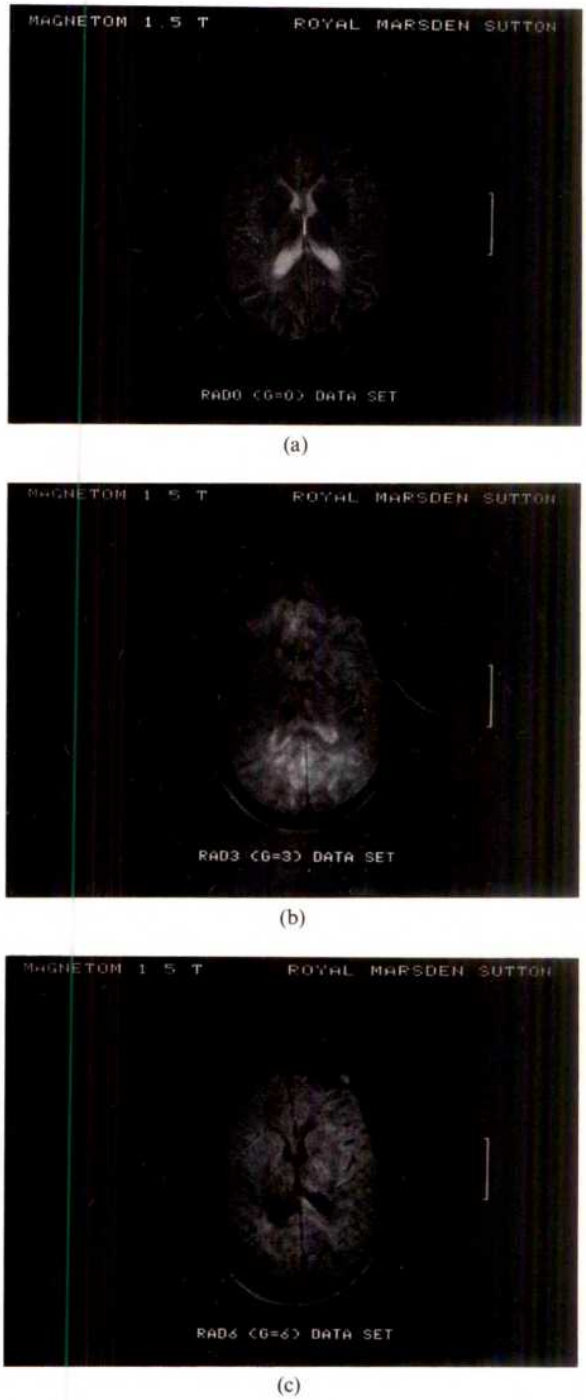
MAGNETOM 1.5 T
ROYAL MARSDEN SUTTON
RAD0 (G=0) DATA SET
RAD3 (G=3) DATA SET
RAD6 (G=6) DATA SET

(a)

(b)

(c)

Figure 6. The (a) RAD0, (b) RAD3 and (c) RAD6 data sets, showing a reduction in CSF intensity when the 6 mT/m gradients are applied.

Table IV. Calculated IVIM/RAD diffusion coefficients in volunteers with ECG

Cerebral region	IVIM diffusion coefficient[a]	RAD diffusion coefficient[a]	Published values[a]	Reference
Regions above or at the top of the ventricles (mean ± SEM):				
CSF	2.9±0.1	2.2±0.3	3.7±0.6	Chien et al (1988)
Grey matter				
(a) Frontal	0.6±0.1	1.8±0.3	0.9±0.3	Chien et al (1988)[b]
(b) Occipital	4.8±0.4	1.1±0.1	1.87	Gehrig et al (1989)[b]
White matter	2.9±0.4	0.6±0.2	1.2±0.2	Chien et al (1988)[b]
			1.45	Gehrig et al (1989)[b]
Regions through the ventricles (mean ± SEM):				
CSF	5.6±0.3	3.0±0.3	3.7±0.6	Chien et al (1988)
Grey matter				
(a) Frontal	1.0±0.2	2.0±0.5	0.9±0.3	Chien et al (1988)[b]
(b) Occipital	2.4±0.8	1.8±0.2	1.87	Gehrig et al (1989)[b]
White matter	2.7±0.5	0.3±0.1	1.2±0.2	Chien et al (1988)[b]
			1.45	(Gehrig et al (1989)[b]

[a] Diffusion coefficients are quoted in units of 10^{-3} mm^2/s.

[b] It was not specified whether the region imaged was above or through the ventricles and whether the grey matter was from the frontal or occipital lobes.

depend on the direction in which the diffusion-encoding gradient was applied in an anisotropic material.

Diffusion is maximum along the long axis of celery owing to the absence of restrictions, and minimum along its short axis owing to the presence of barriers. The RAD technique gives an intermediate value as it represents the normalized effect of diffusion along the three orthogonal axes, one long and two short. The much smaller uncertainty associated with the RAD diffusion values are a consequence of the increased sensitivity of this pulse sequence to diffusion effects. The results confirm the effect of the diffusion-encoding direction on the computed diffusion values (D_e) when imaging materials have a very asymmetrical structure, such as muscle.

In vivo *diffusion studies*

In vivo diffusion coefficients were calculated as described on p. 887 and the results are given in Table IV, whilst the computed diffusion maps are shown in Fig. 5. For Tables IV and V the IVIM and RAD uncertainties are calculated from the standard deviation of the mean

Table V. Comparison of the magnitude of motion artefacts to the signal-to-noise ratio in the IVIM and RAD data sets using ECG

(a) IVIM measurements

Source of artefact	IVIM0 image data	IVIM3 image data	IVIM6 image data
CSF flow/pulsation	13.7±5.8	34.6±10.3	93.5±14.8
Orbital motion	13.3±6.1	26.4±9.2	24.6±12.9
Patient motion or real brain motion	15.4±7.1	47.5±13.1	39.6±13.0
Signal			
Signal in cerebral cortex	151.5±16.4	161.6±20.6	118.0±14.3
Random noise	11.5±5.0	11.3±4.8	11.3±5.2

(b) RAD measurements

Source of artefact	RAD0 image data	RAD3 image data	RAD6 image data
CSF flow/pulsation	18.4±6.2	140.8±33.7	56.6±6.7
Orbital motion	23.8±8.0	66.8±11.9	17.0±6.4
Patient motion or real brain motion	24.6±7.2	74.1±12.9	50.9±7.8
Signal			
Signal in cerebral cortex	206.3±17.6	102.6±16.3	92.9±13.6
Random noise	8.1±3.2	2.3±0.5	2.2±0.4

value in the region of interest by error propagation using Equation 10. As can be seen from Fig. 5, the presence of the 3 mT/m gradients in each of the three orthogonal directions, resulting in a total gradient magnitude of 5.2 mT/m, gives rise to severe motion artefacts, which are not completely eliminated by the ECG gating. The magnitude of these artefacts is summarized in Table V(b). A comparison of these values with those caused by the IVIM sequence [Table V(a)] reveals that application of gradients in all three directions severely accentuates the problem. This may be explained by the fact that cerebrospinal fluid (CSP) flow and pulsation takes place in more than one plane (Feinberg & Mark, 1987), thus the two additional gradients accentuate velocity components along those two directions as well. The magnitude of these artefacts will lead to large measurement uncertainties as it is comparable to or greater than the signal in the cerebral cortex, as indicated in Table V(b). In addition, random patient motion must occur in more than one plane, hence the pronounced motion effects when using all three gradients (Fig. 6).

Application of the 6 mT/m gradients (total resultant gradient of 10.4 mT/m), however, led to a surprising reduction in the artefact intensity caused by the CSF and orbital motion. This finding was reproducible in another volunteer and is in good agreement with the results of Moseley et al (1989). This apparently paradoxical effect may be explained by considering Equation 1. The spin-echo attenuation is determined by the exponential factor $\exp\{-b.D\}$, where $b \propto G^2$. This factor is equal to 0.7 for the RAD3 or IVIM6 sequences (assuming CSF has $D = 2.4 \times 10^{-3}\ \mathrm{mm^2/s}$). However, when the RAD6 gradients are switched on, the exponential factor is reduced to 0.3, thus resulting in a significant reduction in signal compared with either the IVIM6 or RAD3 sequences.

The effect of the gradients is, therefore, to almost completely eliminate signal from fast-diffusing regions, such as the CSF, so that hypointense regions in the RAD6 image (Fig. 6c) correspond to fast-diffusing species, whilst hyperintense regions correspond to slow-diffusing species. Since the CSF is the main source of motion effects (Fig. 6b), this signal attenuation facilitates the production of more accurate diffusion and perfusion maps. The use of higher gradient strengths could, therefore, improve the accuracy of the IVIM data sets since both the CSF and grey matter signals would be significantly attenuated. Almost artefact-free images could then be obtained, which would facilitate the calculation of perfusion fractions as well as diffusion coefficients in different regions in the brain.

Conclusions

The results presented above confirm that sensitivity enhanced diffusion maps may be obtained by employing gradient sensitization in three orthogonal directions. This leads to a two- to five-fold improvement in diffusion sensitivity, which may be valuable when conducting clinical studies. Diffusion measurements are limited by the T_2 of the material under study, which reduces the SNR and hence measurement accuracy. Application of higher gradient strengths would allow the use of shorter echo times, thus reducing T_2 losses. Motion sensitivity remains an important problem, severely limiting the clinical usefulness of both IVIM and RAD diffusion maps. Motion artefacts may be reduced by applying higher gradient strengths in order to eliminate the signal from fast-diffusion compartments, such as the CSF, which are usually the source of significant motion artefacts. Faster imaging sequences could also minimize or eliminate these problems. Implementation of both the IVIM and RAD techniques with higher gradient strengths, better eddy current compensation methods and shorter TE may, therefore, allow quantitative studies of diffusion in tissues.

Acknowledgments

We are grateful to the Cancer Research Campaign for supporting this research and to Dr S. Tanner for performing the T_2 measurements.

References

Ahn, C. B., Lee, S. Y., Nalcioglu, O. & Cho, Z. H., 1986. An improved NMR diffusion coefficient imaging method using an optimised pulse sequence. *Medical Physics, 13*, 43–48.

Avraamidou, A. & Leach, M. O., 1988. Direction independent diffusion coefficient mapping. *Society of Magnetic Resonance in Medicine Book of Abstracts* (Berkeley, California), Vol. 2, p. 747.

Beall, R. T., Amtey, S. R. & Kasturi, S. R., 1984. In *NMR Data Handbook for Biomedical Applications* (Pergamon Press, USA), pp. 101–151.

Cantor, D. M. & Jonas, J., 1977. Automated measurement of self-diffusion coefficients by the spin-echo method. *Journal of Magnetic Resonance, 28*, 157–162.

Chien, D., Buxton, R. B., Kwong, K. K., Brady, T. J. & Rosen, B. R., 1988. Quantitative diffusion imaging in the human brain. *Proceedings of the 7th Annual Meeting of the Society of Magnetic Resonance in Medicine, San Francisco* (SMRM, Berkeley, CA), p. 218.

Feinberg, D. A. & Mark, A. S., 1987. Human brain motion and cerebrospinal fluid circulation demonstrated with MR velocity imaging. *Radiology, 163*, 793–799.

Gehrig, J., Bader, R., Zabel, H. J., Backert-Baumann, P., Gückel, F. & Lorenz, W. J., 1989. Determination of diffusion in humans with ECG triggered PGSE sequences. *Proceedings of the 8th Annual Meeting of the Society of Magnetic Resonance in Medicine, Amsterdam* (SMRM, Berkeley, CA), p. 135.

Gowland, P. A., 1990. The Accurate Measurement of NMR Parameters *in Vivo*, PhD Thesis, University of London, UK.

Hazlewood, C. F., Cleveland, G. & Medina, D., 1974. Relationship between hydration and proton nuclear magnetic resonance relaxation times in tissues of tumor-bearing and non-tumor-bearing mice: implications for cancer detection. *Journal of the National Cancer Institute, 52*, 1849–1853.

Hoult, D. I. & Lauterbur, P. C., 1979. The sensitivity of the Zeugmatographic experiment involving human samples. *Journal of Magnetic Resonance, 34*, 425.

James, T. L. & McDonald, G. G., 1973. Measurement of the self-diffusion coefficient of each component in a complex system using pulsed-gradient Fourier transform NMR. *Journal of Magnetic Resonance, 11*, 58–61.

KÄRGER, J., PFEIFER, H. & HEINK, W., 1988. Principles and applications of self-diffusion measurements by nuclear magnetic resonance. *Advances in Magnetic Resonance, 12*, 1–89.

LE BIHAN, D. & BRETON, E., 1985. Imagerie de diffusion *in vivo* par résonance magnétique nucléaire. *Comptes Rendus de l'Académie des Sciences (Paris), 301* (série II), *15*, 1109–1112.

LE BIHAN, D., BRETON, E., LALLEMAND, D., GRENIER, P., CABANIS, E. & LAVAL-JEANTET, M., 1986. MR imaging of intravoxel incoherent motions: applications to diffusion and perfusion in neurologic disorders. *Radiology, 161*, 401–407.

LE BIHAN, D., BRETON, E., LALLEMAND, D., AUBIN, M. L., VIGNAUD, J. & LAVAL-JEANTET, M., 1988. Separation of diffusion and perfusion in intravoxel incoherent motion MR imaging. *Radiology, 168*, 497–505.

MADDEN, A., 1990. NMR Studies of Tissue Physiology and Metabolism: The Investigation of Perfusion, Diffusion and Intracellular pH, PhD Thesis, University of London, Ch. 5, pp. 132–153.

MOSELEY, M. E., COHEN, Y., MINTOROVITCH, J., CHILEUITT, L., SHIMIZU, H., TSURUDA, J., NORMAN, D. & WEINSTEIN, P., 1989. Evidence for anisotropic self-diffusion in cat brain. *Society of Magnetic Resonance in Medicine Book of Abstracts*, Vol. 1, p. 136.

NEEMAN, M., FREYER, J. P. & SILLERUD, L. O., 1990. Pulsed-gradient spin-echo studies in NMR imaging. Effects of the imaging gradients on the determination of diffusion coefficients. *Journal of Magnetic Resonance, 90*, 303–312.

STEJSKAL, E. O., 1965. Use of spin echoes in a pulsed magnetic field gradient to study anisotropic restricted diffusion and flow. *Journal of Chemical Physics, 43*, 3597–3603.

STEJSKAL, E. O. & TANNER, J. E., 1965. Spin diffusion measurements: spin echoes in the presence of time-dependent field gradient. *Journal of Chemical Physics, 42*, 288–292.

TAYLOR, D. G. & BUSHELL, M. C., 1985. The spatial mapping of translational diffusion coefficients by the NMR imaging technique. *Physics in Medicine and Biology, 30*, 345–349.

WESBEY, G. E., MOSELEY, M. E. & EHMAN, R. L., 1984. Translational molecular self-diffusion in magnetic resonance imaging: effects and applications. In *Biomedical Magnetic Resonance*, ed. by T. L. James and A. R. Margulis (Radiology Research and Education Foundation, San Francisco, USA), pp. 63–78.

1992, *The British Journal of Radiology*, 65, 895–900

Impact of hydration status on body composition as measured by dual energy X-ray absorptiometry in normal volunteers and patients on haemodialysis*

By F. F. Horber, MD, F. Thomi, MS, J. P. Casez, MD, J. Fonteille, MD and Ph. Jaeger, MD

Policlinic of Medicine, University Hospital, Berne, Switzerland

(*Received 13 September 1991 and in revised form 7 February 1992, accepted 26 March 1992*)

Keywords: Dual-energy X-ray absorptiometry, Haemodialysis, Hydration status, Body composition

Abstract. To evaluate the influence of hydration status on the estimation of body composition using dual-energy X-ray absorptiometry (DXA), six normal volunteers and seven patients on maintenance haemodialysis were investigated using two different DXA machines (Lunar DPX, Hologic QDR 1000/W). Normal volunteers were studied (Hologic QDR 1000/W) before and 1 h after ingestion of breakfast, lunch and dinner (drinking various amounts of liquids at each meal, 0.5–2.4 kg). Whereas bone mineral content and body fat mass did not change, lean body mass of the trunk increased as a consequence of the meals. Conversely in patients on haemodialysis (Lunar DPX), lean body mass decreased in all segments of the body as a consequence of removal of 0.9–4.4 kg of salt-containing fluid by haemodialysis (trunk 61%, legs 30%, arms 5.5% and rest of the body 3.5%), whereas bone mineral content and body fat mass remained unchanged. However, this finding(s) did not hold true in one particular patient with bilateral hip prostheses. Measurement of body composition in eight normal volunteers on the same day with both machines showed similar results for lean and fat mass, whereas bone mineral content was found to be 17% higher using the Lunar DPX. In summary, in centres where both machines are available, follow-up of one individual patient should always be performed using the same equipment. In addition, hydration status and food intake must be taken into account when repetitive measurements of lean body mass are performed in the same patient.

Recently, development of dual-energy X-ray absorptiometry (DXA) technology by several manufacturers has allowed the measurement of lean and fat mass in healthy subjects (Heymsfield et al, 1989; Mazess et al, 1990; Wang et al, 1989). Dual-photon absorptiometry (DPA) was first employed using a gadolinium-153 source (Heymsfield et al, 1989). Replacement of the isotope by an X-ray source (DXA) allowed reduction in investigating time and improvement in precision and accuracy owing to the greater radiation fluence of the latter method (Mazess et al, 1990). However, until now only Lunar equipment has been validated with established methods of determining body composition such as whole-body potassium content, underwater weighing, etc. (Heymsfield et al, 1989; Wang et al, 1989). Since it is known that different DXA machines may give different results for bone mineral measurements (McClung & Roberts, 1989; Kelly et al, 1989), it is of obvious importance to compare results of fat and lean mass determinations obtained by machines from different manufacturers.

In addition, it is well known that DXA cannot differentiate between body water and lean body mass. Measuring pure water with DXA *in vitro* revealed that its radiological behaviour is identical to that of a mixture of 91.4% lean tissue and 8.6% fat tissue (Nord & Payne, 1990). However, this is only true if one assumes that body water accounts for a fixed fraction of lean mass (*i.e.* 73.2%). Using this assumption, precise measurement of lean body mass is possible using DXA (Mazess et al, 1990).

Anuric patients with end-stage renal failure usually retain salt-containing fluid (equivalent to pure lean tissue as measured by DXA) between haemodialysis sessions. Accumulated salt and water is removed by dialysis in a short period of time (*i.e.* 3–4 h). By scanning patients with DXA before and after dialysis, effects of removal of several litres of salt-containing fluid on body composition could be assessed. This would be of major interest, since reliable measurements of lean and fat mass in dialysis patients are important to monitor accurately (1) their nutritional status and (2) potential pharmacological or dietary interventions to improve their known impaired body composition (Horber et al, 1986).

For convenience and time efficiency it is important to be able to investigate subjects at any given time of day and without a prior fasting period. On the other hand, hydration status may influence results obtained not only in patients on dialysis but also in normal subjects.

Therefore, the following three studies were designed to answer the following questions:

Address correspondence and reprint requests to F. F. Horber, MD, Medizinische Poliklinik, Freiburgstrasse, Inselspital, CH-3010 Bern, Switzerland.

* This paper was presented in part at the annual meeting of the American Society of Nephrology 1990, Washington DC, and reported in abstract form (*Journal of the American Society of Nephrology, 1*, 362, 1990).

1. Are changes in hydration status of normal volunteers and patients on haemodialysis accurately detected by DXA technology?
2. Does removal of salt-containing fluid by haemodialysis and enteral intake of water and food also influence bone and fat mass measurements?
3. Are results of body composition obtained by DXA from two different manufacturers similar, if not identical?

Methods

Dual-energy X-ray absorptiometry

Equipment from two different manufacturers was used to assess whole-body composition: the Lunar DPX (Lunar Radiation Corp., Madison, WI) and the Hologic QDR 1000/W (Hologic Inc., Waltham, MA).

The Lunar DPX uses one constant potential X-ray source at 78 kVp and a K-edge filter (effective energies of 40 and 70 keV). The DPX unit performs a series of transverse scans moving from head to toe at 1 cm intervals providing a pixel size of approximately 5 mm × 10 mm. Data are analysed using software version 3.1 (Mazess et al, 1990).

The Hologic QDR 1000/W uses a switched pulsed stable dual-energy radiation with two peak kilovoltages of 70 and 140 kVp. An Automatic Internal Reference System, which employs a calibration wheel, achieves a drift-free measurement for bone. The QDR performs a series of transverse scans moving from head to toe at 1.2 cm intervals providing a pixel size of 1.9 mm × 12 mm. Data are analysed using software version 5.35. A calibration phantom for soft tissue is scanned in parallel with the subjects.

For both machines the composition of soft tissue is given by a ratio of beam attenuation at the lower energy relative to that at the higher energy. Radiation dose of a single measurement is less than 0.1 μGy (Mazess et al, 1990). With both machines a scan is completed in less than 20 min.

Electronic balance

For comparison of body weight measurements using DXA, subjects were weighed immediately before each DXA measurement on an electronic balance with a precision of 0.1 kg (Kipfer DPW 150, Jegenstorf, Switzerland).

Subjects: study protocols

Effects of drinking and meals on body composition: assessment by QDR 1000/W (Study 1). Six healthy normal volunteers (three males, three females) were studied. Subjects' characteristics were as follows: age 24–37 years, body weight 50–90 kg and body height 160–178 cm. Subjects were scanned in their underwear and weighed six times the same day, immediately before and 1 h after each meal [breakfast: 400 ml, 155 g, 632 kcal; lunch: 800–2200 ml (median 1950 ml), 310 g, 530 kcal; and dinner: 800–2400 ml (median 1200 ml), 110 g, 530 kcal], which were served in an identical manner to all the subjects. Immediately following lunch and dinner, subjects were encouraged to drink as much as they could. After the post-meal scan, subjects were not allowed to eat or drink. In addition, subjects had to empty their bladder immediately before each scan. Furthermore, all drinking and urine volumes were recorded. No subjects had any stools during the study period.

Effects of haemodialysis treatment on body composition: assessment by DPX (Study 2). Seven patients on long-term haemodialysis (five males, two females) were weighed and scanned immediately before and within 1 h following haemodialysis. Patients were not allowed to eat or drink and did not loose any urine or stool between the two measurements. Subjects' characteristics were as follows: age 23–75 years, body weight before dialysis 45–71 kg and body height 154–175 cm. Reason for end-stage renal disease was glomerulonephritis ($n = 6$) and polycystic kidney disease ($n = 1$). One of the subjects had bilateral hip prostheses because of aseptic necrosis of the femoral heads.

Patients were receiving various drugs such as frusemide, calcium antagonists, beta-adrenergic antagonist agents and vitamin-D derivatives.

Impact of two different DXA technologies on body composition (Study 3). Eight healthy volunteers (four males, four females) were studied. Subjects' characteristics were as follows: age 24–65 years, body weight 50–90 kg and body height 160–178 cm. Prior to the investigation, subjects were fasting for at least 10 h. Subjects were analysed twice, once with the Hologic QDR 1000/W and once with the Lunar DPX.

These studies were approved by the ethical committee at the University of Berne. Informed consent was obtained from all subjects after the nature of the procedure(s) had been fully explained.

Statistical analysis

Values appearing in the text and in the tables are means ±SEM. For comparisons, the Student's paired *t*-test was used.

Results

Effects of drinking and meals on body composition: assessment by QDR 1000/W

Drinking of 0.8–2.4 l (median 0.83 l) of water did not influence DXA measurements of fat and bone mass, whereas lean mass increased ($p < 0.005$) by the difference in body weight (water and food intake minus urinary output minus insensitive losses) both at lunch (between 1200 and 1300 h) and at dinner (between 1700 and 1800 h, Fig. 1a) The changes in weight estimated from the Hologic QDR compared with those from the balance were as follows: increase in weight due to lunch: 1567±210 g *vs.* 1483±217 g; decrease in weight between lunch and dinner: −1609±198 g *vs.* −1633±214 g; increase in weight due to dinner: 1004±239 g *vs.* 983±274 g. However, it is of interest to note that a light breakfast with ingestion of minor amounts of fluid (less than 500 ml) did not significantly change estimates of body composition.

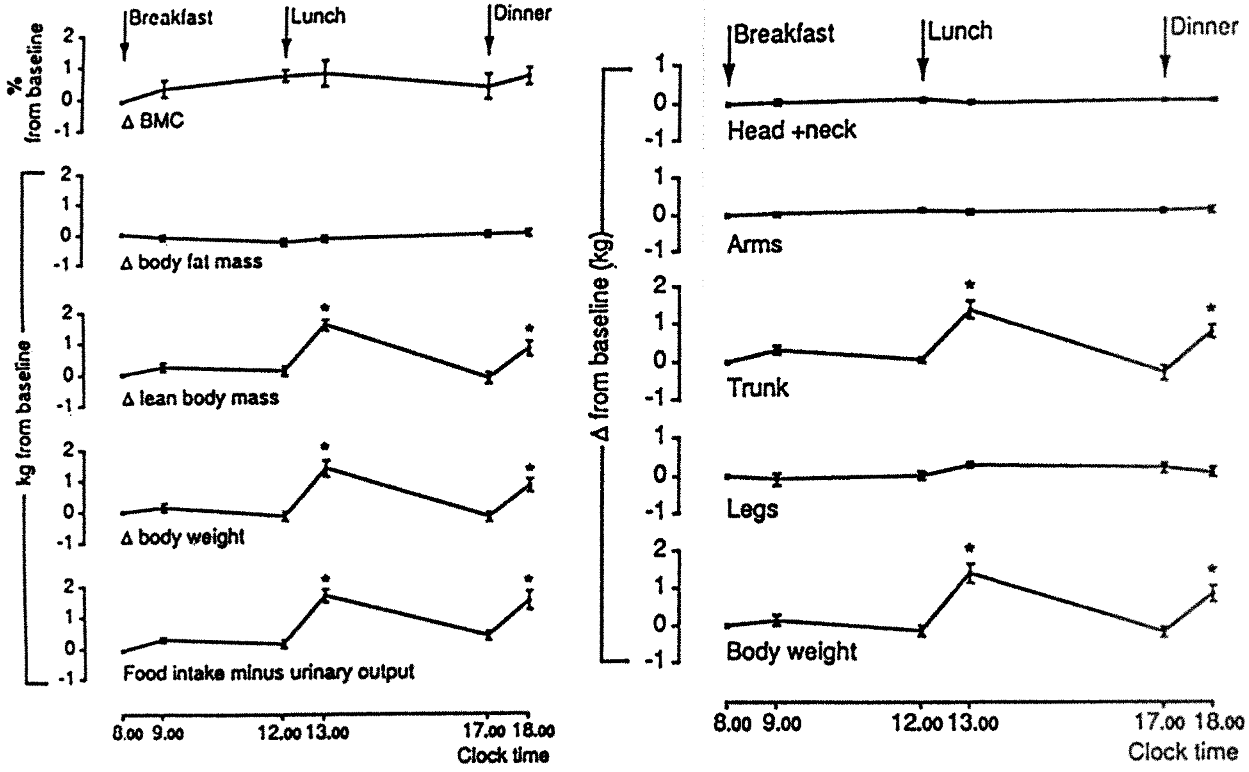

(a) (b)

Figure 1. (a) The effects of fluid and food intake on body composition measurements as assessed by the QDR 1000/W. (b) Repartition of changes in lean body mass induced by fluid and food intake. Values are given as mean ± SEM and reported in kg or percentage from baseline measurements. $^*p < 0.01$: before *vs.* after meal.

Figure 1b depicts the segmental repartition of changes in lean body mass observed over the examination period. Interestingly, increments in lean body mass after lunch and dinner were only detected in the trunk and not in the arms, legs or "head and neck".

The increment in lean mass during the meals was strongly correlated with the differences between water and food intake and urinary output ($r = 0.93$; $p < 0.0001$).

Predicted to observed fat mass changes

According to Nord and Payne (1990), the expected fat mass change as a result of a change in lean mass due to pure water ingestion can be calculated as follows:

$$(8.6/91.4) \times \text{delta lean mass} \qquad (1)$$

Table I demonstrates that no significant differences between expected fat changes and those measured with the Hologic QDR 1000/W were observed at breakfast, lunch and dinner.

Effects of haemodialysis treatment on body composition: assessment by DPX

Effect of haemodialysis on whole-body segments. As a consequence of removal of salt-containing fluid by dialysis therapy, body weight decreased by 0.9–4.4 kg (median 3.1 kg). Bone and fat mass did not change despite salt and water removal during haemodialysis. In contrast, decrease in lean mass ($p < 0.01$) was noted, which accounted for 94±5% of the changes in body weight as a consequence of dialysis therapy. As expected, the amount of weight lost and the change in lean body mass observed during dialysis were strongly correlated with each other ($r = 0.94$, $p < 0.006$).

The loss of fat mass as a consequence of salt-

Table I. Effects of different meals on observed *vs.* predicted fat mass changes

	Observed fat mass change (g) (1)		Predicted fat mass change (g) (2)	
Breakfast	−26±110	(−268 +416)	14±12	(−19 +60)
Lunch	192±65	(−7 +404)	129±20	(+58 +184)
Dinner	134±68	(−94 +307)	81±21	(+23 +157)
All meals	100±51	(−268 +416)	75±75	(−19 +184)

Values are given as mean±SEM, range in parentheses.
(1) As measured by Hologic QDR 1000/W; (2) as estimated by the equation of Nord and Payne (1990).

Table II. Effect of haemodialysis (HD) treatment on body composition measurements as assessed by DXA

	Body fat mass (kg)		Lean body mass (kg)		Bone mineral content (kg)	
Patient	Before HD	After HD	Before HD	After HD	Before HD	After HD
1	5.9	5.8	41.6	40.1	1.64	1.59
2	12.8	12.7	38.5	34.8	2.25	2.25
3	14.9	15.0	41.1	37.7	2.05	2.10
4	18.4	18.8	50.8	45.4	1.70	1.70
5	7.5	7.3	35.5	32.5	1.61	1.60
6	11.4	10.6	51.3	49.5	2.33	2.33
Mean ± SEM	11.8 ± 1.9	11.7 ± 1.8	43.2 ± 2.7	40.0 ± 2.6*	1.93 ± 0.13	1.93 ± 0.14
Patient with hip prostheses	8.3	6.4	52.4	49.8	2.43	2.42

* $p < 0.01$ *vs.* before HD.

containing fluid removal was not significantly different from zero (0.12 ± 0.17 kg, Table II).

It is of interest to note (Table II) that the changes observed during dialysis in the subject with bilateral hip prostheses were different, in that not only lean mass but also fat decreased. These differences remained even after the prostheses were excluded from the analysis (area of exclusion: all transverses containing the prosthetic implant). This indicates that results have to be interpreted with caution in subjects with artificial implants such as metal prostheses.

Effect of haemodialysis on segmental analysis of body segments. When the reduction in body weight as a result of dialysis was analysed according to the segments of the body (*i.e.* trunk, legs, arms and the rest of the body) again no changes were observed for fat and bone mass of all segments. However, with respect to lean mass, the trunk accounted for 61 ± 7% ($p < 0.002$ before *vs.* after haemodialysis), legs 30 ± 4% ($p < 0.02$), arms 5.5 ± 2.5% ($p < 0.04$) and rest of the body 3.5 ± 2.7% for the decrease in lean body mass observed during dialysis. Lean mass removed from the different segments of the body was higher in the trunk (9 ± 1.7%) and legs (6.8 ± 1.2%) than in the arms (3.4 ± 1.0%; $p < 0.05$).

Assessment of body composition with DXA: Hologic or Lunar

Figure 2 depicts the relationship between values obtained with the Hologic QDR 1000/W and Lunar DPX with respect to body weight and its partition into lean, fat and bone mass.

Body weight measured with both machines was virtually identical [$r = 1.00$, $p = 0.0001$, SEE = ±0.97 kg; Hologic measurement (kg) = −0.97 kg + 1.02 × Lunar measurement (kg)]. As expected (Kelly et al, 1989; McClung & Roberts, 1989), bone mineral content was found to be higher with the Lunar than with the Hologic ($p < 0.05$) by about 17 ± 2% [$r = 0.98$, $p = 0.0001$, SEE = ±92 g; Hologic measurement (kg hydroxyapatite) = 0.084 (kg) + 0.82 × Lunar measurement (kg)]. Fat body mass [$r = 0.99$, $p = 0.0001$, SEE = ±0.80 kg; Hologic measurement (kg) = 2.30 (kg) + 0.84 × Lunar measurements (kg)] and lean body mass [$r = 0.99$, $p = 0.0001$, SEE = ±1.40 kg; Hologic measurement (kg) = −1.78 (kg) + 1.05 × Lunar measurement (kg)] were similar using both DXA methodologies.

Assessment of body weight using an electronic balance or DXA

Balance weight was similarly correlated with the weight obtained by the Lunar DPX [balance weight (kg) = 0.92 Lunar DPX weight (kg) + 4.68 kg; $r = 0.988$, $p = 0.0001$] or by the Hologic QDR 1000/W [balance weight (kg) = 0.93 Hologic weight (kg) + 3.49 kg; $r = 0.992$, $p = 0.0001$].

Discussion

The present study demonstrates that acute food and water intake as well as chronic overhydration do not influence measurements of bone using DXA. In contrast, acute changes in whole-body water content markedly influence results of lean body mass in subjects investigated with DXA (Fig. 1). Furthermore, removal of salt-containing fluid by dialysis in chronically overhydrated patients changes lean body mass in all segments of the body (with the exception of the arms) according to their respective contribution to total lean body mass. In contrast, drinking up to 2.4 l of liquids within an hour leads to an increased lean body mass at the level of the trunk only, but not in other segments of the body.

Based on the equation by Nord and Payne (1990), fat mass results have to be adjusted if changes in lean mass measurements are due to intake or removal of pure water, as was the case in our meal study (Fig. 1, Table I). In contrast, if changes in lean mass are due to removal of salt-containing fluids (about 7 g of salt per litre of dialysate) as in our study in dialysis patients, such corrections should not be made. This is due to the fact that water containing 7 g of salt is similar to the lean mass equivalent as described by Nord and Payne (1990). However, despite these potential differences, the

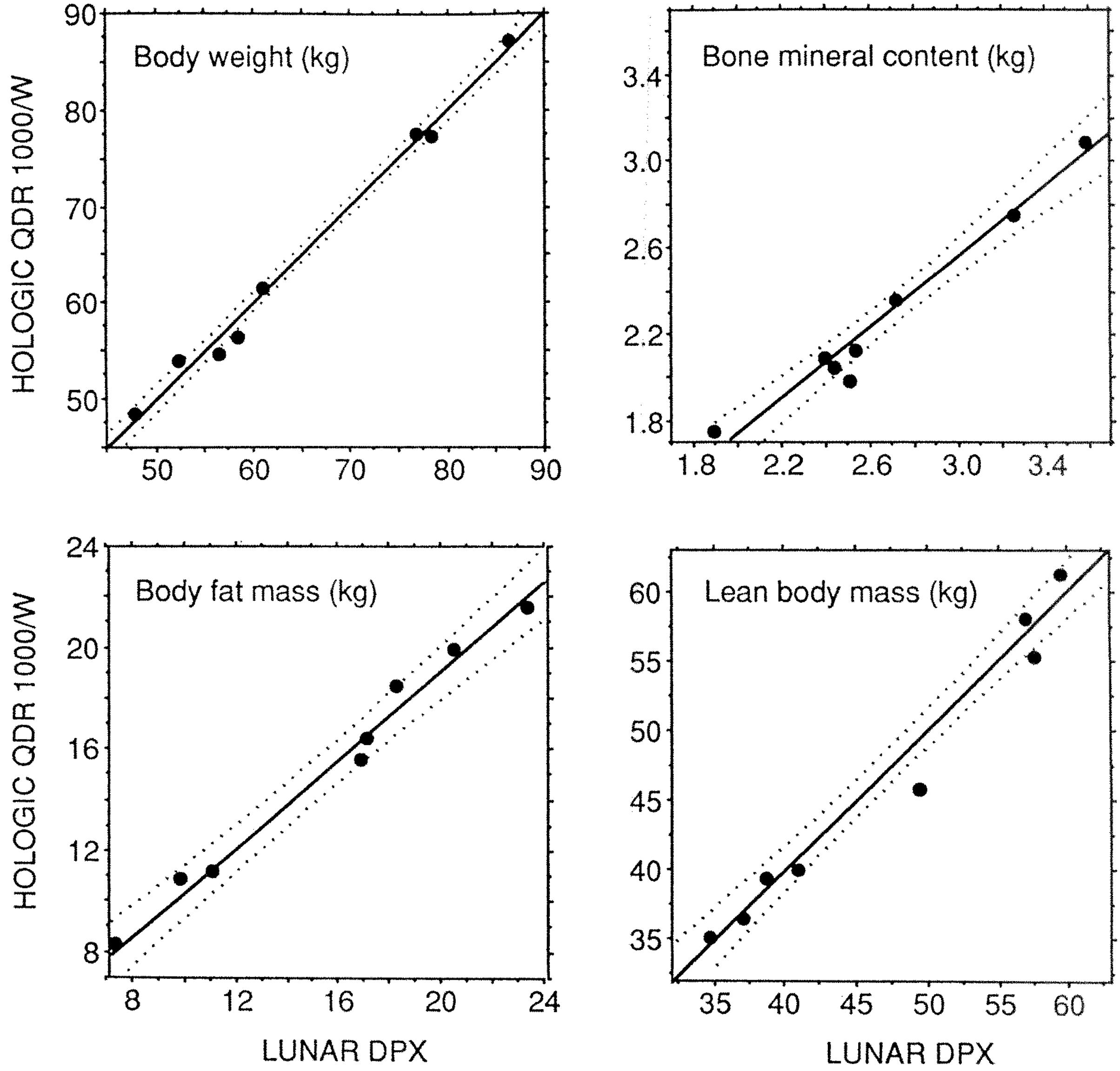

Figure 2. Correlation of Hologic QDR 1000/W *vs.* Lunar DPX for body weight (top left), bone mineral content (top right), body fat mass (bottom left) and lean body mass (bottom right). Grid lines depict 95% confidence intervals for the true mean of Y-axis.

accuracy of fat measurement during changing hydration status seems reasonable for clinical studies.

Collectively these results suggest that using DXA fat mass and bone mineral content can be assessed independently from food and hydration status, at least in normal volunteers and in subjects on haemodialysis. On the other hand, proper assessment of lean mass is clearly dependent on hydration status. However, eating a light meal with less than 500 ml of fluid does not preclude precise measurement of lean body mass, provided subjects empty their bladder prior to the investigation.

Reproducible measurements of body composition in dialysis patients are needed to monitor accurately the nutritional status of these individuals and to assess the efficacy of dietary and pharmacological interventions designed to improve their known impaired body composition (Horber et al, 1986). In contrast to fat mass (with the restrictions discussed above) and bone mineral content, measurements of which are independent of the time lag after the last dialysis, lean body mass is dependent on the hydration status of the patient at the time of measurement. Therefore, patients on haemodialysis should probably be studied immediately following a dialysis session.

As shown by the present studies in a patient on haemodialysis, implantation of metal prostheses may result in erroneous results for whole-body composition, which should be interpreted with caution in such patients.

Recently Heymsfield et al (1989) validated DXA as a powerful, precise and accurate tool to assess whole-body composition using a Lunar DPX (Mazess et al, 1990; Wang et al, 1989). The present paper demonstrates that similar results for lean and fat mass can be obtained using the Hologic QDR 1000/W at least for the height and weight range assessed in the present study. As reported by others, results of both techniques considerably differ in terms of bone mineral content, which seems to be due to an overestimation of bone mineral content by the Lunar DPX (Kelly et al, 1989).

In summary, if both machines are available, follow-up of individual patients should be performed using the same equipment. In addition hydration status and food intake must be taken into account when repetitive measurements are carried out in the same individual.

Acknowledgment

We thank Dr Philippe Pointet and Dr Francis Ducret for their help in haemodialysis patient selection. This study was supported in part by a grant from the Walter Schmid Foundation, Berne, Switzerland, and a grant from Lepetit Laboratories.

References

HEYMSFIELD, S. B., WANG, J., HESHKA, S., KEHAYIAS, J. J. & PIERSON, R. N., 1989. Dual-photon absorptiometry: comparison of bone mineral and soft tissue mass measurements *in vivo* with established methods. *American Journal of Clinical Nutrition, 49,* 1283–1289.

HORBER, F. F., ZUERCHER, R. M., HERREN, H. CRIVELLI, M. & FREY, F. J., 1986. Altered body fat distribution in patients with glucocorticoid treatment and in patients on long-term dialysis. *American Journal of Clinical Nutrition, 43,* 758–769.

KELLY, T. L., SLOVIK, D. M. & NEER, R. M., 1989. Calibration and standardization of bone mineral densitometers. *Journal of Bone Mineral Research, 4,* 663–669.

MAZESS, R. B., HOWARD, S. B., BISEK, J. P. & HANSON, J., 1990. Dual-energy X-ray absorptiometry for total-body and regional bone mineral and soft-tissue composition. *American Journal of Clinical Nutrition, 51,* 1106–1112.

MCCLUNG, M. & ROBERTS, L., 1989. Correlation of bone density measurements by 153-Gd and X-ray dual photon absorptiometry. *Journal of Bone Mineral Research, 4,* S368.

NORD, R. H. & PAYNE, R. K., 1990. Standards for body composition calibration in DEXA. In *Current Research in Osteoporosis and Bone Mineral Measurement* ed. by E. F. J. Ring (British Institute of Radiology, London), pp. 27–28.

WANG, J., HEYMSFIELD, S. B., AULET, M., THORNTON, J. C. & PIERSON, R. N., 1989. Body fat from body density: underwater weighing vs. dual-photon absorptiometry. *American Journal of Physiology (Endocrinology & Metabolism), 256,* E829–834.

1992, *The British Journal of Radiology*, 65, 901–904

Single- versus dual-energy quantitative computed tomography for spinal densitometry in patients with rheumatoid arthritis

By Roland F. J. M. Laan, MD, *Leon J. Th. O. van Erning, MSc, PhD, *J. Albert M. Lemmens, MD, PhD, Levinus B. A. van de Putte, MD, PhD, *Sjef H. J. Ruijs, MD, PhD and Piet L. C. M. van Riel, MD, PhD

Departments of Rheumatology and *Radiology, University Hospital Nijmegen, PO Box 9101, 6500 HB Nijmegen, The Netherlands

(Received 25 October 1991 and in revised form 13 February 1992, accepted 26 March 1992)

Keywords: Single-energy quantitative computed tomography, Dual-energy quantitative computed tomography, Rheumatoid arthritis, Spinal fat content, Osteoporosis

Abstract. Lumbar bone mineral density was measured by both single- and dual-energy quantitative computed tomography in 109 patients with rheumatoid arthritis. The results were corrected for the age-related increase in vertebral fat content by converting them to percentages of expected densities, using sex and energy-level specific regression equations obtained in a normal reference population. The percentages of expected density are approximately 10% lower in the single- than in the dual-energy mode, both in the patients with and without prednisone therapy. This difference is statistically highly significant, and is positively correlated with the duration of the disease and with the degree of radiological joint destruction. The data suggest that the vertebral fat content may be increased in patients with rheumatoid arthritis, as a consequence of disease-dependent mechanisms.

Quantitative computed tomography (QCT) is one of the methods available for spinal densitometry, and can be performed in a single-energy or a dual-energy mode (SEQCT and DEQCT). The results of SEQCT are influenced by the presence of varying amounts of fatty yellow bone marrow within the vertebrae. Correction for this fat-associated error, as offered by DEQCT, is particularly important if densitometry is performed in patients with disorders that might be associated with changes in bone marrow composition (Genant et al, 1988). In the literature, changes in marrow composition, independent of changes in age or bone density, have been described for example in patients with Gaucher disease, or with anorexia nervosa, and after irradiation (Rosenthal et al, 1989; Mayo-Smith et al, 1989; Stevens et al, 1990).

Both SEQCT and DEQCT have been used to evaluate bone mineral density (BMD) in patients with rheumatoid arthritis (RA) (Compston et al, 1988; Laan et al, 1992). The possibility of changes in marrow composition has, however, not been explored in patients with this disease. If such changes exist, the relationship between SEQCT and DEQCT measurements would be different in patients with RA and in normal controls. We report here SEQCT and DEQCT data that were obtained simultaneously in the same patients, and which suggest that the vertebral fat content may be increased in patients with RA.

Patients and methods

Patient selection

The study was performed in 109 patients with rheumatoid arthritis (RA). They were initially selected for two different studies: a cross-sectional survey and a controlled clinical trial, designed to evaluate the influence of low-dose prednisone therapy on bone mineral density in the long term and short term, respectively. The results on these issues are reported elsewhere (Laan et al, 1991, 1992).

To select patients for the cross-sectional survey, the records of all classical or definite RA patients attending the outpatient clinic of a university rheumatology department during a 4-month period were reviewed. Patients on long-term ($\geqslant 6$ months) low-dose ($\leqslant$ 10 mg/day) prednisone therapy ($n = 30$) and patients who had never been treated with systemic corticosteroids, but who had been treated with at least two different disease modifying antirheumatic drugs (DMARD) ($n = 44$) were selected for this study. For the controlled clinical trial, patients with active, classical or definite RA, who were started on intramuscular gold salts, were selected ($n = 35$). Only baseline BMD measurements are used in the present report. At that time no patients were treated with corticosteroids.

Normal controls were not included in the study; instead, we used normal reference data published in the literature (Kalender et al, 1989). To check, however, for systematic errors in the analytical technique, 18 patients with primary osteoarthrosis (OA) were also measured. These patients all had long-standing primary arthrosis of either hip or knee, and were selected from a waiting

---

Address correspondence to Roland F. J. M. Laan, MD.

list for joint replacement. All OA patients had a primary degenerative disorder with no symptoms of inflammatory disease.

Bone densitometry

All measurements were performed with a Siemens Somatom DR3, according to methods described before (Kalender et al, 1987, 1989). This apparatus allows rapid kilovolt switching. The voltage is switched between 85 and 125 kV from pulse to pulse. The absorption data are thus obtained at two kV peak values in a single scan.

Patients are positioned with the lumbar spine over a calibration phantom, consisting of two stable plastics: a water-equivalent and a bone-equivalent standard containing 200 mg hydroxyapatite/ml. Scans are made through the midvertebral level with a slice thickness of 8 mm. While Kalender et al measured L1–L3 we used lumbar vertebrae L2–L4. Three images are reconstructed for each scan: at 125 kV, at 85 kV, and a dual-energy calcium density image after processing by material decomposition techniques. Regions of interest (ROI) are automatically defined for the trabecular part and the cortical rim of the vertebral body separately. The algorithm automatically traces the cortical ridge line and locates a ROI centre point. The inner and outer cortical contour are chosen at 60% between cortical ridge line and trabecular values. The contour for trabecular bone is fixed at 90% of the distance between the ROI centre point and the inner cortical contour. A more extensive description of this ROI definition procedure has been published (Klotz et al, 1989).

The SEQCT data presented in this study refer to the measurements with 85 kV. The DEQCT data are, of course, derived from the calcium density image. The patients with RA were measured over an approximately 3-year period. The patients with OA were measured not as a single cohort, but randomly interspersed with the other patients in the first year of the measurements.

The results are expressed as percentages of expected densities. For this purpose we used energy-level specific linear regression equations, derived from a population that has been measured on the same type of apparatus according to the same analytical techniques as described above, in Germany, Belgium and France. This reference population consists of 135 males and 139 females, who were scheduled for a computed tomography (CT) examination mainly for trauma or neurological disorders, and in whom no conditions were present that could affect bone mass. The exclusion criteria included amongst others spinal and hip fractures, inactivity, steroid use, and bone marrow disorders including anaemia. The normal reference data obtained show a reasonable agreement with normal data obtained in other countries with different apparatus and measurement protocols (Kalender et al, 1989).

Clinical parameters

In the RA patients the severity of the disease was assessed by the following parameters. The radiological destruction of hands and wrists was evaluated independently by two investigators using the Larsen method (Larsen et al, 1977). In case of disagreement, consensus was reached after re-evaluation of the radiographs. A total of 20 joints was examined in each patient (range from 0 to 100; a zero score indicates no radiological destruction).

The functional capacity of each patient was evaluated by the Dutch equivalent of the Stanford Health Assessment Questionnaire (HAQ), which has been validated for RA patients in our department (range from 0.00 to 3.00; a zero score indicates no functional impairment) (van der Heijde et al, 1990).

Statistical analysis

Differences in percentages of expected densities of identical ROIs in the same patient, between the single and dual energy modes, were analysed with a two-sided paired t-test. The use of paired instead of unpaired t-test is justified because SEQCT and DEQCT measurements, obtained in identical regions of interest, are compared in the same patient. Differences in proportions of patients with a negative and a positive difference between SEQCT and DEQCT are tested with the two-tailed Fisher's exact test for 2×2 tables. Pearson correlation coefficients are calculated as indicated in the text.

Results

The clinical data on the participating patients are summarized in Table I. The bone densitometry results are summarized in Table II. In the patients with OA the percentages of expected density are, as expected, quite similar in single- and in dual-energy modes. In the patients with RA, however, the SEQCT measurements are significantly lower than the DEQCT values, both for the trabecular and the cortical ROI. The difference between SEQCT and DEQCT in patients with RA is highly significant ($p < 0.0001$ by paired t-test), suggesting a consistent difference in the same direction in all patients. The difference between SEQCT and DEQCT was negative in 95 (87%) and positive in 14 (13%) patients with RA. In patients with OA the difference was negative in eight (44%) and positive in 10 (56%) patients. This difference in proportion of patients with positive and negative differences between patients with RA and OA is also statistically significant (two-tailed Fisher's exact test, $p = 0.0003$).

The difference between SEQCT and DEQCT is similar in patients with and without low-dose prednisone therapy (data not shown). The difference between the percentages of expected BMD as measured by SEQCT and by DEQCT, respectively, is significantly correlated with the duration of RA ($r = 0.38$, $p = 0.0001$), and with the Larsen score ($r = 0.27$, $p = 0.01$), but not with age or functional capacity at the time of the BMD measurement.

Discussion

Our results indicate that the relation between SEQCT and DEQCT is different in patients with RA than in a

Table I. Clinical data: mean (median, range) values

	Rheumatoid arthritis		Osteoarthrosis
	Females	Males	
Number	73	36	18
Age (years)	56.0 (58.0, 26.1–86.9)	60.6 (61.0, 32.6–87.3)	63.2 (61.5, 43.9–73.6)
Duration of RA (years)	10.9 (9.5, 0.3–54.0)	8.8 (7.8, 0.6–27.9)	Not applicable
Larsen score	32.8 (27.5, 0–87)	26.2 (26, 2–76)	Not applicable
Functional capacity	0.74 (0.65, 0.00–2.08)	0.53 (0.36, 0.00–1.74)	Not applicable

normal reference population reported in the literature. Several hypotheses could be put forward to explain this phenomenom.

At first one may argue that the differences between SEQCT and DEQCT in our RA patients could be either apparatus or procedure related. Although we used the same type of equipment that was used for the normal reference population, apparatus-related artefacts can never be completely ruled out. Our protocol differs from the one used in the normal reference population only in the fact that we measured lumbar vertebrae L3 and L4 instead of L1 to L3. Since no differences between SEQCT and DEQCT were seen in the patients with OA, we do not believe that either type of error could be very important . An alternative hypothesis would be that RA patients develop a different vertebral soft-tissue composition from normal controls during the course of their disease. In SEQCT the measured CT number represents the combined X-ray attenuation of all materials present in a defined volume element. DEQCT allows for the selective measurement of the density of material with a high atomic number (calcium). The differences between SEQCT and DEQCT percentages of expected density in RA patients must therefore be due to differences in the composition of the non-mineralized tissue components. Our results could be explained if more red bone marrow is replaced by fat in the RA patients than in the normal reference population reported in the literature. We have to emphasize, however, that this hypothesis should be tested by directly estimating the vertebral fat content in patients with RA by either CT or nuclear magnetic resonance imaging. To the best of our knowledge such data are not available at the moment.

One may argue that our explanation is less probable for the cortical than for the trabecular ROI. The cortical ROI definition is based, however, on adaptive thresholding and the resulting cortical width depends in part on the trabecular values adjacent to the cortical bone. A lower trabecular level results in a lower cortical value simply because the width will be increased. This effect will be even more pronounced if the subcortical fat content is increased.

The significant positive correlations between the duration of disease and the severity of the RA as judged by the Larsen score on the one hand and the difference between SEQCT and DEQCT percentages of expected densities on the other, further support the hypothesis that a disease-dependent mechanism is responsible for the observed phenomenon. It can not be excluded, however, that it might be caused by the therapies prescribed to these patients rather than by the disease itself. The fact that similiar results were obtained in patients

Table II. BMD measurements by single- and dual-energy QCT in a trabecular and a cortical region of interest (ROI)

		Single energy (85 kV)		Dual energy (85, 125 kV)		Difference: single − dual energy	
	n	Mean	(SD)	Mean	(SD)	Mean	95% CI limits
Trabecular ROI							
RA, females	73	85.4	(33.0)	94.6	(33.2)	−9.2	−11.1, −7.2
RA, males	36	99.0	(28.3)	110.2	(30.4)	−11.1	−15.0, −7.3
Osteoarthrosis	18	102.9	(21.5)	104.1	(21.5)	−1.2	−6.0, +3.6
Cortical ROI							
RA, females	73	92.4	(22.1)	101.0	(26.1)	−8.7	−9.9, −7.4
RA, males	36	99.2	(22.2)	105.7	(26.5)	−6.5	−8.5, −4.4
Osteoarthrosis	18	112.8	(16.4)	113.6	(16.4)	−0.8	−3.6, +2.0

with and without prednisone treatment seems to rule out the possibility that corticosteroid therapy is responsible for the observed differences between SEQCT and DEQCT measurements. This would be in accordance with the data of Mayo-Smith et al (1989) who found no differences in vertebral fat content between patients with Cushing disease and normal controls.

So far one study has been published on SEQCT data in patients with non-steroid-treated RA (Compston et al, 1988). The main finding of this study was an approximately 10% reduction in trabecular BMD compared with normal controls. Our data show that in patients with RA, BMD is underestimated in comparison with normal controls, even when the age-dependent increase in vertebral fat content is corrected for. The present study suggests that the reduction in trabecular BMD reported by Compston et al may in fact have been due to an increased vertebral fat content. We suggest that, certainly for research purposes, DEQCT instead of SEQCT should be used for accurate bone mineral densitometry in patients with RA.

Acknowledgments

The co-operation of the orthopaedic surgeons in the St Maarten Hospital in Nijmegen, who referred the patients with primary osteoarthrosis in this study, is gratefully acknowledged. This study was supported by a grant from the Dutch Ministry of Education (Program for the Stimulation of Health Research, SGO).

References

COMPSTON, J. E., CRAWLEY, E. O., EVANS, C. & O'SULLIVAN, M. M., 1988. Spinal trabecular bone mineral content in patients with non-steroid treated rheumatoid arthritis. *Annals of Rheumatic Diseases, 47,* 660–664.

GENANT, H. K., ETTINGER, B., HARRIS, S. T., BLOCK, J. E. & STEIGER, P., 1988. Quantitative computed tomography in assessment of osteoporosis. In *Osteoporosis. Etiology, Diagnosis, and Management,* ed. by B. L. Riggs and L. J. Melton III (Raven Press, New York), pp. 221–249.

KALENDER, W. A., KLOTZ, E. & SUESS, C., 1987. Vertebral bone mineral analysis: an integrated approach with CT. *Radiology, 164,* 419–423.

KALENDER, W. A., FELSENBERG, D., LOUIS, O., LOPEZ, P., KLOTZ, E., OSTEAUX, M. & FRAGA, J., 1989. Reference values for trabecular and cortical vertebral bone density in single and dual-energy quantitative computed tomography. *European Journal of Radiology, 9,* 75–80.

KLOTZ, E., KALENDER, W. A. & SANDOR, T., 1989. Automated definition and evaluation of anatomical ROI's for bone mineral determination by QCT. *IEEE Transaction on Medical Imaging, 8,* 371–376.

LAAN, R., VAN RIEL, P., VAN ERNING, L., LEMMENS, A., RUIJS, S. & VAN DE PUTTE, L., 1991. Short term effect of low dose prednisone therapy on bone mineral density in patients with rheumatoid arthritis. *Arthritis and Rheumatism, 34* (No. 9 Suppl.), A147.

LAAN, R. F. J. M., VAN RIEL, P. L. C. M., VAN ERNING, L. J. Th. O., LEMMENS, J. A. M., RUIJS, S. H. J. & VAN DE PUTTE, L. B. A., 1992. Vertebral osteoporosis in rheumatoid arthritis patients: effect of low dose prednisone therapy. *British Journal of Rheumatology, 31,* 91–96.

LARSEN, A., DALE, K. & EEK, M., 1977. Radiographic evaluation of rheumatoid arthritis and related conditions by standard reference films. *Acta Radiologica Diagnostica, 18,* 481–491.

MAYO-SMITH, W., ROSENTHAL, D. I., GOODSIT, M. M. & KLIBLANSKI, A., 1989. Intravertebral fat measurement with quantitative CT in patients with Cushing disease and anorexia nervosa. *Radiology, 170,* 835–838.

ROSENTHAL, D. I., MAYO-SMITH, W., GOODSIT, M. M., DOPPELT, S. & MANKIN, H. J., 1989. Bone and bone marrow changes in Gaucher disease: evaluation with quantitative CT. *Radiology, 170,* 143–146.

STEVENS, S. K., MOORE, S. G. & KAPLAN, I. D., 1990. Early and late bone-marrow changes after irradiation: MR evaluation. *American Journal of Roentgenology, 154,* 745–750.

VAN DER HEIJDE, D. M. F. M., VAN RIEL, P. L. C. M. & VAN DE PUTTE, L. B. A., 1990. Sensitivity of a Dutch Health Assessment Questionnaire in a trial comparing hydroxychloroquine and sulphasalazine. *Scandinavian Journal of Rheumatology, 19,* 407–412.

1992, *The British Journal of Radiology*, *65*, 905–909

Efficacy of low-dose iodine-131 ablation of post-operative thyroid remnants: a study of 69 cases

By S. F. Leung, MB, BS, FRCR, Martin W. M. Law, PhD and Stephen K. W. Ho, MPhil

Department of Clinical Oncology, Prince of Wales Hospital, Chinese University of Hong Kong, Hong Kong

(*Received 16 December 1991 and in revised form 14 April 1992, accepted 8 May 1992*)

Keywords: Thyroid cancer, Radioiodine

Abstract. Low-dose iodine-131 of mean activity 1117 MBq was used to ablate post-operative thyroid remnants in 69 patients with differentiated thyroid cancer. Successful ablation was defined as uptake of less than 1% at 48 h and absence of visible image on the post-ablation scan. Ablation by one dose was successful in 95% of patients after total or subtotal thyroidectomy, and 56% of patients after partial or hemithyroidectomy. All patients with uptake of 10% or less on the pre-ablation scan had successful ablation. The results are compared with other reports using low-dose radioiodine ablation and the significance of the findings discussed.

The literature contains discordant views regarding the efficacy of low-dose iodine-131 (^{131}I) ablation of post-operative thyroid remnants in patients with differentiated thyroid cancer, with ablation success rates ranging from 0 to 83% (McCowen et al, 1976; Kuni & Klingensmith, 1980; Siddiqui et al, 1981; DeGroot & Reilly, 1982; Ramacciotti et al, 1982; Snyder et al, 1983; Creutzig, 1987; Johansen et al, 1991). The interest in using a low activity such as 1110 MBq lies in the prospect of outpatient treatment, with attendant economy and convenience. A decreased risk of leukaemogenesis and extrathyroidal organ damage from lower whole-body radiation exposure is another theoretical advantage, and this may be of special concern in young patients with favourable prognostic factors (Pochin, 1961; Brincker et al, 1973). The present study of 69 cases serves to supplement clinical data to help clarify this controversial issue.

Materials amd methods

A retrospective study was undertaken on 69 patients with differentiated thyroid cancers who received ^{131}I ablation of post-surgical thyroid remnants at the Department of Clinical Oncology, Prince of Wales Hospital, Hong Kong between June 1984 and March 1991. Table I details patient characteristics. Patients with the following characteristics were excluded from the study: inoperable local disease; local and/or regional recurrent disease on presentation; known distant metastases on presentation; histologies other than papillary or follicular carcinoma; external radiotherapy given before post-ablation scan. Patients abstained from thyroxine for at least 4 weeks and iodine-containing food for 2 weeks before the diagnostic ^{131}I scan. Diuretics and thyroid-stimulating hormone (TSH) stimulation were not used.

48 h after the administration of a diagnostic dose of 37 MBq of ^{131}I, neck and whole-body images were scanned using a gamma camera with pinhole and parallel hole collimators, respectively. A gamma scintillation detector was used to measure the uptake and the uptake percentage was obtained by comparing the counts from the thyroid remnant with those from a known activity of ^{131}I in a tissue-equivalent neck phantom. Serum T4, T3 and TSH levels (replaced by free hormone and sTSH levels from December 1988) were routinely measured. All patients had TSH levels of above 58 μIU/ml (median level above upper measurable limit) at the time of the post-ablation scan.

Table I. Patient characteristics

	n
Histology	
papillary	54
follicular	15
Extrathyroidal extension	
yes	8
no	61
Surgery	
total/subtotal thyroidectomy	60
partial/hemi-thyroidectomy	9
Sex	
Male	14
Female	55
Age (years)	
< 40	30
⩾ 40	39

Address correspondence to Dr S. F. Leung, Department of Clinical Oncology, Prince of Wales Hospital, Hong Kong.

Table II. Ablation success as related to nature of operation

Nature of operation	No. of patients	Median % uptake pre-ablation scan (range)	% of patients with ≤ 1% uptake on post-ablation scan (ablation success rate)
Total/subtotal thyroidectomy	60	6.7% (1–49%)	57/60 = 95%
Partial/hemithyroidectomy	9	37% (3.4–57%)	5/9 = 56%
All operations	69	10% (1–57%)	62/69 = 90%

Patients with significant residual uptake, considered as uptake of greater than 1% of the ^{131}I diagnostic dose at 48 h or the presence of visible image on the scan, were given an ablation dose of about 1110 MBq (mean 1117 MBq, median 1132 MBq, range 762–1569 MBq). Patients were given replacement thyroid hormone after ablation and a follow-up scan performed 10 weeks later with the same pre-scan preparations and diagnostic ^{131}I activity. Patients with significant residual uptake, *i.e.* failed ablation by the first dose of ^{131}I, were given a higher dose of ^{131}I of about 3700 MBq and re-scanned by the same imaging technique until no significant uptake was present on the follow-up scans. Patients were then put on a suppressive dose of thyroxine.

Results

Ablation success as related to nature of operation

For patients who had total or subtotal thyroidectomies, a 95% success rate of ablation was achieved with one dose of ^{131}I of mean activity 1132 MBq. This is significantly higher than that for patients who had partial or hemithyroidectomies ($p < 0.001$, χ^2 test) (Table II).

Ablation success as related to pre-ablation uptake

Successful ablation by one dose of ^{131}I was achieved in all patients with pre-ablation uptake of 10% or less. Above this level, the failure rate was 20% (Table III).

Failures of first ablation dose

Seven patients had incomplete ablation after the first dose of ^{131}I. All of them had a visible image on the first post-ablation scan with a mean uptake of 4.7% (range 0.74–22%). They required an average of 3 (range 2–4) total doses of ^{131}I of mean cumulative activity 4334 MBq (range 762–5587 MBq) for complete ablation.

Table III. Correlation between pre- and post-ablation uptake

Uptake % in pre-ablation scan	No. of patients	Proportion of patients with ≤ 1% uptake on post-ablation scan
1%–10%	34	34/34 = 100%
>10%–20%	15	13/15 = 87%
>20%–30%	5	4/5 = 80%
>30%–40%	11	9/11 = 82%
>40%–50%	2	2/2 = 100%

The scan image

In the seven patients with a visible image on the first post-ablation scan, the site(s) of uptake was similar to that of the pre-ablation scan in all cases. No patient had new foci of uptake detected in the neck or other parts of the body on the post-ablation scan.

Disease status on follow-up

The median follow-up time of the patients, counting from the date of ablation, was 26 months. One patient had cervical nodal recurrence in the neck at 23 months. No visible image was present on her first post-ablation scan with an uptake of 0.2%. This was similar to the median post-ablation uptake of 0.2% in patients without recurrence in the neck.

Discussion

^{131}I ablation of post-surgical thyroid remnants in patients with differentiated thyroid cancer is widely practised despite controversies regarding its therapeutic impact. Arguments for a policy of achieving complete ablation include the existent, though low, mortality from differentiated cancer and its known response to radioiodine (Pochin, 1971), the multicentric nature of the tumour (Black et al, 1960), the known recurrence of tumour in remaining normal thyroid tissue (Mazzaferri & Young, 1981), the known association between differentiated and anaplastic cancer (Leeper, 1973), the possibility of occult cervical metastases showing up after the ablation dose (Henk et al, 1972; Coakley et al, 1980), the facilitation of follow-up assessment (Beierwaltes, 1978; Pochin, 1971) and improved survival in certain subsets of patients (Varma et al, 1970; Mazzaferri et al, 1977; Beierwaltes, 1978; Young et al, 1980). However, conclusions from some retrospective studies suffer from the drawback of lack of appropriate control groups balanced for factors like age, sex, initial tumour extent and concurrent treatment by hormone and/or external radiotherapy. There still remains uncertainty whether ablation of minimal thyroid remnants contributes independently to improve survival in the setting of present-day follow-up protocols using tumour markers and hormone suppression, especially in young patients with papillary cancers who are generally regarded to have a good prognosis (Halnan, 1966; Byar et al, 1979; Samaan et al, 1983; Simpson, 1990). Given such uncertainty and the effectiveness of low-dose ablation by the criteria in our study, we support the use of a low activity

Table IV. Comparison of patient series using low-dose ^{131}I for ablation

Study group reference	No. of patients	Pre-scan preparation	Diagnostic dose (MBq)	Ablation dose (MBq)	Timing of post-ablation scan (months)	Criteria of succesful ablation	Success rate after first ablation dose
McCowen et al (1976)	36	Stop T4 6 weeks Stop T3 2 weeks	37–74	925–1099	3	-ve scan, PB^{131}I[a] conversion rate < 0.005%/l or whole-body retention < 3% in 7 days	21/36 = 58%
Kuni & Klingensmith (1980)	13	Stop T4 3–12 months Stop T3 1–6 weeks	185	925–1106	3–24	No visible image	0/13 = 0%
Siddiqui et al (1981)	10	Stop T4 4 weeks Stop T3 2 weeks Give TSH	111	1073–1110	9–15	No visible image	1/10 = 10%
DeGroot & Reilly (1982)	18	Stop T3 3 weeks	37	1110	3–12	No visible image, < 0.2% uptake	15/18 = 83%
Ramacciotti et al (1982)	20	Stop T4 6 weeks Stop T3 2 weeks	37–56	1110	6	Uptake < twice background level	5/20 = 25%
Snyder et al (1983)	69	Stop T4 4 weeks Stop T3 2 weeks	37	1084 ± 56	3–12	Uptake < 1%	56/69 = 81%
Creutzig (1987)	10	3 months post-op	5550*	1110	3	< 1% uptake on Day 7	7/10 = 70%
Johansen et al (1991)	36	Stop T4 ± give TSH	1058*	1058	3–4	No pathological uptake	21/36 = 58%
Present study	69	Stop T4 4 weeks Stop T3 2 weeks Low-iodine diet	37	1117	2.5	No visible image and uptake < 1%	62/69 = 90%

*The therapeutic dose also served as the post-ablation diagnostic dose.

[a] Protein-bound iodine-131.

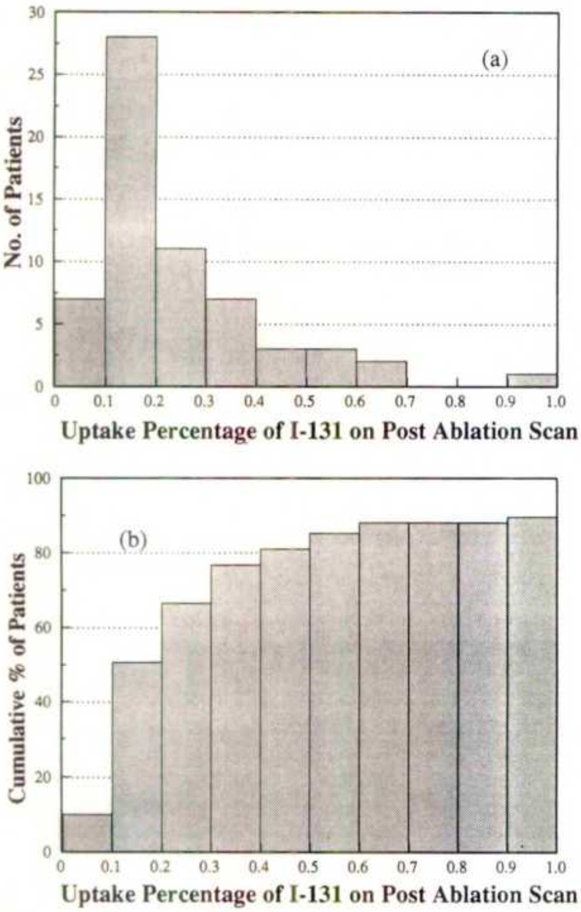

Figure 1. (a) Distribution of patients by uptake percentages on the first post-ablation scan. (b) Cumulative % of patients with increasing uptake levels (up to 1%) on the post-ablation scan. This corresponds to the "success" rates of ablation defined at different post-ablation uptake levels.

of ^{131}I such as 1110 MBq for ablation of small post-operative thyroid remnants. This has the theoretical advantage of minimizing whole-body radiation exposure and hence lowering the potential risk of leukaemogenesis, and the practical advantage of economy and convenience of outpatient treatment in many countries. It should be mentioned, however, that in patients with known distant metastases, it would be more appropriate to use a higher activity such as 3700 MBq or above.

Table IV shows that there is a great variation in the "success" rates of low-dose radioiodine ablation in different reports. High success rates were obtained in reports using similar criteria of successful ablation and diagnostic ^{131}I doses as in the present study (DeGroot & Reilly, 1982; Snyder et al, 1983). The lowest success rates were found in Kuni's and Siddiqui's series, where higher diagnostic doses were used. More stringent criteria for complete ablation were implied, since it is known that higher diagnostic doses increase the visual detection of residual thyroid tissue (Waxman et al, 1981). It would be interesting but impossible (owing to differences in details of the preparation procedure for scanning and instrument design) to interpret our data using the criteria in other reports in an exactly comparable way. However, it is evident that a range of different "success" rates could be obtained by applying different cut-off points for definition of "successful" ablation to our data, as shown in Fig. 1. Our success rate would still be remarkably high at 75% even if successful ablations was defined at an uptake level as low as 0.3%.

Different criteria for definition of successful ablation is a probable explanation for the different results in different reports. This may reflect different opinions regarding the importance of complete ablation and the aggressiveness the clinician should adopt for this purpose. In other words the controversy of the effectiveness of low-dose ablation may in part be a controversy of the desired completeness of ablation. While the criteria used in the present study might be less stringent than those used in some reports, there is lack of evidence to support the effort of pursuing more vigorous ablation with more stringent criteria. The probability of tumour recurrence in the neck in our patients was not related to the exact amount of post-ablation uptake. The attempt to ablate very minute amounts of thyroid remnants may involve the delivery of sub-tumourocidal doses and higher whole-body radiation exposure (Ramanna et al, 1982). Moreover, the estimation of the dose received by tiny thyroid remnants from a given ^{131}I activity involves assumptions that may make correlation with treatment outcome difficult (Snyder et al, 1983). In view of the above-mentioned observations and considerations, we feel that it is practical to employ the clinical practice for successful ablation adopted in our study, which is readily fulfilled by low-dose ^{131}I ablation.

References

BEIERWALTES, W. H., 1978. The treatment of thyroidcarcinoma with radioactive iodine. *Seminars in Nuclear Medicine, 8*, 79–94.

BLACK, B. M., KIRK, T. A., WOOLNER, L. B., 1960. Multicentricity of papillary adenocarcinoma of the thyroid. Influence of treatment. *Journal of Clinical Endocrinology and Metabolism, 22*, 130–135.

BRINCKER, H., HANSEN, H. S. & ANDERSEN, A. P., 1973. Induction of leukaemia by ^{131}I treatment of thyroid carcinoma. *British Journal of Cancer, 28*, 232–237.

BYAR, D. P., SYLVAN, B. G., PIERREDOR, W., JACQUES, C., HENRIETTE, A. V. G., MARCEL, M., RICHARD, J. S., MARTINE, V. G., 1979. A prognostic index for thyroid carcinoma ... an EORTC study. *European Journal of Cancer, 15*, 1033–1042.

COAKLEY, A. J., PAGE, C. J. & CROFT, D., 1980. Scanning dose and detection of thyroid metastases (Letter). *Journal of Nuclear Medicine, 21*, 803.

CREUTZIG, H., 1987. High- or low-dose radioiodine ablation of thyroid remnants. *European Journal of Nuclear Medicine, 12*, 500–502.

DEGROOT, J. & REILLY, M., 1982. Comparison of 30 and 50 mCi doses of iodine-131 for thyroid ablation. *Annals of Internal Medicine, 96*, 51–53.

HALNAN, K. E., 1966. Influence of age and sex on thyroid cancer. *Cancer, 19,* 1534–1536.

HENK, J. M., KIRKMAN, S. & OWEN, G. M., 1972. Whole-body scanning of I-131 therapy in the management of thyroid carcinoma. *British Journal of Radiology, 45,* 369–376.

JOHANSEN, K., WOODHOUSE, N. J. Y. & ODUGBESAN, O., 1991. Comparison of 1073 and 3700 MBq iodine-131 in postoperative ablation of residual thyroid tissue in patients with differentiated thyroid cancer. *Journal of Nuclear Medicine, 32,* 252–254.

KUNI, C. C. & KLINGENSMITH, W. C., 1980. Failure of low doses of ^{131}I to ablate residual thyroid tissue following surgery for thyroid cancer. *Radiology, 137,* 773–774.

LEEPER, R. D., 1973. The effect of ^{131}I therapy on survival of patients with metastatic papillary or follicular thyroid carcinoma. *Journal of Clinical Endocrinology and Metabolism, 36,* 1143–1152.

MAZZAFERRI, E. L. & YOUNG, R. L., 1981. Papillary thyroid cancer. A 10-year follow-up. *American Journal of Medicine, 70,* 511.

MCCOWEN, K. D., ADLER, R. A., GHAED, N., VERDON, T. & HOFELDT, F. D., 1976. Low dose radioiodide thyroid ablation in post surgical patients with thyroid cancer. *American Journal of Medicine, 61,* 52–58.

POCHIN, E. E., 1961. The occurrence of leukemia following radioiodine therapy. In *Advances in Thyroid Research,* ed. by R. Pitt-Rivers (Pergamon Press, Oxford), pp. 392–397.

POCHIN, E. E., 1971. Radioiodine therapy of thyroid cancer. *Seminars in Nuclear Medicine, 1,* 503–515.

RAMACCIOTTI, C., PRETORIUS, H. T., LINE, B. R., GOLDMAN, J. M. & ROBBINS, J., 1982. Ablation of non-malignant thyroid remnants with low doses of radioactive iodine: concise communication. *Journal of Nuclear Medicine, 23,* 483–489.

RAMANNA, L., WAXMAN, A., CHAPMAN, N., BRACHMAN, M., TANASESCU, D., BERMAN, D., CHAMPMAN, D., BRAUNSTEIN, G., 1982. Treatment rationale in thyroid carcinoma: Effect of scan dose. *Journal of Nuclear Medicine 23,* p. 43. (abstract of Proceedings of 29th Annual Meeting of the Society of Nuclear Medicine).

SAMAAN, N. A., MAHESHWARI, Y. K., NADER, S., HILL, C. S., JR., SCHULTZ, P. N., HAYNIE, T. P., HICKEY, R. C., CLARK, R. L., GOEPFERT, H., IBANEZ, M. L., LITTON, C. E., 1983. Impact of therapy for differentiated carcinoma of the thyroid: an analysis of 706 cases. *Journal of Clinical Endocrinology and Metabolism, 56,* 1131–1138.

SIDDIQUI, A. R., EDMONSON, J., WELLMAN, H. H., HAMAKER, R. C., LINGEMAN, R. E., PARK, H. M. & JOHNSTON, C. C., 1981. Feasibility of low doses of ^{131}I for thyroid ablation in postsurgical patients with thyroid carcinoma. *Clinical Nuclear Medicine, 6,* 158–161.

SIMPSON, W. J., 1990. Radioiodine and radiotherapy in the management of thyroid cancers. *Otolaryngological Clinics of North America,* **23,** 509–521.

SNYDER, J., GORMAN, C. & SCANLON, P., 1983. Thyroid remnant ablation: questionable pursuit of an ill-defined goal. *Journal of Nuclear Medicine, 24,* 659–665.

VARMA, V. M., BEIERWALTES, W. H., NOFAL, M. M., NISHIYAMA, R. H. & KOPP, J. E., 1970. Treatment of thyroid cancer: death rates after surgery and after surgery followed by sodium iodide I-131. *Journal of the American Medical Association, 214,* 1437–1442.

WAXMAN, A., RAMANNA, L., CHAPMAN, N., CHAPMAN, D., BRAUNSTEIN, G. & BERMAN, D., 1981. The significance of I-131 scan dose in patients with thyroid cancer: determination of ablation. *Journal of Nuclear Medicine 22,* 861–865.

YOUNG, R. L., MAZZAFERRI, E. L., RAHE, A. J. & DORFMAN, S. G., 1980. Pure follicular thyroid carcinoma: impact of therapy in 214 patients. *Journal of Nuclear Medicine 21,* 733–737.

1992, *The British Journal of Radiology*, *65*, 910–917

Functional changes in the pig kidney following irradiation with fractionated doses of fast neutrons (42 $\mathrm{MeV}_{d\rightarrow Be}$)

By M. E. C. Robbins, PhD, *D. W. H. Barnes, MD, J. W. Hopewell, PhD, *J. F. Knowles, PhD, M. Rezvani, PhD and *J. M. Sansom

CRC Normal Tissue Radiobiology Research Group, Research Institute (University of Oxford), Churchill Hospital, Oxford OX3 7LJ, and *MRC Radiobiology Unit, Chilton, Didcot, Oxfordshire OX11 0RD, UK

(*Received 17 October 1991 and in revised form 27 March 1992, accepted 8 May 1992*)

Keywords: Fast neutrons, Pig kidney, Glomerular filtration rate, Effective renal plasma flow, Kidney weight

Abstract. The right kidney of female Large White pigs, approximately 14 weeks old, was irradiated with fractionated doses of fast neutrons (42 $\mathrm{MeV}_{d\rightarrow Be}$). The total doses used were 6.6–9.2 Gy. Changes in kidney function, assessed as the functional index (FI, where FI = irradiated kidney function/unirradiated kidney function) or as individual kidney glomerular filtration rate (GFR) and effective renal plasma flow (ERPF), were serially determined up to 104 weeks after irradiation using $^{99}\mathrm{Tc^{m}}$-DTPA and ^{131}I-hippuran renography. The animals were then euthanized, the kidneys removed and weighed. A dose-dependent reduction in FI was seen within 13 weeks of irradiation. Measuring individual kidney function revealed a hyperaemic response in both irradiated and unirradiated kidneys 4 weeks after irradiation. This was followed by a dose-dependent reduction in irradiated kidney GFR and particularly ERPF. The ED_{50} value for the impairment in ERPF, assessed as the percentage of irradiated kidneys exhibiting a $\geqslant 50\%$ reduction in ERPF, was significantly lower than that for GFR, *i.e.* 7.20±0.10 Gy compared with 8.44±0.07 Gy ($p < 0.001$). A dose-related reduction in irradiated kidney weight was also observed. These fast neutron-induced changes in renal function and weight are qualitatively similar to those observed following photon irradiation of the pig kidney.

It is well recognized that radiotherapy for abdominal tumours is frequently limited by the adverse reactions of the normal tissues included within the treatment volume. Of these, the kidney is particularly radiosensitive. The radiation tolerance of the human kidney was defined by Kunkler et al (1952), who established that a total dose of 23 Gy, given over 5 weeks, carried with it a high risk of renal damage. Experimental studies of the radiation response of the kidney in a wide variety of systems have confirmed the pronounced radiosensitivity of the kidney (for a review, see Robbins & Hopewell, 1991). The kidney can be considered to be a late-responding normal tissue which exhibits a considerable capacity for repair of sublethal irradiation damage; the size of the dose per fraction of photon irradiation markedly influences renal radiation tolerance (Stewart et al, 1984; Williams & Denekamp, 1984).

Pronounced changes in renal function, assessed in terms of glomerular filtration rate (GFR) and/or effective renal plasma flow (ERPF) have also been observed within weeks of irradiation. An initial hyperaemic response has been reported experimentally (Mendelsohn & Caceres, 1953; Raulston et al, 1978), and also clinically (Avioli et al, 1963; Textor et al, 1987). This initial response is followed by a progressive decline in both GFR and ERPF (Robbins et al, 1985; Stewart et al, 1988). These studies have used photon irradiation. In contrast, there appear to be little data on the effects of neutron irradiation on GFR and ERPF. In a previous report (Robbins et al, 1991a) the response of the pig kidney to fractionated doses of fast neutrons (42 $\mathrm{MeV}_{d\rightarrow Be}$) was compared with that observed after photon irradiation. A major conclusion of th was that there was no influence of fraction overall treatment time on the response of the pig k to fast neutron irradiation. During the course of th investigation individual kidney GFR and ERPF were routinely determined using $^{99}\mathrm{Tc^{m}}$-diethylene-triamine-pentaacetic acid (DTPA) and ^{131}I-hippuran renography, respectively. The lack of any dose fractionation effect with fast neutron irradiation gave an opportunity to consider, in detail, the dose–effect relationships for neutron irradiation alone in terms of both GFR and ERPF, with a relatively large number of animals per dose group. In addition, dose-related effects of fast neutron irradiation on kidney weight were investigated, since a dose-related reduction in kidney weight has been observed following photon irradiation (Jordan et al, 1978; Michalowski, 1986). The determination of fast neutron-induced changes in both renal function and renal weight also enabled the possible relationship between these two parameters to be evaluated.

The pig and man are unique in possessing a multipapillate multipyrimidal kidney (Sperber, 1944); moreover, there are pronounced similarities in renal physiology between the two species (Farebrother et al, 1975; Terris, 1986). These similarities indicate that data on the response of the pig kidney to neutron irradiation may be of direct clinical relevance.

Materials and methods

In this study a total of 37 female pigs of the Large White strain were irradiated with fast neutrons. The animals were brought into the animal house when approximately 12 weeks of age (20–25 kg body weight) and were allowed an acclimatization period of at least 2 weeks before any experimental procedures were undertaken. All procedures were carried out under anaesthesia using a 2% halothane, ~ 70% oxygen, and ~ 30% nitrous oxide gas mixture (Dickinson & Hubbard, 1990).

Before irradiation the position of each kidney was determined by intravenous pyelography and the position of the right kidney included in an 8 cm × 12 cm field tattooed on the overlying skin. Neutron irradiations were carried out using the Variable Energy Cyclotron (VEC) at the Atomic Energy Research Establishment (AERE). The physical characteristics of this beam have been described previously (Goodhead et al, 1977). Neutrons were produced by the bombardment of a 2 mm thick gold-backed beryllium target with 42 MeV deuterons. The target-to-skin distance was 150 cm, giving a dose rate of 0.45–0.5 Gy/min at the midline of the kidney. The right kidney was irradiated with total doses given as 6 or 12 fractions in 18 days or as 6, 12 or 30 fractions in 39 days. For each fractionation schedule animals were irradiated at four dose levels; the total doses were 6.6, 7.4, 8.2 and 9.2 Gy, with 3–13 animals in each dose group.

Prior to irradiation, and at regular intervals from 4 to [illegible] weeks after irradiation, renal function was deter[illegible] by ^{99}Tc^{m}-DTPA and ^{131}I-hippuran renography. [illegible] techniques employed have been reported in detail [illegible] (Robbins et al, 1984) and will only be described briefly. Three matched 5.0 cm diameter NaI scintillation detectors were used, one positioned over each kidney, the other over the heart. The detectors were connected to a multichannel analyser with windows set to record activity in the photopeak regions for ^{99}Tc^{m} and ^{131}I. The analyser was operated in the multiscaling mode, with counts from each tracer from the three detectors integrated over 20 s intervals for the duration of each renogram.

The tracers used were ^{99}Tc^{m}-labelled human serum albumin (HSA) (Byk-Mallincrodkt), ^{131}I-HSA (Cis UK), ^{99}Tc^{m}-DTPA and ^{131}I-hippuran (Byk-Mallincrodkt). Studies were performed using the following standard protocol:

(1) ^{99}Tc^{m}-HSA (2.2–22.2 MBq, depending on the size of the pig) was injected into an ear vein via an indwelling butterfly cannula. Five minutes were allowed for the tracer to equilibrate within the blood, then activity was recorded for 2 min over each detector. These data were used to determine the ^{99}Tc^{m} subtraction factor for each kidney (Robbins et al, 1985).

(2) ^{131}I-HSA (0.2–1.48 MBq) was then injected into the same ear vein. Five minutes later the activity was recorded over each detector for 2 min to determine the ^{131}I subtraction factor. A blood sample (2 ml) was then withdrawn from the contralateral ear vein via an indwelling butterfly cannula.

(3) A solution containing ^{99}Tc^{m}-DTPA (37–296 MBq) and ^{131}I-hippuran (1.85–12.95 MBq) was injected via an ear vein and the time-related changes in activity over both kidneys and the heart were recorded for a period of up to 40 min.

(4) Blood samples were taken at 5, 10, 15, 20, 40, 60 and 120 min intervals after injection of the isotope cocktail. Aliquots (1 ml) of plasma were counted in a well-type NaI detector connected to a multichannel analyser. The activity of both nuclides was determined, and GFR and ERPF calculated from the plasma disappearance curves of ^{99}Tc^{m}-DTPA and ^{131}I-hippuran, respectively (Robbins, 1984).

From the results of the renograms and measurements of tracer activity in plasma samples the following parameters were calculated:

(1) *Individual kidney function*. This was assessed by determining the uptake function for each tracer in each kidney (Robbins et al, 1985). Thus the percentage contribution of K_L ERPF to total ERPF =

$$\frac{\text{Uptake function of } K_L \text{ for } ^{131}\text{I-hippuran}}{\text{Uptake function of } K_L + K_R \text{ for } ^{131}\text{I-hippuran}} \times 100\%$$

Similarly, the uptake constants for ^{99}Tc^{m}-DTPA were determined to obtain values for the percentage contribution of each kidney to the total GFR. Determination of the total GFR and ERPF was from the disappearance curves obtained from the serial blood samples. This enabled the evaluation of absolute values of individual kidney GFR and ERPF (Robbins, 1984; Robbins et al, 1984).

(2) *Functional index*. The functional index (FI) was determined from the ratio of the uptake function of the irradiated kidney to that of the contralateral unirradiated kidney in the same animal. Irradiated kidneys in which the FI was < 30% were defined as having "no significant function" (NF) (Robbins et al, 1991a).

104 weeks after irradiation the pigs were killed by means of nitrous oxide asphyxiation. Both the irradiated right kidneys and the unirradiated left kidneys were removed, weighed and perfusion-fixed with a mixture of 1% acetic acid in 10% formal saline. Four animals were lost from the study prematurely (three at 52 weeks and one at 65 weeks after irradiation). Since the kidney function and weight of these four irradiated kidneys were not significantly different from those seen in animals which were sacrificed 104 weeks after irradiation, they were included in the analysis. Results for individual kidney GFR and ERPF were compared with those previously observed in age-matched historical controls (Robbins et al, 1989a). Results were expressed as mean ± SE.

Results

Functional index

The time-related changes in the FI in pigs receiving total doses of 6.6–9.2 Gy of fast neutrons (42 MeV$_{d \rightarrow Be}$) to the right kidney are shown in Fig. 1. The pattern of response was similar in terms of either GFR or ERPF; FI values were reduced within 4 weeks of irradiation, and by 13 weeks this decrease appeared to be dose-

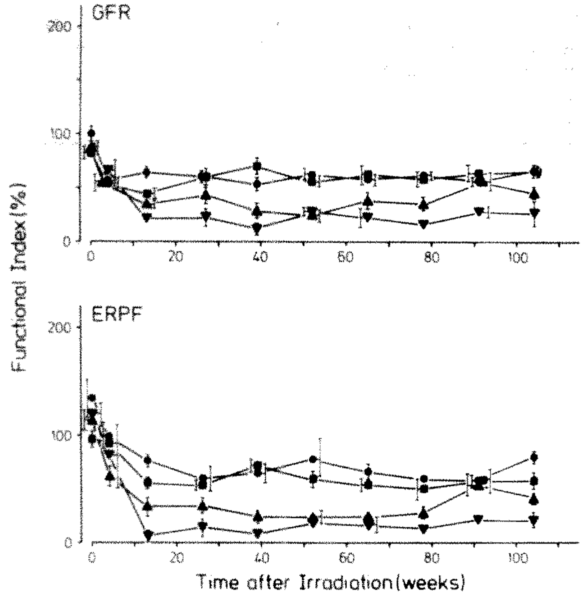

Figure 1. Time-related changes in the mean functional index (upper panel GFR, lower panel ERPF) after irradiation of the right kidney of pigs with fast neutrons (42 $\mathrm{MeV}_{\mathrm{d}\rightarrow\mathrm{Be}}$). ●, 6.6 Gy; ■, 7.4 Gy; ▲, 8.2 Gy; ▼, 9.2 Gy. Error bars, ±SE.

related. FI values remained essentially unchanged between 13 and 104 weeks after irradiation. The dose dependence of these radiation-induced changes in FI was demonstrated by examining the mean values of the FI, in terms of both GFR and ERPF, determined between 13 and 104 weeks after irradiation (Fig. 2). The mean FI values for both GFR and ERPF were well correlated with the radiation dose, $r = -0.99$ and -0.95, respectively ($p \leqslant 0.05$). Moreover, the slopes of the regression lines fitted to the data for GFR and ERPF were not significantly different from one another, *i.e.* -15.76 ± 3.57 and -20.94 ± 2.26, respectively ($p >$ 0.1).

Dose–effect curves were also constructed by assessing, at each dose level, the percentage of renograms performed between 13 and 104 weeks after irradiation in which the FI was < 30%. The dose–response curves for the impairment in FI were fitted by probit analysis (Fig. 3). The doses associated with the 50% level of effect, the ED_{50} value, for GFR and ERPF were determined. The ED_{50} value in terms of ERPF was 8.22 ± 0.05 Gy, a value significantly less ($p < 0.001$) than the value of 8.52 ± 0.06 Gy determined in terms of GFR.

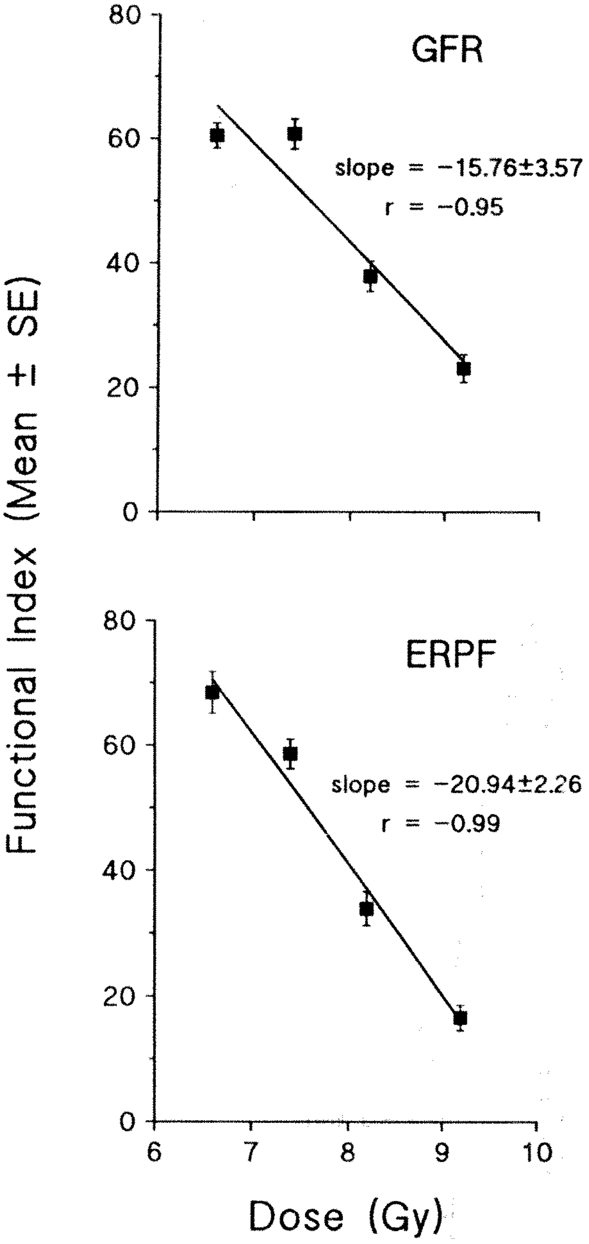

Figure 2. Dose-related reduction in the mean functional index (upper panel GFR, lower panel ERPF) assessed on the basis of renograms carried out 13–104 weeks after irradiation with 6.6–9.2 Gy of fast neutrons (42 $\mathrm{MeV}_{\mathrm{d}\rightarrow\mathrm{Be}}$). Error bars represent ±SE.

Individual kidney function

To illustrate the effects of fast neutrons on individual kidney function, the GFR and ERPF values of both the irradiated and the contralateral unirradiated kidney were plotted as a percentage of age-matched controls (Fig. 4). Four weeks after irradiation, irradiated kidney GFR was slightly increased compared with control values; this was followed by a pronounced dose-related reduction in GFR, with minimal values being observed between 26 and 52 weeks after irradiation. Irradiated kidney GFR then remained essentially unchanged up to the end of the experimental period. The contralateral unirradiated kidney also exhibited a hyperaemic response 4 weeks after irradiation, but the increase in GFR was considerably greater than that seen in the

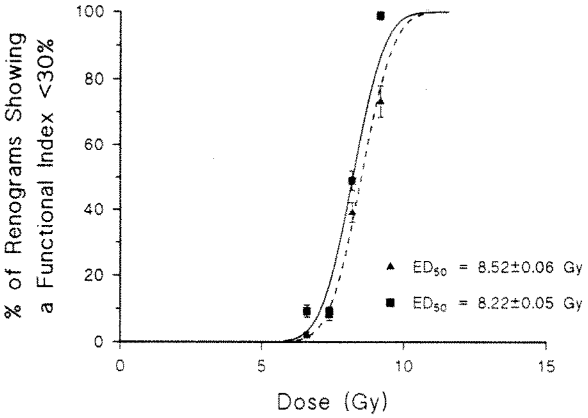

Figure 3. Dose-related changes in the percentage incidence of renograms indicating an FI of < 30% 13–104 weeks after irradiation of the right kidney with fast neutrons (42 $\mathrm{MeV}_{d\rightarrow Be}$). ▲, GFR; ■, ERPF. Error bars represent ±SE.

Table I. Mean values (±SE) of GFR and ERPF (percentage of age-matched controls) measured between 13 and 104 weeks after irradiation of the right kidney alone with total doses of fast neutrons (42 $\mathrm{MeV}_{d\rightarrow Be}$). The numbers of measurements in each group are given in parentheses. Errors indicate ±SE.

	Functional parameter		
Total dose (Gy)	GFR	ERPF	*p* value
6.6	88.27±3.63 (66)	55.32±2.59 (69)	< 0.001
7.4	81.63±4.14 (67)	52.99±3.54 (67)	< 0.001
8.2	60.11±3.65 (55)	33.81±2.40 (60)	< 0.001
9.2	32.41±3.90 (20)	19.10±2.98 (20)	< 0.01

irradiated kidney. GFR increased two- to three-fold compared with age-matched controls. GFR then declined, but generally remained above control values up to 91 weeks after irradiation, indicating functional compensation for the reduction in GFR observed in the irradiated kidney. However, at 104 weeks after irradiation, GFR values in the unirradiated kidney were similar to those of controls. In contrast to the dose-related changes seen in the irradiated kidney, the changes in unirradiated kidney GFR appeared to be independent of dose. The response of the irradiated kidney, in terms of ERPF, was similar to that described for GFR, although the severity of the dose-related reduction in ERPF appeared greater than that noted for GFR (Fig. 4b). Indeed, comparing the mean values of ERPF measured 13–104 weeks after irradiation, for each dose group, with those for GFR indicated a significantly greater reduction ($p \leqslant 0.01$) in terms of ERPF following fast neutron irradiation (Table I).

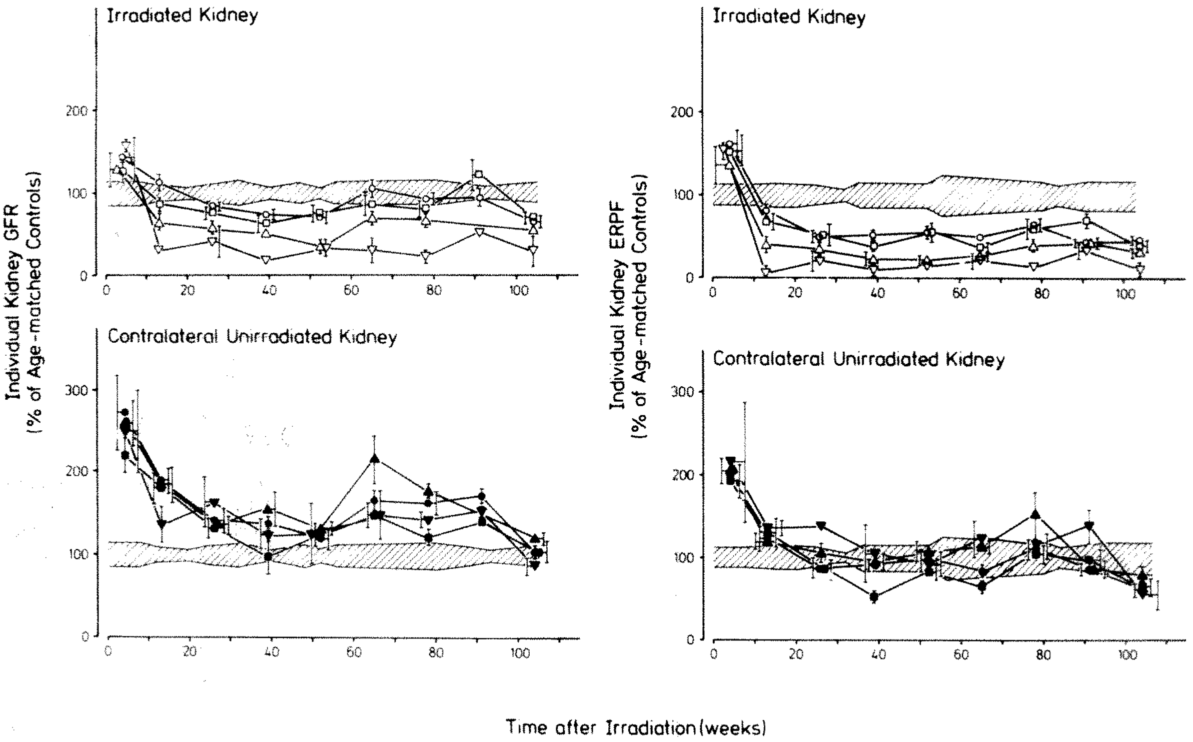

Figure 4. Time-related changes in mean (a) GFR and (b) ERPF in individual kidneys in pigs irradiated with fast neutrons (42 $\mathrm{MeV}_{d\rightarrow Be}$) to the right kidney alone. Open symbols represent the irradiated kidney; for key to symbols see Fig. 1. The hatched area represents the 95% confidence limits of age-matched control animals. Error bars represent ±SE.

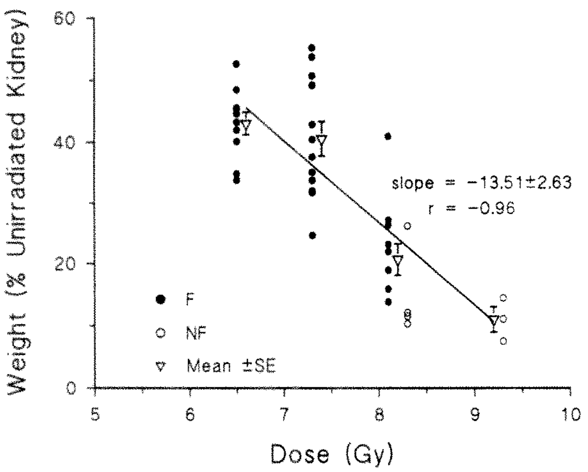

Figure 5. Dose-related changes in irradiated kidney weight, expressed as a percentage of the contralateral unirradiated organ, following fast neutron (42 $\text{MeV}_{d \rightarrow Be}$) irradiation in pigs.

The contralateral unirradiated kidney ERPF was markedly increased 4 weeks after irradiation; values then declined such that by 26–39 weeks after irradiation, unirradiated kidney ERPF levels were similar to those observed in age-matched controls. There was little further change in the parameter up to 104 weeks after irradiation. There was no compensatory increase in ERPF observed in the unirradiated kidney (Fig. 4b).

The dose-dependence of the fast neutron-induced changes in irradiated kidney GFR and ERPF was further demonstrated by examining the mean values of these parameters between 13 and 104 weeks after irradiation. Both the mean GFR and ERPF in the irradiated kidneys were well correlated with the radiation dose, $r = \geqslant -0.97$ ($p < 0.001$). The slope of the dose–response curve for GFR was significantly steeper than that for ERPF ($p < 0.01$). Dose–effect curves were also constructed by assessing, at each dose level, the percentage of renal function tests performed between 13 and 104 weeks after irradiation in which the irradiated kidney exhibited a ⩾ 50% reduction in GFR or ERPF. The ED_{50} value for the impairment in ERPF was significantly lower than that for GFR, *i.e.* 7.20 ± 0.10 Gy as compared with 8.44 ± 0.07 Gy ($p < 0.001$).

Kidney weight

The changes in the weight of the irradiated kidney, expressed as a percentage of the contralateral unirradiated kidney, and plotted as a function of the total dose of fast neutrons, are illustrated in Fig. 5. Kidney weight was well correlated with neutron dose ($r = 0.96$, $p < 0.01$). It is of interest to note that even after doses of 6.6 and 7.4 Gy of fast neutrons, when all kidneys were defined as functioning (FI > 30%), the weights of the irradiated kidneys were < 60% of the contralateral organ. With higher doses, NF kidneys were evident; these were usually associated with a relative weight of < 15%.

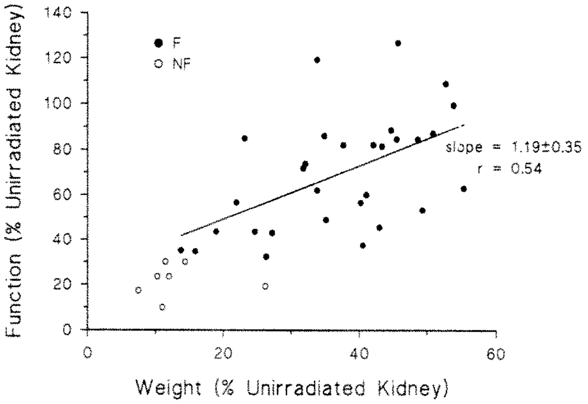

Figure 6. Plot of functional index against the weight of the irradiated kidney, expressed as a percentage of the contralateral unirradiated kidney.

In order to investigate the relationship between organ weight and functional index, the FI, in terms of ERPF, was plotted against irradiated kidney weight (expressed as a percentage of the contralateral organ) (Fig. 6). A regression line of slope 1.19 ± 0.35 ($p = 0.002$) could be fitted to the data for functioning irradiated kidneys (FI > 30%), indicating a positive relationship between function and organ weight. The NF unirradiated kidneys were excluded from this analysis.

Discussion

The present findings indicate that total doses of between 6.6 and 9.2 Gy of fast neutrons (42 $\text{MeV}_{d \rightarrow Be}$), to the right kidney of approximately 14-week-old pigs, caused pronounced changes in renal function within several weeks of irradiation. Evaluating changes in kidney function in terms of the FI suggested a decrease in function, in terms of both GFR and ERPF, within 4 weeks of irradiation; by 13 weeks, this decrease was dose-related. FI values then remained essentially unchanged up to the end of the experimental period. This pattern of response was similar to that seen following irradiation of the right kidney of either 14-week-old (Robbins et al, 1985) or approximately 45-week-old pigs (Robbins et al, 1989a) with single doses of photons.

A major limitation of expressing the function of the irradiated kidney as an FI is that the comparison is between a damaged irradiated kidney and an apparently normal unirradiated kidney; the result obtained will be somewhat biased against the irradiated kidney owing to the compensatory response of the unirradiated kidney. It is therefore necessary to consider changes in individual kidney GFR and ERPF.

Within 4 weeks of fast neutron (42 $\text{MeV}_{d \rightarrow Be}$) irradiation, irradiated kidney GFR and ERPF appeared greater than values observed in age-matched controls, suggesting a hyperaemic response. It is of interest to note that the contralateral unirradiated kidney exhibited a similar but even more marked increase in renal haemodynamics. This accounted for the decrease in the FI seen at this time, since the increase in irradiated kidney GFR and ERPF was less than that seen in the contralateral unirradiated organ. Evidence of a hyperaemic response has also been observed following fast neutron (50 MeV$_{d \rightarrow Be}$) irradiation of a single hypertrophied kidney in the rhesus monkey (Raulston et al, 1978). Moreover, irradiation with photons has also been shown to elicit an initial hyperaemic response in the irradiated kidney of the pig (Robbins et al, 1985, 1989b), monkey (Anderson et al, 1982), dog (Mendelsohn & Caceres, 1953), mouse (Glatstein, 1973), and in patients (Avioli et al, 1963). X-irradiation has also been reported to cause an increase in contralateral unirradiated kidney function in the pig (Robbins et al, 1985). There is little additional information available concerning the effects of unilateral irradiation on the contralateral kidney. Caldwell et al (1967) observed abnormal renograms in the unirradiated kidney of rabbits up to 5 weeks after a dose of 22 Gy to the other kidney; no data on absolute GFR or ERPF values were presented. The mechanisms responsible for this hyperaemic response is seen in both kidneys after unilateral aemmic response is seen in both kidneys after unilateral irradiation is suggestive of a systemic effect. Significant increases in GFR and renal plasma flow are seen in patients receiving total body irradiation prior to allogenic bone marrow transplantation, and these may involve the release of vasodilator prostaglandins, since the haemodynamic changes were associated with a rise in urinary 6-keto α PGF1. No measurements of prostaglandin excretion are yet available following irradiation of the pig.

This initial hyperaemic response was followed, in the irradiated kidney, by a progressive dose-related reduction in GFR, and in particular, ERPF, 26–52 weeks after irradiation; renal haemodynamics then remained at this reduced level up to 104 weeks after irradiation. Both the mean GFR or ERPF (obtained 13–104 weeks after irradiation) exhibited a linear dose–response relationship. However, the slopes of the respective dose–response curves were significantly different ($p < 0.001$), such that there was a 7% reduction in function/Gy for ERPF, compared with an 11% reduction in function/Gy for GFR. These findings are qualitatively similar to those seen following photon irradiation of both kidneys in mature pigs (Robbins et al, 1989b). Moreover, the ED$_{50}$ value determined from the incidence of irradiated kidneys exhibiting a $\geqslant$ 50% reduction in ERPF was significantly lower than that for GFR, an observation seen previously following photon irradiation of the pig kidney (Robbins et al, 1989a, b). Associated with this decrease in irradiated kidney GFR was a concomitant increase in GFR in the unirradiated kidney. This reflects the compensatory response of this kidney to the loss of function in the irradiated organ. It is of interest to note that there was little evidence for any compensatory increase in ERPF by the contralateral unirradiated kidney. A similar difference in the compensatory response of the contralateral unirradiated kidney has also been observed in the pig following X-irradiation (Robbins et al, 1985). The reason for this difference remains unclear.

The compensatory response of the unirradiated kidney following irradiation of the contralateral organ can be explained in terms of the physiological response of the kidneys to injury. Removal or injury of one kidney will lead to compensatory renal growth (CRG) by the other kidney; CRG returns total renal mass and GFR to near normal values, although the causal mechanisms remain ill-defined (Peters, 1978; Fine, 1986). In the context of the present data it is likely that fast neutron-induced damage to the irradiated kidney is recognized and leads to a compensatory response by the unirradiated kidney. Subsequently, total renal function will return to near normal levels with elimination of any further compensatory response.

In the present study the fast neutron-induced reduction in the weight of the irradiated kidney, assessed 104 weeks after irradiation, was dose-related. Similar dose-related reductions in the weight of irradiated kidneys have been reported in the mouse 6 months after fast neutron (Geraci et al, 1978) and 5–24 months after X-irradiation (Jordan et al, 1978). This is further evidence to show that there is no qualitative difference between the response of the kidney to fast neutron or photon irradiation. Although there was a positive correlation between irradiated kidney weight and FI, the data points were rather scattered. A similar scattering was noted when plotting irradiated kidney ERPF, this time expressed as a percentage of age-matched controls, against irradiated kidney weight expressed in this case as a percentage of the mean weight of a single kidney from age-matched controls (data not presented). This scatter in the data is not surprising, since the two variables are not directly related. Renal function is a measure of the number of functioning nephrons present, whereas renal weight will be made up of all renal tissue, consisting of both functioning and non-functioning renal tissue.

It is of interest to note that previous studies have indicated that if the contralateral kidney is removed before irradiation then the irradiated kidney does not undergo shrinkage but remains at its pre-irradiation size (Redd, 1960; Asscher, 1964). In addition, if both kidneys of pigs are irradiated then the reduction in kidney weight with time is markedly less than that seen following irradiation to one kidney while leaving the contralateral kidney intact (Robbins et al, unpublished observations). Thus the presence of the contralateral unirradiated kidney influences the response of the irradiated kidney in terms of both function and weight. This reflects the propensity of the contralateral kidney to exhibit CRG and inhibit any potential for recovery in the irradiated kidney. Although CRG in the undamaged organ will tend to minimize the loss in overall function, it was pointed out by Hinman (1926) in his theory of renal counterbalance, that this response is not necessarily advantageous, since hypertrophy of the normal kidney suppresses recovery of the injured kidney, causing renal hypotrophy in the latter (Hinman, 1970).

More recent studies (Finn, 1986; Churchill et al, 1991) have confirmed the concept of renal counterbalance, *i.e.* the hypertrophied kidney suppresses any recovery of the injured kidney and causes its eventual atrophy. Unilateral renal injury leading to such atrophy, such as ureteral obstruction and ischaemia, can be modified by a reduction in the function of the contralateral kidney (Finn, 1986). The response may be mediated by changes in the ratio of vasodilator and vasoconstrictor substances, or by the accumulation of naturally occurring cytoprotective agents. In either case a prerequisite for full recovery of the damaged organ is a growth stimulus, which appears primarily to involve regeneration of the tubular epithelium. It is, however, unlikely that the irradiated kidney will be able to exhibit such recovery, since the principal site of damage in radiation nephropathy appears to be glomerular rather than tubular (Robbins et al, 1991b). Indeed, experimental studies indicate that the kidney fails to exhibit any significant long-term recovery in function following irradiation (Rockwell & Moulder, 1985; Stewart et al, 1989).

In summary, the response of the pig kidney to fast neutron irradiation, in terms of changes in GFR and ERPF, is similar to that observed after photon irradiation. Moreover, the fast neutron-induced reduction in kidney weight observed following irradiation of the right kidney alone was similar to that seen by other investigators after photon irradiation (Jordan et al, 1978; Michalowski, 1986). These findings are in agreement with those involving other organ systems in the pig (Hopewell et al, 1988; Blekkenhorst et al, 1990; Rezvani et al, 1990). However, there was no strongly defined relationship found between long-term radiation-induced changes in renal function following fast neutron irradiation and the reduction in the mass of the irradiated kidney.

Acknowledgments

The authors gratefully acknowledge the support and collaboration of the staff at the Churchill Hospital Research Institute, the MRC Radiobiology Unit, and the team at the AERE Variable Energy Cyclotron, without whose help these studies could not have been performed. Specific thanks are given to Dr D. Goodhead and D. Bance for calibration of the beam line, M. Corp and Dr T. Yeung for dosimetry, and P. Gray and A. Thompson for providing back-up electronics support. P. Bates, F. Dickinson, N. Hubbard and P. Monk are thanked for their expert help in animal anaesthesia and husbandry. The work was jointly supported by the Cancer Research Campaign and the Medical Research Council, including a special MRC programme grant to Dr J. Hopewell.

References

ANDERSON, R. E., KLINGLER, E. L., BARTELS, P. H. & JORDAN, S. W., 1982. The pathogenesis of radiation injury in complex tissues. *Analytical and Quantitative Cytology, 4,* 165–173.

ASSCHER, A. W., 1964. The delayed effects of renal irradiation. *Clinical Radiology, 15,* 320–325.

AVIOLI, L. V., LAZOR, M. Z., COTLOVE, E., BRACE, K. C. & ANDREWS, J. R., 1963. Early effects of radiation on renal function in man. *American Journal of Medicine, 34,* 329–337.

BLEKKENHORST, G., HENDRIKSE, A., KENT, C., JONES, D. & VAN DEN AARDWEG, G. J. M. J., 1990. Preclinical studies with the Faure high energy neutron facility: response of pig skin to fractionated doses of fast neutrons ($66\,\mathrm{MeV}_{p\rightarrow Be}$). *Radiotherapy and Oncology, 18,* 147–154.

CALDWELL, W. L., BOSCH, A., THOMASSEN, R. W. & IRIZARRY, S., 1967. Effects of unilateral renal irradiation on the ^{131}I-hippuran renogran in rabbits. *Journal of Urology, 98,* 154–158.

CHURCHILL, M., CHURCHILL, P. C., SCHWARTZ, M., BIDANI, A. & MCDONALD, F., 1991. Reversible compensatory hypertrophy in transplanted Brown Norway rat kidneys. *Kidney International, 40,* 13–20.

DICKINSON, F. & HUBBARD, N., 1990. The Large White female pig in research related to cancer treatment: general husbandry and anaesthesia. *Animal Technology, 41,* 35–41.

FAREBBROTHER, D. A., HATFIELD, P., SIMMONDS, H. A., CAMERON, J. S., JONES, A. S. & CADENHEAD, A., 1975. Experimental crystal nephropathy (one year study in the pig). *Clinical Nephrology, 4,* 243–250.

FINE, L., 1986. The biology of renal hypertrophy. *Kidney International, 29,* 619–634.

FINN, W. F., 1986. Renal counterbalance. *Journal of Laboratory and Clinical Medicine, 105,* 1105–1223.

GERACI, J. P., THROWER, P. D. & MARIANO, M., 1978. Cyclotron fast neutron RBE for late kidney damage. *Radiology, 126,* 519–520.

GLATSTEIN, E., 1973. Alterations in rubidium-86 extraction in normal mouse tissues after irradiation. *Radiation Research, 53,* 88–101.

GOODHEAD, D. T., BERRY, R. J., BANCE, D. A., GRAY, P. & STEDEFORD, J. B. H., 1977. High energy fast neutrons from the Harwell variable energy cyclotron. 1. Physical characteristics. *American Journal of Roentgenology, 129,* 709–716.

HINMAN, F., 1926. Renal counterbalance. *Archives of Surgery, 12,* 1105–1223.

HINMAN, F., JR, 1970. The pathophysiology of renal obstruction. In *Urology,* vol. 1, ed. by M. F. Campbell and J. H. Harrison (W. B. Saunders, Philadelphia), pp. 313–348.

HOPEWELL, J. W., BARNES, D. W. H., ROBBINS, M. E. C., SANSOM, J. M., KNOWLES, J. F. & VAN DEN AARDWEG, G. J. M. J., 1988. The relative biological effectiveness of fractionated doses of fast neutrons ($42\,\mathrm{MeV}_{d\rightarrow Be}$) for normal tissues in the pig. I. Effects on the epidermis and dermal vascular/connective tissue. *British Journal of Radiology, 61,* 928–938.

JORDAN, S. W., KEY, C. R., GOMEZ, L. S., AGNEW, J. & BARTON, S. L., 1978. Late effects of radiation on the mouse kidney. *Experimental and Molecular Pathology, 29,* 115–219.

KUNKLER, P. B., FARR, R. F. & LUXTON, R. W., 1952. The limit of renal tolerance to X-rays. *British Journal of Radiology, 25,* 190–201.

MENDELSOHN, M. L. & CACERES, E., 1953. Effects of X-ray to the kidney on the renal function of the dog. *American Journal of Physiology, 173,* 351–354.

MICHALOWSKI, A., 1986. The pathogenesis of the late side-effects of radiotherapy. *Clinical Radiology, 37,* 203–207.

PETERS, G., 1978. History and problems of compensatory adaptations of renal functions and of compensatory hypertrophy of the kidney. *Yale Journal of Biological Medicine, 51,* 235–245.

RAULSTON, G. L., GRAY, K. N., GLEISER, C. A., JARDINE, J. H., FLOW, B. L., HUCHTON, J. I., BENNET, K. R. & HUSSEY, D. H., 1978. A comparison of the effects of $50\,\mathrm{MeV}_{d\rightarrow Be}$ neutron and cobalt-60 irradiation on the kidneys of rhesus monkeys. *Radiology, 128,* 245–249.

REDD, B. L., JR, 1960. Radiation nephritis. Review, case report and animal study. *American Journal of Roentgenology, 83,* 88–106.

REZVANI, M., BARNES, D. W. H., HOPEWELL, J. W., ROBBINS, M. E. C., SANSOM, J. M., ADAMS, P. J. V. & HAMLET, R., 1990. The relative biological effectiveness of fractionated doses of fast neutrons (42 $\mathrm{MeV}_{d\rightarrow Be}$) for normal tissues in the pig. III. Effects on lung function. *British Journal of Radiology, 63,* 875–881.

ROBBINS, M. E. C., 1984. Single injection techniques in determining age-related changes in porcine renal function. *International Journal of Applied Radiation and Isotopes, 35,* 85–91.

ROBBINS, M. E. C. & HOPEWELL, J. W., 1991. Renal and genitourinary system morbidity of radiotherapy. In *Complications of Cancer Management,* ed. by P. N. Plowman, T. McElwain and A. Meadows (Butterworth-Heinemann, Oxford), pp. 193–212.

ROBBINS, M. E. C., SOPER, M. & GUNN, Y., 1984. Techniques for the quantitative measurement of individual kidney function in the pig. *Journal of Applied Radiation and Isotopes, 35,* 853–858.

ROBBINS, M. E. C., HOPEWELL, J. W. & GUNN Y., 1985. Effects of single doses of X-rays on renal function in unilaterally irradiated pigs. *Radiotherapy and Oncology, 4,* 143–151.

ROBBINS, M. E. C., CAMPLING, D., REZVANI, M., GOLDING, S. J. & HOPEWELL, J. W., 1989a. Nephropathy in the mature pig after irradiation of a single kidney: a comparison with the immature pig. *International Journal of Radiation Oncology, Biology, Physics, 16,* 1519–1528.

ROBBINS, M. E. C., CAMPLING, D., REZVANI, M., GOLDING, S. J. & HOPEWELL, J. W., 1989b. Radiation nephropathy in mature pigs following the irradiation of both kidneys. *International Journal of Radiation Biology, 56,* 83–98.

ROBBINS, M. E. C., BARNES, D. W. H., CAMPLING, D., HOPEWELL, J. W., KNOWLES, J. F., SANSOM, J. M. & SIMMONDS, R. H., 1991a. The relative biological effectiveness of fractionated doses of fast neutrons (42 $\mathrm{MeV}_{d\rightarrow Be}$) for normal tissues in the pig. IV. Effects on renal function. *British Journal of Radiology, 64,* 823–830.

ROBBBINS, M. E. C., WOOLDRIDGE, M. J. A., JAENKE, R. S., WHITEHOUSE, E., GOLDING, S. J., REZVANI, M. & HOPEWELL, J. W., 1991b. A morphological study of radiation nephropathy in the pig. *Radiation Research, 126,* 317–327.

ROCKWELL, S. & MOULDER, J. E., 1985. Biological factors of importance in split-course radiotherapy. In *Optimization of Cancer Radiotherapy,* ed. by B. R. Paliwal, D. E. Herbert and C. G. Orkin (American Institute of Physics, New York),, pp. 171–182.

SPERBER, I., 1944. Studies on the mammalian kidney. *Zoologiska Bidrag fran Uppsala, 22,* 249–431.

STEWART, F. A., SORANSON, J. A., ALPEN, E. L., WILLIAMS, M. V. & DENEKAMP, J., 1984. Radiation-induced renal damage. The effects of hyperfractionation. *Radiation Research, 98,* 407–420.

STEWART, F. A., LEBESQUE, J. V. & HART, G. A., 1988. Progressive development of radiation damage in mouse kidneys and the consequences for reirradiation tolerance. *International Journal of Radiation Biology, 53,* 405–416.

STEWART, F. A., LUTS, A. & LEBESQUE, J. V., 1989. The lack of long-term recovery and reirradiation tolerance in the mouse kidney. *International Journal of Radiation Biology, 56,* 449–462.

TERRIS, J. M., 1986. Swine as a model in renal physiology and nephrology: an overview. In *Swine in Biomedical Research,* ed. by M. E. Tumbleson (Plenum, New York), pp. 1673–1689.

TEXTOR, S. C., FORMAN, S. J., ZIPSER, R. D. & CAMERON, J. E., 1987. Changes in renal blood flow, glomerular function, and vasoactive hormones in bone-marrow-transplant recipients after total-body irradiation. In *Prostaglandin and Lipid Metabolism in Radiation Injury,* ed. by T. L. Walden and H. N. Hughes (Plenum, New York), pp. 305–317.

WILLIAMS, M. V. & DENEKAMP, J., 1984. Radiation-induced renal damage in mice: influence of fraction size. *International Journal of Radiation Oncology, Biology, Physics, 10,* 885–893.

1992, *The British Journal of Radiology*, *65*, 918–928

Retrospective analysis of nasopharyngeal carcinoma treated during 1976–1985: late complications following megavoltage irradiation

By Anne W. M. Lee, FRCR, Stephen C. K. Law, FRCR, *S. H. Ng, MRCP, David K. K. Chan, PhD, Y. F. Poon, FRCR, William Foo, FRCR, S. K. O, FRCR, Stewart Y. Tung, FRCR, †Fred K. Cheung, MSc and *John H. C. Ho, MD, DSc, FRCR

Institute of Radiology and Oncology, Queen Elizabeth Hospital, Wylie Road, Kowloon, Hong Kong; *Baptist Hospital, Waterloo Road, Kowloon, Hong Kong; and †Physics Department, Princess Margaret Hospital, 500 Sherbourne Street, Toronto, Canada

(*Received 28 November 1991 and in revised form 15 April 1992, accepted 8 May 1992*)

Keywords: Nasopharyngeal carcinoma, Late irradiation complications

Abstract. A retrospective analysis was undertaken of the late complications observed in 4527 patients with nasopharyngeal carcinoma treated by megavoltage radiotherapy during the years 1976–1985. Unconventional fractionation schedules were used because of serious resource limitations. The median equivalent doses were 65 Gy to the nasopharyngeal region and 53 Gy to the cervical region. 707 patients had reirradiation for local recurrences and 250 for regional relapses. The 10-year actuarial cancer-specific survival was 47%, and the corresponding all-complication-free and neurological-complication-free rates were 40% and 72%, respectively. Altogether, 1395 (31%) patients developed one or more late irradiation sequelae. The majority were mild soft-tissue damages, but 322 (7%) had significant functional disturbances, from which 62 (1%) died. Neurological damage that occurred in 450 (10%) patients constituted the major morbidity and accounted for all but three of the treatment mortalities. The cumulative incidence of the various complications is summarized, and the data recorded in the literature reviewed in order to give a proper perspective of the problem. Patients treated during 1981–1985 had a significantly higher actuarial encephalomyelopathy-free rate than those treated during 1976–1980, but the incidence-free rates for the other neurological complications remained unimproved, suggesting that the improvement could be mainly attributed to additional shielding for the brainstem rather than the reduction of dose from 3.8–4.2 Gy to 2.5 Gy per fraction.

To achieve the highest cure rate with lowest morbidity is undoubtedly the ideal goal of every oncologist. This is especially difficult in the treatment of nasopharyngeal carcinoma (NPC) because of the tumour's characteristic propensity for extensive invasion and its anatomical proximity to critical structures. The balance between the risk of lethal local failure and that of fatal treatment complications poses a constant dilemma.

To maximize the chance of cure, an adequately toxic dose of radiation has to be given to all potential sites of infiltration (Ho, 1982; Hoppe et al, 1976;& Yamashita et al, 1986). Although the optimum dose schedule has yet to be determined, it is agreed that doses below 60 Gy at conventional fractionation of 2 Gy daily are inadequate for tumour eradication. Thus, all normal tissues within the target volume will be exposed to a potentially damaging dose. Neural structures adjacent to the base of the skull are particularly vulnerable, as the usually quoted tolerance limit (Rottenberg et al, 1977; Sheline et al, 1980) will inevitably be exceeded. The risk of late irradiation damage is substantial, and may indeed be unavoidable (Ballantyne, 1975; Qin et al, 1988; Tokars & Griem, 1979).

Because of a serious shortage of treatment machines, schedules with large fractional doses were used in our institute. This, unfortunately, further aggravates the risk of damage, especially for neural tissues. With the accumulation of long-term survivors, the problem of late complications becomes one of our major concerns. To have an accurate assessment of the maximum risk caused by contemporary methods, patients with non-disseminated disease treated by megavoltage radiotherapy during 1976–1985 were analysed. This is a detailed account of our recorded sequelae, together with a review of the incidence reported in the English language literature.

Materials and methods

Patient characteristics

During the study period, 4628 previously untreated patients with squamous cell carcinoma of the nasopharynx were irradiated with megavoltage (4.5–8 MV) photons in our department. Excluding 101 patients with distant metastasis at presentation, 4527 were evaluated in the present study.

Presented in part at the Hong Kong Symposium on Nasopharyngeal Carcinoma, organized by the Asian Oceanian Clinical Oncology Association, in Hong Kong, on 22 April 1990.

Address correspondence to Dr Anne W. M. Lee.

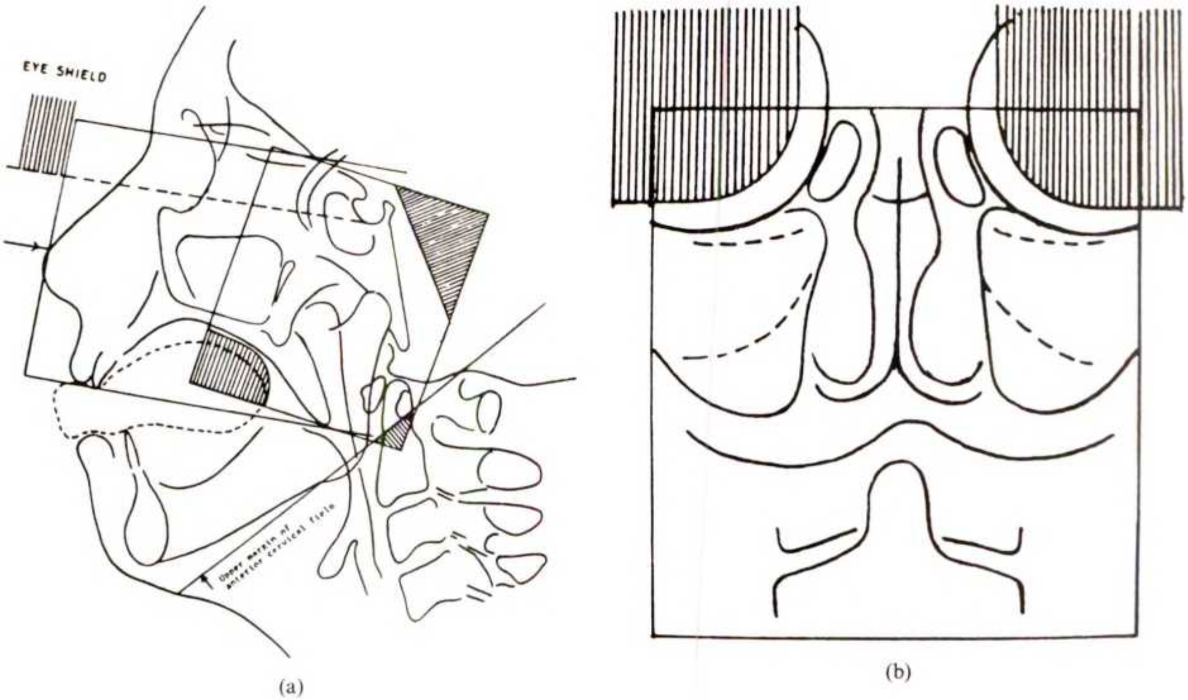

(a)

(b)

The male to female ratio was 2.7 to 1. Their age at the time of treatment ranged from 10 to 88 years (median, 48 years). 93% of patients were regularly observed until death or the time of analysis, while 7% (336) defaulted follow-up after a median period of 3 years from completion of primary radiotherapy (range, 0–12 years).

Radiation therapy

Primary course. The target volume, radiation techniques and dosage schemes have been described in detail in previous publications (Ho, 1978, 1982). Figure 1 shows the standard technique and coverage.

Three modifications to the field arrangement were introduced during this period. In our attempts to reduce late neurological complications, a greater portion of the anterior part of the brainstem was shielded in patients without cranial involvement since 1981, and the hypothalamic–pituitary stalk was shielded in patients with small T1 tumours since 1985. To minimize marginal miss in patients with extensive parapharyngeal involvement, a postero-lateral boost was added since 1983.

Different fractionation schedules were employed in different periods to achieve the best possible results within our practical constraints. It was not until 1981, with the addition of a linear accelerator, that we were able to reduce the mean tumour dose (MTD) from 3.8–4.2 Gy to 2.5 Gy per fraction for all patients. Table I lists the most frequently used fractionation schemes and their biological equivalents as calculated by

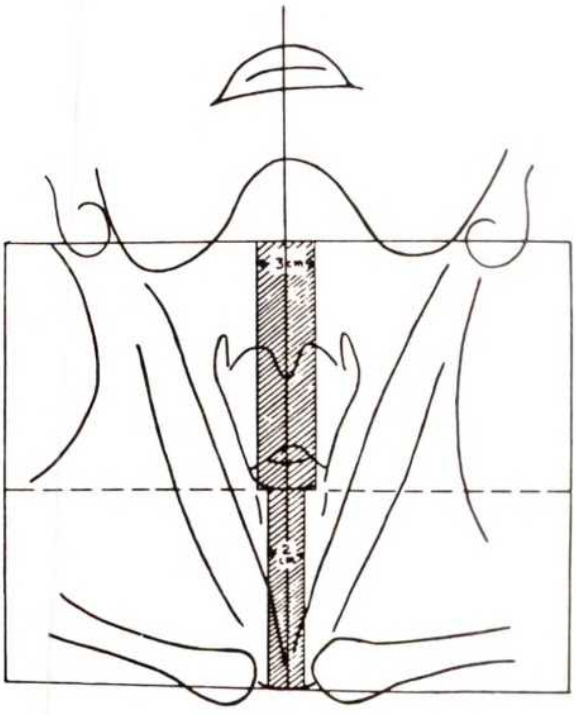

(c)

Figure 1. The standard technique for the primary target consisting of (a) two lateral parallel-opposed facial fields supplemented by (b) an anterior facial field, and for the neck, (c) an anterior cervical field with a median shield for the larynx and the spinal cord.

Table I. The first course of loco-regional radiation therapy
(A) The most frequently used schedules

Schedules (Gy/fractions/days)	Biological equivalent doses TDF			No. of cases
	TDF	BED-Gy10	BED-Gy3	
Nasopharyngeal region				
60.0/24/39	108	75	110	1796
50.4/12/38	107	72	121	869
66.0/33/44	109	79	110	194
62.5/29/42[a]	108	76	108	479
60.0/28/39[a]	102	73	103	387
62.1/31/43[a]	103	75	105	261
Cervical region				
39.2/07/42	88	61	112	2081
33.6/06/35	76	52	96	199
51.2/22/35[a]	91	66	99	586
56.8/23/42[a]	104	74	115	238
50.8/24/37[a]	87	64	96	210

(B) Total dose equivalent to conventional fractionation of 2 Gy daily as estimated by TDF

Dose equivalent	Nasopharyngeal	Cervical[b]
> 66 Gy	20 (< 1%)	3 (< 1%)
64–66 Gy	3463 (76%)	39 (1%)
60–63 Gy	802 (18%)	395 (9%)
55–59 Gy	154 (3%)	191 (4%)
50–54 Gy	16 (< 1%)	2925 (65%)
< 50 Gy	72 (2%)	428 (9%)
No irradiation	—	546 (12%)

TDF, time-dose-fractionation method (Orton & Ellis, 1973).
BED-Gy10, Gy3, biological effective doses assuming $\alpha/\beta = 10$ and 3 Gy, respectively (Barendsen, 1982; Fowler, 1989).
[a] En-bloc technique using different fractionation in two phases.
[b] Total number with at least one course of neck irradiation: 3642 as primary and 339 as salvage treatment.

the linear-quadratic equation (Barendsen, 1982; Fowler, 1989) and the time-dose-fractionation (TDF) method (Orton & Ellis, 1973). To give an easily understood picture of the total dose received, the doses equivalent to conventional fractionation of 2 Gy daily as estimated by TDF are presented in this text. The median dose to the nasopharyngeal region was 65 Gy, as 3463 (76%) patients had an MTD of 64–66 Gy.

Only 3642 patients had neck irradiation during the primary course as it was our policy to withhold prophylactic treatment in node-negative patients. The most commonly employed fractionation schedule was 5.6 Gy at the 90% isodose level (IL), weekly for 7 fractions. But for patients treated with the en-bloc technique, daily fractions of 1.5–2 Gy were used during the initial en-bloc phase, while fractional doses of 2–2.5 Gy were used for the nasopharyngeal and 5.6 Gy for the cervical region during the subsequent phase. The median dose to the neck was 53 Gy.

In addition to the basic course, 199 (4%) patients had booster doses to the nasopharyngeal region: 60 by intracavitary caesium for a median dose of 20 Gy at 10 mm depth, 128 by external irradiation for 11 Gy, and 11 by a combination of both methods at various doses. Boosts to the parapharyngeal space and cervical region for a median dose of 11 Gy were given to 76 (2%) and 1156 (26%) patients, respectively.

Reirradiation for loco-regional recurrences. 707 (16%) patients had reirradiation for local recurrence 0.5–11 years (median, 2 years) after completion of the primary course: 38 by brachytherapy for a median dose of 40 Gy at 10 mm depth, 587 by external radiotherapy for a median MTD of 57 Gy, and 82 by a combination of both at various doses. Of those who suffered further recurrence after remission with a second treatment, 50 had additional irradiation.

Of the patients without previous cervical irradiation, 339 subsequently had therapeutic radiotherapy (302 to whole neck and 37 to involved field) for a median dose of 53 Gy at 90% IL. Hence, 3981 (88%) of the whole series had at least one course of neck irradiation (primary or salvage).

For patients who relapsed despite previous cervical RT, 250 had reirradiation to a median dose of 49 Gy. Of those who recurred again, 19 had additional radiotherapy.

Additional modalities

Chemotherapy was given in conjunction with primary radiotherapy in 378 (8%) patients. Various cytotoxic agents (including methotrexate, vincristine and cis-platinum) were used.

A radiosensitizer (metronidazole) had been given to 41 patients in 1978: 22 for primary treatment and 19 reirradiation. This study was stopped shortly afterwards because of unacceptably severe acute gastrointestinal and neurological toxicities.

Aggravating conditions

Coexisting medical problems (other than treatment factors) that might have aggravated the risk of irradia-

Table II. Possible aggravating condition for irradiation damage

Coexisting medical problem		Complication rate (%)	Risk ratio	Difference (*p* value)
Diabetes mellitus	yes	24/56 (43)	1.397	0.0497
	no	1371/4471 (31)		
Hypertension	yes	49/116 (42)	1.384	0.0071
	no	1346/4411 (31)		
Ischaemic heart	yes	3/11 (27)	0.885	0.7989
	no	1392/4516 (31)		
Dermatomyositis	yes	9/37 (24)	0.788	0.3907
	no	1386/4490 (31)		

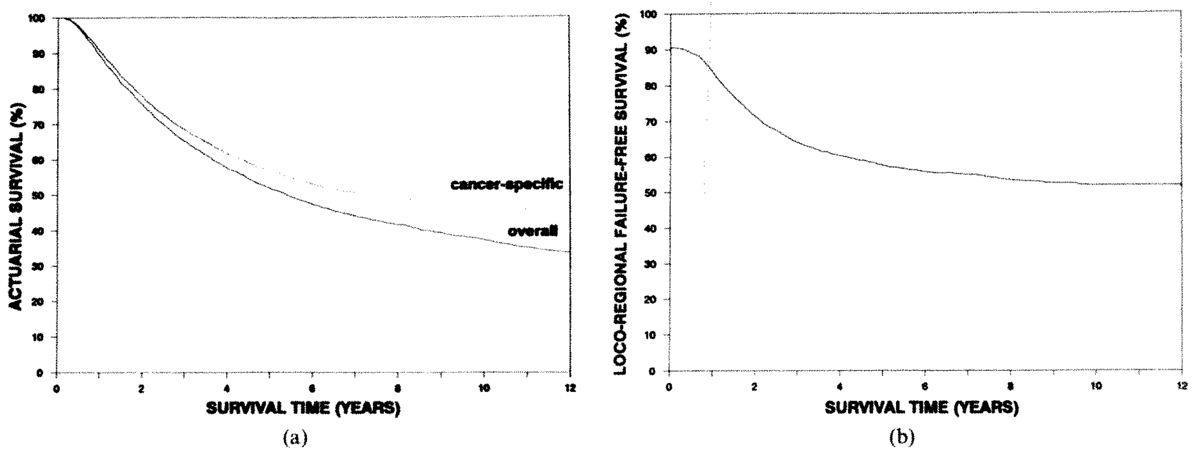

(a) (b)

Figure 2. The actuarial (a) overall survival and cancer-specific survival, and (b) loco-regional failure-free rate as calculated from completion of primary radiotherapy.

tion damage were analysed and the relative risks are listed in Table II.

Statistical methods

All the survival curves were actuarial measurements as calculated by the Kaplan–Meier method (1958), and the differences between the curves compared by the log-rank test (Peto et al, 1977).

Results and discussion

To assess the risk of late irradiation complications, it is necessary to know not only the size of the exposed population, but also the proportion of patients who have survived sufficiently long to develop the sequelae. Assessment of complications is meaningful only when tumour control is also analysed for gauging the therapeutic ratio.

For patients with non-disseminated NPC treated by megavoltage irradiation, we achieved a 10-year actuarial cancer-specific survival of 47%, and an overall survival (taking into account all causes of deaths) of 37% (Fig. 2a). The corresponding loco-regional failure-free rate was 53% (Fig. 2b).

Diagnosis of late complications can be difficult and a high degree of awareness is required. Temporal lobe necrosis and endocrine dysfunctions, in particular, are easily overlooked by the unwary, as the majority of these patients have minimal symptoms and signs. Before attributing abnormalities to irradiation damage, however, every effort must be made to exclude other possible causes. Correct differentiation from tumour recurrence is critical, and a long period of observation may be needed for confirmation.

Altogether, 31% (1395) of our patients developed one or more late radiation-induced sequelae. Significant functional disturbances were noted in 7% (322), from which 1% (62) died. Neurological complications, which occurred in 10% (450) of patients, constituted the major cause of serious disabilities and accounted for all but three of our treatment mortalities. In terms of actuarial calculation, our 10-year all-complication-free rate was 40%, and the neurological-complication-free rate 72% (Fig. 3). Patients with hypertension or diabetes mellitus had a significantly higher risk of complications (Table II), and the various sequelae observed are summarized in Table III.

It is difficult to compare the results between different centres as the period of treatment, number of patients, percentage of survivors, duration of observation, diligence of detection, and tightness of definition differ. Series with 5-year results cannot adequately reflect the gravity of the problems since the median latency of neurological sequelae was 5 years from completion of primary treatment. The few series with 10-year follow-up reported survival ranging from 19% (Haghbin et al, 1985) to 55% (Hoppe et al, 1976). The majority of

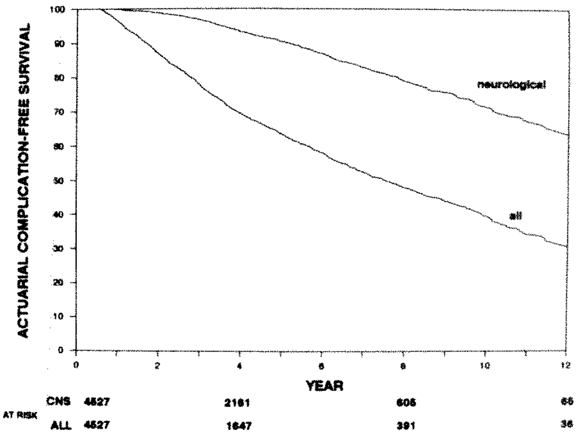

Figure 3. The actuarial all-complication-free and neurological-complication-free rates from completion of primary radiotherapy.

Table III. Cumulative incidence of late irradiation sequelae

Type of complication	Total (%)	Severe	Fatal
Overall	1395 (31)	322	62
Nervous system:			
Temporal lobel necrosis	138 (3)	40	40
Brainstem encephalopathy/myelopathy	44 (1)	26	16
Cranial/sympathetic nerve palsy	241 (5)	51	4
Hypothalamic–pituitary dysfunction	159 (4)	22	0
Nasal/nasopharyngeal fossa:			
Severe mucosal atrophy	28 (1)	7	2
Osteonecrosis	4 (0.1)	1	0
Ear:			
Impairment of hearing	375 (8)	134	0
Persistent otitis	111 (2)	19	0
Eyeball:			
Cataract	6 (0.1)	1	0
Retinitis	3 (0.1)	1	0
Corneal ulceration	5 (0.1)	4	0
Temporo-mandibular joint:			
Trismus	231 (5)	47	0
Oral cavity:			
Osteonecrosis	9 (0.2)	3	0
Soft-tissue necrosis	3 (0.1)	0	0
Neck:			
Soft-tissue fibrosis	721 (16)	15	0
Soft-tissue necrosis	16 (0.4)	6	0
Persistent lymphoedema	5 (0.1)	1	0
Fracture of clavicle	3 (0.1)	1	0
Radiation-induced malignancy	2 (< 0.1)	2	1

authors only list complications in a brief paragraph, very few present a detailed analysis of aggravating factors, and none has included actuarial measurements of incidence.

To assess our incidence of complications in a proper perspective, the cumulative incidence recorded in the literature is reviewed (Table IV). The median overall complication rate reported was 38% (Haghbin et al, 1985), with a serious morbidity rate of 8% (Ballantyne, 1975) and a mortality rate of 3% (Haghbin et al, 1985). Our complication rates were mostly in the middle or lower range except for temporal lobe necrosis, neuropathy, neuroendocrine dysfunction, deafness and neck fibrosis.

Neurological complications

Temporal lobe necrosis. Our cumulative incidence was 3% (138), whilst the highest reported in the literature was 1% (van Andel & Hop, 1982). The latent interval ranged from 1.5 to 13 years (median, 5 years). The confidence of clinical diagnosis based on typical clinical features, computed tomography (CT), magnetic resonance imaging (MRI) and correlation with the distribution of radiation dose has been discussed in previous publications (Lee et al, 1988, 1990).

Temporal lobe necrosis is the most worrying complication as it accounted for 65% (40/62) of our irradiation-induced mortalities or 0.9% (40/4527) of deaths for the whole series.

Complete excision of the necrotic lesion is hazardous because of the bilateral involvement. Hence only eight patients had surgical intervention: 38% (3/8) of them responded but one died in the immediate post-operative period. Conservative treatment with corticosteroids was attempted in 81 patients. Although 33% (27/81) did show a significant clinical and radiological response lasting for more than 6 months, 14% (11/81) died of uncontrolled sepsis resulting from induced immunosuppression. The optimal treatment remains to be explored, but it is difficult to gauge the ultimate value of the various forms of treatment, as the natural rate of progression varies considerably among patients.

With a median observation period of 3 years (range, 0.5–9 years) from the detection of cerebral damage, 29% (40/138) of these patients had progressed to a debilitated state and 20% (28/138) died of cerebral necrosis. However, 71% (98/138) were still alive, and 62% (86/138) had little functional disability. The 5-year probability of surviving from temporal lobe necrosis or its treatment was 59% (Fig. 4a).

Brainstem encephalopathy/cervical spinal cord myelopathy. This is the next most serious sequela in our series. Our cumulative incidence was 1% (44), whilst the reported incidence ranged from 0.2% (Huang & Chu, 1981) to 18% (Qin et al, 1988), with a median of 2% (Marks et al, 1982).

The latent interval ranged from 0.4 to 9 years (median, 3 years). It was often impossible to differen-

Table IV. Review of literature on late complications following radiation therapy for nasopharyngeal carcinoma

Type of complication	Cumulative incidence (%) and reference		
	Lowest	Median	Highest
Overall	6/99 (6) Baker (1980)	30/70 (38) Haghbin et al (1985)	54/82 (66) Hoppe et al (1976)
Serious morbidity	3/49 (6) Stein et al (1988)	17/218 (8) Ballantyne (1975)	10/118 (8) Marks et al (1982)
Treatment death	1/142 (1) Scanlon et al (1967)	2/79 (3) Haghbin et al (1985)	13/218 (6) Ballantyne (1975)
Cerebral necrosis	3/838 (0.4) Chang et al (1980)	1/105 (1) Chatani et al (1986)	1/86 (1) van Andel & Hop (1982)
Encephalomyelopathy	?/1032 (0.2) Huang (1980)	2/118 (2) Marks et al (1982)	254/1379 (18) * Qin et al (1988)
Neuropathy	1/296 (0.3) Flores et al (1986)	3/251 (1) Mesic et al (1981)	5/82 (6) Hoppe et al (1976)
Endocrinopathy	1/138 (1) Cellai et al (1982)	4/118 (3) Marks et al (1982)	15/251 (6) Mesic et al (1981)
Fatal epistaxis	3/251 (1) Mesic et al (1981)		3/218 (1) Ballantyne (1975)
Deafness	1/152 (1) Bohorquez (1976)		18/251 (7) Mesic et al (1981)
Persistent otitis	4/99 (4) Baker (1980)	6/43 (14) Urdaneta et al (1976)	?/1032 (44) Huang (1980)
Cataract	1/105 (1) Chatani et al (1986)		19/650 (3) de Schryver et al (1971)
Retinopathy	12/650 (2) de Schryver et al (1971)		
Trismus	2/43 (5) Urdaneta et al (1976)	8/82 (10) Hoppe et al (1976)	15/118 (13) Marks et al (1982)
Tissue necrosis	3/296 (1) Flores et al (1986)	?/1032 (3) Huang (1980)	11/118 (9) Marks et al (1982)
Neck fibrosis	4/251 (2) Mesic et al (1981)	11/82 (13) Hoppe et al (1976)	19/118 (16) Marks et al (1982)
Malignancy	11/1605 (1) Huang (1980)		2/218 (1) Ballantyne (1975)

All quoted incidences are based on retrospective analyses with the exposed population as denominator.
*Patients with transient L'Hermitte's syndrome included.

tiate between damage of the brainstem and that of the upper cervical spinal cord by clinical signs alone. The protein content in the cerebrospinal fluid (CSF) was only mildly elevated, and both CT and myelograms were non-contributory. Only one patient had MRI performed, and the finding was highly suggestive of demyelination in the irradiated part of the brainstem.

All these patients presented with spastic paraparesis or quadriparesis with unequivocal long tract signs; 23 also had multiple cranial nerve palsies. Sensory defect was absent or mild as the damage was mostly confined to the anteriorly situated corticospinal tract.

There was no effective treatment to arrest this pathological process. 59% (26/44) of these patients progressed rapidly to a debilitated state, and 34% (15/14) died, while the remaining ran a slowly deteriorating course. The 5-year probability of surviving from encephalomyelopathy since its detection was 63% (Fig. 4b). Fortunately no case has occurred since 1983, hence this only accounts for 24% (15/62) of our treatment mortalities or 0.3% (15/4527) of deaths for the whole series.

Cranial/cervical sympathetic nerve palsy. Although peripheral nerves are relatively resistant, radiation-induced cranial and/or cervical sympathetic nerve palsies have been reported with an incidence ranging from 0.3% (Flores et al, 1986) to 6% (Hoppe et al, 1976), and a median of 1% (Mesic et al, 1981). Our cumulative incidence was 5% (241)

The latent interval ranged from 0.5 to 11 years (median, 5 years). 85% (204/241) of these patients had been closely monitored for more than 1 year after detection, and the median duration of observation was 3 years. 23 cases also had long tract signs and hence fell under the brainstem encephalopathy syndrome. 20 of

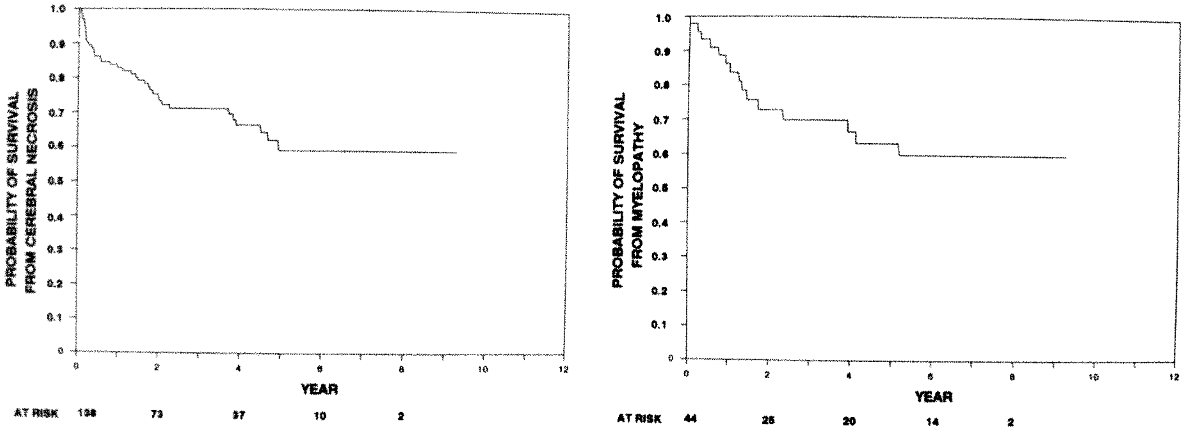

(a) (b)

Figure 4. The probability of surviving from (a) temporal lobe necrosis or its treatment, and (b) brainstem encephalopathy/cervical cord myelopathy from the time of their detection.

the 47 patients with sixth nerve palsy were associated with temporal lobe necrosis, but only five of them had papilloedema, suggesting that the majority were genuine neuropathy rather than a false localizing sign for increased intracranial pressure.

The incidence of various nerve palsies is listed in Table V. In agreement with other workers (Ballantyne, 1975; Flores et al, 1986; Hoppe et al, 1976; Huang & Chu, 1981; Mesic et al, 1981), the last four cranial nerves (the 12th in particular) were by far the commonest affected, our incidence being 4% (166). Although the majority had mild symptoms only, 2% (4/166) of these patients died of aspiration pneumonia due to swallowing dysfunction. 54% (89/166) of our patients had marked fibrosis of the soft tissue of the neck. Perineural fibrosis in the retropharyngeal space may be the major contributing cause for the neuropathy (Cheng & Schulz, 1975; Hoppe et al, 1976; Huang & Chu, 1981), but post-mortem confirmation is still awaited.

Among the other cranial nerves, optic atrophy with an incidence of 1% (51) was functionally and psychologically the most distressing, especially in the 0.4% (16) with bilateral blindness. The largest collection of optic atrophy following radiotherapy for head and neck tumours was reported by Parsons et al (1983), but the incidence rate could not be estimated as there was no information on the total number of NPC patients irradiated.

Involvement of the fourth, fifth and seventh nerves was infrequent, and all were associated with gross signs of brainstem damage. The incidence of eighth nerve palsy could not be assessed, as our patients with impairment of hearing had not been subjected to full otological examination, accurate differentiation between the conductive and the neurogenic elements was difficult, and distinction between damage of the sensory apparatus and that of the nerve was impossible.

Hypothalamic-pituitary dysfunction. The median reported incidence is 3% (Marks et al, 1982), and the highest 6% (Mesic et al, 1981) of the exposed population. Our cumulative incidence of symptomatic dysfunction with a grossly abnormal serum level of thyroxin, cortisol and/or prolactin was 4% (159). Stimulation studies and growth hormone and sex hormones tests were not routinely performed.

The latent interval ranged from 0.8 to 13 years (median, 5 years). The incidence of various hormonal disturbances is listed in Table VI. Hyperprolactinaemia

Table V. Cumulative incidence of cranial/sympathetic nerve palsy

Nerve	Total (%)	Unilateral	Bilateral	Severe
II	51 (1.1)	35	16	24
IV	5 (0.1)	4	1	0
V	18 (0.4)	18	0	0
VI	47 (1.0)	39	8	2
VII	5 (0.1)	5	0	0
IX	15 (0.3)	10	5	3
X	25 (0.6)	19	6	7
XI	52 (1.1)	36	16	4
XII	147 (3.2)	84	63	23
C. Sym.	7 (0.2)	7	0	3

C. Sym., cervical sympathetic nerve.

Table VI. Cumulative incidence of symptomatic hormonal dysfunction

Type of dysfunction	Total (%)	Severe
Secondary hypothyroidism	87 (1.9)	11
Secondary hypoadrenalism	36 (0.8)	3
Hyperprolactineamia		
Female	74 (6.0)	12
Male	3 (0.1)	1

35 patients had more than one dysfunction.

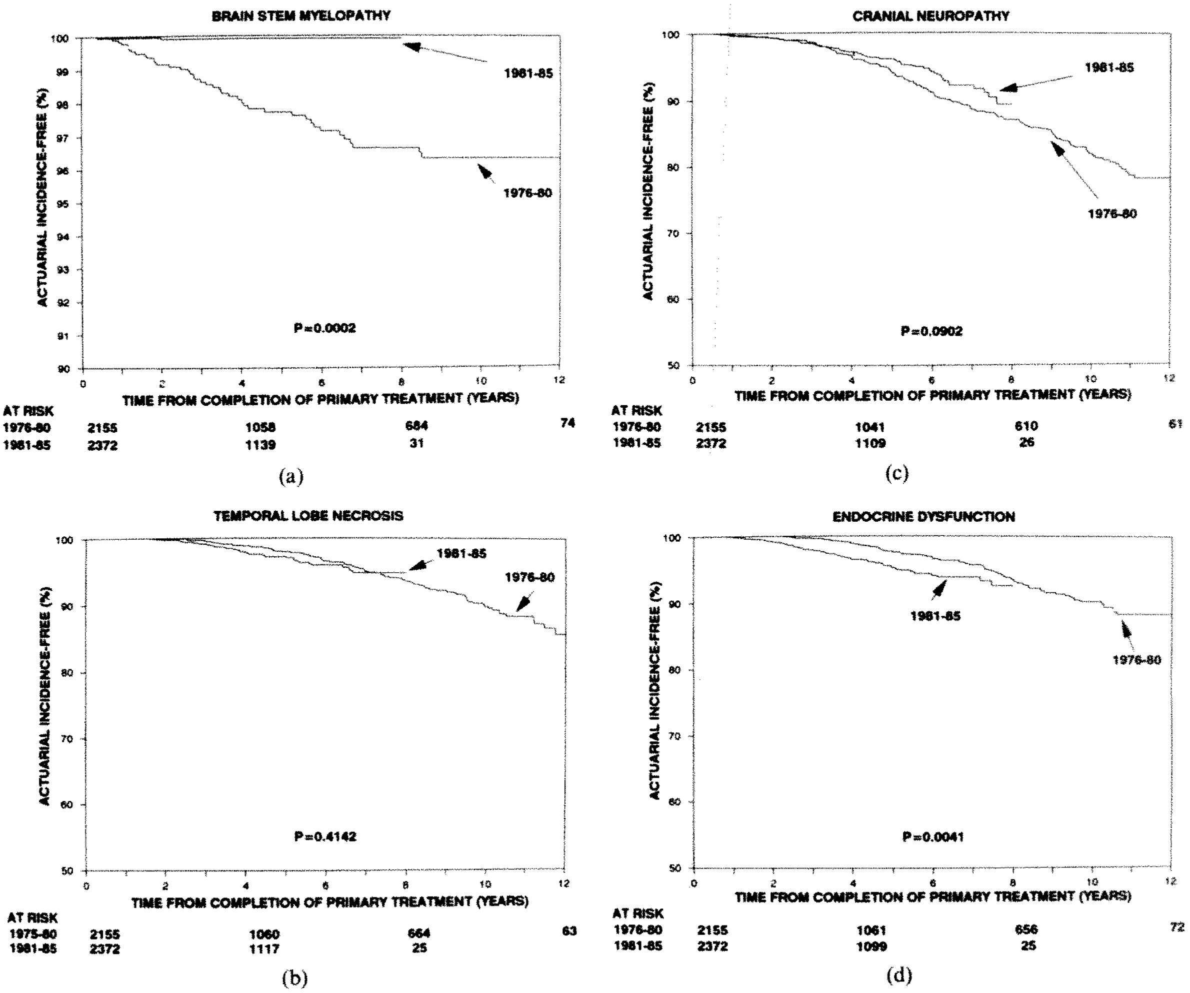

(a) (c)

(b) (d)

Figure 5. The actuarial incidence-free rates for patients treated during 1976–1980 versus those treated during 1981–1985: (a) brainstem encephalopathy/cervical cord myelopathy, (b) temporal lobe necrosis, (c) cranial/cervical sympathetic nerve palsy and (d) hypothalamic–pituitary dysfunction.

leading to amenorrhoea and/or galactorrhoea developed in 6% (74/1227) of our female patients, but only 0.1% (3/3300) of males complained of impotence or decreased libido. Of the 2% (87/4527) of patients with hypothyroidism, none had elevation of thyroid stimulating hormone.

In survivors subjected to full endocrine scrutiny, a much higher incidence of hormonal disturbances was observed (Lam et al, 1987, 1991; Samaan et al, 1982). Studies of our cases by Lam et al (1987, 1991) showed that the hypothalamus was the primary site of radiation-induced damage, biochemical anomalies could occur as early as 1 year after irradiation, and the incidence increased with increasing dosage to the hypothalamic–pituitary stalk.

Comparison between two periods. To assess the effectiveness of the measures introduced for reduction of irradiation complications, patients treated during 1976–1980 were compared with those treated during 1981–1985. While patients treated in the latter period had a significantly higher actuarial encephalomyelopathy-free rate (Fig. 5a), the temporal lobe necrosis-free (Fig. 5b) and the cranial neuropathy-free (Fig. 5c) rates showed no significant improvement, and the hormonal dysfunction-free rate appeared even worse (Fig. 5d).

Our optimism in achieving effective minimization of encephalomyelopathy is not premature as the latency for this sequela was relatively short (median, 3 years). The main attribute for this improvement is probably the additional shielding for the brainstem rather than our present reduction of MTD from 3.8–4.2 Gy to 2.5 Gy per fraction, as the actuarial incidence-free rates for the other neurological sequelae remained unimproved. The paradoxical increase in hormonal dysfunction is most likely to have resulted from an increased awareness and early detection. The effect of additional hypothalamic–pituitary shielding has yet to be assessed. Further reduction of fractional dose to 1.8–2 Gy might be necessary for significant improvement.

Non-neurological complications

Although the dysfunctions caused by damage of non-neurogenic structures are generally mild, serious morbidities and even mortalities can result.

Severe mucosal atrophy. Repeated episodes of epistaxis from the markedly atrophic and telangiectatic mucosa of the nasal/nasopharyngeal fossa occurred in 1% (28) of our patients, and 0.04% (2) died of uncontrolled haemorrhage. The reported incidence of fatal epistaxis is 1% (Ballantyne, 1975; Mesic et al, 1981).

Otological complications. The reported incidence of deafness following irradiation to the nasopharyngeal region ranged from 1% (Bohorquez, 1976) to 7% (Mesic et al, 1981), whilst 8% (375) of our patients had significant impairment of hearing and 3% (134) serious bilateral deafness.

Ear infection is another frequently encountered problem with a median reported incidence of 14% (Urdaneta et al, 1976). Although only 3% (111) of our patients had records of persistent otitis media, 17% (19/111) of them suffered from serious sepsis including meningitis.

Eyeball damage. While the optic chiasma and nerve were inevitably included within the target volume, the eyeballs could be shielded in the majority of patients, hence damage of the eyeball was relatively uncommon. Our incidence was 0.3% (14), and half (7/14) of these patients had an exceptionally high dose to their orbits because of initial tumour involvement.

Accurate assessment of the incidence of radiation-induced cataract is difficult as ageing degeneration cannot be excluded as the basic cause. De Schryver et al (1971) reported an incidence of 3% for radiation-induced cataract and 2% for retinitis, our corresponding incidence rates for both conditions were 0.1%.

Trismus. Five per cent (231) of our patients had marked fibrosis of the temporo-mandibular joints and/or adjacent muscles, and feeding difficulties occurred in the 1% (47) with a dental gap narrower than 0.5 cm. The median incidence recorded in the literature was 10% (Hoppe et al, 1976).

Bone/soft tissue necrosis. The median reported incidence was 3% (Huang & Chu, 1981). Our incidence of necrosis of bone was 0.3% (13), and of soft tissue in the oral cavity 0.1% (3). Almost all patients had varying degrees of xerostomia, and many had dental caries.

Neck complications. The reported incidence of fibrosis of the soft tissue of the neck ranged from 2% (Mesic et al, 1981) to 16% (Marks et al, 1982), with a median of 13% (Hoppe et al, 1976). Our incidence of 16% (721/4527) for the whole series or 18% (721/3981) for those with cervical radiotherapy was among the highest reported. This resulted from the large weekly fraction used for neck irradiation. Although many had a "woody" feel, only 0.3% (15) had significant functional limitation. However, the possible association with neuropathy warrants greater concern.

Soft-tissue necrosis and persistent lymphoedema were detected in 0.4% (16) and 0.1% (5) of our patients, respectively. Almost half (10/21) of them had received additional booster doses or reirradiation.

Radiation-induced malignancy. Two (0.04%) of our patients developed osteosarcoma in the irradiated parts of the maxilla 10 and 13 years after the primary course of radiotherapy. Higher incidence is expected with longer follow-up, the reported rate in the literature being 1% (Ballantyne, 1975; Huang, 1980).

Dose equivalents

To allow for an easy description of this overall summary of late complications, only the dose equivalents estimated by the TDF method (Orton & Ellis, 1973) are presented in the text (see Table I for the exact fractionation schedules and their biological doses by linear-quadratic equation). The nominal standard dose concept (Ellis, 1969), however, is by no means flawless; calculation of brain dose must be interpreted with caution, as the capacity of neural tissues for repair and repopulation is grossly different from that of connective tissues on which Ellis' formula is derived. Special modifications (Pezner & Archambeau, 1981; Sheline et al, 1980), a correction factor for large fractional doses (Turesson & Notter, 1980), and even different basic concepts (Fowler, 1989) have been strongly advocated, and should be considered in future dose prescription.

Owing to the substantial quantity and complexity of the data accumulated, analyses of the factors affecting the incidence, the predictive accuracy of different biological formulae and the magnitude of aggravation by additional boosting and reirradiation will be presented in subsequent papers.

Conclusions

While it is not advisable to compromise the chance of tumour eradication for fear of inducing treatment morbidity, it cannot be overemphasized that meticulous care in planning and administration of radiotherapy is vital in avoiding unnecessary damage. Large fractional doses should not be used if machine availability allows. With increasing accuracy in the delineation of tumour extent by modern investigative methods, additional shielding should be carefully tested in properly staged early cases. Development of effective and non-toxic radioprotectors is awaited. It is important that future efforts be directed not only at improving the chances of survival for patients with NPC, but also towards reducing the price they have to pay for their survival.

Acknowledgments

The authors with to thank Drs Myo Thaw, S. K. Au, T. K. Yau, T. W. Leung, M. Cheung, V. Hsue, W. H. Kwan, P. Choi and C. H. Ying for their assistance in the data entry; Mr W. H. Ho, K. M. Poon and Ms R. Lam for tracing the data; Drs W. H. Lau, V. K. C. Tse, G. K. H. Au and Mr. C. L. Chan for their advice in the data collection; Drs V. K. C. Tse, G. K. H. Au and all staff of the Institute for their contribution in the management of this series of patients; and IBM for their generous donation of computer equipment.

References

BAKER, S. R., 1980. Nasopharyngeal carcinoma: clinical course and results of therapy. *Head and Neck Surgery, 3*, 8–14.

BALLANTYNE, A. J., 1975. Late sequelae of radiation therapy in cancer of the head and neck with particular reference to the nasopharynx. *American Journal of Surgery, 130*, 433–436.

BARENDSEN, G. W., 1982. Dose fractionation, dose rate and isoeffect relationships for normal tissue responses. *International Journal of Radiation Oncology, Biology, Physics, 8*, 1981–1997.

BOHORQUEZ, J., 1976. Factors that modify the radio-response of cancer of the nasopharynx. *American Journal of Roentgenology, 126*, 863–876.

CELLAI, E., CHIAVACCI, P., OLMI, P. & CARCANGIU, M. L., 1982. Carcinoma of the nasopharynx: results of radiation therapy. *Acta Radiologica Oncology, 21* (Fasc. 2), 87–95.

CHANG, C., LIU, T., CHANG, Y. & CAO, S., 1980. Radiation therapy of nasopharyngeal carcinoma. *Acta Radiologica Oncology, 19* (Fasc. 6), 433–438.

CHATANI, M., TESHIMA, T., INOUE, T., AZUMA, I., YOSHIMURA, H., OSHITANI, T., HASHIBA, M., NISHIYAMA, K., TSUTSUI, K., FUJIMURA, T., ARAKI, Y., HISHIYAMA, Y., ARITA, S., YAMADA, C., KONDO, K., KAGEMOTO, M., TANAKA, M. & IMAJO, Y., 1986. Radiation therapy for nasopharyngeal carcinoma: retrospective review of 105 patients based on a survey of Kansai Cancer Therapist Group. *Cancer, 57*, 2267–2271.

CHENG, V. S. T. &SCHULZ, M. D., 1975. Unilateral hypoglossal nerve atrophy as a late complication of radiation therapy of head and neck carcinoma: a report of four cases and a review of the literature on peripheral and cranial nerve damages after radiation therapy. Cancer, 35, 1537–1544.

DE SCHRYVER, A., WACHTMEISTER, L. & BARYD, I., 1971. Ophthalmologic observations on long-term survivors after radiotherapy for nasopharyngeal tumours. *Acta Radiologica Therapy Physics Biology, 10*, 193–209.

ELLIS, F., 1969. Dose, time and fractionation. A clinical hypothesis. *Clinical Radiology, 20*, 1–7.

FLORES, A. D., DICKSON, R. I., RIDING, K. & COY, P., 1986. Cancer of the nasopharynx in British Columbia. *American Journal of Clinical Radiology, 9* (4), 281–291.

FOWLER, J. F., 1989. The linear quadratic formula and progress in fractionated radiotherapy. *British Journal of Radiology, 62*, 679–694.

HAGHBIN, M., KRAMER, S. & PATCHEFSKY, A. S., 1985. Carcinoma of the nasopharynx: a 25-year study. *American Journal of Clinical Radiology, 8*, 384–392.

HO, J. H. C., 1978. An epidemiologic and clinical study of nasopharyngeal carcinoma. *International Journal of Radiation Oncology, Biology, Physics, 4*, 181–198.

HO, J. H. C., 1982. Nasopharynx. In *Treatment of Cancer*, ed. by K. E. Halnan, J. L. Boak, D. Crowther, C. E. von Essen, J. S. Orr and M. J. Peckham (Chapman and Hall, London), pp. 249–267.

HOPPE, R. T., GOFFINET, D. R. & BAGSHAW, M. A., 1976. Carcinoma of the nasopharynx: eighteen years' experience with megavoltage radiation therapy. *Cancer, 37*, 2605–2612.

HUANG, S.-C., 1980. Nasopharyngeal cancer: a review of 1605 patients treated radically with cobalt 60. *International Journal of Radiation Oncology, Biology, Physics, 6*, 401–407.

HUANG, S.-C. & CHU, G.-L., 1981. Nasopharyngeal cancer: study II. *International Journal of Radiation Oncology, Biology, Physics, 7, 713–716.*

KAPLAN, E. L. & MEIER, P., 1958. Nonparametric estimation from incomplete observations. *Journal of American Statistic Association, 53*, 457–481.

LAM, K. S. L., HO, J. H. C., LEE, A. W. M., TSE, V. K. C., CHAN, P. K., WANG, C., MA, J. T. C. & YEUNG, R. T. T., 1987. Symptomatic hypothalamic–pituitary dysfunction in nasopharyngeal carcinoma patients following radiation therapy: a retrospective study. *International Journal of Radiation Oncology, Biology, Physics, 13*, 1343–1350.

LAM, K. S. L., TSE, V. K. C., WANG, C., YEUNG, R. T. T. & HO, J. H. C., 1991. Effects of cranial irradiation on hypothalamic–pituitary function: a 5-year longitudinal study in patients with nasopharyngeal carcinoma. *Quarterly Journal of Medicine, New Series 78* (No. 286), 165–176.

LEE, A. W. M., NG, S. H., HO, J. H. C., TSE, V. K. C., POON, Y. F., TSE, C. C. H., AU, G. K. H., O, S. K., LAU, W. H. & FOO, W., 1988. Clinical diagnosis of late temporal lobe necrosis following radiation therapy for nasopharyngeal carcinoma. *Cancer, 61*, 1535–1542.

LEE, A. W. M., CHENG, L. O. C., NG, S. H., TSE, V. K. C., O, S. K., AU, G. K. H. & POON, Y. F., 1990. Magnetic resonance imaging in the clinical diagnosis of late temporal lobe necrosis following radiotherapy for nasopharyngeal carcinoma. *Clinical Radiology, 41*, 24–41.

MARKS, J. E., BEDWINEK, J. M., LEE, F., PURDY, J. A. & PEREZ, C. A., 1982. Dose–response analysis for nasopharyngeal carcinoma: an historical perspective. *Cancer, 50*, 1042–1050.

MESIC, J. B., FLETCHER, G. H. & GOEPFERT, H., 1981. Megavoltage irradiation of epithelial tumours of the nasopharynx. *International Journal of Radiation Oncology, Biology, Physics, 7*, 447–453.

ORTON, C. G. & ELLIS, F., 1973. A simplification in the use of the NSD concept in practical radiotherapy. *British Journal of Radiology, 46*, 529–537.

PARSONS, J. T., FITZGERALD, C. R., HOOD, C. I., ELLINGWOOD, K. E., BOVA, F. J. & MILLION, R. R., 1983. The effects of irradiation on the eye and optic nerve. *International Journal of Radiation Oncology, Biology, Physics, 9*, 609–622.

PETO, R., PIKE, M. C., ARMITAGE, P., BRESLOW, N. E., COX, D. R., HOWARD, S. V., MANTEL, N., MCPHERSON, K., PETO, J. & SMITH, P. G., 1977. Design and analysis of randomized clinical trials requiring prolonged observation of each patient. *British Journal of Cancer, 35*, 1–39.

PEZNER, R. D. & ARCHAMBEAU, J. O., 1981. Brain tolerance unit: a method to estimate risk of radiation brain injury for various dose schedules. *International Journal of Radiation Oncology, Biology, Physics, 7*, 397–402.

QIN, D., HU, Y., YAN, J., XU, G., CAI, W., WU, X., CAO, D. & GU, X., 1988. Analysis of 1379 patients with nasopharyngeal carcinoma treated by radiation. *Cancer, 61*, 1117–1124.

ROTTENBERG, D. A., CHERNIK, N. L., DECK, M. D. F., ELLIS, F. & POSNER, J. B., 1977. Cerebral necrosis following radiotherapy of extracranial neoplasms. *Annals of Neurology, 1*, 339–357.

SAMAAN, N. A., VIETO, R., SCHULZ, P. N., MAOR, M., MEOZ, R. T., SAMPIERE, V. A., CANGIR, A., RIED, H. L. & JESSE JR, R. H., 1982. Hypothalamic, pituitary and thyroid dysfunction after radiotherapy to the head and neck. *International Journal of Radiation Oncology, Biology, Physics, 8*, 1857–1867.

SCANLON, P. W., RHODES, R. E., WOOLNER, L. B., DEVINE, K. D. & MCBEAN, J. B., 1967. Cancer of the nasopharynx: 142 patients treated in the 11 year period 1950–1960. *American Journal of Roentgenology, 99*, 313–325.

SHELINE, G. E., WARA, W. M. & SMITH, V., 1980. Therapeutic irradiation and brain injury. *International Journal of Radiation Oncology, Biology, Physics, 6*, 1215–1228.

Stein, M., Kuten, A., Arbel, M., Ben-Schachar, M., Epelbaum, R., Wajsbort, R., Klein, B., Cohen, Y. & Robinson, E., 1988. Carcinoma of the nasopharynx in Northern Israel: epidemiology and treatment results. *Journal of Surgical Oncology*, *37*, 84–88.

Tokars, R. P. & Griem, M. L., 1979. Carcinoma of the nasopharynx: an optimization of radiotherapeutic management for tumour control and spinal cord injury. *International Journal of Radiation Oncology, Biology, Physics*, *5*, 1741–1748.

Turesson, I. & Notter, G., 1980. An experimental study of single and fractionated high and continuous low dose rate irradiation on normal tissue. In *British Journal of Radiology, Special Report No. 17* (British Institute of Radiology, London), pp. 165–177.

Urdaneta, N., Fischer, J. J., Vera, R. & Gutierrez, E., 1976. Cancer of the nasopharynx: review of 43 cases treated with supervoltage radiation therapy. *Cancer*, *37*, 1707–1712.

Van Andel, J. G. & Hop, W. C. J., 1982. Carcinoma of the nasopharynx: a review of 86 cases. *Clinical Radiology*, *33*, 95–99.

Yamashita, S., Kondo, M., Inuyama, Y. & Hashimoto, S., 1986. Improved survival of patients with nasopharyngeal squamous cell carcinoma. *International Journal of Radiation Oncology, Biology, Physics*, *12*, 307–312.

1992, *The British Journal of Radiology*, *65*, 929–931

Technical notes

Localization of impalpable breast lesions using the Hawkins needle

By T. M. Walker, FRCR and *H. B. Ross, FRCS

Departments of Radiology and *Surgery, Royal Berkshire Hospital, Reading, Berkshire, UK

(Received 5 August 1991 and in revised form 18 November 1991, accepted 14 January 1992)

Keywords: Breast localization, Impalpable breast lesions

Pre-operative localization of impalpable breast lesions detected by mammography has become a routine procedure, especially in those units involved with breast screening. Various techniques are available to facilitate localization, either with the injection of dyes, or using one of a variety of flexible wires or rigid needles.

A new needle, the Hawkins needle*, has recently become available (Urratia et al, 1988), and we wish to describe its use in 99 patients.

Methods

The Hawkins needle (Fig. 1) is a co-axial system which consists of a rigid 20-gauge outer sheath with a blunt tip and a small window 1.5 cm from the tip; an inner core has a sharp tip and a spring-hook. When the inner core is advanced the needle point protrudes from the outer sheath; if the core is withdrawn the point is hidden in the sheath and the spring-hook protrudes from the window in the outer sheath. Clear markings at 1 cm intervals are etched on the needle shaft. The proximal end of the inner core has an 18-gauge hub welded to it. There is also a two-part removable plastic hub which fits over the proximal end of the needle. It is available in 10 cm or 12.5 cm lengths.

Radiographic localization can be performed with the use of either a fenestrated compression plate or stereotactic equipment; the needle may also be inserted under ultrasound guidance. After skin cleansing and local anaesthesia the needle is inserted at the appropriate site with the point of the inner core protruding from the sheath, and the spring-hook hidden. The needle is sufficiently sharp that a skin incision before insertion is not necessary. The plastic hub provides good purchase for positioning. The approximate depth for insertion can be estimated from a mammogram film taken at right angles to the plane of insertion. Ideally the tip of the needle should be placed about 1 cm distal to the suspect lesion. A check radiograph is taken following removal of the plastic hub to assess the proximity of the needle to the lesion. If the position is unsatisfactory it is very easy to reposition the needle correctly.

When the position is satisfactory the compression plate can be removed; care is needed to ensure that the needle is not dislodged at this stage. It is preferable that compression is released before the spring-hook is engaged. Gentle pressure on the needle during release will ensure that its tip remains at the original depth; once compression is removed the inner core of the needle can be withdrawn, revealing the spring-hook, which fixes the needle in the tissues. The point of fixation is at the site of the hook; if this is proximal to the lesion the needle tip may be withdrawn from the lesion during release of compression. When using a stereotactic localization technique with the tip of the needle accurately sited at the depth of the lesion it is especially important that the hook is not exposed before release of compression.

A radiograph is taken at right angles to the direction of insertion to check the correct depth (Fig. 2); if not satisfactory the needle can be repositioned after advancing the inner core to expose the needle point and conceal the spring-hook. When the position is adequate the needle can be taped to the chest wall; we have not found that the use of the plastic hub is necessary when taping the needle to the skin.

During surgery the initial incision can be made at any appropriate site; as the needle is rigid the area containing its tip can readily be palpated by movement of its exposed proximal end. When the tissue to be excised is located the surgeon can remove the needle intact by advancing the inner core to conceal the hook and withdrawing the whole unit. It is not necessary to cut the needle with wire cutters.

Results

The Hawkins needle has been used for 107 localization procedures in 99 patients; in six women two needles were inserted to localize separate lesions in the same breast, and in two women bilateral needles were inserted. The majority of localizations were performed using a perforated compression plate, but six were inserted using a stereotactic attachment and one under ultrasound guidance. Localization was achieved without repositioning the needle in 77 procedures, while some degree of adjustment was required on 30 occasions, mainly because of inaccurate depth placement. In 44 cases the final films showed that the needle passed through part of the suspect lesion or was within the area of microcalcifications; in 48 cases it was immediately

---

*Available from: E-Z-EM Ltd, 1230 High Road, London N20 0LH, UK.

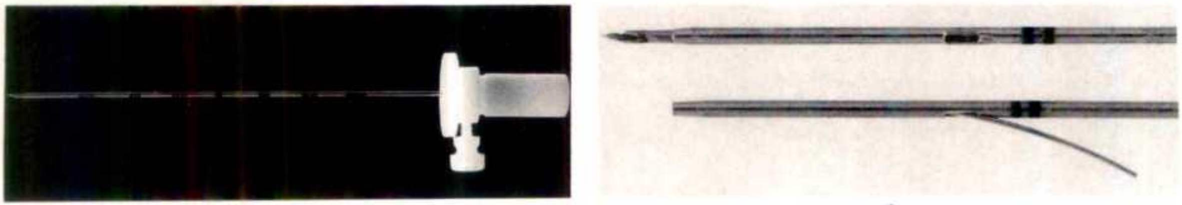
(a) (b)

Figure 1. The Hawkins needle. (a) The complete needle assembly showing the detachable hub; the centimetre markings on the needle shaft are clearly seen. (b) The upper illustration shows the inner core advanced, exposing the sharp tip and hiding the spring-hook. The lower illustration shows the needle with the inner core withdrawn, exposing the hook and concealing the needle tip.

adjacent to the lesion, and in 14 it was within 1 cm of the edge of the abnormality; in only one patient was the needle more than 1 cm from the lesion. Surgery was performed in each patient within 4 h of needle placement.

The suspect lesion was excised in every case except one, although in four cases the lesion was not seen on the inital specimen radiograph and additional tissue was excised. In one patient the suspect lesion was seen on follow-up radiographs after 6 months, even though successful excision was thought to have been performed at the time of surgery.

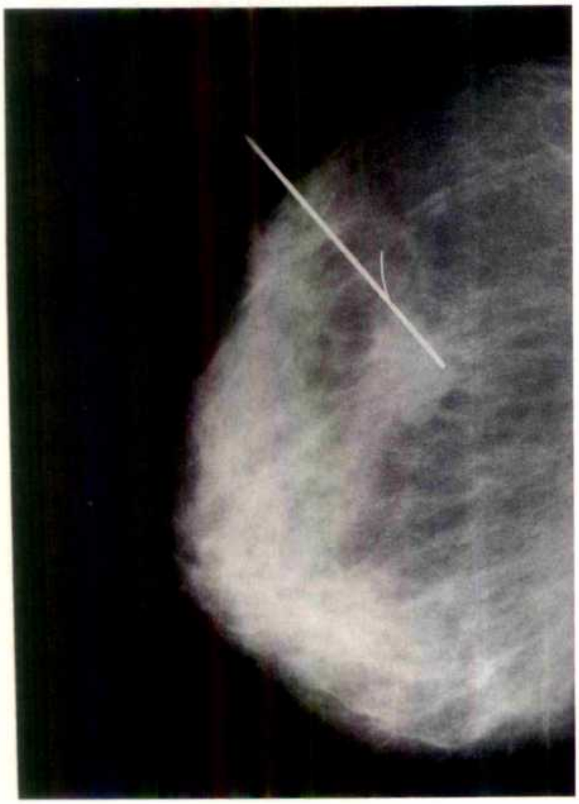

Figure 2. The needle *in situ*. The shaft passes through the posterior edge of an impalpable mass lesion; the spring-hook can clearly be seen, and is placed slightly proximal to the edge of the mass. A 10 mm invasive ductal carcinoma was completely excised.

No complications were encountered during the procedures and no patient complained of undue discomfort. In no case was the needle dislodged from the breast before surgery, although radiographs were not taken immediately before operation to check the position of the needle.

Discussion

Various localization techniques had been used in this unit before the Hawkins needle became available. Initially a flexible spring-hook wire was used (Kopans & DeLuca, 1980), but during surgery it proved difficult to locate the tip of the wire within the breast, and the initial skin incision had to be made at the site of wire insertion. The Homer "Mammolok" needle was then used (Homer, 1985), with the advantage that it was easily palpable in the tissues; however, the hook of this needle was often difficult to advance in dense breast tissue and frequently caused patient discomfort; on some occasions the needle became partially withdrawn after insertion in the X-ray department, particularly during skin cleansing in the operating theatre.

The Hawkins needle overcomes the disadvantages of both these systems. It is a rigid needle and can therefore be palpated by the surgeon, allowing optimal initial skin incision. Its very sharp point does not cause discomfort during insertion, and the patient does not not appear to feel the hook being withdrawn. Its design ensures that, once in position, it is unlikely to move; the blunt tip of the outer sheath makes it difficult to advance the needle inadvertantly, and Urratia et al (1988) have shown that the Hawkins needle will withstand a greater withdrawal tension than either the Kopans wire or the Homer needle.

One problem can arise when using the needle with a stereotactic attachment; our Siemens unit has two needle guides each with a hole through which the needle is inserted. The shaft of the Hawkins needle passes easily through a 0.9 mm hole in the guides, but these cannot be withdrawn over the hub which is slightly larger than the shaft; guides with 1.2 mm holes must be used. A modification of the needle guides is being developed which will allow direct removal of the localization needle from the needle guides.

The Hawkins needle has been found to have significant advantages over other types of localization wire or needle which have been used in this hospital. Although other new localization needles have also become available in Britain the Hawkins needle has been shown to fulfil the requirements of both radiologist and surgeon.

Acknowledgments
We wish to thank the radiographers and nursing staff of the X-ray Department for their help and understanding when using this needle on our patients.

References

HOMER, M. J., 1985. Nonpalpable breast lesion localization using a curved-end retractable wire. *Radiology*, *157*, 259–260.

KOPANS, D. B. & DELUCA, S., 1980. A modified needle-hookwire technique to simplify preoperative localization of occult breast lesions. *Radiology*, *134*, 781.

URRATIA, E. J., HAWKINS, M. C., STEINBACH, B. G., MEACHAM, M. A., BLAND, K. I., COPELAND, E. M. & HAWKINS, I. F., 1988. Retractable-barb needle for breast lesion localization: use in 60 cases. *Radiology*, *169*, 845–847.

Single energy quantitative computed tomography: the effects of phantom calibration material and kVp on QCT bone densitometry

By R. W. Whitehouse, BSc, MB, ChB, FRCR and J. E. Adams MB, BS, FRCP, FRCR

Department of Diagnostic Radiology, University of Manchester, Oxford Road, Manchester M13 9PT, UK

(*Received 21 November 1991 and in revised form 24 February 1992, accepted 26 March 1992*)

Keywords: QCT mineral densitometry, Reference phantom, Effective energy

Introduction

Bone mineral densitometry by quantitative computed tomography (QCT) was introduced in 1976 (Isherwood et al 1976), and is now a clinically established and useful technique. It is usually performed with a reference phantom scanned with the patient. The reference phantom is required to correct for variations that may occur in measured CT numbers due to CT scale drifts or changes in effective beam energy (Cann and Genant 1980). The measured CT number in a region of interest is expressed in mineral density equivalents of phantom reference material.

A saturated solution of dipotassium hydrogen phosphate (K_2HPO_4) in water has been used in dosimetry as a cortical bone equivalent material for many years (Witt and Cameron, 1969) and dilutions of this material are popular for QCT reference phantoms used in trabecular bone mineral densitometry (Cann and Genant, 1980). Several potential sources of error have been identified with reference phantoms containing aqueous solutions of K_2HPO_4, including changes in concentration of the solute with time and displacement effects (Rao et al, 1987). These problems have stimulated searches for alternative reference materials, the most popular of which has been calcium hydroxyapatite. This has been regarded as preferable to K_2HPO_4 as calcium hydroxyapatite is a true constituent of bone. Calcium hydroxyapatite is not water soluble and has to be embedded in a water equivalent plastic. The attenuations of K_2HPO_4 and calcium hydroxyapatite alter with X-ray energy in similar, but not identical, rates to that of bone (Hubbell, 1969; ICRU, 1989). It has been recommended that single energy QCT bone mineral densitometry be performed at the lowest possible kVp as the increasing contribution of the photoelectric effect to the total measured attenuation will then make the measurement more sensitive to high atomic number elements such as calcium in bone mineral (Cann, 1987). Mineral densitometry may be performed on a variety of CT scanners, some of which can scan at energies as low as 70 kVp but many of which have a fixed scanning energy, usually around 120 kVp. The material with the energy-dependent attenuation closest to that of bone over this range of kVps should give the best inter-scanner consistency for bone mineral densitometry *in vivo*.

An alternative approach to avoid the probable energy and reference material dependency of QCT mineral densitometry is to use the phantom to determine the effective energy of the scan and then to calculate the theoretical Hounsfield number of bone at this energy from its assumed composition. A dual energy QCT technique has been described using such an effective energy approach (Nickoloff et al, 1988). This theoretical Hounsfield number and the theoretical mineral content of bone can then be used to construct a new calibration curve of Hounsfield number against true bone mineral content for mixtures of bone in water. An effective energy method of single energy QCT using either K_2HPO_4 or potassium iodide in water as reference materials showed the improved precision of this approach (Crawley et al, 1989), but a tissue modelling approach to express the results after correction for the true composition of bone was not performed. Theoretical analysis of the influence of phantom type

---

Address correspondence to Dr R.W. Whitehouse.

and also marrow composition on QCT mineral densitometry has been described, indicating the probable influence of these factors (Crawley et al, 1988).

The following experiment was performed to test the differential effects of the phantom reference material, the scanner energy and the method of analysis on single energy QCT mineral densitometry of cortical bone and to measure the influence of these factors on the result obtained. Femoral cortical bone was chosen to avoid the complicating influence of marrow composition on the results (Mazess, 1983).

Materials and methods

Informed consent for additional sections to be performed was obtained from 15 patients attending the department for vertebral trabecular bone mineral densitometry by QCT. Three additional scans were performed through the mid-femoral shafts at 80 kVp, 120 kVp and 140 kVp, using either the Cann and Genant University of California, San Francisco (UCSF) phantom (eight patients) containing K_2HPO_4 in water, or the General Electric (GE) phantom (seven patients) containing calcium hydroxyapatite in plastic. The CT numbers of the reference phantom materials, air, water (or water equivalent plastic) and the cortical bone of both femoral shafts were then measured on each scan. Femoral cortical bone mineral density was then calculated by two methods from each scan.

Method 1

Conventional single-energy QCT mineral densitometry (SEQCT): linear regression of each concentration of mineral equivalent material in the phantom against its CT number value was used to produce a calibration curve for each scan. The CT number of cortical bone was converted into a mineral equivalent (in mg/ml) from this calibration curve.

Method 2

Effective energy approach: all CT numbers were first converted to Hounsfield numbers by recalibration against the measured attenuation of air and water on each scan (Brooks, 1977). The Hounsfield number of each concentration of mineral equivalent material in each phantom was then corrected for displacement of the surrounding medium (Rao et al, 1987) before linear regression was performed as above. The slope of this calibration curve was then used to determine the effective energy of the scan after the method of Nickoloff et al (1988). Assuming cortical bone consists of 1.112 g/ml calcium hydroxyapatite, 0.614 g/ml collagen and 0.192 g/ml water (ICRU, 1989), the theoretical Hounsfield number of cortical bone was calculated for each scan at each kVp, using energy dependent coefficients (Nickoloff and Feldman, 1985; Nickoloff et al, 1988), calculated from published tables of linear attenuation coefficients (Hubbell, 1969; ICRU, 1989). Linear attenuation coefficient values for effective energies lying between those tabulated were calculated by interpolation using best-fit polynomial regressions (Nickoloff, personal communication, 1990). A calibration curve for the Hounsfield numbers of mixtures of theoretical bone in water was then constructed and used to convert the Hounsfield number of each region of cortical bone into a mineral density.

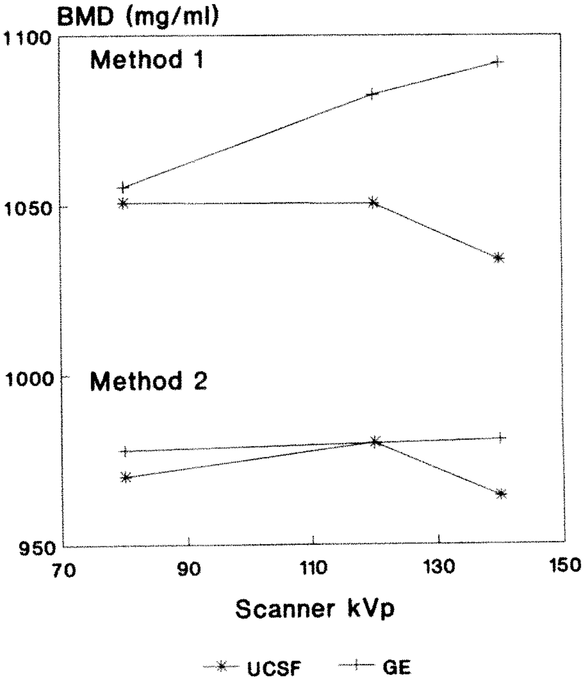

Figure 1. QCT mineral density for femoral cortical bone using two reference phantoms (UCSF containing dipotassium hydrogen phosphate and GE containing calcium hydroxyapatite) and two analysis methods (Method 1—conventional QCT; Method 2—effective energy approach) at three scanner energies.

Mineral density results for the same method in the same femur at different scan energies were compared with a Student's *t*-test for matched pairs; comparisons between the different phantoms using the same method were made using a *t*-test for unmatched groups.

Results

The mean bone mineral densities (BMD) for cortical bone by each method with each reference phantom are expressed graphically in Fig. 1.

Method 1

The mineral density measured using the GE phantom increased significantly with increasing energy ($p < 0.01$) from 1055.6 ± 71.9 mg/ml (mean ± 1SD, $n = 7$) at 80 kVp to 1082.3 ± 73.3 mg/ml at 120 kVp and 1091.7 ± 67.8 mg/ml at 140 kVp. Using the UCSF phantom constant mineral density results were obtained at 80 kVp (1050.8 ± 57.3 mg/ml; mean ± 1SD, $n = 8$) and 120 kVp (1050.5 ± 54.2 mg/ml) but a significant decrease occurred between 120 and 140 kVp (1034 ± 50.5 mg/ml, $p < 0.05$). A significant difference ($p < 0.05$) between cortical bone mineral density as measured by the two phantoms was evident at 140 kVp, but not at 80 or 120 kVp.

Method 2

All mineral density results were significantly lower by this method than by Method 1 ($p < 0.01$). Both phantoms gave similar values for the mineral content of cortical bone at all energies, the GE phantom showing no significant change in mineral density with scan energy (977.4 ± 65.7 mg/ml at 80 kVp, 979.8 ± 65.2 mg/ml at 120 kVp and 980.9 ± 60.3 mg/ml at 140 kVp; means ± 1SD, $n = 7$) whilst the UCSF phantom showed a small but statistically significant variation in mean mineral density with increasing energy (970.2 ± 53.7 mg/ml at 80 kVp, 980 ± 50.2 mg/ml at 120 kVp and 964.1 ± 46.5 mg/ml at 140 kVp; means ± 1SD, $n = 8$). There was no significant difference in mean mineral content measured by the two phantoms at any energy using this second analysis method.

Discussion

The results of the study indicate that the BMD measurements made by conventional SEQCT are dependent on both choice of phantom material and scanner energy. This may explain some of the variation in BMD measurements between scanners noted by previous investigators (Cann, 1987). Not all scanners are capable of scanning at the low energy (80 kVp or lower) recommended for mineral densitometry. The K_2HPO_4 phantom gave a more consistent result for mineral content over the 80–120 kVp range in which most scanners operate. The alternative approach (Method 2) utilizing effective beam energy determination gave results largely independent of both the phantom type and the scanner energy and this was particularly consistent for the GE phantom. The apparent increasing mineral density of bone with increase in scanner energy with the GE phantom reflects the high collagen content of bone, for which no allowance can be made by the phantom (Goodsitt et al, 1988). The Hounsfield number of collagen increases with increasing energy, whilst that of bone mineral decreases. The attenuation of collagen contributes to bone mass measurement and will thus cause the attenuation of bone to decrease less rapidly with increasing energy than that of bone mineral. The presence of collagen also accounts for the higher mineral content as measured by either phantom at any energy by Method 1, as only the contribution made by mineral is calculated in Method 2.

These factors also have significance for post-processing dual-energy QCT mineral densitometry, used to correct trabecular bone estimations for the influence of fat (Cann and Genant, 1983). One basic assumption made of dual-energy QCT is that bone will have the same QCT mineral density at both scan energies, any deviation from this being considered to be due to the influence of marrow components (Genant and Boyd, 1977). For conventional single energy QCT, at 80 and 140 kVp, neither phantom gave the same density for cortical bone. Thus by combining the results of the two scans for a dual-energy calculation errors will be generated. The UCSF phantom shows less energy dependence than the GE phantom in this respect. For the effective energy approach as described by Nickoloff et al (1988), the GE phantom appears ideal, with almost no infuence of scan energy on the measured mineral density of bone.

Over the energy range 80–120 kVp, the UCSF phantom gives more consistent results than the GE phantom for conventional single energy QCT. This reflects the closer relationship between the mass attenuation coefficients of bone and dipotassium hydrogen phosphate in this energy range than that between bone and calcium hydroxapatite. As observed in the ICRU report No.44 (1989), CT reference materials should have mass attenuation coefficients within 1% of the substance being measured over the energy range being used. The current study suggests that calcium hydroxyapatite in water equivalent plastic fails to fulfil this requirement, but describes an effective energy approach which overcomes the problem. Reference phantoms containing other materials (*e.g.* calcium carbonate; Suzuki et al, 1991) are also being produced. The energy-dependent relationship between the attenuation values of these materials and bone should be evaluated before such phantoms become established in clinical use.

In practice SEQCT is most commonly performed to measure trabecular bone density in vertebrae (Genant et al, 1982, 1989) and the presence of red and yellow marrow in varying proportion will affect the results (Crawley et al, 1988). The Hounsfield numbers of red and yellow marrow alter differently with energy, but the Hounsfield number of both increases with increasing scan energy (ICRU, 1989). This may exaggerate the energy-dependent change in measured mineral content with an hydroxyapatite phantom. Further studies to assess these different phantoms and methods of analysis on trabecular bone mineral measurements *in vivo* are required.

Acknowledgments

Provision of the hydroxyapatite phantom and support for the research fellow in computed tomography (RWW) from IGE is gratefully acknowledged.

References

Brooks, R. A., 1977. A quantitative theory of the Hounsfield unit and its application to dual energy scanning. *Journal of Computer Assisted Tomography*, *1*, 487–493.

Cann, C. E., 1987. Quantitative CT applications: Comparison of current scanners. *Radiology*, *162*, 257–261.

Cann, C. E. & Genant, H. K. 1980. Precise measurement of vertebral mineral content using computed tomography. *Journal of Computer Assisted Tomography*, *4*, 493–500.

Cann, C. E. & Genant, H. K., 1983. Single versus dual energy CT for vertebral mineral quantification (abstract). *Journal of Computer Assisted Tomography*, *7*, 551–552.

Crawley, E. O., Evans, EW. D. & Owen, G. M., 1988. A theoretical analysis of the accuracy of single energy CT bone-mineral measurements. *Physics in Medicine and Biology*, *33*, 1113–1127.

Crawley, E. O., Evans, W. D. & Owen, G. M., 1989. CT spinal bone mineral measurement—A method based on effective photon energy. In *Osteoporosis and Bone Mineral Measurement*, ed. by E. F. J. Ring, W. D. Evans and A. S. Dixon (IPSM Publications, York), pp.79–91.

Genant, H. K., Block, J. E., Steiger, P., Glueer, C. C., Ettinger, B. & Harris, S. T., 1989. Appropriate use of bone densitometry. *Radiology, 170*, 817–822.

Genant, H. K. & Boyd, D., 1977. Quantitative bone mineral analysis using dual energy computed tomography. *Investigative Radiology, 12*, 545–551.

Genant, H. K., Cann, C. E., Ettinger, B. & Gordon, G. S., 1982. Quantitative computed tomographs of vertebral spongiosa: a sensitive method for detecting early bone loss after oophorectomy. *Annals of Internal Medicine, 97*, 699–705.

Goodsitt, M. M., Kilcoyne, R. F., Gutcheck, R. A., Richardson, M. L., & Rosenthal, D. I., 1988. Effect of collagen on bone mineral analysis with CT. *Radiology, 167*, 787–791.

Hubbell, J. H., 1969. Photon cross sections, attenuation coefficients and energy absorption coefficients from 10 keV to 100 GeV. National Standard Reference Data System—National Bureau of Standards (US GPO, Washington, DC) *29*, pp. 1–80.

International Commission on Radiation Units and Measurements (ICRU), 1989. *Tissue Substitutes in Radiation Dosimetry and Measurement*. ICRU Report No. 44, 1–189.

Isherwood, I., Rutherford, R. A., Pullan, B. R. & Adams, P. H., 1976. Bone mineral estimation by computer assisted transverse axial tomography. *Lancet, 2*, 712–715.

Mazess, R. B., 1983. Errors in measuring trabecular bone by computed tomography due to marrow and bone composition. *Calcified Tissue International, 35*, 148–152.

Nickoloff, E. & Feldman, F., 1985. Bone mineral assessment with dual energy computerised tomography (CT) imaging. *Seminar Proceedings of the Society of Photo-Optical Instrumentation Engineers, 555*, 178–187.

Nickoloff, E., Feldman, F. & Atherton, J. V., 1988. Bone mineral assessment: New dual energy approach. *Radiology, 168*, 223–228.

Rao, G. U., Yaghmai, I., Wist, A. O. & Arora, G., 1987. Systematic errors in bone-mineral measurements by quantitative computed tomography. *Medical Physics, 14*, 62–69.

Suzuki, S., Yamamuro, T., Okumura, H. & Yamamoto, I., 1991. Quantitative computed tomography: comparative study using different scanners with two calibration phantoms. *British Journal of Radiology, 64*, 1001–1006.

Witt, R. M. & Cameron, J. R., 1969. *Bone Standards, USAEC Progress Report No. COO-1422-42* (US Atomic Energy Comission, Madison, WI).

1992, *The British Journal of Radiology*, *65*, 935–938

Case reports

Second malignant neoplasm following treatment of Hodgkin's disease: a case report

By V. S. N. Rao, DMRT, K. A. Dinshaw, DMRT (Lond), FRCR (Lond), S. K. Shrivastava, MD, DNBR, M. A. Muckaden, MD, S. Susnerwala, DMRT, MD, DNBR, *S. H. Advani, MD, †J. J. Vyas, MS, FACS and ‡N. M. Kavarana, MS

Departments of Radiation Oncology, *Medical Oncology, †Surgical Oncology and ‡Plastic Surgery, Tata Memorial Hospital, Bombay, India

(*Received 28 August 1991 and in revised form 13 December 1991, accepted 11 February 1992*)

Keywords: Hodgkin's disease, Second malignant neoplasms, Second cancers

Improvement in the treatment of Hodgkin's Disease (HD) over the past decade has led to increased survival rates, particularly in the early stages. Recognition of long-term complications of the treatment have also increased. Prolonged survival following aggressive treatment of HD is accompanied by an increased risk of the oncogenic effects of radiotherapy and chemotherapy (Halperin et al, 1984). Second malignant neoplasms (SMN) may also develop after the primary has been successfully treated and cured (Kim et al, 1978; Valagussa et al, 1986; Boivin & O'Brien, 1988). We report a case of HD, successfully treated by combined modality treatment developing a chondrosarcoma arising in the chest wall 9 years later.

Case report

A 5-year-old female child presented to the Tata Memorial Hospital, in February 1980 with bilateral cervical and left axillary lymphadenopathy of 15 months duration. There was no history suggestive of "B" symptoms. The liver and spleen were not palpable. The chest radiography, bone marrow aspiration and biopsy and lymphogram were all normal. A biopsy of a cervical lymphnode revealed Hodgkin's disease of lymphocyte-predominance type. Thus she was staged clinically as Hodgkin's disease IIA as per the Ann-Arbor classification (Carbone, 1971). The child was treated by radical irradiation with ^{60}Co gamma rays to a total dose of 4000 cGy in 20 fractions over 36 days to the mantle field with a further boost of 1000 cGy in 1 week to the left supraclavicular fossa between March and April 1980. As the residual left supraclavicular nodes persisted after irradiation for nearly 3 months, she was given six cycles of COPP chemotherapy consisting of cyclophosphamide 600 mg/m^2 on day 1 and 8, vincristine 1.4 mg/m^2 on day 1 and 8, procarbazine 100 mg/m^2 day 1–15 and prednisolone 20 mg/day, day 1–15 and the cycle repeated every 28th day. She achieved complete remission.

The patient remained asymptomatic and disease-free for 9 years until February 1990. Stunted growth of the thoracic spine and reduction of sitting height were noted. She attained the menarche in 1986 at the age of 11 years. In February 1990, an opacity in the upper and middle zones of the left lung was reported on a routine chest radiograph (Fig. 1). She was treated with antibiotics and antifungal agents but with no apparent response. In July 1990, she presented with gradually increasing swelling in the left infraclavicular area. Radiographs revealed an expansile destruction of the anterior end of the left 2nd rib with punctate calcification. A "J" needle biopsy from the swelling showed a matrix forming chondroid and osteoid lesion. After the biopsy the patient was lost to follow-up.

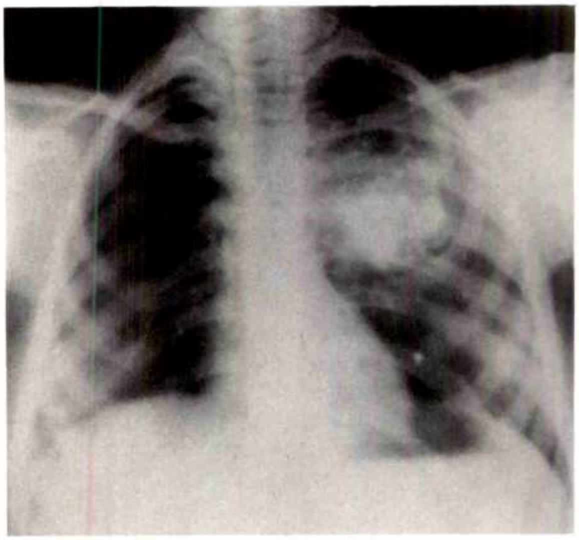

Figure 1. Chest X-ray showing opacity in upper and middle zones of left side of the chest.

In March 1991, she again presented with a large, fixed bony swelling 14 × 7 cm in size in the left upper anterior chest wall, extending to the left axilla (Fig. 2). A bone scan showed increased uptake in the left hemithorax including the sternum, 2nd to 5th left ribs anteriorly, left clavicle and left scapula. A fine needle aspiration cytology (FNAC) revealed "chondroid neoplasia with atypia". Further investigations were carried out to assess the extent and operability of the tumour. Computed tomography showed a large soft tissue mass arising from the

---

Address correspondence to Dr (Ms) K. A. Dinshaw, DMRT (Lond), FRCR (Lond), Head, Department of Radiation Oncology, Tata Memorial Hospital, Parel, Bombay 400 012, India.

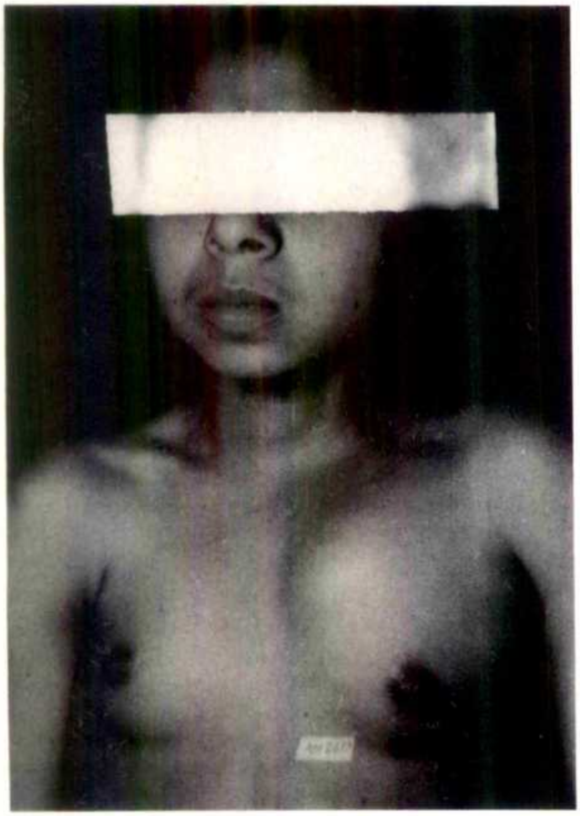

Figure 2. Clinical photograph showing left upper chest wall tumour.

left 2nd rib, infiltrating the thoracic wall, mediastinum, pericardium and surrounding tissues and displacing the major vessels and the trachea towards the right. There was evidence of extensive new bone formation (Fig. 3). An angiogram revealed a hypovascular mass in the left hemithorax with a short segmental occlusion of the left axillary artery. She was diagnosed as having developed a second malignant neoplasm (SMN) following radiotherapy and chemotherapy treatment for Hodgkin's disease.

At surgery, the pericardium was minimally tethered, therefore the tumour was considered operable and was removed together with three ribs, a part of the upper sternum and the medial end of the left clavicle. A left upper lobectomy was also carried out due to adhesions. Resection was incomplete. The chest wall defect was reconstructed by a cadaveric dura and a marlex mesh. The histopathology of the operative specimen was reported as a "moderately differentiated chondrosarcoma showing myxoid areas and foci of osteoid differentiation, infiltrating the ribs. Sections from the lung show no invasion by tumour".

The patient remained symptom free for 5 months following surgery. Thereafter, she developed massive recurrence over the upper chest wall, which was found to be inoperable.

Discussion

Development of a radiation induced sarcoma (RIS) is rare, although ionizing radiation is recognized as being capable of inducing bone tumours (Tucker et al, 1987). The direct cellular effects of radiation combined with immunosuppressive effects of chemotherapy are probably equally important as etiological factors for its induction (Smith et al, 1980).

Cahan et al (1948) described the criteria required to confirm RIS: (1) no antecedent lesion in the affected bone; (2) the sarcoma must develop within the area included in the therapeutic beam; (3) a long asymptomatic latent period between irradiation and clinical appearance of sarcoma must exceed the 5 year cure period; and (4) all sarcomas must be confirmed histologically. These criteria have been accepted by others (Kim et al, 1978; Tountas et al, 1979; Smith et al, 1980; Halperin et al, 1984), and our patient satisfied all these criteria. A pre-treatment chest film was normal. The

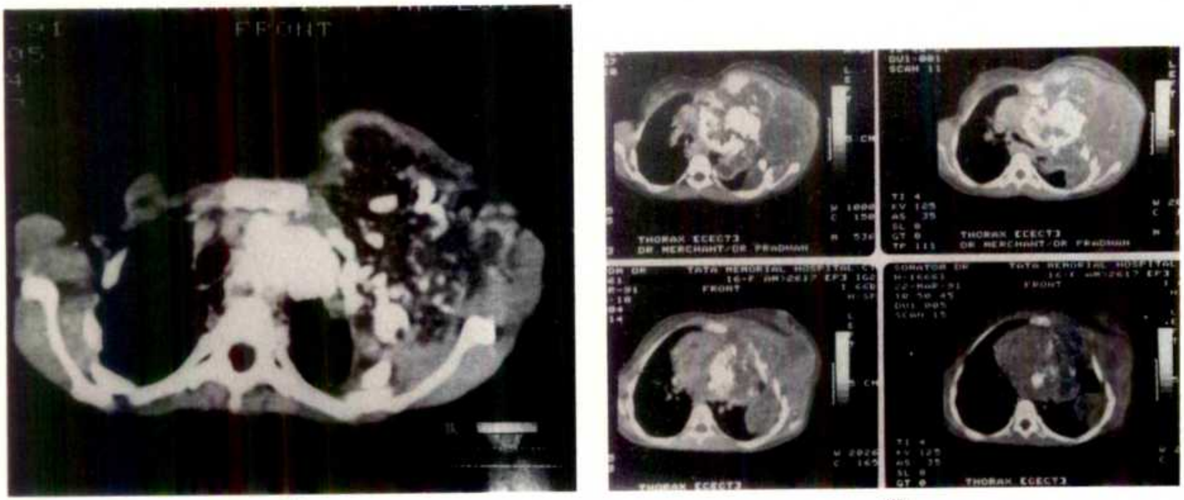

(a) (b)

Figure 3. (a) and (b) CT scan of the chest showing large soft tissue mass arising from left 2nd rib, infiltrating thoracic wall, mediastinum, pericardium and surrounding tissues, pushing the major vessels and trachea towards right side.

anterior end of the left 2nd rib was included in the radiation portal of the mantle field. There was a latent period of more than 9 years and the SMN was histologically confirmed to be chondrosarcoma.

The incidence of second cancers is steadily increasing following the treatment of HD (Smith et al, 1980; Souba et al, 1986; Tucker et al, 1988). The most common second tumours are leukaemias, especially ANLL, non-Hodgkin's lymphoma (NHL) and solid tumours. The increased risk of SMN is 5% and 23% at 10 years and 19 years respectively (Cimino et al, 1991). The Stanford group (Tucker et al, 1988), in their large series of 1507 patients reported the cumulative risk of second cancers at 15 years to be 17.6% as compared to 2.6% in the general population. They have observed a steep increase in the risk of developing solid tumours after 10 years but no new case of leukaemia was reported after 10 years. From McGill University, in a pooled analysis from seven studies, a 2.2-fold increased risk of second cancers in all anatomic sites was reported following radiotherapy (Boivin et al, 1988). An increased risk of second cancers seen in patients treated by a combination of radiotherapy and chemotherapy (Arseneau et al, 1972) has also been documented. In a study at the Princess Margaret Hospital, Toronto, the overall incidence of post-radiation sarcoma of bone is 0.035% of all irradiated 5 year survivors (Tountas et al, 1979). At the Royal Marsden Hospital, London, 38 (29 solid tumours and nine leukaemias) second malignancies were recorded in 36 patients among 730 cases of HD. The overall incidence of solid tumours was 3.8% and the relative risk was 3.2 (Colman et al, 1988). High incidences of leukaemias have been reported with chemotherapy especially with alkylating agents (Valagussa et al, 1986; Coleman et al, 1987; Tucker et al, 1987), whereas solid tumours were observed with radiotherapy alone or with adjuvant chemotherapy (Tucker et al, 1988). Radiotherapy and chemotherapy with alkylating agents for childhood cancers increase the subsequent risk of bone cancer (Tucker et al, 1987). The Stanford series has shown a higher actuarial risk of developing solid tumours in patients who received radiotherapy alone (7.0%) and a combination of radiotherapy and chemotherapy (11.7%), whereas the risk of leukaemia increases (11.5%) in patients treated with chemotherapy alone (Tucker et al, 1988). No excess risk of leukaemias was found with radiotherapy alone or with adjuvant chemotherapy groups. In patients with HD treated with ABVD, no case of acute leukaemia has been recorded (Valagussa et al, 1986; Cimino et al, 1991).

The latent period, which is the time between completion of treatment of primary HD and the development of the second malignancy is reported ranging from 6 to 13 years by many authors (Kim et al, 1978; Smith et al, 1980; Halperin et al, 1984; Souba et al, 1986; Cimino et al, 1991). Radiation-induced leukaemias have a shorter latency period (Kim et al, 1978). The interval for SMN in the field of radiation was 9.3 years compared with 10.3 years for those outside the field (Newton et al, 1991). The relation of radiation dose to the development of a sarcoma has also been documented by some workers. The greater the absorbed dose by bone, the greater the risk of inducing sarcomas (Tountas et al, 1979). A minimum threshold is reported to be 1000 cGy, below which the risk for RIS is minimal. However, a study from Princess Margaret Hospital has observed a low risk of bone sarcoma (0.05%–0.2%) with an absorbed bone dose range between 40 Gy and 70 Gy (Tountas et al, 1979). In their study, Smith et al (1980) found no absolute criteria for establishing a minimum radiation dose or latent period, but Kim et al (1978) concluded that, with a radiation dose of less than 3000 cGy and latent period shorter than 4 years, the development of RIS is unlikely. Tucker et al (1987) found a 40-fold increased risk when the radiation dose was more than 6000 cGy and the pattern of the risk was essentially the same whether the patients were treated with orthovoltage or megavoltage. It has been suggested that for radiation to induce malignant change, the injury to individual cells must be sufficient to cause genetic mutation, but insufficient to cause cell death (Cole et al, 1965), a situation that apparently arises at the margin of a radiation field.

Second cancers are usually more aggressive (Tountas et al, 1979) in nature having a high grade histology, a high tendency for recurrence and proclivity for distant metastasis (Souba et al, 1986). The histopathology is reported mainly as osteogenic sarcoma, fibrosarcoma, malignant fibrous histiocytoma, chondrosarcoma, etc. (Tountas et al, 1979; Halperin et al, 1984; Souba et al, 1986; Tucker et al, 1987). The majority of spontaneous osteogenic sarcoma cases are of the osteoblastic subtype whereas the tumours in irradiated sites tend to be of fibroblastic, telangiectatic, osteoblastic and chondroblastic subtypes (Newton et al, 1991).

Treatment of these cancers is mainly surgical (Smith et al, 1980; Souba et al, 1986). Unfortunately, the extent of resection is often limited by the proximity of the tumour to vital structures. The role of aggressive adjuvant chemotherapy is doubtful (Souba et al, 1986). The overall prognosis is very poor (Smith et al, 1980; Souba et al, 1986). When all sites are included, the 5 year disease-free survival rate is reported to be only 19% (Souba et al, 1986).

In conclusion, second malignant neoplasms are seen occasionally in long-term survivors. New treatment strategies are being explored to reduce these complications especially in childhood cancers, although treatment protocols should attempt to reduce the most serious consequences of therapy without compromising the excellent survival rates. The benefits of aggressive initial treatment outweigh the risk of development of second cancers.

References

Arseneau, J. C., Sponzo, R. W., Levin, D. L., Schnipper, L. E., Bonner, H., Young, R. C., Canellous, G. P., Johnson, R. E. & Devita, V. T., 1972. Nonlymphomatous malignant tumours complicating Hodgkin's Disease. *New England Journal of Medicine, 287*, 1119–1122.

1992, *The British Journal of Radiology*, *65*, 938–940

Boivin, J. F. & O'Brien, K., 1988. Solid cancer risk after treatment of Hodgkin's Disease. *Cancer*, *61*, 2541–2546.

Cahan, W. G., Woodard, H. Q., Higinbotham, N. L., Stewart, F. W. & Coley, B. L., 1948. Sarcoma arising in irradiated bone. *Cancer*, *1*, 3–29.

Carbone, P. P., 1971. Report of committee on Hodgkin's disease staging classification. *Cancer Research*, *31*, 1860–1861.

Cimino, G., Papa, G., Tura, S., Mazza, P., Rossi Ferrini, P. L., Bosi, A., Amadori, S., Lo Coco, F., D'Arcangelo, E., Giannarelli, D. & Mandelli, F., 1991. Second primary cancer following Hodgkin's Disease: Updated results of an Italian multicentric study. *Journal of Clinical Oncology*, *9*, 432–437.

Cole, L. J. & Nowel, P. C., 1965. Radiation carcinogenesis: The sequence of events. *Science*, *150*, 1782–1786.

Colman, M. & Selby, P., 1987. Second malignancies and Hodgkin's Diseases. In *Hodgkin's Disease*, ed. by P. Selby and T. J. McElwain (Blackwell Scientific Publications, Oxford), pp. 361–377.

Colman, M., Easton, D. F., Horwich, A. & Peckham, M. J., 1988. Second malignancies and Hodgkin's Disease: The Royal Marsden Hospital experience. *Radiotherapy and Oncology*, *11*, 229–238.

Halperin, E. C., Greenberg, M. S. & Suit, H. D., 1984. Sarcoma of bone and soft tissue following treatment of Hodgkin's Disease. *Cancer*, *53*, 232–236.

Kim, H. J., Chu, F. C., Woodard, H. Q., Melamed, M. R., Huvos, A. & Cantin, J., 1978. Radiation-induced soft-tissue and bone sarcoma. *Radiology*, *129*, 501–508.

Newton, W. A., Jr., Meadows, A. T., Shimada, H., Bunin, G. R., Vawter, G. F., 1991. Bone sarcomas as second malignant neoplasms following childhood cancer. *Cancer*, *67*, 193–201.

Smith, J., O'Connel, R. S., Huvos, A. G. & Woodard, H. Q., 1980. Hodgkin's Disease complicated by radiation sarcoma in bone. *British Journal of Radiology*, *53*, 314–321.

Souba, W. W., McKenna, R. J., Jr., Meis, J., Benjamin, R., Raymond, A. K. & Mountain, C. F., 1986. Radiation-induced sarcomas of the chest wall. *Cancer*, *57*, 610–615.

Tountas, A. A., Fornasier, V. L., Harwood, A. R., Leung, P. M. K., 1979. Postirradiation sarcoma of bone. A perspective. *Cancer*, *43*, 182–187.

Tucker, M. A., D'Angio, G. J., Boice, J. D., Jr,. Strong, L. C., Li, F. P., Stovall, M., Stone, B. J., Green, D. M., Lombardi, F., Newton, W., Hoover, R. N. & Fraumeni, J. F., Jr., For the Late Effects Study Group, 1987. Bone sarcomas linked to Radiotherapy and Chemotherapy in children. *New England Journal of Medicine*, *317*, 588–593.

Tucker, M. A., Coleman, C. N., Cox, R. S., Varghese, A. & Rosenberg, S. A., 1988. Risk of second cancers after treatment for Hodgkin's Disease. *New England Journal of Medicine*, *318*, 76–81.

Valagussa, P., Santoro, A., Fossati-Bellani, F., Banfi, A. & Bonadonna, G., 1986. Second acute leukaemia and other malignancies following treatment for Hodgkin's Disease. *Journal of Clinical Oncology*, *4*, 830–837.

Extradural paraganglioma with multiple skeletal metastases

By Rajesh Jindel, MD, A. K. Gupta, MD, *A. K. Mahapatra, MS, MCh, †C. S. Bal, MD, and R. M. Singhal, MD

Departments of Radiotherapy, *Neurosurgery and †Nuclear Medicine, All India Institute of Medical Sciences, New Delhi, India

(Received 6 August 1991 and in revised form 2 January 1992, accepted 6 March 1992)

Keywords: Extradural paraganglioma, Skeletal metastases, Radiotherapy, Chemotherapy

Tumours arising from the paraganglia (paragangliomas) are characteristically of low malignant potential, with only 10% developing distant metastases (North et al, 1990). Malignancy in paragangliomas is defined either by local invasion or spread to distant sites normally devoid of paraganglia (Irons et al, 1977; Jackson et al, 1982). We present a case with several unusual features: (1) the primary site of the tumour is in the extradural space at D7 and L3 levels (lesion at L3 not biopsied), (2) multiple skeletal metastases at a short interval after primary diagnosis, and (3) absence of mitoses both in the original specimen and the metastatic deposit.

Case report

A 29-year-old man presented in December 1989 with girdle pain in the upper abdomen for 3 months, descending numbness and paraparesis for 3 weeks and incontinence for 1 week.

He had paraparesis with diminished power in the right (4/5) and the left (3/5) legs, exaggerated knee jerks and extensor plantar responses. All other systems were within normal limits.

Radiographs of the spine showed destruction of the pedicle of the D7 vertebra with a paravertebral soft-tissue mass and collapse of the L3 vertebra. A myelogram revealed an extradural block at D7 level with displacement of the thecal sac anteriorly. There was anterior deviation of the contrast opposite the collapsed L3 vertebral body. This was confirmed by computed tomography (CT) of the spine (Fig. 1). A thyroid scan and urinary HVA and VMA estimation were within normal limits. A routine haemogram and serum chemistry were within normal limits.

Dorsal laminectomy was performed in January 1990 at D7 level with removal of extradural intraosseous tumour.

Address correspondence to Dr R. M. Singhal, MD, Additional Professor, Department of Radiotherapy, All India Institute of Medical Sciences, Ansari Nagar, New Delhi 110029, India.

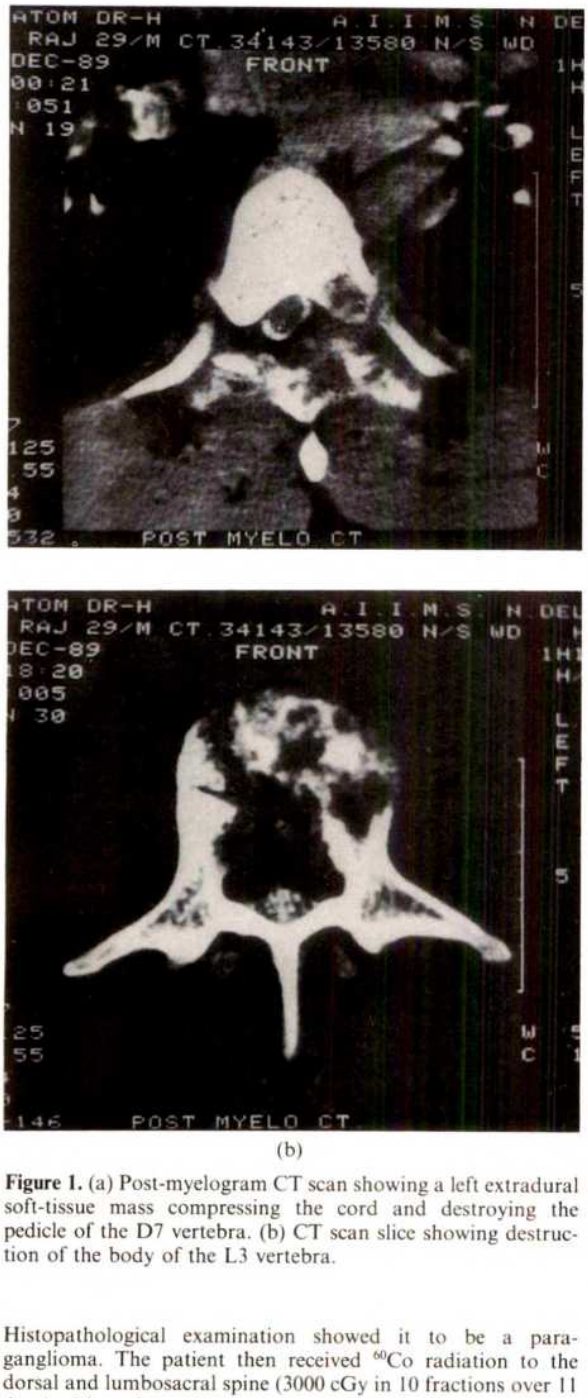

(b)

Figure 1. (a) Post-myelogram CT scan showing a left extradural soft-tissue mass compressing the cord and destroying the pedicle of the D7 vertebra. (b) CT scan slice showing destruction of the body of the L3 vertebra.

Histopathological examination showed it to be a paraganglioma. The patient then received ^{60}Co radiation to the dorsal and lumbosacral spine (3000 cGy in 10 fractions over 11 days) without immediate symptomatic improvement.

The patient returned after 8 months with complete recovery of paraparesis and complete control over bowel and bladder. However, he complained of a rapidly enlarging mass on the left frontal region. Biopsy showed a paraganglioma with histopathological features similar to the original specimen. A DMSA(v) bone scan showed areas of increased uptake compatible with skeletal metastases at the right 6th rib, iliac bone and left frontal bone.

He received radiation to the skull (4746 cGy in 20 treatments over 26 days) and subsequently chemotherapy with monthly cycles of cyclophosphamide, vincristine, adriamycin and DTIC for 2 months. There was a partial response in the swelling on the skull and a repeat DMSA(v) scan in April 1991 showed a reduced uptake at the previous sites.

Discussion

Paraganglioma (carotid body tumour, chemodectoma) may arise in any area of the body where paraganglia are situated (North et al, 1990). Paragangliomas are commonly bilateral and may be multicentric. Multicentricity occurs in approximately 10% of the tumours (Irons et al, 1977; Jackson et al, 1982). The incidence of metastases is close to 10% (range 2–50%) (Gaylis & Mieny, 1977; Zbaren & Lehmann, 1985). Generally, paraganglioma exhibit a prolonged interval (0–20 years) for the development of metastases/recurrence (Coulson, 1970; Whimster & Masson, 1970; Parnell & Dick, 1973; Osborn & Mojtahed, 1986).

Metastatic medullary carcinoma of the thyroid has often been confused with paraganglioma (Gongal et al, 1971). Owing to similarity of pathology, a thyroid scan and serum calcitonin levels are recommended as routine investigations for establishing the diagnosis of metastatic paraganglioma (Harrington et al, 1941; Willis & Berell, 1955; North et al, 1990).

Radiotherapy in conjunction with surgery is effective in the treatment of large, incompletely resected paraganglioma (Kim et al, 1980). Most authors currently recommend a dose of 4500 cGy (Zinreich & Lee, 1986). Kim et al (1980) compiled data from 10 studies and reported 90% (202/225 cases) local control with radiation for short follow-up periods. Konefal et al (1987) reported 80% local control with radiation from 26 cases with a median follow-up of 10.5 years. In patients receiving 4000 cGy post-surgery, the local control rate improved to 90% (Konefal et al, 1987).

No consistent therapy has been given for metastatic paraganglioma. In general, surgical resection of isolated metastases has proved useful. Various chemotherapy agents, including 5-fluorouracil and cisplatinum, have been tried, but without much success (Harrington et al, 1941; Say et al, 1973; Poster et al, 1979).

The reported case represents a multicentric origin of paraganglioma in the extradural space with multiple skeletal metastases.

References

Coulson, W. F., 1970. A metastasizing carotid body tumor. *Journal of Bone & Joint Surgery*, *52*(5), 355–360.

Gaylis, H. & Mieny, C. J., 1977. The incidence of malignancy in carotid body tumours. *British Journal of Surgery*, *64*, 885–889.

Gongal, D. N., Mack, G. J. & Vaidya, B. B., 1971. Extradural metastases form a presumed carotid body tumor producing paraplegia. A case report. *Canadian Journal of Surgery*, *14*, 410–412.

Harrington, S. W., Clagget, O. T. & Dockerty, M. B., 1941. Tumors of the carotid body: clinical and pathological considerations of 20 tumors affecting 19 patients (1 bilateral). *Annals of Surgery*, *114*, 820–823.

1992, *The British Journal of Radiology*, *65*, 940–942

IRONS, G. B., WIELAND, L. H. & BROWN, W. L., 1977. Paragangliomas of the neck. Clinical and pathological analysis of 116 cases. *Surgical Clinics of North America*, *57*, 575–583.

JACKSON, C. G., GLASSOCK, M. E. & NISSEN, A. J., 1982. Glomus tumor surgery: the approach, results and problems. *Otolaryngological Clinics of North America*, *15*, 897–916.

KIM, J. A., ELKON, D., LIM, M. L. & CONSTABLE, W. C., 1980. Optimum dose of radiotherapy for chemodectomas of the middle ear. *International Journal of Radiation Oncology, Biology, Physics*, *6*, 815–819.

KONEFAL, J. B., PILEPICH, M. V., SPECTOR, G. J. & PEREZ, C. A., 1987. Radiation therapy in the treatment of chemodectomas. *Laryngoscope*, *97*, 1331–1335.

NORTH, N. A., ZINREICH, E. S., CHRISTENSEN, W. N. & NORTH, R. B., 1990. Multiple spinal metastasis from paraganglioma. *Cancer*, *66*, 2224–2228.

OSBORN, R. E. & MOJTAHED, S., 1986. Paraganglioma metastatic to cervical spine. *Computers in Radiology*, *10*, 167–170.

PARNELL, A. P. & DICK, D. J., 1973. Extradural metastases from paraganglioma: report of two cases. *American Journal of Surgery*, *39*, 333–341.

POSTER, D. S., SCHAPIRO, H. & WORONOF, F. R., 1979. Chemodectomas: review and report of nine cases. *Journal of Medicine*, *10*(3), 207–223.

SAY, C. C., HORI, J. & SPRATT, JR, 1973. Chemodectomas with distant metastasis: case report and review of the literature. *American Journal of Surgery*, *39*, 333–341.

WHIMSTER, W. F. & MASSON, A. F., 1970. Malignant carotid body tumor with extradural metastases. *Cancer*, *26*, 239–244.

WILLIS, A. G. & BERELL, J. H. W., 1955. The structure of a carotid body tumor. *Acta Anatomica*, *25*, 220–225.

ZBAREN, P. & LEHMANN, W., 1985. Carotid body paraganglioma with metastasis. *Laryngoscope*, *95*, 450–454.

ZINREICH, E. S. & LEE, D. J., 1986. Radiotherapy for the treatment of paraganglioma in the temporal bone. *Ear Nose Throat Journal*, *65*(4), 181–184.

Intrathoracic lymphadenopathy and HIV infection

By N. C. Cowan, MA, MB, BChir, FRCR, *J. R. Salisbury, BSc, MB, BS, MRCPath and †J. Moxham, MD, FRCP

Departments of Radiology and *Pathology, King's College Hospital, London SE5 9RS, and †Department of Thoracic Medicine, King's College School of Medicine and Dentistry, Bessemer Road, London SE5 9PJ, UK

(Received 16 December 1991 and in revised form 6 April 1992, accepted 30 April 1992)

Keywords: Human immunodeficiency virus (HIV) infection, Intrathoracic lymphadenopathy, Bronchogenic carcinoma, Computed tomography

Case report

A 32-year-old homosexual man, known to be HIV-seropositive for 7 years, presented with a 2-month history of a productive cough, night sweats, lethargy, right-sided upper chest discomfort and exertional dyspnoea. He smoked 10–20 cigarettes per day. There was no other relevant past medical history.

The patient looked thin and unwell but was afebrile. Small lymph nodes were palpable in the neck, axillae and groin. A chest radiograph showed right paratracheal lymphadenopathy with adjacent ill-defined air-space consolidation in the right upper lobe (Fig. 1). At fibreoptic bronchoscopy the only abnormality was tracheal indentation from the right. Other investigations at presentation included a blood CD4 lymphocyte count of 386/mm^3 (normal value > 1000/mm^3), a CD8 lymphocyte count of 1819/mm^3, Hb 13.6 g/dl, WBC 10.6×10^9, granulocytes 7.7×10^9/l, lymphocytes 2.7×10^9/l; urea, electrolytes and liver function tests were normal except for an elevated alkaline phosphatase (105 IU/l).

Computed tomography (CT) of the thorax showed a large soft-tissue mediastinal mass that did not enhance significantly following intravenous contrast medium. The mass encased the ascending aorta, right pulmonary artery, trachea and carina and invaded the superior vena cava (Fig. 2). Cytological examination of a percutaneous mediastinal biopsy of the mass demonstrated large numbers of malignant cells, possibly lymphoid in origin. To achieve a definite diagnosis a second percutaneous biopsy was performed and yielded irregular fragments of pinkish-grey tissue with areas of haemorrhage. Histological examination of the biopsy showed dense fibrous tissue infiltrated by a pleomorphic tumour with a high mitotic index and extensive areas of necrosis. There was focal glandular configuration and neutral mucins could be demonstrated at the luminal border and in the cytoplasm of the tumour cells (Fig. 3). Immunohistochemistry, using the avidin–biotin–peroxidase complex technique, showed the presence of cytokeratins, epithelial membrane antigen and vimentin, patchily. The tumour was negative for leucocyte common antigen, excluding a lymphoma, and for Leu 7 and placental alkaline phosphatase, excluding an embryonal carcinoma of germ cell origin. The tumour was therefore demonstrated to be a poorly differentiated adenocarcinoma of the bronchus with spread to mediastinal lymph nodes.

The patient rapidly deteriorated with dyspnoea, dysphagia for solids and further upper chest pain. He developed superior vena caval obstruction and pain in his left arm. A radiograph showed a poorly defined lucent area of bony destruction in the proximal diaphysis of the left humerus which on biopsy was demonstrated to be metastatic adenocarcinoma.

Palliative treatment with chemotherapy plus radiotherapy was given to the mediastinum and humerus. The patient died at home several weeks later.

Address correspondence to Professor J. Moxham.

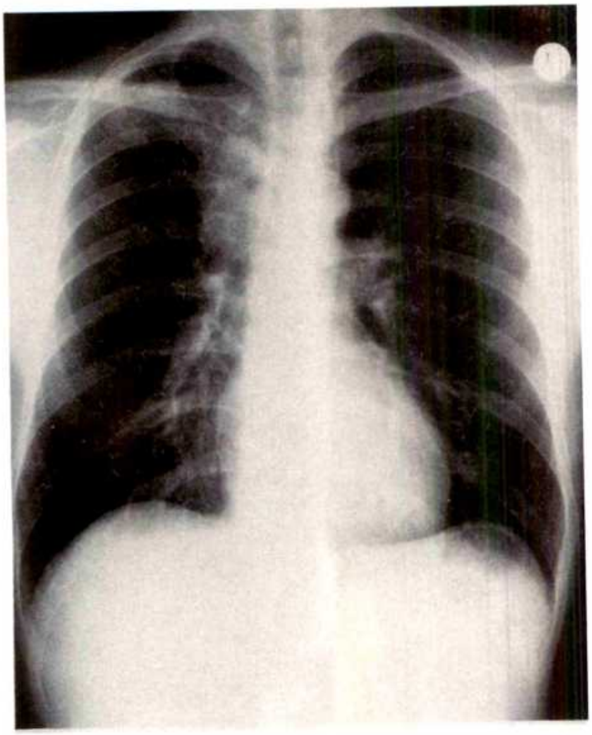

Figure 1. Chest radiograph showing right paratracheal lymphadenopathy with adjacent ill-defined air-space consolidation in the right upper lobe.

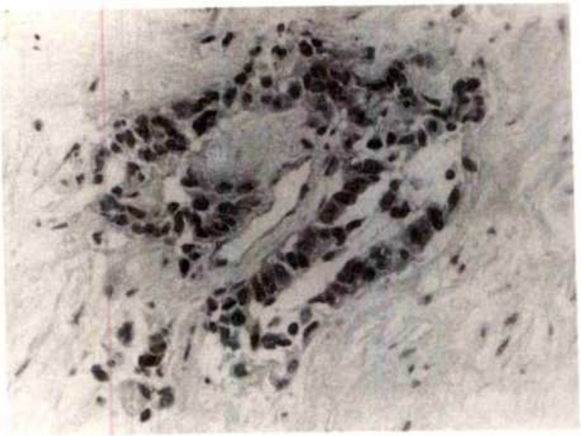

Figure 3. Mediastinal biopsy specimen showing fibrous tissue infiltrated by poorly formed glandular structures. The appearances were those of poorly differentiated adenocarcinoma of the bronchus.

Discussion

The aim of this report is to emphasize that lung cancer may occur in the young HIV-infected population and should be included in the differential diagnosis of intrathoracic lymphadenopathy in this patient group. Diagnosis may be delayed for two reasons. Firstly, patients are in a younger age group than is usually associated with bronchogenic carcinoma. Secondly, they commonly have opportunistic infections and HIV-related malignancies with radiographic signs similar to those of bronchogenic carcinoma.

Intrathoracic lymphadenopathy in HIV-seropositive patients most commonly indicates *Mycobacterium tuberculosis* infection (Hewlett et al, 1988). Other causes include Kaposi's sarcoma and less commonly non-Hodgkin's lymphoma, or *Mycobacterium avium* complex infection. Pathogenic fungi such as *Cryptococcus neoformans, Histoplasma capsulatum* and *Coccidioides immitis* may also cause intrathoracic lymphadenopathy in HIV infection, but this is much more common in the USA than, in the UK. Lymphadenopathy may be due to simultaneous infection and neoplasm in the same nodes. Hilar and mediastinal lymphadenopathy are not part of the HIV-related generalized lymphadenopathy syndrome and their presence should prompt investigation for tumour or infection, even in the absence of symptoms, clinical signs or

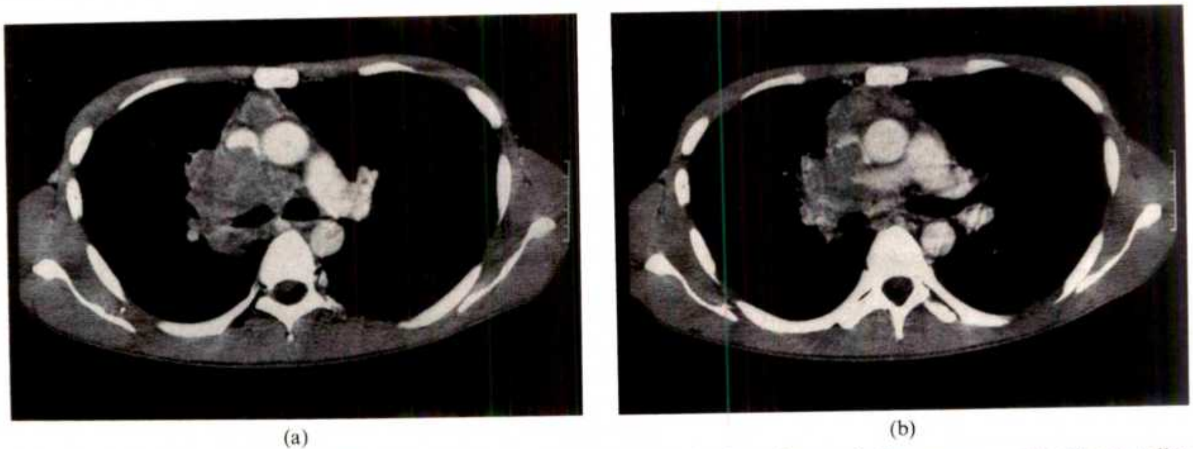

(a) (b)

Figure 2. (a, b) Contrast-enhanced CT sections at the level of the carina showing a large soft-tissue mass encasing the ascending aorta, right pulmonary artery, trachea and carina, and invading the superior vena cava.

additional radiological findings (Stern et al, 1984). Investigation should usually include bronchoscopy and nodal biopsy.

A small number of case studies suggest that primary lung carcinoma occurs with increased frequency in HIV-infected patients. One small series reported a 14-fold increased risk compared with the overall risk for white male persons (Braun et al, 1990). Adenocarcinoma was the commonest cell type but small cell and squamous cell carcinomas were also reported. All reported patients were smokers.

When tuberculosis develops early in the evolution of HIV-related immunosuppression, the clinical and radiographic signs may be indistinguishable from classical reactivation tuberculosis (Colebunders et al, 1989). Upper lobe infiltrates and lung cavities are commonly seen on the chest radiograph but hilar and/or mediastinal lymphadenopathy is unusual. When tuberculosis complicates the late stages of HIV disease, hilar and mediastinal lymphadenopathy is commonly seen, occurring in approximately 60% of cases. Pulmonary infiltrates occur with similar frequency in upper and lower lung zones and do not cavitate or heal with a scar. Lastly, disseminated disease is found in a high percentage of patients (Pitchenik & Rubinson, 1985). These unusual features often suggest a diagnosis other than tuberculosis, which may delay both diagnosis and treatment.

Kaposi's sarcoma (KS) in the chest, is typically characterized by pleural effusions and ill-defined pulmonary nodules superimposed on a background of diffuse reticular lung disease. Hilar or mediastinal adenopathy occurs in 50% of cases of intrathoracic KS. KS may be difficult to distinguish radiologically from AIDS-related lymphoma (ARL). In both KS and ARL, extranodal involvement is common. Open lung biopsy may be required for diagnosis (Davis et al, 1987).

Hilar or mediastinal lymphadenopathy is unusual in ARL and is more commonly due to co-existent infection with tuberculosis (Nyberg & Federle, 1987). The most common radiological manifestations of thoracic ARL are pleural effusions and pulmonary disease appearing as multiple nodules, interstitial infiltrates or air-space lung disease. There is no predominant pattern of involvement of the lung parenchyma. When adenopathy is due to ARL it is often not as bulky as lymphoma in the general population (Sider et al, 1989).

CT has an important role in the investigation of HIV-related chest conditions. CT readily confirms the presence or absence of significant pulmonary parenchymal disease when the chest radiographs are equivocal or difficult to interpret. Visualizing the location and distribution of the pulmonary parenchymal disease on CT allows direction of transbronchial biopsy or percutaneous needle aspiration to the region of the lung that will provide the highest diagnostic yield (Kuhlman et al, 1989). CT is much more sensitive than plain radiography for detecting small pulmonary nodules which may be the first indication of metastatic spread to the lung from KS or lymphoma. CT accurately maps the extent of adenopathy, helpful in staging ARL, and may provide a guide as to which lymph node groups are most accessible for biopsy.

Conclusion

Intrathoracic lymph node enlargement in a patient with HIV infection usually indicates *Mycobacterium* tuberculosis. KS, lymphoma or *Mycobacterium avium* complex infection are less common. Bronchogenic carcinoma should be included in the differential diagnosis of intrathoracic lymphadenopathy in patients with HIV infection. Hilar and mediastinal lymphadenopathy are not part of the HIV-related generalized lymphadenopathy syndrome. Intrathoracic lymphadenopathy in HIV-seropositive patients should prompt CT examination of the thorax, followed by nodal biopsy.

References

Braun, M. A., Killam, D. A., Remick, S. C. & Ruckdeschel, J. C., 1990. Lung cancer in patients seropositive for human immunodefiency virus. *Radiology, 175,* 341–343.

Colebunders, R. L., Ryder, R. W. & Nzilambi, N., 1989. HIV infection in patients with tuberculosis in Kinshasa, Zaire. *American Review of Respiratory Disease, 139,* 1082–1085.

Davis, S. D., Henschke, C. I., Chamides, B. K. & Westcott, J. L., 1987. Intrathoracic Kaposi sarcoma in AIDS patients: radiographic—pathologic correlation. *Radiology, 163,* 495–500.

Hewlett, D., Jr, Duncanson, F. P., Jagadha, V., Lieberman, J., Lenox, T. H. & Wormser, G. P., 1988. Lymphadenopathy in an inner city population consisting principally of intravenous drug abusers with suspected acquired immunodeficiency syndrome. *American Review of Respiratory Disease, 137,* 1275–1279.

Kuhlman, J. E., Knowles, M., Fishman, E. K., Zerhouni, E. A., Hruban, R. H. & Siegelman, S. S., 1989. Diseases of the chest in AIDS: CT diagnosis. *Radiographics, 9,* 827–857.

Nyberg, D. A. & Federle, M. P., 1987. AIDS-related Kaposi sarcoma and lymphomas. *Seminars in Roentgenology, 22,* 54–65.

Pitchenik, A. E. & Rubinson, H. A., 1985. The radiographic appearance of tuberculosis in patients with the acquired immune deficiency syndrome (AIDS) and pre-AIDS. *American Review of Respiratory Disease, 131,* 393–396.

Sider, L., Weiss, A. J., Smith, M. D., VonRoenn, J. H. & Glassroth, J., 1989. Varied appearance of AIDS-related lymphoma in the chest. *Radiology, 171,* 629–632.

Stern, R. G., Gamsu, G., Golden, J. A., Hirji, M., Webb, W. R. & Abrams, D. I., 1984. Intrathoracic adenopathy: differential feature of AIDS and diffuse lymphadenopathy syndrome. *American Journal of Roentgenology, 142,* 689–692.

1992, *The British Journal of Radiology*, *65*, 943–944

Basal cell carcinomas do metastasize

By Elizabeth J. Junor, MRCP, FRCR, *Ian Campbell, FRCPath and R. Paul Symonds, MD, FRCP, FRCR

Beatson Oncology Centre, and *Stobhill Hospital, Glasgow, UK

(*Received 16 September 1991 and in revised form 15 January 1992, accepted 11 February 1992*)

Keywords: Basal cell carcinoma

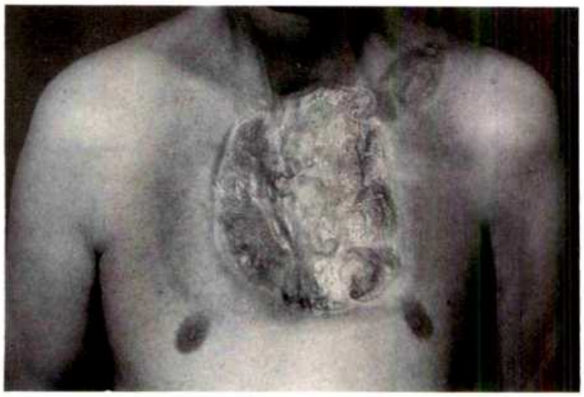

Figure 1. Large ulcerated basal cell carcinoma immediately after radical radiotherapy and prior to excision and reconstructive surgery.

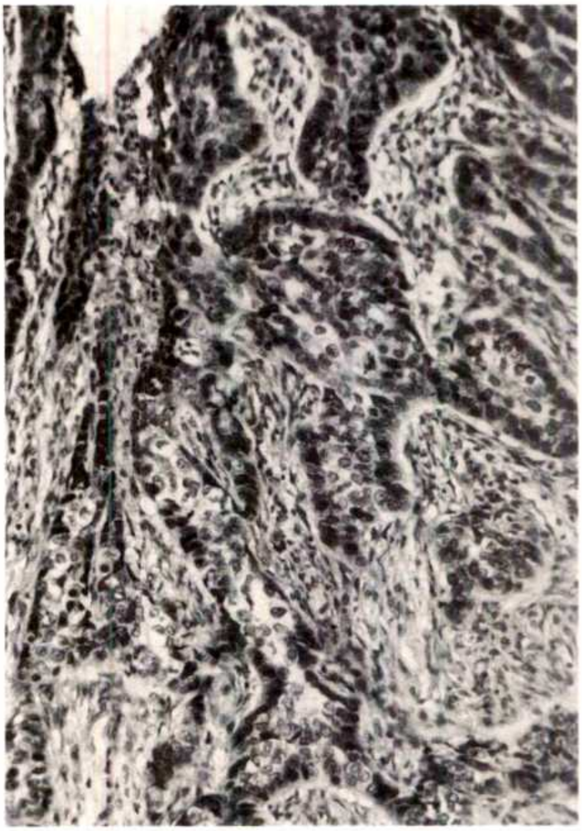

Figure 2. Skin of chest. This high power field shows palisading of the basal cells of the tumour (haematoxylin and eosin stain × 150).

The incidence of metastasis in basal cell carcinomas is calculated to be approximately 0.1%. We would like to report a case with some interesting features. This 55-year-old male presented with a large ulcerated lesion on his anterior chest wall. It had been present for 6 years but had enlarged more rapidly over the past 2 years. He had noticed a red itchy patch 32 years previously when he was performing military service in the Middle East. It was slow to heal and he was sure that it had originated as an insect bite. There was no other medical history of note and in particular he had not been exposed to arsenic, mineral oil or radiation. When seen at the clinic his anterior chest wall had a 20 × 20 cm ulcerated lesion with a rolled edge through which the tendons of sternomastoid could clearly be seen. Biopsy was reported as metatypical basal cell carcinoma (Fig. 2).

Surgical resection was attempted and skin grafting performed soon after presentation but the tumour had recurred locally within 6 weeks. He then underwent a course of radical radiotherapy receiving 60 Gy delivered in 2 Gy daily fractions over 6 weeks to the anterior chest wall by a combination of 4 MV photons and electrons. Partial regression of the lesion occurred (Fig. 1) and he then underwent radical surgical excision, removing part of both clavicles, the greatest part of the sternum and the first four ribs on both sides. The defect was closed by latissimus dorsi flaps. Pathological examination of the specimen showed complete excision of the lesion but there was evidence of tumour within the marrow cavity of the sternum. The graft healed well and there was no sign of local recurrence when the patient was admitted to hospital 7 months later, jaundiced and in a debilitated state. He died soon after, which was 14 months after his original presentation to hospital.

Postmortem examination revealed no evidence of local recurrence on the chest wall. There were no

---

Address correspondence to Elizabeth J. Junor, Beatson Oncology Centre, Western Infirmary, Glasgow.

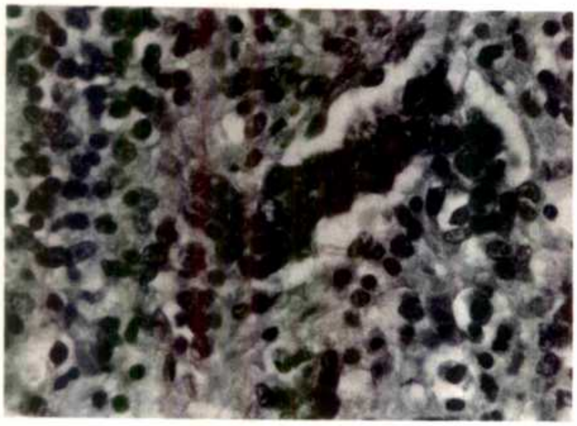

Figure 3. Metastasis to spleen. Groups of tumour cells are present in the splenic sinusoids (haematoxylin and eosin stain × 600).

mediastinal lymph nodes involved and no lung metastases. Several peri-pancreatic lymph nodes were involved by metastatic tumour. The liver contained multiple metastatic nodules ranging in size from 1–7 cm. Metastases were also found in the spleen (Fig. 3) and in one rib. All lesions were confirmed histologically as metastasis from basal cell carcinoma.

Although there are approximately 180 published cases of definite metastasizing basal cell carcinoma, this case raises some interesting points. In an excellent review of the world literature published by Domarus & Stevens (1984), the median age at presentation was 45 years, median age at first sign of metastasis was 59 and median survival after first sign of metastasis 8 months. They also found that the median interval between onset of tumour and first metastasis was 9 years. This reported case fits closely with the findings of Domarus.

As with most cases of metastasizing basal cell carcinoma, the lesion in our patient repeatedly recurred locally but unlike most there was control of the local site at the time of death from metastatic disease. This may have been associated with the extensive surgical resection performed soon after radical radiotherapy.

The history of a red itchy patch possibly linked to an insect bite during a period spent in the Middle East is interesting in that one other patient in the literature, a 27-year-old male, thought that his metastasizing basal cell carcinoma had originated at the sight of a sandfly bite which failed to heal, although there was no evidence of systemic Leishmaniasis.

It is unusual to find metastases in the spleen from any malignant disease other than lymphoma and is exceedingly rare for basal cell carcinoma to metastasize to the spleen. Our patient had both liver and spleen metastasis both of which are very rare in basal cell carcinoma, the commonest sites being lung and bone.

Although basal cell carcinoma is a common malignancy we should obviously be alert to the possibility of metastatic potential when presented with a large lesion in a relatively young man, especially if the histology is metatypical.

Acknowledgment

The authors would like to acknowledge Mr Andrew Batchelor who performed the reconstructive surgery.

References

Domarus, H. V. & Stevens, P. J., 1984. Metastatic basal cell carcinoma. *Journal of the American Academy of Dermatology*, *11*(6), 1043–1060.

1992, *The British Journal of Radiology*, *65*, 945–946

Case of the month

A curious case of pelvic calcification

By D. J. Grier, MRCP, FRCR and *G. N. A. Sibley, DM, MCh, FRCS

Departments of Clinical Radiology and *Urology, Bristol Royal Infirmary, Marlborough Street,
Bristol BS2 8HW, UK

(Received 28 May 1991 and accepted 2 July 1991)

A 48-year-old woman complained of chronic dysuria, urinary frequency and incontinence. 20 years ago invasive carcinoma of the cervix had been treated by Wertheim's hysterectomy and radiotherapy (cobalt 60). Between 5200–6000 rads tumour dose were administered over 36 days with no immediate complication.

A colostomy was performed 2 years later for colonic obstruction due to a stricture of the recto-sigmoid. She subsequently developed bilateral ureteric strictures and required an ileal interposition for this, the distal end of the ileal segment being anastomosed to the bladder dome. Both of these episodes were ascribed to fibrosis secondary to radiotherapy.

Multiple urine cultures showed persistent growths of proteus and coliform organisms, and urinary pH was frequently raised. During this time there had been several episodes of metabolic acidosis and renal calculi had been treated with lithotripsy. 10 years after this a pneumonectomy was performed for an anaplastic bronchial carcinoma. Her general health was good with no evidence of recurrence of either tumour to date.

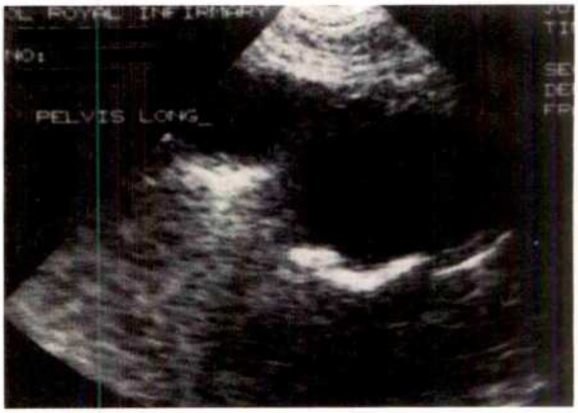

Figure 2. Longitudinal ultrasound scan of the pelvis.

The following investigations were performed in the investigation of her urinary tract (Figs 1–3).

What is the most likely cause for these appearances? What is the most appropriate management?

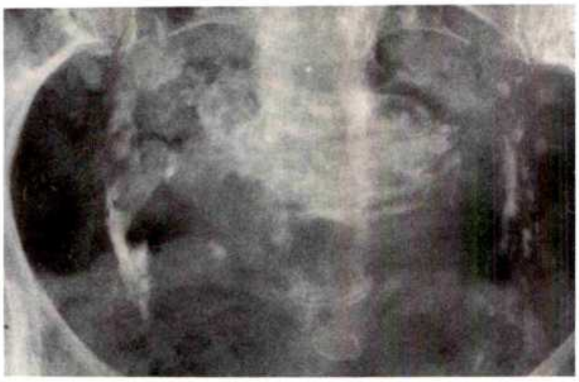

Figure 1. Plain film of the pelvis.

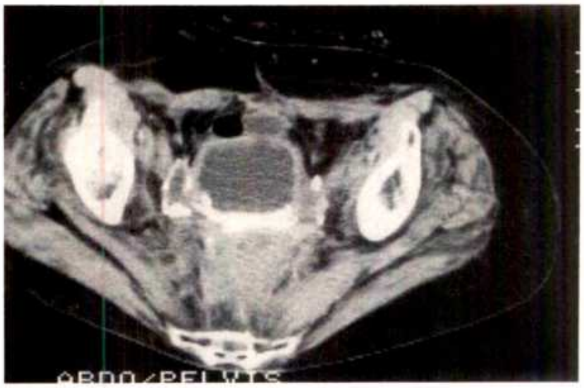

Figure 3. CT scan of the pelvis.

Address correspondence to D. J. Grier.

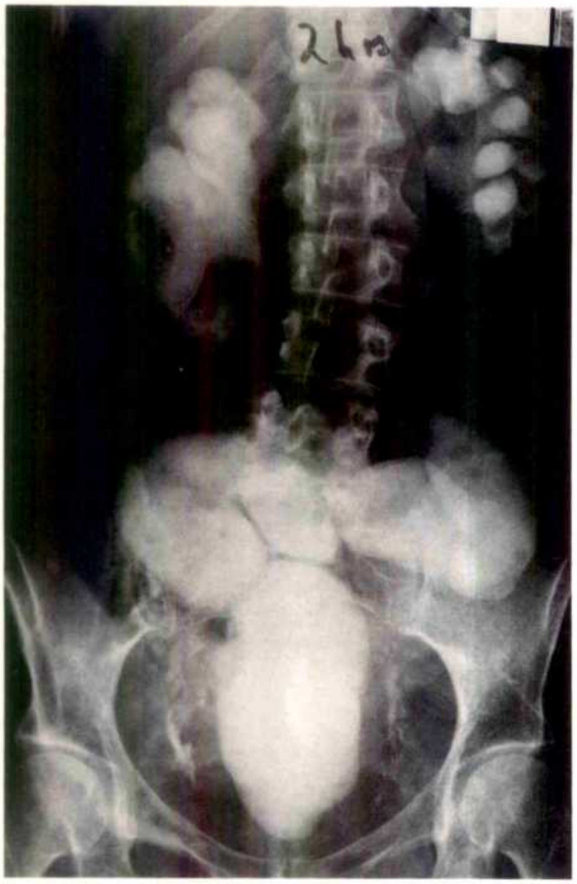

Figure 4. Intravenous urogram; delayed film showing bilateral hydronephroses and ileal interposition.

The plain radiograph (Fig. 1) shows extensive calcification within the pelvis. Ultrasound (Fig. 2) demonstrates an echogenic posterior bladder wall with distal acoustic shadowing. Computed tomography (CT) (Fig. 3) confirms extensive calcification, thickening and deformity of the posterior and lateral bladder wall, and also shows para-vesical calcification.

Cystoscopy was performed revealing a calcareous slough on the posterior bladder wall, some of which could be scraped away only with difficulty. Intravenous urography (Fig. 4) demonstrates the overall appearance of the urinary tract.

The diagnosis is dystrophic calcification of the bladder wall due to alkaline encrusting cystitis. In this condition there is deposition of urinary phosphate on the bladder wall, a process facilitated by chronic inflammation and fibrosis of the bladder wall and alkaline urine in which phosphate is less soluble. Infection with proteus spp. is implicated in the aetiology, as it is a urea splitting organism leading to raised urinary pH. This patient had persistent urinary growths of proteus and other organisms. Management of this condition is by acidification and sterilization of the urine. Occasionally cystoscopic removal of adherent calcareous slough is required (Jamieson, 1966).

This patient has since undergone an ileal conduit urinary diversion in view of persistent infection and troublesome incontinence.

Discussion

Radiographically visible calcification of the urinary bladder (other than calculi) is rare. Recognized causes include transitional cell carcinoma, schistosomiasis and tuberculosis, and cyclophosphamide cystitis (Gross, 1979).

Visible bladder wall calcification in association with non-granulomatous infection is very rare. There is only one other report of a case 6 years after radiotherapy for carcinoma of the cervix (Harrison et al, 1978).

Alkaline encrusting cystitis was a common diagnosis before the widespread use of antibiotics, usually affecting women of childbearing age. Typical symptoms were of dysuria, suprapubic pain and often haematuria. An increased incidence of this condition was noted in patients undergoing radiotherapy for bladder tumours (Jamieson, 1966). Injury to the bladder wall as a result of radiotherapy, leading to inflammation, necrosis and fibrosis, in the presence of alkaline urine was felt to favour deposition of urinary phosphate.

That the calcification in this case predominantly affected the posterior bladder wall is probably due to its proximity to the cervix. The region of the interureteric ridge of the bladder wall is considered the most vulnerable site for damage. Further, its vascular supply may have been compromised by the Wertheim's hysterectomy.

As this patient has had several complications secondary to pelvic radiotherapy, it is not surprising that the radiological appearances of encrusting cystitis are so florid. Recognition of this condition is helpful because prompt treatment of urinary tract infection, particularly proteus, and acidification of the urine at an early stage may prevent, or even reverse, progression.

Acknowledgments

We would like to thank Professor E. R. Davies and Dr J. Bullimore for their assistance in the preparation of this manuscript.

References

Gross, B. H., 1979. Bladder and ureteral calcifications. *Seminars in Roentgenology, 14,* 261–262.

Harrison, R. B., Stier, F. M. & Cochrane, J. A., 1978. Alkaline encrusting cystitis. *American Journal of Roentgenology, 130,* 575–577.

Jamieson, R. M., 1966. The treatment of phosphatic encrusted cystitis (alkaline cystitis) with nalidixic acid. *British Journal of Urology, 38,* 89–92.

1992, *The British Journal of Radiology*, *65*, 947–948

Short communication

Visualization of the axillary vein during ^{99}Tc^{m} methoxy-isobutyl-isonitrile (MIBI) myocardial imaging

By P. W. P. Bearcroft, MB, MRCP and E. P. Wraight, MB, PhD, FRCR

Department of Nuclear Medicine, Addenbrooke's Hospital, Hills Road, Cambridge CB1 2QQ, UK

(Received 20 November 1991, accepted 12 March 1992)

Keywords: MIBI, Vein, Cardiac imaging

^{99}Tc^{m} methoxy-isobutyl-isonitrile (MIBI) is a cationic complex which is replacing thallium in the investigation of cardiac ischaemia in many centres (Wackers et al, 1989) and is also finding non-cardiac applications (Piwnica-Worms & Holman, 1990). We wish to report on the visualization of the axillary vein after injection in two patients undergoing myocardial scintigraphy at rest using this agent. Incidental venous visualization has been reported after intravenous injection of thallium-201. This was shown not to be a trivial finding since arm vein uptake compromised myocardial counting statistics significantly and was associated with a lower myocardial washout of thallium (Gal & Port, 1986). In that study, venous uptake appeared to be associated with the site of injection.

Case 1

A 45-year-old non-smoking male presented with a 5 year history of mild chest pain on effort for which he took no medication. There was no history of trauma or catheterization to his right arm. Exercise electrocardiogram (ECG) was normal. An exercise ^{99}Tc^{m}-MIBI study demonstrated no evidence of myocardial ischaemia at rest nor during exercise, but on the rest study the injected vein was seen to have taken up tracer (Fig. 1a).

Case 2

A 44-year-old ex-smoker presented with a 4 month history of angina on effort following an episode of documented mycoplasma pneumonia. Other than nifedipine, he took no medication. Examination was normal. An exercise ^{99}Tc^{m}-MIBI cardiac study demonstrated small areas of reversible ischaemia near the apex anteriorly and posterolaterally corresponding with ischaemic changes on the ECG. Again, there was tracer uptake in the injected vein on the rest study (Fig. 1b).

Discussion

The cases described confirm that venous uptake is seen with ^{99}Tc^{m}-MIBI as with thallium. This has not, to our knowledge, been described previously. ^{99}Tc^{m}-MIBI has been found to accumulate in viable myocardial tissue in proportion to regional blood flow, as has thallous chloride (^{201}Tl) (Wackers et al, 1989). Pharmacokinetic studies demonstrate a high initial uptake in the lung, heart, liver and skeletal muscle with

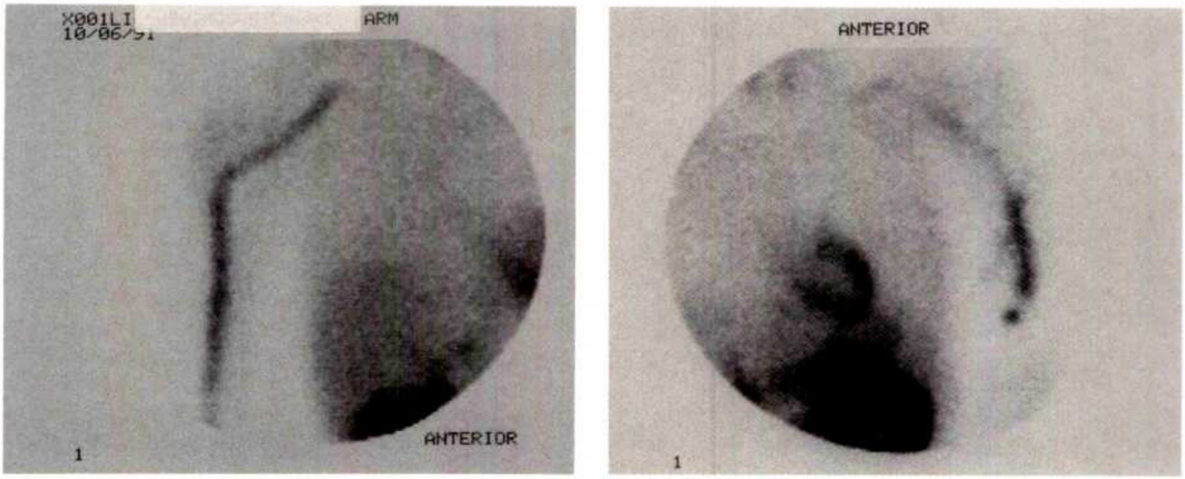

(a) (b)

Figure 1. (a) and (b): venous uptake of ^{99}Tc^{m}-MIBI in the injected vein in two patients undergoing resting cardiac studies.

rapid subsequent pulmonary clearance relative to the steady activity in the heart (Jones et al, 1984). MIBI diffuses passively across the cell membrane by a Na-K-ATPase-independent mechanism and binds to a specific cytosolic site with high affinity (Mousa et al, 1987). A possible mechanism for the uptake described is the direct uptake of MIBI by endothelial cells, associated with stasis within the vein. Figs 1a, b were recorded over 1 h after injection of tracer, so excluding a blood pool effect.

We have neither made a formal study of the frequency of venous uptake of ^{99}Tc^{m}-MIBI nor of its effect on myocardial counting statistics. The effect on axillary vein uptake of the site and manner in which the radiopharmaceutical is injected needs to be determined and, in particular, whether a saline flush has any beneficial effect. Because we were aware of the possibility of uptake of radiopharmaceuticals in the vein used for injection, it has been our standard practice to administer ^{99}Tc^{m}-MIBI using a saline flush technique for both exercise and rest studies, although no mention of the need for this technique is made in the manufacturer's guidance notes. In the cases reported the flush was inadvertently omitted, and in both the cephalic vein was used for injection. We have not observed radiopharmaceutical uptake in veins from injections that have been flushed, regardless of the injection site chose. This suggests that this is not simply an anatomical phenomenon related to hold up of the cephalic vein drainage at the clavipectoral fascia.

The effect of possible clinical factors should also be investigated. Smoking was found to be inversely related to venous uptake of thallous chloride (Gal & Port, 1986), although the significance of this fact is uncertain. Neither of our cases had any past medical history of diabetes mellitus, congestive heart failure or pulmonary disease. Other than nifedipine, neither was on any medication and neither had had venous catheterization at that site.

The prolonged visualization of the injected vein also points to a possible further use for ^{99}Tc^{m}-MIBI as a venographic agent both in the investigation of thrombosis of the peripheral venous systems and also in the study of other venous systems. Attempts to use thallium as a venographic agent have been limited due to poor resolution (Silberstein & Robbins, 1984), but it is expected that this would be less of a problem with ^{99}Tc^{m}-MIBI.

Conclusion

We have reported two cases where venous uptake of ^{99}Tc^{m}-MIBI has been clearly demonstrated during a resting cardiac study. This has important implications for these examinations and may influence the method used for injection of the radiopharmaceutical.

References

Gal, R. & Port, S. C., 1986. Arm vein uptake of thallium-201 during exercise; incidence and clinical significance. *Journal of Nuclear Medicine, 27*(8), 1353–1357.

Jones, A. G., Abrams, M. J., Davison, A., Brodaek, J. W., Toothaker, A. K., Adelstein, S. J. & Kassis, A. I., 1984. Biological studies of a new class of technetium complexes: the hexakis (alkylisonitrile) technetium(I) cations. *International Journal of Nuclear Medicine and Biology, 11*, 225–234.

Mousa, S. A., Williams, S. J. & Sands, H., 1987. Characterisation of *in vivo* chemistry of cations in the heart. *Journal of Nuclear Medicine, 28*(8), 1351–1357.

Piwnica-Worms, D. & Holman, B. L., 1990. Non-cardiac applications of hexakis- (alkonylisonitrile) Technetium-99m complexes. *Journal of Nuclear Medicine, 31*(7), 1166–1167.

Silberstein, E. B., Robbins, P. J., Fortman, D. L., Thomas, S. R. & Sill, P., 1984. Venous uptake of 201-Tl as Thallous chloride. *Nuclear Medicine Communications, 5*, 329–337.

Wackers, F. J. Th., Berman, D. S., Maddahi, J., Watson, D. D., Beller, G. A., Strauss, H. W., Boucher, C. A., Picard, M., Holman, B. L., Fridrich, R., Inglese, E., Delaloye, B., Bischof-Delaloye, A., Camin, L. & McKusick, K., 1989. Technetium-99m hexakis 2-methoxyisobutyl isonitrile: human biodistribution, dosimetry, safety, and preliminary comparison to thallium-201 for myocardial perfusion imaging. *Journal of Nuclear Medicine, 30*, 301–311.

1992, *The British Journal of Radiology*, *65*, 949–953

Correspondence

(The Editors do not hold themselves responsible for opinions expressed by correspondents)

Radiation protection associated with well woman screening

The Editor—Sir,
It was of interest to see the issues on this topic which Moores and Henshaw considered worthy to be raised in your pages (Moores & Henshaw, 1992).

The principle issue in their eyes seems to be the classification for radiation protection purposes of women presenting for breast screening. An examination of the design and structure of the NHS Breast Screening Programme will confirm that in no way can this be confused with a research project. Breast screening is offered to (a section of) the public, just like any other service in the NHS. In common with all the other medical services, this offer can be accepted or rejected. All patients are, in this sense, "volunteers" and simply to accept an offer of an established service does not make one the subject of a research project. There is, I believe, no justification whatsoever to create two standards of care by treating women who happen to have symptoms in any way less rigorously for radiation protection purposes than those presenting for screening. Both should receive a dose of radiation "as low as reasonably possible to achieve the purpose".

Differences of opinion may be encountered as to the definition of "purpose". It would not be realistic to use as the "purpose" the objective of the screening programme—a reduction in mortality from breast cancer—we don't expect to be able to identify any improvement for about 5 years rising to maximal in about 20. To pick out any one from a list of standards, each of which has been arbitrarily agreed as a measure of a particular quality assurance criterion (and as such are all likely to be changed in the course of the normal, regular, routine QA review processes), would, with respect to Moores and Henshaw, be nonsensical. It seems perfectly obvious that the "purpose" of a mammographic exposure must be identical to that of any other radiological examination, namely to produce a radiograph of such quality as to be acceptable to the radiologist concerned.

The calculations put forward in the letter are impressive, but we must never forget the fact that no case of breast cancer has ever been shown to result from a mammographic dose of radiation. Moreover, there has been no excess of cancers detected in the many thousands of women screened and subjected to close follow-up under rigid clinical trial conditions to indicate that radiation induced cancers have occurred. All the assumptions upon which we wisely base our practice are derived from calculated extrapolations from studies which found excess cancers resulting from much higher doses of much higher energy radiation to much smaller numbers of much younger women.

Evidence from the UK screening programme to date, shows that some 60% of women, who have had their cancers detected at an early stage by screening, have a life expectancy equal to that of a woman who has never had breast cancer (Wilson, 1992).

Surely, we should be endeavouring to quantify and publicise the proven risks to the female population of not being screened in comparison with the theoretical risks of being screened, rather than to concentrate only on one side of the equation and to indulge in flights of fancy based upon assumptions and EEC Commissioners' guidelines.

Yours etc.,
E. J. Roebuck

Nottingham Breast Screening Service,
City Hospital,
Hucknall Road,
Nottingham NG5 1PB

(*Received 9 July 1992, accepted 1 September 1992*)

References

Moores, B. M. & Henshaw, E. T., 1992. Radiation protection associated with well woman breast cancer screening. *British Journal of Radiology*, *65*, 552–553.

Wilson, A. R. M., 1992. *The Nottingham Breast Screening Results, 1990/2* (British Breast Group, London), February, 1992.

Wilson, A. R. M., 1992. *Early Cancers Detected by Breast Screening* (European Group for Breast Cancer Screening, Rhodes), May, 1992.

Radiation protection associated with well woman breast cancer screening

The Editor—Sir,
Moores and Henshaw's letter (1992) suggests that the NHS Breast Screening Programme (NHS BSP), is a research project. The NHS BSP is, in fact, an accepted health programme based on established policies and its specific purpose is to diagnose breast cancer early, thus reducing mortality in the target population by 25%. While it is not in itself research, as it is the first national breast screening programme in the world, it naturally generates various research projects and questions arise which are best answered by research. Such issues, and other matters of policy are considered in the first instance by the Department of Health Breast Screening Advisory Committee, chaired by Professor Martin Vessey.

Moores and Henshaw suggest that certain aspects of radiation protection within the screening process have not been fully appraised. In fact, the NHS BSP is building up an extensive set of literature dealing with all aspects of quality assurance of the programme. This includes the "Pritchard" report (1989), which was prepared by a subcommittee of the Radiological Advisory Committee at the department. In Table I of the report, the acceptable value for the average glandular dose to a 45 mm thick standard breast using a grid was set at less than 5 mGy per view. The method of measurement to be used was described in the Pritchard report. The methods described in this report were further developed and refined in IPSM Report No. 59 (1989).

The NHS BSP in 1990 established a national mammography physics centre at St. Luke's Hospital, Guildford. This centre carried out a survey of dose given by all mammography sets used in the NHS BSP. The measurements were taken using the described methods in IPSM 59 by physicists working regularly, some full time, in mammography physics. The data were presented by Dr K. C. Young of the centre at Symposium Mammographicum in April 1992 and will be published shortly by the NHS BSP. All sets measured had a mean glandular dose less than 3 mGy, with 98% less than 2 mGy.

I will leave it to others to deal with the detailed technical questions Moores and Henshaw pose, but I can assure you that the NHS BSP takes radiation protection and the issues of benefits and disadvantages in screening very seriously indeed.

Yours etc.,

J. PATNICK

Trent Regional Health Authority,
Fulwood House,
Old Fulwood Road,
Sheffield S10 3TH

(Received 28 July 1992 and accepted 1 September 1992)

References

MOORES, B. M. & HENSHAW, E. T., 1992. Radiation protection associated with well woman breast cancer screening. *British Journal of Radiology, 65*, 552–553.

NHS BSP, 1989. *Quality Assurance Guidelines for Mammography, The Pritchard Report.*

IPSM, 1989. *The Commissioning and Routine Testing of Mammographic X-ray Systems*, Report No 59 (IPSM, York).

Standards of radiation protection in mammographic screening

THE EDITOR—SIR,

We wish to clarify some of the radiological protection issues raised by Moores and Henshaw (1992) in connection with the UK breast cancer screening programme using X-ray mammography.

The International Commission on Radiological Protection (ICRP) has defined the category of "medical exposure" as principally the exposure of persons as part of their diagnosis or treatment with such exposure usually intended to provide a direct benefit to the exposed individual (ICRP, 1991). If the practice is justified and the protection optimized, the dose to the patient will be as low as is compatible with the medical purpose. ICRP suggests that the application of limits might be to the patient's detriment and therefore does not recommend dose limits for medical exposures.

The purpose of mammographic screening is clearly the diagnosis of breast cancer, although the probability that any particular woman will have breast cancer is quite low. The irradiation of well women as part of such a programme should therefore be regarded as medical exposure according to the ICRP definition and so dose limits for members of the public are not relevant.

British law (IRR, 1988) incorporates the ICRP principles of justification and optimization by requiring that all medical exposures be conducted in accordance with accepted diagnostic or therapeutic practice (justification), and with procedures selected to ensure that the dose to the patient is as low as reasonably practicable in order to achieve the required diagnostic or therapeutic purpose (optimization).

In the case of mass screening by X-ray examination, justification requires the demonstration of a net positive benefit when weighing, in commensurate terms, all the benefits (both to individual persons and to the population) against all the costs (including radiation detriment). This has already been carried out for the UK breast cancer screening programme where, for women aged between 50 and 65 years of age, the number of cancers detected and susceptible to cure was predicted to outweigh greatly the number of cancers induced (Department of Health and Social Security, 1986). The screening programme is therefore not a research project, as Moores and Henshaw suggest, since it has been justified and is now an accepted diagnostic practice.

Although not recommending dose limits for medical exposures, ICRP has recently advocated the use of dose constraints in the process of optimization: these constraints should be set for common diagnostic procedures by professional and advisory bodies and applied with flexibility to allow higher doses when indicated by sound clinical judgement. The National Radiological Protection Board (1991) proposes to endorse this approach and will be giving further guidance in due course. For the purposes of optimization, dose constraints will relate to typical practices within a radiology department for various examinations and not to individual patients. The action to be taken if dose constraints are exceeded would be a local investigation of the circumstances and either modifications to techniques and equipment or justification of the need for the high doses.

In summary, the 1990 recommendations of ICRP provide a framework for standards of radiation protection in mammography that are common to all medical and other types of exposure to ionizing radiation.

Yours etc.,

P. C. SHRIMPTON
B. F. WALL

National Radiological Protection Board,
Chilton, Didcot,
Oxon OX11 0RD

(Received 30 July 1992 and accepted 1 September 1992)

References

DHSS, 1986. *Report of a DHSS Working Group (Forrest, P., Chairman) to the Health Ministers of England, Wales, Scotland and Northern Ireland* (Breast Cancer Screening, HMSO, London).

ICRP, 1991. 1990 Recommendations of the International Commission on Radiological Protection. Publication 60. *Annals of the ICRP, 21*, Nos 1–3.

IRR, 1988. *The Ionising Radiation (Protection of Persons Undergoing Medical Examination or Treatment) Regulations.* (HMSO, London) SI (1988), p. 778.

MOORES, B. M. & HENSHAW, E. T., 1992. Radiation protection associated with well woman breast cancer screening. *British Journal of Radiology, 65*, 552–553.

NRPB, 1991. *Board Advice Following Publication of the 1990 Recommendations of the ICRP. Consultative Document* (NRPB, Chilton), M321.

Radiation protection associated with well women breast cancer screening

THE EDITOR—SIR,

The letter from Moores and Henshaw (1992) raises several points which must be answered. However, we believe the answers are relatively simple provided certain points are kept clearly in mind. We wish to make the following comments:

1. To answer the first question in their second paragraph, "Irradiation of well women for screening purposes" does constitute medical exposure, for which there is no dose limit. Paragraph 2.16 of the Guidance Notes to the Ionising Radiations Regulations 1985 (NRPB, 1988) applies, which states: "Screening programmes... should be undertaken only if the expected medical benefits to the individuals examined and to the population as a whole exceed the economic and social costs, including the risks associated with the radiation dose involved. Since benefits are not always the same for all members of the population, screening should be limited normally to particular groups". This aspect of the NHS Breast Screening Programme (BSP) was fully considered by the Forrest Committee when recommending that the BSP should be set up, in the light of information then available and a knowledge of breast doses at that time, as outlined in Annex D of the Forrest Report (DHSS, 1986). This has been confirmed to us recently by members of the Forrest Committee. Paragraphs 2.19–2.29 of the Guidance Notes refer specifically to medical research and thus plainly do not apply to the NHS BSP. It then follows that paragraphs 3–8 and paragraph 10 of their letter are irrelevant.

2. Returning to paragraph 2 of their letter, the "required diagnostic purpose" of breast cancer screening is the early detection of breast cancer. The "upper level of dose considered acceptable to achieve this purpose" was given in the Pritchard Report (Department of Health, 1989) as 5 mGy per film to a standard breast using a grid but may be revised to 3 mGy shortly. However, this value is intended only as a guideline and not as a limit.

3. Regarding the last sentence of paragraph 2 of their letter, the original target of the NHS BSP was a detection rate of 5 cancers per 1000 women on the first screen, and about 3.7 per 1000 on later rounds (Forrest report, paragraph 8.5). The target for the first screening round is understood to have been exceeded in all parts of the UK, but for present and future discussion the detection rate on subsequent screening rounds will be more important. Early indications are that this may be around 4 per 1000 and it should be noted that in the Edinburgh trial (Roberts et al, 1990) just over 3 cancers per 1000 were detected on the 2nd, 3rd and 4th rounds at 2 yearly intervals (in contrast to the 3 yearly interval at present employed in the NHS BSP). The important point here is not just the numerical value, but its constancy for repeated screening rounds. At each successive screening round the benefit/risk ratio increases, because the greater age of the women results in reduced risk of radiation induced cancers appearing while the detection rate remains about the same.

4. Regarding paragraph 9 of their letter, the UK Mammography Physics Group study referred to was an early and provisional survey carried out informally in 1989 by a group of physicists in the field, and intended for their information only, but was subsequently used by the Commission of the European Communities (CEC) with permission as the best up-to-date figures then available. The CEC guidelines referred to the upper quartile so that inevitably 25% of centres exceeded this value!

5. To answer those questions at the end of their letter which relate to the physics of mammography:

Question 1. This has been answered in paragraph 1 above, and is also covered in a letter from Mrs J. Patnick, National Co-ordinator of the NHS BSP.

Question 2. "Actual levels of radiation employed" have been measured in some regions for compressed breasts 4.5 cm thick and found not to differ significantly from those predicted employing phantoms of 4 cm Perspex, although compressed breast thicknesses are more usually around 5.5 cm rather than the 4.5 cm initially assumed.

Question 3. Perspex phantoms have been employed because they provide a quick, practical check of dose by a standard method which can be used and repeated in all centres. As stated in IPSM Report 59, p. 34, "Dose will also be affected by the size and composition of the breast with the former varying both within and between populations and the latter throughout the life of the woman. This diversity of both dose specification and breast dimensions and composition makes dose comparisons very difficult and it is important for such purposes that doses be specified for a standard breast and in a standard way" (IPSM, 1989). The use of phantoms is not unknown in other radiological examinations, as shown by the recent CEC workshop on phantoms held in Wurzburg, and their use should probably be encouraged.

Questions 4 and 5. It is important to distinguish dose limits from reference dose levels for diagnostic X-ray examinations. There are no dose limits for medical exposure.

We leave the remaining question for others to answer.

We believe that the fundamental radiation protection aspects of the NHS BSP were properly considered at its inception, and are being kept under review. In view of the relatively high benefit to risk ratio, it is probably more important to ensure that image quality remains high (to maximize cancer detection rate), than to show excessive concern over minimizing the dose involved.

Yours etc.,

J. Law
D. R. Dance
K. Faulkner
M. C. Fitzgerald
M. L. Ramsdale
A. Robinson
(IPSM Mammography Working Party)
Department of Medical Physics and Medical Engineering
Western General Hospital
Crewe Road
Edinburgh EH4 2XU

(Received 30 July 1992 and accepted 1 September 1992)

References

Department of Health, 1989. *Guidelines on the Establishment of a Quality Assurance System for the Radiological Aspects of Mammography Used for Breast Screening* (Department of Health, London).

DHSS, 1986. *Breast Cancer Screening. A Report of a Working Group Chaired by Professor Sir Patrick Forrest* (HMSO, London), pp. 81–82.

NRPB, 1988. *Guidance Notes for the Protection of Persons Against Ionising Radiations Arising from Medical and Dental Use* (HMSO, London).

IPSM, 1989. *Commissioning and Routine Testing of Mammographic X-ray Systems. Report No. 59* (IPSM, York).

Moores, B. M. & Henshaw, E. T., 1992. Radiation protection associated with well woman breast cancer screening. *British Journal of Radiology, 65*, 552–553.

Roberts, M. M., Alexander, F. E., Anderson, T. J., Chetty, U., Donnan, P. T., Forrest, P., Hepburn, W., Huggins, A., Kirkpatrick, A. E., Lamb, J., Muir, B. B., Prescott, R. J., 1990. Edinburgh trial of screening for breast cancer: mortality at seven years. *Lancet, 335*, 241–246.

Authors' reply

The Editor—Sir,

We would like to thank all those who responded to our letter (Moores & Henshaw, 1992). We are fully conversant with the views expressed in all of the replies but unfortunately we feel that none address the fundamental operational radiation protection issues raised in our letter. Therefore, we would like to make the following comments to these replies.

1. Law et al quite rightly point out that: "Screening programmes.... should be undertaken only if the expected medical benefits to the individuals examined and to the population as a whole exceed the economic and social costs, including the risks associated with the radiation involved. Since benefits are not always the same for all members of the population screening should be limited normally to particular groups". The main elements of this statement are:

(a) A screening programme has responsibilities to the individual as well as to the population.

(b) Since well women participating in a breast screening programme are volunteers all those participating should be provided with information appropriate to their own circumstances if they are expected to give informed consent.

(c) Particular groups may need to be considered separately, particularly if items (a) and (b) are to be effectively implemented.

To date a particular group has been defined solely in terms of age in order to evaluate risks and benefits arising from breast screening. However, of equal relevance and sensitivity in terms of affecting both benefits and risks is breast size and composition. Thus, in order to reemphasize the points raised in our letter we would like to pose the question as to whether or not the existing quality control/radiation protection framework adequately takes into account, say, that group of women aged 50-54 with breast thickness greater than 6 cm. Breast thickness encountered range from 1 to 8 cm and approximately 25% of women have thicknesses greater than 6 cm. Consequently the above group will consist of roughly 350,000 women who are eligible for screening and comprose approximately 10% of the screened population. However, this group will in fact represent potentially more than 10% of the overall benefits and risks which occur in the whole screened population.

2. In order to provide informed consent, are we able to indicate the magnitude and range of doses which the above mentioned group of women might expect to encounter at any individual breast screening unit? Also can these doses be related to "average" dose received by the total screened population?

The breast dose to well women depends upon a number of factors including breast thickness and compostion, technical performance of X-ray equipment, radiographers' performance, ergonomics of equipment design including the effectiveness of breast compression. At present breast dose is implied solely from dose measurements undertaken on a Perspex phantom of standard thickness which only depends upon technical performance of the equipment and does not necessarily relate to clinical practice. In fact a recently published "Protocol for Patient Dose Measurements in Diagnostic Radiology" produced jointly be the Institute of Physical Sciences in Medicine, National Radiological Protection Board and College of Radiographers, states "Direct measurements (of dose) during the course of real examinations on real patients provide the best indication of actual clinical practice". If this is the case then why have such measurements not formed part of the routine quality control in well women breast screening during the past 2 years. After all, the population eligible for screening comprise over 4 million women with a potential collective dose equivalent of over 2000 women Sv, which is roughly the same as that arising annually in the UK from all barium enemas.

All X-ray sets employed in the Breast Screening Programme are checked at least bi-annually, including an output calibration and assessment of beam quality. The periodic assessment of breast dose on a sample of women of differing breast sizes is, therefore, an extremely easy, and inexpensive undertaking from a knowledge of the radiographic factors employed.

The Commission of European Communities has undertaken European wide trials of breast dose and image quality in mammography. Dose assessments were performed on women undergoing an examination and image quality assessed from the corresponding clinical images by a panel of expert radiologists. The following preliminary conclusions may be drawn from the study:

(a) Dose measurements performed upon screened women of average breast size placed some UK units at the high end of the European dose range, even though they had "IPSM" test phantom doses below 2 mGy.

(b) European units who do not perform standard phantom measurements had doses at the low end of the European range.

(c) Actual measured breast dose can vary by a factor of 50 or more and average doses for individual screening units by a factor of 5.

Consequently at present it is not possible to predict with any certitude what the actual dose to the previously defined population (50-54 years age group, breast thickness of 6 cm or more) would be at any particular screening unit nor whether or not it fulfilled the requirements of ALARA.

3. The true benefits arising from the Breast Screening Programme are not provided by breast cancer detection rates. It would be relatively straightforward to establish a screening programme which detected virtually all cancers with minimal risk. However, the cancers detected might be at an advanced stage of development. Benefit-risk assessment in terms of cancers detected are, therefore, of limited value.

As pointed out by Mrs Patnick, "... the specific purpose is to diagnose breast cancer early, thus reducing mortality in the target population by 25%." This statement refers specifically to a reduction in breast cancer mortality, normally assesssed by a reduction in death rate in the screened population as compared to an equivalent unscreened control group. Since breast cancer contributes approximately 5% of the annual cause of death in the UK; the proposed reduction would represent an overall reduction in death rate, from all sources, of 1%. In order to ensure statistical accuracy in assessing these changes a sufficiently large screened and unscreened population must be investigated, which are equivalent not only in terms of age but also socio-economic, possibly geographic and other indicators.

It is worth noting that since the mortality associated with breast cancer incidence is appoximately 50% then roughly 50% of women with breast cancer, will demonstrate the same mortality as an equivalent group of women who do not have breast cancer.

In terms of cost-benefit analysis, however, the most relevant measure of benefit arising frm a screening programme is expressed in terms of women -years or life-expectancy gained in the screened population. This measure of benefit takes into account not only any changes in death-rate but also the age-group in which any gains occur. Years of life-expectancy gained at 70 years of age will have a different cost-benefit compared with that at 50. Thus, any comprehensive evaluation of benefits arising from breast screening should take account of the age at which cancers are detected and thus the potential life-expectancy remaining, as well as the size or stage of cancers detected. The detection of early or minimal cancers being a prime requirement for effective screening.

The existing UK Breast Screening Programme was established following the results obtained from a number of trials including the Swedish. Two countries, Swedish Malmo, UK Trial and Nijmegen Project. The organization and structure of these trials was varied in terms of numbers and age groups screened, employment of randomized selection or matched data analysis. Similarly the results presented were in a variety of different formats and indicated variations in terms of the observed reduction in mortality, age group dependence of cancer detection and distribution of cancer sizes or staging within the population as well as the magnitude of mortality difference between a screened and unscreened population with time following the commencement of screening.

For example the UK Trial (Chamberlain et al, 1988) observed a reduction in mortality of 14% when no allowance was made for underlying differences in breast cancer mortality between the screened and unscreened populations but rose to 20% when adjusted for differences in pre-trial mortalityrates. These differences fell short of statistical significance. Also no difference in mortality was observed during the first 5 years. The two Swedish Trials observed a higher mortality amongst younger women implying a possible difference in tumour biology between younger and older women. The two Swedish studies also presented some conflicting results.

All of these studies appear to pose many questions and in most other scientific activites the pursuit of answers to these questions would be deemed primary research. However, within the framework of the UK Programme it is not as yet possible to predict the specific benefits to individual women or groups of women arising from the Programme until supporting research provides this information. At present well women are being irradiated at an indeterminate level for indeterminate future benefit.

4. Because the early detection of breast cancer in all women is of prime importance but particularly in younger age-groups 50-54, 55-59 any factor which can influence this is of great importance.

A loss of image quality with increasing breast thickness for a molybdenum anode X-ray tube and screen-film combination has been extensively documented. Since image quality and detection of minimal cancers must be intimately related, women with larger compressed breast thickness may be affected.

The effect on image quality of increasing absorber thickness has recently been studied together with the effect of kV (Young & Ramsdale, 1992). This work indicates that the loss in image quality in performing an examination at 28 kV on an "average" breast thickness between 6 and 8 cm comared with an "average" between 1 and 6 cm is approximately the same as the loss in performing an examination on an average sized breast at 34 kV compared with 28 kV. This work was performed on physical test phantoms. To relate it to the clinical domain requires the radiological assessment of the image quality of a mammogram of an average sized breast, produced at both 28 and 34 kV, and performed on a symptomatic patient with an assessed minimal carcinoma. Preferably high contrast detail such as micro calcifications should not be present and reasonable amounts of breast parenchyma or structural noise should be present. If the radiologist considers the loss of image quality impairs the previous diagnostic outcome then there is every indication that existing mammographic practice may significantly affect clinical diagnosis of minimal cancers in women with compressed breast thickness of 6 cm or more. If the radiologist does not feel that image quality has been seriously affected then it would presumably be necessary to reconsider the existing tolerances on kV calibration. Also kV dependence of clincial image quality may need to be reviewed.

5. The purpose of our original letter and this response has been to try and insert a "human aspect" into the breast screening radiation protection framework. At present inanimate test phantoms and all age cancer mortality statistics are employed in assessing performance. We believe it to be inadequate to treat over 4 million women with ages ranging from 50 to 64 and possessing compressed breast thicknesses ranging from 1 to 8 cm as a homogeneous group in respect of radiation protection philosophy, including cost-risk benefits, particularly when considering the aims and objectives of this philosophy, including its responsibility to the individual.

For any screening programme to take place benefit/risk ratios must be acceptable and, therefore, known to a reasonable degree of certitude for all individuals. It is not permissible to transfer benefit or risks from one group to another to justify the whole activity. Therefore, unlike the situation which exists with a sick patient there must exist some notional lower limit for benefit or upper limit for dose to a well individual. Otherwise is it seriously being suggested that no upper dose limit exists for the irradiation of a large group of women who are fit and well.

We feel that variations in risk with age group, breast thickness and composition, also possible variations in tumour biology with age and variations in image quality with breast thickness all tend to support this viewpoint.

Yours etc.,

B. M. Moores
E. T. Henshaw

Integrated Radiological Services Ltd,
Unit 188, Century Building,
102 Tower Street,
Brunswick Business Park,
Liverpool L3 4BJ

(Received 26 August 1992 and accepted 1 September 1992)

References

Chamberlain, J., Coleman, D., Ellman, R. & Moss, S. M., 1988. First results on mortality reduction in the UK trial of early detection of breast cancer. *Lamat*, 411–416.

Young, K. C. & Ramsdale, M. L., 1992. Evaluation of mammography image quality phantoms. In *Proceedings of the Workshop Test Phantoms and Optimisation in Diagnostic Radiology and Nuclear Medicine. Wurzburg*, in press.

1992, *The British Journal of Radiology*, *65*, 954

Book review

The Physics and Radiobiology of Fast Neutron Beams. By D. K. Bewley, pp. xii + 179, 1989 (Medical Science Series, Adam Hilger, Bristol), £29.50
ISBN 0 85 274 093X

Ten years after the publication *of Fast Neutrons in the Treatment of Cancers* by Mary Catterall and David K. Bewley in 1979, David Bewley has published an update on fast neutron therapy which concentrates on physical and radiobiological aspects. Since the first applications of fast neutrons at Hammersmith Hospital in the 1970s significant improvments have been achieved. Improvements have also been seen in the neutron generators and collimation systems as well as in dosimetry and radiobiology. Therefore, it was a good time to present an updated overview and synthesis of the situation of fast neutron therapy, or at least, the developments in its physical and radiobiological aspects.

The first two chapters deal with the production of neutron beams and their interactions with matter. Useful tables and figures present the neutron spectra, cross sections and kerma ratios. Neutron dosimetry is discussed in Chapter 3. The important problem of the separation between the neutron and the gamma components is stressed. Typical dose distributions are presented in Chapter 4, with several illustrating examples. Comparison is always made with the dose distribution for high-energy photons (beam penetration and skin sparing). The improvement made in the physical selectivity of fast neutron therapy during these last two decades is obvious. In the best equipped neutron therapy facilities, the isodose curves for neutrons and photons become very similar.

Protection problems are more important in neutron therapy than in photon therapy. They will become even more difficult with the application of the new ICRP recommendations. Some methods for reducing the dose to staff are indicated. As pointed out, survey instruments based on microdosimetric principles are promising. Two additional methods used at the Louvain-la-Neuve facility should have been added—a construction of a neutron pit (especially when a fixed vertical beam is used) and a shutter to protect the hands of the radiographers.

Chapter 7 on radiobiology is important and well presented. It starts from the rationale of introduing fast neutrons in therapy (hypoxic cells) and discusses the other additional mechanisms through which fast neutrons could bring a potential benefit compared with photons: less differences in cell radiosensitivity related to mitotic cycle, less repair, etc. Detailed information on RBE is presented, especially RBE variation with dose, differences between RBE for early and late effects, etc. The point is made that a single conversion factor is not sufficient to take into account the RBE differences when comparing neutrons with photons, but even when comparing two neutron beams of different energy (*e.g.* when comparing d(16)+Be and p(62)+Be neutron beams, which are the lowest and the highest neutron energies used in therapy). The concept of effective neutron dose D_n, eff is developed in some length, although the author is fair to recognize that international opinion (*e.g.* the ICRU) recommends that dose specification for treatment should be in terms of total dose ($D_n + D_\gamma$) with the γ-component noted separately.

A rather short review of the clinical results of neutron therapy is given in Chapter 8, with evident care to remain objective. A clinical discussion was obviously not the purpose of the book. The heavy ions are briefly mentioned and the radiation hazards of neutrons are discussed in Chapter 9.

This book by David Bewley has certainly been welcomed by all those who are involved in fast neutron therapy, namely engineers, physicists, radiobiologists and radiation oncologists. The structure of the book is clear and concise. The reader immediately realizes that it has been written by somebody who has been personally and deeply involved. In addition, the book is a useful source of information for those groups of scientists interested in different types of applications of neutrons. Finally, it provides a valuable set of data for those radiation oncologists who are confronted with the debates about fast neutron therapy, and who want to build up their own knowledge.

The only regret, especially from the neutron radiobiology teams on the continent, is that so little from their own data has been quoted.

André Wambersie

1992, *The British Journal of Radiology*, *65*, 955–960

VOLUME 65 NUMBER 779 NOVEMBER 1992

The British Journal of Radiology

Direct coronal computed tomography of the temporomandibular joint in patients with rheumatoid arthritis

By P. Goupille, MD, B. Fouquet, MD, *P. Cotty, MD, †D. Goga, MD and J.-P. Valat, MD

Departments of Rheumatology, *Neuroradiology and †Maxillofacial Surgery, University of Tours, Trousseau Hospital, 37044 Tours Cedex, France

(*Received 17 June 1991 and in final form 9 March 1992, accepted 6 May 1992*)

Keywords: Rheumatoid arthritis, Temporomandibular joint, Computed tomography

Abstract. Direct coronal computed tomography (CT) of the temporomandibular joint (TMJ) was performed in 26 patients with rheumatoid arthritis (RA) and 26 control subjects. Erosions and cysts of the mandibular condyle had a significantly higher frequency in the RA group than in the control group ($p < 0.05$) but there was no significant difference in the incidence of other abnormalities. Bone changes were bilateral in RA. A wide range of CT abnormalities was present in patients with RA and in the control group. There are no CT abnormalities specific for RA, but the incidence of erosions and cysts of the mandibular condyle was significantly higher in the RA group and should suggest the diagnosis.

Reports on the extent of the involvement of the temporomandibular joint (TMJ) in rheumatoid arthritis (RA) differ widely. Clinical TMJ involvement in RA varies from 4.7% (Ragan, 1979) to 84% (Friez & Le Goc, 1982). The incidence of radiographic abnormalities on conventional radiography varies from 19 to 86% (Uotila, 1964; Ericson & Lundberg, 1967; Larheim et al, 1983; Syrjanen, 1985). There has been one previous direct coronal computed tomography (CT) study of the TMJ in adult RA (Avrahami et al, 1989), which found bone lesions in 68% of the joints. More recently, Larheim and Kolbenstvedt (1990) reported 70% of TMJ abnormalities on axial CT in patients with RA.

These variations might be due to different types of examination, the selection of patients, the use of different criteria for classifying joint involvement and the presence or absence of a control group which could lead to an overestimation of the frequency of TMJ involvement in RA. Radiological examination of the TMJ is difficult owing to its location and its relation to other cranial structures. The aims of this study were: (1) To investigate the frequency, character and severity of TMJ bone changes on direct coronal CT in RA. The significance of the findings was evaluated by comparison with a control group; (2) To determine the specific lesions of RA on TMJ.

Materials and methods

RA group

26 patients with clinically established RA based on the criteria of the American Rheumatism Association were included. The mean age of the patients was 62.1 years (SD 11.8). The female to male ratio was 22 : 4. The mean duration of the disease was 105 months (SD 133 months, range 0.5–51 years).

Control group

26 patients (mean age 62 years, SD 11.4 years) without general joint disease and admitted for sciatica were included. The selection was based on age and sex to match the RA group.

Ethical committee permission was granted and informed consent was obtained after the nature of the procedure had been fully explained.

Coronal CT examination of the TMJ

26 RA and 26 control subjects underwent coronal CT examination of the TMJ. The patients who had no evidence of cervical spine instability on neck radiography were examined in the supine position, with hyperextension of the neck. The radiographic beam was directed cephalad through the TMJ by a 20° tilt of the gantry. CT sections were selected on the lateral scout view, making certain that each condyle was imaged (Fig. 1). Contiguous 1.5 mm thick scans were obtained and a retrospective target reconstruction was made with a hard filter. Interpretation was made on a computer console with bone and soft-tissue windows settings. All CT scans were examined "blind" and in random order by a single observer. In each CT scan, the shape (convex, concave or flattened) and the height (normal, hypoplasic or hyperplasic) of the mandibular condyle were estimated. The presence or absence of the following features was evaluated: flattening of the articular eminence, bone demineralization, erosions and bone cysts of the mandibular condyle and glenoid fossa (none, one, two or more), condylar head resorption (none, mild, severe), mandibular fracture, decreased

---

Address correspondence to Dr P. Goupille.

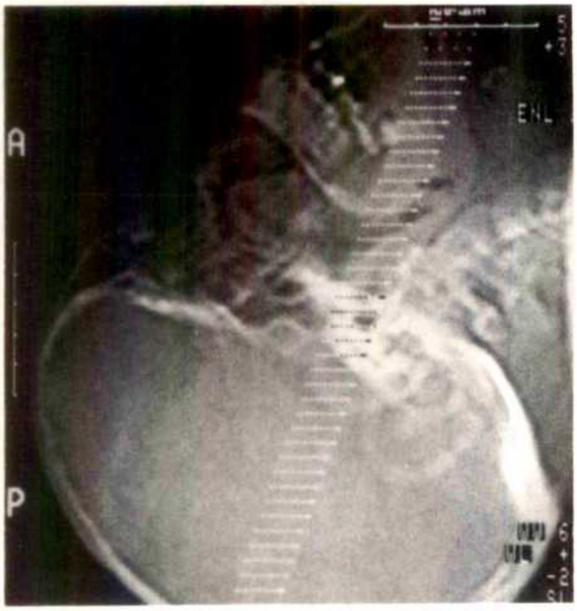

Figure 1. CT scan showing coronal section.

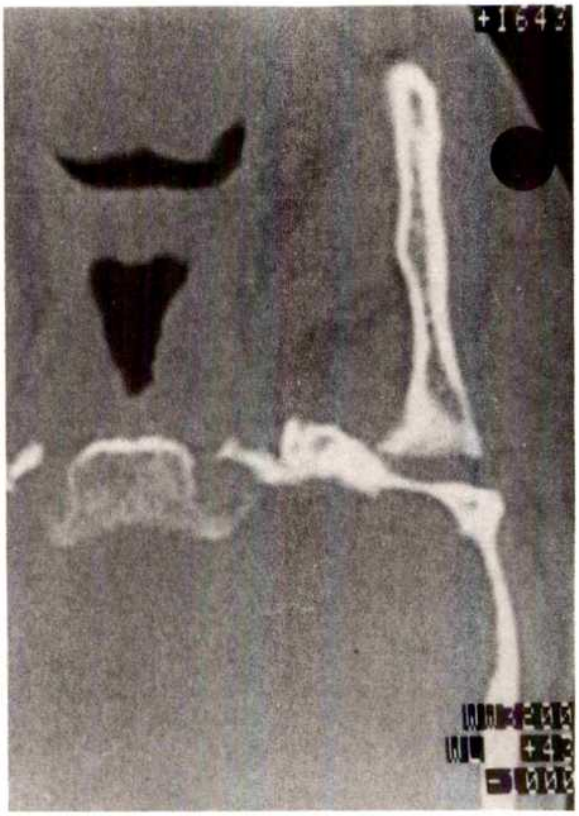

Figure 3. Extensive erosion of the condylar surface of the mandibular condyle in RA.

joint space (less than 0.5 mm), bony ankylosis, temporal or mandibular subchondral sclerosis, osteophytosis and calcification of the articular disc.

Statistics

For each parameter, the significance of differences between the two groups was analysed by means of the χ^2 test. The level of statistical significance was $p < 0.05$, otherwise denoted NS.

Results

Only five control subjects were free of bone changes; most (20) had flattening of the articular eminence.

Changes in condylar shape, erosions and cysts of the mandibular condyle and condylar head resorption were more frequent in the RA group than the control group (Table I). A statistically significant difference was only found for erosions and cysts of the mandibular condyle (Table I). Osteophytic changes were more frequent in the RA group than in the control group, without a statistically significant difference (Table I).

Erosions and bone cysts were demonstrated in 88% of the TMJ in RA compared with 58% in the control group ($p < 0.05$). In most cases, the bone changes in RA were bilateral.

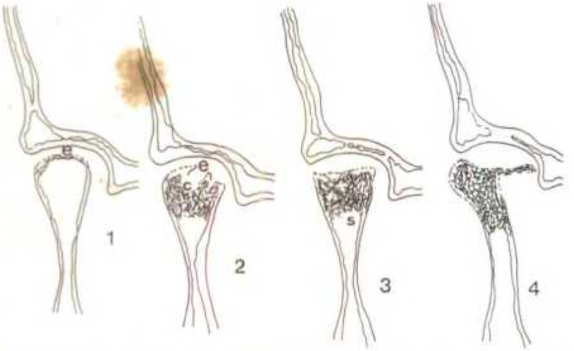

Figure 2. Four stages of bone changes of the mandibular condyle on CT in RA. e, erosion; c, cysts; s, sclerosis.

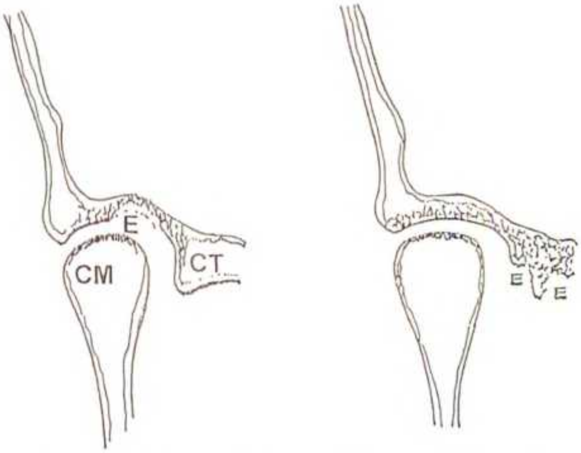

Figure 4. Bony changes of the glenoid fossa on CT in RA. E, erosions; CT, glenoid fossa; CM, mandibular condyle.

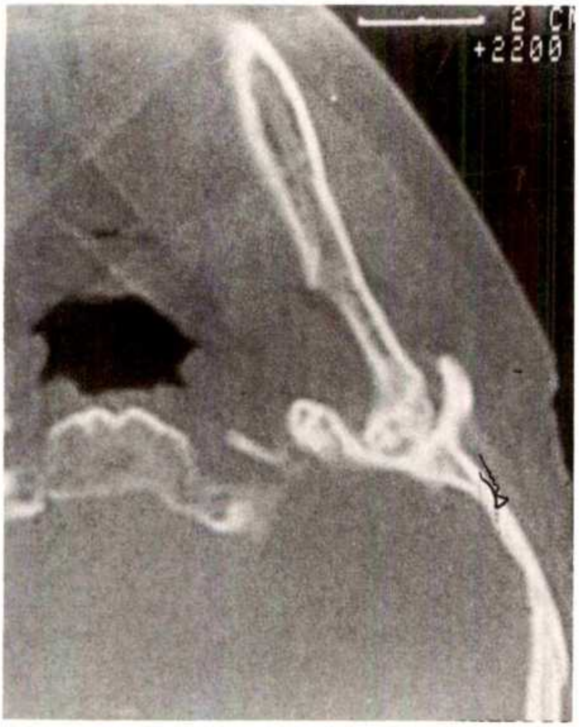

Figure 5. Osteophyte arising from the glenoid fossa in RA.

Bone changes of the mandibular condyle among the RA group were classified into four grades (Fig. 2):

Grade 1: erosions of the subchondral bone.
Grade 2: erosions with deep cysts.
Grade 3: extensive erosion of the condylar surface (Fig. 3).
Grade 4: flattening and resorption of the condylar surface.

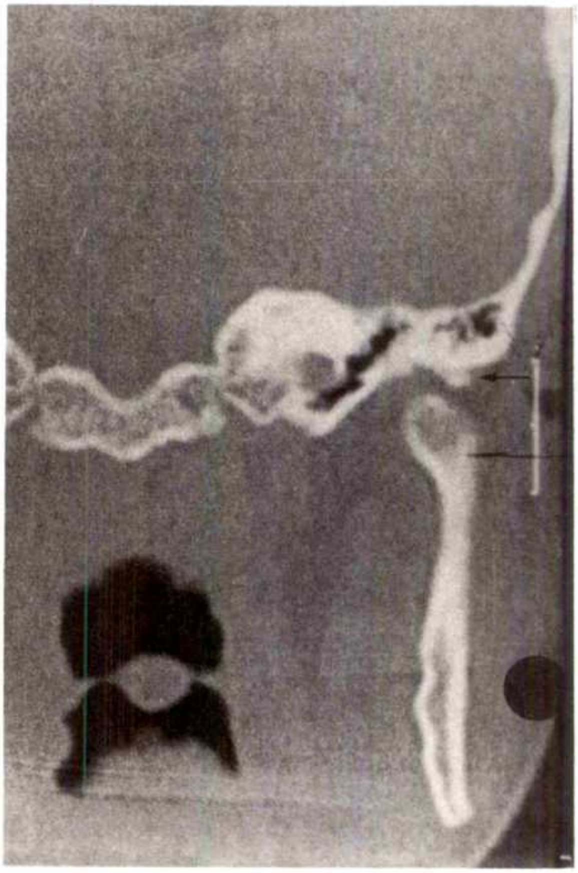

Figure 6. Meniscus calcification in RA (arrow).

Bone changes of the glenoid fossa were less frequent (Table I). Erosions and cysts involved either the floor or the internal part of the glenoid fossa (Fig. 4).

Table I. Bone changes among 26 patients with RA and 26 control subjects on coronal CT of the TMJ

	Control ($n = 26$)		RA ($n = 26$)	
	Right TMJ	Left TMJ	Right TMJ	Left TMJ
		$p < 0.001$		
Erosions of the mandibular condyle	4	3	19	17
		$p < 0.001$		
		$p < 0.001$		
Cysts of the mandibular condyle	7	8	20	17
		$p < 0.001$		
Condylar head resorption	5	4	10	11
Deformity of the mandibular condyle	11	12	17	20
Osteophytes arising from mandibular condyle	5	3	6	7
Erosions of the glenoid fossa	6	6	9	9
Cysts of the glenoid fossa	5	4	7	10
Flattening of the articular eminence	19	18	14	16
Meniscus calcification	4	1	4	1
Decreased joint space	13	13	12	9

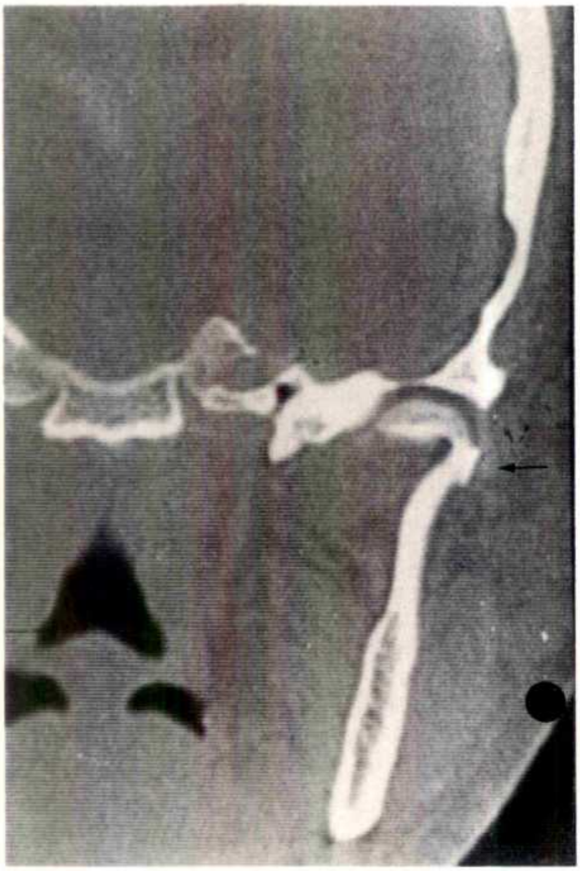

Figure 7. Calcification adjacent to the lateral aspect of the mandibular condyle in RA (arrow).

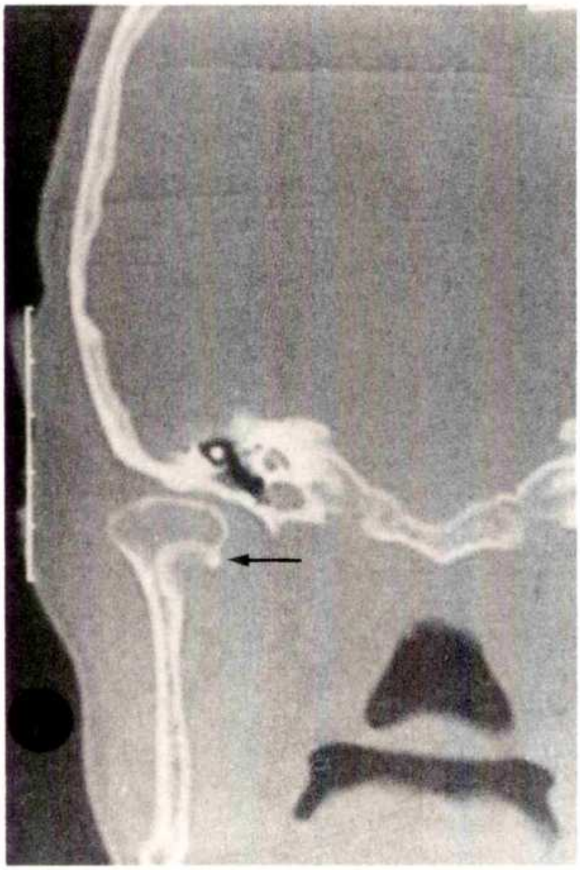

Figure 8. Medial osteophyte of the mandibular condyle in a "teardrop" configuration in RA (arrow).

Six patients with RA had large destructive lesions: (a) flattening of the mandibular condyle and glenoid fossa with erosions of the articular surfaces, sclerosis and decreased joint space; (b) multiple cysts of the articular surfaces, erosions, more decreased joint space and changes of the glenoid fossa; (c) osteophyte arising from the glenoid fossa (Fig. 5); and (d) an osteocartilaginous loose body was noted in one case.

Intra-articular calcification was also seen: meniscal calcification in six cases (Fig. 6); larger intra-articular calcification in one case; and calcification along the outer part of the mandibular condyle in one case (Fig. 7). Ankylosis of the TMJ in RA was observed in two TMJs. Other changes (one in each case) were noted: (a) decreased joint space and sclerosis of the articular surfaces; (b) "teardrop" osteophyte of the mandibular condyle (Fig. 8); (c) osseous bridging between the glenoid fossa and the mandibular condyle; and (d) bone sequestra within an area of bone sclerosis (Fig. 9).

Discussion

Since Suarez et al (1980) made their preliminary study on CT of the TMJ, the technique has rapidly proved to be highly accurate for evaluating both bony changes and the meniscal position (Helms et al, 1984a; Manzione et al, 1984; Sartoris et al, 1984; Thompson et al, 1984). The sagittal view may give more information regarding the position of the meniscus than the coronal view (Helms et al, 1984b; Manzione et al, 1984a; Manco et al, 1985; Raustia et al, 1985), but the coronal plane allows better visualization of the osseous elements of the TMJ (Horowitz et al, 1982; Larheim & Kolbenstvedt, 1984; Reck & Fielding, 1986). Axial sections cut the articular surfaces of the condylar head and glenoid fossa tangentially, precluding the demonstration of fine bone changes (Avrahami et al, 1989). The aim of our study was to estimate the osseous involvement of TMJ in RA, so the coronal plane was used.

Erosions and cysts of the TMJ in RA on coronal CT were frequent in our study (88%). The only previous coronal CT study of the TMJ in adult RA found 68% of bone lesions of various degrees, but without a control group (Avrahami et al, 1989).

Contrary to some other studies obtained with conventional radiography or tomography (Mayne & Hatch, 1969; Blair, 1973; Trenwith & Beale, 1977; Syrjanen, 1985), some bone changes were equally distributed in the two groups in our study, namely flattening of the

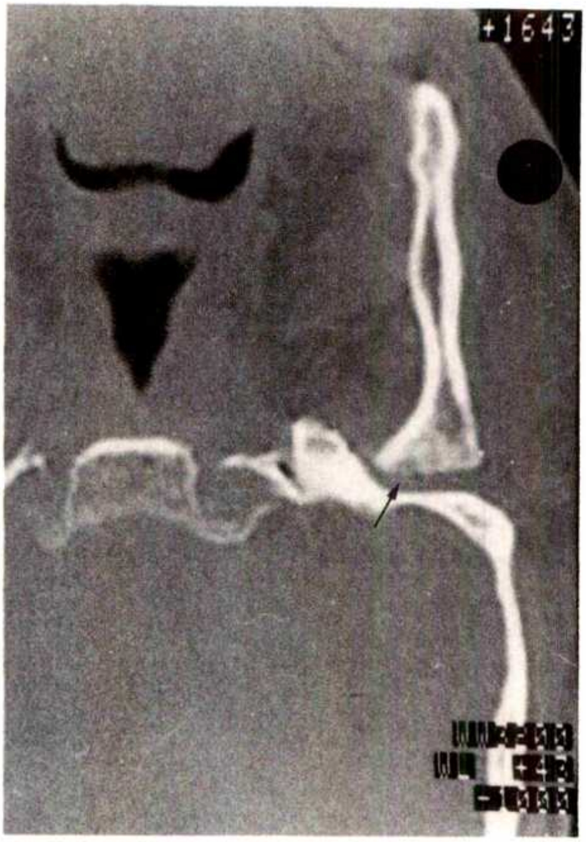

Figure 9. Bone sequestrum (arrow) within a sclerotic area of the mandibular condyle in RA.

articular eminence, decreased joint space, calcification of the articular disc, osteophytosis and subchondral sclerosis. Erosions and changes in the shape of the mandibular condyle have been described as osteoarthritic lesions (Toller, 1973, 1974; Rasmussen, 1981).

We found that the lesions most suggestive of RA were erosions and cysts of the mandibular condyle, and this agrees with some previous papers (Blanc, 1959; Mayne & Hatch, 1969; Chalmers & Blair, 1973). Bilateral involvement of the TMJ was more common in the RA group than in the control group, and this also agrees with previous papers (Resnick, 1974; Lowry, 1975; Seymour et al, 1975).

In conclusion, coronal CT scanning is an accurate technique for evaluating bone changes in the TMJ. Erosions and cysts of the mandibular condyle and the bilateral nature of these abnormalities are suggestive of RA.

Acknowledgment

We wish to thank Mrs S. Gardès for typing the manuscript.

References

Avrahami, E., Segal, R., Solomon, A., Garti, A., Horowitz, I., Caspi, D., Wigler, I. & Yaron, M., 1989. Direct coronal high resolution computed tomography of the temporomandibular joints in patients with rheumatoid arthritis. *Journal of Rheumatology, 16,* 298–301.

Blanc, P., 1959. L'atteinte de l'articulation temporo-maxillaire au cours du rhumatisme inflamatoire chronique. *Cahiers Odonto-stomatologiques, 9,* 17–73.

Chalmers, I. M. & Blair, G. S., 1973. Rheumatoid arthritis of the temporomandibular joint. A clinical and radiological study using circular tomography. *Quarterly Journal of Medicine (New series), 42,* 369–386.

Ericson, S. & Lundberg, M., 1967. Alterations in the TMJ at various stages of rheumatoid arthritis. *Acta Rheumatologica Scandinavica, 13,* 257–274.

Friez, L. & Le Goc, Y., 1982. Articulations temporo-maxillaires et polyarthrite rhumatoïde. *Rhumatologie, 34,* 193–196.

Helms, C. A., Vogler, J. B. & Morrish, R. B., 1984a. Diagnosis by computed tomography of temporomandibular joint meniscus displacement. *Journal of Prosthetic Dentistry, 51,* 544–547.

Helms, C. A., Vogler, J. B., Morrish, R. B., Goldman, S. M., Capra, R. E. & Proctor, E., 1984b. Temporomandibular joint internal derangements: CT diagnosis. *Radiology, 152,* 459–462.

Horowitz, I., Avrahami, E. & Mintz, S. S., 1982. Demonstration of condylar fractures of the mandible by computed tomography. *Oral Surgery, Oral Medicine, Oral Pathology, 54,* 263–268.

Larheim, T. A. & Kolbensvedt, A., 1984. High-resolution computed tomography of the osseous temporomandibular joint. Some normal and abnormal appearances. *Acta Radiologica, 25,* 465–469.

Larheim, T. A. & Kolbenstved, A., 1990. Osseous temporomandibular joint abnormalities in rheumatic disease. Computed tomography versus hypocycloidal tomography. *Acta Radiologica, 31,* 383–387.

Larheim, T. A., Storhaug, K. & Tveito, L., 1983. Temporomandibular joint involvement and dental occlusion in a group of adults with rheumatoid arthritis. *Acta Odontologica Scandinavica, 41,* 301–309.

Lowry, J. C., 1975. Psoriatic arthritis involving the temporomandibular joint. *Journal of Oral Surgery, 33,* 206–208.

Manco, L. G., Messing, S. G., Busino, L. J., Fasulo, C. P. & Sordill, W. C., 1985. Internal derangements of the temporomandibular joint evaluated with direct sagittal CT: a prospective study. *Radiology, 157,* 407–412.

Manzione, J. V., Katzberg, R. W., Brodsky, G. L., Seltzer, S. E. & Mellins, H. Z., 1984. Internal derangement of the temporomandibular joint: diagnosis by direct sagittal computed tomography. *Radiology, 150,* 111–115.

Mayne, J. G. & Hatch, G. S., 1969. Arthritis of the temporomandibular joint. *Journal of the American Dental Association, 79,* 125–130.

Ragan, C., 1979. General management of rheumatoid arthritis. *Journal of the American Medical Association, 141,* 124.

Rasmussen, O. C., 1981. Description of population and progress of symptoms in a longitudinal study of temporomandibular arthropathy. *Scandinavian Journal of Dental Research, 89,* 196–203.

Raustia, A. M., Pyhtinen, J. & Virtanen, K., 1985. Examination of the temporomandibular joint by direct sagittal computed tomography. *Clinical Radiology, 36,* 291–296.

Reck, S. F. & Fielding, A. F., 1986. Computed tomography in temporomandibular joint diagnosis. *New York State Dental Journal, 52,* 37–40.

RESNICK, D., 1974. TMJ involvement in ankylosing spondylitis. Comparison with rheumatoid arthritis and psoriasis. *Radiology, 112,* 587–591.

SARTORIS, D. J., NEUMANN, C. H. & RILEY, R. W., 1984. The temporomandibular joint: true sagittal computed tomography with meniscus visualization. *Radiology, 150,* 250–254.

SEYMOUR, R. L., CROUSE, V. L. & IRBY, W. B., 1975. Temporomandibular ankylosis secondary to rheumatoid arthritis. *Oral Surgery, Oral Medicine, Oral Pathology, 40,* 584–589.

SUAREZ, F., BHUSSRY, B., NEFF, P., HUANG, H. & VAUGHN, D., 1980. A preliminary study of computerized tomography of the temporomandibular joint. *Compendium of Continuing Education in Dentistry, 1,* 217–222.

SYRJANEN, S. M., 1985. The temporomandibular joint in rheumatoid arthritis. *Acta Radiologica, 26,* 235–243.

THOMPSON, J. R., CHRISTIANSEN, E., HASSO, A. N. & HINSHAW, D. B., 1984. TMJ: high-resolution computed tomographic evaluation. *Radiology, 150,* 105–110.

TOLLER, P. A., 1973. Osteoarthritis of the mandibular condyle. *British Dental Journal, 124,* 223–231.

TOLLER, P. A., 1974. Temporomandibular arthropathy. *Proceedings of the Royal Society of Medicine, 67,* 153–159.

TRENWITH, J. A. & BEALE, G., 1977. Rheumatoid arthritis in the temporomandibular joint. *New Zealand Dental Journal, 73,* 195–199.

UOTILA, E., 1964. The temporomandibular joint in adult rheumatoid arthritis: a clinical and roentgenologic study. *Acta Odontologica. Scandinavica, 22* (suppl. 39), 22.

1992, *The British Journal of Radiology*, *65*, 961–967

Vasoconstriction by angiographic contrast media in isolated canine arteries

By Naoya Gomi, MD

Department of Radiology, Tokyo Medical and Dental University, Faculty of Medicine, 5–45 Yushima
1-chome, Bunkyo-ku, Tokyo 113, Japan

(*Received 17 February 1992 and accepted 6 May 1992*)

Keywords: Diatrizoate, Iopamidol, Ioxaglate, Iotrolan, Meglumine, Mannitol, Dog arteries, Vasoconstriction, Vasodilatation, Osmolality, Vascular pain

Abstract. To study the mechanism of the pain produced by contrast media (CM) in peripheral arteriography, we examined the direct effects of low concentrations (1.85–100 mg I/ml) of CM (diatrizoate, iopamidol, ioxaglate, and iotrolan) on helically cut strips of canine blood vessels taken from six different regions. We found that: (a) low concentrations of CM induced vasoconstriction. (b) This occurred immediately after the application of CM and produced sustained constriction. (c) The constriction produced in arteries was dose-dependent. (d) The production and intensity of constriction in the arterial strips differed as follows: cranial mesenteric artery > renal artery > femoral artery > common carotid artery > thoracic aorta > coronary artery. The effects of the CM were, in order of magnitude: diatrizoate > iopamidol > ioxaglate > iotrolan. Differences between CM corresponded with the differences in osmolality of the CM solutions. (e) Low concentrations of meglumine and mannitol also produced vasoconstriction. (f) Constriction caused by all drug samples used was reversible, but the process of relaxation to the original tension was much slower in CM-treated arterial strips than in the other strips. From these results, we confirmed that the incidence and degree of vasoconstriction produced by all drug samples used in this experiment depended on solution osmolality, rather than on chemotoxicity or ionicity. We discuss the physiological mechanism of these results and stress the importance of CM hyperosmolality in vasoconstriction and vascular pain production.

The pain produced by intra-arterial injection of conventional contrast media is well known and presents a significant clinical problem. Recent thinking suggests that the pain is probably due to the high osmolality (Speck et al, 1980; Morris, 1988; Sovak et al, 1988) of the contrast media, the mechanism being induction of pain by vasodilatation in the local peripheral vascular bed (Grainger, 1980; Steiner et al, 1980). (1) The more serious the circulatory insufficiency, the greater is the pain (Amundsen, 1965). (2) The effect on the blood vessels of contrast media injected into the femoral artery of lumbar-sympathectomized humans can be studied by toe plethysmography. There is evidence of an immediate and striking degree of vasoconstriction on intra-arterial injection of contrast media, followed in a few minutes by vasodilatation. This vasoconstriction is independent of the sympathetic innervation and is presumed to be the result of a direct effect of contrast media on the arteries (Shaw, 1956). (3) In the hind limb of conscious rats (Nishiki et al, 1984), the infusion of 200 mg I/ml (1090 mosmol/kg H_2O) of iothalamate into the femoral artery at a rate of 2.4 ml/min and a dose of 6 ml/kg body weight immediately produces strong pain with distinct local ischaemia, which continues during infusion for about 1 min, and then is followed by definite local flushing which is not associated with vascular pain. Because pain and skin changes in the hind limb cannot be observed in saline experiments, this report suggests that the former is due to vasoconstriction and the latter vasodilatation. The intensity of pain and skin changes are lower with metrizamide (310 mosmol/kg H_2O) than with iothalamate. These indicate to us that the direct effects of lower concentrations of the contrast media on arteries (*i.e.* vasoconstriction) may be important in pain production, because in the early stage of contrast medium infusion or injection, there is a low concentration of contrast medium in the blood.

In the present experiment, the direct effects of conventional and new low-osmolar contrast media (ionic and non-ionic) and of meglumine and mannitol (for the effect of osmolality) were studied in different isolated canine arteries.

Materials and methods

Mongrel dogs of both sexes, weighing 10–15 kg, were anaesthetized with sodium pentobarbital (30 mg/kg, intravenously) and sacrificed by bleeding from the carotid arteries. The cranial mesenteric artery (CMA), renal artery (RA), femoral artery (FA), common carotid artery (CCA), coronary artery (CA) and thoracic aorta (TA) were isolated. The vessels were cut spirally into strips of approximately 15 mm × 3 mm. Each strip was fixed vertically between hooks under a resting tension of 1–2 g in a 20 ml organ bath containing Krebs' solution. The upper end of the strip was connected to the lever arm of a force-displacement transducer. The bathing solution (pH 7.2–7.4) was bubbled with a mixture of 95% O_2–5% CO_2 and was maintained at 37 ± 0.5°C. Constituents of the solution (mmol/l) were: Na^+, 143.5; K^+, 5.9; Ca^{2+}, 2.5; Mg^{2+}, 2.5; Cl^-, 125.8; $H_2PO_4^-$, 1.2; SO_4^{2-}, 2.5; HCO_3^-, 25.0; dextrose, 5.0. Before the

Table I. Iodine concentration and osmolality of contrast media used in this experiment

Contrast medium	Iodine concentration (mg I/ml)	Osmolality (mosmol/kg H_2O)
Diatrizoate (Urografin 60%)	292	1500
Iopamidol (Iopamiron 300)	300	612
Ioxaglate (Hexabrix 320)	320	600
Iotrolan (Isovist 240)	240	300

experiments the preparations were allowed to equilibrate for 90–120 min in the bathing medium. They were then primed by adding 2.7×10^{-6} mol/l norepinephrine (TA and CA) and 1.4×10^{-6} mol/l norepinephrine (CMA, RA, FA and CCA) twice, to establish a constant contractile response. In experiments using modified Krebs' solution, the strips were exposed for 100 min and the solution was replaced every 20 min during the exposure period. Norepinephrine was used to establish that each specimen was still intact.

Drugs used were: contrast media, diatrizoate, iopamidol, ioxaglate and iotrolan (the iodine concentration and osmolality of contrast media are shown in Table I); meglumine HCl; mannitol; and norepinephrine hydrochloride.

The vasomotor responses of strips to drugs were recorded on an ink-writing oscillograph. The response of each strip to each agent in normal nutrient solution, Krebs' solution, was measured as length and expressed as an absolute tension value (1.0 cm = 1.0 g). Mannitol solution (280 mosmol/kg H_2O) was used as a control. After the effect of each drug concentration on tension was tested, each sample solution in the bath was analysed for osmolality, using a vapour pressure osmometer. Results shown in the text, tables and figures are expressed as mean values ± standard deviation of the means. Statistical analyses were made using Student's t-test and values of $p < 0.05$ were regarded as significant. The effects of drugs on tension under various conditions are described below.

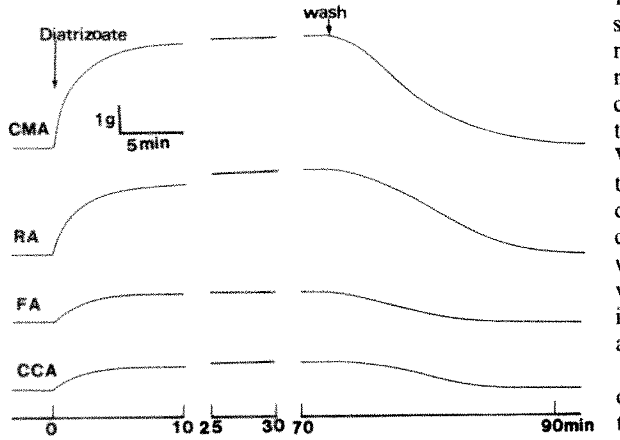

Figure 1. Typical responses of isolated strips of different arteries to diatrizoate (51.6 mg I/ml). CMA, cranial mesenteric artery; RA, renal artery; FA, femoral artery; CCA, common carotid artery.

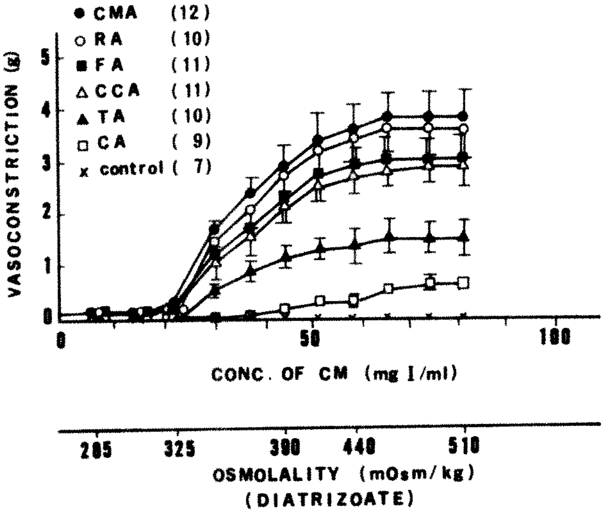

Figure 2. Constrictive responses of different isolated arteries to diatrizoate at different concentrations. Figures in parentheses indicate the number of preparations tested. CMA, cranial mesenteric artery; RA, renal artery; FA, femoral artery; CCA, common carotid artery; TA, thoracic aorta; CA, coronary artery; CM, contrast medium.

Results

Effects of contrast media on isolated strips of different arteries

Each of the CM, at varying concentrations of 1.85–100 mg I/ml, were added directly to the bathing solution. A typical experiment with one contrast medium (51.6 mg I/ml diatrizoate, an ionic monomeric medium) is shown in Fig. 1. Sustained constriction, consisting of an initial phasic constriction followed by a tonic phase, was induced by diatrizoate in all arteries. Vasoconstriction developed immediately after application of diatrizoate, but production and degree of tension differed with their origin. The rate of increase of constrictive response and the intensity of constriction were less in FA and CCA than in CMA and RA. The vasomotor effects of this contrast medium were reversible, but more than 15 min was required to relax the arteries to their initial tension level.

Figures 2–5 show the results when CM were added directly to the bathing medium in cumulative concentrations (1.85–100 mg I/ml). Figure 2 shows the dose–response curves of diatrizoate. The control solution and 1.85–14.8 mg I/ml diatrizoate had no effect on arterial strips from any of the six regions. The threshold concentration of diatrizoate for inducing constriction in

Table II. Relationship between CM iodine concentration of 74.0 mg I/ml and vascular constriction in different regional arterial segments

CM solution	Vascular constriction (g)					
	CMA	RA	FA	TA	CCA	CA
Diatrizoate	3.75 ± 0.47	3.55 ± 0.45	2.98 ± 0.36^{a}	1.45 ± 0.31^{a}	2.85 ± 0.25^{a}	0.55 ± 0.07^{a}
Iopamidol	2.75 ± 0.33^{b}	2.50 ± 0.41^{b}	1.85 ± 0.26^{ab}	1.95 ± 0.05^{ab}	0.80 ± 0.52^{ab}	0
Ioxaglate	1.00 ± 0.36^{b}	0.85 ± 0.35^{b}	0.55 ± 0.42^{ab}	0.25 ± 0.09^{ab}	0.60 ± 0.28^{ab}	0
Iotrolan	0	0	0	0	0	0

CM, contrast media; CMA, cranial mesenteric artery; RA, renal artery; FA, femoral artery; TA, thoracic aorta; CCA, common carotid artery; CA, coronary artery.

[a] Significant difference from CMA in each group ($p < 0.05$).

[b] Significant difference from diatrizoate in each group ($p < 0.05$).

arteries, except for CA, was 22.2 mg I/ml and tension was in the range of 0.1–0.3 g. The threshold concentration for inducing constriction in CA was 29.6 mg I/ml; this concentration induced severe constrictions in all other arteries about five times the constriction produced by a concentration of 22.2 mg I/ml: 1.65±0.21 g in CMA, 1.50±0.33 g in RA, 1.2±0.53 g in FA, 1.13±0.21 g in CCA, 0.63±0.11 g in TA, and 0.05±0.01 g in CA. Vasoconstriction increased with increasing iodine concentrations; maximum constriction was induced by 74.0 mg I/ml. The values of vascular constriction in different regional arterial segments caused by each CM containing 74.0 mg I/ml are shown in Table II. However, as can be seen in Fig. 2, there was a marked difference between the responses to diatrizoate in arteries from different regions.

Figure 3 shows the responses to iopamidol, a non-ionic monomeric medium, in isolated arteries. The threshold concentration of iopamidol for eliciting constriction was higher than that of diatrizoate: 29.6 mg I/ml in CMA, RA, FA and CCA, 37.0 mg I/ml in TA, and 81.4 mg I/ml in CA. The dose–response curves of iopamidol were almost linear, although regional differences were observed in the vascular reactivity to this contrast medium. Maximum constriction, obtained by a concentration of 100 mg I/ml was: 3.60±0.37 g in CMA, 3.52±0.31 g in RA, 3.10±0.25 g in FA, 2.45±0.38 g in CCA, 1.55±0.22 g in TA, and 0.23±0.09 g in CA. The relationship between the production and degree of vasoconstriction and the iodine concentration of iopamidol differed from that of diatrizoate, higher concentrations of iodine in iopamidol being required to produce vasoconstrictive responses similar to those of diatrizoate.

Figure 4 shows the responses to ioxaglate, an ionic dimeric medium. All the responses of isolated strips of

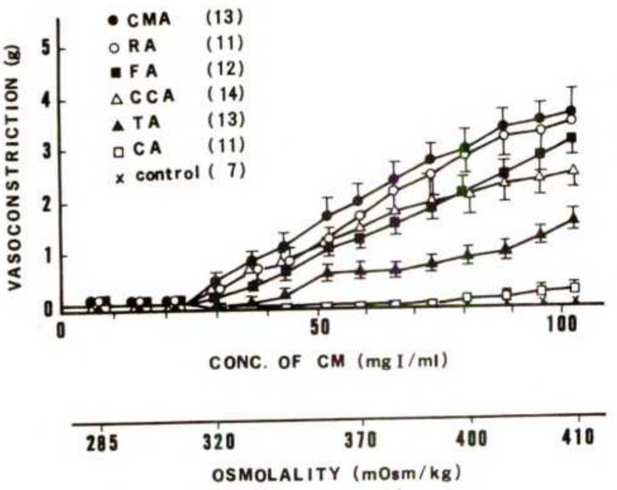

Figure 3. Constrictive responses of different isolated arteries to iopamidol at different concentrations. Figures in parentheses indicate the number of preparations tested. CMA, cranial mesenteric artery; RA, renal artery; FA, femoral artery; CCA, common carotid artery; TA, thoracic aorta; CA, coronary artery; CM, contrast medium.

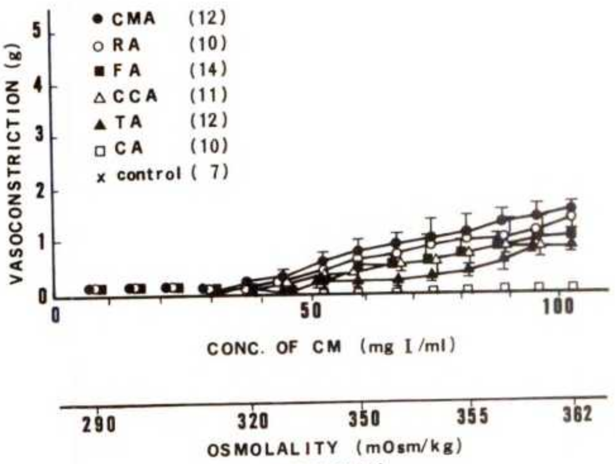

Figure 4. Constrictive responses of different isolated arteries to ioxaglate at different concentrations. Figures in parentheses indicate the number of preparations tested. CMA, cranial mesenteric artery; RA, renal artery; FA, femoral artery; CCA, common carotid artery; TA, thoracic aorta; CA, coronary artery; CM, contrast medium.

Table III. Relationship between equiosmolar solution (360 mosmol/kg H_2O) of contrast media and vascular constriction in different regional arterial segments

CM solution	Vascular constriction (g)					
	CMA	RA	FA	TA	CCA	CA
Diatrizoate	1.65 ±0.11	1.50 ±0.23	1.20 ±0.17	0.63 ±0.04	1.13 ±0.32	0.05 ±0.01
Iopamidol	1.65 ±0.28	1.35 ±0.19	1.10 ±0.09	0.60 ±0.05	1.20 ±0.12	0
Ioxaglate	1.50 ±0.10	1.38 ±0.24	1.00 ±0.03	0.68 ±0.08	0.95 ±0.11	0

CM, contrast media; CMA, cranial mesenteric artery; RA, renal artery; FA, femoral artery; TA, thoracic aorta; CCA, common carotid artery; CA, coronary artery.
No statistically significant difference from diatrizoate was found in any group.

different arteries to ioxaglate were similar to those in Figs 1, 2 and 3, and dose–response curves were similar to those in Fig. 3. However, the threshold concentration of ioxaglate for inducing constriction in arteries was higher than that of diatrizoate and iopamidol, being 37.0 mg I/ml in CMA and RA, 44.4 mg I/ml in FA and CCA, and 51.6 mg I/ml in TA. The maximum constriction produced by 100 mg I/ml was: 1.50±0.42 g in CMA, 1.20±0.13 g in RA, 1.00±0.33 g in FA, 0.90±0.18 g in CCA, and 0.75±0.11 g in TA. However, these values were below one-half of those observed for diatrizoate. No response of CA could be observed during this experiment.

Values of vasoconstriction in different regional arterial segments caused by each of three contrast media of the same osmolality (360 mosmol/kg H_2O) are shown in Table III.

Figure 5 shows the responses to iotrolan, a non-ionic dimeric medium. None of the solutions of iotrolan, or the control solution, had any effect on the isolated strips of different arteries (Table II).

Effects of meglumine on isolated strips of different arteries

Meglumine solutions produced a phasic constriction followed by a sustained one, as can be seen in Fig. 1 for the sodium/meglumine salt diatrizoate. The constriction was reversible, but about 2 min was required for the relaxation of the tissues to their initial tension level. Figure 6 shows responses to meglumine. Meglumine (0.03–1.0 mol/l) in Krebs' solution was added to the arteries. None of the arteries responded to 0.03 mol/l meglumine or the control solution. Application of 0.1 mol/l induced significant constriction in the following order: CMA > RA > FA > CCA > TA. However, the constrictive effect of 0.3 mol/l meglumine on the vascular strips was below one-third that of the 0.1 mol/l-applied strips. The constrictive effect of meglumine on the arteries decreased with increasing concentration of meglumine, and application of 1.0 mol/l completely inhibited the production of any constrictive effect. No effects were observed in CA with any concentration of meglumine used.

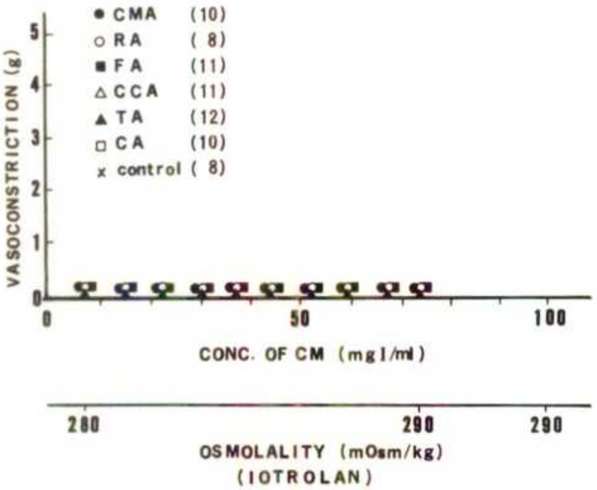

Figure 5. Constrictive responses of different isolated arteries to iotrolan at different concentrations. Figures in parentheses indicate the number of preparations tested. CMA, cranial mesenteric artery; RA, renal artery; FA, femoral artery; CCA, common carotid artery; TA, thoracic aorta; CA, coronary artery; CM, contrast medium.

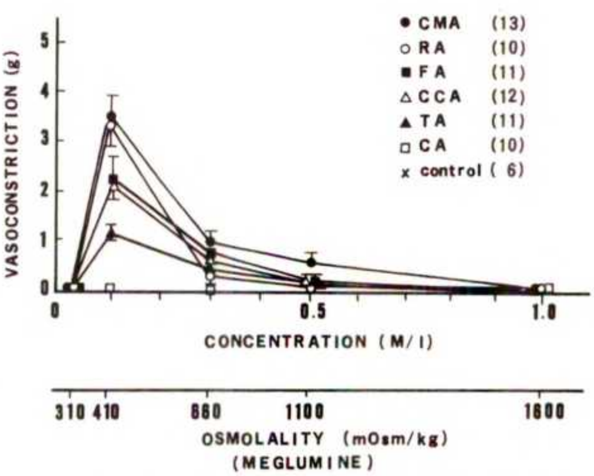

Figure 6. Effects of meglumine at different concentrations on the vasomotor responses of different isolated arteries. Figures in parentheses indicate the number of preparations tested. CMA, cranial mesenteric artery; RA, renal artery; FA, femoral artery; CCA, common carotid artery; TA, thoracic aorta; CA, coronary artery.

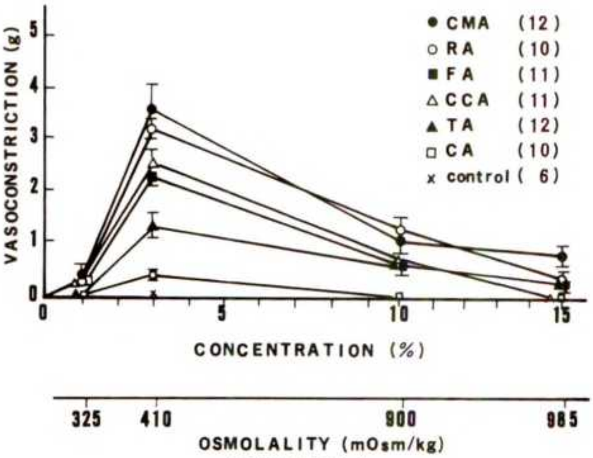

Figure 7. Effects of mannitol at different concentrations on the vasomotor responses of different isolated arteries. Figures in parentheses indicate the number of preparations tested. CMA, cranial mesenteric artery; RA, renal artery; FA, femoral artery; CCA, common carotid artery; TA, thoracic aorta; CA, coronary artery.

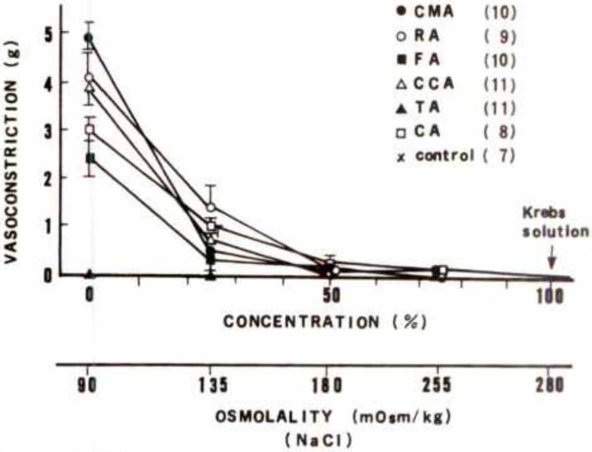

Figure 8. Effects of hypo-osmotic solutions at different concentrations on the vasomotor responses of different isolated arteries. Figures in parentheses indicate the number of preparations tested. CMA, cranial mesenteric artery; RA, renal artery; FA, femoral artery; CCA, common carotid artery; TA, thoracic aorta; CA, coronary artery. Hypo-osmotic solutions were prepared by removing NaCl from Krebs' solution.

Effects of osmolality on isolated strips of different arteries

Effect of high osmolality. Hyperosmotic solution was prepared by adding excess mannitol to isotonic Krebs' solution. All the vascular responses of the isolated strips of different arteries to hyperosmotic solution were similar to those induced by meglumine (Fig. 6). Figure 7 shows responses to hyperosmotic solution. Application of control (280 mosmol/kg H_2O) or Krebs' solution (280 mosmol/kg H_20) had no effect on any of the arteries used. The production and degree of vasoconstriction increased with increasing mannitol concentration (osmolality) up to 3% mannitol (410 mosmol/kg H_2O), which induced significant vasoconstriction under almost the same conditions as those in the CM- and meglumine-applied strips. However, the intensity of tension due to 10% mannitol (900 mosmol/kg H_2O) was one-third that of the strips treated with 3% mannitol. This trend continued with increasing hyperosmolality.

The values of vasoconstriction in different regional arterial segments caused by diatrizoate, iopamidol, meglumine and mannitol of the same osmolality (410 mosmol/kg H_2O) are shown in Table IV.

Effect of low osmolality. A hypo-osmotic solution was prepared by removing NaCl from isotonic Krebs' solution (280 mosmol/kg H_2O). Exposure of the isolated strips of different arteries to this hypo-osmotic solution induced constriction of a sustained nature, similar to the effect of the hyperosmotic CM diatrizoate, as seen in Fig. 1. Figure 8 shows responses to low osmolality. The production and degree of vasoconstriction increased with increasing hypo-osmolality in almost the same manner as those in the strips described above.

Discussion

Relationship between CM vasomotor effects and pain production

It has been reported (Schneider & Rand, 1988) that the vasomotor effects of CM are due chiefly to a direct effect on blood vessels. We were unable to find any

Table IV. Relationship between equiosmolar solution (410 mosmol/kg H_2O) of contrast media, meglumine and mannitol and vascular constriction in different regional arterial segments

CM solution	Vascular constriction (g)					
	CMA	RA	FA	TA	CCA	CA
Diatrizoate	3.35 ±0.47	3.20 ±0.35	2.65 ±0.41	1.30 ±0.16	2.45 ±0.22	0.30 ±0.02
Iopamidol	3.50 ±0.28	3.25 ±0.33	2.80 ±0.24	1.25 ±0.08	2.40 ±0.27	0.20 ±0.01
Meglumine	3.52 ±0.36	3.25 ±0.35	2.33 ±0.42	1.24 ±0.09	2.20 ±0.28	0
Mannitol	3.60 ±0.45	3.22 ±0.06	2.42 ±0.12	1.31 ±0.19	2.50 ±0.26	0.30 ±0.02

CM, contrast media; CMA, cranial mesenteric artery; RA, renal artery; FA, femoral artery; TA, thoracic aorta; CCA, common carotid artery; CA, coronary artery.

No statistically significant difference from diatrizoate was found in any group.

detailed reports of the direct effects of low concentrations of CM on arteries. In this study, topical application of low concentrations of CM induced vasoconstriction. The production of vasoconstriction changed significantly ($p < 0.05$) with the chemical structure of the CM, as shown in Table II (in which the iodine concentration was the same for all media), in the order: diatrizoate > iopamidol > ioxaglate > iotrolan. Iotrolan had no constrictive effects on the vascular strips during these experiments. Moreover, meglumine (used to increase the solubility of CM) and mannitol (used to test the relation of vasomotor effects and hyperosmolality) also induced vasoconstriction when applied in low concentrations.

The threshold concentration of CM for eliciting constriction of the vascular strips was 22.2 mg I/ml for diatrizoate, 29.6 mg I/ml for iopamidol, and 37.0 mg I/ml for ioxaglate, but the osmolality of all these CM solutions was the same (318 mosmol/kg H_2O). The results shown in Fig. 5 are explained by the fact that the osmolality of the highest concentration of iotrolan used in this experiment was 290 mosmol/kg H_2O, and therefore too low for an effect to be seen.

The relationship between degree of vasoconstriction and hyperosmolality was examined in solutions of the same osmolality. As can be seen in Tables III and IV, the intensity of constriction caused by CM, meglumine and mannitol (all in equiosmolar solution) was almost the same in each artery. From these results, we hypothesized that the production and intensity of vasoconstriction induced by all the drug samples used in this experiment depended on the osmolality of the solution, rather than on its chemotoxicity or ionicity. The same osmolality-dependent concept has been suggested for the production and intensity of vascular pain (Sovak et al, 1988). A possible mechanism of the constriction produced by CM is depolarization of smooth muscle cells in arteries exposed to hyperosmolality (Kuriyama et al, 1971).

In cases (Figs 6 and 7) where sample solutions of higher osmolality than about 600 mosmol/kg H_2O were used, the intensity of the vascular tension was weakened with increasing osmolality; solutions of 1600 mosmol/kg H_2O and above completely inhibited the production of vascular constriction, as shown in Fig. 6. This mechanism may be due to the hyperosmotic solution "pulling" water out of cells, increasing smooth muscle cell electrolyte concentration, and hyperpolarizing the cell (Dean et al, 1983; Morris, 1988). However, hyperosmotic solution-induced damage (Almén et al, 1973; Nyman & Almén, 1980; Thiesen & Mützel, 1990) to the vascular walls is also suggested as another mechanism.

In this experiment using canine arteries, vasodilatation induced by CM could *not* be observed. Moreover, we were unable to find any reports studying vasodilatation caused by CM, based on *in vitro* vascular preparations. However, hyperosmotic solutions (about 600 mosmol/kg H_2O and above) of CM also weakened the intensity of vascular tension with increasing osmolality, and then completely inhibited the production of vascular constriction as can be seen in Figs 6 and 7 (unpublished data). Therefore, it is suggested that vasodilatation in the local peripheral vascular bed induced by intra-arterial injecton of CM occurs via the effects of both an inhibition of the production of vascular constriction and an increase of blood volume, caused by the effects of hyperosmotic solutions.

In this study, the characteristics of vasoconstriction caused by hyperosmotic solutions were: (a) muscle tension developed immediately after application. (b) Sustained constrictions were induced by all the sample solutions used in this experiment. (c) The constrictions produced in arteries were dose-dependent. (d) The production and intensity of muscle tension differed in different arteries in the order: CMA > RA > FA > CCA > TA > CA, the threshold concentration for constriction in CA being higher than that in the other arteries. The same results were observed in arteries treated with meglumine or mannitol. The results suggest that the production and intensity of vascular pain are very low in CA when CM was injected intra-arterially. (e) The vasoconstriction caused by CM was reversible, but the time taken for the tissues to relax to the original tension was much longer than that required after meglumine and mannitol treatment. This suggests that an affinity of CM for smooth muscle cells in arteries may be important in the elucidation of the mechanism of the intensity of vascular pain, because the degree of pain elicited at the same osmolality was in the order: meglumine diatrizoate ≫ meglumine chloride (Speck et al, 1980). (f) Constriction of arteries was also induced by low NaCl concentration Krebs' solution (hypo-osmolality) as well as by a hyperosmolar solution. The mechanism of action of the former solution seemed to be depolarization of smooth muscle cells (Ozaki & Urakawa, 1981).

Possible mechanism of the relationship between vasoconstriction and the incidence of pain

When barium chloride, which produces vasoconstriction (Toda et al, 1976) under the same condition as those induced by CM, is injected into CMA, it induces visceral pain (Taira et al, 1968). The degree of visceral pain increases with increasing concentrations of barium chloride (Taira et al, 1968). The vascular pain produced by intra-arterial injections of CM is considered to be the result of a mechanism in which hyperosmotic CM solutions induce depolarization of smooth muscle cells in arteries, this effect stimulating paravascular sensory nerve terminals, or extending the vasoconstriction to the nerve terminals.

However, because the vasodilatation is mainly due to hyperpolarization of smooth muscle cells in arteries, it is difficult to explain the relationship between local vasodilatation and the pain production by this theory.

To prevent vascular pain, it is desirable that the osmolality of CM solutions should be the same as, or as near as possible to, that of blood.

Acknowledgments

I thank Professor Dr Soji Suzuki for his considerable assistance.

References

ALMÉN, T., HÄRTEL, M., NYLANDER, G. & OLIVEGRONA, H., 1973. Effects of metrizamide on silver staining of aortic endothelium. *Acta Radiologica Supplmentum, 335*, 233–238.

AMUNDSEN, P., 1965. Double-blind test in comparison of angiographic contrast media for intravascular use. *Acta Radiologica (Diagnosis) 3*, 335–343.

DEAN, P. B., KIVISAARI, L. & KORMANO, M., 1983. Contrast enhancement pharmacokinetics of six ionic and non-ionic contrast media. *Investigative Radiology, 18*, 368–374.

GRAINGER, R. G., 1980. Osmolality of intravascular radiological contrast media. *British Journal of Radiology, 53*, 739–746.

KURIYAMA, H., OHSHIMA, K. & SAKAMOTO, Y., 1971. The membrane properties of the smooth muscle of the guinea-pig portal vein in isotonic and hypertonic solutions. *Journal of Physiology (London), 217*, 179–199.

MORRIS, T. W., 1988. The cardiovascular effects of iodinated contrast media injections. *Investigative Radiology, 23* (Suppl. 1), S133–S136.

NISHIKI, K., TOKIYORI, Y., NAKADA, Y. & OSHINO, N., 1984. Minor evocation by iopamidol of vascular pain in conscious rats (in Japanese, English abstract). *Japan Pharmacology & Therapeutics, 12* (Suppl. 1), 79–87.

NYMAN, U. & ALMÉN, T., 1980. Effects of contrast media on aortic endothelium. *Acta Radiologica Supplmentum, 362*, 65–71.

OZAKI, H. & URAKAWA, N., 1981. Involvement of a Na–Ca exchange mechanism in contraction induced by low-Na solution in isolated guinea-pig aorta. *Pflügers Archiv, 390*, 107–112.

SCHNEIDER, K. M., & RAND, M. J., 1988. Vasodilation and vasoconstriction in the rabbit isolated aorta: effect of ioxilan, iohexol, and diatrizoate. *Investigative Radiology, 23* (Suppl. 1), S150–S152.

SHAW, R. S., 1956. Vascular responses to intra-arterial Diodrast and Urokon during arteriography. *Surgery, 39*, 385–398.

SOVAK, M., HALKVICH, C. & FOSTER, S. J., 1988. Current contrast media and ioxilan comparative evaluation of vascular pain by aversion conditioning. *Investigative Radiology, 23* (Suppl. 1), S84–S87.

SPECK, U., SIEFERT, H. & KLINK, G., 1980. Contrast media and pain in peripheral angiography. *Investigative Radiology, 15*, S335–S339.

STEINER, R. M., GRAINGER, R. G., MEMON, N., WEISS, D., KANOFSKY, P. B. & MENDUKE, H., 1980. The effect of contrast media of low osmolality on the peripheral arterial blood flow in the dog. *Clinical Radiology, 31*, 621–627.

TAIRA, N., NAKAYAMA, K. & HASHIMOTO, K., 1968. Vocalization response of puppies to intra-arterial administration of bradykinin and other algesic agents, and mode of actions of blocking agents. *Tohoku Journal of Experimental Medicine, 96*, 365–377.

THIESEN, B. & MÜTZEL, W., 1990. Effects of angiographic contrast media on venous endothelium of rabbits. *Investigative Radiology, 25*, 121–126.

TODA, N., HOJO, M. & SAKAE, K., 1976. Modification by temperature of the response of isolated aorta to stimulatory agents and transmural stimulation. *Blood Vessels, 13*, 210–221.

1992, *The British Journal of Radiology*, *65*, 968–970

Percutaneous drainage of splenic abscesses: an effective and safe procedure

By I. Hadas-Halpren, N. Hiller and M. Dolberg

Department of Radiology, Shaare Zedek Medical Center, POB 3235, Jerusalem 91031, Israel

(*Received 16 September 1991 and in revised form 1 May 1992, accepted 3 June 1992*)

Keywords: Spleen, Splenic abscess, Abscess drainage

Abstract. Percutaneous drainage of splenic abscesses has not yet become a common procedure due to the potential risk of bleeding and the danger of damage to neighbouring organs. We present our experience of percutaneous drainage in eight patients with splenic abscesses. Four patients were treated by therapeutic percutaneous needle aspiration of the fluid collection, and four by percutaneous trocar catheter insertion. All procedures were guided by ultrasound or computed tomography. The procedure was successful in all eight patients with no complications.

Focal diseases of the spleen can easily be demonstrated by a variety of imaging modalities and thus are accessible to interventional procedures.

Despite the common, widespread use of interventional radiology in abdominal and thoracic organs, splenic punctures are still avoided due to the risk of uncontrolled haemorrhage and possible damage to neighbouring structures (Quinn et al, 1986). In recent years only a few series reporting interventional radiology of the spleen have been published (Berkman et al, 1983; Lerner & Spataro, 1984; Quinn et al, 1986; Ramakrishnan et al, 1987; Shah et al, 1987).

Our experience with therapeutic drainage of splenic abscesses is described, emphasizing the technique, precautions, complications and results.

Materials and methods

Eight patients are presented ranging from 16 to 92 years in age (Table I).

Four had developed splenic abscesses after undergoing abdominal surgery. In the other four patients, the aetiology remains unknown.

All eight patients presented with fever and sepsis. Diagnosis of a splenic abscess was established by means of ultrasound or CT. Only patients without bleeding diatheses were considered for intervention.

The size of the intrasplenic collection was measured, and the nature of the fluid it contained was characterized. An optimal route of access (traversing the least possible amount of splenic parenchyma, and avoiding bowel and pleura) was planned using ultrasound or CT (Quinn et al, 1986).

Inflammatory processes that were very small, in a deep location, or not liquid were not considered for catheter insertion. Instead, as much fluid as possible was aspirated using a 19 gauge needle. When the abscess was large enough, liquid and accessible, drainage was feasible.

Local anaesthetic was administered and the spleen punctured using a 19–22 gauge Chiba type needle. After aspiration of fluid or pus, the needle was withdrawn. Through a small skin incision a 12–16 F trocar catheter was inserted in the direction and to the depth of the needle puncture. The catheter was left in place for 1–15 days, was regularly flushed, and was withdrawn only when pus or fluid no longer drained.

The post-procedural management included frequent pulse and blood pressure measurements as well as blood counts for early detection of haemorrhage.

Table I. Therapeutic drainage of splenic fluid collections

Age (yrs)	Predisposing factors	Type of drainage	Catheter duration (days)	Outcome	Complications
52	Gastric ulcer perforation	Aspiration	—	Cure	None
67	None	Aspiration	—	Cure	None
16	Serratia sepsis	Aspiration	—	Cure	None
89	Left hemicolectomy	Aspiration	—	Cure	None
56	Right hemicolectomy	Catheter	1	Cure	None
88	None	Catheter	13	Cure	None
80	None	Catheter	15	Cure	None
92	Left hemicolectomy	Catheter	11	Cure	None

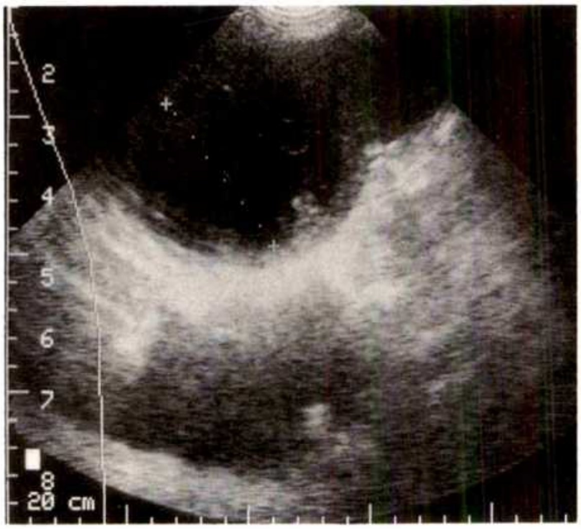

Figure 1. A 92-year-old patient suspected clinically to have urinary tract infection. Sagittal sonogram shows a large hypoechoic, thick-walled fluid collection with scattered internal echoes within the spleen.

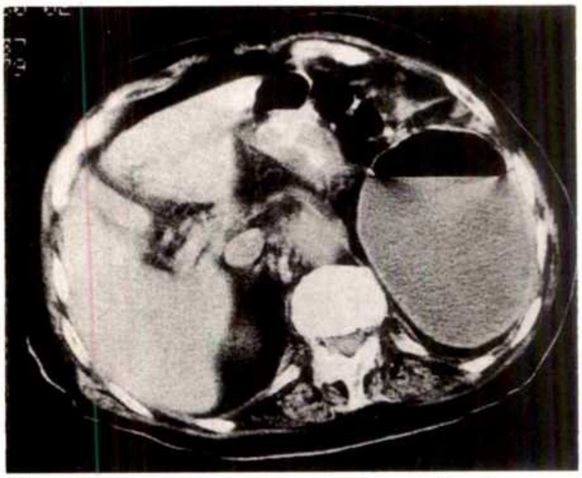

Figure 2. CT examination (same patient as Fig. 1) shows a large splenic abscess with air fluid level.

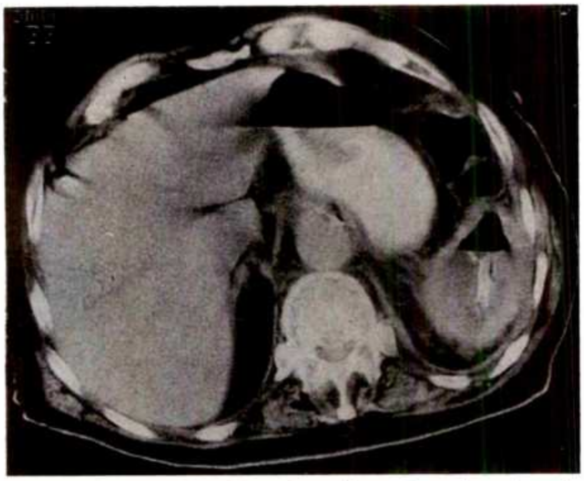

Figure 3. Same patient. Two days after catheter insertion, the abscess is much smaller.

Results

Four patients underwent therapeutic needle aspiration, and four patients were treated by placement of a trocar catheter for continuous drainage. The results are summarized in Table I.

All the patients recovered from their septic state, and follow-up examinations showed improvement until the abscess disappeared (Figs 1–3). This was true even in those cases in which not all the purulent collection was aspirated.

Discussion

Percutaneous radiologically guided biopsies and drainage are now common but rarely applied to the spleen, perhaps because of possible capsular injury and bleeding or damage to neighbouring organs (pleura and bowel) (Quinn et al, 1986).

Splenic punctures for splenoportography were performed as early as the 1950s with a relatively large (16 gauge) needle, with a low complication rate (Gzozdanovic & Hauptmann, 1955). However, interventional procedures concerning the spleen are not commonly performed. Only a few reports of drainage of splenic abscesses via a percutaneous route are available (Berkman et al, 1983; Lerner & Spataro, 1984; Quinn et al, 1986; Ramakrishnan et al, 1987; Shah et al, 1987).

Splenic abscesses are not very common. In several autopsy series, their frequency ranged from 0.14% to 0.7% (Chun et al, 1980). If left untreated, the mortality rate approaches 100% (Simpson, 1980). In the past splenectomy was the only available treatment. It is well established that the spleen is of great importance for proper immunological function and that splenectomy carries an increased morbidity rate, with danger of overwhelming post-splenectomy infections. In addition splenectomy has a significant mortality rate, especially in the elderly.

Percutaneous drainage enables preservation of the spleen and spares patients who are usually septic, severely ill and at high surgical risk, from surgery and anaesthesia, and is safe and efficient.

References

BERKMAN, W. A., HARRIS, S. A., JR & BERNARDINO, M. E., 1983. Non surgical drainage of splenic abscess. *American Journal of Roentgenology, 141*, 395–396.

CHUN, C. H., RAFF, M. J. & CONTRERAS, L., 1980. Splenic abscess. *Medicine, 59*, 50–65.

GZOZDANOVIC, V. & HAUPTMANN, E., 1955. Further experience with percutaneous lienoportal venography. *Acta Radiologica, 43*, 177–200.

LERNER, R. M. & SPATARO, R. F., 1984. Splenic abscess: percutaneous drainage. *Radiology, 153*, 643–645.

Quinn, S. F., VanSonnenberg, E., Casola, G., Wittich, G. R. & Neff, C. C., 1986. Interventional radiology of the spleen. *Radiology, 161,* 289–291.

Ramakrishnan, M. R., Sarathy, T. K. & Balu, M., 1987. Percutaneous drainage of splenic abscesses: case report and review of literature. *Pediatrics, 79,* 1029–1031.

Shah, H. R., Cue, J. I., Boyd, C. M. & Cone, J. B., 1987. Solitary splenic abscess: a new complication of splenic salvage treated by percutaneous drainage. *Journal of Trauma, 27,* 337–338.

Simpson, J. H., 1980. Solitary abscess of the spleen. *British Journal of Surgery, 67,* 106–110.

1992, *The British Journal of Radiology*, *65*, 971–976

One-view *versus* two-view mammography in baseline screening for breast cancer: a review

By *J. A. A. M. van Dijck, MSc, *A. L. M. Verbeek, MD, PhD, J. H. C. L. Hendriks, MD, PhD and R. Holland, MD, PhD

National Expert and Training Centre for Breast Cancer Screening, St Radboud University Hospital, Box 9101, NL-6500 HB Nijmegen and *Department of Medical Informatics and Epidemiology, University of Nijmegen, Kapittelweg 54, NL-6525 EP Nijmegen, The Netherlands

(*Received 18 February 1992 and in revised form 21 May 1992, accepted 22 June 1992*)

Keywords: Cancer screening, Mammography, Number of views

Abstract. Two-view mammography is generally preferred as an initial screening examination because the number of missed carcinomas and false positive results in one-view mammography is considered too large. The present review was performed to assess the difference in screening quality between one- and two-view mammography. Nineteen previous studies were reviewed and differences in sensitivity as well as specificity between two-view and one-view mammography were calculated. The results ranged from −5.7% to 19.4% (median 3.9%), and 2.7% to 36.1% (median 14.8%), respectively, and indicate a higher screening quality of two-view mammography. However, in the studies considered there is a large variation in study population, screening tests used and assessment of disease outcome, which makes the numerical results less conclusive. None of the studies provided adequate information for deciding whether two-view mammography in baseline screening for breast cancer is preferable to one-view mammography. If a screening programme using one-view mammography has already achieved high sensitivity and specificity, the value of an additional craniocaudal view is only marginal.

The maximum reduction in breast cancer mortality that can be achieved by mammographic screening depends to a large extent on the quality of the screening test. Ideally all women with preclinical breast cancer should show positive, and all others negative, screening test results.

Since the introduction of mammography in breast cancer screening, the number of views to be used, particularly for the first screening examination, has been debated. Two-view mammography, *i.e.* mediolateral oblique and craniocaudal projections of each breast, has been criticized because compared with one-view, *i.e.* the oblique projection, the radiation dose is twice as high, the costs are higher, and it takes longer to perform and interpret. However, sensitivity and specificity may both decrease if only one view is used.

In theory, if two independent screening tests instead of one are used, more cases of the disease will be detected (higher sensitivity), and more women without the disease will have a false positive test result (lower specificity) because the combined result is positive if both tests are positive as well as if either one of the tests is positive (Weinstein & Fineberg, 1980). The test result of a two-view mammogram, however, is not the same as the combined result of an oblique and a craniocaudal projection read separately because further evaluation of the lesion on the second view may lead to a negative two-view result. This means that the sensitivity of two-view mammography is not necessarily higher and the specificity is not necessarily lower than that of one-view.

Different studies on this subject have reached different conclusions. Some authors recommend one-view mammography because only very few cancers would be missed (Lundgren & Jakobsson, 1976; Weishaar et al, 1976; Locker et al, 1988). Others argue that in one-view mammography the number of false negative results or the number of false positive results is too high (Moskowitz & Libshitz, 1977; Andersson et al, 1978; Andersson, 1981; Muir et al, 1984; Sickles et al, 1986; Bassett et al, 1989), especially in women with dense breast tissue (Cukier et al, 1977; Ikeda & Sickles, 1988). The extensive and expensive diagnostic tests which will follow a false positive screening result may cause severe strain or physical harm to women and will lead to extra costs.

The best way to evaluate the screening quality of one-view versus two-view mammography would be to conduct a randomized controlled trial. Random allocation of the target population, *i.e.* women who are having a baseline screening for breast cancer, to one- or two-view mammography would ensure comparability of populations in terms of prevalence and spectrum of malignant and benign breast disease as well as breast parenchyma. Only one screening centre and one radiologist should be involved, to avoid variation in technical quality of the mammograms and between observers. Follow-up for a year should allow for clinical diagnosis of those with false negative results.

Address correspondence to: Mrs J. A. A. M. van Dijck, MSc, Department of Medical Informatics and Epidemiology, University of Nijmegen, Kapittelweg 54, NL-6525 EP Nijmegen, The Netherlands.

The population of such a study would have to be very large to be able to estimate the sensitivities and specificities with acceptable precision because breast cancer is a relatively rare disease (at initial screening about seven breast cancer cases may be detected in 1000 women screened). Before deciding whether or not such a large-scale randomized study would be justified, the difference in sensitivity and specificity between two-view and one-view mammography was quantified in the present literature review, with special emphasis on design and study population.

Studies and methods

Identification and selection of published studies

A list of published studies was compiled by checking literature references and by performing a MEDLINE CD-ROM search covering the period up to July 1991. The index terms used were "breast neoplasms" and "mammography", followed by a search for "view(s)" and "projection(s)" in title and abstract. Studies could only be included if the test results had been related to the diagnosis and if the numbers of true and false positive results and true and false negative results of both mammographic tests had been presented. Nineteen studies were included. All the studies were reviewed for the methods of sampling the study population, the mammographic tests compared, and the proper assessment of disease outcome of the study population (particularly women with a negative screening test result).

Test characteristics of two- against one-view mammography

If the tests are evaluated in the same population, the respective numbers of women with and without the disease are equal for the two- and one-view situations: $A+C = a+c$ and $B+D = b+d$ (Table I).

Test results reported in more than two alternatives, for instance "negative", "additional views required" and "positive" or "negative", "probably malignant" and "malignant", were made dichotomous by regarding "negative" as the negative test result, and all other alternatives as positive.

The percentage difference in sensitivity between two- and one-view mammography, D_{sens}, was calculated as the difference in true positive results divided by the number of breast cancer patients, multiplied by 100 (see Equation (1), Table I). The percentage difference in specificity between the two- and one-view test, D_{spec}, was calculated as the difference in true negative results divided by the number of "non-cases", multiplied by 100 (Equation (2), Table I).

The reciprocal of the number of cases $[1/(A+C)]$ and the reciprocal of the number of non-cases $[1/(B+D)]$ were defined as indicators of the precision of D_{sens} and D_{spec}, respectively, and were calculated. If in any study two or more radiologists had read both the one- and two-view mammograms, a combined difference in sensitivity and specificity was calculated, using the mean difference in true positives and true negatives, respectively.

Table I. Sensitivity and specificity of two-view and one-view screening test

Two-view mammography

		Breast cancer yes	Breast cancer no
Test result	+	A	B
	−	C	D
		$A+C$	$B+D$

$$\text{Sensitivity} = \frac{A}{A+C}$$

$$\text{Specificity} = \frac{D}{B+D}$$

One-view mammography

		Breast cancer yes	Breast cancer no
Test result	+	a	b
	−	c	d
		$a+c$	$b+d$

$$\text{Sensitivity} = \frac{a}{a+c}$$

$$\text{Specificity} = \frac{d}{b+d}$$

$$D_{sens} = \frac{A-a}{A+C} \times 100\% = \frac{A-a}{a+c} \times 100\% \qquad (1)$$

$$D_{spec} = \frac{D-d}{B+D} \times 100\% = \frac{D-d}{b+d} \times 100\% \qquad (2)$$

D_{sens}: Difference in sensitivity between two-view and one-view mammography.
D_{spec}: Difference in specificity between two-view and one-view mammography.

Results

Eighteen publications were selected. Buchanan & Jager (1977) described two substudies, both of which were included; Muir et al (1984) reported three substudies of which only the first one could be used, so that in all, we included 19 studies. Table II summarizes the studies according to population size, age, and modifiers of D_{sens} and D_{spec}. These modifiers include population characteristics, such as screening or patient population, tests applied and assessment of disease outcome, on which the sensitivity and specificity are dependent. By implication, D_{sens} and D_{spec} will depend on these factors as well. A more detailed description of these modifiers is given in the Discussion section, below.

All studies can be criticized with regard to at least one modifier. The studies listed in the upper part of Table II report on populations or compare tests that are inadequate to answer the question posed by this review.

Table III shows the sensitivity and specificity of two-view mammography, as well as D_{sens} and D_{spec}. D_{sens} was calculated from 17 studies and ranged from −5.7% to 19.4% (median 3.9%, mean 5.0%, standard deviation 6.5%). D_{spec} was calculated from nine studies and varied from 2.7% to 36.1% (median 14.8%, mean 14.9%, standard deviation 11.6%).

Figure 1 shows D_{sens} (vertical axis) in relation to the precision (horizontal axis). In 14 out of 17 studies the sensitivity of two-view mammography was higher than that of one-view ($D_{sens} > 0\%$), while one study showed no difference. In two studies D_{sens} was very high (18.4% and 19.4%), but these studies lacked precision. In the studies listed in the lower part of Table III D_{sens} does not

Table II. Studies according to population size, age and modifiers of D_{sens} and D_{spec}

Study	No. of cases	No. of "non-cases"	Age (yrs)	Population				Tests applied					Outcome*
				A	B	C	D	E	F	G	H	I	
Weishaar et al, 1976	223	0	nm	−	−	−	nr	−	+	−	+	+	nr
Locker et al, 1988	352	0	nm	−	−	+	nr	+	+	±	+	+	nr
Moskowitz & Libshitz, 1977	31	119	nm	+	−	−	−	−	−	−	+	+	±
Andersson et al, 1978	478	0	nm	−	−	+	nr	+	+	±	+	+	nr
Bassett & Gold, 1983	80	0	33–87	−	−	−	nr	+	+	±	+	+	nr
Muir et al, 1984	0	303	45–64	−	−	nr	+	+	+	+	+	+	−
Bassett et al, 1987	169	194	28–94	−	−	+	−	+	+	+	+	−	+
Bassett et al, 1989	169	0	nm	−	−	+	nr	+	+	±	−	+	nr
Cukier et al, 1977	106	0	nm	±	−	−	nr	−	−	+	+	+	nr
Buchanan & Jager, 1977 (1st)	160	0	nm	±	−	−	nr	−	−	−	+	−	nr
Buchanan & Jager, 1977 (2nd)	50	30	nm	±	−	+	nr	−	−	−	+	−	+
Hüppe & Schneider, 1977	277	0	nm	−	−	−	nr	+	+	+	+	+	nr
Libshitz et al, 1976	88	0	nm	−	−	+	nr	−	−	−	−	−	nr
Pagani et al, 1980	53	20	nm	−	−	+	nr	−	+	+	+	+	+
Lundgren & Jakobsson, 1976	34	860	35+	+	+	−	−	−	+	+	+	+	−
Andersson, 1981	117	100	45–69	+	+	−	−	+	+	−	+	+	±
Sickles et al, 1986	27	2473	nm	+	+	+	+	+	+	+	+	+	−
Anttinen et al, 1989	34	269	50–52	+	+	−	−	+	+	+	+	+	+
Ikeda & Sickles, 1988	5	995	av 57	+	−	nr	+	+	+	+	−	+	−

+ = yes, − = no, ± = partly, nm: not mentioned, nr: not relevant (in column D and Outcome because no non-cases were included, in column C because D_{sens} was not calculated), av: average.

A: asymptomatic population (breast cancer screening programme); B: baseline screening; C: cases include those with initially false negative results; D: non-cases randomly sampled from initially true negatives and false positives.

E: cc + oblique versus oblique (if −: lateral view or three-view); F: film-mammography (if −: xero); G: revision of both tests (if ±: two-view results by combining separately read oblique and craniocaudal views); H: revision without additional information; I: no use of "additional views requested/equivocal"

*Diagnostic work-up/follow-up of the screening test negatives (if ±: women with false positive one-view result were free of breast cancer).

NOTE: Bassett et al, 1987, and Bassett et al, 1989 were based on the same patients and including the 80 patients of Bassett & Gold, 1983.

Table III. Sensitivity of two-view mammography, D_{sens}, and two-view specificity D_{spec}, according to study

Study	Sensitivity 2-view	D_{sens}*	Specificity 2-view	D_{spec}*
Weishaar et al, 1976	100%†	1.3% (0.004)	—	—
Locker et al, 1988	81.8%	3.9% (0.003)	—	—
Moskowitz & Libshitz, 1977	100%†	19.4% (0.032)	100%†	36.1% (0.008)
Andersson et al, 1978	94.3%	4.7% (0.002)	—	—
Bassett & Gold, 1983	100%	1.3% (0.013)	—	—
Muir et al, 1984	—	—	95.7%	5.3% (0.003)
Bassett et al, 1987	84.0%	−5.7% (0.006)	87.7%	26.3% (0.005)
Bassett et al, 1989	91.9%	6.4% (0.006)	—	—
Cukier et al, 1977	99.1%	1.4% (0.009)	—	—
Buchanan & Jager, 1977, 1st substudy	100%†	1.3% (0.006)	—	—
Buchanan & Jager, 1977, 2nd substudy	96.0%†	−2.0% (0.020)	90.0%†	21.0% (0.033)
Hüppe & Schneider, 1977	96.4%	8.7% (0.004)	—	—
Libshitz et al, 1976	96.6%†	3.4% (0.011)	—	—
Pagani et al, 1980‡	81.6%	8.5% (0.019)	—	—
Lundgren & Jakobsson, 1976	100%	0% (0.029)	93.8%	14.8% (0.001)
Andersson, 1981	100%†	6.3% (0.009)	97.4%†	4.4% (0.010)
Sickles et al, 1986	100%	7.4% (0.037)	93.9%	18.8% (0.0004)
Anttinen et al, 1989	87.5%	18.4% (0.029)	66.9%	2.7% (0.004)
Ikeda & Sickles, 1988§	—	—	98.8%	4.9% (0.001)

*In parentheses: precision of D_{sens} ($1/(A+C)$: see text) and D_{spec} ($1/(B+D)$: see text).

†Based on original screening or diagnostic test result.

‡D_{spec} not calculated because no test results of the non-cases were given by the author.

§D_{sens} not calculated because of small number of cases.

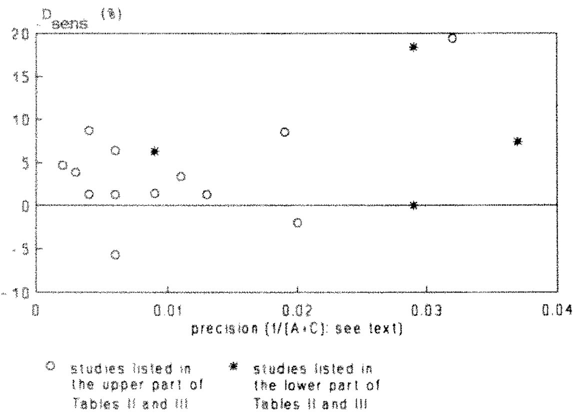

Figure 1. D_{sens} (%) and corresponding precision in 17 studies.

seem to differ from the values for the studies in the upper part, although tending to be less precise.

Figure 2 shows D_{spec} (vertical axis) against precision (horizontal axis). The variation is very large. In four studies D_{spec} varies from 2.5% to 5.5%, but in five other studies it varies from 14.8% to 36.1%. D_{spec} tends to be larger and less precise for the studies listed in the upper part of Tables II and III.

Figure 3 shows D_{sens} and D_{spec} together for those studies (only seven) that report both sensitivity and specificity. No relation between D_{sens} and D_{spec} can be observed.

Discussion

The sensitivity and specificity of a screening test are influenced by characteristics of the study population, the test applied, and the assessment of disease outcome. As a consequence, D_{sens} and D_{spec} may also be affected by these modifiers. Table II presents the studies according to numbers of breast cancer cases and "non-cases", age (which was rarely mentioned), and presence (+) or absence (−) of several items on which the modifiers were scored.

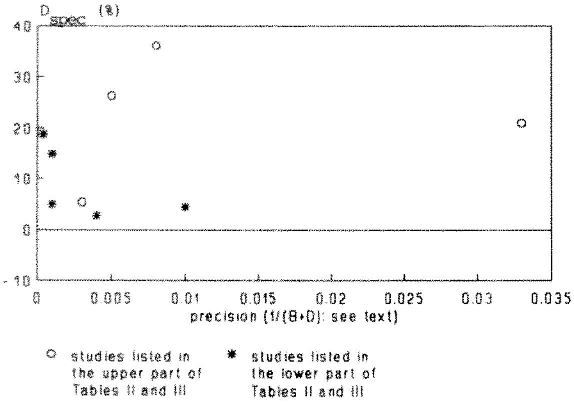

Figure 2. D_{spec} (%) and corresponding precision in 9 studies.

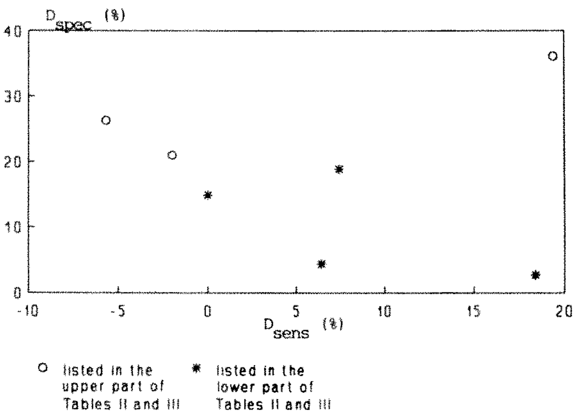

Figure 3. D_{sens} (%) and D_{spec} (%) in 7 studies reporting both sensitivity and specificity.

First, study populations should be samples of the general population and not taken from a clinic where women present with breast complaints. The larger tumour size at diagnosis yields higher sensitivities and the presence of benign breast disease yields lower specificities, which increase the likelihood of differences in D_{sens} and D_{spec}. Furthermore, cases as well as controls should be included. In populations of breast cancer cases only, the sensitivity cannot be assessed properly because visibility of the tumour on one projection will almost certainly lead to a positive test result if the radiologist is aware of the diagnosis of breast cancer for the whole set of cases. Also, case series should include women with false negative mammographic screening results, whereas control series should be a random sample of all "non-cases" (those with initially true negative or false positive results). In populations of only women with initially (true or false) positive test results some kind of lesion will be present on all mammograms, which will make it very difficult to decide which are negative. Even if a large sample of screen-negatives are included the results will be biased, as can be illustrated by Lundgren and Jakobsson's study (1976). Here 210 women with positive one-view screening results, 65 women with a positive history and 618 of 5804 with negative screening results had three-view mammography. One- and three-view mammograms were reviewed by a blinded radiologist. In this study population, specificities were 79.5% and 94.3%, respectively, but in the unselected screening population, one-view specificity was as high as 97.0%. In conclusion, unbiased estimates of D_{spec} can only be obtained if the non-cases are a random sample of those with initially true negative or false positive screening results.

The technical quality of the mammograms and the reading ability of the reviewing radiologists vary between the studies. Interobserver variation can be illustrated by Anttinen's study in which four radiologists read the same mammograms (Anttinen et al, 1989). Radiologist 1's reading of one-view mammograms had a higher sensitivity than radiologist 4's of two-view. However, Radiologist 1's specificity on two-view reading was much lower than that of Radiologist 4 on one-view reading.

Furthermore, the use of xerography, three-view mammography, the lateral view, or the availability of previous mammograms will influence results. Moreover, if in any study only the oblique view is reviewed and the results are compared with the screening results of two-view mammography, work-up bias and interobserver variation can occur. Finally, in some studies one of the alternative qualifications was "additional views required for confirmation of malignancy" or "equivocal". It will be clear that many more verdicts of "additional views required" are found at one-view readings. If the radiologist must choose between "positive" and "negative" without the option of "additional views", they will sometimes choose "negative", which leads to different cut-off points for a positive test result for one- and two-view mammography.

A final modifier of D_{sens} and D_{spec} is the assessment of disease outcome. The definitive diagnosis (presence or absence of breast cancer), which is required for the calculation of sensitivity and specificity, will be known for women whose screening yielded positive results who then underwent diagnostic tests. Those whose test results were negative, on the other hand, are not tested further; and some may be falsely negative because not all breast cancers show mammographically suspect signs at the screening examination (Peeters et al, 1989b). D_{sens} will thus be overestimated because the denominator does not include these false negatives, while the numerator remains constant (see Table I). D_{spec} will hardly change because the number of true negatives is usually large and constant. Therefore, follow-up data must be available to provide information on the number of cancers missed at the screening but diagnosed clinically later on, allowing for an unbiased estimation of D_{sens}.

Tables II and III show two groups of studies. Those in the upper part of the Tables reported on the population and/or applied tests which were not very suitable for answering the question of this review. The median D_{sens} of the studies of the lower part of Table III was 6.9%. The negative sign for D_{sens} and the very large D_{spec} in Bassett's and Buchanan's studies (Bassett et al, 1987; Buchanan & Jager, 1977) have probably been caused by the use of the alternative score "additional views required". In Lundgren and Jakobsson's study (1976) D_{sens} might have been larger than zero if follow-up data had been available to adjust for cancers missed at one-view screening but detectable at two-view.

According to Fig. 2, all nine studies had fewer false positive results with two-view mammography. D_{spec} was largest in studies listed in the upper part of Table III. Considering only studies listed in the lower part of Table III, the median for D_{spec} was 4.9%. Assuming $D_{spec} = 5\%$ and a two-view specificity of 90%, then of 10000 women screened 1000 will have a false positive result on two-view mammography and 1500 on one-view mammography. If the two-view specificity is 99%, then these numbers will be 100 and 600, respectively. In both examples the difference is 500 false positive results, but in the first, one view yields 50% more false positive results, and in the second, 500%.

It can be concluded that two-view mammography detects more cases and reduces the number of unnecessary diagnostic tests. However, the differences can hardly be assessed. Propably the gain in sensitivity and specificity by the addition of the craniocaudal view is highest for radiologists who are relatively inexperienced in reading mammograms. They may not be able to achieve a high sensitivity as well as a high specificity even when two views are available.

Whether the two-view screening test is more effective depends not only on D_{sens} and D_{spec}, but also on the sensitivities and specificities themselves. For example, Peeters and colleagues (1989a) reported a sensitivity of 93% and a specificity of 99% for screening test consisting of one-view mammography only. If with the oblique view alone 93% of the breast cancer cases can be detected and only 1% of the women without breast cancer must undergo unnecessary diagnostic tests, it may be concluded that although two-view screening may yield more true positive and true negative results, it will probably be less cost-effective. If the baseline mammograms are read by less experienced radiologists, the specificity of one-view mammography may be too low, and then two-view may be more cost-effective.

Acknowledgments

We thank F. de Groot for his comments.

References

ANDERSSON, I., 1981. Radiographic screening for breast carcinoma III. Appearance of carcinoma and number of projections to be used at screening. *Acta Radiologica Diagnosis*, *22*, 407–420.

ANDERSSON, I., HILDELL, J., MÜHLOW, A. & PETTERSSON, H., 1978. Number of projections in mammography: influence on detection of breast disease. *American Journal of Roentgenology*, *130*, 349–351.

ANTTINEN, I., PAMILO, M., ROIHA, M., SOIVA, M. & SURAMO, I., 1989. Baseline screening mammography with one versus two views. *European Journal of Radiology*, *9*, 241–243.

BASSETT, L. W. & GOLD, R. H., 1983. Breast radiography using the oblique projection. *Radiology*, *149*, 585–587.

BASSETT, L. W., BUNNEL, D. H., JAHANSHAHI, R., GOLD, R. H., ARNDT, R. D. & LINSMAN, J., 1987. Breast cancer detection: one versus two views. *Radiology*, *165*, 95–97.

BASSETT, L. W., BUNNEL, D. H., GOLD, R. H. & JAHANSHAHI, R., 1989. Film-screen mammography: comparison of views. *Journal of the National Medical Association*, *81*, 391–394.

BUCHANAN, J. B. & JAGER, R. M., 1977. Single view negative mode xeromammography: an approach to reduce radiation exposure in breast cancer screening. *Radiology*, *123*, 63–68.

CUKIER, D. S., LOPEZ, F. A. & MARAVILLA, R. B., 1977. One-view follow-up mammogram. Efficacy in screening for breast cancer. *Journal of Applied Medical-Technology Assessment*, *237*, 661–662.

HÜPPE, J. R. & SCHNEIDER, H. J., 1977. Über die Effizienz und Praktikabilität der Schrägaufnahme als 1-Ebenen-Mammographie. *Radiologe*, *17*, 211–212.

IKEDA, D. M. & SICKLES, E. A., 1988. Second-screening mammography: on versus two views per breast. *Radiology, 168,* 651–656.

LIBSCHITZ, H. I., FETOUH, F., ISLEY, J. & LESTER, R. G., 1976. One view mammographic screening? *Radiology, 120,* 719–722.

LOCKER, A. P., MANHIRE, A. R., CASELDINE, J. & BLAMEY, R. W., 1988. A comparison of the detection of breast carcinoma by mammography using one and two views. (*Proceedings of Symposium Mammographicum '87*). *British Journal of Radiology, 61,* 440.

LUNDGREN, B. & JAKOBSSON, S., 1976. Single view mammography. A simple and efficient approach to breast cancer screening. *Cancer, 38,* 1124–1129.

MOSKOWITZ, M. & LIBSHITZ, H. I., 1977. Mammographic screening for breast canncer by lateral view only: is it practical? *Journal of the Canadian Association of Radiology, 28,* 259–261.

MUIR, B. B., KIRKPATRICK, A. E., ROBERTS, M. M. & DUFFY, S. W., 1984. Oblique-view mammography: adequacy for screening. Work in progress. *Radiology, 151,* 39–41.

PAGANI, J. J., BASSETT, L. W., GOLD, R. H., BENEDETTI, J., ARNDT, R. D., LINSMAN, J. & SCANLAN, R. L., 1980. Efficacy of combined film-screen/xeromammography: preliminary report. *American Journal of Roentgenology, 135,* 141–146.

PEETERS, P. H. M., VERBEEK, A. L. M., HENDRIKS, J. H. C. L. & BON, M. J. H. VAN, 1989a. Screening for breast cancer in Nijmegen. Report of 6 screening rounds, 1975–1986. *International Journal of Cancer, 43,* 226–230.

PEETERS, P. H. M., VERBEEK, A. L. M., HENDRIKS, J. H. C. L., HOLLAND, R., MRAVUNAC, M. & VOOIJS, G. P., 1989b. The occurrence of interval cancers in the Nijmegen screening programme. *British Journal of Cancer, 59,* 929–932.

SICKLES, E. A., WEBER, W. N., GALVIN, H. B., OMINSKY, S. H. & SOLLITTO, R. A., 1986. Baseline screening mammography, one vs two views per breast. *American Journal of Roentgenology, 147,* 1149–1153.

WEINSTEIN, M. C. & FINEBERG, H. V., 1980. *Clinical Decision Analysis.* 1st edn. (W. B. Saunders, Philadelphia), pp. 148–159.

WEISHAAR, J., PATEROK, E. M., MÜLLER, A. & WILLGEROTH, F., 1976. Zur Mammographie mit einer Aufnahme. *Deutsche Medizinische Wochenschrift, 101,* 1865–1866.

1992, *The British Journal of Radiology*, *65*, 977–982

Sonography in thyroid carcinoma in children

By †Cristian J. Garcia, MD, Alan Daneman, MD, BCh, FRCPC, Kieran McHugh, MB, FRCR, *Helen Chan, MD and *Denis Daneman, MB, BCh, FRCPC

Department of Radiology and the *Department of Pediatrics, The Hospital for Sick Children, 555 University Avenue, Toronto, Ontario, Canada, M5G 1X8

(Received 7 January 1992 and in revised form 14 May 1992, accepted 3 June 1992)

Keywords: Carcinoma, Children, Sonography, Thyroid

Abstract. This paper reviews the clinical, sonographic and pathological findings of 20 children with thyroid carcinoma in an attempt to determine the value and limitations of sonography in thyroid neoplasms in this age group. Although sonography is an excellent technique for the evaluation of thyroid disorders and masses, certain limitations must be kept in mind. Microscopic foci of tumour might be missed and sonography cannot predictably differentiate benign from malignant disease. Previous radiation exposure should increase the level of suspicion for malignancy.

In children thyroid carcinoma is uncommon and constitutes 1–1.5% of all malignancies (Miller, 1985; Desjardins et al, 1988). Although sonography has been successfully used to study thyroid and extrathyroid neck masses in children (Friedmann et al, 1983; Sherman et al, 1985), its value and limitations in paediatric thyroid neoplasms have not been assessed. During the past 13 years, 40 children with thyroid carcinoma were treated at our institution and sonography was performed pre-operatively in 20 of them. This report correlates the data for these 20 patients.

Material and methods

We reviewed the clinical, sonographic and pathological findings of 20 patients diagnosed as having thyroid carcinoma at the Hospital for Sick Children, Toronto, between 1977 and 1990: 10 girls and 10 boys, whose age at the time of diagnosis ranged from 6.3 to 19 years (mean = 13.1 years).

The sonographic examinations were performed with the patient in the supine position with a pillow under the shoulders and the neck hyperextended. No patient preparation or sedation was used. The thyroid lesions were considered hyper-, iso- or hypoechoic relative to the normal thyroid gland, echo-free or of mixed echogenicity.

Six patients also had pre-operative computed tomography (CT) of the neck and 17 had at least one pre-operative radionuclide thyroid scan (technetium-99m pertechnetate and/or iodine-131 scans). All patients had a chest radiograph and eight had chest CT pre-operatively.

19 patients were treated surgically with total or partial thyroidectomy and in one patient the diagnosis of metastatic medullary thyroid carcinoma was made by a cervical node biopsy. Histology was available from all patients.

Results

17 patients presented with an asymptomatic mass or thyroid nodule that had been present for up to two years; in three of these it was an incidental finding during routine examination. The neck mass was felt to be thyroid in origin in 14 cases and only one had multiple palpable thyroid nodules. One patient presented with hoarseness and cough and a mass was found. Two patients with known multiple endocrine neoplasia (MEN) syndrome Type IIb had raised serum calcitonin levels; one of these did not have a palpable neck mass. All patients were clinically and biochemically euthyroid at the time of presentation. Five patients also had cervical lymphadenopathy.

Seven patients had a history of neck or chest radiation, between two and 16 years previously, for Hodgkin's lymphoma, leukaemia, Ewing's sarcoma, metastatic Wilms' tumour or abdominal neuroblastoma.

19 patients were treated with total or partial thyroid resection. Post-operatively, ablative doses of radioactive iodine and/or L-thyroxine suppression were utilized.

Histology

Histology revealed papillary carcinoma in 12 cases (two with mixed papillary-follicular features), follicular carcinoma in six, and medullary carcinoma in two. The thyroid carcinoma was unicentric in 10 cases (follicular carcinoma 6, papillary carcinoma 4); in four of these it co-existed with one or two benign nodules (adenoma or colloid nodule). The carcinoma was multifocal in the other 10 (papillary carcinoma 8, medullary carcinoma 2). Of the 10 multifocal carcinomas, seven were bilateral in the gland and three unilateral.

Identification of lesions on sonography

Sonography identified a single thyroid nodule or mass in 12 patients (Fig. 1) and two or more nodules in seven (Fig. 2). In one patient with medullary carcinoma and

---

Address correspondence to Dr Alan Daneman, Radiologist-in-Chief, Department of Diagnostic Imaging, Hospital for Sick Children, 555 University Avenue, Toronto, Ontario, M5G 1X8, Canada.

†Present address: Departamento de Radiologia, Hospital Clinico Universidad Catolica de Chile, Marcoleta 347, Santiago, Chile, South America.

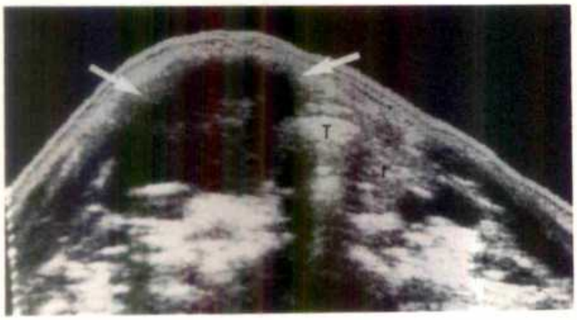

Figure 1. Transverse sonogram of the thyroid in a 12-year-old girl shows a large, unicentric mass (arrows) in the right lobe. The mass has a mixed echogenicity with an echo-free periphery and echogenic centre. The trachea (T) is displaced to the left and the left lobe (t) is normal. Diagnosis: unicentric follicular carcinoma.

without a palpable thyroid mass, no definite thyroid nodules were detected and only a hyperechoic linear density was noted in the right lobe. In one patient with metastatic bilateral multifocal papillary carcinoma, contralateral involvement was suspected but the findings were equivocal. Sonography failed to detect carcinomatous involvement of the contralateral lobe in five of the seven cases with histologically proven multifocal bilateral carcinoma and in six of these the contralateral tumour foci were microscopic on histological examination (Fig. 3). Sonography also failed to detect a second 1 cm tumour nodule in the isthmus in a case of metastatic papillary carcinoma and a 0.5 cm nodule in a case of bilateral multifocal medullary carcinomas. In one patient who presented with a neck mass and extensive cervical lymphadenopathy, a metastatic lymph node was mistaken for a thyroid nodule on ultrasound examination: in this case the thyroid was small but diffusely infiltrated by a papillary carcinoma. In the three cases of unilateral multifocal involvement, sonography detected a single nodule: in two of these multiplicity was determined by multiple microscopic tumour foci.

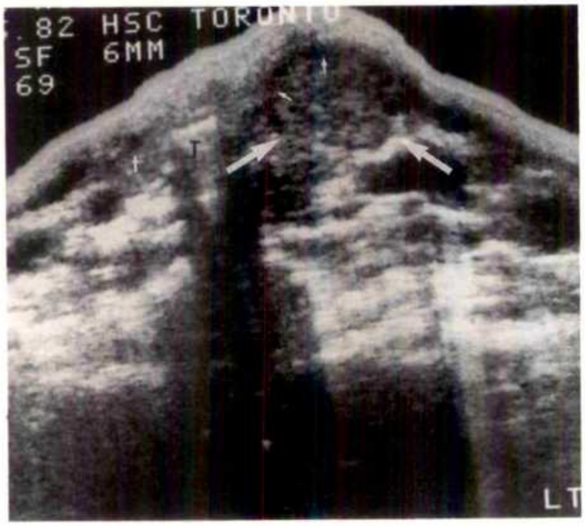

Figure 3. Transverse sonogram of the thyroid in a 7-year-old girl shows a slightly hypoechoic, well defined nodule in the left lobe (large arrows) surrounded by a hypoechoic rim or halo (small arrows). This was shown to be a papillary carcinoma. The trachea (T) has been displaced towards the right and the right lobe of the thyroid (t) appears normal. However multiple microscopic tumour foci were noted histologically on the right.

Appearance of lesions on sonography

The malignant lesions had an ill-defined margin in eight cases (Fig. 4) and were relatively well defined in 11 (Figs 1, 3). In the four patients in whom a unicentric carcinoma co-existed with benign nodules, the margins of the benign nodules were well defined in three and slightly ill-defined in one (Fig. 2).

The size of the lesions varied from 1.5 to 4.5 cm in maximum diameter and the echogenicity was variable (Figs 1–4). The lesions were hyperechoic in six cases,

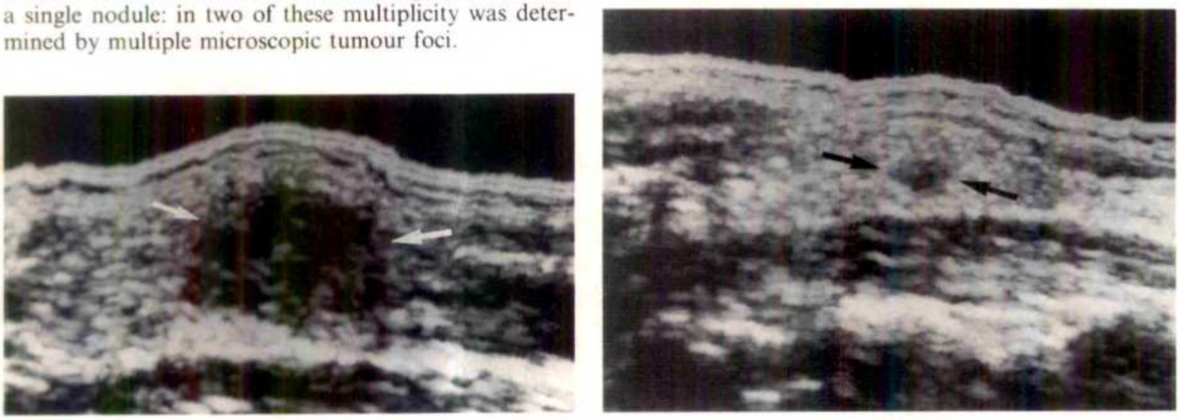

(a) (b)

Figure 2. Multinodular thyroid gland in a 19-year-old boy with a history of chest and abdominal radiation 16 years previously because of pulmonary metastases from Wilms' tumour. (a) Longitudinal sonogram of the right lobe of the thyroid shows a relatively well defined nodule (arrows) of mixed echogenicity with multiple echo-free areas, shown to be a unicentric follicular carcinoma. (b) Longitudinal sonogram of the left lobe shows a smaller hypoechoic nodule (arrows) that was shown histologically to be an adenoma.

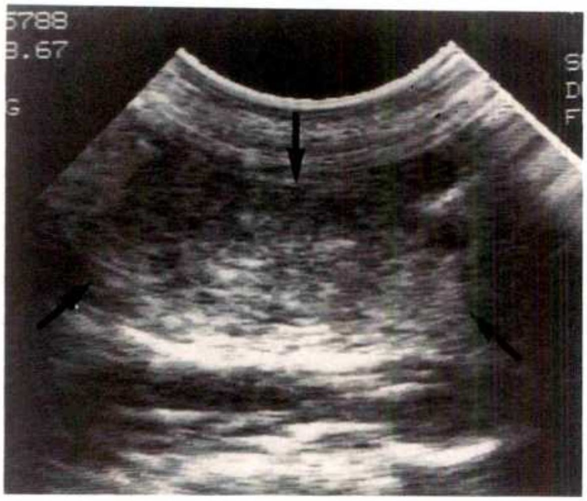

Figure 4. Longitudinal sonogram of the left lobe of the thyroid in a 16-year-old girl shows marked enlargement of the lobe (arrows) and a diffuse, ill-defined inhomogenous echo pattern. This was shown histologically to be a multifocal, unilateral papillary carcinoma.

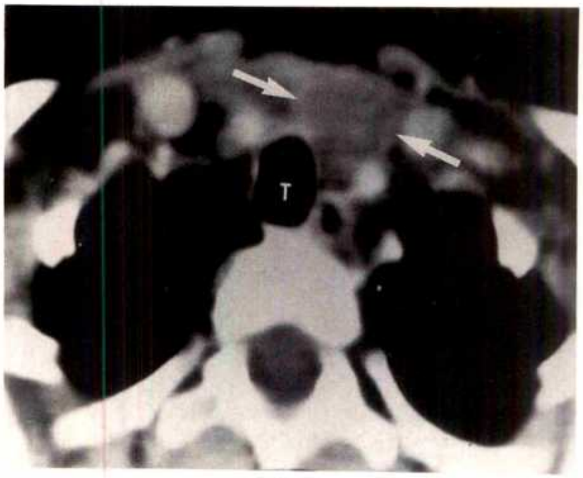

Figure 5. Computed tomograph (after intravenous contrast medium enhancement) of the upper chest in a 7-year-old girl with a mixed papillary-follicular carcinoma. The scan shows a mass of low attenuation (arrows) extending from the lower part of the thyroid through the thoracic inlet into the upper mediastinum on the left. The mass lies anterolateral to the trachea (T).

hypoechoic in five, and isoechoic in three. In five cases the lesions were of mixed echogenicity with some echo-free cystic areas, and in one case the echo pattern was inhomogenous. In none of the cases was a completely echo-free lesion noted. A halo or hypoechoic rim surrounding the nodule was present in four cases of bilateral multifocal papillary carcinoma. Calcified nodules were detected bilaterally in one case of multifocal medullary carcinoma and in one multifocal papillary carcinoma.

The benign lesions also had variable echogenicity (hyperechoic 2 (one with halo), hypoechoic 1, echo-free 1).

Radionuclide scans

15 of the radionuclude studies were considered abnormal and demonstrated a single "cold" lesion in nine patients, multiple cold lesions in three, single "hot" lesions in two and both cold and hot lesions in one. In two cases (medullary carcinoma 1, papillary carcinoma 1) the radionuclide study was normal.

Other diagnostic modalities employed

Six patients had *computed tomography (CT)* of the neck and in four of these the thyroid mass or masses were easily identified. In the fifth it was difficult to identify the thyroid mass separately from the adjacent extensive cervical lymphadenopathy. In the sixth patient (medullary carcinoma) the gland was extremely small and CT, like sonography, failed to document a thyroid mass.

The thyroid masses showed low or patchy attenuation. In one case of medullary carcinoma, calcified nodules were noted that had been demonstrated by sonography. In one patient, CT identified extension of the tumour into the thoracic inlet (Fig. 5) and in two extensive adenopathy was noted.

In two patients, lung metastases were detected on *chest radiography* and chest CT at the time of presentation and in one of these (medullary carcinoma) the lung metastases were calcified. This latter patient also had bony, hepatic and retroperitoneal metastases. The chest radiograph and/or chest CT were negative in all the other cases.

Discussion

Thyroid carcinoma may occur at any age and approximately 5–10% of cases occur in patients younger than 21 years (Zohar et al, 1986; Desjardins et al, 1988; Ceccarelli et al, 1988; Zimmerman et al, 1988). It accounts for approximately 1.5% of all paediatric cancers and 5% of malignancies involving the head and neck in children (Miller, 1985; Desjardins et al, 1988). Although in most series it is at least twice as common in girls as in boys (Joppich et al, 1983; Desjardins et al, 1988; Ceccarelli et al, 1988; Zimmerman et al, 1988), we found no difference in sex distribution. Although thyroid carcinoma tends to be more advanced both locally and systemically at the time of the diagnosis in children than in adults, the prognosis is better in patients younger than 21 years than in older people (Joppich et al, 1983; Zohar et al, 1986; Zimmerman et al, 1988). This is based on an excellent response in children to surgical treatment, followed by ablation of the thyroid remnant by radioactive iodine and thyroid suppression with L-thyroxine.

Metastatic involvement of the cervical lymph nodes has been reported to be the most common presenting symptom of thyroid carcinoma in children and may be present in 30–90% of cases at the time of diagnosis (Reiter et al, 1981; Zohar et al, 1986; Desjardins et al, 1988; Zimmerman et al, 1988). In our series only seven cases (35%) had cervical lymphadenopathy at the time of presentation, but six of them also had thyroid nodules. However, a painless thyroid nodule or mass without associated symptoms may also be the first sign (Sherman et al, 1985) occurring in the majority of our cases (60%). Less frequently they metastasize to the lungs and occasionally to bone and other structures. Approximately 6–14% present with lung metastases at the time of diagnosis (Hopwood et al, 1976; Ceccarelli et al, 1988; Zimmerman et al, 1988), as occurred in two of our patients (10%). Most children with thyroid carcinoma are euthyroid although rarely they may present with hyperthyroidism (Kirkland et al, 1973; Hopwood et al, 1976).

There is a significant association between thyroid neoplasms and previous exposure to ionizing radiation to the head and neck (Hagler et al, 1966; Refetoff et al, 1975; Cerletty et al, 1978; Walsh et al, 1978; Fleming et al, 1985), with a latency period that may be as long as 25 years (Miller, 1985; Zohar et al, 1986). This predisposing factor has been reported in 20–50% of children with thyroid carcinoma (Segal et al, 1985; Zohar et al, 1986) and occurred in 35% of our patients. However, the number of cases of thyroid malignancy related to radiation might increase with the improved survival of childhood malignancies in general.

It has been reported that the incidence of malignancy in multinodular glands is lower (1–7%) than that in solitary nodules (10–25%) (Brown, 1981; Miller, 1985). However, according to McCall et al (quoted by Austin, 1982) there is no significant difference between the incidence of carcinoma in multinodular goitre and in that of solitary cold nodules after exclusion of those patients with factors which predispose to neoplasia (*e.g.* history of radiation exposure, multiple endocrine neoplasia syndrome). In a review of 16 cases with multinodular gland in children at our institution, we found four (25%) to be associated with carcinoma, three of whom had had neck radiation.

In general a history of previous radiation, rapid enlargement of a thyroid nodule, cervical lymphadenopathy and hoarseness are all suggestive of malignancy (Reiter et al, 1981).

Histologically the most common types are the well differentiated pure or mixed papillary and follicular carcinomas (90% in our series). Medullary carcinoma (10%) is far less frequent and anaplastic carcinomas are extremely rare in children (McCook et al, 1982; Miller, 1985; Zohar et al, 1986). Papillary or mixed papillary follicular carcinomas are frequently multicentric and bilateral and it is unclear whether they represent metastases or multifocal origin of the neoplasm (Reiter et al, 1981; Desjardins et al, 1988), and this is in accordance with our series. Multifocal thyroid carcinoma is more commonly associated with radiation (Cerletty et al, 1978; Walsh et al, 1978; Fleming et al, 1985) but often the lesions are less than 1 cm in size (Hagler et al, 1966). In our series, all patients with a history of irradiation had multiple thyroid nodules, because of multifocal carcinoma in three cases and associated benign lesions in four (adenomas in two and a colloid nodule in two) (Fig. 2). Benign and malignant lesions may therefore coexist following radiation, as previously reported. (Hagler et al, 1966; Austin, 1982).

Medullary thyroid carcinoma accounts for approximately 3.5–10% of all thyroid cancers at all ages (McCook et al, 1982) and occurs most commonly between the ages of 30 and 60. Although rarely diagnosed before 10 years, it has been reported even during the second year of life (Stjerholm et al, 1980), but C-cell hyperplasia is more likely to be seen in younger patients (Graze et al, 1978; Stjerholm et al, 1980; Jones & Sisson, 1983; Desjardins et al, 1988). The lesion most commonly occurs sporadically (80–90%) but may occur in families as a component of the multiple endocrine neoplasia II (MEN-II) syndrome (20%) (McCook et al, 1982; Desjardins et al, 1988). In the latter it is commonly associated with adrenal phaeochromocytoma and hyperplasia of the parathyroid glands (MEN-IIa). MEN-IIb is a less common form and consists of elements of MEN-IIa together with features of marfanoid habitus, mucosal neuromas and intestinal ganglioneuromatosis (McCook et al, 1982; Desjardins et al, 1988). This neoplasm is always associated with raised serum calcitonin levels (McCook et al, 1982; Jones & Sisson, 1983) which may be detected in screening studies performed because of the presence of other clinical features of the syndrome or of a neck mass (McCook et al, 1982; Desjardins et al, 1988). The thyroid lesions may be bilateral in approximately 20% of sporadic cases and 90% of those lesions associated with MEN II syndromes (Graze et al, 1978; McCook et al, 1982; Jones & Sisson, 1983) and was present in our two patients with MEN IIb.

Thyroid sonography has been used mainly in adults to differentiate solid from cystic lesions, solitary from multifocal lesions and thyroid from extrathyroidal lesions (Sackler et al, 1977; Scheible et al, 1979; Simeone et al, 1982; Walker et al, 1985). High resolution equipment allows detection of nodules as small as 2–3 mm (Sackler et al, 1977; Walker et al, 1985). Although sonographic criteria for the differentiation of benign and malignant nodules have been described (Propper et al, 1980; Simeone et al, 1982), these are not entirely reliable (Sackler et al, 1977; Propper et al, 1980; Hung et al, 1982). Poor definition of the margin of a nodule is more commonly seen in malignant lesions (Fig. 4). A halo or echo-free rim around the thyroid nodule has been described particularly in relation to benign nodules (Scheible et al, 1979) but has also been seen in some malignant nodules (Sackler et al, 1977; Propper et al, 1980), as was noted in four of our cases of carcinoma (Fig. 3). This sign should therefore be considered non-specific and not useful in the differentiation of benign from malignant disease.

Purely cystic lesions of the thyroid are generally considered to be benign (Becker et al, 1980), with an incidence of malignancy of about 2% in cysts less than 3 cm in diameter (Hayles et al, 1956; Allen et al, 1979; Hammer et al, 1982). Most cysts however result from necrosis or degeneration of benign nodules, usually adenomas, adenomatous nodules or colloid cysts (Becker et al, 1980). In our present series four malignant thyroid nodules presented with a mixed echogenicity with echo-free or cystic areas (Figs 1, 2), but none as a pure cyst. The ability of sonography to differentiate purely cystic lesions from those that are echogenic or of mixed echogenicity is a distinct advantage over thyroid scintigraphy.

On sonography, thyroid carcinomas may have a heterogenous echo pattern but are more often less echogenic than the rest of the gland, with ill-defined margins (Scheible et al, 1979; Simeone et al, 1982), but may appear well circumscribed. In our series, the echogenicity of the nodules was variable, as were the margins (Figs 1–4). This finding of non-specific echo patterns in carcinoma strongly suggests that sonographic features should be correlated with the clinical findings. Sonography is more sensitive than clinical examination or thyroid scintigraphy in the detection of additional nodules. However, it may be difficult to define separate additional nodules with sonography when they are very numerous, when they are located in the isthmus and the gland is not enlarged or when there is associated extensive lymphadenopathy as occurred in two of our patients. Sonography has also been reported to have a higher sensitivity and specificity than clinical examination in the detection of local recurrence after thyroidectomy (Simeone et al, 1987).

On radionuclide study thyroid carcinomas are usually "cold" (non-functioning) but rarely may be "hot" (functioning) as was found in three of our patients. Purely cystic lesions (on sonography) are very unlikely to be malignant and also are usually "cold" on radionuclide studies. The functional information obtained on a radionuclide scan is therefore likely to be quite limited in terms of differentiating benign and malignant nodules.

Primary and metastatic medullary carcinomas tend to calcify and this can be detected on plain films, sonography or CT (Wallace et al, 1970; Pearson et al, 1973; McCook et al, 1982; Schwerk et al, 1985). Lung metastases (20%), bony metastases (17%), liver metastases (20%) and a fibronodular interstitial pattern in both lungs (Wallace et al, 1970; McCook et al, 1982) may occur, as noted in one patient of our series. On sonography hypoechoic nodules with calcification have been described (Schwerk et al, 1985) and this was seen in one of our patients. Sonography has thus been recommended in the screening of members of families affected by medullary carcinoma. Radionuclide studies are not useful since the tumour does not arise from the follicular cells. However, bone and liver scintigraphy are very useful for the detection of metastatic disease (McCook et al, 1982).

Although thyroid carcinoma has been found in association with Hashimoto's thyroiditis (Mauras et al, 1985; Desjardins et al, 1988), we did not see this association in the present series.

In the presence of large thyroid masses and/or extensive cervical lymphadenopathy, CT proved to be more useful than sonography in the delineation of the extent of the mass, particularly into the thoracic inlet and mediastinum (Fig. 5) and for the differentiation of the primary thyroid lesion from the lymphadenopathy. We feel that cervical CT (and/or magnetic resonance imaging) is specifically indicated in those unusual cases of large thyroid masses and/or extensive lymphadenopathy.

Sonography is therefore an excellent technique for the evaluation of thyroid disorders in children, especially for the study of thyroid nodules and masses, and has been shown in adults to be extremely valuable for the documentation of local recurrence following thyroidectomy (Simeone et al, 1987). However, certain limitations should be kept in mind. Sonography cannot detect very small microscopic foci of malignancy (but continuing technical advances with equipment providing greater spatial resolution should improve its ability to do so). Furthermore, sonography cannot predictably differentiate benign from malignant disease and the findings must be correlated with the clinical features and histology. Although sonography can delineate the exact location of thyroid nodules and masses and their relationship to adjacent structures in the vast majority of cases, it might be difficult to achieve this in the presence of an unusually large mass or in association with extensive cervical lymphadenopathy.

We therefore recommend thyroid sonography in children with single or multiple thyroid nodules. Cystic nodules which are completely echo-free on sonography are highly unlikely to be malignant. The incidence of malignancy is markedly increased in those nodules that have a varying degree of echogenicity or are of mixed echogenicity on sonography. Furthermore, an ill-defined margin to the nodule is suggestive of a more aggressive lesion. A history of previous irradiation exposure should also increase the level of suspicion for malignancy.

References

Allen, F. H., Krook, P. M. & Degroot, W. P. H., 1979. Ultrasound demonstration of a thyroid carcinoma within a benign cyst. *American Journal of Roentgenology*, *132*, 136–137.

Austin, C. W., 1982. Ultrasound evaluation of thyroid and parathyroid disease. *Seminars in Ultrasound*, *3*, 250–262.

Becker, S. P., Skolnik, E. M. & O'Neill, J. V., 1980. The nodular thyroid. *Otology Clinics of North America*, *13*, 53–58.

Brown, C. L., 1981. Pathology of the cold nodule. *Journal of Clinical Endocrinology and Metabolism*, *10*, 235–245.

Ceccarelli, C., Pacini, F., Lippi, F., Elisei, R., Arganini, M., Miccoli, P. & Pinchera, A., 1988. Thyroid cancer in children and adolescents. *Surgery*, *104*, 1143–1148.

Cerletty, J. M., Guansing, A. R., Engbring, N. H., Hagen, T. C., Kim, H. J. Shetty, K. R., Rosenfeld, P. S. & Wilson, S., 1978. Radiation-related thyroid carcinoma. *Archives of Surgery*, *113*, 1072–1076.

Desjardins, J. G., Bass, J., Leboeuf, G., Lorenzo, M. D., Letarte, J., Khan, A. H. & Simard, P., 1988. A twenty-year experience with thyroid carcinoma in children. *Journal of Pediatric Surgery, 23,* 709–713.

Fleming, I. D., Black, T. L., Thompson, E. I., Pratt, C., Rao, B. & Hustu, O., 1985. Thyroid dysfunction and neoplasia in children receiving neck irradiation for cancer. *Cancer, 55,* 1190–1194.

Friedmann, A. P., Haller, J. I., Goodman, J. D. & Hager, H., 1983. Sonographic evaluation on non-inflammatory neck masses in children. *Radiology, 147,* 693–697.

Graze, K., Spiler, I. J., Tashjian, A. H., Melvin, K. E. W., Cervi-Skinner, S., Gagel, R. F., Miller, H. H., Wolfe, H. J., Delellis, R. A., Leape, L., Feldman, Z. T. & Reichlin, S., 1978. Natural history of medullary thyroid carcinoma. *New England Journal of Medicine, 299,* 980–985.

Hagler, S., Rosenblum, P. & Rosenblum, A., 1966. Carcinoma of the thyroid in children and young adults: iatrogenic relation to previous irradiation. *Pediatrics, 38,* 77–81.

Hammer, M., Wortsman, J. & Folse, R., 1982. Cancer in cystic lesions of the thyroid. *Archives of Surgery, 117,* 1020–1023.

Hayles, A. B., Kennedy, R. L. J., Woolner, L. B. & Black, B. M., 1956. Nodular lesions of the thyroid gland in children. *Journal of Clinical Endocrinology and Metabolism, 16,* 1580–1594.

Hopwood, N. H., Carroll, R. G., Kenny, F. M. & Foley, T. P., 1976. Functioning thyroid masses in childhood and adolescence. *Journal of Pediatrics, 89,* 710–718.

Hung, W., August, G. P., Randolph, J. G., Schiggall, R. M. & Chandra, R., 1982. Solitary thyroid nodules in children and adolescents. *Journal of Pediatric Surgery, 17,* 225–229.

Kirkland, R. T., Kirkland, J. L., Rosenberg, H. S., Harberg, F. J., Librik, L. & Clayton, G. W., 1973. Solitary thyroid nodules in 30 children and report of a child with a thyroid abscess. *Pediatrics, 51,* 85–90.

Jones, B. A. & Sisson, J. C., 1983. Early diagnosis and thyroidectomy in multiple endocrine neoplasia. *Journal of Pediatrics, 102,* 219–223.

Joppich, I., Roher, H. D., Hecker, W. C. H., Knorr, D. & Dawn, R., 1983. Thyroid carcinoma in childhood. *Progress in Pediatric Surgery, 16,* 23–27.

McCook, T., Putman, C. E., Dale, J. K. & Wells, S. A., 1982. Medullary carcinoma of the thyroid: radiographic features of a unique tumor. *American Journal of Roentgenology, 139,* 149–155.

Mauras, N., Zimmerman, D. & Goellner, J. R., 1985. Hashimoto thyroiditis associated with thyroid cancer in adolescent patients. *Journal of Pediatrics, 106,* 895–898.

Miller, J. H., 1985. Thyroid malignancies. In *Imaging in Pediatric Oncology* (Williams and Wilkins, Baltimore), pp. 127–136.

Pearson, K. D., Wells, S. A. & Keiser, H. R., 1973. Familiar medullary carcinoma of the thyroid, adrenal pheocromocytoma and parathyroid hyperplasia: a syndrome of multiple endocrine neoplasia. *Radiology, 107,* 249–256.

Propper, R. A., Skolnick, M. L., Weinstein, B. J. & Dekker, A., 1980. The non-specificity of the thyroid halo sign. *Journal of Clinical Ultrasound, 8,* 129–132.

Refetoff, S., Harrison, J., Karanfilski, B. T., Kaplan, E. L., Degrott, L. J. & Bekerman, C., 1975. Continuing occurrence of thyroid carcinoma after irradiation to the neck in infancy and childhood. *New England Journal of Medicine, 292,* 171–175.

Reiter, E. O., Root, A. W., Rettig, K. & Vargas, A., 1981. Childhood thyromegaly: recent developments. *Journal of Pediatrics, 99,* 507–518.

Sackler, J. P., Passalaqua, A. M., Blum, M. & Amorocho, L., 1977. A spectrum of the thyroid gland as imaged by gray scale water bath sonography. *Radiology, 125,* 467–472.

Scheible, W., Leopold, G. R., Woo, V. L. & Gosink, B. B., 1979. High-resolution real-time ultrasonography of thyroid nodules. *Radiology, 133,* 413–417.

Schwerk, W. B., Grum, R. & Wahl, R., 1985. Ultrasound diagnosis of C-cell carcinoma of the thyroid. *Cancer, 55,* 624–630.

Segal, K., Fidi, J., Levy, R. & Aristede, A., 1985 Thyroid carcinoma in children and adolescents. *Annals of Otology, Rhinology and Laryngology, 94,* 346–349.

Sherman, N. H., Rosenberg, H. K., Heyman, S. & Templeton, J., 1985. Ultrasound evaluation of neck masses in children. *Ultrasound in Medicine and Biology, 4,* 127–134.

Simeone, J. F., Daniels, G. H., Mueller, P. R., Maloof, F., Vansonnenberg, E., Hall, D. A., O'Connell, R. S., Ferrucci, J. T. & Wittenberg, J., 1982. High-resolution real-time sonography of the thyroid. *Radiology, 145,* 431–435.

Simeone, J. F., Daniels, G. H., Hall, D. A., McCarthy, K., Kopans, D. B., Butch, R. J., Mueller, P. R., Stark, D. D., Ferrucci, J. T. & Wang, C. A., 1987. Sonography in the follow-up of 100 patients with thyroid carcinoma. *American Journal of Roentgenology, 148,* 45–49.

Stjerholm, M. R., Freudenbourg, J. C., Mooney, H. S., Kinney, F. J. & Deftos, L. J., 1980. Medullary carcinoma of the thyroid before age 2 years. *Journal of Clinical Endocrinology and Metabolism, 51,* 252–253.

Walker, B. J., Finlay, D., Amar, S. S., Small, P. G., Wastie, M. L. & Pegg, C. A. S., 1985. A prospective study of thyroid ultrasound scan in the clinically solitary nodule. *British Journal of Radiology, 58,* 617–619.

Wallace, S., Hill, C. S., Paulus, D. D., Ibanez, M. L. & Clark, R. L., 1970. The radiologic aspects of medullary (solid) thyroid carcinoma. *Radiologic Clinics of North America, 8,* 463–474.

Walsh, P. G. & Volpe, R., 1978. Irradiation-related thyroid cancer. *Annals of Internal Medicine, 88,* 261–262.

Zimmerman, D., Hay, I. D., Gough, I. R., Goellner, J. R., Ryan, J. J., Grant, C. S. & McConahey, W. H., 1988. Papillary thyroid carcinoma in children and adults: Long-term follow-up of 1039 patients conservatively treated at one institution during three decades. *Surgery, 104,* 1157–1166.

Zohar, Y., Strauss, M. & Laurian, N., 1986. Adolescent versus adult thyroid carcinoma. *Laryngoscope, 96,* 555–559.

1992, *The British Journal of Radiology*, 66, 983–986

Enlarged mediastinal lymph nodes in the fibrosing alveolitis of systemic sclerosis

By S. J. Garber, MRCP, FRCR, *A. U. Wells, MRCP, *R. M. duBois, MD, FRCP and D. M. Hansell, MRCP, FRCR

Departments of Radiology and *Thoracic Medicine, Royal Brompton National Heart and Lung Hospital, Sydney Street, London SW3 6NP, UK

(*Received 3 January 1992 and in revised form 5 May 1922, accepted 3 June 1992*)

Keywords: Systemic sclerosis, Fibrosing alveolitis, High resolution computed tomography

Abstract. The aim of this study was to determine the prevalence of enlarged mediastinal lymph nodes in systemic sclerosis (SSc) and relate this to the extent of pulmonary disease and disease activity as judged by high resolution computed tomography (HRCT). The HRCT scans of 78 patients with SSc were reviewed. The extent of lung disease and HRCT pattern were analysed and CT scans examined on soft tissue window settings for evidence of mediastinal lymph node enlargement. Sixty six (85%) patients had evidence of lung involvement on CT. Enlarged mediastinal lymph nodes were present in 21 (32%) patients with lung involvement but in only 1 (8%) patient without. The prevalence of enlarged mediastinal nodes increased with more extensive lung involvement on CT ($p < 0.025$), but correlated poorly with the type of CT appearance and concurrent erythrocyte sedimentation rate. Mediastinal lymph node enlargement occurs frequently in patients with SSc, particularly if lung involvement is extensive.

It is now recognized that mediastinal lymph node enlargement may occur in cryptogenic fibrosing alveolitis (CFA) without associated neoplastic disease. A recent study (Bergin & Castellino, 1990) has demonstrated mediastinal nodes greater than the threshold size for abnormality, as defined by the American Thoracic Society (Glazer et al, 1985), in 11/12 patients with CFA. Computed tomography (CT) has now an established role in the diagnosis of interstitial lung disease (Hansell & Kerr, 1991). Furthermore, using a visual estimation of parenchymal involvement, good correlation of the extent of disease with clinical and functional impairment in patients with sarcoidosis and other diffuse lung diseases has been demonstrated (Aberle et al, 1990; Müller et al, 1989).

Lung fibrosis in CFA and systemic sclerosis (SSc) are histologically identical and radiologically similar. Two types of CT appearances in SSc are recognized: a characteristic peripheral reticular pattern corresponding with a histological appearance of established fibrosis (Müller et al, 1986) and an amorphous increase in lung density, or "ground-glass" appearance, again with a peripheral distribution, correlating with an intra-alveolar and interstitial cellular infiltrate (Vedal et al, 1988). To some extent both ends of the disease spectrum coexist in the same histological sections. These HRCT patterns have been shown to be reliable predictors of the histological appearances of open lung biopsy specimens (Müller et al, 1987; Wells et al, 1992).

This study was designed to define the prevalence of enlarged mediastinal lymph nodes in SSc and correlate this with the extent of lung involvement and disease activity, reflected by HRCT appearances.

Methods

CT scans of 78 patients fulfilling the American Rheumatology Association preliminary criteria for the diagnosis of SSc (Subcommittee for Scleroderma Criteria, 1980), with a ratio M : F = 1 : 3.5 and mean age 49.7 years (range 38.1 to 61.3 years), were reviewed. Patients with concurrent pulmonary infection or neoplasm were excluded from the study.

CT scans were performed on an Elscint 2002 scanner with a scanning time of 5.5 s. Interspaced 3 mm sections were taken at 10 mm intervals and reconstructed using a high resolution "bone" algorithm. Original images were photographed on wide window settings ($C = -600$, $W = 1600$).

First, lung appearances were categorized as either parenchymal opacification equal to or exceeding reticulation or as predominantly reticulation. Second, the extent of disease or the area of involvement was calculated by a subjective assessment of the percentage of abnormal lung, to the nearest 5%, at five levels. A weighting factor was applied, as in the method detailed by Müller et al (1989). This method has been applied to other diffuse lung diseases and interobserver variation is slight (Aberle et al, 1990).

Scans were re-imagined for mediastinal detail ($C = 22$, $W = 450$) and mediastinal lymph nodes measured on hard copy. The number and site of lymph nodes with maximum transverse diameter $\geqslant 12$ mm were documented. The position of lymph nodes was recorded using the four anatomical areas described by Ingram et al (1989). Measurements were initially made by one

---

Address correspondence to: Dr D. M. Hansell, Department of Radiology, Royal Brompton National Heart and Lung Hospital, Sydney Street, London SW3 6NP.

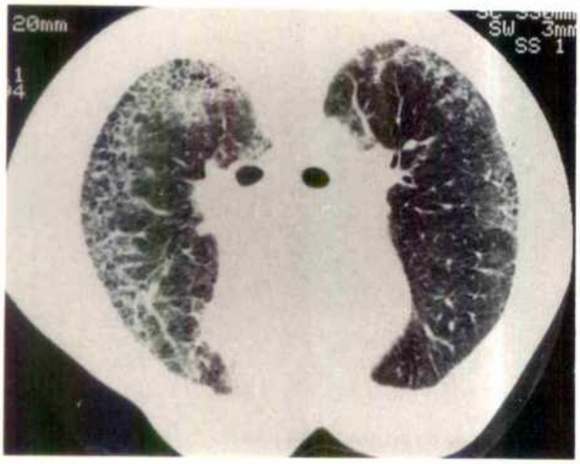

Figure 1. HRCT scan demonstrating a predominantly reticular pattern in the lungs predictive of a fibrotic lung biopsy.

observer (S.J.G.) and then verified by a second (D.M.H).

As intravenous contrast medium was not given no attempt was made to assess the hilar regions for the presence of enlarged lymph nodes.

Patients were subdivided into those with no evidence of lung disease on CT (Group A) and the remainder into three equal groups: Group B with the least extensive lung disease, Group C with intermediate disease and Group D with the most extensive disease. The differences in prevalence of enlarged mediastinal lymph nodes for each group were analysed using the chi-squared test for trend.

To define whether mediastinal lymph node enlargement had any relationship to a systemic disturbance, the prevalence of enlarged nodes was determined in patients with an erythrocyte sedimentation rate (ESR), performed within 7 days of the CT scan, greater than 20 mm/h and compared with that in those with one less than or equal to 20 mm/h.

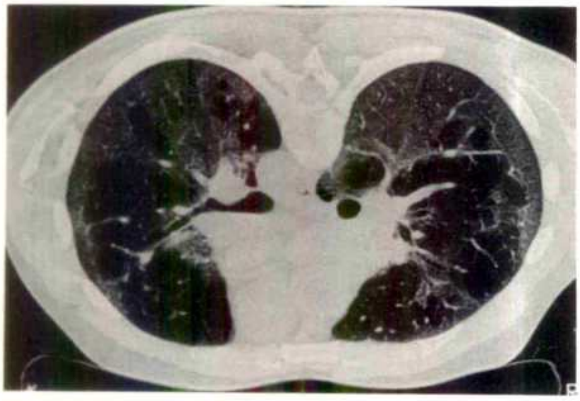

Figure 2. HRCT scan demonstrating amorphous parenchymal opacification in a subpleural distribution indicating an inflammatory cellular infiltrate.

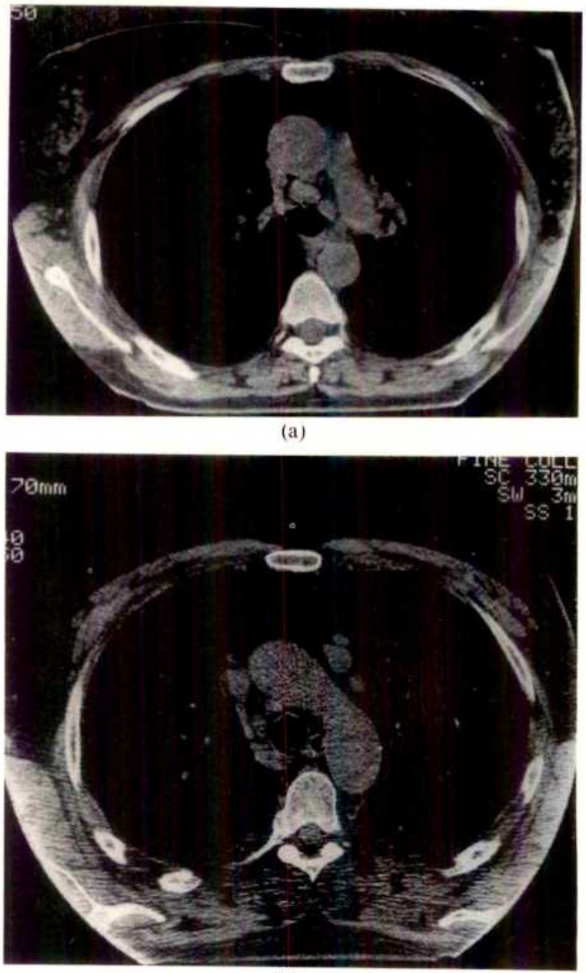

Figure 3. CT scans demonstrating enlarged mediastinal nodes in (a) the pretracheal region (max. diam. 16 mm) and (b) the left superior mediastinum (max. diam. 18 mm).

All patients were followed clinically and radiologically for a minimum of two years.

Results

Evidence of lung disease on HRCT was identified in 66 (85%) patients with SSc. CT appearances were of a predominantly reticular pattern in 30 patients (Fig. 1) and with parenchymal opacification equal to or exceeding reticulation in 36 patients (Fig. 2).

At least one lymph node greater than or equal to 12 mm in diameter was present in 21/66 (32%) patients with CT evidence of lung involvement and 1/12 (8%) without. Of the 22 patients with lymph node enlargement, 13 had one node, four had two nodes, one had three nodes, two had five nodes and two had six nodes.

Ten nodes were located in the left superior mediastinum, one in the right superior mediastinum, 26 in the pretracheal and retrocaval space and nine in the precarinal and subcarinal area (Figs. 3a, b).

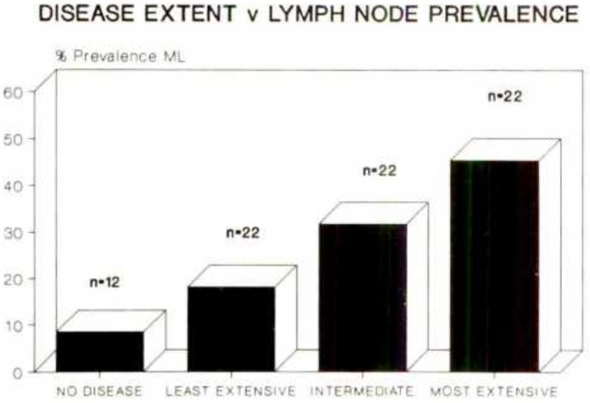

Figure 4. Bar chart of enlarged mediastinal lymph node (ML) prevalence and disease extent. Nodal prevalence increased significantly with increasing extent of lung disease ($p < 0.025$).

No significant difference in the prevalence of enlarged mediastinal lymph nodes was found between those cases with a predominantly reticular pattern (9/30) and those with parenchymal opacification equal to or exceeding reticulation (12/36). There was no significant difference in the prevalence of mediastinal lymph node enlargement between patients with an ESR > 20 mm/h (4/16) and those with an ESR $\leqslant 20$ mm/h (15/49).

The prevalence of enlarged mediastinal lymph nodes increased progressively with increasing extent of disease (Fig. 4). In Group A, one (8%), had significantly enlarged mediatinal nodes, in Group B four (18%), in Group C seven (32%) and in Group D 10 (45%). The difference was significant at the $p < 0.025$ level.

No evidence of supervening malignant or pulmonary infection was detected during the two-year follow-up.

Discussion

The lung parenchymal changes on CT in patients with SSc have been well documented (Schurawitzki et al, 1990). The aim of this study was to determine the prevalence of mediastinal lymph node enlargement in SSc and correlate this with disease extent and degree of inflammatory change. In our series of patients with CT evidence of lung disease secondary to SSc, the prevalence of significantly enlarged mediastinal lymph nodes was 32%. Bergin and Castellino (1990) reported enlarged nodes in 11 out of 12 (92%) patients with CFA. In the American study, patients had advanced disease and underwent CT scanning because of clinically significant chronic pulmonary symptoms. Our patients with SSc were scanned as part of an assessment for pulmonary involvement and a significant proportion had no clinical evidence of chest disease at the time of scanning. The higher prevalence of mediastinal lymph node enlargement in the American series in part relates to the more extensive lung changes seen in their cases. This observation is in agreement with our demonstration of a positive trend between increasing lymph node prevalence and extent of lung disease. However, even in patients with extensive disease, the prevalence of mediastinal lymph node enlargement in SSc was significantly lower than that seen in CFA. If, as suggested by Bergin, mediastinal lymph node enlargement simply reflects disease activity, differences in the prevalence of enlarged nodes may partially reflect differences in intensity of the underlying disease processes. There is epidemiological support for this idea; the fibrosing alveolitis of SSc has a better prognosis than lone CFA, even with matching of demographic factors and severity of pulmonary dysfunction (Wells et al, 1991).

To examine the hypothesis that the mediastinal lymph node enlargement was part of a systemic inflammatory process, the prevalence of enlarged mediastinal lymph nodes was correlated with the ESR; in this series no significant correlation was found.

The grading of CT appearances in this study was based on the observations of Müller; patchy parenchymal opacification predicts a high likelihood of inflammatory histology, whereas a fibrotic biopsy is obtained from areas with a reticular pattern on HRCT (Müller et al, 1987). Bergin and Castellino (1990) suggested that the enlarged nodes reflect reactive hyperplasia secondary to chronic inflammation. We found no significant difference in lymph node prevalence between patients with inflammatory lung changes and those with predominantly fibrotic lung disease as judged by HRCT. This unexpected finding may reflect the presence of considerable underlying inflammation, possibly due to subclinical infection in "traction" bronchiectasis secondary to the more fibrotic pattern of lung disease. Fibrotic histology in CFA is associated with a worse prognosis (Turner-Warwick et al, 1980); additionally extensive fibrotic disease, as judged by HRCT, is associated with a bronchoalveolar lavage neutrophilia, indicating respiratory tract inflammation (Hansell et al, 1991).

Lymph node prevalence correlated strongly with the extent of lung disease. Enlarged nodes were present in only one fifth of the group of patients with the least extensive lung changes, whilst almost half the patients with the most extensive lung disease had evidence of mediastinal lymph node enlargement.

Inaccuracies in measuring lymph node size, affecting the estimation of the prevalence of enlarged mediastinal lymph nodes in this series, may have occurred in two ways: first, scans 3 mm in thickness spaced at 10 mm intervals were performed, rather than contiguous scans; and second, because intravenous contrast medium was not given, assessment for hilar lymphadenopathy was not possible. These two factors are likely to have produced an underestimate of the prevalence of enlarged lymph nodes in our patients. Additionally there is a higher prevalence of enlarged mediastinal lymph nodes in parts of North America than in the United Kingdom.

There is an increased prevalence of malignancy in all fibrotic lung diseases, including SSc (Rickards et al, 1958). It is important to appreciate that mediastinal lymph node enlargement identified on CT may be present without concomitant neoplastic disease. None of our patients developed malignancy during the subsequent follow-up for a minimum of two years.

In conclusion, patients with evidence of interstitial lung fibrosis secondary to SSc have an increased prevalence of enlarged mediastinal lymph nodes when compared with those with no CT evidence of lung disease. The prevalence of these enlarged lymph nodes increases with the extent of pulmonary involvement but does not correlate with the disease activity, as judged by the HRCT pattern, or the ESR. Enlarged mediastinal lymph nodes in patients with SSc do not necessarily indicate supervening malignant disease.

References

Aberle, D. R., Hansell, D. M., Brown, K. & Tashkin, D. P., 1990. Lymphangiomyomatosis: CT, chest radiographic and functional correlations. *Radiology*, *176*, 381–387.

Bergin, C. & Castellino, R. A., 1990. Mediastinal lymph node enlargement on CT scans in patients with Usual Interstitial Pneumonitis. *American Journal of Roentgenology*, *154*, 251–254.

Glazer, H. S., Gross, B. H., Quint, L. E., Francis, R., Bookstein, F. L. & Orringer, M. B., 1985. Normal mediastinal lymph nodes: number and size according to American Thoracic Society mapping. *American Journal of Roentgenology*, *144*, 261–265

Hansell, D. M. & Kerr, I. H., 1991. The role of high resolution computed tomography in the diagnosis of interstitial lung disease. *Thorax*, *46*, 77–84.

Hansell, D. M., Wells, A. U., Cullinan, P., Black, C. M. & duBois, R. M., 1992. High resolution computed tomography and bronchoalveolar lavage cell profiles in fibrosing alveolitis: a correlation. *Clinical Radiology*, Abstract, *45*, 48.

Ingram, C. E., Belli, A. M., Lewars, M. D., Reznek, R. H. & Husband, J. E., 1989. Normal lymph node size in the mediastinum: a retrospective study in two patient groups. *Clinical Radiology*, *40*, 35–39.

Müller, N. L., Miller, R. R., Webb, W. R., Evans, K. G. & Ostrow, D. N., 1986. Fibrosing alveolitis: CT–pathologic correlation. *Radiology*, *160*, 585–588.

Müller, N. L., Staples, C. A., Miller, R. R., Vedal, S., Thurlbeck, W. M. & Ostrow, D. N., 1987. Disease activity in idiopathic pulmonary fibrosis: CT and pathologic correlation. *Radiology*, *165*, 731–734.

Müller, N. L., Mawson, J. B., Mathieson, J. R., Abboud, R., Ostrow, D. N. & Champion, P., 1989. Sarcoidosis: correlation of extent of disease at CT with clinical, functional and radiographic findings. *Radiology*, *171*, 613–618.

Rickards, R. L. & Milne, J. A., 1958. Cancer of the lung in progressive systemic sclerosis. *Thorax*, *13*, 238–245.

Schurawitzki, H., Stiglbauer, R., Graninger, W., Herold, C., Polzleitner, D., Burghuber, O. C. & Tscholakoff, D., 1990. Interstitial lung disease in systemic sclerosis: high resolution CT versus radiography. *Radiology*, *176*, 755–799.

Subcommittee for Scleroderma Criteria of the American Rheumatism Association Diagnostic and Therapeutic Criteria Committee, 1980. Preliminary criteria for the classification of systemic sclerosis (scleroderma). *Arthritis and Rheumatology*, *23*, 581–590.

Turner-Warwick, M., Burrows, B. & Johnson, A., 1980. Cryptogenic fibrosing alveolitis: clinical features and their influence on survival. *Thorax*, *35*, 581–590.

Vedal, S. V., Welsh, V. E., Miller, R. R. & Müller, N. L., 1988. Desquamative interstitial pneumonia; computed tomographic findings before and after treatment with corticosteroids. *Chest*, *93*, 215–217.

Wells, A. U., Hansell, D. M., Corrin, B., Harrison, N. K., Goldstraw, P., Black, C. M. & duBois, R. M., 1990. High resolution computed tomography assessment of disease activity in the fibrosing alveolitis of systemic sclerosis: a histological correlation. *Thorax*, *47*, 508–512.

Wells, A. U., Cullinan, P., Black, C. M. & duBois, R. M., 1991. Lone cryptogenic fibrosing alveolitis carries a worse prognosis than the fibrosing alveolitis of systemic sclerosis. *American Review of Respiratory Disease*, 143(4), A52.

1992, *The British Journal of Radiology*, 66, 987–989

Prediction of birthweight by fetal ultrasound biometry

By D. A. Nzeh, MBBS, FMCR, S. Rimmer, FRCR, *W. M. O. Moore, FRCOG and †L. Hunt, PhD

Departments of Radiology, *Obstetrics and Gynaecology and †Faculty of Medicine and Computational Group, St. Mary's Hospital for Women and Children, Manchester, UK.

(*Received 7 August 1991 and in revised form 3 December 1991, accepted 3 June 1992*)

Keywords: Birthweight, Fetal biometry

Abstract. A total of 104 women with singleton pregnancies who were delivered between 37 and 42 weeks gestation had ultrasound scans during the fortnight before delivery. The biparietal diameter (BPD), abdominal circumference (AC) and femur length (FL) were measured in all cases. Estimation of fetal weight (EFW) was done by four different methods: using AC alone, AC/BPD, AC/FL and AC/BPD/FL. Results were compared with values of actual birthweights at delivery. There was no significant difference between the mean birthweights of the 47 boy and 57 girl fetuses studied. The $EFW_{(Shepard)}$ method showed the least bias overall: mean percentage error 1.7%, standard deviation (SD) 10.6%. The other three methods significantly underestimated birthweights on average: $EFW_{(Deter)}$, mean error 2.2%, SD 9.3%, $p < 0.02$; $EFW_{(Campbell)}$, mean error 5.4%, SD 9.5%, $p < 0.001$; $EFW_{(Hadlock)}$, mean error 5.6%, SD 9.3%, $p < 0.001$. The percentage error in each group was significantly negatively correlated ($p < 0.001$) with the scan–delivery interval. Two new equations were generated which gave more accurate predictions for the cases under study using AC, BPD and FL as a combination and also in addition to scan–delivery interval (SDI) in days.

Several methods are now available for estimation of birthweight using fetal measurements obtained by ultrasound. Initial approach to fetal weight estimation utilized measurements of abdominal circumference (AC) alone (Campbell & Wilkin, 1975). Different combinations of fetal parameters have also been employed: AC has been used in conjunction with biparietal diameter (BPD) (Shepard et al, 1982), AC and femur length (FL) have also been combined (Hadlock et al, 1984). The three commonly measured fetal parameters of AC, BPD and FL have also been applied together (Hadlock et al, 1985). Accurate estimation of fetal weight (EFW) is useful in successful management of labour and care of the newborn baby in the early days of life. Birth trauma, perinatal asphyxia and maternal morbidity are some of the problems associated with vaginal delivery of the macrosomic fetus (Hirata et al, 1990).

The aim of this study was to evaluate the accuracy of fetal biometry in the prediction of birthweight by means of formulae currently in use and to see whether a more reliable formula could be produced using AC, BPD and FL combined and in addition to scan–delivery interval (SDI).

Patients and methods

One hundred and four women who had singleton pregnancies and were delivered between 37 and 42 weeks gestation had ultrasound scans done from day 0 to 15 prior to delivery. The age range of cases in the study was 16–42 years with a mean of 27.3 years.

AC, BPD and FL measurements were obtained in cm in all cases. Fetal weight (EFW) was estimated using the following formulae and recorded in grams.

$$\begin{aligned}
EFW_{(Campbell)} &= 1000e^{-4.564 + 0.282AC - 0.00331AC^2}\\
EFW_{(Shepard)} &= 10^{1.25 - 0.00265BPD \times AC + 0.046AC + 0.166BPD}\\
EFW_{(Hadlock)} &= 10^{1.3598 - 0.0037AC \times FL + 0.051AC + 0.1844FL}\\
EFW_{(Deter)} &= 10^{1.335 - 0.0034AC \times FL + 0.0316BPD + 0.0457AC + 0.1623FL}
\end{aligned}$$

Results of EFW obtained using the above formulae were compared with actual birthweights. There were 47 boy and 57 girl fetuses in the series.

Results

The range of actual birthweights was 1940–4700 g, mean 3194 g, SD 499 g. There was no statistically significant difference between the mean birthweights of the male and female fetuses. $EFW_{(Shepard)}$ showed the least bias overall (mean error 1.7%, SD 10.6%). The other three methods significantly underestimated birthweights on average:

$EFW_{(Deter)}$ mean −2.2%, SD 9.3%, $p < 0.02$,
$EFW_{(Campbell)}$ mean −5.4%, SD 9.5%, $p < 0.001$,
$EFW_{(Hadlock)}$ mean −5.6%, SD 9.3%, $p < 0.001$.

The percentage error in each group was significantly negatively correlated ($p < 0.001$) with the scan–delivery interval. For intervals up to five days, the Deter and the Shepard methods significantly overestimated the birthweight (mean 2.9%, SD 9.1%, $p < 0.05$ and mean 6.7%, SD 12.0%, $p < 0.001$ respectively) whereas the other two methods had negligible bias (Campbell: mean −0.3%, SD 9.3%; Hadlock: mean −0.6%, SD 8.4%).

$EFW_{(Shepard)}$ was the most accurate in the 6–10 days interval (mean −0.5%, SD 7.6%) while the Hadlock, Campbell and Deter methods significantly underestimated birthweight in this range (mean −7.5%, SD

This paper was presented in part at the 48th annual congress of the British Institute of Radiology, Harrogate, 11–13 June 1990.

Address for correspondence: Dr D. A. Nzeh, Department of Radiology, University of Ilorin, Ilorin, Nigeria.

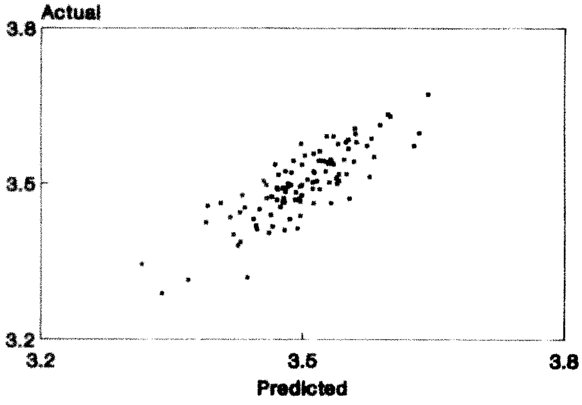

Figure 1. Scatter plot of actual $\log_{10}$(birthweight) versus $\log_{10}$(birthweight) predicted using Equation (1).

7.1%, $p < 0.001$; mean −7.0%, SD 7.6%, $p < 0.001$ and mean −4.1%, SD 7.0%, $p < 0.002$ respectively).

All four methods significantly underestimated birthweight at intervals of 11 days or more: $EFW_{(Shepard)}$ mean −3.8%, SD 8.1%, $p < 0.05$; $EFW_{(Deter)}$ mean −8.1%, SD 8.3%, $p < 0.001$; $EFW_{(Campbell)}$ mean −11.7%, SD 7.7%, $p < 0.001$; and $EFW_{(Hadlock)}$ mean −11.7%, SD 9.1%, $p < 0.001$.

Using linear regression analysis, two new equations were generated which gave closer predictions for the cases under study using AC, BPD and FL in combination and in addition to SDI as follows:

$$\log_{10}(\text{birthweight}) = 0.470 + 0.488\log_{10}\text{BPD} + 0.554\log_{10}\text{FL} + 1.377\log_{10}\text{AC} \quad (1)$$

$$\log_{10}(\text{birthweight}) = 0.326 + 0.00451(\text{SDI}) + 0.383\log_{10}\text{BPD} + 0.614\log_{10}\text{FL} + 1.485\log_{10}\text{AC} \quad (2)$$

The two new equations for predicting birthweight gave negligible bias when subjected to the same statistical analysis as the four equations under review.

Figure 1 is a scatter plot of actual $\log_{10}$(birthweight) versus predicted $\log_{10}$(birthweight) using Equation (1) and shows close correlation between predicted and actual values.

Discussion

Comparison of fetal weight models from different studies has shown that the use of multiple parameters, and in particular the combination of head, abdomen and femur length measurements, provide the most adequate estimations of fetal weight with 95% confidence interval in the range of 15–16% (Hadlock, 1990). Studying the weight estimation for fetuses small and large for their gestational age, it was observed that only formulae dependent on femur length (FL) fitted both groups well (Miller et al, 1988). Abdominal diameter measurement has been found to be less accurate in cases of oligohydramnios because the fetal skin edge may be difficult to identify when liquor volume is diminished (Valea et al, 1990).

The accuracy of a given model in predicting birthweight decreases further as the population deviates further from that used to generate such a model (Hirata et al, 1990). It is therefore important that each institution should determine which formula best suits its cases, especially when no model has yet been generated locally.

In the present study, $EFW_{(Shepard)}$ showed the least bias overall. This finding is at variance with reports from some other studies which concluded that Shepard's model, which combined AC and BPD, was less accurate than other formulae which used AC and FL (Miller, 1988).

Although it has been claimed in the past that there is cessation of fetal growth at 38 weeks gestation (Rossavik et al, 1988), results from the current series did not support this observation and showed that fetal growth continued until term.

When the two new equations were subjected to the same statistical analysis as the four equations under review, the newly generated equations gave more accurate results.

The lapse time or scan–delivery interval (SDI) has been noted as a critical element in the accuracy of remote estimates of fetal weight (Spinnato et al, 1988). Findings from the present report corroborate this view when the newly generated equation from this study, which incorporated SDI, is applied. It is interesting that all the four formulae under review underestimated birthweight at intervals of 11 days or more because the daily incremental gain in fetal weight during the last two weeks of gestation was not taken into consideration in developing these equations.

The formulae found most useful for prediction of birthweight among the cases studied were the newly generated equations and they are recommended for use, especially when applied in conjunction with SDI.

References

Campbell, S. & Wilkin, D., 1975. Ultrasonic measurement of fetal abdomen circumference in the estimation of fetal weight. *British Journal of Obstetrics and Gynaecology*, *82*, 689–697.

Hadlock, F. P., Harrist, R. B., Carpenter, R. J., Deter, R. L. & Park, S. K., 1984. Sonographic estimation of fetal weight. *Radiology*, *150*, 535–540.

Hadlock, F. P., Harrist, R. B., Sharman, R. S., Deter, R. L. & Park, S. K., 1985. Estimation of fetal weight with the use of head, body and femur measurements—a prospective study. *American Journal of Obstetrics and Gynecology*, *151*, 333–337.

Hadlock, F. P., 1990. Sonographic estimation of fetal weight. *Radiologic Clinics of North America*, *28*, 47–50.

Hirata, G. I., Medearis, A. L., Horenstein, J., Bear, M. B. & Platt, L. D., 1990. Ultrasonographic estimation of fetal weight in the clinically macrosomic fetus. *American Journal of Obstetrics and Gynecology*, *162*, 238–242.

Miller, J. M., Kissling, G. A., Brown, H. L. & Gabert, H. A., 1988. Estimated fetal weight: applicability to small- and large-for-gestational-age fetus. *Journal of Clinical Ultrasound*, *16*, 95–97.

Rossavik, I. K., Deter, R. L. & Wasserstrum, N., 1988. Mathematical modeling of fetal growth v. fetal weight changes at term. *Journal of Clinical Ultrasound*, *16*, 9–15.

SHEPARD, M. J., RICHARDS, V. A., BERKOWITZ, A. L., WARSOP, S. L. & HOBBINS, J. C., 1982. An evaluation of two equations for predicting fetal weight by ultrasound. *American Journal of Obstetrics and Gynecology*, *142*, 47–54.

SPINNATO, J. A., ALLEN, E. D. & MENDENHALL, H. W., 1988. Birthweight prediction from remote ultrasound examination. *Obstetrics and Gynecology*, *71*, 893–898.

VALEA, F. A., WATSON, W. J. & SEEDS, J. W., 1990. Accuracy of ultrasonic weight prediction in the fetus with preterm premature ruptures of membranes. *Obstetrics and Gynecology*, *75*, 183–185.

1992, *The British Journal of Radiology*, *65*, 990–995

The effect of thin K-edge filters on radiation dose in dental radiography

By D. S. MacDonald-Jankowski, MSc, FDSRCPS, DDRRCR and *C. P. Lawinski, BSc, MSc, MPhil

Department of Dental Radiology, King's College School of Medicine and Dentistry, Denmark Hill, London SE5 9RS and *Department of Medical Physics and Medical Engineering, King's College Hospital, Denmark Hill, London SE5 9RS, UK

(Received 30 September 1991 and in revised form 11 March 1992, accepted 6 May 1992)

Keywords: Dental radiography, Filtration, Radiation dosage

Abstract. The use of thin K-edge filters has been found to reduce considerably the radiation dose in intra-oral radiography. The aim of this study was to investigate the effect of filtration on the skin entrance dose and several sites (representing organs or areas of interest within the head) along the central beam axis, at other points within the primary beam and at two points just outside the primary beam. The subject was a sliced head phantom (a human skull embedded in tissue-equivalent material) which was exposed to X rays from a conventional dental X-ray unit in the range of tube voltage 55–85 kVp for each of four filter systems. These were 2.7 mm of aluminium alone (the existing total filtration) or with an added 0.1 mm erbium, 0.1 mm yttrium or 0.05 mm niobium metal foils. Measurements of radiation dose were made using thermoluminescent dosemeters (TLD rods) and were adjusted to simulate the exposure resulting from a typical dental radiograph of a maxillary molar. The results suggest that the use of thin K-edge filters significantly reduces the entrance skin dose and to a certain extent reduces the total dose imparted to the head. However, the dose to the ipsilateral orbit at higher tube voltages may be increased.

In a previous paper the authors reported that in dental radiography the use of K-edge filters significantly reduced the potential dose delivered along the central ray of the primary beam (MacDonald-Jankowski & Lawinski, 1991).

The aim of this study was to assess the effect of filtration on the skin entrance dose and on the radiation dose reaching the organs or areas of the head lying both within and outside the primary radiation beam. Dose measurements were made using thermoluminescent dosemeter (TLD) rods placed in a sliced head phantom. These were chosen in preference to the ionization chamber system used in the previous study because of the convenience of their small size.

The term K-edge filter as used in this study describes the use of any filtering material that demonstrates a K-edge within the useful energy range of the X-ray beam employed. However, in previous studies the term K-edge filter was applied to those materials that not only filtered the lower photon energy end of the spectrum but also the higher photon energies, resulting in a "bandpass" effect (Nagel, 1989). This is the case for erbium. The term pseudo-K-edge filters was applied to those filters that only removed the lower photon energies (Nagel, 1989) as is the case with niobium and yttrium.

Materials and methods

As in the previous study a General Electric GE1000 dental X-ray unit with a total filtration equivalent to 2.7 mm of aluminium was employed for all measurements made. A 36 cm open-ended cylindrical long cone with a diameter of 6 cm provided collimation of the beam and resulted in a 50 cm focus–film distance.

The following filter systems were investigated. These were selected as they are all commercially available products that have been offered to the dental profession.

1. The existing 2.7 mm aluminium (Al) equivalent filtration alone (referred to as aluminium).
2. 0.1 mm erbium (Er) foil (Reactor Experiment Inc.) in addition to the 2.7 mm aluminium equivalent filtration (referred to as erbium).
3. 0.05 mm niobium (Nb) foil (Niobex Inc.) in addition to the 2.7 mm aluminium equivalent filtration (referred to as niobium).
4. 0.1 mm yttrium (Y) foil (Yttro Corporation) in addition to the 2.7 mm aluminium equivalent filtration (referred to as yttrium).

The additional foils were affixed to the added aluminium filter (accessible through the tube port) on the side facing the patient. The radiation spectra of the four filter systems were computed as previously using the methods of Birch et al (1979).

Radiation dose measurements for each filter system were made on a head phantom (a human skull embedded in temex tissue-equivalent material) sliced horizontally (55 mm slices) to allow easy placement of the TLD rods (Fig. 1). A non-screen intra-oral dental film packet incorporating a lead foil backing was placed palatal to the upper right molar teeth in the usual manner and the dental X-ray unit was positioned for a typical periapical view. The downward angulation employed prevented the possibility of rays within the

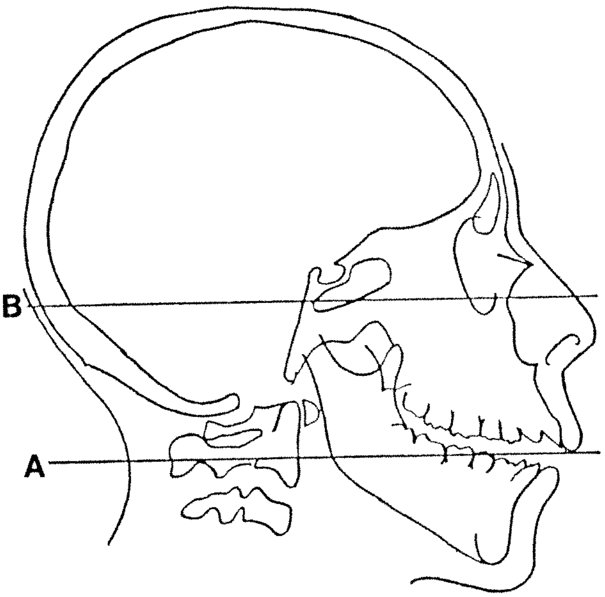

Figure 1. A lateral projection of the head phantom showing the two horizontal planes of section (A and B).

primary beam from travelling unattenuated along the air spaces that can occur between the slices of the head phantom.

The radiation exposure to the various sites was measured using a batch of 100 lithium fluoride TLD rods (6 mm × 1 mm) in conjunction with a Toledo TLD reader (supplied by Vinten Instruments Ltd). All the TLD rods had previously been calibrated against a 37D exposure meter system with a 3.5 cm^3 volume ionization chamber (supplied by Vinten Instruments Ltd).

Measurements were made at five selected sites along the central beam axis, at five sites elsewhere within the primary beam and at two sites outside the primary beam for a series of tube voltage values (55–85 kVp in 5 kV increments) for each of the four filter systems. The selected sites along the central beam axis were the entrance skin dose, the inside of the cheek, both in front of and behind the film packet, and the exit skin dose. The sites elsewhere in the primary beam were the ipsilateral orbit, the ipsilateral and contralateral tonsil, the contralateral masseter and the sublingual mucosa. The scattered radiation sites were the contralateral orbit and below the pituitary. Unfortunately, owing to the design of the head phantom employed, a reliable assessment of the dose to the thyroid could not be made. The positions of these sites are shown in Figs 2 and 3.

For each measurement a series of 20 1 s exposures was made on the X-ray unit to deliver sufficient radiation exposure to the TLD dosemeters to provide reliable readings.

Results and discussion

The calculated mean energy for each filter system, the half-value layer and derived total filtration have been

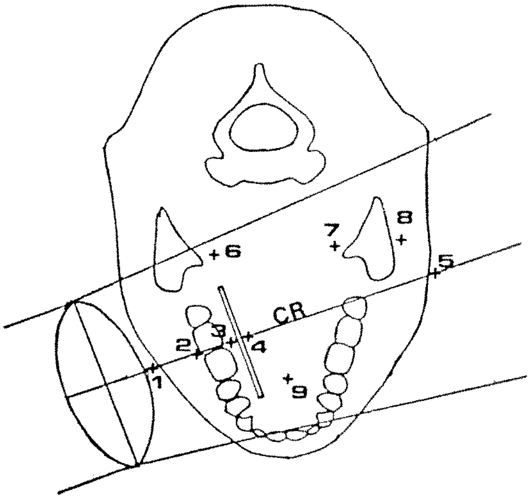

Figure 2. Section A demonstrates the sites of dose measurement along the central ray: 1, skin entrance; 2, inside of the cheek; 3, in front of film; 4, behind the film; 5, skin exit. Other sites within the primary beam are: 6, ipsilateral tonsil; 7, contralateral tonsil; 8, contralateral masseter; 9, sublingual mucosa.

shown previously (MacDonald-Jankowski & Lawinski, 1991). In each case the total filtration was well within the minimum requirements given in the *Guidance Notes for the Protection of Persons against Ionising Radiations Arising from Medical and Dental Use* (NRPB, 1988).

One consequence of using a thin K-edge filter in addition to the existing aluminium is that the extra beam attenuation introduced by the filter will require an increase in the radiographic exposure time.

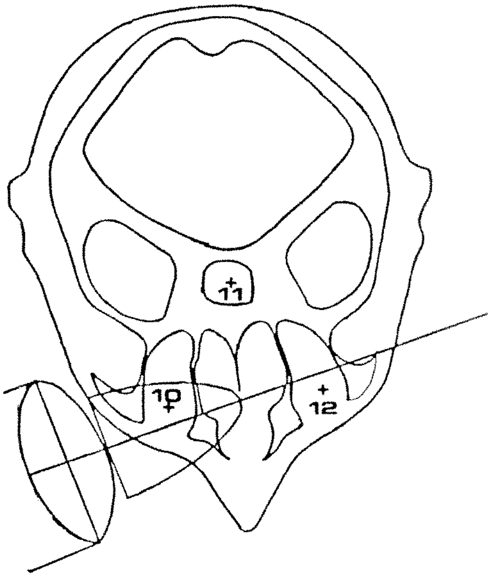

Figure 3. Section B demonstrates other sites within the primary beam (the D-shaped area); 10, ipsilateral orbit; and sites outside the primary beam; 11, below the pituitary; 12, contralateral orbit.

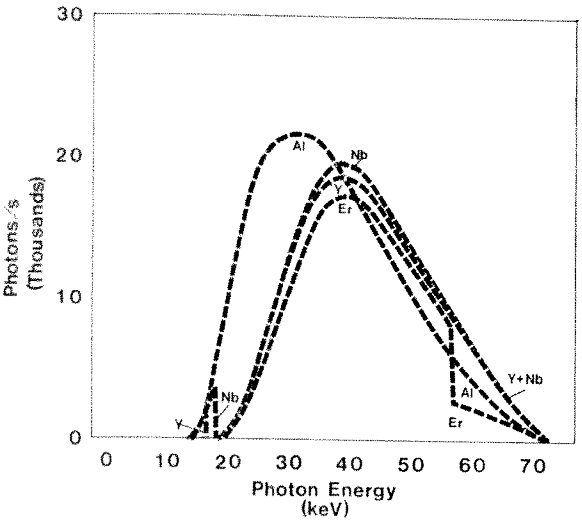

Figure 4. The computed beam spectra modified by the relative exposure time factor for the four filter systems.

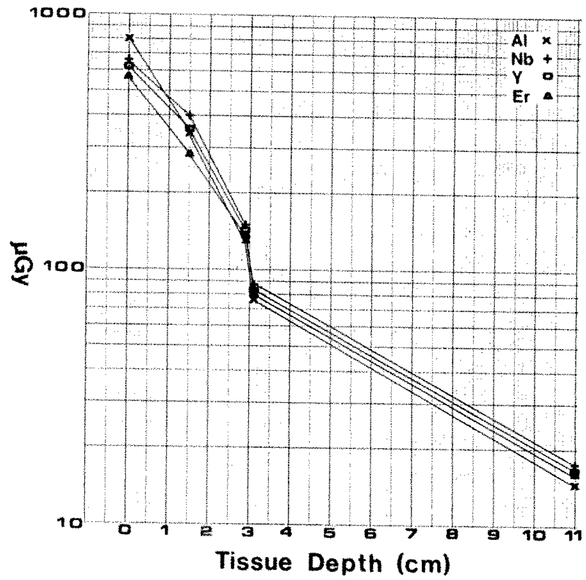

Figure 5. A semi-log plot of the fall in dose with increase in depth of tissue along the central ray axis for each of the four filter systems (at 75 kVp).

The computed beam spectra (at 75 kVp) for the four filter systems have been detailed previously (MacDonald-Jankowski & Lawinski, 1991). These spectra were adjusted to take into consideration the higher radiographic exposure times for the K-edge filter systems to show the relative radiation intensities reaching the patient, in addition to the relative photon energies in the beam (Fig. 4).

It is seen that the computed intensities are in approximately the same proportions as the measured values of the entrance skin dose at 75 kVp shown in Fig. 5. The shaping of the spectra resulting from the additional thin K-edge filters is clearly illustrated. From our previous study (Fig. 4 in MacDonald-Jankowski & Lawinski, 1991) there is greater filtration of the low-energy photons with the K-edge filters; the erbium additionally, to a certain extent, filters the high-energy photons. In this work all the measured radiation doses approximate to those resulting from the exposure of a typical dental radiograph of the maxillary molars.

The data for radiation dose measured along the central ray of the primary beam were almost identical to, and therefore confirmed, those presented earlier (MacDonald-Jankowski & Lawinski, 1991). These are summarized in Fig. 5, which shows a semi-log plot of the fall in radiation dose with increase in depth of tissue along the central ray axis for each of the four filter systems (at 75 kVp).

The results for the site on the inside of the cheek (Fig. 6, not presented previously) show a fall in dose with increasing kilovoltage for all the filter systems. However, an interesting observation is that the curve for aluminium filtration crosses over the curves for the other filter systems (top to bottom).

Inspection of the film dose and the post-film dose (Fig. 5) demonstrates that the lead backing in the dental film packet absorbs approximately one-half of the radiation dose that has passed through the object and the film.

The radiation doses at the other sites within the primary beam (other than along the central ray axis) exhibit different patterns dependent on the position and depth of the site relative to the entrance beam. The ipsilateral orbit (Fig. 7), which lies approximately 2 cm deep to the skin surface, exhibits the crossover of the aluminium curve similar to the site on the inside of the cheek. The deeper sites (Fig. 8–11) show the pattern already observed for the film dose of all four filter systems with a gradual increase with increase in kVp. The curve for aluminium filtration lies below those of the other filter systems.

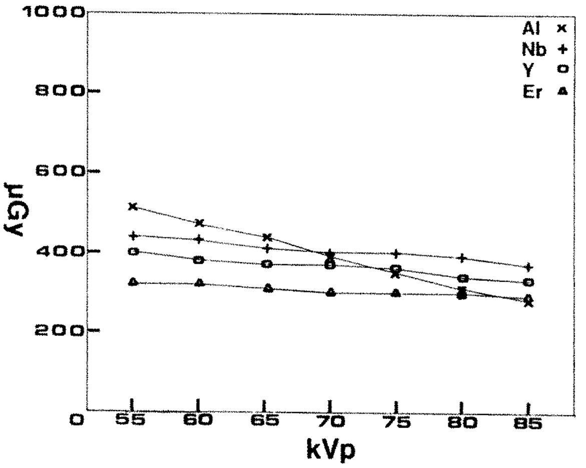

Figure 6. The dose for the inside of the cheek for the four filter systems.

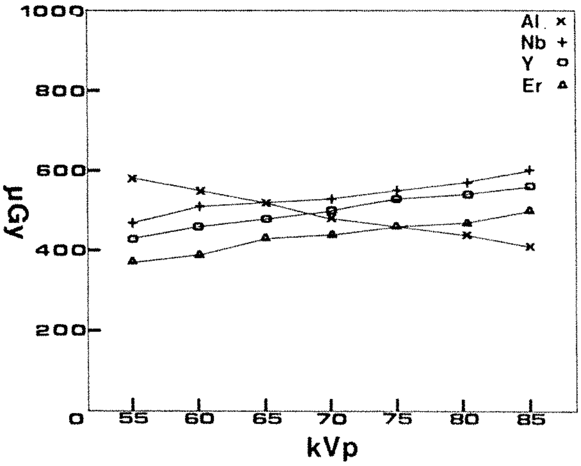

Figure 7. The ipsilateral orbit dose for the four filter systems.

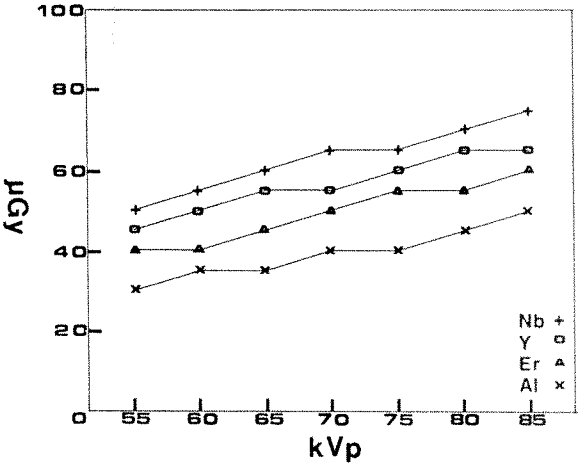

Figure 9. The contralateral tonsil dose for the four filter systems.

A comparison of the results for the contralateral tonsil and the contralateral masseter suggests that the effect of the ramus of the mandible (bone) is to absorb approximately half of the radiation passing through it (Figs 9, 10). The measurements outside the primary beam (below the pituitary, Fig. 12, and the contralateral orbit, Fig. 13) represent the distribution of scattered radiation at these sites. Both sets of curves show little change in scattered dose with kilovoltage.

An examination of the errors involved in the experimental methods used suggested a typical error of ±10% in the measurements of radiation dose and ±1 kV in tube voltage (Figs 6–13).

Conclusions

Reviewing all the observations within the primary beam, it is seen, as expected, that most of the radiation dose is absorbed in the first 1–2 cm of tissue (Fig. 5). The effect is especially marked for the aluminium filtration. Our results are in good agreement with previous work on the use of K-edge filtration in intra-oral radiography (Richards et al, 1970; Gelskey & Baker, 1981; Tyndall, 1986; Mauriello et al, 1987; Ponce et al, 1988; Horner et al, 1988; Farman et al, 1989; Kircos et al, 1989; Kapa et al, 1990) which, in general, reported a substantial reduction in dose. However, it should be noted that unlike our work these studies only assessed the skin dose as a measure of the overall radiation dose imparted to the patient.

For an optimally exposed dental radiograph the thin K-edge filter systems produce a significantly smaller entrance skin dose in comparison to that with the aluminium filtration. For example, at 75 kVp with erbium filtration the skin entrance dose is reduced to 70% of that with aluminium alone. Additionally, the thin K-edge filters exhibit a slightly higher exit skin dose than aluminium. With erbium the exit dose is 110% of that with aluminium (at 75 kVp). Thus, in combination, these findings suggest a reduction of the overall radia-

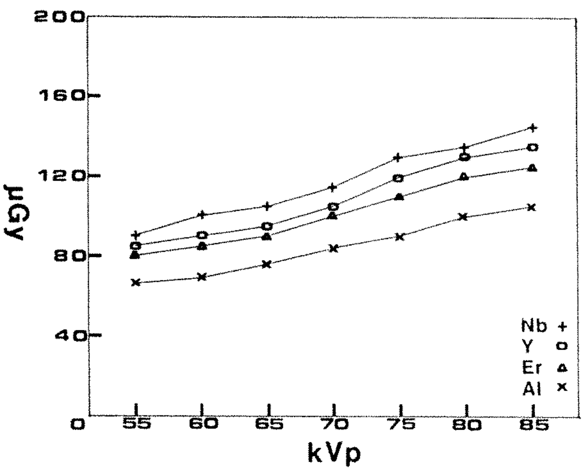

Figure 8. The ipsilateral tonsil dose for the four filter systems.

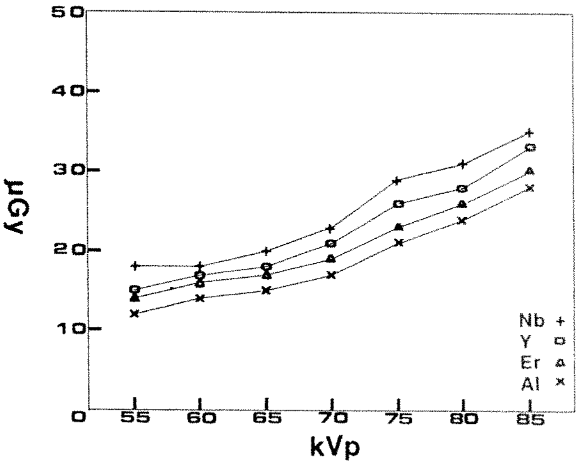

Figure 10. The contralateral masseter dose for the four filter systems.

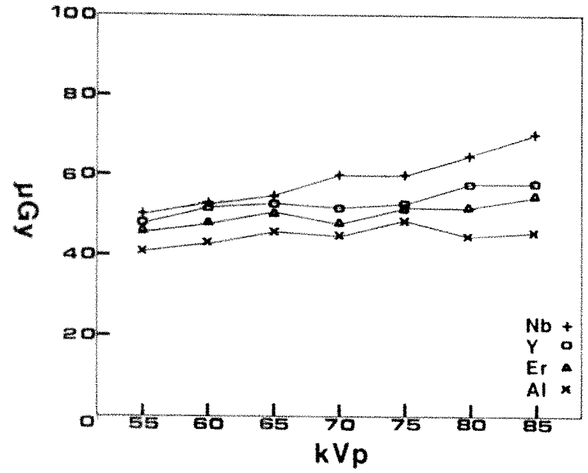

Figure 11. The sublingual mucosa dose for the four filter systems.

tion dose absorbed by the head when using a K-edge filter. Overall, the results for the erbium system appear most promising; when compared with those of aluminium they demonstrate the greatest reduction in radiation dose within the first 1–2 cm of tissue with only a slightly larger scattered radiation dose.

A slight increase in the dose delivered to deep structures was observed with the K-edge filter systems when compared with aluminium alone. This has also been reported by Byrne et al (1991) for niobium at 70 kVp. White and Gratt (1991) have suggested that an aluminium filter system delivered a higher deep dose than niobium. However, in this work the accumulated dose to various sites within the head delivered during a full radiographical survey of the mouth (using 18 intra-oral films) was measured. Thus for a certain number of the 18 exposures (at least three) many of the sites would be comparatively close to the surface of the skin adjacent to the entrance site of the primary beam. This would

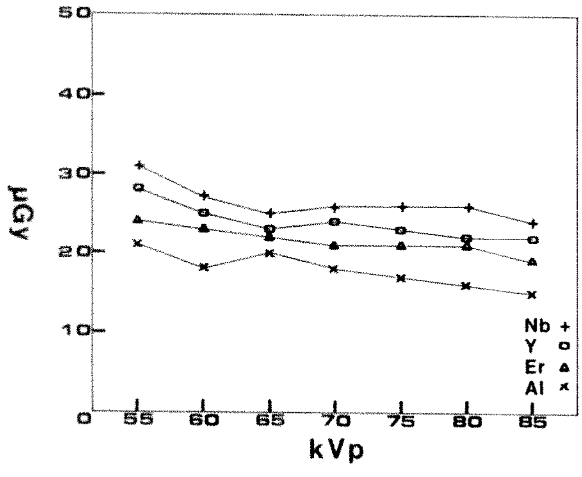

Figure 12. The dose delivered just below the pituitary for the four filter systems.

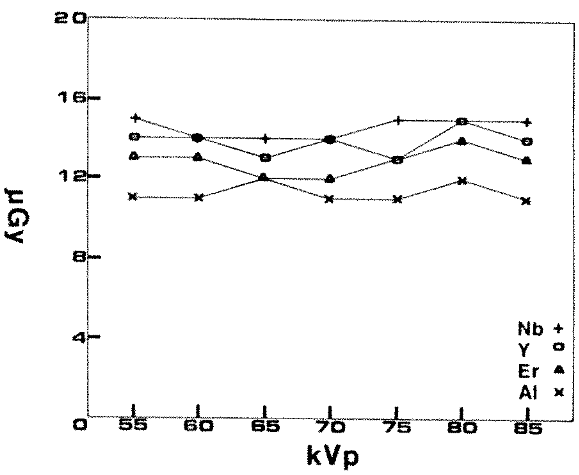

Figure 13. The contralateral orbit dose for the four filter systems.

favour a higher deep dose with the aluminium filtration owing to the higher skin dose associated with this filter system.

The position and extent of the crossover effect seen in Figs 6 and 7 is dependent on the site of measurement. The crossover is thought to be due to the changing relationship of the mean beam energy of the four filter systems with increase in tissue depth and change in tube voltage. One result of this crossover at the site of the ipsilateral orbit suggests that the use of a K-edge filter (in dental radiology) at higher tube voltages does not reduce the radiation dose to the eye. Although radiation-induced cataract is a non-stochastic phenomenon with a threshold in the range 0.5–2 Gy for a single exposure and 5 Gy for a highly fractionated or protracted exposure (ICRP, 1989) and therefore above that of dental exposure, the dentist is not exempt from minimizing unnecessary radiation. However, this reduction in radiation dose to the lens of the eye would be better produced by the use of a collimator providing a small rectangular beam.

Acknowledgments

We would like to thank Dr K. Cranley of the Royal Victoria Hospital, Belfast, for computing the spectra and Lorna Vassell for preparing the typescript.

References

Birch, R., Marshall, M. & Ardran, G. M., 1979. *Catalogue of Spectral Data for Diagnostic X-rays*, Scientific Report Series No 30 (Hospital Physicists' Association, London).

Byrne, C. M., Pharoah, M. J. & Wood, R. E., 1991. Skin exposure and thyroid dose distribution using niobium filtration. *Journal of Canadian Dental Association, 57*, 663–665.

Farman, A. G., Perez, C., Jacobson, A. & Kelly, M. S., 1989. Evaluation of aluminium-yttrium filtration for intra-oral radiography. *Oral Surgery, Oral Medicine, Oral Pathology, 67*, 224–226.

Gelskey, D. E. & Baker, C. G., 1981. Energy selective filtration of dental X ray beams. *Oral Surgery, Oral Medicine, Oral Pathology, 52*, 565–567.

HORNER, K., LAWINSKI, C. P. & SMITH, N. J. D., 1988. Erbium filtration for dose reduction in dental radiography. *British Journal of Radiology, 61*, 609–612.

ICRP, 1989. *RBE for Deterministic Effects, Annals of the ICRP*. International Commission on Radiological Protection Publication 58.

KAPA, S. F., TYNDALL, D. A. & OUELLETTE, T. E., 1990. The application of added beam filtration to intra-oral radiography. *Dento-maxillofacial Radiology, 19*, 67–74.

KIRCOS, L. T., STANINEC, M. & CHOU, L., 1989. Rare earth filters for intraoral radiography: exposure reduction as a function of kV(p) with comparisons of image quality. *Journal of the American Dental Association, 118*, 605–609.

MACDONALD-JANKOWSKI, D. S. & LAWINSKI, C. P., 1991. The reduction in radiation dose for intra-oral radiography by the use of thin K-edge filters. *British Journal of Radiology, 64*, 524–528.

MAURIELLO, S. M., WASHBURN, D. B. & MATTESON, S. R., 1987. Effects of rare earth filters on patient exposure and image contrast. *Journal of Dental Research, 66*, 1326–1330.

NAGEL, H. D., 1989. Comparison of performance characteristics of conventional and K-edge filters in general diagnostic radiology. *Physics in Medicine and Biology, 34*, 1269–1287.

NRPB, 1988. National Radiological Protection Board, Health and Safety Executive and Health Departments, 1988. *Guidance Notes for the Protection of Persons against Ionizing Radiations Arising from Medical and Dental Use* (HMSO, London).

PONCE, A. Z., MCDAVID, W. D. & LANGLAND, O. E., 1988. The use of added erbium filtration in intraoral radiology. *Oral Surgery, Oral Medicine, Oral Pathology, 66*, 513–517.

RICHARDS, A. B., BARBOR, G. L., BADER, J. D. & HALE, J. D., 1970. Samarium filtration in dental radiology. *Oral Surgery, Oral Medicine, Oral Pathology, 29*, 704–715.

TYNDALL, D. A., 1986. Spectroscopic analysis and dosimetry of diagnostic X-ray beams filtered by rare earth materials. *Oral Surgery, Oral Medicine, Oral Pathology, 62*, 205–211.

WHITE, S. C. & GRATT, B. M., 1991. Evaluation of niobi-X filtration in intraoral radiology. *Oral Surgery, Oral Medicine, Oral Pathology, 72*, 746–755.

1992, *The British Journal of Radiology*, 65, 996–1002

The distribution of medical X-ray doses amongst individuals in the British population

By D. Hart, PhD and *J. C. Le Heron, BSc

National Radiological Protection Board, Chilton, Didcot, Oxon OX11 0RQ, UK and *National Radiation Laboratory, PO Box 25099, Christchurch, New Zealand

(*Received 13 November 1991 and in revised form 12 March 1992, accepted 6 May 1992*)

Keywords: Diagnostic X rays, Patient doses, Cumulative doses, Distribution, Britain

Abstract. This study has estimated the distribution of diagnostic X-ray doses amongst individuals in the British population by sampling the records kept by general practitioners (GPs) on their patients and the records held by the radiology department of a district general hospital. Deceased patients were chosen in the former case in order to evaluate the dose acquired over a complete lifetime. In each case, several hundred records were sampled. The GP data obtained have enabled an estimate to be made of the likelihood of reaching various dose levels in a lifetime. It is estimated that about 1% of the population has received a lifetime effective dose-equivalent of more than 100 mSv. The largest cumulative dose revealed by the samples of GP and radiology department records was about 200 mSv. The GP data have also shown that the last year of life sees a four-fold increase in the number of X-ray examinations experienced compared with the previous 9 years. The hospital data have allowed an estimate to be made of current rates of dose acquisition amongst the population of a District Health Authority.

Information was collected in Great Britain during the 1980s on typical radiation doses from common X-ray examinations (Shrimpton et al, 1986), and on the frequency of occurrence of specific types of X-ray examination (Wall et al, 1986). On that basis, an estimate was made of the annual collective effective dose-equivalent to the population of Great Britain from medical X rays, which amounted to 16 000 man-Sv (Shrimpton & Wall, 1986). This collective dose implied a per caput annual effective dose-equivalent for the British population of about 0.3 mSv. This was an average annual dose, which took no account of the way in which the doses were actually spread amongst the population.

Some people may have a considerable number of X-ray examinations in their lifetime, whereas others may have none at all. No attempt ever appears to have been made to estimate the distribution of cumulative lifetime doses for Great Britain. The aim of this study was to find the distribution amongst individuals in the population of: (1) cumulative lifetime doses from diagnostic X rays; and (2) current annual doses from diagnostic X rays.

Methods

Two types of record were investigated with this aim: (1) medical records kept by general practitioners (GPs) on their patients; and (2) records kept in the radiology department of a general hospital. Radiotherapy, nuclear medicine and dental X rays were all excluded from the scope of this study.

GPs' records

Sampling GPs' records is akin to sampling the general population. In England the total number of people on GPs' lists exceeds the total population (Department of Health, 1990). This is because names are retained on the lists despite the persons having died or emigrated. It seems likely that virtually the whole population is registered with GPs.

Only patients who had died were included in the analysis of GPs' records, so that doses acquired over a complete lifetime could be assessed. People who had recently died were chosen in order to produce as up-to-date an analysis as possible. The records of people who had died in the county of Oxfordshire were stored alphabetically by surname. 519 of these were selected from throughout the alphabet to give a stratified representative sample. Each individual's file was read in its entirety, and the type and date of each X-ray examination were noted. This process took an average of about 30 min per patient. The earliest date to which an individual's record went back was 1920. On average, about 50% of an individual's lifetime was covered by the medical record. The earliest reference to an X-ray examination was in 1935.

Hospital radiology department records

People who have received a high cumulative dose from diagnostic X rays can feasibly have done so only through a number of visits to hospital radiology departments with facilities for complex high-dose examinations. A study of the records of such a department should therefore reveal high cumulative doses more frequently than the survey of GPs' records. (Concentration on patients undergoing very high-dose examinations, such as interventional and cardiac radiology, was not pursued in this study, but might reveal very high cumulative doses.)

A specific hospital was chosen for study because it carried out the overwhelming majority of radiological

Table I. Relative levels of historical doses in Great Britain (with sources)

Decade	Bone marrow doses per examination	Effective dose-equivalents per fluoroscopic examination	Entrance surface doses per film	Dose per examination (based on previous column)	Vetter's ratios	Dose adjustment per examination
1980s	1 (A)	1 (A, B)	1 (A)	1	1980 = 1	1
					1975 = 1.4	
1970s		1.8 (C, D)	1.5 (E)	1.5	1970 = 2.8	2
1960s		3.2 (F, G)			1960 = 2.8	3
1950s	3.2 (H)	4.2 (I, J, K)	5.5 (J, L)	4.1	1950 = 4.2	4
1940s			8 (M)	6	1940 = 5.6	6
1930s			20 (N)	15	1930 = 5.6	10

Sources: A NRPB-R200, Shrimpton et al (1986)
B Rowley et al (1987)
C Takeshita et al (1972)
D Levy et al (1972)
E Van Elegem et al (1972)
F Ardran & Crooks (1969)
G Reinsma (1962)
H Adrian (1966)
I Adrian (1960)
J Ardran & Crooks (1953)
K Ardran & Crooks (1957)
L Stanford & Vance (1955)
M Martin (1947)
N Ardran (1956).

examinations in the District Health Authority in which it is located. The population of the district was 230 000. The hospital had 600 beds and carried out a wide range of X-ray examinations, including barium studies, angiography and computed tomography (CT). Radiological records were kept for a recommended minimum period of 3 years and in practice were kept for 4 years. After this time they were stored elsewhere for legal purposes only, and were not retrieved if the patient returned to the radiology department. Thus records going back over a considerable period of time were available only for those patients who attended regularly, *i.e.* at intervals of 4 years or less. This type of record-keeping system is inappropriate for the purposes of a definitive study of lifetime cumulative doses. Nevertheless, quite a few patients were found to have dose records going back over a considerable period of time.

The initial approach to finding patients with a considerable cumulative dose was to select the thicker film packets, and about 100 of these were chosen for study. However, it became clear that this method of searching was not satisfactory. Some thick film packets contained only a large number of chest radiographs, which implied a small radiation dose. Some thin film packets contained one or more CT examinations, which implied a fairly considerable dose. Therefore a different approach was adopted by estimating the combined dose from the types of examinations listed on the front of the film packet as a means of selecting patients who had cumulative doses greater than 30 mSv. Nearly 5000 records were scanned in this way. For all the patients selected as receiving over 30 mSv, an accurate total dose was subsequently calculated and the type and date of each X-ray examination were noted.

Another set of 1000 patients was analysed; not for high doses, but as a representative sample of the patients in the radiology department records. This analysis allowed an estimate to be made of the current distribution of X-ray doses in the population served by the District Health Authority, rather than looking back into the more distant past as in the lifetime dose study.

Corrections to the data

In order to compile an estimate of cumulative lifetime doses, an effective dose-equivalent that was typical of national practice was assigned to each recorded examination. As X-ray examinations going back over 50 years were being dealt with, it was necessary to make a correction for the higher doses incurred per examination in the past. Table I shows how this correction was made. To estimate the relative levels of medical X-ray dose per examination in the past in Great Britain, various types of dose measurement were compared. Bone marrow doses for eight types of non-fluoroscopic examination were compared between the 1980s and the 1950s, *i.e.* between NRPB-R200 (Shrimpton et al, 1986) and the final report of the Adrian Committee. Effective dose-equivalents for fluoroscopic examinations were also compared over the decades. For the 1970s, doses in France and Japan from barium meals and enemas were used, since no published doses were found for Great Britain. The Japanese examinations involved both direct fluoroscopy and image intensifiers, whereas all the French examinations used image intensifiers. Comparisons were also made with NRPB-R200 for entrance surface doses per film in non-fluoroscopic examinations, for five types of radiograph in the case of Ardran and Crooks and nine types for Stanford and Vance (both covering the 1950s), four types for Martin (referring to the 1940s), and one type for Ardran (referring to the 1930s). No published entrance surface doses per film for the 1970s were found for Great Britain; the result of a Belgian study using phantoms has been added to Table I for comparison. The number of films used per examination in the 1950s was about 75% of the number used in the 1980s, as shown in Table II. It was assumed that the number of films per examination was the same in the 1930s and 1940s as in the 1950s. In

Table II. Numbers of films per examination

Examination	1957 (Adrian, 1960)	1983 (Shrimpton et al, 1986)
Lumbar spine	2.6	3.4
Chest	1.2	1.3
Skull	2.6	3.0
Abdomen	1.4	1.4
Thoracic spine	2.1	2.4
Pelvis	1.3	1.1
IVU	6.1	8.2
Barium meal	5.4	7.8
Barium enema	4.1	8.5
Cholecystography	3.4	4.7
Average	3.0	4.2

column 5 of Table I allowance has been made for the increase in films/examination.

Gonad doses per examination are not likely to be comparable over long periods of time. This is because the choice of projecctions may well change with time and because gonad doses vary considerably with technique, depending, for instance, on whether gonad shields are used or not. Gonad doses were therefore not compared.

The ratios used by Vetter et al (1991) in calculating historical exposures for the USA are shown in the penultimate column in Table I. The changes in dose per examination in Great Britain over the decades were found to be similar to the ratios used by Vetter, with the exception of the 1930s. Since for Great Britain this was based on only a single observation, an adjustment factor of 10 was chosen, being halfway between Vetter's ratio and the ratio derived from Ardran. Only a few examinations, all of low dose, were found for the 1930s, so the factor for that decade was not of crucial importance.

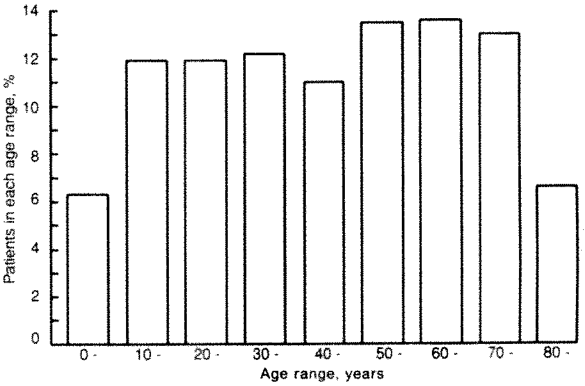

Figure 1. Age distribution for all X-ray examinations, both sexes.

The dose adjustments per examination in the final column of Table I were used to convert current doses to historic dose levels when compiling individual patient's dose histories.

Figure 1 is derived from an earlier national survey (Wall et al, 1986) and shows that the frequency of X-ray examinations is fairly evenly distributed with age, so that people between the ages of 10 and 80 years have about the same number of X-ray examinations per annum, although young people tend to have low-dose examinations whereas the elderly tend to have high-dose examinations. This simplifies the analysis because there is virtually no need to correct for the age range of the sample at any point in time. The main determinant of frequency of examination is not the age of the patient but the period of the century under consideration, as explained in the next paragraph.

Table III shows how some published surveys indicate that the annual number of medical X-ray examinations performed in Britain has changed over the last 50 years.

Table III. Annual number of medical X-ray examinations in Britain

Year	Area	Population (millions)	Annual number of medical X-ray examinations (millions)[a]	Source	Annual number of medical X-ray examinations per thousand population
1939	GB	46.4	~ 2.8	1	~ 60
1945	GB	48.1	~ 6	1	~ 125
1951	E+W	43.8	7.7	2+3	176
1953	E+W	44.1	9.8	2+3	222
1955	E+W	44.4	12.2	2+3	275
1957	GB	50.6	13	4	257
1964	GB	52.6	16.3	5	310
1977	GB	54.4	21.3	6	392
1983	GB	54.6	24.6	7	450

GB, Great Britain; E+W, England and Wales.

[a] Excluding private hospitals.

Sources:
1 Barclay (1949)
2 MRC (1956)
3 Osborn & Smith (1956)
4 Adrian (1960)
5 Matthews & Miller (1969)
6 Kendall et al (1980)
7 Wall et al (1986).

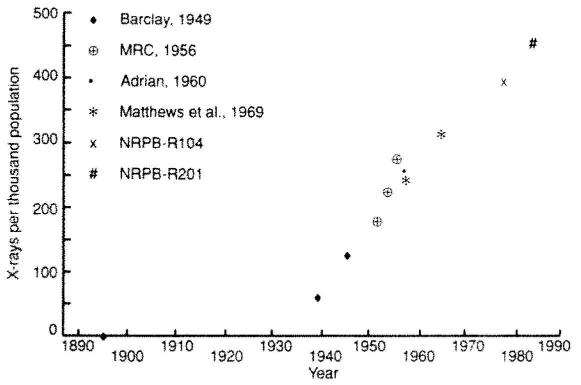

Figure 2. Annual X-ray examinations in Britain per thousand population (excluding mass surveys).

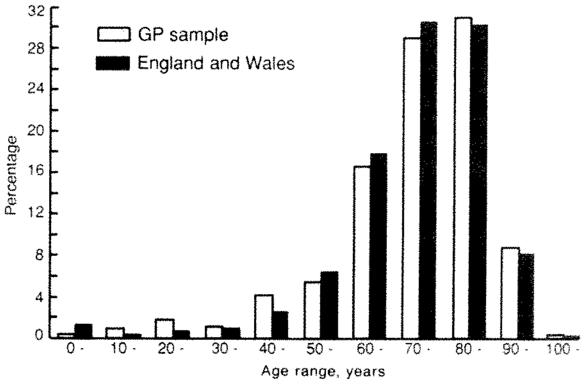

Figure 3. Age distribution of patients at death.

Since the population has also grown in that period, and since the geographical area covered has not always been the same, it is helpful to derive the number of examinations per thousand population, and this is shown in the final column of Table III. Figure 2 presents these numbers graphically and clearly shows an almost linear increase over this period with no sign of falling off in the 1980s. The numbers for 1939 and 1945 are only approximate since they rely merely on a statement (Barclay, 1949) that the volume of X-ray work during World War II more than doubled. Nevertheless, it seems clear that the frequency of X-ray examinations was very low in the period 1895–1940 in comparison with current practice.

Comparison of these estimates with the frequency of X-ray examinations observed in each decade for the sample of 519 GP records, made it possible to calculate that the records of X-ray examinations in the sample were about 81% complete for the 1980s, but were only about 17% complete for the 1930s, with a steady improvement over the decades in between. Throughout the whole period from 1930 to 1990, the GPs' records appeared to be about 54% complete. These results are shown in Table IV. When considering the cumulative lifetime dose that was estimated for each individual, one must bear this level of completeness in mind. The cumulative lifetime doses quoted in this paper could conceivably be underestimated by a factor of two from this source of uncertainty alone.

Results

Cumulative lifetime doses

Figure 3 shows the age distribution at time of death of the patients in the sample of GPs' records compared with national data for England and Wales in 1988 (Office of Population Censuses and Surveys, 1990). The data cover 515 patients since an exact date of death could not be established for four patients. It can be seen that the sample matches the national pattern reasonably well. A slight exception occurs in the under-10 years age range, where deaths immediately after birth are under-represented because these babies are seldom registered with a GP.

Figure 4 shows the distribution of cumulative lifetime effective dose-equivalents that have been estimated from the sample of GPs' records. Allowance has been made here for higher dose levels in the past, but not for the possible incompleteness of the records. The first bar shows the percentage of patients who have received less than 10 mSv effective dose-equivalent, the second bar the percentage who have received 10–20 mSv, and so on. Some 50% of the sample received less than 10 mSv, and 75% received less than 20 mSv in a lifetime. Only

Table IV. Percentage completeness of GPs' records

Decade	No of patients in GPs' records covering each decade	Annual number of examinations per thousand people		Percentage of completeness
		GPs' records	Historic estimates (from Table III)	
1930s	42	10	~ 60	~ 17
1940s	92	38	~ 125	~ 30
1950s	263	91	250	36
1960s	370	138	310	45
1970s	467	218	390	56
1980s	503	363	450	81
Total	519	858	1585	54

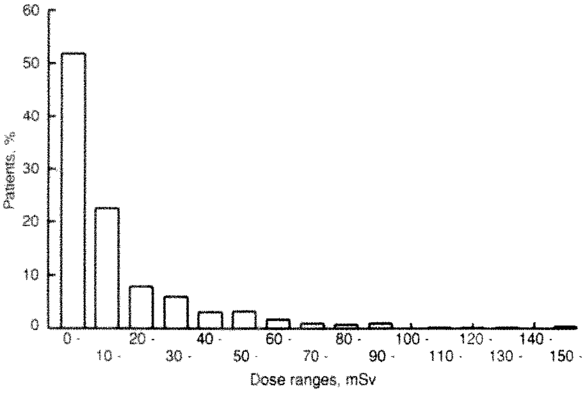

Figure 4. Distribution of lifetime doses.

about 1% received more than 100 mSv. The average lifetime dose for the sample was 17 mSv, which implies an average annual dose over a lifetime of 75 years of 0.2 mSv. This is similar to the average annual dose from medical exposures estimated for the UK population in the 1980s, which was 0.3 mSv per head, despite the dissimilarity of the time periods.

Since all the GPs' patients who were studied had died, it was possible to analyse the frequency of examinations in the last few years of life. Figure 5 shows the proportion of lifetime X-ray examinations that occur in each of the last 10 years of life. Death occurs at the origin of the chart, the first bar shows the percentage of lifetime examinations in the last year of life, the second bar shows the percentage in the penultimate year of life, and so on. The data in this diagram have been corrected to eliminate the incompleteness of records in past decades by using the historic estimates of examination frequencies over the decades shown in Table IV, *i.e.* the proportion of an average lifetime's examinations that occur in the last decade of life (the 1980s) was fixed at 450/1585 = 28%. This percentage was based purely on historic estimates and not on direct observation of individual patients. It effectively assumes a lifespan of only 60 years, but is insensitive to the use of different lifespans. The proportion is as high as 28% primarily because of the steadily rising trend in examination frequencies as shown in Fig. 2. As a result of this correction, an average of 8% of lifetime examinations was estimated to occur in the last year of life. There is an increase by a factor of approximately four in the number of examinations carried out in the last year of life compared with the average of the previous 9 years. There will, of course, be a much reduced opportunity for the expression of radiation-induced health effects following exposures received so late in life.

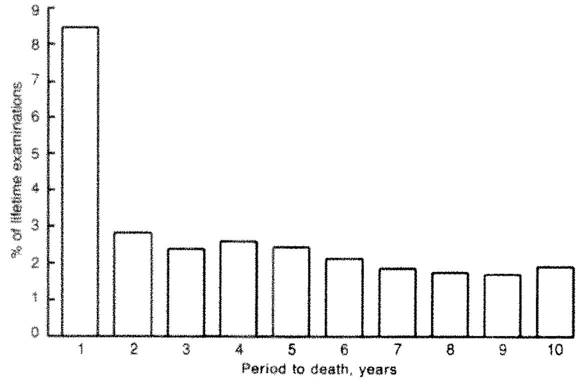

Figure 5. X-ray examinations in the last 10 years of life.

Table V. Twelve patients with the highest cumulative dose (hospital and GP data)

Total dose (mSv)	Age range (years)	Sex	Examination types and number (in order of highest combined effective dose-equivalent)
186[a]	37–60	F	5 Barium enemas, 3 IVUs, 5 lumbar spine, 2 barium meals
182[a]	38–64	F	4 Barium enemas, 7 barium meals, 4 IVUs
182[a]	56–78	M	7 Barium enemas, 4 IVUs
177	46–87	F	5 Barium enemas, 3 IVUs, 2 lumbar spine
154	46–86	F	3 Barium enemas, 2 IVUs, 2 barium meals, 5 pelvis, 2 lumbar spine
149[a]	43–66	F	7 IVUs, 3 barium enemas, 12 abdomen, 2 barium meals, 2 lumbar spine, 10 hip
135	37–82	F	6 Barium meals, 4 lumbar spine, 2 IVUs, 1 barium enema, 4 cholecystography
130[a]	62–82	F	5 Barium meals, 2 barium enemas, 7 abdomen, 2 IVUs, 2 lumbar spine
124[a]	25–56	M	4 Barium enemas, 3 IVUs, 2 barium meals, 2 lumbar spine
123[a]	47–73	F	2 Barium enemas, 3 IVUs, 30 hip, 7 pelvis, 3 lumbar spine
121	43–79	F	4 IVUs, 4 barium meals, 2 barium enemas
113[a]	44–60	F	5 barium enemas, 4 barium meals, 2 IVUs, 4 abdomen

IVU, intravenous urogram.

[a] Not a lifetime dose (hospital patient).

This analysis of the frequency of X-ray examinations in the later stages of life differs from that of Russell (1988) in two ways, which makes direct comparison of the results of the two studies difficult. During his investigation of the "last illness factor", Russell included only examinations that were both connected with, and occurred during, fatal illness. In this study no attempt has been made to link X-ray examinations to the cause of death. This analysis has calculated the percentage of patients' lifetime examinations that occur in the final year of life, whereas Russell calculated the percentage of the District Health Authority's diagnostic radiology workload that was last-illness related.

Table V gives a summary of the 12 patients with the highest cumulative doses found in either the hospital radiology department records or GPs' records. Doses in the hospital records are marked with superscripts.

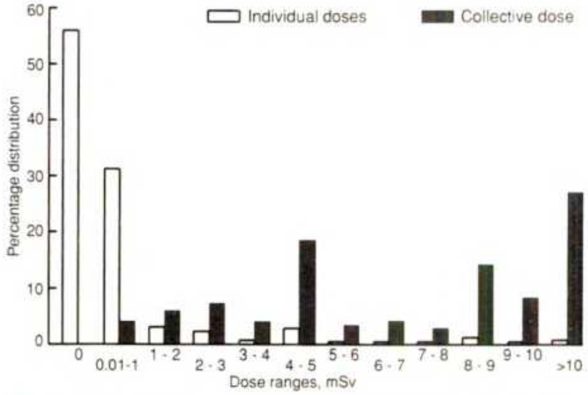

Figure 6. Distribution of doses accumulated over 3 years in a District Health Authority, 1988–90.

Most of the hospital patients were still alive at the time of the study, so their cumulative dose will underestimate their lifetime dose. It can be seen that the highest total effective dose-equivalent was about 190 mSv. This was incurred by a hospital patient in a 23-year period from age 37 to age 60 years.

Table V also shows the types of examination giving a significant contribution to the patient's lifetime dose. The examination types are listed with the number of such examinations and in the order of the current magnitude of dose from a set of examinations, the largest being given first. CT examinations do not appear on this list, despite, in many cases, giving comparable or higher doses than barium enemas. The absence of CT examinations is almost certainly a result of higher doses being used in the past for conventional examinations. High lifetime doses in this study tend to be produced by having high-dose examinations in the 1950s and 1960s, whereas CT was not introduced until the 1970s.

Current dose distribution in the population

The analysis of radiology department records allowed an estimate to be made of the current distribution of medical X-ray doses amongst the population. Figure 6 shows an estimate of the distribution of effective dose-equivalents accumulated over a recent 3-year period amongst the population of the District Health Authority served by the hospital. Examinations carried out at the only other NHS hospital in the District (a 60-bed hospital) were allowed for in this analysis, but not those performed outside the District. The diagram has two items of information. The white bars indicate the percentage of the population within individual dose ranges. The dose ranges are zero, up to 1 mSv, 1–2 mSv, and so on until the final bars, which include anything over 10 mSv. The shaded bars indicate the percentage of the collective dose that is accounted for by each of these dose ranges. Two minor peaks occur in the data at 4 and 8 mSv, which coincide with the typical dose from an intravenous urogram (IVU) or barium meal and a barium enema, respectively.

Since the X-ray records were fully complete for 1988–1990, it was possible to estimate the percentage of the population that did not have an X-ray examination in this period. It can be seen that 56% of the population had no dose in the 3 years, whereas those who acquired more than 10 mSv effective dose-equivalent in 3 years amounted to only 0.8% of the population and yet they incurred the largest proportion (27%) of the collective dose. On average, 93% of the population receives an effective dose-equivalent from diagnostic X rays of less than 1 mSv in any one year. But of course the corollary to the fact that most people receive relatively low doses of diagnostic X rays is that a few people receive the majority of the dose: 82% of the collective dose is incurred by the other 7% of the population.

Discussion and conclusions

It should be borne in mind that there are large uncertainties in the evaluation of long-term cumulative doses as attempted here. For instance, all examinations would not have been carried out at typical dose levels. Furthermore, the level of completeness of the records comprising each individual case history is unknown and would generally appear to be quite low, to the extent that lifetime doses estimated from the sample of GPs' records could be underestimated by a factor of two. Despite the uncertainty revealed by these considerations, this first attempt at assessing the distribution of doses should be of some value.

The important results of the study may be summarized as follows:

1. The last year of life sees a four-fold increase in the number of X-ray examinations compared with the previous 9 years. On average, 8% of lifetime examinations occur in the last year of life.
2. The distribution of doses from diagnostic X rays suggests that about 75% of the population receives a lifetime dose of less than 20 mSv, but at least 1% receives a lifetime dose greater than 100 mSv.
3. The largest lifetime dose revealed by the samples of GP and radiology department records was about 200 mSv, around two and a half times the typical radiation dose from natural background, excluding radon, in a lifetime.
4. Future estimates of lifetime dose may well be higher, owing to the increasing frequency of examinations and a greater prevalence of high-dose CT examinations.
5. The distribution of annual doses to individuals from diagnostic X rays is very skewed, with about 7% of the population receiving around 80% of the collective dose.

Acknowledgments

We wish to thank Carolyne McKinlay, Alun Davies and Geoff Phillips for allowing access to patient records. Ella Barclay, Mark Hillier, Barry Wall, Mary Whitham and Sarah Whitham helped considerably by collecting data from GPs' files.

References

ADRIAN, LORD, 1960. *Radiological Hazards to Patients: Second Report of the Committee* (HMSO, London).

—— 1966. *Radiological Hazards to Patients: Final Report of the Committee* (HMSO, London).

ARDRAN, G. M., 1956. The dose to operator and patient in X-ray diagnostic procedures. *British Journal of Radiology, 29*, 266–269.

ARDRAN, G. M. & CROOKS, H. E., 1953. A comparison of radiographic techniques with special reference to dosage. *British Journal of Radiology, 26*, 352–357.

—— 1957. Gonad radiation dose from diagnostic procedures. *British Journal of Radiology, 30*, 295–297.

—— 1969. Dose reduction in fluoroscopy. *British Journal of Radiology, 42*, 554.

BARCLAY, A. E., 1949. The old order changes. *British Journal of Radiology, 22*, 300–308.

DEPARTMENT OF HEALTH, 1990. *Health and Personal Social Services Statistics for England* (HMSO, London).

KENDALL, G. M., DARBY, S. C., HARRIES, S. V. & RAE, S., 1980. *A Frequency Survey of Radiological Examinations Carried out in NHS Hospitals in Great Britain in 1977 for Diagnostic Purposes*, NRPB-R104 (HMSO, London).

LEVY, P., PALLARDY, G. & LEDOUX-LEBARD, G., 1972. Dose reçue au cours des examens radiologiques digestifs. *Journal de Radiologie et d'Electrologie, 53*, 777–782.

MARTIN, J. H., 1947. Radiation doses received by the skin of a patient during routine diagnostic X-ray examinations. *British Journal of Radiology, 20*, 279–283.

MATTHEWS, J. C. & MILLER, H., 1969. Radiation hazards from diagnostic radiology. *British Journal of Radiology, 42*, 814–817.

MRC, 1956. *The Hazards to Man of Nuclear and Allied Radiations* (Medical Research Council, London).

OFFICE OF POPULATION CENSUSES AND SURVEYS, 1990. *Mortality Statistics: General*, Series DH1, No 21 (HMSO, London).

OSBORN, S. B. & SMITH E. E., 1956. The genetically significant radiation dose from the diagnostic use of x-rays in England and Wales. *Lancet, 16 June*, 949–953.

REINSMA, K., 1962. *Dosemeters for X-ray Diagnosis* (Philips Technical Library, Eindhoven).

ROWLEY, K. A., HILL, S. J., WATKINS, R. A. & MOORES, B. M., 1987. An investigation into the levels of radiation exposure in diagnostic examinations involving fluoroscopy. *British Journal of Radiology, 60*, 167–173.

RUSSELL, J. G. B., 1988. The last illness factor: a District experience. *British Journal of Radiology, 61*, 1037–1038.

SHRIMPTON, P. C. & WALL, B. F., 1986. Doses to patients from medical radiological examinations in Great Britain. *Radiological Protection Bulletin, 77*, 10–14.

SHRIMPTON, P. C., WALL, B. F., JONES, D. G., FISHER, E. S., HILLER, M. C., KENDALL, G. M. & HARRISON, R. M., 1986. *A National Survey of Doses to Patients Undergoing a Selection of Routine X-ray Examinations in English Hospitals*, NRBP-R200 (HMSO, London).

STANFORD, R. W. & VANCE, J., 1955. The quantity of radiation received by the reproductive organs of patients during routine diagnostic X-ray examinations. *British Journal of Radiology, 28*, 266–273.

TAKESHITA, K., ANTOKU, S. & SAWADA, S., 1972. Exposure pattern, surface, bone marrow integral and gonadal dose from fluoroscopy. *British Journal of Radiology, 45*, 53–58.

VAN ELEGEM, P., BRUNFAUT, C. & LEJEUNE, S., 1972. Dosimetrie en radiodiagnostic. *Journal Belge de Radiologie, 55*, 271–284.

VETTER, R. J., GRAY, J. E. & KOFLER, J. M., 1991. Patient radiation doses at a large tertiary care medical center. In *Statistics of Human Exposure to Ionising Radiation*, Proceedings of a meeting held in Oxford, April 1990. Special issue of *Radiation Protection Dosimetry, 36*, 2–4.

WALL, B. F., HILLIER, M. C. & KENDALL, G. M., 1986. *An Update on the Frequency of Medical and Dental X-ray Examinations in Great Britain–1983*. NRPB-R201 (HMSO, London).

1992, *The British Journal of Radiology*, *66*, 1003–1006

Efficiency of a lead-containing tie for radiation protection of the thyroid gland

By Hans-Martin Klein, MD and Achim Stargardt, PhD

Clinic of Diagnostic Radiology, University of Technology, 5100 Aachen, Germany

(Received 24 January 1992 and in revised form 11 May 1992, accepted 25 June 1992)

Keywords: Thyroid gland, Radiation dose, Lead shielding

Abstract. During fluoroscopy the examiner is usually protected by a radiation-reducing body shield, leaving the thyroid unprotected. The fact that the thyroid is located in a region of the neck usually covered by the shirt collar led to the idea of designing a tie with lead core, providing easy and "decorative" reduction of the radiation dose. Sonographic examinations were carried out in 20 volunteers (10 men, 10 women) to determine the size of the gland and its coverage by such a tie. The reduction of the surface and organ dose was assessed using film dosimetry with scattered radiation, the body of the examiner being simulated by an Alderson phantom. On average 88% of the thyroid gland surface area was covered. Surface dose was reduced to 1%, and organ dose to 10% of the value without the protection tie.

The radiation dose acquired by the radiologist during diagnostic or therapeutic fluoroscopy has been reduced continuously in the last decades. This has been made possible by technical improvements in fluoroscopy such as better shielding, higher sensitivity of image intensifiers and screen–film systems, and intermittent fluoroscopy with digital image acquisition and storage. Furthermore, better protective clothing has been developed.

However, protection of two sensitive organs in the examiner—the lens of the eye and the thyroid gland—has remained unsatisfactory. The latter can be shielded by a lead-armed collar, but this is somewhat hampering and may therefore not be used regularly by all radiologists.

The anatomical location of the thyroid (Figs 1, 2) suggests that a tie-shaped lead shield could be designed which would be easy to wear and might also be decorative (Fig. 3). The reduced size of this shield certainly reduces the protective effect on the thyroid (as compared with a collar). The aim of our investigations has been to determine the potential use of such a lead tie.

Material and methods

The projected area over the thyroid gland covered by the test tie was determined by ultrasound in 20 volunteers (10 men and 10 women) with normal thyroid function.

The volume of both lobes was estimated sonographically. Upper, lower, left and right margins of each lobe were marked on the skin through the centre of an ultrasound biopsy probe. Taking into account the anatomical size, shape and location of the thyroid gland, a test tie was manufactured with a lead equivalent of 0.5 mm (Hänel Inc., München/FRG). The mass

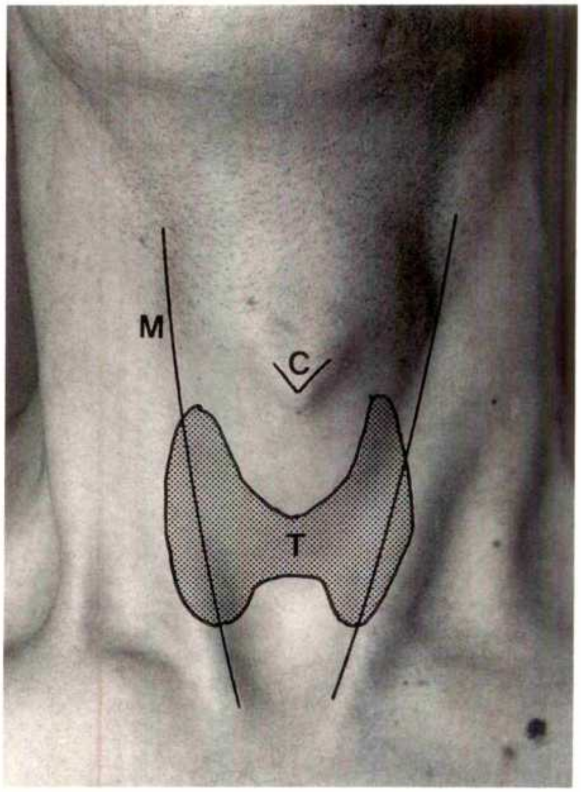

Figure 1. Cervical anatomy. The upper poles of the thyroid gland are usually situated caudal to the incisura thyroidea of the thyroid cartilage. C = incisura of thyroid cartilage, M = sternocleidomastoid muscle, T = thyroid gland.

Address for correspondence Dr Hans-Martin Klein, Klinik für Radiologische Diagnostik, Klinikum der RWTH Aachen, 5100 Aachen, Germany.

German patent registered (G 91 08 312.5).

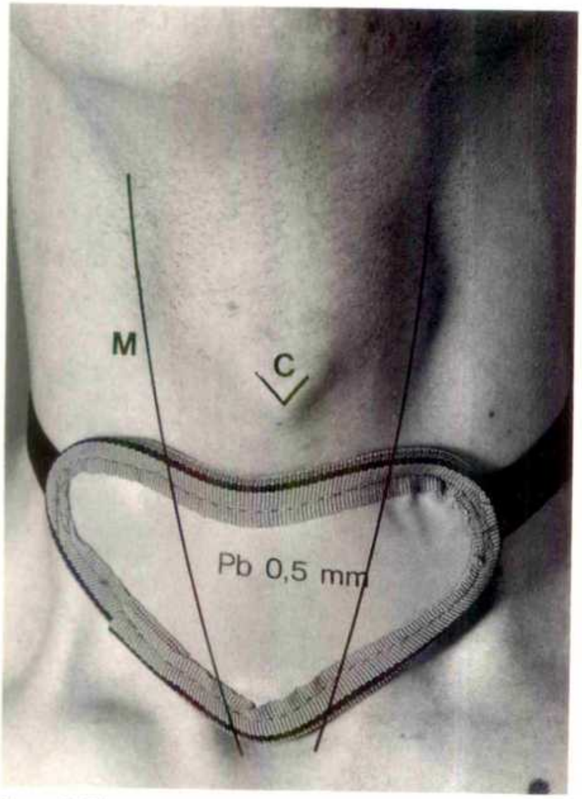

Figure 2. The test model of the lead tie positioned adequately over the thyroid gland. C = incisura of thyroid cartilage, M = sternocleidomastoid muscle.

of this tie is 40 g, compared with that of a conventional collar, 0.5 mm lead equivalent, which has a mass of 350 g.

The distance between the tie and the margins of the thyroid lobes were determined. The projected thyroid gland area F_{thy} was assumed to be rectangular, and was estimated using equation (1).

$$F_{thy} = L \times W \qquad (1)$$

where L = songraphically determined length and W = sonographically determined width of the thyroid lobe.

The percentage of thyroid area covered was estimated by

$$F_{cov} = \frac{(L-d_l)\times(W-d_w)}{F_{thy}} \times 100 \qquad (2)$$

where d_l = sum of distance between tie and upper/lower pole and d_w = sum of distance between tie and lateral/medial pole.

The efficiency of protection was tested with film dosimetry by a method similar to that used in clinical routine (Fig. 4). Test exposures with standardized parameters were obtained for a fluoroscopy unit with an overhead tube (Siregraph, Siemens Inc.). The X-ray tube voltage was 80 kV, and the current–time product was 80 mAs. The focus-object distance was 1 m. To

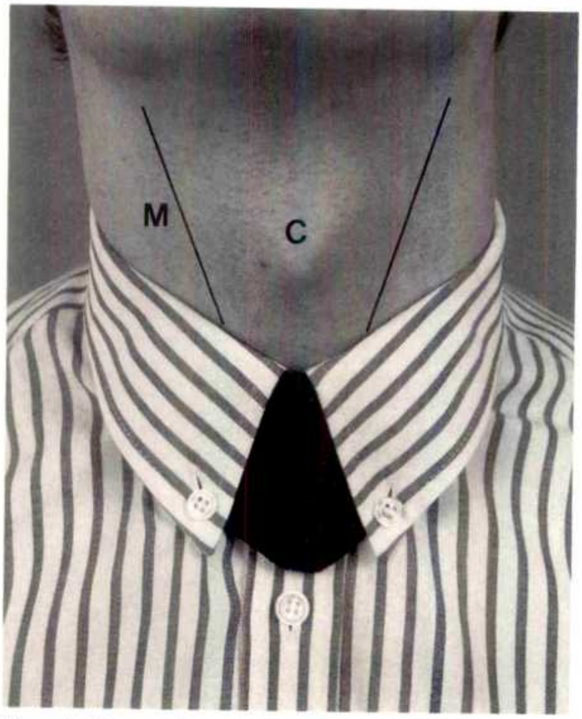

Figure 3. The test tie with textile shade, the lateral parts of the lead tie lying under the collars of the shirt. C = incisura of thyroid cartilage, M = sternocleidomastoid muscle.

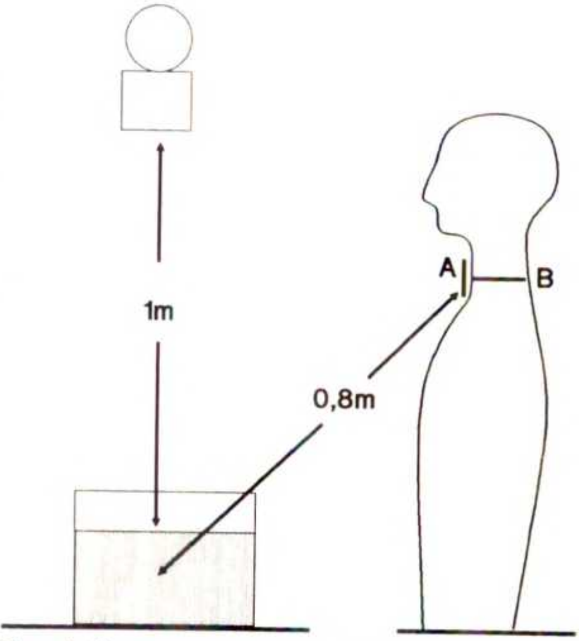

Figure 4. Measurement setting. An overhead X-ray tube is situated 1 m above a scattering phantom (20 l water). The body of the examiner is simulated by an Alderson phantom. The distance between the centre of the scattering phantom and the thyroid gland is 80 cm (arm length).

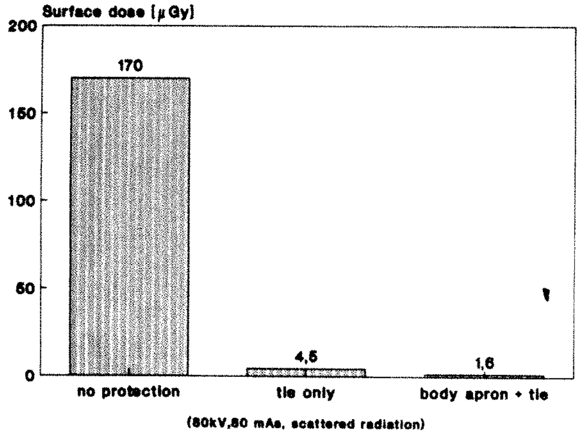

Figure 5. Surface dose in the thyroid gland region with lead apron and with and without tie. Scattered radiation 80 kV, 80 mAs photon flux.

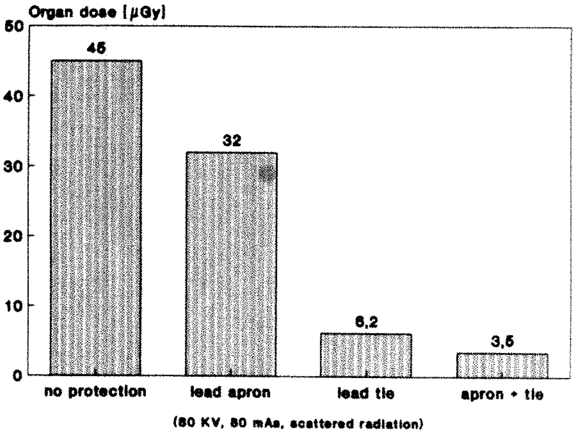

Figure 6. Organ dose in the covered thyroid gland. Measurements were carried out (1) without any protection, (2) with body apron only, (3) with lead tie only and (4) with lead apron and tie. All values given for scattered radiation, 80 kV, 80 mAs photon flux.

achieve the appropriate scattering conditions and energy spectrum, a 20-litre water container was used as a scattering phantom. The body of the radiologist was simulated by an Alderson phantom. The radiation dose was determined by a screen–film system in a flexible cassette with a sensitivity of 200 (a dose of 5 µGy is necessary to achieve an optical density of 1). It was positioned on the cervical surface and between the horizontal slices of the Alderson phantom in the thyroid region. A calibration curve was determined by directly measuring the scattered radiation dose with a dose meter (Dali, Wellhöfer Inc.) and relating it graphically to the resulting optical density.

The distance between the centre of the scattering phantom and the dosemeter film was 0.8 m (arm length). Measurements were carried out with and without a body apron, with and without a tie, on the surface and between the phantom slices in the thyroid region. Every value was obtained from the arithmetic mean of the measured optical density at four points located in the anatomical region of the thyroid gland.

Results

In three of the 20 cases examined sonographically, the thyroid gland area was completely covered by the protective tie. These three volunteers had relatively short necks. In 10 cases, one thyroid pole remained uncovered, in seven cases this being the upper pole of the right lobe. The mean distance between the unprotected pole and the margin of the protective tie was 9 mm. In seven cases, two or more poles were not covered. The mean distance between the tie and the free poles was 10.4 mm. There was no difference between men and women. Average covering (F_{cov}) of the right lobe was 86.5%, and of the left lobe 89%. The minimum coverage of the total thyroid gland, in one test person, was 73%. The average percentage of total thyroid area (for both lobes) covered by the tie was 88%, with a standard deviation of 9.7%.

Dosimetry showed that the surface dose in the covered skin area was reduced by 99%, from 170 µGy to 1.6 µGy, for 80 mAs if tie and apron were used. Measurements without body lead apron showed an increase of surface dose from 1.6 to 4.5 µGy (Fig. 5). The organ dose in the thyroid region was 45 µGy if no protection was used, 32 µGy if only body apron was used, 6.2 µGy if only the protective tie was used and 3.5 µGy if both body apron and tie were present. The radiation reduction using the tie in addition to the lead apron is therefore 89.1% (Fig. 6) for the thyroid parts lying under the lead tie.

Discussion

The radiation dose acquired by the examiner during fluoroscopy is considerable. In the course of carotid, visceral and peripheral angiography, Tryhus et al (1987) found an organ dose of 40 µGy in the thyroid. A thyroid dose of up to 400 µGy was measured during cardiac catheterization by Malsky et al (1971) and Miller et al (1985). Riley et al (1973) found a thyroid dose of 210 µGy in abdominal angiography.

It is known that chronic radiation exposure of the thyroid can lead to adenoma and probably increases the number of thyroid malignancies (Kaplan et al, 1987). Conventional means of protection are mostly hampering and inconvenient in diagnostic procedures (Kaffe et al, 1986). Additionally, the patients feel that the radiologist's "armament" emphasizes the "radiation danger" they are exposed to. To avoid these disadvantages, we thought of combining protection and convenience by designing an easy-to-wear tie with a lead core.

We found the efficiency of this tie to depend on anatomical constitution. People with short, stout necks can achieve almost complete covering of the thyroid, while those with lean, long necks gain less benefit.

Nevertheless, in none of the test subjects was less than 73% of the thyroid area covered. In our measurement setting, the organ dose is caused mainly by direct radiation, though the influence of radiation scattered throughout the examiner's body is also important, as was seen if only the tie was used with no lead apron. A considerable protective effect is therefore achieved even if the tie does not completely cover the thyroid. The reduction in thyroid organ dose was found to be 89% under our measurement conditions.

Compared with conventional cervical lead shields, the protective effect is less, particularly if the position of the examiner is not at right angles to the scattering source. Furthermore, depending on the body apron used, a gap remains between lead tie and protective apron, which can be avoided if a conventional cervical shield is used.

Radiation protection for the radiologist can never be complete. It must always be a compromise between convenience and efficiency. Within these limitations, we hope the proposed tie will be an adequate aid for radiation protection.

References

KAFFE, I., LITTNER, M. M., SHLEZINGER, T. & SEGAL, P., 1986. Efficiency of the cervical lead shield during intraoral radiography. *Oral Surgery, Oral Medicine, Oral Pathology, 62*, 732–736.

KAPLAN, M. M., BOICE, J. D., AMES, D. B. & ROSENSTEIN, M., 1987. Thyroid, parathyroid and salivary gland evaluations in patients exposed to multiple fluoroscopic examinations during tuberculosis therapy: A pilot study. *Journal of Clinical Endocrinology and Metabolism, 66*, 376–382.

MALSKY, S. J., ROSWIT, B., REID, C. B. & HAFT, J., 1971. Radiation exposure to personnel during cardiac catheterization. *Radiology, 100*, 671–674.

MILLER, S. W., & CASTRONOVO, F. P., 1985. Radiation exposure and protection in cardiac catheterization laboratories. *American Journal of Cardiology, 55*, 171–176.

RILEY, R. C., BIRKS, J. W., PALACIOS, E. & TEMPLETON, A. W., 1973. Exposure of radiologists during special procedures. *Radiology, 104*, 679–683.

TRYHUS, M., METTLER, F. A. & KELSEY, C., 1987. The radiologist and angiographic procedures. Absorbed radiation dose. *Investigative Radiology, 22*, 747–750.

1992, *The British Journal of Radiology*, 66, 1007–1010

Measuring radiation exposure during percutaneous drainages: can shoulder dosemeters be used to estimate finger doses?

By Tapio Vehmas, MD and *Heikki Tikkanen, MD

From the Department of Radiology, University of Helsinki, and the *Department of Clinical Physiology, Helsinki University Central Hospital, Haartmaninkatu 4, SF-00290 Helsinki, Finland

(*Received 20 February 1992 and in revised form 11 June 1992, accepted 29 June 1992*)

Keywords: Dosimetry, Interventional radiology, Occupational safety, Percutaneous drainage, Radiation monitoring

Abstract. Some previous studies have shown remarkably high finger doses to radiologists performing percutaneous drainage under fluoroscopy. To assess the possible need for extra finger dosemeters in addition to the general dosemeter, radiologists' and assistants' radiation exposure at both shoulders and at the third fingers of both hands were recorded using thermoluminescent dosemeters during 27 interventional drainage procedures. Under couch screening was used. Mean dose rates were calculated by dividing the doses by the screening time. The dose rates for the sites measured were correlated with each other. The radiologists' bilateral finger dose rates did not correlate with each other; nor did dose rates between the left shoulder and the right hand. The radiologists' dose rates at both shoulders, however, correlated with each other, as did the shoulder dose rates with the dose rates at the ispilateral hand. The right shoulder dose rates correlated with the left hand dose rates. The assistants' dose rates at the places of measurement all showed significant correlations with each other. It is therefore concluded that radiologists involved in percutaneous drainages should use finger dosemeters on both hands; for assistants this may not be necessary.

Pathological fluid collections are commonly treated using percutaneous drainages. The predecessor of these procedures was percutaneous nephrostomy, which is used today also as a preliminary measure before some complicated interventions such as percutaneous lithotomy. Some recent papers have demonstrated high radiation exposure of radiologists during fluoroscopically guided interventional drainages. Mean doses are usually reported. Finger doses of up to 18 mGy were reported by Krahe et al (1986), and Ramsdale et al (1991) measured average values of 35 mSv during percutaneous biliary procedures. Considering the ICRP yearly maximum occupational exposure limits, finger doses have been shown to be the most limiting features during transhepatic cholangiographies and portographies (Gustafsson & Lunderquist 1981), percutaneous renal stone removal (Geterud et al, 1989) and percutaneous nephrostomy (data concerning 11 unilateral and 5 bilateral nephrostomies given by Vehmas et al, 1991). During all these procedures the fingers of the radiologist are likely to be close to the primary radiation field.

The radiation exposure of radiologists is routinely measured using personal dosemeters, which are generally fixed to the unprotected area high on the trunk (ICRP, 1982). No other dosemeters are in routine use in Finland. This study was therefore undertaken to determine whether a dosemeter thus located is also able to predict the finger doses.

Material and methods

Radiation doses during 27 percutaneous drainage procedures (Table I) were recorded. In 20 procedures a resident was assisting the performing radiologist. In all the procedures, the target for puncture was localized and the puncture was performed using sonographic guidance. After this, a modified Seldinger technique under fluoroscopic guidance was used to finally introduce the chosen catheter into the target. The technique varied somewhat depending on the type of the procedure, on the working practice of the radiologist and on the type of catheter. The detailed technique of percutaneous nephrostomy has previously been described (Vehmas et al, 1988). The procedures were performed by six radiologists, one of whom was left-handed (six procedures).

Fluoroscopy was carried out in 25 cases (including all the 20 cases in which an assistant participated) with Siemens angiographic equipment, supplied with a Siemens Sirecon 2 RBV image intensifier system and an Elema-Schönander Multix table. The kV/mA factors

Table I. Types of the 27 percutaneous drainages and side of the body containing the drainage target

Drainage type	Side	Number
Percutaneous nephrostomy	right	8
Percutaneous nephrostomy	left	4
Percutaneous nephrostomy	bilateral	5
Percutaneous nephrostomy/ change of nephrostomy catheter	bilateral	3
Placement of ureteric stent	left, right	2
Percutaneous biliary drainage	middle	2
Percutaneous abscess/pseudocyst drainage	middle, right	2
Change of abscess catheter	left	1

Table II. Radiologists' ($n = 27$) and assistants' ($n = 20$) dose rates (10^{-9} Gy/s)

TLD site	Mean dose rate	Median dose rate	Range
Radiologist			
Right shoulder	25	14	0–130
Left shoulder	26	17	4.0–80
Right III finger	310	200	6.9–2600
Left III finger	340	130	72–2500
Assistant			
Right shoulder	7.7	4.4	0–12
Left shoulder	7.6	3.8	0–18
Right III finger	40	13	0–330
Left III finger	27	13	0–140

were controlled automatically. A Philips Diagnost 73 fluoroscopy apparatus with an automatic brightness control and equipped with a Philips ST Titan 9/5" image intensifier system was used in two cases.

Calcium sulphate ($CaSO_4$:Dy) thermoluminescent dosemeters (TLDs) were fixed on the unprotected body parts of the radiologist and the assistant, on both shoulders and on the palmar aspects of the middle phalanges of the third fingers. The TLDs were analyzed and calibrated at the Finnish Centre for Radiation and Nuclear Safety. The thermoluminescent output of $CaSO_4$:Dy powder was measured using a Vinten Toledo 654 TLD reader. Three samples of powder for each dosemeter were analyzed and the mean value was accepted. The background dose was measured with TLDs and subtracted from the measured doses. Only doses of 1 μGy or more were considered.

Assuming the causes of error in the TLD measurements to be independent of each other, the estimated combined uncertainty (standard deviation) is $\pm 22\%$ (statement of the Finnish Centre for Radiation and Nuclear safety). The measured radiation doses were converted to the mean dose rates (10^{-9} Gy/s) by dividing the measured dose by the particular screening time. The correlation of the dose rates for each of the two dosemeter sites was calculated using Spearman's rank correlation.

Results

The screening time averaged 18 minutes (range 0.5–66 mins). Radiologists' and assistants' dose rates are given in Table II. Spearman's rank correlation (p-values) between all pairs of dosemeter sites are shown in Fig. 1. Most of the radiologists' dosemeter sites showed statistically significant correlations, with the exceptions of not significant ($p > 0.05$) correlations between the contralateral hands and between the left shoulder and the right hand. Correlations were also calculated between dominant/non-dominant hands and the corresponding shoulders. Neither dominant versus non-dominant hands nor non-dominant hands versus dominant shoulders correlated significantly with each other, while all other correlations in this analysis were significant. Assistants' dose rates measured at the different sites all correlated significantly with each other.

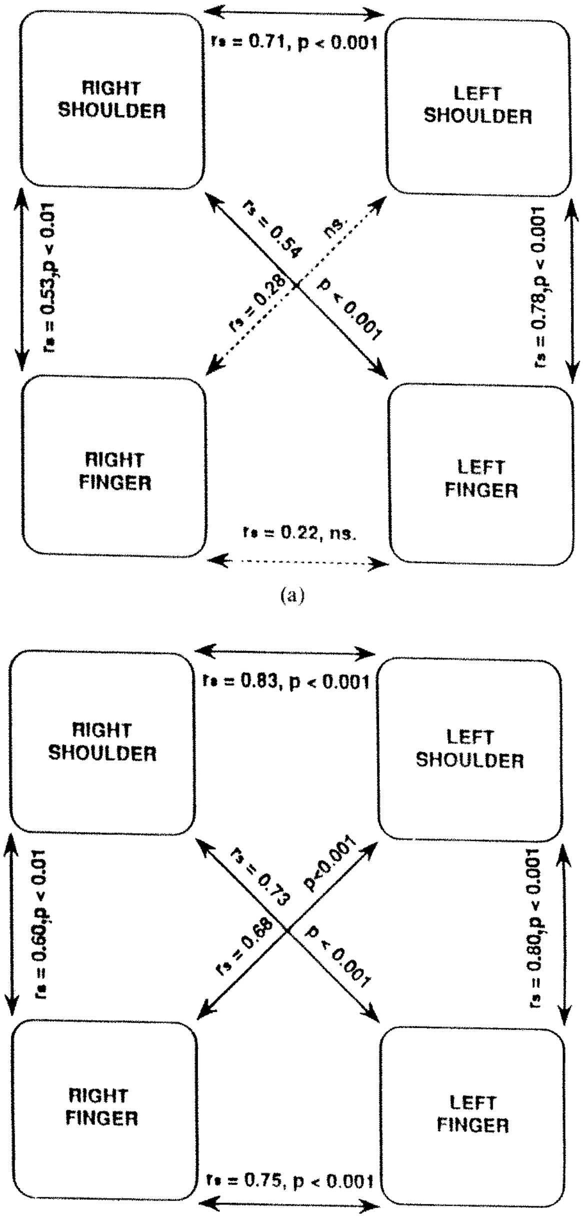

(a)

(b)

Figure 1. (a) Spearman's rank correlation (correlation coefficients r_s and p-values) between radiologists' (a) and assistants' (b) dose rates at all pairs of dosemeter sites. ns. = not significant ($p > 0.05$).

The frequency distributions of dose rates (shoulders and fingers) in both the radiologists and the assistants were skewed. Most dose rates were modest, but some were very high. Natural logarithmic transformation of the hand dose rates gave frequency distributions very

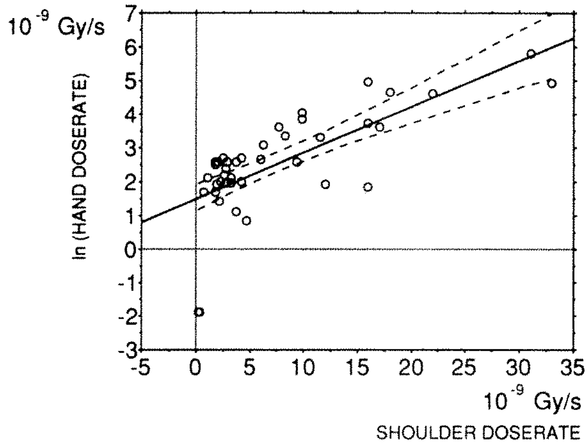

Figure 2. Linear regression model with 90% confidence limits of dose rates to assistants between (combined right and left) shoulders (*x*-axis) and hands (*y*-axis; dose rates after natural logarithmic transformation). $y = 0.136x + 1.508$; $r_s = 0.717$, $p = 0.0001$.

close to the normal distribution, enabling the comparison of the transformed values using regression analysis (Fig. 2).

Discussion

When doses or dose rates are measured, mean values and ranges are usually given. In this study, the range of dose rates in each category was wide, up to differences of several hundred-times. The frequency distributions of dose rates showed that most measured dose rates were concentrated at relatively low levels, with occasional high dose rates. Mean dose rates are higher than "typical dose rates". Median doses or dose rates, for example, are better indicators of "typical doses/typical dose rates" and should be used more often in reporting.

For the radiologists, most dosemeter sites correlated significantly with each other, but the dose rates at both hands as well as the dose rates at the left shoulders versus the right hands showed no significant correlations with each other.

The fingers of the performing radiologist are very close to the primary radiation field during percutaneous drainages. The radiologist can perhaps not avoid placing his hands into the primary field during some difficult moments of catheterization. His hands may also accidentally slip into the field and remain there until he notices the situation. Contact with the primary radiation is likely to be random, to differ from one examination to the other and differ between the two hands, which would explain why there is no correlation between the dose rates for the hands. The calculation of correlations in terms of dominant/non-dominant hands did not clarify the matter further; it seems likely that finger technique during catheterization varies from one individual to another regardless of which hand is dominant.

The varying correlations between the shoulders and fingers are more difficult to explain. The random exposure of the fingers in the primary beam, mentioned above, is probably the most important reason causing a low correlation between hand and shoulder doses. If the radiologist is working in an oblique position towards the beam, one of the shoulder dosemeters may occasionally be hidden behind the edge of the lead apron or behind his body. It is therefore concluded that:

(1) because the correlation between shoulder and finger dose rates is uncertain, the radiologist should have an extra finger dosemeter;
(2) because there is no correlation between the hands, finger dosemeters should be placed on both hands.

Finger dosemeters should be used systematically, although this may be awkward during normal clinical work.

Dose rates measured for the assistants at all the sites showed significant correlations with each other. Assistants generally work at some distance from the primary beam, and the amount of secondary radiation received on the X-ray tube side of their body is inversely proportional to the square of the distance to the primary beam. Finger dose rates may be roughly estimated from the measured shoulder dose rates using regression equations such as that derived from Figure 2. This formula would probably hold true precisely only in this particular study, but similar measurements and calculations may be done in other conditions. Separating the left and right side measurements makes these models more accurate.

In this study, calculated dose rates have been used instead of the more common raw dose measurements. Analysis using doses gave significant correlations between all pairs of sites for both radiologists and assistants, because screening time is the dominant factor determining dose at any site. For example, a short screening time will result in both low finger and shoulder doses, ensuring good correlation between these sites. Since the aim of the study was to investigate the relationship between doses at different sites in an individual, results independent of screening time were obtained by calculating dose rates.

All the studies referred to in the introductory paragraph which point to the limiting nature of the finger doses (Gustafsson et al, 1981; Geterud et al, 1989; Vehmas et al, 1991) have been performed using undercouch X-ray tubes. Using overcouch tubes, the radiation geometry is different. Overcouch fluoroscopic tubes produce more radiation to the unprotected upper part of the radiologist's body than undercouch tubes (Law, 1985; Inglis et al, 1989). Our results therefore apply only to undercouch tubes.

The present findings hold true only if the worker is mainly employed with percutaneous drainages with little other exposure. If interventional radiologists and their assistants are involved in other types of radiology (*e.g.* barium examinations) the evaluation of finger doses is more difficult, and so this is an extra indication for finger dosimetry.

In conclusion, a radiologist should use extra dosemeters on both his hands when performing percutaneous drainage procedures. Assistants' finger dose rates correlate significantly with the shoulder dose rates measured with general dosemeter badges and the use of extra dosemeters may not be necessary for them. These statements may not apply to overcouch screening or to cases where the interventional radiologist and his assistant are exposed during other kinds of radiation work.

Acknowledgment

We wish to thank the staff of the Finnish Centre for Radiation and Nuclear Safety and the Department of Radiology of the University Central Hospital, and to express our appreciation to Donald Smart, BSc, MEd, for the language revision.

References

GETERUD, K., LARSSON, A. & MATTSON, S., 1989. Radiation doses to patients and personnel during fluoroscopy at percutaneous renal stone extraction. *Acta Radiologica, 30*, 201–206.

GUSTAFSSON, M. & LUNDERQUIST, A., 1981. Personnel exposure to radiation at some angiographic procedures. *Radiology, 140*, 807–811.

INGLIS, J. A., TOLLEY, D. A. & LAW J., 1989. Radiation safety during percutaneous nephrolithotomy. *British Journal of Urology, 63*, 591–593.

INTERNATIONAL COMMITTEE FOR RADIOLOGICAL PROTECTION (ICRP), 1982. General principles of monitoring for radiation protection of workers. *Annals of the ICRP*, Publication 35 (Pergamon Press, Oxford).

KRAHE, TH. VON, EWEN, K., LACKNER, K., KÖSTER, O. & NICHOLAS, V., 1986. Die Strahlenexposition des Patientes und Untersuchers in der interventionellen Radiologie. *Fortshcritte auf dem Gebiete der Röntgenstrahlen und der neuen bildgebenden Verfahren, 145*, 217–220.

LAW, J., 1985. Doses to head and arms of radiologists during fluoroscopy. *British Journal of Radiology, 58*, 187–188.

RAMSDALE, M. L., WALKER, W. J. & HORTON, P. W., 1991. Extremity doses during interventional radiology. *Clinical Radiology, 41*, 34–36.

VEHMAS, T., HAVUKAINEN, R., TAPIOVAARA, M., MANKINEN, P., PITKÄRANTA, P., TERVAHARTIALA, P., SAVIKURKI, S. & KIVISAARI, L., 1991. Radiation exposure during percutaneous nephrostomy. *Fortschritte auf dem Gebiete der Röntgenstrahlen und der neuen bildgebenden Verfahren, 154*, 238–241.

VEHMAS, T., KIVISAARI, L., MANKINEN, P., TIERALA, E., SOMER, K., LEHTONEN, T. & STANDERTSKJÖLD-NORDENSTAM, C-G., 1988. Results and complications of percutaneous nephrostomy. *Annals of Clinical Research, 20*, 423–427.

1992, *The British Journal of Radiology*, *65*, 1011–1017

Effect of diatrizoate on the function of the isolated perfused rat kidney

By P. Brown, MB, ChB, FRCS, ‡J. Haylor, BPharm, PhD, S. K. Morcos, FRCS, FFRRCSI, FRCR, §G. H. Cope, PhD and †A. M. El Nahas, PhD, FRCP

Department of Diagnostic Imaging and †Sheffield Kidney Institute, Northern General Hospital NHS Trust, Sheffield S5 7AU, and Departments of ‡Medicine and Pharmacology and §Biomedical Sciences, University of Sheffield, Sheffield S10 2TH, UK

(*Received 29 October 1991 and in revised form 27 March 1992, accepted 6 May 1992*)

Keywords: Diatrizoate, Water-soluble contrast medium, Isolated perfused rat kidney, Glomerular filtration rate, Proteinuria

Abstract. The mechanism of the nephrotoxicity of water-soluble contrast media (WSCM) remains ill defined. We have studied the effect of diatrizoate on the isolated perfused rat kidney (IPRK). Emphasis was on the effect of low- and high-dose diatrizoate on glomerular filtration rate (GFR), renal perfusate flow (RPF), fractional excretion of albumin (FE Alb) and fractional reabsorption of sodium (FR Na). The addition of diatrizoate to the IPRK led to a dose-dependent biphasic change in RPF and GFR characterized by an initial transient increase followed by a marked and sustained decrease. Diatrizoate induced a diuresis and a parallel increase in urinary sodium excretion (fall of FR Na). FE Alb was also increased in kidneys exposed to diatrizoate. Electron microscopy of a control kidney showed preservation of cellular architecture, which contrasted with the observed cytoplasmic vacuolation of proximal tubular cells after perfusion with diatrizoate. This study confirms a direct effect of WSCM on the function of the IPRK. In this experimental model, diatrizoate reproduces the effects observed *in vivo* on GFR and renal perfusion.

The pathophysiology of the nephrotoxicity of water-soluble contrast media (WSCM) remains unclear with conflicting experimental data (Katzberg et al, 1983, 1986; Vari et al, 1988; Katzberg, 1989; Vaamonde et al, 1989). The mechanisms postulated include reduced renal perfusion, glomerular injury, tubular damage and obstructive nephropathy (Dawson, 1985; Vari et al, 1988).

Relying on a new experimental approach based on the isolated perfused rat kidney (IPRK), we have recently demonstrated that WSCM exert a direct haemodynamic effect on the kidney, characterized by increased renal vascular resistance leading to reduced renal perfusion (El Sayed et al, 1991; Haylor et al, 1991).

This study was designed to extend these observations by studying the direct effect of diatrizoate, a high-osmolar WSCM, on other functional parameters of the IPRK. We compared the effects of low and high doses of diatrizoate (Urografin, Schering AG) on renal vascular resistance and glomerular filtration rate (GFR) as well as urinary albumin and sodium excretions.

Materials and methods

The isolated perfused rat kidney

Male Wistar rats (Sheffield University, 400–450 g) were anaesthetized with pentobarbitone (60 mg/kg, intraperitoneally). The right ureter was cannulated for the collection of urine and the right renal artery was cannulated via the superior mesenteric artery. Perfusion was initiated *in situ* and the right kidney transferred to a perfusion circuit as described previously (El Sayed et al, 1991). Kidneys were perfused at constant pressure (100 mmHg) using a servo-controlled peristaltic pump with a Krebs–Henseleit solution containing 6.7% (w/v) bovine serum albumin and 14 mmol/l mixed amino acids. Amino acids were included in the perfusate to stabilize the GFR (Epstein et al, 1982; El Sayed et al, 1990). The volume of the perfusion system was 150 ml and the perfusate was maintained at 37°C and gassed with 95% O_2/5% CO_2.

Materials

The mixed amino acids solution used was Vamin 14 electrolyte-free (Kabi Pharmacia Ltd). The perfusate was prepared by dissolving bovine serum albumin (Pentex Fraction V, Miles, UK) in Krebs–Henseleit solution, dialysing for 8 h to remove small molecular weight fragments, adjusting the albumin concentration to 6.7% and sterilizing by filtration. Both glucose and amino acids were added to the perfusate immediately prior to use. 1 μCi [^{14}C]-inulin carboxylic acid (4.76 mCi/mmol, Amersham, UK) was added to each perfusion to measure the GFR and was measured in perfusate and urine samples on a beta scintillation counter (Tricarb 460 CD) using Scintran Cocktail T (BDH). Protein was assayed by the comassie blue method using a diagnostic assay kit (Sigma, Total Protein Micro 610–A). The flame photometer (Corning 410 C) was standardized by machine standard solutions at 140 mmol/l. The osmometer (Roebling Automatik)

Address correspondence to Dr S. K. Morcos, Department of Diagnostic Imaging, Northern General Hospital, Herries Road, Sheffield S5 7AU, UK.

was standardized by machine standards at 300 mosmol/kg H_2O.

Experimental protocol

Each kidney was perfused for a 90-min period, the first 40 min (0–40 min) being an equilibration period. Subsequently, a 20-min baseline period (40–60 min) was studied. At 60 min, either 2 ml (producing an iodine concentration in the perfusate of 4 mg I/ml, $n = 10$) or 10 ml (20 mg I/ml of perfusate, $n = 9$) of a solution of sodium meglumine diatrizoate (300 mg I/ml, osmolality 1590 mosmol/kg H_2O) were added to the renal perfusate. The solution of diatrizoate was prepared by diluting the commercially available Urografin 325 (Schering AG) with sterile water. The low dose of diatrizoate was chosen to reproduce in the IPRK the maximum serum iodine concentrations observed *in vivo* after an intravenous injection of 100 ml of Urografin 370 (Feldman et al, 1984). The high dose aimed at reproducing iodine concentrations comparable to those achieved with angiographic studies in humans and the maximum tolerated intravenous dose in rats (Reed et al, 1983).

The effect of diatrizoate on the function of the IPRK was studied over a 30-min experimental period (60–90 min). During the baseline (B) and experimental (E) periods, clearance studies (inulin, albumin and sodium) were undertaken at 5 min intervals while renal perfusate flow (RPF) was monitored continuously. The control group consisted of kidneys ($n = 6$) perfused over 90 min without the addition of contrast medium.

Parameters

GFR was measured as the clearance of [^{14}C]-inulin determined from sequential measurements of the urinary excretion rate and perfusate concentration of ^{14}C. The RPF was estimated by the continuous recording of the pump speed. Urine sodium was measured by flame photometry. Urine albumin was detected by the comassie blue method (Bradford, 1976), which, unlike the Lowry assay (Morcos et al, 1992), showed no interaction *in vitro* with diatrizoate. The fractional reabsorption of sodium (FR Na) was calculated from the formula 100 − (sodium clearance × 100/GFR), and the fractional excretion of albumin (FE Alb) was equal to albumin clearance × 100/GFR. Filtration fraction (FF) was calculated as (GFR × 100/RPF). The osmolality of the renal perfusate was measured using a freezing point depression osmometer.

Renal morphology

The effect of high-dose diatrizoate on renal morphology was assessed by electron microscopy. One kidney from the control group and one kidney from the diatrizoate group were examined. At the end of the experiment, the kidneys were perfused with 2% (w/v) glutaraldehyde in 0.1 mol/l sodium phosphate buffer (pH 7.3, 450 mosmol) at room temperature and fixed for 2–3 h. Thereafter, the kidneys were diced into 1 mm^3 cubes and washed in buffer overnight. Next morning, the tissues were refixed in 1% (w/v) osmium tetroxide in 0.1 mol/l phosphate buffer for 2 h, dehydrated with alcohol and embedded in Araldite. Ultrathin sections were stained with uranyl acetate and lead citrate and examined in a Philips CM10 electron microscope.

Statistical analysis

Results are expressed as mean ± standard error of the mean ($X \pm$SEM). Both renal perfusate flow and [^{14}C]-inulin clearance were expressed per gram wet weight of the non-perfused rat kidney. In each preparation, the results were also expressed as percentage of baseline measurement obtained during the period 55–60 min. Results were compared within groups using paired Student's t-test and between groups using the Mann–Whitney U-test relying on Microtab software. A p value of < 0.05 was considered to be significant.

Results

Baseline parameters

The baseline (40–60 min) functional criteria of the IPRK preparations ($n = 25$) were satisfactory, as GFR was 0.97 ± 0.05 ml/min/g, FR Na 88.5 ± 1.6% and FE Alb 0.93 ± 0.1%. As with all IPRK preparations, the RPF was high (49.2 ± 1.3 ml/min/g) and consequently FF was low (2.1 ± 0.2%).

Whilst the GFR of the control IPRK was stable (Fig. 1a), the RPF increased with time (Fig. 1b). Consequently, a time-dependent fall in FF was observed in these kidneys (Fig. 2). The gradual increase in RPF is likely to be due to the vasodilatory effect of the amino acids included in the perfusate. Over the 90 min observation period, FR Na remained stable (Fig. 3) and a slight increase of 0.3% in FE Alb was noted.

Electron microscopic examination of the kidney from this group showed excellent preservation of cellular architecture, with structurally normal glomeruli showing fenestrated endothelium, intact basement membrane and epithelial foot processes (Fig. 4a). Tubular architecture was also preserved as shown by the absence of significant cytoplasmic vacuolation and the preservation of the brush border (Fig. 4b).

Effect of diatrizoate on the IPRK

The addition of 2 ml (4 mg I/ml) and 10 ml (20 mg I/ml) of diatrizoate to the perfusate increased its osmolality from 314 ± 7 mosmol/kg H_2O ($n = 25$) to 346 ± 4 mosmol/kg H_2O and 452 ± 7 mosmol/kg H_2O, respectively ($p < 0.001$).

Glomerular filtration rate

The addition of diatrizoate to the perfusate of the IPRK led to an immediate and transient increase in GFR followed by a significant dose-dependent and sustained fall (Fig. 1a). At the end of the experimental period, the reduction in GFR induced by low-dose diatrizoate was −15% compared with −45% for the high-dose group (Fig. 1a).

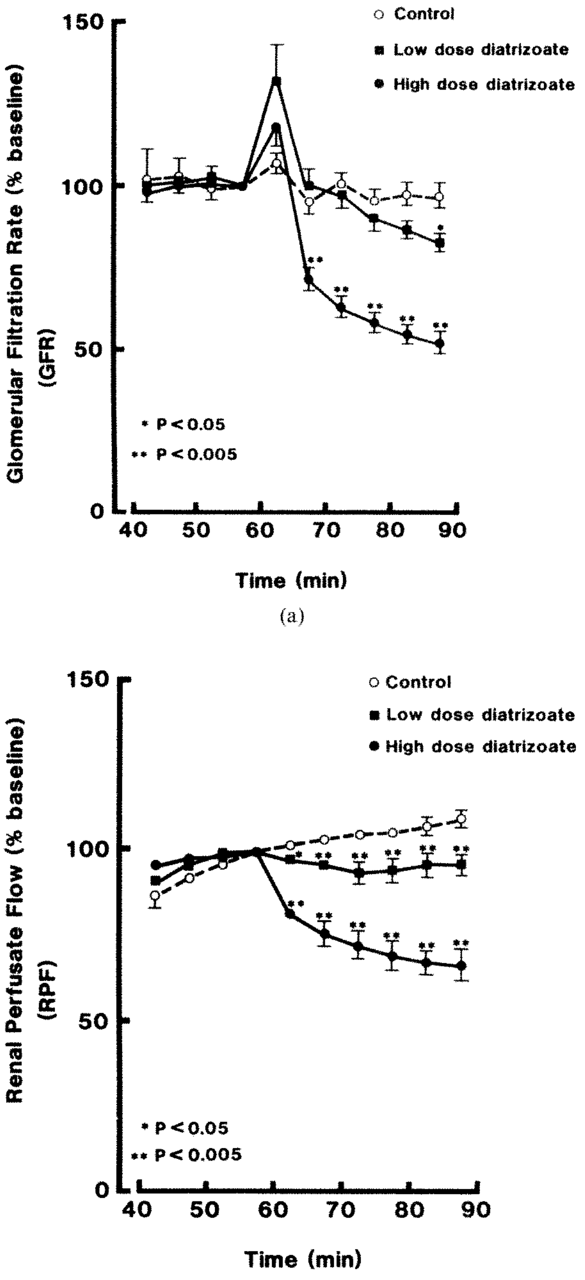

(a)

(b)

Figure 1. (a) Changes in GFR (expressed as percentage of baseline) with time. Statistical comparisons with the control group. (b) Changes in RPF (expressed as percentage of baseline) with time. Statistical comparisons between the experimental groups and the control.

Renal perfusate flow

A biphasic change in RPF was also noted on addition of diatrizoate. As previously described, this consisted of an initial transient increase in RPF (2–3 s) followed by a sustained dose-dependent decrease (El Sayed et al,

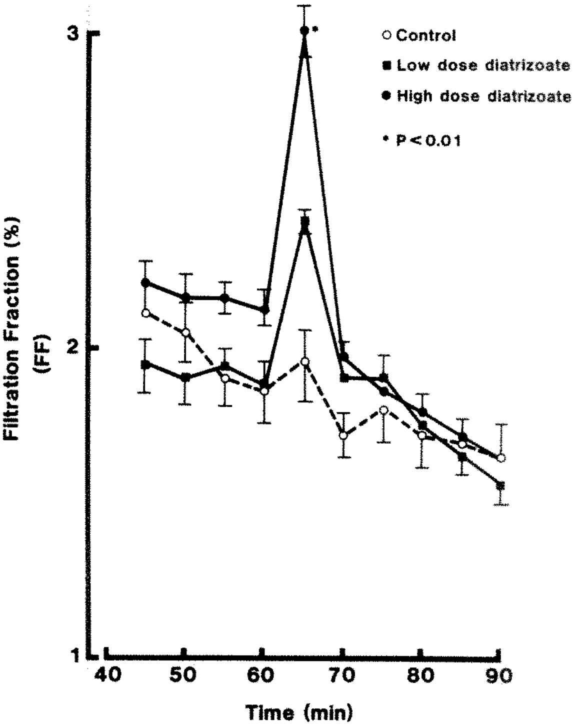

Figure 2. Changes in FF with time. Statistical comparison with the control group.

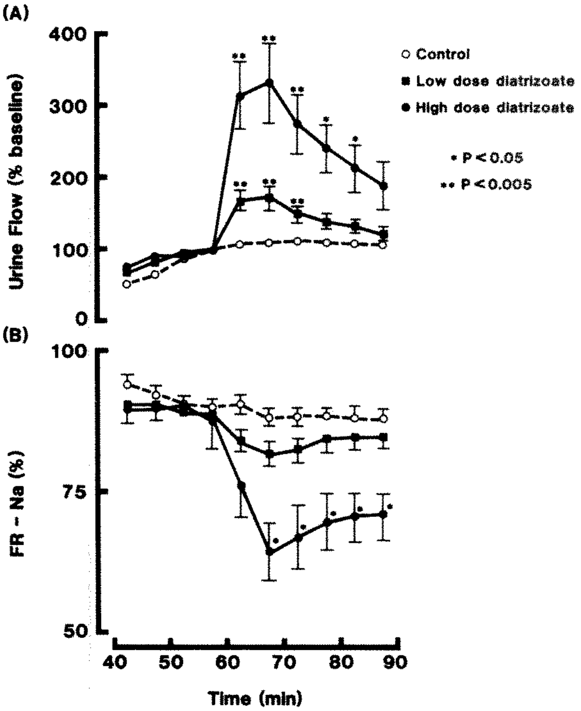

Figure 3. Changes in urine flow (a) and fractional reabsorption of sodium (FR Na %) (b) with time. Statistical comparisons with the control group.

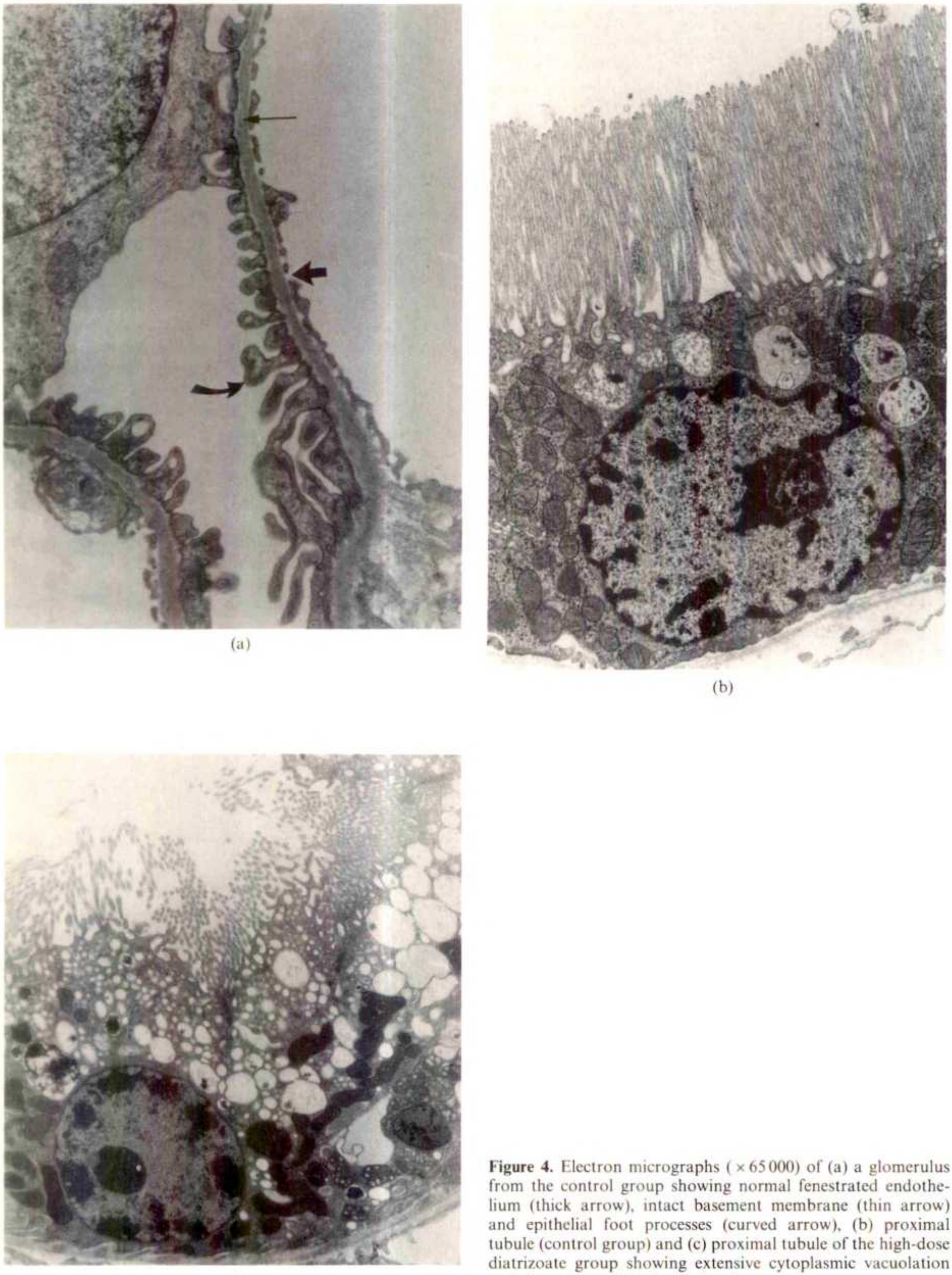

(a)

(b)

(c)

Figure 4. Electron micrographs (×65 000) of (a) a glomerulus from the control group showing normal fenestrated endothelium (thick arrow), intact basement membrane (thin arrow) and epithelial foot processes (curved arrow), (b) proximal tubule (control group) and (c) proximal tubule of the high-dose diatrizoate group showing extensive cytoplasmic vacuolation and disruption of the brush border.

Table I. Effects of diatrizoate (low and high doses) on the functional parameters of the IPRK. Mean ± SEM is given of baseline (B) measurements taken in the period 50–60 min and experimental measurements (E) taken in the period 80–90 min.

	Control ($n = 6$)		Low-dose diatrizoate ($n = 10$)		High-dose diatrizoate ($n = 9$)	
	B	E	B	E	B	E
GFR (ml/min/g)	0.92 ± 0.13	0.91 ± 0.17	0.89 ± 0.9	0.73 ± 0.6	1.1 ± 0.7	0.58 ± 0.5*
RPF (ml/min/g)	48.6 ± 2.1	53.0 ± 2.3*	46.6 ± 2.0	45.2 ± 2.4	52.3 ± 2.2	34.8 ± 1.8*
FF (%)	1.9 ± 0.2	1.6 ± 0.2	2.1 ± 0.3	1.7 ± 0.1	2.2 ± 0.2	1.6 ± 0.1*
Urine flow (μl/min/g)	130 ± 20	160 ± 30	150 ± 20	170 ± 20	150 ± 30	230 ± 30
FR Na (%)	90.3 ± 5.1	88.5 ± 5.1	88.3 ± 2.2	84.9 ± 2.5	88.6 ± 2.4	71.0 ± 4.4*
Osmolality perfusate (mosmol/kg H_2O)	311 ± 15	318 ± 20	313 ± 4	346 ± 4**	320 ± 2	452 ± 7*

GFR, glomerular filtration rate; RPF, renal perfusate flow; FF, filtration fraction; FR Na, fractional reabsorption of sodium. *$p < 0.05$, **$p < 0.001$ (paired *t*-test).

1991). Within-group comparisons showed the fall in RPF to be significant in the high-dose experimental group (Table I). When compared with the control group, the fall in RPF was significant in the low (−12%) and the high (−42%) dose groups (Fig. 1b).

Filtration fraction

No significant change was noted in the filtration fraction (FF) of kidneys in the control or in the low-dose groups (Table I). The addition of high-dose diatrizoate led to an acute and transient increase in FF (Fig. 2). Within this group, comparisons showed a significant fall in FF during the experimental period. However, when compared with the experimental period of control kidneys, no significant difference was detected. This may be due to the time-dependent fall in FF observed in control kidneys as the result of the steady increase in RPF (Fig. 2).

Sodium excretion

In the high-dose diatrizoate group, a significant fall (−22.5%) in the fractional reabsorption of sodium (FR Na) was observed, leading to increased urinary sodium excretion. Increased urinary flow was also observed in the experimental period of the diatrizoate groups; the maximum increase reached was +70% in the low-dose group and +230% in the high-dose group compared with controls (Fig. 3).

Albumin excretion

Fractional excretion of albumin (FE Alb) during the baseline period (50–60 min) was 0.92 ± 0.15% (control group, $n = 6$), 1.07 ± 0.07% (low-dose group, $n = 4$) and 0.69 ± 0.12% (high-dose group, $n = 4$). The measurements during the experimental period (80–90 min) were 1.23 ± 0.3%, 2.15 ± 0.21% and 2.6 ± 0.14%, respectively. This represents a significant increase within each group ($p < 0.05$). In addition, both high- and low-dose diatrizoate kidneys showed a significant increase compared with the control group during the experimental period ($p < 0.01$).

Ultrastructural changes

The addition of diatrizoate did not alter the structure of the glomeruli. On the other hand, marked cytoplasmic vacuolation and disruption of the brush border was observed in the cells of the proximal tubules (Fig. 4c).

Discussion

This study confirms our previous observations of a direct haemodynamic effect of WSCM on the IPRK (El Sayed et al, 1991; Haylor et al, 1991). It also extends these observations by showing that diatrizoate induces a dose-dependent fall in GFR as well as an increase in urinary excretion of both albumin and sodium.

Using the IPRK, we reproduced the biphasic effect of WSCM on GFR observed *in vivo* (Webb, 1984; Leeming et al, 1985; Katzberg et al, 1986). This consisted of a transient increase followed by a sustained and significant fall. The early increase in GFR observed has been attributed to the osmotic diuresis induced by WSCM (Katzberg et al, 1983). In the IPRK, this transient increase in GFR was associated with a parallel increase in filtration fraction suggesting a predominant glomerular efferent arteriolar vasoconstruction. Alternatively, changes in glomerular permeability may have contributed to the increased GFR. The more sustained fall in GFR that followed the initial response took place in parallel with the reduction in RPF and the increased urinary sodium excretion. Whether the fall in GFR is causally related to changes in RPF or renal sodium handling remains to be determined. Reed et al (1983) suggested a direct effect of WSCM on GFR independently of changes in renal blood flow. They have linked the fall in GFR induced by diatrizoate *in vivo* to the natriuresis, postulating that the increased sodium delivery to the macula densa may have triggered the tubuloglomerular feedback mechanism and induced glomerular afferent arteriolar vasonconstriction. Our study cannot dissociate the fall in GFR from the changes in RPF and sodium excretion. Finally, Katzberg et al (1983, 1986) implied that the reduction in GFR was secondary to the osmotic diuresis-induced increase in intratubular pressure. This hypothesis was questioned by Webb (1984) who pointed out that the fall in GFR was maintained well after the expected changes in tubular hydrostatic pressure have returned to normal. Our preliminary data on the effect of a low-osmolar non-ionic dimer (iotrolan) on the IPRK also cast doubt on the role of osmotic diuresis. This iso-osmolar agent produced a significant fall in GFR comparable to that induced by diatrizoate in the absence of increased urine flow (Brown et al, 1991). This may suggest that the pathophysiology of nephrotoxicity is multifactorial with different mechanisms involved in low- and high-osmolar agents.

We have also observed that diatrizoate increases urinary albumin excretion in a dose-dependent fashion. Proteinuria is a well documented complication of WSCM in experimental animals (Golman & Holtas, 1980) and in humans (Khoury et al, 1983). Whilst WSCM can give false positive reactions with different reagents used to measure urinary protein (Dawson & Howell, 1985), we have excluded in preliminary experiments such an interaction between diatrizoate and the comassie blue reagents (Morcos et al, 1992). However, our study cannot differentiate between a direct glomerular or tubular origin of the proteinuria. Although no structural changes were observed in the glomeruli, this does not rule out changes in permeability. By contrast, the observed structural changes induced by diatrizoate in the proximal tubules may have contributed to diminished reabsorption of albumin. These tubular morphological changes are typical of those observed *in vivo* after the administration of radiocontrast agents (Moreau et al, 1980; Katzberg et al, 1986). Proximal tubular reabsorption of protein may also be affected by the osmotic diuresis and the reduction of urinary transit time within this segment of the nephron.

This study supports clinical observations of a dose-dependent nephrotoxicity of WSCM. High-dose administration of WSCM in angiographic investigations is associated with an increased risk of inducing renal functional impairment (Gomes et al, 1985). The IPRK, in spite of its inherent limitations, clearly demonstrates direct nephrotoxicity of WSCM independently from changes in systemic haemodynamics or humoral mediators. This experimental approach is expected to prove helpful in clarifying the different aspects of the pathophysiology of contrast media nephrotoxicity.

Acknowledgments

The authors would like to thank Schering AG, Berlin, Kodak Trust of the Royal College of Radiologists, Trent Regional Health Authority and Northern General Hospital NHS Trust (Sheffield) for their financial support. We are grateful to Professor U. Speck of Schering AG for his help and encouragement to carry out this work and to Mrs J. D. Towers, Miss J. Chowdry and Mr K. Nasseem for their technical assistance.

References

Bradford, M. M., 1976. A rapid and sensitive method for the quantitation of microgram quantities of protein utilising the principle of protein-dye binding. *Analytical Biochemistry, 72,* 248–254.

Brown, P., Haylor, J. L., El Nahas, A. M. & Morcos, S. K., 1991. A comparison of the functional effects of diatrizoate, ioxaglate and iotrolan on the isolated perfused rat kidney. *British Journal of Radiology, 64* (Congress Suppl.), 131 (Abstract).

Dawson, P., 1985. Contrast agent nephrotoxicity. An appraisal. *British Journal of Radiology, 58,* 121–124.

Dawson, P. & Howell, M., 1985. Misleading urine tests after using contrast media. *British Journal of Radiology, 58,* 785.

El Sayed, A. A., Haylor, J. L. & El Nahas, A. M., 1990. The differential effects of amino acids on the isolated rat kidney. *Clinical Science, 79,* 381–386.

El Sayed, A. A., Haylor, J. L., El Nahas, A. M., Salzano, S. & Morcos, S. K., 1991. Haemodynamic effects of water-soluble contrast media on the isolated perfused rat kidney. *British Journal of Radiology, 64,* 435–439.

Epstein, F. H., Brosnan, J. T., Tange, T. D. & Ross, B. D., 1982. Improved function with amino acids in the isolated perfused kidney. *American Journal of Physiology, 243,* F284–F292.

Feldman, S., Hayman, L. A. & Hulse, M., 1984. Pharmacokinetics of low and high dose intravenous diatrizoate contrast media administration. *Investigative Radiology, 19,* 54–57.

Golman, K. & Holtas, S., 1980. Proteinuria produced by urographic contrast media. *Investigative Radiology, 15,* S61–S66.

Gomes, A. S., Baker, J. D., Martin-Paredero, V., Dixon, S. M., Takiff, H., Machleder, H. I. & Moore, W. S., 1985. Acute renal dysfunction after major arteriography. *American Journal of Roentgenology, 145,* 1249–1253.

Haylor, J. L., El Sayed, A. A., El Nahas, A. M. & Morcos, S. K., 1991. The effect of sodium iothalamate on the vascular resistance of the isolated perfused rat kidney. *British Journal of Radiology, 64,* 50–54.

Katzberg, R. W., 1989. What do we really know about contrast medium-induced acute renal failure? *Investigative Radiology, 24,* 219–220.

Katzberg, R. W., Schulman., G, Meggs, L. G., Caldicott, W. J. H., Damiano, M. M. & Hollenberg, N. K., 1983. Mechanism of the renal response to contrast medium in dogs, decrease in renal function due to hypertonicity. *Investigative Radiology, 18,* 74–80.

Katzberg, R. W., Pabico, R. C., Morris, T. W., Hayakawa, K., McKenna, B. A., Panner, B. J., Ventura, J. A. & Fischer, H. W., 1986. Effects of contrast media on renal function and subcellular morphology in the dog. *Investigative Radiology, 21,* 64–70.

Khoury, G. A., Hopper, J. C., Varghese, Z., Farrington, K., Dick, R., Irving, J. D., Sweny, P., Fernando, O. & Moorhead, J. F., 1983. Nephrotoxicity of ionic and non-ionic contrast material in digital vascular imaging and selective renal arteriography. *British Journal of Radiology, 56,* 631–635.

Leeming, B. W., Spokes, K. C. & Silva, P., 1985. Effect of meglumine iothalamate on renal haemodynamics and function in the diabetic rat. *Investigative Radiology, 20,* 971–977.

Morcos, S. K., Haylor, J., Brown, P. & Nahas, A. M., 1992. Iodinated water soluble contrast media (WSCM) interfere with urinary protein assays. *British Medical Journal, 29,* 305.

Moreau, J. F., Droz, D., Noel, L. H., Leibowitch, J., Jungers, P. & Michel, J. R., 1980. Tubular nephrotoxicity of water-soluble iodinated contrast media. *Investigative Radiology, 15,* S54–S60.

REED, J. R., WILLIAMS, R. H. & LUKE, R. G., 1983. The renal haemodynamic response to diatrizoate in normal and diabetic rats. *Investigative Radiology, 18*, 536–540.

VAAMONDE, C. A., BIER, R. T., PAPENDICK, R., ALBERT, H., GOUVEA, W., OWENS, B. & PARDO, V., 1989. Acute and chronic effects of radiocontrast in diabetic rats. Role of anesthesia and risk factors. *Investigative Radiology, 24*, 206–218.

VARI, C. R., NATARAJAN, L. A., WHITESCARVER, S. A., JACKSON, B. A. & OTT, C. E., 1988. Induction, prevention and mechanisms of contrast media-induced acute renal failure. *Kidney International, 33*, 699–707.

WEBB, J. A., 1984. The effect of intravenous contrast medium on glomerular filtration rate. *British Journal of Radiology, 57*, 387–393.

1992, *The British Journal of Radiology*, *65*, 1018–1024

Stage IB cervical carcinoma: a clinical audit

By M. N. Gaze, MRCP (UK), FRCR, C. G. Kelly, MRCP (UK), FRCR, *P. R. C. Dunlop, MD, FRCR, A. T. Redpath, BSc, PhD, G. R. Kerr, MSc and V. J. Cowie, MD, FRCR

Department of Clinical Oncology, Western General Hospital, Edinburgh EH4 2XU, UK

(*Received 2 January 1992 and accepted 6 May 1992*)

Keywords: Cervical carcinoma, Clinical audit, Radiotherapy, Surgery, Treatment-related morbidity

Abstract. All patients with FIGO Stage IB cervical cancer registered with the Department of Clinical Oncology at the Western General Hospital, Edinburgh, during the 6 years from 1979 to 1984 have been reviewed, as part of a continuing programme of clinical audit. Of the 140 patients with Stage IB disease, 68 (49%) were treated by primary surgery of whom 44 (31%) also received adjuvant radiotherapy. Radical radiotherapy was the definitive treatment for 69 patients (49%). Three patients (2%) were not treated with curative intent. The crude 5-year survival rate for all cases was 72% and the cause-specific 5-year survival rate was 78%. Local tumour control at 5 years was 72%. There was no significant difference in outcome between the surgically treated and irradiated groups of patients. Age, histology and nodal status did not influence outcome. Irradiated patients with bulky tumours fared significantly worse than the other patients who received radical radiotherapy. Multivariate analysis of all patients revealed no significant independent prognostic variables. Primary surgery appears to confer no benefit over radical radiotherapy in terms of either survival or local control. Treatment-related late bladder and bowel morbidity was, however, significantly worse in irradiated patients.

Two new radical treatments for carcinoma of the uterine cervix were being pioneered at the turn of the century. Radium was first used shortly after its discovery by the Curies in 1898 and a woman with cervix cancer "well radiumised" in 1905 was reported cured 8 years later (Abbe, 1913). At the same time, a radical operation for cervical cancer was being developed (Wertheim, 1912). Since then, both surgery and radiotherapy have been important in the management of this disease.

In the 6-year period from 1979 to 1984, 140 patients with FIGO Stage IB carcinoma of the uterine cervix were referred to the Regional Department of Clinical Oncology at the Western General Hospital, Edinburgh. The majority of patients were treated by radical hysterectomy or radical radiotherapy. This paper is an audit of the management of these patients in terms of survival, local tumour control and treatment-related morbidity. Possible important prognostic factors in Stage IB carcinoma of the cervix are evaluated and the place of lymphangiography in the assessment of new patients is discussed.

Patients and methods

Patients and staging procedure

The case notes of all 546 new patients with carcinoma of the uterine cervix registered in the Department of Clinical Oncology at the Western General Hospital, Edinburgh, from 1979 to 1984 have been reviewed. This audit is of the 140 patients (26%) who were staged as having FIGO Stage IB carcinoma of the cervix. Routine staging investigations included examination under anaesthesia, cystoscopy, intravenous urography and chest radiography. Bipedal lymphangiography was not performed in all patients.

Treatment policy

Radical hysterectomy and pelvic lymphadenectomy tended to be the preferred treatment for younger, fitter patients. Some patients with bulky or poorly differentiated tumour received pre-operative radiotherapy, usually 20 Gy in 10 fractions over 2 weeks to the true pelvis using megavoltage X rays. If the histology of the excised pelvic lymph nodes revealed involvement with metastatic carcinoma, post-operative pelvic radiotherapy was administered. A dose of 40 Gy in 20 fractions over 4 weeks or its equivalent (including the pre-operative treatment if that had been given) was prescribed. In a few patients the diagnosis of invasive carcinoma was made following simple hysterectomy. Most of these received post-operative pelvic radiotherapy. All patients treated surgically are analysed together irrespective of whether or not they received adjuvant pelvic radiotherapy. Patients considered unsuitable for radical hysterectomy were treated with radical radiotherapy.

Radiotherapy technique

A combination of external-beam therapy and intracavitary caesium was used in all patients. The radiotherapeutic technique changed during the period of this audit. From 1979 to 1981 patients were treated with the wedge technique. Megavoltage external-beam radiation

---

Address correspondence to Dr M. N. Gaze, Department of Radiation Oncology, University of Glasgow, CRC Beatson Laboratories, Alexander Stone Building, Garscube Estate, Glasgow G61 1BD, UK.

*Present address: Department of Radiotherapy and Oncology, South Cleveland Hospital, Marton Road, Middlesbrough, Cleveland TS4 3BW, UK.

Table I. Treatment of patients with FIGO Stage IB cervical carcinoma

	No radiotherapy	Pre-operative radiotherapy	Post-operative radiotherapy	Pre- and post-operative radiotherapy	Total
Radical hysterectomy and pelvic lymphadenectomy	22	15	12	5	54
Simple hysterectomy	2	0	12	0	14
Radiotherapy technique		Wedge	Low-dose brick	High-dose brick	Total
		25	40	4	69
Total					137

was administered to the whole pelvis using parallel opposed fields with midline lead shielding to give a dose of 20 Gy to the central pelvis and to point A, and 40 Gy to the pelvic sidewall in 20 fractions over 4 weeks. Intracavitary treatment was given using the Edinburgh line source applicator and a manual afterloading system with caesium sources (Campbell & Douglas, 1966; Redpath et al, 1976). The dose prescribed from intracavitary caesium was 55 Gy to point A in two insertions. From 1981 to 1984 the low-dose brick technique was used. External-beam therapy was given using a three-field brick technique usually prescribing 40 Gy in 20 fractions over 4 weeks with no central shielding. A single intracavitary caesium insertion was prescribed to give 35 Gy to point A. Patients considered to have advanced disease by virtue of abnormal lymphangiograms (UICC Stage IIIB), were treated with the high-dose brick technique. A dose of 55 Gy in 30 fractions over 6 weeks was administered by a three-field brick technique to the pelvis followed by a single intracavitary caesium insertion prescribing a dose of 27 Gy to point A (Quilty, 1988). In 1984 a Selectron remote afterloading machine was installed and replaced the manual afterloading technique of Redpath et al (1976). The Edinburgh line source was adapted for use with the Selectron. The loading of the active sources was programmed to reproduce the dosimetry and dose rate at point A of the manual system. Patients treated by radical radiotherapy are analysed together irrespective of the radiotherapy technique used.

Follow-up

Data are available until death or the 1989 anniversary of treatment in all except two patients who were lost to follow-up at 1 and 24 months.

Analysis

The case notes of all patients were reviewed and standard data were entered into a computer for analysis. Survival curves were calculated by the life table method and compared using the log rank test. Proportional hazards analysis (Cox, 1982) was used to detect independent prognostic variables. The Mann–Whitney test was used to compare the incidence of morbidity in different treatment groups.

Results

Treatment intent and modality

This audit relates to 140 patients with FIGO Stage IB carcinoma of the cervix. Because of serious intercurrent illness or poor general condition, two patients received only palliative treatment and one was untreated. The treatments received by the 137 patients (98%) treated radically are shown in Table I.

Age

Patients treated surgically had a mean age of 41.2 (range 23–80) years and patients treated by radical radiotherapy had a mean age of 53.3 (range 26–79) years. Patients receiving radical radiotherapy were significantly older than those treated by surgery ($t = 5.4$, $p < 0.0001$).

Histology

Table II shows the distribution of pathological types and tumour grade. Histological confirmation of the diagnosis was available in all cases.

Lymph node involvement

Bipedal lymphangiography was performed in 84 patients (60%). The results are shown in Table III. Pre-operative lymphangiograms were performed in only 36 of the 54 patients who underwent radical hysterectomy and pelvic lymphadenectomy. Table IV shows the correlation between radiological abnormalities and

Table II. Histological type and grade

Tumour type	Degree of differentiation					
	Well	Moderate	Poor	Not stated	Total	(%)
Squamous carcinoma	8	28	63	17	116	(83)
Adenocarcinoma	7	2	2	7	18	(13)
Adenosquamous carcinoma	0	1	2	1	4	(3)
Clear cell carcinoma	0	0	0	2	2	(1)
Total	15	31	67	27	140	(100)
(%)	(11)	(22)	(48)	(19)	(100)	

Table III. Results of lymphangiograms

	Not done	Normal appearances	Abnormal appearances	Total
Patients treated with radical hysterectomy and pelvic lymphadenectomy	18	24	12	54
Patients treated with simple hysterectomy	8	3	3	14
Patients treated with radical radiotherapy	27	28	14	69
Total	53	55	29	137

histological node involvement. The specificity of a test indicates the proportion of those without the disease who give a negative test result, and the sensitivity indicates the proportion of those with the disease who have a positive test result. The specificity of lymphangiography in detecting abnormal nodes in this group of patients was 73%, although the sensitivity was only 50%. Lymph node histology is available for 56 patients. Of the 54 patients treated by radical hysterectomy and pelvic lymphadenectomy, 42 patients were pathologically node negative and 12 had involved nodes. Two patients underwent laparotomy with a view to radical hysterectomy, but at operation nodal involvement was obvious and lymph node biopsy only was performed. Subsequent treatment was by radical radiotherapy. 42 patients underwent lymphangiography prior to radical radiotherapy. Outcome in the 14 patients with radiological evidence of nodal involvement was not significantly different from that in patients with normal lymphangiograms.

Survival

For all 140 patients, crude survival at 5 years was 71.8% (95% confidence interval (CI): 64.2–79.4%) and cause-specific survival (obtained by censoring 11 intercurrent deaths) was 77.5% (95% CI: 70.1–84.9%). However, patients continue to die of cervical cancer after 5 years and the cause-specific actuarial survival at 8 years was only 64.1% (95% CI: 50.3–77.9%). There was no significant difference ($p = 0.302$) in cause-specific survival between patients treated with radical radiotherapy and those treated surgically (Fig. 1). The local recurrence-free survival curves similarly show no significant difference ($p = 0.539$) between the two treatment groups (Fig. 2).

Table IV. Correlation of lymphangiographic appearances with pathological nodal involvement

	Node histology positive	Node histology negative	Total
Lymphangiogram abnormal	5	7	12
Lymphangiogram normal	5	19	24
Total	10	26	36

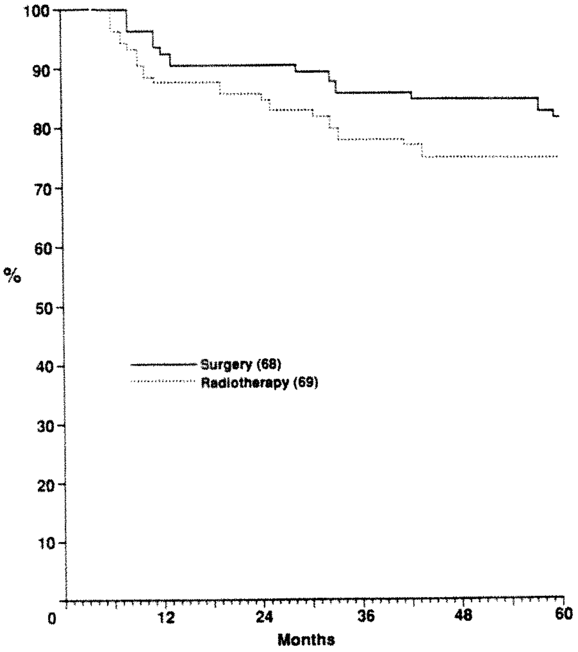

Figure 1. Cause-specific survival for patients treated with surgery and radical radiotherapy.

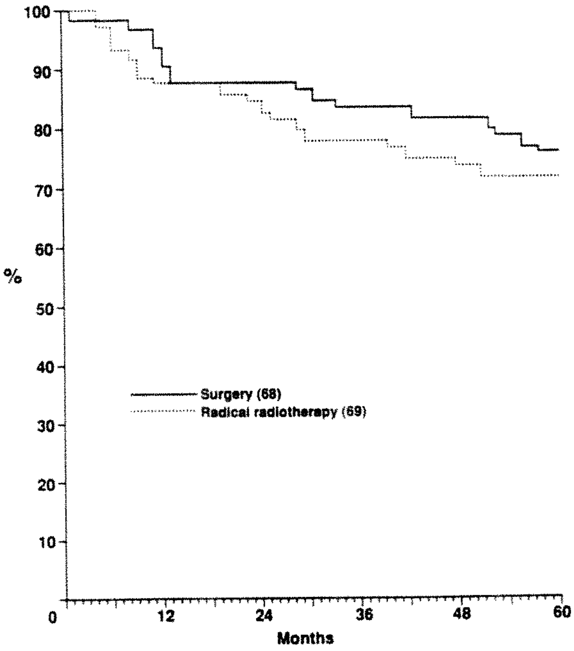

Figure 2. Local recurrence-free survival for patients treated with surgery and radical radiotherapy.

Table V. Causes of death

	Intercurrent illness	Pelvic disease only	Metastatic disease only	Pelvic and metastatic disease	Total dead	Alive
Patients treated by surgery	2	6	7	1	16	52
Patients treated by radiotherapy alone	9	8	12	6	35	34
Total	11	14	19	7	51	86

Patterns of failure

Of the 137 radically treated patients, 84 remain alive 5–10 years after presentation. Causes of death are shown in Table V. No patient died from treatment-related morbidity.

Prognostic factors

There was no discernible difference in survival or local control when the effect of age, histological type, differentiation and radiological and pathological node status were subjected to univariate analysis. Tumour size was not routinely measured, nevertheless the EUA report in 18 of the patients treated with radical radiotherapy describes the lesion as "bulky" or "extensive". Outcome for these patients was significantly worse ($p = 0.021$) than for the other 51 radically irradiated patients (Fig. 3). Multivariate analysis of the effect of age, cell type, tumour grade, lymphangiographic appearances, nodal status at operation and treatment modality failed to reveal any significant independent prognostic factors. Tumour bulk could not be included in this analysis as data were not available for most patients.

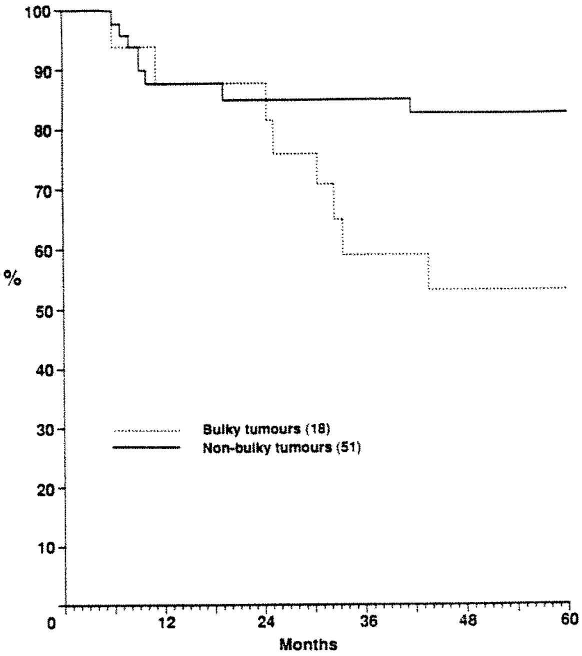

Figure 3. Cause-specific overall survival following radical radiotherapy for patients with "bulky" tumours compared with the other irradiated patients ($p = 0.021$).

Morbidity

Late bladder and bowel morbidity was graded retrospectively according to the EORTC/RTOG scale

Table VI. EORTC/RTOG scoring system for late radiation reactions

Bladder	
Grade 1	Slight epithelial atrophy. Minor telangiectasia (microscopic haematuria)
Grade 2	Moderate frequency, generalized telangiectasia. Intermittent macroscopic haematuria
Grade 3	Severe frequency and dysuria. Severe generalized telangiectasia (often with petechiae). Frequent haematuria. Reduction in bladder capacity (< 150 ml)
Grade 4	Necrosis. Contracted bladder (capacity < 100 ml). Severe haemorrhagic cystitis
Grade 5	Death directly related to radiation-induced effects
Bowel	
Grade 1	Mild diarrhoea. Mild cramping. Bowel movement less than five times daily. Slight rectal discharge or bleeding
Grade 2	Moderate diarrhoea and colic. Bowel movement greater than five times daily. Excessive rectal mucus or intermittent bleeding
Grade 3	Obstruction or bleeding requiring surgery
Grade 4	Necrosis, perforation or fistula
Grade 5	Death directly related to radiation-induced effects

Table VII. Treatment-related morbidity

	Grade						Total
	0	1	2	3	4	5	
Late bladder morbidity							
Radical radiotherapy alone	54	3	5	3	4	0	69
Surgery alone	24	0	0	0	0	0	24
Combined treatment	39	1	0	2	2	0	44
Late bowel morbidity							
Radical radiotherapy alone	47	8	5	4	5	0	69
Surgery alone	24	0	0	0	0	0	24
Combined treatment	36	3	1	3	1	0	44

(Table VI). The incidence of normal-tissue damage in each treatment group is shown in Table VII. Grade 3 or 4 bladder damage occurred in 10% of patients treated by radical radiotherapy compared with 6% of patients treated surgically ($z = 2.30$, $p = 0.02$). Grade 3 or 4 bowel damage occurred in 13% of patients treated by radical radiotherapy compared with 6% of patients treated surgically ($z = 2.82$, $p = 0.005$). Within the group treated by surgery, no morbidity was documented in patients treated by surgery alone whereas Grade 3 or 4 bladder and bowel damage each occurred in 9% of patients receiving surgery and adjuvant radiotherapy ($z = 1.76$, $p = 0.08$ for bladder morbidity, $z = 2.27$, $p = 0.02$ for bowel morbidity). There was no difference in the morbidity between the patients receiving radical radiotherapy and those treated by surgery with adjuvant radiotherapy.

Discussion

Clinical audit is defined as "a systematic critical analysis of the quality of medical care, including the procedures used for diagnosis and treatment, the use of resources, and the resulting outcome for the patient" (H. M. Secretaries of State, 1989). It has recently been enccouraged by the Government, although there is a long tradition of audit in clinical oncology. This dates back to the establishment in 1929 of The National Radium Commission, which made record keeping and submission of annual reports of treatment results a condition for lending radium sources to hospitals for the treatment of malignant disease (Raven, 1990). In oncology, survival has traditionally been the principal measure chosen to reflect outcome of treatment. Other important outcome measures include local control and treatment-associated morbidity. Disease-related factors are, however, not the only aspects of patient management that must be considered. In times of increasing financial accountability, audit takes into account use of available resources and the cost of treatment. Also, in an era of informed consent, patient preference may influence treatment choice. If a cancer or a particular stage of the disease can be treated by different modalities with an equivalent chance of cure, morbidity, patient preference and economics become important factors.

An audit of cervical cancer treatment in this department for the period from 1960 to 1976 has been published previously (Brand & Kerr, 1982). The 5-year survival rate was 72.0% for 442 patients with Stage IB disease treated radically by surgery or radiotherapy. Although conclusions drawn from comparison with historical controls can only be tentative, the present crude overall survival rate of 71.3% is remarkably similar.

These results are, however, poor compared with those reported from other centres. For patients treated with radical radiotherapy, 5-year survival rates greater than 85% are commonly reported (Fletcher, 1971; Park et al, 1973; Perez et al, 1986). Similar figures are also given for patients treated by surgery (Park et al, 1973; Hoskins et al, 1976). The reasons for this discrepancy are not clear. There appears to be no difference in survival rates, either in the current series or in the literature, between patients treated with surgery or radiotherapy (Hopkins & Morley, 1991) or between patients treated with radiotherapy alone or combined modalities (Mendenhall et al, 1991). It would be unwise, however, to attempt to draw conclusions about the relative efficacy of surgery and radiotherapy from the present study. It must be emphasized that this is not a randomized trial but an audit of clinical practice in which the two groups of patients are not comparable.

Although it has been suggested that there is a more aggressive form of cervical cancer carrying a poorer prognosis emerging in younger patients (Prempree et al, 1983; Lybeert et al, 1987, Elliot et al, 1989), there is no evidence to support this in the present data. Age is not a significant prognostic factor in our series and this is in keeping with other recent reports (Russell et al, 1987; Junor et al, 1989).

The proportion of patients with adenocarcinoma (13%) is slightly higher than that reported from other centres (Park et al, 1973; Perez et al, 1986; Alcock & Toplis, 1987), which is from 6 to 8%. Although cervical adenocarcinoma was once thought to be less radiosensitive than squamous carcinoma (Fletcher, 1971) prognosis in our series is independent of cell type, and accords well with the findings of Grigsby et al (1988).

Lymphangiography is generally recognized to be an investigation of high specificity (85–100%) but somewhat poorer sensitivity (27–77%) (Piver et al, 1971; de Muylder et al, 1984; Smales et al, 1986). Our figures of 73% and 50% for sensitivity and specificity are not markedly different. These results may not reflect the accuracy of lymphangiography in all patients who underwent the investigation, however, as no pathological data were obtained for those patients treated with radiotherapy because of positive lymphangiograms. Thus the true sensitivity may be greater than indicated. Lymph node status is usually found to be a major prognostic factor, whether assessed radiologically (Smales et al, 1986) or pathologically (Alcock & Toplis, 1987). It is surprising, therefore, that we have not demonstrated either radiological or histological lymph node involvement to be an adverse factor. Prognosis in the surgically treated group was similar whether or not the nodes were histologically involved, and not different from that achieved by radical radiotherapy. The routine use of lymphangiography does not, therefore, seem to be justified.

The increase in tumour size that generally occurs along with increasing FIGO stage is recognized to correlate with worsening prognosis. The FIGO system does not take account of tumour volume within each stage, although it has been recognized by Fletcher (1971), Grigsby et al (1988) and Kovalic et al (1991) as well as the present series to be a relevant factor. Most series fail to report measurements of tumour volume, and this is clearly a weakness of the present staging system. The reason for the poorer prognosis in patients with bulky tumours is not clear, as the patterns of failure in these patients are not significantly different from those seen in patients with non-bulky tumours. 19 of 40 patients dying from their malignancy had distant metastases in the absence of local recurrence. This indicates that cervical carcinoma, even when at an apparently early stage, may be a systemic disease. Although improvements in local methods of treatment may diminish mortality, effective systemic therapy is needed.

The incidence of late morbidity is an important factor in the assessment of results of treatment of cervical carcinoma. However, only limited weight can be given to a retrospective analysis of unclassified clinical observations recorded in case notes. While severe morbidity is likely to be relatively well documented, milder degrees may not be uniformly recorded by different observers. Sismondi et al (1989), surveying 96 papers that refer to complications of cervix cancer treatment, found that 59 made no attempt to grade severity. 22 different classifications were used in the 39 papers in which some sort of scale was used to quantify problems. It is against this background that one must evaluate the observation that significant late bladder and bowel morbidity is documented for patients receiving radiotherapy and no morbidity in patients treated by surgery alone. While our figures for severe radiotherapy-related morbidity are similar to the 11% national benchmark figure reported in the Patterns of Care Outcome Survey (Hanks et al, 1982), they are greater than is desirable. This relatively high incidence is not accounted for by the excessive late radiation damage noted in patients treated with the high-dose brick technique (Quilty, 1988).

This audit has all the deficiencies inherent in any retrospective analysis. For example, some important data were missing from the case notes, pathological and radiological findings were not uniformly reported and tumour size, which may be a particularly important prognostic factor, was not systematically recorded. In addition, radiotherapy techniques changed and morbidity was not always documented.

To try to improve the clinical service and standards of care for our patients, a new practice has evolved in Edinburgh. We attempt to ensure that all new patients with carcinoma of the cervix, irrespective of where in south-east Scotland they may have presented, are jointly assessed together with a central review of pathology in a combined gynaecological/oncology clinic. This is staffed by consultant gynaecological, radiation and medical oncologists, all with special expertise and experience in the management of gynaecological malignancy. Protocols for staging, treatment and follow-up have been agreed. This enables multidisciplinary discussion with a view to optimal and consistent management of all patients. Prospective recording of clinical and pathological data, results of staging investigations and full treatment details are performed. At each follow-up attendance, standardized documentation of bowel, bladder and sexual function and morbidity and disease status is made. This will ensure that future audits are more reliable and that patient care is improved.

Acknowledgments

We wish to thank Dr J. R. B. Livingstone, Dr S. M. Ludgate and Dr G. E. Smart under whose care the majority of these patients were treated.

References

ABBE, R., 1913. The use of radium in malignant disease. *Lancet, ii*, 524–527.

ALCOCK, C. J. & TOPLIS, P. J., 1987. The influence of pelvic lymph node disease on survival for stage I and II carcinoma of the cervix. *Clinical Radiology, 38*, 13–16.

BRAND, M. A. J. T. & KERR, G. R., 1982. The results of treatment of carcinoma of the uterine cervix using a linear vaginal source and 4MV X rays. *British Journal of Radiology, 55*, 352–355.

CAMPBELL, E. M. & DOUGLAS, M., 1966. The treatment of carcinoma of the cervix using a linear vaginal source and 4MeV X rays. *British Journal of Radiology, 39*, 537–546.

COX, D. R., 1982. Regression models and life tables. *Journal of the Royal Statistical Society Series, 34*, 187–220.

DE MUYLDER, X., BÉLANGER, R., VAUCLAIR, R., AUDET-LAPOINTE, P., CORMIER, A. & METHOT, Y., 1984. Value of lymphography in stage IB cancer of the uterine cervix. *American Journal of Obstetrics and Gynecology, 148*, 610–613.

ELLIOT, P. M., TATTERSALL, M. H. N., COPPLESON, M., RUSSELL, P., WONG, F., COATES, A. S., SOLOMON, H. J., BANNATYNE, P. M., ATKINSON, K. H. & MURRAY, J. C., 1989. Changing character of cervical cancer in young women. *British Medical Journal, 298*, 288–290.

FLETCHER, G. H., 1971. Cancer of the uterine cervix. *American Journal of Roentgenology, 111*, 225–242.

GRIGSBY, P. W., PEREZ, C. A., KUSKE, R. R., CAMEL, H. M., KAO, M. S., GALAKATOS, A. E. & HEDERMAN, M. A., 1988. Adenocarcinoma of the uterine cervix: lack of evidence for a poor prognosis. *Radiotherapy and Oncology, 12*, 289–296.

HANKS, G. E., KRAMER, S., DIAMOND, J. J. & HERRING, D. F., 1982. Patterns of care outcome survey: national outcome data for six disease sites. *American Journal of Clinical Oncology, 5*, 349–353.

H. M. SECRETARIES OF STATE FOR HEALTH, WALES, NORTHERN IRELAND AND SCOTLAND, 1989. *Working for Patients* (HMSO, London), p. 39.

HOPKINS, M. P. & MORLEY, G. W., 1991. Radical hysterectomy *versus* radiation therapy for Stage IB squamous cell carcinoma of the cervix. *Cancer, 68*, 272–277.

HOSKINS, W. J., FORD, J. H., LUTZ, M. H. & AVERETTE, H. E., 1976. Radical hysterectomy and pelvic lymphadenectomy for the management of early invasive cancer of the cervix. *Gynecologic Oncology, 4*, 278–290.

JUNOR, E. J., SYMONDS, R. P., WATSON, E. R. & LAMONT, D. W., 1989. Survival of younger cervical carcinoma patients treated by radical radiotherapy in the West of Scotland 1964–1984. *British Journal of Obstetrics and Gynaecology, 96*, 525–528.

KOVALIC, J. J., PEREZ, C. A., GRIGSBY, P. W. & LOCKETT, M. A., 1991. The effect of volume of disease in patients with carcinoma of the uterine cervix. *International Journal of Radiation Oncology, Biology, Physics, 21*, 905–910.

LYBEERT, M. L. M., MEERWALDT, J. H. & VAN PUTTEN, W. L. J. 1987. Age as a prognostic factor in carcinoma of the cervix. *Radiotherapy and Oncology, 9*, 147–151.

MENDENHALL, W. M., MCCARTY, P. J., MORGAN, L. S., CHAFE, W. E. & MILLION, R. R., 1991. Stage IB or IIA-B carcinoma of the intact uterine cervix $\geqslant$ 6cm in diagmeter: is adjuvant extrafascial hysterectomy beneficial? *International Journal of Radiation Oncology, Biology, Physics, 21*, 899–904.

Park, R. C., Patow, W. E., Rogers, R. E. & Zimmerman, E. A., 1973. Treatment of stage I carcinoma of the cervix. *Obstetrics and Gynecology, 41*, 117–122.

Perez, C. A., Camel, H. M., Kuske, R. R., Kao, M.-S., Galakatos, A., Hederman, M. A. & Powers, W. E., 1986. Radiation therapy alone in the treatment of carcinoma of the uterine cervix: a 20-year experience. *Gynecologic Oncology, 23*, 127–140.

Piver, M. S., Wallace, S. & Castro, J. R., 1971. The accuracy of lymphangiography in carcinoma of the uterine cervix. *American Journal of Roentgenology, Radium Therapeutics and Nuclear Medicine, 111*, 278–283.

Prempree, T., Patanaphan, V., Sewchand, W. & Scott, R. M., 1983. The influence of patients' age and tumour grade on the prognosis of carcinoma of the cervix. *Cancer, 51*, 1764–1771.

Quilty, P. M., 1988. A report of late rectosigmoid morbidity in patients with advanced cancer of the cervix, treated by a six week pelvic brick technique. *Clinical Radiology, 39*, 297–300.

Raven, R. W., 1990. *The Theory and Practice of Oncology: Historical Evolution and Present Principles* (Parthenon Publishing, Carnforth), p. 232.

Redpath, A. T., Douglas, M. A. J. T. & Orr, J. A., 1976. The Edinburgh afterloading technique for carcinoma of the uterine cervix. *British Journal of Radiology, 49*, 963–965.

Russell, J. M., Blair, V. & Hunter, R. D., 1987. Cervical carcinoma: prognosis in younger patients. *British Medical Journal, 295*, 300–303.

Sismondi, P., Sinistrero, G., Zola, P., Volpe, T., Ferraris, R., Castelli, G. L. & Giai, M., 1989. Complications of uterine cervix carcinoma treatments: the problem of a uniform classification. *Radiotherapy and Oncology, 14*, 9–17.

Smales, E., Perry, C. M., MacDonald, J. S. & Baker, J. W., 1986. The value of lymphography in the management of carcinoma of the cervix. *Clinical Radiology, 37*, 19–22.

Wertheim, E., 1912. The extended abdominal operation for carcinoma uteri. *American Journal of Obstetrics, 66*, 169–232.

1992, *The British Journal of Radiology*, 65, 1025–1029

Calcium antagonists protect mice against lethal doses of ionizing radiation

By G. L. Floersheim

Department of Research, University Hospitals, Hebelstrasse 20, 4031 Basel, Switzerland

(Received 28 October 1991 and in final form 8 June 1992, accepted 29 June 1992)

Keywords: Radioprotection, Calcium antagonists, Diltiazem, Nifedipine, Nimodipine

Abstract. Currently available radioprotectors are poorly tolerated in man and the general use of aminothiol radioprotectors is compromised by their side-effects. In a search for less toxic radioprotective agents, diltiazem, a calcium antagonist with a benzothiazepine structure, was found to protect mice against a lethal (LD_{100}) γ radiation dose allowing survival of up to 93%. Dihydropyridine calcium antagonists such as nifedipine, nimodipine, isradipine and nitrendipine also provided radioprotection. Calcium antagonists might attenuate radiation-induced injury by inhibiting cellular calcium overload, subsequent to cell membrane damage caused by radiation-generated free radicals. In view of their good tolerance, calcium antagonists may be applied safely in situations of radiation exposure, including radiotherapy and internal radionuclide contamination. These calcium antagonists may also be viewed in other contexts where free radicals are implicated in pathological processes.

The search for chemical agents which protect against the tissue damage caused by exposure to ionizing radiation has led to the identification of thiol (sulfhydryl) compounds with marked activity in experimental models (Sweeney, 1979). However, the use of the most promising agent, WR 2721 (S-2-(3-aminopropylamino)-ethylphosphorothioic acid), has been limited by its poor clinical tolerance (Cairnie, 1983; Turrisi et al, 1983). In this study a different approach has been initiated by testing thiol substances not designed for radioprotective activity but known from their use in other contexts to have a favourable therapeutic index. This included diltiazem, a benzothiazepine whose use as a calcium antagonist in cardiovascular pharmacology is based on extensive clinical experience. Since diltiazem protected against radiation-induced damage, the effects of other calcium antagonists were also investigated.

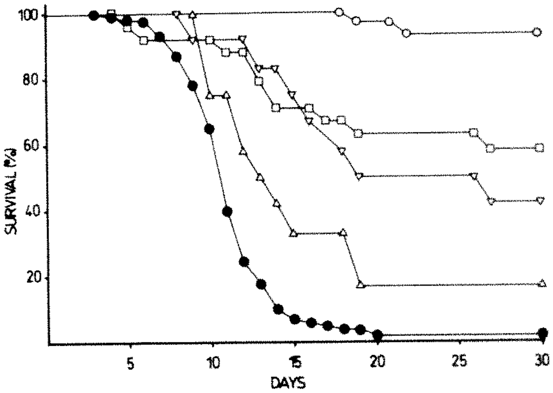

Figure 1. Survival of female C3H mice irradiated with 10.5 Gy (dose rate ~ 0.15 Gy/min). A small number of the mice (6 treated with 110 mg/kg diltiazem at −15 min, 6 treated with 110 mg/kg diltiazem at +10 min and 6 controls) were irradiated with 8.5 Gy at a dose rate of 0.9 Gy/min. The mice were treated subcutaneously with diltiazem before or after irradiation. The doses of diltiazem were as follows: 110 mg/kg (n = 29) at −15 min (○); 55 mg/kg (n = 24) at −15 min (□); 27.5 mg/kg (n = 12) at −15 min (△); 110 mg/kg (n = 12) at +10 min (▽). Controls (n = 114) were injected with 0.1 ml distilled water per 10 g body weight (●).

Materials and methods

Mice and irradiation

The experiments were carried out using C3H mice of both sexes (Gl. Bomholtgard, Ry, Denmark) weighing 22–24 g and fed Nafag pellets and water *ad libitum*. Groups of mice were irradiated in a perforated plexiglass chamber from a ^{60}Co source (Gammatron). The target distance was 80 cm. Dosimetry was performed with a strontium-calibrated ionization chamber. For the experiments with diltiazem, the results of which are illustrated in Fig. 1, female mice (n = 173) were irradiated with 10.5 Gy (dose rate ~ 0.15 Gy/min). A smaller scale experiment (n = 18) was also peformed with a dose of 8.5 Gy from a source delivering 0.9 Gy/min. The doses delivered by the two radiation sources corresponded to the respective LD_{100} values and resulted in the same mean survival times. Accordingly, they were assumed to be biologically isoeffective and results obtained with both radiation dose rates were pooled.

The female mice used for the experiments whose results are shown in Fig. 2 received 8.5 Gy at a rate of 0.9 Gy/min. In the experiments with male mice, the results of which are illustrated in Fig. 3, the irradiation doses were 8.1 and 9.0 Gy at a rate of 0.9 Gy/min.

The efficacy of a compound was measured by its ability to protect mice against a lethal dose of whole-

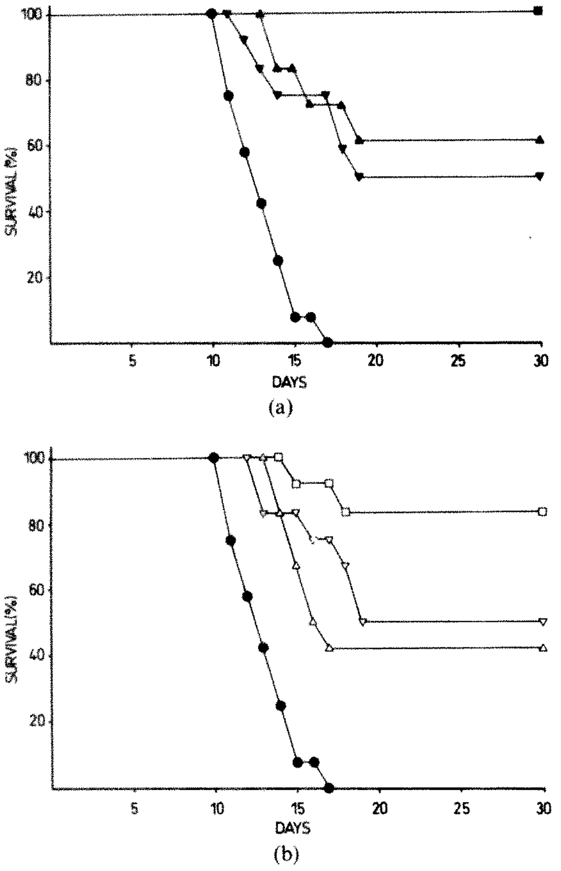

(a)

(b)

Figure 2. Groups of 12 female C3H mice irradiated with 8.5 Gy (dose rate 0.9 Gy/min). Their radiation LD_{50} was ~ 7.75 Gy. The mice were injected intraperitoneally 30 min before irradiation. For a better detection of the relative contributions, the agents were applied at only half their optimal dose. (a) The mice received 1.5 mg/kg body weight nifedipine in 0.15 ml/10 g standard solvent (■), 0.15 ml/10 g standard solvent containing 18% ethanol (▲), or 0.15 ml/10 g of an 18% ethanol solution in distilled water, corresponding to 2295 mg/kg ethanol (▼). Controls received 0.15 ml/10 g distilled water (●). (b) The mice were injected with 2.0 mg/kg nimodipine in 0.1 ml/10 g standard solvent (□); 0.1 ml/10 g standard solvent containing 23.7% ethanol (△), or 0.1 ml/10 g of a 23.7% ethanol solution in distilled water corresponding to 2015 mg/kg ethanol (▽). Controls recevied 0.1 ml/10 g distilled water (●).

body γ radiation, protection being identified by animal survival at 30 days. The agents were first tested at 50% of the LD_{50} and, in case of efficacy, at progressively halved doses. The figures for survival after the respective treatments are presented in the Figures. Since, in general, the mice succumbed at approximately day 10 after irradiation, their death can be attributed to bone marrow damage. However, in the experiments in which a supralethal radiation dose was applied, the results of which are depicted in Figure 3b, gut-related deaths may have occurred.

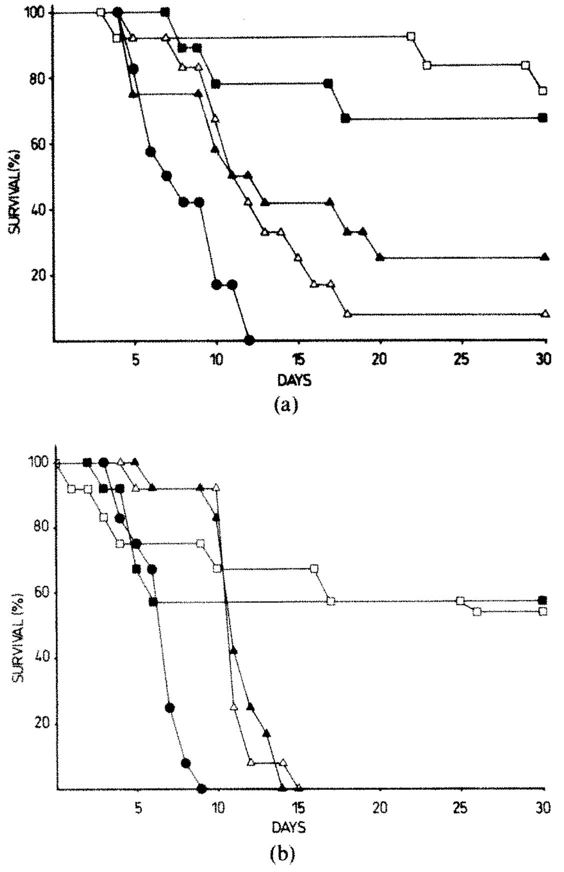

(a)

(b)

Figure 3. Survival in groups of 12 male C3H mice irradiated with 8.1 Gy (a) or 9.0 Gy (b) at the dose rate 0.9 Gy/min. The radiation LD_{50} in these mice was ~ 6.35 Gy (dose rate 0.9 Gy/min). The mice were injected intraperitoneally 30 min before irradiation with either nifedipine or nimodipine in their solvents or with ethanol at the dose corresponding to that present in the solvent. Treatments were as follows: Controls: 0.2 ml distilled water/10 g body weight (●); nifedipine, 3 mg/kg in 0.3 ml solvent/10 g (■); 0.3 ml/10 g of an 18% ethanol solution in distilled water corresponding to 4590 mg/kg ethanol (▲); nimodipine, 4 mg/kg in 0.2 ml solvent/10 g (□); 0.2 ml/10 g of an 23.7% ethanol solution (4050 mg ethanol/kg) in distilled water (△).

Drugs

Diltiazem was provided in ampoules containing 25 mg diltiazem hydrochloride and 150 mg mannitol (Warner-Lambert). The content of the ampoules was dissolved in distilled water and 0.1 ml/10 g body weight was administered by the subcutaneous route to the mice. In control experiments, it was ascertained that mannitol alone did not exert any radioprotection.

Nifedipine and nimodipine were available as commercial solutions (Bayer) and applied by the intraperitoneal route. The solvents for nifedipine and nimodipine contained 18% and 23.7% ethanol, respectively. In addition, the solvent included polyethylene glycol 400, sodium citrate and citric acid (courtesy Prof. S. Kazda). Since standard solvent and ethanol alone, in the quantity contained in the solvent, afforded equivalent radioprotection (Fig. 2), it can be assumed that the components of the standard solvent other than ethanol did not contribute to the protective activity afforded by the standard solvent. It was ascertained in separate experiments that polyethylene glycol 400 alone had no radioprotective activity.

Nitrendipine (Bayer) was administered as a suspension in distilled water (0.1 ml/10 g body weight) by the intraperitoneal route. Isradipine (Sandoz) was dissolved in olive oil and was also injected intraperitoneally (0.1 ml/10 g body weight). Olive oil alone did not protect. Verapamil (Knoll) was administered intraperitoneally in distilled water (0.1 ml/10 g body weight) and flunarizine (Janssen) was given orally as a suspension in distilled water (0.1 ml/10 g body weight).

Statistical evaluation

The statistical significance of the differences in survival rates, as compared to controls, was determined according to the two-tailed chi-square test. Differences in survival time were evaluated according to a two-tailed *t*-test.

Results

The survival at 30 days of female C3H mice irradiated over the whole body with γ-rays at approximately LD_{100} was increased to 93% by 110 mg/kg of subcutaneous diltiazem, a dose corresponding to 50% of the LD_{50} of the drug (Fig. 1). Survival with 55 mg/kg and 27.5 mg/kg of diltiazem was 58% and 17% respectively (Fig. 1). Significant survival (42%) was also obtained when diltiazem was administered 10 min after the completion of irradiation (Fig. 1). The protection produced by diltiazem occurred irrespective of the dose rate at which the radiation was given.

A similar dose-dependent improvement in survival in lethally irradiated female C3H mice was achieved following the intraperitoneal administration of nifedipine and nimodipine. These agents were administered in combination with their standard solvents, which contained ethanol (18% for nifedipine and 23.7% for nimodipine). Ethanol has long been known to exert radioprotective activity (Paterson & Matthews, 1950). Therefore to avoid confounding the additive or synergistic effects of ethanol with those of nifedipine and nimodipine, it was necessary to distinguish between the relative protective contributions of solvent and calcium antagonist. Figures 2a and 2b present the results of experiments in which the efficacy of nifedipine and nimodipine (both at a dose corresponding to 25% of their LD_{50}) are compared with those of their respective standard solvents, and with that of ethanol at an appropriate standard solvent concentration. The survival in lethally irradiated female C3H mice was 100% with 1.5 mg/kg nifedipine, 61% with the standard solvent and 50% with ethanol (Fig. 2a).

With 2.0 mg/kg nimodipine, 82% of the mice survived, but only 42% with the standard solvent and 50% with ethanol (Fig. 2b). The radioprotective effects afforded by standard solvents and ethanol *per se* were not significantly different. The differences in survival rate (chi-square test) between either nifedipine or nimodipine (each in standard solvents) and their respective solvents alone, were statistically significant ($p < 0.001$ and $p < 0.01$, respectively). Accordingly, after subtractive correction for the solvent effect, the residual radioprotection (39% with nifedipine and 40% with nimodipine) can be ascribed to the calcium antagonists.

The intrinsic radioprotective potential of these calcium antagonists was confirmed in irradiation experiments on male C3H mice, which are more radiosensitive than female mice. For mice irradiated with 8.1 Gy (Fig. 3a), survival after treatment with 3 mg/kg nifedipine or 4 mg/kg nimodipine (*i.e.* at doses corresponding to 50% of their LD_{50}) was 67% ($p < 0.005$) and 75% ($p < 0.001$), respectively, compared to survival on treatment with the corresponding doses of ethanol alone of 25% and 8%, respectively. For mice irradiated with the supralethal dose of 9.0 Gy (Fig. 3b), survival was 58% ($p < 0.0025$) with 3 mg/kg nifedipine and 55% ($p < 0.0025$) with 4 mg/kg nimodipine as compared with the corresponding doses of ethanol which afforded no survival advantage at 30 days, only a prolongation of the mean survival time from 6.6 ± 1.6 days (controls) to 11.1 ± 2.1 and 11.0 ± 2.2 days ($p < 0.01$; *t*-test), respectively.

The results obtained with other calcium antagonists are presented in Table I. Survival of 58% ($p < 0.001$) was achieved with isradipine applied at 27.5 mg/kg ($n = 24$) to female C3H mice irradiated with 8.5 Gy at a dose rate of 0.9 Gy/min. Nitrendipine (100 or 50 mg/kg) administered intraperitoneally as a suspension in distilled water to female C3H mice irradiated with 10.5 Gy (dose rate of 0.15 Gy/min) resulted in survival of 29% or 25%, respectively. No animal survival was produced by pretreatment with verapamil or flunarizine.

Discussion

These experiments demonstrate that some calcium antagonists—particularly diltiazem, but also nifedipine and nimodipine—are effective radioprotectors. One explanation for the observed effect could be related to the radiation-induced lipid peroxidation of cell membrane structures by oxygen-derived free radicals with ionic leakage through cellular membranes and excessive calcium influx with ensuing cellular dysfunction and death from Ca^{2+} overload. In reperfusion injury, another situation involving peroxidative membrane injury by free radicals (Ip & Levin, 1988; Janero et al, 1988; Bolli et al, 1989; Opie, 1989; Nayler et al, 1990; Watts et al, 1990), Ca^{2+} channel blockers have also been shown to be protective.

On the other hand, antioxidative effects by calcium antagonists such as nifedipine (Shridi & Robak, 1988; Ondrias et al, 1989) and diltiazem (Koller & Bergmann, 1989) have been reported and their radioprotective activity could also be linked more generally to the

Table I. Survival (30 days) of lethally irradiated female C3H mice pretreated with various calcium antagonists

Treatment	Dose (mg/kg)	Route of application	Time (min)	Survival[a]	%	p[b]
Controls (0.1 ml aq. dest./10 g)		i.p.	−30	0/30	0	
Controls (0.1 ml olive oil/10 g		i.p.	−30	0/6	0	
Isradipine	27.5	i.p.	−30	14/24	58	< 0.001
Isradipine	27.5	i.p.	−120	5/18	28	< 0.01
Nitrendipine	100	i.p.	−30	7/24	29	< 0.005
Nitrendipine	50	i.p.	−30	3/12	25	< 0.005
Verapamil	16	i.p.	−30	0/12	0	n.s.
Flunarizine	25	p.o.	−30	0/12	0	n.s.

[a] No. of surviving mice/total no. of mice.
[b] Chi-square test, compared to the relative controls.
n.s. = Not significant.

scavenging of free radicals (Janero et al, 1988). Thiol radioprotectors are believed to act principally by neutralizing radiation-induced free radicals via the formation of disulphides. Therefore, the particular efficacy of diltiazem may be explained by the fact that this molecule is capable of functioning not only as a calcium antagonist, but also as a thiol.

No class dependency can be observed, since both a benzothiazepine (diltiazem) and dihydropyridine (nifedipine and nimodipine) calcium antagonists were active. To the latter class belong also the moderately effective compounds nitrendipine and isradipine (Table I). Variations in efficacy between these calcium antagonists may be due to differences in bioavailability or tissue specificity. The relatively high dose of diltiazem required for radioprotection in mice may be explained by its low bioavailability and high metabolic rate in the mouse. The calcium channel blockers flunarizine and verapamil which differ in their chemical structure from benzothiazepines and dihydropyridines exhibited no radioprotective activity (Table I).

Diltiazem also displayed some activity when administered after the completion of irradiation (Fig. 1). This important property is not shared with thiols such as WR 2721, cysteamine or cysteine.

Whether calcium antagonists protect from ionizing radiation has not been studied previously. Some attenuation of the radiation response has been reported by treatment with nifedipine in patients developing radiation oesophagitis after thoracic radiation (Finkelstein, 1986). Nifedipine was applied when pain on swallowing was severe, after radiation, and was thought to reduce oesophageal spasm. In other work, variation in blood flow caused by calcium channel blockers was proposed to explain a modified sensitivity of mouse tumours to X rays (Wood & Hirst, 1989). With non-ionizing radiation, *in vitro* studies revealed that cell changes occurring after exposure to magnetic fields were influenced by calcium channel blockers (Papatheofanis, 1990).

Since calcium antagonists lower blood pressure, antihypertensive agents from other classes were tested (unpublished). Neither the thiol captopril, an angiotensin-converting enzyme inhibitor, nor the β-adrenergic blocking agent propranolol or various other vasoactive drugs used in the management of hypertension, coronary disease and cardiac arrhythmias (including clonidine, diazoxide, prazosine, hydrochlorothiazide, amiodarone, debrisoquine, sodium nitroprusside, molsidamine and ketanserine) exhibited significant radioprotective activity, suggesting that hypotension accompanied by tissue hypoxia is not the cause of the radioprotection produced by calcium antagonists.

Calcium antagonists are well tolerated and thus display a significant advantage over other agents providing effective radioprotection. In addition to their use in nuclear emergencies, more gentle radioprotectors may be useful in cancer radiotherapy and in situations involving internal radionuclide contamination. If it could be established that calcium antagonists inhibit radiation carcinogenesis, they might be useful in extensive medical radiological procedures, exposure to radon or to cosmic radiation at high altitudes.

Since radiation injury typically exemplifies tissue damage due to reactive oxygen species, radioprotective calcium antagonists may also be viewed in the context of an evergrowing body of degenerative diseases in which free radicals are thought to be implicated in the pathogenesis (Halliwell & Gutteridge, 1985; Cross et al, 1987; Cotgreave et al, 1988).

Acknowledgments

This work was supported by Grant No. 3981-0.87 of the Swiss National Foundation and the Mildner Stueckrath Foundation for Cancer Research. I thank F. R. Bühler for discussions and Armin Bieri, Ronald König and Chantal Racine for technical assistance.

References

Bolli, R., Triana, F. & Jeroudi, M. O., 1989. Postischemic mechanical and vascular dysfunction (myocardial 'stunning' and microvascular 'stunning') and the effects of calcium-channel blockers on ischemia/reperfusion injury. *Clinical Cardiology, 12,* 16–25.

Cairnie, A. B., 1983. Adverse effects of the radioprotector WR 2721. *Radiation Research, 94,* 221–226.

Cotgreave, I. A., Moldéus, P. & Orrenius, S., 1988. Host biochemical defense mechanism against prooxidants. *Annual Review of Pharmacology and Toxicology, 28,* 189–212.

Cross, E. C., Halliwell, B., Borish, E. T., Pryor, W. A., Ames, B. N., Saul, R. L., McCord, J. M. & Harmann, D., 1987. Oxygen radicals and human disease. *Annals of Internal Medicine, 107,* 526–545.

Finkelstein, E., 1986. Nifedipine for radiation oesophagitis. *Lancet, i,* 1205–1206.

Halliwell, B. & Gutteridge, J. M. C., 1985. *Free Radicals in Biology and Medicine* (Clarendon, Oxford).

Ip, J. H. & Levin, R. I., 1988. Myocardial preservation during ischemia and reperfusion. *American Heart Journal, 115,* 1094–1104.

Janero, D. R., Burghardt, B. & Lopez, R., 1988. Protection of cardiac membrane phospholipid against oxidative injury by calcium antagonists. *Biochemical Pharmacology, 37,* 4197–4203.

Koller, P. T. & Bergmann, S. R., 1989. Reduction of lipid peroxidation in reperfused isolated rabbit hearts by diltiazem. *Circulation Research, 65,* 838–846.

Nayler, W. G., Liu, J. & Panagiotopoulos, S., 1990. Nifedipine and experimental cardioprotection. *Cardiovascular Drugs and Therapy, 4,* 879–886.

Ondrias, K., Misik, V., Gergel, D. & Stasko, A., 1989. Lipid peroxidation of phosphatidilcholine liposomes depressed by the calcium channel blockers nifedipine and verapamil and by the antiarrhythmic-antihypoxic drug stobadine. *Biochimica Biophysica Acta, 1003,* 238–245.

Opie, L. H., 1989. Reperfusion injury and its pharmacologic modification. *Circulation, 80,* 1049–1062.

Papatheofanis, F. J., 1990. Use of calcium channel antagonists as magnetoprotective agents. *Radiation Research, 122,* 24–28.

Paterson, E. & Matthews, J. J., 1950. Protective action of ethyl alcohol on irradiated mice. *Nature, 168,* 1126–1127.

Shridi, F. & Robak, J., 1988. The influence of calcium channel blockers on superoxide anions. *Pharmacological Research Communications, 20,* 13–21.

Sweeney, T. R., 1979. *A Survey of Compounds from the Anti-radiation Drug Development Program of the U.S. Army Medical Research and Development Command.* (Walter Reed Army Institute of Research, Washington, DC).

Turrisi, A. T., Kligerman, M. M., Glover, D. J., Glick, J. H., Norfleet, L. & Gramkowski, M., 1983. Experience with phase I trials of WR 2721 preceding radiation therapy. In *Radioprotectors and Anticarcinogens.* Ed. by Nygaard, F. O. & Simic, M. G. (Academic Press, London), pp. 681–694.

Watts, J. A., Norris, T. A., London, R. E., Steenbergen, C. & Murphy, E., 1990. Effects of diltiazem on lactate, ATP, and cytosolic free calcium levels in ischemic hearts. *Journal of Cardiovascular Pharmacology, 15,* 44–49.

Wood, P. J. & Hirst, D. G., 1989. Calcium antagonists as radiation modifiers: site specificity in relation to tumor response. *International Journal of Radiation Oncology, Biology Physics, 16,* 1141–1144.

1992, *The British Journal of Radiology*, *65*, 1030–1034

Technical note

Phantoms for evaluating the performance characteristics of bone densitometers

By G. J. Royle, BSc, ARCS and R.D. Speller, BSc, ARCS, PhD

Medical Physics Department, University College London, 11–20 Capper Street, London WC1E 6JA, UK

(*Received 24 October 1991 and in revised form 27 February 1992, accepted 6 May 1992*)

Keywords: Phantoms, Bone density, Osteoporosis

Osteoporosis is characterized by a gradual loss of osseous tissue within the framework of the bone, which lowers bone strength and so increases the risk of fracture. A variety of techniques exist for identifying early bone loss, such as single- or dual-photon absorptiometry (SPA, DPA), quantitative computed tomography (QCT), etc. (Speller et al, 1989). Those commonly employed concentrate on the rate of decrease in bone density or bone mineral content within a particular site. The skeletal sites that become most susceptible to fracture are those with high trabecular content, namely the distal radius, the femoral neck and the lumbar vertebrae. For diagnosis of osteoporosis serial density measurements need to be performed at regular intervals over a period of many months. The frequency at which measurements are performed must be determined by the precision of the machine as compared with the decrease in bone density over that period of time. The reported rates of bone loss for normal post-menopausal women are 1.2% per year for trabecular bone (vertebral QCT measurements; Cann et al, 1985) and 0.9% per year for cortical bone (SPA measurements of mid-radius; Mazess, 1982). Therefore, the precision of the method must be sufficient to allow the machine to detect the small changes in bone density that occur in the space of a few months. Thus, knowledge of the precision and accuracy of the machine is essential. All systems when installed are supplied with a calibration phantom. These phantoms are either simple representations of the patient, or in the case of QCT, they are permanent inserts in the scanning table. At present, no phantoms that allow varying density inserts simulate sections of the body. The variable inserts often require liquid standards to be made. In general, these phantoms are used to determine the accuracy of a system under a single set of conditions and do not lend themselves to simulating varying degrees of osteoporosis in realistic conditions. This underlines the need for a set of test tools for evaluating the performance of bone density machines that can simulate accurately the progression of osteoporosis in bone tissue.

This paper describes the design and construction of anthropomorphic phantoms composed of tissue-equivalent materials with solid inserts of various densities which may be used for this purpose.

Design of the anthropomorphic phantoms

Phantoms are commonly used within the development of new techniques to simulate the conditions encountered by ionizing radiation in a patient and to investigate the administered dose. A set of anthropomorphic phantoms, intended for use as test tools in bone densitometry, has been designed and constructed for the most common measurement sites, namely the lower forearm, the upper thigh and the abdomen. To ensure universal application of the finished test objects, a survey of the relevant anatomical dimensions was performed at University College and Middlesex School of Medicine anatomy department. The dimensions of the various tissues closely approximate the corresponding tissues within a healthy, adult subject of average size. The requirement of realistic phantoms is that the dimensions, attenuation and density of the various tissues are similar to those of a standard adult subject. Another condition included within the design of the phantoms was for the shapes of the various tissues to be simplified for ease in construction and to avoid complicating the use of the phantoms. Symmetrical shapes, in particular those with circular symmetry, are used where possible to minimize errors in the repositioning of the phantoms in the machine. This approach has been used in previous phantoms for CT evaluation (White et al, 1981) and has proved very successful. Symmetrical tissue models are used without compromising the shape and dimensions of the tissues as shown in the phantoms of the lower forearm and upper thigh (see Figs 1, 4).

The anthropomorphic phantoms can be used to simulate a patient at various stages of osteoporosis by using removable bone inserts of the same dimensions but with varying densities. The ability of a densitometer to distinguish small differences in bone mineral content can thereby be assessed.

The lower forearm phantom

The lower forearm, in particular the radius at mid and distal positions, is the site commonly measured in SPA. The mid-radius (> 95% cortical bone) provides a measurement of cortical bone and the distal radius (~ 75% cortical bone) indicates the state of total bone. Many SPA machines provide a routine for correct

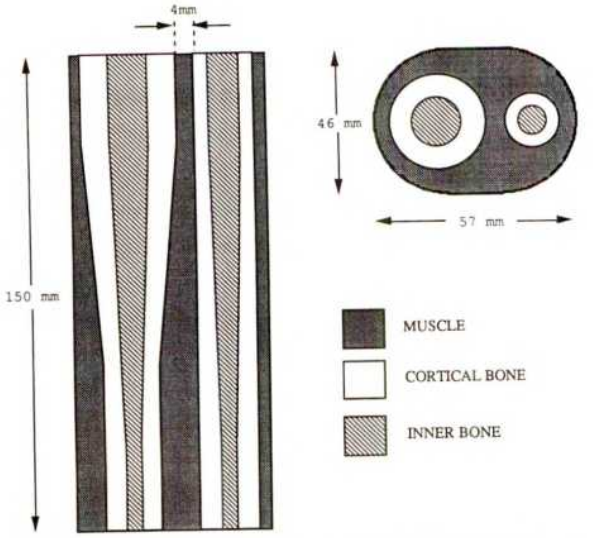

Figure. 1. Top view and cross-section of the lower forearm phantom. The radius is to the left and the ulna to the right.

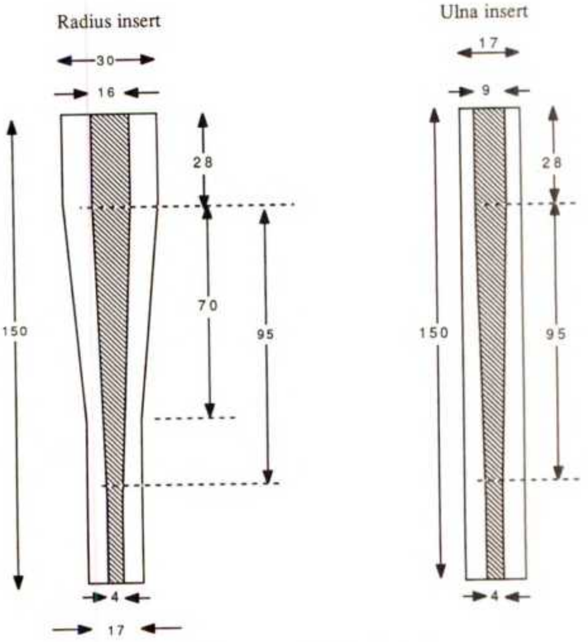

(All dimensions are in millimetres)

Figure 2. Longitudinal cross-sectional views of the radius and ulna inserts showing the dimensions of each. The transverse cross-sections of both inserts are circular throughout the length.

repositioning of the measurement site by scanning the forearm in search of a particular separation of the radius and ulna (commonly 6 or 8 mm). Therefore the important factors that should be incorporated within the design of the forearm phantom are the inclusion of the distal and mid-radius positions, correct separation of the radius and ulna bone models throughout their lengths, and the relative proportions of inner and outer bone at each site.

The design of the lower forearm phantom is shown in Figs 1 and 2. The radius and ulna are fabricated as removable inserts consisting of an outer cortical shell containing inner bone (a homogeneous tissue with the average properties of trabeculae filled with marrow). The variation that has been observed in these two bone components has been incorporated in a set of inserts to simulate changes that occur in women from normal to 2–4 years of progressive osteoporosis. The density changes are:

1. Insert 1: normal density values of inner and outer bone.
2. Insert 2: 2.5% reduction in cortical density, 3% reduction in inner bone.
3. Insert 3: 4% reduction in cortical density, 4.8% reduction in inner bone.

The phantom is elongated at either end so that the distal and mid-radius positions, at which measurements are often made, do not occur at the edge of the phantom.

The outer dimensions (*i.e.* cortical bone dimensions) of the radius and ulna bone models (Fig. 2) were taken from a study of 20 cross-sections of adult anatomical samples. The dimensions of the inner, medullary cavity were calculated assuming that the radius is 95% cortical bone at mid-radius and 75% cortical bone at the distal position. The same relative percentages were assumed for the ulna.

The surrounding tissue is taken to be muscle tissue. Other tissues present, such as adipose or blood vessels were assumed to be small components and their properties do not differ significantly from muscle to warrant inclusion. The outer dimensions of the finished phantom were taken from the mean values of 20 female wrists. The variation in soft-tissue thickness over this region would serve only to complicate the phantom without contributing significantly to the phantom requirements. A photograph of the finished wrist phantom is shown in Figure 3.

The upper thigh phantom

Bone remodelling in the femoral neck correlates well with other skeletal regions. For this reason, as well as it having high fracture risk in osteoporotics, it is a region often chosen for bone measurement. DPA and QCT are able to account for the overlying soft-tissue thickness and hence can use this site.

Repositioning errors are a problem in these two techniques, so simple, symmetrical shapes are required, although the ability to introduce asymmetry in order to test the system response is also important. These requirements are fulfilled by the upper thigh phantom shown in Figs 4 and 5. The diameter of the outer adipose layer was taken as the average from a sample of seven adult females. The effect of soft-tissue thickness

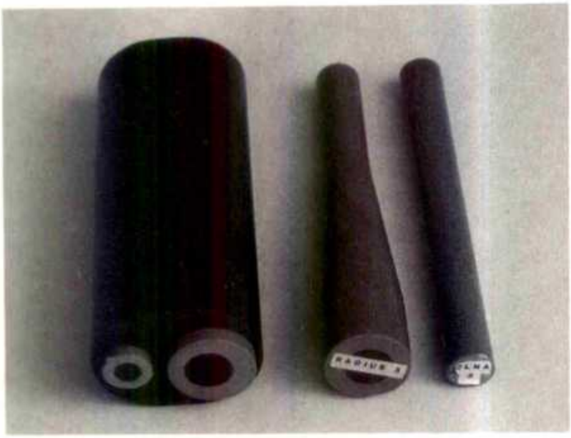

Figure 3. The lower forearm phantom.

and asymmetry can be investigated by enclosing the phantom in a non-concentric sleeve of soft-tissue material. The cortical and trabecular bone models (Fig. 5) were taken from the work of Woodard and White (1982). The femoral neck is mainly trabecular bone filled with marrow and therefore it is this section that is made replaceable. The variation in the cortical shell was assumed to not represent a significant effect owing to the proportion of the bone it occupies. A set of inner bone models of varying densities was developed to provide changes in bone mineral content from a normal value to a 10.5% decrease. Reductions in density much below this value are difficult to manufacture. This is due to the volume of microspheres preventing the mixture behaving as a liquid that is essential for mixing and moulding. Figure 6 shows the components of the completed femoral neck phantom.

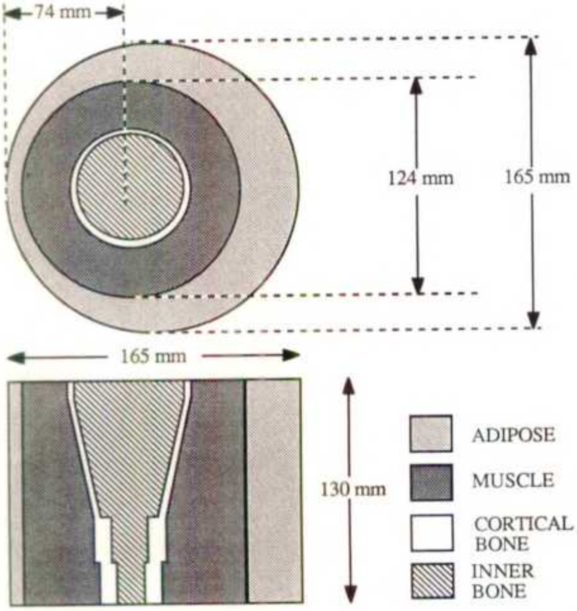

Figure 4. Top view and cross-section of the upper thigh phantom.

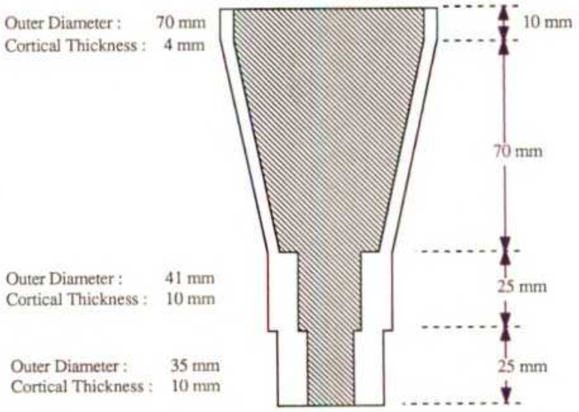

Figure 5. The femoral neck bone models (described by Woodard & White, 1982).

The abdomen phantom

The lumbar vertebrae from L1 to L3 enclosed within the abdomen is a region of great clinical interest within the study of bone disease. Osteoporosis is commonly recognized by vertebral crush fractures, and so this site is often measured for diagnosis. As with measurement of the femoral neck, the spine is measured by techniques that can account for the overlying soft-tissue thickness.

The abdomen is a very complex region of the body encompassing a large range of tissues of intricate shapes, thus presenting problems in the design of a realistic body phantom. However, a study of the properties of the tissues in this region showed that some tissues have similar density and attenuation and so can be grouped together as one tissue for the purposes of building the phantom. This greatly reduces the number of tissue types that need to be simulated. The substitute materials eventually made were muscle, adipose, cortical and trabecular bone, liver, kidney, gut, pancreas and a blood/fat mixture used to simulate the central group of

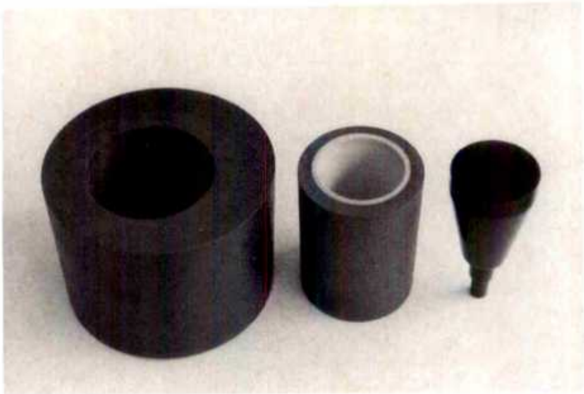

Figure 6. The femoral neck phantom.

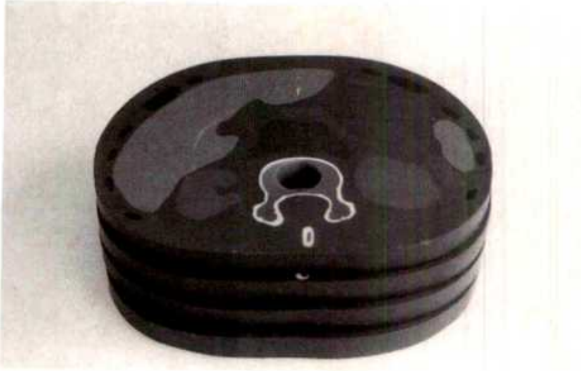

Figure 7. The abdomen phantom.

arteries (namely the aorta). Furthermore, slight simplification of the shapes of each of the tissues made the phantom easier to construct and reduced the effect of repositioning errors. For each of the organs a slab of the relevant material was made, from which the simplified organ shape was cut. These were arranged in the correct anatomical positions and the connective tissue (adipose and muscle) poured to produce a solid slab. These were then machined to size.

Owing to the extreme difficulties of building a three-dimensional (3-D) phantom of this region, four thin layers have been used to create a solid structure, each layer representing the anatomical dimensions at a particular location as imaged with a CT-type investigation within an average, adult subject. Correct positioning of the four slices provides a "3-D" simulation. When used, care must be taken to ensure that slab interfaces are inclined to the radiation beam at small angles to avoid the effects of the slice edges. Figure 7 shows the completed phantom, which consists of four 2.5 cm thick slices to form a total 10 cm thick abdominal section. The anatomical shapes and dimensions at each of these layers were given by Koritke and Sick (1983). Different degrees of osteoporosis are simulated by replacing the rod of inner bone passing down the vertebral column. The rod represents the inner bone section and was designed to allow changes from normal values to a 10% decrease.

Tissue substitute materials

The materials used to construct these phantoms are epoxy-resin-based tissue-substitute materials (White et al, 1977). The material consists of an epoxy resin base (namely Araldite with a suitable hardener) into which particulate fillers, such as polyethylene, calcium carbonate, PVC, etc., are added to produce the density and attenuation values of the required tissue. To ensure quality control of material production, all constituents were dispensed to ±0.2% by weight prior to mixing. For construction of the body cross-sections, individual tissues were produced in slabs. These were checked for homogeneity. The density and attenuation properties of the substitutes provide a close approximation to the tissue simulated; furthermore, Hardie-Brown et al (1987) reported the degree of scatter from these substitutes to be a good approximation to that of the real tissues.

Table I. The percentage weights of the constituents for both healthy and low-density bone substitute materials. CB1 is a medium-viscosity epoxy resin system consisting of 100 parts by weight Araldite MY750 and 60 parts by weight Synolide 960. PVC is polyvinyl chloride, and PMS is phenolic microspheres of specific gravity 0.2 and mean particle size 50 μm. Density measurements were made to ±0.5%

Tissue	Percentage weights of constituents	Density (g/cm^3)
Inner bone 1	CB1 (75.17); PVC (24.83)	1.18 (healthy)
Inner bone 2	CB1 (74.61); PVC (24.83); PMS (0.56)	1.15 (~ 2% drop)
Inner bone 3	CB1 (74.05); PVC (24.83); PMS (1.12)	1.13 (~ 4% drop)
Inner bone 4	CB1 (73.42); PVC (24.83); PMS (1.75)	1.11 (~ 6% drop)
Inner bone 5	CB1 (72.90); PVC (24.83); PMS (2.27)	1.09 (~ 8% drop)
Inner bone 6	CB1 (72.12); PVC (24.83); PMS (3.05)	1.06 (~ 10% drop)

The formulae used for the inner bone and cortical bone tissue substitutes to represent healthy bone (*i.e.* normal-density bone) were taken from White et al (1977). To produce the osteoporotic bone substitutes (*i.e.* low-density bone), specific quantities of phenolic microspheres (PMS) were added to the mixture for healthy bone. PMS is a powder made of hollow, gas-filled spheres having a low density of ~ 0.2 g/cm^3. A small quantity of this material, when added to the mixture, can reduce the density by a suitable amount.

Table I shows the percentage weights of the chemical constituents required to produce the substitutes to simulate both healthy and osteoporotic bone.

Conclusions

A series of phantoms for use in the evaluation of accuracy and precision in any bone densitometer have been designed and built. The design criteria have included the tissue types to be simulated, the geometry of suitable phantoms, the sites at which clinical measurements are made and the degradation in bone tissue that is encountered in osteoporosis. Three phantoms have been built: the lower forearm, the lumbar spine and the neck of the femur. Each phantom correctly simulates the anatomical site but at the same time allows reproducible results both in the positioning of the phantom and in the simulation of a given bone density. The bone elements are replaceable, solid tissue substitutes that do not suffer from the problems associated with the use of liquid bone substitutes such as K_2HPO_4.

References

CANN, C. E., GENANT, H. K., KOLB, F. O. & ETTINGER, B., 1985. Quantitative computed tomography for prediction of vertebral fracture risk. *Bone*, *6*, 1–7.

HARDIE-BROWN, D., LILLICRAP, S. C. & SCOTT, J., 1987. Phantom materials for photon-scattering measurements. *Physics in Medicine and Biology*, *32*, 1175–1178.

KORITKE, J. G. & SICK, H., 1983. In *Atlas of Sectional Human Anatomy* (Urban and Schwarzenberg, Munich), pp. 255–281.

MAZESS, R. B., 1982. On aging bone loss. *Clinical Orthopaedics and Related Research*, *165*, 239–252.

SPELLER, R. D., ROYLE, G. J. & HORROCKS, J. A., 1989. Instrumentation and techniques in bone density measurement. *Journal of Physics E. Science and Instrumentation*, *22*, 202–214.

WHITE, D. R., MARTIN, R. J. & DARLISON, R., 1977. Epoxy resin based tissue substitutes. *British Journal of Radiology*, *50*, 814–821.

WHITE, D. R., SPELLER, R. D. & TAYLOR, P. M., 1981. Evaluating performance characteristics in computerized tomography. *British Journal of Radiology*, *54*, 211–229.

WOODARD, H. Q. & WHITE, D. R., 1982. Bone models for use in radiotherapy dosimetry. *British Journal of Radiology*, *55*, 277–282.

1992, *The British Journal of Radiology*, 66, 1035–1038

Case reports

Segmental reversal of intrahepatic portal flow due to a liver metastasis

By Riwa Kishimoto, MD, *Kiyoshi Choji, MD, *Tarik F. Massoud, FRCR, Shin-ichi Matsuoka, MD, Minhua Chen, MD, Nobuyuki Fujita, MD and Goro Irie, MD

Department of Radiology, Hokkaido University School of Medicine, Sapporo, Japan, and *Department of Clinical Radiology, John Radcliffe Hospital, Oxford, UK

(*Received 8 November 1991 and in revised form 28 April 1992, accepted 22 June 1992*)

Keywords: Liver neoplasms, Angiography, Doppler ultrasound, Portal vein

Case report

A 60-year-old woman who had a Dukes C colonic adenocarcinoma resected four years previously presented with malaise, hepatomegaly and elevated serum tumour markers. Her radiological investigations included liver ultrasonography, computed tomography (CT) (Fig. 1), and magnetic resonance imaging. These revealed a 6 cm solitary metastasis mainly in the right lobe (segments S8 and S4) not extending to the porta hepatis. The tumour compressed the inferior vena cava (IVC) and the right hepatic vein. No portal vein thrombosis was demonstrated. Angiography was performed prior to surgical removal of the tumour. The portal phase of a selective superior mesenteric arteriogram unexpectedly revealed abrupt "cut-off" of the main right portal branch at the porta hepatis, and no portal branches were demonstrated within the right lobe of the liver (Fig. 2). A selective common hepatic arteriogram demonstrated the tumour blush in the upper part of the right lobe of the liver as well as a faint blush-like impression of the main branch of the right portal vein in the late phase.

In view of these portal venographic appearances, a duplex ultrasonographic examination was performed for further assessment (Fig. 3a). Due to the patient's abdominal discomfort, she was most at ease whilst lying supine with her knees flexed. In this position, normal flow in all the hepatic veins as well as the intrahepatic portal branches was observed (Fig. 3b). However, when the patient extended her knees fully the haemodynamics altered. Thus, temporary flow reversal was seen within the right hepatic vein (Fig. 3c) and the right portal branches including the main right portal trunk at the porta hepatis. During this period the normal pulsatile flow within the right hepatic vein was replaced by continuous flow characteristic of the portal system. This flow pattern returned to normal when the patient adopted the flexed knee position. Normal flow was present in the left portal branches and in the left and middle hepatic veins.

Address correspondence to Dr R. Kishimoto, Department of Radiology, Hokkaido University School of Medicine, N-15, W-7, Kita-ku, Sapporo 060, Japan.

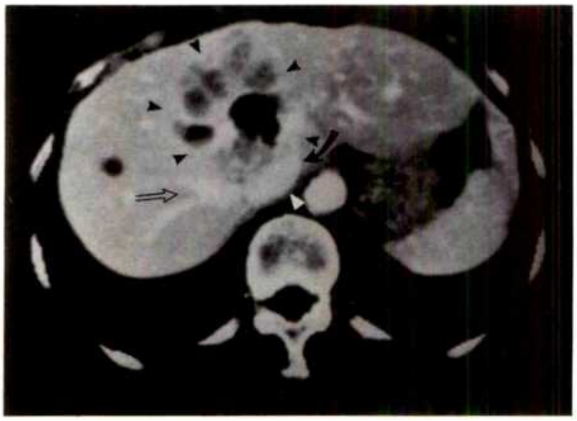

Figure 1. Liver CT. CT following intravenous enhancement. An inhomogeneously enhancing mass (black arrowheads) was seen attached to the IVC (white arrowhead), the right hepatic vein (open arrow) and the middle and left hepatic vein trunk (curved arrow). The middle and left hepatic vein trunk was compressed.

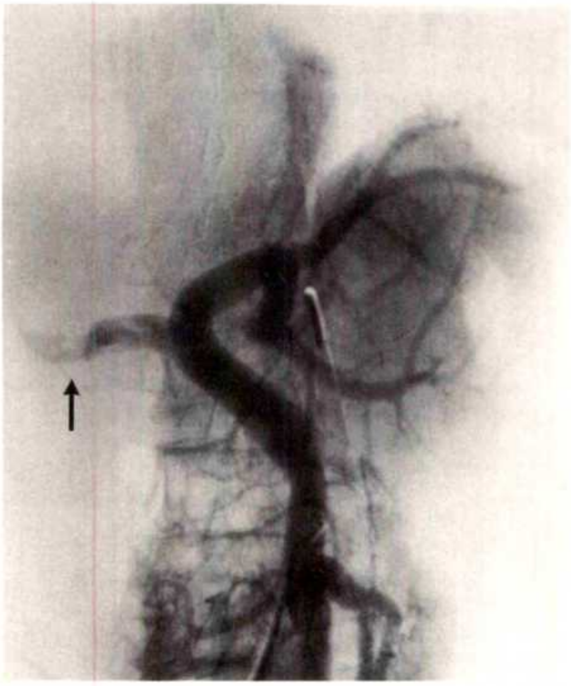

Figure 2. Presurgical portography. A superior mesenteric portogram showed an abrupt cut-off of the main right portal branch (arrow).

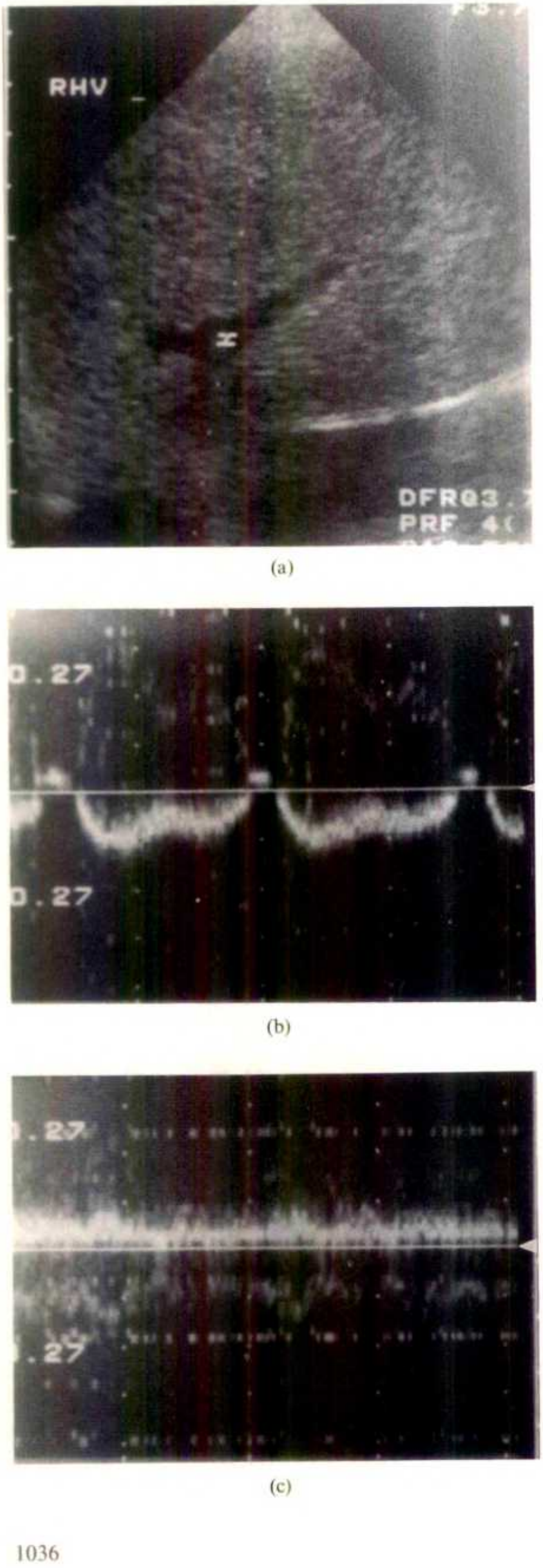

(a)

(b)

(c)

Further assessment of the venous circulation within the right lobe of the liver was undertaken by digital subtraction venography of the IVC. This confirmed the tumour compression of the IVC and the right hepatic vein. It also outlined the extent of intrahepatic venous flow reversal with the patient in the extended knee position. Thus reflux was observed from the IVC and the right hepatic vein at the tumour periphery mainly to the left hepatic vein via intrahepatic venous collaterals (Fig. 4a) and partly to the right portal branches, emptying into the left hepatic vein (Fig. 4b). Blood within the left hepatic vein emptied into the IVC proximal to the tumour.

An extended right hepatectomy was performed with complete removal of the tumour. The patient remains well 14 months after surgery.

Discussion

The liver offers a moderate amount of resistance to blood flow from the portal system to the vena cava. As a result, the pressure in the portal vein averages 10 mmHg, which is considerably higher than in the IVC, which is almost zero pressure. Because of this high portal venous pressure, the pressures in the portal vessels and capillaries have a much greater tendency to become abnormally high than is true elsewhere in the body (Guyton, 1976). As flow rate is determined by the ratio of pressure and resistance, circumstances leading to increased resistance may ultimately lead to reversal of blood flow from a normally hepatopetal to a hepatofugal direction. Several causes of portal venous flow reversal have been described. Extrahepatic conditions include congestive cardiac failure (Diebold et al, 1983; Smith et al, 1985; Hosoki et al, 1990; Duerinckx et al, 1990), Budd-Chiari syndrome (Mathieu, 1990), and large retroperitoneal tumours (Mathieu, 1990). Intrahepatic conditions include portal hypertension (Moreno et al, 1967; Okuda et al, 1973), hepatic venocclusive disease (Brown et al, 1990), fistulas from the hepatic artery to the portal vein (congenital or acquired) (Okuda et al, 1977), tumours (especially hepatomas) (Okuda et al, 1973, 1977), and hepatic haematoma/contusion (Mathieu, 1990). Depending on the part of the liver involved and the source of increase in portal venous resistance, the flow reversal may be global or segmental. In the case we present, we observed segmental flow reversal in the portal vein branches due to a large solitary liver metastasis that did not invade adjacent vessels. We believe this is a previously undocumented cause of alteration in portal venous haemodynamics.

The haemodynamic mechanisms involved in

Figure 3. Duplex sonography. (a) Right intercostal scan. The sampling point is in the right hepatic vein. (b) Examination in flexed knee position. Normal flow directions and patterns were observed. The base-line of the flowmetry is shown by a white line with a white arrowhead in Figs 3b and 3c. (c) Examination in extended knee position. Reversal of the flow direction was noted. The Doppler flow pattern in the right hepatic vein became continuous, similar to that of the normal portal vein. Doppler flowmetry from the right portal branches, also with the knee extended showed continuous and reversed flow.

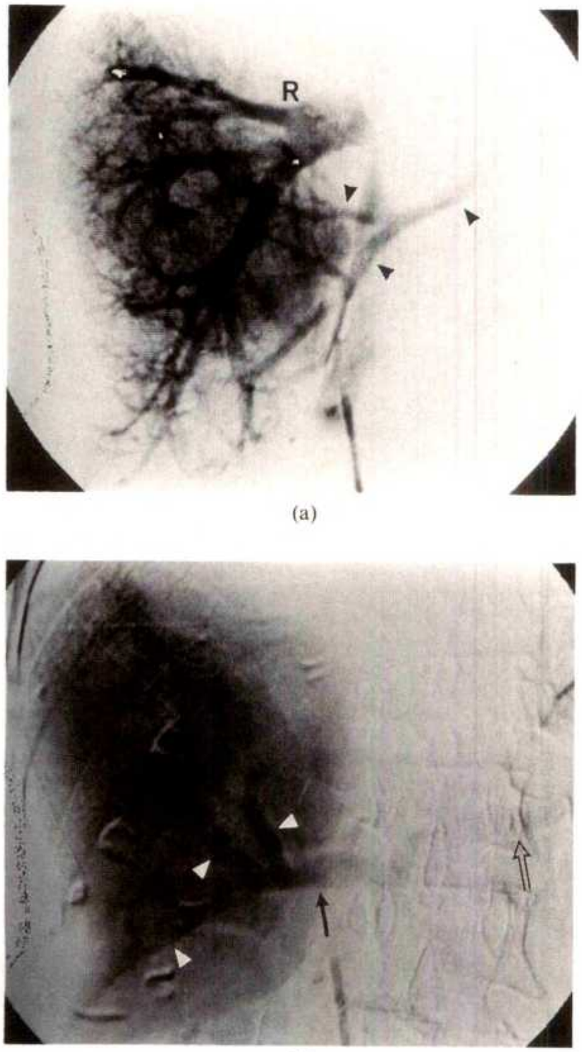

(a)

(b)

Figure 4. Digital subtraction venography of the IVC. The catheter was placed in the IVC distal to the lesion. (a) There was filling of the right hepatic vein (R) as well as short branches of the hepatic vein, due to reversed flow from the IVC. Diversion of the contrast material in the right hepatic vein (R) to the left hepatic vein (arrowheads) was noted. A filling defect due to tumour compression was seen in the IVC at the junction with the hepatic veins. (b) Late phase. Intrahepatic branches of the right portal vein (arrowheads) as well as the right main branch of the portal vein at the porta hepatis (arrow), which were not seen on superior mesenteric portography (Fig. 2), were clearly demonstrated. Furthermore, the left portal vein was faintly opacified (open arrow).

segmental reversal of intrahepatic portal flow have been considered by Mathieu (1990). Intrahepatic lesions may at times produce compression of the surrounding venous bed severe enough to result in interruption of the portal inflow to this area. As a result, hepatic arterial flow increases to compensate for the loss of portal flow. Intrahepatic arterioportal communications develop that allow the arterial blood to flow back through portal veins once the obstruction has become too tight. When the reversed portal flow reaches a collateral portal vein with normal inflow into nondiseased hepatic territory, it drains through this portal branch in a hepatopetal direction. This portal flow reversal is a haemodynamic phenomenon that can result from any obstruction of the hepatic venous bed. As in our case, involvement of hepatic veins close to a hepatic tumour can give rise to a segmental postsinusoidal obstruction.

Imaging modalities that may provide information regarding the portal venous system include angiography and duplex sonography. Both techniques have certain intrinsic limitations. Angiography can yield anatomical information but cannot measure detailed flow rate and the direction of flow is sometimes difficult to establish when insufficient contrast is present. Duplex sonography, on the other hand, can determine relative flow rates and definite direction but only in the limited area under examination. Dynamic CT, providing segmental studies of the phases of arterial and portal parenchymal enhancement, may also be of some value.

Angiographically, a stagnant portal system may be suggested if minimal forward portal flow is documented on portography, along with retrograde flow following coeliac or superior mesenteric arteriography (Okuda et al, 1973). Such stagnation as observed in our patient, leading to "cut-off" of the right intrahepatic portal venous branch on the superior mesenteric portogram, is reminiscent of changes seen in portal tumour thrombosis. It is of interest to note that angiographically there was no evidence of invasion of either the IVC or the right hepatic vein by the tumour in our case, suggesting either the presence of sufficient compliance in these veins to allow external compression by the adjacent tumour, or else involvement of hepatic sinusoids and venules by tumour while the larger veins remain patent (Mathieu, 1990). These changes are unlike those due to hepatoma, where arterioportal shunting is most commonly due to tumour invasion of the portal vein identified angiographically as tumour thrombus. In that case perivenous and peribiliary arterial plexi supply the tumour thrombus, thus creating a shunt with the venous lumen, leading to portal flow reversal (Morse et al, 1985).

Provided an adequate tracing can be obtained, duplex sonography is accurate in determining the direction of portal flow (Nelson et al, 1987). The normal portal vein and its branches show almost continuous flow except for some increase during inspiration (Smith et al, 1985). Moreover, normal portal venous flow varies in the same individual, increasing after a meal (Madjar et al, 1985), and decreasing after exercise and in the upright portion (Ohnishi et al, 1985). Reversed or "to and fro" flow in the portal vein is abnormal and is encountered in those conditions outlined previously. Interestingly, the change in direction of flow seen on duplex sonography in our patient following the change in knee position suggests that mechanical compression of liver parenchyma by the anterior abdominal wall was contributory to these altered haemodynamics. This mechanism remains speculative but may be similar to that suggested previously for reduced portal flow with posture change (Moreno et al, 1967; Okuda et al, 1973; Ohnishi et al, 1985), and due to huge retroperitoneal tumours externally compressing liver parenchyma and vessels (Mathieu, 1990).

References

Brown, B. P., Abu-Yousef, M., Farner, R., LaBrecque, D. & Gingrich, R., 1990. Doppler sonography: a noninvasive method for evaluation of hepatic venocclusive disease. *American Journal of Roentgenology*, *154*, 721–724.

Diebold, B., Touati, R., Blanchard, D., Colonna, G., Guermonprez, J. L., Peronnean, P., Forman, J. & Maurice, P., 1983. Quantitative assessment of tricuspid regurgitation using pulsed Doppler echocardiography. *British Heart Journal*, *50*, 443–449.

Duerinckx, A. J., Grant, E. G., Perrella, R. R., Szeto, A. & Tessler, F. N., 1990. The pulsatile portal vein in cases of congestive heart failure: correlation of duplex Doppler findings with right atrial pressures. *Radiology*, *176*, 655–658.

Guyton, A. C., 1976. The systemic circulation. In: *Textbook of Medical Physiology*, 5th edn., ed. by A. C. Guyton (W. B. Saunders, Philadelphia), p. 375.

Hosoki, T., Arisawa, J., Marukawa, T., Tokunaga, K., Kuroda, C., Kozuka, T. & Nakano S., 1990. Portal blood flow in congestive heart failure: pulsed duplex sonographic findings. *Radiology*, *174*, 733–736.

Madjar, H., Gill, R. W., Griffiths, K. A. & Kossoff, G., 1985. Liver function tested by pulsed Doppler measurements of portal venous flow fasting and following a standard meal. In: *Proceedings of the 4th meeting of the World Federation of Ultrasound in Medicine and Biology*, ed. by R. W. Gill and M. J. Dadd (Pergamon Press, Sydney), p. 70.

Mathieu, D., 1990. Dynamic CT in hepatic vascular disorders. In: *Gastrointestinal Radiology Reviews*, Vol. 1, ed. by H. Herlinger & A. Megibow (Dekker, New York), pp. 67–120.

Moreno, A. H., Burchell, A. R., Rousselot, L. M., Panke, W. F., Slafsky, F. & Burke, J. H., 1967. Portal blood flow in cirrhosis of liver. *Journal of Clinical Investigation*, *46*, 436–445.

Morse, S. S., Sniderman, K. W., Galloway, S., Rapoport, S., Ross, G. R. & Glickman, M. G., 1985. Hepatoma, arterioportal shunting, and hyperkinetic portal hypertension: therapeutic embolization. *Radiology*, *155*, 77–82.

Nelson, R. C., Lovett, K. E., Chezmar, J. L., Moyers, J. H., Torres, W. E., Murphy, F. B. & Bernardino, M. E., 1987. Comparison of pulsed Doppler sonography and angiography in patients with portal hypertension. *American Journal of Roentgenology*, *149*, 77–81.

Ohnishi, K., Saito, M., Nakayama, T., Iida, S., Nomura, F., Koen, H. & Okuda, K., 1985. Portal venous hemodynamics in chronic liver disease: effects of posture change and exercise. *Radiology*, *155*, 757–761.

Okuda, K., Moriyama, M., Yasumoto, M., Jinnouchi, S., Shimokawa, Y., Nakayama, T., Kanda, Y., Fukuyama, Y., Musha, H., Kuratomi, S. & Nakashima, T., 1973. Roentgenologic demonstration of spontaneous reversal of portal blood flow in cirrhosis and primary carcinoma of the liver. *American Journal of Roentgenology*, *119*, 419–428.

Okuda, K., Musha, H., Yamasaki, T., Jinnouchi, S., Nagasaki, Y., Kubo, Y., Shimokawa, Y., Nakayama, T., Kojiro, M., Sakamoto, K. & Nakashima, T., 1977. Angiographic demonstration of intrahepatic arterioportal anastomoses in hepatocellular carcinoma. *Radiology*, *122*, 53–58.

Smith, H. J., Groettum, P. & Simonsen, S., 1985. Ultrasonic assessment of abdominal venous return. I. Effect of cardiac action and respiration on mean velocity pattern, cross-sectional area and flow in the inferior vena cava and portal vein. *Acta Radiologica Diagnosis*, *26*, 581–588.

Intrarenal varices mimicking hydronephrosis

By W. Kincaid, FRCR and R. Edwards, MRCP, FRCR

Department of Diagnostic Radiology, Western Infirmary, Glasgow G11 6NT, UK

(*Received 9 January 1991 and in revised form 7 May 1992, accepted 22 June 1992*)

Keywords: Intrarenal varices, Colour Doppler ultrasound

A case of intrarenal varices mimicking hydronephrosis on ultrasound examination is described. This is an important differential diagnosis if intervention is being considered.

Case report

A 20-year-old male with portal hypertension secondary to idiopathic portal vein thrombosis presented with left loin pain. 3 years previously he had a successful end-to-side distal splenorenal shunt. Ultrasound examination was reported as showing a mild left hydronephrosis and multiple splenic varices. Doppler examination was not performed. On intravenous urography the left kidney excreted promptly. There was widespread deformity of the calyces but no dilatation. His pain settled and he was discharged.

The patient presented again 18 months later with increasing left loin pain. The findings on ultrasound examination were typical of a moderate left hydronephrosis (Fig. 1), but on colour Doppler examination the separation of the renal sinus echoes was found to be due to dilated venous channels (Fig. 2). The symptoms were relieved by simple analgesia and to date there has been no alteration in managment.

Address correspondence to W. Kincaid, Department of Diagnostic Radiology, Western Infirmary, Glasgow G11 6NT.

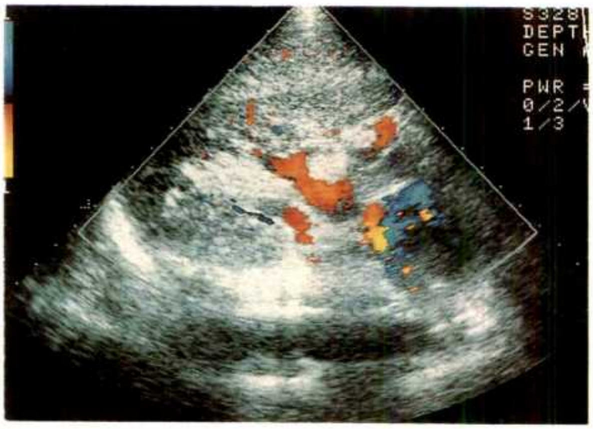

Figure 1. Longitudinal scan of the left kidney showing separation of the renal sinus echoes.

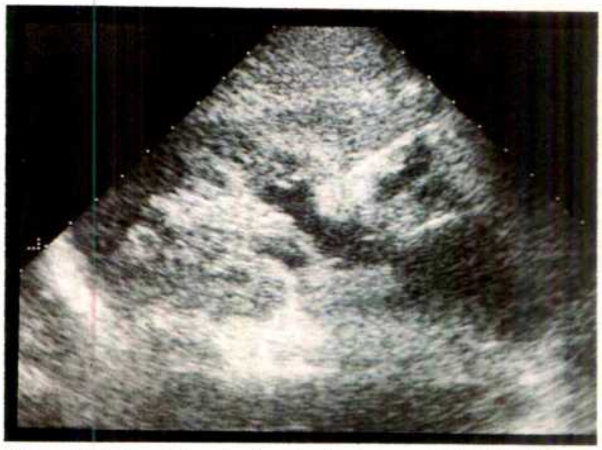

Figure 2. Colour Doppler longitudinal scan of the left kidney showing intrarenal varices.

Discussion

Portal hypertension may result from any process causing increased resistance to portal blood flow into or through the liver or to hepatic venous outflow. Hepatic cirrhosis is the commonest cause. Idiopathic portal vein thrombosis is rare. Patterns of collateral flow in portal hypertension are varied (Doehner et al, 1956). The gastro-oesophageal veins are most frequently involved. In this patient an end-to-side distal splenorenal shunt had been performed for recurrent haematemesis from oesophageal varices. Following successful decompression patent portosystemic collaterals may persist or reappear (Rikkers et al, 1978; Nasbeth et al, 1979; Widrich et al, 1980). Renal collaterals are described but are uncommon. Many entities that may cause a false positive diagnosis of hydronephrosis on ultrasound have been reported. These include a full bladder, increased urine output, renal sinus cysts and vesico-ureteric reflux (Gill & Curtis, 1977; McClennan, 1979; Morin & Baker, 1979; Cronan et al, 1982; Amis & Cronan, 1988). Pericalyceal varices causing filling defects on intravenous urography simulating transitional cell carcinoma have been described in the "nutcracker phenomenon" (Trambert et al, 1990). This is a rare condition of venous hypertension caused by extrinsic compression of the left renal vein between the superior mesenteric artery and the aorta. In our case the calyceal deformity on the intravenous urogram was secondary to extrinsic compression from the varices. Scola et al (1989) reported that in 43 of 100 patients with Grade 1 hydronephrosis on ultrasound, separation of the renal sinus echoes was due to blood vessels mimicking hydronephrosis.

Colour Doppler ultrasound is a valuable non-invasive method for differentiating hydronephrosis from intrarenal blood vessels. It is particularly recommended if any interventional procedure on the kidney is being considered.

References

AMIS, E. S. & CRONAN, J. J., 1988. The renal sinus: an imaging review and proposed nomenclature for sinus cysts. *Journal of Urology*, *139*, 1151–1159.

AMIS, E. S., CRONAN, J. J., PFISTER, R. C. & YODER, I. C., 1982. Ultrasonic inaccuracies in diagnosing renal obstruction. *Urology*, *19*, 101–105

CRONAN, J. J., AMIS, E. S., YODER, I. C., KOPANS, D. B., SINEONE, J. F. & PFISTER, R. C., 1982. Peripelvic cysts: an imposter of sonographic hydronephorisis. *Radiology*, *144*, 149–152.

DOEHNER, G. A., RUZICKA, F. F. JR, ROUSSELOT, L. M. & HOFFMAN, G., 1956. The portal venous system: on its pathological roentgen anatomy. *Radiology*, *66*, 206–217.

GILL, W. B. & CURTIS, G. A., 1977. The influence of bladder fullness in upper urinary tract distension and renal excretory function. *Journal of Urology*, *117*, 573–576.

MCCLENNAN, B. L., 1979. Current approaches to the azotemic patient. *Radiologic Clinics of North America*, *17*, 197–211.

MORIN, M. E. & BAKER, D. A., 1979. Influence of hydration and bladder distension on the sonographic diagnosis of hydronephrosis. *Journal of Clinical Ultrasound*, *7*, 192–194.

NABSETH, D. C., JOHNSON, W. C., WIDRICH, W. C., O'HARA, E. T. & VOLLMAN, R. W., 1979. Splenorenal shunts in portal hypertension. *Journal of Cardiovascular Surgery*, *20*, 201–207.

RIKKERS, L. F., RUDMAN, D., GALAMBOS, J. T., FULENWIDER, J. T., MILLIKAN, W. J., KUTNER, M., SMITH, R. B., 3RD, SALAMN, A. A., JONES, P. J. JR & WARREN, W. D., 1978. A randomised controlled trial of the distal splenorenal shunt. *Annals of Surgery*, *188*, 271–282.

SCOLA, F. H., CRONAN, J. J. & SCHEPPS, B., 1989. Grade 1 hydronephrosis: pulsed Doppler ultrasound evaluation. *Radiology*, *171*, 519–520.

TRAMBERT, J. J., RABIN, A. M., WEISS, K. L. & TEIN, A. B., 1990. Pericalyceal varices due to the nutcracker phenomenon. *American Journal of Roentgenology*, *154*, 305–306.

WIDRICH, W. C., ROBBINS A. H., JOHNSON, W. C. & NABSETH, D. C., 1980. Long term followup of distal spenorenal shunts. *Radiology*, *134*, 341–345.

Transitional cell carcinoma of the bladder associated with Crohn's disease: case report and review of the literature

By *Y. Fujimura, MD, T. Kihara, MD, J. Uchida, MD, K. Hoshika, MD, *I. Sato, MD, †T. Eimoto, MD, Y. Furukawa, MD, ‡A. Sone, MD and §K. Ohashi, MD

Divisions of *Gastroenterology and †Nephrology, Department of Internal Medicine; and Departments of ‡Urology and §Family Practice, Kawasaki Medical School, 577 Matsushima, Kurashiki, Okayama 701–01, Japan

(Received 25 November 1991 and in revised form 12 March 1992, accepted 26 March 1992)

Keywords: Transitional cell carcinoma, Bladder tumour, Crohn's disease, Adolescent

Transitional cell carcinoma of the bladder rarely occurs within the first two decades of life. We report a case of transitional cell cancer of the bladder complicating Crohn's disease and review the relevant literature.

Case report

The patient was a 15-year-old boy admitted to hospital in May 1990 with a fever and diarrhoea of four years' duration. There was no relevant past or family history. On admission, his temperature was 38.2°C and there was tenderness on palpation of the right lower quadrant. Laboratory findings on admission were as follows: white blood cell count was normal, C-reactive protein was 4.2 mg/dl (normal < 0.3 mg/dl), the erythrocyte sedimentation rate was 30 mm/h, albumin was 2.2 g/dl (normal, 3.5–4.5 g/dl), cholesterol was 92 mg/dl (normal, 130–220 mg/dl) and other blood tests were within normal limits. There were 20–25 red blood cells per high-power field in his urine. A chest radiograph was normal. A double-contrast examination of the upper gastrointestinal tract and a barium enema revealed typical Crohn's disease changes involving the ileum and proximal caecum, and a fistulous tract between the ileum and ascending and sigmoid colon. Treatment with total parenteral nutrition and elemental enteral hyperalimentation was commenced.

Two months later, abdomen ultrasound with a full bladder showed an unexpected 1.5 cm papillary tumour localized in the lower right posterior wall of the bladder (Fig. 1). An excretory urogram (Fig. 2) was performed and showed a filling defect. The tumour was resected at cystoscopy and shown to be a finger-like papillary tumour with a stalk (Fig. 3). The pathological finding was a Grade II transitional cell carcinoma

Address for correspondence: Yoshinori Fujimura, MD, Division of Gastroenterology, Department of Internal Medicine,- Kawasaki Medical School, 577 Matsushima, Kurashiki, Okayama 701–01, Japan.

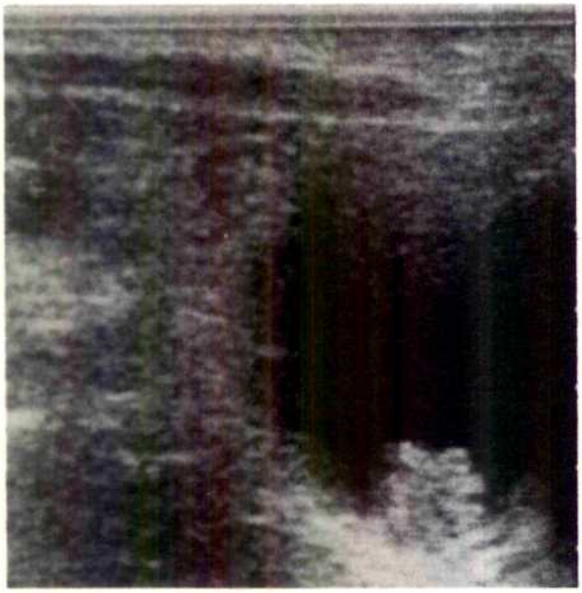

Figure 1. Ultrasonogram of the bladder, showing a papillary tumour.

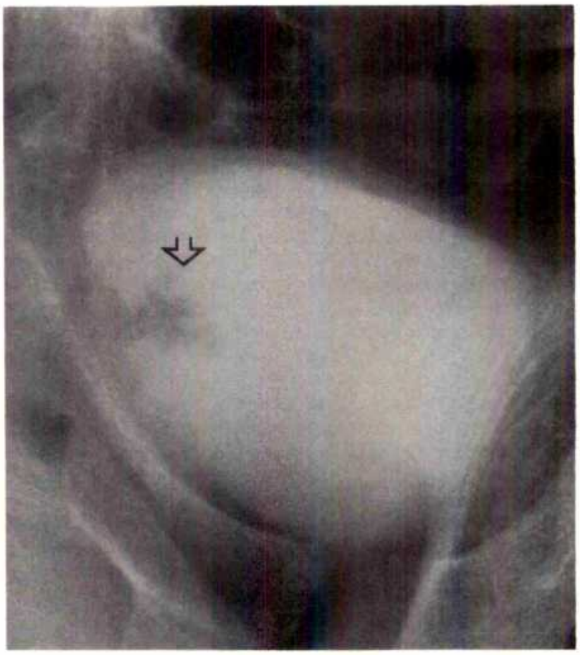

Figure 2. Excretory urography demonstrating a filling defect on the right lateral wall of the bladder (arrow).

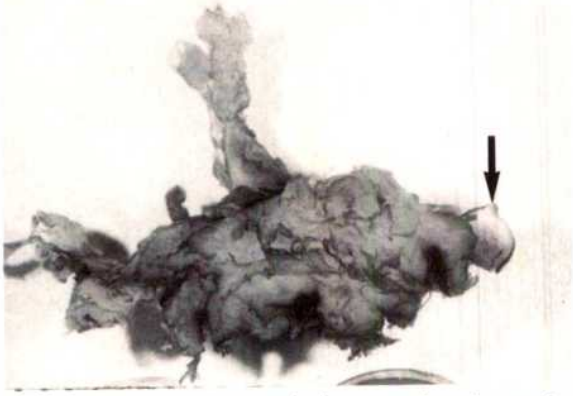

Figure 3. Dissecting micrograph of a resected specimen using transurethral electrocoagulation. A stalk (arrow) is recognized at bottom of the specimen.

without muscular invasion. The stalk was free of tumour. No recurrence was seen on ultrasound and cystoscopy 14 months later.

Discussion

Javadpour and Mostofi (1969) reported that primary epithelial tumour of the bladder in the first two decades of life is rare. Transitional cell carcinoma of the bladder is uncommon in this age group and approximately 100 patients have been described in the literature (Mauermayer et al, 1977; MacCarthy et al, 1979; Benson et al, 1983). The majority of cases presented with macrohaematuria. Our patient had transient and asymptomatic microhaematuria recognized on urinalysis only at admission. Although the diagnosis of bladder tumours is confirmed at cystoscopy, their discovery may be delayed, as in our case, by transient and asymptomatic microhaematuria.

Recently, ultrasound examination as a noninvasive method has been widely used in Japan. In this case, we found a papillary tumour of the bladder on ultrasound examination of the abdomen. Ultrasound may be useful as the initial screening test for patients with haematuria.

Most reports (Mauermayer et al, 1977; MacCarthy et al, 1979; Benson et al, 1983; Lalmand et al, 1988) have indicated that epithelial bladder tumours in children and adolescents are morphologically and clinically benign with favorable prognoses because of both low rate of recurrence and low grade of malignancy. In general, it is considered that potentially carcinogenic predisposing conditions for bladder cancer in the young are cigarette smoking (Benson et al, 1983), schistosomiasis (Brumskine et al, 1977) and unusual exposure to paints, solvents, and chemicals (Benton & Henderson, 1973). However, we found no evidence of these conditions in this case.

It is well known that Crohn's disease may involve the urinary tract and may appear as a mass in the bladder due to compression and invasion by an enlarging intraabdominal abscess. This was not true in this case. Radiographic features mimicking a primary bladder tumour have rarely been reported in Crohn's disease with ileovesical and rectovesical fistulas (Goldstein et al, 1971; Joffe, 1976; Edelman & Sternberg, 1980; Evans, 1990). It should be noted that the inflammatory changes in Crohn's disease closely resemble bladder tumours on radiography and cystoscopy.

Recently, extraintestinal cancers associated with Crohn's disease have been reported. A review of the literature (Fielding et al, 1972; Gyde et al, 1980; Greenstein et al, 1985; Kvist et al, 1986; Madjlessi et al, 1986; Ball et al, 1988; Nakajima et al, 1990) showed reports of extraintestinal cancer complicating Crohn's disease in a total of 96 cases. Our case of transitional cell carcinoma of the bladder complicating Crohn's disease in an adolescent is rare. Although extraintestinal cancers occur at various sites in Crohn's disease, early reports (Gyde et al, 1980; Greenstein et al, 1980, 1981) failed to identify a statistically significant increase of any particular site of cancer in Crohn's disease patients. In 1985, Greenstein et al reported a significant increase in both genito-urinary tumours and reticuloendothelial neoplasms in Crohn's disease. Genito-urinary tumours, especially squamous cell carcinomas of the perianal region and vulva, are thought to be related to long-term chronic irritation and alteration of immune status due to medication with immunosuppressive drugs. Bladder cancer complicating Crohn's disease has been reported in only five cases, including ours, in this review of the literature.

Acknowledgment

We thank Miss H. Nakaishi for typing the manuscript.

References

Ball, C. S., Wujanto, R., Haboubi, N. Y. & Schofield, P. F., 1988. Carcinoma in anal Crohn's disease; discussion paper. *Journal of the Royal Society of Medicine*, *81*, 217–219

Benson, R. C., Jr., Tomeiza, K. M. & Kelalis, P. P., 1983. Transitional cell carcinoma of the bladder in children and adolescents. *Journal of Urology*, *130*, 54–55.

Benton, B. & Henderson, B. E., 1973. Environmental exposure and bladder cancer in young males. *Journal of the National Cancer Institute*, *51*, 269–270.

Brumskine, W., Dragan, P. & Sanvee, L., 1977. Transitional cell carcinoma and schistosomiasis in a 5-year-old boy. *British Journal of Urology*, *49*, 540.

Edelman, M. J. & Sternberg, S. S., 1980. A pseudotumor of the urinary bladder. *Clinical Bulletin*, *10*, 35–37.

Evans, R. H., 1990. Crohn's disease mimicking primary bladder tumour. *British Journal of Urology*, *65*, 299–300.

Fielding, J. F., Prior, P., Waterhouse, J. A. & Cooke, W. T., 1972. Malignancy in Crohn's disease. *Scandinavian Journal of Gastroenterology*, *7*, 3–7.

Goldstein, M. J., Bragg, D. & Sherlock, P., 1971. Granulomatous bowel disease presenting as a bladder tumour. *American Journal of Digestive Disease*, *16*, 337–341.

Greenstein, A. J., Sachar, D. B., Smith, H., Janowitz, H. D. & Aufses, A. H., Jr., 1980. Patterns of neoplasia in Crohn's disease and ulcerative colitis. *Cancer*, *46*, 403–407.

Greenstein, A. J., Sachar, D. B., Smith, H., Janowitz, H. D. & Aufses, A. H., Jr. 1981. A comparison of cancer risk in Crohn's disease and ulcerative colitis. *Cancer*, *48*, 2742–2745.

GREENSTEIN, A. J., GENNUSSO, R., SACHAR, D. B., HEIMANN, T., SMITH, H., JANOWITZ, H. D. & AUFSES, A. H., JR., 1985. Extraintestinal cancers in inflammatory bowel disease. *Cancer*, *56*, 2914–2921.

GYDE, S. N., PRIOR, P., MACARTNEY, J. C., THOMPSON, H., WATERHOUSE, J. A. H. & ALLAN, R. N., 1980. Malignancy in Crohn's disease. *Gut*, *21*, 1024–1029.

JAVADPOUR, N. & MOSTOFI, F. K., 1969. Primary epithelial tumors of the bladder in the first two decades of life. *Journal of Urology*, *101*, 706–710.

JOFFE, N., 1976. Roentgenologic abnormalities of the urinary bladder secondary to Crohn's disease. *American Journal of Roentgenology*, *127*, 297–302.

KVIST, N., JACOBSEN, O., NØRGAARD, P., OCKELMANN, H. H., KVIST, H. K., SCHOU, G. & JARNUM, S., 1986. Malignancy in Crohn's disease. *Scandinavian Journal of Gastroenterology*, *21*, 82–86.

LALMAND, B., AVNI, E. F., SIMON, J., VERHEST, A., SCHULMAN, C. C. & STRUYVEN, J., 1988. Transitional cell papillary carcinoma of the bladder in a child. *Pediatric Radiology*, *17*, 77–79.

MACCARTHY, J. P., GAVRELL, G. J. & LEBLANC, G. A., 1979. Transitional cell carcinoma of the bladder in patients under thirty years of age. *Urology*, *13*, 487.

MADJLESSI, S. H. M., FARMER, R. G. & WEICK, J. K., 1986. Inflammatory bowel disease and leukemia. *Digestive Diseases and Sciences*, *31*, 1025–1031.

MAUERMAYER, W., TAUBER, R. & STEUER, G., 1977. Epitheliale Harnblasentumoren im Kindesalter und beim Jugendlichen. *Urologe (A)*, *16*, 286.

NAKAJIMA, H., MUNAKATA, A. & YOSHIDA, Y., 1990. Extraintestinal cancers in Crohn's disease. *Digestion*, *47*, 1–7.

The Swiss cheese brain

By A. Jackson, PhD, MRCP, FRCR, M. J. Dobson, MB, ChB, MRCP and P. N. Cooper, MA, MRCP

Department of Neuroradiology, Manchester Royal Infirmary, Oxford Rd, Manchester M13 9WL, UK

(Received 15 November 1991 and accepted 12 March 1992)

Keywords: Cysticercosis, Magnetic resonance imaging, Computed tomography

Case report

A 37-year-old Indian man presented with a 6-month history of focal and grand mal convulsions. He had emigrated from India 2 years previously and was working as a chef in a local restaurant. There was no significant past medical history. Initial investigations included a computed tomogram (CT) of his brain (Fig. 1), which demonstrated a number of small enhancing parenchymal lesions with surrounding low-attenuation changes which were attributed to oedema. A magnetic resonance (MR) scan was performed and is illustrated (Figs 2–4).

What are the radiological findings? What is the diagnosis and what other information would you seek to confirm this?

The MR images demonstrate multiple, well-defined lesions throughout the brain, which show a predilection for grey matter. On short repetition time (TR) images the lesions appear as well-defined, low-signal foci (Fig. 2). On long TR images the lesions demonstrate a central nidus ranging from low to high signal and greatly varying degrees of associated oedema (Fig. 3). The lesions show a variable degree of ring enhancement following gadolinium (Fig. 4). Close examination demonstrates a small focus of irregularity in some of the cyst walls particularly on the post-contrast image (Fig. 4, arrows).

These appearances are pathognomonic of neurocysticercosis (Bowen & Post, 1991). The findings of similar cysts within skeletal muscle (Fig. 5) or positive radioimmunoassay of serum or cerebrospinal fluid (CSF) may support the diagnosis. Although they are specific, immunological tests are insensitive (Rodriguez-Carbajal & Boleaga-Duran, 1982) and CT and magnetic resonance imaging (MRI) currently form the most sensitive and specific diagnostic indicator.

Discussion

Neurocysticercosis is an infestation of the central nervous system by *Taenia solium*, the pork tapeworm. Faecal shedding of eggs by the definitive host, man, leads to ingestion of eggs by the intermediate host, usually pig or man. The primary larvae, oncospheres, hatch in the intestine and are distributed haematogenously to the brain and other tissues where they develop into secondary larvae, cysticerci (Marquez-Monter, 1971). Human morbidity results from dead larvae within the central nervous system leading to seizures intracranial hypertension, basal arachnoiditis, focal neurological deficits or dementia (Torrealba et al, 1984).

The use of MRI allows the recognition of live cysts, which has been of great significance since the introduction of effective chemotherapy using praziquantel (Sotelo et al, 1984). The MRI appearances of the cysticerci vary with the stage of development and with the area of involvement, which may be parenchymal, meningeal or ventricular (Carbajal et al, 1977). Parenchymal cysts are found primarily in cerebral grey matter although histologically many cortical cysticerci lie within sulci from which they burrow into the cortex. When a viable larva is present within the cyst, MRI will demonstrate an homogeneous CSF-like intensity on both long and short TR images except for a mural nodule, slightly hyperintense to grey matter on the long TR images, which represents the scolex of the larvae (Suss et al, 1986; Bowen & Post, 1991). In these early stages there is usually no evidence of contrast enhance-

---

Address correspondence to Dr A. Jackson.

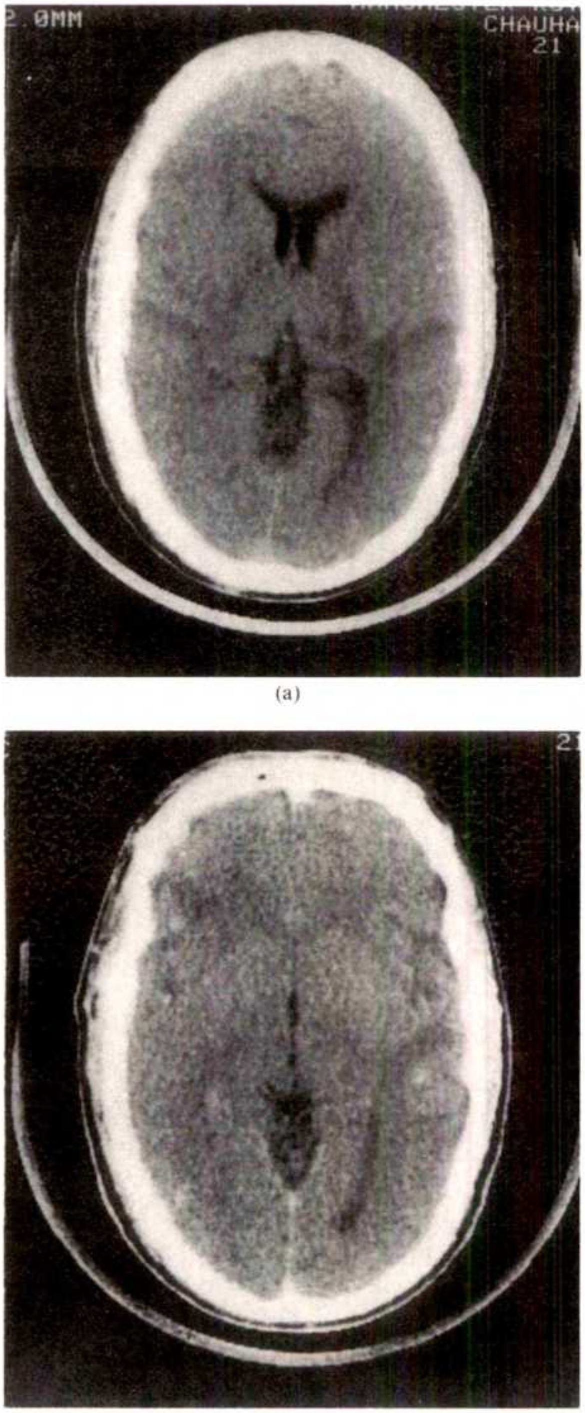

(a)

(b)

Figure 1. (a) Pre- and (b) post-contrast CT scans.

ment in the cyst wall or of surrounding oedema. The appearances of multiple cysts in the brain on short TR images has been likened to "Gruyere (Swiss) cheese" (Rodriguez-Carbajal & Boleaga-Duran, 1982).

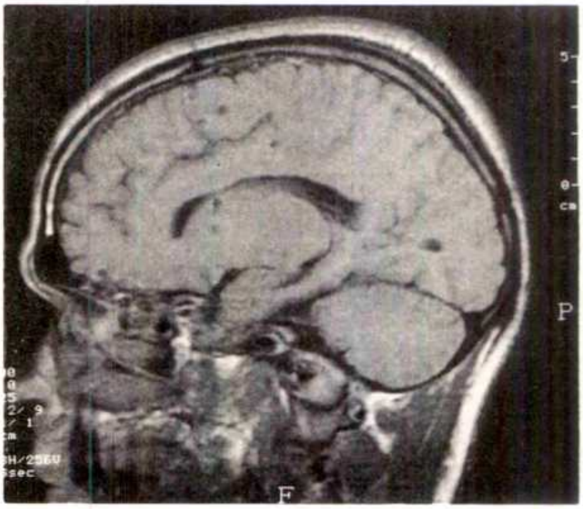

Figure 2. T_1-weighted parasagittal image.

As the larva dies, long TR images show a surrounding rim of hyperintensity representing inflammation and surrounding oedema; the cyst also becomes more hyperintense on long TR images and can become indistinguishable from surrounding oedema. At this stage, short TR images display cyst and mural nodule more

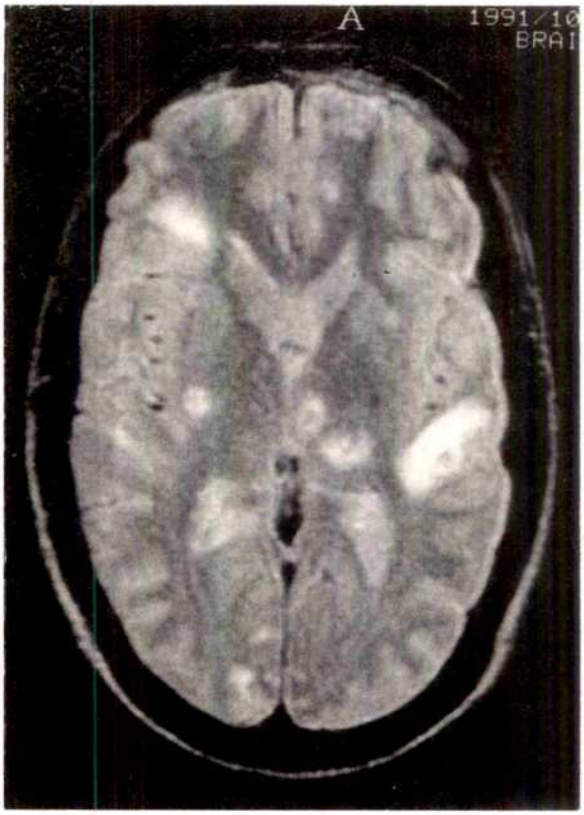

Figure 3. T_2-weighted axial image.

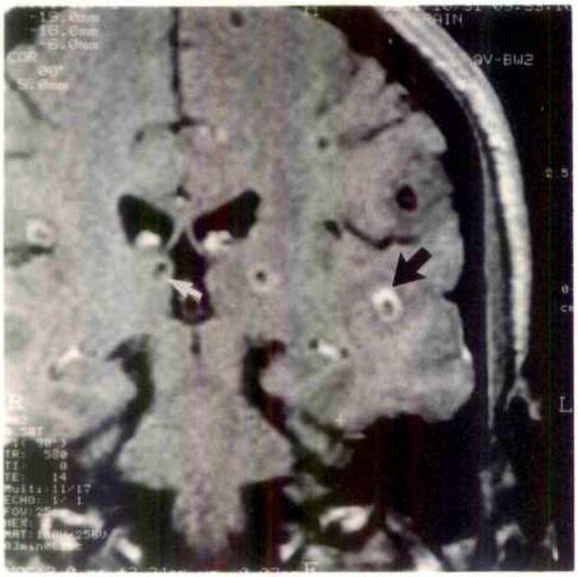

Figure 4. T_1-weighted coronal section following gadolinium.

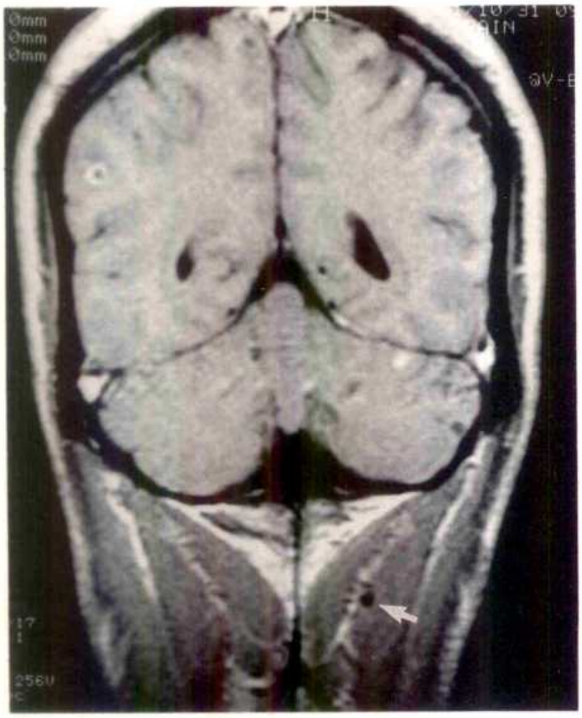

Figure 5. Post-contrast coronal CT scan showing multiple cerebral lesions and a single cystic lesion in the extensor muscles of the neck on the left (arrows).

effectively and will show marked cyst wall enhancement following gadolinium. After the parasite dies and calcifies, MRI may show a focal signal void, particularly on gradient echo images, and a fibrous, enhancing capsule is formed. As the lesion regresses the oedema and surrounding reactive changes reduce but ring enhancement persists. Finally the lesion will cease to enhance and the surrounding brain will return to normal. The time taken for this evolution of imaging appearances varies but is generally about a year (Suss et al, 1986; Bowen & Post, 1991).

CT is superior to MRI in the detection of calcified lesions but is far less sensitive in the detection of early chronic cysticerci, subarachnoid cysts and pericystic oedema (Teitelbaum et al, 1989).

Cysticercus lesions in the basal cisterns may degenerate to form a multilobular "racemose" cyst, several centimetres in diameter. These cysts are most commonly located in the cerebellopontine angle and are associated with extensive granulomatous meningitis of the basal cisterns, which is well demonstrated by MRI (Bowen & Post, 1991).

References

Bowen C. B. & Post, J. D., 1991. Intracranial infection. In *Magnetic Resonance Imaging of the Brain and Spine*, ed. by S. W. Atlas (Raven Press, New York), pp. 530–533.

Carbajal, J. R., Palacios, E. & Azar-Kia, B., 1977. Radiology of cysticercosis of the central nervous system including computed tomography. *Radiology, 125*, 127–131.

Marquez-Monter, 1971. Cysticercosis. In *Pathology of Protozoal and Helminthic Diseases with Clinical Correlation*. (Williams & Wilkins, Baltimore), pp. 592–617.

Rodriguez-Carbajal, J. & Boleaga-Duran, B., 1982. Neuroradiology of human cysticercosis. In *Cysticercosis: Present State of Knowledge and Perspectives*, ed. by A. Flisser, K. Williams, J. P. Laclette, C. Larralde, C. Ridaura and F. Beltran (Academic Press New York), pp. 139–162.

Sotelo, J., Escobedo, F., Rodriguez-Carbajal, J., Torres, B. & Rubio-Donnadieu, F., 1984. Therapy of parenchymal brain cysticercosis wih praziquantel. *New England Journal of Medicine, 310*, 1001–1007.

Suss, R. A., Maravilla, K. R. & Thompson, J., 1986. MR imaging of intracranial cysticercosis: comparison with CT and anatomopathological features. *American Journal of Neuroradiology, 7*, 235–242.

Teitelbaum, G. P., Otto, R. J., & Lin M., 1989. MR imaging of neural cysticercosis. *American Journal of Roentgenology, 153*, 857–866.

Torrealba, G., Del-Villar, S., Tagle P. & Kase, C. S., 1984. Cysticercosis of the central nervous system: clinical and therapeutic considerations. *Journal of Neurology, Neurosurgery and Psychiatry, 47*, 784–790.

1992, *The British Journal of Radiology*, *66*, 1045–1046

Demonstration by computed tomography of a case of internal small bowel herniation

By J. C. Hoeffel, MD, *J. Zimberger, MD, B. Pocard, MD and C. Hoeffel, MD

Department of Radiology, Hôpital Jeanne d'Arc, BP 303, 54201 Toul Cédex, France and *Department of Surgery, Hôpital Bel Air, 57312 Thionville, France

(Received 23 Janaury 1992 and accepted 7 May 1992)

Keywords: Computed tomography, Small bowel hernia, Internal hernia

Internal hernia is a rare condition. We report a case where computed tomography (CT) demonstrated a saclike encapsulation of small bowel loops which suggested a diagnosis of internal hernia.

Case report

A 76-year-old woman presented with abdominal pain and vomiting. Ultrasound examination revealed a 10 cm heterogenous mass posterior to the bladder, close to the ovaries, associated with bilateral hydronephrosis affecting mainly the left side. Contrast-enhanced CT showed a large pelvic mass (Fig. 1), behind the bladder, of fluid density and containing septations. The appearance suggested dilated loops of small bowel. Both ureters were dilated, and a plain film of the abdomen 24 h after injection of contrast medium (Fig. 2) showed marked left hydronephrosis and less severe dilatation of the right renal tract. Forty-eight hours after injection (Fig. 3) the left ureter was still opacified.

At laparotomy a cluster of dilated and congested loops of small bowel were found posterior to the bladder and these were strangulated in the pouch of Douglas. Resection of 50 cm of ileum was necessary, following which the patient made a full recovery.

Histology showed acute ischaemia of the small bowel. Two months after surgery, renal ultrasound showed complete resolution of the left hydronephrosis.

Address for reprints: Dr J. C. Hoeffel, Dept. of Radiology, Hôpital Jeanne d'Arc, BP 303, 54201 Toul, Cédex, France.

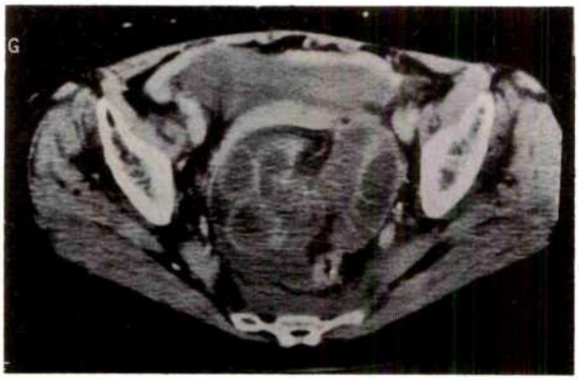

Figure 1. CT of the pelvis after injection of contrast medium showing a huge mass behind the bladder with septa suggesting a cluster of intestinal loops.

Discussion

An internal hernia is a rare condition where herniation of a viscus through a normal or abnormal aperture occurs within the peritoneal cavity.

Three basic forms of hernia through a normal aperture have been described (Jones, 1964). The first is herniation of the small intestine through the foramen of Winslow (53% of cases) and this is termed a paraduodenal henia; it is at least three times more common on the left than on the right and frequently involves only a few small bowel loops which usually reduce spontaneously (Meyers, 1970). The second form is where

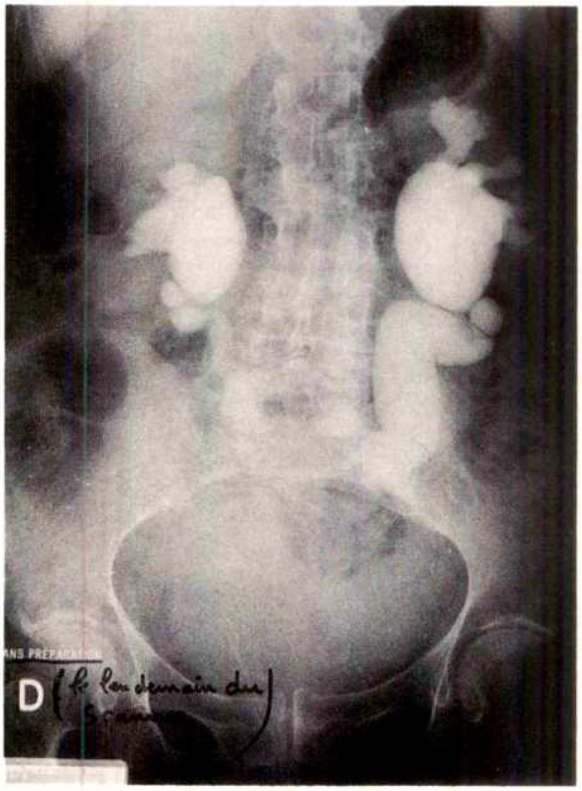

Figure 2. Plain film of the abdomen 14 h after CT showing left hydronephrosis and mild right hydronephrosis.

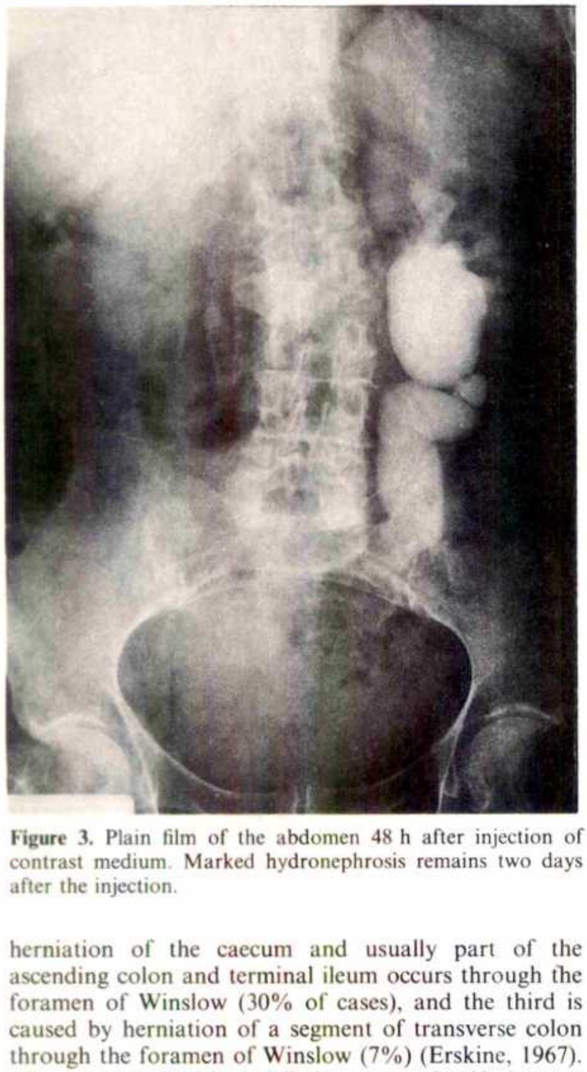

Figure 3. Plain film of the abdomen 48 h after injection of contrast medium. Marked hydronephrosis remains two days after the injection.

herniation of the caecum and usually part of the ascending colon and terminal ileum occurs through the foramen of Winslow (30% of cases), and the third is caused by herniation of a segment of transverse colon through the foramen of Winslow (7%) (Erskine, 1967). The case described here falls into an unclassified group which represent 10% of all internal hernias.

Bates et al (1983) reported a strangulated hernia through the broad ligament causing ureteric obstruction. A 49-year-old housewife presented with a 10-hour history of severe colicky pain of rapid onset in the left loin and left iliac fossa. An intravenous urogram showed obstruction of the left ureter at the pelvic brim. Laparotomy was performed and 30 cm of small bowel was found to have herniated through a defect in the left broad ligament. At the neck of the hernia, the bowel had strangulated and subsequently perforated during reduction. The hernial mass had been compressing the left ureter. The small bowel on either side of the perforation was resected and the Fallopian tube divided to prevent recurrence. A hernia through a defect in the broad ligament is rare. Our case is unique in that it presented with ureteric obstruction.

Cases of ureteral obstruction secondary to other intestinal abnormalities are rare. Ney & Hyman (1954), Lal & Brown (1967), Ravich (1976), Klousia & Belman (1977) and Emmott & Tanagho (1980) reported cases of urinary obstruction and dilatation caused by massive faecal impaction. Siegelbaum & Rabinovich (1988) reported a two-month-old infant with bowel obstruction secondary to a colonic intussusception and Cook (1969) reported on an appendical abscess causing urinary obstruction. Kyosola (1977) also published a case of simultaneous ovarian torsion and gangrenous strangulation of bowel through a congenital opening in the mesosalpinx.

In the case described here, CT was suggestive of an unusual internal hernia by its demonstration of intestinal loops in the pouch of Douglas. Hydronephrosis secondary to compression of the ureters by the cluster of loops is an unusual feature and regressed after surgical correction.

Acknowledgments

The authors would like to thank Dr P. B. Guyer of Southampton (Great Britain) for his help in reviewing the manuscript.

References

BATES, G. J., BENNETT, I. C., FURNIVAL, C. M. & GOUGH, I. R., 1983. A strangulated hernia through the broad ligament causing ureteric obstruction. *Journal of the Royal College of Surgeons of Edinburgh*, *28*, 335.

COOK, G. T., 1969. Appendiceal abscess causing urinary obstruction. *Journal of Urology*, *101*, 212–215.

EMMOTT, R. C. & TANAGHO, E. A., 1980. Ureteral obstruction due to fecal impaction in patient with colonic loop urinary diversion. *Urology*, *15*, 496–497.

ERSKINE, J. M., 1967. Hernia through the foramen of Winslow. A case report of the cecum incarcerated in the lesser omental cavity. *American Journal of Surgery*, *114*, 941–947.

JONES, T. W., 1964. Paraduodenal hernia and hernias of the foramen of Winslow. In: *Hernia*, Ed. by L. M. Nyhus and H. N. Harkins (Lippincott, J. B., Philadelphia) pp. 577–601.

KLOUSIA, J. W. & BELMAN, A. B., 1977. Unilateral hydronephrosis secondary to mid ureteral extrinsic fecal obstruction. *Journal of Urology*, *118*, 107.

KYOSOLA, K., 1977. Simultaneous occurence of ovarian torsion and gangrenous strangulation through a congenital opening in the mesosalpinx. *Annales Chirurgiae et Gynaecologiae (Helsinki)*, *66*, 290–291.

LAL, S. & BROWN, G. N., 1967. Some unusual complications of fecal impaction. *American Journal of Proctology*, *18*, 226–231.

MEYERS, M. A., 1970. Paraduodenal hernias. Radiologic and arteriographic diagnosis. *Radiology*, *95*. 29–37.

NEY, C. & HYMAN, R. M., 1954. Complete urinary retention in the female. *American Journal of Surgery*, *87*, 34–40.

RAVICH, L., 1976. Constipation: a cause of urinary tract obstruction and infection. *Urology*, *7*, 236–237.

SIEGELBAUM, M. H. & RABINOVITCH, H. H., 1988. Hydronephrosis secondary to colonic intussusception. *Urology*, *32*, 421–423.

1992, *The British Journal of Radiology*, *65*, 1047–1048

Caecal herniation through the foramen of Winslow: diagnosis by computed tomography

By M. R. Schuster, MD, R. K. Tu, MD and K. A. Scanlan, MD

Department of Diagnostic Radiology, University of Wisconsin Hospital and Clinics, Clinical Science Center, E3/311, 600 Highland Avenue, Madison, WI 53792–3252, USA

(*Received 7 January 1992 and accepted 12 March 1992*)

Keywords: Internal hernia, Foramen of Winslow, Colon, Computed tomography

Herniation of viscera through the foramen of Winslow comprises 0.08% of all hernias, with caecal involvement in nearly a third (Valenziano et al, 1987). Due to the difficulty in diagnosis, only 10% are diagnosed on plain films prior to surgery (Okhuma & Miyazake, 1977); therefore, other imaging methods are being utilized to assist in the diagnosis. This example of caecal herniation through the foramen of Winslow was diagnosed by dynamic abdominal computed tomography (CT) and its important diagnostic points are reviewed.

Case report

A 64-year-old woman presented with 12-hour history of shortness of breath and chest pain. Vital signs and laboratory studies were normal. The physical examination was normal with the exception of a mildly tympanitic abdomen. A plain radiograph on admission showed an air-filled loop of bowel over the mid-abdomen, thought to represent a dilated loop of colon (Fig. 1).

Two days later, the patient developed increased abdominal pain with an elevated white cell count. An abdominal film showed free intraperitoneal air. Dynamic CT scan with bolus intravenous contrast medium and full bowel opacification with oral contrast medium showed a contrast/gas level in the lesser sac. This was traced to a stretched mesenteric segment passing through the foramen of Winslow. The ascending colon was identified in the subhepatic space and the terminal ileum entered this region via the major hepatic fissure. Free intraperitoneal gas was present (Fig. 2).

The radiographic findings were confirmed at laparotomy. The caecum and terminal ileum were found to have herniated through the foramen of Winslow, and the caecum had perforated near the attachment of the appendix. The entire ascending colon was mobile without the retroperitoneal fixation.

Discussion

Blandin first reported herniation through the foramen of Winslow in 1834 (Blandin, 1834). The terminal ileum, caecum, and right colon were contained within the lesser sac (Harned & Farley, 1974). To date, 138 cases have been reported: 63% of epiploic hernias contained small bowel only, 30% contained terminal ileum and caecum, 7% involved transverse colon, and a few cases of herniation of the gallbladder have been reported (McCrea, 1951; Richardson & Anastopoulos, 1951).

The plain film findings of epiploic herniation of the caecum are: (a) a collection of fluid and gas in the lesser sac displacing the stomach and duodenum to the left; and (b) failure to visualize the caecum in its normal position. The plain film appearance may also suggest a lesser sac abscess (Henisz et al, 1974).

CT is a primary differentiating imaging modality (Wojtasek et al, 1991). The findings are: (a) the presence of mesentery between the inferior vena cava and main portal vein; (b) a collection of gas/fluid in the lesser sac

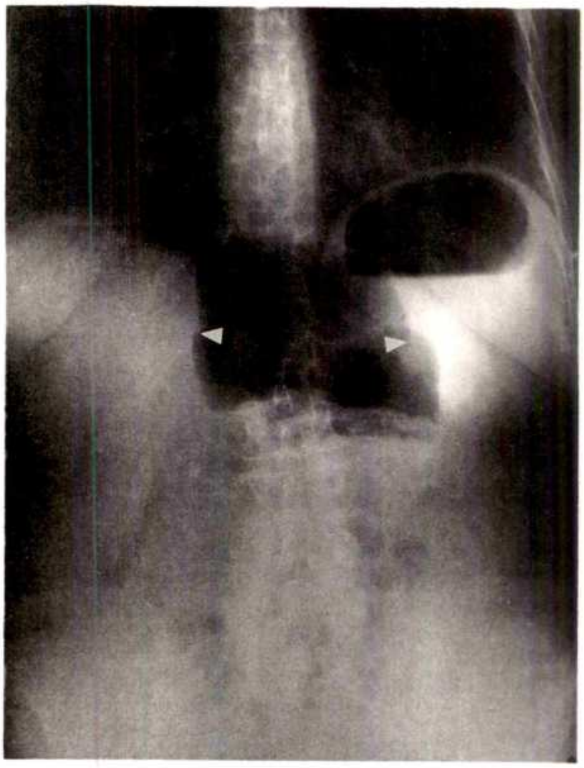

Figure 1. Erect abdominal radiograph. The caecum (arrowheads) is within the lesser sac and projects over the epigastrium. No colonic gas is visualized over the right flank

---

Reprint requests and correspondence to: Kathleen A. Scanlan, MD, Department of Diagnostic Radiology, University of Wisconsin Hospital and Clinics, 600 Highland Avenue E3/311, Madison, Wisconsin 53792–3252 USA.

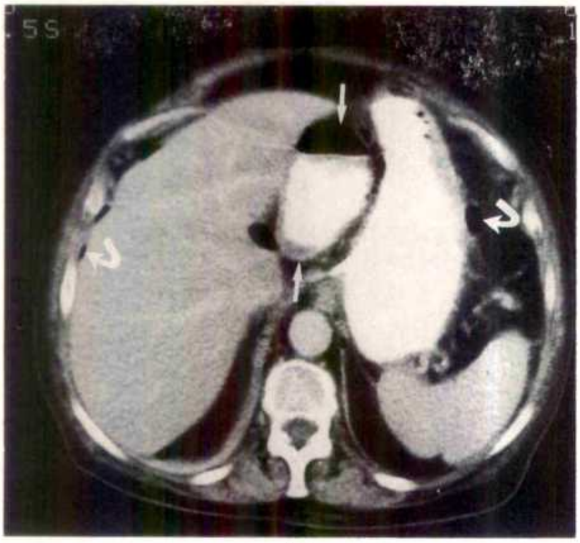

(a)

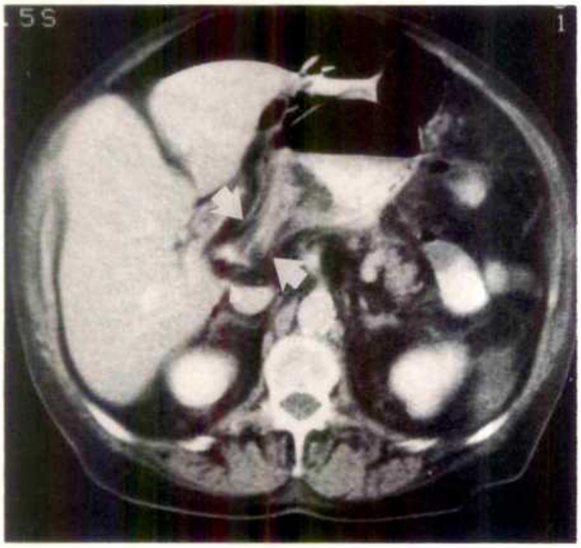

(b)

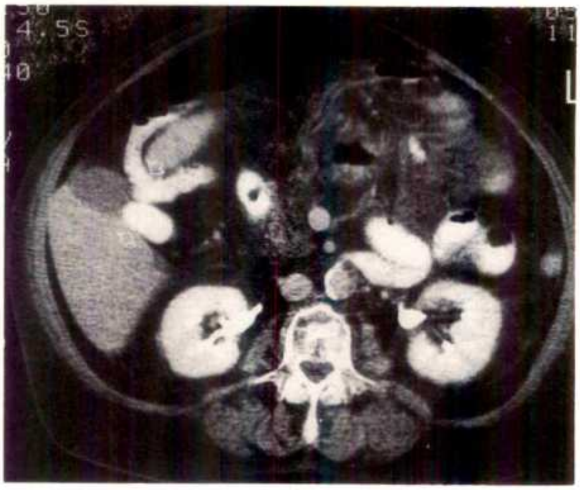

(c)

Figure 2. Axial CT slices through the upper and mid-abdomen with intravenous contrast bolus and oral contrast medium. The gas contrast-filled caecum (a) is present within the lesser sac (arrows). Free intraperitoneal air (curved arrows) resulted from perforation of the caecum. The caecal and ileal mesentery (b) pass through the foramen of Winslow (short arrows). The ascending colon is present in the high subhepatic space (arrowhead) and the caecum is within lesser sac. The subhepatic location of the terminal ileum and ascending colon (c) reflect the migration of the caecum through the foramen of Winslow (open arrows).

with a "beak" directed toward the epiploic foramen; (c) absence of the ascending colon in the right gutter; and (d) two or more loops of bowel (representing the displaced ascending colon and terminal ileum) in the high subhepatic space near the porta hepatis. This surgically proven example illustrates the diagnostic points.

Conclusions

Though the diagnosis of caecal herniation through the foramen of Winslow may be suggested by plain film, CT with oral and intravenous contrast medium supports the diagnosis with a great degree of confidence. The untreated mortality rate of 49% (Erskine, 1967) should improve with radiological diagnosis at an earlier stage.

References

BLANDIN, P. F., 1834. *Traité D'anatomie Topographique, ou Anatomie des Régions du Corps Humain*, 2nd edn (Germer-Baillière, Paris).

ERSKINE, J. M., 1967. Hernia through the foramen of Winslow. *Surgery, Gynecology and Obstetrics*, *125*, 1903–1909.

HARNED, R. K. & FARLEY, G. E., 1974. Herniation of cecum and terminal ileum through the foramen of Winslow. *American Journal of Gastroenterology*, *61*, 304–307.

HENISZ, A., MATESANZ, J. & WESTCOTT, J. L., 1974. Cecal herniation through the foramen of Winslow. *Radiology*, *112*, 575–578.

MCCREA, A. N., 1951. Herniation of gallbladder through the foramen of Winslow. *British Journal of Surgery*, *38*, 386–387.

OKHUMA, R. & MIYAZAKE, K., 1977. Herniation through the foramen of Winslow. *Japan Journal of Surgery*, *152*, 151–157.

RICHARDSON, J. B. & ANASTOPOULOS, H. A., 1981. Hernia through the foramen of Winslow. *Maryland State Medical Journal*, *30*, 56–59.

VALENZIANO, C. P., HOWARD, W. B. & CRIADO, F. J., 1987. Hernia through the foramen of Winslow: a complication of cholecystectomy. *American Journal of Surgery*, *53*, 254–257.

WOJTASEK, D. A., CODNER, M. A. & NOWAK, E. J., 1991. CT diagnosis of cecal herniation through the foramen of Winslow. *Gastrointestinal Radiology*, *16*, 77–79.

1992, *The British Journal of Radiology*, *65*, 1049–1050

Case of the month

Dense bones

By Sarah Vinnicombe, BSc, MRCP, Christine Heron, MRCP, FRCR and *Mark Wansbrough-Jones, MSc, FRCP

Departments of Radiology and *Infectious Diseases, St George's Hospital, Blackshaw Road, London SW17, UK

(Received 3 June 1991 and accepted 2 July 1991)

A 39-year-old Asian woman was investigated for a 4 year history of generalized aches and pains and more recent malaise, fevers and cervical adenopathy. On admission, her erythrocyte sedimentation rate (ESR) was 62 and there was a mild polyclonal gammopathy. Mantoux and Kveim tests were negative and screening cultures of urine and sputum (including for acid and alcohol fast bacilli) were also negative. The chest radiograph is shown in Fig. 1. At this time, radiographs of the skull, pelvis and hands were normal.

The patient received a 6 month trial of antituberculous chemotherapy, but this resulted in minimal symptomatic improvement and her lymphadenopathy persisted. In addition, she complained of increasing pelvic pain. A pelvic radiograph was obtained, followed by isotope scintigraphy with $^{99}Tc^{m}$-methylene diphosphonate (Figs 2 & 3, respectively).

What investigation(s) would you do next? What diagnoses would you consider?

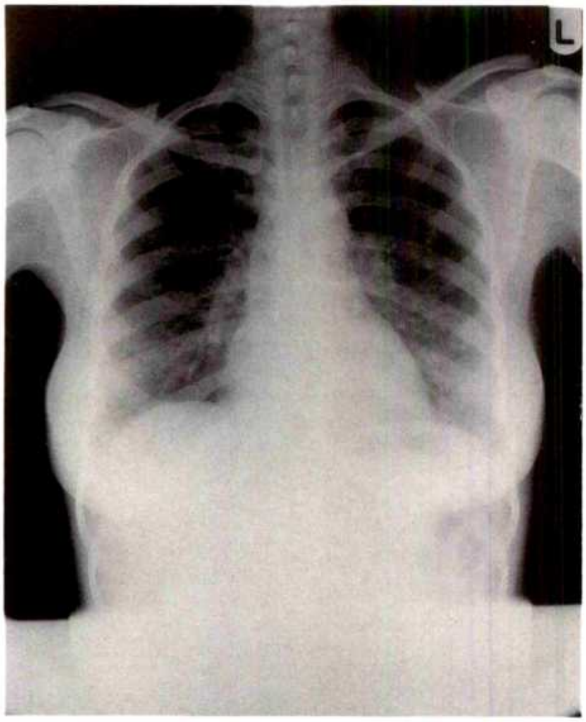

Figure 1. Chest radiograph.

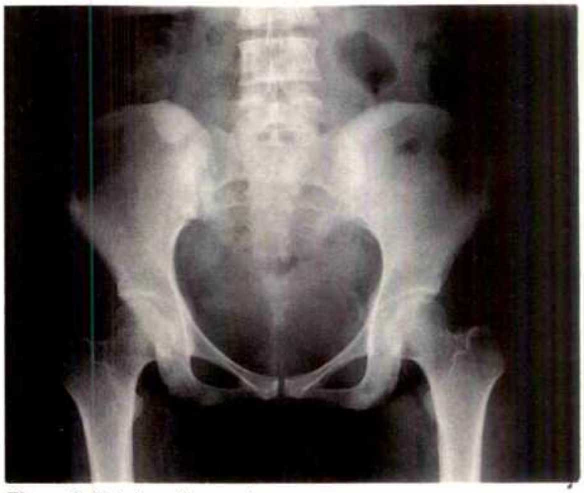

Figure 2. Pelvic radiograph.

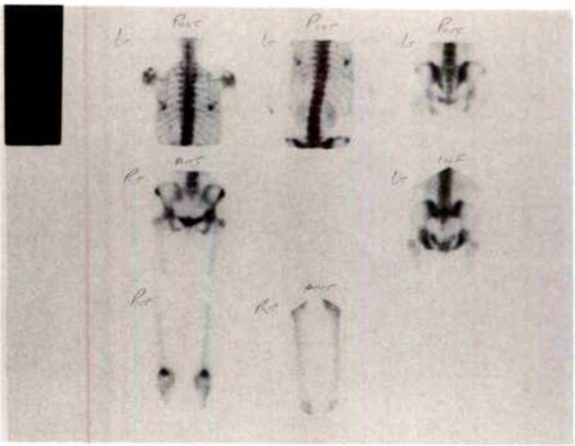

Figure 3. Isotope bone scan using $^{99}Tc^{m}$-methylene diphosphonate; views of the axial skeleton.

Address correspondence to Dr S. Vinnicombe, Department of Radiology, St George's Hospital, Blackshaw Road, London SW17 0QT.

The chest radiograph shows mild nodularity in the lungs, particularly in the midzones. There is also some prominence of the hila, which is more marked on the left, and a suggestion of right paratracheal adenopathy. In the pelvis, there are areas of sclerosis, without expansion, around the sacroiliac joints, ischial tuberosities and iliac blades bilaterally. The radioisotope bone scan shows a small area of increased uptake around the right ischial tuberosity and in the posteromedial part of the right iliac crest

A bone biopsy was performed under computed tomography (CT) guidance and one of the cervical lymph nodes was also biopsied. Non-caseating granulomata were found on histological examination of both specimens. A diagnosis of sclerosing sarcoidosis of bone was made and treatment with steroids commenced. Over the next 6 months the patient improved symptomatically and her ESR fell slowly to 30.

Discussion

The differential diagnosis of sclerotic bone lesions is large, including metastatic carcinoma (notably of prostate and breast), lymphoma (particularly Hodgkin's disease) and Paget's disease. Other rarer causes include systemic mastocytosis and osteopetrosis. Most of these are readily excluded, either radiologically or clinically, but this may be difficult in the case of lymphoma even after bone biopsy. The clinical course in the two conditions is of value, as sclerotic sarcoidosis tends to be indolent in nature (Weston & Duffy, 1975).

Sarcoidosis is a chronic granulomatous condition of unknown aetiology. The reported incidence of bony involvement in the literature varies from 6 to 26% of cases (Lin et al, 1973). The usual pattern is of osteolytic lesions, predominantly in the small tubular bones of the hands and feet. The vertebrae are occasionally affected. The lesions tend to occur in association with pulmonary and dermatological manifestations of the disease and they are strongly predictive of chronicity of disease.

Purely osteoblastic lesions are rare in sarcoidosis. They were first documented in 1971 by Bonakdarpour et al and a small number of reports have appeared since then. Certain features are common to all the cases described. Firstly, sclerotic lesions have a marked tendency to involve the axial skeleton, in particular the pelvis, spine and occasionally the ribs and skull. The bones of the hands and feet are nearly always spared. This is in contrast with the more usual osteolytic sarcoidosis. The involvement is often strikingly symmetrical and there is little evidence of bony destruction. Patients frequently experience bone pain, unlike those with osteolytic sarcoid of the extremities. Sclerotic lesions may antedate or post-date other manifestations of the disease and skin involvement need not be present. However, lymphadenopathy is a frequent accompaniment. Finally, all the patients reported except one have been middle-aged and of negroid extraction.

Isotope scintigraphy in this patient seriously underestimated the extent of bony involvement. This, again, contrasts with osteolytic sarcoidosis, where it has been shown that bone scintigraphy with $^{99}Tc^{m}$-diphosphonate is much more sensitive than plain radiography (Rohatgi, 1980). In the one other report of the use of scintigraphy in osteosclerotic sarcoid, the lesions exhibited avid uptake (Abdelwahab & Norman, 1988).

The fact that patients may present with symptomatic sclerotic lesions before the development of the more obvious manifestations of sarcoidosis may pose a diagnostic difficulty. This diagnosis should always be considered in the differential of sclerotic bone especially in patients of an appropriate age and racial background.

References

ABDELWAHAB, I. F. & NORMAN, A., 1988. Osteosclerotic sarcoidosis. *American Journal of Roentgenology, 150,* 161–162.

BONAKDARPOUR, A., LEVY, W. & AEGERTER, E. E., 1971. Osteosclerotic changes in sarcoidosis. *American Journal of Roentgenology, Radiologic Therapeutics and Nuclear Medicine, 113,* 646–649.

LIN, S. R., LEVY, W., GO, E. B., LEE, I. & WONG, W. K., 1973. Unusual osteosclerotic changes in sarcoidosis, simulating osteoblastic metastases. *Radiology, 106,* 311–312.

ROHATGI, P. K., 1980. Radioisotope scanning in osseous sarcoidosis. *American Journal of Roentgenology, 134,* 189–191.

WESTON, M. & DUFFY, P., 1975. Osteosclerosis in sarcoidosis. *Australasian Radiology, XIX* (2), 191–193.

Keywords: Sarcoidosis, Osteosclerosis, Isotope scintigraphy

1992, *The British Journal of Radiology*, *65*, 1051–1054

Short communication

Correlations between α/β and $T_{\frac{1}{2}}$: implications for clinical biological modelling

By D. J. Brenner, PhD

Center for Radiological Research, Columbia University, 630 W. 168th Street, New York, NY 10032, USA

(*Received 12 June 1991 and in revised form 16 September 1991, accepted 6 May 1992*)

Keywords: Linear-quadratic model, Fractionation, Low dose rate, Modelling

There seems little question that future directions in radiotherapy will involve altered or customized fractionation schedules (Cooper, 1990). Recent interest in accelerated fractionation and hyperfractionation, high dose-rate brachytherapy, and the search for predictive assays for tumour proliferation all exemplify this trend.

The linear–quadratic model, the formalism for which was first described by Lea and Catcheside (1942), is now the modelling tool of choice (*e.g.* Fowler, 1989) for investigating alternative fractionation schedules. In this model the biological effect, E, of an acute dose of radiation, D, is related to a combination of dose and dose-squared terms:

$$\frac{E}{\beta} = \frac{\alpha}{\beta} D + D^2 \qquad (1)$$

where α/β is an empirically-determined parameter. When the dose is protracted (with fractionation or low dose rate), there is time for sublethal damage repair to act on the dose-squared component, but the linear dose term will be unchanged. Thus the dose-squared term is reduced and the effect is now related to D by

$$\frac{E}{\beta} = \frac{\alpha}{\beta} D + \mathrm{G}\, D^2 \qquad (2)$$

where the quantity G ($\leqslant 1$) can be calculated from the particular fractionation/LDR scheme used, and to a parameter to represent the speed of sublethal damage repair. For repair governed by first-order kinetics, this parameter can be represented by one (or more) half-times for sublethal damage repair, $T_{\frac{1}{2}}$.

Thus, in principle, knowing α/β and $T_{\frac{1}{2}}$ (and/or their distributions), it is possible to investigate the equivalence of any fractionation scheme to any other, either for early or for late effects. There are, in fact, some situations where α/β but not $T_{\frac{1}{2}}$ need be known—in particular, a fractionation schedule with many hours between treatments, where time for full sublethal damage repair is allowed; for brachytherapy, or accelerated or hyperfractionated regimes, however, both parameters need to be known.

Note that, in general, we also need to consider proliferation during the overall times of the treatments; here, for illustrative purposes, we avoid this by assuming that the various treatments take the same overall time.

Available data for α/β and $T_{\frac{1}{2}}$ derived from results in the clinic have been summarized by Thames et al (1990), for normal tissues in animals by Thames and Hendry (1987), and for animal tumours by Williams et al (1985) and Guttenberger et al (1990). *In-vitro* data for [α, $T_{\frac{1}{2}}$] from cells of human origin have been reviewed by Brenner and Hall (1991). Figure 1 indicates that, for the parameter α/β, the human, animal, and *in-vitro* data appear consistent with each other, all showing a very broad range of values.

There are many more data available for α/β than for $T_{\frac{1}{2}}$. From the clinic, there is really only one published report in which both α/β and $T_{\frac{1}{2}}$ were obtained from the same clinical results; this was from Turesson and Thames (1989) for post-mastectomy irradiation. For normal tissues in animals, there are at least 16 data sets in which α/β and $T_{\frac{1}{2}}$ were obtained together (Thames et al, 1984, 1988; Ang et al, 1985, 1987; Travis et al, 1985, 1987; Vegesna et al, 1985, 1989; Dewit et al, 1987; Dale et al, 1988; Rojas et al, 1989; Scalliet et al, 1989; Steel et al, 1989; Stuben et al, 1991). The data are shown in Fig. 2. Only two such data sets are known for animal tumours, from Guttenberger et al (1990) and Rojas et al (1989). *In vitro*, where experiments may be performed rather more easily and with better statistics, 36 paired data sets for [α/β, $T_{\frac{1}{2}}$] from cells of human origin were reviewed by Brenner and Hall (1991).

The normal-tissue animal data in Fig. 2 show an inverse correlation—as α/β increases, $T_{\frac{1}{2}}$ decreases. Appropriate non-parametric (i.e. model-independent) tests for correlation are the Spearman rank test (Spearman, 1904) or the Kendall τ test (Kendall, 1938). For these normal-tissue animal data, both tests indicate that the probability of α/β and $T_{\frac{1}{2}}$ being independent is less than 0.1%. On the other hand, the animal-tumour data of Guttenberger et al (1990) and Rojas et al (1989), though limited in number for correlation analysis, do not show this inverse correlation, and suggest a possible positive correlation (significant at 80% confidence level).

In light of the highly significant correlation found in the normal-tissue animal data, we have investigated possible relationships between α/β and $T_{\frac{1}{2}}$ in *in-vitro* data for cells of human origin. The data for cells of human origin are shown in Figs 3 and 4. Figure 3 shows these *in-vitro* data for normal cells of human origin and, using the non-parametric tests described above, we can say, at the 90% confidence level, that the data are inversely correlated (the probability that the parameters are independent is 9.2%). Figure 4 shows the corresponding *in-vitro* data for *tumour* cells of human origin. In this case we can say with 90% (or 95%) confidence that the parameters α/β and $T_{\frac{1}{2}}$ have a positive correlation (the probability that they are independent is 4.6%).

Thus both the *in-vivo* and the *in-vitro* data appear to suggest that α/β and $T_{\frac{1}{2}}$ are correlated—an inverse correlation for normal cells, and a positive correlation for tumour cells. As pointed out by Ang et al (1987), if all other factors (the effect, E, and the quadratic term, β) were kept constant, then a fluctuation (say upward) in the regression estimate of α/β would necessitate a compensating downward fluctuation in the estimate of G (see Equation (2)), and hence in $T_{\frac{1}{2}}$, thus making for an inverse correlation. However, there is no reason to suppose that the estimate of β would not also fluctuate in such estimates, which would eliminate this "curve-fitting" explanation of the observed correlations. It should be noted that

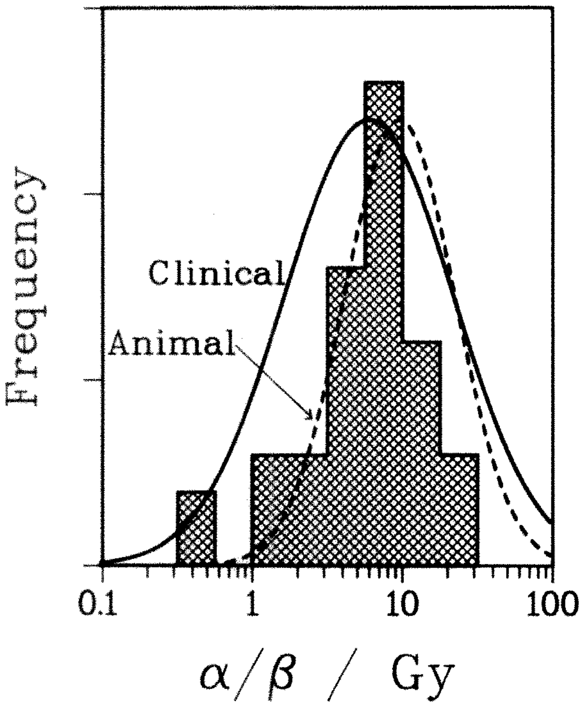

Figure 1. Comparison of α/β values derived from cells of human origin *in vitro* (shaded histogram; Brenner & Hall, 1991), from clinical data (full curve: log-normal distribution fitted to data for human tumours from review by Thames et al (1990)), and from animal tumour data (dashed curve: log-normal distribution fitted to data for clamped tumours from review by Williams et al (1985).

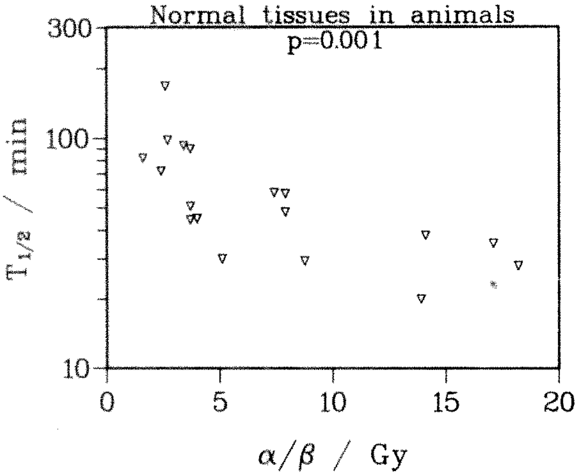

Figure 2. Summary of α/β and $T_{\frac{1}{2}}$ data for normal tissues in animals, where these parameters were obtained together. Data are from Thames et al, 1984, 1988; Dale et al, 1988; Ang et al, 1985, 1987; Travis et al, 1985, 1987; Vegesna et al, 1985, 1989; Dewit et al, 1987; Rojas et al, 1989, Scalliet et al, 1989; Steel et al, 1989 and Stuben et al, 1991. The p value refers to the probability, estimated using Kendall's τ test (Kendall, 1938), that α/β and $T_{\frac{1}{2}}$ are independent.

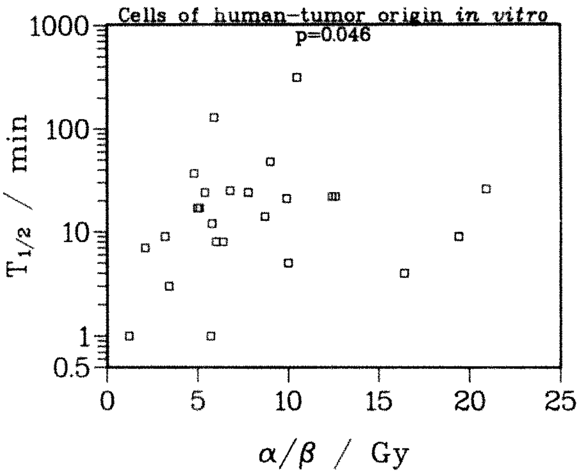

Figure 3. Summary of α/β and $T_{\frac{1}{2}}$ data for cells of human tumour origin, *in vitro*, where these parameters were obtained together (Brenner & Hall, 1991). The p value refers to the probability, estimated using Kendall's τ test (Kendall, 1938), that α/β and $T_{\frac{1}{2}}$ are independent.

maximum-likelihood methods were used to obtain most of the data sets discussed here (Thames et al, 1986; Brenner & Hall, 1991), and it is thus unlikely that these correlations are spuriously produced by the data fitting procedures used.

If these correlations are real, they may well represent the influence of a third "hidden" variable. For example, cellular proliferation—and thus the fraction of cells in different parts of the cell cycle—is often considered to be a determinant of the α/β ratio (Hall, 1988), and it is quite plausible to suppose that repair rates will also be different in different parts of the cell

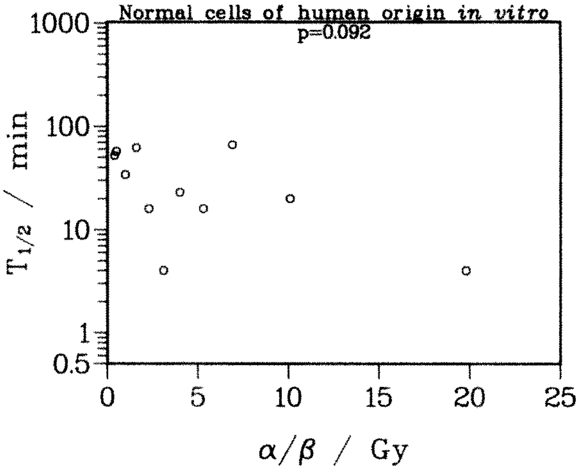

Figure 4. Summary of α/β and $T_{\frac{1}{2}}$ data for normal cells of human origin *in vitro*, where these parameters were obtained together (Brenner & Hall, 1991). The p value refers to the probability, estimated using Kendall's τ test (Kendall, 1938), that α/β and $T_{\frac{1}{2}}$ are independent.

cycle, due to such factors as chromatin structure and enzymatic availability.

Apart from the mechanistic questions raised, there are important methodological implications for the use of the linear-quadratic model in designing alternative fractionation regimes. From Fig. 1, it is clear that the use of single "representative" values of α/β is unwise; this is also true for $T_{1/2}$, which has an even broader range of measured values (Brenner & Hall, 1991). *Prima facie*, a reasonable approach would be to consider an appropriate range of α/β values and $T_{1/2}$ values, and repeat the calculations for parameter values covering these ranges; this is implicitly done, for example, by Fowler (1989, 1990), Dale (1986) and Thames and Hendry (1987); at that point the results might be averaged, or the most conservative accepted, or the results examined to see which are in best accord with clinical data.

Such an approach, however, will not work if the α/β and $T_{1/2}$ really are correlated. If this is the case, as the discussions above seem to suggest, then only paired sets of parameters, *i.e.* $[\alpha/\beta, T_{1/2}]$ sets obtained from analysis of the same data set, should be used. This approach will certainly decrease the number of parameter sets that can be used for such calculations, but should lead to more reliable design of new fractionated and brachytherapy regimens.

Acknowledgements

The advice of Drs Eric Hall and Charles Geard is gratefully acknowledged. This work was supported by Grants CA-24232 and CA-12536 from the National Cancer Institute, and grant PDT-438 from the American Cancer Society.

References

ANG, K. K., XU, F.-X., LANDUYT, W., & VAN DER SCHUEREN, E., 1985. The kinetics and capacity for repair of sublethal damage in mouse lip mucosa during fractionated irradiations. *International Journal of Radiation Oncology, Biology and Physics, 11*, 1977–1983.

ANG, K. K., THAMES, H. D., VAN DER KOGEL, A. J. & VAN DER SCHUEREN, E., 1987. Is the rate of repair of radiation-induced sublethal damage in rat spinal chord dependent on the size of dose per fraction? *International Journal of Radiation Oncology, Biology and Physics, 13*, 557–562.

BRENNER, D. J. & HALL, E. J., 1991. Conditions for the equivalence of continuous to pulsed low dose rate brachytherapy. *International Journal of Radiation Oncology, Biology and Physics, 20*, 181–190.

COOPER, J. S., 1990. Will altered fractionation schemes alter the future? *International Journal of Radiation Oncology, Biology and Physics, 19*, 1621–1622.

DALE, R. G., 1986. The application of the linear-quadratic models to fractionated radiotherapy when there is incomplete normal tissue recovery between fractions, and possible implications for treatments involving multiple fractions per day. *British Journal of Radiology, 59*, 919–927.

DALE, R. G., TROTT, K. R. & HUCZKOWSKI, J., 1988. Possible dose rate dependence of recovery kinetics as deduced from a preliminary analysis of the effects of fractionated irradiations at varying dose rates. *British Journal of Radiology, 61*, 153–157.

DEWIT, L., OUSSOREN, Y. & HART, G., 1987. Modification by cis-diamminedichloroplatinum (II) of the radiation dose response for intestinal crypt cells in mice. *Radiation Research, 111*, 445–456.

FOWLER, J. F., 1989. The linear-quadratic formula and progress in fractionated radiotherapy. *British Journal of Radiology, 62*, 679–694.

FOWLER, J. F., 1990. How worthwhile are short schedules in radiotherapy?: A series of exploratory calculations. *Radiotherapy and Oncology, 18*, 165–181.

GUTTENBERGER, R., KUMMERMEHR, J. & CHMELEVSKY, D., 1990. Kinetics of recovery from sublethal damage in four murine tumors. *Radiotherapy and Oncology, 18*, 79–88.

HALL, E. J., 1988. *Radiobiology for the Radiologist* (J. P. Lippincott, Philadelphia).

KENDALL, M. G., 1938. A new measure of rank correlation. *Biometrika, 30*, 81–93.

LEA, D. E. & CATCHESIDE, D. G., 1942. The mechanism of the induction by radiation of chromosome aberrations in *Tradescantia*. *Journal of Genetics, 44*, 216–245.

ROJAS, A., JOINER, M. C., & JOHNS, H., 1989. Recovery kinetics in mouse skin and CaNT tumours. *Radiotherapy and Oncology, 16*, 211–220.

SCALLIET, P., LANDUYT, W. & VAN DER SCHUEREN, E., 1989. Repair kinetics as a determining factor for late tolerance of central nervous system to low dose rate irradiation. *Radiotherapy and Oncology, 14*, 345–353.

SPEARMAN, C., 1904. The proof and measurement of association between two things. *American Journal of Psychology, 15*, 72–101.

STEEL, G. G., KELLAND, L. R. & PEACOCK, J. H., 1989. The radiobiological basis for low dose rate. In *Brachytherapy 2*, ed. by R. F. Mould (Nucletron, The Netherlands).

STUBEN, G., LANDUYT, W., VAN DER SCHUEREN, E., VAN DER KOGEL, A. & REIJNDERS, A., 1991. Estimation of repair parameters in mouse lip mucosa during continuous and fractionated low dose-rate irradiation. *Radiotherapy and Oncology, 20*, 38–45.

THAMES, H. D. & HENDRY, J. H., 1987. *Fractionation in Radiotherapy*. (Taylor & Francis, London).

THAMES, H. D., WITHERS, H. R. & PETERS, L. J., 1984. Tissue repair capacity and repair kinetics deduced from multifractionated or continuous irradiation regimens with incomplete repair. *British Journal of Cancer, 49*, Suppl. VI, 263–269.

THAMES, H. D., ROZELL, M. E., TUCKER, S. L., ANG, K. K., FISHER, D. R. & TRAVIS, E. L., 1986. Direct analysis of quantal response data. *International Journal of Radiation Biology, 49*, 999–1009.

THAMES, H. D., ANG, K. K., STEWART, F. A. & VAN DER SCHUEREN, E., 1988. Does incomplete repair explain the apparent failure of the basic LQ model to predict spinal cord and kidney responses to low doses per fraction? *International Journal of Radiation Biology, 54*, 13–19.

THAMES, H. D., BENTZEN, S. M., TURESSON, I., OVERGAARD, M. & VAN DEN BOGAERT, W., 1990. Time-dose factors in radiotherapy: a review of the human data. *Radiotherapy and Oncology, 19*, 219–235.

TRAVIS, E. L., PETERS, L. J., MCNEILL, J., THAMES, H. D. & KAROLIS, C., 1985. Effect of dose-rate on total body irradiation: Lethality and pathologic findings. *Radiotherapy and Oncology, 4*, 341–351.

TRAVIS, E. L., THAMES, H. D., WATKINS, T. L. & KISS, I., 1987. The kinetics of repair in mouse lung after fractionated irradiation. *International Journal of Radiation Biology, 52*, 903–919.

TURESSON, I. & THAMES, H. D., 1989. Repair capacity and kinetics of human skin during fractionated radiotherapy, erythema, desquamation, and telangiectasia after 3 and 5 years' follow-up. *Radiotherapy and Oncology, 15*, 169–188.

VEGESNA, V., WITHERS, H. R., THAMES, H. D. & MASON, K. A., 1985. Multifraction radiation response of mouse lung. *International Journal of Radiation Biology, 47*, 413–422.

VEGESNA, V., WITHERS, H. R. & TAYLOR, J. M., 1989. Repair kinetics of mouse lung. *Radiotherapy and Oncology*, *15*, 115–123.

WILLIAMS, M. V., DENEKAMP, J. & FOWLER, J. F., 1985. A review of α/β ratios for experimental tumors: implications for clinical studies of altered fractionation. *International Journal of Radiation Oncology, Biology and Physics*, *11*, 87–96.

1992, *The British Journal of Radiology*, *65*, 1055–1057

Correspondence

(The Editors do not hold themselves responsible for opinions expressed by correspondents)

The role of ^{99}Tc^{m}-HMPAO white cell imaging in suspected orthopaedic infection

The Editor—Sir,

I wonder why we need a new nuclear medicine technique for the clinical problem of suspected infection of total joint prosthesis. It seems to me that if this diagnosis is strongly suspected the appropriate investigation is aspiration of the joint. If the tap is dry, contrast should be injected to confirm that the nededle was correctly placed. This will exclude infection that warrants early treatment, avoid the unneccessary contamination of operating theatres used for aseptic orthopaedic surgery and provide the organism in infected cases. A nuclear medicine study is appropriate in borderline cases when the risk of infecting a normal joint outweighs the suspicion of sepsis. Here nuclear medicine has a place as a screening tool. The investigation should be designed to suffer the minimum of false negative results. In this role the new and more complex technique that the authors describe, appears less effective than routine ^{99}Tc^{m}-MDP scintigraphy. Positive cases should all undergo aspiration of the joint.

To confound my quandary regarding the author's recommendations for clinical practice, I see problems in method that may throw further doubt on their conclusions. They assume that a patient who responds to antibiotics must have been infected. Would not an uninfected prosthesis do as well on antibiotics? Equally, how can they be sure that low grade infection did not resolve or at least improve on conservative treatment.

Yours etc.,
D. Wilson

Nuffield Orthopaedic Centre,
Windmill Road,
Headington,
Oxford OX3 7LD
(*Received 16 April 1992 and accepted 18 June 1992*)

Reference

Copping, C., Dalgliesh, S. M., Dudley, N. J., Griffiths, P. A., Harrington, M., Potter, R. & Smith, B. D., 1992. The role of ^{99}Tc^{m}-HMPAO white cell imaging in suspected orthopaedic infection. *British Journal of Radiology*, *65*, 309-312.

Authors' reply

The Editor—Sir,

We thank you for the opportunity to respond to the interesting letter from Dr Wilson concerning our recent article (Copping et al, 1992).

The group of patients included in the study were those with suspected latent infection. They presented with pain, no elevation of temperature and subsequent negative blood tests. In our opinion, aspiration is not the primary investigation of choice for such patients. Only when florid infection is strongly suspected do patients undergo routine aspiration prior to surgery. If the tap is dry, contrast is used in conjunction with an image intensifier. Such patients are not referred for nuclear medicine tests and were, therefore, not included in the study. However, following scanning, aspiration was conducted in our study when it was considered appropriate.

With regard to using the response of patients to antibiotics following positive scans as confirmation of the presence of infection, we found that long term follow-up revealed no recurrence of their initial symptoms. Similarly, those patients having negative scans who were conservatively managed have remained symptom free since discharge. We therefore feel that our assumptions are justified.

Yours etc.,

C. Copping
S. M. Dalgliesh
N. J. Dudley
P. A. Griffiths
M. Harrington
R. Potter
B. D. Smith

Departments of Medical Physics and Computing
and Orthopaedic Surgery,
County Hospital,
Lincoln L12 5QY
(*Received 18 May and accepted 18 June 1992*)

Reference

Copping, C., Dalgliesh, S. M., Dudley, N. J., Griffiths, P. A., Harrington, M., Potter, R. & Smith, B. D., 1992. The role of ^{99}Tc^{m}-HMPAO white cell imaging in suspected orthopaedic infection. *British Journal of Radiology*, *65*, 309-312.

Coil embolization using a saline flush technique

The Editor—Sir,

We read with great interest the article by Makita et al (1991). We would like to report our experience with the saline flush technique for coil embolization.

We have been using a similar technique since 1982. The saline flush manoeuvre was carried out in about 200 patients (approximately 400 coils). The splenic, hepatic, renal and hypogastric arteries were successfully embolized. We used 5 F, 7 F or (in early years) 9 F sized catheters and home-made coils (Ryzhkov et al, 1988) prepared from suitable guidewires (0.95 mm or 1.38 mm in diameter, respectively). The coils had 3-10 rings and were 4-15 cm long when stretched. In most cases coils could be accurately placed using the flush technique.

A few serious complications occurred, however. In spite of a carefully checked catheter position by making a strong hand injection of saline under fluoroscopic control, there were four cases of unwanted movement of the catheter tip. Inadvertent embolization of the left common femoral artery by a coil occurred in one patient with gynaecological cancer during therapeutic occlusion of the left hypogastric artery; emergency surgical removal of the coil was needed. In two other patients (both with renal carcinoma), the proximal coil was partially situated in the abdominal aorta post-embolization. Fortunately both devices were gently removed during subsequent elective nephrectomy 1 week later. Inadvertent embolization of the coeliac trunk caused no sequelae in the remaining patient with liver cancer.

Following this, we now use the saline flush technique with particular caution. We usually perform this manoeuvre for passing the coil to the catheter tip or for positioning the coil partially extruded from the catheter. The final extrusion is made with a guidewire.

Coiling inside the catheter occurred in three of six cases, when relatively large (9 F) catheters and smaller coils (made from 7 F corresponded guidewire) were used. Removal of the catheter together with the impacted coil and repeat catheterization were needed in all three patients.

We would like to congratulate Dr Makita and colleagues on their excellent results. We feel that our complications with flush technique are related to the use of our home-made coils which are longer and had more rings than the standard ones. It should be considered, however, that extensive experience in embolization procedures and undoubted caution are essential prerequisites for the clinical use of saline flush technique.

Yours etc.,

P. G. Tarazov
E. M. Gapchenko
I. A. Dmitrieva
V. K. Ryzhkov

Department of Diagnostic Radiology,
Central Research Institute of Roentgenology and Radiology,
Pesochny-2,
St Petersburg 189646,
Russia

(*Received 21 May 1992 and accepted 18 June 1992*)

References

Makita, K., Furui, S., Irie, T., Hirata, J., Yamauchi, T., Tsuchiqa, K., Takenaka, E., Ohtomo, K. & Ibukuro, K., 1991. Embolization with steel coils using a saline flush technique. *British Journal of Radiology*, *64*, 708-710.

Ryzhkov, V. K., Borisova, N. A., Gapchenko, E. M. & Dmitrijeva, I. A., 1988. Verschluss von Arterien durch vergrossert Spiralembolisate. *Radiologia Diagnostica* (Berlin), *29*, 713-717.

Imaging of organ function

The Editor—Sir,

Although the main emphasis of radiology has been the demonstration of disease through observation of changes in structure, imaging of organ function is becoming an increasingly important part of diagnostic radiology. A brief review of papers published in the British Journal of Radiology over a 1 year period (May 1991-April 1992) revealed 23 articles concerned with functional aspects of imaging, comprising 24% of the non-therapy papers in this period. 11 of these papers involved Doppler ultrasound, 8 nuclear medicine, 2 computed tomography and 2 magnetic resonance imaging. (There were no papers involving digital subtraction angiography which can be used to estimate blood flow.)

Despite this trend towards increasing involvement in functional aspects of disease, there remains very little formal training in physiology within the FRCR. Also workers in these areas frequently appear to be unaware of what functional information can be derived from the techniques other than their own. There seems to be a need for a forum to allow an exchange of ideas between the different groups with an interest in imaging organ function and I would be keen to hear from anybody interested in becoming involved in such a forum. This would inevitably involve input from multiple disciplines and thus perhaps would be most appropriately organized within the British Institute of Radiology.

Yours etc.,

K. A. Miles

Department of Nuclear Medicine,
Addenbrooke's Hospital,
Hills Road,
Cambridge CB2 2QQ

(*Received 26 May 1992 and accepted 18 June 1992*)

Fluid levels in a spinal aneurysmal bone cyst following biopsy

The Editor—Sir,

In their recent article on computed tomography (CT) of osseous lesions (Davies et al, 1992) the authors emphasize the high sensitivity and specificity of the presence of fluid–fluid levels within a lesion for the diagnosis of aneurysmal bone cyst (ABC). In their experience fluid–fluid levels were not seen on CT of ABC following disruption of the tumour by biopsy or previous surgery even when they had been present before the intervention. We have recently seen a spinal ABC with multiple fluid levels following open biopsy.

A 14-year-old boy presented with a 2 week history of a painful lump in the mid lumbar spine and signs and symptoms of progressive cauda equina compression. Plain radiographs showed a lytic lesion involving L3 and L4. Surgical exploration revealed a blood filled cavity approximately 3 cm in diameter. Two biopsies of the lining were taken. Curettage was considered unwise in view of the proximity to the cauda equina. Histology of the specimens confirmed the diagnosis of ABC. He subsequently made rapid neurological improvement but, 3 weeks later, he was readmitted as an emergency unable to walk. A plain radiograph (Fig. 1) showed the lesion now had a calcified rim and extended into the paravertebral soft tissues.

Computed tomography of the spine (Fig. 2) showed an extensive mass with a partly calcified rim. Multiple fluid levels were present within the lesion. The mass encroached on the spinal canal and a subsequent myelogram showed a complete block at the level of the L2/3 disc space. The patient was treated with radiotherapy and has made an almost complete neurological recovery.

This case illustrates that fluid–fluid levels may occur in ABC following surgical intervention although it would appear that they are uncommon. The cause for their disappearance is uncertain but presumably reflects healing of the lesion which commonly occurs within 2 months of any form of treatment including biopsy alone (Hay et al, 1978; Ohry et al, 1988; DeRosa et al, 1990). It is possible that fluid–fluid levels would not have been seen lesion if it had not

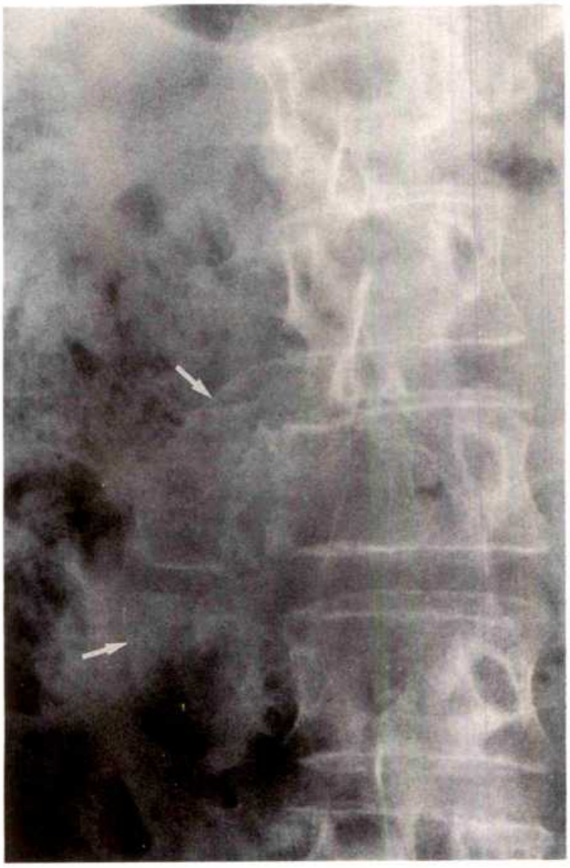

Figure 1. Radiograph of the lumbar spine 3 weeks after the initial surgery, the lesion has a thin peripheral rim of calcification (arrows).

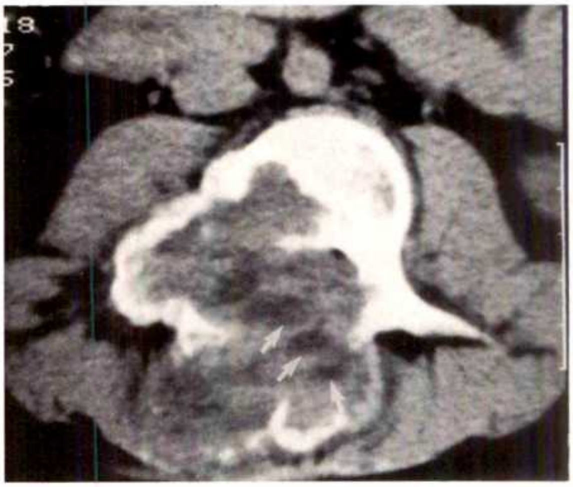

Figure 2. Unenhanced CT scan at the level of L3, the extent of the lesion is clearly seen. Multiple fluid levels (arrows) are seen within it.

been necessary to scan the patient so soon after biopsy due to the deterioration in his condition.

Yours etc.,
D. Kessel

Department of Radiology,
Middlesex Hospital,
Mortimer Street,
London W1N 8AA

(Received 7 June 1992 and accepted 28 August 1992)

References

Davies, A. M., Cassar-Pullicino, V. N. & Grimer, R. J., 1992. The incidence and significance of fluid-fluid levels on computed tomography of osseous lesions. *British Journal of Radiology*, *65*, 193-198.

DeRosa, G. P., Graziano, G. P. & Scoot, J., 1990. Arterial embolisation of aneurysmal bone cyst of the lumbar spine. *Journal of Bone and Joint Surgery*, *72* (A), 777-780.

Hay, M. C., Paterson, D. & Taylor, T. K., 1978. Aneurysmal bone cysts of the spine. *Journal of Bone and Joint Surgery*, *60* (B), 406-411.

Ohry, A., Lipschitz, M., Shemesh, Y., Lipschitz, L. & Tadmor, R., 1988. Disappearance of quadriparesis due to a huge cervicothoracic aneurysmal bone cyst. *Surgical Neurology*, *29*, 307-310.

1992, *The British Journal of Radiology*, *65*, 1058–1063

Proceedings of the Scottish Radiological Society

Autumn Meeting held in Glasgow, November 9, 1991

Radiodiagnosis Programme

Chairman: N. McMillan

MR evaluation of supraspinatus outlet narrowing in shoulder impingement syndrome, by J. Namasivayam, W. P. Chan, M. Valensieck and H. K. Genant

The role of CT in calcaneal fracture assessment, by E. Robertson and J. Addison

An "eye" for audit, by W. Kincaid, N. McMillan and G. Dutton

Audit of outpatient barium services, by G. Houston and N. McMillan

The role of CT in the diagnosis and assessment of malignant pleural mesothelioma, by K. Buchan, S. Miller, C. J. Clark, A. N. Jilaihawi and D. Prakash

Metastatic disease and the equivocal bone scan—the value of MRI, by F. Aitchison, F. W. Poon, D. Hadley, H. W. Gray and A. W. Forrester

Colour Doppler of the normal paediatric testis, by S. Ingram and A. Hollman

Radiotherapy and oncology programme

Chairman: A. N. Harnett

Tape recording outpatient consultations in oncology improves patient understanding and decision making, by M. A. Cornbleet, G. Knowles, N. North and R. C. F. Leonard

Physiological sequelae of breast irradiation—a comparison of two radiation therapy techniques, by P. D. J. Hardman, G. R. Kerr, A. Rodger and P. Tweedale

Treatment of relapsed ovarian carcinoma in Edinburgh 1980–1991, by P. Bliss, M. Stewart, R. C. F. Leonard and J. F. Smyth

An audit of orthopaedic surgery and radiotherapy in the management of upper and lower limb girdle bone metastases, by P. D. J. Hardman, J. Robb, G. R. Kerr and A. Rodger

Buying cancer care, by G. J. G. Rees

Improving clinical management through diagnostic imaging: the role of health services research, by I. Russell

MR evaluation of supraspinatus outlet narrowing in shoulder impingement syndrome

By J. Namasivayam, *W P. Chan, *M. Valensieck and *H. K. Genant

*Department of Radiology, Royal Infirmary, Glasgow and *Department of Radiology, University of California Medical Center, San Francisco*

Rotator cuff pathology resulting from supraspinatus outlet narrowing as a result of acromion and acromio-clavicular joint abnormalities was analysed in 53 patients with clinical impingement syndrome. MR imaging of the 55 shoulders demonstrated two different types of downward slope of the anterior third of acromion compromising the supraspinatus outlet. In the first, an anterior slope was assessed on oblique sagittal plane; in the second, a lateral slope was evaluated on oblique coronal plane at constant levels of bony (coracoid process) and joint (acromio-clavicular joint) landmarks. Surgical correlation was available in 16 shoulders. MR imaging enabled us to distinguish between tendonitis, partial tear and complete tear in all but one shoulder. A significant (confidence level $> 95\%$, p value < 0.01) direct correlation was observed between decreasing anterior slope of acromion and severity of supraspinatus disease; increasing age of patients and severity of supraspinatus disease. MR is a highly effective method of evaluating the bony and joint abnormalities which contribute to the narrowing of the supraspinatus outlet resulting in impingement of the supraspinatus, and thus aids the planning of the appropriate treatment.

The role of CT in calcaneal fracture assessment

By E. M. Robertson, J. Addison and *J. Hutchison

*Departments of Radiology and *Orthopaedics, Aberdeen Royal Infirmary*

Accurate assessment of calcaneal fractures is necessary to estimate the need for reconstruction, to minimize long-term deformity and early degenerative change. The complexity of calcaneal anatomy makes plain film assessment of trauma difficult. In Aberdeen, CT assessment has been used for a number of years. 83 patients (70 male, 13 female) with plain film calcaneal fractures were investigated with CT over a five-year period. Eleven patients had bilateral fractures, giving a total of 94 fractures. Review of the radiographs and CT scans showed that CT offered additional information in almost all cases: in particular, the size and number of bone fragments, degree of displacement, presence of steps in the articular surface and fibular impingement by bone spurs were all clearly demonstrated. In three cases, the fracture did not involve the subtalar joint as had been suspected from the plain films. On CT, the calcaneal fractures could be divided into six groups: 36 inverted 'Y' fractures, with essentially a 3-part fracture; 28 badly comminuted fractures; 12 downward impaction fractures with an intact subtalar facet; 8 vertical, longitudinal splint fractures with two large fragments; 4, a combination of the longitudinal and extra-articular fractures; and 6 purely extra-articular fractures. A study relating clinical outcome to CT appearance is currently under way.

An "eye" for audit

By W. Kincaid, N. C. McMillan and G. Dutton
Western Infirmary, Glasgow G11 6NT

A retrospective study of patients referred for brain CT by ophthalmologists was carried out to assess its effect on clinical management. 53 patients, aged 1–80, were included in the study. The most common presenting complaints were visual field defects, headaches, and glaucoma. Of 21 patients who had had plain skull X-rays earlier in the investigation process, only 7 (33%) were reported as abnormal, 5 of which were false positives. In 38 patients the CT was reported as normal and in most cases resulted in the patient's discharge from the clinic. Similarly in the majority of the 15 patients who had an abnormal CT the examination was conclusive, leading again to discharge or neurosurgical referral. In the 6 patients who presented with a homonymous hemianopia, the CT was positive: 4 posterior cerebral infarcts, 1 meningioma and 1 primary malignant tumour.

As a result of this study we recommend the following practice: (1) plain skull X-rays have very little value in non-traumatic ophthalmic conditions and should not be performed in these circumstances:; (2) brain CT is usually normal in patients presenting with headaches and is not indicated in the absence of localizing signs; (3) brain CT is rarely helpful in glaucoma, except in some cases of low-tension glaucoma for which more research is required; (4) brain CT should be the first imaging examination in patients with a homonymous hemianopia; (5) brain CT should be considered early in the test sequence as this would reduce the number of additional investigations and follow-up clinic appointments, with considerable cost savings.

Audit of outpatient barium services

By J. G. Houston and N. McMillan
Western Infirmary, Gartnavel General Hospital, Glasgow

Over 3000 patients attend the X-ray departments of two city hospitals annually for outpatient barium examinations, accounting for 15–30% of radiologists' work. With this size of service and the particular demands made on patients by these examinations an audit of the appointment system and patients' attitudes to the service was undertaken. One hundred patients (50 from each centre) were asked to fill out questionnaires before and after their outpatient examination, and the delays in the appointment sytem were quantified. The average age was 51 years (range 18–83 years), 61 women and 49 men, equally referred by GPs and outpatient clinics. 40% of patients arrived late for their appointment, delays in public transport and insufficient parking possible causes. 60% are seen within 15 min of their appointment. The level of information about examination that patients receive was thought too low. 60% were not told by the referring clinician what the procedure involved, 5% did not know what examination they had come for, 14% thought the preparation inadequately explained, and 50% thought the examination better than expected, indicating unnecessary anxiety which might be allayed by further information while waiting for the procedure. 96% thought staff very helpful and 98% were overall satisfied with the service.

The role of computed tomography in the diagnosis and assessment of malignant pleural mesothelioma

By K. Buchan, S. Miller, C. J. Clark, A. N.. Jilaihawi and D. Prakash
Regional Thoracic Surgical Unit, Hairmyres Hospital, East Kilbride, Glasgow G75 8RG

The diagnostic specificity and sensitivity of computed tomography in malignant pleural mesothelioma was assessed in patients attending Hairmyres Hospital over a 4-year period. The specificity of this investigation was 100% when CT appearances were typical ($n = 15$), 80% when suggestive or typical ($n = 35$) and 65% when suggestive ($n = 20$). The sensitivity was 97% when appearances were suggestive or typical ($n = 59$) and 57% when typical ($n = 35$). When compared with findings at thoracotomy in 38 cases, CT proved accurate in demonstrating the location of gross disease but less helpful in predicting infiltration of contiguous structures and mediastinal lymph node involvement. CT features indicating inoperability by radical extrapleural pneumonectomy were present in 12% of 58 patients referred for a surgical opinion.

Metastatic disease and the equivocal bone scan—value of MRI

By F. Aitchison, F. W. Poon, D. Hadley, H. W. Gray and A. W. Forrester
Royal Infirmary, Glasgow G31 2ER

Bone scintigraphy is a highly sensitive though non-specific examination in the detection of skeletal metastases. Although the results are normally read in conjunction with plain X-rays of the areas showing abnormal isotope uptake, a fair proportion of patients will still have equivocal findings. Previously these patients would have had either a repeat isotope bone scan after three to six months or a bone biopsy. In a prospective study, we found that in patients with equivocal isotope uptake over the spinal area, MRI is able to demonstrate evidence of metastases in 46% of the patients studied and concluded that MRI is a useful non-invasive complementary investigation for detecting spinal metastases.

Colour Doppler of the normal paediatric testis

By S. Ingram and A. Hollman
The Royal Hospital for Sick Children, Glasgow

Recent reports suggest that colour Doppler sonography (CDS) is a useful tool in the diagnosis of testicular torsion in children. However, little is known regarding the sensitivity of colour Doppler in the normal paediatric testis. In this prospective study we scanned the testes of 50 boys (mean age 6.5 years, range 10 weeks–13 years) who came for renal tract ultrasound in the investigation of urinary tract infection. Ethical committee approval was granted and informal consent obtained from parents. All boys had clinically normal testes. Testicular blood flow and volume measurements were taken. 58% of children had flow detected in both testes, 34% had no flow detected in either testis and 8% had detectable flow in one testis only. No flow was detected in children below the age of 2 years and flow was always detected above the age of 10 years. There were approximately equal numbers of patients in the two age groups, 2–6 years (28) and 7–10 years (22) The proportion of children who had flow detected in both testes was no higher in the 7–10 age group than in the 2–6 age group (47% *vs.* 62%). The combined testicular volume ranged between 0.21 ml and 9.44 ml (median: 1 ml, mean: 1.3 ml). 84% of patients with a combined testicular volume greater than the median had detectable flow. These results suggest that up to one third of a random selection of children with normal testes may not have blood flow demonstrable by CDS. Detectable blood flow correlates better with testicular volume than age. These facts should be borne in mind when diagnosing torsion by CDS.

Tape recording outpatient consultations in oncology improves patient understanding and decision making

By M. A. Cornbleet, G. Knowles, N. North and R. C. F. Leonard
ICRF Department of Medical Oncology, Western General Hospital, Edinburgh

Patients with advanced cancer may not gain maximal benefit from explanations of their situation, because anxiety levels are high when there is much information to absorb. In a prospective randomized trial, new patients referred to a Medical Oncology clinic were invited to have their consultation tape recorded for them to take away (18 patients) or not (16 patients). All patients completed Hospital Anxiety and Depression (HAD) scales prior to their consultation, together with a questionnaire about their understanding of their diagnosis. 1 week later, repeating the questionnaires revealed a significant reduction in anxiety scores (6.9 to 3.1, *vs.* 7.1 to 6.1, $p = 0.0035$) and a substantial improvement in information score (3.3 to 9.3, *vs.* 3.3 to 4.4, $p = 0.0001$) among those with a tape. All patients were enthusiastic about the tape, and none reported any distress among family members who also listened. Tape recording substantially improves the efficiency of the outpatient consultation by reducing anxiety levels and enhancing understanding of the diagnosis and treatment options without increasing depression.

Physiological sequelae of breast irradiation—a comparison of two radiation therapy techniques

By P. D. J. Hardman, G. R. Kerr, A. Rodger and *P. Tweedale
*Department of Clinical Oncology, Western General Hospital, Crewe Road, Edinburgh, and *Lothian Area Respiratory Function Service, City Hospital, Edinburgh*

During the period January 1990 to October 1991, 110 consecutive patients treated with radiotherapy (RT) for breast cancer underwent sequential assessment of dynamic ventilatory function (FeV$_1$, VC, and FeV$_1$/VC) and of carbon monoxide gas transfer (T_{LCO}, K_{LCO}) following surgery but immediately prior to RT (control values), 10 weeks following completion of RT (acute phase values), and one year following completion of RT (late phase values). 94 patients underwent RT to the breast (if present), the chest wall and the supraclavicular/axillary lymph nodes (4-field technique). 16 patients underwent RT to the breast/chest wall (tangential fields technique). Comparison of control and acute phase data show reductions in mean physiological values.

	4-field technique ($n = 94$)			Tangential fields ($n = 16$)		
	Control	Acute phase	p value	Control	Acute phase	p value
FeV$_1$	2.42	2.29	< 0.0001	2.49	2.50	0.98
VC	3.08	2.95	< 0.0001	3.17	3.16	0.90
FeV/VC	0.78	0.77	0.176	0.78	0.79	0.57
T_{LCO}	7.03	6.19	< 0.0001	7.86	7.21	0.002
K_{LCO}	1.59	1.47	< 0.0001	1.72	1.62	0.008

These results show that the 4-field technique is associated with greater impairment of pulmonary function in the acute phase than is the tangential technique. Data examining the late phase changes in pulmonary function associated with each technique were also presented.

Treatment of relapsed ovarian carcinoma in Edinburgh 1980–1991

By P. Bliss, M. Stewart, R. C. F. Leonard and J. F. Smyth
Department of Clinical Oncology, Western General Hospital, Edinburgh EH4 2XU

The treatment of relapsed ovarian carcinoma in Edinburgh was reviewed retrospectively with particular reference to the use of platinum-containing compounds. 193 patients have been treated for relapsed ovarian carcinoma over this period. 115 patients (60.5%) received cis-platinum alone or in combination as first-line therapy, 47 (24%) received chlorambucil initially and 28 (14%) received prednimustine. On relapse 65 patients (33.7%) were prescribed cis-platinum, 52 (27%) were prescribed chlorambucil, and 29 patients (15%) received carboplatinum upon relapse. Of the 115 patients initially treated with cis-platinum, 23 were retreated with cisplatinum; there was a 13% response rate amongst these patients (1 CR 2 PR). 23 of the 115 were retreated with carboplatinum, the response rate was 26% (6 PR). Finally 43 were retreated with chlorambucil, giving a response rate of just 7% for these patients. It appeared that patients who responded well to the reintroduction of platinum were those who had a longer disease-free interval and who responded to platinum-based chemotherapy given as first line. However the numbers involved were too small to draw significant conclusions. In general it seems that conventional chemotherapy has poor activity as second line therapy and novel drugs and approaches are justified for first relapse.

An audit of orthopaedic surgery and radiotherapy in the management of upper and lower limb girdle bone metastases

By P. D. J. Hardman, *J. Robb, G. R. Kerr and A. Rodger
*Department of Clinical Oncology and *Department of Orthopaedic Surgery, Western General Hospital, Edinburgh EH4 2XU*

54 consecutive patients have been identified who underwent 61 orthopaedic operations for metastatic bone disease affecting the upper and lower girdles. These patients were subsequently managed with a consistent post-operative radiotherapy (RT) treatment policy. There were 27 prophylactic bone fixations and 34 fixations of pathological fracture. There was a marked difference in survival between these groups. The median post-operative survival of the prophylactic (P) group was 15 months whereas that of the fracture (F) group was 2 months ($p < 0.0001$). Mobility following surgery and RT in the lower limb girdle was significantly improved in both the P group

($p < 0.05$) and in the F group ($p < 0.0001$), 58% and 91%, respectively, of these patients being subsequently able to walk with or without aids. 78% of the P group and 62% of the F group had a good functional result without further sequelae at the operation site until the time of death. 92% of the P group and 59% of the F group were able to be discharged home following treatment. Further local fracture occurred in 9% of the P group and in none of the F group. Fixation of pathological fracture, in combination with post-operative RT, provides effective palliation until the time of death in most patients and is well justified. These results suggest that patients undergoing prophylactic fixation do well following surgical stabilization + RT although the extent to which subsequent fracture may be prevented remains uncertain.

Buying cancer care

By G.J.G. Rees
Royal United Hospital, Combe Park, Bath BA1 3NG

An ideal service for a patient with cancer includes: prompt referral by GP; prompt and expert assessment by consultant(s); rapid completion of investigations; "state of the art" treatment supervised personally by consultant(s) highly experienced in the management of the particular tumour; provision of all necessary facilities for prompt and proper treatment of complications; unlimited time for discussion of diagnosis, prognosis, side effects; where beneficial, unlimited input from specialized nurses and a suitably trained counsellor; all this provided near to the patient's home. In general there is a marked discrepancy between the cost per patient benefit year between palliative and radical treatments. It is illogical to spend money on palliative treatments if the same amount of money stands to purchase a greater benefit if spent on radical treatments that are not being offered, *e.g.* adjuvant chemotherapy for breast and, possibly, for unfavourable bowel cancer. However, whilst there is still scope for utilizing the resources currently available more equitably, there is also unlimited scope for improving the service by paying more. It is the duty of doctors to use available resources equitably with the maximum efficiency. It is also their duty to inform purchasers what can and what cannot be provided for a given amount of money. A patient has a right to know about all possibly beneficial treatment options for which there is reasonable evidence of efficacy, whether or not the purchaser has decided to provide funding for them. We need more public discussion on deciding priorities for spending.

Improving clinical managment through diagnostic imaging: the role of health services research

By Ian Russell
Health Services Research Unit, University of Aberdeen

The late Professor Archie Cochrane proposed that the adoption of the new diagnostic technologies should be conditional on objective evidence, preferably derived from randomized trials, that their use either alters the natural history of disease or otherwise benefits patients. Although this advice is sound in principle, there are many problems in applying it. First, the chain of events linking improved imaging to improved patient outcome is long and complex. Secondly, most diagnostic technologies cover a wide range of diseases. Thirdly, the benefits of improved imaging are often intangible or otherwise difficult to estimate. Fortunately, there are published studies to show that these problems can be overcome by persistence and ingenuity. It is also important to improve the selection of patients for established diagnostic technologies. This needs prospective observational studies rather than randomized trials. Both before requesting a scan and after receiving the result, doctors are asked to specify both their differential diagnosis and their current management plan. Only those scans that change or strengthen that management plan are regarded as beneficial. Careful data collection, followed by multivariate statistical analysis, yields decision rules that discriminate effectively between scans that will benefit clinical management and those that will not. Diagnostic imaging has a major role to play in improving clinical management, and thus patient outcome, with the Scottish Health Service. Pragmatic yet rigorous research can help in two ways—by evaluating new diagnostic technologies through randomized trials, and by improving patient selection for existing technologies through prospective observational studies.

Proceedings of the Scottish Radiological Society

Abstracts presented to a meeting organised by the Scottish Radiological Society, held on Saturday, 14 March 1992

Radiodiagnosis Programme

An evaluation of head CT in three centres, by B. C. M. Macpherson, E. L. S. Lindsay and P. Macpherson
Biopsy made easy, by W. Kincaid, I. Robertson and R. Edwards
Diagnosis and embolization of vein of Galen aneurysm in a neonate, by A. Jain, A. S. Hollman, J. Dervin and T. L. Turner
The effect of pharyngeal tonicity on the outcome of alaryngeal speech in laryngectomees? by J. Guse, A. E. Camilleri and C. Dunnett
Early experience with a self-expandable metallic stent for the treatment of malignant biliary obstruction, by A. Ramsay, I. S. Stewart and F. W. Poon
Paediatric pelvic ultrasound, by K. A. Duncan, A. S. Hollman and M. D. C. Donaldson
Assessment of results of gallbladder ultrasound in general radiological practice, by J. Walker, R. T. A. Chalmers and P. L. A. Allan
Ultrasound guided biopsy of the kidneys, by N. J. A. Cozens, J. T. Murchison, P. L. Allan and R. J. Winney

An evaluation of head CT and three centres

B. C. M. Macpherson, E. L. S. Lindsay and P. Macpherson
Department of Radiology, Glasgow Royal Infirmary, Crosshouse Hospital, Ayrshire and Institute of Neurological Sciences, Glasgow

All computed tomograms (CT's) of the head performed over a 3 month period in a Regional Neurological Unit (Institute of Neurological Sciences (INS), Glasgow), a teaching hospital (Glasgow Royal Infirmary (GRI)) and a District General Hospital (Crosshouse Hospital, Kilmarnock) were evaluated. The age/sex profiles of the patients were similar for the three hospitals, but the reason for referral showed more variation—the commonest indication was head injury at the INS (16% of scans), and suspected space occupying lesion in GRI (29%) and Crosshouse (36%). Suspected acoustic neuroma accounted for 13% of scans in Crosshouse. Cross-checking of computerized data at the INS revealed coding errors for the clinical or radiological diagnosis in 5% and duplication of "unique" identification number in 1%; 2.5% of scans recorded in the departmental day book were omitted from the computerized record. For each referral category, the rate of positive scans was highest in the INS, and for certain categories, *e.g.* non-acute headache and cerebellopontine angle, virtually all scans were normal. Improved vetting of requests and the limitation of CT scanning to a second-line investigation for conditions, such as putuitary adenoma and acoustic neuroma, where non-invasive screening tests exist, is recommended.

Biopsy made easy

W. Kincaid, I. Robertson and R. Edwards
Western Infirmary, Glasgow G11 6NT

Percutaneous ultrasound guided biopsy has become standard practice in many hospitals. A number of biopsy devices are now available and we have compared our experience with manual and automated biopsy systems. Over a 15 month period prospective data was collected in over 50 ultrasound guided biopsies utilising an automated system (Biopty system, Bard UK). This was compared with retrospective data of our previous experience over the preceding 15 month period. We have compared procedural time, patient discomfort, post procedural complications and quality and accuracy of pathological specimens. Biopsies were performed by different radiologists with widely varying experience. In both groups approximately half of the biopsies were from liver and the remainder from other abdominal sites and chest lesions. The automated biopsy device consistently provided higher quality and more diagnostic tissue samples in less time with significantly less patient discomfort and with no greater prevalence of complications than a manual biopsy system.

Diagnosis and embolization of vein of Galen aneurysm in a neonate

A. Jain, A. S. Hollman, J. Dervin and *T. L. Turner
Royal Hospital for Sick Children, Yorkhill Hospital and
**Institute of Neurological Sciences, Glasgow*

Malformation of the vein of Galen is rare and constitutes less than 1% of all cerebral arteriovenous malformation. The malformation is extracerebral and has a complex system of feeder vessels including the anterior and posterior parietal, the pericallosal, thalamoperforatior and the superior cerebellar arteries. Neonates may present with severe cardiac failure with an associated cranial bruit. Later presentation in infancy or in childhood, is characterized by progressive hydrocephalus and subarachnoid haemorrhage. This case report highlights the efficacy of colour Doppler ultrasound in the diagnosis of vein of Galen aneurysm in infancy and illustrates that prompt embolization can give excellent results and may avert the high mortality associated with this condition.

The effect of pharyngeal tonicity of the outcome of alaryngeal speech in laryngectomees?

J. Guse, A. E. Camilleri and C. Dunnett
Royal Infirmary, Glasgow G11 6NT

Insufflation videofluoroscopy is used to assess laryngectomy patients for speech restoration. It has been reported to predict the success rate of tracheo-oesophageal fistula creation with a voice prosthesis. The aim of this audit study was to measure the correlation between videofluoroscopy (VF) and successful alaryngeal speech in our laryngectomy population. The patients were categorized by speech, *i.e.* oesophageal and fistula and by the VF diagnosis, *i.e.* pharyngeal hypotonicity, normal tonicity, hypertonicity, spasm and stricture. Success was defined as audible intelligible speech. Radiological diagnosis was carried out by one observer on two occasions to assess repeatability. 26 patients were included in the study, mean age 62 (range 44–77). VF results were four hyotonic, 11 normal tonicity, eight hypertonic, two spasm and one stricture. The percentage success rate for fistula speech was 50% hypotonic, 100% normal tonicity, 57% hypertonic, 50% spasm and none stricture. The percentage success rate for oesophageal speech was 100% normal tonicity, none hypertonic. The intraobserver repeatability of VF was 56% for exact category agreement and 90% for variation of one category or less. Our VF distribution is very similar to the previous English study and demonstrates that normal tonicity is associated with very good results. The lack of repeatability suggests that the radiological diagnosis should be left to a few specialized centres.

Early experience with a self-expandable metallic stent for the treatment of malignant biliary obstruction

A. Ramsay, I. S. Stewart and F. W. Poon
Department of Radiology, Glasgow Royal Infirmary, Glasgow

The treatment of malignant biliary obstruction increasingly demands the placement of internal biliary stents, with the use of external or internal/external drainage catheters being unacceptable to many patients and clinicians. 21 patients underwent percutaneous transhepatic placement of self-expandable metallic stents (Wallstent, Medinvent). All patients were referred following failed attempted access at ERCP, or because previous surgery had made ERCP impossible. Initial stent position was considered satisfactory in all cases, with minimal initial complications. The advantages over conventional plastic stents are described with an assessment of survival duration, stent patency and length of stay at home. The technique offers important advantages in patient tolerance, the use of a small (7 F) introducer system, with a large internal diameter and a relatively high patency rate. Disadvantages include expense, difficulty in stent removal when placed and stent shortening when released. Metallic stents offer a significant role in palliative treatment of malignant obstructive jaundice with some important advantages over existing drainage procedures.

Paediatric pelvic ultrasound

K. A. Duncan, A. S. Hollman and M. D. C. Donaldson
Royal Hospital for Sick Children, Yorkhill, Glasgow

Pelvic ultrasound is being employed increasingly in the evaluation of pubertal and other associated disorders in the female child. However, there have been few large studies to date and these have shown some variance as to the range of normal appearances including the frequency of non-visualization of the normal ovary. We report on prospective sonographic findings in a control group of 99 girls between the ages of 3 months and 16 years. The uterus was visualized in 100%. It was noted to enlarge slowly throughout childhood with a pubertal growth spurt: changing in shape from the infantile inverted pear configuration, through a cylindrical shape seen in the pre-pubertal girls, to the post-pubertal pear shape. Both ovaries were visualized in 67% of controls, the right ovary only in 13% and the left only in 5%. Neither was demonstrated in 15%. Ovarian volume also showed a progressive increase with a growth spurt in puberty. In the evaluation of patients with pubertal disorders comparison with these normal ranges is proving very useful. In combination with an LHRH test, the sonographic appearances of the uterus and ovaries allow such conditions as premature thelarche (breast development), thelarche variant and precocious puberty to be distinguished. As a non-invasive investigation with high patient acceptability, pelvic ultrasonography is also of great value in monitoring the response of these girls to treatment. Other situations where we have found pelvic ultrasound useful include delayed puberty and Turner's syndrome.

Assessment of results of gallbladder ultrasound in general radiological practice

J. Walker, *R. T. A. Chalmers and P. L. A. Allan
*Departments of Radiology and *Surgery, Royal Infirmary, Lauriston Place, Edinburgh EH3 9YW*

Ultrasound has generally established its role as the imaging investigation of choice to diagnose cholethithiasis. This is because it requires minimal patient preparation, does not entail ionizing radiation, can be extended to visualize other organs and, moreover, has been determined as accurate. This accuracy has been reported as 96% or greater in many series, but these are often prospective and the examinations performed by senior sonographers. We sought to address whether the accuracy is maintained in a department where sonographers of varying experience work and both emergency and routine patients are scanned. We reviewed and compared the pre-operative ultrasound and cholecystectomy findings of 128 patients. In eight patients the findings were at variance. Five patients were reported as having gallstones on ultrasound but none were found at operation; an ultrasound false positive rate of 3.9%. Three patients had gallstones at operation though none were reported on ultrasound; a 2.3% false negative rate. Any incorrect diagnosis is to be avoided, but it is more important to avoid false positives than false negatives as inappropriate surgery will be performed; specificity should be maintained at slight cost to sensitivity. False positive diagnoses may be avoided by performing an optimal examination, repeating it if necessary and by performing alternative imaging, either cholescintigraphy or oral cholecystography on occasion. Some false negatives may be avoided by repeating the examination if the gallbladder appears abnormal initially but no stones are identified. We conclude that with these provisos ultrasound correctly diagnoses cholelithiasis in daily practice.

Ultrasound guided biopsy of the kidneys

N. J. A. Cozens, J. T. Murchison, P. L. Allan and *R. J. Winney
*Departments of Radiology and *Renal Medicine, Royal Infirmary of Edinburgh, Edinburgh*

Various methods of location and guidance have been used to facilitate percutaneous renal biopsy since its introduction in the 1950s. Plain films and anatomical landmarks, fluoroscopy, pyelography, radioisotope scan, retrograde pyelography and computed tomography (CT) scanning have been utilized. Real-time ultrasound has superseded these to become the method of choice. We reviewed renal biopsies performed by a renal physician after ultrasound localization of the kidney with our early experience of renal biopsies performed using a spring loaded biopsy device (Biopty). The Biopty biopsies were performed under real-time ultrasound guidance by a single radiologist. The smaller Biopty needle more frequently provides satisfactory histologically diagnostic specimens (93%) than the previous cutting needle technique (79%) ($p < 0.05$). No statistically significant difference in complications occurred. The average length of stay in hospital was significantly shorter for elective biopsies with the Biopty device; 1.80 compared with 2.93 nights ($p < 0.01$). We now perform all our renal biopsies with the Biopty device under real-time ultrasound guidance.

1992, *The British Journal of Radiology*, *65*, 1064–1067

Book reviews

Imaging of the Pelvis; MRI with Correlations to CT and Ultrasound. Ed. by M. C. Fishman-Javitt, H. L. Stein and J. L. Lovecchio, pp. xiv + 303, 1990 (Little, Brown & Company, Boston), $85.00.
ISBN 0–316–28396–7

This book presents a comprehensive and honest review of the various imaging modalities currently available for interrogating the pelvis, with an emphasis on the burgeoning role of Magnetic Resonance Imaging (MRI). Although ultrasound is clearly the method of choice for the investigation of benign disease, Computed Tomography (CT) scanning has for years now been the workhorse of any X-ray department with an oncology commitment; and MRI has yet to supersede CT in some fundamental areas of diagnosis, particularly staging of abdominopelvic malignancy. The authors present the case for MRI clearly in terms of better tissue contrast, non-invasiveness, the facility of direct multiplanar imaging and clarity of vascular structures; the illustrations provided are indeed excellent. However, serious limitations of MRI *vs.* CT currently still include poorer spatial resolution, lack of useful bowel contrast, long scanning times, inability to accurately image the peritoneum and expense. Whilst it is hoped that all of these factors will improve over the next few years; the authors preface all their comments in favour of MRI with phrases such as "holds great promise", "likely to prove comparable to CT", "rapidly becoming as accurate". It is a somewhat naive concept to address imaging of pelvic malignancy entirely in terms of the pelvis since although MRI is undoubtedly comparable with CT for many pelvic cancers; the key to their staging is the ability to examine the abdominal contents accurately as well, and this claim cannot currently be met by existing MRI technology. In terms of layout, editorial style and illustrations, the book is very readable; chapters address each pelvic organ separately, describing anatomy, benign disease and malignancy in an orderly fashion with up-to-date references and clear illustrations. The authors display a good knowledge of individual diseases including behaviour of tumours and patterns of spread. This is an excellent text for learning about state-of-the-art imaging in the pelvis; it will appeal to both diagnosticians and therapists. The message is loud and clear: at present CT is still quicker, cheaper, and globally more accurate than MRI for the day-to-day management of abdominopelvic malignancy and ultrasound more valuable in benign disease; until MRI technology is further improved it will only provide a fascinating complement to existing techniques. However, that day may not be too distant.

E. Moskovic

MRI of the Wrist and Hand. By M. A. Reicher and L. E. Kellerhouse, pp. xiii + 214 (Raven Press, New York), $107.00.
ISBN 0–88167–664–0

Following the early appreciation of the value of Magnetic Resonance Imaging (MRI) in large joints such as the knee and hip, MRI has been increasingly employed to evaluate smaller joints including the wrist and hand. This book is intended to provide a source of reference for radiologists and orthopaedic surgeons who are interested in wrist disease and MRI. As the application of MRI to this region is at a relatively early stage the authors also hope to provide a focal point for further discussion and research in MRI of hand and wrist disease.

Murray Reicher and Leland Kellerhouse are two of a group of radiologists from California who have published a wide range of authoritative texts on musculoskeletal MRI. Murray Reicher is also co-author of a successful book on MRI of the knee, written in the same style as the present text and also published by Raven Press, in 1987. In both books the introduction is followed by a chapter on technical considerations which includes a description of MR physics and documents state-of-the-art MRI techniques. The rationale for the selection of various imaging protocols is presented and although it has been considerably updated the content of this chapter is similar to that in the earlier publication and many of the diagrams have been reproduced. The next chapter is devoted to a description of the various imaging protocols employed at the authors' centre plus a comprehensive and detailed description of normal anatomy with well annotated cross-sectional images in multiple planes.

MRI is increasingly employed in the evaluation of patients with carpal tunnel syndrome and the next chapter provides a clear account of the appearances which have been described, and the way in which MR may be of value in assessing the aetiology of carpal tunnel syndrome. Post-operative changes are also discussed to familiarize the reader with both the appearances following successful decompression and the reasons for failed surgery. An extensive review of the current literature on MRI in carpal tunnel syndrome and the way in which it is employed is presented.

The following two chapters are devoted to descriptions of carpal instability, distal ulnar instability and other problems which may affect the distal radioulnar joint. As the authors state "the relationship of the carpal bones and ligaments is extremely complex" and they have succeeded in producing a simplified explanation of wrist pathomechanics.

By the very nature of the subject, however, these chapters remain complicated and will be of most value to radiologists and orthopaedic surgeons with a particular interest in this field. MRI is well suited to assessing the relationship of the carpal bones in various types of instability because of its multiplanar imaging capability. These relationships are well described but in some instances I found it difficult to visualize the associated ligamentous injuries. Imaging of the distal radioulnar joint is also a challenging subject and the authors clearly illustrate how assessment of the triangular fibrocartilage forms only one part of the complete evaluation of this region; which is why MRI offers considerable advantages over arthrography.

Osteonecrosis and fractures of the wrist are covered in the next chapter. These disorders occur relatively commonly and MRI is gaining acceptance as the imaging procedure of choice for the primary detection and staging of early avascular necrosis. This chapter is therefore of interest to the general radiologist and clinician who are likely to be required to assess such conditions or to evaluate fractures and the important associated soft tissue injuries which occur in the wrist and hand.

The chapter on the imaging of tumours and synovial processes provides specific information about tumours which may be encountered in the hand and indicates the role of MRI in their evaluation.

The following two chapters are concerned with the normal anatomy of the finger and experience of imaging finger pathology. The authors admit that their descriptions of finger pathology are somewhat anecdotal since experience in finger imaging is at an early stage. However, the chapter does provide a useful insight into the abnormalities which may be recognized and the possible areas for development.

The final two chapters discuss firstly an orthopaedic surgeon's perspective and secondly, a radiologist's perspective of the value of MRI in particular circumstances. They serve to consolidate and in some cases expand on the information contained in the preceeding chapters.

This book is well written and illustrated and although certain chapters are directed to the specialist radiologist or orthopaedic surgeon, others are of more general interest. It is hard to image that anyone could undertake MR imaging of the hand and wrist without access to a book of this nature.

C. Heron

Radiology of Organ Transplantation. Ed. by J. G. Letourneau, D. L. Day and N. L. Ascher, pp. xvi + 359, 1991 (Wolfe Publishing Ltd, London), £77.00.
ISBN 0-8151-5372-4

This multi-author work is based upon more than 20 years' experience of solid-organ transplantation at the University of Minnesota, and is a worthy testament to the considerable teamwork between physicians, surgeons, radiologists and pathologists of all the different subspecialities that form the essence of this exciting and rapidly advancing area of medical practice.

An initial section deals with the general systemic complications of all forms of transplantation and the inevitably associated immunosuppression. Each of the four subsequent sections is devoted to a specific solid organ (*i.e.* kidney, liver, pancreas, heart and lungs), and for each organ there are chapters covering the roles of plain film radiology, scintigraphy, sonography, arteriography, Computed Tomography (CT) scanning, Magnetic Resonance (MR) imaging and interventional radiology. The diagnostic and therapeutic potential and limitations of all these techniques are thoroughly discussed and amply illustrated, and there are extensive lists of references that will prove extremely useful to other workers in the field.

This book is a valuable contribution to the literature. It is packed with facts and figures that will be of interest to all radiologists and clinicians involved in organ transplantation, and although it represents the practice at a single institution and is therefore not entirely comprehensive in its coverage, it is highly recommended to imaging departments at all transplant centres.

H. C. Irving

A Practical Guide to Echocardiography and Cardiac Doppler Ultrasound. By I. A. Jawad, pp. x + 379, 1990 (Churchill Livingstone, Edinburgh), £24.95.
ISBN 0-316-45832-5

This paperback is aimed at the cardiovascular technicans and cardiologists learning adult cardiac ultrasonography. It includes a brief discussion of the presentation of congenital heart disease in adults.

The first chapter deals with anatomy and physiology and the principles of ultrasound, Doppler and cardiac imaging. The second chapter deals with specific disease entities such as valvular disease and prostheses, cardiac masses and pericardial disease. The third section deals with application in cardiac diagnosis and management of certain topics such as heart failure, left ventricular dysfunction and heart murmur. The sequence of chapters is comprehensive, simple and easy to follow.

The quality of the illustrations, both black and white and colour Doppler is good and they are well annotated.

In general this book is easy to read with small subject sections within chapters. It explains both pathology and the associated findings on echoes very well. My only minor criticism of the book is that there is a lack of cross referencing within the text. The indexing in general, however, is more than adequate. I think this is a very suitable book both for cardiac technicians and for radiologists beginning to grapple with the techniques of echocardiography.

A. Jones

Phototherapy of Cancer. Ed. by G. Morstyn and A. Kaye, pp. ix + 224, 1990 (Harwood Academic Publishers, New York), $108.00.
ISBN 3-7186-0510-4

This multi-author text is comprised of 12 chapters, the initial four of which are concerned with basic biology, photochemistry, laser systems and light delivery. Chapters 5–11 review clinical applications and the book concludes with a discussion of the future directions for Photodynamic Therapy (PDT)/Phototherapy. With few exceptions, all the discussion relates to PDT and, in this sense, the book's title may appear misleading to those unfamiliar with the subject. For those seeking information about all aspects of the use of light in the diagnosis and management of cancer, this text will appear wanting.

The first chapter, discussing the biological basis for Phototherapy, is well-presented and will be read easily by all those familiar with basic radiobiology: it is very comprehensively referenced. A relatively succinct and well-presented chapter on the chemistry of sensitizers is followed by two which present delivery systems and dosimetry in considerable detail. The first of these, concerned with laser systems for PDT, is 35 pages in length. For the unqualified reader, these two chapters may seem too detailed with numerous diagrams and formulae supporting the text. For those already involved in PDT, they are unlikely to provide new information, as they are essentially concerned with reviewing areas with which the specialized reader is likely to be familiar.

The seven chapters that follow present, to a differing extent, laboratory and clinical data by site (brain, eye, gastrointestinal tract, skin/head and neck, lung and bladder); one chapter being concerned with 'early' cancers. The presentations are very varied in style, with no attempt having been made by the editors to produce diagrams, tables and charts to a single format. PDT is a discipline that is, in terms of its clinical application, in its infancy—a point made by many of the authors. It is, therefore, not surprising that there is a dearth of comparative data, most authors quoting personal series of patients that are, unavoidably, anecdotal. These chapters are variably illustrated but many clinical figures are endocsopic in origin and copy rather poorly into print.

The concluding chapter by Russo and Mitchell considers future directions for PDT. As one would expect, it poses many questions and hints at the directions that may be taken to provide some of the answers. It is clear that the authors, like the book's editors and many of its contributors, feel that the future for PDT is promising as there are many clinical areas in which reproducible responses have been reported. It is also very clear that good comparative studies are required, incorporating PDT into the definitive management of malignant disease. It clearly has no future as a treatment modality if it is only to have a limited role as a palliative measure.

Any book that considers a new discipline sets itself a difficult task, particularly when that discipline has yet to be accepted as having any routine clinical role. It is difficult to produce an authoritative text when there is little in the way of hard data to present. Perhaps this book has, in some senses, appeared a little too early because the wealth of basic science detail seems rather unsupported by the clinical chapters, although these comprise over half the text. If current clinical research advances the application of PDT as rapidly as some suggest, this part of the book may date rather too quickly.

R. BUCHANAN

Genetic Basis for Carciogenesis—Tumour Suppressor Genes and Oncogenes. Ed. by A. G. Knudson, E. J. Stanbridge, T. Sugimura, M. Terada and S. Watanabe, pp. xviii + 318, 1990 (Taylor & Francis, Hampshire), £48.00.
ISBN 7484–0017–6

This book is based upon the proceedings of the 20th International Symposium of The Princess Takamatsu Cancer Research Fund, Tokyo, 1989. The text addresses the very pertinent and exciting subject of the genetics of carcinogenisis and cancer. The first two chapters introduce the reader to the evidence for human tumour supressor genes and hereditary cancer, oncogenes and anti-oncogenes.

The current evidence for multistep carcinogenisis is discussed and there are chapters which detail the evidence for and the understanding of oncogenes and tumour suppressor genes, including the molecular biology of retinoblastoma.

A basic understanding of molecular biology is assumed. However, the text is well written and presented, each chapter being preceeded by a brief abstract and completed with a clear conclusion.

I have no hesitation in recommending this book to both clinical scientists and oncologists.

J. GLAHOLM

Treatment of Prostatic Cancer Facts and Controversies. Ed. by F. H. Schroeder, pp. xiii + 255, 1990 (John Wiley & Sons, New York), $69.95.
ISBN 0–471–56833–3

This book is based upon the proceedings of an EORTC Genitourinary Group Sponsored Meeting held in Italy on October 12–15, 1989. The text addresses some of the issues relevant to the local and systemic management of this disease, however there are a number of serious ommissions. Current high resolution Computed Tomography (CT) scanning is particularly valuable for the detection of macroscopic pelvic lymph node involvement, yet contrary statements are made, apparently on the basis of outdated reference material.

A chapter is dedicated to the role of radiotherapy for localized prostatic carcinoma, yet without scientific discussion of the value of prophylactic pelvic lymph node irradiation. Even though the discussion relates to the Stanford experience, at the time of writing the results of the randomized prospective trial from RTOG 77–06 were available which at the very least deserves mention!

Several chapters discuss the role of endocrine therapy, including total androgen blockade, and the limited value of chemotherapy. However, the issue of immediate versus deferred endocrine therapy for asymptomatic systemic disease is discussed in a presumptive and non scientific manner, yet the MRC trial addressing this question is only mentioned in passing.

Finally, the value of prostate specific antigen is discussed in a number of chapters. However, the information is scattered throughout the text, reflecting the multiple authorship of this monograph.

In summary, the text is somewhat disjointed with several serious omissions. It neither fulfills the criteria of a textbook nor of a scientific update and I would regard its value as somewhat limited.

J. GLAHOLM

Endoscopic Approaches to Cancer Diagnosis and Treatment. Japanese Cancer Association, Gann Monography on Cancer Research No. 37. Ed. by Y. Oguro and K. Takagi, pp. vi + 166, 1990 (Taylor & Francis Ltd, Hampshire), £48.00.
ISBN 7484–0016–8

This is a delightful book, one to be savoured rather than studied. Japan is the mother of endoscopy where virtually all technical advances and experimentation are born. Endoscopists will enjoy the clear descriptions of the remarkable developments that are occurring and I think many radiologists will be amazed at what endoscopy can now achieve. Within these covers there are descriptions of video endoscopic views of colonic polyps using 30 × magnification power (allowing a differential diagnosis according to surface pattern); data from both transhepatic cholangioscopy and per-oral cholangioscopy; discussion on the value of trans-oral endoscopy of the pancreatic duct and indication of the place of endoscopic treatment in early gastric cancer (with high frequency electro-surgical resection and laser therapy) to name just a few of the techniques that are becoming available. How much will ever prove valuable or become routine therapy is arguable. What is perhaps depressing for the conventional radiologist is that it is almost certain that, in time, the mucosal surface of the gut will no longer be his domain. What is also perhaps depressing for the practitioner in the UK is that it is unlikely that we will ever match the resources available to these Japanese investigators. For instance, one author says that he routinely takes two rolls of 16 mm colour film for each patient for photographic documentation of upper gastrointestinal endoscopy which he says is essential for good results! All this may seem completely over the top but it is difficult to deny the existence of excellent results within this monography, such as an increase in the diagnosis of early gastric cancer from 19% of all cases of gastric cancer up to 1975, to 47% up to 1985 with the introduction of the endoscopy-first policy.

I cannot recommend this book as essential reading for the hard pressed funds of most departmental libraries or personal collections. Clearly, its relevance will be limited. However, if you do have an opportunity to flick through the pages I think you will enjoy and be amazed at what is now possible. A word of warning however for barium based radiologists; this book may well not be good for your health!

P. J. SHORVON

Ultrasound of Appendicitis and its Differential Diagnosis. By J. B. C. M. Puylaert, pp. 118, 1990 (Springer-Verlag, Heidelberg), DM 98.00.
ISBN 3–540–52727–3

Dr Puylaert was one of the first ultrasonologists to employ ultrasound routinely for the diagnosis of appendicitis. In the introduction he states that this book reflects a 4 year experience with ultrasound examination in patients with clinical signs of appendicitis. The comprehensive text and the 169 figures in the book demonstrate the considerable expertise he has gained in this field during this time.

The layout and format of the book are clear and easy to follow. A brief introductory chapter is followed by a chapter entitled "Review of the Literature". The anatomy, pathophysiology, epidemiology and clinical diagnosis are discussed in some detail with a section at the end of the chapter on the limited role played by radiology in the diagnosis of acute appendicitis prior to the use of ultrasound. The next two chapters describe the method of graded compression ultrasound and the normal anatomy of the right iliac fossa as seen on ultrasound examination. An illustration demonstrating simulation of graded compression on computed tomography (CT) scanning vividly illustrates the technique. Following this there is a chapter on the diagnosis of appendicitis by ultrasound, which includes sections on acute, abortive and recurrent appendicitis as well as an appendiceal mass. As in the remainder of the book the illustrations in this section are of a very high quality with, in many cases, correlation between the ultrasound images and the pathological specimens. Anyone considering using ultrasound in the diagnosis of acute appendicitis should be particularly interested in the final section of this chapter on pitfalls in the ultrasound diagnosis of appendicitis. The role of ultrasound in the differential diagnosis of right iliac fossa pain is well covered in the next chapter, which begins with a long section on bacterial ileocaecitis. Gynaecological, urological and caecal pathology are all discussed with good description of the ultrasound features which aid in differentiating between the various conditions. Overlap in the ultrasound appearances may sometimes occur, especially if an abscess is present. The valuable role that CT may play in these difficult cases is well illustrated.

In the final chapter the author states that ultrasound deserves liberal use in all patients with suspected appendicitis with the possible exception of 15–30 year old males. In his own practice ultrasound has led to a "beneficial change in therapeutic management in 26% of patients with clinical signs of appendicitis". He also states that "extensive experience with ultrasound of the abdomen as well as dedication are absolute requirements for obtaining reliable results". There is no doubt that this reasonably priced book should be an essential text for any ultrasonologist wishing to obtain such results.

A. L. Hine

Frontiers in Radiation Biology, Proceedings of the 21st Annual Meeting of the European Society for Radiation Biology. Ed. by E. Riklis, pp. xviii + 712, 1990 (VCH, Germany), DM 268.00. ISBN 3-527-27813-3

The publication of conference proceedings in the form of articles which are neither extended abstracts nor full length peer reviewed papers is becoming increasingly prevalent. It is almost as though no meeting can be considered as scientifically worthy unless a compilation of manuscripts appears in print within a couple of years. Whether you like this trend or not it seems to be here to stay. These proceedings do, however, form an excellent record of the meeting appreciated by the participants and those who could not attend but might have wished to do so. They can also constitute an important addition to the literature, particularly where they form part of an ongoing series on a given topic. This aspect is enhanced where the scientific standard of the individual papers is maintained by peer review.

This book contains a diverse selection of topics covering a wide spectrum of subject areas from experimental radiotherapy to carcinogenesis, from free radical chemistry to environmental radiation protection. While it cannot, therefore, serve as a readily accessible reference work it provides an extensive (75 papers in all) series of short articles, some of which are of a high standard. The quality of the publication has been enhanced by the resetting of the manuscripts into a consistent font and format so that this book looks highly professional, is well laid out and is pleasing to read. This process undoubtedly contributed to the long delay before publication, but it does set this book apart from the many meeting proceedings in which camera ready format leads to a rather messy result.

It is obvious that no peer review process was applied to the submitted papers and that the Editor did not attempt to correct the rather poor use of English in a few of the papers that renders them almost unintelligible. In this respect it is no worse than many meeting proceedings and I should emphasize that there is a lot of excellent science in this book, most of it highly readable.

D. Hirst

Meetings and Courses

Modern methods of Detecting and Measuring Ionizing Radiations
November 6, 1992
London
Further details: Dr J P Nicholson, 64 Dalkeith Road, Harpenden, Herts AL5 5PW

A Practical Approach to Breast Imaging
November 9-13, 1992
Rancho Mirage, California, USA
Further details: Radiology Postgraduate Education, UCSF School of Medicine, Box 0628, Room C-324, San Francisco, CA 94143-0628, USA. Tel. 415 476 5731

Screening for Breast Cancer Multi-Disciplinary Courses and Radiologists Specialist Courses
November 30-December 2, 1992, and 2 days Specialist course
Nottingham
Further details: Mrs B Price, Nottingham Breast Screening Training Unit, City Road, Hucknall, Nottingham NG5 1PB. Tel. 0602 691689

Emerging Targets in Cancer Chemotherapy
December 10-11, 1992
London
Further details: Lucinda Middleton, IBC Technical Services Ltd, Gilmoora House, 57-61 Mortimer Street, London W1N 7TD. Tel. 071 637 4383

Annual Meeting and Course: Imaging and Intervention of the Genitourinary Tract: The Cutting Edge
January 9-10, 1993 (Meeting)
January 11-15, 1993 (Course)
Naples, Florida, USA
Further details: Dawne Ryals and Associates, PO Box 1925, Roswell, Georgia 30077-1925, USA. Tel. 404 641 9773

Miami Neuro-oncology Symposium
21-23 January, 1993
Key Biscayne, Florida, USA
Further details: Division of Continuing Medicine (D23-3), PO Box 016960, Miami, FL 33101, USA. Tel. 305 547 6716

The Bart's/Royal London FRCR II Revision Course (MCQs, Film Reporting and Practice Vivas)
February 9-11, 1993
London
Further details: Mrs J Jessop, Course Secretary, Academic Department of Radiology, St Bartholomew's Hospital, London EC1A 7BE. Tel. 071 601 8864

The Epidemiology of Nutrition and Cancer. An International Course
1-12 March, 1993
Lyon, France
Further details: The Unit of Education and Training, International Agency for Research on Cancer, 150, cours Albert Thomas, F-69372, Lyon Cedex 08, France

PET and SPECT Imaging of Living Brain Chemistry
March 10-12, 1993
Baltimore, Maryland, USA
Further details: Patty Campbell, Johns Hopkins Medical Institutions, Office of Continuing Education, Turner Building, 720 Rutland Avenue, Baltimore, Maryland 21205, USA. Tel. 410 955 6046

General Radiology Review
March 28-April 2, 1993
Marina Del Rey, California, USA
Further details: Mila Wayne, UCLA Radiological Sciences, 10833 LeConte Avenue, Los Angeles, CA 90024-1721, USA. Tel. 310 206 7435

MRI Teaching Course
April 14-16, 1993
London
Further details: Conference Office, The Royal College of Radiologists, 38 Portland Place, London W1N. Tel. 071 636 4432

Second Consensus Development Conference on the Treatment of Radiation Injuries
April 14-17, 1993
Bethesda, Maryland, USA
Further details: Doris Browne, Defense Nuclear Agency, Armed Forces Radiobiology Research Institute, Bethesda, Maryland 20889 5145, USA

Medical and Biological Implant Technology. Second International Conference
April 19-22, 1993
Warwick
Further details: Dr J P Nicholson, 64 Dalkeith Road, Harpenden, Herts AL5 5PW

Principles and practice of clinical MRI
April 22-25, 1993
Baltimore, Maryland
Further details: Program Coordinator, Johns Hopkins Medical Institutions, Office of Continuing Education, Turner Building, 720 Rutland Avenue, Baltimore, Maryland 21205, USA. Tel. 410 955 2959

CT Course
May 6, 1993
London
Further details: Conference Office, The Royal College of Radiologists, 38 Portland Place, London W1N 3DG. Tel. 071 636 4432

Sixth International Conference on Behcet's Disease
June 30-July 1, 1993
Paris
Further details: B Wechsler, Service de Médicine Interne, Pitié-Salpêtriere, 47/83 Boulevarde de L'Hopital, 75013 Paris Cedex France. Tel. 45 70 26 6

6th International Congress on Interventional Ultrasound
September 7-10, 1993
Copenhagen
Further details: C Nolsøe, Department of Ultrasound, Herlev Hospital, University of Copenhagen, DK-2730 Herlev, Denmark

Royal College of Radiologists Annual Scientific Meeting
September 21-25, 1993
Warwick
Further details: Conference Office, The Royal College of Radiologists, 38 Portland Place, London W1N 3DG. Tel. 071 636 4432

As a service to our readers, notices of meetings or courses will be inserted free of charge.
Please send information to the The Managing Editor, The British Journal of Radiology, 36 Portland Place, London W1N 4AT.

© 1992, *The British Journal of Radiology*, 65, 1069–1074

VOLUME 65 NUMBER 780 DECEMBER 1992

The British Journal of Radiology

The assessment of carotid and vertebral arteries: a comparison of CFM duplex ultrasound with intravenous digital subtraction angiography

By I. Colquhoun, *C. P. Oates, *K. Martin, K. Hall and *T. A. Whittingham

Department of Neuroradiology and *Regional Medical Physics Department, Newcastle General Hospital, Newcastle Upon Tyne, UK

(*Received 13 September 1991 and in revised form 5 May 1992, accepted 3 June 1992*)

Keywords: Ultrasound, DSA, Carotid artery, Vertebral artery

Abstract. The use of duplex ultrasound with colour flow mapping is compared with that of intravenous digital subtraction angiography (IVDSA) in the investigation of carotid and vertebral artery disease. Ninety-nine carotid and vertebral arteries were examined independently by IVDSA and ultrasound for location and degree of disease in 30 men (mean age 58) and 20 women (mean age 53). For purposes of comparison the carotid tree was divided into six segments. In 46% of cases no disease was detected by either modality. In 36% of cases where disease was found, ultrasound found mild disease in arteries reported as normal by IVDSA. Both modalities detected the six cases of total occlusion found in the study. IVDSA underestimated five cases of major disease found by ultrasound at the bifurcation or in the bulb. Overall agreement in grading vessel segments was good, with 74.5% in complete agreement and 90.3% grading stenoses to within ±25% of the other modality. There was good qualitative agreement in the findings for vertebral arteries. In four patients conventional arteriography was also available for comparison.

The introduction of colour flow mapping (CFM) to duplex ultrasound scanning has improved the ease of performing ultrasound investigations of the carotid and vertebral arteries. The vessels may be located quickly and the presence of echoes in the vessel lumen which indicate pathological conditions are more easily distinguished from echoes due to artefacts. Regions of turbulent flow are readily identifiable. Previous studies have shown that duplex ultrasound is an effective screening investigation for carotid artery disease (Glover et al, 1982; Hames et al, 1985a,b; Jacobs et al, 1985; Cardullo et al, 1986). Since it is a non-invasive screening test that is highly acceptable to patients we wished to compare duplex ultrasound plus CFM with intravenous digital subtraction angiography (IVDSA), which has been the investigation of choice used to screen for carotid disease in Newcastle.

Methods

The study cohort was composed of 52 consecutive patients referred by their clinicians for IVDSA examination of the carotid arteries. With the approval of the clinicians each patient was given an explanation of the study and their consent for the ultrasound examination obtained. The ultrasound examinations were performed within four weeks of IVDSA without knowledge of the patients' clinical problem or of the IVDSA findings. The results of the IVDSA and ultrasound examinations were subsequently analysed independently. Two patients did not attend for ultrasound and in one patient the IVDSA image from one side was spoilt by a swallowing artefact. Results were therefore obtained from 99 carotid arteries: 30 men, mean age 58 (44–70) and 20 women, mean age 53 (38–68).

To compare the two modalities at different sites, the carotid tree was divided into six segments, shown in Figure 1. A further comparison was made in the vertebral artery using the Doppler waveform obtained from the vertebral artery at the level of the carotid bifurcation. For both modalities, the maximum degree of stenosis in each segment was noted and graded on a scale 0–V as shown in Table I. Where possible the length and site of the lesion within the vessel were also noted. This could not be done where the presence of disease was inferred from the Doppler waveform alone. In addition, any calcification and ulceration were noted.

The IVDSA examinations were performed using dedicated digital subtraction angiographic equipment. The catheter was introduced over a guidewire following puncture of either the basilic or cephalic vein in the antecubital fossa under local anaesthesia, and the tip positioned in the right atrium. Forty millilitres of 370 mg I/ml non-ionic contrast medium were injected at a rate of 20 ml/s for each run. Images were obtained of

---

Address correspondence to C. P. Oates, Regional Medical Physics Department, Newcastle General Hospital, Newcastle Upon Tyne, NE4 6BE.

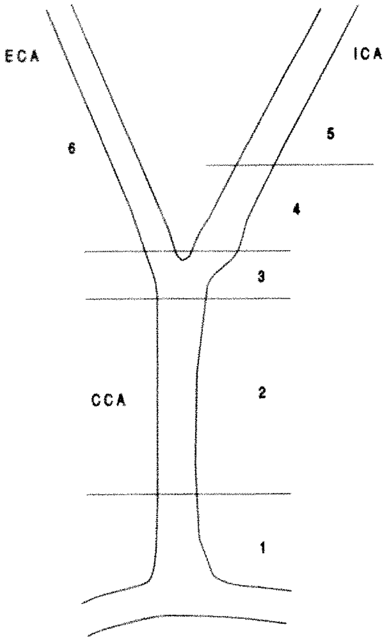

Figure 1. The carotid artery tree showing the segments into which the vessels were divided for analysis. ECA = external carotid artery; ICA = internal carotid artery; CCA = common carotid artery.

Table I. The grading scheme used to classify disease in a vessel segment

Grade	Degree (% stenosis)
0	no disease
I	0–24
II	25–49
III	50–74
IV	75–99
V	total occlusion

the aortic arch and great vessels' origins (LAO), the extracranial carotid and vertebral arteries (both 45° obliques, supplemented when necessary by a PA with the chin extended) and the intracranial circulation (PA 25°). No complications were recorded. The degree of stenosis for each area was assessed using callipers to measure the width of the lumen at the site of maximal stenosis and expressing this as a percentage of the true lumen, predicted by extrapolation from above and below the stenosis.

The ultrasound examination was performed with an Acuson 128 duplex scanner with colour flow mapping using a 5 MHz small parts linear array probe (L538). The scans were performed by one of three people (C.P.O., I.C., K.M.). The patient lay supine with the head rotated away from the side being examined, to expose the lateral side of the neck. The base of the common carotid artery was located in transverse section on the image and followed distally to locate the position and orientation of the bifurcation. The vessels were then imaged in longitudinal section. The images were examined for site and length of stenotic disease and for the presence of ulceration and calcification. Doppler waveforms were recorded at the base of the common carotid artery, 2 cm below the bifurcation, 2 cm above the bifurcation in both the internal and external carotid arteries, and in the internal carotid artery at the level of the angle of the mandible. Doppler waveforms were obtained with the Doppler range gate set to straddle the vessel. Incidental findings were recorded. A further Doppler waveform was recorded from the vertebral artery at the level of the carotid bifurcation. Diagnosis was made from the images and assessment of the Doppler waveforms. When possible the percentage diameter stenosis was measured directly from the image with electronic callipers. This could not always be done with certainty, particularly in the case of higher grade stenoses, and the degree of disease was then assessed from the Doppler waveforms. Low grade stenoses cause spectral broadening and spike turbulence over the systolic peak. Higher grade stenoses cause significant increases in peak systolic velocity, with turbulence appearing as bi-directional flow over the systolic peak. For example, a peak systolic velocity of 120 cm/s in the internal carotid artery was taken to indicate > 50% diameter stenosis, and > 250 cm/s with diastolic velocities > 100 cm/s was taken to indicate > 80% diameter stenosis (Zwiebel, 1987; Jacobs et al, 1985).

Results

Of the 50 patients examined, 27 were referred with transient ischaemic attacks, two with amaurosis fugax, 15 with stroke and six with non-specific complaints.

In only one patient examined by ultrasound was the examination judged of poor quality, compared with five patients examined by IVDSA, where in one patient the images of one carotid artery were rendered non-diagnostic by a swallowing artefact.

In 46 of the 99 carotid arteries successfully scanned, no abnormality was detected by either IVDSA or ultrasound. Results for the 53 arteries where pathology was found are shown in Table II. In 10 (19%) cases there was complete agreement on the site of disease throughout the carotid tree and of these, six also agreed in grade of stenosis and three were within one grade. In 19 (36%) cases IVDSA reported all the carotid arteries as normal. In 13 of these, ultrasound reported Grade I disease, in five Grade II disease, and in one external carotid artery (ECA) Grade III disease was detected. In 14 of these cases the position and extent of the disease were seen on the ultrasound image and five cases were reported from the waveform alone. In one case ultrasound reported normal vessels and IVDSA reported Grade I disease. Of 49 cases where ultrasound reported mild disease (Grade I–II) in a vessel segment and IVDSA reported the segment as normal, the diagnosis was made on the basis of lesions seen on the image in 31 (63%) vessel segments

Table II. Comparison of ultrasound with IVDSA for each vessel segment

a) Segment 1

	Ultrasound Grade						
IVDSA Grade	0	I	II	III	IV	V	Total
0	44	5	2	—	—	—	51
I	—	—	—	—	—	—	—
II	—	—	—	—	—	—	—
III	—	—	—	—	—	—	—
IV	—	—	—	—	—	—	—
V	—	—	—	—	—	2	2
Total	44	5	2	—	—	2	53

b) Segment 2

	Ultrasound Grade						
IVDSA Grade	0	I	II	III	IV	V	Total
0	31	13	5	—	—	—	49
I	—	2	—	—	—	—	2
II	—	—	—	—	—	—	—
III	—	—	—	—	—	—	—
IV	—	—	—	—	—	—	—
V	—	—	—	—	—	2	2
Total	31	15	5	—	—	2	53

c) Segment 3

	Ultrasound Grade						
IVDSA Grade	0	I	II	III	IV	V	Total
0	18	9	4	—	—	—	31
I	2	9	2	—	1	—	14
II	1	1	1	2	1	—	6
III	—	—	—	—	—	—	—
IV	—	—	—	—	2	—	2
V	—	—	—	—	—	—	—
Total	21	19	7	2	4	—	53

d) Segment 4

	Ultrasound Grade						
IVDSA Grade	0	I	II	III	IV	V	Total
0	22	4	1	—	—	—	27
I	1	—	—	—	—	—	1
II	1	3	4	—	3	—	11
III	—	—	—	3	—	—	3
IV	—	—	—	—	7	—	7
V	—	—	—	—	—	4	4
Total	24	7	5	3	10	4	53

Table II.—*continued*

e) Segment 5

	Ultrasound Grade						
IVDSA Grade	0	I	II	III	IV	V	Total
0	42	3	1	—	—	—	46
I	—	—	—	—	—	—	—
II	1	—	—	—	—	—	1
III	—	—	1	—	—	—	1
IV	—	—	—	—	1	—	1
V	—	—	—	—	—	4	4
Total	43	3	2	—	1	4	53

f) Segment 6

	Ultrasound Grade						
IVDSA Grade	0	I	II	III	IV	V	Total
0	36	1	1	2	1	—	41
I	2	2	—	1	—	—	5
II	1	—	—	—	—	—	1
III	1	—	1	—	—	—	2
IV	2	—	1	—	1	—	4
V	—	—	—	—	—	—	—
Total	42	3	3	3	2	—	53

g) All Segments

	Ultrasound Grade						
IVDSA Grade	0	I	II	III	IV	V	Total
0	193	35	14	2	1	—	245
I	5	13	2	1	1	—	22
II	4	4	5	2	4	—	19
III	1	—	2	3	—	—	6
IV	2	—	1	—	11	—	14
V	—	—	—	—	—	12	12
Total	205	52	24	8	17	12	318

and on the waveforms alone in 18 (37%) vessel segments.

There was good agreement in detecting major disease (Grades IV–V). Both modalities detected the six cases of total occlusion found (two in the common carotid artery (CCA), four in the internal carotid artery (ICA)). In the two cases of CCA occlusion, retrograde flow in ECA to ICA was observed on IVDSA and colour Doppler. IVDSA found 14 cases of Grade IV stenosis and ultrasound found 17 cases, 11 of which were in agreement with IVDSA. Two cases of Grade IV found by IVDSA were reported as Grade 0 and one as Grade II by ultrasound, all in the ECA. Four cases of Grade IV found by ultrasound were reported as Grade II by IVDSA: three in the bulb and one at the bifurcation. One case of Grade IV found by ultrasound was reported as Grade I (at the bifurcation) and one as Grade 0 (at the origin of ECA) by IVDSA.

Overall the agreement in grading for each vessel segment was good; 74.5% agreed, 90.3% were within one grade and 97.8% were within two grades.

A number of incidental findings were also reported. Calcification was observed in 15 vessel segments by ultrasound alone and a further two by both IVDSA and ultrasound. Ulceration was reported in three vessel segments by IVDSA alone. IVDSA also found one case of a small arteriovenous malformation in the left frontal lobe and one case of a dural arteriovenous fistula of the left sigmoid sinus.

With reference to the vertebral artery, 78 cases were reported normal by both modalities. Only two vertebral arteries shown on IVDSA to be very narrow were not detected by ultrasound. Four vessels were reported as large by IVDSA and ultrasound showed a high flow rate. Of nine vessels reported as small or irregular by IVDSA, ultrasound found small damped flows in five and reported four as normal. In one case IVDSA reported a small vessel with slow filling and the ultrasound Doppler waveform showed no end-diastolic flow, consistent with increased peripheral resistance. In two cases reported normal by IVDSA, ultrasound found velocities less than normal.

Only four patients subsequently underwent conventional selective carotid arteriography. There was good correlation between the results obtained from these studies and those obtained from the initial IVDSA and ultrasound studies, as shown in Table III. The one major area of disparity is in Area 6 on the left for patient 4, where there was a severe stenosis at the carotid bifurcation involving the origins of the internal and external carotid arteries. The IVDSA and ultrasound demonstrated this but showed no stenosis in the external carotid artery above its origin (Area 6). However, the selective carotid arteriogram performed five weeks later demonstrated occlusion of the external carotid artery. Review of the studies demonstrate that the external carotid artery occlusion occurred in the interval between the IVDSA/ultrasound and the selective carotid arteriogram.

Discussion

Intravenous DSA has been compared with duplex ultrasound previously (Glover et al, 1982), as has intra-arterial DSA (Zietler et al, 1989). Predictably, the best results obtained with DSA are by selective catheterization of the carotid arteries. However, Zietler et al (1989) point out that this is only strictly necessary when detailed investigation of intracranial vessels is required.

The ultrasound investigations in this study were performed using a 5 MHz probe as this was the only probe available throughout the study. In many subjects a 7.5 MHz probe can give better visualization of the bifurcation. However, it has been our experience when we have used a 7.5 MHz probe on the Acuson that examination of the distal internal carotid artery is more difficult and that in obese patients visualization of the carotid bifurcation itself is not as clear as when using a 5 MHz probe. This study has shown the 5 MHz probe to give adequate results in all of the patients investigated.

Previous ultrasound studies have shown that duplex ultrasound is better at detecting > 50% stenosis in ICA than conventional angiography (Hames et al, 1985a) and that it is able to separate 0–24% and 25–49% stenosis in cases of early disease (Hames et al, 1985b). Glover et al (1982) showed that duplex ultrasound was as good as IVDSA but that where differences arose, IVDSA tended to underestimate the degree of disease. The combined use of ultrasound for imaging and Doppler waveforms allows both > 50% and < 50% stenosis to be reliably detected. In particular, the use of high resolution B-mode imaging allows low grade plaques to be seen whilst the Doppler waveform gives a more accurate indication of the degree of stenosis in high grade disease (Hames et al, 1985a,b; Jacobs et al, 1985). Jacobs et al (1985) and Cardullo et al (1986) also say that B-mode imaging visualized small plaques that were missed by conventional angiography.

Our findings agree with these. Of the 19 cases in which IVDSA reported all the carotid arteries as

Table III. Correlation of results obtained from IVDSA and ultrasound (US) studies with those subsequently obtained in the four patients who underwent selective carotid arteriography (SCA). Area 1 was not examined by SCA and has therefore not been included

	Patient 1			Patient 2			Patient 3			Patient 4		
Area	DSA	US	SCA	DSA	US	SCA	DSA	US	SCA	DSA	US	SCA
Right												
2	0	0	0	all normal			0	0	0	0	I	I
3	0	0	0				0	0	I	0	II	I
4	II	II	II				0	0	I	0	II	I
5	0	0	0				0	0	0	V	V	V
6	0	0	0				0	0	0	0	III	II
Left												
2	0	II	0	all normal			0	0	0	0	0	I
3	0	0	0				I	I	I	IV	IV	IV
4	0	0	0				I	I	I	0	0	0
5	0	0	0				0	0	0	0	0	0
6	0	0	0				0	0	0	0	0	V

normal, small plaques (Grade I–II) were visualized by ultrasound in 14 (74%) cases. In considering the individual vessel segments reported normal by IVDSA, again, ultrasound visualized lesions in 31/46 (67%), of which two (4%) were in the ECA. Conversely there were only nine segments where the ultrasound was reported normal and IVDSA found minor disease, of which three (33%) were in the ECA.

The segment in which there was greatest discrepancy between ultrasound and IVDSA, that is two or more grades of difference, was the ECA. IVDSA and ultrasound each reported five cases in which the grade was higher than in the other modality. In the bifurcation–carotid bulb segment (Areas 3 and 4) there were five cases where ultrasound reported Grade IV and IVSDA reported only minor disease. This may be due to the plane of the IVDSA image being such as to underestimate the degree of stenosis, or it may be due to overestimation by Doppler ultrasound. However, on all four ultrasound studies an intraluminal plaque was clearly identified. The degree of occlusion was confirmed by imaging the vessel transversely with CFM, and Doppler velocities were high in every case (3–6 m/s). There was therefore a high degree of confidence in all four ultrasound results.

No attempt was made in this study to classify plaque morphology. However the presence of calcification and ulceration were noted. The difficulty of classifying plaque morphology by ultrasound has been reviewed by Cardullo et al (1986). Ratliff et al (1985), comparing Doppler ultrasound findings with histological specimens, concluded that ulceration, thrombus and fibrous intimal thickening could not be detected reliably by ultrasound imaging, but calcification could be identified. A more recent study using an ultrasound frequency of 7.5 MHz suggests that plaques may be categorized into one of four groups according to their morphology and that these categories give a guide to prognosis (Steffen et al, 1989). In the present study calcification was seen by ultrasound in 17 vessel segments, but ulceration was noted in only three cases, all by IVDSA.

The results we report for the vertebral artery are of a more qualitative nature than for the carotid artery as the former artery was only examined at one point, level with the carotid bifurcation. In spite of the limited examination the comparison between IVDSA and ultrasound was good. There was qualitative agreement in 88/94 (93.6%) of cases.

The advantages of having the additional information of CFM in duplex ultrasound have been described before (Steinke et al, 1990). It leads to a technically more competent investigation and enables intraluminal disease to be readily identified and confirmed, so that it does not take so long to perform a scan. In the study by Cardullo et al (1986), 76% of arteries reported to be totally occluded on duplex ultrasound were found to be patent, although with major disease, on arteriography. In the present study both modalities agreed on which vessels were totally occluded, and the CFM provided confirmation, including the presence of retrograde flow in the ECA in two cases of CCA total occlusion. In cases of suspected total occlusion the CFM colour scale could be reduced to show mean velocities of 2–9 cm/s. We also found CFM particularly helpful in following tortuous vessels and in locating the vertebral arteries.

Conclusion

The ease of obtaining reliable ultrasound scans of the carotid arteries has been improved by CFM. Overall we found good agreement between ultrasound and IVDSA in determining both the degree and location of carotid disease. In assessing the degree of stenosis, there was complete agreement in 74.5% of cases, 90.3% of results were within one grade of each other and 97.8% were within two grades. Duplex ultrasound detected all six cases of total occlusion of ICA or CCA found by IVDSA. The three cases of Grade IV stenosis shown by IVDSA but under-reported by ultrasound were all within the ECA, whereas of six cases of Grade IV detected by ultrasound and under-reported by IVDSA, five were at the bifurcation or in the bulb and just one in the ECA. There was only one set of carotid arteries reported as normal by ultrasound but abnormal by IVDSA which reported Grade I disease. However, in 19 cases reported as normal by IVDSA, ultrasound showed Grade I–III disease. This suggests that ultrasound is more sensitive in detecting mild disease than IVDSA. IVDSA reported three cases of ulceration, none of which were detected by ultrasound. Ultrasound detected 97/99 vertebral arteries. The two not found both showed very narrow vessels on IVDSA. In conclusion, ultrasound with CFM performs as well as IVDSA in detecting major disease, and is better than IVDSA in detecting mild disease. This was confirmed by the four patients whose results were also compared with those of conventional arteriography.

References

CARDULLO, P. A., CUTLER, B. S. & BROWNELL WHEELER, H., 1986. Detection of carotid artery disease by duplex ultrasound. *Journal of Diagnostic Medical Sonography, 2*, 63–73.

GLOVER, J. L., BENDICK, P. J., JACKSON, V. P., BECKER, G. J., DILLEY, R. S. & HOLDEN, R. W., 1984. Duplex ultrasonography, digital subtraction angiography, and conventional angiography in assessing carotid atherosclerosis. *Archives of Surgery, 119*, 664–669.

HAMES, T. K., HUMPHERIES, K. N., RATLIFF, D. A., BIRCH, S. J., GAZZARD, V. M. & CHANT, A. D. B., 1985a. The validation of duplex scanning and continuous wave Doppler imaging: a comparison with conventional angiography. *Ultrasound in Medicine and Biology, 11*, 827–834..

HAMES, T. K., RATLIFF, D. A., HUMPHERIES, K. N., GAZZARD, V. M., BIRCH, S. J. & CHANT, A. D. B., 1985b. The accuracy of duplex scanning in the evaluation of early carotid disease. *Ultrasound in Medicine and Biology, 11*, 819–825.

JACOBS, N. M., GRANT, E. G., SCHELLINGER, D., BYRD, M. C., RICHARDSON, J. D. & COHAN, S. L., 1985. Duplex carotid sonography: Criteria for stenosis, accuracy, and pitfalls. *Radiology, 154*, 385–391.

RATLIFF, D. A., GALLAGHER, P. J., HAMES, T. K., HUMPHERIES, K. N., WEBSTER, J. H. H. & CHANT, A. D. B., 1985.

Characterisation of carotid artery disease: comparison of duplex scanning with histology. *Ultrasound in Medicine and Biology*, *11*, 835–840.

STEFFEN, C. M., GRAY-WEALE, A. C., BYRNE, K. E. & LUSBY, R. J., 1989. Carotid artery atheroma: ultrasound appearance in symptomatic and asymptomatic vessels. *Australian and New Zealand Journal of Surgery*, *59*, 529–534.

STEINKE, W., KLOETZSCH, C. & HENNERICI, M., 1990. Carotid artery disease assessed by colour Doppler flow imaging: correlation with standard Doppler sonography and angiography. *American Journal of Neuroradiology*, *11*, 259–266.

ZEITLER, E., SEYFARTH, W., RICHTER, E. J., RITTER, W. & LEONHARDI, J., 1989. The value of angiography in cerebrovascular disease. *Thoracic and Cardiovascular Surgeon*, *37*, 259–263.

ZWIEBEL, W. J., 1987. Spectrum analysis in carotid sonography. *Ultrasound in Medicine and Biology*, *13*, 625–636.

1992, *The British Journal of Radiology*, *65*, 1075–1082

$^{99}Tc^{m}$Technegas and krypton-81m ventilation scintigraphy: a comparison in known respiratory disease

By J. M. James, MB, ChB, MRCGP, J. J. Lloyd, BSc, MSc, *†B. C. Leahy, MB, ChB, MRCP, *‡S. Church, MRCP, MD, C. C. Hardy, MRCP, MD, R. A. Shields, MSc, PhD, FIPSM, M. C. Prescott, MB, ChB, MD and H. J. Testa, PhD, FRCP, FRCR

Departments of Nuclear Medicine and Medical Physics and *Respiratory Medicine, Manchester Royal Infirmary, Oxford Road, Manchester, M13 9WL, UK

(*Received 28 May 1992 and accepted 12 August 1992*)

Keywords: Tc-Technegas, Krypton-81m, Scintigraphy, Respiratory disease

Abstract. Krypton-81m gas, by virtue of its imaging characteristics, is often considered the "gold standard" for ventilation scintigraphy but its use is restricted by its high cost and limited availability. The new radiopharmaceutical $^{99}Tc^{m}$-Technegas, a suspension of ultrafine technetium-99m labelled carbon particles, produces high-quality images of ventilation and has the advantage of continuous availability. As part of our evaluation of Technegas the two were compared in 40 patients with a variety of established respiratory diseases. Disparities were seen in five patients in five diagnostic groups and may be a consequence of the differing physical properties of the two agents and the different inhalation techniques used. In addition two interesting features were noted on the Technegas images. (1) Hot spots were seen in 50% of patients, particularly in those with a degree of airways obstruction; (2) preferential basal deposition of activity was seen in 30%, particularly in patients with idiopathic pulmonary fibrosis. Both features were significantly associated with parameters of pulmonary function indicating obstructive lung disease in the former case and restrictive lung disease in the latter.

The value of ventilation-perfusion scintigraphy in the diagnosis of pulmonary embolism is widely recognized. Whilst the technique and radiopharmaceutical used for perfusion imaging are well established, a number of differing techniques and agents are currently available for ventilation scintigraphy, each having advantages and disadvantages.

A previously reported study from this department comparing krypton-81m and Technegas in patients with pulmonary embolism (James et al, 1991) found disparities between the two sets of ventilation images in 1 of 31 (3.2%) of cases. In addition 14% of the Technegas images contained hot spots (small regions of high count density) and 16% showed preferential basal deposition of activity. Other studies have compared images by Technegas with those by krypton-81m (Peltier et al, 1990; De Geeter et al, 1990) and with xenon-133 (Fawdry & Gruenewald, 1988; Sullivan et al, 1988). Significant disparities were not documented by Peltier et al but were seen in 1 of 17 (6%) patients by De Geeter et al who judged the Technegas images to be technically superior in 11 patients. The xenon-133 comparisons found the Technegas images to be diagnostically superior in 3 of 20 (15%) (Fawdry & Gruenewald, 1988) and 21 of 46 (46%) (Sullivan et al, 1988). Hot spots were recorded in varying numbers in each of these studies. The presence of a posterior gradient of Technegas activity was noted by De Geeter et al. Sullivan et al comment that "ventilation parallels perfusion in its distribution in normal lungs" and Peltier et al that "the apex to base distribution of technetium-99m and krypton-81m appeared to be similar." In all three of these studies the patients were supine.

The aim of this further study, undertaken in a group of patients with established respiratory disease, was twofold: firstly, to assess the incidence and significance of disparities between Technegas and krypton-81 images and secondly, to evaluate the diagnostic potential of the two features previously noted and the correlation of these with indices of pulmonary function.

Materials and methods

Patients

The study was approved by the local Ethical Committee. Forty patients were recruited in eight diagnostic groups, the diagnosis in each case being advised and determined by a senior physician in the Department of Respiratory Medicine. The relevant factors regarding the patients are detailed in Table I.

Procedure

The patients' pulmonary function was tested just before imaging. Measurement of forced expiratory volume in one second ($FEVI_1$) and forced vital capacity (FVC) were made in all patients using Vitalograph dry spirometry. Transfer factor, alveolar volume, residual volume (RV) and total lung capacity (TLC) were also measured in the majority. Lung volumes were measured using helium dilution. Transfer factor was measured using a carbon monoxide 10 s breath-hold technique. In

---

†Present address: Department of Medicine, Trafford General Hospital, Moorside Road, Urmston, Manchester, M31 3SL, UK.

‡Present address: Department of Medicine, Charing Cross Hospital, Fulham Palace Rd, London, W6 8RF, UK.

Table I. Patients

Disease	No. of patients	Description
Pleurisy	1	1 male, 58 years, ex-smoker
Left ventricular failure	1	1 male, 72 years, non-smoker
Sarcoidosis	4	3 male, 1 female; 33–47 years (mean 40); 1 smoker, 2 non-smokers, 1 ex-smoker
Emphysema	4	1 male, 3 female; 31–75 years (mean 54); 2 smokers, 2 ex-smokers; 1 of the group was known to have bullae and 1 had additional bronchiectasis
Asthma	6	4 male, 2 female; 21–70 years (mean 57); 1 smoker, 3 non-smokers, 2 ex-smokers; 1 patient had additional bronchiectasis
Chronic obstructive airways disease	6	3 male, 3 female; 61–72 years (mean 67); 3 smokers, 3 ex-smokers; 1 patient had concurrent pneumonia
Space-occupying lesion	8	7 male, 1 female; 30–74 years (mean 58); 5 smokers, 1 non-smoker, 2 ex-smokers; 7 patients had bronchoscopy-proven bronchial carcinoma and 1 had a long-standing aspergilloma
Idiopathic pulmonary fibrosis	10	5 male, 5 female; 53–75 years (mean 63); 2 smokers, 4 non-smokers, 4 ex-smokers

some patients functional residual capacity, peak expiratory flow (PEF) rate and diffusion coefficient were also measured. Tables of predicted values for these measurements are available based on age, sex and height (Quanjer, 1983). A figure for "percentage of predicted value" was therefore calculated for each measurement made. It was not possible to perform full testing in all patients as in many cases the severity of the underlying respiratory disease prevented compliance with the test procedure.

In all cases radiopharmaceutical administration and imaging were performed with the patient seated. The gamma camera (either an IGE 400A/T maxicamera or an Elscint Dymax LF, each fitted with a low-energy general-purpose collimator) was positioned as for a posterior lung view. Technegas was generated as previously described (James et al, 1991). The patient was then instructed as to the mode of inhalation required using a mouthpiece connected, via a filter, to a delivery tube which was in turn connected to the Technegas generator. Wearing a nose clip and from functional residual capacity the patient was asked to take a slow deep inspiration of Technegas, hold their breath for 5 s and then expire before returning to tidal breathing of room air. Ample time was allowed for practice runs. Patients who were unable to co-operate fully with this inhalation technique either did a mixture of breath-holding and tidal breathing or tidal breathing alone. Administration was continued until either a posterior count rate of approximately 1600 cps was achieved or the 10 min for which Technegas is available after generation had elapsed.

Krypton-81m gas was obtained by passing air through a rubidium-81/krypton-81m generator (Clark et al, 1978); it was then inhaled via a face mask during tidal breathing. In the majority of cases Technegas and krypton-81m images were obtained in succession in each of four projections—posterior, right posterior oblique, left posterior oblique and anterior. 200kcount analogue and computer images (128 × 128 matrix) were acquired in each case, image acquisition times being 2–3 min for Technegas and 30–60 s for krypton-81m.

Following acquisition the two sets of images were assessed and compared by two independent experienced observers. The Technegas images were classified according to the presence or absence of hot spots and preferential basal deposition of activity. Differences between the mean indices of pulmonary function within these two groups were then evaluated using the unpaired *t*-test (Unistat 4.5 computer package).

Table II. Breathing patterns used

Breathing pattern	No. of patients	No. of inhalations (mean)	Final posterior count rate (mean), cps
Breath holding alone	28 (70%)	1–10 (3.4)	1275–2230 (1728)
Breath holding + tidal	9 (23%)	2–10 (4) + tidal breaths	1250–1700 (1517)
Tidal alone	3 (8%)	Tidal breaths	700 1500 2010

Table III. The incidence of Technegas image features in relation to the pulmonary disease groups studied

Diagnosis	Total no. of patients	Hot spots	Preferential basal deposition
Pleurisy	1	0	1 (100%)
Left ventricular failure	1	0	0
Sarcoidosis	4	0	1 (25%)
Emphysema	4	3 (75%)	0
Asthma	6	4 (67%)	0
Chronic airways disease	6	5 (83%)	0
Space-occupying lesion	8	4 (50%)	3 (38%)
Idiopathic pulmonary fibrosis	10	4 (40%)	7 (70%)
Totals	40	20 (50%)	12 (30%)

Results

The breathing patterns used by patients in this series are summarized in Table II. High-quality images were obtained in all cases, although in those performing tidal breathing the Technegas administration took longer than in those holding their breath. Hot spots were seen on the Technegas images in 50% of the patients overall, in seven of nine undergoing a mixture of breath holding and tidal breathing and in all of those performing tidal breathing alone. Preferential basal deposition of Technegas was found in 30% of the scans; breathing patterns in these patients paralleled those for the whole series. The incidence of each feature in the various disease groups studied is indicated in Table III and

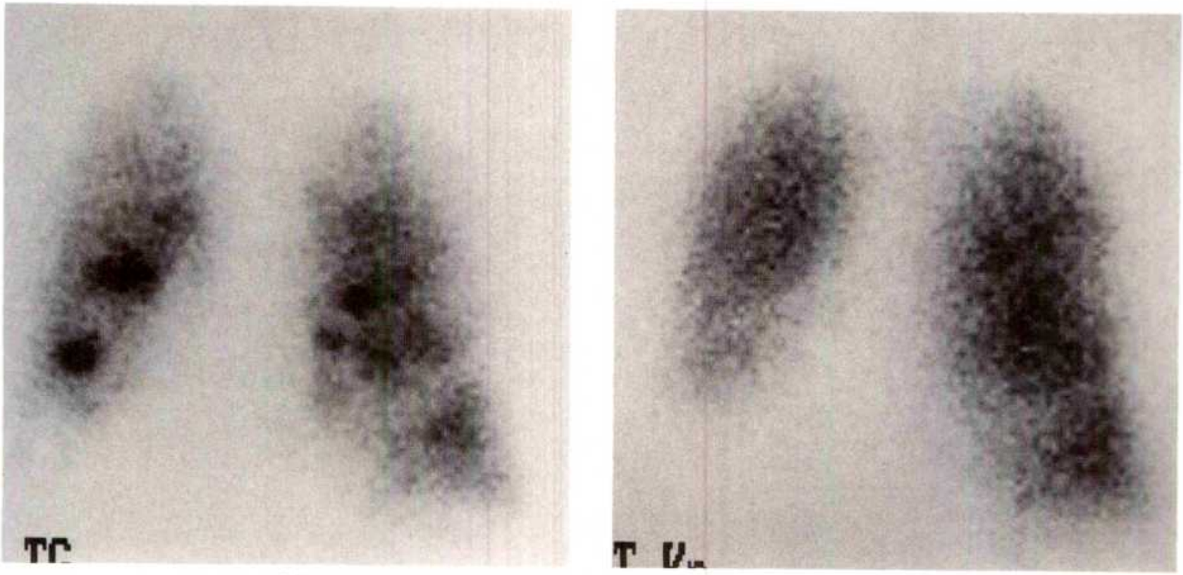

(a) (b)

Figure 1. Posterior view of the lungs: (a) Technegas, (b) krypton-81m. A number of hot spots, both central and peripheral, are seen on the Technegas image.

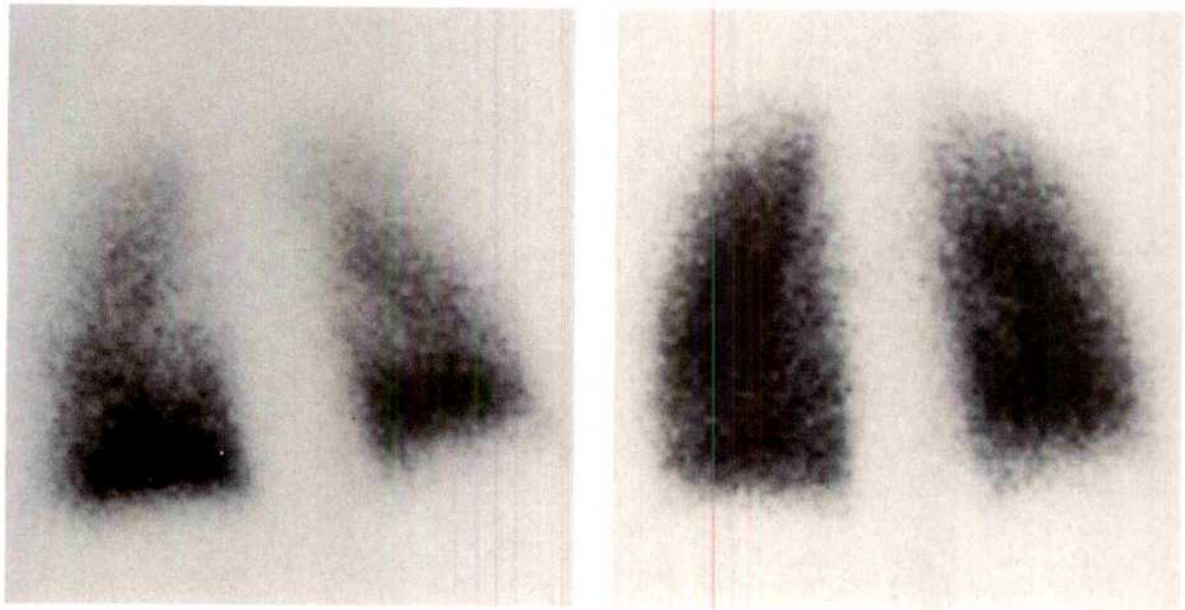

(a) (b)

Figure 2. Posterior view of the lungs: (a) Technegas, (b) krypton-81m. There is pronounced basal deposition of Technegas. The krypton-81m image is more uniform.

examples of each illustrated in Figs 1 and 2. Hot spots are most common in chronic obstructive airways disease, emphysema and asthma, being seen in 83%, 75% and 67% of these groups. Preferential basal deposition of activity is seen in 70% of those with idiopathic pulmonary fibrosis.

Detailed analysis of the pulmonary function test results (Table IV) revealed that in patients with scan images showing hot spots there were significant differences between the mean values for FEV$_1$, FEV$_1$%P ($p < 0.001$), FEV$_1$/FVC, PEF, PEF%P, RV/TLC ($p < 0.01$) and FEV$_1$/FVC%P, FVC, FVC%P and TCO/VA%P ($p < 0.05$). These differences were apparent whether the patient group with space-occupying lesions were included or excluded. In those patients whose scans showed preferential basal deposition of activity, significant differences were found for FEV$_1$/FVC, FEV$_1$FVC%P ($p < 0.01$) and FEV$_1$%P ($p < 0.05$).

The Technegas and krypton-81m images were directly comparable in 35 of the 40 patients (88% of the series). A single disparity was seen in each of the following five disease categories: sarcoidosis, asthma, chronic obstructive airways disease, space-occupying lesion and idiopathic pulmonary fibrosis.

In two instances (one patient with a space-occupying lesion and one with sarcoidosis) ventilatory defects in the lower regions of the lungs appeared larger with krypton. In a further three cases there was patchy, irregular apical deposition of Technegas and a more uniform krypton image (one patient with idiopathic pulmonary fibrosis, one with chronic obstructive airways disease and one asthmatic). An example of each disparity is shown in Figs 3 and 4.

Table IV. Summarized pulmonary function test results

Parameter	No. of patients	Hot spots		Preferential basal deposition	
		Present	Absent	Present	Absent
		Mean ± SEM	Mean ± SEM	Mean ± SEM	Mean ± SEM
FEV$_1$	40	1.3±0.14	2.4±0.18^{c}	2.2±0.2	1.7±0.2
FEV$_1$%P	40	51.3±4.1	80.0±3.7^{c}	76.8±6.4	60.9±4.0^{a}
FVC	40	2.4±0.2	3.2±0.2^{a}	2.8±0.3	2.8±0.2
FVC%P	40	72.8±5.6	89.8±4.2^{a}	81.7±8.0	80.4±4.2
FEV$_1$/FVC	40	59.0±4.8	73.9±2.7^{b}	80.3±3.0	60.5±3.5^{b}
FEV$_1$/FVC%P	40	77.9±6.5	94.7±3.4^{a}	103±4	78.9±4.6^{b}
PEF	38	252±24	378±36^{b}	360±42	294±30
PEF%P	38	59.6±4.8	80.8±5.7^{b}	80.2±8.2	66.4±4.5
RV	36	2.0±0.2	1.6±0.1	1.5±0.1	1.9±0.1
RV%P	36	83.1±7.9	92.7±5.2	74.5±7.3	92.4±5.6
RV/TLC	36	43.2±2.1	35.6±1.8^{b}	36.0±2.1	40.5±1.9
RV/TLC%P	36	113±6	102±4	102±6	110±5
TLC	36	4·7±0.4	4.7±0.3	4.3±0.4	4.8±0.3
TLC%P	36	79.6±6.3	80.0±3.9	71.3±7.0	82.7±4.2
FRC	33	3.0±0.3	2.5±0.2	2.4±0.3	2.7±0.2
FRC%P	33	96.9±9.0	82.4±4.6	76.1±8.7	93.8±5.6
TLCO	36	16.5±1.9	21.6±2.2	19.1±2.5	19.5±1.9
TLCO%P	36	64.5±5.3	81.0±6.8	70.0±8.3	75.4±5.6
TLCO/VA	29	5.5±1.9	5.0±0.4	5.7±0.4	4.25±1.4
TLCO/VA%P	29	66.4±6.7	88.4±6.0^{a}	75.6±6.9	78.9±6.6

FEV$_1$ = Forced Expiratory Volume (litres) in 1 s.
FVC = Forced Vital Capacity (litres).
FEV$_1$/FVC = FEV$_1$ expressed as a % of FVC.
PEF = Peak Expiratory Flow rate (litres/min).
RV = Residual Volume (litres).
TLC = Total Lung Capacity (litres).
RV/TLC = RV expressed as a % of TLC.
FRC = Functional Residual Capacity (litres).
TLCO = Transfer Factor (ml/min/mmHg).
TLCO/VA = Diffusion Coefficient (ml/min/mmHg/litre).
%P = Percentage of predicted value for age, sex and height.
SEM = Standard error of the mean.
^{a} = Significance $p < 0.05$.
^{b} = Significance $p < 0.01$.
^{c} = Significance $p < 0.001$.

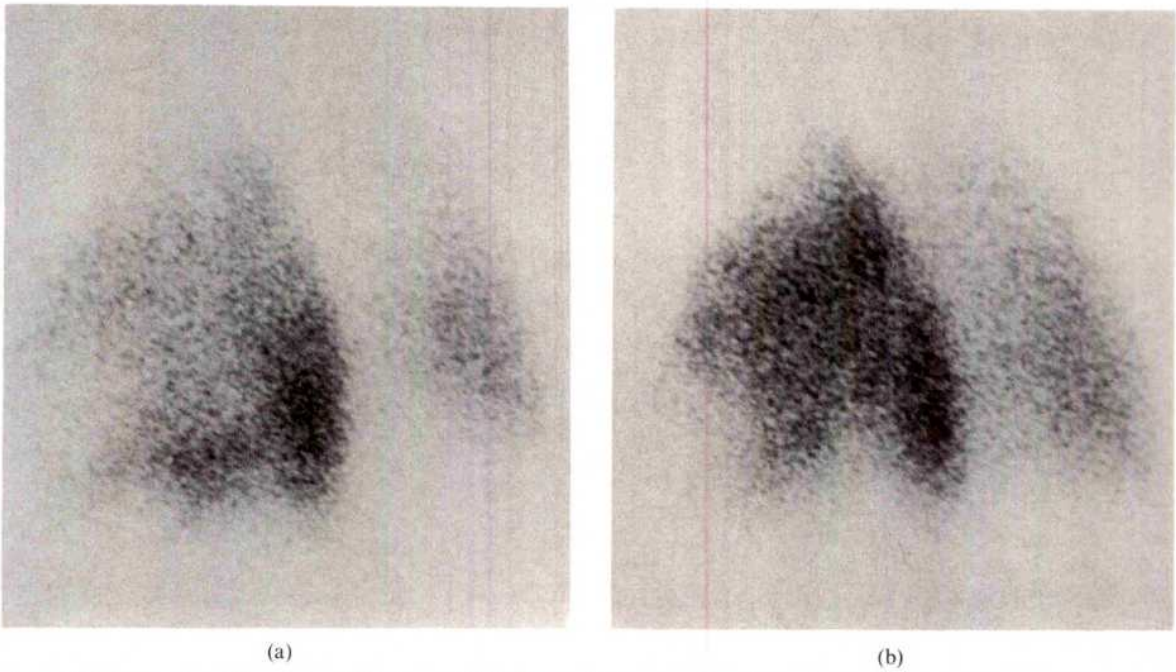

(a) (b)

Figure 3. Left posterior oblique view of the lungs (a) Technegas (b) krypton-81m. A ventilatory defect is seen in the lower zone of the left lung which appears larger on the krypton-81m image.

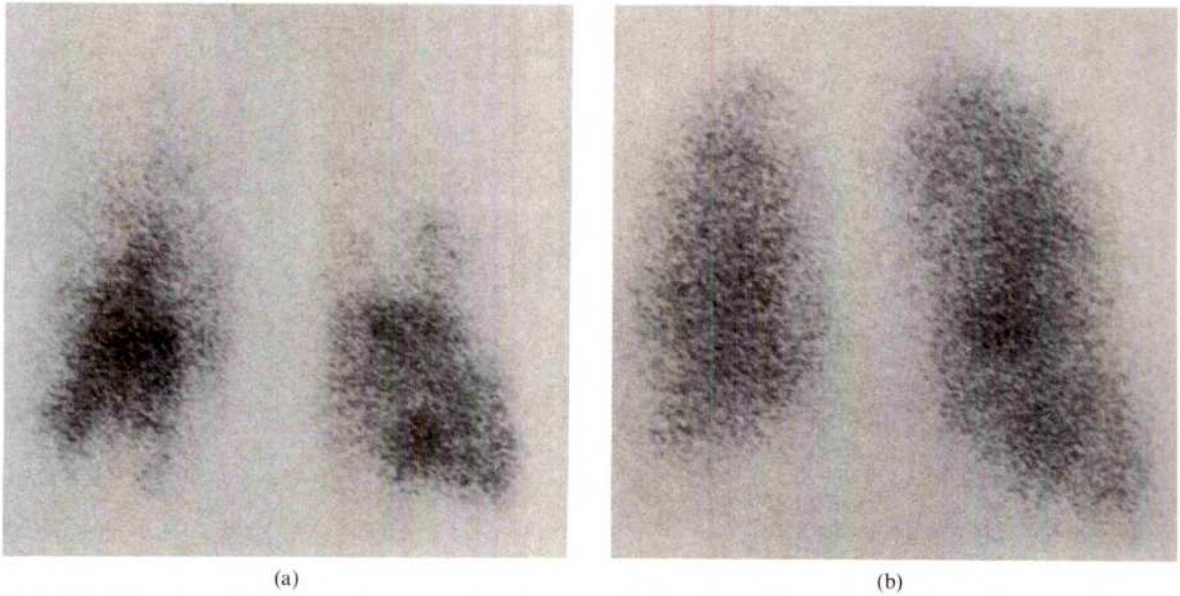

(a) (b)

Figure 4. Posterior view of the lungs (a) Technegas (b) krypton-81m. There is patchy Technegas deposition in the upper zone of the right lung. The krypton-81m image appears more uniform.

Discussion

Hot spots

The presence of hot spots or regions of high count density together with decreased lung penetration or predominantly central airway deposition has been well documented on radioaerosol ventilation images in patients with airways obstruction (Santolicandro et al, 1975; Fazio et al, 1978; Hayes for Taplin, 1980). Central/large airway deposition can arise as a direct consequence of narrowing of the large airways but may also result from altered ventilatory flow due to small/peripheral airway disease or changes in compliance within peripheral lung units. Non-uniform patterns of small airway constriction coupled with uneven distribution of ventilation may produce peripheral hot spots. Partial obstruction of a bronchus will lead to increased flow through neighbouring bronchi and increased particle deposition by impaction as well as localized deposition at the site of the obstruction (Agnew, 1984). Varying degrees of obstruction may arise from factors such as smooth muscle constriction, submucosal oedema or inflammation and mucous hypersecretion with mucous plugging or formation of mucoid strands (Mossberg, 1984).

It has yet to be established whether the hot spots seen on the Technegas ventilation images are indicative of airways dysfunction, as appears to be the case with other radioaerosols. Although different authors report varying sizes for Technegas particles, all agree that they are probably less than 0.2 μm in diameter (Burch et al, 1986; Strong & Agnew, 1989; Isawa et al, 1991): considerably smaller than other radioaerosols. Particles of this size are unlikely to impact on airway walls in regions of increased flow velocity and local turbulence caused by narrowing, unless considerable effective increase in size occurs either by aggregation or hydration. However, on theoretical grounds, hot spots can arise at airway bifurcations or in areas of non-stable flow (Gradon & Orlicki, 1990). Arnot et al (1986), using a ^{99}Tc^{m}-aerosol with particles of a similar size to Technegas, noted hot spots in a number of patients with airway disease. They postulated that small regions of lung existed whose airways were almost completely obstructed and into which particles could drift by diffusion, deposit and accumulate further with each inspiration/expiration cycle.

In order to be able to attribute diagnostic significance to the presence of hot spots on Technegas ventilation images, correlation with indices of pulmonary function is desirable. In obstructive disease such as asthma or chronic airways obstruction, FEV$_1$ is reduced much more than FVC, giving a low FEV$_1$/FVC ratio. Peak expiratory flow (PEF) is also reduced and both RV and TLC are high due to lung hyperinflation. In our present study, hot spots were demonstrated particularly in patients with chronic obstructive airways disease, emphysema and asthma. Significantly different values were found for a number of lung function parameters associated with airways obstruction. These differences remained significant when the subgroup with space-occupying lesions was excluded from the analysis, and overall it seemed that images containing hot spots were associated with severe airways obstruction. It is not surprising, therefore, that the patients with hot spots experience greater difficulty with Technegas inhalation, more patients resorting to tidal breathing or a mixture of breath holding and tidal breathing. These findings suggest that the presence of hot spots on Technegas ventilation images may have clinical significance, but as current diagnostic parameters are well established the use of this technique as a clinical tool is unlikely.

Preferential basal deposition of activity

The presence of increased basal deposition of Technegas and a gradation of activity from apex to base when compared to krypton-81m images was noted in 30% of this series of patients. Such gradients have also been noted, as have anterior-posterior gradients in patients studied supine, with other ^{99}Tc^{m}-labelled aerosols and with Technegas, by various authors (Santolicandro et al, 1975; Alderson et al, 1984; Arnot et al, 1986; Finn et al, 1986; De Geeter et al, 1990).

The distribution of alveolar ventilation is influenced by:—

(1) gravitational effects consequent upon the intrapleural pressure, which in the upright position lead to an increase in ventilation per unit volume of the lung by 1.5–2 times between the upper and lower zones (Secker-Walker, 1978; Chamberlain et al, 1983);
(2) local alveolar compliance, upon which the fractional exchange of air is dependent (Alderson & Line, 1980);
(3) local airways resistance, which for a given change in inflation pressure bears an inverse relationship with flow (Alderson & Line, 1980);
(4) the rate and depth of respiration; and
(5) the lung volume; following forced expiration to residual volume, airway closure occurs in the lower lobes so that more of the next inhalation enters the upper lobes (Kaneko et al, 1966).

Excess basal deposition of Technegas is likely to reflect primarily the gravitational effects leading to increased basal ventilation in the upright posture. The performance of slow inhalation from functional residual capacity will also tend to increase basal deposition. However, the use of a standard Technegas administration technique for the majority of patients means that differences in apex–base activity between patients could possibly reflect specific abnormalities of lung function: if all patients had normal lung function and inhaled Technegas in the same manner in the same position, then the same pattern of deposition should be seen in all. Breathing patterns in patients showing preferential basal deposition are very similar to those for the group as a whole and are therefore not thought to have influenced the pattern of deposition noted with this group. Other authors (Chamberlain et al, 1983; Agnew et al, 1984) have noted decreased apical aerosol activity in the upper lung zones in smokers. They suggest that this may be related either to early anatomical changes within the respiratory bronchioles or to loss of elastic lung recoil, with consequent alteration in the compliance–resistance balance and thereby in the vertical distribution of aerosol. In the patient group studied here, preferential basal deposition was seen in 30%, of whom 20% were current smokers and 40% ex-smokers. The incidence of smoking in this subgroup was lower than within the group as a whole so cannot be implicated. Perhaps reflecting the preferential decrease in ventilation to the lower lung regions in airways obstruction, this feature was not seen in the asthmatics, those with emphysema or those with chronic obstruction. It was however much more commonly seen in patients with idiopathic pulmonary fibrosis (IPF) (70%) than in those with other lung diseases (17%). In restrictive lung disease such as IPF, the FEV_1/FVC ratio tends to be normal or increased. In those showing preferential basal deposition the FEV_1/FVC ratios, both measured and predicted, were significantly higher.

The diagnosis of idiopathic pulmonary fibrosis is usually made by a combination of bronchoalveolar lavage, open lung biopsy and computed tomographic imaging (Raghu, 1987; Strickland, 1988). The latter provides information on the anatomical extent of the disease but fails to clarify its functional extent. An imaging technique which could assist in the diagnosis of IPF and provide information on functional lung capacity might prove useful. It is possible that the preponderance of basal activity seen on Technegas images reflects the functional impairment in this disease, which commences in the lower zones. The low-compliance alveoli are small in volume so receive less air, but exchange a larger than normal fraction of their volume with each inspiration. Presumably both factors contribute to the increased basal deposition. Technegas administration is terminated by count rate and not by the number of breaths taken. Patients with IPF compensate for the smaller volume of air received by taking more breaths to reach the desired count rate (mean: 4 breath-holds in patients with IPF compared to 3 for the patients with other respiratory disease).

Technegas/krypton-81m disparities

Disparities between the Technegas and krypton-81m images are seen in five of the 40 patients studied in five disease categories. These disparities may arise from:

(1) the radiolabelling of the inspired air, which differs for the two agents, and the different modes of inhalation used;
(2) the reflection by krypton-81m images of ventilation rather than volume; and
(3) the different photon energies of the two isotopes.

The air inspired during radioaerosol or Technegas inhalation is uniformly labelled, being drawn from a large reservoir via a small external dead space. With krypton-81m the concentration of activity in the inspired air varies markedly: the activity available builds up towards the end of expiration, producing a bolus of activity at the start of the next inspiration followed by lower activity throughout the remainder of inhalation. In the normal situation such uneven labelling of inspiratory flow is probably insignificant, as the regional distribution of flow differs little between early and late inspiration. Apical penetration may, however, be enhanced by both the distribution of the inspired krypton and the occurrence of preferential apical ventilation early in inspiration. When there is airways obstruction the basal airways may be closed during the early part of inspiration and will therefore only receive activity late in inspiration, at a time when the inspiratory concentration is also dependent on the patient's respiratory rate, tidal volume and the dead space of the delivery system (Alderson & Line, 1980). With Technegas, as already discussed, there is no tendency for preferential apical deposition of activity.

Krypton-81m images reflect the regional arrival of gas or tidal ventilation. When minute ventilation is greater than normal the regional count rate becomes more dependent on regional lung volume than on ventilation. As a result krypton-81m images may underestimate ventilation in regions with high ventilatory flow (Fazio & Jones, 1975). Conversely, krypton-81m may dilute into areas of low ventilatory tidal volume and may not truly reflect regional ventilatory abnormalities (Hoshi et al, 1990).

Within this series, the basal defects which appear larger with krypton-81m occur in one patient with sarcoidosis and one with a space-occupying lesion. These defects perhaps represent regions of high ventilatory flow, consequent upon some degree of bronchial obstruction, into which Technegas penetrates better than krypton-81m. Uniform apical krypton-81m penetration associated with patchy Technegas deposition is seen in one asthmatic patient, one patient with chronic airways obstruction and one with idiopathic pulmonary fibrosis. It is possible that in these cases we are seeing the effect of enhanced apical penetration of krypton-81m due to the uneven labelling of inspired gas, together with the occurrence of preferential apical ventilation early in inspiration and basal airway closure consequent upon increased airway resistance. Krypton-81m could also be diffusing into apical areas of low ventilatory tidal volume and overestimating ventilation. The patchy distribution of Technegas may be presenting a truer functional picture.

The energy of photons emitted from krypton-81m is 190 keV which is significantly higher than the 140 keV of photons from technetium-99m, for which most low-energy collimators are designed. The increased septal penetration at 190 keV may be expected to degrade krypton-81m images slightly, thus possibly making them appear to be more uniform than the underlying distribution of ventilation. Technegas images, conversely, may be expected to be "sharper". Our experimental observations suggest that this is not, however, a major effect.

Conclusions

Two important conclusions can be drawn from this study.

1. In the majority of instances Technegas and krypton-81m images are comparable. In this series of patients known to have respiratory disease, disparities arose in 12.5% of patients. In our usual population studied for suspected pulmonary embolism, co-existent respiratory disease is found in 30% of cases. Therefore disparities between Technegas and krypton-81m might be expected to occur in only 4% of the population with pulmonary embolism. This number is small and unlikely to result in clinical problems, unless the scan results are

interpreted in isolation without knowledge of the patient's history and radiological findings.

2. Two distinct features on the Technegas images which could have diagnostic significance in respiratory disease other than pulmonary embolism are noted. The presence of hot spots was significantly associated with indices of lung function indicating airways obstruction. The preferential basal deposition of Technegas (leading to an increased apex-to-base gradient of activity) was significantly associated with parameters found in restrictive lung disease. In no case would the occurrence of either feature detract from the diagnostic quality of the images as an overall picture of ventilation if performed in conjunction with perfusion imaging for suspected pulmonary embolism.

Acknowledgments

The support of the North West Regional Health Authority in providing funds for purchase of the Technegas generator is acknowledged. We are grateful to Mrs Shirley Turner and Mrs Barbara Bosch for efficient performance of the pulmonary function tests and to the Nuclear Medicine technicians for their assistance with the patient imaging studies.

References

AGNEW, J. E., 1984. Aerosol contributions to the investigation of lung structure and ventilatory function. In *Aerosols and the Lung*, ed. by S. W. Clarke and D. Pavia, (Butterworth & Co., London), pp. 92–126.

AGNEW, J. E., BATEMAN, J. R. M., PAVIA, D. & CLARKE, S. W., 1984. Radionuclide demonstration of ventilatory abnormalities in mild asthma. *Clinical Science, 66*, 525–531.

ALDERSON, P. O. & LINE, B. R., 1980. Scintigraphic evaluation of regional pulmonary ventilation. *Seminars in Nuclear Medicine, 10*, 218–242.

ALDERSON, P. O., BIELLO, D. R., GOTTSCHALK, A., HOFFER, P. B., KROOP, S. A., LEE, M. E., RAMANNA, L., SIEGAL, B. A. & WAXMAN, A. D., 1984. Tc-99m-DTPA aerosol and radioactive gases compared as adjuncts to perfusion scintigraphy in patients with suspected pulmonary embolism. *Radiology, 153*, 515–521.

ARNOT, R. N., BURCH, W. M., ORFANIDOU, D. G., GWILLIAM, M. E., ABER, V. R. & HUGHES, J. M. B., 1986. Distributions of an ultra-fine ^{99m}Tc aerosol and ^{91m}Kr gas in human lungs compared using a gamma camera. *Clinical Physics and Physiological Measurement, 17*, 345–359.

BURCH, W. M., SULLIVAN, P. J., MCLAREN, C. J., 1986. Technegas—a new ventilation agent for lung scanning. *Nuclear Medicine Communications, 7*, 865–871.

CHAMBERLAIN, M. J., MORGAN, W. K. C., VINITSKI, S., 1983. Factors influencing the regional deposition of inhaled particles in man. *Clinical Science, 64*, 69–78.

CLARK, J. C., HORLOCK, P. L., WATSON, I. A., 1978. Krypton 81m in generators for ventilation and perfusion. In *Clinical and Experimental Applications of Krypton-81m*, ed. by J. P. Lavender (British Institute of Radiology Special Report No. 15) (BIR, London), pp. 7–15.

DE GEETER, F., BOSSUYT, A. & JONCKHEER, M., 1990. Comparison of Technegas to ^{81m}Kr as ventilation agent. In *Nuclear Medicine Quantitative Analysis in Imaging and Function* (Proceedings of the 1989 European Association of Nuclear Medicine Conference) ed. by H. A. E. Schmidt and J. Chambron (Schattauer, Stuttgart, New York), pp. 386–388.

FAWDRY, R. M. & GRUENEWALD, S. M., 1988. Initial experience with Technegas—A new ventilation agent. *Australasian Radiology, 32*, 232–238.

FAZIO, F. & JONES, T., 1975. Assessment of regional ventilation by continuous inhalation of radioactive krypton-81m. *British Medical Journal, iii*, 673–676.

FAZIO, F., SANTOLICANDRO, A., SOLFANELLI, S., PALLA, A., FORNAI, E. & GUINTINI, C., 1978. Lung imaging following inhalation of technetium-99m-labelled microspheres: A comparison with the krypton-81m technique. In *Clinical and Experimental Applications of Krypton-81m*, ed. by J. P. Lavender (British Institute of Radiology Special Report No. 15) (BIR, London), pp. 130–140.

FINN, J. P., MYERS, M. J., NAIR, K. M. & LAVENDER, J. P., 1986. Clinical comparison of a new technetium-99m DTPA aerosol delivery system with krypton-81m. *British Journal of Radiology, 59*, 19–24.

GRADON, L. & ORLICKI, D., 1990. Deposition of inhaled aerosol particles in a generation of the tracheobronchial tree. *Journal of Aerosol Science, 21*, 3–19.

HAYES, M. for TAPLIN, G. V., 1980. Lung imaging with radioaerosols for the assessment of airway disease. *Seminars in Nuclear Medicine, 10*, 243–251.

HOSHI, H., DADPARVAR, S., PROMISLOFF, R., SLIZOFSKI, W. J., BROWN, S., GLAB, L. B. & BRADY, L. W., 1990. Mismatch between ^{99m}Tc-DTPA aerosol and ^{81m}Kr lung ventilation scintigraphy: a pitfall of radionuclude imaging. *European Journal of Nuclear Medicine, 16*, 121–123.

ISAWA, T., TESHIMA, T., ANAZAWA, Y., MIKI, M. & MOTOMIYA, M., 1991. Technegas for inhalation lung imaging. *Nuclear Medicine Communications, 12*, 47–55.

JAMES, J. M., HERMAN, K. J., LLOYD, J. J., SHIELDS, R. A., TESTA, H. J., CHURCH, S. & STRETTON, T. B., 1991. Evaluation of ^{99m}Tc-Technegas ventilation scintigraphy in the diagnosis of pulmonary embolism. *British Journal of Radiology, 64*, 711–719.

KANEKO, K., MILIC-EMILI, J., DOLOVICH, M. B., DAWSON, A. & BATES, D. V., 1966. Regional distribution of ventilation and perfusion as a function of body position. *Journal of Applied Physiology, 21*, 767–777.

MOSSBERG, B., 1984. Asthma—sites of airway obstruction and aerosol deposition. *European Journal of Respiratory Disease, Supplement 136, 65*, 49–53.

PELTIER, P., DE FAUCAL, P., CHETANNEAU, A. & CHATAL, J.-F., 1990. Comparison of Technetium-99m aerosol and krypton-81m in ventilation studies for the diagnosis of pulmonary embolism. *Nuclear Medicine Communications, 11*, 631–638.

QUANJER, Ph.H., 1983. Clinical Respiratory Physiology. Standardized lung function testing—report of working party. *Bulletin Européen de Physiopathologie Respiratoire, 19* (Suppl. 5), 7–10.

RAGHU, G., 1987. Idiopathic pulmonary fibrosis—A rational clinical approach. *Chest, 92*, 148–154.

SANTOLICANDRO, A., FORNAI, E., MARINI, C., PALLA, A., SOLFANELLI, S. & GIUNTINI, C., 1975. Uneven deposition of minimicrospheres in patients with obstructive lung disease. *Journal of Nuclear Biology and Medicine, 19*, 112–120.

SECKER-WALKER, R. H., 1978. Pulmonary physiology, pathology and ventilation-perfusion studies. *Journal of Nuclear Medicine, 19*, 961–968.

STRICKLAND, B., 1988. Imaging fibrosing alveolitis. *Postgraduate Medical Journal, 64* (Suppl. 4), 35–40.

STRONG, J. C. & AGNEW, J. E., 1989. The particle size distribution of Technegas and its influence on regional lung deposition. *Nuclear Medicine Communications, 10*, 425–430.

SULLIVAN, P. J., BURKE, W. M. & BURCH, W. M., 1988. A clinical comparison of Technegas and xenon-133 in 50 patients with suspected pulmonary embolus. *Chest, 44*, 300–304.

1992, *The British Journal of Radiology*, *65*, 1083–1085

Comparison of a subjective and a quantitative assessment of the neonatal chest radiograph

By B. Yuksel, MD, A. Greenough, MD, FRCP, DCH and *J. Karani, BSc, MB, BS, FRCR

Departments of Child Health and *Radiology, King's College Hospital, London SE5 9RS, UK

(*Received 11 June 1992 and accepted 10 August 1992*)

Keywords: Chronic lung disease, Prematurity

Abstract. The aim of this study was to assess if quantitative classification of the chest radiograph appearance at 7 days predicted chronic oxygen dependency (oxygen dependency beyond 8 weeks of age) more accurately than did subjective classification at 28 days of age. Thirty preterm infants, median gestational age 27 weeks, who had chest radiographs taken for clinical purposes at 7 and 28 days of age, were recruited into the study. The 7-day chest radiograph was scored according to the lung volume, presence of opacification, interstitial changes, pulmonary interstitial emphysema and cystic elements. The range of chest radiograph scores was from 0–18, a score of 18 indicating the most abnormal appearance. The 28-day chest radiograph was classified as Type I or Type II chronic lung disease (CLD), according to the presence or absence, respectively, of coarse reticulation. The median chest radiograph score at 7 days of the 30 infants was 5 (range 2–14). In predicting chronic oxygen dependency, a chest radiograph score of 5 at 7 days had 83% sensitivity and 75% specificity, but a diagnosis of Type II CLD at 28 days of age had only 67% sensitivity and 67% specificity. We conclude that a quantitative assessment of the chest radiograph appearance at 7 days is more useful than a subjective assessment at 28 days of age.

During the last decade the survival of low-birthweight (LBW) infants, even those born after very short gestations, has improved (Greenough & Roberton, 1985; Chan et al, 1992). As a consequence, many infants now remain oxygen-dependent until at least 28 days of age. However, the ultimate prognosis for this group of infants varies, relatively few remaining chronically oxygen-dependent beyond the neonatal period (Horbar et al, 1988). It has been suggested that the prognosis for LBW infants may be deduced from the appearance of their chest radiograph at 28 days, a diagnosis of Type I rather than Type II chronic lung disease (CLD) being associated with a better outcome (Hyde et al, 1989). We preferred to classify the chest radiograph by means of a scoring system and found this also useful in prognosis (Yuksel et al, 1991). Infants whose chest radiographs had the highest scores had the worst lung function abnormalities at six months of age (Yuksel et al, 1991) and were most likely to be oxygen-dependent at 36 weeks post-conception (Maconochie et al, 1991). We have now applied this scoring system to the chest radiograph at 7 days, and the aim of the present study was to determine whether this, or diagnosis of Type II CLD from the chest radiograph at 28 days, is the better predictor of chronic oxygen dependency.

Methods

Premature infants were eligible for entry into the study if they had been ventilated and/or required supplementary oxygen in the perinatal period and remained oxygen-dependent up to and including 28 days of age. Consecutive infants who had a chest radiograph taken at 7 and 28 (±1) days for clinical purposes were recruited into the study.

The 7-day chest radiographs were scored according to the lung volume and degree of inflation of the lung fields, the presence of an endotracheal tube, opacification, interstitial changes, air bronchogram, pulmonary interstitial emphysema and cystic elements (Table I). The range of scores was from 0 to 18, a score of 18 indicating the most abnormal appearance. The 28-day chest radiographs were classified as Type I or Type II CLD, as defined by Hyde et al (1989). Type I CLD was diagnosed if there were pulmonary opacities that were predominantly perihilar and homogeneous, sometimes patchy, but without coarse reticulation. Type II CLD was diagnosed if there was coarse reticulation characterized by streaky densities interspersed with small cystic translucencies which were sometimes due to air cysts with well-defined walls.

Analysis

The median chest radiograph score was calculated. The duration of ventilation and oxygen dependency of infants with a chest radiograph score equal to or above the median score were compared with those of infants whose score was below the median. The chest radiograph scores of the infants who had Type I or Type II CLD were also compared, as was their duration of ventilation and oxygen dependency. Differences between the groups were assessed for statistical analysis using the Wilcoxon rank sum test. The sensitivity and specificity of a chest radiograph score greater than the median, and of a diagnosis of Type II CLD, to predict prolonged (i.e.

Address correspondence to Dr A. Greenough, Department of Child Health, King's College Hospital, London SE5 9RS, UK.

Table I. Chest radiograph scoring system

Score	0	1	2	3	4
Intubated	No	Yes			
Lung volume	Normal	Reduced	Increased		
Degree of inflation of lung fields	Normal	Under-inflation	Over-inflation		
Opacification ("haziness")	Normal	Perihilar or regional	Perihilar and regional	Complete opacification	
Interstitial changes ("coarse shadowing")	Absent	Present (1 zone)	Present (2 zones)	Present (3 zones)	Present (4 or more zones)
Air bronchogram	Absent	Present			
Pulmonary interstitial emphysema	Absent	Present			
Cystic elements	None	Simple	Multiple		
Size of cyst	None	< one-third of lung field	> one-third of lung field		

beyond 8 weeks of age) oxygen dependency were calculated.

Patients

Thirty infants were entered into the study. They had a median gestational age of 26.5 weeks (range 23–35) and birthweight of 880 g (range 506–1780). They were ventilated for a median of 16 days (range 3–45) and required supplementary oxygen for 59 days (range 29–340). During the course of this study it was the neonatal unit's policy to administer corticosteroids only after 28 days of age. As a consequence, none of our study population had received dexamethasone prior to the 28-day chest radiograph.

This study was approved by the King's College Hospital Ethics Committee.

Results

The median chest radiograph score was 5 (range 2–14). Ten infants had interstitial shadows on their chest radiographs; all of these scored 6 or more. Only four infants had cysts present on their radiographs, and all four chest radiographs scored 9 or more; these were the highest scores of our study population. The infants with a chest radiograph score of 5 or more required mechanical ventilation for a median of 20 days (range 3–40), showing no significant difference from the infants whose chest radiograph score was less than 5, whose median ventilation dependency was 9 days (range 2–45). A chest radiograph score of 5 or more was associated with significantly longer oxygen dependency: median 79 days (range 31–340), compared to a median of 43 days (range 29–73) in those infants with a score less than 5 ($p < 0.01$).

Fourteen infants were diagnosed as suffering from Type I CLD, and their median chest radiograph score was 4 (range 2–11), which did not differ significantly from the median score of the 16 infants with Type II CLD, which was 7.5 (range 2–14). The infants with Type I CLD were ventilated for a median of 8 days (range 2–40) and needed supplementary oxygen for 50 days (range 29–180). The infants with Type II CLD were ventilated for a median of 19 days (range 4–45) and received supplementary oxygen for a median of 72 days (range 29–340); this did not differ significantly from the requirements of the infants with Type I CLD.

A chest radiograph score of 5 had 83% sensitivity and 75% specificity in predicting oxygen dependency beyond 8 weeks of age. A diagnosis of Type II CLD had a 67% sensitivity and 67% specificity in predicting oxygen dependency beyond 8 weeks.

Discussion

We have demonstrated that the quantitative rather than the subjective assessment of the chest radiograph correlates better with the length of time supplementary oxygen is required and is a better predictor of chronic oxygen dependency. We used chronic oxygen dependency as our outcome criterion as nowadays mortality amongst even very immature infants is very low but, unfortunately, increasing numbers of infants survive to be chronically oxygen-dependent. This chronic oxygen dependency has important implications both for neonatal resources and for parents; such infants frequently require prolonged admission to the neonatal unit and may even require home oxygen therapy (Greenough et al, 1991). Thus accurate prediction of chronic oxygen dependency beyond the neonatal period would be extremely useful.

The subjective classification (Hyde et al, 1989) which we assessed differentiated the radiograph appearances into one of only two diagnoses. It is likely that in a large series (Hyde et al, 1989) some radiographs would fail to fulfill the criteria for either diagnosis. In contrast, our present scoring system assesses a number of components of the appearance of the radiograph, so that it would be possible to use it to quantify any radiograph. In addition, we have previously showed the scoring system to be extremely reproducible (Yuksel et al, 1991).

Differentiation of Type II from Type I CLD was based on the presence of coarse reticulation. Our scoring system, on the other hand, assessed the presence of a variety of features on the chest radiograph, including opacification and interstitial shadows, and also differentiates between the size of cysts. Inclusion of these categories increases the discriminative ability of the scoring system, as interestitial changes and cystic elements were present only on the chest radiographs of infants with the highest scores.

The quantitative assessment was applied at 7 days of age, yet still correlated better with our outcome criterion than the subjective classification at 28 days of age. Early treatment with dexamethasone (i.e. given at 14 rather than 28 days or later) is much more effective in improving long-term outcome (Cummings et al, 1989). Thus our quantitative assessment of the chest radiograph at 7 days, by accurately predicting chronic oxygen dependency at that early age, would be able to facilitate effective intervention to prevent chronic lung disease.

References

CHAN, V., GREENOUGH, A. & GAMSU, H. R., 1992. Neonatal complications of mechanical ventilation in extremely preterm infants. *European Journal of Pediatrics, 151*, 693–696.

CUMMINGS, J. J., D'EUGENIO, D. B. & GROSS, S. J., 1989. A controlled trial of dexamethasone in preterm infants at high risk for bronchopulmonary dysplasia. *New England Journal of Medicine, 320*, 1505–1510.

GREENOUGH, A., HIRD, M. F. & GAMSU, H. R., 1991. Home oxygen therapy following neonatal intensive care. *Early Human Development, 26*, 29–35.

GREENOUGH, A. & ROBERTON, N. R. C., 1985. Morbidity and survival in neonates ventilated for the respiratory distress syndrome. *British Medical Journal, 290*, 597–600.

HORBAR, J. D., MCAULIFFE, T. L., ADLER, S. M., ALBERSHEIM, S., CASSADY, G., EDWARDS, W., JONES, R., KATTWINKEL, J., KRAYBILL, E. N., KRISHNAN, V., RASCHKO, P. & WILKINSON, A. R., 1988. Variability in 28-day outcomes for very low birthweight infants: An analysis of 11 neonatal intensive care unit. *Pediatrics, 82*, 554–559.

HYDE, I., ENGLISH, R. E. & WILLIAMS, J. A., 1989. The changing pattern of chronic lung disease of prematurity. *Archives of Disease in Childhood, 64*, 448–451.

MACONOCHIE, I., GREENOUGH, A., YUKSEL, B., PAGE, A. & KARANI, J., 1991. A chest radiograph scoring system to predict chronic oxygen dependency in low birth weight infants. *Early Human Development, 26*, 37–43.

YUKSEL, B., GREENOUGH, A., KARANI, J. & PAGE, A., 1991. Chest radiograph scoring system for use in preterm infants. *British Journal of Radiology, 64*, 1015–1018.

1992, *The British Journal of Radiology*, *65*, 1086–1092

Myocardial damage following coronary bypass surgery: assessment with antimyosin antibody uptake

By A. Jiménez-Heffernan, MD, J. M. Latre, MD, *M. Concha, MD, M. Torres, MD, M. Martínez-Paredes, MD, J. M. Llamas-Elvira, MD, F. M. González, MD, A. Valverde, MD and A. Mateo, MD

Nuclear Medicine and *Cardiovascular Surgery Services, Hospital Reina Sofia, Cordoba, Spain

(*Received 14 January 1992 and in final form 8 July 1992, accepted 10 August 1992*)

Keywords: Antimyosin antibody uptake, Myocardial damage, Coronary bypass surgery

Abstract. To assess the role of ^{111}In antimyosin antibody (AbAm) in the delineation of myocardial damage following coronary bypass surgery, we studied 51 consecutive patients who underwent coronary surgery, 27 of whom had a history of prior myocardial infarction. All patients underwent a diagnostic protocol comprising: (1) ^{99}Tc^{m} pyrophosphate (PYP) and AbAm injection 48 h after surgery (AbAm imaging 24 and 48 h post-injection) (myocardial/background and myocardial/lung ratios were obtained respectively from the computer image); (2) Radioimmunoassay (RIA) serum CK-B levels from samples obtained immediately before surgery, and 24 and 48 h later; (3) clinical and ECG follow-up. Twenty-five patients showed positive AbAm studies, 10 had positive PYP images, and 21 had CK-B levels above normal limits at 24 h. One patient with abnormal AbAm, PYP and CK-B studies had new Q waves on the ECG after surgery. This patient was considered to have sustained a peri-operative myocardial infarction. The large number of positive AbAm studies probably reflects myocardial damage frequently associated with coronary bypass surgery.

Antimyosin antibody (AbAm) imaging has been gaining popularity due to its specificity for myocardial necrosis (Khaw et al, 1986, 1987a,b). Myocyte necrosis associated with acute myocardial infarction (Antunes et al, 1989), acute myocarditis (Yasuda et al, 1987) and heart transplant rejection (Carrio et al, 1988; Latre et al, 1992) have been successfully delineated by AbAm uptake. Loss of sarcolemmal integrity permits exposure of intracellular myosin to circulating fab fragments of antibody (Khaw et al, 1979) with subsequent antigen–antibody reaction and binding.

Coronary bypass surgery is widely used as treatment for coronary disease in a number of situations. A serious complication of bypass surgery is peri-operative myocardial infarction (PMI), frequently subendocardial and small (Roberts, 1983), which may represent the end of a spectrum beginning with minimal myocardial damage due to non-specific surgical trauma, with various intermediate degrees of severity. PMIs may occur at the time of anaesthesia induction, during cardiopulmonary bypass or post-operatively (Schaff et al, 1984). Several factors may play a role in the development of perioperative damage, including reperfusion injury of previously ischaemic myocardium (Miyazaki et al, 1987) following a period of operative non-perfusion (Bulkley & Hutchins, 1977).

Our purpose was to assess the role of AbAm scintigraphy in the delineation of myocardial damage in patients following coronary bypass surgery, comparing it with ^{99}Tc^{m} pyrophosphate (PYP), and serum CK-B radioimmunoassay (RIA) measurements.

Patients and methods

Fifty-one consecutive patients who underwent aortocoronary bypass surgery were studied in a prospective protocol comprising the following procedures: ^{99}Tc^{m} PYP and ^{111}In AbAm injection on the same day, 48 h after surgery, obtaining PYP images 3–4 h after injection and AbAm images 24 and 48 h later (AbAm injection immediately following PYP scintigraphy). CK-B serum levels were measured from samples obtained immediately before, 24 h and 48 h after surgery. All patients were followed up clinically and electrocardiographically. The protocol was approved by the hospital's research committee and patients provided informed consent in all cases. The effective dose equivalent from both radionuclide procedures was estimated to be 10.5 mSv.

Twenty-four patients had no history of myocardial infarction (MI) but 27 did, nine of whom received thrombolytic therapy. The age of the infarct ranged from 10 days to 2.7 years (Table I). Patients underwent bypass surgery because of unstable angina in 19 cases and stable angina in 25; seven patients were asymptomatic early affter i.v. thrombolysis for acute myocardial infarction (and underwent surgery within a protocol of early surgical revascularization after thrombolysis). Localization of necrosis was assessed by electrocardiography, with additional data obtained from the preoperative coronary angiography, and from PYP scintigraphy in four cases. Forty-eight patients had signifi-

---

Address correspondence to: Amelia Jiménez-Heffernan, MD, Apartado de Correos n 3041, 14004 Cordoba, Spain.

Table I. Patients with prior myocardial infarction (MI).

Age of MI	No. of patients	Thrombolysis
10 days	1	1
21–30 days	7	7
1.5–3 months	6	—
4–6 months	2	1
> 2 years	11	—
Total	27	9

cant disease of the left anterior descending artery. The number of diseased vessels and the coronary arteries bypassed are shown in Tables II and III. The coronary arteries were grafted with saphenous vein in 30 patients, with internal mammary artery in four patients, and with both in 17 patients. An average of 2.7 vessels were grafted. The mean cardiopulmonary bypass time was 107±35.9 min; the mean aortic cross-clamp time was 48±19.6 min. Cardiopulmonary bypass was prolonged in two patients because of bleeding.

Protocol

^{99}Tc^{m} PYP scanning was performed with 700 MBq injected intravenously. Four-view planar images were obtained 3–4 h after injection and registered on a 256×256 resolution computer matrix (450 Kcts/view). The ratio of myocardial to background (M/B) uptake was obtained from an irregular region of interest (ROI) over the myocardial area, in counts per pixel, from the anterior view. A computer-generated mirror image in the right hemithorax was used as the background region. The upper normal limit for M/B ratio was set at 1.21. This limit was obtained from the mean plus 2 standard deviations (SDs) (0.99+0.11) of a control group of 17 patients with non-coronary chest pain who underwent PYP scanning as part of a protocol for the differential diagnosis of thoracic pain, and who were found to have oesophageal (11 patients) or thoracic soft tissue (6 patients) lesions. PYP images were negative in all cases. The estimated effective dose equivalent from PYP imaging is 2.4 mSv.

Following the PYP scintigraphy, a 70 MBq dose of ^{111}In-labelled AbAm (MYOSCINT, Centocor) was injected intravenously. Four-view planar images (450 Kcts/view) were obtained 24 and 48 h after injection and registered on a 256×256 computer matrix. Myocardial/lung (M/L) activity ratios, in counts per pixel, were calculated from myocardial and lung irregular ROIs on the anterior view image. The cut-off level used for M/L uptake ratio was 1.86, and was obtained from the mean value plus 2 SDs (1.62+0.12) of a control group of 18 heart transplant patients with no biopsy evidence of rejection and normal resting left ventricular function as assessed by MUGA ventriculography (Latre et al, 1992). Only patients with elevated M/L ratios at 24 and 48 h were considered to have a positive antimyosin study. The estimated effective dose equivalent from AbAm imaging is 8.1 mSv.

CK-B measurements were performed by RIA (NMS Pharmaceuticals). Venous blood samples were obtained immediately before surgery and at 24 and 48 h after the operation. The normal upper limit of serum CK-B was set at 12.5 ng/ml as recommended by the manufacturer.

Quantitative and visual analysis of imaging procedures was carried out by two independent experienced observers.

Quantitative results were expressed in terms of mean±SD. Kolmogorov-Smirnov's test was used to verify that numerical parameters followed a normal distribution. Student's *t*-test and one-factor variance analysis, followed by Newman Keul's test, were used to compare the means of quantitative parameters in different situations. The relations between quantitative parameters were assessed obtaining Pearson's correlation coefficient and qualitative parameters were assessed by the chi-squared test.

Results

Twenty-five patients presented positive AbAm uptake (M/L > 1.86) at 24 and 48 h post-injection, with means of 2.09±0.1 and 2.10±0.1 respectively; their M/L ratios ranged from 1.91 to 2.43 at 24 h and from 1.87 to 2.43 at 48 h. Myocardial uptake was diffuse (Fig. 1) in 17 cases and segmental in seven (Fig. 2), with three patients showing uptake in more than one myocardial segment. Table IV summarizes these results and shows myocardial localization of uptake. Figure 3 represents a negative antimyosin image in a patient with 24 and 48 h M/L ratios of 1.69 and 1.67 respectively.

Ten patients had positive PYP M/B uptake ratios (> 1.21), with a mean of 1.33±0.1 (range 1.25–1.73). Table IV shows the myocardial segments involved. Seven of these patients had positive antimyosin M/L ratios.

Serum CK-B levels were elevated (> 12.5 ng/ml) in 21 patients at 24 h (mean 22.6±11.2 ng/ml), and the

Table II. Patients: number of significantly diseased and bypassed vessels

No. of vessels	No. of patients
1	7
2	19
3	12
4	12
5	1

Table III. Coronary arteries bypassed

Artery	No. of patients
Left anterior descending	48
Right coronary	28
Circumflex	17
Obtuse marginal	16
Posterolateral left ventricular branch	11
First diagonal	11

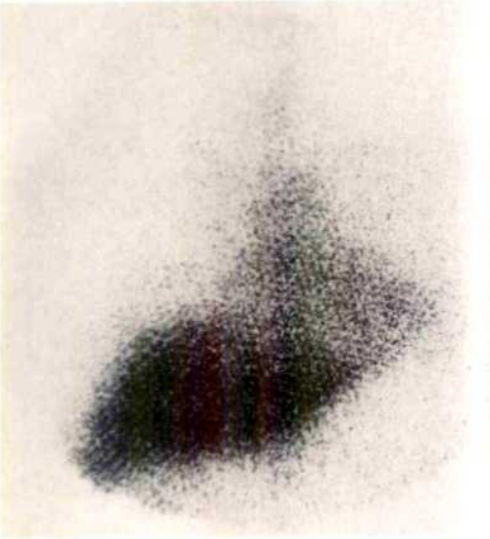

Figure 1. Diffuse myocardial uptake of ^{111}In antimyosin antibody 48 h after injection. This patient had M/L AbAm ratios of 2.29 and 2.39 at 24 and 48 h post-injection, respectively.

elevation persisted at 48 h in six of these patients (mean 17 ± 3.9 ng/ml). Baseline measurements were negative in all patients. Figure 4 shows the distribution of CK-B levels in all patients. Five of the seven patients with positive AbAm and PYP studies had elevated CK-B serum levels at 24 h. Positive CK-B levels at 24 h were found in 11/25 (44%) patients with a positive AbAm study and in 6/10 (60%) patients with a positive PYP study.

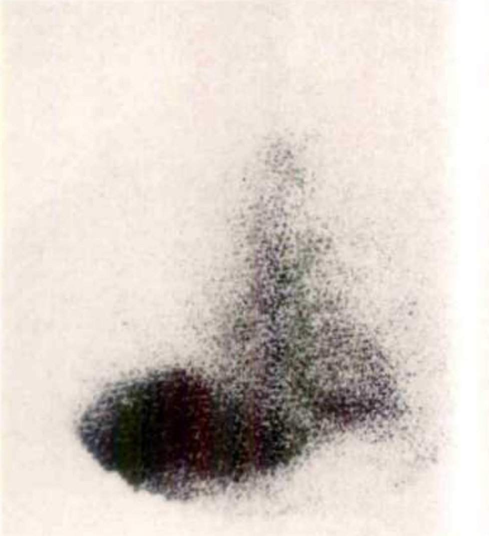

Figure 2. Inferior and anterolateral myocardial uptake of ^{111}In antimyosin antibody 48 h after injection. This patient had M/L AbAm ratios of 2.13 and 2.25 at 24 and 48 h post-injection respectively.

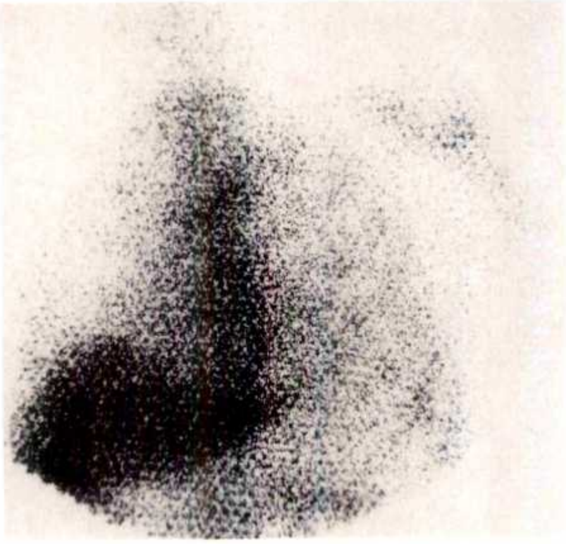

Figure 3. Negative antimyosin image in a patient with M/L ratios of 1.69 and 1.67 at 24 and 48 h respectively. Note prominent non-specific hepatic activity and some degree of bone marrow uptake.

No good correlation was found between PYP M/B and AbAm M/L ratios. There was some correlation, although low, between AbAm M/L ratios at 24 and 48 h

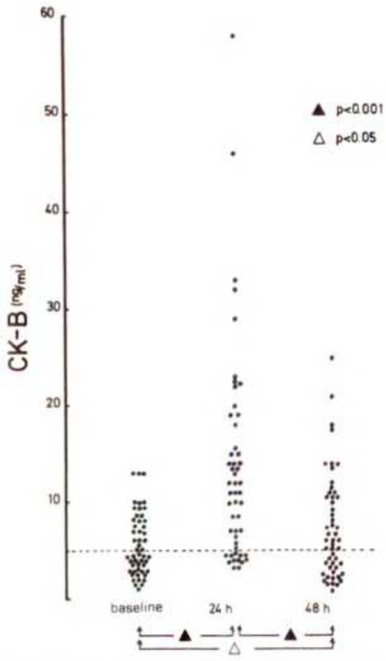

Figure 4. CK-B serum levels at baseline, and after 24 and 48 h. The dotted line is the level of detectability of the assay, 5 ng/ml. Differences were observed at $p < 0.001$ between mean levels at the three moments studied. Differences between baseline and 48 h measurements were significant ($p < 0.05$).

Table IV. Antimyosin, pyrophosphate and CK-B (ng/ml). Results and post-operative ECG changes

	AbAm M/L			PYP		CK-B		
Patient no.	24 h	48 h	Location	M/B	Location	24 h	48 h	ECG
1[a]	1.88	1.62	—	1.08	—	5	< 5	N
2	1.86	1.79	—	1.07	—	5	< 5	ST
3	1.49	1.41	—	1.09	—	5	< 5	N
4[a]	1.85	1.73	—	1.06	—	5	< 5	ST
5	2.17	2	D	1.21	—	5	< 5	ST
6	1.92	1.87	D	1.11	—	10	< 5	N
7	1.78	1.9	—	1.16	—	22	< 5	ST
8[a]	2.39	2.37	AL	1.13	—	29	< 5	ST
9[a]	1.81	1.84	—	1.27	PL	13	< 5	ST
10	2.37	2.43	D	1.05	—	8	< 5	ST
11	2.11	1.97	D	1.05	—	8	< 5	N
12	1.78	1.9	—	1.26	A	5	< 5	ST
13[a]	1.85	1.67	—	1.22	A	5	< 5	N
14[a]	2.1	2	D	1.12	—	11	< 5	ST
15[a]	2.05	2.03	D	1.18	—	5	< 5	ST
16[a]	1.97	2.09	D	1.10	—	7	< 5	ST
17	1.85	1.89	—	1.01	—	5	< 5	ST
18	1.71	1.7	—	1.02	—	5	< 5	N
19[a]	1.43	1.55	—	1.14	—	12	< 5	N
20	1.93	1.99	AS	1.3	AS	22	< 5	N
21	1.77	1.86	—	1.09	—	5	< 5	ST
22[a]	2.22	2.09	D	1.09	—	5	< 5	N
23[a]	1.57	1.6	—	1.07	—	7	< 5	ST
24	1.69	1.67	—	1.03	—	19	< 5	ST
25	1.92	2.12	D	1.15	—	10	< 5	N
26[a]	1.7	1.7	—	1.07	—	58	18	N
27[a]	1.72	1.86	—	1.11	—	5	< 5	ST
28[a]	1.85	2.17	—	1.12	—	13	< 5	ST
29	1.62	1.76	—	1.05	—	10	< 5	ST
30[a]	1.99	1.86	D	1.43	S	7	< 5	ST
31[a]	1.93	2.12	D	1.33	A	15	< 5	N
32[a]	2.04	2.06	D	1.30	AL	6	< 5	ST
33	2.43	2.13	AL	1.15	—	11	< 5	N
34[a]	2.04	2	I	1.09	—	33	< 5	ST
35	1.65	1.82	—	1.17	—	14	14	ST
36[a]	1.8	1.64	—	1.19	—	19	< 5	N
37[a]	1.8	1.65	—	1.15	—	20	< 5	ST
38	2.13	2.25	I, AL	1.73	I, AL	22	< 5	Q
39	2.33	2.34	A	1.25	A	23	13	Q
40[a]	2.29	2.39	D	1.27	A	18	< 5	N
41[a]	1.91	1.94	D	0.99	—	14	25	ST
42	1.98	1.98	D	1.01	—	32	< 5	N
43	1.49	1.32	—	1.10	—	46	21	ST
44[a]	1.69	1.80	—	0.97	—	15	14	N
45[a]	1.95	1.97	PL, I	1.08	—	10	< 5	ST
46[a]	1.83	1.58	—	0.87	—	13	< 5	ST
47	1.98	2.01	D	0.73	—	5	< 5	N
48	1.98	2.22	D	1.07	—	12	< 5	ST
49[a]	2.01	1.77	—	0.76	—	12	< 5	N
50[a]	2.08	2.12	IAP	1.09	—	15	< 5	ST
51	1.75	1.75	—	1.2	—	10	< 5	ST

[a] = patients with prior myocardial infarction.
Myocardial localization of uptake: D = diffuse, AL = anterolateral, AS = anteroseptal, PL = posterolateral, A = anterior, I = inferior, IAP = inferoapical.
ECG: N = no changes; ST = ST segment or T-wave abnormalities.

and cross-clamp time ($n = 51$): $r = 0.33$ and $r = 0.37$ respectively, at $p < 0.05$. AbAm M/L ratios also showed low but significant ($p < 0.05$) correlation with bypass time ($n = 51$): $r = 0.28$ and 0.30 at 24 and 48 h respectively. There was no correlation between CK-B levels at 24 or 48 h and PYP or AbAm ratios, and the type of

Table V. Mean values of AbAm M/L, PYP M/B, and 24 h CK-B for different types of graft

Graft	24 h AbAm	48 h AbAm	PYP	CK-B 24 h
Saphenous ($n = 30$)	1.87	1.85	1.15	14.9
Saphenous + mammary ($n = 17$)	2	2.03	1.13	12.3
Significance	$p < 0.05$	$p < 0.05$	NS	NS

NS = not significant.

myocardial uptake of AbAm was not found to be related to enzyme levels. CK-B levels at 24 h showed low but significant correlation with bypass time, $r = 0.31$, $p < 0.05$, but not with aortic cross-clamp time.

The following variables did not influence the results of either AbAm (levels and type of uptake), PYP or CK-B levels: bypass time, cross-clamp time, presence of prior MI, age of prior MI, stable or unstable angina.

AbAm M/L ratios, both at 24 and 48 h, were significantly higher in patients in whom both the saphenous vein and the internal mammary artery were used (mean 2.00 and 2.03) than in patients in whom only the saphenous vein was used (mean 1.87 and 1.85), $p < 0.05$. The form of graft performed had no apparent influence on the PYP or CK-B levels (unlike the AbAm ratios) (Table V).

Transitory ST segment and T-wave abnormalities following surgery were seen in 30 patients, and new Q waves after surgery were apparent in two patients (nos. 38 and 39) (Table IV).

Discussion

High specificity of antimyosin in the diagnosis of acute myocardial necrosis has been extensively reported (Khaw et al, 1979, 1986, 1987a,b), even in subendocardial lesions (Hendel et al, 1990). There is some evidence indicating uptake of antimyosin by ischaemic but viable myocytes (Bhattacharya & Lahiri, 1991). Animal (Morguet et al, 1992) and human (Latre et al, 1990) studies of infarcts undergoing successful thrombolysis have shown AbAm uptake in ischaemic but viable myocardium (demonstrated by $^{99}\mathrm{Tc}^{\mathrm{m}}$ isonitrile uptake) in the transitional zone between necrosis and normal tissue. Hyperpermeability of myocyte membranes is not therefore exclusively associated with irreversible necrosis. Narula et al (1990) have demonstrated a reduction in infarct size measured by AbAm using a membrane stabilizing agent.

Considering the second day after surgery as the optimum time for injecting PYP and AbAm as hot spot–acute phase tracers, we have found important differences in their behaviour. AbAm studies were abnormal in 25 patients and PYP studies were abnormal in 10, with seven patients showing positive uptake of both. In addition, the distribution of uptake with AbAm was diffuse in 17 cases and restricted to myocardial segments in eight, while PYP uptake was segmental in all cases. Persistent AbAm uptake occurring late after infarction (two weeks and more) in the absence of ongoing necrosis has been reported (Tamaki et al, 1990; Matsumori et al, 1990). These authors proposed prolonged breakdown of membrane integrity with persistent exposure of myosin in damaged myocardium to explain their findings. Thirteen of our patients with positive AbAm studies had a history of prior MI, and six of them had relatively recent infarcts (within 4 months). We cannot therefore exclude prolonged AbAm uptake in these patients (AbAm uptake was diffuse in five of them). Persistent uptake of PYP for several months after acute MI was reported earlier (Buja et al, 1977) and again may account for some of our positive PYP studies. Interestingly, Tamaki et al (1990) assessed PYP uptake together with AbAm, and PYP images were positive in 29% of their patients 1–2 weeks after infarction, whereas AbAm studies were positive in 100% of patients. In our series, six patients with positive PYP studies had a history of prior MI and three of these were relatively recent (within 4 months). Although persistent uptake of either AbAm or PYP after MI may have played a role in some of our patients, it would not have in the majority of them.

The finding of significantly higher levels of antimyosin uptake in patients whose LAD coronary artery was grafted with internal mammary artery than in patients grafted with saphenous vein is important but controversial. Chest tissues overlie myocardial and lung regions in planar images; if antimyosin uptake were present in thoracic tissues due to abnormalities from dissection of the internal mammary artery it would elevate the activity measured in either ROI, depending on the level of the abnormality. If included in the lung ROI, it would lower the M/L ratio; if included in the myocardial ROI, it would elevate it. Another possibility would be heavier surgical manipulation of myocardium while performing a mammary artery bypass of LAD, reflecting direct myocardial damage that would elevate the M/L ratio. We have no clear evidence indicating which mechanism is responsible for higher AbAm M/L ratios in patients in whom bypass was performed with a mammary artery graft.

Our results in relation to AbAm agree with the findings of Van Vlies et al (1990). After studying 23 CABS patients with AbAm and finding positive uptake in 19 (82%), they conclude that some degree of myocardial damage may be common following uncomplicated surgery.

The weak but existing correlations between AbAm levels and bypass and cross-clamp times in our study may indicate a relationship between these variables in the production of myocardial damage.

The significantly lower number of patients with positive PYP studies in relation to AbAm in our series could be explained by the lower sensitivity of PYP for subendocardial lesions, although three patients had positive PYP and negative AbAm studies. CK-B levels at 24 h were negative in two and just above normal limits in the third patient. These three cases may represent false-positive PYP results due to conditions other than myocardial damage.

CK-MB levels are known to be transiently elevated during the first 24 h after surgery, due to myocardial injury from the surgical procedure (Tonkin et al, 1975; Klein et al, 1976). CK-B measurements include MB and BB chains. Elevation of CK-BB serum levels has been reported following thoracotomy with an accompanying rise in CK-MB (Graeber et al, 1980). We believe the contribution of CK-BB in our measurements of total CK-B has been similar in all patients, and since all other situations in which CK-BB is known to be elevated were excluded in our patients, we agreed to use CK-B because CK-MB RIA measurements were not available at the time this study was undertaken.

CK-B levels were above normal limits at 24 h in 21 patients and remained elevated at 48 h in six. The first post-operative measurement in our study was performed at 24 h, a time when elevation due to surgical manipulation is decreasing but the level may still be above normal. We therefore missed the peak elevation of enzyme which (if due solely to surgical manipulation) may have occurred around 6 h post-operatively. Persistence of CK-B elevation at 48 h in six patients indicated more severe myocardial injury.

If surgical trauma producing minimal myocardial injury causes the release of MB chains from myocytes into the circulation, it seems logical on theoretical grounds that fab fragments of AbAm may come into contact with myosin in this context of increased membrane permeability. Only 11 patients with positive CK-B levels at 24 h had abnormal AbAm, with no significant differences in the mean values of CK-B levels in patients with positive and negative AbAm studies. If the mechanisms of CK-B release and AbAm uptake are similar, we cannot explain the finding of 14 patients with positive AbAm uptake and no CK-B elevation. Only six of these patients had prior infarction, so prolonged AbAm uptake is not the complete explanation. It could be that AbAm is more sensitive than the release of intracellular CK-MB in the delineation of myocardial damage, but then, as with PYP studies, we can find no explanation for the 10 patients with elevated CK-B levels and a negative AbAm study. Van Vlies et al (1990) found no clear relation between antimyosin uptake (negative, local or diffuse) and creatine kinase MB levels. We consider, therefore, that the mechanisms of AbAm uptake and CK-MB release are not the same in patients undergoing CABS.

We found transmural peri-operative myocardial infarction in one patient with abnormal PYP and AbAm studies, elevated CK-B levels at 24 and 48 h and new Q waves. The large number of patients with abnormal AbAm and CK-B levels at 24 h, and the smaller number with abnormal PYP and CK-B levels at 48 h, either in isolation or in combination, without Q waves, probably relate to differing grades of myocardial damage due to surgical manipulation and reperfusion injury.

References

ANTUNES, M. L., SELDIN, D. W., WALL, R. M. & JOHNSON, L. L., 1989. Measurement of acute Q-wave myocardial infarct size with single-emission computed tomography imaging of indium-111-antimyosin. *American Journal of Cardiology, 63*, 777–783.

BHATTACHARYA, S. & LAHIRI, A., 1991. Clinical role of indium-111 antimyosin imaging. *European Journal of Nuclear Medicine, 18*, 889–895.

BUJA, L. M., POLINER, L. R., PARKEY, R. W., PULIDO, J. I., HUTCHESON, D., PLATT, M. R., MILLS, L. J., BONTE, F. J. & WILLERSON, J. T., 1977. Clinicopathologic study of persistently positive technetium-99m stannous pyrophosphate myocardial scintigrams and myocytolytic degeneration after myocardial infarction. *Circulation, 56*, 1016–1023.

BULKLEY, B. H., & HUTCHINS, G. M., 1977. Myocardial consequences of coronary artery bypass graft surgery. The paradox of necrosis in areas of revascularization. *Circulation, 56*, 906–913.

CARRIO, I., BERNA, L., BALLESTER, M., ESTORCH, M., OBRADOR, D., CLADELLAS, M., ABADAL, L. & GINJAUME, M., 1988. Indium-111 antimyosin scintigraphy to assess myocardial damage in patients with suspected myocarditis and cardiac rejection. *Journal of Nuclear Medicine, 29*, 1893–1900.

GRAEBER, G. M., SNYDER R. J., & ZAJTCHUK, R., 1980. A comparison of serum isoenzyme levels of creatine phosphokinase and lactic dehydrogenase in patients undergoing thoracic operations and patients admitted to a coronary care unit. *Annals of Thoracic Surgery, 30*, 364–369.

HENDEL, R. C., MCSHERRY, B. A. & LEPPO, J. A., 1990. Myocardial uptake of indium-111-labeled antimyosin in acute subendocardial infarction: clinical, histochemical and autoradiographic correlation of myocardial necrosis. *Journal of Nuclear Medicine, 31*, 1851–1853.

KHAW, B. A., FALLON, J. T., BELLER, G. A. & HABER E., 1979. Specificity of localization of myosin-specific antibody fragments in experimental myocardial infarction: histologic, histochemical, autoradiographic and scintigraphic studies. *Circulation, 60*, 1527–1531.

KHAW, B. A., GOLD, H. K., YASUDA, T., LEINBACH, R. C., KANKE, M., FALLON, J. T., BARLAS-KOVACH, M., STRAUSS, H. W., SHEEHAN, F. & HABER, E., 1986. Scintigraphic quantification of myocardial necrosis in patients after intravenous injection of myosin-specific antibody. *Circulation, 74*, 501–508.

KHAW B. A., STRAUSS, H. W., MOORE, R., FALLON, J. T., YASUDA, T., GOLD, H. K., & HABER, E., 1987a. Myocardial damage delineated by 111 In antimyosin Fab and 99mTc-pyrophosphate. *Journal of Nuclear Medicine, 28*, 76–82.

KHAW, B. A., YASUDA, T., GOLD, H. K., LEINBACH, R. C., JOHNS, J. A., KANKE, M., BARLAS-KOVACH, M., STRAUSS, H. W. & HABER, E., 1987b. Acute myocardial infarct imaging with indium-111-labeled monoclonal antimyosin fab. *Journal of Nuclear Medicine, 28*, 1671–1678.

KLEIN, M. S., COLEMAN, R. E., WELDON, C. S., SOBEL, B. E., & ROBERTS, R., 1976. Concordance of electrocardiographic and scintigraphic criteria of myocardial injury after cardiac surgery. *Journal of Thoracic and Cardiovascular Surgery, 71*, 934–937.

LATRE, J. M., ARIZON, J. M., JIMENEZ-HEFFERNAN, A., ANGUITA, M., GONZALEZ, F. M., RUBIO, F. L., MESA, M. D., MONTERO, A., VALLES, F. & CONCHA, M., 1992. Noninvasive radioisotopic diagnosis of acute cardiac rejection. *Journal of Heart and Lung Transplantation, 11*, 453–457.

LATRE, J. M., JIMENEZ-HEFFERNAN, A., PAN, M., TORRES, M., Llamas, J. M., Gonzalez, F. M. & Mateo, A., 1990. Residual myocardial necrosis assessment after effective thrombolysis. In *Nuclear Medicine Quantitative Analysis in Imaging and Function*, ed. by H. A. E. Schmidt and J. Chambron (F. K. Schauttauer Verlag GmbH, Stuttgart—New York), pp. 251–253.

Watanabe, Y., Yonekura, Y., Endo, K., Konishi, J., Yoshida, A. & Tamaki, S., 1990. Persistent uptake of indium-111-antimyosin monoclonal antibody in patients with myocardial infarction. *American Heart Journal, 120,* 1026–1030.

Miyazaki, S., Fujiwara, H., Onodera, T., Kihara, Y., Matsuda, M., Wu, D. J., Nakamura, Y., Kumada, T., Sasayama, S., Kawai, C., & Hamashima Y., 1987. Quantitative analysis of contraction band necrosis after ischemia and reperfusion in the porcine heart. *Circulation, 75,* 1074–1082.

Morguet, A., Munz, D. L., Klein, H. H., Pich, S., Conrady, A., Nebendahl, K., Kreuzer, H. & Emrich, D., 1992. Myocardial distribution of indium-111-antimyosin fab and technetium-99m-sestamibi in experimental nontransmural infarction. *Journal of Nuclear Medicine, 33,* 223–228.

Narula, J., Nicol, P. D., O'Donnell, S. M., Newell, J. B., Pieri, P. L., Guerrero, J. L., Nossiff, N., Strauss, H. W. & Khaw, B. A., 1990. Documentation of reperfusion myocardial injury by dual radio-labelled anti-myosin imaging: reversibility by membrane stabilizing agents (abstract). *Journal of Nuclear Medicine, 31,* 805.

Roberts, A. J., 1983. Perioperative myocardial infarction and changes in left ventricular performance related to coronary artery bypass graft surgery. *Annals of Thoracic Surgery, 35,* 208–225.

Schaff, H. V., Gersh, B. J., Phil, D., Fisher, L. D., Frye, R. L., Mock, M. B., Ryan, T. J., Ellis, R. B., Chaitman, B. R., Alderman, E. L., Kaiser, G. C., Faxon, D. P. & Bourassa, M. G., 1984. Detrimental effect of perioperative myocardial infarction on late survival after coronary artery bypass. *Journal of Thoracic and Cardiovascular Surgery, 88,* 972–981.

Tamaki, N., Yamada, T., Matsumori, A., Yoshhida, A., Fujita, T., Ohtani, H., Watanabe, Y., Yonekura, Y., Endo, K., Konishi, J. & Kawai, C., 1990. Indium-111-antimyosin antibody imaging for detecting different stages of myocardial infarction: comparison with technetium-99m-pyrophosphate imaging. *Journal of Nuclear Medicine, 31,* 136–142.

Tonkin, A. M., Lester, R. M. & Guthrow, C. E., 1975. Persistence of MB isoenzymes of creatine phosphokinase in the serum after minor iatrogenic cardiac trauma. Absence of postmortem evidence of myocardial infarction. *Circulation, 51,* 627–631.

Van Vlies, B., Van Royen, E. A., Visser, C. A., Meyne, N. G., Van Buul, M. M. G., Peters, R. J. G. & Dunning, A. J., 1990. Frequency of myocardial-111 antimyosin uptake after uncomplicated coronary artery bypass grafting. *American Journal of Cardiology, 66,* 1191–1195.

Yasuda, T., Palacios, I. F., Dec, G. W., Fallon, J. T., Gold, H. K., Leinbach, R. C., Strauss, H. W., Khaw, B. A. & Haber, E., 1987. Indium-111 monoclonal antimyosin antibody imaging in the diagnosis of acute myocarditis. *Circulation, 76,* 306–311.

1992, *The British Journal of Radiology*, *65*, 1093–1096

Computed tomographic appearances of the pelvis following hindquarter amputation

By J. Fowler, FRCR, A. M. Davies, FRCR, *S. R. Carter, FRCS, *R. J. Grimer, FRCS and *R. S. Sneath, FRCS

Department of Radiology and the *Birmingham Bone Tumour Treatment Service, Royal Orthopaedic Hospital, Birmingham, UK

(*Received 30 April 1992 and in revised form 6 July 1992, accepted 30 July 1992*)

Keywords: Computed tomography, Bone tumours, Hindquarter amputation

Abstract. Bilateral and midline symmetry of the normal pelvic anatomy is an aid to the interpretation of computed tomographic (CT) examinations. Following hindquarter amputation (HQA) or partial hemipelvectomy (PHP) the normal anatomical relationships are disturbed. The CT examinations of 15 patients who had undergone either an HQA or a PHP for an advanced musculoskeletal malignancy are reviewed. The new "normal" anatomy revealed displacement of the bladder and small bowel to the side of surgery in one third of patients, more commonly in the PHP cases. There were varying degrees of wasting of the ipsilateral musculature, gluteus maximus muscle flap, erector spinae and psoas muscles, etc., because of partial denervation and disruption of their origin or insertion. Recurrent tumour was identified in eight of 10 cases in which it was clinically suspected prior to the CT examination. Invariably the recurrence arose within the muscle flap at the resection margin. Bone involvement by direct tumour spread was present in three cases. Pitfalls in differentiating recurrent tumour from scar tissue are discussed.

Lesions of the pelvis are frequently difficult to evaluate because of the curved orientation of the pelvic bones and overlying bowel shadows. Computed tomography (CT), with its ability to demonstrate cross-sectional anatomy, is well suited to image the osseous pelvis and associated abnormalities (Weis et al, 1978; Gilula et al, 1979; Amendola et al, 1983). The anatomical features of the pelvis that are advantageous for CT interpretation include midline or bilaterally symmetrical structures with the relationships kept constant by the confines of the bony pelvis (Levitt et al, 1978). These features however no longer apply when a patient has undergone mutilating surgery such as a hindquarter amputation (HQA) or partial hemipelvectomy (PHP) (Fig. 1). The purpose of this study is to review the normal and abnormal CT appearances of the pelvis in a series of patients who have undergone either HQA or PHP.

Patients and methods

The Birmingham Bone Tumour Treatment Service has performed 61 HQAs or PHPs for musculoskeletal malignancies of the pelvis since 1971. The indications and long-term results have been reported previously (Carter et al, 1990), covering either a full HQA or a partial hemipelvectomy (PHP) through the ilium (King & Steelquist, 1943). Fifteen patients subsequently underwent 20 CT examinations of the pelvis and these form the basis of the present study.

There were six male and nine female patients, with ages ranging from 22 to 61 years (mean 42 years). Uncontrasted examinations were obtained using either a Siemens DRH or a HiQ CT scanner with 8 mm contiguous slices. The images were reviewed retrospectively, paying particular attention to pelvic symmetry, the surgical scar and the presence or absence of recurrent disease.

Results

The histology of the primary tumours in the 15 cases was as follows: 6 chondrosarcomas, 4 malignant fibrous histiocytomas, 2 osteosarcomas, 1 Ewing's tumour and 2 soft tissue liposarcomas.

The "new" normal anatomy is based around the pre-existing contralateral bony pelvic wall and sacrum, together with a remnant of ipsilateral ilium (minimal in HQA and moderate in PHP). The post-operative ipsilateral pelvic wall is made up of a gluteal muscle flap stretching from the sacroiliac remnant anteriorly to the midline anterior abdominal wall and perineum, with a covering of subcutaneous fat and skin (Fig. 1).

Following HQA or PHP the pelvic contents may remain in their normal position with relative symmetry about the midline. Loss of the bony and fascial support can result in lateral and caudal displacement of the bladder and small bowel to the side of surgery. True herniation through the muscle flap was not seen. Displacement of the bladder was seen in 3 of 4 cases with a PHP as compared with only 2 of 11 cases with an HQA (Fig. 2). The bladder base and the prostate or uterus remained in a midline position.

Address correspondence to Dr A. M. Davies, MRI Centre, Royal Orthopaedic Hospital, Woodlands, Northfield, Birmingham B31 2AP, UK.

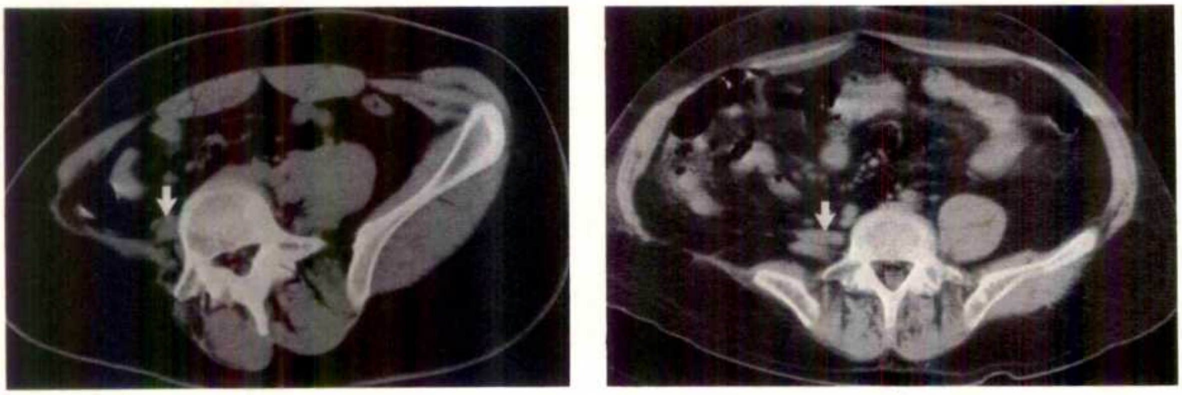

Figure 1. Wasting of the right psoas muscle (arrows). (a) Right HQA. Thin gluteal muscle flap inserting into the abdominal muscles laterally. (b) Right PHP with a thin gluteal flap arising from the iliac remnant inserting into the external abdominis oblique muscle laterally.

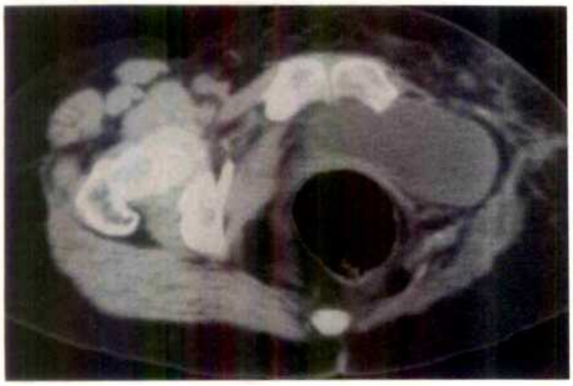

Figure 2. Left PHP with wasting of the muscle flap posterolaterally and caudal and ipsilateral displacement of the bladder deep to the subcutaneous scar.

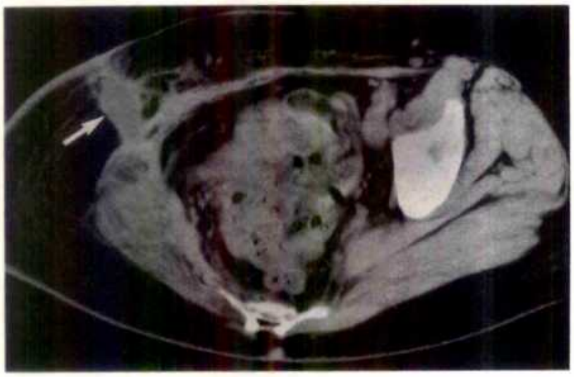

Figure 3. Three weeks after right HQA, with a serous collection in the subcutaneous scar (arrow) and engorgement of the vessels in the adjacent subcutaneous fat.

Atrophy of the ipsilateral musculature was identified as follows: rectus abdominis 3 cases, gluteal flap 10 cases, erector spinae 7 cases, psoas 14 cases with the muscle in the remaining case being replaced by recurrent tumour (Figs 1, 2).

The surgical scar could be identified in all cases, usually as a linear soft tissue density extending at right angles to an overlying skin dimple, through the subcutaneous fat (Fig. 2). Prominence of the vessels within the subcutaneous fat around the scar was more common in those examinations performed a few weeks after surgery (Fig. 3). The scar was thickened in three cases and enlarged in four. This thickening was due to a localised serous collection in one case (Fig. 3) and recurrent tumour in three other cases.

Tumour recurrence was identified on CT in 8 of 10 cases in which it was clinically suspected prior to the examination. The remaining five CT examinations were performed as part of the current study. The size of the recurrence varied from 3 cm to 20 cm in diameter (mean 10 cm). Recurrence was invariably within the muscle flap at the margin of resection (Figs 4, 5). The subcutaneous scar was involved in three cases. Invasion of the adjacent iliac remnant or the sacrum was identified in three cases. All bony involvement was by direct spread (Fig. 5).

The ipsilateral vascular bundle was only visible in half the patients because it was tied off relatively proximally. In those examinations in which it was visible (predominantly PHP cases) it was never enlarged and was not confused with lymphadenopathy.

Discussion

HQA or PHP has been employed in the surgical management of advanced musculoskeletal malignancies of the pelvis for 100 years (Hogarth-Pringle, 1916). The current study was prompted by an HQA case in which a mass, palpable deep to the surgical scar, was subse-

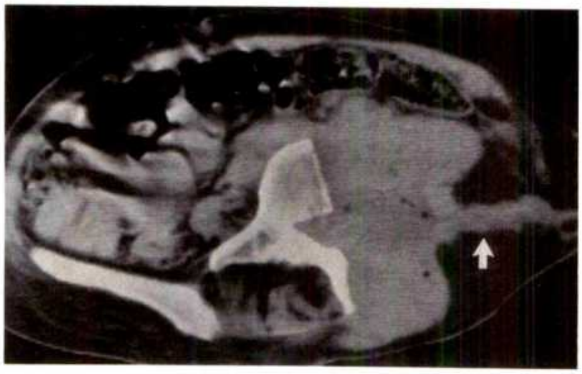

Figure 4. Left HQA with a partial sacrectomy. Large recurrent liposarcoma obliterating the left paravertebral tissues and extending into the scar (arrow).

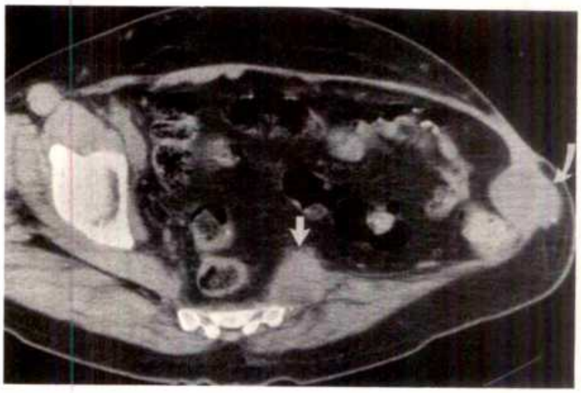

Figure 6. Left HQA with two foci of recurrent chondrosarcoma—on the inner aspect of the gluteal muscle flap adjacent to the left side of the distal sacrum (straight arrow) and in the subcutaneous scar laterally (curved arrow).

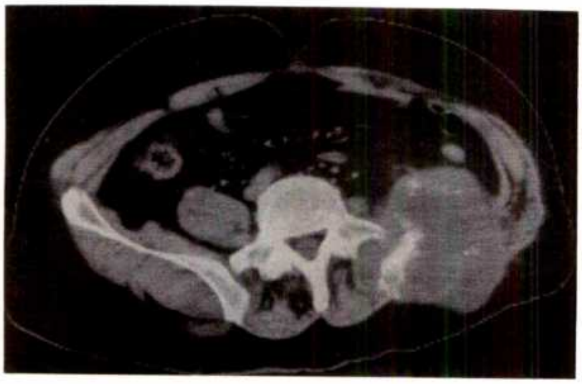

Figure 5. Left PHP with a recurrent chondrosarcoma obliterating the posterior portion of the gluteal flap and invasion of the iliac remnant.

quently shown on CT to be a displaced bladder (Fig. 2). This particular case highlighted the importance of appreciating the anatomical alterations which may occur after surgical treatment and which can complicate detection of recurrence.

The most important anatomical change following HQA or PHP is loss of midline symmetry. Removal of the bony and fascial support allows for caudal and ipsilateral displacement of the bladder (Fig. 2). This feature was more commonly seen in the PHP patients and may be due to the more lateral origin of the muscle flap from the iliac remnant, resulting in a larger pelvis.

The reduction in the ipsilateral musle bulk contributes to the loss of symmetry. The loss of muscle bulk is due to excision of muscle and wasting of the remaining muscle (Fig. 2). Muscle wasting is typified by reduced muscle volume and accentuation of the intramuscular fat planes (Fig. 1). Wasting of the muscle flap is to be expected because of partial denervation and disruption of some of its attachments. An increase in size of the ipsilateral muscles invariably denoted recurrent tumour (Figs 4, 5).

In this series, the site of recurrence, adjacent to the iliac remnant or sacrum, is to be expected because it is at this point that the resection margin is typically closest to the tumour. This is therefore the critical area for review on follow-up CT examinations. The other area that merits close attention is the surgical scar. Considering the mutilating nature of the surgery, remarkably little scar tissue is visible on CT within the pelvis. Characteristically the only scar tissue visible is that which traverses the subcutaneous fat deep to the skin incision. When tumour is shown to extend from the main site of recurrence directly into the scar (Fig. 4) there can be little doubt as to the diagnosis.

The situation is less straightforward when there is focal enlargement of the scar remote from the resection margin (Figs 3, 6). If the soft tissue mass is of low attenuation on CT and is revealed only weeks after surgery, a post-operative serous collection is the most likely diagnosis (Fig. 3). The low attenuation alone is not pathognomonic of a fluid collection; the lobules of tumour cartilage found in chondrosarcomas, the commonest histology in this series, are characteristically of a similar low attenuation (Fig. 6). The majority of chondrosarcomas arising in the pelvis are low-grade sarcomas; recurrences would therefore be expected to take several months to develop. In this context intravenous contrast medium is unlikely to be helpful as chondrosarcomas, due to their low vascularity, rarely show significant enhancement.

The differential diagnosis of any mass lesion at the site of previous surgery must also include infection with abscess formation. Such a complication might be expected because some of these cases, chondrosarcoma excepted, will be immuno-compromised by chemotherapy and the vascularity of the muscle flap is not always optimal. This complication was not seen in any of the current series. One important point to stress, however, is that the presence of an abscess does not exclude a concomitant local recurrence and therefore cytology of any drained fluid is advisable. The same principle applies to aspiration of any serous collection.

Prominence of the subcutaneous vessels (Fig. 3) was most commonly seen in those examinations performed within a few weeks of operation. This is presumed to be due to engorgement of the vessels secondary to the trauma of the surgery. In a few cases similar changes were also visible a considerable time after surgery (Fig. 2). Possible explanations in those cases are either that the surgery has resulted in a compromise of the local venous drainage, or that the prominence is a local response to radiotherapy, although the latter was not the case in Fig. 2.

In our experience primary musculoskeletal malignancies of the pelvis are difficult to diagnose, and it is often more than a year from the commencement of symptoms to detection (Grimer & Sneath, 1990). Consequently most of these primary tumours are large at the time of initial staging, which is why HQA or PHP may be necessary rather than limb-salvage surgery. To a degree the same applies to the recurrent tumours in this selected series, in that CT easily demonstrated all the lesions with a mean diameter of 10 cm (Figs 4, 5, 6). Were these patients to undergo regular CT following surgery, irrespective of symptoms, the detection of early subclinical recurrences would be more problematical and the routine use of intravenous contrast medium probably advantageous. In the hunt for these small recurrences, magnetic resonance imaging (MRI) would be the examination of choice because of its high contrast resolution and multiplanar capability (Vanel et al, 1990). The sensitivity of MRI is superior to that of CT in the detection of local recurrences of disease < 15 ml in volume (Reuther & Mutschler, 1990) and MRI could be expected to reveal the same anatomical alterations as demonstrated on CT in this study following HQA or PHP.

References

AMENDOLA, M. A., SHIRAZI, K., AMENDOLA, B. E., KUHNS, L. R., TISNADO, J. & YAGHMAI, I., 1983. CT of malignant tumors of the osseous pelvis. *Computerized Radiology, 7*, 107–117.

CARTER, S. R., EASTWOOD, D. M., GRIMER, R. J. & SNEATH, R. S., 1990. Hindquarter amputation for tumours of the musculoskeletal system. *Journal of Bone & Joint Surgery, 72B*, 490–493.

GILULA, L. A., MURPHY, W. A., TAILOR, C. C. & PATEL, R. B., 1979. CT of the osseous pelvis. *Radiology, 132*, 107–114.

GRIMER, R. J. & SNEATH, R. S., 1990. Diagnosing malignant bone tumours (Editorial). *Journal of Bone & Joint Surgery, 72B*, 754–756.

HOGARTH-PRINGLE, J., 1916. The interpelvic–abdominal amputation. *British Journal of Surgery, 4*, 283–296.

KING, D. & STEELQUIST, J., 1943. Transiliac amputation. *Journal of Bone & Joint Surgery, 25A*, 351–367.

LEVITT, R. G., SEIGEL, S. S., STANLEY, R. J. & EVENS, R. G., 1978. CT of the pelvis. *Seminars in Roentgenology, 13*, 193–200.

REUTHER, G. & MUTSCHLER, W., 1990. Detection of local recurrent disease in musculoskeletal tumors: MRI versus CT. *Skeletal Radiology, 19*, 85–90.

VANEL, D., BROSSEL, R., BONNEROT, V., COFFRE, C. & CONTESSO, G., 1990. MRI in the follow-up of primary musculoskeletal tumors. *Contrast Media in MRI, International Workshop, Berlin, 1–3 Feb. 1990*. (Medicom Europe, Bussum, Netherlands), pp 391–399.

WEIS, L., HEELAN, R. T. & WATSON, R. C., 1978. CT of orthopedic tumors of the pelvis and lower extremity. *Clinical Orthopedics & Related Research, 130*, 254–259.

1992, *The British Journal of Radiology*, 66, 1097–1101

Assessment of mammographic film processor performance in a hospital and mobile screening unit

By J. G. Murray, MRCPI, D. J. Dowsett, MSc, O. Laird, DCR and J. T. Ennis, MD, FRCR, FRCPI

Eccles Street Breast Screening Centre, Mater Misericordiae Hospital, Dublin 7, Ireland

(Received 20 February 1992 and in revised form 22 June 1992, accepted 16 July 1992)

Keywords: Screening mammography, Film processor, Image quality

Abstract. In contrast to the majority of mammographic breast screening programmes, film processing at this centre occurs on site in both hospital and mobile trailer units. Initial (1989) quality control (QC) sensitometric tests revealed a large variation in film processor performance in the mobile unit. The clinical significance of these variations was assessed and acceptance limits for processor performance determined. Abnormal mammograms were used as reference material and copied using high definition 35 mm film over a range of exposure settings. The copies were than matched with QC film density variation from the mobile unit. All films were subsequently ranked for spatial and contrast resolution. Optimal values for processing time of 2 min (equivalent to film transit time 3 min and developer time 46 s) and temperature of 36°C were obtained. The widespread anomaly of reporting film transit time as processing time is highlighted. Use of mammogram copies as a means of measuring the influence of film processor variation is advocated. Careful monitoring of the mobile unit film processor performance has produced stable quality comparable with the hospital based unit. The advantages of on site film processing are outlined. The addition of a sensitometric step wedge to all mammography film stock as a means of assessing image quality is recommended.

Since 1989 the Mater Hospital has operated an urban and rural mammographic breast screening service. Asymptomatic women aged over 50 years and resident in either region are invited for two-view screening mammography sessions. These take place at both the hospital itself and a mobile trailer unit. Radiography and technical staff alternate between both units and all films are double read by the same two screening radiologists. Identical radiographic systems (Siemens Mammomat II), film–screen combinations (Agfa Mammo-Ray) and film processors (Agfa Curix Compact) are used by both units.

In contrast to the majority of screening programmes, processing of film is undertaken on site in the mobile unit. This allows film viewing at time of initial patient presentation. Repeat or supplementary views are obtained as required thereby avoiding further recall and unnecessary patient anxiety. This facility also improves overall efficiency by allowing a more definite diagnosis to be made at initial film viewing.

Despite data which suggest an equal prevalence of breast carcinoma in both regions (International Agency for Research on Cancer, 1989), detection rate differences of 4/1000 (rural/mobile) *vs.* 7/1000 (urban/hospital) were initially obtained.

Quality assurance monitoring at the mobile unit confirmed consistent performance figures (kVp, mAs, etc) for the X ray machine over a 3 month period. Daily step wedge sensitometric measurements from the mobile film processor, however, revealed large variations (Fig. 1).

The identification of the film processor as the weakest link in the mammographic chain, and poor film processing as the major reason for low contrast and high dose values, was described previously by Galkin et al (1988), Russell & Carmichael (1987) Tabar & Dean (1983), Karila (1988), Hendrick (1990) and Leitz (1990).

The aim of this study was to assess if observed differences in film quality between both units could influence diagnostic accuracy and to determine acceptable limits of processor performance (time/temp.). The reliability of on-site film processing in the mobile unit was also studied.

Method

Quality control tests at both centres were carried out according to guidelines of the Institute of Physical Sciences in Medicine (1989). The film processor was tested using a standard 16 step aluminium wedge and Mammoray Cassette/MR3 II film combination exposed at fixed settings (26 kV, 6.3 mAs) (Fig. 1). Relating the observed variations in test film quality from the mobile unit to differences in diagnostic accuracy could only convincingly be demonstrated by studying their effect on real breast pathology as seen in routine mammography. Accordingly 10 good quality abnormal mammograms containing microcalcifications (resolution examples) and parenchymal changes (contrast examples) were selected and displayed under optimal viewing conditions. They were copied using Kodak Ektachrome 100 HC colour-slide film, under and over exposing +and −2 f stops in half stop intervals.

This colour film has a high spatial resolution (75 line pairs/mm) and excellent contrast range (Kodak Technical Publication E-27(H). Its gamma (as measured from step wedge exposure) is very similar to the MR3 II film (Fig. 2). Thus we can extrapolate that its grey scale response closely mimics the range of contrast variations

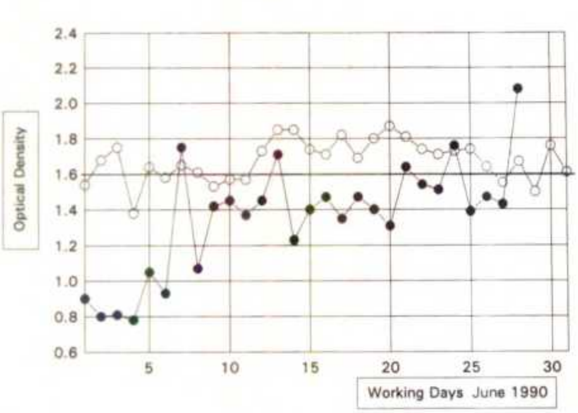

Figure. 1. Optical density variation seen in the daily test films from the hospital assessment centre (open symbols) and the mobile screening unit (closed symbols) for the month of June 1990. The reference optical density, 1.6, is Step 8 on the grey scale wedge from an optimally processed film. This is seen to vary from 0.8 to over 2.0 on the test films from the mobile centre.

seen on the original mammogram. A single-process colour film, yielding a direct positive, avoids the two processes necessary with black and white film. These film qualitites ensure that image degradation normally associated with film copying is negligible.

A sensitometric grey scale is now a standard feature on our mammorgaphy stock (Fig. 3) and was replicated on all copy films. Absolute optical density (OD) was measured from a central point on the sensitometric scale using an Agfa D-120 densitometer. Values thus obtained from copy films were matched with the range of optical density seen in quality control films from the mobile unit in June 1990. Nine levels of exposure variation in the film copies (including correctly exposed copy) represented the range of film quality seen in Fig. 1. Ten original mammograms thus yielded 90 film copies of mixed exposure. All copies were independently ranked 0–5 for spatial and contrast resolution by both screening radiologists (Fig. 4).

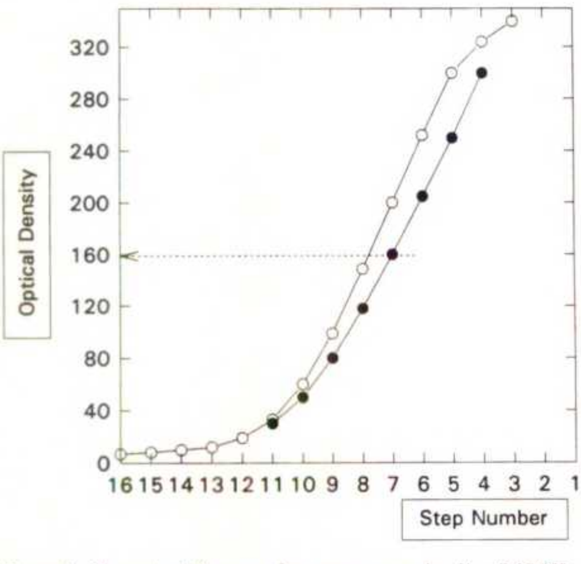

Figure 2. Characteristic curve for mammography film (MR3II: open symbols) and the colour copying film (Kodak 100 HC: filled symbols), showing similarity of response. Since the Kodak 100 HC is a positive-image film the slope should be shown reversed; the curve has been transposed for clarity. Optical density 1.6 was chosen as the reference point on these curves for exposure comparisons.

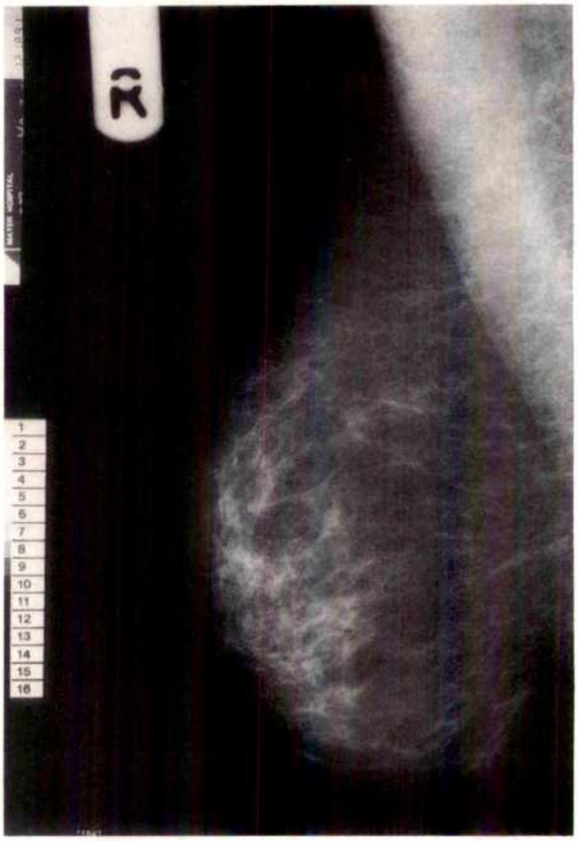

Figure 3. An example of an optimally exposed mammogram showing pre-exposed optical step wedge use for assessing film processor performance.

To determine the relationships of the proposed limits of optical density to processing time and temperature a sensitometer was used to pre-expose a series of films with a 16 step grey scale. These films were used to assess three different temperature settings (32, 34 and 36°C) while maintaining a constant 3 min film cycle (Fig. 5).

Results

Figure 4 shows the combined results for all 90 copied mammograms in terms of spatial and contrast resolution. At the extremes of exposure dark images were adequate for visualization of microcalcification but poor

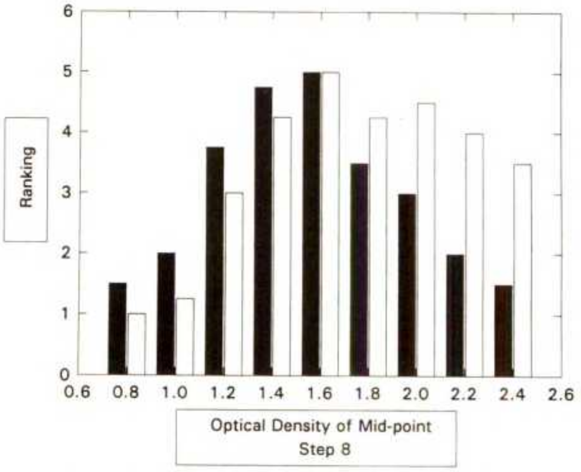

Figure 4. The total result from ranking 90 copy films. Optical densities ranging from 0.8 to 2.4, obtained for Step 8 on the reference wedge, are plotted on the X axis. The optical density of 1.6 identifies the correctly exposed copy-mammogram that exactly matches the quality of the original. The black bars represent ranking for contrast, the white bars that for resolution.

for parenchymal detail while light images were non-diagnostic for both. A ranking of greater than three was deemed acceptable for diagnostic purposes and so our acceptance limits were 1.3–1.9 OD.

Two film transport speeds, 30 and 40 cm/min, are possible in this model processor, and since longer processing times are most beneficial in terms of lower patient radiation dose (Law & Kirkpatrick, 1987; Haus, 1990) the slower film transport setting of 30 cm/min was chosen as optimal. Acceptance limits of 1.3–1.9 OD correspond to temperature range 34 ± 2°C (Fig. 5). Film transport speed of 30 cm/min is equivalent to a film transit time of 3 min, a processing time of 2 min and a two tank developer time of 46 s (Table I).

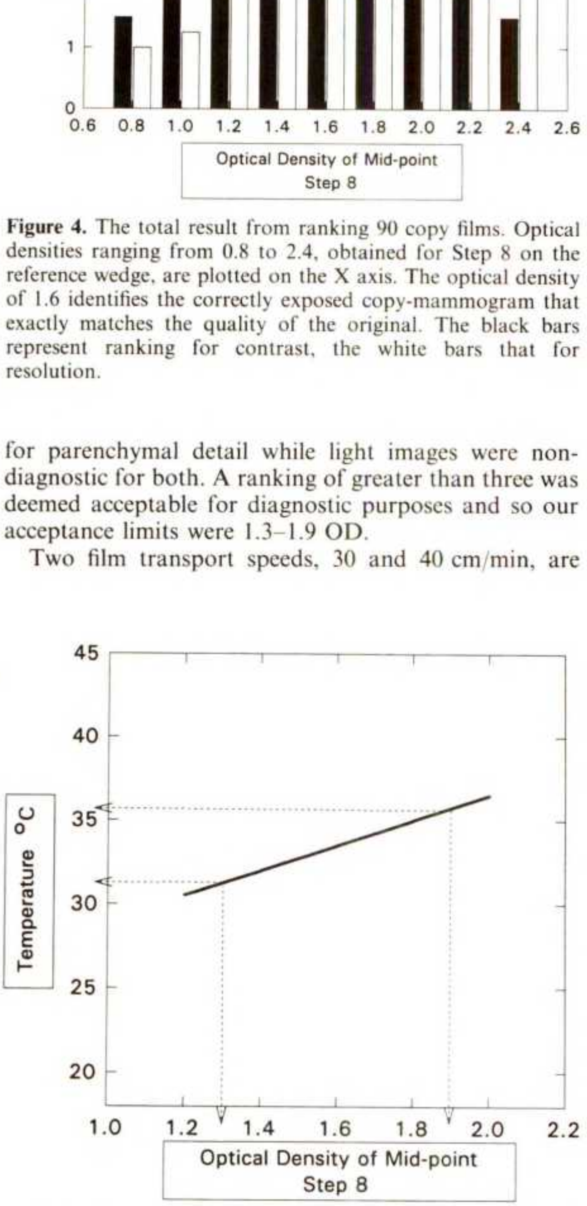

Figure 5. The density change for Step 8 of the reference wedge seen on films processed at different temperatures using a 3.0 min film transit (30 cm/min). Acceptable density variations are 1.3 to 1.9 for Step 8. This corresponded to a temperature range of 34 ± 2°C.

Table I. Breakdown of cycle times for Agfa Curix Compact film processor at 30 cm/min film speed

Developer time	46 seconds
Processing time (developing, fixing, washing, drying)	120 seconds
Film transit time (cassette in to film out)	180 seconds

Discussion

In contrast to the marked technical improvements in mammography equipment over the past decade, recent data by Galkin et al (1988) and Hendrick, 1990 have highlighted the wide ranges of image quality and patient dose that still exist. The importance of quality assurance was shown by Karila (1988) who achieved an 84% reduction in average breast radiation dose with no loss of diagnostic accuracy by a quality control project over a 5 year period.

Despite extensive use of mammographic phantoms in quality control and recent advances in their construction (Caldwell & Yaffo 1990), there are a number of inherent disadvantages in their use to mimic breast pathology. Firstly, their tissue-equivalence is only approximate to breast tissue (Friedrick, 1991). Secondly, continuous usage of a single phantom results in the production of multiples of a single abnormal image. In time an observer learns to recognize this fixed abnormal pattern and therefore bias is introduced for subsequent viewing. In order to overcome these problems we chose a range of abnormal mammograms containing real pathology as our reference material. Law & Kirkpatrick (1988) and De Parades et al (1987) have both used breast phantoms to examine mammographic film processor temperature and time and their effect on patient dose and image quality. The former recommend acceptance limits for time at 3–3.5 min and a temperature of 35 or 36°C. The latter recommend a processing temperature of 92–95°F, (equivalent 33.3–35°C). Our figures correlate well with these at 3 min and 34 ± 2°C.

From the above results, it would seem that photographic copying of real pathology may indeed be an alternative means of assessing processor performance. While further studies would be necessary to substantiate these findings, this method has a number of advantages: (a) real and not simulated pathology (phantom) is studied; (b) potential bias from use of a solitary phantom is avoided; (c) a wide range of pathology is freely available for copying and (d) cost-effectiveness.

It is important to note that while processing temperature accurately reflects the temperature in the developer tank, processing time reflects overall film transit through the film processor (film transit time) and not the duration of transit through the developer solution (developer time). This is a potential source of error, as firstly it is developer time and not duration in fixing, washing and drying tanks which most influences image quality and required patient dose. Secondly, the relationship between processing and developer times varies with the rate of film transport. All articles referenced have failed to address adequately these anomalies. In order to allow comparison with previous studies, we have stated overall film transit time, but have related this to true processor and developer times for suggested optimal limits (Table I). We suggest that future studies state all three parameters, thus allowing a more direct and potentially more accurate means of assessing film processor performance.

Russell & Carmichael (1987) reported that a decrease of 2–3°C processing temperature required a compensatory increase in patient dose of 25% for older films and 5–10% for newer films. In addition Law & Kirkpatrick (1988), Kimme-Smith et al (1988) and Haus (1990) report that upper limits of processing time and temperature can allow an appreciably lower patient radiation dose. On the basis of these findings we recommend that our upper limits of acceptance, *i.e.* 36°C and 2 min be taken as most beneficial in terms of patient dose and image quality. Brenner (1989) has shown the medico-legal implications of QC in mammography. The possible reduction in patient dosage and improvement in diagnostic accuracy as outlined above are of obvious importance in this regard.

On-board film processing in mobile units has not gained widespread acceptance amongst breast screening programmes. This is despite a number of inherent advantages: (1) It reduces patient recall for repeat/supplementary film views and thereby allays patient anxiety. (2) Supplementary views at initial presentation improve diagnostic accuracy and patient management. (3) It allows staff on site to assess image quality throughout the working day. (4) Constant film feedback motivates staff on site. (5) It avoids potential film fogging associated with a delay in film transfer to a central processor.

Constant QC monitoring of film processor performance at both centres is now possible as pre-exposed sensitometric grey scales have been placed on our mammography film stock. The grey scale lies in a shielded area adjacent to the identity label (Fig. 3). Thus image quality can be checked against an optimal grey scale kept on the film viewer. Variation in image quality can be quickly assessed; changes in grey scale density indicate film processing faults, no changes in grey scale density but variations in image density indicate X ray exposure variation.

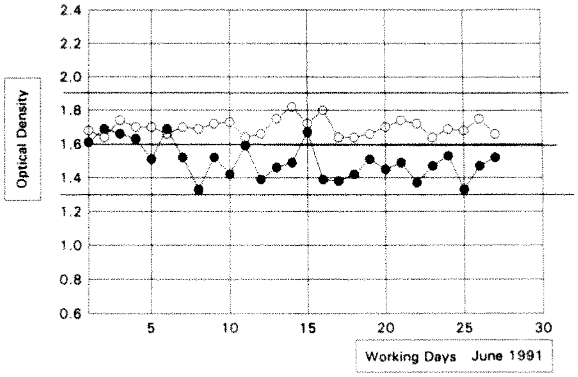

Figure 6. Optical density variations for Step 8 seen one year later when the mobile screening centre was subject to approximately the same ambient temperature variations.

Problems exist with film processors in mobile units, the major one being the control of ambient temperatures in these small often poorly insulated units. The variations in processor performance have been seen to correspond with large variations in ambient temperature and an immediate improvement in film quality was seen when the ventilation system in our mobile was upgraded. Further small improvements at both centres were obtained by adjusting replenishment rates in the small volume developer tanks. One year later film quality proved consistent and within our denisty variation limits (Fig. 6). The remaining small variations seen in both centres does not influence diagnostic accuracy and on-site film processing in our mobile screening unit continues to be an invaluable asset. Both film processors, to date, give reliable and consistent results.

Conclusion

Image quality is paramount to the success of high quality mammography. The film processor has been identified as the weakest link in the mammographic chain.

The anomaly that exists in reporting overall film transit time in the absence of true processing and developer times is discussed. The use of all three parameters when reporting film processor performance is advocated. Processing time and temperature have been shown to influence both patient dose and image quality. Optimal values for processing time of 2 min and processing temperature of 36°C are proposed.

The use of photographic copies of real pathology as an adjunct to quality assurance has been investigated. Initial results are comparable to those of previous phantom studies. The abolition of observer bias normally associated with phantom usage is an obvious advantage. The addition of a step wedge grey scale to pre-exposed mammography film thereby allowing constant monitoring of image quality is advocated. The resulting ease with which the film processor or X ray machine can be differentiated as sources of possible image degradation is outlined.

Regular quality control testing and attention to design have ensured that our mobile unit processing is now comparable to the central hospital based unit. From these findings we now recommend on-site processing of all mammography film with its inherent advantages.

Acknowledgments

The authors wish to acknowledge the generous financial support to the Eccles Street Breast Screening Centre from the European Community, The Mater Foundation, FEMSCAN, and Quinnsworth Ltd.

References

BRENNER, R. J., 1989. Medicolegal aspects of screening mammography. *American Journal of Radiology, 153*, 53–56.

CALDWELL, C. B. & YAFFE, M. J., 1990. Development of an anthropomorphic breast phantom. *Medical Physics, 17*, 273–280.

DE PARADES, E. S., FRAZIER, E. B., HARTWELL, G. D., STRASH, A. M., SCHEER, C., SMITH, D. C., BARNETTE, P. A., NOEL, W. & KENNEWEG, D., 1987. Development and implementation of a quality assurance programme for mammography. *Radiology, 163*, 83–85.

FRIEDRICH, M. A., 1991. Mammographic equipment, technique, and quality control. *Current Opinion in Radiology, 3*, 571–578.

GALKIN, B. M., FEIG, S. A. & MUIR, H. D., 1988. The technical quality of mammography in centres participating in a regional breast cancer awareness programme. *Radiographics, 8*, 133–145.

HAUS, A. G., 1990. Technological improvements in screen film mammography. *Radiology, 174*, 628–637.

HENDRICK, R. E., 1990. Standardization of image quality and radiation dose in mammography. *Radiology, 174*, 648–654.

INSTITUTE OF PHYSICAL SCIENCES IN MEDICINE, 1989. Report 59. *Commissioning and routine testing of mammographic X-Ray systems.* Obtainable from Institute of Physical Sciences in Medicine, 2 Low Owegate, York YO1 1QU, England.

INTERNATIONAL AGENCY FOR RESEARCH ON CANCER, 1989. *Geographical map for breast cancer mortality 1970s.* Obtainable from Europe Against Cancer Programme, Commission of the European Communities, Rue de la Loi 200–1049, Brussels, Belgium.

KARILA, K. T. A., 1988. Quality control of mammographic equipment—a 5 year follow-up. *British Journal of Radiology, 61*, 1155–1167.

KIMME-SMITH, C., ROTHSCHILD, P. A., BASSETT, L. W., GOLD, R. H. & MOLER, C., 1989. Mammographic film-processor temperature, development time and chemistry: effect on dose, contrast, and noise. *American Journal of Radiology, 152*, 35–40.

KODAK, 1988. Publication No. E-27H. Obtainable from Kodak International Lab Ltd.

LAW, J. & KIRKPATRICK, A. E., 1988. Film processing for mammography. *British Journal of Radiology, 61*, 939–942.

LEITZ, W., 1990. Quality requirements in mammographic screening in Sweden. *Recent Results Cancer Research, 119*, 75–80.

RUSSELL, J. G. B. & CARMICHAEL, J. H. E., 1987. Developer temperature in diagnostic departments. *British Journal of Radiology, 60*, 781–782.

TABAR, L. & DEAN, P. B., 1983. *Screen Film Mammography: Quality Control in Breast Cancer, Current Diagnosis and Treatment*, ed. by S. A. Feig & R. McLelland (Mahon, New York), pp. 161–168.

1992, *The British Journal of Radiology*, 65, 1102–1104

The influence of needle size on post-myelography headache: a controlled trial

By Garrett M. McGann, FRCR, Fergus V. Gleeson, FRCR, Ian Kelly, FRCR, Alan R. Valentine, FRCR, Andrew Platts, FRCR, Paul Butler, FRCR and *Bernard J. Crump, MFCM

Department of Radiodiagnosis, Royal Free Hospital, Pond Street, London NW3 2QG and *Department of Public Health Medicine, Central Birmingham Health Authority, Birmingham B15 2TZ, UK

(*Received 28 April 1992 and accepted 10 August 1992*)

Keywords: Myelography, Headache

Abstract. This study aimed to test the hypothesis that the use of fine rather than larger calibre needles for myelography reduces the incidence of post-procedural headache. 160 patients were randomized in a prospective controlled trial of 22 gauge versus 26 gauge needles. The incidence and overall severity of headache as measured at 1, 4 and 21 days after myelography was not significantly different in the two groups.

Headache is by far the most common and most disabling adverse effect of myelography, occurring in 4–49% of patients (Skalpe et al, 1988; Sand, 1989). There is general consensus that headache is attributable to continuing cerebrospinal fluid (CSF) leakage from the dural puncture site after withdrawal of the needle, resulting in relative CSF hypotension and stretching of pain-sensitive intracranial structures. The evidence for this includes the following: the headache is almost always influenced by posture, being relieved by lying down (Smith et al, 1980); low CSF pressures have been measured in patients with persistent symptoms (Hilton-Jones, 1984); continued dural leak has been seen at surgery (Brown & Jones, 1962) and has been demonstrated by radioisotopes (Leiberman et al, 1971) and a lower incidence of headache is encountered when the puncture is made at the C1/2 level (Skalpe et al, 1988). If the use of fine calibre needles compared with larger needles were to reduce the rate of CSF leak after lumbar puncture, the incidence or severity of post-procedural headache should fall. Several studies have addressed this issue. A controlled trial involving 100 volunteers, 50 randomized to lumbar puncture with 22 gauge and 50 to puncture with 26 gauge, detected no difference in the frequency of complaints overall, but found an incidence of severe headache of 44% in the 22 gauge group and zero in the 26 gauge group (Tourtellotte et al, 1972). In a study of post-procedural headache after myelography comparing 20 gauge with 22 gauge needles, using unblinded observers to question the subjects, a significant reduction in headache was seen in the 22 gauge group (Sand et al, 1989). However, a further study involving 18, 20 and 22 gauge needles found no significant difference in the incidence of headache attributable to different needle sizes, but a higher rate was noted in females (Rolfe & Maguire, 1980).

An uncontrolled survey of symptoms after outpatient myelography using 25 and 26 gauge needles had suggested a low incidence of headache and other symptoms; 90% of patients were said to have had no adverse effects after puncture with a 26 gauge needle (Vezina et al, 1989). We sought to validate this conclusion in a double blind controlled trial. After completion of this study, a controlled trial of 22 versus 26 gauge needles has been published (Wilkinson & Sellar, 1991) which found a significant reduction in moderate and severe headache incidence after puncture with the finer gauge.

Subjects and methods

160 consecutive patients attending for myelography were randomized to undergo the lumbar puncture with either a 22 or a 26 gauge needle. Both calibres were already being used regularly in the department. Patients with marked obstruction to CSF flow (mostly those with thecal compression due to metastatic tumour) were excluded from the study. Conditions during and following the examination were standardized: no local anaesthetic was used and lumbar puncture was performed with the patient in the sitting position with the cutting axis of the needle orientated in the rostrocaudal direction (the direction of the majority of the fibres of the dura mater). 7 ml of CSF were removed for laboratory analysis and 17 ml of iohexol, 240 mg iodine/ml, were injected. It was recorded whether the examination was limited to the lumbosacral segments or included thoracic and cervical examination which involves running contrast up from the puncture site by tilting the patient head down. The radiologist recorded whether the needle insertion and examination were straightforward or technically difficult. After the study, the patients rested in bed with head elevated for 24 hours, during which time oral fluids were encouraged. The patients were questioned by an independent observer at 24 hours and the presence and severity of headache was assessed using a visual analogue scale. The scale ranged

---

Address correspondence to Dr G. McGann, Radiology Department, Pilgrim Hospital, Boston, Lincs PE21 9QS, UK.

Table I. Analysis of headache scores as obtained with visual analogue scales at Days 1, 4 and 21

Day	Needle	Number in group	Total headache score of group	Mean	Variance	Standard deviation
1	22	75	230	3.067	15.198	3.898
	26	71	189	2.662	13.913	3.730
4	22	75	186	2.480	13.145	3.626
	26	71	133	1.873	9.6	3.103
21	22	75	70	0.933	5.874	2.424
	26	71	24	0.338	2.227	1.492

from 0 to 10 with 0 representing no headache and 10 an extremely severe headache. The patients' perception of the unpleasantness of the procedure ("procedure tolerability") was similarly assessed. The occurrence of other symptoms was noted. Further interviews were carried out by telephone at 4 and 21 days.

Results

160 patients were entered into the trial and randomized; due to incomplete follow-up or death, adequate data were available in 146. 75 (51.4%) were male. 84 patients (57.5%) suffered headache at some time during the follow-up period which they attributed to the procedure. 39 of 71 patients (55%) who underwent puncture with a 26 gauge needle reported headache; 45 of 75 patients (60%) in the 22 gauge group reported headache. The results of the visual analogue and subsequent verbal inquiry of pain scores of headache were not normally distributed and therefore required analysis with non-parametric statistics (Kruskal-Wallis test for two groups). There was no significant difference in pain scores between the two groups at any stage of follow up, ($p = 0.42$ at day 1, $p = 0.50$ at day 4, $p = 0.20$ at day 21). See Table I.

The incidence of "procedural difficulty" was statistically similar in both groups. 12 difficult procedures were reported in the 22 gauge group and 11 in the 26 gauge group. This analysis does not include two patients in whom puncture was not achieved with a 26 gauge who were removed from the trial and were subsequently punctured with a 22 gauge. Likewise, procedural tolerability showed no difference in the two groups ($p = 0.199$). The only finding to reach statistical significance was in other post-procedural symptoms, namely a reported increase in back or neck pain, nausea, vomiting or dizziness. Data were available in 143 patients. Of the 74 in the 22 gauge group, 37 (50%) admitted to at least one of these symptoms; of the 69 patients in the 26 group, only 19 (28%) did ($p = 0.0099$).

Disregarding needle diameter, the incidence of headache was similar in those having cervical examinations to those having lumbar views only ($p = 0.686$ at day 1, $p = 0.472$ at day 4, $p = 0.589$ at day 21).

Sample size calculations would suggest that a trial of this size might be expected to detect a difference of between two and three points in the pain score, with 80% power, at conventional levels of significance.

Discussion

As a result mainly of uncontrolled trials, the use of very fine gauge spinal needles has been advocated both for myelography and for diagnostic LP. It is frequently more difficult and time consuming to obtain CSF samples through these needles. Injection of contrast is slower and so the inexperienced radiologist may less easily recognize subdural injection of contrast medium. Failure to puncture the theca was experienced twice with 26 gauge needles.

The incidence and character of headache and other complaints after lumbar puncture and after myelography following lumbar puncture, with the modern non-ionic contrast agents is similar (Sand et al, 1987) and are thus possibly attributable to the dural puncture rather than to any effect that contrast medium may have.

The similarity in our results between those who had lumbar studies and those in whom the contrast was run to the cervical region is consistent with a relative lack of influence of the contrast medium on post-myelogram symptoms, possibly indicating that our results could be applied to diagnostic lumbar punctures without contrast injection. Although there was a statistically significant increase in symptoms other than headache after puncture with 22 gauge needle, the overall morbidity attributable to this group of symptoms is clinically minor compared with headache.

In conclusion, our data show no reduction in headache following myelography with the different needle sizes employed in our study. Other less frequent and less troublesome symptoms may be reduced by the use of the smaller gauge needle.

Acknowledgment

We thank radiographers and nurses of the "special investigations suite" in the Royal Free Hospital, without whose patient assistance this trial would not have been possible.

References

BROWN, B. A. & JONES, O. W., 1962. Prolonged headache following spinal puncture, response to surgical treatment. *Journal of Neurosurgery*, *19*, 349–350.

HILTON-JONES, D., 1984. What is postlumbar puncture headache and is it avoidable? In *Dilemmas in the Management of the Neurological Patient*, ed. by C. Warlow and J. Garfield (Churchill Livingstone, Edinburgh), pp. 144–157.

LEIBERMAN, L. M., TOURTELLOTTE, W. W., NEWKIRK, T. A., 1971. Prolonged post-lumbar puncture cerebrospinal fluid leakage from lumbar subarachnoid space demonstrated by radioisotope myelography. *Neurology 21*, 925–928.

ROLFE, E. B. & MAGUIRE, P. D., 1980. The incidence of headache following various techniques of metrizamide myelography. *British Journal of Radiology*, *53*, 840–844.

SAND, T., 1989. Which factors affect reported headache incidences after lumbar myelography? *Neuroradiology, 31,* 55–59.

SAND, T., STOVNER, L. J., DALE, L. & SALVESON, R. 1987. Side effects after diagnostic lumbar puncture and lumbar iohexol myelography. *Neuroradiology, 29,* 385–388.

SAND, T., MYHR, G., STOVNER, L. J., DALE, L. G. & TANGERUD, A., 1989. Side effects after ambulatory lumbar iohexol myelography. *Neuroradiology, 31,* 49–54.

SKALPE, I. O. & NAKSTAD, P., 1988. Myelography with iohexol (Omnipaque); clinical report with special reference to the adverse effects. *Neuroradiology, 30,* 169–174.

SMITH, F. R., PERKIN, G. D. & CLIFFORD ROSE, F., 1980. Posture and headache after lumbar puncture. *Lancet, 1,* 1245.

TOURTELLOTTE, W. W., HENDERSON, W. G., TUCKER, R. P., GILLAND, O., WALKER, J. E. & KOKMAN, E., 1972. A randomised, double-blind clinical trial comparing the 22 versus 26 gauge needle in the production of the post-lumbar puncture syndrome in normal individuals. *Headache 12,* 73–78.

VEZINA, J. L., FONTAINE, S. & LAPERRIERE, J., 1989. Outpatient myelography with fine needle technique: an appraisal. *American Journal of Roentgenology, 153,* 383–385.

WILKINSON, A. G. & SELLAR, R. J., 1991. The influence of needle size and other factors on the incidence of adverse effects caused by myelography. *Clinical Radiology, 44,* 338–341.

1992, *The British Journal of Radiology*, *65*, 1105–1107

Does Myodil introduced for ventriculography lead to symptomatic lumbar arachnoiditis?

By C. A. Rowland Hill, J. V. Hunter, I. F. Moseley and B. E. Kendall

Lysholm Department of Radiology, National Hospital for Neurology and Neurosurgery, Queen Square, London WC1N 3BG, UK

(*Received 2 March 1992 and accepted 3 June 1992*)

Keywords: Arachnoiditis, Myelography, Myodil, Pantopaque

Abstract. Although there is a substantial body of evidence implicating Myodil or Pantopaque as a cause of lumbar arachnoiditis, assessment of the clinically based evidence is complicated by the additional potentially causative factors present in a high proportion of cases. These include pre-existing spinal pathology, traumatic lumbar puncture and surgery. The aim of this retrospective study was to attempt to ascertain whether Myodil introduced via ventricular catheter was associated with subsequent development of symptomatic lumbar arachnoiditis. In 222 patients in whom clinical records were reviewed there was no excess of back pain following ventriculography compared to the general population. Myodil ventriculography does not appear to be a major cause of symptomatic lumbar arachnoiditis. Several unavoidable problems with the methodology of this study are discussed.

Spinal arachnoiditis is a non-infectious or post-infectious aseptic inflammatory process of the leptomeninges. The imaging of this condition has recently been reviewed (Kendall et al, 1991). Circumscribed and diffuse forms have been described with a variety of aetiologies including trauma, surgery, neoplasia, infection, haemorrhage and a range of irritants, foremost among which are radiographic contrast media, both oily and ionic water-soluble. Of particular interest is ethyl iodophenylundecylate (Pantopaque or Myodil) which was widely used as a positive myelographic contrast medium from the mid-1940s until the general acceptance of non-ionic water soluble media during the early 1980s.

The incidence of clinically significant arachnoiditis associated with Myodil or Pantopaque myelography is difficult to assess but has been estimated to be between "probably only a fraction of one per cent" (Peterson, 1975) and approximately 1% (Shaw et al, 1978). However, the relative contribution of the contrast medium compared to other factors also known to be associated with arachnoiditis and which are present in many of the described cases is less certain. Lumbar disc disease in the absence of any intervention (Ransford & Harries, 1972) and surgery without myelography (Jorgensen et al, 1975) are the most important in this context but spinal neoplastic disease and haemorrhage are also known causes of arachnoiditis. In a review of 80 myelographically-diagnosed cases of arachnoiditis (Shaw et al, 1978) 42 had previous Myodil myelography but only three of these (4%) had had no complications during myelography, no spinal surgery and no previous spinal disease. In another series of 50 patients (Guyer et al, 1989) 47 had Myodil myelography but 46 had also undergone lumbar surgery.

The aim of this retrospective study was to attempt to remove some of these possible additional contributory factors by studying a group of patients in whom Myodil was introduced via a burr hole and ventricular catheter and thus in whom the primary pathology and any later intervention was not expected to be spinal. Subsequent development of symptomatic lumbar arachnoiditis, indicated by their re-presentation with low back pain, and clinical and radiological assessment might then be more directly attributed to Myodil.

Methods

Patients who underwent Myodil ventriculography were identified from post-World War II radiology department records. Clinical case notes were then obtained where possible. A proforma was constructed and completed as far as possible for each patient as follows: presentation; nature of Myodil study; volume of Myodil injected; Myodil flow into normal fourth ventricle; previous back pain (0–3); post-Myodil back pain or sensory symptoms; length of follow-up; final diagnosis; confirmation of arachnoiditis; other, including surgery and other treatment.

The endpoint for the study was death of the patient or the last entry in the notes. For many patients data were incomplete; for example, the volume of Myodil injected was sometimes not recorded.

Two 'null hypotheses' were constructed:

(1) that the prevalence of low back pain (as evidence of symptomatic arachnoiditis) in post-Myodil ventriculography patients is no different from that of the general population; and

(2) that the prevalence of low back pain (as evidence of symptomatic arachnoiditis) before Myodil ventriculography is no different from the prevalence of back pain following exposure to Myodil.

Results

We were able to identify 477 patients (M = 268, F = 209 M:F = 1.28:1) with a mean age of 35 years (n = 358) who underwent Myodil ventriculography between 1949 and 1979. The mean volume of Myodil introduced was 2.1 ml (range 0.8–6 ml, n = 299).

Examination of all the available notes resulted in a completed study group of 222 patients (M = 141, F = 81 M:F = 1.74:1). Mean follow-up was 40 months (n = 222), range less than 1 month to 30 years. 84 patients were followed up for 12 months or more. The mean age of the completed study group was 34 years (n = 222), age range 5 months to 72 years. The mean volume of Myodil used was 2.2 ml (range 0.8–6 ml, n = 149). In 70 patients the radiologist's report specifically commented on flow of contrast into the (normal) fourth ventricle. In only seven cases was there confirmation by screening or plain radiography of Myodil in the lumbosacral sac.

There was a range of pathologies including 39 patients with aqueduct stenosis. 61 patients were shunted, including 37 Torkildsen's procedures. 19 subjects underwent post-mortem examination, of whom 16 showed no evidence of arachnoiditis, one demonstrated a ventriculitis, one a neoplastic leptomeningitis and one (a 5-year-old child) a chronic leptomeningitis.

Three patients re-presented with back pain following Myodil ventriculography: one had a temporal lobe glioma complicated by blood clot in the left lateral ventricle, one was an achondroplastic with spinal stenosis who had pre-existing low back pain, and the third had an episode of acute back pain associated with shunt infection a year following ventriculography, resolving on antibiotics.

Three cases of spinal arachnoiditis were diagnosed at myelography: one was associated with an infected Torkildsen's shunt, one with tuberculous meningitis and the third with a past history of taboparesis.

At follow-up surgery five patients were diagnosed as suffering from posterior cranial fossa arachnoiditis, four of whom had had at least one previous operation on the posterior fossa.

Discussion

Experimental work in animals has shown that introduction of Pantopaque into the spinal subarachnoid space by lumbar puncture (Fisher, 1965) or cisternal puncture (Howland & Curry, 1966; Bergeron et al, 1971; Pasaoglu et al, 1988) invariably results in the development of an arachnoiditis varying from mild to severe. The deliberate introduction of blood with Pantopaque (Howland & Curry, 1966) or the occurrence of a traumatic puncture (Bergeron et al, 1971) are associated with severe arachnoiditis.

Although some early reports found no adverse effects attributable to the clinical use of Myodil or Pantopaque for myelography (Bering, 1950; Bull, 1950; Shipp, 1953), the last in a series of 1800 myelograms, this contrasts dramatically with the experience of others. There are numerous reports of arachnoiditis demonstrated surgically, radiologically or post-mortem in patients who have undergone Myodil or Pantopaque myelography (Tarlov, 1945; Hurteau et al, 1954; Davies, 1956; Shaw et al, 1978). In Davies's series 14 of 119 patients (12%) developed chronic symptoms attributed to Myodil. Erikson & van Baaren (1953) and Mason & Raaf (1962) both described single cases where a patient died with severe basal arachnoiditis 15 and 7 months respectively after myelography. In a group of patients who underwent repeat myelography (for indications undisclosed by the authors), radiological signs of arachnoiditis were demonstrated in 66% of patients who underwent Myodil myelography and 80% of patients who had surgery in addition to myelography (Johnson & Burrows, 1978).

There was no statistically significant incidence of low back pain in our study group and no excess of unexplained low back pain in patients pre- and post-ventriculography. (Interestingly, the prevalence of low back pain in the study group was less than that reported in the literature). As such both the null hypotheses proposed are sustained and no case of back pain need be attributed to Myodil-induced arachnoiditis.

We recognize that there are many potential problems with both the methodology and interpretation of this study. Approximately half of the patients went on to craniotomy or shunting and subarachnoid blood may rarely be associated with arachnoiditis (Shaw et al, 1978). Neoplasia is another recognized cause of arachnoiditis and drop metastases from a cerebral lesion could have been a complicating factor. However, these would tend to lead to a higher incidence of clinical spinal manifestations. The length of follow-up is limited by several factors, not least that patients were frequently sent back for further care at their referring hospitals after investigation at this centre. However it is probably true that patients with persistent or recurrent symptoms were more likely to be referred back to the specialist centre. Thus, the likelihood that many patients with short or incomplete follow-up had complications of Myodil injection is low. In the Glasgow series (Shaw et al, 1978) 49% of their cases presented within 1 year of initial investigation and 20% within 1 month although it is not stated which of these cases underwent Myodil myelography.

A more serious flaw in the study is the uncertainty as to whether Myodil ever reached the lumbosacral sac. Aqueduct stenosis without a Torkildsen's procedure represents a particular problem in this respect as this would be expected to have prevented caudal passage of contrast medium. In only 32% of our patients was there a specific comment in the study report that Myodil had flowed into a normal fourth ventricle. Only 3% of patients had subsequent lumbar spine radiographs or fluoroscopy confirming the presence of Myodil. Nevertheless, in patients without obstruction Myodil would be expected to flow into the lumbosacral sac when the patient was sat up at the end of the procedure (Bull, 1950). Only 27.5% of the patients were shunted after the ventriculogram, suggesting that most of the remainder did not have a blockage proximal to the outlet foramina of the fourth ventricle. A further potential problem is that the volume of Myodil used for ventriculography tended to be at the lower limit of normal for the amount used for lumbar myelography; however although one of the operators routinely used a 6 ml volume for the latter investigation, very many patients received only 3 ml, much of which was removed. Furthermore there is no evidence relating the development of arachnoiditis to the volume of contrast medium used.

Finally, if the incidence of symptomatic arachnoiditis following myelography is of the order of 1% then the study group is not of sufficient size to significantly demonstrate a lower incidence of arachnoiditis.

Conclusion

Only half the potential cohort could be studied adequately but these preliminary results suggest that symptomatic lumbar arachnoiditis is not a major complication of Myodil ventriculography. As indicated above, incomplete records are more likely to indicate lack of complications. Pooled data from a number of centres would be required to achieve a much larger series to look for a statistically significant result. Age- and sex-matched controls may also be required. A more appropriate study to answer the question as to whether or not Myodil myelography is a cause of symptomatic arachnoiditis may be to use two cohorts of spontaneously presenting patients with low back pain following either Myodil or non-ionic water-soluble contrast medium, age, sex and clinically matched, utilizing an historic cohort analysis. A diagnostic test, high quality MRI being the most appropriate (Delamarker et al, 1990; Kendall et al, 1991), may be used to confirm arachnoiditis, although water soluble myelography with modern agents probably remains the "gold standard".

Like other centres we are now receiving many queries relating to chronic spinal problems following myelography. Many are from patients who have only been exposed to non-ionic water-soluble media used in doses not associated with arachnoiditis. Some of the earlier ionic water soluble media (Conray, Dimer-X) have also been associated with changes of arachnoiditis on subsequent radiculography in the absence of surgical intervention (Castan et al, 1977; Picard et al, 1977), but these were never used at our hospital.

References

Bergeron, R. T., Rumbaugh, C. L., Fang, H. & Cravioto, H., 1971. Experimental Pantopaque arachnoiditis in the monkey. *Radiology*, *99*, 95–101.

Bering, E. A., 1950. Notes on the retention of Pantopaque in the subarachnoid space. *American Journal of Surgery*, *80*, 455–458.

Bull, J., 1950. Positive contrast ventriculography. *Acta Radiologica*, *34*, 253–268.

Castan, P., Bourbotte, G., Herail, J. P. & Maurel, J., 1977. Follow-up and postoperative radiculography. A radiological analysis of 640 patients. *Journal of Neuroradiology*, *4*, 49–93.

Davies, F. L., 1956. Effect of unabsorbed radiographic contrast media on the central nervous system. *Lancet*, *ii*, 747–748.

Delamarker, R. B., Ross, J. S., Masaryk, T. J., Modic, M. T. & Bohlman, H., 1990. Diagnosis of lumbar arachnoiditis by magnetic resonance imaging. *Spine*, *15*, 304–310.

Erickson, T. C. & Van Baaren, H. J., 1953. Late meningeal reaction to ethyl iodophenylundecylate used in myelography. *JAMA*, *153*, 636–639.

Fisher, R. L., 1965. An experimental evaluation of Pantopaque and other recently developed myelographic contrast media. *Radiology*, *85*, 537–545.

Guyer, D. W., Wiltse, L. L., Eskay, M. L. & Guyer, B. H., 1989. The long range prognosis of arachnoiditis. *Spine 14*, 1332–1341.

Howland, W. J. & Curry, J. L., 1965. Experimental studies of Pantopaque arachnoiditis. *Radiology*, *87*, 253–261.

Hurteau, E. F., Baird, W. C. & Sinclair, E., 1954. Arachnoiditis following use of iodized oil. *Journal of Bone and Joint Surgery*. *36*A, 393–400.

Johnson, A. J. & Burrows, E. H., 1978. Thecal deformity after lumbar myelography with iopherdylate (Myodil) and meglumine iothalomate (Conray 280). *British Journal of Radiology*, *51*, 196–202.

Jorgenson, J., Hansen, P. H., Steenskov, V. & Oveson, N., 1975. A clinical and radiological study of chronic lower spinal arachnoiditis. *Neuroradiology*, *9*, 139–144.

Kendall, B. E., Stevens, J. M. & Thomas D., 1991. Arachnoiditis. *Current Imaging*, *3*, 113–119.

Mason, M. S. & Raaf, J., 1962. Complications of Pantopaque myelography. Case report and review. *Journal of Neurosurgery*, *19*, 302–311.

Pasaoglu, A., Gok, A. & Patioglu, T. E., 1988. An experimental evaluation of response to contrast media Pantopaque, iopamidol and iohexol in the subarachnoid space. *Investigative Radiology*, *23*, 762–66.

Peterson, H. O., 1975. The hazards of myelography. *Radiology*, *115*, 237–239.

Picard, L., Roland, J., Blanchot, P., David, R., Montaut, J. & Pourel, J., 1977. Scarring of the theca and the nerve roots as seen at radiculography. *Journal of Radiology*, *4*, 29–48.

Ransford, A. O. & Harries, B. J., 1972. Localised arachnoiditis complicating lumbar disc lesions. *Journal of Bone and Joint Surgery*, *54*B, 656–665.

Shaw, M. D. M., Russell, J. A. & Grossart, K. W., 1978. The changing pattern of spinal arachnoiditis. *Journal of Neurology, Neurosurgery and Psychiatry*, *41*, 97–107.

Shipp, F. L., 1953. Technique and value of myelography. *JAMA*, *151*, 185–187.

Tarlov, I. M., 1945. Pantopaque meningitis disclosed at operation. *JAMA*, *129*, 1014–1016.

1992, *The British Journal of Radiology*, *65*, 1108–1113

Clearance of iopamidol, a non-ionic contrast medium, by CAPD in patients with end-stage renal failure

By P. K. Donnelly, BSc, MD, FRCS, N. Burwell, RGN, *A. McBurney, BSc, MPhil, PhD, †J. W. Ward, BPharm, MBChB, FRCP, ‡J. Walls, MBBS, FRCP and §E. M. Watkin, MBBS, FRCR, DMRD

Department of Surgery, Leicester General Hospital, Gwendolen Road, Leicester LE5 4PW; *Department of Chemical Pathology, †Department of Clinical Pharmacology, Glenfield General Hospital, Groby Road, Leicester LE3 9QP; ‡Department of Nephrology, §Department of Radiology, Leicester General Hospital, Gwendolen Road, Leicester LE5 4PW, UK

(*Received 12 February 1992 and in revised form 4 June 1992, accepted 16 July 1992*)

Keywords: Iopamidol, Non-ionic contrast, Clearance, Continuous ambulatory peritoneal dialysis

Abstract. In normal healthy subjects radiographic contrast media are cleared by the kidneys with a half-life of approximately 2 h and a total body clearance of 8 l/h. The mechanism of contrast clearance has not been previously investigated in chronic renal failure patients undergoing continuous ambulatory peritoneal dialysis (CAPD). A study was undertaken to investigate the pharmacokinetics of a non-ionic water soluble radiographic contrast medium (iopamidol) in 10 patients stabilized on CAPD. All patients (eight male, two female) aged 22–68 years (median 53 years) had injection of 30 ml of iopamidol 300 via a forearm vein to investigate subclavian vein patency following previous cannulation for haemodialysis. Venous blood samples, CAPD dialysate and urine were collected for seven days post injection. The mean plasma half-life was 37.9 h (SD 10.6) (range 24.1–57.2 h) for the CAPD patients and was greatly prolonged in comparison to healthy subjects. The total body clearance of iopamidol was also greatly reduced (0.377 l/h). CAPD removed an average of 53.6% of the administered dose (range 36.3–80.8%) whilst an average of 26.9% was excreted in the urine (range 1.3–56.3%). The combined renal and dialysate clearance was up to 93% of the administered dose over the period of the study. There is therefore some evidence for a small extra renal clearance of iopamidol in end-stage renal failure patients. This study has shown for the first time that patients with end-stage renal failure undergoing CAPD have significantly delayed elimination of contrast medium. This should be taken into consideration when extensive or prolonged investigations using contrast medium are proposed.

Iopamidol is a non-ionic water soluble radiographic contrast medium with low osmolarity, chemical toxicity and an absence of ionic charge (Partridge et al, 1981). These factors have led to its increased use in high risk patients such as those with end-stage renal disease (Bettmann, 1987). It is rapidly eliminated unchanged by the renal route in patients with normal renal function, with half of the dose eliminated within two hours, and 85–90% recovered in 72 h (Tirone et al, 1982; McKinstry et al, 1984). There is negligible plasma protein binding of the medium. The clearance of iopamidol has not been fully investigated in end-stage renal failure although other iodine-based contrast media are known to have delayed elimination (Bahlmann & Kruskemper, 1973). Whilst haemodialysis is an effective method of removing iodine containing contrast media, approximately 50% of patients with chronic renal failure are currently treated by continuous ambulatory peritoneal dialysis (CAPD) (Wing et al, 1988). Angiographic investigations in CAPD patients are frequently necessary to assess subclavian vein patency prior to creation of forearm fistulae (Donnelly et al, 1989). A study was therefore performed to define the pharmacokinetics of iopamidol in patients with end-stage renal failure who were having subclavian venography whilst undergoing CAPD.

Patients and methods

10 patients (eight male, two female) with end-stage renal failure and age range 22–68 (median 53 years) were studied (Table I). The project was approved by the Leicestershire District Ethical Committee and all patients gave written consent. They were stabilized on CAPD and had previously undergone temporary subclavian vein cannulation for acute access to haemodialysis. Each received an intravenous bolus dose of 30 ml Niopam (iopamidol) 300 (612.4 mg/ml) following an overnight fast. Blood samples were taken from the opposite arm at intervals: 5, 20, 40, 60 min and 2, 4, 6, 8, 12, 24, 72 and 144 h post-dose. Plasma was separated by centrifugation and stored at −20°C prior to analysis. Total urine output was collected for seven days in 24 h periods. The 24 h volume was recorded and aliquots stored at −20°C. For most patients (Table I) a daily dialysis consisted of 2 litres of hyperosmolar dialysate (alternating 2 litre bags of glucose 3.86% (RPB5415R) and glucose 1.36% (RPB5406R), Baxter Healthcare, Wallingford Road, Compton, Newbury, Berkshire) over 15 min with a dwell time of 6–8 h followed by drainage and discarded. This cycle was repeated four times in 24 h, and for the next 7 days the volume of each dialysate bag drained was recorded and an aliquot stored at −20°C.

Iopamidol assay

Iopamidol, chemically (S)-N,N'-bis [2-hydroxy-1-(hydroxy-methyl)ethyl]-5-[-hydroxy-1-(oxopropyl) amino]-2,4,6-triiodo-1,3-benzenedicarboxamide, and the internal standard, (S,S)-N,N,'-bis-[2-hydroxy-1-

Table I. Details of CAPD patients

Patient number	Initial	Age	Sex	Duration on dialysis	Body weight (kg)	Urine volume ml/day	Dialysis cycles	Cause of renal failure
1	SL	22	M	6 months	56.9	nil	4 (2 l) bags/day	Alports syndrome
2	EW	64	M	10 months	62.2	1425	4 (2 l) bags/day	Small kidneys
3	AM	47	M	24 months	71.6	2015	4 (2 l) bags/day	Membranous glomerulonephritis
4	HP	66	M	36 months	72.5	953	4 (2 l) bags/day	Hypertension
5	AM	59	M	5 months	67.5	365	4 (2 l) bags/day	Obstructive nephropathy
6	JK	36	M	21 months	64.5	15	4 (2 l) bags/day	Hypertensive renal disease
7	AJ	67	M	24 months	70.5	209	4 (2 l) bags/day	Renal carcinoma
8	GS	64	M	17 months	74.7	52	4 (3 l) bags/day	Membranous glomerulonephritis
9	SA	28	F	54 months	49.0	195	3 (2 l) bags/day	Post-partum haemolytic-uraemic syndrome
10	GN	42	F	17 months	88.6	725	4 (2 l) bags/day	Chronic pyelonephritis

(hydroxy - methyl) ethyl] - 5 - [hydroxy - 1 - (oxoethyl) amino]-2,4,6-triiodo-1,3-benzenedicarboxamide, were supplied by Bracco SpA, Milan. All other reagents were Analar grade.

Determination of iopamidol in plasma, urine and dialysate was performed as follows; 200 μl sample, standard or quality control (QC) plus 25 μl internal standard (1 mg/ml in distilled water) plus 200 μl saturated ammonium sulphate solution were pipetted into an Eppendorf tube, vortex mixed for 60 s and centrifuged at 12000 revs/min for 6 min. 200 μl of the supernatant was transferred to an autosampler vial and aliquots analysed by high pressure liquid chromatography (HPLC). All samples were assayed in duplicate. The calibration was linear up to 5 mg/ml and passed through zero. Quality control samples contained 75 and 600 μg/ml. The coefficients of variation of the assay at 20, 100 and 500 μg/ml were 8.4, 4.1 and 1.2%, respectively ($n = 7$). The inter assay coefficients of variation were 9.2 and 2.8% for QCs I and II, respectively ($n = 10$).

HPLC was performed using a Perkin Elmer ISS-101 autosampler, an LDC/Milton Roy variable wavelength Spectromonitor 3100 detector, and LDC/Milton Roy Constametric 3000 pump and a Hypersil ODS 5 μm column 30 × 0.4 cm. Chromatographic conditions were: wavelength — 240 nm; sensitivity — 1.0 AUFS; flow rate — 2 ml/min; temperature — ambient; eluent — 1% glacial acetic acid in water. The retention times of the internal standard and iopamidol were 4 and 6 min, respectively.

Details of pharmacokinetic analysis

Pharmacokinetic parameters (Keller et al, 1990) were obtained using SIPHAR, an integrated computer system for pharmacokinetic data analysis (Simed, France). The programme utilized the following equations to determine the main pharmacokinetic parameters:

Total body clearance (CL) = Dose/AUC_∞
where AUC_∞ is the area under the plasma concentration *vs.* time curve extrapolated to infinity.

Volume of distribution (β phase) [model independent] = CL/β
where β is the slope of the terminal phase of the plasma concentration *vs.* time curve.

Volume of distribution (steady state) [model dependent] = CL × MRT
where MRT = Σcoef i/exp i^2

fe = fraction of drug excreted unchanged = cumulative excretion/dose

Renal clearance = fraction excreted unchanged in urine × CL

Dialysate clearance = fraction excreted unchanged in dialysate × CL.

Elimination half-lives from urine and dialysate data were calculated using the Sigma Minus method (ARE plots or amount remaining to be excreted plots). This procedure consists of plotting log (AUC_∞ − Aet) *vs.* time, where Ae_∞ represents the cumulative excretion of drug over the period of study and Aet is the cumulative excretion of drug up to time(t). The half-life of elimination is then given by 0.693/slope of the terminal section of the plot.

Results

The mean plasma concentration *vs.* time profile for all subjects studied is shown in Fig. 1 and pharmacokinetic parameters derived from plasma data in Table IIa. For two subjects, the data were best represented by a two-term exponential function, with a fast distribution phase followed by a prolonged terminal elimination phase whilst the remaining data from eight subjects were best described by a three-term exponential function, with an intermediary phase having a half-life of about 2 h. The terminal plasma elimination half-life (mean ± SD) was 37.9 ± 10.6 h. This value is in marked contrast to those reported for healthy volunteers, *i.e.* 2.14 ± 0.48 h (McKinstry et al, 1984) and 1.91 ± 0.33 h (Tirone et al, 1982). The delayed removal of iopamidol can be related primarily to a decrease in total body clearance of drug since mean clearance was only 0.371 l/h in the CAPD

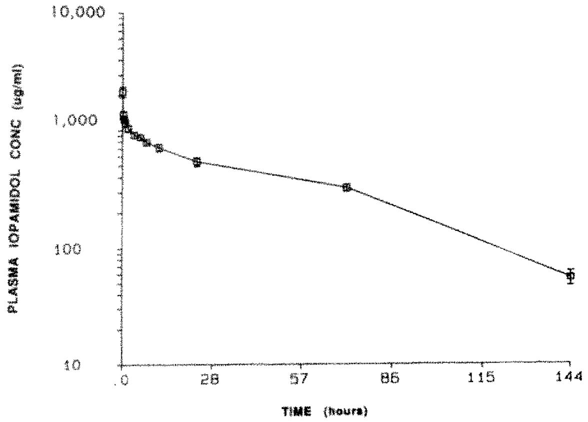

Figure 1. Iopamidol plasma concentration *vs.* time curve following intravenous administration of 30 ml Niopam 300. Values are the mean ± SEM of duplicate estimations in 10 subjects with end-stage renal failure undergoing CAPD for 7 days.

Table II. Pharmacokinetic parameters obtained following the administration of 30 ml Niopam 300 (18 372 mg iopamidol) intravenously to 10 subjects with end-stage renal failure undergoing CAPD for 7 days. Parameters are derived from (a) plasma, (b) urine, (c) dialysate data.

(a) Plasma data

Subject	$t\frac{1}{2},z$	CL_t l/h	Vd,β l	Vd,SS l
1	32.8	0.281	13.3	13.3
2	33.3	0.354	17.0	18.3
3	24.1	0.445	15.5	17.5
4	32.2	0.412	19.1	19.2
5	47.7	0.399	27.6	27.4
6	45.6	0.316	20.8	21.5
7	35.0	0.409	20.6	22.7
8	57.2	0.399	33.0	33.9
9	25.8	0.340	12.7	14.1
10	45.1	0.353	22.9	21.8
Mean	37.9	0.371	20.3	21.0
SD	10.6	0.050	6.4	6.2

$t\frac{1}{2},z$ = elimination half life, CL_t = total body clearance, $Vd\beta$ = volume of distribution (model independent), Vd,SS = volume of distribution (using the fitted model).

(b) Urine data

Subject	$t\frac{1}{2},z$	CL_2	fe
2	33.3	0.131	0.369
3	28.1	0.251	0.563
4	35.1	0.172	0.416
5	48.3	0.054	0.134
7	34.2	0.027	0.065
8	69.2	0.005	0.013
9	24.7	0.125	0.378
10	29.2	0.078	0.221
Mean	37.8	0.105	0.269
SD	14.5	0.081	0.191

CL_2 = renal clearance, fe = fraction of dose excreted as unchanged drug.

(c) Dialsyate data

Subject	$t\frac{1}{2},z$	Cl_{pd}	fe
1	36.5	0.227	0.809
2*	48.6	0.135	0.382
3	23.3	0.162	0.363
4	26.0	0.174	0.422
5	45.0	0.232	0.581
6*	38.9	0.187	0.593
7	35.5	0.224	0.549
8	50.0	0.246	0.616
9	24.0	0.191	0.562
10	25.9	0.172	0.488
Mean	35.4	0.195	0.536
SD	10.3	0.036	0.132

Cl_{pd} = dialysate clearance, * = 1 dialysate bag lost.

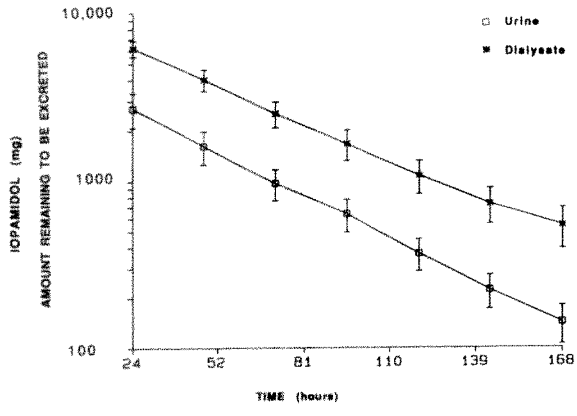

Figure 2. The amount of iopamidol remaining to be excreted *vs.* time plots for both urine and dialysate data from subjects with end-stage renal failure undergoing CAPD for 7 days. Each subject was given 30 ml Niopam 300 intravenously (total dose given 18 372 mg) on Day 1 of the study. Values are the mean ± SEM of duplicate estimations in each subject. The number of subjects (n) = 9 for urine data and 10 for dialysate data.

patients, compared with reported values in healthy subjects of about 8 l/h (McKinstry et al, 1984). The volume of distribution was increased slightly in CAPD patients, 21.0 ± 6.2 l compared with 16.8 l (McKinstry et al, 1984) and just over 15 l (Tirone et al, 1982) in healthy volunteers.

Pharmacokinetic parameters derived from urine and dialysate data are shown as Tables IIb and IIc. Half-life of elimination of iopamidol in urine and dialysate was determined using Sigma Minus plots as described in the methods section (Fig. 2). Statistical analysis using one-way Anova revealed no significant differences in the terminal elimination half-life calculated from the different sets of data. Linear regression analysis revealed

Table III. Recovery of iopamidol in urine and dialysate from 10 subjects with end-stage renal failure undergoing CAPD for 7 days

Subject	Amount unchanged drug recovered in urine and dialysate mg (total dose gives 18 372 mg)	% Dose
1	14 862	80.9
2*	13 802	75.1
3	17 012	92.6
4	15 396	83.8
5	13 128	71.5
6**	10 943	59.6
7	11 287	61.4
8	11 556	62.9
9	17 094	93.0
10	13 038	71.0
Mean	13 839	75.2
SD	2 237	12.2

* = 1 dialysis bag lost, ** = 2 dialysis bags lost and urine collection incomplete on Days 1 and 2. Each subject received 30 ml Niopam 300 intravenously on Day 1 of the study. One subject (Subject 1) was anuric throughout the study.

a significant negative correlation between renal clearance and dialysate clearance ($r = -0.7507$, $p < 0.05$), indicating that clearance by dialysate increased as renal clearance declined.

The recovery of iopamidol from both urine and dialysate is shown in Table III. Over the period of study, up to 93% of the administered dose was recovered, mean ±SD 75.2±12.2%. During the course of the study one patient experienced a possible reaction to the contrast medium. 20 h after injection of contrast, patient HP felt generally unwell and developed bilateral submandibular swelling. This gradually resolved over the next 7 days. During that time throat swabs, Paul Bunnel test and viral titres were unexceptional. There were no past or subsequent submandibular problems.

Discussion

In recent years the range and number of radiological procedures performed on patients with end-stage renal failure has increased. One reason for this is the success of renal replacement therapy by dialysis and transplantation, with an increase in the number of older patients accepted for treatment (Wing et al, 1988). Since accelerated cardiovascular disease is a frequent accompaniment of renal failure, high risk patients are increasingly referred for interventional procedures which are screened radiographically.

Renal impairment increases susceptibility to the toxic effects of radiographic contrast media (Bettmann, 1987). Since contrast media are normally distributed throughout the body fluids and excreted in relation to glomerular filtration rate, toxicity is said to increase with the duration in the circulation and the total dose given (Dawson, 1985; Goodfellow et al, 1986). Bahlmann & Kruskemper (1973) and Ackrill et al (1976) showed that, in the absence of renal function, ionic contrast medium (diatrizoate) remained at high levels in the circulation but that > 85% of a given dose could be cleared by a 12 h haemodialysis which was the norm at that time. Using modern techniques 69% of the ionic medium (iothalamate) is cleared during 4 h of haemodialysis (Evans et al, 1988). Iopamidol excretion is delayed in patients with renal dysfunction (Oshima et al, 1988) and in end-stage renal disease 73% may be cleared by a 4 h haemodialysis although the total excretion varies with the time after dosage (Harasawa et al, 1990). Other non-ionic contrast media include iopromide and iohexol. Haemodialysis produced an almost 60% decrease in serum concentration of iopromide (Kierdorf et al, 1989) whilst for iohexol a 4 h haemodialysis reduced body load by 36% (Waaler et al, 1990). It has been argued that in order to reduce risk, radiographic examinations of renal failure patients should be followed by haemodialysis (Evans et al, 1988; Chamberlain & Sherwood, 1966). A small but significant amount of contrast is cleared by biliary excretion as shown in early studies (Hansson & Lindholm, 1963; Ackrill et al, 1976; Harasawa et al, 1990).

Since its introduction in the late 1970s CAPD has rapidly become the first line method of treating end-stage renal failure in the USA and within Europe and of the 7000 patients in the UK on regular dialysis half are treated by CAPD (Wing et al, 1988). CAPD patients are increasingly referred for radiographic contrast studies in the investigation of cardiovascular disease. For example, when CAPD functions poorly a forearm fistula is needed and a venogram is frequently necessary to unmask subclavian stenosis arising from previous temporary access. There are two previous reports (Evans et al, 1988; Milman & Christensen, 1974) concerning ionic contrast clearance in patients undergoing acute or "stab" peritoneal dialysis with short "dwell times". Both studies document a substantially delayed clearance of contrast media with half-life approximated at 24–30 h. This study is however the first to rigorously investigate the clearance of non-ionic contrast media in patients undergoing long term CAPD.

Results obtained in the present study show decreased clearance of iopamidol in renal failure patients undergoing CAPD and are in agreement with theoretical considerations of drug excretion (Keller et al, 1990). The study has shown that CAPD can remove up to 80% of the administered iopamidol in 7 days. Nonetheless, high levels of contrast media are present in the circulation for several days during CAPD. There is some evidence that even in renal failure, the urine provides a significant route for excretion and supplements peritoneal function. Examination of the data for clearance indicated that combined renal and dialysate clearance accounted for 61.4–92.9% of the total body clearance. The data also suggest a further route of clearance for iopamidol, which is likely to be enhanced hepatic metabolism and biliary excretion. The aforementioned assumption is valid in the present study as less than 1% of the total dialysate excretion was collected in the final dialysate sample and less than 10% of the urine excretion in the first 24 h urine sample. Furthermore, calculation of the amount of the iopamidol dose remaining in the body at the end of the study period revealed that at least 90% of the dose had been removed.

If large doses of contrast media are needed or frequent studies performed then renal failure patients treated by CAPD may be at increased risk of delayed chemotoxicity due to prolonged exposure of the circulation to abnormally high levels of medium. Late onset reactions, including arm pain, following a variety of contrast media injections are well recognized (Panto & Davies, 1986). A possible delayed reaction with iopamidol (involving arm pain and arthropathy) has been reported in two CAPD patients 16 h after undergoing subclavian venography (Donnelly et al, 1989). Fatal vascilitis has also been reported in a patient with chronic renal impairment 48 h following radiographic investigation with the non-ionic contrast medium, iohexol (Goodfellow et al, 1986). Although the precise aetiology of these responses is unclear, a toxic effect of contrast on vascular endothelium has been postulated (Panto & Davies, 1986; Goodfellow et al, 1986).

Mersereau & Robertson (1961) originally demonstrated endothelial damage of vessels histologically following exposure to ionic contrast media and more recently *in vitro* assays have shown the differential effect of ionic and non-ionic media on the function and morphology of cultured endothelial cells (Laerum et al, 1983; Morettin et al, 1984). Although iopamidol was found to be minimally toxic to endothelium, in these assays the exposure time was no more than 24 h. Exposure to contrast at relatively high levels for up to 7 days as occurs in CAPD patients may be more harmful. An approach to reducing the risk of adverse reaction to contrast media in CAPD patients may include acute haemodialysis via temporary vascular access following contrast study. Given the hazards associated with acute haemodialysis access this option would be contraindicated in most cases. Administration of steroid 12–24 h before contrast may also be helpful, particularly in patients giving a history of allergy, asthma or previous contrast reaction (Lasser et al, 1987; Reidy, 1988). Alternatively, frequent cycling of peritoneal dialysis by continuous cycling peritoneal dialysis (CCPD) may possibly clear contrast more efficiently than conventional CAPD and is currently undergoing investigation. Meanwhile, it would seem prudent to observe carefully all patients undergoing contrast medium studies whilst on treatment with CAPD and to limit the dose to the minimum necessary.

Acknowledgments

The authors are most grateful to Dr Peter Cox and Bracco SpA for their support and for generously providing iopamidol standards for the pharmacokinetic studies. Miss Sue Massey kindly typed the manuscript.

References

Ackrill, P., McIntosh, C. S., Nimmon, C., Baker, L.R. I. & Cattell, W. R. 1976. A comparison of the clearance of urographic contrast medium (sodium diatrizoate) by peritoneal and haemodialysis. *Clinical Science and Molecular Medicine*, *50*, 69–74.

Bahlmann, J. & Kruskemper, H. L., 1973. Elimination of iodine-containing contrast media by haemodialysis. *Nephron* *10*, 250–255.

Bettmann, M. A., 1987. Radiographic contrast agents—a perspective. *New England Journal of Medicine*, *317*(14), 891–893.

Chamberlain, M. J. & Sherwood, T., 1966. The extra-renal excretion of diatrizoate in renal failure. *British Journal of Radiology*, *39*, 765–770.

Dawson, P., 1985. Chemotoxicity of contrast media and clinical adverse effects. *Investigative Radiology*, *20*, S84–S91.

Donnelly, P. K., Belton, I., Chapman, P. & Watkin, E. M., 1989. New radionuclide method of visualising subclavian vein occlusion following temporary venous access. *British Journal of Surgery*, *76*, 1024–1025.

Evans, J. R., Cutler, R. E. & Forland, S. C., 1988. Pharmacokinetics of iothalamate in end-stage renal disease. *Journal of Clinical Pharmacology*, *28*, 826–830.

Goodfellow, T., Holdstock, G. E., Brunton, F. J. & Bamforth, J., 1986. Fatal acute vasculitis after high dose urography with iohexol. *British Journal of Radiology*, *59*, 620–621.

Hansson, R. & Lindholm, T., 1983. Elimination of hypaque (sodium-3,5-diacetamido-2,4,6-triiodobenzoate) and the effect of haemodialysis in anuria. *Acta Medica Scandinavica*, *174*, 611.

Harasawa, H., Yamazaki, C. & Masuko, K., 1990. Side effects and pharmacokinetics of non ionic iodinated contrast medium in hemodialized patients. *Nippon Igaku Hoshasen Gakki Zassh*, *50*(12), 1524–1531.

Keller, E., Reetze, P. & Schollmeyer, P., 1990. Drug therapy in patients undergoing continuous ambulatory peritoneal dialysis, clinical pharmacokinetic considerations. *Clinical Pharmacokinetics*, *18*(2), 104–117.

Kierdorf, H., Kinder, J., Winterscheid, R., Hollmann, H. J., Vorwerk, D. & Speck, U., 1989. Elimination of the non-ionic contrast medium Iopromide in end-stage renal failure by hemodialysis. *Kidneys and the Urinary Tract*, *128*, 119–123.

Laerum, F., Borsum, T. & Reisvaag, A., 1983. Human endothelial cell culture as an evaluation system for the toxicity of intravascular contrast media. *Investigative Radiology*, *18*(2), 199–206.

Lasser, E. C., Berry, C., Talner, L. B., Santinl, L. C., Lang, E. K., Gerber, F. H. & Stolberg, H. O., 1987. Pretreatment with corticosteroids to alleviate reactions to intravenous contrast material. *New England Journal of Medicine*, *317*(14), 815–819.

McKinstry, D. N., Rommel, A. J. & Sugerman, A. A., 1984. Pharmacokinetics, metabolism and excretion of iopamidol in healthy subjects. *Investigative Radiology*, *19*, S171–174.

Mersereau, W. A. & Robertson, H. R., 1961. Observations on venous endothelial injury following the injection of various radiographic contrast media in the rat. *Journal of Neurosurgery* *18*, 289–294.

Milman, N. & Christensen, E., 1974. Elimination of diatrizoate by peritoneal dialysis in renal failure. *Acta Radiologica Diagnosis*, *15*, 265–272.

Morettin, L. B., Olifant, D. M. & Brown, R. T., 1984. Comparative evaluation of the effects of ionic *vs.* a non ionic contrast medium on the venous endothelium. *Investigative Radiology*, *19*(6), 594–586.

Oshima, K., Seko, S., Usui, T., Nagaoka, S. & Hayashi, M., 1988. Clinical studies of excretory urography in patients with renal dysfunction. *Nishinihon Journal of Urology, 50,* 765–768.

PANTO, P. N. & DAVIES, P. M., 1986. Delayed reactions to urographic contrast media. *British Journal of Radiology, 59,* 41–44.

PARTRIDGE, J. B., ROBINSON, P. J., TURNBULL, C. M., STOKER, J. B., BOYLE, R. M. & MORRISON, G. W., 1981. Clinical cardiovascular experiences with Iopamidol a new non-ionic contrast medium. *Clinical Radiology, 32,* 451–455.

REIDY, J. F., 1988. Reactions to contrast media and steroid treatment. *British Medical Journal, 296,* 801–809.

TIRONE, P., FERRARI, D. & VIVIANI, G., 1982. Pharmacokinetics of iopamidol, a clinical study. *Diagnostic Radiology, 7,* 83–86.

WAALER, A., SVALAND, M., FAUCHALD, P., JAKOBSEN, J. A., KOLMANNSKOG, F. & BERG, K. J., 1990. Elimination of iohexol, a low osmolar non-ionic contrast medium by hemodialysis in patients with chronic renal failure. *Nephron, 56,* 81–85.

WING, A. J., BROYER, M. & BRUMMER, F. P., 1988. Demography of dialysis and transplantation in Europe 1985–1986. Trends over a decade. *Nephrology Dialysis and Transplantation, 3,* 714–727.

1992, *The British Journal of Radiology*, 66, 1114–1118

Late follow-up of lung function after whole lung irradiation for Wilms' tumour

By S. P. Attard-Montalto, J. E. Kingston, O. B. Eden, and *P. N. Plowman

Departments of Paediatric Oncology and *Radiotherapy, St Bartholomew's Hospital, West Smithfield,
London EC1A 7BE, UK

(*Received 14 April 1992 and in revised form 8 July 1992, accepted 10 August 1992*)

Keywords: Wilms' tumour, Pulmonary irradiation, Lung function

Abstract. Radiotherapy is known to have acute and long term deleterious effects on lung tissue. However, pulmonary irradiation is an established treatment in advanced childhood tumours with pulmonary metastases not responsive to chemotherapy. In this study eight patients with Wilms' tumours and lung metastases treated with whole lung irradiation (1200–1837 cGy) and chemotherapy were reassessed clinically, radiologically and with lung function tests 6–26 years after radiotherapy. One patient was breathless after mild exertion, four after strenuous exercise and three were asymptomatic. Clinically all had small chests and four of five females had underdeveloped breasts. A chest radiograph showed clear lung fields in all cases. Lung volumes, especially total lung capacity (TLC) and vital capacity (VC), were decreased when compared with predicted values for age and height. However, gas transfer per unit lung volume (KCO) was normal. This study suggests that pulmonary irradiation in childhood results primarily in underdevelopment of the thorax and that diffuse interstitial lung fibrosis is not a significant feature at this dose level.

The late effects of the treatment of childhood tumours are now the focus of much attention since survival has improved so dramatically over the last two decades. For nephroblastoma, more than 80% of all patients appear to be long-term survivors so that the documentation of sequelae and the initiation of preventative measures is proving increasingly important. Whole lung radiotherapy retains a place in the management of children presenting with stage IV Wilms' tumour, despite an ever increasing awareness of the relative radiosensitivity of the lungs. "Dose ranging" studies in this disease over the last 20 years have helped us to understand the potential for clinical toxicity. This study was set up to assess lung function in a group of patients who had received whole lung irradiation for pulmonary metastases between 6 and 26 years previously.

Method and patients

We have studied eight patients now aged 11–32 years with nephroblastoma who had received treatment 6–26 years previously. This included a nephrectomy, actinomycin D and whole lung irradiation (1200–1837 cGy) in all patients. Four received lung irradiation within 6 weeks of actinomycin D. Seven had radiotherapy to the tumour bed and abdomen (2850–3500 cGy), six were treated with cyclophosphamide, and one patient received ifosfamide followed by high dose melphalan and an autologous bone marrow transplant for refractory disease. This last patient (H) developed a pneumothorax during radiotherapy but no other acute complications were noted. One patient (A) had a right upper lobectomy for excision of metastases, and another (F) had a rib osteochondroma excised.

For each patient respiratory symptoms, exercise tolerance, smoking habits and current medication were noted. Full physical examination, a chest radiograph and pulmonary function tests were performed when free of any respiratory infection. Pulmonary function tests included the measurement of forced expiratory volume in one second (FEV_1), forced vital capacity (FVC), functional residual capacity (FRC), expiratory reserve volume (ERV), and vital capacity (VC) using a P.K. Morgan spirometer (Spiroflow). Transfer factor for carbon monoxide (T_LCO) was measured by the single breath method P.K. Morgan transfer test and gas transfer per unit lung volume (KCO) was calculated using the alveolar volume obtained during the same procedure. For FEV_1, FVC, FRC, ERV, and VC, the greatest of three values was recorded. Residual lung volume was calculated by subtracting ERV from FRC; the total lung capacity (TLC) by adding residual volume to vital capacity. Absolute values were recorded and then expressed as a percentage of the predicted mean value for the patients' sex, height and age. Values greater than two standard deviations from the predicted mean value were recorded as abnormal.

Results

Clinical

Table I gives details of patient characteristics, including sex, tumour site, age at treatment, radiotherapy and chemotherapy administered, plus clinical symptoms and signs. Patient H, aged 5 years at the time of treatment, was short of breath after minimal exertion 6 years later, and required frequent courses of salbutamol for recurrent wheezing episodes. This patient had received the highest irradiation dose (1837 cGy)

Address reprint requests to Dr P. N. Plowman.

Table I. Clinical, chemotherapy and radiotherapy details

Patient	Sex	Tumour site	Age at RT (year/month)	Dose of RT to lung (cGy)	Chemotherapy	Symptoms	Signs
A	F	left	3 yr	1500 (107/fraction)	AVAct** Cyclo	SOBOE (mild) backache	small chest small breasts flank hypoplasia scoliosis
B	M	right	11 yr 2 m	1200 (120/fraction)	AVAct Cyclo	none	small chest flank hypoplasia scoliosis
C	F	right	6 yr 10 m	1500 (125/fraction)	AVAct* Cyclo	none	small chest flank hypoplasia
D	F	left	6 yr 1 m	1550 (130/fraction)	Act*	none	small chest small breasts flank hypoplasia scoliosis
E	M	left	1 yr 10 m	1500 (136/fraction)	AVAct* Cyclo	SOBOE (mild)	small chest flank hypoplasia
F	M	left	5 yr 3 m	1650 (138/fraction)	AVAct	SOBOE (mild)	small chest flank hypoplasia scoliosis
G	F	right	6 yr 6 m	1500 (150/fraction)	AVAct Cyclo	SOBOE (mild)	small chest small breasts flank hypoplasia
H	F	left	5 yr	1837 (167/fraction)	AVAct Cyclo If Mel ABMT	SOBOE (severe)	small chest small breasts flank hypoplasia

RT = radiotherapy; A = adriamycin; V = vincristine; Act = actinomycin D; Cyclo = cyclophosphamide; If = ifosfamide; Mel = melphalan; ABMT = autogous bone marrow transplant; ** = actinomycin and cyclophosphamide received within 6 weeks of lung radiotherapy; * = actinomycin received within 6 weeks of lung radiotherapy; SOBOE = short of breath on exertion.

and had also developed a pneumothorax during radiotherapy. Four other patients reported that they were short of breath after moderate exertion compared with their peer group. One of these patients (F) also used salbutamol on an intermittent basis. The remaining three patients were asymptomatic including two patients (B and C) who were the oldest of this cohort at the time of pulmonary irradiation, being 11 years 2 months and 6 years 10 months when they received 1200 and 1500 cGy respectively. However, all patients had a small chest cage and flank hypoplasia. Four of five females had underdeveloped breasts and one (Patient D) had undergone breast augmentation with silicone implants. Four had a scoliosis, convex away from the irradiated flank, and one had persistent and recurrent backache (Patient A). None had focal chest signs on clinical examination.

Table II. Results of pulmonary function tests

Patient	Age at RT (year/month)	Assessment after RT (years	FEV_1 (%)	FEV_1/FVC (%)	VC (%)	TLC (%)	FRC (%)	RV (%)	T_LCO (%)	KCO (%)
A	3 years	13	79	95	71	49	95	131	73	109
B	11 years 2 months	10	88	95	74	76	95	98	80	108
C	6 years 10 months	15	66	83	67	62	63	73	84	120
D	6 years 1 month	27	80	98	71	73	62	45	69	102
E	1 years 10 months	20	69	87	77	68	51	85	77	114
F	5 years 3 months	16	73	95	66	62	61	67	79	123
G	6 years 6 months	11	69	98	66	80	67	103	66	104
H	5 years	6	48	85	48	52	75	73		

RT = radiotherapy; (%) = % of predicted value for sex and height.

Chest radiography

The only abnormalities seen were post-operative changes in the two patients who had a thoracotomy for removal of metastases (Patient A) and excision of a rib osteochondroma (Patient F).

Pulmonary function

Results are shown in Table II.

Spirometry. FEV_1 was less than two standard deviations of the predicted value in six out of eight patients (48–79%, with a mean of 67%) and just greater in two (80 and 88%). FVC was reduced in all eight patients (53–77%, mean 65%). FEV_1/FVC was normal (83–98%, mean 92%).

Lung volume. Vital capacity ranged from 48–77% (mean 67.5%) of the predicted mean and total lung capacity 49–80% (mean 65%). These values were reduced in all patients. Functional residual capacity was normal in two patients (95%) and low in six (51–75%, mean 63%), whereas the residual volume was normal in three (85–103%), low in four (45–73%) and greater than expected in one patient (131%)

Gas transfer. Patient H was unable to perform these tests satisfactorily. In the remaining patients gas transfer of carbon monoxide (T_LCO) was reduced in five patients (69–79%; mean 75.4%) and just less than two standard deviations below the predicted mean in two patients (80 and 84%). Transfer of CO per unit lung volume (KCO) was either normal (five patients) with a range of 102–114%, mean 107%, or increased in two patients (120 and 123%).

Discussion

Pulmonary irradiation is established as the treatment of childhood malignancies especially for lung metastases resistant to chemotherapy and its use in patients with stage IV Wilms' tumours has apparently improved the 2-year survival to at least 50% (Cassady et al, 1973). Though the morbidity associated with pulmonary irradiation has diminished by reducing the radiation dose per fraction (Cassady et al, 1973; Gross, 1977; Abbatucci et al, 1978; Travis et al, 1991), both acute and long term complications still arise (Gross, 1977; Tefft, 1977; Jones et al, 1984; Thomas et al 1988; Travis 1991). Work on adults has shown that the predominant late abnormality following pulmonary irradiation is a restrictive defect due to fibrosis (Sutton, 1960; Weir & Michaelson, 1971; Cassady et al, 1973). This may be a contributory factor in children, but the most significant long term abnormality appears to be thoracic wall, musculoskeletal and alveolar hypoplasia resulting in small volume lungs (Wohl et al, 1975; Littman et al, 1976; Benoist et al, 1982; Miller et al, 1986).

Patients who have received whole lung irradiation for stage IV Wilms' tumour and who have survived are usually asymptomatic, or slightly short of breath on exertion (Wohl et al, 1975; Littman et al, 1976; Gross 1977; Benoist et al, 1982; Shaw et al, 1991). In our study only one out of eight patients had significant symptoms. She had suffered acute complications during radiotherapy and had received the highest total dose. Four others felt disadvantaged compared with their peers regarding exercise tolerance. Underdevelopment of the chest wall and breasts was obvious but clinical examination of the chest and chest radiography did not reveal any significant pulmonary abnormalities. Pulmonary function tests performed on patients in our study showed that they had small volume lungs with normal gas transfer per unit lung volume. The results were further from the predicted mean in patients treated at a younger age, and those who received higher total doses of radiation, and more significantly higher dose fractions.

In the first National Wilms' Tumor Study (NWTS I), 24 children presenting with pulmonary metastases received whole lung radiotherapy (parallel opposed, megavoltage photon portals and 1400 cGy mid-plane dose in 7–10 fractions), concomitantly with actinomycin, and with an optional boost of 3000 cGy to restricted lung volumes not exceeding 25% of the total lung volume (Tefft, 1977). Four out of 21 patients who received the recommended dose developed evidence of pulmonary damage and one patient died of pneumocystis pneumonia. Three patients received a higher radiotherapy dose than the protocol dictated and two of these died. Using a similar protocol as in NWTS I, the whole lungs of 49 children were irradiated in NWTS II (Thomas et al, 1988). Four (8%) developed toxicity and three died. Concomitant actinomycin and/or doxorubicin was a noteworthy feature as was the (off-protocol) dose of 1800 cGy in one of the fatalities. The long term follow-up of the survivors of NWTS I and II has not been published.

However, late follow-up data from other studies have been published. Littman et al (1976) compared the lung function in 15 children with nephroblastomas who had received whole lung radiotherapy, either for treatment of pulmonary metastases (10 patients) or as prophylaxis (five patients). The patients had received orthovoltage X rays (whose RBE relative to megavoltage X rays for pulmonary toxicity is unknown but estimated at 0.85–0.90) in doses of 1163–1370 cGy mid-plane and concomitant chemotherapy. Examining lung function tests 4–20 years after radiation, Littman et al found a reduction in vital capacity (VC), total lung capacity (TLC) and forced expiratory volume in one second (FEV_1) in both groups of children, especially in those presenting with metastases (*e.g.* 35% versus 21% reduction in VC). The authors concluded that decreased lung compliance, perhaps as a result of diffuse interstitial fibrosis, led to restrictive lung disease and hence reduced lung volumes. The reduced FEV_1 was thought to be due to limited expiratory effort or an obstructive element in the larger airways.

Wohl et al (1975) studied a group of six patients who had received orthovoltage (250 kV) therapy of 850–1240 cGy to the lung in 11 days, and described a reduction of TLC and VC to 70% of normal. Transfer factor for carbon monoxide (T_LCO) was reduced to the same extent as lung volume. Pressure-volume lung studies were performed in three patients and these showed normal resting elastic properties of the lungs when lung volume was expressed as a percentage of the observed TLC. This and the observation that transpulmonary pressures at TLC and FRC were normal, suggested that the size and the mechanical properties of the chest wall had been affected either directly by the radiation or in response to the presence of a small lung during a period of chest growth.

Furthermore, Benoist et al (1982) reviewed 48 children receiving whole lung radiotherapy (2000 cGy in 15 fractions) in conjunction with actinomycin. From their results the authors concluded that a restrictive ventilatory defect and thoracic hypoplasia were late sequelae of pulmonary radiotherapy. They also concluded that pulmonary fibrosis was, at these radiation doses, unlikely in view of: (i) the normal pressure/volume curves relative to the measured lung volumes; (ii) the absent dip in the arterial saturation after exercise; and (iii) the normal T_LCO in all of their measurements when related to the TLC. Benoist et al argued that retarded musculoskeletal/chest growth or a reduction in the number of functioning alveoli (the surviving alveoli functioning normally) could each singly or in part explain the observed abnormalities.

In contrast Shaw et al (1991) described the late follow-up of three children who had received megavoltage photon radiation to the whole lung to a dose of 1200 cGY in 8 daily fractions with actinomycin. These workers claimed a 20% reduction in T_LCO and a smaller 7% (but significant) reduction in the T_LCO corrected for lung volume (KCO). This claim has reopened the debate as to the effect of low dose radiotherapy on the lungs of these children and prompted the current study.

The radiobiology of lung damage following radiotherapy falls into two well recognised and distinct histopathological phases. The first, radiation pneumonitis, occurs within six months of radiotherapy and is exacerbated by concomitant radiosensitising chemotherapy (Ware et al, 1973; Makipernaa et al, 1989). It is characterized histologically by the deposition of fibrin-like material in the alveolar spaces and swelling and degeneration of the epithelial type 2 cells lining the alveolar walls. In contrast, the predominant lesion of the chronic phase is progressive diffuse fibrosis of the septa resulting in a thickening of the alveolar walls. It is generally believed that acute radiation pneumonitis leads on to chronic fibrosis. Following the not insignificant number of deaths due to radiation pneumonitis in the early Wilms' tumour series, and the description of restrictive lung function tests in the late follow-up of these patients, it was assumed that these changes in lung function were due to diffuse fibrosis. However, in patients treated with lower total radiation doses by more carefully fractionated prescriptions and without concomitant radiosensitizing chemotherapy, radiation pneumonitis is rarely observed clinically or radiologically but, as we have confirmed here, there are late changes in lung function. Therefore, diffuse fibrosis may not be the mechanism behind these late changes in lung function.

Indeed, Wohl et al (1975) and Benoist et al (1982) produced lung function data which were inconsistent with diffuse interstitial fibrosis. In our series on patients who had received similar doses of radiation, the gas transfer per unit lung volume (KCO) was not reduced despite reductions in VC, TLC and T_LCO comparable with other series. This observation strongly supports the thesis that even minor diffuse lung fibrosis does not occur in these children as they grow and develop. Retardation of the skeletal chest wall growth would tend to produce the lung function test abnormalities demonstrated. Radiation induced spinal growth stunting, further accentuated by flank irradiation, will tend to skew standard lung function tables, estimated partly on height, towards a predicted underestimate of lung volume if spinal growth stunting is the only abnormality. However, if thoracic cage growth is also retarded, the changes in lung function may well be commensurate. In addition, these changes in lung function tests could also be observed if some alveoli were irreparably damaged whilst others (the majority) continued to function normally. Indeed in a study on mice Sharplin and Franko (1989) found that sometimes the histopathological changes in the lungs following radiation were those of multiple focal clusters of "foamy cells" and small accumulations of lymphocytes, rather than diffuse fibrosis.

We would conclude that whole lung radiotherapy in a dose of 1200 cGy in eight fractions over 9–12 days by opposed megavoltage photon portals, and without concomitant radiosensitizing drugs, gives rise to mild to moderate restrictive lung function tests (probably worse the younger the patient). This is consistent with the degree of thoracic hypoplasia induced by the treatment. We find no evidence of transfer factor deficiency when allowances are made for the observed lung volume and conclude that there is no evidence favouring diffuse lung fibrosis in these patients.

References

ABBATUCCI, J. S., BOULIER, A., FABRE, J. & LOZIER, J. C., 1978. Functional evaluation of pulmonary bilateral irradiation effects. *European Journal of Cancer*, *14*, 781–785.

BENOIST, M. R., LEMERLE, J., JEAN, R., RUFIN, P., SCHEINMANN, P. & PAUPE, J., 1982. Effects on pulmonary function of whole lung irradiation for Wilms' tumour in children. *Thorax*, *37*, 175–180.

CASSADY, J. R., TEFFT, M., FILLER, R. M., JAFFE, N. & HELLMAN, S., 1973. Considerations in the radiation therapy of Wilms' tumour. *Cancer*, *32*, 598–608.

GROSS, N. J., 1977. Pulmonary effects of radiation therapy. *Annals of Internal Medicine*, *86(1)*, 81–92.

JONES, B., BRESLOW, N. E. & TAKASHIMA, J., 1984. Toxic deaths in the second National Wilms' Tumor Study. *Journal of Clinical Oncology*, 1028–1033.

LITTMAN, P., MEADOWS, A. T., POLGAR, G., BORNS, P. F. & RUBIN, E., 1976. Pulmonary function in survivors of Wilms' tumour. Patterns of impairment. *Cancer*, *37(6)*, 2773–2776.

MAKIPERNAA, A., HEIPO, M., LAITINEN, L. A. & SIIMES, M. A.,

1989. Lung function following treatment of malignant tumours with surgery, radiotherapy or cyclophosphamide in childhood: a follow up study after 11 to 27 years. *Cancer*, *63*, 625–630.

MILLER, R. W., FUSNER, J. E., FINK, R. J., MURPHY, T. M., GETSON, P. R., VOJTOVA, J. A. & REAMAN, G. H., 1986. Pulmonary function abnormalities in long term survivors of childhood cancer. *Medical and Pediatric Oncology*, *14*, 202–207.

SHARPLIN, J. & FRANKO, A. J., 1989. A quantative histology study of strain-dependent differences in the effects of irradiation on mouse lung during the intermediate and late phases. *Radiation Research*, *119*, 15–31.

SHAW, N. J., EDEN, O. B., JENNEY, M. E. M., STEVENS, R. F., MORRIS-JONES, P. H., CRAFT, A. W. & CASTILLO, L., 1991. Pulmonary function in survivors of Wilms' tumour. *Pediatric Hematology and Oncology*, *8*, 131–137.

SUTTON, M. M., 1960. The functional effect of pulmonary irradiation. *British Medical Journal*, 11, 838.

TEFFT, M., 1977. Radiation related toxicities in National Wilms' Tumor Study Number 1. *International Journal of Radiation Oncology, Biology, Physics*, *2*, 455–463.

THOMAS, P. R. M., TEFFT, M., D'ANGIO, G. J. & NORKOOL, P., 1988. Acute toxicities associated with radiotherapy in the second National Wilms' Tumor Study. *Journal of Clinical Oncology*, *6*(11), 1694–1698.

TRAVIS, E. L., 1991. *Lung Morbidity of Radiotherapy. Complications of Cancer Management*, ed. by P. N. Plowman, T. J. McElwain & A. Meadows (Butterworth/Heinemann, London), pp. 232–249.

WARA, W. M., PHILLIPS, T. L., MARGOLIS, L. W. & SMITH, V., 1973. Radiation pneumonitis: a new approach to the determination of time-dose factors. *Cancer*, *32*, 547–552.

WEIR, G. J. & MICHAELSON, S. M., 1971. *Pulmonary Radiation Reactions*. (Charles C. Thomas, Springfield, Illinois).

WOHL, M. E., THORN GRISCOM, N., TRAGGIS, D. G. & JAFFE, N., 1975. Effects of therapeutic irradiation delivered in early childhood upon subsequent lung function. *Pediatrics*, *55*(4), 507–516.

1992, *The British Journal of Radiology*, *65*, 1119–1123

Influence of radiologist grade on fluoroscopic patient dose

By P. R. Hoskins, BA, MSc, PhD and J. R. Williams, BA, MSc, FIPSM

Department of Medical Physics and Medical Engineering, Western General Hospital, Edinburgh, EH3 9YW, UK

(*Received 17 February 1992 and in revised form 8 June 1992, accepted 26 June 1992*)

Keywords: Fluoroscopy, Radiologist, Patient dose, X ray

Abstract. The effect of radiologist grade on patient dose during fluoroscopic barium studies was assessed over a one-year period in a large teaching hospital using area–kerma measurements made with a Diamentor M2 system. The number of studies investigated was 164 for barium swallows, 274 for barium meals and 1288 for barium enemas. The patient's AP thickness was assessed at the abdominal level from a formula combining the patient's estimated height and weight. For each study there was no significant change in AP thickness as a function of radiologist grade. For all barium studies there was a trend for both the screening time and the patient dose to fall to a minimum for the grades third-year registrar/first-year senior registrar. From this group to consultant level the dose and screening time rose.

Medical X-ray examinations contribute about 87% of the radiation dose from all man-made sources of radiation to the UK population (NRPB, 1990). Fluoroscopic examinations such as barium studies give relatively high patient doses, barium enemas contributing 14% to the above figure and barium meals 12% (NRPB, 1990). The factors influencing the patient dose from a fluoroscopic examination can be split into machine factors, patient factors and operator factors. Modern fluoroscopic devices have a number of features which will result in lower patient doses. These include the use of lower input intensifier exposure rates due to improvements in intensifier efficiency and camera sensitivity, the use of collimation which adjusts automatically with field size and tube-intensifier distance, and the use of digital facilities allowing freeze frame and digital fluorography. Patient factors include the size of the patient; larger patients will be associated with higher entrance surface skin dose rates. It would also be expected that longer studies would be associated with uncooperative patients and those where diagnosis was difficult. It is commonly believed that radiologists early in their training will give longer screening times than their more experienced colleagues. However, there is no quantitative evidence in the literature to support this. In this study all patient doses were measured over a period of a year in one screening room in a large teaching hospital in order to investigate the effect of the experience of the radiologist on the dose to the patient.

Method

Area–kerma measurements may in general be made using an ionization chamber placed over the end of the X-ray tube which fully intercepts the beam. It has been shown that the energy imparted to the patient can be estimated from the area–kerma product, the fluoroscopic kV and the total X-ray beam filtration (Shrimpton et al, 1984). In turn it has been shown for a range of common X-ray studies that the energy imparted expressed in mJ and the effective dose equivalent expressed in mSv are closely correlated (Shrimpton, 1988) so that in practice energy imparted can be used as a measure of patient dose.

The X-ray room was equipped with a Siemens Pantascope 4 table with an undercouch tube and a Siemens 2 image intensifier system. The generator was a Tridoros 5S. An undercouch tube was used for screening. Spot films were taken with the undercouch tube using cassette film. An overcouch tube was used for additional views taken for barium enema studies.

In this study area–kerma measurements were made using a Diamentor M2 system with the chamber attached to the undercouch tube. The films taken using the undercouch tube were under the radiologist's control whereas the films taken using the overcouch tube were under the control of the radiographer. The data from the overcouch tube will not be considered in this study. Radiographers were asked to note the following information for each patient: date, examination, radiologist, patient's height and weight, average fluroscopic kV, area–kerma reading, total screening time. To ensure that this did not intrude on the normal running of the X-ray examination, the height and weight were obtained by asking each patient rather than by direct measurement. Data were acquired on all studies over a period of one year from the beginning of October 1990 to the end of September 1991; this period corresponded to the academic year for medical staff in Edinburgh.

Analysis was performed using an Archimedes microcomputer. Examination details were entered into a database. For each patient the energy imparted was calculated from the area–kerma reading and the average fluoroscopic kV using the data of Shrimpton et al (1984); the total beam filtration was 3 mm.

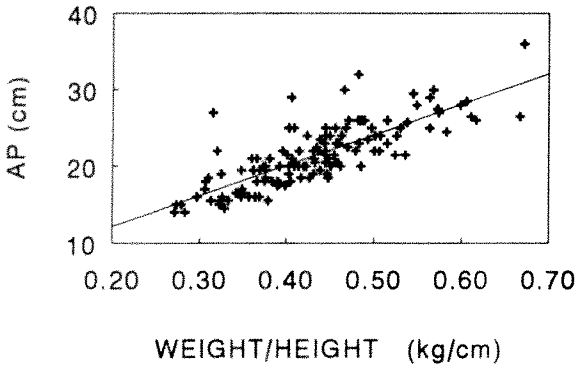

Figure 1. AP thickness as a function of the ratio of weight (kg) to height (cm) for 130 patients.

One of the factors which affects radiation dose is the size of the patient. In order to assess the effect of size, the patient's AP thickness was selected as an appropriate parameter. The AP thickness was estimated from the recorded height and weight. A formula for the derivation of AP thickness was derived from a separate study in which measurements had been made of height, weight and AP thickness.

There was no policy of patient selection for radiologists other than that two of the consultant radiologists were referred some of the more difficult cases. The first-year registrars were supervised by a consultant for the first two to five sessions at the beginning of their training.

Results

Calculation of AP thickness

Figure 1 shows the AP thickness plotted against the ratio (weight/height) for the 130 patients of the separate study. There is a high correlation ($r = 0.81$). The regression line from these data, shown below in equation (1), was used in this study to estimate AP thickness from the recorded height and weight.

$$\text{AP thickness (cm)} = 4.22 + 39.81[\text{weight(kg)}/\text{height (cm)}] \quad (1)$$

The effect of errors can be estimated by considering a 2 cm error in height and a 5 kg error in weight, when applied to an average man of 170 cm and 70 kg. From the regression curve this leads to an error in AP thickness of 6%. Measurements taken indicate that this would have a 10% effect on patient dose. For the average AP thickness for the group of patients in the following sections it is likely that some patients would have overestimated and some underestimated their height and weight so that on average the true picture would emerge.

Table I. Number of patients per study

Examination	No. of patients
Barium swallow	164
Barium meal	274
Barium enema	1288
Other	143
Data incomplete	56

Effect of radiologist grade on patient dose and screening time

56 patients had incomplete data and these were excluded from the analysis. Table I shows the number of examinations for which there were complete data. Of the 143 studies in the "other" examinations group, no single examination was performed on enough patients (the greatest number was 20) to enable meaningful statistical analysis of the effect of radiologist grade. Radiologists were grouped according to grade (Table II). It should be noted that the staffing figures included radiologists who rotated between hospitals, and locum radiologists. Figure 2 shows the patient dose and screening time as a function of radiologist grade. The mean and standard error of the mean are indicated for each group. For the groups not shown, the number of patients was too low (4 or less) to warrant statistical analysis. For all three studies there is a trend for both the screening time and the dose to fall as experience increases, to reach a minimum for third-year registrars and first-year senior registrars. From this grade to consultant level the dose and screening time rise. The average patient thicknesses were 19.7 cm, 19.9 cm and 20.2 cm for barium swallows, meals and enemas respectively. The variation of dose with thickness showed no consistent trend, indicating that the changes observed in dose and screening time are not due to differences in referral pattern associated with patient size.

Table II. Radiologist groups and number of patient examinations for each group

Code	Grade	No. of radioligists	BS	BM	BE
R1	Registrar (1st year)	3	44	87	371
R2	Registrar (2nd year)	6	45	67	378
R3	Registrar (3rd year)	2	0	0	25
S1	Senior registrar (1st year)	5	3	15	279
S2	Senior registrar (2nd–4th year)	6	3	4	76
CO	Consultant	6	69	101	159

BS = barium swallow, BM = barium meal, BE = barium enema.

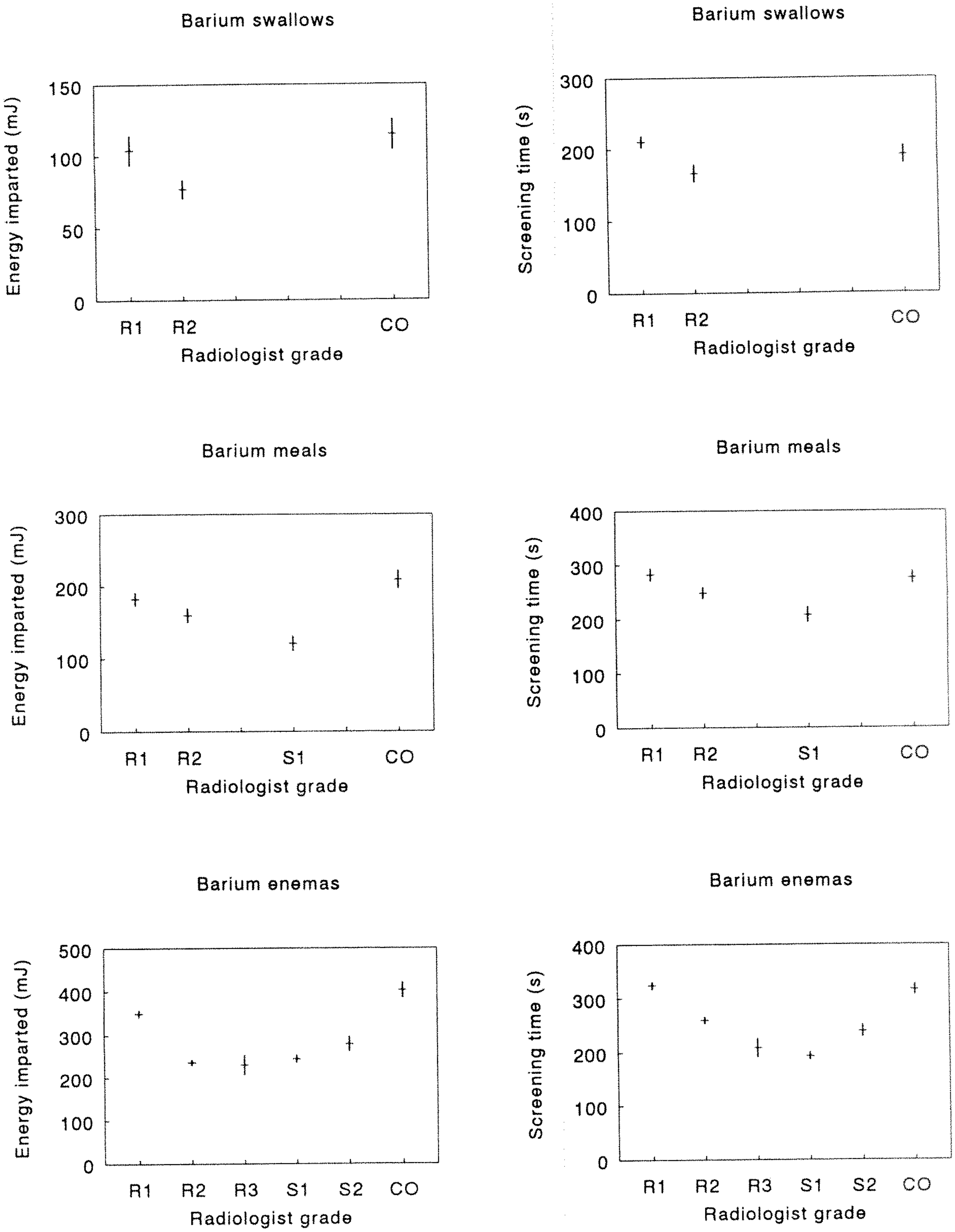

Figure 2. Patient dose and screening time as a function of radiologist grade. The mean ± standard error of the mean is indicated in each case.

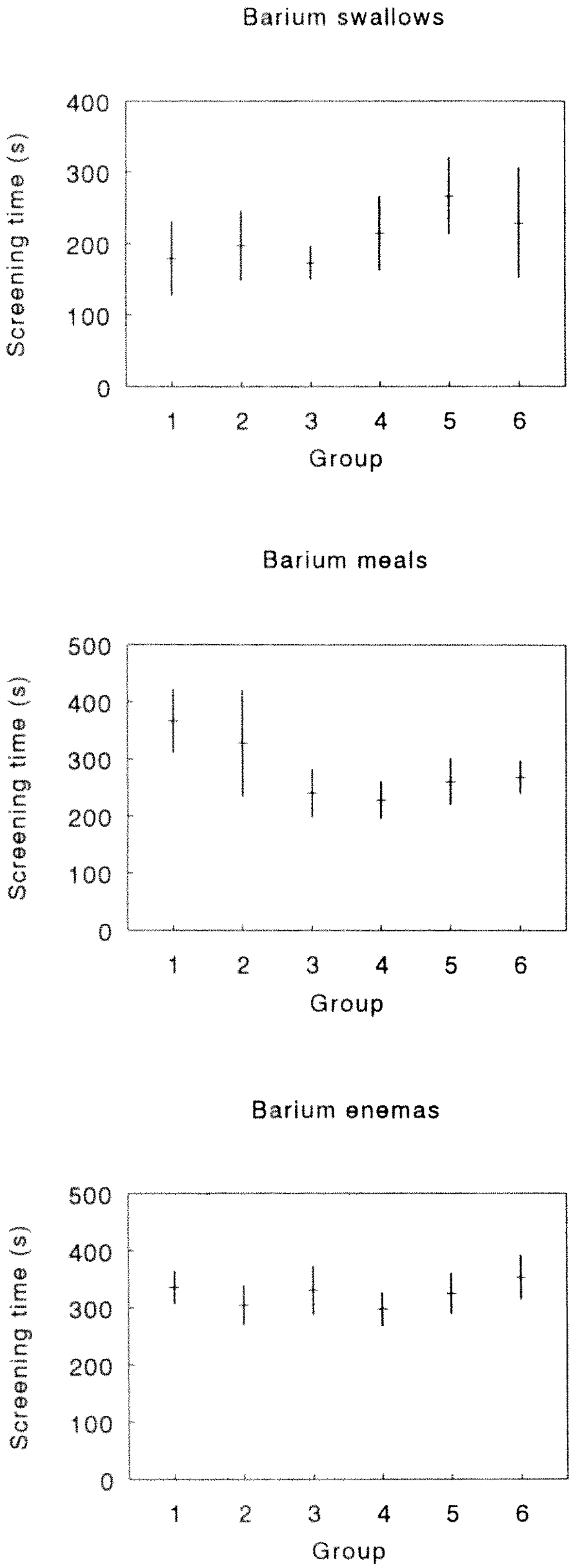

Figure 3. Screening times for first-year registrars for barium swallows (BS), meals (BM) and enemas (BE). In each case the data have been divided into six groups containing equal numbers of patients. The mean ± standard error of the mean is indicated in each case.

Trends in dose and screening time throughout the duration of the study

It might be expected that the largest falls in patient dose and screening time would occur for the first-year registrar group in the first few weeks or months of their training. Examination of dose as a function of time indicates a general fall for most radiologist groups throughout the year. It is thought that a large part of this fall is associated with reductions of the input intensifier exposure rate (from 26 to 20 μR s^{-1}) by service engineers, and also adjustment to the automatic exposure control system for radiography as a result of changes to the film processor, which resulted in lower doses to the patient. These effects will then to a large extent mask any changes for individual grades associated with increase in experience gained by the most junior radiologists through the year of study.

The change in patient screening time as the year progressed can also be studied. For barium meals there was a significant reduction in the screening time over the first four months of the study; however this is not reproduced for barium enemas or for barium swallows (Fig. 3).

Discussion

Discussion with radiological colleagues revealed a number of factors which could explain the changes in patient dose and screening time observed in this study. There was no policy of patient selection for radiologists, other than that two of the consultant radiologists dealt with some of the more difficult cases; it would be expected that more difficult cases would be associated with higher screening times and consequently higher doses. It was thought that the more senior radiologists would concentrate mainly on the performance of a study which was diagnostic, whereas junior radiologists would concentrate mainly on the production of a technically satisfactory study. With increasing experience the junior radiologists would become highly proficient, which may explain the decrease in screening times and doses. The production of a diagnostic study may in practice require longer screening times, which would contribute to the relatively high doses produced by the senior radiologists.

There is a maximum difference in dose produced by different grades of a factor of 1.74. As indicated in the introduction, there will be other factors related to the machines and the patients which influence patient dose. Measurements made by ourselves on patient doses from barium studies throughout the region indicate that in practice there is a large variation in doses between centres, the greatest difference being a factor of eight. As expected, the lowest doses were obtained using a digital fluorographic system. This indicates that the effect of radiologist grade on patient dose is not as important as other factors, especially those connected with the X-ray set itself.

In this study there is no strong evidence of a large fall in screening time or dose for first-year trainee radiologists in their first few weeks or months. It is more the case that a fall in patient dose occurs throughout the period of training.

Conclusion

For the fluoroscopic barium studies of this investigation there is a fall in patient dose associated with a fall in screening time throughout the period of radiologist training. There is then a gradual rise in both dose and screening time as the radiologist rises in seniority.

Acknowledgments

We should like to thank all the radiologists and radiographers from Edinburgh Royal Infirmary who took part in this study; to Miss J. Brown and Miss Palmer for providing access to rooms in the X-ray department of Edinburgh Royal Infirmary; and to Dr I. Prossor and Dr D. Redhead for discussion of the study results.

References

National Radiation Protection Board (NRPB), 1990. *Patient Dose Reduction in Diagnostic Radiology*. Documents of the NRPB Vol. 1, No. 3 (HMSO, London).

Shrimpton, P. C., 1988. Organ doses, energy imparted and effective dose equivalents from routine X-ray examinations. In *Are X-rays Safe Enough? Patient Doses and Risks in Diagnostic Radiology*, ed. by K. Faulkner and B. F. Wall (IPSM, York), pp. 32–39.

Shrimpton, P. C., Wall, B. F., Jones, D. G. & Fisher, E. S., 1984. The measurement of energy imparted to patients during diagnostic X-ray examinations using the Diamentor exposure-area product meter. *Physics in Medicine and Biology*, *29*, 1199–1208.

1992, *The British Journal of Radiology*, 65, 1124–1129

Comparison of the effect of different reference data on Lunar DPX and Hologic QDR-1000 dual-energy X-ray absorptiometers

By M. A. Laskey, DPhil, *A. J. Crisp, FRCP, †T. J. Cole, PhD and §J. E. Compston, FRCP

Bone Density Unit, Department of Nuclear Medicine, *Department of Rheumatology, Addenbrooke's Hospital, §Department of Medicine, University of Cambridge Clinical School, Addenbrooke's Hospital, Cambridge CB2 2QQ and †MRC Dunn Nutritional Laboratory, Downhams Lane, Milton Road, Cambridge CB4 1XJ, UK

(Received 8 May 1992 and in revised form 25 June 1992, accepted 13 July 1992)

Keywords: Dual-energy X-ray absorptiometry, Reference data, Lunar DPX, Hologic QDR-1000

Abstract. We have investigated whether the Lunar DPX (software 3.4) and Hologic QDR-1000 dual-energy X-ray absorptiometers have comparable normal reference databases for the spine and femur of white UK and USA subjects. After conversion for systematic differences in absolute bone density values between the two systems, the reference databases were very similar for the spine in young subjects, but there were clear differences in the femur databases of young females and males of all ages. These differences were confirmed by comparing the percent age-matched and young values determined by the two systems for subjects scanned on both systems. Thus the diagnosis and management of a patient could differ, depending on the system used for the bone density measurements.

Bone density measurements are used widely in the clinical management of osteoporosis. Manufacturers of dual-energy X-ray absorptiometers have provided reference data for spine and femur bone density values derived from healthy ambulatory subjects, so that the bone density in an individual can be expressed as a percentage of the expected peak bone mass for a Caucasian subject of the same sex, or as a percentage of the expected bone density value for a subject of the same age and sex (percent young and age-matched values). It is assumed that the lower the percent age-matched value, the greater is the risk of osteoporosis for a subject of that age. Most reference data have been compiled in the USA and various centres are now investigating whether they are appropropiate for UK subjects. In this study we have compared the reference databases for the spine and femur as supplied by the manufacturers of the Hologic QDR-1000 and the Lunar DPX (software version 3.4).

Methods

Compilation of Lunar DPX and Hologic QDR-1000 databases

The Hologic QDR-1000 (Hologic Inc., Waltham, MA, USA) reference ranges of bone densities were derived in the USA by measuring the bone density of 605 spines and 747 femurs of females, and 294 spines and 725 femurs of males. There were between 70 and 156 female subjects in each decade for the female femur database and between 14 and 180 subjects in each decade for the female spine database. Data on the number of male subjects in each decade and the heights of the subjects were not available. The mean weights of the males and females were 79 kg and 65 kg, respectively. Subjects with renal or hepatic disease, hyperparathyroidism, hyperthyroidism, amenorrhoea (in young women), oophorectomy, hypogonadism, rheumatoid arthritis, ankylosing spondylitis, Paget's disease, malabsorption or cancer were excluded. Subjects on steroids, anticonvulsants, diuretics, oestrogens or sodium fluoride were also excluded, as were subjects with vertebral compression or fracture, laminectomy, the presence of radio-opaque dye, severe osteophytes or scoliosis. Outliers (± 3 SD) were removed on a statistical basis (Kelly, 1990). At present Hologic supply only one Caucasian reference range of bone densities. This is being used for white Americans and Europeans.

The Lunar DPX (Lunar Corp., Madison, Wisconsin, USA) American reference data (software version 3.4) were collected from university medical centres and clinics. 968 spine and 792 femur scans were obtained from women. The mean weights of the male and female subjects were 78 kg and 65 kg, respectively. The total number of male subjects, number of female subjects in each decade and heights of the subjects used to compile their reference data were not stated. Lunar have also compiled 11 sets of reference ranges of bone densities for Caucasian and Oriental subjects. There is no difference between their USA and UK database. The reference data for the Lunar DPX are based on ambulatory subjects who were free from chronic diseases affecting bone. In addition, the subjects were not taking medica-

---

Present address and address for correspondence and reprint requests to Dr M. A. Laskey, Dunn Nutritional Laboratory, Downhams Lane, Milton Road, Cambridge CB4 1XJ, UK.

tions that are known to influence bone. Subjects with deformed spines were excluded, but some subjects with marked osteophytes were included in Lunar's reference data. Elderly subjects with one wedge fracture were not excluded.

Database comparison using subjects scanned on both systems

The Lunar DPX and the Hologic QDR-1000 databases were investigated by measuring the bone densities of 53 (seven males and 46 females) subjects on both systems. Each subject's spine (L1–L4) and femur bone density was measured on the same day. The subjects ages ranged from 26–72 years. Their spine bone densities ranged from 0.54–1.60 g cm^{-2}, femur densities from 0.43–1.21 g cm^{-2}, greater trochanter densities from 0.38–1.10 g cm^{-2} and Ward's triangle densities from 0.22–1.15 g cm^{-2}. The relationship between the bone density values of the two systems was examined by linear regression analysis and by the method of Bland and Altman (1986).

The mean bone density for males and females at each bone site and for each 5 year age group (20–85 years) was determined from the manufacturer's reference databases. These databases could only be compared in detail after conversion for the systematic differences in the absolute bone density values of the two absorptiometers (Gundry et al, 1990; Nijs et al, 1990; Reid et al, 1990; Laskey et al, 1991; Mazess et al, 1991; Svendsen et al, 1992). The derived regression equations were used to convert the supplied Hologic QDR-1000 database bone density values for spine and femur to equivalent Lunar bone density values. The significance of the bone density differences between the two populations used to compile the databases was assessed as described in Appendix I. The standard deviations (SD) of reference bone density values supplied for the Lunar DPX and Hologic QDR-1000 systems are shown in Table I.

The percent young and age-matched values for spine and femur regions were noted for the 53 subjects scanned on both systems. The Lunar minus Hologic percent young and age-matched bias and the 95% confidence limits were determined for the spine and femur regions of the 53 subjects scanned on both machines.

Table I. Standard deviations of reference bone densities (g cm^{-2}) of Lunar DPX and Hologic QDR-1000

	Lunar		Hologic	
	Male	Female	Male	Female
Spine (L2–L4)	0.16	0.17	0.11	0.11
Neck of femur	0.13	0.12	0.11	0.10
Trochanter	0.10	0.09	0.11	0.09
Ward's triangle	0.13	0.13	0.12	0.11

Results

Comparison of Lunar and Hologic databases

Table II shows that despite the systematic differences in spine and femur bone density between the Lunar DPX and Hologic QDR-1000 reported previously (Laskey et al, 1991), the correlation coefficients were high. This is because the correlation coefficient is not a measure of agreement between two methods (Bland & Altman, 1986).

Using the regression equations shown in Table II, the reference databases for spine and femur bone density (BMD) provided by Hologic were converted to Lunar-equivalent bone density values. The results expressed as Lunar BMD minus converted Hologic BMD (Figs 1 and 2) were then calculated for each bone site investigated and for male and female subjects of different ages. If both systems had identical normal reference bone density values, these values would be approaching zero.

Figures 1 and 2 demonstrate that there was good agreement between the normal reference databases for the spine for young male and female subjects. The agreement was less good for spines of elderly subjects, the Lunar reference bone density values being higher than the converted Hologic values. The irregularity in the female spine data at the age of 45 years (Fig. 2) is because the Lunar spine database is constant from 20–45 years and then decreases rapidly. In contrast there is a gradual decrease in the Hologic female spine database from the early thirties followed by a more rapid decrease in the mid-forties.

For the neck of femur region, Lunar reference data were about 0.05 g cm^{-2} lower than the converted Hologic values for females under 70 years old, but about 0.10 g cm^{-2} lower for males of all ages. The greater trochanter bone density reference values for males were consistently about 0.10 g cm^{-2} lower for the Lunar DPX than the converted Hologic QDR-1000 values. The difference in reference BMD values for the neck of femur and greater trochanter in the two popula-

Table II. Correlation coefficients and regression equations derived by scanning 50 subjects on both the Lunar DPX and Hologic QDR-1000 systems

Site	r	Standard error of estimate (SEE)	Regression equation
Spine	0.993	0.025	DPX = 1.08 (±0.019) QDR + 0.043 (±0.017)
Neck of femur	0.946	0.053	DPX = 1.07 (±0.053) QDR + 0.092 (±0.037)
Trochanter	0.919	0.062	DPX = 1.21 (±0.075) QDR − 0.007 (±0.045)
Ward's triangle	0.940	0.066	DPX = 1.14 (±0.059) QDR + 0.141 (±0.031)

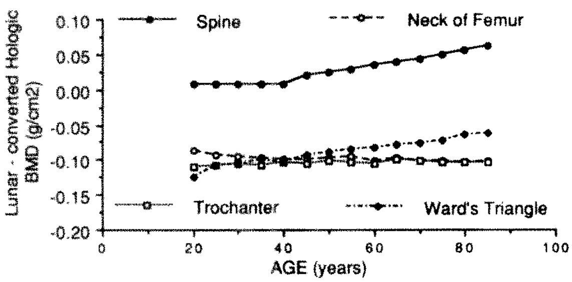

Figure 1. Difference between Lunar and converted Hologic bone densities of reference populations of normal males. The results are expressed as Lunar BMD – converted Hologic BMD.

tions was highly significant at all ages of males ($p < 0.001$). The greater trochanter values for females in the Lunar reference database were about 0.07 g cm^{-2} lower up to the age of 60 years, but then gradually increased relative to the converted Hologic values, so that at 85 years they were about 0.05 g cm^{-2} higher than the converted Hologic values. These differences in the two female reference populations were highly significant ($p < 0.001$) up to the age of 40 years. The Lunar reference values for Ward's triangle were about 0.09 g cm^{-2} lower than the converted Hologic reference values for males. These differences between the two male reference populations were highly significant ($p < 0.001$) up to the age of 50 years. For females the Lunar reference values for Ward's triangle were also about 0.10 g cm^{-2} lower than the converted Hologic values for young subjects ($p < 0.001$ for subjects under 40 years) but gradually increased to 0.06 g cm^{-2} higher for 85-year-old women.

In vivo *comparison of percent age-matched and young values*

Figures 3 and 4 show the Lunar minus Hologic bias and 95% confidence limits for the percent age-matched and young values for the spine and femur measurements of the 53 subjects who had bone density measurements performed on the Lunar DPX and Hologic QDR-1000.

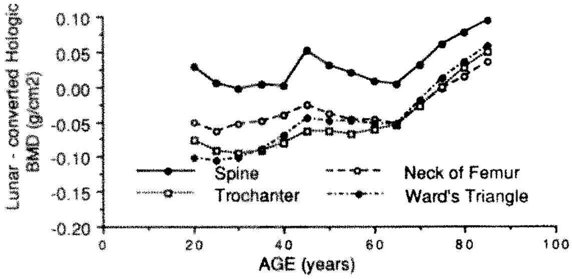

Figure 2. Difference between Lunar and converted Hologic bone densities of reference populations of normal females. The results are expressed as Lunar BMD minus converted Hologic BMD.

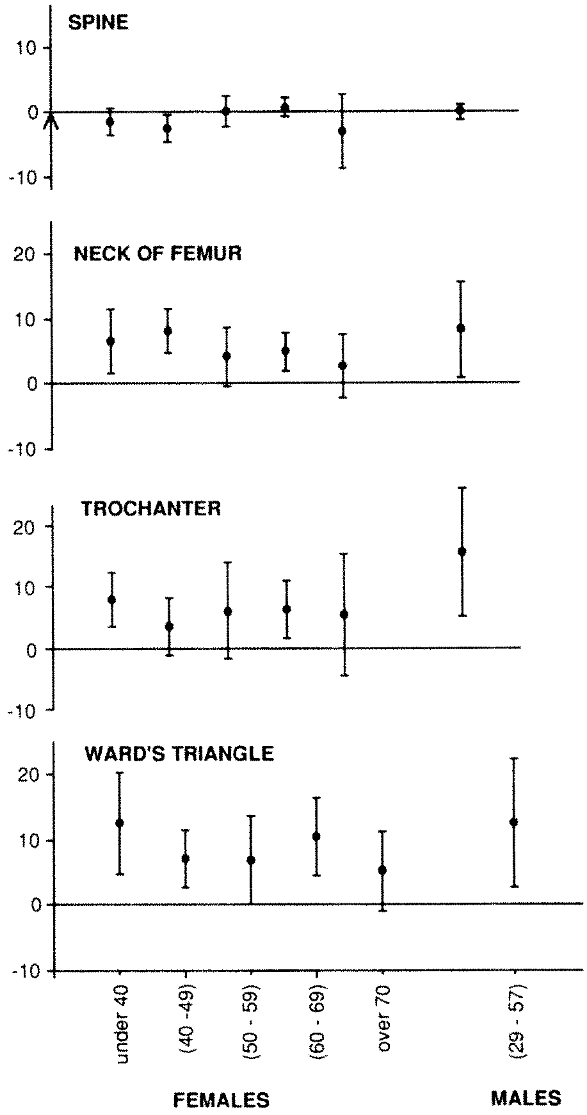

Figure 3. Lunar minus Hologic bias and 95% confidence limits of percent age-matched BMD values. Women under 40 years (mean age 30.7 years, $n = 7$); women 40–49 years (mean age 44.9 years, $n = 10$); women 50–59 years (mean age 55.1 years, $n = 9$); women 60–69 years (mean age 64.3 years, $n = 15$); women over 70 years (mean age 71.2 years, $n = 5$); men 27–59 years (mean age 43 years, $n = 7$).

For the spine the Lunar minus Hologic percent age-matched and young biases were close to zero (−3.0% to +1.80%) at all ages. However, the Lunar minus Hologic percent age-matched and young biases for the femur measurements of all male and female subjects were consistently positive and ranged from +2.8% to +18.0% (Figs 3 and 4). The biases were generally greatest for Ward's triangle measurements. The Lunar minus Hologic percent age-matched femur biases were

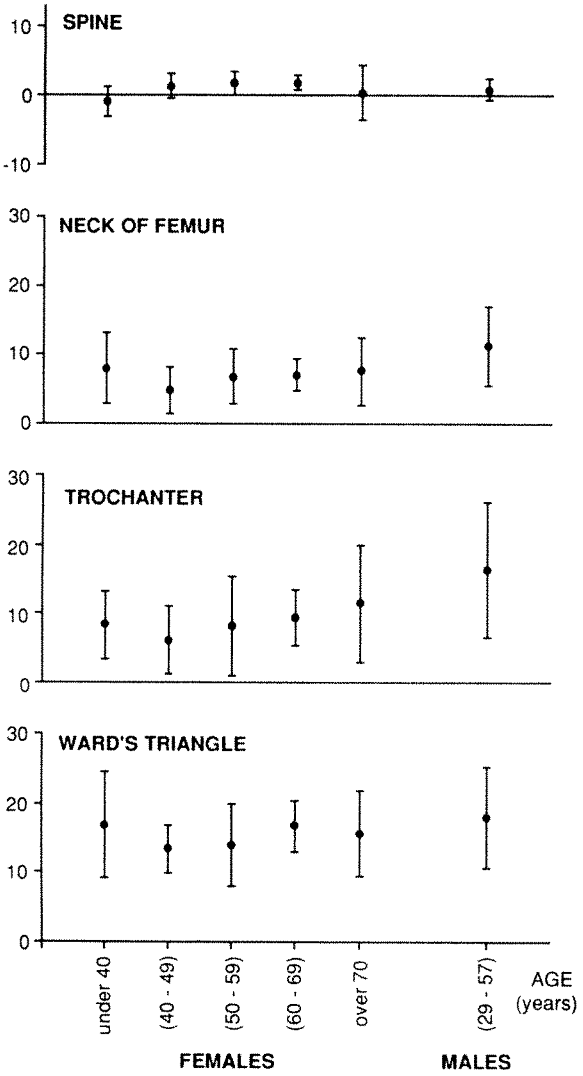

Figure 4. Lunar minus Hologic bias and 95% confidence limits of percent young BMD values. Subjects as described in Fig. 3.

smaller than the percent young values of females. The 95% confidence intervals for the bias were very large for all femur measurements. However, the 95% confidence limits did not include zero for any of the femur percent young values (Fig. 4).

Discussion

Bone density values obtained from one machine cannot be used to predict very accurately the values provided by another machine (Laskey et al, 1991). This is especially true for femur measurements and is demonstrated by the very large confidence intervals of the Lunar/Hologic bone density ratios and of the Lunar minus Hologic percent age-matched and young values (Figs 3 and 4). This variability is because there are subject (*e.g.* depth of subject, degree of osteoporosis) and site-dependent (*e.g.* selection of femur regions) factors, as well as machine variables (*e.g.* calibration, differences in edge detection, approach to dual-energy production) which influence the bone density difference between the two absorptiometers (Cullum et al, 1989; Mazess et al, 1989, 1991; Adachi & Webber, 1991; Laskey et al, 1991). Thus, even if the reference databases were identical (*i.e.* Lunar BMD minus converted Hologic BMD values equalled zero), one would not expect the percent age-matched and young values for subjects scanned on both machines always to be exactly the same, although the mean biases should be close to zero. However, if the calculated age-related differences in reference databases are correct (Figs 1 and 2), one would predict that the percent age-matched values for the femur of women and men would be systematically higher for subjects scanned on the Lunar DPX than on the Hologic QDR-1000. Only very small biases would be predicted for most spine measurements.

These predictions were confirmed *in vivo* (Figs 3 and 4). Thus the percent age-matched and young biases for spine measurements were small, but the irregularities in spine databases for subjects around 45 and over 70 years were demonstrated by the negative Lunar minus Hologic biases at these age-groups (Fig 3). The small discrepancies between the Lunar and Hologic databases calculated for older subjects may relate to the inclusion or exclusion of subjects with osteophytes or wedge fractures into the database. Few elderly subjects are completely free of these phenomena and they are very difficult to diagnose accurately even when lateral spine radiographs are obtained.

Figures 3 and 4 demonstrated that, as predicted by Figs 1 and 2, Lunar percent age-matched and young values for the femur of males and females were consistently higher than the corresponding Hologic values. The discrepancies in the manufacturer's femur databases could be due to the different selection of normal subjects. However, the weights of the male and female subjects used to compile the Lunar and Hologic reference data were very similar. The different methods of locating the various regions of the femur may also be a contributing factor.

Another method of assessing risk of osteoporosis is to use *Z*-scores (Parfitt, 1990). The *Z*-score is calculated as follows:

$$Z\text{-score} = \frac{P - \text{Mam}}{\text{SDam}}$$

where P is the patient's measured bone density value; Mam is the mean bone density value for sex and age-matched normals; SDam is the standard deviation of the bone density for sex and age-matched controls.

The manufacturers of the Lunar DPX and Hologic QDR-1000 quote femur mean bone density, SDs ranging from 0.09–$0.13\ \mathrm{g\,cm^{-2}}$, depending on bone site measured and sex of the subject, but not on the age of the subject (Table I). The calculated differences between the Lunar and converted Hologic femur database bone density values were about 0.10 g cm^{-2} for males and about 0.05–0.10 g cm^{-2} for young females depending on age and region of femur investigated (Figs 1 and 2). These differences are approximately the same as the SD of the database bone densities (Table I). Hence, the *Z*-score for Lunar femur measurements (software 3.4) will be about 0.5–1.0 higher than Hologic femur measurements for males and young females. A subject with a *Z*-score of -1 and above is usually considered to have a normal bone density but a *Z*-score of -2 indicates severe osteopenia. Hence these database discrepancies could lead to different diagnoses.

The ratios of the SDs for the bone densities of the Lunar and Hologic databases should be similar to the Lunar/Hologic BMD bias, *e.g.* 1.13 for spine, 1.2 for femoral neck and greater trochanter and 1.44 for Ward's triangle (Laskey et al, 1991). From Table I it can be calculated that the Lunar/Hologic ratios of the SD for the databases are greater than these values for the spine, about the same for the neck of femur and smaller for the greater trochanter and Ward's triangle. Hence, even if the Lunar and Hologic databases were strictly comparable, *Z*-scores would only be similar for the neck of femur. The Lunar *Z*-scores would be of smaller magnitude (either positive or negative) for the spine, but of greater magnitude for the greater trochanter and Ward's triangle. Clearly *Z*-scores will be inaccurate in identifying the 25% of the population most at risk of developing osteoporosis if the reference bone density value or the SD of the reference bone density is not appropriate for the population under investigation.

Both Lunar and Hologic are collecting more reference data from different countries and it is probable that there will be updates to their reference data. Lunar have published more reference data for US and European women (Lunar Corporation, 1991) compiled from about 2500 women. The two sets of Lunar spine data were similar except for women aged 40–59 years and over 70 years when the Lunar News data were about 0.03 g cm^{-2} lower. Most Lunar News femur data were slightly higher: greater trochanter data by on average 0.022 g cm^{-2}, neck of femur data by 0.003 g cm^{-2}, and Ward's triangle by 0.005 g cm^{-2}. The SD for all bone regions was stated in Lunar News to be 0.12 g cm^{-2}. These changes will decrease but not remove the database differences.

The variability in bone density measurements between machines from the same manufacturer must be negligible, if centrally compiled reference data are to be used. Blake et al (1991) determined the coefficient of variation for bone density results to be 1.4% for the spine and 2.1% for the femoral neck for Hologic QDR-1000 systems, but Morita et al (1990) found that the coefficient of variation of bone density results of the different systems they studied varied from 1% to 10%.

In conclusion, at present there are clear differences between the femur databases supplied with the Lunar DPX and the Hologic QDR-1000 being used by USA and UK investigators, which could affect the clinical management of individual subjects. There is a European Committee (COMAC) which aims to standardize the bone density measurements of the four major manufacturers of dual-energy X-ray absorptiometers (Lunar, Hologic, Norland and Sopha Medical) and a quasi-anthropomorphic spine phantom has been constructed to use for the cross-calibration of all these systems. Hopefully this collaboration will also facilitate the collation of normal reference data for dual-energy X-ray absorptiometers.

Appendix I

The following method was used to determine the significance of the differences between the Lunar and the Hologic databases.

Consider the three samples of subjects:

(1) Hologic database; (2) Lunar database; (3) Cambridge comparison database. Sample (1) is measured on a Hologic QDR-1000, Sample (2) on a Lunar DPX, and Sample (3) on both systems. In what follows, the suffices 1, 2 or 3 indicate which sample is referred to, while the suffices H or L indicate the system used (Hologic or Lunar) to make the measurements.

The size of each sample is n_i $(i = 1 \ldots 3)$, the mean bone density for the sample is $\mathrm{M}_{\mathrm{H}i}$ or $\mathrm{M}_{\mathrm{L}i}$ depending on the machine used, and the SD of the bone density correspondingly is $\mathrm{SD}_{\mathrm{H}i}$ or $\mathrm{SD}_{\mathrm{L}i}$.

Sample 3 is used to predict L from H, based on the regression equation

$$\text{Lunar DPX} = c\,.\,\text{Hologic QDR} + d \qquad \text{(A1)}$$

where c is the regression coefficient and d the intercept, given by $(\mathrm{M}_{\mathrm{L}3} - c.\mathrm{M}_{\mathrm{H}3})$. The regression has a standard error of estimate of $\mathrm{SEE}_{\mathrm{L}3}$.

Equation (A1) is used to convert the Hologic values of Sample 1 to Lunar, so that $\mathrm{M}_{\mathrm{L}1} = (c.\mathrm{M}_{\mathrm{H}1} + d)$. The difference between the Lunar and Hologic databases is then given, in Lunar units, by $(\mathrm{M}_{\mathrm{L}2} - \mathrm{M}_{\mathrm{L}1})$ or $(\mathrm{M}_{\mathrm{L}2} - c.\mathrm{M}_{\mathrm{H}1} - d)$. Substituting for d gives the difference as

$$(\mathrm{M}_{\mathrm{L}2} - c\,.\,\mathrm{M}_{\mathrm{H}1}) - (\mathrm{M}_{\mathrm{L}3} - c\,.\,\mathrm{M}_{\mathrm{H}3}) \qquad \text{(A2)}$$

The variance of this difference is given by

$$\begin{aligned}\mathrm{Var}(\mathrm{M}_{\mathrm{L}2}) - c^2\mathrm{Var}(\mathrm{M}_{\mathrm{H}1}) + {\mathrm{M}_{\mathrm{H}1}}^2\mathrm{Var}(c)&\\ + \mathrm{Var}(d) - 2\,\mathrm{M}_{\mathrm{H}1}\,\mathrm{M}_{\mathrm{H}3}\,\mathrm{Var}(c)&\end{aligned}$$

which simplifies to

$$\frac{{\mathrm{SD}_{\mathrm{L}2}}^2}{n_2} + c^2\,\frac{{\mathrm{SD}_{\mathrm{H}1}}^2}{n_1} + {\mathrm{SEE}_{\mathrm{L}3}}^2\left(\frac{1}{n_3} + \frac{(\mathrm{M}_{\mathrm{H}1} - \mathrm{M}_{\mathrm{H}3})^2}{(n_3 - 1)\,{\mathrm{SD}_{\mathrm{H}3}}^2}\right) \qquad \text{(A3)}$$

The significance of the difference is then given by the *t*-statistic

$$t = \frac{\text{difference as given by (A2)}}{\sqrt{\text{variance of difference as given by (A3)}}}$$

on $(n_1 + n_2 + n_3 - 3)$ degrees of freedom. In practice the two terms of (A3) involving SD^2 are much larger than the SEE^2 term, so that the SEE^2 term can be ignored for all practical purposes.

Appendix II

Lunar software version 3.6 (due for global release summer 1992) includes refined reference data. The reference data changes appear small for all female data and for male spine and Ward's triangle data. The female data are almost identical to the reference data reported in Lunar News (March 1991). However, there are substantial changes to the male neck of femur and greater trochanter reference data. These greatly improve the agreement between the two systems. Thus, the maximum differences between the Lunar (software 3.6) and converted Hologic database will be $-0.030\ \text{g cm}^{-2}$ for the neck of femur of young males and $+0.03\ \text{g cm}^{-2}$ for the greater trochanter of elderly males.

References

Adachi, J. D. & Webber, C. E., 1991. The interchangeability of radioisotope and X-ray based measurements of bone mineral density. *British Journal of Radiology, 64,* 217–220.

Blake, G. M., Tong, C. M. & Fogelman, I., 1991. Intersite comparison of the Hologic QDR-1000 dual energy X-ray bone densitometer. *British Journal of Radiology, 64,* 440–446.

Bland, J. M. & Altman, D. G., 1986. Statistical methods for assessing agreement between two methods of clinical measurement. *Lancet, 1,* 307–310.

Cullum, I.D., Ell, P. J. & Ryder, J. P., 1989. X-ray dual photon absorptiometry: a new method for the measurement of bone density. *British Journal of Radiology, 62,* 587–592.

Gundry, C. R., Miller, C. W., Ramos, E., Moscona, A., Stein, J. A., Mazess, R. B., Sartoris, D. J. & Resnick, D., 1990. Dual-energy radiographic absorptiometry of the lumbar spine: clinical experience with two different systems. *Radiology, 174,* 539–541.

Kelly, T. L., 1990. Bone density reference databases for American men and women. *Journal of Bone and Mineral Research, 5,* Suppl. 2, 702.

Laskey, M. A., Flaxman, M. E., Barber, R. W., Trafford, S., Hayball, M. P., Crisp, A. J. & Compston, J. E., 1991. Comparative performance *in vitro* and *in vivo* of Lunar DPX and Hologic QDR-1000 dual energy X-ray absorptiometers. *British Journal of Radiology, 64,* 1023–1029.

Mazess, R., Collick, B., Trempe, J., Barden, H. & Hansen, J., 1989. Performance evaluation of a dual-energy X-ray bone densitometer. *Calcified Tissue International, 44,* 228–232.

Mazess, R. B., Trempe, J. A., Bisek, J. P., Hanson, J. A. & Hans, D., 1991. Calibration of dual-energy X-ray absorptiometry for bone density. *Journal of Bone and Mineral Research, 6,* 799–806.

Morita, R., Fukunaga, M., Shiraki, M., Orimo, H., Nakamura, T., Fujita, T., Inoue, T., Kaneda, K., Tomita, A., Yamamoto, K. & Norimatsu, H., 1990. Cross calibration of BMD values among the different bone densitometric equipments. In *Osteoporosis 1990, 2. Third International Symposium on Osteoporosis, Copenhagen, Denmark, 14–18 October, 1990,* ed. by C. Christiansen and K. Overgaard (Osteopress Aps, Copenhagen) pp. 796–798.

Nijs, J., Geusens, P., Dumortier, F., Wouters, C. & Dequeker, J., 1990. *In vitro* evaluation of DPA and DEXA systems. In *Osteoporosis 1990, 2. Third International Symposium on Osteoporosis, Copenhagen, Denmark, 14–18 October, 1990,* ed. by C. Christiansen and K. Overgaard (Osteopress Aps, Copenhagen) pp. 728–729.

Lunar Corporation (1991). Normal reference data. *Lunar News,* March 1991 (Madison, USA) p. 3.

Parfitt, A. M., 1990. Interpretation of bone densitometry measurements: disadvantages of a percentage scale and a discussion of some alternatives. *Journal of Bone and Mineral Research, 5,* 537–540.

Reid, D. M., Lanham, S. A., McDonald, A. G., Avenell, A., Fenner, J. A. K., Boyle, I. T., Pye, D. & Nuki, G., 1990. Speed and comparability of 3 dual-energy X-ray absorptiometers (DXA) models. In *Osteoporosis 1990, 2. Third International Symposium on Osteoporosis, Copenhagen, Denmark, 14–18 October, 1990,* ed. by C. Christiansen and K. Overgaard (Osteopress Aps, Copenhagen) pp. 575–577.

Svendsen, O. L., Marslew, U., Hassager, C. & Christiansen, C., 1992. Measurements of bone mineral density of the proximal femur by two commercially available dual energy X-ray absorptiometric systems. *European Journal of Nuclear Medicine, 19,* 41–46.

1992, *The British Journal of Radiology*, *65*, 1130

Technical note

Sialography using a paediatric intravenous cannula

By G. D. Walker, MB, MRCP(UK), FRCR

Department of Radiology, Southampton General Hospital, Tremona Road, Southampton SO9 4XY, UK

(Received 19 March 1992 and accepted 6 May 1992)

Keyword: Sialography

Sialography is the best way of assessing disease of the duct system of the parotid and submandibular glands. However, it can often be difficult to cannulate the orifices of Stenson's and Wharton's ducts with the available range of plastic and metal instruments.

A 24 G Jelco Teflon intravenous cannula (Critikon Ltd) offers practical benefits whilst costing less than 5% of one commercially produced alternative in use in the department.

Technique

The sharp introducer needle is withdrawn and discarded, although its plastic end cap is retained. The outer Teflon sheath is then used for duct cannulation. Under direct vision, sufficient contrast is injected via a 2 ml syringe to fill the duct system before exchanging the syringe for the plastic end cap which prevents premature drainage of contrast whilst radiographs are made.

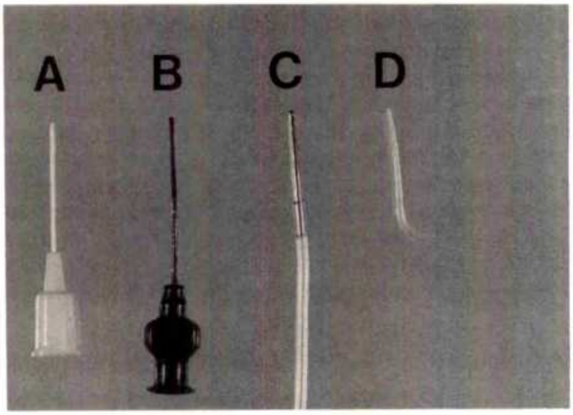

Figure 1. A: Jelco 24 G Teflon catheter (Critikon Ltd); B: metal sialography needle; C: Rabinov sialography catheter (SCS T-32S William Cook) and D: polythene sialography catheter (Meadox (UK) Ltd).

Discussion

The cannula is 2 cm in length with a radio-opaque female Luer-lok hub. Its Teflon sheath has an outside diameter of 0.75 mm and a lumen of 0.5 mm diameter. The catheter end is tapered, reducing from 0.75 mm to just over 0.55 mm. Fig. 1 shows a magnified view of the ends of other cannulae available in the radiology department.

This device has several advantages over the other available cannulae. It is disposable and sterile when supplied and is easily procurable as a stock item on most paediatric wards.

The cannula has good strength in its long axis and its short length also helps to direct the tapered end into the duct orifice. Its light weight means that it can be left *in situ* whilst radiographs are made without taping to the skin or risk of displacement. This avoids unnecessary trauma to the duct caused by repeated reinsertion of the cannula and allows injection of the duct under direct vision. Occlusion of the cannula using the end cap prevents premature drainage of contrast. The Teflon sheath is radiolucent which ensures that distal duct calculi are not obscured. Its short length, Teflon manufacture and thin walled structure all mean contrast injection is achieved with lower pressure than with the alternatives.

It costs much less than the alternative disposable devices; locally the Jelco cannula costs £0.52, the Meadox cannula £11.34 and the Rabinov £19.04 (all prices including VAT).

1992, *The British Journal of Radiology*, *65*, 1131–1132

Case reports

Primary leiomyosarcoma of the superior vena cava with massive thrombosis treated by local fibrinolysis

By M. Marini, *E. Tovar, †Mª F. López-Fernández, F. Pombo and E. Rodríguez

Departments of Radiology, *Vascular Surgery and †Haematology, Hospital Juan Canalejo, La Coruña, Spain

(*Received 2 December 1991 and in final form 25 June 1992, accepted 10 August 1992*)

Keywords: Leiomyosarcoma, Superior vena cava, Neoplasm, Thrombolytic therapy, Computed tomography

Occlusion of the superior vena cava (SVC) is usually related to malignant or benign disease involving the mediastinum (Putnam et al, 1988) or secondary to central venous catheters and pacemakers (Capek & Cope, 1989). Acute superior vena cava syndrome (SVCS) caused by massive thrombosis secondary to leiomyosarcoma is a very rare event. Primary leiomyosarcoma of the SVC has been reported in only a few cases and special attention to radiological findings has been described in only two cases (Vogel et al, 1981; Lupetin et al, 1986).

We report a case of massive thrombosis of the SVC and its branches treated by local thrombolytic therapy that achieved complete lysis. Subsequently an intraluminal tumour mass was demonstrated on an enhanced computed tomographic (CT) study. Local fibrinolytic treatment should be given in SVCS due to thrombosis. The CT studies are of value in the search for the aetiology of SVCS. To our knowledge, this case is the first one in which the CT findings of leiomyosarcoma of the SVC are reported.

Case report

A 75-year-old male smoker, with no personal or family history of thrombosis, presented with acute swelling of the face, neck, upper thorax and extremities, exophthalmus, severe dyspnoea and cyanosis. Tracheostomy had already been performed at the referring hospital.

Thoracic computed tomography (CT) performed after a 100 ml bolus of contrast medium had been injected in the left antecubital vein showed obliteration of the lumen of the left innominate and right internal jugular veins and superior vena cava, suggesting thrombosis. Small venous collaterals were evident throughout the mediastinum. No mediastinal or pulmonary masses were found. Venography performed via 4F catheters placed percutaneously through both antecubital veins showed a large volume of thrombus in the subclavian and innominate veins bilaterally as well as in the SVC. Both catheters were then advanced, so that the tips were embedded in the thrombus in the innominate veins (Fig. 1). An initial bolus of 250 000 units of urokinase was infused, followed by 75 000 units/h through each catheter for 72 h. Plasma fibrinogen levels remained within normal limits, and the patient became asymptomatic. Follow-up venography demonstrated complete clearance of thrombus and an intraluminal filling defect was revealed in the SVC (Fig. 2). A further CT study was performed and an intraluminal mass, which enhanced after injection of contrast medium, was seen in the SVC (Fig. 3). A tumour of the SVC, probably leiomyosarcoma, was suspected and a thoracotomy was performed. At operation a pedunculated intravascular mass was resected together with a part of the vessel wall, and the defect was closed by direct suture. Pathological examination confirmed the diagnosis of leiomyosarcoma of high-grade malignancy. A post-operative cavogram showed patency, but a respiratory infection developed on the 15th post-operative day and the patient died.

Discussion

Primary leiomyosarcoma of the SVC is a very rare malignant tumour and to our knowldge only six cases

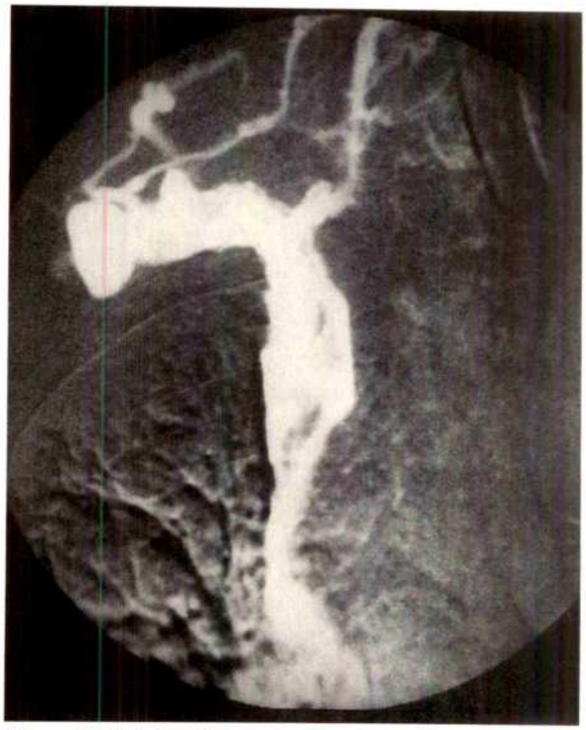

Figure 1. (*left*) Baseline cavogram reveals large amounts of thrombus in the SVC and its main tributaries.

Address correspondence and reprint requests to: Milagros Marini, Department of Radiology, Hospital Juan Canalejo, Xubias de Arriba 84, 15006, La Coruña, Spain.

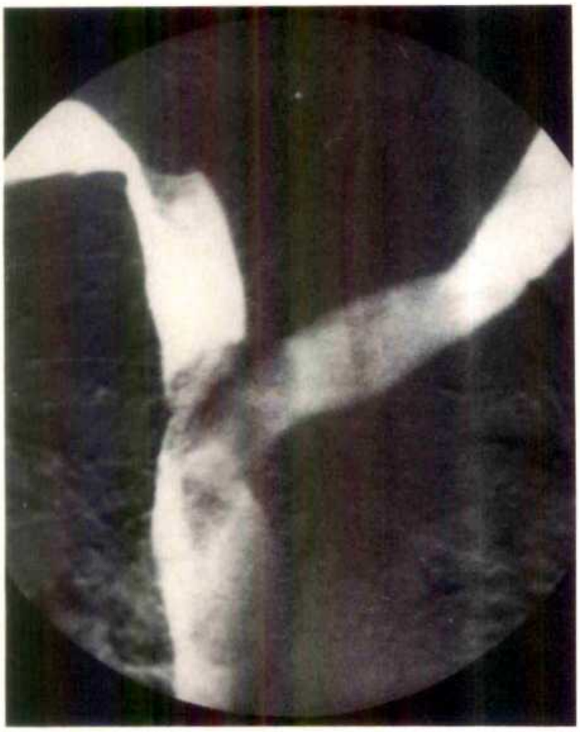

Figure 2. (*right*) Follow-up cavogram obtained after 72 h local infusion of urokinase shows lysis of thrombi and an intrinsic defect on the left wall of the SVC.

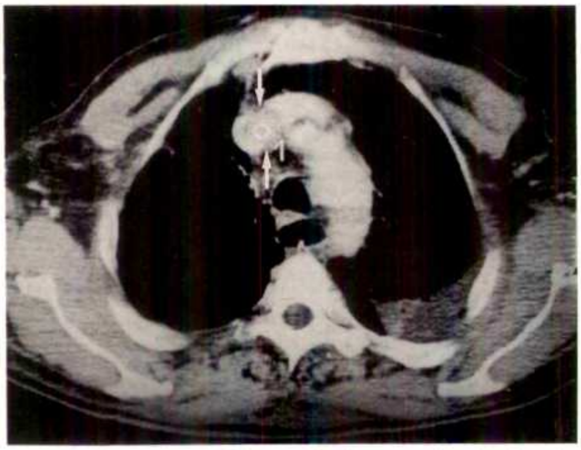

Figure 3. Post-contrast CT scan showing an enhancing intraluminal mass (attenuation value, 96.5 HU) involving the confluence of innominate veins (arrows).

have been previously reported, two in the radiological literature (Vogel et al, 1981; Lupetin et al, 1986). Leiomyosarcomas originate from the vessel walls and their growth can be intra- or extraluminal, although they commonly exhibit both components (Van Rooij et al, 1988). When, as in our case, the growth of a leiomyosarcoma is purely intraluminal, the differential diagnosis lies between tumour and thrombosis. If thrombus is excluded, then leiomyosarcoma is likely to be the diagnosis as this is the most common intramural venous tumour (Van Rooij et al, 1988). Dynamic CT is the most appropriate imaging test in establishing the diagnosis. Contrast enhancement of the intraluminal filling defect, which is related to hypervascularity of the mass, is the hallmark of tumoral thrombosis (Zeman et al, 1988). However, when thrombosis is associated with intraluminal tumour, dynamic CT is unable to demonstrate the hypervascularity of the mass. Recently, gadolinium diethylene triaminepenta-acetic acid (Gd-DTPA) enhanced magnetic resonance (MR) has been shown to be useful in differentiating blood clot from tumour (Gehl et al, 1990).

Local fibrinolytic therapy has been applied in a few cases of total thrombosis with SVCS (Becker et al, 1985; Putnam et al, 1988; Capek & Cope, 1989). The advantage off this form of therapy is the local effect of the thrombolytic agent on the thrombus, producing lysis but with a low incidence of haemorrhagic complications.

Symptoms and resectability of the leiomyosarcoma (resection is the treatment of choice) depend on the location and extent of the tumour and associated thrombosis (Van Rooij et al, 1988). In this case, local thrombolytic therapy lysed the thrombus, allowing us to establish the diagnosis of intraluminal leiomyosarcoma and also improving the SVCS symptoms. Complete lysis of the thrombus allowed appropriate surgical excision.

References

BECKER, G. J., HOLDEN, R. W., MAIL, J. T., OLSON, E. W. & CASTANEDA-ZUNIGA, W. R., 1985. Local thrombolytic therapy for "thoracic inlet syndrome". *Seminars in Interventional Radiology*, *2*, 349–353.

CAPEK, P. & Cope, C., 1989. Percutaneous treatment of superior vena cava syndrome. *American Journal of Roentgenology*, *152*, 183–184.

GEHL, H. B., BOHNDORF, K. & KLOSE, K. C., 1990. Inferior vena cava tumor thrombus: demonstration by Gd-DTPA enhanced MR. *Journal of Computed Assisted Tomography*, *14*, 479–481.

LUPETIN, A. R., DASH, N. & BECKMAN, I., 1986. Leiomyosarcoma of the superior vena cava: diagnosis by cardiac gated MR. *Cardiovascular Interventional Radiology*, *9*, 103–105.

PUTNAM, J. S., UCHIDA, B. T., ANTONOVIC, R. & RÖCH, J., 1988. Superior vena cava syndrome associated with massive thrombosis: treatment with expandable wire stents. *Radiology*, *167*, 727–728.

VAN ROOIJ, W. J., MARTENS, F., VERBEETEN, B., JR. & DIJKSTRA, J., 1988. CT and MR imaging of leiomyosarcoma of the inferior vena cava. *Journal of Computed Assisted Tomography*, *12*, 415–419.

VOGEL, H., KALMAR, P., KNOP, J., RUNGE, M. & WOLF, W., 1981. Leiomyosarcoma of the superior vena cava. *Fortschritte auf dem Gebiete der Röntgenstrahlen und der neuen bildgeberden Verfahren*, *134*, 691–692.

ZEMAN, R. K., CRONAN, J. J., ROSENFIELD, A. T., LYNCH, J. H., JAFFE, M. H. & CLARK, L. R., 1988. Renal cell carcinoma: dynamic thin section CT assessment of vascular invasion and tumor vascularity. *Radiology 167*, 393–396.

1992, *The British Journal of Radiology*, *66*, 1133–1134

Hodgkin's disease—a very late recurrence

By I. J M. Johnson, FRCS and R. Pillai, FRCS

Department of Cardiothoracic Surgery, John Radcliffe Hospital, Oxford, UK

(*Received 23 October 1991 and in revised form 22 April 1992, accepted 3 June 1922*)

Keywords: Hodgkin's, Diagnosis

Hodgkin's disease represents 0.7% of all malignancies excluding skin cancer in England and Wales (Mead & Whitehouse, 1988) and, although the therapeutic regimes produce good results, achievement of cure remains ill defined. There is an increasing awareness of problems with treatment, appearance of a second malignancy and possible relapse. We present an extremely rare case of very late relapse (23 years) and discuss its relevance to the much debated question of the length of time required to follow patients after remission.

Case report

A Caucasian male originally presented in 1968 aged 21 years with an 18 month history of a swelling on the left side of the neck. Biopsy revealed this to be Hodgkin's disease, the classification of which has changed since 1968. Current review of the original histopathological slides suggests this was nodular sclerosing in type, but by no means typical. The Ann Arbor Stage I tumour was treated with radiotherapy to the neck, axilla and mediastinum using separate fields with a total dose in the order of 4000 cGy. The patient made a good recovery and was followed yearly until discharged from the Specialist Clinic in 1980. He remained well until early 1991 when he attended his general practitioner complaining of back pains following mild trauma. Chest radiograph revealed, as an incidental finding, a virtual whiteout of the left lung field but no other pathology (Fig. 1). Bronchoscopy and bronchial lavage both proved negative. Computerized axial tomography showed several filling defects in the liver and spleen, but these were thought to represent "burn-out" Hodgkin's disease and not active disease. In view of the patient's age, left thoracotomy was performed. The left lung was completely replaced by tumour which extended into the left atrium and involved the pulmonary artery. Left pneumonectomy was performed. Histology demonstrated this to be atypical nodular sclerosing-type Hodgkin's. He is currently undergoing chemotherapy for the recurrence.

Discussion

The results of treatment, especially Stage I and II disease, are good with 70–80% of patients remaining disease free (Mead & Whitehouse, 1988). The majority who relapse do so within the first 36 months (defined as early relapse) and approximately 90% fall into this group (Herman et al, 1985). Those who present with late relapse (after 36 months) have a mean onset of symptoms at 66 months after termination of therapy. The majority who relapse, especially in the late group, are male even once the overall male predominance in the disease is taken into account.

The other risk factors for late recurrence are having disease in Stage I or II and most importantly having the nodular sclerosing pathological type (Collaborative study, 1984). The last factor may be explained by Lukes et al (1966) as to whether nodular sclerosing histology represents a stronger host resistance to the tumour than seen in other groups. The greater response inhibits the proliferation of neoplastic cells and results in a more indolent course with a higher tendency for delayed reemergence. There are various modes of surveillance open to a physician and these vary between units. At Stanford University for example, 70% of relapses are detected by history and examination with 25% of patients being detected by radiographs (Collaborative study, 1984). A greater emphasis is placed on haematological screening in the UK. There seems to be no significant difference in pick-up rates with the various regimes.

A recurrence of Hodgkin's disease at 23 years after treatment is almost unique, but it raises two important points in relation to the management of these patients. Firstly, should the patient ever be discharged from care as there appears to be no time limit where they could be considered safe from further disease? Secondly, a diagnosis of Hodgkin's disease should always head the list of differential diagnosis and should be actively excluded in any patient considered to be in remission. As this case

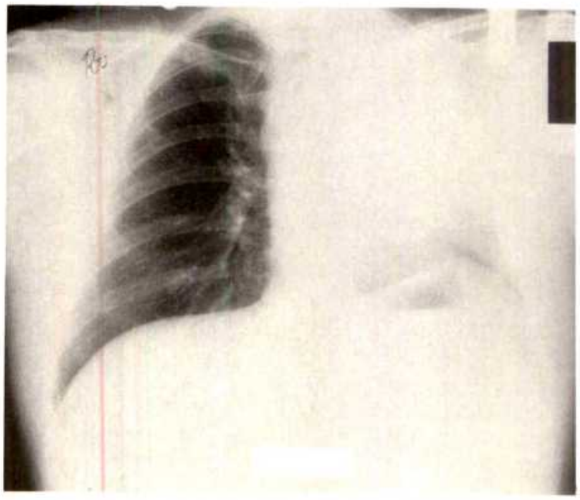

Figure 1. Chest radiograph revealing virtual whiteout of the left lung field.

1992, *The British Journal of Radiology*, *65*, 1134–1136

illustrates, Hodgkin's disease represents a life-long threat to the patient and requires constant vigilance by medical practitioners.

References

COLLABORATIVE STUDY, 1984. Radiotherapy of Stage I and II Hodgkin's. *Cancer*, *54*, 1928–1942.

HERMAN, T. S., HOPPE, R. T., DONALDSON, S. S., COX, R. S., ROSENBERG, S. A. & KAPLAN, H., 1985. Late relapse among patients treated for Hodgkin's disease. *Annals of Internal Medicine*, *102*, 292–297.

LUKES, R. J., BUTLER, J. J. & HICKS, E. D., 1966. Natural History of Hodgkin's disease as related to its pathological picture. *Cancer*, *19*, 317–344.

MEAD, G. M. & WHITEHOUSE, J. M. A., 1988. Clinical aspects of Hodgkin's disease. *British Medical Journal*, *297*, 1562–1564.

Dural venous sinus thrombosis following myelography: demonstration by magnetic resonance imaging

By R. W. J. Hartley, MRCP, A. Jackson, PhD, MCRP, FRCR and *R. S. Cooke, FRCS

Departments of Neuroradiology and *Neurosurgery, Manchester Royal Infirmary, Oxford Road, Manchester, M13 9WL, UK

(*Received 21 January 1992 and in revised form 21 May 1992, accepted 22 June 1992*)

Keywords: Myelography, Complications, Dural venous thrombosis, Magnetic resonance imaging

Headache is a common complication of myelography, occurring in approximately 30% of cases (Wilkinson & Sellar, 1991). The headaches may be severe and are frequently postural in nature. We present a case in which a severe post-myelographic headache progressed over a period of six weeks. The development of fundal haemorrhages with visual impairment prompted investigation by magnetic resonance imaging (MRI) which demonstrated thrombosis of the right transverse sinus. Anticoagulant therapy led to prompt relief of symptoms and improvement of visual acuity.

Case report

A 51-year-old man presented to another hospital with three days of severe low back pain and right-sided sciatica. Initial examination demonstrated reduced straight leg raising on the right but no other abnormality. Initial treatment with seven days bed rest resulted in no improvement and a lumbar myelogram was performed using iohexol (Omnipaque, 240 mg/ml, Nycomed Ltd). Myelography demonstrated no evidence of significant abnormality and the patient's symptoms resolved spontaneously.

During the 24 h following myelography the patient developed severe postural headaches associated with nausea and vomiting. This was considered to be post-myelographic in nature and was treated conservatively. Symptoms worsened over the following four weeks and examination at this stage revealed bilateral papilloedema, slight left afferent pupil defect and an enlarged right blind spot. Computed tomography (CT) of the brain (IGE 8800) performed without intravenous contrast was normal. Over the following two weeks the patient's visual acuity deteriorated and bilateral fundal flame haemorrhages developed, prompting further investigation including MRI. Coronal and axial T_2 and proton-density-weighted dual echo (SE 2000/80, 20) and T_1-weighted (SE 420–500/25) axial sagittal and coronal images were obtained. All images demonstrated loss of flow void in the right transverse sinus. On T_1-weighted images an area of signal isointense with grey matter was demonstrated within the right transverse sinus on all images (Figs 1, 2). On T_2- and proton-density-

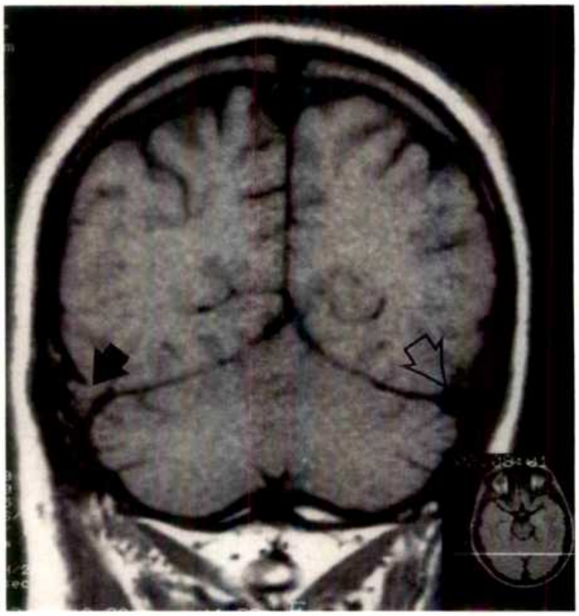

Figure 1. Coronal T_1-weighted image (SE 500/25) demonstrating intermediate signal in the right transverse sinus (arrow). The left transverse sinus demonstrates a normal signal void (open arrow).

Address correspondence to Dr A. Jackson, Department of Neuroradiology, Manchester Royal Infirmary, Oxford Road, Manchester, M13 9WL, UK.

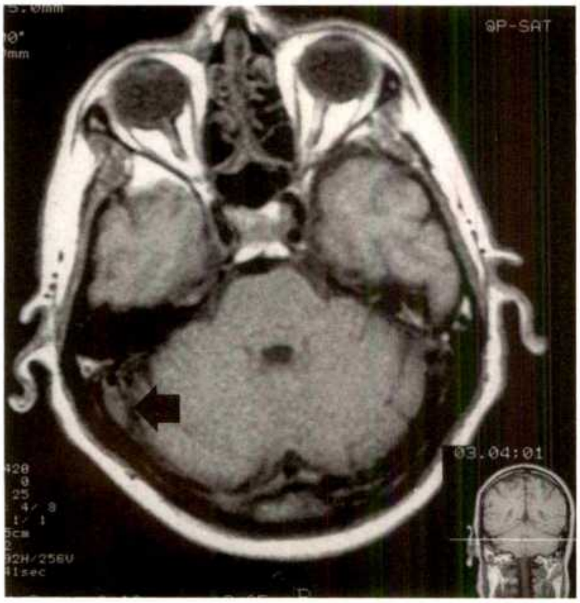

Figure 2. Axial T_1-weighted image (SE 500/25) also demonstrating thrombus in the right transverse sinus (arrow).

weighted images an area of high signal was identified in the same position (Fig. 3). The distal portion of the sigmoid sinus immediately proximal to the jugular foramen demonstrated flow void on all sequences, indicating vascular patency, and was shown to receive blood from superficial cerebral veins (Figs 1, 2). A diagnosis of right transverse dural sinus thrombosis was made and was confirmed using intravenous digital subtraction angiography. The patient was treated with anticoagulation and his symptoms resolved dramatically within the first week; papilloedema and changes in visual acuity resolved more steadily over the following month. Anticoagulation was continued for a period of four months.

Extensive haematological and biochemical investigations and an ultrasound scan of the upper abdomen were performed on the advice of a haematologist to exclude any underlying thrombotic tendency. All test results were normal.

Discussion

Cerebral venous or dural sinus thrombosis most commonly presents with symptoms and signs of raised intracranial pressure. Postural headache, nausea, vomiting, convulsions and depressed alertness are common (Bansal et al, 1980). Focal signs are often subtle or absent and the clinical diagnosis is frequently overlooked (Bousser et al, 1985).

Before the widespread introduction of antibiotic therapy, dural sinus thrombosis was most commonly attributed to infective phlebitis secondary to craniofacial infections, particularly otitis media. At the present time the majority of cases are non-septic and the condition is most commonly seen in premature neonates, post-partum patients and those with a malignancy (Bansal et al, 1980; Hickey et al, 1982). Aseptic intracranial venous thrombosis has also been associated with a wide variety of other disorders which predispose to intravascular thrombosis (Harris et al, 1989) (Table I) but has not been described as a complication of myelography.

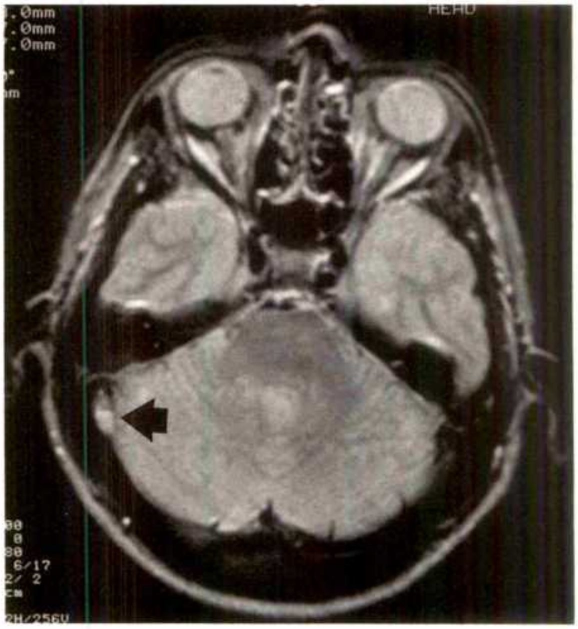

Figure 3. Axial T_2-weighted image (SE 2000/80) showing high signals from the thrombus (arrowed).

We think that dural sinus thrombosis in the case presented here resulted from a period of prolonged dehydration induced by the nausea and vomiting associated with post-myelographic headache. Dehydration is certainly a known predisposing factor for the development of dural sinus thrombosis and extensive investigation has failed to reveal any other aetiology in this case.

The finding of isolated unilateral thrombosis of the transverse sinus in this case does not entirely explain the spectrum of clinical features observed. Lateral sinus thrombosis is often asymptomatic although it may be associated with signs of raised intracranial pressure as in this case (Adams & Biller, 1989). The development of

Table I. Causes of aseptic intracranial venous thrombosis

Pregnancy and childbirth
Oral Contraceptives
Carcinoma
Haemolytic anaemia
Paraoxysmal nocturnal haemoglobinuria
Sick cell disease
Polycythaemia vera
Afrinrinogenaemia
Disseminated intravascular coagulation
Antithrombin III deficiency
Dehydration
Marasmus
Androgen therapy
Head injury
Diabetes mellitus
Wegener's granulomatosis
Polyarteritis nodosa
Sarcoidosis
Ulcerative colitis
Nephrotic syndrome
Cardiac failure
Chronic lung disease
Intravenous catheters

papilloedema and fundal haemorrhage is more usually associated with extensive thrombosis of the sagittal sinus, or thrombosis of the cavernous sinus. Although these were not demonstrated in the present case, the rapid therapeutic response to anticoagulation leads us to believe that venous thrombosis was the underlying cause. It seems possible that venous thrombosis was more extensive than was demonstrated, possibly involving small vessels beyond the resolution of MRI.

MRI is now accepted as the method of choice for the demonstration of dural sinus thrombosis (Hulcelle et al, 1989). Acute thrombosis initially appears as a region of iso-intensity relative to normal brain on T_1-weighted images, becoming progressively hyperintense with the formation of methaemoglobin. Rephasing of spins, caused by even-echo re-phasing and/or gradient-moment nulling, may also give rise to signal within a patient sinus, as may unilateral slow flow in the transverse sinus (Listerud et al, 1991). These problems can be overcome by the use of multi-planar imaging using heavily T_1-weighted short TR spin echo techniques as in the current case (Hulcelle et al, 1989). The potential pitfalls of spin echo imaging may also be overcome by use of gadolinium enhancement although contrast enhancement in low flow states may be misleading (Tsuruda et al, 1991). A number of flow-related imaging sequences have also been described which will allow improved demonstration of venous thrombosis even in the presence of unilateral slow flow (Harris et al, 1989; Tavares et al, 1989; Tsuruda et al, 1991; Ridgeway & Smith, 1986).

Although the development of dural sinus thrombosis has not been previously associated with myelography, the similarity of the symptoms to those of post-myelographic headache is potentially misleading. We think that any case of unduly prolonged post-myelographic headache, particularly if associated with focal neurological signs or with confirmatory signs of raised intracranial pressure, should raise the suspicion of venous thrombosis. The diagnosis of venous thrombosis is of importance since it can give rise to significant morbidity and is effectively treated by anticoagulation. MRI is the method of choice for the evaluation of venous thrombosis but is prone to a number of flow-related artefacts which may be misleading if appropriate imaging sequences are not performed.

Acknowledgments

The authors would like to thank Mrs J. Ford for typing the manuscript.

References

Adams, H. P. & Biller, J., 1989. Ischaemic cerebrovascular disease. In: *Neurology in Clinical Practice*, Vol. 2, ed. by W. G. Bradley, R. B. Daroff, G. M. Fenichel and C. D. Marsden (Butterworth-Heinemann, London) pp. 936–938.

Bansal, B. C., Gupta, R. R. & Prakash, C., 1980. Stroke during pregnancy and puerperium in young females below the age of 40 as a result of cerebral venous/venous sinus thrombosis. *Japanese Heart Journal, 21*, 171–183.

Bousser, M., Chiras, J., Bories, J. & Castaigne, P., 1985. Cerebral venous thrombosis: a review of 38 cases. *Stroke, 16*, 199–213.

Harris, T., Smith, R. & Koch, K., 1989. Gadolinium DTPA enhanced MR imaging of septic dural sinus thrombosis. *Journal of Computer Assisted Tomography, 13*, 682–684.

Hickey, W. F., Garnick, M. B. & Henderson, I. C., 1982. Primary cerebral venous thrombosis in patients with cancer—a rarely diagnosed paraneoplastic syndrome. *American Journal of Medicine, 73*, 740–750.

Hulcelle, P. J., Dooms, G. C., Mathurin, P. & Cornelis, G., 1989. MRI assessment of unsuspected dural sinus thrombosis. *Neuroradiology, 31*, 217–221.

Listerud, J., Atlas, S. W. & Axel, L., 1991. Flow theory and MR techniques. In: *Magnetic Resonance Imaging of the Brain and Spine*, ed. by S. W. Atlas (Raven Press, New York), pp. 49–68.

Ridgeway, J. & Smith, M., 1986. A technique for velocity imaging using magnetic resonance imaging. *British Journal of Radiology, 59*, 603–607.

Tavares, N., Auffermann, W., Brown, J., Gilbert, T., Sommerhoff, C. & Higgins, C., 1989. Detection of thrombus by using phase image MR scans: ROC curve analysis. *American Journal of Roentgenology, 153*, 173–178.

Tsuruda, J. S., Shimakawa, A., Pelc, N. J. & Saloner, D., 1991. Dural sinus occlusion: Evaluation with phase-sensitive gradient echo MR imaging. *American Journal of Neuroradiology, 157*, 139–146.

Wilkinson, A. G. & Sellar, R. J., 1991. The influence of needle size and other factors on the incidence of adverse effects caused by myelography. *Clinical Radiology, 44*, 338–341.

1992, *The British Journal of Radiology*, *65*, 1137–1139

Lethal micromelic facial bones sclerosis dysplasia

By D. Müller, *K. Kozlowski, FRACR and †D. Sillence, FRACP

Säuglingsklinik Chemnitz, Germany and Departments of *Radiology and †Genetics, Royal Alexandra Hospital for Children, Sydney, Australia

(Received 25 November 1991 and in revised form 23 March 1992, accepted 6 May 1992)

Keywords: Dysplasia, Newborn skeletal, Osteopenia, Metaphyseal defects, Facial sclerosis

This stillborn female, the third born of unrelated parents, was delivered by spontaneous vaginal delivery at 31 weeks gestation after a pregnancy complicated by polyhydramnios. The birth weight was 2750 g and the length 42 cm. Severe hydrops foetalis was present (Fig. 1).

The mother had been treated for insulin dependent diabetes mellitus for the past 10 years. The first child, delivered at 31 weeks of gestation, died aged 7 days with a diagnosis of diabetic fetopathy. There was neither clinical, radiographic nor anatomo-pathological evidence of bone dysplasia. The second child was normal. The father had no history of bone dysplasia.

At autopsy, severe hydrops foetalis and placentae were present. There were bilateral hydrothoraces and ascites. The subcutaneous fatty tissue was well developed. Minor hepatosplenomegaly (liver 170 g) and struma connata (7 g) were present. Microscopic examination of all tissue except chondro-osseous tissues showed no gross abnormality apart from generalized oedema, moderate amniotic fluid aspiration and lung atelectasis.

The radiographic examination revealed a dense, well ossified spine, base of skull and facial bones. There was poor mineralization of the remaining skeleton. There was rhizomelic shortening of the extremities with markedly shortened and deformed long tubular bones. The ends of the long bones were mushroom-shaped and showed small, round, irregular defects. Some fractures were present in the shafts of the long bones. The short tubular bones of the hands and feet were relatively little affected. The clavicles were not mineralized. The scapulae and the pelvis were poorly mineralized with round, radiolucent defects similar to those in the metaphyses of the long bones. The ribs were thin and only short segments of the posterior parts were demonstrated. They were separated from the spine (Fig. 2).

Chondro-osseous tissues stained with H&E and a silver-stain were reviewed. These showed a relatively normal reserve zone, although most reserve zone chondrocytes had relatively condensed pyknotic often spherical nuclei. Reserve zone matrix was within normal limits. The proliferative zone was foreshortened in all growth plates examined with clusters of proliferative chrondrocytes blending with clusters of hypertrophic chondrocytes with overall expansion of the hypertrophic zone and loss of columniation. The zone of chondro-osseous transformation was accordingly irregular with bridging between primary trabeculae. The primary trabeculae were foreshortened leading abruptly into a zone of intense fibroblastic proliferation with replacement of normal marrow by a fibrocellular matrix. Osteoclasts were prominent throughout this fibroblastic matrix. Cortical bone and osseous trabeculae in many areas were discontinuous forming islands surrounded by the fibrocellular matrix. The close association of osteoclasts with these islands of bone was similar to the appearances seen in osteolytic disorders. These sections

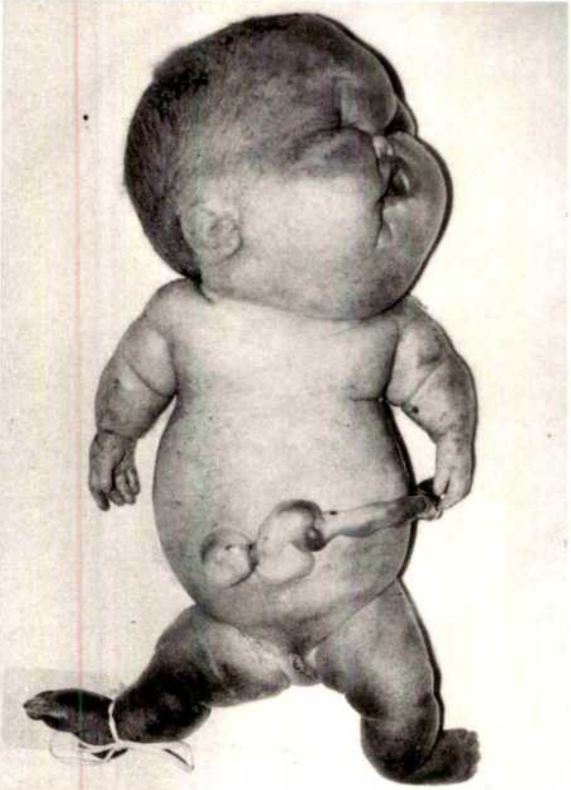

Figure 1. Hydrops foetalis. The abnormal face is predominantly the result of oedema. Shortening of the extremities.

Address correspondence to Dr K. Kozlowski, Royal Alexandra Hospital for Children, Camperdown 2050, New South Wales, Australia.

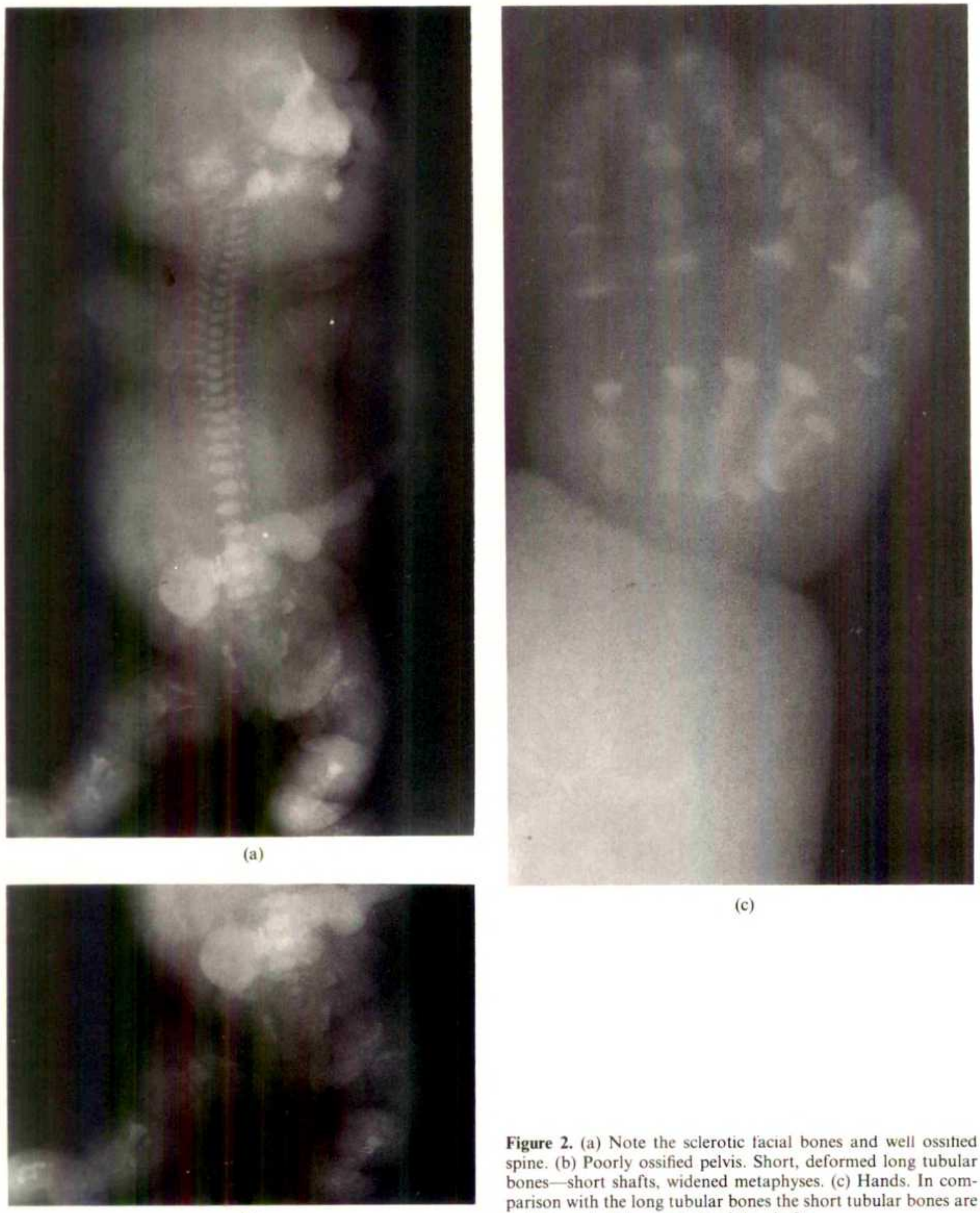

(a)

(b)

(c)

Figure 2. (a) Note the sclerotic facial bones and well ossified spine. (b) Poorly ossified pelvis. Short, deformed long tubular bones—short shafts, widened metaphyses. (c) Hands. In comparison with the long tubular bones the short tubular bones are well formed. Sclerotic ends of the shafts.

showed evidence of an osteochondrodysplasia in which the epiphyseal and growth plate cartilage were abnormal, but the most abnormal pathology, *i.e.* the osseous pathology, had close similarities to the changes in hyperparathyroidism (osteitis fibrosa cystica) or the "generalized" osteolytic disorders such as the

Winchester syndrome. The cartilaginous abnormalities were similar to the pathologic disturbance in opsimodysplasia and some metaphyseal dysplasias.

Discussion

This newborn represents a new hitherto undescribed case of lethal newborn skeletal dysplasia.

There is a superficial resemblance of this stillborn infant to osteogenesis imperfecta Type IIA and hypophosphatasia and to a lesser extent to a severe form of metatropic dysplasia, fibrochondrogenesis, opsismodysplasia and achondrogenesis. All these entities can be easily excluded both on X-ray examination and microscopic chondro-osseous analysis.

The severe, fatal, osteogenesis imperfecta Type IIA (Sillence, 1988) is characterized by generalized osteopenia, thick ribs with multiple fractures and platyspondyly and short broad long bones which are characteristically compressed and have a "concertina" appearance. Central osteosclerosis, deficient rib ossification and well developed vertebral bodies are distinguished in this present infant from OI Type II.

While the fibrous medullary matrix is suggestive, congenital osteitis fibrosa cystica due to fetal hyperparathyroidism usually shows more asymmetric changes in the fetal skeleton. It may result from a fetal response to maternal hypoparathyroidism or hyperparathyroidism in the fetus of a normal mother where the fetus has inherited paternal idiopathic hypercalcaemia.

The congenital, lethal form of hypophosphatasia may show extreme delay in bone mineralization, but then the axial skeleton is also affected and the short tubular bones are not spared. The long bones are usually thin and mushroom-like metaphyses are not a feature of hypophosphatasia. Finally, the alkaline phosphatase levels were normal in both the parents (Kozlowski et al, 1976; Caswell et al, 1989).

The severe form of metatropic dysplasia shows severe shortening of the long tubular bones with marked metaphyseal flaring. However the long bones show no fractures and the mineralization of the skeleton is normal. The bones of the cranial vault and the clavicles are well developed. Finally, generalized platyspondyly is a characteristic feature of metatropic dysplasia, a feature absent in our case (Kozlowski et al, 1976).

Shortened tubular bones with metaphyseal flare are features of fibrochondrogenesis. All the bones are well mineralized and the peculiar pear-shaped platyspondyly is a distinctive feature of the disease. The cartilage histopathology is distinctive with spindle like chondrocytes arranged in a fibrinous matrix (Eteson et al, 1984).

Opsismodysplasia is characterized by shortening of the diaphyses and considerable irregularities of enlarged metaphyses. The most characteristic feature is extreme shortness of the short tubular bones. The metacarpals, metatarsals and phalanges show the epiphyseal and the non-epiphyseal ends of the shafts which are cup-shaped. There is also a severe platyspondyly. The histopathology is similar but different (Maroteaux et al, 1984).

Achondrogenesis Type I shows a well mineralized skeleton with the exception of the vertebral bodies. There is extreme shortening of the long tubular bones. The femora and the iliac bones are almost round-shaped and project spurs which gives them a star-like appearance (Buyse, 1990).

Severe diabetic foetopathy may present radiologically as the Caudal Regression syndrome. It is characterized radiologically by variable sacral malformations (Carlo et al, 1982). No sacral deformity was present in our case.

In conclusion, the newborn reported here represents a new lethal newborn skeletal dysplasia with distinctive radiographic features and characteristic microscopic chondro-osseous appearances. As the facial bones are most affected by the sclerotic changes we propose for this condition the name "lethal micromelic facial bones sclerosis dysplasia".

References

Buyse, M. L., 1990. *Birth Defects Encyclopedia 1990*, (Blackwell Scientific Publications, Dover, MA) pp. 8–10.

Carlo, W. A., Kliegman, R. M., Dixon, M. S., Fletcher, B. D. & Fanaroff, A. A., 1982. Vertebral agenesis. *American Journal of Diseases of Children, 136*, 533–537.

Caswell, A. M., Russell, R. G. R. & Whyte, M. P., 1989. Hypophosphatasia pediatric forms. *Journal of Pediatric Endocrinology, 3*, 73–139.

Eteson, D. J., Adomian, G. E., Ornoy, A., Koide, T., Sugiura, Y., Calabro, A., Lungarotti, S., Mastroiacovo, P., Lachman, R. S. & Rimoin, D. L., 1984. Fibrochondrogenesis: radiologic and histologic studies. *American Journal of Medical Genetics, 19*, 277–290.

Kozlowski, K., Sutcliffe, J., Barylak, A., Harrington, G., Kemperdick, H., Nolte, K., Rheinwein, H., Thomas, P. S. & Uniecka, W., 1976. Hypophosphatasia: review of 24 cases. *Pediatric Radiology, 5*, 103–117.

Kozlowski, K., Campbell, J., Anderson, B., Erken, E. H. W., Jequier, S., Nelson, M., Sliman, N., Sprague, P. & Tamaela, L. A., 1988. Metatropic dysplasia and its variants (analysis of 14 cases). *Australasian Radiology, 32*, 325–337.

Maroteaux, P., Stanescu, V., Stanescu, R., Le Marec, B., Moraine, C. & Lejarraga, H., 1984. Opsismodysplasia: a new type of chondrodysplasia with predominant involvement of the bones of the hand and the vertebrae. *American Journal of Medical Genetics, 19*, 171–182.

Sillence, D. O., 1988. Osteogenesis imperfecta: nosology and genetics. *Annals of the New York Academy of Sciences, 543*, 47–61.

1992, *The British Journal of Radiology*, *65*, 1140–1142

Non-endoscopic per oral biliary stent insertion

By J. Singanayagam, MB, BS, FRCS (Ed), H. K. Chow, MB, ChB, FRCR, FFRRCS (I) and D. J. West, MB, ChB, FRCR

Department of Diagnostic Radiology, City General Hospital, London Road, Newcastle-under-Lyme, Staffordshire ST4 6QG, UK

(*Received 4 February 1992 and in revised form 29 May 1992, accepted 22 June 1992*)

Keywords: Polya gastrectomy, Obstructive jaundice, Cholangiogram, Biliary stricture, Biliary stent

We describe a new technique of biliary stent insertion which is particularly suitable for patients with previous gastric surgery where endoscopic or combined endoscopic and percutaneous biliary stent insertion would be technically difficult.

Case report

A 64-year-old lady with previous history of palliative polya gastrectomy for antral carcinoma presented with obstructive jaundice due to recurrent tumour. Under local anaesthesia and light sedation a percutaneous transhepatic approach was made into the dilated right intrahepatic biliary tree using a van Sonnenberg two part needle. A percutaneous transhepatic cholangiogram confirmed a dilated biliary tree, occlusion of the common bile duct and multiple stones in the gallbladder (Fig. 1). A hydrophilic guide wire (150 cm long, 0.035″ diameter, Radifocus angled type from Terumo Corporation, Tokyo) was manipulated through the occluded segment of the common bile duct into the proximal duodenal loop. A 110 cm long 5 F cobra catheter was inserted over the guide wire and was used to steer the guide wire through the gastro jejunal anastomosis into the stomach and thereafter through the gastro oesophageal junction into the oesophagus and mouth (Fig. 2). The hydrophilic guide wire was removed and replaced by a 400 cm long guide wire (Cotton Leung Biliary Stent from Wilson-Cook Medical, Inc.). A 10 F biliary stent was passed over the guide wire and cobra catheter in retrograde fashion with the aid of a pusher catheter and positioned at the site of the biliary occlusion (Figs 3 & 4). Injection of contrast into the biliary tree showed free drainage of contrast through the stent into the duodenal loop (Fig. 4). Adequate biliary drainage was maintained with no immediate or early complications. The screening time for the whole procedure was 6 min and the technique proved to be just as simple and quick as a totally percutaneous approach.

Discussion

Insertion of stents by the endoscopic or percutaneous route is the preferred treatment for most patients with neoplastic biliary strictures. The endoscopic route of stent placement utilizes the natural passages of the body, avoids liver puncture and has been shown to be safer than the percutaneous route (Speer et al, 1987). However, the percutaneous route has been shown to be more successful in negotiating difficult strictures, especially those in the hilar region where it would be

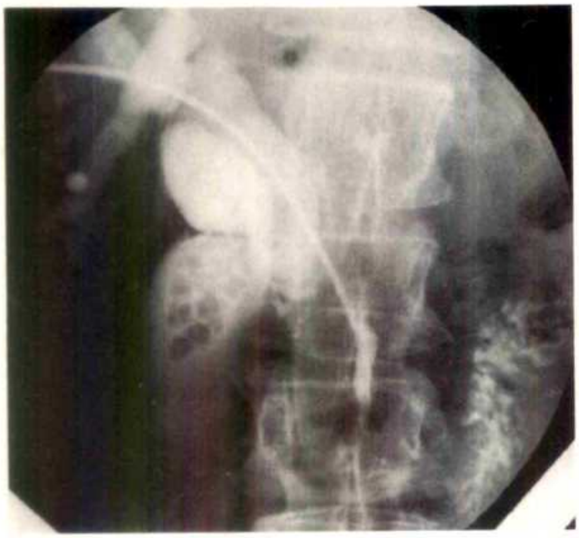

Figure 1. Percutaneous transhepatic cholangiogram showing occlusion of common bile duct, dilated biliary tree and multiple gallstones in the gallbladder.

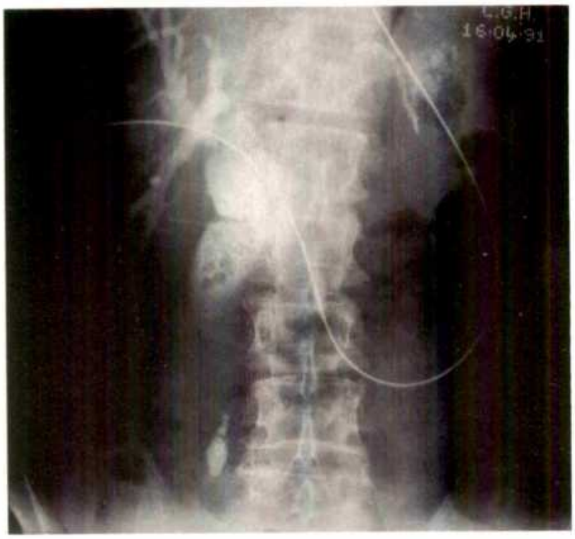

Figure 2. Cobra catheter inserted through biliary structure into stomach, oesophagus and mouth.

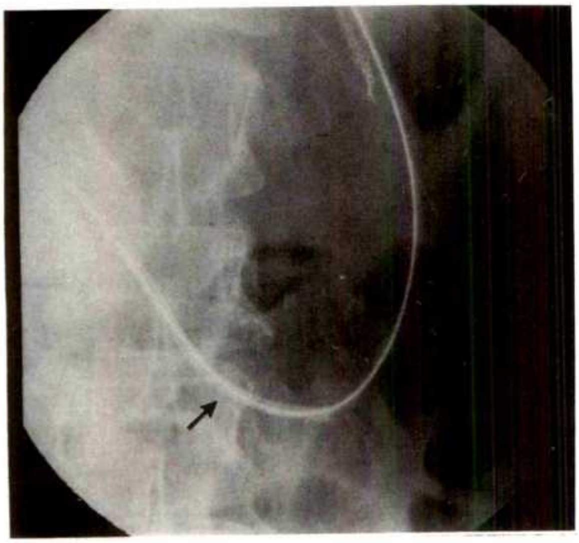

Figure 3. Biliary stent insertion in retrograde fashion using a pusher catheter.

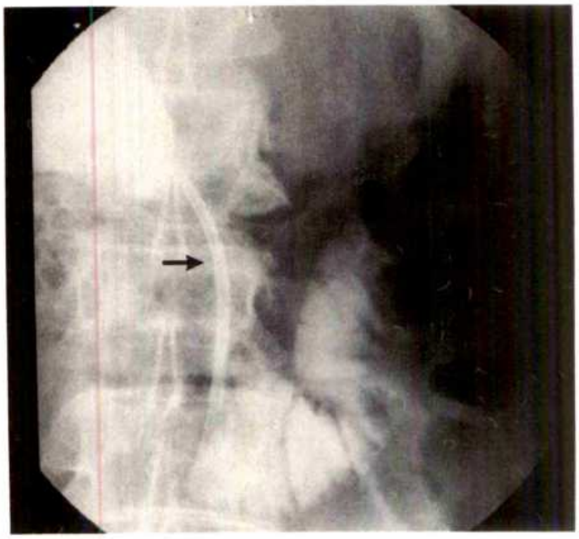

Figure 4. Biliary stent positioned in place at site of biliary stricture. Free drainage of contrast seen through the stent into the duodenum.

necessary to drain both lobes of the liver to prevent cholangitis (Dooley et al, 1984; Stoker et al, 1985; Lammer et al, 1986; Gibson et al, 1988; Huibregtse et al, 1988; Lameris et al, 1987).

To overcome difficult strictures but avoid the complication of a large liver puncture some centres have advocated a combined approach. Here a guide wire and catheter are passed by the percutaneous transhepatic route through the occlusion into the duodenum and retrograde insertion of endoscopic stent is carried out.

The most recent advance in hepato-biliary interventional radiology has been the introduction of self-expanding metallic endoprostheses (Dick et al, 1989; Irving et al, 1989). Some of these stents which are made of closely woven mesh of stainless steel (Wall stent, Medinvent SA, Lausanne) are relatively resistant to tumour ingrowth and have a lower occlusion rate (Adam, 1990). They are introduced over a catheter (7 French gauge) percutaneously and when released expand and achieve a maximum internal diameter of 10 mm. As the introducing catheter is smaller than most internal/external drainage catheters it eliminates most of the problems associated with percutaneous stent insertion. However, the major disadvantage of this stent at present is its high cost which prevents its routine use in all centres. Obviously, if the occlusion rate of the metallic stent is significantly lower then the initial cost of metallic stents would be outweighed by the added cost of reinsertion of plastic stents.

The endoscopic and combined methods of stent insertion are successful in the majority of patients with biliary strictures (Robertson et al, 1987; Speer et al, 1987). However, in patients following previous gastric surgery like polya gastrectomy, it may prove technically difficult and time consuming to negotiate the gastro jejunal anastomosis, enter the proximal duodenal loop and line up the approach to allow stent insertion by these methods.

The method we have described would be useful in selected difficult patients, especially following gastric surgery, as an alternative method of stent insertion avoiding the technical difficulties of the endoscopic and combined methods and the increased morbidity of the percutaneous method. Although a 10 F stent was used in this patient, as this was the only size available at the time, this method will also allow the use of much larger plastic stents and both self-expanding and balloon expandable metallic stents thus reducing the incidence of stent occlusion. The 5 F catheter used in this patient could be replaced by a 4 F catheter thus enabling significant reduction in the size of the liver puncture compared with percutaneous stent insertion alone.

With practice and experience it may be possible to use this technique in patients with normal anatomy thereby significantly reducing the costs and the logistical difficulties of organizing two separate clinical teams (gastroenterology and radiology) together for the combined approach.

References

Adam, A., 1990. Percutaneous biliary drainage for malignancy—an expanding field. *Clinical Radiology*, *42*, 225–227.

Dick, R., Gillams, A., Dooley, J. S. & Hobbs, K. E. F., 1989. Stainless steel mesh stents for biliary strictures. *Interventional Radiology*, *4*, 95–98.

Dooley, J. S., Dick, R., George, P., Kirk, R. M., Hobbs, K. E. F. & Sherlock, S., 1984. Percutaneous transhepatic endoprosthesis for bile duct obstruction. *Gastroenterology*, *86*, 905–909.

Gibson, R. N., Yeung, E., Hadjis, N., Adam, A., Benjamin, I. S., Allison, D. J. & Blumgart, L. H., 1988. Percutaneous transhepatic endoprosthesis for hilar

1992, *The British Journal of Radiology*, *65*, 1142–1144 *Case reports*

cholangiocarcinoma. Value in patients unsuitable for surgical resection or bypass. *American Journal of Surgery*, *156*, 363–367.

Huibregtse, K., Katon, R. M. & Tytgat, G. N., 1988. Endoscopic management of biliary and periampullary cancer. In *Surgery of the Liver and Biliary Tract*, ed. by L. H. Blumgart (Churchill Livingstone, Edinburgh), pp. 889–896.

Irving, J. D., Adam, A., Dick, R., Dondelinger, R. F., Lunderquist, A. & Roche, A., 1989. Gianturco expandable metallic biliary stents; results of a European clinician trial. *Radiology*, *172*, 321–326.

Lameris, J. S., Stoker, J., Dees, J., Nix, D. A. F. F., van Blankenstein, M. & Jeekel, J., 1987. Non-surgical palliative treatment of patients with malignant biliary obstruction—the place of endoscopic and percutaneous drainage. *Clinical Radiology*, *38*, 603–608.

Lammer, J. & Neumayer, K., 1986. Biliary drainage endoprostheses: experience with 201 placements. *Radiology*, *159*, 625–629.

Robertson, D. A. F., Ayres, R., Hacking, C. N., Shepherd, H., Birch, S. & Wright, R., 1987. Experience with a combined percutaneous and endoscopic approach to stent insertion in malignant obstructive jaundice. *Lancet*, 1449–1452.

Speer, A. G., Russel, R. C. G., Hatfield, A. R. W., Macrae, K. D., Cotton, P. B., Mason, R. M., Leung, J. W. C., Houghton, J. & Lennon, C. A., 1987. Randomised trial of endoscopic versus percutaneous stent insertion in malignant obstructive jaundice. *Lancet*, *ii*, 57–62.

Stoker, J., Dees, J., van Blankenstein, M. & Nix, G. A. J. J., 1985. Results of endoscopic stenting in malignant strictures of the biliary tract. *Gut*, *26*, AM35.

Yolk sac tumour of the testis in childhood

By V. Thava, MRCPI, FRCR, *N. Cooper, MB, ChB and J. A. Egginton, DCH, FRCR

Departments of Radiology and *Pathology, North Staffordshire Hospital Centre, City General Hospital,
Stoke-on-Trent ST4 6QG, UK

(Received 17 February 1992 and in revised form 26 May 1992, accepted 22 June 1992)

Keywords: Yolk sac tumour, Testis, Ultrasound

Despite being a rare neoplasm, yolk sac tumour is the commonest of all childhood testicular malignancies. Early detection and treatment result in an excellent prognosis. Ultrasound can play a valuable role in differentiating benign and malignant forms of testicular pathology at any age. Detailed description of ultrasonic appearances of specific tumours with pathological correlation is, however, as yet incomplete.

Case report

A 13-month-old child was admitted with a scrotal swelling that was thought by the mother to have been present since birth but had increased considerably in size over the previous 4 weeks. Clinical examination revealed a large, tense, non-tender swelling which did not transilluminate. A complicated hydrocele was suspected.

Testicular ultrasound was performed with a 5 MHz probe. The lesion measured 5 × 4 cm and proved to be a well defined, predominantly solid, ovoid mass of generally heterogeneous echogenicity with randomly distributed anechoic spaces. These spaces were mainly round or ovoid with one or two being of more tubular shape, consistent with fluid containing spaces or channels. The background matrix was extremely variable in texture, with a cluster of strikingly hyperechoic foci at the upper pole (Fig. 1a,b). No ultrasonic evidence of infiltration into the adjacent tissues was demonstrated and the right testis was uninvolved. In view of the solid nature of the lesion a left inguinal hemi-orchidectomy was performed.

The bisected testis showed almost total replacement by tumour, consisting of solid yellow tissue, multiple cysts and small haemorrhagic areas (Fig. 2a). On microscopy a heterologous appearance of papillary, microcystic, macrocystic and endodermal sinus types was demonstrated with numerous Schiller-Duval bodies. There were large areas of necrosis and multiple dilated vascular channels. These histological findings are of classical yolk sac pattern (Fig. 2b).

Human chorionic gonadotrophin level was normal at less than 1 IU per litre, but the pre-operative alpha fetoprotein level (AFP) was 95 kilo units per litre (normal less than 9 kU/l). AFP dropped to 22 kU/l 6 weeks after surgery. Chest radiography and contrast enhanced computed tomography (CT) of the abdomen and pelvis performed post-operatively were normal; no evidence was seen of lymphadenopathy. Monthly follow-up of the infant with AFP assay and 6 monthly chest radiographs over a 12 month period have been arranged, followed by 6 monthly AFP estimations for a further year. To date neither radiotherapy nor chemotherapy have been administered.

Discussion

Complicated hydroceles, adherent scrotal hernias, chronic torsions and testicular tumours form most of the differential diagnoses of scrotal swellings which do not transilluminate. They can be difficult to differentiate by clinical examination alone and the value of ultrasonography as a non-invasive investigation in the diagnosis of such scrotal swelling is well documented (Fuse et al, 1990). The incidence of malignant testicular tumours has been quoted as approximately 1 per million in children under 15 years of age (Young et al, 1986),

---

Address correspondence to J. A. Egginton, Department of Radiology, City General Hospital, Newcastle Road, Stoke-on-Trent, ST4 6QG.

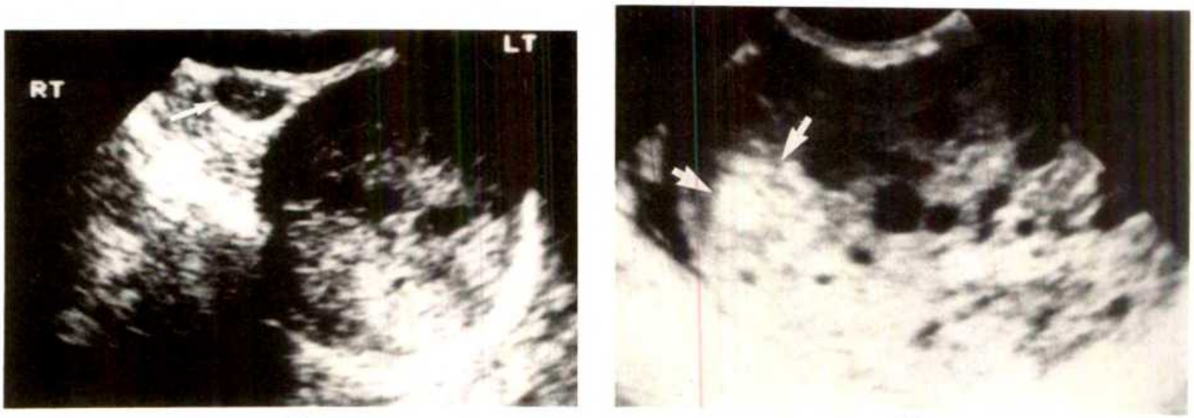

(a) (b)

Figure 1. (a) Ultrasonic appearances of left testicular tumour in transverse section showing mixed echogenicity and anechoic areas. The uninvolved right testis is also shown (arrow). (b) Longitudinal section of tumour showing in addition the hyperochoic foci at the upper pole (small arrows).

and 75% of these testicular malignancies in childhood are yolk sac tumours (Green, 1985). The reported median age at presentation is 17 months, with a right sided predominance of 1.2 to 1 (Kaplan et al, 1988). The usual mode of presentation is as a painless scrotal swelling which does not transilluminate.

Kaplan and others have staged the disease into four categories based on the AFP level and the presence of metastatic spread. Our case would be classed as Stage I as tumour was limited to the scrotum, there was no CT evidence of retroperitoneal spread and a marked (80%) fall in AFP level at the first post-operative follow-up at 6 weeks was recorded. Prognosis for Stage I yolk sac tumour treated by high orchidectomy alone is excellent (Green, 1986). In their report Kaplan et al (1988) found normal AFP levels in 13.8% of their patients with prepubertal yolk sac tumours, but in those cases where it was elevated the AFP was shown to be a reliable indicator of the presence of tumour and, hence, a potentially useful tumour marker. We suggest that in a young, Stage I patient such as ours, particularly exhibiting a rapid fall in the post-operative AFP, more extensive investigation of metastatic spread is not indicated and would only become necessary should recurrence be suspected.

Of 20 patients with testicular tumour evaluated by ultrasound by Fuse et al (1990) only two yolk sac tumours were found. One showed a heterogeneous pattern which was not described in detail, while the other was homogeneous. Yolk sac tumours resemble the rat yolk sac which tends to outgrow its blood supply causing central necrotic areas to develop. Histological findings of multiple sinus types reflect the heterogeneous

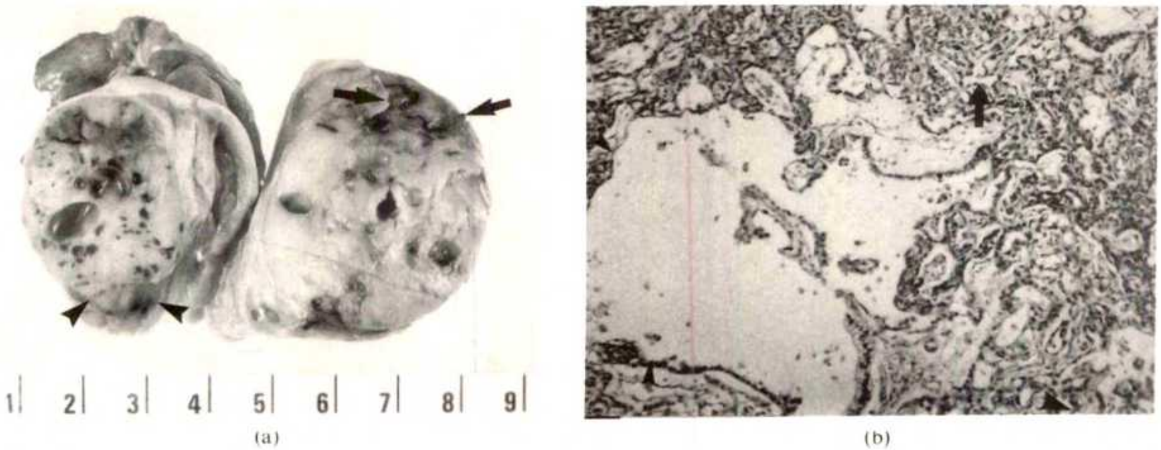

(a) (b)

Figure 2. (a) Bisected testis with attached epididymis showing almost total replacement by tumour, with haemorrhagic (arrows) and cystic (arrow heads) areas. (b) Microscopic section (× 40) showing papillary (large arrow head), microcystic (arrow) and macrocystic (small arrow head) sinus types.

ultrasonic appearance of the matrix in our patient. The Schiller-Duval bodies are characteristic of this type of tumour. The prominent cystic spaces seen on ultrasound no doubt represent the macroscopic cysts, as well as vascular channels and necrotic areas seen in the sections. However, the cause of cluster of hyperechoic foci has not been established. Apart from tumour tissue, only haemorrhagic areas were identified histologically at the upper pole, and there was no fatty tissue to account for it. Avery et al (1991) have recently described a focal hyperechoic appearance on ultrasound in a Leydig cell testicular tumour, the cause of which they were similarly unable to explain histologically. In their patient microscopy was identical to tumour in the other testis which did not however, contain any areas of increased density. The occurrence of reflective foci such as these is not tumour specific.

The normal testis is homogeneous in texture and of moderate echogenicity. In the majority of cases tumour involvement results in a hypoechoic texture replacing part or all of the normal tissue. Leukaemic infiltration in children also frequently produces a diffusely hypoechoic appearance in association with testicular enlargement (Bland et al, 1986) and focal hypoechoic lesions in a heterogeneous matrix have been reported in metastatic neuroblastoma (Casola et al, 1984). A further cause of a swollen, inhomogeneously hypoechoic testis in the newborn is testicular infarction (Zarin et al, 1990), the involved testis also showing a surrounding echogenic rim. Small dense areas due to fibrosis may develop within the infarcted testis (Carrol & Gross, 1983).

Yolk sac tumour is the infantile equivalent of embryonal cell tumour. They belong to a relatively small group which also includes teratomas and teratocarcinomas, having a disorganized hyperechoic pattern and frequently showing cysts of variable size. Embryonal cell tumours tend to the be rather less heterogeneous than teratomas and may contain densely echogenic foci (Schwerk et al, 1987). Recurrent rhabdomyosarcoma has been reported as giving rise to an irregular complex mass of mixed echogenicity (Fowler et al, 1987). A disorganized pattern can also be seen in chronic low grade infection and is often associated with changes in the epididymis.

While it is not possible to make a tumour specific diagnosis on the basis of ultrasound appearance, ultrasound will aid the differential diagnosis and distinguish benign from malignant lesions in the majority of cases.

Acknowledgments

We thank Mr P. Higgins for permission to present his patient, as well as Dr Hill and Dr Stevens for their help.

References

Avery, G. R., Peakman, D. J. & Young, J. R., 1991. Unusual hyperechoic ultrasound appearance of testicular Leydig cell tumour. *Clinical Radiology*, *43*, 260–261.

Bland, P. H., Dipietro, M. A., Chenevert, T. L., Hutchinson, R. J. & Carson, P. L., 1986. Tissue characterisation of the testis using ultrasonic CT. *Radiology*, *159*, 101–105.

Caroll, B. A. & Gross, D. M., 1983. High-frequency scrotal sonography. *American Journal of Roentgenology*, *140*, 511–515.

Casola, G., Scheible, W. & Leopold, G. R., 1984. Neuroblastoma metastatic to the testis: ultrasonographic screening as an aid to clinical staging. *Radiology*, *151*, 475–476.

Fowler, R. C., Chennells, P. M. & Ewing, R., 1987. Scrotal ultrasonography: a clinical evaluation. *British Journal of Radiology 60*, 649–654.

Fuse, H., Shimazaki, J. & Katayama, T., 1990. Ultrasonography of testicular tumours. *European Urology*, *17*, 273–275.

Green, D. M., 1985. *The Diagnosis and Management of Malignant Tumours in Infants and Children* (Martinus-Nijhoff Publishing, Boston).

——, 1986. Testicular tumours in infants and children. *Seminars in Surgical Oncology*, *2*, 156–162.

Kaplan, G. W., Cromie, W. C., Panayotis, P., Kelalis, P., Silber, I. & Tank, E. S., 1988. Prepubertal yolk sac testicular tumours—report of the testicular tumour registry. *Journal of Urology*, part 2, *140*, 1109–1112.

Schwerk, W. B., Schwerk, W. N. & Rodeck, G., 1987. Testicular tumours: prospective analysis of real-time US patterns and abdominal staging. *Radiology*, *164*, 369–374.

Young, J. L., Ries, L. G., Silverbery, E., Horm, J. W. & Miller, R. W., 1986. Cancer incidence-survival and mortality for children under 15 years of age. *Cancer*, *58*, 598–602.

Zerin, J. M., Dipietro, M. A., Grignon, A. & Shea, D., 1990. Testicular infarction in the newborn: ultrasound findings. *Pediatric Radiology*, *20*, 329–330.

1992, *The British Journal of Radiology*, *65*, 1145–1146

Case of the month

Fit and . . . well

By *R. D. Thomas, MRCP and A. J. Gould, FRCR

Department of Radiology, Poole General Hospital, Longfleet Road, Poole, Dorset BH15 2JB, UK

(*Received 25 July 1991 and accepted 4 September 1991*)

Previously fit and well, a 65-year-old gentleman awoke at 3 am with searing interscapular pain. The general practitioner administered morphine and referred him urgently to hospital. On arrival he was found to be pale and sweaty with a mild tachycardia and he refused to move his arms. Physical examination was otherwise unremarkable and, of note, his blood pressure was normal. He was considered likely to have suffered a myocardial infarction though an electrocardiogram (ECG) showed only the tachycardia. A chest radiograph was considered normal by the admitting clinicians.

The "arrest team" was called 2 h after admission and found the patient cyanosed and having a grand mal epileptic attack. He recovered spontaneously.

He continued to complain of severe pain between his shoulders to the extent that the admitting junior staff tentatively diagnosed acute myalgia and requested urgent ESR. Concern that the pain may represent an aortic dissection prompted a request for a mediastinal computed tomogram (CT). The chest radiograph was not available to the radiologist supervising the CT, from which 3 images are reproduced (Fig. 1). Is there any evidence of an aortic dissection? What is your diagnosis?

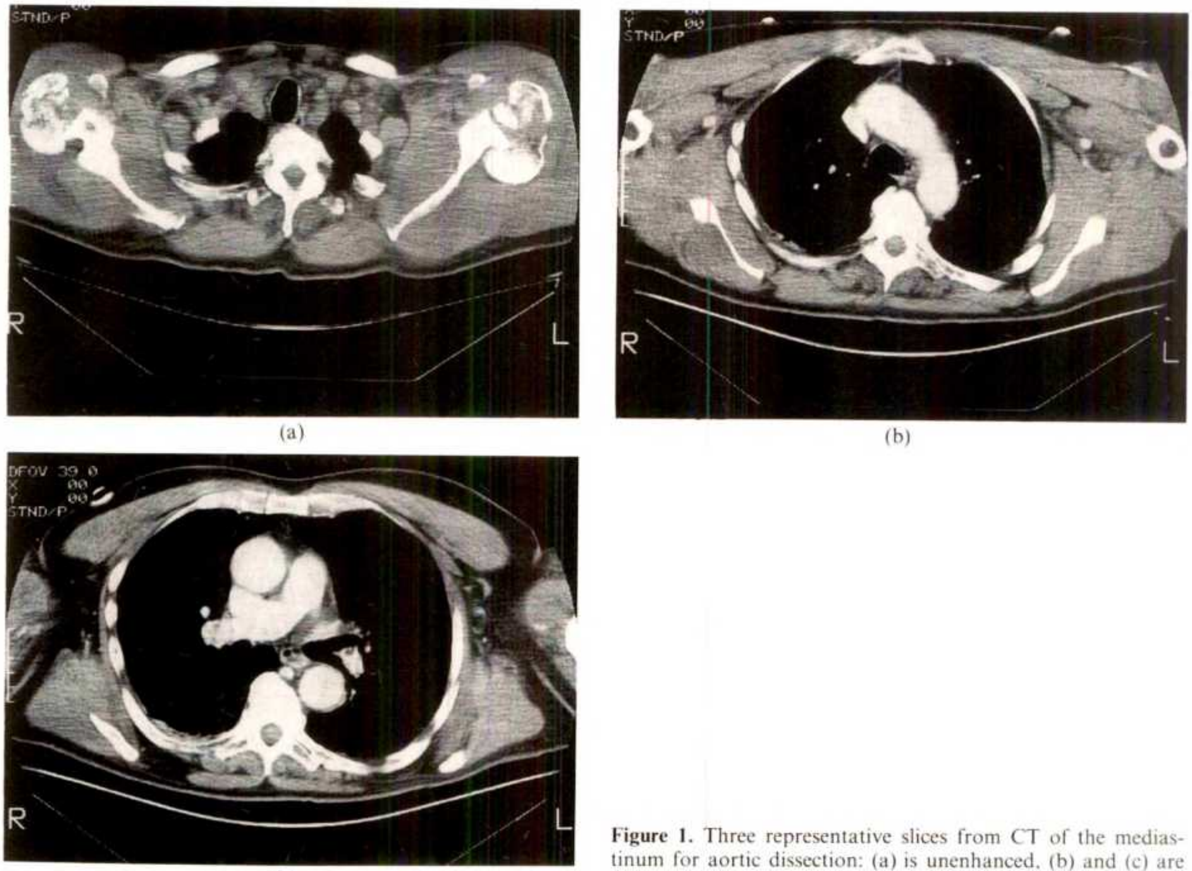

(a)

(b)

(c)

Figure 1. Three representative slices from CT of the mediastinum for aortic dissection: (a) is unenhanced, (b) and (c) are enhanced.

---

*Present address: X-ray Department, Southampton General Hospital, Tremona Road, Southampton, SO9 4XY.

Address correspondence to A. J. Gould.

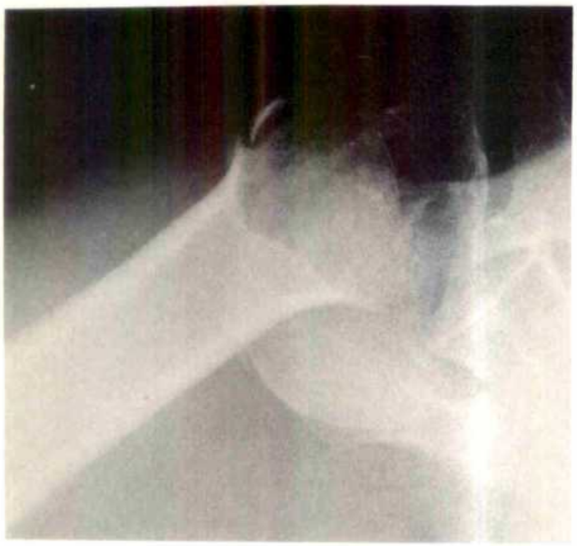

Figure 2. Axial plain radiograph of the right shoulder.

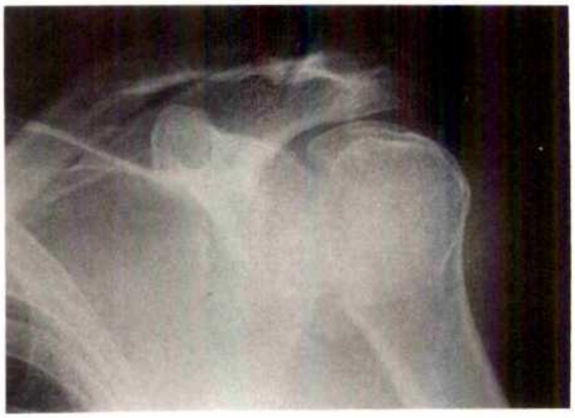

Figure 3. Antero-posterior plain radiograph of the left shoulder.

The aorta is normal and there are no accessory findings (such as pleural fluid) to suggest a dissection. The shoulders, however, can be seen to be fractured (Figs 2 & 3). Plain radiographs of the shoulders are illustrated and show bilateral posterior fracture-dislocation. This is an uncommon event. Dislocation of the shoulders is usually in an anterior direction. Posterior dislocation accounts for perhaps 15% (Samilson & Prieto, 1983) and occurs as a result of violent muscle contraction, the posterior muscle groups being stronger than the anterior.

Bilateral posterior fracture-dislocation of the shoulders are almost all accounted for by two aetiologies: epiletic fits and electric shock, typically historically, electro-convulsive therapy. Trauma more commonly results in a unilateral injury, though bilateral injury may occur. The incidence of ECT induced shoulder injury has been markedly reduced leaving epileptic seizures as the overwhelmingly dominant cause of bilateral fracture-dislocation of the shoulders (Shaw & Kansas, 1971). The association of posterior dislocation with a seizure has long been known (Cooper, 1839) and the first bilateral dislocation due to epilepsy was reported by Coover in 1932. The injury may be the only evidence of a seizure (Pear, 1970). However, it is not widely recognized as a complication of epilepsy and both the fit and resultant injury frequently go undetected for a considerable time.

Keywords: Posterior dislocation, Shoulder joint, Epilepsy

We believe that our patient suffered his first epileptic fit while asleep, injured both shoulders and awoke from his post-ictal sleep as a result of the pain. The right shoulder injury was just visible on the chest radiograph when it was viewed by a radiologist, but unfortunately this film is again unavailable. Missing this subtle radiographic sign, combined with failure to recognize the association of epilepsy with fracture-dislocation of the shoulder, meant that the correct diagnosis was not suspected, despite an epileptic fit being witnessed. Cardiac investigations and CT of the brain were normal.

The final diagnosis is late-onset idiopathic grand mal epilepsy resulting in bilateral posterior fracture-dislocation of the shoulders.

References

COOPER, A., 1839. On the dislocation of the os humeri upon the dorsum scapulae and upon fractures near the shoulder joint. *Guys Hospital Report*, *4*, 265.

COOVER, C., 1932. Double posterior luxation of the shoulder. *Pennsylvania Medical Journal*, *35*, 566.

PEAR, B. L., 1970. Bilateral posterior fracture dislocation of the shoulder—an uncommon complication of a convulsive seizure. *The New England Journal of Medicine*, *283*, 135–136.

SAMILSON, R. L. & PRIETO, V., 1983. Dislocation arthropathy of the shoulder. *The Journal of Bone and Joint Surgery*, *65*A, 456–460.

SHAW, J. L. & KANSAS, T., 1971. Bilateral posterior fracture-dislocation of the shoulder and other trauma caused by convulsive seizures. *The Journal of Bone and Joint Surgery*, *53*A, 1437–1440.

1992, *The British Journal of Radiology*, 65, 1147–1149

Correspondence

(The Editors do not hold themselves responsible for opinions expressed by correspondents)

Fluid levels in a spinal aneurysmal bone cyst following biopsy

Author's reply

The Editor—Sir,

Dr Kessel reports that he has seen a fluid–fluid level in an ABC following which is contrary to the experience expressed in our recent paper (Davies et al, 1992). It is interesting to note that, since the publication of this paper I too have seen a persistent fluid–fluid level in an ABC following biopsy. I would suggest that the presence or absence of a fluid–fluid level will depend on the extent of the biopsy. Dr Kessel states that, in his case, the biopsies were obtained from the lining of the tumour. In that situation it is likely that the internal architecture of the tumour will not have been significantly disturbed hence the persistence of the fluid–fluid levels.

Yours etc.,
A. M. DAVIES

MRI Centre,
Royal Orthopaedic Hospital,
Birmingham

(*Received 18 June 1992 and accepted 25 June 1992*)

Reference

DAVIES, A. M., CASSSAR-PULLICINO, V. N. & GRIMER, R. J., 1992. The incidence and significance of fluid–fluid levels on computed tomography of osseous lesions. *British Journal of Radiology*, 65, 193–198.

Cranial stereotactic multiple arc radiotherapy

The Editor—Sir,

The paper by Thomson & Clegg (1992) does not discuss the verification of the dose calculation on a case by case basis. We presented our method of SMART at the ICR meeting in which we described a procedure for verification of the "full-blown" 3-D dose calculation using a separate, fast program (MUSET), which takes as input the dimensions of the major axes of an ellipsoid. We concur with the authors that the assumption of ellipsoidal shape is reasonable but would like to hear how they verify the accuracy of their computer calculation for each case.

Yours etc.,
D. JONES

Northwest Medical Physics Center,
Roentgen Hall,
21031 67th Avenue,
Lynnwood,
WA 98036, USA
(*Received 13 May 1992 and accepted 8 July 1992*)

References

JONES, D., CHRISTOPHERSON, D. & HAFERMANN, M. D., 1989. A technique for fractionated radiosurgery. Paper No. 766, (ICR, Paris).

THOMSON, E. S. & CLEGG, P., 1992. Cranial stereotactic multiple arc radiotherapy, treatment planning using angiographic images. *British Journal of Radiology*, 65, 317–320.

Authors' reply

The Editor—Sir,

We thank Douglas Jones for his interest in our work. We are glad that their computer program based on a similar principle has been shown to produce good results. With regard to their question about case by case verificaiton, we would refer them to the third paragraph in the Results section of Thomson & Clegg (1992) in which our case by case analysis is discussed. At St Bartholomew's Hospital we also have a "full-Blown" 3-D calculation program based on CT patient data, which is briefly described in the paper. The case by case analysis carried out included a comparison with this program (as described). Since the time of submission, this case by case comparison has continued.

In these relatively early days of stereotactic radiotherapy, second order verification (on a case by case basis) of the three dimensional algorithms used can be considered almost a luxury. Many centres throughout the world, using the "Gamma Knife" technique (Walton et al, 1987), have successfully treated patients over a number of years without such verification.

Yours etc.,
E. S. THOMSON
D. DOUGHTY

Department of Medical Physics & Bioengineering,
Norfolk and Norwich Hospital,
Brunswick Road,
Norwich
NR1 3SR
(*Received 29 June 1992 and accepted 8 July 1992*)

References

THOMSON, E. S. & CLEGG, P., 1992. Cranial stereotactic multiple arc radiotherapy, treatment planning using angiographic images. *British Journal of Radiology*, 65, 317–320.

Walton, L., Bomford, C. K. & Ramsden, D., 1987. The Sheffield stereotactic radiosurgery unit: physical characteristics and principles of operation. *British Journal of Radiology, 60*, 897–906.

Acronyms in bone densitometry

The Editor—Sir,

In response to our publication (Gluer et al, 1990a), Wilson and colleagues (1990) proposed the adoption of a uniform terminology and corresponding abbreviation for Dual X-ray Absorptiometry (DXA).

We supported this suggestion (Gluer et al, 1990b). Since then, the number of papers on DXA has increased considerably. Still, different abbreviations (DEXA, DER, DRA, QDR and DPX) for this technique for bone densitometry are used, several of which are proprietary in origin. DXA is the upgraded version of DPA (Dual Photon Absorptiometry). The nuclear source has been replaced by an X-ray source and this improved technology has gained widespread acceptance and distribution. Recently, similar developments in SPA (Single Photon Absorptiometry) have occurred, which will add yet another abbreviation to densitometry-terminology: SXA for Single X-ray Absorptiometry, not the alternative "SEXA".

Users and manufacturers of these techniques have now joined efforts in an International Standards Committee (Nord et al, 1991). In this Committee, standards of calibration, measurement units and terminology are discussed. There is a general agreement that standard abbreviations for bone densitometry techniques are necessary and the term DXA has been accepted.

Therefore, again we would like to emphasize the use of the acronym DXA for Dual X-ray Absorptiometry and add the acronym SXA for Single X-ray Absorptiometry. When we confine ourselves to SPA, SXA, DPA and DXA, next to QCT for Quantitative Computed Tomography, both researchers and clinicians will understand what we mean.

Still, good acronyms for ultrasound attenuation and velocity measurements and for magnetic resonance measurements, both for quantifying bone mineral density and structure, have to be agreed upon. Acronyms such as QUS for quantitative ultrasound and QMR for quantitative magnetic resonance would be consistent with QCT. Such terminology, however, would clearly need consensus development.

Yours etc.,

H. K. Genant
C. C. Gluer
K. G. Faulkner
S. Majumdar
S. T. Harris
K. Engelke
C. van Kuijk

Osteoporosis Research Group,
Department of Radiology,
University of California San Francisco,
San Francisco,
CA 94143-0628,
USA

(*Received 29 June 1992 and accepted 16 July 1992*)

References

Gluer, C. C., Steiger, P., Selvidge, R., Elliesen-Kliefoth, K., Hayashi, C. & Genant, H. K., 1990a. Comparative assessment of dual-photon absorptiometry and dual-energy radiography. *Radiology, 174*, 223–228.

Gluer, C. C., Steiger, P. & Genant, H. K., 1990b. Reply. *Radiology, 176*, 875-876.

Nord, R. H., Stein, J. A., Mazess, R. B. & Pommet, R. P., 1991. Letter. *Bone Mineral, 13*, 85.

Wilson, C. R., Collier, D., Carrera, G. F. & Jacobson, D. R., 1990. Acronym for dual-energy X-ray absorptiometry. *Radiology, 176*, 875

Latent image fading and mean glandular dose in mobile mammographic screening

The Editor—Sir,

The phenomenon of latent image fading, although well known (*e.g.* Kofler & Gray, 1991) is not often considered as a cause of film optical density variations in conventional radiography because of the short times between exposure and processing normally encountered. In mammography used for breast screening, however, the range of times between film exposure and processing can be much greater than in conventional radiology. When a mammogram is taken at a screening or assessment centre where processing is undertaken on site, the delay will be only a few minutes or less, but when films from mobile breast screening trailers are being returned to the centre for processing on the same working day, the delay could be in the region of 7 h. At some centres, processing of films from mobile units may be carried out on the next working day, giving a delay ranging from approximately 16 h, up to a maximum of 5 days for an extended bank holiday weekend. One reason for using centralized film processing is that the processor can be kept under strict quality control to ensure optimal imaging performance for all films pasing through the centre, but it is possible that this may not be achieved with working practices that can lead to long delays between film exposure and processing.

An investigation was performed into the effect of delayed processing in mammography. Kodak MinR-E film was used and processed on a Kodak M6B processor operating on a 180 second

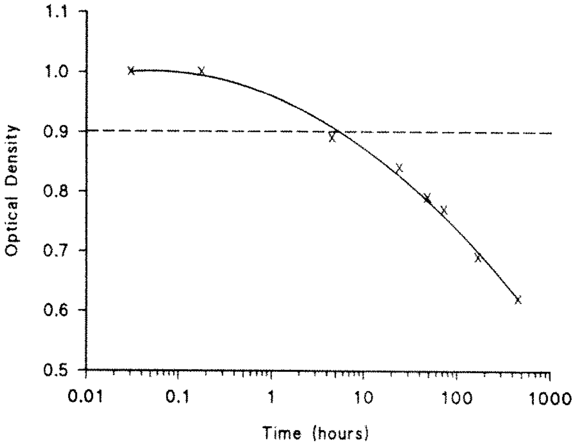

Figure 1. Graph of speed index (optical density of sensitometry step 11) against time between exposure and processing for Kodak MinR-E film with Kodak RP X-omat chemistry. The dotted line shows the lower tolerance limit on this parameter as recommended in IPSM (1989). The tolerance limit is exceeded after approximately 6 h.

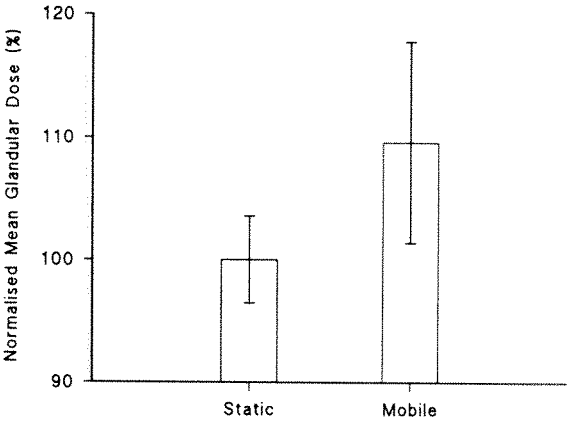

Figure 2. Graph showing the normalized mean glandular dose for units employing immediate and delayed processing. The standard deviations on each mean are also shown.

cycle at 36°C with Kodak RP X-omat chemistry. A number of films were exposed with a green light sensitometer and stored in light tignt conditions. A further sensitometric strip was exposed and processed immediately. At intervals, one of the stored sensitometric strips was processed along with another freshly exposed strip which was used to correct for any variation in processor performance. Strips stored for times between 0 and 456 h were used. After processing, the sensitometric strips were read on a transmission densitometer.

The optical density for the 11th step on the strip (the step giving an optical denstiy closest to 1.0 above base plus fog, commonly used as an indicator of speed for film processor quality control) is shown plotted against a logarithmic time scale in Figure 1. The guidelines for quality assurance in the National Health Service Breast Screening Programme given in the Institute of Physical Sciences in Medicine Report no. 59 (IPSM, 1989) recommend a tolerance of +- 10% on this speed index. The lower tolerance limit is indicated by the dotted line in Figure 1 which shows that this toloerance is exceeded (even for a stable film processor) for delays between exposure and processing greater than approximately 6 h. The value of the maximum slope of the characteristic curve was also calculated for each set of results but was found not to vary significantly.

In practice, latent image fading will be expressed as a drop in speed for films subject to delayed processing. Values of mean glandular dose calculated according to the method described in IPSM Report 59 using data acquired during QA surveys were studied in order to assess the size of this effect. The data were normalized in order to remove the effect of different film processors and target densities for each centre. For each centre, the mean dose for the static units was calculated and defined as 100%. This value was then used to normalize each of the mean glandular dose measurements relating to that centre. The results are shown graphically in Figure 2.

The magnitude of the latent image fading effect in mammography is known to vary between film types (Kimme-Smith et al, 1991), but this study shows that this effect can be a significant factor in practice when attempting to apply stringent quality control in breast screening mammography using X-ray units remote from the central processor. Preliminary studies of the mean glandular dose show a statistically significant difference at the 97½% level of confidence between the doses delivered by static and mobile units. The results obtained suggest that batch processing of films on the same working day as their exposure is to be preferred over longer delays.

Yours etc.,

K. J. Robson
C. J. Kotre
K. Faulkner

Regional Medical Physics Department,
Newcastle General Hospital,
Newcastle-upon-Tyne,
NE4 6BE UK

(Received 10 July 1992 and accepted 10 August 1992)

References

IPSM, 1989. *Commissioning and routine testing of mammographic X-ray systems*. Report No. 59 (Institute of Physical Sciences in Medicine, York).

Kimme-Smith, C., Bassett, L. W., Gold, R. H. & Chow, S., 1991. Increased radiation dose at mammography due to prolonged exposure, delayed processing, and increased film darkening. *Radiology*, *178*, 387–391.

Kofler, J. M. & Gray, J. E., 1991. Sensitometric responses of selected medical radiographic films. *Radiology*, *181*, 879–883.

1992, *The British Journal of Radiology*, *65*, 1150–1153

Book reviews

Physical Properties of Tissue: Comprehensive Reference Book. By F. A. Duck, pp. x + 346, 1990 (Academic Press, London), £30.00.
ISBN 0–12–222800–6
This book is excellent: it is the "Kaye & Laby" and "Geigy Scientific Tables" for those who work or are connected with the medical sciences.

The book consists of nine chapters covering the thermal, optical (including ultraviolet and infrared), acoustic (*i.e.*, ultrasonic), mechanical and electrical properties of tissue; together with the effects of ionizing radiation and nuclear magnetism within tissues. An additional chapter and appendices provide information on tissue composition and perfusion rates. The introduction is essential reading since it sets out the limitations of the information provided. In particular, Francis Duck has made a book reviewer's task easier and quoting from the introduction: "Each chapter is organised in a similar way. Firstly, basic definitions are given of the quantities to be used. No values are tabulated without an associated definition. Standard units are given, together with acceptable alternatives. Simple statements of the theoretical basis of the properties under discussion are also given. Sufficient discussion is included to allow a correct interpretation of the data included in the tables, but without being tutorial in nature. Fuller texts are referenced for those whose knowledge is limited". The book fulfills these objectives clearly and concisely.

The Index is an important feature of such a book and works well, giving both reference to text and tabulated values.

This book is unique and is a valuable source of reference. It is surprising that a similar textbook has not been compiled before—the obvious is often overlooked. Doubtless Francis Duck will continue to wander libraries ensuring that future editions will contain the latest reference value!

This book is highly recommended for all libraries, departments and individuals who have to make use of fundamental data and information.

P. C. Jackson

Contrast-enhanced MRI of the Breast. By S. H. Heywang-Kobrunner, pp. 244, 1990 (Karger AG, Basel), £35.70.
ISBN 3–8055–5293–9
This monograph encompasses the extensive experience and expertise of its author, who has pioneered the technique of magnetic resonance imaging (MRI) of the breast using gadolinium enhancement, and has been eagerly awaited by those who practise in this field. Dr Heywang-Kobrunner's technique uses a 3D gradient echo fast imaging sequence with a slice thickness of no more than 5 mm. Using the special coil, the functional design features of which are fully described, the breast is scanned before and twice after the injection of gadolinium. The method is described in detail within the opening section. This is followed by illustrative examples of breast carcinoma in a number of guises and a wide range of benign conditions. The diagnosis depends not only upon the morphological pattern but also upon the rate and degree of enhancement. The author constantly refers to, and illustrates, the adjunctive role of enhanced MR imaging in relation to mammography and ultrasound in the investigation of breast abnormalities. Applications of the technique are precisely drawn and include the evaluation of palpable abnormalities in negative mammographs which show a dense parenchymal pattern, in markedly asymmetrical mammographic patterns, in the evaluation of scanning after surgery and radiotherapy and in the assessment of breasts containing implants. The very high sensitivity of enhanced MRI in the demonstration of carcinoma is unfortunately counterbalanced by the low specificity. Nevertheless, the author's balanced evaluation presents a compelling case for the selective use of this technique in breast assessment. The national breast screening programme is revealing a large number of cases in which enhanced MRI would be a useful, if expensive, procedure.

G. H. Whitehouse

Musculoskeletal Imaging–MRI, CT, Nuclear Medicine and Ultrasound In Clinical Practice. Ed. by J. A. Markisz, pp. 432, 1991 (Churchill Livingstone, Edinburgh), £90.00.
This is a multi-author American text with the editor contributing to six of the 12 chapters. The first chapter comprising in excess of one quarter of the whole book, is basically a magnetic resonance imaging (MRI) atlas of the joints. The quality of the images is acceptable but these could be found in many of the numerous MRI atlases recently published. There is also an adequate chapter on the principles of MRI but there again, similar chapters are reproduced in almost every MRI text book, regardless of the subspeciality interest.

The remaining chapters review the applications and appropriate uses of the recently developed modalities—computed tomography (CT), ultrasound, nuclear medicine and MRI in musculoskeletal disease. The emphasis is on MRI being the newest and least familiar technique. Whilst this approach is understandable the result is that the coverage of the remaining modalities is limited. The failure to even mention the potential role of ultrasound in the evaluation of congenital dislocation of the hip and irritable hip syndromes is a serious omission as is limited the mention of CT arthrography to just two sentences. On the other hand the MRI chapters are generally good with numerous illustrations of the commoner pathologies.

In conclusion, the problem with this book is that it contains insufficient to be considered authoritative but it is too costly to be used as a basic primer on the subject. Were the publishers to consider a second edition, then the first 110 pages might be put to better use.

A. M. Davies

Fundamentals of Skeletal Radiology. By C. A. Helms, pp. xii + 209, 1989, (WB Saunders, Philadelphia), £25.00.
ISBN 0–7216–2346–8
In his preface, Dr Helms describes his book as "a small compendium of pearls, differential diagnoses and lessons learned in the reality of skeletal radiology". This is indeed true. This is a slim volume of 200 pages, dealing almost entirely with plain film diagnosis of bone lesions. The emphasis is on differentiating features of largely common conditions, nowhere better demonstrated than in the chapter on benign cystic

lesions. Such a potential minefield for the radiologist in training, the subject is considerably simplified and learning greatly facilitated. The chapter on "Don't Touch Lesions" is useful, particularly for those with little experience in the field.

The radiographs throughout, of which there are an abundance (over 250 plates), are excellently reproduced. The text is not meant to provide a complete overview of the subject, but merely an introduction to skeletal radiology, and certainly further reading from a larger textbook will be required. At a price of £25, radiologists wishing to acquaint or reacquaint themselves with basic skeletal radiology would find this book not only readable, but also enjoyable.

P. N. M. TYRRELL

Quantitative Coronary Arteriography. Ed. by J. H. C. Reiber and P. W. Serryus, pp. 385, 1990, (Kluwer Academic Publishers, Dordereft), £97.50.
ISBN 0792309138

This book is essentially the proceedings of a conference held in June 1989 on the progress in quantitative coronary arteriography and related techniques. It consists of a *pot pourri* of topics. Part I, some 132 pages long, considers the problems and solutions in directly measuring coronary arteries and their stenoses. Part 4 considers the methods of measuring coronary flow reserve and their potential pitfalls. Both sections are essentially methodologic and extremely valuable to anyone working in the field. The remainder of this 385 page book consists of a mixture of applications of coronary quantitation, coronary angioscopy and intracoronary ultrasound, the consideration of intracoronary stents, and a brief and now dated review of a variety of recanalization techniques. The final chapter, on the history of coronary arteriography, complete with illustrations taken from the various important publications, is of great interest but unrelated to the rest of the material.

As in the three previous books edited by the same group and with some of the same contributors, the methodological chapters stand out as excellent introductions to their subjects and give well balanced descriptions of the techniques and their roles in cardiology. The majority of the other chapters on intracoronary techniques are good on the descriptions but considerable experience of their use has developed since the chapters were written and the reader would have his appetite whetted, but would not be entirely up-to-date with the role of these various procedures.

M. J. RAPHAEL

Report No 62: Computers in Diagnostic Radiology. Ed. by J. Robertson, P. F. Wankling, K. Faulkner and M. R. Holubinka, pp. iii+164, 1990 (The Institute of Physical Sciences in Medicine, York).
ISBN 0-904181-61-8

This book is a compilation of papers that were presented at a meeting entitled "Computers in Diagnostic Radiology" organized by the Institute of Physical Sciences in Medicine, which was held at Newcastle upon Tyne during 1989. The book consists of 24 chapters from authors who originate mainly from UK centres. At first sight some of the chapters seem sparse with almost 50% being five or less pages in length. However, when grouped together and read in conjunction much useful information can be gained.

In broad terms there are four chapters on patient administration type systems in radiology, 12 chapters on image processing, two chapters on non-imaging uses of computers and four chapters on the use of computers in performance analysis of imaging equipment. There is also a chapter on computer software safety which is becoming more topical and, rather disappointingly, only one chapter, which was very sparse, on PACS.

This book, as one has become used to expect, is a high quality production of well written chapters. This book will certainly appeal to all professions within clinical radiology who require a working knowledge and overview of the use of computers in modern diagnostic imaging departments.

P. C. JACKSON

A Short Textbook of Clinical Imaging. Ed. by D. Sutton and W. R. Young, 1990 (Springer Verlag, Heidelberg), £59.50.
ISBN 3-540-19592-0

This basic text is aimed at the trainee radiologist. Its anglo-american co-editors and several well-known authors from both sides of the Atlantic have produced a comprehensive and readable book that covers general radiology with sections on neuroradiology, obstetric ultrasound and nuclear medicine. It does not aim to cover techniques in radiology but confines itself to the use of the various modalities when dealing with each body system. It is extremely well illustrated incorporating magnetic resonance imaging and colour flow Doppler where appropriate.

Descriptions of conditions are short and not discursive, reference to specialist textbooks would be necessary for lengthier descriptions and more information about most conditions. The text is annotated with several lists: again these are concise and deal with the commonest causes of the radiological appearance in question and happily do not include long lists of esoteric conditions.

In comparison with *A Textbook of Radiology and Imaging* (4th edition), edited by D. Sutton, it is more compact, briefer in description but better illustrated. It is an excellent starting point for a trainee radiologist but would fall far short of the information required by the Fellowship Part 2 candidate. It is an extremely useful book for the department library, particularly where there are radiologists in training. Its strengths are the numerous illustrations and helpful lists, but as it aims to cover all of basic radiology it needs supplementation with specialist books to achieve the required level of knowledge for the Fellowship examination.

N. DESOUZA

MRI Primer. By W. Oldendorf and W. Oldendorf Junior, pp. xiii+222, 1991 (Raven Press, New York), $60.00.
ISBN 0-88167-769-8

This book has been written as an introduction for non-experts to the expanding world of magnetic resonance imaging (MRI). This book will appeal to the non-mathematically inclined since the use of equations is avoided completely. There are 11 chapters, taking the reader through a brief description of the requirements for various clinical imaging procedures and the basic concepts of nuclear magnetic resonance (NMR). Relatively, very little is written on the actual image formation and, for instance, there are no explanations at all about phase and frequency encoding and the use of the 2DFT for image reconstruction. This may not be important for clinical staff who may have only a peripheral interest in the actual image formation process.

The book succeeds well in describing tissue characterization using NMR and many useful analogies are described to help the reader understand the physical processes occurring in the NMR experiment. The authors have invested many words to assist the reader in truly understanding the physical processes occurring in different tissue types.

There are several chapters concerned with the technology used to obtain images and comparisons are made with computed tomography (CT); such text is probably useful for referring physicians in the USA, but probably less appropriate for radiologists in the UK.

It would have been useful if the authors could have maintained a consistency on the use of the Tesla throughout the book without resorting to the gauss: it is very difficulty to make comparisons between magnetic fields from various sources when quoted in different units.

Overall I was pleasantly suprised by this book; it was easy reading and informative. However, the title may be misleading since it is more a description of NMR, with imaging presented as a supplementary item. This book is recommended to all those who do not require an in depth knowledge of the imaging techniques involved in MRI.

P. C. JACKSON

The Radiotherapy of Malignant Disease, (2nd Edn). Ed. by R. C. S. Pointon, 1991 (Springer Verlag, London), £99.50.
ISBN 3-540-19622-6

This book is a useful basic introduction to radiotherapy practice for trainees, particularly at the Manchester school. It describes a didactic approach to radiation technique and treatment policy which will be most helpful in the early stages of training. There are, however, serious disadvantages for those who want to appreciate widely differing treatment philosophies in radiation oncology. The reader is left with the overriding impression that management policies described in this book are recommended because they have been in use for a long period of time, rather than because they have been subject to critical statistical analysis. There are many general statements as to the benefit of a particular technique or dose-fractionation regimen which are not backed up by literature references. Clearly this department has enormous experience and therefore it seems a pity that this book cannot go into more detail with respect to outcome.

The book opens with brief introductions to radiotherapy physics and radiobiology and the trainee will need to rely on the recommendations for further reading at the end of the chapters. The review of Mould Room techniques should have wide appeal and is well illustrated.

The concept of the "optimum dose" is described with clarity. Adherence to a few standard radiotherapy regimens using a small number of fractions and short overall treatment times permits an analysis of outcome with dose-response and morbidity data. I was disappointed that there is not more detailed discussion of this data throughout the chapters dealing with specific disease sites. This book has a particular onus to discuss moderate degrees of late radiation morbidity in detail, bearing in mind the fractionation schedules that are used, and this omission represents a serious shortcoming. For example, the chapter discussing head and neck cancer does not deal with the problem of spinal cord tolerance. Similarly, the chapter on CNS neoplasma gives insufficient analysis of outcome.

Another major philosophy of the Manchester school is to separate the various specialist disciplines in cancer medicine. This is contrary to the training requirements in clinical oncology in the United Kingdom and gives the impression of a fragmented approach to patient management. The radiotherapist requires a knowledge of cancer surgery, medical oncology and continuing care which is not provided in this book. For example, the chapter on oral cancer opens with the statement that there should be medical oncology input into the management of the patient but then fails to make any further mention of the role of chemotherapy. Likewise, the chapter on breast cancer gives a very limited and unbalanced view of the overall management of the patient.

In summary this book is an interesting description of Manchester practice which all trainees in radiotherapy should be aware of but I would not advise them to use it as their main textbook. Thus it will find a place on the library bookshelf rather than in every radiotherapist's office.

D. J. COLE

Guidelines on Patient Care in Radiography (2nd Edn). By C. Gunn and C. S. Jackson, pp. 232, 1991 (Churchill and Livingstone, Edinburgh), £8.95.
ISBN 0-443-04391-4

On a cursory first reading of this edition, the book seemed to have little more to offer than a collection of short notes concerning patient care in a radiographic department. However, deeper reading revealed a systematic and concise quick reference work, not only useful to student radiographers for whom the book is intended but to anyone having recourse to work within the fields of radiography/radiotherapy.

25 relatively short chapters proved to contain a wealth of information on subjects as divers as hygiene and radiographic contrast agents to transport and the unconscious patient. Included in these sections is an excellent newcomer to this edition, Chapter one, outlining not only departmental and local organization but also organization at national level, taking into account recent changes in the NHS set out in the White Paper. Information on computer data gathering technology systems and Korner Units as well as brief notes on COSHH and RIDDOR were included in this section along with a very good piece on hazards in the work place. A little more on informed consent would have been useful and we would point out that the age of consent is 16 years and not 18 years as stated in the book.

The third chapter which dealt with patient psychology was a joy and we are sure this will make new and more experienced members of staff reading it much more aware of the ways in which they approach and deal with patients. It was felt that, whilst racial and ethnic issues were touched upon in this chapter, perhaps a more full account of the needs and problems of particular groups would have been beneficial as would some notes on religious observance. It was also felt that perhaps some notes on the response to death of patients and dealing with relatives and friends as well as one's own emotions in such stressful times, would not have been out of place in this section, particularly for those members of staff working in radiotherapy who have longterm contact with patients and also for staff working in accident and emergency departments.

Chapter four deals with the needs of the unconscious patient very well, though we are of the opinion that in the notes dealing with the sedated patient in the department, especially those who are to undergo lengthy procedures, some mention of the need for pulse oximetry should have been included for the sake of completeness.

We were worried by the notes on page 36 dealing with the lifting and handling of patients and felt that one lift in particular should no longer be advocated as it can be dangerous to both staff and patients alike. We were surprised that no mention of the superb range of hoists and patient lifting equipment was made and felt it would have been useful to emphasize the need for correct lifting training sessions with more diagrams. We felt more diagrams would have been beneficial in the otherwise good section on resuscitation.

The new notes dealing with patients who are suffering from HIV related conditions we thought were particularly well written and non-judgemental in their approach though we wondered why no mention of hepatitis was included. We were cautious about the recommendation for the use of 2% gluteraldehyde for the disinfection of blood spillages as no mention of the toxic nature of this substance or the strict guidelines controlling its use was made. We felt that perhaps this was not the most appropriate substance to recommend for this purpose. We were also concerned about the mention of hypochlorite preparations for general wound care as well as the use of silicone sprays to protect the skin, touched upon in other chapters. We feel that some mention of pre-investigative preparations were lacking *e.g.* antibiotic cover; full blood counts etc., for invasive work.

On the whole we were impressed by the scope of the book, covering as it did such a variety of subjects whilst not getting too bogged down in detail. We understand the difficulties of tackling a broad area such as this and feel that the authors have done a good job. There are of course anomalies which may simply reflect local policy.

We recommend this volume with minimal reservations.

N. A. Franks
J. E. Maynard

Applied Radiobiology and Radiation Protection. By R. Granier and D. J. Gambini. Translated by Roy Lisker, pp. 355, 1990 (Prentice-Hall), £45.00.
ISBN 13-039991-4

This is an important area with much good and competitive literature and this book is aimed at students and practitioners in ionising radiation subjects covering medical and industrial applications. The contents list and index are comprehensive and thus useful. As a translation it retains traces of its Gallic origins and many of the references and official documents quoted tend to be French and not necessarily easily accessible. The subject emphasis is on "applied" rather than academic radiobiology but the authors have included adequate and sufficiently detailed backgrounds of physics and biology to support the text. There is a particularly useful review, in quite good detail, of much of radiotherapeutic and nuclear medicine technology, methods of measurement of natural radioactivity, medical radio-exposure, industrial applications and a particularly fascinating discussion of nuclear explosion and its human consequence.

In addition to the general review in these areas the book becomes a reference manual when seeking the particular. For example there is: a table of procedures to follow in the case of radio-exposure at the onset of pregnancy based on a quite resonable philosophy; tables from the MIRD calculations and sufficient explanation to use these, plus references; useful tables of medical isotopes with their principle emanations. The subject coverage is amazingly comprehensive for a single book and, although rather condensed, the text is still quite readable. Typesetting, particularly the use of bold, uppercase and italics, helps point the way through this compact text and perhaps the only grumble is the variation in print density, particularly on the photo reproduced text in diagrams, which sometimes hinders readability.

In comparison with other books on the subject this one is wide ranging, is particularly good on radiation protection and has surprising details in some areas. It is not as easily read as, for example, Hall's book, but it does have a different emphasis in exploring the practical relationship between man and radioactivity and its attendant consequences. As such, I have found its text tables a useful addition to my stock of radiobiology books.

In summary, this is a good general reference and source book which is wide ranging and up to date and an excellent acquisition for both medical library and laboratory.

A. W. Preece

Deutsches Röntgen-Museum Remscheid-Lennep. By Ulrich Hennig, pp. 128, March 1989 (Georg-Westermann-Verlag, Braunschweig), 10DM.
ISBN 0341-8634

This paperback pocket book is one of a monthly series devoted to the museums of the German-speaking world. Each issue is self-contained and devoted to a single museum.

The book includes a map of the locality, a plan of the museum and details of its opening hours. A chronology of Wilhelm Conrad Röntgen's life is followed by his portrait and a biography, personal and scientific. A brief history of the museum itself introduces the main part of the book, which is a description of the collection. Although an important part of the museum is devoted to the historical heritage of radiology and imaging, and particularly to Röntgen's life and work, the museum's directors have devoted a large proportion of its four buildings to educational exhibits related to the physics and applications of radiation.

There are many high quality illustrations, over half in colour, relating to Röntgen's life and to the exhibits. The book is a pleasure to hold and read, even for someone like myself whose knowledge of the German language is as skeletal as the 1895 radiograph of Frau Röntgen's hand which decorates the front cover. A more fluent reader of German with an interest in radiological history will find the purchase price well worth while.

J. Guy

Meetings and Courses

Screening for Breast Cancer Multi-Disciplinary Courses and Radiologists Specialist Courses
November 30-December 2, 1992, and 2 days Specialist course
Nottingham, UK
Further details: Mrs B Price, Nottingham Breast Screening Training Unit, City Road, Hucknall, Nottingham NG5 1PB. Tel. 0602 691689

Methods for Monitoring Bone Joint Disease
16-17 December 1992
London, UK
Further details: Lucinda Middleton, IBC Technical Services Ltd, Gilmoora House, 57-61 Mortimer Street, London W1N 7TD. Tel. 071 637 4383

Interventional Radiology Update
16-17 January, 1993
Laguna Niguel, California, USA
Further details: Dawne Ryals and Associates, PO Box 1925, Roswell, Georgia 30077-1925, USA. Tel. 404 641 9773

The Bart's/Royal London FRCR II Revision Course (MCQs, Film Reporting and Practice Vivas)
February 9-11, 1993
London, UK
Further details: Mrs J Jessop, Course Secretary, Academic Department of Radiology, St Bartholomew's Hospital, London EC1A 7BE. Tel. 071 601 8864

The Epidemiology of Nutrition and Cancer. An International Course
1-12 March, 1993
Lyon, France
Further details: The Unit of Education and Training, International Agency for Research on Cancer, 150, cours Albert Thomas, F-69372, Lyon Cedex 08, France

Principles and practice of clinical MRI
April 22-25, 1993
Baltimore, Maryland
Further details: Program Coordinator, Johns Hopkins Medical Institutions, Office of Continuing Education, Turner Building, 720 Rutland Avenue, Baltimore, Maryland 21205, USA. Tel. 410 955 2959

Fetal Assessment: Advanced Aspects
11-13 March, 1993
Orlando, Florida
Further details: Program Coordinator, Office of Continuing Education, John Hopkins Medical Institutions, Turner Building 20, 720 Rutland Avenue, Baltimore, Maryland 21205-2195, USA. Tel. 410 955 2959

UCLA: General Radiology Review Course
28 March-2 April, 1993
Marina Del Rey, California, USA
Further details: Mila Wayne, UCLA Medical Center, Department of Radiological Sciences, 10833 Le Conte Avenue, BL-428 CHS, Los Angeles, California, USA. Tel. 310 206 7435

A Fine Needle Aspiration Cytology of the Breast Course
29-30 March, 1993
Nottingham, UK
Further details: Mrs B Price, Nottingham Breast Screening Training Unit, City Road, Hucknall, Nottingham NG5 1PB. Tel. 0602 691689

Second Consensus Development Conference on the Treatment of Radiation Injuries
April 14-17, 1993
Bethesda, Maryland, USA
Further details: Doris Browne, Defense Nuclear Agency, Armed Forces Radiobiology Research Institute, Bethesda, Maryland 20889 5145, USA

Principles and practice of clinical MRI
April 22-25, 1993
Baltimore, Maryland, USA
Further details: Program Coordinator, Johns Hopkins Medical Institutions, Office of Continuing Education, Turner Building, 720 Rutland Avenue, Baltimore, Maryland 21205, USA. Tel. 410 955 2959

International Conference & Course on Stereotactic Radiotherapy/Surgery
6-8 May, 1993
Amsterdam, The Netherlands
Further details: Congress Secretariat, VU Ziekenhuis, Afd. Radiotherapie, Postbus 7057, 1007 MB Amsterdam, The Netherlands.
Tel. 31 20 548 6163

Society of Pediatric Radiology
9-11 June, 1993
London, UK
Further details: Congress Secretariat, Conference Associates and Services Ltd, ESPR, 55 New Cavendish Street, London W1M 7RE. Tel. 071 486 0531

6th International Congress on Interventional Ultrasound
September 7-10, 1993
Copenhagen, Denmark
Further details: C Nolsøe, Department of Ultrasound, Herlev Hospital, University of Copenhagen, DK-2730 Herlev, Denmark

Royal College of Radiologists Annual Scientific Meeting
September 21-25, 1993
Warwick, UK
Further details: Conference Office, The Royal College of Radiologists, 38 Portland Place, London W1N 3DG. Tel. 071 636 4432

RCR Breast Group Mammography Meeting
21-22 October, 1993
Cheltenham, UK
Further details: Conference Office, The Royal College of Radiologists, 38 Portland Place, London W1N 3DG. Tel. 071 636 4432

As a service to our readers, notices of meetings or courses will be inserted free of charge.
Please send information to the The Managing Editor, The British Journal of Radiology, 36 Portland Place, London W1N 4AT.

BJR THE BRITISH JOURNAL OF RADIOLOGY
Established 1896

The Editorial Board

Honorary Editors
D. G. Shaw, FRCP, FRCR (Jan.-Sept.)
D. M. King, MB, BS, FRCR, DMRD (Sept.-Dec.)
F. A. Duck, BSc, MSc, PhD

Diagnostic Radiology
Deputy Editor
D. M. King, MB, BS, FRCR, DMRD (Jan.-Sept.)
G. H. Whitehouse, MB, BS, FRCP, FRCR, DMRD (Oct.-Dec.)

Associate Editors
H. Baddeley, MB, BS, DMRD, FRCR, MRACR
J. B. Bingham, MA, MRCP, MSc, FRCR
A. M. Davies, MB, ChB, DMRD, FRCR
P. Dawson, BSc, PhD, MB, BS, MRCP, MInstP, FRCR
A. H. Freeman, MB, BS, FRCR
P. R. Goddard, BSc, MB, BS, MD, DMRD, FRCR
H. C. Irving, MB, BS, DMRD, FRCR
J. B. Karani, FRCR
J. Pemberton, BSc, MB, BS, MRCP, LRCS, FFR, FRCR,DMRD
A. M. Peters, BSc, MSc, MB, ChB, MD, MRCPath
D. W. Pilling, MB, ChB, DCH, DMRD, FRCR
J. F. Reidy MB, BS, FRCP, FRCR
M. B. Rubens, MB, BS, LRCP, MRCS, DMR, FRCR
P. J. Shorvon, MB, BS, MRCP, FRCR
J. Tudor, MB, BS, FRCR
A. R. Valentine, MB, BS, MRCS, LRCP, FRCR, DMRD
J. Virjee, MB, ChB, FRCR
G. H. Whitehouse, MB, BS, FRCP, FRCR, DMRD (Jan.-Sept.)

Physics and Technology
Deputy Editor
C. K. Bomford, BSc, MPhil, FInstP

Associate Editors
D. R. Dance, MA, PhD, FIPSM
R. M. Harrison, BSc, MSc, PhD, FInstP
P. C. Jackson, BSc, PhD, FInstP, CPhys, FIPSM
R. A. Shields, PhD

Radiotherapy and Oncology
Deputy Editor
D. M. Tait, MB, ChB, MRCP, FRCR

Associate Editors
R. Beaney, BSc, MB, ChB, MD, MRCP, FRCR
P. R. Blake, MD, MB, BS, BSc, FRCR
D. J. Cole, MB, BS, MRCP, FRCR
J. Glaholm, BSc, MRCP, FRCR

Radiobiology
Deputy Editor
J. W. Hopewell, BSc, PhD

Associate Editors
D. Hirst, BSc, PhD
A. J. Mill, BSc, ARCS, PhD
T. E. Wheldon, BSc, PhD, FInstP

Associate Editors Overseas
S. G. A. Chenery, PhD, FCCPM (North America)
B. J. Cremin, MD, FRCR, FRACR (South Africa)
R. Fox, DPhil (Australia)
M. Takahashi, MD (Japan)

Managing Editor: T. R. Hogan, BSc, PhD
Sales and Promotions Manager: H. D. Smith
Production Editor: J. A. Rodd, BA
Publications Secretary: R. Needham, BA, MPhil

© 1992 The British Institute of Radiology

New Series
VOLUME 65
JANUARY TO DECEMBER, 1992

Published by
THE BRITISH INSTITUTE OF RADIOLOGY
36 Portland Place, London W1N 4AT

INDEX TO AUTHORS
1992

A
Abdelwahab, I.F., 14, 485
Aber, C. P., 818
Adam, A., 538
Adams, J. E., 931
Advani, S. H., 935
Aitken, A. G. F., 95
Alcock, C. J., 148
Al-Dawoud, A., 349
Al-Hindawi, M. K., 313
Allan, P. L., 581, 594
Al-Mulhim, F. A., 774
Al-Saigh, A. H., 390
Alvarez, F., 289
Aman, S., 13
Aprill, C., 61
Argent, A. C., 221
Armstrong, P., 438
Arunasalam, M., 190
Ashida, H., 668
Astor, M., 66
Attard-Montalto, S. P., 1114
Avni, E. F., 302

B
Babich, J. W., 787
Baer, H. U., 871
Bal, C. S., 938
Banerjee, A. K., 268
Banerjee, B., 342, 604, 611
Bar Ziv, J., 585
Bard, D. R., 112
Barnes, D. W. H., 910
Barratt, T. M., 137
Barron, J. A., 185
Bates, J. A., 207
Bates, N. P., 460
Battaglia, A. P., 187
Baudouin, C. J., 132
Baum, M., 30
Beale, D. J., 495
Beales, J. S. M., 803
Bearcroft, P. W. P., 947
Bearn, P. E., 556
Bedmarek, D. R., 162
Belton, R. R., 148
Belton, I., 491
Beluffi, G., 348
Berlis, A., 653
Berry, R. J., 1
Bhattacharya, J., 598
Bilbao, J. I., 248
Bishop, M. C., 81
Blake, G. M., 127
Blethyn, A. J., 33
Bloom, R. A., 585
Bloom, P. A., 845
Blumgart, L. H., 871
Bogduk, N., 361
Bomford, C. K., 92
Bongain, A., 63
Bonnett, D. E., 327
Bottomley, F., 564
Boultbee, J. E., 264
Bowler, J. V., 47
Boxer, D. I., 476
Boyes, B. E., 342
Bradley, S. A., 105
Bradley, D. A., 190
Brakel, K., 779
Brenecker, P., 393
Brenner, D. J., 66, 242, 1051
Brettle, D. S., 528
Brown, E. F., 21
Brown, P., 459, 838, 1011
Brueton, R. N., 384
Brunt, A. M., 726
Bryant, D. J., 132
Buckenham, T. M., 545
Bull, A. R., 554
Bulman, A. S., 553
Burwell, N., 1108
Bussaka, H., 140
Butler, P., 1102
Butler-Manuel, P. A., 119, 384

C
Calne, R. Y., 397
Campbell, S., 459, 838
Campbell, I., 943
Carter, S. R., 1093
Carty, H. L. M., 281
Casez, J. P., 895
Cassar-Pullicino, V. N., 193
Castellano, I. A., 878
Catling, M. K., 188
Chalmers, R. T. A., 581
Chammas, M. Y., 774
Chan, D. K. K., 918
Chan, H., 977
Chang, W.-Y., 202
Chapple. C.-L., 225
Chauvel, P., 63
Chen, S.-C., 202
Chen, M., 1035
Cheung, F. K., 918
Choi, B. I., 9
Choji, K., 1035
Chokshi, N. C., 442
Chow, H. K., 1140
Chuang, W.-L., 202
Church, S., 1075
Clarke, O., 268, 598
Clarke, P., 799
Clegg, P., 317
Clements, L., 397
Clements, R., 861
Close, P. J., 729
Cole, D. J., 792
Cole, T. J., 1124
Coleman, N. J., 528
Coles, I. P., 252
Coles, R., 701
Colquhoun, I., 1069
Compston, J. E., 1124
Concha, M., 1086
Condon, B. R., 816
Conford, E. J., 75
Cook, P., 375
Cook, A. M., 507
Cooke, R. S., 1134
Cooper, T., 306
Cooper, P. N., 1042
Cooper, N., 1142
Cope, G. H., 1011
Copping, C., 309, 1055
Cornali, M., 187
Cory, D., 75
Cotty, P., 955
Courdi, A., 63
Cowan, N. C., 940
Cowen, A. R., 528, 818
Cowie, V. J., 1018
Cozens, N. J. A., 594
Craciun, E., 585
Cranage, R. W., 232
Cremin, B. J., 221
Crisp, A. J., 1124
Crump, B. J., 1102
Cull, R. E., 344
Cumberland, D. C., 283

D
Dale, R. G., 252
Dalgleish, S. M., 309, 1055
Dance, D. R., 950

INDEX TO VOLUME 65

Daneman, A., 977
Daneman, D., 977
Das, I. J., 92
Davie, M. W. J., 213
Davies, A. M., 105, 193, 1093, 1147
Davies, P. T. G., 447
Davies, S., 94
Davis, J. B., 517
Dawes, P. J. T. K., 792
Dawson, P., 538
de Boo, T., 857
de Bruyn, R., 137
de Guise, J. A., 273
de la Riva, A., 289
de Vries, E. H., 868
Dean, E. M., 517
Dendy, P. P., 167
Derbyshire, N. D. J., 576
Desai, A., 185
Dhillon, M. S., 722
Dicks-Mireaux, C., 724
Dilhuydy, H. P., 273
Dinshaw, K. A., 935
Dische, S., 87
Dixon, A. K., 167, 397
Dmitrieva, I. A., 1055
Dobrowsky, W., 143
Dobson, M. J., 1042
Doherty, M., 271
Dolberg, M., 968
Dolke, G., 438
Donnell, S., 281
Donnelly, P. K., 1108
Doughty,D., 94, 461, 1147
Dourthe, O., 541
Dowsett, D. J., 1097
duBois, R. M., 983
Duck, F. A., 557
Dudley, N. J., 309, 1055
Duforestel, Th., 63
Duhrrant, K. R., 792
Dunlop, P. R. C., 1018
Dyer, J., 701
Dyet, J. F., 818

E
Eden, O. B., 1114
Edwards, R. D., 453, 538, 1038
Eeles, R., 672
Egginton, J. A., 1142
Eimoto, T., 1040
El Nahas, A. M., 459, 838, 1011
El-Hassan, A. Y., 774
El-Tahir M. I., 390
Engelke, K., 1148
Ennis, J. T., 1097
Errington, R. D., 691
Ettore, F., 63
Evans, J. A., 570
Evans, P. M., 701

F
Faulkner, K., 44, 225, 334, 686, 799, 950, 1148
Fenger, C., 218
Ferraro, M., 701
Ferris, J. D., 845
Finch, J., 327
Finlay, D. B. L., 491
Fiori, P., 348
Fisher, C., 72
Fitzgerald, R., 822
Fitzgerald, M. C., 950
Fitzpatrick, M. M., 137
Floersheim, G. L., 1025
Flower, M. A., 787
Fogelman, I., 127
Fonteille, J., 895
Foo, W., 918
Foreman, N. K., 78
Fouquet, B., 955
Fowler, J., 1093
Franklin, K., 21
Fujimura, Y., 1040
Fumita, N., 1035
Furukawa, Y., 1040

G
Gandhi, M. R., 459, 838
Ganesan, G. S., 175
Gapchenko, E. M., 1055
Garber, S. J., 983
Garcia, C. J., 977
Garvie, N., 803
Gaze, M. N., 1018
Genant, H. K., 1148
George, N. J. R., 172
Gevenois, P. A., 766
Gildersleve, J. Q., 701
Gillard, I., 766
Gillet, J. Y., 63
Ginai, A. Z., 779, 868
Gioanni, J., 63
Glaros, D., 417
Gleeson, F. V., 137, 1102
Glew, D., 306
Gluer, C. C., 1148
Goddard, P. R., 306, 375, 845
Goga, D., 955
Golding, S., 199, 470
Goldstraw, P., 672
Gomi, N., 961
Gonzalez, F. M., 289, 1086
Gordon, H., 609
Gould, A. J., 1145
Goupille, P., 955
Graham, J. D., 157
Grant, D. S., 731
Gray, T. A., 459, 838
Grech, P., 354
Greenough, A., 355, 1083
Gregson, H. S., 81
Gresch, P., 458
Grier, D., 283, 945
Griffiths, P. A., 309, 1055
Grimer, R. J., 193, 1093
Guerrero, R., 289
Gupta, B. D., 722
Gupta, S. K., 769
Gupta, A. K., 938
Guy, R. L., 119, 384, 445

H
Hadas-Halpren, I., 968
Haddaway, M. J., 213
Haddock, J. A. A., 674
Hadley, D. M., 816
Hall, E. J., 66, 242
Hall, K., 1069
Han, J. K., 9
Han, M. C., 9
Hancock, A. P., 878
Hansell, D. M., 674, 852, 983
Haque, Q. M., 604
Harada, K., 662
Hardy, C. C., 1075
Harner, C. L., 157
Harper, W. M., 491
Harrington, M., 309, 1055
Harris, I., 95
Harris, S. T., 1148
Hart, D., 189, 996
Hartley, W., 818
Hartley, R. W. J., 1134
Hartnell, G. G., 283
Hartog, M., 306

INDEX TO AUTHORS—continued

Hatanaka, Y., 140
Hatzikonstantinou, J., 417
Haylor, J., 1011
Heatley, F. W., 119
Hebisch, G., 298
Hemingway, A. P., 351
Hendriks, J. H. C. L., 971
Henshaw, E. T., 552, 952
Hermann, G., 14, 485
Hermus, A. R. M. M., 542
Heron, C., 1049
Heuston, P. M., 425
Hey, E. N., 298
Hiller, N., 968
Hine, A. L., 476, 831
Ho, S. K. W., 905
Ho, J. H. C., 918
Hoeffel, J. C., 1045
Hoeffel, C., 1045
Hofman, P., 56
Holbrook, M. C., 185
Holder, P., 384, 451
Holland, R., 971
Hong, A., 87
Hop, W. C. J., 868
Hopewell, J. W., 152, 792, 910
Horber, F. F., 895
Horton, D., 507
Horwich, A., 672
Hoshika, K., 1040
Hoskins, P. R., 1119
Hounsell, A. R., 321
Howard, C. J., 232
Hsieh, M.-Y., 202
Huda, W., 91
Hughes, P. M., 181, 295
Hughes, D., 754, 758
Hunt, L., 987
Hunter, E. W., 225
Hunter, J. V., 1105
Husband, D. J., 691
Hutchinson, C. E., 822
Hyde, I., 355

I

Ibrahim, E. M., 774
Ikezoe, J., 662
Imamura, K., 668
Inoue, M., 662
Irie, G., 1035
Irving, H. C., 207
Isherwood, I., 39, 758
Ishida, T., 502
Ishikawa, T., 668
Itoh, T., 668

J

Jackson, A., 754, 1042, 1134
Jaeger, Ph., 895
James, J. M., 403, 1075
Janse Van Rensburg, L., 445
Jennings, P., 852
Jimenez-Heffernan, A., 289, 1086
Jindel, R., 938
Johansen, B., 93
Johnson, A. E., 92
Johnson, R. J., 181
Johnson, I. J. M., 1133
Jones, A. C., 271
Jones, D., 1147
Jones, J. A., 175
Jones, M., 281
Jones, T., 697
Junor, E. J., 943

K

Kabala, J., 375
Kalef-Ezra, J., 417
Karani, J., 355, 1083
Karantanas, A., 417
Kase, K. R., 92
Kavarana, N. M., 938
Kean, D., 344
Keevil, S. F., 438
Kelly, C. G., 1018
Kelly, I., 1102
Kenan, S., 485
Kendall, B. E., 1105
Kennedy, C., 137
Kerr, D. J., 349
Kerr, G. R., 1018
Kerslake, R. W., 170
Kessel, D., 556, 1056
Kihara, T., 1040
Kikuchi, Y., 668
Kincaid, W., 453, 1038
King, C. M. P., 827
King, A. D., 831
Kingston, J. E., 827, 1114
Kinsella, D., 85, 681
Kirkbride, P., 510, 833
Kishimoto, R., 1035
Klein, M. J., 14, 485
Klein, H.-M., 1003
Klouvas, G., 417
Knight, C. G., 112
Knowles, S., 349
Knowles, J. F., 910
Kono, M., 502
Korogi, Y., 140
Kotre, C. J., 334, 686, 1148
Kozlowski, K., 1137
Kozuka, T., 662
Kreel, L., 710
Krexner, E., 393
Kronborg, O., 218

L

Laan, R. F. J. M., 901
Lagendijk, J. J. W., 56
Lagrange, J. L., 63
Laidlaw, A., 845
Laird, O., 1097
Lamb, G., 94
Lambilliotte, J. P., 547
Lambrecht, R. M., 787
Lameris, J. S., 779
Lammertsma, A. A., 697
Lamont, R. F., 609
Langston, J. W., 78
Laskey, M. A., 1124
Latre, J. M., 289, 1086
Law, J., 50, 353, 950
Law, M. W. M., 905
Law, S. C. K., 918
Lawinski, C. P., 93, 339, 990
Lawrie, B. W., 33
Le Heron, J. C., 996
Leach, M. O., 885
Leahy, B. C., 403, 1075
Lebensart, P. D., 585
Lee, T. Y., 91
Lee, R. E. J., 225
Lee, A. W. M., 918
Lemieux, R. J., 273
Lemmens, J. A. M., 901
Leonard, R. C. O., 803
Leung, S. F., 710, 905
Levy, P., 585
Lewis, M. M., 14, 485
Lin, Z.-Y., 202
Lindskoug, B. A., 431
Lipton, M. E., 95
Littler, J. A. H., 691
Liu, F. -F., 833
Llamas-Elvira, J. M., 289, 1086

INDEX TO VOLUME 65

Lloyd, M. N. H., 95
Lloyd, J. J., 403, 1075
Loft, S. M., 252
Logie, J., 95
Longo, J. M., 248
Looser, C., 871
Lopez, M. F., 1131
Ludman, C. N., 724
Lund, M. B., 93

M

MacDonald, L. M., 598
MacDonald-Jankowski, D. S., 93, 990
Madden, A., 885
Magee, B., 94
Mahapatra, A. K., 938
Mahmoud, H. H., 78
Majumdar, S., 1148
Malatani, T., 390
Manhire, A. R., 81
Mansilla, F., 248
Mantell, B. S., 355, 814
Maquin, P., 541
Marco, M., 258, 523
Marini, M., 1131
Marsh, J. I., 74
Marshall, N. W., 44, 686, 799
Martel, Y., 273
Martijn, A., 720
Martin, K., 1069
Martinez, M., 289
Martinez-Paredes, M., 1086
Mason, M., 445, 672
Massoud, T. F., 1035
Masterson, J. B., 425, 607
Mateo, A., 289, 1086
Matos, C., 766
Matsumoto, H., 668
Matsuoka, S., 1035
Maughan, T. S., 112
McBride, K., 607
McBruney, A., 1108
McCall, I. W., 213
McCoy, C. T., 425
McDonald, L. M., 268
McGann, G. M., 1102
McGivern, D., 178
McHugh, K., 977
McHugo, J. M., 849
McIntosh, C., 95
McLoughhlin, R. F., 425
McNamara, D., 273
McNicol, M., 476
McRobbie, D. W., 264, 878
Mehta, S., 549
Melsom, H., 93
Merrick, M. V., 803
Metcalfe, C. S., 570
Michael, B. D., 87
Michalowski, A., 731
Miettunen R. H., 238, 551
Miles, K. A., 491, 555, 1056
Millar, J. S., 183
Miller, T. T., 14
Mitchell, M. E., 175
Mitchelmore, A. E., 306
Monks, P. L., 729
Moore, C. J., 321
Moore, N. R., 470
Moore, W. M. O., 987
Moores, B. M., 552, 952
Morcos, S. K., 459, 838, 1011
Morgan, D. A. L., 75
Morgan, H. M., 409
Morgan, R. A., 825
Morris, A. D., 152
Morris, G. M., 152
Morton, E. J., 701
Moseley, I. F., 1105
Moskovic, E., 30
Mosley, J. G., 185
Moxham, J., 940
Muckaden, M. A., 935
Muller, N. L., 74
Muller, D., 1137
Mulvey, P. J., 536
Munk, P. L., 74
Munoz-Galindo, L., 248
Munro, A., 95
Murakami, T., 662
Murali, D., 722
Murchison, J., 95, 594
Murphy, D., 295
Murray, J. G., 1097
Myhre, K. I., 93
Myint, S., 691

N

Nabhan, A. A., 774
Nakajima, Y., 668
Nakamura, H., 662
Nakanishi, K., 662
Namasivayam, J., 761
Nath, A. K., 649
Ng, K. H., 190
Ng, S. H., 918
Nias, A. H. W., 784
Nijs, H. G. T., 779
Norman, P., 85
Norton, A. J., 827
Nzeh, D. A., 987

O

O, S. K., 918
Oates, C. P., 1069
Obhrai, M., 849
O'Connor, S. A., 178
Ogunbiyi, O. A., 390
Ohashi, K., 1040
Okizuka, H., 502
Oldroyd, B., 523
Omojola, M. F., 390
Ott, R. J., 787
Oyama, Y., 668

P

Padhani, A. R., 397
Padley, S. P. G., 852
Page, A., 355
Page, J. E., 545
Page-Thomas, D. P., 112
Pandiscia, A. T., 348
Panizza, B. J., 754
Park, J. H., 9
Parker, S. C., 451
Parkin, G. J. S., 528
Parsons, C., 30, 72
Parsons, D., 306
Pastma, C. T., 857
Patel, U., 181
Patnick, J., 949
Pavlidis, N., 417
Paxton, R. M., 825
Payne, M., 339
Peeling, W. B., 861
Peh, W. C. G., 442
Pellegrini, V., 95
Pemberton, J., 451, 480
Penney, M. D., 861
Perez-Fontan, J., 555
Perkin, G. D., 447
Perry, P. M., 784
Phelps, P. D., 370
Pickuth, D., 672
Pickworth, F. E., 21

INDEX TO AUTHORS—continued

Pietschmann, P., 393
Pillai, R., 1133
Plane, J. H., 717
Platts, A., 1102
Plowman, P. N., 94, 461, 510, 1114
Pocard, B., 1045
Podd, T. J., 187
Pombo, F., 555, 1131
Poon, Y. F., 918
Potter, R., 309, 1055
Powell, T., 449
Papachrysostomou, M., 715
Pradere, B., 541
Pratt, C., 476
Prescott, M. C., 403, 1075
Preston, B. J., 271
Pujara, C. M., 421
Pumphery, C., 672
Putz, R., 653
Pye, S. D., 715
Pye, D. W., 807

R
Rafaelsen, S. R., 218
Railhac, J.-J., 541
Rajah, R., 849
Ramsdale, M. L., 950
Rao, V. S. N., 935
Ratcliffe, J., 459
Rawlings, C., 701
Rebollo, J., 248
Redpath, T. W., 495
Redpath, A. T., 1018
Rees, S., 554
Reid, H., 754
Reiff, D., 545
Reiner, I., 281
Rennison, A., 342, 604, 611
Renwick, M., 298
Resch, H., 393
Reznek, R. H., 827
Rezvani, M., 910
Rhymer, J. C., 264
Richardson, W., 816
Richwood, A. M. K., 281
Rimmer, S., 987
Ritchie, D. A., 178
Robben, S. G. F., 868
Robbins, M. E. C., 910
Roberts, J. T., 792
Robinson, A., 950
Robinson, M. H., 157
Robinson, V. P., 564
Robson, K. J., 334, 1148
Rodesch, F., 302
Rodgers, P. M., 207
Rodriguez, E., 555, 1131
Roebuck, E. J., 949
Rojas, A., 87
Romanowski, C. A. J., 459, 838
Rosenbusch, G. R., 542, 857
Ross, H. B., 929
Rowland Hill, C. A., 1105
Royle, G. J., 1030
Rudin, S., 162
Rugg, T., 87
Ruijs, S. H. J., 901
Ryan, P. J., 127
Ryan, M. V., 425
Rypens, F., 547
Ryzkhov, V. K., 1055

S
Saeki, M., 668
Sagar, S. M., 421
Salisbury, J. R., 940
Sambrook, P., 172
Sandhu, D. P. S., 172
Sandison, G. A., 91
Sansom, J. M., 910
Sato, I., 1040
Saunders, A. J., 724
Scanlan, K. A., 1047
Schultheiss, T. E., 737
Schumacher, M., 653
Schuster, M. R., 1047
Sebag-Montefiore, D., 461
Sethu, A. U., 649
Sharma, O. P., 769
Sharma, S. V.,769
Sharrock, P. J., 321
Shaw, A. J., 321
Sheppard, L., 731
Shields, R. A., 403, 1075
Shirley, I. M, 564
Shrimpton, P. C., 189, 950
Shrivastava, S. K., 935
Siamopoulos, K. C., 417
Sibley, G. N. A., 945
Sidhu, R., 722
Sieber, V. K., 148
Siegel, A., 266
Sillence, D., 1137
Simpson, A. H. R. W., 576
Singanayagam, J., 1140
Singh, D. P., 722
Singhal, R. M., 938
Sintzoff, S. A. Jr, 766
Sissons, G., 681, 861
Smart, H. E., 349
Smith, A. N., 715
Smith, B. D., 309, 1055
Smith, M. A., 438
Sneath, R. S., 1093
Somers, J., 137
Sone, A., 1040
Sood, B., 769
Speller, R. D., 1030
Spencer, J., 199
Sprigg, A., 589
Stain, S. C., 871
Stallenberg, B., 766
Stargardt, A., 1003
Starritt, H. C., 557
Steiner, G. M., 589
Stephens, L. C., 737
Stephenson, B. M., 279
Stinchcombe, S. J., 81
Struyven, J., 547, 766
Stubbs, F., 283
Sugden, E. M., 148
Sugimura, K., 502
Sugiura, M., 502
Sule-Suso, J., 726
Sur, R. K., 722
Susnerwala, S. H., 935
Swindell, W., 701
Swingler, R. J., 344
Symonds, R. P., 943

T
Tait, D., 787
Takahashi, M., 140
Takemori, M., 502
Tarazov, P. G., 1055
Taylor, A. D., 507
Taylor, R. S., 545
Teasdale, E., 761
Terpstra, O. T., 779
Testa, H. J., 403, 1075
Thava, V., 1142
Thien, T., 857
Thomas, G. V., 33
Thomas, S. J., 167
Thomas, R. J., 553
Thomas, R., 609

INDEX TO VOLUME 65

Thomas, R. D., 1145
Thomi, F., 895
Thompson, R. P. H., 451
Thomson, E. S., 317, 1147
Tierney, A. M., 814
Tikkanen, H., 1007
Torres, M., 289, 1086
Tothill, P., 807
Tovar, E., 1131
Trevor, M. M., 717
Triller, J., 871
Troughton, A. H., 825
Tsai, J.-F., 202
Tsao, S. Y., 710
Tu, R. K., 1047
Tung, K. T., 72
Tung, S. Y., 918
Turnbull, L., 344
Twining, P., 455

U
Uchida, J., 1040

V
Valat, J.-P., 955
Valentine, A. R., 1102
Valverde, A., 1086
van den Berg, J. C., 542
Van Gansbeke, D., 547
Van Regemorter, G., 547
van der Vliet, A. M., 720
van Waarde, W. M., 720
van Aalderen, W. M. C., 720
van Aalen, J., 857
van Gelderen, W. F. C., 865
van Erning, L. J. Th., 901
van de Putte, L. B. A., 901
van Riel, P. L. C. M., 901
van Dijck, J. A. A. M., 971
van Kuijk, C., 1148
Vandemerckt, C., 302
Vehmas, T., 1007
Verbeek, A. L. M., 971
Verhest, A., 547
Vermeylen, D., 302
Vidal, E., 289
Vieitez, J. M., 248
Vinall, A. J., 536
Vinnicombe, S., 1049
Vivian, G. C., 21
Vyas, J. J., 935

W
Wade, J. P., 261
Waker, A. J., 258, 523
Walkden, S. E., 187
Walker, J., 581
Walker, T. M., 929
Walker, G. D., 1130
Walkinshaw, S. A., 298
Wall, B. F., 950
Walls, J., 1108
Wang, L.-Y., 202
Wansborough-Jones, M., 1049
Ward, J. W., 1108
Warenius, H. M., 691
Warnock, N. G., 449
Wastie, M. L., 75
Watkin, E. M., 1108
Watson, C. J. E., 397
Wax, M. K., 833
Wayte, S. C., 495
Webb, S., 835
Wells, A. U., 983
Wells, I. P., 825
Welsh, A. D., 232
West, D. J., 1140
Whitehouse, R., 549, 931
Whittingham, T. A., 1069
Wild, S. R., 715
Wilkinson, I. D., 167
Wilkinson, J. M., 321
Wilks, R.,93
Williams, J. R., 188, 1119
Williams, H., 266
Williams, M. P., 681
Williams, M. V., 460
Williams, P. C., 321
Williams, P. H., 351
Willvomseder, R., 393
Wilson, D., 1055
Winkelbauer, F., 393
Winney, R. J., 594
Wong, W. L., 451, 480, 598
Worswick, L., 609
Worthington, B. S., 170
Wraight, E. P., 112, 947
Wright, F. W., 553

X
Xiao, Z. R., 701

Y
Yosef, H., 792
Young, W. T., 33
Young, I. R., 132
Young, C. H., 442
Yuksel, B., 355, 1083

Z
Zammit-Maempel, I., 181, 295
Zhao, S., 39
Zhu, X. P., 39
Zimberger, J., 1045

SUBJECT INDEX
1992

- Radiodiagnosis
  - Bones and joints (excluding skull)
  - Neuroradiology (including skull)
  - Cardiovascular system
  - Respiratory tract
  - Digestive tract
  - Liver and biliary tract, spleen, pancreas
  - Urinary tract
  - Haemopoietic, lymphatic, reticulo-endothelial systems
  - Reproductive system
  - Endocrine system
  - Breast and soft tissues
  - Paediatrics
  - Contrast media and other drugs
  - Apparatus and technical aspects
  - Organizations, statistics and economics
  - Computed tomography (head)
  - Computed tomography (whole body)
  - Computed tomography (apparatus and technical aspects)
  - Interventional radiology
- Ultrasound
  - Clinical aspects
  - Apparatus and technical aspects
- Nuclear medicine
  - Clinical aspects
  - Apparatus and technical aspects
- Nuclear magnetic resonance
- Physics and technology
  - Applied to radiograms
  - Applied to radiotherapy
  - Applied to nuclear medicine
  - applied to magnetic resonance
  - Applied to ultrasound
- Radiotherapy
  - Results and clinical aspects
  - Apparatus and technical aspects
- Cancer chemotherapy
- Radiobiology
  - Applied to radiotherapy
  - Fractionation studies
  - Sensitizers and protectors
  - Other studies
- Hazards and radiation protection
- Lectures and addresses
- Education
- Proceedings
- Book reviews
- Instructions to authors

RADIODIAGNOSIS

Bones and joints

(excluding skull)

CT of a unicameral bone cyst in a rib (Case report), 74
Is the coned lateral lumbosacral junction radiograph necessary for radiological diagnosis? (Correspondence), 94
Computed tomographic assessment of soft tissue abnormalities following calcaneal fractures, 105
Measurement of tibial torsion—a new technique applicable to ultrasound and computed tomography, 119
Measurement of forearm bone mineral density in normal women by dual-energy X-ray absorptiometry, 127
An unusual presentation of pulmonary alveolar microlithiasis and diaphyseal aclasia (Case report), 178
The incidence and significance of fluid–fluid levels on computed tomography of osseous lesions, 193
Bone mineral density in healthy normal women and reproducibility of measurements in spine and hip using dual-energy X-ray absorptiometry, 213
Linear scleroderma and melorheostosis (Case report), 266
An unusual osteochondral body in association with calcium pyrophosphate dihydrate crystal deposition disease (Case report), 271
Relapsing polychondritis (Correspondence), 355
High-intensity zone: a diagnostic sign of painful lumbar disc on magnetic resonance imaging, 361
The role of 3D CT in the assessment of acetabular fractures, 384
The spine deformity index in osteoporosis is not related to bone mineral and ultrasound measurements, 393
New evidence that tamoxifen does not induce osteoporosis: a nuclear activation analysis and absorptiometry study, 417
Radiological features during and following treatment of spinal tuberculosis, 476
The musculoskeletal manifestations of epidermolysis bullosa: an analysis of 19 cases with a review of the literature, 480
Scintigraphic abnormalities in patients with painful hip replacements treated conservatively, 491
The application of microdosimetry in clinical bone densitometry using a dual-photon absorptiometer, 523
The value of ultrasound in the assessment of bone, 589
Use of ultrasound in osteomyelitis, 649
Subluxation of the patella: evaluation of patellar articular cartilage with MR imaging, 662
Gadolinium-DTPA enhanced MRI in neonatal osteomyelitis of the cervical spine (Case report), 720
Patellar metastasis: a rare presentation (Case report), 722
Transverse geniculate ligament of the knee: appearance and frequency on plain radiographs, 766
Evaluation of skeletal metastases, 803
Tuberculosis of the ribs: computed tomographic findings (Case report), 822
A curious case of pelvic calcification (Case of the month), 945
Direct coronal computed tomography of the temporomandibular joint in patients with rheumatoid arthritis, 955
Fluid levels in a spinal aneurysmal bone cyst following biopsy (Correspondence), 1056
Computed tomographic appearances of the pelvis following hindquarter amputation, 1093
Lethal micromelic facial bones sclerosis dysplasia (Case report), 1137

INDEX TO SUBJECTS—continued

Fit and...well (Case of the month), 1145
Fluid levels in a spinal aneurysmal bone cyst following biopsy (Correspondence), 1147

Neuroradiology
(including skull)

The use of MRI in the investigation of spinal cord compression (Correspondence), 187
Diagnosis of brain death: superiority of perfusion studies with ^{99}Tc^{m}-HMPAO over conventional radionuclide cerebral angiography, 289
Peripheral neuropathy simulating lymphoma (Case report), 344
The basal turn of the cochlea, 370
Magnetic resonance imaging and treatment of an unusual seminoma metastasis occurring in the parasellar region (Case report), 445
^{99}Tc^{m} HMPAO SPECT in progressive multifocal leucoencephalopathy (Case report), 447
Increased attenuation value of a colloid cyst of the third ventricle following ventricular decompression (Case report), 449
Magnetic resonance imaging of pulsatile cerebrospinal fluid flow by spatial modulation of magnetization, 495
Prenatal ultrasonographic diagnosis of an aneurysm of the vein of Galen (Case report), 609
Direct and CT measurements of canals and foramina of the skull base, 653
Primary choroid plexus papilloma of the cerebellopontine angle: magnetic resonance imaging, computed tomographic and angiographic appearances, 754
How frequent is chronic lumbar arachnoiditis following intrathecal Myodil?, 758
The prognostic importance of CT features in primary intracranial lymphoma, 761
External carotid angioplasty in the treatment of developing stroke (Case report), 825
Extradural paraganglioma with multiple skeletal metastases (Case report), 938
The Swiss cheese brain (Case report), 1042
The influence of needle size on post-myelography headache: a controlled trial, 1102
Does Myodil introduced for ventriculography lead to symptomatic lumbar arachnoiditis?, 1105
Dural venous sinus thrombosis following myelography: demonstration by magnetic resonance imaging (Case report), 1134

Cardiovascular system

Renal arterial fibromuscular dysplasia: acute renal infarction in three patients with angiographic evidence of medial fibroplasia (Case report), 81
Percutaneous transluminal angioplasty: pain during balloon inflation, 140
Three-dimensional imaging of dual isotope data-sets in a case of acute myocardial infarction (Case report), 273
Anatomy of percutaneous femoral puncture (Correspondence), 283
Impedance plethysmography and thrombo-embolic disease, 306
Contrast extravasation from a Pulse-Tec graft: a complication of high-dose recombinant tissue-type plasminogen activator therapy (Case report), 545
Intracardiac metastases from germ cell tumours—an unusual but important site of metastasis, 672
Digital cardiac imaging—the death knell of cineangiography (Technical note), 818
External carotid angioplasty in the treatment of developing stroke (Case report), 825
Doppler ultrasound scanning in the detection of renal artery stenosis in hypertensive patients, 857
Localized loss of the infrabronchial descending aortic interface as a normal variant, 865
Pelvic phleboliths: is there an association with diverticulitis?, 868
Vascoconstriction by angiographic contrast media in isolated canine arteries, 961
Segmental reversal of intrahepatic portal flow due to a liver metastatis (Case report), 1035
Coil embolization using a saline flush technique (Correspondence), 1055
The assessment of carotid and vertebral arteries; a comparison of CFM duplex ultrasound with intravenous digital subtraction angiography, 1069
Myocardial damage following coronary bypass surgery. Assessment with antimyosin antibody uptake, 1086

Respiratory tract

An unusual presentation of pulmonary alveolar microlithiasis and diaphyseal aclasia (Case report), 178
Computed tomography in agenesis of the lung in infants, 221
Chest radiograph scoring system for use in pre-term infants (Correspondence), 355
The incidence and severity of hypoxia associated with ^{99}Tc^{m} Technegas ventilation scintigraphy and ^{99}Tc^{m} MAA perfusion scintigraphy, 403
A sense of déjà vu (Correspondence), 459
Magnetic resonance imaging of pulsatile cerebrospinal fluid flow by spatial modulation of magnetization, 495
Mistaken hilar mass (Correspondence), 553
The radiology and terminology of cryptogenic organizing pneumonia, 674
The radiological imaging of bronchial atresia, 681
A flexion and extension device for dynamic MR imaging of the neck (Technical note), 816
Portable chest radiography in intensive care: a comparison of computed and conventional radiography, 852
Enlarged mediastinal lymph nodes in the fibrosing alveolitis of systemic sclerosis, 983
^{99}Tc^{m}-Technegas and krypton-81m ventilation scintigraphy: a comparison in known respiratory disease, 1075
Comparison of a subjective and a quantitative assessment of the neonatal chest radiograph, 1083

Digestive tract

Echo pattern of lymph nodes in colorectal cancer: an *in vitro* study, 218
Small bowel fistula secondary to endarteritis obliterans, complicating chemotherapy for small bowel lymphoma (Case report), 349
Diagnosis and treatment of an oesophageal stricture due to lichen planus (Case report), 451
Audit in action: significant reduction of double-contrast barium enema screening time with no loss of examination quality, 507
Now you see it . . . now you don't (Correspondence), 556
The ultrasound appearances of intramural bowel gas: the bright ring appearance and the effervescent bowel. A report of three cases, 585
Anal endosonography: which endoprobe? (Technical note), 715
Pelvic phleboliths: is there an association with diverticulitis?, 868
Demonstration by computed tomography of a case of internal small bowel herniation (Case report), 1045
Caecal herniation through the foramen of Winslow: diagnosis by computed tomography (Case report), 1047

INDEX TO VOLUME 65

Sialography using a paediatric intravenous cannula (Technical note), 1130

Liver and biliary tract, spleen, pancreas

Percutaneous removal of retained intrahepatic stones with a pre-shaped angulated catheter: review of 96 patients, 9
Choledochal cyst and congenital anomalies of the pancreatico-biliary junction: the clinical findings, radiology and outcome in nine cases, 33
An association between leakage of contrast seen on T-tube cholangiogram and subsequent biliary peritonitis (Short communication), 185
Duplex pulsed Doppler sonography in the differential diagnosis of hepatocellular carcinoma and other common hepatic tumours, 202
Hydatid disease of the liver: evaluation of ultrasound and computed tomography, 390
Biliary dilatation and pseudo-tumour of the liver (Correspondence), 458
Splenic cyst: demonstration of the relationship between subcapsular haematoma and false cyst by imaging (Case report), 541
Pancreatic metastasis from renal cell carcinoma (Case report), 547
An audit of ultrasound diagnosis of gallbladder calculi, 581
Ultrasound demonstration of a leaking hydatid cyst of the liver causing "cyst within a cyst" appearance (Case report), 604
The thread and streak sign of portal vein tumour thrombus demonstrated by colour Doppler imaging (Case report), 607
Epitheloid haemangioendothelioma of liver: a vascular tumour easily mistaken for metastatic carcinoma on ultrasound imaging (Case report), 611
Fatty infiltration of the liver: analysis of prevalence, radiological and clinical features and influence on patient management, 774
Accuracy of ultrasound and oral cholecystography in assessing the number and size of gallstones: implications for non-surgical therapy, 779
Staging of hilar cholangiocarcinoma by ultrasound and duplex sonography: a comparison with angiography and operative findings, 871
Percutaneous drainage of splenic abscesses: an effective and safe procedure, 968
Segmental reversal of intrahepatic portal flow due to a liver metastatis (Case report), 1035
Non-endoscopic per oral biliary stent insertion (Case report), 1140

Urinary tract

^{99}Tc^{m}-mercapto acetyl triglycine in paediatric renal tract disease, 21
Renal arterial fibromuscular dysplasia: acute renal infarction in three patients with angiographic evidence of medial fibroplasia (Case report), 81
Duplex Doppler ultrasound in the investigation of occult nephropathy following haemolytic uraemic syndrome, 137
The use of ^{123}I-Hippuran renography in the management of synchronous bilateral upper urinary tract transitional cell carcinomata (Case report), 172
Intrarenal Doppler ultrasound studies in normal and acutely obstructed kidneys, 207
Percutaneous sclerotherapy for simple renal cysts in children (Short communication), 281
Benign non-infected urachal cyst in an adult: review of the literature and a case report, 313
The disappearing bladder—modifying imaging techniques after rectal excision (Technical note), 442
The use of theophylline, an adenosine antagonist in the prevention of contrast media induced nephrotoxicity (Correspondence), 459
Juxtaglomerular cell tumour of the kidney as cause of hypertension: a case report (Case report), 542
Pancreatic metastasis from renal cell carcinoma (Case report), 547
Conventional 15 G needle technique for renal biopsy compared with ultrasound-guided springloaded 18 G needle biopsy, 594
Renal ultrasonographic appearances at presentation in an infant with Lesch-Nyhan syndrome (Case report), 724
Spontaneous disappearance of staghorn calculus (Correspondence), 731
Osteosarcoma metastatic to the kidney with invasion of the inferior vena cava (Case report), 827
Effect of diatrizoate on the function of the isolated perfused rat kidney, 1011
Intrarenal varices mimicking hydronephrosis (Case report), 1038
Clearance of iopamidol, a non-ionic contrast medium, by CAPD in patients with end-stage renal failure, 1108

Haemopoietic, lymphatic, reticulo-endothelial systems

CT evaluation of lymph node status at presentation of prostatic carcinoma, 199
Echo pattern of lymph nodes in colorectal cancer: an *in vitro* study, 218
Small bowel fistula secondary to endarteritis obliterans, complicating chemotherapy for small bowel lymphoma (Case report), 349
Mesenteric lymphadenopathy in idiopathic retroperitoneal fibrosis (Correspondence), 555
The prognostic importance of CT features in primary intracranial lymphoma, 761
Intrathoracic lymphadenopathy and HIV infection (Case report), 940
Hodgkin's disease—a very late recurrence (Case report), 1133

Reproductive system

Magnetic resonance imaging of penile rhabdomyosarcoma (Case report), 175
Carcinoma of the ovary: a diagnostic hitch (Case report), 181
CT evaluation of lymph node status at presentation of prostatic carcinoma, 199
Accuracy of pelvimetry measurements on CT scanners (Technical note), 261
Sonographic detection of neonatal hydrometrocolpos (Case report), 268
Computed tomographic assessment of intraperitoneal fluid distribution prior to intraperitoneal chemotherapy for ovarian cancer, 295
Magnetic resonance imaging and treatment of an unusual seminoma metastasis occurring in the parasellar region (Case report), 445
The value of transvaginal scanning in the assessment of second trimester oligohydramnios (Short communication), 455
The value of magnetic resonance relaxation time in staging ovarian endometrial cysts, 502
The role of hysterosalpingography in modern gynaecological practice, 849

INDEX TO SUBJECTS—continued

Endocrine system

Detection and evaluation of fetal goitre by ultrasound, 302

Breast and soft tissues

Tumour and tumour-like conditions of the soft tissue: magnetic resonance imaging features differentiating benign from malignant masses, 14

Chest radiography in the management of breast cancer, 30

Magnetization transfer contrast (MTC) imaging of skeletal muscle at 0.26 Tesla—changes in signal intensity following exercise, 39

Improved image quality for dense breasts in mammography, 50

Malignant paraganglioma of the mediastinum: a further diagnostic and therapeutic use of radiolabelled mIBG (Case report), 75

Computed tomographic assessment of soft tissue abnormalities following calcaneal fractures, 105

The use of a chelating derivative of alpha melanocyte stimulating hormone for the clinical imaging of malignant melanoma, 112

Magnetic resonance imaging of peritoneal leiomyosarcomatosis (Case report), 170

Magnetic resonance imaging of extracranial head and neck tumours, 375

The musculoskeletal manifestations of epidermolysis bullosa: an analysis of 19 cases with a review of the literature, 480

Intramuscular myxoma: magnetic resonance features, 485

A preliminary investigation of the imaging performance of photostimulable phosphor computed radiography using a new design of mammographic quality control test object, 528

Results from the HAD psychometric questionnaire in 54 breast cancer patients treated with breast conservation (Correspondence), 553

Macrodystrophia lipomatosa: radiographic observations, 769

Localization of impalpable breast lesions using the Hawkins needle (Technical note), 929

^{99}Tc^{m}-Technegas and krypton-81m ventilation scintigraphy: a comparison in known respiratory disease, 1075

Primary leiomyosarcoma of the superior vena cava with massive thrombosis treated by local fibrinolysis (Case report), 1131

Paediatrics

Computed tomography in agenesis of the lung in infants, 221

Results of a survey of doses to paediatric patients undergoing common radiological examinations, 225

Sonographic detection of neonatal hydrometrocolpos (Case report), 268

Percutaneous sclerotherapy for simple renal cysts in children (Short communication), 281

Detection and evaluation of fetal goitre by ultrasound, 302

Dystrophic umbilical artery calcifications in an infant (Case report), 348

Chest radiograph scoring system for use in pre-term infants (Correspondence), 355

Two cases of isolated deficiency of all four limbs diagnosed antenatally with a review of the literature (Case report), 598

Renal ultrasonographic appearances at presentation in an infant with Lesch-Nyhan syndrome (Case report), 724

Comparison of a subjective and a quantitative assessment of the neonatal chest radiograph, 1083

Lethal micromelic facial bones sclerosis dysplasia (Case report), 1137

Contrast media and other drugs

The use of theophylline, an adenosine antagonist in the prevention of contrast media induced nephrotoxicity (Correspondence), 459

Vascoconstriction by angiographic contrast media in isolated canine arteries, 961

Effect of diatrizoate on the function of the isolated perfused rat kidney, 1011

Does Myodil introduced for ventriculography lead to symptomatic lumbar arachnoiditis, 1105

Clearance of iopamidol, a non-ionic contrast medium, by CAPD in patients with end-stage renal failure, 1108

Dural venous sinus thrombosis following myelography: demonstration by magnetic resonance imaging (Case report), 1134

Apparatus and technical aspects

Improved image quality for dense breasts in mammography, 50

Measurement of forearm bone mineral density in normal women by dual-energy X-ray absorptiometry, 127

Bone mineral density in healthy normal women and reproducibility of measurements in spine and hip using dual-energy X-ray absorptiometry, 213

A fine needle aspiration technique using high negative pressure (Technical note), 264

Impedance plethysmography and thrombo-embolic disease, 306

New evidence that tamoxifen does not induce osteoporosis: a nuclear activation analysis and absorptiometry study, 417

Quantitative analysis of CT brain images: a statistical model incorporating partial volume and beam hardening effects, 425

The application of microdosimetry in clinical bone densitometry using a dual-photon absorptiometer, 523

A preliminary investigation of the imaging performance of photostimulable phosphor computed radiography using a new design of mammographic quality control test object, 528

Contrast extravasation from a Pulse-Tec graft: a complication of high-dose recombinant tissue-type plasminogen activator therapy (Case report), 545

Measurement of tissue perfusion by dynamic computed tomography (Correspondence), 554

Digital cardiac imaging—the death knell of cineangiography (Technical note), 818

Portable chest radiography in intensive care: a comparison of computed and conventional radiography, 852

Organization, statistics and economics

What to do with the biopsy specimen—practice in an oncology setting (Technical Note), 72

Computer-based teaching file (Correspondence), 187

Computed tomography in abdominal trauma: an audit of usage and image quality, 397

Increasing patient throughput in magnetic resonance imaging: a practical approach, 470

Audit in action: significant reduction of double-contrast barium enema screening time with no loss of examination quality, 507

What is the clinical disadvantage of discarding old radiographs? Survey of patients not re-examined for a long time, 668

INDEX TO VOLUME 65

Computed tomography
(head)

Quantitative analysis of CT brain images: a statistical model incorporating partial volume and beam hardening effects, 425
Increased attenuation value of a colloid cyst of the third ventricle following ventricular decompression (Case report), 449
Direct and CT measurements of canals and foramina of the skull base, 653
Primary choroid plexus papilloma of the cerebellopontine angle: magnetic resonance imaging, computed tomographic and angiographic appearances, 754
The prognostic importance of CT featues in primary intracranial lymphoma, 761
Appearances of choroidal osteomas with diagnostic imaging, 845
The Swiss cheese brain (Case report), 1042
Demonstration by computed tomography of a case of internal small bowel herniation (Case report), 1045
Caecal herniation through the foramen of Winslow: diagnosis by computed tomography (Case report), 1047

Computed tomography
(whole body)

CT of a unicameral bone cyst in a rib (Case report), 74
Computed tomographic assessment of soft tissue abnormalities following calcaneal fractures, 105
Measurement of tibial torsion—a new technique applicable to ultrasound and computed tomography, 119
The incidence and significance of fluid–fluid levels on computed tomography of osseous lesions, 193
CT evaluation of lymph node status at presentation of prostatic carcinoma, 199
Computed tomography in agenesis of the lung in infants, 221
Accuracy of pelvimetry measurements on CT scanners (Technical note), 261
Computed tomographic assessment of intraperitoneal fluid distribution prior to intraperitoneal chemotherapy for ovarian cancer, 295
Peripheral neuropathy simulating lymphoma (Case report), 344
The role of 3D CT in the assessment of acetabular fractures, 384
Hydatid disease of the liver: evaluation of ultrasound and computed tomography, 390
Computed tomography in abdominal trauma: an audit of usage and image quality, 397
Biliary dilatation and pseudo-tumour of the liver (Correspondence), 458
Measurement of tissue perfusion by dynamic computed tomography (Correspondence), 554
Mesenteric lymphadenopathy in idiopathic retroperitoneal fibrosis (Correspondence), 555
Small cell carcinoma of the prostate (Case report), 726
Tuberculosis of the ribs: computed tomographic findings (Case report), 822
Intrathoracic lymphadenopathy and HIV infection (Case report), 940
Direct coronal computed tomography of the temporomandibular joint in patients with rheumatoid arthritis, 955
Enlarged mediastinal lymph nodes in the fibrosing alveolitis of systemic sclerosis, 983
Fluid levels in a spinal aneurysmal bone cyst following biopsy (Correspondence), 1056
Computed tomographic appearances of the pelvis following hindquarter amputation, 1093
Fit and...well (Case of the month), 1145
Fluid levels in a spinal aneurysmal bone cyst following biopsy (Correspondence), 1147

Interventional radiology

Percutaneous removal of retained intrahepatic stones with a pre-shaped angulated catheter: review of 96 patients, 9
What to do with the biopsy specimen—practice in an oncology setting (Technical Note), 72
Percutaneous transluminal angioplasty: pain during balloon inflation, 140
A fine needle aspiration technique using high negative pressure (Technical note), 264
Diagnosis and treatment of an oesophageal stricture due to lichen planus (Case report), 451
Technique for steel coil embolization of biopsy track for use with the "Biopty" needle (Technical note), 538
Conventional 15 G needle technique for renal biopsy compared with ultrasound-guided springloaded 18 G needle biopsy, 594
External carotid angioplasty in the treatment of developing stroke (Case report), 825
Appearances of choroidal osteomas with diagnostic imaging, 845
Percutaneous drainage of splenic abscesses: an effective and safe procedure, 968
Coil embolization using a saline flush technique (Correspondence), 1055
Primary leiomyosarcoma of the superior vena cava with massive thrombosis treated by local fibrinolysis (Case report), 1131
Non-endoscopic per oral biliary stent insertion (Case report), 1140

ULTRASOUND
Clinical aspects

Ultrasonic detection of parathyroid adenomas (Correspondence), 95
Measurement of tibial torsion—a new technique applicable to ultrasound and computed tomography, 119
Duplex Doppler ultrasound in the investigation of occult nephropathy following haemolytic uraemic syndrome, 137
Duplex pulsed Doppler sonography in the differential diagnosis of hepatocellular carcinoma and other common hepatic tumours, 202
Intrarenal Doppler ultrasound studies in normal and acutely obstructed kidneys, 207
Echo pattern of lymph nodes in colorectal cancer: an *in vitro* study, 218
Sonographic detection of neonatal hydrometrocolpos (Case report), 268
How good is ultrasound in the detection and evaluation of anterior abdominal wall defects?, 298
Detection and evaluation of fetal goitre by ultrasound, 302
Sonographic features in a case of Fitz-Hugh-Curtis syndrome masquerading as malignancy (Case report), 342
Ultrasonic findings in visceral *Pneumocystis carinii* infection in AIDS (Correspondence), 354
Hydatid disease of the liver: evaluation of ultrasound and computed tomography, 390
The value of transvaginal scanning in the assessment of second trimester oligohydramnios (Short communication), 455
Routine radiographer screening for fetal abnormalities by ultrasound in an unselected low risk population, 564
A role for ultrasound in limb lengthening, 576
An audit of ultrasound diagnosis of gallbladder calculi, 581

INDEX TO SUBJECTS—continued

The value of ultrasound in the assessment of bone, 589
Conventional 15 G needle technique for renal biopsy compared with ultrasound-guided springloaded 18 G needle biopsy, 594
Two cases of isolated deficiency of all four limbs diagnosed antenatally with a review of the literature (Case report), 598
Ultrasound demonstration of a leaking hydatid cyst of the liver causing "cyst within a cyst" appearance (Case report), 604
The thread and streak sign of portal vein tumour thrombus demonstrated by colour Doppler imaging (Case report), 607
Prenatal ultrasonographic diagnosis of an aneurysm of the vein of Galen (Case report), 609
Epitheloid haemangioendothelioma of liver: a vascular tumour easily mistaken for metastatic carcinoma on ultrasound imaging (Case report), 611
Use of ultrasound in osteomyelitis, 649
Renal ultrasonographic appearances at presentation in an infant with Lesch-Nyhan syndrome (Case report), 724
Accuracy of ultrasound and oral cholecystography in assessing the number and size of gallstones: implications for non-surgical therapy, 779
Appearances of choroidal osteomas with diagnostic imaging, 845
Doppler ultrasound scanning in the detection of renal artery stenosis in hypertensive patients, 857
Staging of hilar cholangiocarcinoma by ultrasound and duplex sonography: a comparison with angiography and operative findings, 871
Sonography in thyroid carcinoma in children, 977
Prediction of birthweight by fetal ultrasound biometry, 987

Apparatus and technical aspects

A study of the relationship between routine ultrasound quality assurance parameters and subjective operator image assessment, 570
Anal endosonography: which endoprobe? (Technical note), 715
The assessment of carotid and vertebral arteries; a comparison of CFM duplex ultrasound with intravenous digital subtraction angiography, 1069

NUCLEAR MEDICINE

Clinical aspects

^{99}Tc^{m} mercapto acetyl triglycine in paediatric renal tract disease, 21
Malignant paraganglioma of the mediastinum: a further diagnostic and therapeutic use of radiolabelled mIBG (Case report), 75
The use of a chelating derivative of alpha melanocyte stimulating hormone for the clinical imaging of malignant melanoma, 112
The use of ^{123}I-Hippuran renography in the management of synchronous bilateral upper urinary tract transitional cell carcinomata (Case report), 172
Three-dimensional imaging of dual isotope data-sets in a case of acute myocardial infarction (Case report), 273
Diagnosis of brain death: superiority of perfusion studies with ^{99}Tc^{m}-HMPAO over conventional radionuclide cerebral angiography, 289
The role of ^{99}Tc^{m}-HMPAO white cell imaging in suspected orthopaedic infection, 309
The spine deformity index in osteoporosis is not related to bone mineral and ultrasound measurements, 393
The incidence and severity of hypoxia associated with ^{99}Tc^{m} Technegas ventilation scintigraphy and ^{99}Tc^{m} MAA perfusion scintigraphy, 403
^{99}Tc^{m} HMPAO SPECT in progressive multifocal leucoencephalopathy (Case report), 447
Scintigraphic abnormalities in patients with painful hip replacements treated conservatively, 491
Treatment planning for ^{131}I-mIBG radiotherapy of neural crest tumours using ^{124}I-mIBG positron emission tomography, 787
Evaluation of skeletal metastases, 803
Can serum prostate-specific antigen replace bone scintigraphy in the follow-up of metastatic prostatic cancer?, 861
Efficacy of low-dose iodine-131 ablation of post-operative thyroid remnants: a study of 69 cases, 905
Visualization of the axillary vein during ^{99}Tc^{m} methoxy-isobutyl-isonitrile (MIBI) myocardial imaging (Short communication), 947
The role of ^{99}Tc^{m}-HMPAO white cell imaging in suspected orthopaedic infection (Correspondence), 1055
^{99}Tc^{m}-Technegas and krypton-81m ventilation scintigraphy: a comparison in known respiratory disease, 1075
Myocardial damage following coronary bypass surgery. Assessment with antimyosin antibody uptake, 1086

Apparatus and technical aspects

^{99}Tc^{m}-HMPAO SPECT and magnetic resonance studies in L-asparaginase induced cerebrovascular accident (Case report), 78
Three-dimensional imaging of dual isotope data-sets in a case of acute myocardial infarction (Case report), 273
Acronyms in bone densitometry (Correspondence), 1148

NUCLEAR MAGNETIC RESONANCE

Tumour and tumour-like conditions of the soft tissue: magnetic resonance imaging features differentiating benign from malignant masses, 14
Magnetization transfer contrast (MTC) imaging of skeletal muscle at 0.26 Tesla—changes in signal intensity following exercise, 39
Fat suppression in magnetic resonance imaging at low field strength using binomial pulse sequences, 132
Magnetic resonance imaging of peritoneal leiomyosarcomatosis (Case report), 170
Magnetic resonance imaging of penile rhabdomyosarcoma (Case report), 175
The use of MRI in the investigation of spinal cord compression (Correspondence), 187
Peripheral neuropathy simulating lymphoma (Case report), 344
High-intensity zone: a diagnostic sign of painful lumbar disc on magnetic resonance imaging, 361
Magnetic resonance imaging of extracranial head and neck tumours, 375
Magnetic resonance imaging and treatment of an unusual seminoma metastasis occurring in the parasellar region (Case report), 445
Increasing patient throughput in magnetic resonance imaging: a practical approach, 470
Intramuscular myxoma: magnetic resonance features, 485
Magnetic resonance imaging of pulsatile cerebrospinal fluid flow by spatial modulation of magnetization, 495
The value of magnetic resonance relaxation time in staging ovarian endometrial cysts, 502
Subluxation of the patella: evaluation of patellar articular cartilage with MR imaging, 662

INDEX TO VOLUME 65

Gadolinium-DTPA enhanced MRI in neonatal osteomyelitis of the cervical spine (Case report), 720
Primary choroid plexus papilloma of the cerebellopontine angle: magnetic resonance imaging, computed tomographic and angiographic appearances, 754
A flexion and extension device for dynamic MR imaging of the neck (Technical note), 816
Appearances of choroidal osteomas with diagnostic imaging, 845
Radial diffusion coefficient mapping, 885
Dural venous sinus thrombosis following myelography: demonstration by magnetic resonance imaging (Case report), 1134

PHYSICS AND TECHNOLOGY
Applied to radiodiagnosis
The dependence of the scattered radiation dose to personnel on technique factors in diagnostic radiology, 44
The reduction in radiation dose for intra-oral radiographs by the use of thin K-edge filters (Correspondence), 93
Minimizing radiation dose to patient and staff during fluoroscopic, nasoenteral tube insertions, 162
The significance of patient weight when comparing X-ray room performance against guideline levels of dose (Correspondence), 188
Scattered X-ray intensities from fluoroscopy units (Correspondence), 190
Results of a survey of doses to paediatric patients undergoing common radiological examinations, 225
Dose reduction by the use of erbium filtration in a general radiographic room, 232
Measurement of extrafocal radiation by computed radiography, 238
Accuracy of pelvimetry measurements on CT scanners (Technical note), 261
The Reference Man in diagnostic radiology dosimetry, 431
An alternative approach to contrast-detail testing of X-ray image intensifier systems, 686
An investigation into the effect of protective devices on the dose to radiosensitive organs in the head and neck, 799
Digital cardiac imaging—the death knell of cineangiography (Technical note), 818
Historical experiments predating commercially available computed tomography (Short communication), 835
A figure of merit for the assessment of image intensifier systems, 878
Single- versus dual-energy quantitative computed tomography for spinal densitometry in patients with rheumatoid arthritis, 901
Single energy quantitative computed tomography: the effects of phantom calibration material and kVp on QCT bone densitometry (Technical note), 931
The effect of thin K-edge filters on radiation dose in dental radiography, 990
Efficiency of a lead-containing tie for radiation protection of the thyroid gland, 1003
Comparison of a subjective and a quantitative assessment of the neonatal chest radiograph, 1083
Influence of radiologist grade on fluoroscopic patient dose, 1119

Applied to radiotherapy
A standardized multifield irradiation technique for breast tumours using asymmetrical collimators and beam angulation, 56
Biological intercomparisons of neutron beams used for radiotherapy generated by p^{+}→Be in hospital-based cyclotrons, 66
Dosimetric accuracy at low monitor unit settings (Correspondence), 92
Reduction in the diameter of human hairs following irradiation, 148
Magnetic resonance imaging of Fricke-doped agarose gels for the visualization of radiotherapy dose distributions in a lung phantom (Technical note), 167
The dose-rate effect in interstitial brachytherapy: a controversy resolved, 242
The potential of ytterbium 169 in brachytherapy: a brief physical and radiobiological assessment, 252
Cranial stereotactic multiple arc radiotherapy; treatment planning using angiographic images, 317
Computer-assisted generation of multi-leaf collimator settings for conformation therapy, 321
Quality assurance of computer controlled radiotherapy treatments, 409
Radical treatment of angiosarcoma of the scalp using megavoltage electron beam therapy, 421
Output factors for blocked fields, 517
A manual afterloading technique for the treatment of patients with bronchial carcinoma using iridium-192 wire (Technical note), 536
Image comparison techniques for use with megavoltage imaging systems, 701
Virtual source distances and field geometry independent output factors for 5–14 MeV electron beams from a Siemens Mevatron M7145 (Technical note), 717
An afterloading technique utilizing The Royal London Hospital caesium-137 brain needle in an oral obturator (Technical note), 814
Cranial sterotactic multiple arc radiotherapy (Correspondence), 1056
Cranial stereotactic multiple arc radiotherapy (Correspondence), 1147

Applied to nuclear medicine
The role of ^{99}Tc^{m}-HMPAO white cell imaging in suspected orthopaedic infection, 309
The incidence and severity of hypoxia associated with ^{99}Tc^{m} Technegas ventilation scintigraphy and ^{99}Tc^{m} MAA perfusion scintigraphy, 403
Treatment planning for ^{131}I-mIBG radiotherapy of neural crest tumours using ^{124}I-mIBG positron emission tomography, 787
Sonography in thyroid carcinoma in children, 977
The role of ^{99}Tc^{m}-HMPAO white cell imaging in suspected orthopaedic infection (Correspondence), 1055
Imaging of organ function (Correspondence), 1056

Applied to magnetic resonance
Magnetization transfer contrast (MTC) imaging of skeletal muscle at 0.26 Tesla—changes in signal intensity following exercise, 39
Fat suppression in magnetic resonance imaging at low field strength using binomial pulse sequences, 132
Magnetic resonance imaging of Fricke-doped agarose gels for the visualization of radiotherapy dose distributions in a lung phantom (Technical note), 167
Calibration of a 0.08 Tesla magnetic resonance imager for *in vivo* T_1 and T_2 measurement (Technical note), 438
Magnetic resonance imaging of pulsatile cerebrospinal fluid flow by spatial modulation of magnetization, 495

A flexion and extension device for dynamic MR imaging of the neck (Technical note), 816
Radial diffusion coefficient mapping, 885

Applied to ultrasound
A comparison of ultrasound exposure in therapy and pulsed Doppler fields, 557
A study of the relationship between routine ultrasound quality assurance parameters and subjective operator image assessment, 570
Doppler ultrasound scanning in the detection of renal artery stenosis in hypertensive patients, 857
Staging of hilar cholangiocarcinoma by ultrasound and duplex sonography: a comparison with angiography and operative findings, 871
Prediction of birthweight by fetal ultrasound biometry, 987

Applied to mammography
Improved image quality for dense breasts in mammography, 50
The application of microdosimetry to the metrology of low-energy X rays used in mammography (Technical note), 258
The determination of total filtration on mammographic X-ray sets, 334
A comparison of four mammographic image quality test objects (Technical note), 339
The application of microdosimetry in clinical bone densitometry using a dual-photon absorptiometer, 523
Radiation protection associated with well women breast cancer screening (Correspondence), 552
Localization of impalpable breast lesions using the Hawkins needle (Technical note), 929
Radiation protection associated with well woman screening (Correspondence), 949
Radiation protection associated with well woman breast cancer screening (Correspondence), 949
Standards of radiation protection in mammographic screening (Correspondence), 950
Radiation protection associated with well women breast cancer screening (Correspondence), 950
One-view *versus* two-view mammography in baseline screening for breast cancer: a review, 971
Assessment of mammographic film processor performance in a hospital and mobile screening unit, 1097
Latent image fading and mean glandular dose in mobile mammographic screening (Correspondence), 1148

Applied to densitometry
Measurement of forearm bone mineral density in normal women by dual-energy X-ray absorptiometry, 127
Bone mineral density in healthy normal women and reproducibility of measurements in spine and hip using dual-energy X-ray absorptiometry, 213
Errors due to non-uniform distribution of fat in dual X-ray absorptiometry of the lumbar spine, 807
Impact of hydration status on body composition as measured by dual energy X-ray absorptiometry in normal volunteers and patients on haemodialysis, 895
Single- versus dual-energy quantitative computed tomography for spinal densitometry in patients with rheumatoid arthritis, 901
Single energy quantitative computed tomography: the effects of phantom calibration material and kVp on QCT bone densitometry (Technical note), 931
Phantoms for evaluating the performance characteristics of bone densitometers (Technical note), 1030
Comparison of the effect of difference reference data of Lunar DPX and Hologic QDR-1000 dual-energy X-ray absorptiometers, 1124
Acronyms in bone densitometry (Correspondence), 1148

RADIOTHERAPY
Results and clinical aspects
Tumour and tumour-like conditions of the soft tissue: magnetic resonance imaging features differentiating benign from malignant masses, 14
Chest radiography in the management of breast cancer, 30
A standardized multifield irradiation technique for breast tumours using asymmetrical collimators and beam angulation, 56
The labelling index in carcinoma of the uterine cervix: its correlation with tumour sterilization, 63
Carbogen breathing: a system for use in man (Short communication), 87
The effect on pulmonary function of tangential field technique in radiotherapy for carcinoma of the breast (Correspondence), 92
The use of a chelating derivative of alpha melanocyte stimulating hormone for the clinical imaging of malignant melanoma, 112
Mitomycin C, 5-fluorouracil and radiation in advanced, locally recurrent rectal cancer, 143
Reduction in the diameter of human hairs following irradiation, 148
Re-irradiation of soft-tissue sarcoma, 157
Carcinoma of the ovary: a diagnostic hitch (Case report), 181
CT evaluation of lymph node status at presentation of prostatic carcinoma, 199
The dose-rate effect in interstitial brachytherapy: a controversy resolved, 242
The potential of ytterbium 169 in brachytherapy: a brief physical and radiobiological assessment, 252
Magnetic resonance imaging of extracranial head and neck tumours, 375
Radical treatment of angiosarcoma of the scalp using megavoltage electron beam therapy, 421
Altered radiotherapy fractionation in medulloblastoma (Correspondence), 460
Radiotherapy to the surviving kidney after unilateral nephrectomy in bilateral Wilms' tumour, 510
Accelerated fast neutron therapy: a pilot study, 691
Low oxygen extraction fraction in tumours measured with the oxygen-15 steady state technique: effect of tissue heterogeneity, 697
Asymptomatic temporal lobe injury after radiotherapy for nasopharyngeal carcinoma: incidence and determinants, 710
Small cell carcinoma of the prostate (Case report), 726
Permanent radiation myelopathy (Invited review), 737
A pilot study of accelerated fractionation in the radiotherapy of invasive carcinoma of the bladder, 792
Osteosarcoma metastatic to the kidney with invasion of the inferior vena cava (Case report), 827
Radiation-induced hearing impairment—a pilot study in patients treated for malignant parotid tumours (Short communication), 833
Efficacy of low-dose iodine-131 ablation of post-operative thyroid remnants: a study of 69 cases, 905
Retrospective analysis of nasopharyngeal carcinoma treated during 1976-1985: late complications following megavoltage irradiation, 918
Second malignant neoplasm following treatment of Hodgkin's disease: a case report (Case report), 935

INDEX TO VOLUME 65

Extradural paraganglioma with multiple skeletal metastases (Case report), 938
Basal cell carcinomas do metastasize (Case report), 943
Sonography in thyroid carcinoma in children, 977
Stage IB cervical carcinoma: a clinical audit, 1018
Transitional cell carcinoma of the bladder associated with Crohn's disease: case report and review of the literature (Case report), 1040
Correlations between a/b and $T_{1/2}$: implications for clinical biological modelling (Short communication), 1051
Late follow-up of lung function after whole lung irradiation for Wilms' tumour, 1114
Yolk sac tumour of the testis in childhood (Case report), 1142

Apparatus and technical aspects
A standardized multifield irradiation technique for breast tumours using asymmetrical collimators and beam angulation, 56
Biological intercomparisons of neutron beams used for radiotherapy generated by $p^+ \rightarrow Be$ in hospital-based cyclotrons, 66
Dosimetric accuracy at low monitor unit settings (Correspondence), 92
An innovative method for neuraxis radiotherapy using partial transmission block technique (Correspondence), 94
Cranial stereotactic multiple arc radiotherapy; treatment planning using angiographic images, 317
Computer-assisted generation of multi-leaf collimator settings for conformation therapy, 321
Quality assurance of computer controlled radiotherapy treatments, 409
Output factors for blocked fields, 517
A manual afterloading technique for the treatment of patients with bronchial carcinoma using iridium-192 wire (Technical note), 536
Image comparison techniques for use with megavoltage imaging systems, 701
Virtual source distances and field geometry independent output factors for 5–14 MeV electron beams from a Siemens Mevatron M7145 (Technical note), 717
Treatment planning for ^{131}I-mIBG radiotherapy of neural crest tumours using ^{124}I-mIBG positron emission tomography, 787
An afterloading technique utilizing The Royal London Hospital caesium-137 brain needle in an oral obturator (Technical note), 814
Cranial sterotactic multiple arc radiotherapy (Correspondence), 1056
Cranial stereotactic multiple arc radiotherapy (Correspondence), 1147

CANCER CHEMOTHERAPY
Neoadjuvant intra-arterial chemotherapy in inflammatory carcinoma of the breast, 248
Small cell carcinoma of the prostate (Case report), 726

RADIOBIOLOGY
Applied to radiotherapy
Biological intercomparisons of neutron beams used for radiotherapy generated by $p^+ \rightarrow Be$ in hospital-based cyclotrons, 66
Carbogen breathing: a system for use in man (Short communication), 87
The influence of methotrexate on radiation-induced damage to different lengths of the rat spinal cord, 152
Measurement of extrafocal radiation by computed radiography, 238
The dose-rate effect in interstitial brachytherapy: a controversy resolved, 242
The potential of ytterbium 169 in brachytherapy: a brief physical and radiobiological assessment, 252
The optimum pressure of oxygen for radiotherapy of a mouse tumour, 784
Functional changes in the pig kidney following irradiation with fractionated doses of fast neutrons (42 $MeV_{d \rightarrow Be}$), 910

Fractionation studies
Altered radiotherapy fractionation in medulloblastoma (Correspondence), 460
Permanent radiation myelopathy (Invited review), 737
Correlations between a/b and $T_{1/2}$: implications for clinical biological modelling (Short communication), 1051

Sensitizers and protectors
Carbogen breathing: a system for use in man (Short communication), 87
Calcium antagonists protect mice against lethal doses of ionizing radiation, 1025

Other studies
Reduction in the diameter of human hairs following irradiation, 148
Radiation damage to mouse skin and oesophagus (Correspondence), 731

HAZARDS AND RADIATION PROTECTION
Striking a balance: benefit and risk in man's exposure to man-made radiations (Review article), 1
The dependence of the scattered radiation dose to personnel on technique factors in diagnostic radiology, 44
Minimizing radiation dose to patient and staff during fluoroscopic, nasoenteral tube insertions, 162
Scattered X-ray intensities from fluoroscopy units (Correspondence), 190
An investigation of the dose equivalent to radiographers from a high-energy neutron therapy facility, 327
The Reference Man in diagnostic radiology dosimetry, 431
Radiation protection associated with well women breast cancer screening (Correspondence), 552
An investigation into the effect of protective devices on the dose to radiosensitive organs in the head and neck, 799
Radiation protection associated with well woman screening (Correspondence), 949
Radiation protection associated with well woman breast cancer screening (Correspondence), 949
Standards of radiation protection in mammographic screening (Correspondence), 950
Radiation protection associated with well women breast cancer screening (Correspondence), 950
The distribution of medical X-ray doses amongst individuals in the British population, 996
Efficiency of a lead-containing tie for radiation protection of the thyroid gland, 1003
Measuring radiation exposure during percutaneous drainages: can shoulder dosemeters be used to estimate finger doses?, 1007
Influence of radiologist grade on fluoroscopic patient dose, 1119

INDEX TO SUBJECTS—continued

LECTURES AND ADDRESSES

Striking a balance: benefit and risk in man's exposure to man-made radiations (The Silvanus Thompson Memorial Lecture, 1991), 1

EDUCATION

A persistent offender (Case of the month), 85
Now you see it ... now you don't (Case of the month), 183
Dysphagia paediatrica (Case of the month), 279
A case of malignant hypertension (Case of the month), 351
An underdiagnosed abdominal mass? (Case of the month), 453
Contralateral thinking (Case of the month), 549
A rare cause of a common symptom (Case of the month), 729
The third dimension (Case of the month), 831
A curious case of pelvic calcification (Case of the month), 945
Dense bones (Case of the month), 1049
Fit and ... well (Case of the month), 1145

PROCEEDINGS

Cerebral blood flow—practical measurement and clinical relevance, a mulimodality approach, 12 February 1991, 463
Ultrasonic assessment of bone, 29 May 1991, 96
International particle therapy meeting, 7 June 1991, 284
The new legislation—friend or foe (after the White Paper and into Europe), 13 June 1991, 733
Progress in MRI: scientific and clinical developments in the United Kingdom, 14 October 1991, 839
Proceedings of the Scottish Radiological Society. Radiodiagnosis programme, 9 November 1991, 1058
Hypoxic cell sensitizers: back in fashion? 15 November 1991, 356
Proceedings of the British Medical Ultrasound Society 23rd Annual Meeting, 614
Proceedings of the Scottish Radiological Society. Radiodiagnosis programme, 14 March 1992, 1058

BOOK REVIEWS

Anderson, L. L. et al. *Interstitial Brachytherapy: Physical Biological and Clinical Considerations*, 191
Bewley, D. K. *The Physics and Radiobiology of Fast Neutron Beams*, 954
Bradac, G. B., Ferszt, R. and Kendall, B. E. (Eds). *Cranial Meningiomas—Diagnosis Biology and Therapy*, 191
Browne, D., Weiss, J. F., MacVittie, T. J. and Pillai, M. V. (Eds). *Treatment of Radiation Injuries*, 287
Burhenne, H. J. (Ed.). *The Radiologic Clinics of North America*, 288
Dik, K. and Gunsser, I. *Atlas of Diagnostic Radiology of the Horse Part 3: Diseases of the Head, Neck and Thorax*, 360
Dobelbower, R. (Ed.). *Gastrointestinal Cancer: Radiation Therapy*, 100
Duck, F. A. *Physical Properties of Tissue: Comprehensive Reference Book*, 1150
Fishman-Javitt, M. C., Stein, H. L. and Lovecchio, J. L. (Eds). *Imaging of the Pelvis: MRI and Correlations to CT and Ultrasound*, 1064
Gautherie, M. (Ed.). *Methods of Hyperthermia Control*, 100
Granier, R. and Gambini, D. J. *Applied Radiobiology and Radiation Protection*, 1153
Gunn, C. and Jackson, C. S. *Guidelines and Patient Care in Radiography*, 1152
Hartman, D. S. *Renal Cystic Disease AFIP Atlas of Radiologic-Pathologic Correlation Fascicle I*, 467
Helms, C. A. *Fundamentals of Skeletal Radiology*, 1150
Hennig, U. *Deutsches Rontgen-Museum Remscheid-Lennep*, 1153
Heywang-Kobrunner, S. H. *Contrast-enhanced MRI of the Breast*, 1150
Jawad, I. A. *A Practical Guide to Echocardiography and Cardiac Doppler Ultrasound*, 1065
Johnson, F. L. and Pochedly, C. *Bone Marrow Transplantation in Children*, 192
Kang, H. S. and Resnick, D. *MRI of the Extremities*, 360
Kirkwood, J. R. *Essentials of Neuroimaging*, 468
Knudson, A. G., Stanbridge, E. J., Sugimura, T., Terada, M. and Watanabe, S. (Eds). *Genetic Basis for Carciogenesis—Tumour Suppressor Genes and Oncogenes*, 1066
Kreel, L. and Thornton, A. *Outline of Medical Imaging*, 1155
Letourneau, J. G., Day, D. L. and Ascher, N. L. (Ed.). *Radiology of Organ Transplantation*, 1065
Markisz, J. A. (Ed.). *Musculoskeletal Imaging—MRI, CT, Nuclear Medicine and Ultrasound in Clinical Practice*, 1150
Morstyn, G. and Kaye, A. (Eds). *Phototherapy of Cancer*, 1065
Newell, J. D. and Kelsey, C. A. (Eds). *Digital Imaging in Diagnostic Radiology*, 287
Nias, A. H. W. *An Introduction to Radiology*, 191
Oguro, Y. and Takagi, K. (Eds). *Endoscopic Approaches to Cancer Diagnosis and Treatment. Japanese Cancer Association, Gann Monography on Cancer Research No. 37*, 1066
Oldendorf, W. and Oldendorf Junior, W. *MRI Primer*, 1151
Pointon, R. C. S. (Ed.). *The Radiotherapy of Malignant Disease (2nd Edn)*, 1152
Puylaert, J. B. C. M. *Ultrasound of Appendicitis and its Differential Diagnosis*, 1066
Reed, N., McCallum, R. W. and Sandler, C. M. *Textbook of Uroradiology*, 467
Reiber, J. H. C. and Serryus, P. W. (Eds). *Quantitative Coronary Arteriography*, 1151
Reicher, M. A. and Kellerhouse, L. E. *MRI of the Wrist and Hand*, 1064
Riklis, E. (Ed.). *Frontiers in Radiation Biology, Proceedings of the 21st Annual Meeting of the European Society for Radiation Biology*, 1067
Riddervold, H. O. *Easily Missed Fractures and Corner Signs in Radiology*, 736
Robertson, J., Wankling, P. F., Faulkner, K. and Holubinka, M. R. (Eds). *Report No. 62: Computers in Diagnostic Radiology*, 1151
Sampson, C. B. (Ed.). *Textbook of Radiopharmacy: Theory and Practice*, 467
Schroeder, F. H. (Ed.). *Treatment of Prostatic Cancer Facts and Controversies*, 1066
Seibel, R. M. M. and Gonemeyer, D. H. W. *Interventional Computed Tomography*, 287
Soto, B. and Pacifico, A. D. *Angiocardiography in Congenital Heart Malformations*, 191
Sutton, D. and Young, W. R. (Eds). *A short Textbook on Clinical Imaging*, 115
Tubiana, M., Dutreix, J. and Wambersie, A. *Introduction to Radiobiology*, 736
Von Hagens, G., Romrell, L. J., Ross, M. H. and Tiedemann, K. *The Visible Human Body: An Atlas of Sectional Anatomy*, 736
Instructions to Authors, 101

PUBLICATIONS OF THE BRITISH INSTITUTE OF RADIOLOGY

BJR Supplements

☐	**24. Radiation Science of Molecules, Mice and Men**, 1992, 256 pp, ISBN 0 905749 316	50.00
☐	**23. Treatment Simulators**, 1989, 48 pp, ISBN: 0 905 74919 7	10.00
☐	**22. Megavoltage Radiotherapy 1937-1987**, 1988, 158 pp, ISBN: 0 905 74916 2	28.50
☐	**21. Radionuclides in Brachytherapy: Radium and After**, 1987, 54 pp, ISBN: 0 905 74915 4	15.00
☐	**20. The Safety of Diagnostic Ultrasound**, 1987, 48 pp, ISBN: 0 905 74914 6	12.00
☐	**18. Criteria and Methods for Quality Assurance in Medical X-ray Diagnosis**, 1985, 180 pp, ISBN: 0 905 74912 X	27.50
☐	**17. Central Axis Depth Dose Data for use in Radiotherapy** This standard work replaces BJR Supplement 11 (1972), 1983, 148 pp, ISBN: 0 905 74911 1	25.00

BIR Reports

☐	**Report 22: The Future of Human Radiation Research**, 1991, 174 pp, ISBN: 0 905749 27 8	27.50
☐	**Report 21: Risks from Radium and Thorotrast**, 1989, 188 pp, ISBN: 0 905 74922 7	40.00
☐	**Report 20: Optimization of Image Quality and Patient Exposure in Diagnostic Radiology**, 1989, 288 pp, ISBN: 0 905 74921 9	30.00
☐	**Report 19: The Scientific Basis of Modern Radiotherapy**, 1989, 142 pp,ISBN: 0 905 74920 0	30.00
☐	**Report 18: Technical and Physical Parameters for Quality Assurance in Medical Diagnostic Radiology**, 1989, 166 pp, ISBN: 0 905 74918 9	30.00
☐	**Special Report 17: High Dose Rate Afterloading in the Treatment of Cancer of the Uterus**, 1980, 200 pp, ISBN: 0 905 74907 3	18.50

Other Publications:

☐	**Pregnancy and Work in Diagnostic Imaging** , 1992 , 8pp, ISBN 0 905 749 308	4.00
☐	**Assurance of Quality in the Diagnostic X-ray Department**, 1988, 108 pp, ISBN: 0 905 74917 0	20.00
☐	**Basic Clinical Ultrasound** Hylton B Meire and Pat Farrant, 1982 (BIR Teaching Series No 4 170 pp, ISBN: 0 905 74910 3	12.50
☐	**Current Research in Osteoporosis and Bone Mineral Measurement II**: 1992 120pp, ISBN 0 905749 29 4.	28.00
☐	**Current Research in Osteoporosis and Bone Mineral Measurement**, 1990, 96 pp, ISBN: 0 905749 23 5	22.00
☐	**Clinical Applications of Ultrasonic Fetal Measurements**, 1991,30 pp, ISBN: 0 905749 24 3	13.50
☐	**Guidelines for the Evaluation of Radiological Technologies**, 1991, 28 pp, ISBN: 0 905 74925 1	13.50
☐	**Medical Radiation Protection Practice within the EEC**, 1991, 56 pp, ISBN: 0 905749 26 X	13.50
☐	**The Safe Use of Diagnostic Ultrasound**, 1991, 48 pp, ISBN: 0 905749 28 6	16.00

The British Institute of Radiology 36 Portland Place, London W1N 4AT Tel. 071-580 4189 Fax. 071-255 3209
American orders to: Medical Physics Publishing Corporation, 27B, 1300 University Avenue,
Madison WI 53706, USA. Fax: 608 262 2413 for dollar price.

25% discount to BIR Members if cheque received with order. Please quote membership number.

Please add £1 per book for postage/packing. Overseas orders will be sent by surface post.

For airmail add £2 per book.

I enclose payment to the sum of £. ☐ by cheque ☐ Barclaycard/Visa

My card number is ☐☐☐☐☐☐☐☐☐☐☐☐☐☐☐☐ ☐ Access

Signature ☐ Please send to this address: (BLOCK CAPITALS)

Name ☐ Membership No ☐

Address. ☐

Postcode ☐ Country ☐

BJR

THE BRITISH
JOURNAL
OF RADIOLOGY

Volume 65 Congress Supplement

Radiology and Oncology '92

Proceedings of the 50th Annual Congress of The British Institute of Radiology

X-ray Diagnosis • Ultrasound • Interventional Radiology
Radiotherapy • Oncology • Hyperthermia
Nuclear Medicine • Nuclear Magnetic Resonance
Radiation Physics • Radiobiology • Radiation Protection

BJR is published by The British Institute of Radiology BIR

NEW!

Self-Developing Radiation Sensitive Film for Quality Control Measurements and Routine Dosimetry in Radiation Therapy

GAFCHROMIC™ Dosimetry Media

Easy To Use...
NO Dark Rooms,
NO Film Cassettes,
NO Processing Required!

- Sensitive to Gamma, Electron, and X-Ray Radiations.
- Self-Developing – No Chemical Processing Required.
- Insensitive to Ambient Room Light.
- Dose Rate and Energy Independent Response.

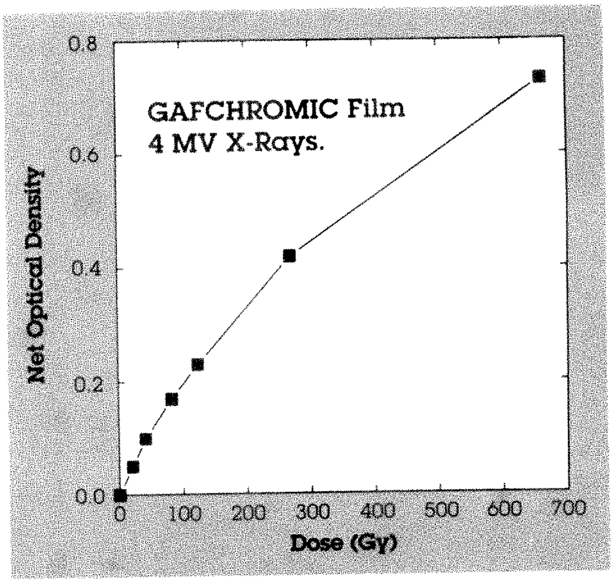

GAFCHROMIC™ dose response curve for 4 Mv X-rays.

FREE SAMPLE!

GAFCHROMIC is a colorless, grainless film that registers a deep blue color when irradiated.

For detailed information and a FREE SAMPLE of GAFCHROMIC, phone 516-741-6360, FAX 516-741-5414, or write and request Bulletin 5021-14.

TM, GAF Chemicals Corporation

NUCLEAR ASSOCIATES

VICTOREEN

Division of VICTOREEN, INC.
100 VOICE ROAD • P.O. BOX 349
CARLE PLACE, NY 11514-0349 U.S.A.
(516) 741-6360
FAX (516) 741-5414

Work in Progress Contents

MONDAY 18 May 4.15–5.30

HALL 10a

ONCOLOGY WORK IN PROGRESS

Chairman: Dr J T Roberts, Newcastle upon Tyne

4.15–4.23 **Strontium-89 versus external beam radiotherapy for pallation of prostate cancer bony metastases**
P M Quilty, Dundee

4.23–4.27 **Correlation of serum prostate specific antigen (PSA) levels and bone scintigraphy in carcinoma prostate**
R Oommen, Vellor, India

4.27–4.35 **Prognostic variables and patterns of relapse in 443 patients with localized prostatic carcinoma**
I M Syndikus, London

4.35–4.43 **Combined radio-chemotherapy for anal canal carcinoma: results of a propsective multicentre trial**
G G Grabenbauer, Frankfurt, Germany

4.43–4.51 **The AXIS trial: an update**
L L Garten, Cambridge

4.51–4.55 **Assessment of tumour cell proliferation in carcinoma of the uterine cervix**
I Bravo, Porto, Portugal

4.55–5.03 **Lectin staining as a possible predictor of radiosensitivity**
V N Bhattathiri, Trivandrum, India

5.03–5.11 **Bladder carcinoma: response-guided treatment allocation after external radiotherapy**
M L M Lybeert, Eindhoven

5.11–5.19 **Risk factors for second primary tumours of oral cavity in lip cancer treated by interstitital implantation**
V N Bhattathiri, Trivandrum, India

TUESDAY 19 May 9.00–10.15

HALL 10b

DIAGNOSTIC WORK IN PROGRESS I

Chairman: Dr R H Corbett, East Kilbride

9.00–9.08 **Double contras barium enema—an extended role for radiographers**
R A J Mannion, Leeds

9.08–9.16 **The ultrasonographic demonstration of peritoneal/omental masses**
G Stewart, Salford

9.16–9.20 **Barium enema examination—when to give Buscopan**
R A J Mannion, Leeds

9.20–9.24 **Prediction of lean body mass from ultrasound measurements of muscle thickness**
R E England, Manchester

9.24–9.28 **Do the lung changes of adult respiratory distress syndrome resolve?**
B Trotman-Dickenson, Oxford

9.28–9.32 **Percutaneous aspiration lung biopsy (PALS): A beginners approach**
J M Fields, Manchester

9.32–9.40 **MRI of soft tissue haemorrhage in haemophiliac patients**
B Trotman-Dickenson, Oxford

9.40–9.48 **Use of ultrasound in osteomyelitis**
A K Nath, Ruwi, Oman

9.48–9.56 **Computerized data processing for a dose area product meter**
A J Hunt, Poole

9.56–10.04 **An economic evaluation of a hospital-wide picture archiving and communication system (PACS)**
G C Weatherburn, Uxbridge

10.04–10.08 **3D reconstruction using CT of an ancient Egyptian mummy**
S W Hughes, London

10.08–10.16 **Tissue characterization at ultrasonic frequencies**
J Behari, New Delhi, India

TUESDAY 19 May 10.45—12.00

HALL 10b

DIAGNOSTIC WORK IN PROGRESS II

Chairman: Dr D Hadley, Glasgow

10.45–10.53 **Magnetic resonance imaging of focal liver lesions: comparison of scanning sequences**
Q Arafat, Birmingham

10.53–11.01 **Experimental studies of ^{99}Tc^{m} (V)-DMS hepatic carcinoma image and observations of preliminary clinical application**
Z Cai, Chongqing, P R China

11.01–11.09 **Detection and characterization of breast tumours by dielectric imaging**
M P Robinson, Bristol

11.09–11.17 **A clinical comparison between conventional and digital mammography utilizing computed radiology**
S C Ward, Leeds

11.17–11.25 **Axillary staging using MRI and radioimmunoscintigraphy**
S M Allen, London

11.25–11.29 **Applications of combined MR and CT imaging of the nasopharynx in patients with nasopharyngeal carcinoma**
W L Wong, London

11.29–11.37 **Determination of unchanged 18 F-DOPA in plasma: a new SPE method**
R F Wang, Orsay, France

11.37–11.41 **Multimodality imaging of the extra-cranial carotids: benefits and pitfalls**
M Gibson, London

11.41–11.45 **Emerging techniques in the design and installation of MRI systems**
D Baker, London

11.45–11.53 **Audit of casualty X-rays**
G M Quaghebeur, London

11.53–12.01 **Workforce reprofiling in imaging**
P N Noble, Bradford

TUESDAY 19 May 12.15—1.15

Hall 10b

DIAGNOSTIC WORK IN PROGRESS III

Chairman: Dr B E M Clay, Swindon

12.15–12.53 **Comparison between planar and tomographic radionuclide ventriculography for detecting inferior myocardial infarction**
H S Lee, Aberdeen

12.23–12.31 **Analgesia and pre-medication to coronary angiography: a patient-controlled audit**
F Stubbs, Sheffield

12.31–12.39 **Sedation and patient monitoring in vascular and interventional radiology**
V G M McDermott, Edinburgh

12.39–12.47 **Post angioplasty ankle brachial index: when should it be measured?**
S J Vinnicombe, London

12.47–12.55 **Direct demonstration of incompetence in recurrent varicose veins—a new technique**
K D McBride, Sheffield

12.55–12.59 **Identification of incompetent mid-thigh (Hunter's Canal) communicating veins: A comparison of varicography with phlebography combined with Valsalva manoeuvre**
T Y K Chan, London

12.59–1.07 **The effects of radiographic contrast media on white blood cell function**
R Farrow, Plymouth

1.07–1.15 **Lower leg DVT's—how good is colour flow ultrasound?**
M J Bradley, Rotherham

1.15—1.19 **Comparison of colour Doppler and phlebography in the diagnosis of deep vein thrombosis**
A Vargha, Sopron, Hungary

Monday 18 May

4.15 – 5.30

Oncology Work in Progress

Hall 10a

Strontium-89 versus external beam radiotherapy for palliation of prostate cancer bony metastases (final results of UK Metastron trial)

*P. M. Quilty, D. Kirk, J. M. Russell, N. S. Reed, D. P. Dearnaley, J. J. Bolger, V. P. Lewington and members of UK Metastron investigators group
*Departments of Radiotherapy and *Oncology, Ninewells Hospital and Medical School, Dundee DD1 9SY, Scotland*

260 patients were randomly selected to receive strontium-89 or external beam radiotherapy (XRT), according to suitability for either local radiotherapy (130 patients: 68 Sr, 62 XRT) or hemibody radiotherapy (130 patients: 65 Sr, 65 XRT). Patients were followed for 3 months to assess pain improvement. 103 patients in the local arm and 96 in the hemibody arm were assessable at 3 months at the time of reporting. In both local and hemibody arms there was no significant difference in pain improvement at original site(s) at 3 months: 55.9% improved after Sr *vs.* 50% after local XRT; 56% after Sr *vs.* 39.1% after hemibody XRT. In the local arm of the trial there was a significant difference in those showing both pain improvement at the original site and no new sites of pain having developed by 3 months—40.7% after Sr *vs.* 18.2% following local XRT ($p < 0.05$). In the hemibody arm the difference was not significant (46% *vs.* 28.3% following hemibody XRT). Pooled results (^{89}Sr *vs.* XRT) showed no significant difference in pain improvement at original site(s) at 3 months (56% Sr *vs.* 44.4% XRT), but there was a significant difference in those with pain improvement and no new sites of pain (43.1% *vs.* 23.3% XRT, $p < 0.01$). Nadir platelet counts and white cell counts were lower after Sr treatment (71.2% of baseline *vs.* 87.2%, 72.4% *vs.* 98%, respectively; $p < 0.01$). There was no significant difference in the proportion of patients requiring blood products (overall, 18% *vs.* 26% XRT). ^{89}Sr (Metastron) appears to be as effective as local or hemibody XRT in palliating bone pain from metastatic prostate cancer. In addition there is a benefit in delaying the occurrence of new sites of pain.

Correlation of serum prostate specific antigen (PSA) levels and bone scintigraphy in carcinoma prostate

R. O. Geetanjali, G. Gopalakrishnan, A. Kanagasabapathy, R. K. Roul
Department of Radiation Oncology, Christian Medical College Hospital, Vellore, India

24 patients with adenocarcinoma prostate, who had undergone ^{99}Tc^{m} MDP bone scintigraphy had serum prostate specific antigen (PSA) assays concurrently. Among 12 patients with bone metastases on scintigraphy (Group I), 11 cases had markedly elevated PSA levels with a mean level of 120.5 ng/ml (normal 0–4 ng/ml). In 12 patients with normal bone scans (Group II), six cases with elevated PSA levels (mean 49.1 ng/ml) had evidence of disease activity in the prostate and/or in the regional lymph nodes. The remaining six cases with normal PSA levels had normal bone scans, thus confirming both the utility of normal PSA levels in excluding bone metastases and the high levels of PSA being suggestive of the presence of bone metastases in asymptomatic patients.

Prognostic variables and patterns of relapse in 443 patients with localized prostatic carcinoma

I. Syndikus, R. Eeles, J. Gadd, J. Davies, M. Law, J. Gellister and D. P. Dearnaley
Department of Radiotherapy, The Royal Marsden Hospital and Institute of Cancer Research, Sutton, Surrey SM2 5PT, UK

From 1970 to 1988, 1846 patients with prostatic carcinoma were treated at The Royal Marsden Hospital. Of these, 443 had disease localized to the pelvis which was treated by radiotherapy. Median follow-up is 4 years, 7 months (3 months–18.6 years). Presenting Stages were T1 in 13%, T2 in 24%, T3 in 33% and 21% presented with positive pelvic nodes on lymphangiogram or computed tomographic (CT) imaging. The median age was 67 (47–85 years), and 73%

were diagnosed by TURP. Radiotherapy was performed on the pelvis in addition to the prostate in 38% and of these, 46% had pelvic nodal disease at presentation. 68% were CT planned. No deaths occurred as a result of radiation treatment. Severe side effects were seen in 8% and all were in the urinary tract. One patient also had a severe bowel complication. The 5 and 10 year survival rates were 55 and 23%, respectively, with metastases causing 61% of deaths. Univariate prognostic factors for survival were T Stage; nodal involvement; obstructive uropathy; grade; performance status; haemoglobin level, acid phosphatase and age ($p < 0.05$). Disease free survival rate was 42% at 5 years, but local recurrence occurred as late as 15 years and distant metastasis as late as 18 years. Overall, 16% had a local recurrence. Only 0.2% had a perineal relapse. Univariate prognostic factors for local recurrence were the same as for survival with the exception of haemoglobin. Patients with nodal disease only had a 34% 5 year disease free survival rate and had a greater chance of developing distant metastases ($p < 0.001$). Of all those who relapsed locally, 60% developed distant metastases with a median latent interval of 1.1 years. We have determined the patient and tumour factors which predict for the development of distant metastases in prostatic cancer that presents with disease confined to the pelvis and have shown that radiotherapy usually achieves good local control.

Combined radio-chemotherapy for anal canal carcinoma: results of a prospective multicentre trial

G. G. Grabenbauer, V. Budach, H. Hutter, V. Gressner-Brocks, R. Döker, U. Rühl and R. Sauer
Department of Radiotherapy, University Hospitals of Erlangen, Essen, Frankfurt, Düsseldorf and Frankfurt/NW, Berlin-Moabit, Germany

From 1985 to 1990, 88 patients with epidermoid or cloacogenic carcinoma of the anal canal were prospectively treated by a combination of radiation and chemotherapy. The primary tumour region including inguinal and pelvic nodes received a total dose of 45–60 Gy (median 50 Gy, single fraction 1.6–2 Gy). Two courses of chemotherapy consisting of 5-fluorouracil (800–1000 mg/sqm Days 1–4, 29–32) and mitomycin C (10 mg/sqm Days 29, 32) were administered. Histologic findings revealed cloacogenic carcinoma in 20 patients and epidermoid carcinoma in 68 patients. The T-stages (TNM 1987) were: T1(21), T2(36), T3(23), T4(6), T0(1), TX(1) with clinically positive regional nodes in 14 of the 88 patients. The female to male ratio was 65:13, median age was 60 years (range 26–87). 61 patients had an incisional biopsy, 17 had incomplete local excision and 10 patients had a colostomy (no abdominoperineal resection). 81 of the 88 (92%) patients were analysed for primary treatment response and follow-up. The complete response rate (assessed 6–8 weeks after treatment) was 93% (75/81). Local recurrence occurred in 7 of the 81 (9%) patients, regional or distant metastases in 12 of the 81 (15%) patients. The colostomy free local control rate was 79%. Actuarial disease free and overall survival at 3 years were 64% and 80%, respectively.

The AXIS trial: an update

L. L. Garten, on behalf of AXIS Steering Group
MRC Cancer Trials Office, Cambridge CB2 2BB, UK

The AXIS trial was initiated in 1989 as an attempt to determine the value of adjuvant radiotherapy and chemotherapy in colorectal cancer treatment. To this end, the trial was designed to include large numbers of patients with minimal data collection for each patient, therefore minimizing extra work for the collaborators. To compare adjuvant chemotherapy with surgery alone, patients with cancer of the colon or rectum are randomized to receive surgery only or sugery with 5-fluorouracil via perioperative intrahepatic infusion. In addition, rectal cancer patients may be randomized for radiotherapy *vs.* no radiotherapy. The choice of pre-or post-operative radiotherapy is left to the clinician. There are no formal eligibility criteria; only that a patient is fit to receive treatment and that the clinician is uncertain as to whether adjuvant treatment is indicated or not. Entry into AXIS continues to increase; at the time of writing nearly 1100 patients had been randomized by 98 clinicians. 61 centres in the UK and Europe have contributed patients, these include district general, teaching and specialist hospitals. Thanks to the outstanding work of collaborating clinicians, AXIS is now the largest UK randomized study of colorectal cancer treatment.

Assessment of tumour cell proliferation in carcinoma of the uterine cervix

I. Bravo, *F. Sansonetty, R. Craveriro, *R. Correia, G. Figueiredo and E. Vieira
*Department of Radiotherapy, Português ituto de Inst Oncologia *Cytometry Laboratoria, Ipatimup, Faciltio de Medicina, 4200 Porto*

Several factors have been considered as influencing the prognosis of carcinoma of the cervix and they are already considered in clinical practice. New biological parameters would be valuable in the selection of therapy for individual patients. In addition to DNA content analysis, S-phase fraction has particular importance as an indicator of proliferative activity. DNA index, in combination with S-phase fraction, is being assessed in over 140 carcinomas using flow cytometry. Preliminary results show that S-phase values range from 2.3% to 48% (with a mean value of 16.32%) and 52% of all tumours are aneuploid. Tumour proliferation is also being evaluated by studying the reactivity to ^{67}Ki proliferative antigen, using immunohistochemical methods. The growth fraction thus determined ranges from 2% to 62.5% (with a mean value of 20.64%). The assessment of the prognostic relevance of these values is presented in association with clinicopathological features.

Lectin staining as a possible predictor of radiosensitivity

V. N. Bhattathiri, P. Remani, R. Pillai, R. Ankathil,
T. T. Sreelekha, T. Vijayakumar and M. K. Nair
Regional Cancer Centre, Trivandrum-695 011, India

Induction of chromosomal damage is recognized as the main method of cell kill by radiation. Micronuclei estimation, which indicates loss of genetic material subsequent to chromosomal damage, has been suggested as a predictive test of radiosensitivity. It is possible that the cell membrane also suffers damage, which assumes significance at the high radiation doses used clinically. The following study shows that the extent of membrane damage possibly reflects tumour control and lectin staining alterations correlates with this. Smears from the tumours of 15 patients with accessible squamous cell cancers of the oral cavity and soft palate were taken before radiotherapy and after various doses of radiation. These were stained with Jack fruit lectin conjugated with Horseradish peroxidase (JFL-HRP) and counterstained with haematoxylin. In each occasion the proportion of cells with lectin staining of the cell membrane was noted and analysed. Before treatment an average of 65% of tumour cells showed lectin staining. This mean percentage decreased with an increasing dose of radiation. Individual tumours showed one of three types of change; rapid decrease, slow decrease or no decrease in the percentage of cells showing staining. Four of the nine patients with slow or rapid decrease had control of primary tumour at 8–10 months, whereas none of those without decrease had primary tumour control. Since lectins bind to specific carbohydrate residues on the cell surface, the decrease in binding reflects the loss or masking of these binding sites owing to radiation induced membrane damage or release of blocking factors. The different types of change reflects the difference in propensity for this damage. The correlation between type of change and the treatment results indicate that lectin staining alterations might prove to be a useful predictive tool of radiosensitivity.

Bladder carcinoma: response-guided treatment allocation after external radiotherapy

M. L. M. Lybeert, *W. De Neve, *C. Goor, M. A. Crommelin, J. G. Ribot
*Department of Radiotherapy, Catharina Hospital, Eindhoven and *Department of Radiotherapy, Academic Hospital, Free University Brussels, Belgium*

Between January 1974 and December 1984, 496 patients with M0 urinary bladder cancer, were treated at the Catharina Hospital by radiotherapy followed by surgery (RTS) (189 patients (T1:44; T2:52, T3:85; T4:6; Tx:2)) or radiotherapy only (RT) (307 patients (T1:67; T2:70; T3:107; T4:59; Tx:4)). To investigate if inferior (global or stratified per stage) survival (S) and locoregional relapse (LRR) observed in RT were related to unfavourable tumour allocation 93 patients with treatment allocation guided by response to radiotherapy (40 Gy median), were analysed. 39 patients further received surgery (CR:$n = 7$; PR:$n = 10$; NC:$n = 22$) (RTS) and 54 patients (CR:$n = 33$; PR:$n = 6$; NC:$n = 14$; unspecified:$n = 1$) received boost radiotherapy (RT). In RTS there were five T1 tumours (CR:$n = 4$; PR:$n = 0$; NC:$n = 1$) with 20%; nine T2 tumours (CR$n = 1$; PR:$n = 1$; NC:$n = 7$) with 11% and 24 T3 tumours (CR:$n = 2$; PR:$n = 9$; NC:$n = 13$) with 22% LRR. One Tx (CR) also relapsed. In RT there were eight T1 tumours (CR:$n = 7$; PR:$n = 0$; NC:$n = 1$) with 88% LRR; 18 T2 tumours (CR:$n = 14$; PR:$n = 1$; NC:$n = 3$) with 50% LRR; 21 T3 tumours (CR:$n = 11$; PR:$n = 3$; NC:$n = 6$; unspecified:$n = 1$) with 69% LRR; and seven T4 tumours (CR:$n = 1$, PR:$n = 2$; NC:n = 4) with 29% LRR. In these 93 patients, multivariate analysis showed response ($p < 0.01$) and surgery ($p = 0.08$, borderline) as independent prognostic factors for S. Response ($p = 0.01$), number of TUR ($p = 0.05$) and surgery ($p < 0.001$) were significant multivariate prognostic factors for LRR. We conclude that, after medium dose radiotherapy, surgery was more efficient than boost irradiation to achieve local control, in spite of allocation of unfavourable patients.

Risk factors for second primary tumours of oral cavity in lip cancer treated by interstitital implantation

V. N . Bhattathiri, C. A. Davis, A. Mathew, K. Ratheesan, F. V. James and M. K. Nair
Regional Cancer Centre, Trivandrum-695 011, India

During the period from January 1984 to December 1988, 44 patients with cancer of the lip had interstitital implantation (ISI) with radium. Of these, 12 patients developed second primary tumours (SPT) of the oral cavity, all of them epidermoid carcinomas and only one arising in the commissural area close to the original lesion. A univariate analysis of certain variables was done with the 12 SPT patients as one group and the other group consisting of 21 patients who had more than 1 year follow-up. (11 having developed locoregional recurrence and/or lost from follow-up). Age, sex, stage, extent of involvement of lip by the index tumour and lifetime exposure to habits (daily frequency × number of years of habit) did not show any influence as a risk factor. Presence of submucous fibrosis (SMF) and leukoplakia in the oral cavity showed borderline significance as a risk factor ($0.05 < p < 0.1$). Exposure of the oral cavity to radiation during the time of ISI was analysed in terms of the milligramme hours (mgh) of radium used. There was no significant risk in developing SPT exerted by this. Interestingly, there was a correlation (0.39) between the mgh used and the time interval between the ISI for the lip cancer and the occurrence of the SPT. If the one case with SPT in the commissure (which might have been a recurrence) and another case where the patient was only 30 years old (and hence might be expected to deviate from the general pattern) are excluded, the correlation reached significance. The conclusion, tempered with the knowledge that the number of cases are rather small, is that patients with SMF and leukoplakia stand a higher risk for a SPT, radiation possibly does not have a role in their induction, however, in those with higher risk radiation it may be having a retardant effect on the SPT.

Tuesday 19 May

9.00 – 10.15

Diagnostic Work in Progress I

Hall 10b

Double contrast barium enema—an extended role for radiographers

R. A. J. Mannion and A. H. Chapman
Department of Radiology, St James' University Hospital, Leeds LS9 7TF, UK

We describe the results of an audit of a training programme designed to instruct radiographers in the performance of the double contrast barium enema on ambulent outpatients. The programme consists of a series of lectures followed by an apprenticeship with a consultant radiologist. We compare the initial 50 unsupervised examinations performed by the first two radiographers to have completed the training programme, with 50 studies performed by senior registrars in radiology. The examinations were matched in terms of age and reason for referral, and the comparison was made by marking each study blind in terms of barium coating, colonic distension, radiography, screening time and number of X-ray exposures. No difference was found in any of these parameters when comparing the two groups. A much larger study would be required to assess any difference in the detection of pathology, but these initial results have encouraged us to continue with the training programme.

The ultrasonographic demonstration of peritoneal/omental masses

G. Stewart and R. Chisholm
Department of Ultrasound, Hope Hospital, Salford M6 8HD, UK

15 patients with ultrasonographic evidence of peritoneal or omental masses, who were examined over a 2 year period, were reviewed. There were nine male patients and six female patients, with a mean age of 73 years (range 55–86). Three of the patients had a known primary malignancy and a further two had a presumed clinical diagnosis of malignancy. In the remaining 10 patients the diagnosis was unknown. Ascites was present in 10 patients but malignant cells were only found in two of these after diagnostic aspiration. High resolution (5 MHz) ultrasound with a linear array transducer demonstrated peritoneal/omental masses in all patients. Ultrasound guided biopsy (18 gauge "Biopty" needle) produced a tissue diagnosis of malignancy in all of the six patients in whom it was performed. There were no complications from the biopsy procedures. Final diagnoses from biopsy or postmortem included 12 carcinomas and one case of a thickened omentum secondary to pelvic sepsis. A high index of suspicion and the correct ultrasonographic technique using a transducer with good "near field" characteristics are necessary for the diagnosis of peritoneal masses. These may be missed when using both a conventional sector transducer and computed tomography. Needle biopsy for tissue diagnosis is a relatively simple and safe procedure.

Barium enema examination—when to give Buscopan

R. A. J. Mannion and A. H. Chapman
Department of Radiology, St James' University Hospital, Leeds LS9 7TF, UK

Buscopan (Hyoscine-N-butylbromide) is used routinely as a hypotonic agent in barium enema examinations, but the optimum route and timing of the injection has not been determined previously. The problem has been addressed in this study by allocating patients, referred for double contrast barium enemas and able to receive Buscopan, into one of three groups. One third received 20 mg intravenously and one third 40 mg intramuscularly at the beginning of the study, the remaining third received a delayed injection of 20 mg intravenously after instillation of the barium. For each patient the barium column was timed round to the mid-transverse colon and the distance measured on the films. Patients with pathology and incontinence were excluded. Routine film series were obtained and the films reviewed for evidence of spasm. Further injections were administered intravenously if necessary. Thus from each study a transit time was obtained in centimetres per second.

Our initial results, based on a total of 102 patients, suggest that intramuscular Buscopan is less effective but produces adequate relaxation in most cases. The delayed intravenous injection does not impede the transit time and reduces the risk of requiring a second injection due to the short duration of action. We would, therefore, recommend a delayed intravenous injection with the intramuscular route as a suitable alternative in cases of poor intravenous access.

Prediction of lean body mass from ultrasound measurements of muscle thickness

D. J. Withers, R. E. England, T. Watt, I. T. Campbell and D. F. Martin
Department of Radiology and University Department of Anaesthesia, Withington Hospital, University Hospital of South Manchester, Manchester M20 8LR, UK

A simple non-invasive method is required to assess lean body mass in intensive care unit patients to monitor the effectiveness of nutritional support. Normal anthropometric techniques are frequently confounded in these patients by oedema occurring predominantly in subcutaneous tissues. In a preliminary study to establish whether ultrasound measurements of muscle thickness can predict lean body mass, 70 volunteers underwent assessment of fat-free mass derived from skinfold measurements. Muscle thicknesses were recorded using a portable ultrasound machine equipped with a 3.5 MHz linear array. Selected sites were the mid-arm level anteriorly (biceps), lateral head of triceps, mid-forearm anteriorly, mid-thigh anteriorly, mid-calf posteriorly and rectus abdominis adjacent to the umbilicus. The correlations between muscle thickness measurements and fat-free mass were highly significant, the highest being for biceps ($r = 0.84$). Multiple regression analysis indicated that thickness measurements were largely, independently correlated with fat-free mass. A simple linear regression involving only biceps thickness accounted for over 70% of the variation in fat-free mass and adding in linear terms for the mid-thigh and forearm increased this proportion to almost 76%. In normal volunteers ultrasound measurements of muscle thickness can predict lean body mass. A study using this method to assess critically ill patients is currently underway.

Do the lung changes of adult respiratory distress syndrome resolve?

B. Trotman-Dickenson, F. W. Wright and C. Woodham
Department of Radiology, Churchill Hospital, Oxford OX3 7LJ, UK

Adult respiratory distress syndrome (ARDS) may follow a variety of insults including major trauma, shock, septicaemia and pulmonary infections. The pathogenesis is multifactorial; activated neutrophils, complement and lipid metabolites are important mediators in the development of pulmonary inflammation. Despite ventilatory support 50% of patients die, however most survivors recover completely. A minority who require prolonged treatment have persistent lung damage due to tissue necrosis and barotrauma producing bullae and pneumothoraces. We studied four patients who survived and developed chronic lung disease with HRCT. These studies show localized areas of lung fibrosis, minute and larger lung cysts and diffuse persistent ground glass opacification. Serial scans show that whilst lung opacification may clear the other changes are irreversible. Bronchiectasis has not been a feature. As in other chronic lung diseases HRCT clearly demonstrated abnormalities poorly shown by conventional radiography.

Percutaneous aspiration lung biopsy (PALB): a beginner's approach

R. A. L. Bisset and J. M. Fields
Department of Radiology, North Manchester General Hospital, Delauneys Road, Crumpsall M8 6RB, UK

The objectives of this study are to assess whether a general radiologist can reliably and safely biopsy pulmonary masses and if complications can be reduced by using an oblique approach rather than the standard anterior or posterior approaches. A total of 41 biopsies were performed on 37 patients (four patients had repeat biopsies) by a single consultant. There were 28 males and nine females with an average age of 62.5 years. All biopsies were performed using a "C" arm X-ray tube. Biopsies were taken with the patient in an oblique position, allowing the needle to enter the lesion through the shortest route. The lung and pleura were punctured once with an 18 or 20 gauge Franceen or Westcott needle. Of the 37 patients 32 had clinical or histological proof of malignancy, a diagnosis which was confirmed at the first or second percutaneous aspiration lung biopsy (PALB) in 27 (92.8%) of patients. There were only six small pneumothoraces, only one requiring aspiration. We conclude that PALB is a safe procedure for the district general hospital consultant to perform and by using the oblique approach complications may be reduced.

MRI of soft tissue haemorrhage in haemophiliac patients

B. Trotman-Dickenson and D. J. Wilson
Department of Radiology, Nuffield Orthopaedic Centre, Oxford OX3 7LD, UK

Clinically, intramuscular bleeding may be indistinguishable from intra-articular haemorrhage or other musculo-skeletal disease, whilst bleeding into the deep muscles of the pelvis or retroperitoneum may mimic a variety of medical and surgical emergencies. The site and severity of the haemorrhage dictates the immediate therapy and subsequent rehabilitation. The aim of our study was to determine whether magnetic resonance imaging (MRI) of soft tissue haemorrhage contributed to the management of the patient. All patients with coagulation disorders and clinical suspicion of soft tissue haemorrhage were scanned using a 1 Tesla superconducting magnet. Intramuscular haematoma were demonstrated in two thirds of the patients. One third had haematomas involving the deep muscles of the pelvis and a similar proportion of haematomas of the thigh muscles. Complications identified included pseudo tumour, osteomyelitis and subcutaneous haemorrhage with sinus formation. Follow-up scans assisted by confirming treatment response and allowing more precise management of the patient. We believe MRI has an important role in the management of soft tissue haemorrhage, providing early diagnosis, precise anatomical localization and the identification of complications.

Use of ultrasound in osteomyelitis

A. K. Nath and A. U. Sethu
Mustafa and Jawad Trading Company LLC, PO Box 4918, Ruwi, Sultanate of Oman

Objective: To evaluate the use of ultrasound in osteomyelitis. *Materials, methods and procedures:* Sonography was performed in 25 patients clinically suspected of having osteomyelitis. Patients ranged in age from 2 to 45 years. All patients underwent a thorough clinical evaluation, chest radiograph, plain radiograph of the affected area, sonography of the affected area and opposite normal area for comparison. Sonograms were obtained using a 7.5 MHz phased linear array transducer. Needle aspiration or surgery was performed for fluid collection in contact with bone, diagnosing osteomyelitis or for fluid collection in diagnosing soft tissue abscesses. *Results:* Sonographic criterion for diagnosing osteomyelitis—fluid in contact with bone with no intervening soft tissue. This fluid was thought to represent exudate dissecting in a subperiosteal and/or extraperiosteal location. Sonographic diagnosis of soft tissue abscesses—fluid in soft tissues. Needle aspiration or surgery was performed to confirm pus. 15 of the 25 patients had osteomyelitis: (a) plain radiograph and ultrasound positive—8 patients (b) plain radiograph normal at initial examination but ultrasound positive—7 patients. Seven patients had soft tissue abscesses, one patient had cellulitis and two patients had no abnormality. *Conclusion:* Our findings indicate that ultrasound is useful in (a) preliminary screening of all patients suspected of osteomyelitis; (b) predicting osteomyelitis if fluid is demonstrated in contact with bone even if the initial plain radiograph is normal; (c) differentiating osteomyelitis from soft tissue abscesses; (d) localization of the lesion before aspiration or surgery and (e) detecting reactivity of chronic osteomyelitis in patients who have had inadequate treatment in the past.

Computerized data processing for a dose area product meter

A. J. Hunt
Medical Physics Department, Poole General Hospital, Poole, Dorset BH15 2JB, UK

The aim of this study is to implement a labour saving method of recording and reporting data from a PTW Diamentor M2 dose area product meter in routine use. Manual data collection has proven cumbersome and time consuming, the result has been that users find the Diamentor to be a limited tool. We have used a Cambridge Computers Z88 portable computer with appropriate software to prompt the user for key patient examination parameters and then to store the dose area product and exposure times with this data. The data can then be transferred to a database on a PC for further analysis and summary report generation. The reports for each room will be analysed by patient, examination, view, sex and age. Further comparison between each room's current and previous data, between rooms within each hospital, between hospitals and with the national picture will be made. Each of the two "systems" available will transfer between X-ray rooms in the participating hospitals, each room will be monitored for a period of 4–6 weeks on an annual basis. We have initially chosen to monitor those examinations measured in NRPB Report R200. It is anticipated that simple data collection, together with fast and easy analysis will considerably aid the quality assurance effort and make the dose area product meter a more accepted tool.

An economic evaluation of a hospital-wide picture archiving and communication system (PACS)

G. C. Weatherburn, S. Bryan, M. J. Buxton and J. Keen
Health Economics Research Group, Brunel University, Uxbridge, Middlesex UB8 3PH, UK

The health economics research group (HERG) at Brunel University has been commissioned by the Department of Health to conduct an independent evaluation of the hospital-wide picture archiving communication system (PACS) at the Hammersmith Hospital. The research project is studying the costs and benefits of the important aspects of PACS, namely digital imaging, communication via electronic cables and electronic archiving. The evaluation is complex because of the nature of the technology itself and there are many confounding factors, not least of which is the move to a new department of radiology. The 4 year project has three main components: a before and after study at the Hammersmith Hospital; research concentrating on the effectiveness of PACS in four clinical case study areas and the concurrent monitoring of trends at hospitals pursuing alternative strategies. The implementation process is also being monitored in order to draw lessons for the wider use of PACS in other NHS hospitals.

3D reconstruction using CT of an ancient Egyptian mummy

S. W. Hughes, †A. Sofat, C. Baldock, *W. Wong, *K. Tong and R. Davis
*Departments of Medical Physics and *Radiology, St Thomas' Hospital, London, †Institute of Neurology, London, UK*

The study of ancient Egyptian mummies has always been difficult because of the reluctance of researchers to disturb the wrappings and sealed caskets in which they are contained. Most studies in the past have been conducted using conventional radiography, xeroradiography and, more recently, computerized tomography (CT), the latter having advantages over other techniques. We scanned the entire body of an Egyptian mummy in its sealed painted casket. This work was done in collaboration with the British Museum. Consecutive high resolution CT images in a 512×512 matrix on a Siemens Somatom DRH scanner were performed. Data were acquired at 2 mm slice intervals through the head and neck and at 4 mm intervals through the rest of the body. This information comprising of 500 CT slices, was processed using a Stardent supercomputer and 3D reconstructions of this entire data set were performed. By depicting bony and soft tissue structures, previously unknown information has been obtained. So far, this technique has proved to be an invaluable method for studying ancient antiquities.

Tissue characterization at ultrasonic frequencies

J. Behari and A. K. Singh
School of Environmental Sciences, Jawaharlal Nehru University, New Delhi-110067, India

Attenuation and sound speed measurement appears to be the promising quantitative parameters for biological tissue characterization. We examined the effect of fixation on velocity and its temperature dependence. Fixing the tissue was accomplished by placing it in 10% formaline. The data reported on soft tissues (liver and kidney) were obtained after freshly sacrificing a goat. The data are presented in the frequency range 4–10.0 MHz. Characterization of attenuation of ultrasound in materials by the measurement of spectral shift is adopted. The ultrasound attenuation coefficient was used to detect a large number of abnormalities in tissues, and hence it has a broader applicability in the field of medicine and biology. The slope attenuation can be estimated from a down shift in the frequency of the reflected spectra with range. We have used the reflection from the same sample at different depths for the location of the centre frequency. A typical value of attenuation for liver is 0.91 db cm^{-1} at 30.5°C, while that of attenuation coefficient is 0.13 db cm^{-1} MHz^{-1}. The speed of sound in freshly sacrificed and in formalin fixed samples differs significantly as does their temperature variation. We conclude that measurement of these parameters along with their temperature dependence offers a reliable estimate of tissue characteristics.

Tuesday 19 May

10.45 – 12.00

Diagnostic Work in Progress II

Hall 10b

Magnetic resonance imaging of focal liver lesions: comparison of scanning sequences

Q. Arafat, J. F. C. Olliff and E. B. Rolfe
Department of Diagnostic X-ray, Queen Elizabeth Hospital, Birmingham B15 2TH, UK

Advantages of gradient echo (GRE) breath-hold techniques include reduction of respiratory and motion induced artefact. Good signal to noise (S/N) characteristics and good contrast has been reported using this technique. We compare the conspicuity of liver lesions using this technique with conventional T_1 and T_2-weighted spin echo (SE) techniques at 0.5 T. 26 patients with suspected hepatic lesions were prospectively examined. All scans were performed on a General Electric MR MAX operating at 0.5 T. Axial GRE sequences (time to repeat (TR) 150 ms, time to echo (TE) 12 ms, flip angle 80°) were obtained using a breath-hold of 18 s (3 slices). Axial T_1-weighted SE (TR 520 ms, TE 25 ms) and T_2-weighted SE (TR 2000 ms, TE 80 ms) were also obtained. The number of intrahepatic lesions and their size was noted for each sequence on each patient (performed retrospectively and randomly). On T_1-weighted SE sequences, 37 lesions were indentified in 6 of the 26 patients. On T_2-weighted SE sequences, 70 lesions were identified in 12 of the 26 patients. On T_1-weighted GRE sequences, 81 lesions were identified in 14 of the 26 patients. Statistical analysis using the Wilcoxon signal rank test on the differences between individuals show the difference between T_1-weighted SE and T_1-weighted GRE to be highly significant ($p < 0.005$) and that between T_1-weighted SE and T_2-weighted SE to be significant ($p < 0.03$). The difference between T_2-weighted SE and T_1-weighted GRE did not reach significance. We conclude that T_1-weighted GRE should be used to examine the liver in preference to T_1-weighted SE.

Experimental studies of ${}^{99}\text{Tc}^{m}$ (V)–DMS hepatic carcinoma image and observation of preliminary clinical application

C. Zongping, *L. Shaolin, L. Weidao, W. Guiying, *W. Dingnian, Z. Jinlan, L. Jiajuan, L. Ming, Z. Ping, W. Xianyang and T. Ming
*Department of Nuclear Medicine and The Liver and Gall Research Unit of Chongqing Cancer Institute, Chongqing, China and *Department of Basic Nuclear Medicine of Chongqing University of Medical Science, Chongqing, China*

This is a report on experimental studies of ${}^{99}\text{Tc}^{m}$ (V)–DMS in a group of rats with hepatic carcinoma. The rate of tumour to liver was 2.36–0.48, after improving the method of labelling ${}^{99}\text{Tc}^{m}$ (V)–DMS. We obtained clinical results for 36 cases of different hepatic focus image. The sensitivity of 23 cases of hepatic carcinoma was 91.30%. The specificity of 23 cases of the same group was 92.30% and the accurate rate was 91.67%. This result was higher than the sensitivity of TCT, US and AFP in the same group. The false positive rate of 13 cases of benign hepatic focus was 7.69%. We believe that ${}^{99}\text{Tc}^{m}$ (V)–DMS may be a good hepatic carcinoma image agent.

Detection and characterization of breast tumours by dielectric imaging

M. P. Robinson, J. L. Creen and A. W. Preece
Biophysics Research Unit, Department of Medical Physics, Bristol Oncology Centre, Birstol BS2 8ED, UK

A non-invasive, non-ionizing imaging system has been developed to detect and characterize breast tumours using low power radio-frequency radiation. Significant differences exist in the complex permittivities of breast tumours and healthy breast tissue at radio- and microwave frequencies, this is mainly due to differences in water content. Our system measures complex permittivity with an automatic network analyser coupled to a resonant sensor (resonant frequency 500 MHz). When the latter is placed against tissue, changes in resonant frequency and O-factor of the sensor enable reconstruction of complex permittivity to a depth of 3–4 cm. By combining such measurements with measurements of the position of the sensor, it is possible to build up an image of tissue permittivity. The system has been tested on dielectric phantoms and been found capable of detecting buried structures of anomalous complex permittivity. We are currently evaluating the performance of the system on patients with clinically proven breast malignancies.

A clinical comparison between conventional and digital mammography utilizing computed radiology

S. C. Ward, G. J. S. Parkin and *D. S. Brettle
*Department of Clinical Radiology and *University Department of Medical Physics, The General Infirmary at Leeds, Leeds LS1 3EX, UK*

Previous work utilizing a specially designed mammographic test object has indicated that the image quality of computed radiology (CR) approaches that of a conventional film/screen technique of equivalent radiographic speed. We are currently assessing the suitability of the CR system for use in clinical mammography by comparing similar images of the same breast obtained using the two techniques. Using a randomized viewing sequence, two observers were asked to score the images subjectively utilizing a 5 level scale with regard to noise, sharpness, contrast, overall presentation of the image and ability to demonstrate abnormal features. Initial results indicate that CR is a suitable alternative to conventional film/screen mammography in the clinical setting. Digital films show greater image contrast while standard films are better in terms of overall sharpness. Microcalcifications are clearly seen using both systems, but are more precisely defined on conventional films. Several of the digital images scored poorly with respect to noise, this was due to contamination by dust particles, and in one case this resulted in a false positive identification of a cluster of calcifications. This problem is felt to be related to the siting of the CR unit at our hospital, and particular attention should be paid to this during future installations.

Axillary staging using MRI and radioimmunoscintigraphy

S. Allan, N. Sacks, D. MacVicar and V. R. McCready
Departments of Surgery, Radiology and Nuclear Medicine, The Royal Marsden Hospital, Sutton, Surrey SM2 5PT, UK

Axillary node status is still the most important staging information to have in the management of breast cancer. At present the only accurate method of acquiring this data is from axillary surgery. We present a progress report on a project that aims to provide equivalent data by a combination of radioimmunoscintigraphy (RIS) and magnetic resonance imaging (MRI). A panel of antibodies is used to increase the accuracy of the technique. The optimum antibody was pre-selected for each patient by immunocytochemical staining of fine needle aspirates from the tumour. All patients underwent MRI of their axillae with T_1- and T_2-weighted scans in two axes of reconstruction. The results of RIS and MRI were correlated with histology of the resected specimens. Five patients had RIS; two controls, two positive scans and one negative. Six patients had MRI; enlarged lymph nodes were correctly identified in five patients and normal nodes were seen in the sixth. One of the positives was restaged from clinical assessment as a direct result of MRI. The project continues to recruit patients and the early results are encouraging as to the future prospects of the techniques.

Applications of combined MR and CT imaging of the nasopharynx in patients with nasopharyngeal carcinoma

W. L. Wong, D. L. G. Hill, *R. Beaney, K. Tonge and D. J. Hawkes
*Division of Radiological Sciences and *Department of Radiotherapy, United Medical and Dental Schools, St Thomas' and Guy's Hospital, London, UK*

In the UK nasopharyngeal carcinoma (NPC) accounts for less than 0.5% of all cancers. The disease, however, is much more common in other parts of the world, especially in the Far East where it can account for up to 50% of patients attending cancer clinics. The clinical features vary as they reflect the possible spread of the tumour to surrounding important structures including the skull base, sinuses, orbit and lymph nodes. Computed tomography (CT) and more recently magnetic resonance imaging (MRI) have greatly improved the radiographic evaluation of NPC enabling more accurate staging which in turn permits more specifically tailored treatment and accurate prediction of outcome. Both modalities provide complimentary information. CT is useful for its ability to visualize bone and soft tissue. MRI with its superior "soft tissue contrast" accurately depicts tumour-soft tissue interfaces and tumour margins. Bone integrity is not well shown on MRI. We believe that combined MR and CT datasets will improve the ability to visualize, characterize and stage these tumours. The images were registered in 3D by identifying eight or more homologous 3D points in the two modalities and hence calculating the rigid transformation relating the coordinate systems of the two scanners. We present one patient to demonstrate the advantages of this technique. A 45-year-old woman presented with a short history of nasal stuffiness and deafness. An EUA and endoscopy revealed a nasopharygeal mass, biopsy of which confirmed a squamous cell carcinoma. The images produced clearly show the full tumour extent. The work is being extended in two ways—incorporation of functional information from positron emission tomography into the combined MR and CT images, and by making use of the information for improving external beam 3D radiotherapy planning.

Determination of unchanged 18 F-dopa in plasma: a new SPE method

R. F. Wang, C. Loc'h and B. Mazière
Service Hospitalier Frédéric Joliot, DRIPP-DSV-CEA, 91401 Orsay, Cedex, France

For the assessment and quantification of the pre-synaptic dopaminergic function in the basal ganglia using positron emission tomography (PET) and 18 F-dopa, as the radiolabelled dopamine precursor, an accurate knowledge of the unchanged fraction of the radiotracer in plasmatic sample, as a function of time, is mandatory. This determination which has to be performed on a routine basis must be simple, cheap, rapid, accurate and reliable. Here, we compare the results obtained with a new solid phase extraction (SPE) technique with that of the tedious, classical TLC technique. After intravenous injection of 200 MBq 6-(18 F) Fluoro-L-dopa for PET studies, arterial blood samples were withdrawn in heparinized tubes and centrifugated. 0.2 ml of plasma was added to 0.5 ml of 0.5 M Tris-HCl buffer and poured on a buffer pre-wetted neutral alumina cartridge (Waters). The column was then washed with 2 ml Tris-HCl buffer and 5 ml water to eliminate the radiolabelled metabolites. The radioactivity remaining on the column, and corresponding to unchanged 18 F-L-dopa, was measured in a gamma counter, which compared with that of the untreated plasma sample. The results obtained in healthy volunteers ($n = 2$), patients ($n = 4$) with Parkinson's disease and schizophrenia, and non-human primates show that the two methods are closely correlated (coefficient of variation 2.6 ± 1.3%). Therefore, this SPE technique appears to be an analytical method suitable for correcting the input aterial function in routine clinical PET neurotransmission studies.

Multimodality imaging of the extracranial carotids: benefits and pitfalls

M. Gibson, S. Pickman, *A. Harwood, G. McGann, A. Platts, A. Valentine and †G. Hamilton
*Departments of Radiology, *Vascular Studies and †Vascular Surgery, Royal Free Hospital, London NW3 2QG, UK*

A wide variety of imaging methods are available for the assessment of carotid bifurcation atheromatous disease, but selective intra-arterial studies (IAS) are still regarded by many as the gold standard. Magnetic resonance imaging (MRI) "time of flight" angiography and high definition colour duplex Doppler are newer, non-invasive technique which are compared in this study in eight patients and correlated with IAS. They are graded as to their clinical use by examination of the surgically removed specimens. Several preliminary conclusions have been drawn. (1) Angiography is not the gold standard in all cases. (2) Duplex is the only method that can characterize plaque morphology which is thought to be a major determinant of outcome and so should be performed even when satisfactory angiography has been obtained. (3) Doppler blood flow velocities can be used to grade stenoses when still in doubt after IAS. (4) MRI tends to over estimate stenoses andd may give false positive results. Illustrative imaging and surgical specimen photography presented.

Emerging techniques in the design and installation of MRI systems

D. Baker
David Baker Architects Ltd, 109d Regents Park Road, London NW1 8UR, UK

The objective of our work is to facilitate the installation of magnetic resonance imaging (MRI) systems into often very difficult sites. Five specific cases are discussed, each illustrating particular problems that have resulted in some generally applicable solutions. The installations are as follows: (1) basement installation (case study: Royal Cornwall Hospital, Truro—access and cryogenic gas venting issues). (2) Courtyard installation (case study: St George's Hospital, Tooting—cranage and stray field issues with 1.5 T system). (3) Multistorey installation (case study: The London Clinic—structural supports, acoustic and magnetic shielding issues with 0.5 T system). (4) Twin MR system installation (case study: Mount Vernon Hospital, Northwood—field proximity and installation sequence issues with 0.5 T and 2.0 T systems). (5) Twin MR/CT installation (case study: Central Middlesex Hospital—field proximity and installation issues with 0.5 T MR and CT scanner). The methods, results and conclusions of each case study are explained.

Audit of casualty X-rays

G. M. Quaghebeur and M. Shute
Department of Radiology, King's College Hospital, London SE5 9RS, UK

An audit of casualty X-rays was carried out over a 1 month period at a teaching hospital. The aims of the study, the methodology and the results obtained are presented, as are the conclusions drawn and the new methods of practice. The aims included: (1) to identify the total number of films reported in a 24 h period. (2) To trace unreported films and and assess whether clinical management would have been altered by a radiology report. (3) To assess the standard of radiology intepretation by accident and emergency doctors. (4) To undertake an in-house assessment of a proposed film flagging system by radiographers. The problems encountered in obtaining the data are discussed. All results are presented, but the overall number of films that were reported was 52%. Our results are presented, but the overall number of films that were reported was 52%. Our results are analysed and compared with other published or available figures. The conclusions drawn and alterations to our method of practice are given and a discussion about these will hopefully follow.

Workforce reprofiling in imaging

P. N. Noble
Department of Diagnostic Imaging, Bradford Royal Infirmary, Bradford BD9 6RJ, UK

This paper shall focus on current national and international work which is currently in progress on workforce reprofiling in imaging. I have recently received the 1992 Institute of Health Service Management award for research in relation to imaging reprofiling and has established networks with experts in the field. *i.e.* Professor Roger Dyson. The work will incorporate visits to Europe, Canada and the United States in relation to current utilization of manpower. The work shall indicate the implications of the 1991 NHS and Community Care Act on imaging services, with particular emphasis on the imaging workforce in Bradford since the granting of trust status in 1991. To remain competitive within the internal market, the imaging directorate has successfully implemented new concepts such as self-employed radiographers and self-management teams. The latter has shared experiences at Nissan UK Ltd and has applied these concepts to the Bradford ultrasound service, involving clinicians and radiographers. Successful reprofiling in the workforce has attributed to the devolution of responsibility and accountability of the staff by the formulation of task groups. This methodology has enabled a reduction in costs, an improvement in quality and the provision of rewards for the staff. In the future, experiences and limitation shall be drawn on the role of the graduate radiographer and the inevitable prediction of a technical grade comparable with many European countries.

Tuesday 19 May

12.15 – 1.20

Diagnostic Work in Progress III

Hall 10b

Comparison between planar and tomographic radionuclide ventriculography for detecting inferior myocardial infarction

H. S. Lee, S. J. Cross, *M. Y. Norton and S. Walton
*Department of Cardiology and *Medical Physics, Aberdeen Royal Infirmary, Aberdeen AB9 2ZB, UK*

Planar radionuclide ventriculography (RNV) is routinely used for the detection of regional wall motion abnormalities (RWMA) of the left ventricle (LV). However, for inferior RWMA, sensitivity is known to be low in the conventional left anterior oblique (LAO) projection although it can be improved if a left posterior oblique (LPO) view is also taken. *Objective:* To compare the sensitivity of planar LAO, LPO and tomographic radionuclide ventriculography in the detection of inferior RWMA. *Patients:* 25, consisting of 15 with inferior RWMA on contrast LV angiogram and 10 normal controls. *Methods:* All patients underwent equilibrium planar LAO, LPO then tomographic RNV. All LV images were objectively analyzed for phase. Planar studies were divided into 12 segments and RWMA was defined as >2 SD from normal controls in two adjacent segments. *Results:* Inferior RWMA were detected in LAO in six (40%) patients, LPO in eight (60%) and tomography in 14 (93%) patients, respectively. *Conclusion:* Tomographic RNV has the highest sensitivity in detecting RWMA while planar LPO projection is better than LAO.

Analgesia and pre-medication in coronary angiography: a patient-controlled audit

F. Stubbs, P. Norman, D. C. Cumberland and A. Violaris
Department of Radiology, Northern General Hospital, Sheffield S5 7AU, UK

Coronary angiography is now routine, but no reliable data exists on exactly how painful or distressing patients find it. Consequently, the use of pre-medication and analgesia varies widely between practitioners. This was confirmed by a survey of 100 angiographers which we conducted. The main study was concerned with patients' reactions to coronary angiography and the use of pre-medication. 120 patients, in groups of 30, completed the Spielberger state-trait anxiety questionnaire after angiography. This well established measure quantifies patient's anxiety levels. The four groups were as follows: (a) Day patients—pre-medicated; (b) day patients—not pre-medicated; (c) in-patients—pre-medicated and (d) in-patients—not pre-medicated. Data from the four groups was analysed using the statistical package for social sciences (SPSS). Conclusions include: (1) whether patients find angiography significantly distressing; (2) whether pre-medication effectively reduces anxiety and (3) differences in anxiety levels between day patients and in-patients. Conclusions will be used in formulating guidelines for analgesia in coronary angiography.

Sedation and patient monitoring in vascular and interventional radiology

V. G. M. McDermott, M. Chapman and I. Gillespie
Department of Diagnostic Radiology, Royal Infirmary Edinburgh, Edinburgh EH4, UK

Objective: To assess current practice in Britain and Ireland regarding sedation and monitoring of patients during angiography and interventional radiological procedures. *Method:* Postal survey of the members of the British Society of Interventional Radiology. The response rate was 59%. *Results:* Patients are often (34–50%) sedated for angiography and usually (60–95%) sedated for interventional procedures. Nurses are present for all procedures performed by day and 70% of those performed at night. However, they are specifically given the task of monitoring the patient's vital signs in only 50% of cases. Pulse oximetry is routinely used in 20% of departments and automatic blood pressure monitors in 15%. Anesthetists are present for less than 10% of interventional procedures. 42% of departments have a staffed recovery area. Most vascular/interventional suites are stocked with emergency drugs (88–96%) and a defibrillator (78%). 24% of departments report at least one death during or shortly after a procedure during the last 10 years. 20% of interventional radiologists have taken a refresher course in cardiopulmonary resusitation in the past year. *Conclusions:* There is marked variation in practice regarding sedation and monitoring of patients in vascular/interventional radiology. Guidelines should be made available to maintain a uniform high standard of practice.

Post-angioplasty ankle brachial index: when should it be measured?

C. D. George, T. M. Buckenham and S. J. Vinnicombe
Department of Diagnostic Radiology, St. George's Hospital, London SW17 0QT, UK

The ankle brachial index (ABI) is used as a measure of the severity of lower limb peripheral vascular disease and an increase in the ABI of 0·1 or more following percutaneous transluminal angioplasty (PTA) is an accepted objective measure of a successful dilation. After PTA the ABI is usually measured at 24 h, however, there is little evidence to indicate that this is the optimum time for assessment. To investigate this the ABI was measured, before and at 24 h and 1 month after technically successful PTA of the superficial femoral artery (SFA), in 12 consecutive patients. ABI before PTA was 0·48 ± 0·07 (mean ± SEM). 24 h following PTA the mean ABI was significantly higher 0·77 ± 0·05 but the rise in four individuals was less than 0.1. At 1 month the mean ABI was 0·94 ± 0·04, significantly higher than the measurements obtained both before and at 24 h. Moreover, at 1 month all individuals demonstrated ABI rises of 0·1 or more over the pre-PTA measurement. This suggests that the current practice of quoting the ABI 24 h after PTA as a quantitive measure of improved perfusion may result in under reporting of both the number of successful SFA angioplasties and the degree of improvement. The majority of patients will show further improvement in their ABI between 24 h and 1 month.

Direct demonstration of incompetence in recurrent varicose veins—a new technique

K. D. McBride, *J. D. Beard and P. A. Gaines
*Departments of Radiology and *Vascular Surgery, Royal Hallamshire Hospital, Sheffield S10 2JF, UK*

A significant proportion of patients who have had surgery for varicose veins will present with recurrent disease. These can be difficult cases to manage and accurate pre-operative assessment of the reasons for and the extent of recurrence is essential. Varicography plays an important role in these patients but venous incompetence is inferred with this technique. In a series of 16 legs in 12 patients, varicography was compared with modified ascending phlebography using a pneumatic compressive device. There was a good correlation of findings between both techniques, but direct demonstration of perforator vein incompetence was only shown by the new method. Varicography, however, better demonstrated sapheno-femoral recurrence. The results compare favourably with operative findings. Compression phlebography has limitations, but with further modification may prove more useful in the assessment of perforator vein incompetence.

Identification of incompetent mid-thigh (Hunter's Canal) communicating veins: a comparison of varicography with phlebography combined with Valsalva manoeuvre

T. Y. K. Chan, O. Chan and M. Lea Thomas
Department of Radiology, St Thomas's Hospital, London SE1 7EH, UK

Varicography was performed on 50 legs in 40 patients who had recurrent varicose veins after previous ligation of sapheno-femoral junction with or without stripping of the long saphenous vein. The features, number and locations of the communicating veins in the mid-thigh region (Hunter's Canal) were recorded. Comparison was then made with ascending phlebography with Valsalva manoeuvre which identified only the incompetent communicating veins. The diameter of the competent communicating veins ranged from 0.5 mm to 5.0 mm, mean 1.54 mm, and the diameter of the incompetent ones ranged from 2.5 mm to 8.0 mm, mean 4.9 mm. We found that features on varicography, such as dilatation, turtuosity, luminal irregularity and widening of the distal end of the communicating vein, did not necessarily indicate incompetence. Only a diameter of larger than 5.0 mm would strongly suggest incompetence. We conclude that, whilst varicography is the most useful primary investigation for recurrent varicose veins to show the presence of communicating veins in mid-thigh (Hunter's Canal), ascending phlebography should be carried out to confirm their incompetence. This would help obviate unnecessary extensive surgical exploration and ligation of communicating, yet competent, veins.

The effects of radiographic contrast media on white blood cell function

R. Farrow, C. A. Roobottom and I. P. Wells
Department of Radiology, Derriford Hospital, Plymouth PL6 8DH, UK

There has been extensive research on the effects of radiographic contrast media on red cell rheology. However, there is a paucity of data on the effects of these agents on white cell function. The objectives of our study are to assess the effects of different types of contrast media on white cell function. We studied the effects of neutrophil orientation, chemotaxis and phagocytosis using Zigmond Chamber, underagarose migration and the NBT test, respectively. All of these are well validated in the literature. Results indicate that there is an adverse effect on all measured parameters of white cell function. This occurred at concentrations routinely achieved in clinical imaging and with all contrast agents studied. However, the adverse effects varied significantly depending on the contrast agent used. These effects were greatest with ionic monomers and least with non-ionic dimers. In conclusion all radiographic contrast media affect white cell function but this effect is variable. These findings may be of relevance in the selection of appropriate contrast agents in certain patient subgroups.

Lower leg DVT's—how good is colour flow ultrasound?

M. Bradley, P. Spencer, L. Alexander and G. Milner
X-ray Department, District General Hospital, Rotherham S60 2UD, UK

The first 50 patients in this double blind prospective study of 100 patients have been assessed. The aim is to identify the sensitivity for diagnosis of the deep vein thrombosis (DVT) using colour flow Doppler ultrasound. All patients entered in the trial had venography on the same day. Other studies have suffered from the small number of isolated lower leg DVT diagnosed, whereas we have already identified seven lower leg DVT in this series. 25 examination were positive for thrombus. Of these, seven had isolated lower leg DVT which were all identified by both venography and colour flow. Popliteal vein extension was seen in three cases with both modalities, but in one case by venography only. Preliminary results suggest that where there is underfilling of the deep veins due to clot during venography, colour flow may better delineate the true extent of thrombus. The ultrasound also picked up several other abnormalities in the calf in the other 25 "normal" studies. These included three cases of ruptured Baker's cysts, four cases of superficial thrombophlebitis and two cases of gastronemius tears.

Comparison of colour Doppler and phlebography in the diagnosis of deep vein thrombosis

A. Vargha, T. Baranyai, N. Bodrogi and I. Gergely
Department of Radiology, Hospital of Sopron, Hungary

A prospective study is being undertaken to compare colour Doppler (CD) with phlebography in the diagnosis of lower limb deep vein thrombosis. Phlebography is still a "gold standard" in the diagnosis but complications may occur even with modern non-ionic contrast media. It would be useful to have a non-invasive, simple, quick but accurate method instead. CD is non-invasive, easy to perform and only takes about 20 min per examination. Femoral and popliteal veins are visible even in the adductor canal. Calf veins can also be seen, the only problem is the visibility of the anterior tibial vein.

RADIOLOGY AND ONCOLOGY '93
AND MED X RAY

17–19 May 1993

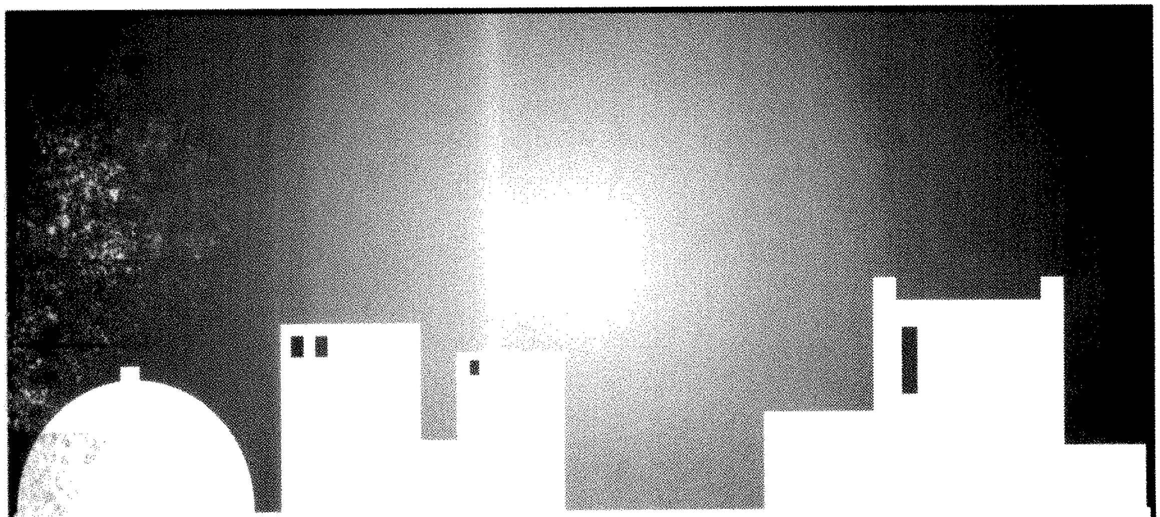

Glasgow, the cultural, commercial and tourist centre of Scotland is the venue for next year's conference and exhibition — make a note in your diary now!

Further information is available from
The British Institute of Radiology
36 Portland Place, London W1N 4AT
Telephone: 071-436 7807

Medical Radiation Protection Practice within the EEC

Editors: M Fitzgerald and J M Courades

Proceedings of a meeting held in London on 5th December 1990, organized by the **BIR** and the **CEC**.

Medical Radiation Protection Practice within the EEC will be of interest to everyone concerned with radiation protection. It contains:

- 11 papers by experts from 6 countries directly involved in the formulation and implementation of Directives.
- Overview of European Safety Legislation and the impact of Harmonization.
- Implementation of Directives affecting the general public, healthworkers and patients.
- Calibration requirements for radiation dosemeters.
- Review of scientific basis for standardization in radiology.

ISBN 0 905749 26 X, 56pp, 265x197mm, Softcover, £13.50
(£10 for BIR members)

The Future of Human Radiation Research (BIR Report 22)

Editors: G B Gerber, D M Taylor, E Cardis and J W Thiessen.

Contains the full review papers presented at a workshop held at Schloss Elmau on 4th-8th March 1991 under the joint sponsorship of the US Department of Energy, the Radiation Effects Research Foundation of Japan, the International Agency for Research on Cancer and the Commission of the European Communities.

This publication complements BIR Report 21 Risks from Radium and Thorotrast. It covers the important and topical subject of cancer risk prediction and contains papers from the worlds leading experts.

ISBN 0 905749 27 8, 174pp, 265mm x 197mm, Illustrated, Softcover, £27.50
(25% discount for BIR members)

THE SAFE USE OF
DIAGNOSTIC ULTRASOUND

Editors: M F Docker & F A Duck

Contributors: F A Duck, M, Dyson, J A Evans, G ter Haar, A R Williams

- Explains how to operate equipment to minimize risk of hazard to patients.
- Practical reference for everyone working in ultrasound.
- Discount for BIR and BMUS members.

ISBN 0 905749 28 6, 48pp, 297mm x 210mm, Illustrated, Softcover, £16
(£12 for BIR and BMUS members).

CURRENT RESEARCH IN OSTEOPOROSIS AND BONE MINERAL MEASUREMENT II: 1992

Edited by E F J Ring

ISBN 0 905749 29 4 softback 120 pages 265 x 197 mm
Publication date: 1 June 1992 Price: £28.00

- ▼ Pathophysiology of bone
- ▼ Radiological measurement of bone
- ▼ Ultrasonic measurement of bone
- ▼ Clinical spectrum of osteoporosis
- ▼ Screening for osteoporosis
- ▼ Pharmaceutical treatment of osteoporosis

Proceedings of the Third Bath Conference held 23-26 June 1992 organised by the National Osteoporosis Society (UK) and the Royal National Hospital for Rheumatic Diseases Bath. A follow up to the 1990 volume.

BJR CONGRESS SUPPLEMENT, VOLUME 65, 1992

Programme and Abstracts Book and Work in Progress Abstracts Booklet combined.

Containing Abstracts of all the presentations at the British Institute of Radiology's 50th Annual Congress: Radiology and Oncology '92, held on 18–20 May 1992 at the International Convention Centre, Birmingham.

Full Contents

Page

Minor amendments See overleaf

Programme and Abstracts Book

Programme and Abstracts Book Contents List iii

Abstracts Congress 1

Index to authors Congress 152

Work in Progress Booklet

Index to authors Facing Work in Progress i

Contents List Work in Progress i

Abstracts Work in Progress 1

Minor amendments

Please note the following corrections brought to our attention following the Congress but too late to be incorporated in the main text:

1. Work in Progress p. 6, "Prediction of lean body mass from ultrasound measurements of muscle thickness".

The order of the authors should be R. E. England, D. J. Withers, T. Watt, I. T. Campbell and D. F. Martin.

2. Work in Progress p. 7, "Use of ultrasound in osteomyelitis", by A. K. Nath and A. U. Sethu.

Please disregard the address provided with the abstract and instead read "Department of Radiology, Khoula Hospital, P.O. Box 51090, Mina Al-Fahal, Muscat - Sultanate of Oman".

3. Work in Progress p. 8, "3D reconstruction using CT of an ancient Egyptian mummy".

Please note that the authors and their corresponding addresses are as follows:

[1] S. Hughes, [1] C. Baldock, [3] A. Sofat, [4] R. Davis, [5] G. Spencer, [2] W. Wong and [2] K. Tonge

[1] *Department of Medical Physics,* [2] *Department of Radiology, St. Thomas' Hospital;* [3] *Institute of Neurology;* [4] *Formerly of Department of Physics, Royal Marsden Hospital;* [5] *Department of Egyptian Antiquities, British Museum; London, UK*

4. MED X RAY Exhibitors (see Programme and Abstracts page viii)

The following companies should be included with the list of Exhibitors:

APPLEFORD INSTRUMENTS LTD
C N SOFTWARE LTD
DANUM INTERNATIONAL LTD
IMC
INTERACTIVE IMAGING SYSTEMS LTD
MEDICAL PORTFOLIO LTD
MEGASOURCE
N E TECHNOLOGY LTD
SMS UNITED KINGDOM LTD
VISTEC BUSINESS SYSTEMS

RADIOLOGY & ONCOLOGY '92

Birmingham 18 – 20 May 1992

The 50th Annual Congress of the British Institute of Radiology incorporating the joint Spring Meeting of the Royal College of Radiologists and the Radiology Section of the Royal Society of Medicine and held in association with the Institute of Physical Sciences in Medicine.

For participants from the USA, application for CME Accreditation has been made. (Fifteen hours were offered at Radiology & Oncology '91).

Published by
The British Institute of Radiology, London, 1992

Phototypeset by BPCC Whitefriars Ltd, Tunbridge Wells,
and printed and bound by BPCC Wheatons Ltd, Exeter.

ORGANISING COMMITTEES

Congress Committee

Professor S C Lillicrap	BIR President and Chairman
Ms E C Beckmann	BIR Vice President and Med X Ray Advisor
Dr R H Corbett	Co-opted Scientific Programme Vice Chairman
Dr A M Davies	Local Representative
Dr P Dawson	BIR Vice President
Dr N W Garvie	BIR Honorary Secretary
Dr J A Glaholm	Local Representative
Dr S J Golding	Scientific Programme Chairman
Dr W Hately	BIR Vice President
Professor C A Joslin	BIR Past President
Dr M P Law	BIR Honorary Secretary & Scientific Poster Exhibition Co-ordinator
Dr D S McIntosh	BIR Honorary Treasurer
Dr W D Morgan	Local Representative
Mr J Twydle	Med X Ray Advisor
Ms V Whitehead	BIR Conference and Events Manager
Ms M-A Piggott	BIR General Secretary
Dr T Hogan	BIR Publications Manager
Miss E Carruthers	BIR Congress and Events Co-ordinator

Scientific Programme Committee

Dr S J Golding (Chairman)
Dr R H Corbett (Vice-Chairman)
Dr T Bates (RCR & RSM)
Ms E C Beckmann
Dr A M Davies
Dr P Dawson
Dr N W Garvie
Dr J A Glaholm
Dr R Harrison (IPSM)
Dr W Hately
Professor C A Joslin
Dr M P Law
Professor S C Lillicrap
Dr W D Morgan
Dr D Stoker (RCR)
Ms V Whitehead

Acknowledgements

The BIR acknowledges with gratitude the help and support of the following:

3M UK plc
Agfa-Gevaert Ltd
Amersham International plc
Anglo-Japanese Radiological Society
The Birmingham School of Radiography
Birmingham Reps and their Hospital Departments
British Nuclear Fuels plc
Du Pont (UK) Ltd
IGE Medical Systems Ltd
Kodak Ltd
Mitsubishi Electric UK Ltd
Nycomed (UK) Ltd
Mr A M Oxley and his team
RAD Magazine, Kingsmoor Publications
Schering Health Care Ltd
Schneider UK plc
Siemens plc
The University of Oxford

CONTENTS

Organising Committees ii
Acknowledgements ii
Message from the President iv
General Information v
List of MED X RAY Exhibitors viii

Scientific Programme and Timetable ix
Personal Planner xii
Monday xv
Tuesday xx
Wednesday xxvi

Abstracts

Monday Congress 1
Tuesday Congress 45
Wednesday Congress 95

Index to authors Congress 152
Map of International Convention Centre and Birmingham Inside back cover and facing page

RADIOLOGY & ONCOLOGY '93

Scottish Exhibition and Conference Centre, Glasgow 17 – 19 May 1993
British Institute of Radiology 51st Annual Conference

Held in association with the Royal College of Radiologists, the Scottish Radiological Society, the Institute of Physical Sciences in Medicine and the Radiology Section of the Royal Society of Medicine.

Radiology & Oncology '93 will incorporate all aspects of modern radiology for all those concerned with diagnostic radiology, radiotherapy and allied sciences.

Proffered abstracts are invited for oral and poster presentations and will form a major element of the meeting.

Deadline for receipt of abstracts: **FRIDAY NOVEMBER 27, 1992**

MESSAGE FROM THE PRESIDENT

Thank you for participating in Radiology & Oncology '92 and the MED X RAY exhibition at this our Golden Jubilee Congress which, we are pleased to report at the time of writing, is proving to be our largest ever.

The Scientific Programme Committee, chaired by Stephen Golding, has provided an interesting and stimulating programme designed to bring together practising professionals, to share experiences and exchange information to help provide for the best practices in Radiology and Oncology. These activities are the major ongoing function of our large multidisciplinary Institute.

We are especially honoured by having three outstanding speakers for the eponymous lectures and bid them a special welcome. The programme also includes teach-ins and work-in-progress sessions. We hope the mix will prove to be to your satisfaction and invite you to let us know of your views following the meeting.

We again have a splendid MED X RAY exhibition and hope you will make the maximum use of the opportunity to exchange views and discuss the latest developments with industry colleagues.

I also wish you a most enjoyable time socially, meeting old friends and making new ones. Vanessa Whitehead and the Conference Team have been dedicated to preparing for this Congress, and will be found at the Registration desk to help with any queries you may have.

Thank you for joining us. I wish you a successful and enjoyable meeting.

STEPHEN LILLICRAP

GENERAL INFORMATION

Congress Site

Radiology & Oncology '92 takes place at the International Convention Centre in Birmingham. Plenary lectures are held in Hall 9; all other sessions take place as shown on the timetable grid (see pages ix to xi). A layout map of the Centre is included on the inside back cover.

Registration

Your delegate's pack contains all relevant tickets (please check these), list of delegates, the MED X RAY handbook and your Congress badge.

Your badge entitles you to admission to all lectures at Radiology & Oncology '92 and to MED X RAY for the days on which you are registered and must be worn throughout the Congress.

Registration Desk Opening Times

The Registration desk will be situated in the Registration area of the International Convention Centre and will be open at the following times:

Sunday	4.00pm - 7.00pm
Monday & Tuesday	8.00am - 4.30pm
Wednesday	8.00am - 2.00pm

MED X RAY

MED X RAY runs for the three days of the Congress, from Monday 18 May - Wednesday 20 May, to span the annual meetings of the British Institute of Radiology and The College of Radiographers. MED X RAY is sited in halls 3 & 4 of the ICC. The opening times are:

Monday-Wednesday 18-20 May   9.00am - 5.30pm

Full details of the companies exhibiting are given in the MED X RAY handbook in your delegates pack.

Scientific Poster Exhibition

The large scientific poster exhibition is on the balcony of Hall 3, within MED X RAY. Opening times are the same as for MED X RAY.

BIR posters will be discussed in chaired sessions and a note of the date, time and session of oral presentation will be on the poster. Abstracts are included within the relevant sessions. The BIR poster exhibition includes presentations on the following topics:

Computed Tomography
Interventional Radiology
Magnetic Resonance Imaging
Nuclear Medicine
Radiation Physics
Radiobiology
Radiological Physics
Radiotherapy and Oncology
Ultrasound

RAD Magazine Poster Prize

The judging of the best proffered poster (content and presentation) will take place on Monday.

Finzi Prize for Junior Radiologists

The Royal Society of Medicine will hold their Finzi Prize for Junior Radiologists on Wednesday 20 May at 2.00pm in Hall 11a.

BIR Information Stand

The BIR stand will be situated on the balcony in Hall 3, within MED X RAY. Further details can be found in the MED X RAY handbook. BIR staff will be available to discuss any aspect of the Institute's activities. We welcome both members and non-members to come and discover the benefits of membership.

Messages

Please check the notice board by the registration desk for messages.

Telephone

There will be a telephone manned during Congress registration opening hours for urgent messages: Birmingham 021-200 2000. This is the main Convention Centre number. Messages will be posted on the message board for delegates' attention.

A number of telephones, both cash and card phones, are located on each floor of the International Convention Centre.

Refreshments

Free tea and coffee will be available within MED X RAY from Monday to Wednesday. Refreshments will be available throughout the day.

Lunch

Light snacks are also available on a cash basis from refreshment points in MED X RAY.

Facilities in the Mall

The Mall, open to the public from 7am until 1am, offers the following facilities:

- * The Box Office for booking concert tickets for events in Symphony Hall, National Indoor Arena and the NEC Arena. Details of forthcoming events can be obtained here.
- * The Coffee Terrace, open from 9am to 9pm provides non-alcoholic beverages and snacks. This is a spacious area allowing easy access to wheelchair users.
- * Located next to the Coffee Terrace is a post box and postage stamp machine for national and international mail.
- * A Visitors' Services Centre incorporates an office providing fax, photocopying and other business services and also an information and booking facility from the Birmingham Convention and Visitor Bureau.
- * The National Westminster Bank has opened a branch for basic counter transactions. There is also a foreign exchange service, please allow 3 days when ordering currency. This bank will be open from 9am until 4.30pm on weekdays.
- * A special freephone service linking the ICC directly to the control centre of the Taxi Owners Association, ensuring a swift response to any requests for taxis.

Cloakrooms

Cloakrooms are available in the Mall during event hours only.

Medical Centre

A Medical Centre is located on Level 3, close to the Coffee Terrace. A full emergency service is provided by professionally trained staff.

Car Parking

2,600 car parking spaces are available at the National Indoor Arena. These are run on a pay and display basis, however spaces can be pre-booked (please contact the BIR Conference Office). The ICC can be reached from here by a short walk or by shuttle bus.

Special Needs

The ICC has been designed with careful consideration for the special needs of people with disabilities. All Halls have wheelchair access.

Good Companions Programme

(admission by ticket only)

It may be possible to accept last-minute bookings for the following at the Registration desk. All tours will depart from the International Convention Centre by 9.30am.

Monday 18 May, Black Crystal Works and Museum, £19.60
A coach tour through the Black Country, an important part of the Midland heritage, has been arranged. The surroundings are no longer black but it is still the home of many internationally renowned glass companies. A stop will be made at the Stuart Crystal shop where a souvenir may be purchased. Watch skilled craftsmen demonstrating the art of glass manufacture at the Royal Brierley Crystal works. The Black Country Museum has preserved the rich industrial heritage of 18th century Midlands. Take a ride on a narrow boat on the canal into the Singing Cavern. Lunch is not included.

Tuesday 19 May, Warwick Castle and Stratford-upon-Avon, £21.20
Travelling via Meriden and Kenilworth Castle, one of the chief strongholds in Tudor England, to Warwick Castle which dates back to the early 17th century. It is one of the finest medieval castles in England, with fine State Rooms and Great Hall, and an impressive array of pictures, furniture, armoury, dungeon and 60 acres of gracious gardens and parkland. The tour will continue on through the beautiful Warwickshire countryside, and on to Stratford-upon-Avon, the very attractive market town set on the banks of the River Avon.

Visit the birthplace of William Shakespeare and the Shakespeare Centre containing many interesting exhibits and souvenirs. The coach will then take you for a panoramic tour of Stratford and make a brief stop at Mary Arden's House, the home of Shakespeare's mother.

Wednesday 20 May, Cadbury World, £13.50
This is a must for all chocoholics. Take this opportunity to experience the magic of chocolate at Cadbury World, located in the heart of the company's historic Bournville site - the original 'factory in the garden'. The Cadbury World experience traces the story of chocolate from its Central American origins through its arrival in Europe and the growth of the Cadbury business from its small family beginnings. The tour includes a demonstration of chocolate making.

Social Programme

(admission by ticket only)

It may be possible to obtain tickets from the BIR office.

Sunday, 17 May:

Radiology & Oncology '92 Fishing Competition:
Enjoy a splendid day's fly fishing for trout at the internationally famous fishery at Packington Hall, Meriden. The day will end with the traditional dinner. Prices from £12.00. Further details can be obtained from Dr W G Jones, Academic Unit of Radiotherapy, Tunbridge Building, Cookridge Hospital, Leeds LS16 6QB. Telephone: Leeds (0532) 673411.

Radiology Golfing Society Golf Match, 11.30am:
The traditional Golf match will take place at the Belfry, over the Brabazon Course. A buffet lunch will be provided beforehand and dinner will be served in the Worcester Suite in the evening. Cost £35.00. Please contact the BIR Conference Office.

Informal Welcome Gathering, 6.00pm - 8.00pm:
This will be held in the foyer of Hall 1 in the International Convention Centre. Meet your fellow delegates, have a drink and pick up your conference folder on Sunday evening. (Free.)

Monday, 18 May:

Civic Reception, 6.15pm - 7.00pm:
This will be held in the Town Hall, Centenary Square, Birmingham. (Free.)

Patrick Collection and buffet supper, 7.00pm - 10.30pm:
This evening includes a tour of Autoworld - a unique collection of over 200 vehicles ranging from 1904 to the present day. They are displayed in period settings within a Victorian Paper Mill in Kings Norton. Price including coach, buffet, wine and VAT is £25.50 per person.

Symphony Hall Evening, 6.30pm-10.30pm:
(Supported by Schering Health Care Ltd)
Music from Swan Lake by Tchaikovsky, Prokofiev's Violin Concerto No 1 in D and Shostakovich's Symphony No 5 in D minor (his most popular symphony) will be performed by the Philharmonic Orchestra of Novosibirsk. The soloist violin is Nicolai Modayan, conducted by Arnold Katz. Price including pre-concert buffet, admission to the concert (usual ticket price £21), drinks and VAT is £22.00 per person.

Tuesday, 19 May:

Topic Lunch, 1.20pm:
(Supported by Nycomed (UK) Ltd)
A chance for informal discussion over lunch with leading experts, on any subject of the participant's choice. Price £5.00.

Annual Dinner 7.30pm for 8.00pm:
This will be held in the Botanical Gardens, Birmingham. There will be free seating. Dress is black tie/dark suit. Cost including transport, drinks reception, wine and VAT is £34.50 per person.

[While all information was correct at the time of going to press, we regret that it was impossible to make changes notified later.]

MED X RAY EXHIBITORS

Listed below are the companies booked to exhibit at MED X RAY, the UK's largest exhibition devoted to the radiological sciences. It is held jointly with The College of Radiographers and is open to all delegates at Radiology & Oncology '92 throughout the Congress. This is the ideal opportunity to view the very latest in equipment and services to the whole industry, and to meet the leading manufacturers to discuss how modern technology can help your concern. Further information can be found in your MED X RAY handbook which is in your delegates pack.

AGFA-GEVAERT LTD
ART COLENTA INTERNATIONAL
ATHRODAX SURGICAL LTD
AURA SCIENTIFIC
BARTEC MEDICAL SYSTEMS LTD
BIOGLAN LABORATORIES LTD
BOC LTD, SPECIAL GASES
BRITISH INSTITUTE OF RADIOLOGY
BRITISH LEAD MILLS SPECIAL PRODUCTS
BRITISH NUCLEAR FUELS PLC
BURLINGTON MEDICAL SUPPLIES LTD
BVM MEDICAL LTD
CALUMET COACH COMPANY
CEA (UK) LTD
CERNER LTD
CHAMPION PHOTOCHEMISTRY INT. LTD
CIS (UK) LTD
THE COLLEGE OF RADIOGRAPHERS
COOK (UK) LTD
CORDIS (UK) LTD
CORINTH MEDICAL
D C BAYMAN CONSTRUCTION LTD
DATA-MED COMPUTER SERVICES LTD
DELLADENE LTD
DEPARTMENT OF HEALTH
DIASONICS SONOTRON LTD
DU PONT (UK) LTD
E MERCK PHARMACEUTICALS
ELSCINT (GB) LTD
EMS EUROPEAN MEDICAL SERVICES
E-Z-EM LTD
FUJI PHOTO FILM (UK) LTD
FUMEO VIDEO SYSTEMS LTD
GAMMEX-RMI LTD
GRANTA BOOK EXHIBITIONS
HENLEYS MEDICAL SUPPLIES LTD
HITACHI MEDICAL SYSTEMS EUROPE GMBH
HTS/PHOENIX IMAGING SYSTEMS LTD
I G E MEDICAL SYSTEMS LTD
IGP (UK) LTD
IMPEX IMAGING SYSTEMS LTD
ISG TECHNOLOGIES EUROPE
KIMAL SCIENTIFIC PRODUCTS LTD
KODAK LTD
KONICA UK LTD
LANDAUER INC
LANMARK
LASER LINES LTD
MAB SERVICES LTD
MALLINCKRODT MEDICAL UK LTD
MARPAUL GROUP
MAS MEDICAL LTD
MEADOX (UK) LTD
MEDICAL X-RAY SUPPLIES LTD
MEDIGRAPH IMAGING LTD
MEDIVANCE INSTRUMENTS LTD
NATIONAL PHYSICAL LABORATORY
NORGINE LTD
NRPB
NUCLETRON TRADING LTD
NYCOMED (UK) LTD
OBS ENTERPRISES LTD
PHILIPS MEDICAL SYSTEMS
PHOTOSOL LTD
PLANMED
PLH MEDICAL LTD
POLAROID (UK) LTD
PREMISE ENGINEERING LTD
QADOS LTD
RADIATRON COMPONENTS LTD
RADIOLOGIC (UK) LTD
RAPITECH (UK) LTD
ROTHBAND W S & CO LTD
SABRE SCIENTIFIC LTD
SCHERING HEALTH CARE LTD
SCHNEIDER UK
SIEL IMAGING EQUIPMENT LTD
SIEMENS PLC
SIEMENS NIXDORF INFORMATION SERVICE
SIMIS MEDICAL IMAGING LTD
SMITH & NEPHEW PHARMACEUTICALS LTD
SURGICAL MEDICAL RADIOLOGICAL X-RAY LTD
TOSHIBA MEDICAL SYSTEMS LTD
VARIAN
VERTEC SCIENTIFIC LTD
WALLAC (NEWBURY) LTD
WARDRAY PRODUCTS LTD
WISEPRESS LTD
WOLTERS KLUWER US CORPORATION
WOLVERSON X-RAY & ELECTRO-MEDICAL LTD
X-OGRAPH LTD
X-RITE (H MILLER GRAPHICS LTD)
ZENITH MEDICAL SYSTEMS LTD
3M UK PLC

[List correct at time of going to press]

MON	Hall 9	Hall 10a	Hall 10b	Hall 11a	Hall 11b
8.45	OPENING — Professor S C Lillicrap				
9.00 — 10.15	**THE CENTRAL NERVOUS SYSTEM** Invited Review Lecture Professor G Bydder, London	**RADIOTHERAPY TREATMENT I** Invited Review Lectures Dr H J Dobbs, London Dr T Landberg, Sweden	**NUCLEAR MEDICINE I** Invited Review Lecture Dr K E Britton, London	**APPLICATION OF BS5750 TO RADIOLOGY** Invited Review Lectures Mr I Hendra, London Dr R Warren, Epping Mr A O'Neill, Kodak, London	**WORKSHOP** HOW DOES RADIOLOGY PROSPER IN THE TRUST HOSPITAL? Organiser: Dr H Loose, Newcastle
COFFEE IN MED X RAY					
10.45 — 12.00	**THE CHEST - BIOPSY TECHNIQUES AND HIGH TECHNOLOGY IMAGING**	**RADIOTHERAPY TREATMENT II** Invited Review Lecture Dr P C Williams, Manchester	**NUCLEAR MEDICINE II** Invited Review Lecture Dr I Gordon, London	**MUSCULOSKELETAL IMAGING — JOINT DISEASE** Invited Review Lecture Dr A M Davies, Birmingham	
12.15 — 1.15	**MACKENZIE DAVIDSON MEMORIAL LECTURE** Professor Sir David Weatherall, Oxford				
LUNCH IN MED X RAY					
2.15 — 3.45	**ULTRASOUND** Invited Review Lecture Dr F A Duck, Bath	**RADIOTHERAPY TREATMENT III** Invited Review Lectures Mrs S Griffiths, Leeds Dr W Swindell, Sutton	**National Centre of Responsibility / BIR Seminar** COMMITTED FOR LIFE	**NUCLEAR MEDICINE III** Invited Review Lectures Dr M Merrick, Edinburgh Dr I Fogelman, London	**CARDIOVASCULAR ADVANCES** Invited Review Lecture Dr D M Nichols, Inverness
TEA IN MED X RAY					
4.15 — 5.30	**PRESIDENTIAL ADDRESS** Professor S C Lillicrap	**ONCOLOGY WORK IN PROGRESS**			**GASTROINTESTINAL IMAGING**

TUES	Hall 9	Hall 10a	Hall 10b	Hall 11a	Hall 11b
8.15	AGM (BIR members only)				
9.00 — 10.15	**MRI TECHNOLOGY** Invited Review Lecture Professor M A Smith, Leeds	**COMBINED CHEMOTHERAPY & RADIOTHERAPY - PROMISES & PROBLEMS** Invited Review Lectures Dr M H Cullen, Birmingham Dr D Spooner, Birmingham	**DIAGNOSTIC WORK IN PROGRESS I**	**RADIOLOGICAL AUDIT**	**HEPATOBILIARY AND PANCREATIC IMAGING** Invited Review Lecture Dr S P Olliff, Birmingham
COFFEE IN MED X RAY					**RADIOBIOLOGY DAY** **in memory of Dr N McNally**
10.45 — 12.00	**TRAUMA** Invited Review Lecture Dr J W R Young, Maryland, USA	**BREAST ONCOLOGY** Invited Review Lecture Dr J R Yarnold, Sutton	**DIAGNOSTIC WORK IN PROGRESS II**	**DEVELOPMENT OF PRODUCTS FOR RADIOLOGY** Invited Review Lectures Dr T Renaa, Nycomed, Birmingham Dr G Elsner, Du Pont, Germany	**SESSION I** Invited Review Lecture Dr M C Joiner, Middlesex
12.15 — 1.15	**SILVANUS THOMPSON MEMORIAL LECTURE** Professor E Hall, USA		**DIAGNOSTIC WORK IN PROGRESS III**		
LUNCH IN MED X RAY					
2.15 — 3.45	**NON-VASCULAR INTERVENTIONAL PROCEDURES** Invited Review Lecture Professor C L Zollikofer, Switzerland	**RADIOLOGICAL HISTORY** Invited Review Lectures Dr N Trott, Cheam Dr J G L Cole, Birmingham	**MUSCULOSKELETAL IMAGING**	**WORKSHOP** GREENING THE RADIOLOGY DEPARTMENT Organiser: Dr E Ison, Oxford	**SESSION II** Invited Review Lecture Dr M Saunders, Middlesex
TEA IN MED X RAY					
4.15 — 5.30	**ADVANCES IN IMAGING THE LIVER** Invited Review Lecture Prof Y Itai, Tokyo, Japan	**AUDIT, TEACHING AND MANAGEMENT APPROACHES IN RADIOLOGY**	**TEACH-IN** **THROMBO-EMBOLIC PHENOMENA IN CLINICAL ANGIOGRAPHY - ROLE OF MATERIALS & TECHNIQUE** Organiser: Dr P Dawson, London Dr A-M Belli, London		**SESSION III** Invited Review Lecture Prof H Bartelink, Amsterdam

WED	Hall 9	Hall 10a	Hall 10b	Hall 11a	Hall 11b
9.00 — 10.15	**MAMMOGRAPHY — QUALITY CONTROL AND SCREENING** Invited Review Lecture Dr R Warren, Epping	**IMAGING AND INVESTIGATION IN CLINICAL ONCOLOGY**	**GENITOURINARY IMAGING** Invited Review Lecture Dr R Johnson, Manchester	**ANGIOPLASTY** Invited Review Lecture Dr W Seyferth, Germany	**PHYSICS I** **BODY COMPOSITION** Invited Review Lecture Professor S Mattsson, Malmö, Sweden
COFFEE IN MED X RAY					
10.45 — 12.00	**NEW APPLICATIONS OF MRI** Invited Review Lecture Dr S Harms, Dallas, USA	**COUNSELLING AND QUALITY OF CARE IN ONCOLOGY** Invited Review Lectures Dr E J Maher, Middlesex Dr J Morris, York	**MEASUREMENTS OF BONE MINERAL** Invited Review Lecture Dr D Felsenberg, Berlin, Germany	**CHEST RADIOLOGY** Invited Review Lecture Dr M McCarty, London	**PHYSICS II** **IMAGE ASSESSMENT** Invited Review Lecture Dr M S Chesters, Leeds
12.15 — 1.15	**3M MAYNEORD MEMORIAL LECTURE** Dr W Vennart, Exeter				
LUNCH IN MED X RAY					
2.15 — 3.45	**ANGIOGRAPHY & INTERVENTIONAL RADIOLOGY**	**TEACH-IN** **IMAGING IN PAEDIATRIC ONCOLOGY** Organiser: Dr S Chapman, Birmingham Invited Review Lectures Dr S Chapman, Birmingham Dr J McHugo, Birmingham Dr C Dicks-Mireaux, London	**ENT IMAGING** Invited Review Lecture Dr P Anslow, Oxford	**ROYAL SOCIETY OF MEDICINE** **FINZI PRIZE** **FOR JUNIOR** **RADIOLOGISTS**	**PHYSICS III** **RADIATION PROTECTION & RISKS AFTER ICRP 60** Invited Review Lecture Dr P J Roberts, Southampton
TEA IN MED X RAY					
4.15 — 5.30	**ADVANCES IN DOPPLER ULTRASOUND**	**BODY CT — CLINICAL & TECHNICAL ADVANCES** **THE BREAST — CLINICAL & TECHNICAL ADVANCES**			**PHYSICS IV** **RADIATION PROTECTION & RISKS** Invited Review Lecture Mr B F Wall, NRPB, Didcot

PERSONAL PLANNER MONDAY 18 MAY

Morning	Afternoon	Evening

08.45 - 09.00am
Opening by BIR President

09.00 - 10.15am
Scientific Sessions
The Central Nervous System
Radiotherapy Treatment I
Nuclear Medicine I
The Application of BS5750 to Radiology

09.00 - 12.00pm
How does Radiology Prosper in the Trust Hospital?

10.45 - 12.00pm
Scientific Sessions
Musculoskeletal Imaging - Joint Disease
Nuclear Medicine II
Radiotherapy Treatment II
The Chest: Biopsy Techniques and High Technology Imaging

12.15pm
MACKENZIE DAVIDSON MEMORIAL LECTURE
"Molecular biology in common disease", Professor Sir David Weatherall, Oxford

2.15 - 5.00pm
Committed for Life: Equipment Seminar

2.15 - 3.45pm
Scientific Sessions
Cardiovascular Advances
Ultrasound
Radiotherapy Treatment III
Nuclear Medicine III

4.15 - 5.30pm
PRESIDENTIAL ADDRESS
"Exploring the niches: some lesser known research areas at the Congress", Professor Stephen Lillicrap, Bath

4.15 - 5.30pm
Scientific Sessions
Oncology Work In Progress
Gastrointestinal Imaging

6.15pm
Civic Reception
6.30pm
Concert at Symphony Hall
7.00pm
The Patrick Collection

PERSONAL PLANNER TUESDAY 19 MAY

Morning	Afternoon	Evening

08.15am BIR AGM

09.00 - 10.15am
Scientific Sessions
MRI Technology
Combined Chemotherapy and Radiotherapy - Promises and Problems
Radiological Audit
Hepatobiliary and Pancreatic Imaging
Diagnostic Work in Progress I

09.00 - 12.00pm
How does Radiology Prosper in the Trust Hospital?

10.45 - 12.00pm
Scientific Sessions
Trauma
Breast Oncology
Radiobiology Day Session I
Developments of Products for Radiology
Diagnostic Work in Progress II

12.15pm
SILVANUS THOMPSON MEMORIAL LECTURE
"The gene as a theme in the paradigm of cancer", Professor Eric Hall, New York

12.15 - 1.15pm *Scientific Session*
Diagnostic Work in Progress III

1.20pm Topic Lunch

2.15 - 3.45pm *Scientific Sessions*
Non-Vascular Interventional Techniques
Radiological History
Musculoskeletal Imaging
Radiobiology Day Session II

2.15 - 5.30pm
Greening the Radiology Department

4.15 - 5.30pm *Scientific Sessions*
Advances in Imaging the Liver
Audit Teaching and Management Approaches in Radiology
Thrombo-Embolic Phenomena in Clinical Angiography - Role of Materials and Technique
Radiobiology Day Session III

7.30pm
BIR Annual Dinner

PERSONAL PLANNER WEDNESDAY 20 MAY

Morning	Afternoon	Evening

09.00 - 10.15am
Scientific Sessions
Mammography - Quality Control and Screening
Imaging and Investigation in Clinical Oncology
Genitourinary Imaging
Angioplasty
Physics I - Body Composition

10.45 - 12.00pm
Scientific Sessions
New Applications of MRI
Counselling and Quality of Care in Oncology
Measurements of Bone Mineral
Chest Radiology
Physics II - Image Assessment

12.15pm
3M MAYNEORD MEMORIAL LECTURE
"Targeted magnetic resonance imaging", Dr William Vennart, Exeter

2.00 - 5.30pm RSM Finzi Prize

2.15 - 3.45pm
Scientific Sessions
Angiography and Interventional Radiology
Imaging in Paediatric Oncology
ENT Imaging
Physics III - Radiation Protection and Risks after ICRP 60

4.15 - 5.30pm
Scientific Sessions
Advances in Doppler Ultrasound
Body CT - Clinical and Technical Advances
The Breast - Clinical and Technical Advances
Physics IV - Radiation Protection and Risks

MONDAY 18 MAY 8.45–9.00

HALL 9

Opening of Radiology & Oncology '92 by BIR President, Professor S C Lillicrap

MONDAY 18 MAY 9.00–10.15

HALL 9

THE CENTRAL NERVOUS SYSTEM

Chairman: Dr D A Yates, Smethwick

9.00–9.25 **Diffusional MRI of the brain**
Invited Review Professor G M Bydder, London (*p. 1*)

9.25–9.33 **CT and MR in the diagnosis of intraventricular cerebral masses**
E J Cornford, Nottingham (*p. 1*)

9.33–9.41 **Fast Spin Echo (FSE) techniques in cranial MR imaging**
J V Byrne, Oxford (*p. 1*)

9.41–9.45 **MRI of meningeal enhancement in malignant disease**
R Guy, Sutton (*p. 2*)

9.45–9.49 **Assessment of meningeal pathology by MRI and CT**
C E Hutchinson, Manchester (*p. 2*)

9.49–9.57 **The role of CT scanning in the investigation of low tension glaucoma**
P G White, Cardiff (*p. 2*)

9.57–10.01 **Ophthalmology referrals for brain CT — a retrospective audit**
W Kincaid, Glasgow (*p. 2*)

10.01–10.09 **Computed tomography of the brain in psychiatric patients: an audit**
D J Grier, Bristol (*p. 3*)

10.09–10.17 **The outcome of fetal ventriculomegaly**
P Twining, Nottingham (*p. 3*)

HALL 10a

RADIOTHERAPY TREATMENT I

Chairman: Dr C H Paine, Oxford

9.00–9.25 **Dose specification: is there a consensus?**
Invited Review Dr H J Dobbs, London (*p. 4*)

9.25–9.33 **Radiobiological implications of physical dose inhomogeneity in radiotherapy treatment planning**
A E Amin, Glasgow (*p. 4*)

9.33–9.41 **Non-coplanar radiotherapy treatment planning**
S G McNee, Glasgow (*p. 4*)

9.41–9.45 **Dose distributions for chest wall conformation therapy using 6 MV X-rays and cobalt beams**
M E Oatey, London (*p. 5*)

9.45–9.49 **Staging of head and neck cancer using magnetic resonance imaging**
M McCarty, Northwood (*p. 5*)

9.49–10.14 **The clinician's expectations from treatment**
Invited Review Dr T Landberg, Malmö, Sweden (*p. 5*)

HALL 10b

NUCLEAR MEDICINE I

Chairman: Dr K E Britton, London

9.00–9.25 **Progress in the radionuclide therapy of cancer**
Invited Review Dr K E Britton, London (*p. 6*)

9.25–9.33 **Dobutamine thallium tomography in the investigation of Syndrome X**
P J Thorley, Leeds (*p. 6*)

9.33–9.39 **Study of left ventricular function in two families with Romano-Ward syndrome**
S J Cross, Aberdeen (*p. 7*)

9.39–9.43 **Detection of viable myocardium with gated F18 fluorodeoxyglucose (FDG) positron emission tomography (PET)**
H S Lee, Aberdeen (*p. 7*)

9.43–9.51 **Regional left ventricular function following CABG: evidence for hibernating myocardium**
M J Metcalfe, Aberdeen (*p. 7*)

9.51–9.55 **Autologous platelet survival in volunteer blood donors**
V S Turner, Birmingham (*p. 8*)

9.55–10.03 **Technetium-HMPAO labelled leucocyte scanning in the initial diagnosis of inflammatory bowel disease**
P N Malcolm, London (*p. 8*)

10.03–10.07 **The use of HMPAO-labelled white cell scintigraphy in the assessment in the assessment of recurrent Crohn's disease**
R P McAvinchey, London (*p. 8*)

HALL 11a

THE APPLICATION OF BS5750 TO RADIOLOGY

Chairman: Dr R H Corbett, East Kilbride

9.00–9.25 **Management and audit — BS5750 in radiology**
Invited Review Dr I R F Hendra, London (*p. 9*)

9.25–9.50 **Total quality management in a clinical radiology department**
Invited Review Dr R Warren, Epping (*p. 9*)

9.50–10.15 **The value of BS5750 to any work or business activity — a company view**
Invited Review Mr A O'Neill, Kodak, London (*p. 9*)

HALL 11b

WORKSHOP (9.00–12.00)
HOW DOES RADIOLOGY PROSPER IN THE TRUST HOSPITAL?

Organizer and Chairman: Dr H Loose, Newcastle-upon-Tyne

Invited Lectures **The status of the Radiology department in the provider — purchaser philosophy**
D Perry, Oxford

The administration and staffing of a trust hospital — our solutions
P Wright, Newcastle-upon-Tyne

How to ensure equipment purchase and minimize capital charges
A Carty, Liverpool

How to cost procedures and the factors to be included
P Davies, Nottingham

Internal cross-charging and external contracts — essential to economic survival
A Saunders, London

MONDAY 18 MAY 10.45–12.00

HALL 9

THE CHEST: BIOPSY TECHNIQUES AND HIGH TECHNOLOGY IMAGING

Chairman: Dr J Ollif, Birmingham

10.45–10.53 **The use of a powered cutting needle (biopty) for obtaining histopathological material in intrapulmonary lesions**
J A A Haddock, London (*p. 11*)

10.53–11.01 **Radiologically guided mediastinal biopsy: a 10 year review**
B Morrissey, Penarth (*p. 11*)

11.01–11.09 **Ultrasound guided biopsy of peripheral lung and pleural lesions**
L Robinson, London (*p.11*)

11.09–11.17 **Avoidance of pneumothorax during percutaneous biopsy of the chest: creating an extrapleural "window"**
S J Golding, Oxford (*p. 12*)

11.17–11.21 **CT assessment of the size of pulmonary nodules: an *in vitro* study**
K M Harris, Penarth (*p. 12*)

11.21–11.29 **Computed tomography in the assessment of the opaque hemithorax in children**
J M E Kirk, London (*p. 12*)

11.29–11.33 **A quantitative HRCT technique for the serial assessment of bronchiectasis**
S R Desai, London (*p. 13*)

11.33–11.37 **High resolution CT appearances in pulmonary complications of rheumatoid disease**
F K Cheah, London (*p. 13*)

11.37–11.41 **High resolution CT appearances in pulmonary haemosiderosis with pathological correlation**
F K Cheah, London (*p. 13*)

11.41–11.45 **The ATS nodal map — a CT demonstration**
J G Murray, Dublin (*p. 13*)

11.45–11.53 **Anterior mediastinal lymphoma**
I R Brand, Leeds (*p. 14*)

11.53–12.01 **MRI of residual lymphoma masses**
D MacVicar, Sutton (*p. 14*)

HALL 10a

RADIOTHERAPY TREATMENT II

Chairman: Dr W Swindell, Sutton

10.45–11.10 **Shaping the treatment volume**
Invited Review Dr P C Williams, Manchester (p. 15)

11.10–11.18 **Optimizing dose with a multileaf collimator for conformal radiotherapy**
S Webb, Sutton (*p. 15*)

11.18–11.26 **Potential advantages of 3D conformal planning in extremity soft tissue sarcoma**
A M Bidmead, London (*p. 16*)

11.26–11.34 **Technical aspects of fractionated stereotactic radiotherapy**
A P Warrington, London (*p. 16*)

11.34–11.38 **Fractionated stereotactic external beam radiotherapy for the treatment of recurrent gliomas and solitary brain metastases: a dose escalation study**
R W Laing, Sutton (*p. 16*)

11.38–11.46 **A computer program for scheduling radiotherapy courses**
E Claridge, Birmingham (*p. 17*)

11.46–11.50 **Use of CT planning to improve mantle radiotherapy dosimetry**
A J Rathmell, Leeds (*p. 17*)

HALL 10b

NUCLEAR MEDICINE II

Chairman: Dr I Gordon, London

10.45–11.10 **The influence of nuclear medicine in paediatric imaging**
Invited Review Dr I Gordon, London (*p. 18*)

11.10–11.18 **Multipurpose scintigraphy with ^{99}Tc^{m} pyrphotech in paediatric oncology**
B F Sinyuta, Kiev, Russia (*p. 18*)

11.18–11.26 **The external radiation hazard from parents and infants undergoing nuclear medicine procedures**
P J Mountford, Birmingham (*p. 19*)

11.26–11.30 **An evaluation of the clinical usefulness of captopril renal scintigraphy**
G C Ooi, Leicester (*p. 19*)

11.30–11.38 **Diagnosis of pulmonary embolism: clinical practice and the use of diagnostic imaging**
C S Romaniuk, Leeds (*p. 19*)

11.38–11.42 **A comparison of SPECT and planar imaging in pulmonary embolus**
S Eustace, Dublin (*p. 19*)

11.42–11.50 **Closing the feedback loop of audit**
J Griffith, Birmingham (*p. 20*)

HALL 11a

MUSCULOSKELETAL IMAGING — JOINT DISEASE

Chairman: Dr N Evans, Birmingham

10.45–11.10 **Advanced imaging of the hindfoot**
Invited Review Dr A M Davies, Birmingham (*p. 21*)

11.10–11.18 **Magnetic resonance and CT arthrography of the shoulder**
I W McCall, Oswestry (*p. 21*)

11.18–11.22 **Superior image quality of high field MR system in comparison with low field MR system in joint disease**
A Mundinger, Freiburg (*p. 21*)

11.22–11.30 **Magnetic resonance tomography of the shoulder: a comparative study with arthroscopy**
C Gückel, Basel (*p. 22*)

11.30–11.34 **The contribution of variations of acromial morphology in rotator cuff disorder — MR imaging**
J Namasivayam, Glasgow (*p. 22*)

11.34–11.38 **Comparison of contrast media in CT arthography of the shoulder**
R Wellings, Birmingham (*p. 22*)

11.38–11.46 **Ultrasound evaluation of displacement in the ossified hip**
L H Berman, Cambridge (*p. 23*)

11.46–11.50 **Demonstration of osteochondritis dissecans of the elbow by computed tomographic arthrography**
P Holland, Birmingham (*p. 23*)

11.50–11.54 **Automated measurement of interbone distance on macroradiographs of osteoarthritic knees using the symmetric axis transformation**
J A Lynch, London (*p. 23*)

11.54–12.02 **The patello-femoral joint — a comparison of geometry measured on the "skyline" view and axial computed tomography**
C P Walker, Birmingham (*p. 24*)

MONDAY 18 MAY 12.15–1.15

HALL 9

MACKENZIE DAVIDSON MEMORIAL LECTURE

Molecular biology in common disease
Professor Sir David Weatherall, Oxford (*p. 25*)

MONDAY 18 MAY 2.15—3.45

HALL 9

ULTRASOUND

Chairman: Dr W Hately, London

2.15–2.40 **Ultrasound exposure measurement for safety**
Invited Review Dr F A Duck, Bath (*p. 26*)

2.40–2.48 **Three-dimensional US of the fetus**
I M G Kelly, London (*p. 26*)

2.48–2.56 **Measurement of ultrasound exposure *in utero***
F A Duck, Bath (*p. 26*)

2.56–3.00 **Comparison of antenatal ultrasonography and postmortem findings in abortuses for lethal renal disease**
R Rajah, Birmingham (*p. 27*)

3.00–3.08 **Correlation of antenatal ultrasound and pathological examination in 153 malformed fetuses**
M J Weston, Bristol (*p. 27*)

3.08–3.16 **Antenatal detection of congenital diaphragmatic hernias: the Northern Region experience**

E Dillon, Stockton-on-Tees (*p. 27*)

3.16–3.20 **Evaluation of "echo-shadow" complex in sonographic diagnosis of cholelithiasis in non-visualized gallbladders**

B Banerjee, Ashton-under-Lyne (*p. 27*)

3.20–3.24 **Ultrasound monitoring of diabetic injection technique**

A Coulthard, Newcastle upon Tyne (*p. 28*)

3.24–3.32 **Endo-anal ultrasound is reliable in mapping anorectal sphincter defects**

K I Deen, Birmingham (*p. 28*)

HALL 10a

RADIOTHERAPY TREATMENT III

Chairman: Dr P C Williams, Manchester

2.15–2.40 **Quality assurance — what is possible?**

Invited Review Mrs S Griffiths, Leeds (*p. 29*)

2.40–3.05 **Imaging and portal verification**

Invited Review Dr W Swindell, Sutton (*p. 29*)

3.05–3.13 **Precision radiation therapy using on-line portal imaging**

S Shalev, Winnipeg, Canada (*p. 29*)

3.13–3.21 **The implementation of patient position correction using on-line radiotherapy imaging**

P M Evans, Sutton (*p. 30*)

3.21–3.29 **The use of an integrated megavoltage imaging system for studies of patient positioning reproducibility**

J Gildersleve, Sutton (*p. 30*)

3.29–3.37 **Ovarian tumours: a prospective study to audit the role of CT scanning**

J Brailsford, Leeds (*p. 30*)

3.37–3.41 **An investigation into radiotherapy treatment couch sag**

G Quinn, Leeds (*p. 30*)

3.41–3.45 **A simple method of verifying dose distribution around a Selectron applicator**

M S Tarakanath, Kuwait (*p. 31*)

HALL 10b

COMMITTED FOR LIFE: EQUIPMENT SEMINAR (2.00–5.15)

Chairman: Dr P Goddard, Bristol

Invited Lectures:

2.05–2.25 **Purchasing — art or science?**

Mr M R Eddy, Bexhill-on-Sea (*p. 32*)

2.25–2.45 **Quality issues**

Mr C E Davis, London (*p. 32*)

2.45–3.05 **Department profiles**

Dr D J Manton, Camberley (*p. 32*)

3.35–3.55 **The outward tender**

Ms E M Pitcher, Bristol (*p. 32*)

3.55–4.15 **Reply to the outward tender**

Mr R W Mark, London (*p. 33*)

4.15–4.35 **Maintenance**

Mr J A Garrett, Bristol (*p. 33*)

4.35–4.55 **Alternative finance and leasing**

Mr E H W Luxton, London (*p. 33*)

HALL 11a

NUCLEAR MEDICINE III

Chairman: Dr M Merrick, Edinburgh

2.15–2.40 **The metastatic survey revisited**

Invited Review Dr M Merrick, Edinburgh (*p. 34*)

2.40–3.05 **The role of bone scan in trauma**

Invited Review Dr I Fogelman, London (*p. 34*)

3.05–3.13 **Clinical high resolution skeletal SPET in 8 min utilizing a multi-detector gamma camera**

J R Buscombe, London (*p. 34*)

3.13–3.17 **The role of isotope bone scanning in patients with foot/ankle pathology**

M Bengoechea, Cardiff (*p. 34*)

3.17–3.25 **Radiology in the clinical management of osteoid osteoma**

C E Hutchinson, Manchester (*p. 35*)

3.25–3.29 **Metastatic disease and the equivocal bone scan: the value of magnetic resonance imaging**

F Aitchison, Glasgow (*p. 35*)

3.29–3.37 **A study of two anti-CEA monoclonal antibodies for immunoscintigraphy of small cell lung cancer**

M L Wastie, Nottingham (*p. 35*)

HALL 11b

CARDIOVASCULAR ADVANCES

Chairman: Dr P Dawson, London

2.15–2.40 **The current role of diagnostic and interventional bronchial angiography**

Invited Review Dr D M Nichols, Inverness (*p. 36*)

2.40–2.44 **Preliminary experience with the Palmaz coronary artery stent**

M R Rees, Leeds (*p. 36*)

2.44–2.48 **Observer variability of contrast echocardiography for the detection of patent foramen ovale**
S J Cross, Aberdeen (*p. 36*)

2.48–2.56 **Functional parameters of the right ventricle evaluated by magnetic resonance imaging in patients with single lung transplantation**
C S Richter, London (*p. 37*)

2.56–3.00 **The value of coronary angioscopy in coronary angioplasty**
M R Rees, Leeds (*p. 37*)

3.00–3.08 **Various manifestations of hypertrophic cardiomyopathy on ultrafast computed tomography**
T Sekiya, Tokyo (*p. 37*)

3.08–3.12 **MR imaging of heart after correction of tetralogy of Fallot**
U M Sivananthan, Leeds (*p. 38*)

3.12–3.20 **Feasibility of left ventricular aneurysm resection assessed using tomographic radionuclide ventriculography**
M J Metcalfe, Aberdeen (*p. 38*)

3.20–3.24 **Radiology of the Churg-Strauss syndrome**
W L Wong, London (*p. 38*)

3.24–3.28 **Artefacts in the ascending aorta on computed tomography: yet another measure of aortic distensibility?**
P Set, Cambridge (*p. 38*)

3.28–3.36 **Magnetic resonance flow mapping in the thoracic aorta of patients with aortic coarctation**
R H Mohiaddin, London (*p. 39*)

MONDAY 18 MAY 4.15–5.30

HALL 9

PRESIDENTIAL ADDRESS

Exploring the niches: some lesser known research areas at the congress

Professor S C Lillicrap, Bath

HALL 10a

ONCOLOGY WORK IN PROGRESS

Chairman: Dr J T Roberts, Newcastle upon Tyne

HALL 11b

GASTROINTESTINAL IMAGING

Chairman: Dr A Cole, Middlesbrough

4.15–4.23 **Videofluoroscopy in the assessment of dysphagia following neurological disease**
A S Ahmed, West Bromwich (*p. 40*)

4.23–4.27 **A swallow assessment clinic: why and how**
F R Wright, Belfast (*p. 40*)

4.27–4.31 **A new chair of radiology—a purpose designed seat to assist fluoroscopy**
D F Martin, Manchester (*p. 40*)

4.31–4.39 **Patterns of colonic transit in severe intractable constipation using oral ^{111}In-DTPA scintigraphy**
J P Roberts, London (*p. 41*)

4.39–4.43 **Validation of region of interest drawing in oral colonic transit scintigraphy**
J P Roberts, London (*p. 41*)

4.43–4.47 **Oesophageal scintigraphy in the assessment of balloon dilatation of the oesophagus for achalasia**
D C F Lloyd, Penarth (*p. 41*)

4.47–4.51 **Radiology of Crohn's disease in Asian immigrants of East Birmingham**
K Jeyapalan, Birmingham (*p. 42*)

4.51–4.59 **Long linear ulceration in Crohn's disease**
P Holland, Birmingham (*p. 42*)

4.59–5.07 **Peritoneal slide: an observation to identify peritoneal adhesions**
A K H Hasan, Dundee (*p. 42*)

5.07–5.11 **Radiological evaluation of the ileoanal (Parke's) pouch: should we continue to do pouchograms?**
M T Keogan, Cambridge (*p. 42*)

5.11–5.15 **Small bowel changes following the modified Scopinaro procedure for morbid obesity**
M Murray, London (*p. 43*)

5.15–5.19 **Magnetic resonance imaging following surgery for ano-rectal anomalies**
D J Grier, Bristol (*p. 43*)

5.19–5.23 **Congenital duodenal obstruction: diagnostic features in 53 neonates**
S Eustace, Dublin (*p. 43*)

5.23–5.31 **Ultrasound in the investigation of the gastrointestinal tract**
W Kincaid, Glasgow (*p. 44*)

TUESDAY 19 MAY 9.00–10.15

HALL 9

MRI TECHNOLOGY

Chairman: Professor I Isherwood, Manchester

9.00–9.25 **The current status of MR angiography and flow measurement technique**
Invited Review Professor M A Smith, Leeds (*p. 45*)

9.25–9.33 **An evaluation of signal properties for MRI**
J P Bean, London (*p. 45*)

9.33–9.37 **Radio frequency eddy current losses for an annular conductor in MRI**
D W McRobbie, London (*p. 45*)

9.37–9.45 **Applications for machine design of the use of superconducting coils**
A S Hall, Wembley (*p. 46*)

9.45–9.53 **3D MR imaging—manipulation and display on an independent console and independent workstation—a comparative study**
C E Hutchinson, Manchester (*p. 46*)

9.53–10.01 **Applications of a simple method of 3D MR image reconstruction from regular 2D images**
L Shapiro, Rochester, USA (*p. 46*)

10.01–10.05 **The phase-inverting harness: a new method of dual surface coil imaging**
N R Moore, Oxford (*p. 47*)

10.05–10.13 **APT—hard pulse trains for fat suppressed MRI at 0.5 T**
T W Redpath, Coventry (*p. 47*)

10.13–10.21 **Magnetization transfer imaging of the brain**
C J Baudouin, London (*p. 47*)

HALL 10a

COMBINED CHEMOTHERAPY & RADIOTHERAPY — PROMISES AND PROBLEMS

Chairman: Dr J A Glaholm, Birmingham

9.00–9.25 **Combined chemotherapy and radiotherapy in non-small cell lung cancer**
Invited Review Dr M H Cullen, Birmingham (*p. 48*)

9.25–9.33 **Adjuvant and adjunctive chemotherapy in head and neck cancer, a meta-analysis**
S El-Sayed, Winnipeg (*p. 48*)

9.33–9.58 **Interrupted hyper-fractionation radiotherapy with concomitant chemotherapy for bulky, inoperable Ewing's sarcoma**
Invited Review Dr D Spooner, Birmingham (*p. 49*)

9.58–10.06 **Acute toxicity study of synchronous chemotherapy and radiotherapy as adjuvant treatment after primary surgery in early breast cancer**
I N Fernando, Sutton (*p. 49*)

10.06–10.10 **Metastatectomy in patients with soft tissue sarcoma**
M H Robinson, London (*p. 49*)

10.10–10.14 **Measurements of platinum uptake in head and neck tumours using X-ray fluorescence**
A El-Sharkawi, Swansea (*p. 50*)

10.14–10.18 **MRI of osteosarcomas and Ewing's sarcomas: the potential of dynamic Gd-DTPA scanning for quantifying the chemotherapy response**
R Maas, Hamburg (*p. 50*)

HALL 10b

DIAGNOSTIC WORK IN PROGRESS I

Chairman: Dr R H Corbett, East Kilbride

HALL 11a

RADIOLOGICAL AUDIT

Chairman: Dr J E Adams, Manchester

9.00–9.08 **The role of hysterosalpingography in the evaluation of infertility — a clinical audit**
M Callaghan, Glasgow (*p. 51*)

9.08–9.16 **Observation of significant abnormalities on lumbar spine radiographs**
J Fowler, Birmingham (*p. 51*)

9.16–9.24 **Audit—the admission chest radiograph in a sickle cell crisis**
W L Wong, London (*p. 51*)

9.24–9.32 **Chest radiography for general practitioners: effects of request review on referral patterns**
A R Padhani, Cambridge (*p. 52*)

9.32–9.40 **General practitioner access to radiology services**
I R Brand, Leeds (*p. 52*)

9.40–9.48 **General practitioners' opinions on the role of barium meals and endoscopy**
J P Owen, Newcastle upon Tyne (*p. 52*)

9.48–9.52 **Diagnostic yield of barium enema in a district general hospital**
T Y K Chan, London (*p. 52*)

9.52–10.00 **Audit of outpatient barium services: user friendly or friendly abuse?**
J G Houston, Glasgow (*p. 53*)

10.00–10.08 **Audit on the management of patients for barium enema**
T Y K Chan, London (*p. 53*)

HALL 11b

HEPATOBILIARY AND PANCREATIC IMAGING

Chairman: Dr R Dick, London

9.00–9.25 **Imaging complications of liver transplantation**
Invited Review Dr S P Olliff, Birmingham (*p. 55*)

9.25–9.33 **Radiological evaluation of pancreatic allografts**
S Meecham Jones, Cardiff (*p. 55*)

9.33–9.37 **Scintigraphic differentiation of surgical jaundice from medical jaundice of viral / schistosomal origin**
A T Khairy, Cairo, Egypt (*p. 55*)

9.37–9.41 **Ultrasound assessment of the normal and obstructed roux loop following surgical biliary diversion**
C L Holland, Birmingham (*p. 55*)

9.41–9.49 **The role of pre-operative intravenous cholangiography in patients undergoing laparoscopic cholecystectomy**
G C McInnes, Aberdeen (*p. 56*)

9.49–9.53 **Antegrade cholecystography following percutaneous cholecystostomy for acute cholecystitis**
T S Creasy, Copenhagen (*p. 56*)

9.53–10.01 **Gallstone recurrence following percutaneous cholecystolithotomy**
J J Donald, London (*p. 56*)

10.01–10.05 **CT assessment of gallstones: correlation with physicochemical properties**
M Blomley, London (*p. 57*)

10.05–10.13 **Intravenous cholangiography—is there life after death?**
P N M Tyrrell, Birmingham (*p. 57*)

TUESDAY 19 MAY 10.45—12.00

HALL 9

TRAUMA

Chairman: Dr S J Golding, Oxford

10.45–11.10 **The advancement of trauma radiology**
Invited Review J W R Young, Maryland, USA (*p. 58*)

11.10–11.18 **Usefulness of three-dimensional computed tomography in craniofacial traumatology**
P Pelotti, Bologna, Italy (*p. 58*)

11.18–11.22 **Instant MRI diagnosis and exclusion of occult femoral neck fractures**
K Lyons, Cardiff (*p. 58*)

11.22–11.30 **MR imaging in vertebra compression fractures**
L A Mitchell, Nottingham (*p. 59*)

11.30–11.38 **Is unilateral facet dislocation of the cervical spine a stable injury?**
V N Cassar-Pullicino, Oswestry (*p. 59*)

11.38–11.42 **Missed fractures in children from an accident service department**
H G Thomas, Oxford (*p. 59*)

11.42–11.46 **Analysis of lateral cervical spine X ray in the assessment of 134 consecutive multiply injured trauma patients from the Helicopter Emergency Service**
R P McAvinchey, London (*p. 60*)

11.46–11.54 **The value of radiograph audit in an accident service department**
H G Thomas, Oxford (*p. 60*)

11.54–12.02 **Computed tomography in blunt abdominal trauma: how helpful for management?**
A R Padhani, Cambridge (*p. 60*)

HALL 10a

BREAST ONCOLOGY

Chairman: Professor C A Joslin, Leeds

10.45–11.10 **Planning radiotherapy treatment for breast cancer**
Invited Review Dr J R Yarnold, Sutton (*p. 61*)

11.10–11.18 **Patterns of axillary lymph node metastasis in breast cancer**
M Van Lancker, Brussels (*p. 61*)

11.18–11.26 **Which imaging modality should be used in assessing response to treatment in breast cancer patients?**
G Needham, Aberdeen (*p. 61*)

11.26–11.34 **Imaging of local recurrence of breast carcinoma**
T J Rissanen, Oulu (*p. 62*)

11.34–11.42 **High dose-rate breast implants**
C G Rowland, Exeter (*p. 62*)

11.42–11.50 **Breast conservative therapy: preliminary report with HDR afterloading iridium-192 implants**
S S Sun, Sichuan (*p. 62*)

11.50–11.54 **Breast cancer and thyroid dysfunction—risk and influence on the prognosis**
V Parvanova, Sofia (*p. 62*)

HALL 10b

DIAGNOSTIC WORK IN PROGRESS II

Chairman: Dr D Hadley, Glasgow

HALL 11a

DEVELOPMENTS OF PRODUCTS FOR RADIOLOGY

Chairman: Dr R H Corbett, East Kilbride

10.45–11.10 **Non-ionic contrast media—the golden idea that was hard to sell**
Invited Review Mr T Renaa, Nycomed, Birmingham (*p. 64*)

11.10–11.35 **Development of new X-ray films: experience and opportunity**
Invited Review Dr G Elsner, Du Pont, Germany (*p. 64*)

HALL 11b

RADIOBIOLOGY DAY: SESSION I

In memory of Dr N McNally
Chairman: Dr J Denekamp, Northwood

10.45–11.15 **Theoretical and experimental aspects of fractionation**
Invited Review Dr M C Joiner, Middlesex (*p. 65*)

11.15–11.23 **Effects of repopulation of an HDR-, MDR- and LDR-radiotherapy on epidermoidal cervix carcinoma cells (CA-Ski cells) and primary human keratinocytes (HPK-cells)**
R Schulz-Wendtland, Freiburg (*p. 65*)

11.23–11.31 **Tumour-dependent changes in the metabolic steady-state of CaNT tumours**
D Szeinfeld, Tygerberg (*p. 66*)

11.31–11.39 **Chemical protection of normal rodent tissue by exogenous ATP after neutron irradiation**
D Szeinfeld, Tygerberg (*p. 66*)

11.39–11.47 **The interaction of radiation and cisplatin in a transplantable hepatocarcinoma**
M J Tomlinson, Bristol (*p. 66*)

11.47–11.55 **Effect of transfected EBV EBNA-1 on the radiation survival curve of BALB/C 3T3 cell line**
Y.-S. Tyan, Taoyuan (*p. 67*)

11.55–11.59 ***In vivo* study of rabbit irradiated skeletal muscle by NMR imaging**
A Francois-Joubert, Grenoble (*p. 67*)

TUESDAY 19 MAY 12.15–1.15

HALL 9

SILVANUS THOMPSON MEMORIAL LECTURE

The gene as a theme in the paradigm of cancer
Professor Eric Hall, Centre for Radiological Research, Columbia University, New York (*p. 68*)

HALL 10b

DIAGNOSTIC WORK IN PROGRESS III

Chariman: Dr B E M Clay, Swindon

TUESDAY 19 MAY 2.15–3.45

HALL 9

NON-VASCULAR INTERVENTIONAL PROCEDURES

Chairman: Dr W Hately, London

2.15–2.40 **Non vascular interventional techniques—biliary disease and stents**
Invited Review Professor C L Zollikofer, Winterthur (*p. 69*)

2.40–2.48 **Flouroscopically guided percutaneous gastrostomy**
R F McLoughlin, Dublin (*p. 69*)

2.48–2.56 **The Holmium-YAG laser: safety in the biliary tract and elsewhere**
M Blomley, London (*p. 69*)

2.56–3.00 **An assessment of the Holmium-YAG laser for fragmenting gallstones**
D A Nicholson, London (*p. 70*)

3.00–3.08 **Pelvi-ureteric junction obstruction—treatment by balloon dilatation in 21 patients**
S Garber, London (*p. 70*)

3.08–3.12 **Renal biopsy in diffuse renal disease—experience with a 14-gauge biopsy gun**
M O Downes, Canterbury (*p. 70*)

3.12–3.20 **Mechanical and ultrasonic properties of urinary stones**
N P Cohen, London (*p. 71*)

3.20–3.24 **Percutaneous balloon dilatation for transplant ureteral stenosis**
D A Nicholson, London (*p. 71*)

3.24–3.32 **Complication rate of combined endoscopic and percutaneous stent insertion**
M B Sheridan, Manchester (*p. 71*)

3.32–3.36 **Transuretheral ureteric stent retrieval using the Amplatz snare**
I Robertson, Glasgow (*p. 72*)

HALL 10a

RADIOLOGICAL HISTORY

Co-Chairmen: Dr J Guy, Yeovil: Professor I Isherwood, Manchester

2.15–2.40 **1927 and after: the Annual Congress in retrospect**
Invited Review Dr N Trott, Cheam (*p. 73*)

2.40–2.48 **Encephalography. Development and introduction into clinical (neuro-) radiology**
H-J Maurer, Kuala Lumpur (*p. 73*)

2.48–2.56 **The birth and development of the X-ray motor car**
J M Guy, Yeovil (*p. 73*)

2.56–3.04 **The Nuffield Institute for Medical Research, Oxford, and radiology of the throat**
S J Golding, Oxford (*p. 74*)

3.04–3.29 **Dr John Hall Edwards: Birmingham's X-ray martyr and first radiologist**
Invited Review Dr J G Latham Cole, Birmingham (*p. 74*)

HALL 10b

MUSCULOSKELETAL IMAGING

Chairman: Dr A M Davies, Birmingham

2.15–2.23 **Ultrasound of the spine in infants with lumbosacral skin lesions**
J Vive, Leicester (*p. 75*)

2.23–2.27 **Ankylosing spondylitis, a comparison of clinical and radiographic features in men and women**
S Eustace, Dublin (*p. 75*)

2.27–2.31 **First metatarsal pronation in hallux valgus**
S Eustace, Dublin (*p. 75*)

2.31–2.39 **The influence of clinical data on the interpretation of MRI scans of the lumbar spine in disc disease**
B S Worthington, Nottingham (*p. 76*)

2.39–2.43 **Cervical spondylosis: correlation of MR imaging and plain film findings**
B C M Macpherson, Glasgow (*p. 76*)

2.43–2.51 **MRI of discitis / osteomyelitis**
A J Tottle, Bristol (*p. 76*)

2.51–2.55 **CT scanning of L3/4 in suspected disc prolapse: is it necessary?**
P de Vos Meiring, Sheffield (*p. 77*)

2.55–3.03 **The influence of smoking on adverse effects following iohexol lumbar myelography**
M Greaves, Consett (*p. 77*)

3.03–3.07 **Sonographic features of plantar fasciitis**
W W Gibbon, Cardiff (*p. 77*)

3.07–3.11 **CT anatomy of the pelvis following hindquarter amputation**
J Fowler, Birmingham (*p. 77*)

3.11–3.15 **If it isn't a soft tissue sarcoma, what is it? A review of one year's referrals to the sarcoma unit—CT findings with pathological correlation**
E C Moskovic, London (*p. 78*)

3.15–3.23 **Bone cortical and periosteal changes as seen on MRI**
G B Greenfield, Tampa (*p. 78*)

3.23–3.27 **MRI of musculoskeletal tumours: a comparative study with X-ray and CT**
V Lozano, Madrid (*p. 78*)

3.27–3.31 **The accessory navicular — a cause of medial foot pain**
C A J Romanowski, Sheffield (*p. 79*)

HALL 11a

WORKSHOP (2.15–5.30): GREENING THE RADIOLOGY DEPARTMENT

Organizer and Chairman: Miss E Ison, Oxford (*p. 80*)

HALL 11b

RADIOBIOLOGY DAY: SESSION II

In memory of Dr N McNally

Chairman: Dr I Stratford, Harwell

2.15–2.45 **Clinical experience with CHART in the UK**
Invited Review Dr M Saunders, Northwood (*p. 81*)

2.45–2.49 **Hyperfractionated accelerated radio-therapy for carcinoma of the oesophagus**
J Sule-Suso, Stoke-on-Trent (*p. 81*)

2.49–2.57 **Early changes in flow and pH of saliva when treating with radiotherapy**
M D Leslie, Northwood (*p. 81*)

2.57–3.05 **Tumour cell kinetics in lung cancer**
B E Lyn, Northwood (*p. 82*)

3.05–3.13 **Tumour proliferation assessed by combined histological and flow cytometric analysis: implications for therapy in squamous cell carcinoma in the head and neck**
G D Wilson, Northwood (*p. 82*)

3.13–3.21 **$TGF\beta_1$, collagen I and III gene expression in human skin fibrosis induced by therapeutic irradiation**
S Delanian, Gif sur Yvette (*p. 82*)

3.21–3.29 **Significance of carbohydrate metabolism control during pre-operative beam therapy of colorectal cancer on the background of short-term artificial hyperglycemia and synchronization of tumour cells on division cycle**
S K Karamian, Armenia (*p. 83*)

3.29–3.37 **Functional state of antioxidant system under the influence of low doses or radiation**
E Kostyushov, St Petersburg (*p. 83*)

TUESDAY 19 MAY 4.15–5.30

HALL 9

ADVANCES IN IMAGING THE LIVER

Chairman: Professor V R McCready, Sutton

4.15–4.40 **Imaging of liver tumours: Japanese experience in detection and characterization**
Invited Review Professor Y Itai, Tsukuba (*p. 84*)

4.40–4.48 **Round flow defects in CT arterial portography — a potential pitfall in interpretation**
M E Roddie, London (*p. 84*)

4.48–4.52 **Dynamic and delayed contrast-enhanced MR scanning of hepatic haemangioma**
C Allen, London (*p. 84*)

4.52–4.56 **The detection, localization and characterization of hepatic mass lesions with MRI at 1.5 T**
M W Bourne, Liverpool (*p. 85*)

4.56–5.04 **Differential diagnosis of space occupying lesions of the liver with MR imaging**
L Vlahos, Athens (*p. 85*)

5.04–5.08 **CT-fluoroscopy (CTF) in the diagnostic and therapeutic approach to hepatic lesions**
L F Frigerio, Milan (*p. 85*)

5.08–5.12 **The liver surface in cirrhosis**
R C V Bhatt, West Bromwich (*p. 86*)

5.12–5.20 **Liver fat estimation using magnetic resonance imaging**
N R Moore, Oxford (*p. 86*)

5.20–5.24 **Sonography versus scintigraphy in chronic liver disease due to hepatitis B / Schistosomiasis**
A T Khairy, Cairo (*p. 86*)

5.24–5.32 **Quantitative volumetric study of the liver**
L F Frigerio, Milan (*p. 86*)

HALL 10a

AUDIT, TEACHING AND MANAGEMENT APPROACHES IN RADIOLOGY

Chairman: Dr K Shah, Birmingham

4.15–4.23 **A computer-assisted method for teaching basic radiology**
A R Wright, Newcastle upon Tyne (*p. 88*)

4.23–4.27 **Awareness of the popumet regulations at a teaching hospital and medical school**
A K M Taylor, Glasgow (*p. 88*)

4.27–4.35 **Clinical audit — developing solutions for the unreported film**
D F Ettles, Bristol (*p. 88*)

4.35–4.43 **Systematic audit of radiology reports by computer link with a pathology computer**
R H Sawyer, Manchester (*p. 89*)

4.43–4.51 **The cost-effectiveness of duplex scanning in peripheral vascular disease**
S Morris, Bristol (*p. 89*)

4.51–4.59 **Audit of MRI for internal derangement of the knee**
K Lyons, Cardiff (*p. 89*)

4.59–5.03 **A protocol for radiological investigation of the renal tract: 1 year on**
U L Udeshi, Kidderminster (*p. 89*)

5.03–5.11 **The use of the CT scanner in ophthalmology**
D Kinsella, Bristol (*p. 90*)

5.11–5.19 **Audit of mesenteric angiography for gastrointestinal haemorrhage**
M E Lipton, Liverpool (*p. 90*)

5.19–5.27 **A simplified approach to the antenatal diagnosis of skeletal dysplasias**
P Twining, Nottingham (*p. 90*)

HALL 10b

TEACH-IN:

THROMBO-EMBOLIC PHENOMENA IN CLINICAL ANGIOGRAPHY—ROLE OF MATERIALS AND TECHNIQUE

Organizers
and Chairmen: Dr P Dawson, London; Dr A-M Belli, London (*p. 91*)

HALL 11b

RADIOBIOLOGY DAY: SESSION III

In memory of Dr N McNally

Chairman: Professor G Steel, Sutton

4.15–4.45 **EORTC fractionation trials in head and neck cancer**
Invited Review Professor H Bartelink, Amsterdam (*p. 92*)

4.45–4.53 **Hyperfractionated radiotherapy of head and neck cancers—preliminary results**
M Niewald, Homburg/Saar (*p. 92*)

4.53–5.01 **Prognostic factors for acute and long-term side effects after radiotherapy of head and neck tumours**
M Niewald, Homburg/Saar (*p. 93*)

5.01–5.09 **Logical presentation and mechanical analogies in the development of mucositis in the oral cavity**
T Ljubenov, Sofia (*p. 93*)

5.09–5.17 **Non-specific cellular resistance disorders induced by low doses of radiation**
I Voltchek, St Petersburg (*p. 93*)

5.17–5.25 **Measurement of normal cell radiosensitivity—a possible path to improve tumour cure?**
N G Burnet, Sutton (*p. 93*)

WEDNESDAY 20 MAY 9.00–10.15

HALL 9

MAMMOGRAPHY—QUALITY CONTROL AND SCREENING

Chairman:	Professor G R Cherryman, Leicester
9.00–9.25 *Invited Review*	**Excellence our only aim—total quality management in mammography** Dr R Warren, Epping (*p. 95*)
9.25–9.33	**National self-assessment of radiologists' film reading performance in breast screening** A G Gale, Nottingham (*p. 95*)
9.33–9.37	**Breast cancer and screening Asian populations** A G Gale, Nottingham (*p. 95*)
9.37–9.41	**Changes in mammographic image quality due to film processor variation** J G Murray, Dublin (*p. 96*)
9.41–9.45	**Image quality in contact and magnification mammography** J Czajka, Manchester (*p. 96*)
9.45–9.49	**Patterns of breast calcification in patients on renal dialysis** A J Evans, Derby (*p. 96*)
9.49–9.57	**Breast screening: deciphering the structure of mammographic microcalcification** A G Gale, Nottingham (*p. 96*)
9.57–10.01	**Image analysis of microcalcifications in X-ray microscopy of paraffin-embedded breast tissues** D A Bradley, Birmingham (*p. 97*)
10.01–10.09	**Performance of mammography screening units in Finland** A Servomaa, Helsinki (*p. 97*)

HALL 10a

IMAGING AND INVESTIGATION IN CLINICAL ONCOLOGY

Chairman:	Dr T Landberg, Malmö, Sweden
9.00–9.08	**Scrotal neoplasms—possibilities using real-time ultrasound** S I Mattila, Oulu (*p. 98*)
9.08–9.12	**Prognosis of cystic change in residual masses following chemotherapy for metastatic teratoma** D J Wilcock, Nottingham (*p. 98*)
9.12–9.20	**Hepatoblastoma: CT findings pre- and post-therapy** S J King, Toronto (*p. 98*)
9.20–9.28	**Assessment of CT measurements of tumour volume as an indicator of response to chemotherapy in osteosarcoma** R Wellings, Birmingham (*p. 99*)
9.28–9.32	**MRI—as a predictor of tumour invasion of the mandible and oral region** J F Griffith, Coventry (*p. 99*)
9.32–9.40	**5 FU modulation and metabolism in colonic cancer monitored by 19 F MRS** M O Leach, Sutton (*p. 99*)
9.40–9.48	**Interstitial laser hyperthermia: the importance of imaging in tumour therapy** J J Donald, London (*p. 100*)
9.48–9.52	**Accuracy of MRI in staging of prostate carcinoma. Cost-effective analysis** V Lozano, Madrid (*p. 100*)
9.52–10.00	**Diagnosing prostate cancer at normal PSA levels: importance of clinico-sonographic correlation** J A Spencer, Philadelphia (*p. 100*)
10.00–10.04	**Serum prostate-specific antigen: before, during and after radical radiotherapy in localized adenocarcinoma prostate** M McLean, Ontario (*p. 100*)
10.04–10.08	**Neoplasia induced renal vascular changes: sonographic evaluation of 48 hypernephromas** B Banerjee, Ashton-under-Lyne (*p. 101*)
10.08–10.16	**Quantitative T_1 and T_2 measurements of lumbar vertebrae in multiple myeloma** V Nicolson, Sutton (*p. 101*)

HALL 10b

GENITOURINARY IMAGING

Chairman:	Dr J P Owen, Newcastle-upon-Tyne
9.00–9.25 *Invited Review*	**A modern imaging approach to pelvic malignancy** Dr R Johnson, Manchester (*p. 102*)
9.25–9.29	**Clinical significance of prostate**

calcification. Transrectal ultrasound and plain film correlation
H Roberts, London (*p. 102*)

9.29–9.33 **MRI of solid renal mass lesions**
J Houston, Reading (*p. 102*)

9.33–9.37 **Observer error in pelvimetry**
A J Liddicoat, Cardiff (*p. 103*)

9.37–9.45 **The age-dependency of the renal resistive index in healthy children**
R O Bude, Ann Arbor (*p. 103*)

9.45–9.49 **Assessment of Gd-DTPA as a CT contrast agent within the renal tract**
R J Gibson, Reading (*p. 103*)

9.49–9.53 **Furosemide and fluid-load Doppler sonography in non-obstructive pyelocaliectasis**
R O Bude, Ann Arbor (*p. 103*)

9.53–10.01 **Ultrasound evaluation of the urethral sphincter in women with obstructed voiding dysfunction**
J G Noble, London (*p. 104*)

10.01–10.05 **Diagnostic features of bladder neck dyssynergia on ultrasonography: a new radiological sign?**
J G Noble, London (*p. 104*)

10.05–10.09 **Ultrasonic appearance of the epididymis and chronic post-vasectomy testicular pain**
A K M Taylor, Glasgow (*p. 104*)

10.09–10.17 **Evaluation of impotence by pharmaco-cavernosometrography**
A M Parikh, London (*p. 105*)

HALL 11a

ANGIOPLASTY

Chairman: Dr J Li, Birmingham

9.00–9.25 **Current trends in PTA**
Invited Review Dr W Seyferth, Ansbach (*p. 106*)

9.25–9.33 **Monitoring platelet deposition following angioplasty using a platelet-specific monoclonal antibody**
A C Perkins, Nottingham (*p. 106*)

9.33–9.37 **Use of human tissue type plasminogen activator in the prevention of early rethrombosis following the treatment of femoral occlusions by percutaneous angioplasty**
J N P Higgins, London (*p. 106*)

9.37–9.45 **Thermal angioplasty using high-frequency ablator**
T A Houghton, Liverpool (*p. 106*)

9.45–9.53 **Angioplasty of long femoral occlusions —can the success rates be improved?**
M R E Dean, Shrewsbury (*p. 107*)

9.53–9.57 **Changes in lower limb blood flow following angioplasty: assessment with duplex Doppler ultrasound**
S C Whitaker, Nottingham (*p. 107*)

9.57–10.05 **Percutaneous transluminal angioplasty of crural arteries—results in 32 patients**
U M Sivananthan, Leeds (*p. 107*)

10.05–10.13 **Prospective randomized trial of PTA versus supervised exercise therapy for intermittent claudication**
T S Creasy, Oxford (*p. 108*)

10.13–10.21 **Angioplasty above the arch**
R A Morgan, Plymouth (*p. 108*)

HALL 11b

PHYSICS I — BODY COMPOSTITION

Chairman: Dr W D Morgan, Birmingham

9.00–9.25 **Radiological assessment of body composition**
Invited Review Professor S Mattsson, Malmö (*p. 109*)

9.25–9.33 **Energy-dispersive X-ray scattering for assessment of crystalline tissues**
G J Royle, London (*p. 109*)

9.33–9.41 **Comparison between radionuclide and polarized X-ray sources for *in vivo* X-ray fluorescence**
P Tothill, Edinburgh (*p. 109*)

9.41–9.45 **The long-term retention of platinum in human tissues following cancer chemotherapy**
P Tothill, Edinburgh (*p. 110*)

9.45–9.49 **X-ray fluorescence for the determination of gold *in vivo***
J Shakeshaft, Bath (*p. 110*)

9.49–9.57 **Determination of body fat by DEXA: a comparison with neutron activation**
S J S Ryde, Swansea (*p. 110*)

9.57–10.01 **A comparison of techniques for the assessment of body fat**
S J S Ryde, Swansea (*p. 110*)

10.01–10.05 **Approaches to the determination of total body protein**
W D Morgan, Birmingham (*p. 111*)

10.05–10.09 **The effects of very low calorie diet on total body nitrogen**
S J S Ryde, Swansea (*p. 111*)

WEDNESDAY 20 MAY 10.45–12.00

HALL 9

NEW APPLICATIONS OF MRI

Chairman: Professor B Worthington, Nottingham

10.45–11.10 **New MRI techniques for musculoskeletal imaging**
Invited Review Dr S E Harms, Texas (*p. 112*)

11.10–11.18 **MRI in the evaluation of the thoracic outlet syndrome**
R J Gibson, Oxford (*p. 112*)

11.18–11.22 **Magnetic resonance imaging in the assessment of peripheral arteriovenous malformations**
D Kinsella, Bristol (*p. 112*)

11.22–11.30 **Initial experiences using fast spin echo**
S J Golding, Oxford (*p. 113*)

11.30–11.38 **Dynamic MRI of the pancreas — gadolinium enhancement in normal tissue**
J A D Brailsford, Leeds (*p. 113*)

11.38–11.46 **A fast technique for demonstrating vascular anatomy and patency using contrast-enhanced turboFLASH**
J P Ridgway, Leeds (*p. 113*)

11.46–11.50 **Fast MR angiography using turboFLASH sequences in advanced aorto iliac disease**
U M Sivananthan, Leeds (*p. 113*)

11.50–11.58 **Quantitative T_1 and T_2 measurements of CSF in patients with multiple myeloma**
V Nicolson, Sutton (*p. 114*)

HALL 10a

COUNSELLING AND QUALITY OF CARE IN ONCOLOGY

Chairman: Dr M Spittle, London

10.45–11.10 **Costs and benefits of counselling**
Invited Review Dr E J Maher, Northwood (*p. 115*)

11.10-11.35 **Comparison of methods for obtaining quality of life assessments in oncology**
Invited Review Dr J Morris, York (*p. 115*)

11.35–11.43 **Treatment of oesophageal carcinoma with combined external beam and intracavitary radiotherapy**
R K Agrawal, Newcastle upon Tyne (*p. 115*)

11.43–11.47 **Radiological audit in oncology: improving the diagnostic algorithm for today's cancer patient**
E C Moskovic, London (*p. 115*)

11.47–11.55 **Percutaneous nephrostomy in malignant disease**
A F Watkinson, London (*p. 116*)

11.55–11.59 **The role of pulmonary computed tomography in the management of Wilms' tumour. 1: Clinical management**
C M Owens, London (*p. 116*)

11.59–12.01 **The role of pulmonary computed tomography in the management of Wilms' tumour. 2: Cost-benefit analysis**
S J D Burnett, London (*p. 116*)

HALL 10b

MEASUREMENTS OF BONE MINERAL

Chairman: Dr F Ring, Bath

10.45–11.10 **Measurement of bone mineral**
Invited Review Dr D Felsenberg, Berlin (*p. 117*)

11.10–11.18 **Non-invasive vertebral texture analysis based on HRCT — a new diagnostic tool in osteoporosis**
A Mundinger, Freiburg (*p. 117*)

11.18–11.26 **SPA, QCT and DXA reference range for British women and correlations between the techniques**
J E Adams, Manchester (*p. 117*)

11.26–11.30 **Methods of assessment of spinal deformity**
G L Thomas, Nottingham (*p. 118*)

11.30–11.34 **Assessment of axial osteopenia: plain radiography versus dual energy X-ray absorptiometry**
M J Garton, Aberdeen (*p. 118*)

11.34–11.42 **Spinal bone mass measurement: QCT or DXA?**
R W Whitehouse, Manchester (*p. 118*)

11.42–11.50 **Increased bone mineral density in the hip and spine by dual X-ray absorptiometry (DEXA)**
E F J Ring, Bath (*p. 119*)

11.50–11.58 **Assessment of bone growth activity in leg lengthening procedures using DEXA**
M J Haddaway, Oswestry (*p. 119*)

HALL 11a

CHEST RADIOLOGY

Chairman: Dr A Wilson, London

10.45–11.10 **Aids and the chest**
Invited Review Dr M McCarty, London (*p. 120*)

11.10–11.18 **The terminology and radiology of cryptogenic organizing pneumonia (COP)**
J A A Haddock, London (*p. 120*)

11.18–11.26 **Organizing pneumonia — "BOOP" or "COP" — a review**
O Constant, Midhurst (*p. 120*)

11.26–11.30 **Lympocytic interstitial pneumonitis in HIV infected children**
C M Owens, London (*p. 121*)

11.30–11.34 **The role of computed tomography in stable cystic fibrosis**
M Logan, Dublin (*p. 121*)

11.34–11.42 **Ultrafast CT appearances of obliterative bronchiolitis and bronchomalacia in lung transplant recipients: early experience**
C M Allen, London (*p. 121*)

11.42–11.46 **Chest magnetic resonance imaging in sarcoidosis**
D Kinsella, Bristol (*p. 122*)

11.46–11.50 **MRI of lung signal intensity and dimensions in patients with chronic lung disease before and after single lung transplantation**
R H Mohiaddin, London (*p. 122*)

11.50–11.58 **High-resolution CT appearances of the lung in alpha-1-antitrypsin deficiency**
P M Taylor, Manchester (*p. 122*)

HALL 11b

PHYSICS II — IMAGE ASSESSMENT

Chairman: Dr R Harrison, Newcastle-upon-Tyne

10.45–11.10 **Human visual perception and ROC methodology in medical imaging**
Invited Review Dr M S Chesters, Leeds (*p. 123*)

11.10–11.14 **"All the better to see you with" — the use of a minifying lens in radiology**
B S Worthington, Nottingham (*p. 123*)

11.14–11.22 **The SDRD: a novel digital radiographic system**
A Martinez, London (*p. 123*)

11.22–11.30 **Monte Carlo study of the design and performance of anti-scatter grids**
D R Dance, London (*p. 124*)

11.30–11.38 **Quantitative assessment of TV fluoroscopy**
D W McRobbie, London (*p. 124*)

11.38–11.42 **First experiences with a DSI digital image review workstation**
A G Davies, Leeds (*p. 124*)

11.42–11.46 **Density profile measurements for quality assurance in digital radiology**
S D Tabakov, London (*p. 124*)

11.46–11.50 **Development of a test object for evaluating image quality of photostimulable phosphor computed radiography systems in clinical service**
J S Price, Leeds (*p. 125*)

11.50–11.54 **Variability of X-ray image intensifier—TV system performance**
A J Shaw, Manchester (*p. 125*)

11.54–11.58 **Phosphor screens image characteristics**
G E Giakoumakis, Ioannina (*p. 125*)

11.58–12.02 **An approach to assessing the adequacy of fluoroscopy equipment to produce adequate images over a wide range of clinical conditions under automatic control**
M Holnbinka, Portsmouth (*p. 125*)

WEDNESDAY 20 MAY 12.15–1.15

HALL 9

3M MAYNEORD MEMORIAL LECTURE

Targeted magnetic resonance imaging
Dr William Vennart, Department of Physics, University of Exeter (*p. 127*)

WEDNESDAY 20 MAY 2.15–3.45

HALL9

ANGIOGRAPHY AND INTERVENTIONAL RADIOLOGY

Chairman: Dr P Dawson, London

2.15–2.23 **Digital versus conventional angiography: a comparative study**
E Jurriaans, Plymouth (*p. 128*)

2.23–2.27 **Enhancing the thrombogenicity of embolization coils**
J Cockburn, London (*p. 128*)

2.27–2.35 **A comparison of pulse-generated run-off and arteriographic assessment of the pedal arch in the outcome of femoro-distal bypass grafting**
D Kinsella, Bristol (*p. 128*)

2.35–2.39 **Calf vessel preservation in peripheral vascular disease — angiography versus pulse generated run-off**
H G Thomas, Oxford (*p. 129*)

2.39–2.47 **Colour duplex, impedance analysis and DSA in femorodistal vein bypass graft surveillance**
D Glew, Bristol (*p. 129*)

2.47—2.51 **Intra-arterial femoral studies in anticoagulated patients using 3 French catheters**
C N Ludman, London (*p. 129*)

2.51–2.59 **A comparative study of the effects of ionic and non-ionic contrast media on oxygen desaturation following intravenous/intra-arterial administration**
Dr P S Sidhu, London (*p. 129*)

2.59–3.03 **Inoculation hazards during interventional radiological procedures**
S Eustace, Dublin (*p. 130*)

3.03–3.07 **Embolization of peri-pancreatic visceral artery pseudo-aneurysms**
J E Jackson, London (*p. 130*)

3.07–3.15 **Approaching and lysing the thrombosed prosthetic graft**
P Guest, London (*p. 130*)

3.15–3.23 **TIPSS. The Edinburgh experience**
N Chalmers, Edinburgh (*p. 130*)

3.23–3.31 **Utility of trans-jugular intrahepatic portosystemic shunting for treatment of portal hypertension**
W K Chong, Nashville (*p. 131*)

HALL 10a

TEACH-IN: IMAGING IN PAEDIATRIC ONCOLOGY

Organizer and Chairman: Dr S Chapman, Birmingham

Invited Lectures **Orbital tumours in childhood and their differential diagnosis**
Dr S Chapman, Birmingham (*p. 132*)

Neonatal tumours — antenatal and post-natal diagnosis
J M McHugo, Birmingham (*p. 132*)

The role of radiology in the management of neuroblastoma
C Dicks-Mireaux, London (*p. 132*)

HALL 10b

ENT IMAGING

Chairman: Dr G A Lloyd, London

2.15–2.40 **The investigation of sinus disease and its intracranial complications**
Invited Review Dr P Anslow, Oxford (*p. 133*)

2.40–2.48 **Subtraction magnetic resonance imaging for tumours of the skull base and paranasal sinuses**
G A Lloyd, London (*p. 133*)

2.48–2.56 **MR appearances of skull base lesions**
S Amin, Sutton (*p. 133*)

2.56–3.04 **Extension of malignant neoplasms upwards through the skull base: role of enhanced MRI**
D J Beale, Coventry (*p. 134*)

3.04–3.12 **Clinical evaluation of combined MRI, CT and MRA in skull-base surgery planning**
S E M Green, London (*p. 134*)

3.12–3.16 **Benign and malignant enlargement of the pterygo-masseteric muscle complex**
P Set, Cambridge (*p. 134*)

3.16–3.24 **The basal turn of the cochlea**
A Duncan, Coventry (*p. 134*)

3.24–3.28 **The parotid node—a pitfall in diagnosis?**
M J Bradley, Rotherham (*p. 135*)

3.28–3.32 **Salivary gland scinitigraphy—a suitable substitute for sialography?**
W J Pilbrow, Chester (*p. 135*)

3.32–3.40 **CT in diagnosis of naso-pharyngeal carcinoma (NPC)**
H-J Maurer, Kuala Lumpur (*p. 135*)

3.40–3.44 **Diagostic—therapeutic possibilities of interventional sonography on pathologic processes of the neck**
A Nedeva, Plovdiv (*p. 136*)

3.44–3.52 **The ultrasonic appearances of normal vocal cords**
J C Hacking, Cambridge (*p. 136*)

HALL 11b

PHYSICS III — RADIATION PROTECTION AND RISKS AFTER ICRP 60

Chairman: Mr B F Wall, Didcot

2.15–2.40 **Reappraisal of risks to the patient in diagnostic radiology**
Invited Review Dr P J Roberts, Southampton (*p. 137*)

2.40–2.48 **The dilemma of leakage radiation — how much should we accept?**
H M Morgan, Bath (*p. 137*)

2.48–2.52 **Direct measurement of the radiation doses to relations of nuclear medicine outpatients**
L K Harding, Birmingham (*p. 137*)

2.52–2.56 **Practical application of ICRP Publication 60 dose quantities to personal monitoring of staff who wear protective aprons**
J R Gill, Bootle (*p. 138*)

2.56–3.00 **Radiation beam alignment at the chest-wall in mammography**
A G Brennan, Manchester (*p. 138*)

3.00–3.04 **Comparison of high and low kVp techniques for PA chest radiographs**
J P Wade, Cambridge (*p. 138*)

3.04–3.08 **Patient dose measurement and reduction—a collaborative experience in East Anglia**
J P Wade, Cambridge (*p. 138*)

3.08–3.16 **Validation of software designed to calculate patient entrance exposures in diagnostic radiology**
C L Skinner, London (*p. 139*)

3.16–3.24 **A portable system for measuring area kerma product during fluoroscopic examinations**
U Reynolds, London (*p. 139*)

3.24–3.28 **Radiation dose to the breast from screening mammography in the West Midlands**
E A McNeil, Birmingham (*p. 139*)

3.28–3.32 **Patient doses received using digital subtraction angiography and Puck serial film changer**
H R Steele, Birmingham (*p. 139*)

3.32–3.36 **Assessment of organ radiation dose and associated risk for digital femoral arteriography**
I A Castellano, London (*p. 140*)

3.36–3.40 **Radiation doses during cardiac catheterization**
C Reek, Leicester (*p. 140*)

WEDNESDAY 20 MAY 4.15–5.30

HALL 9

ADVANCES IN DOPPLER ULTRASOUND

Chairman: Dr W Hately, London

4.15–4.23 **Doppler ultrasound flow measurement in the assessment of arterio-venous access for haemodialysis**
J E Stutley, Toronto (*p. 141*)

4.23–4.27 **Colour flow mapping: does variance correspond to turbulence?**
G M Baxter, Boston (*p. 141*)

4.27–4.35 **A simple device to demonstrate heating patterns in pulsed Doppler ultrasound beams**
H C Starritt, Bath (*p. 141*)

4.35–4.39 **Transcutaneous Doppler ultrasound imaging of the internal mammary arteries**
N Pugh, Cardiff (*p. 142*)

4.39–4.47 **Colour Doppler studies of axillary nodes in patients with breast cancer**
J S Walsh, Edinburgh (*p. 142*)

4.47–4.51 **Colour and duplex Doppler in the diagnosis of hepatic venous outflow obstruction**
M A Collins, Birmingham (*p. 142*)

4.51–4.55 **Colour Doppler ultrasound in suspected scaphoid fracture — the way forward**
D A Nicholson, Manchester (*p. 143*)

4.55–5.03 **Doppler pressure 1/2 time estimation of valve area following percutaneous mitral balloon valvotomy**
R L Parry, Bristol (*p. 143*)

5.03–5.07 **Prediction of vesicoureteric reflux in children using colour Doppler imaging**
S Sukumar, Pendlebury (*p. 143*)

5.07–5.11 **Ultrasound diagnosis of Peyronie's disease in impotence**
Z Amin, London (*p. 143*)

5.11–5.19 **Colour Doppler imaging and prostatic disease**
I M G Kelly, London (*p. 144*)

5.19–5.27 **Colour Doppler imaging in the investigation of impotence**
U Patel, London (*p. 144*)

HALL 10a

BODY CT — CLINICAL AND TECHNICAL ADVANCES

Chairman: Dr S P Olliff, Birmingham

4.15–4.23 **Spiral versus conventional dynamic CT: a randomized trial**
J C Hacking, Cambridge (*p. 145*)

4.23–4.27 **Congenital abnormalities of the inferior vena cava: dianosis by computed tomography**
D I Boxer, London (*p. 145*)

4.27–4.35 **Computed tomography of the abdominal wall**
R Fitzgerald, Wolverhampton (*p. 145*)

4.35–4.43 **Optimum dose of non-ionic contrast media in abdominal and pelvic CT**
K Choji, Sapporo, Japan (*p. 145*)

HALL 10a

THE BREAST — CLINICAL AND TECHNICAL ADVANCES

Chairman: Dr S P Olliff, Birmingham

4.45–4.53 **Mammography in the assessment of response to treatment in patients with large primary breast cancer**
E C Moskovic, London (*p. 147*)

4.53–5.01 **Interval cancers in the breast screening programme**
B E Nathan, Edgware (*p. 147*)

5.01–5.09 **The indeterminate breast mass. Does gadolinium-enhanced MRI have a role?**
P F Hickman, Oxford (*p. 147*)

5.09–5.13 **Digital mammography: evaluation of digitizers**
D H Davies, London (*p. 148*)

5.13–5.21 **Computer detection of soft tissue masses in digital mammograms: automatic region segmentation**
D H Davies, London (*p. 148*)

5.21–5.29 **Ultrasound demonstration of small cancers detected by mammographic screening**
A J Potterton, Gateshead (*p. 148*)

5.29–5.37 **Colour flow characteristics of benign and malignant breast lesions**
M McNicholas, Dublin (*p. 148*)

HALL 11b

PHYSICS IV — RADIATION PROTECTION AND RISKS

Chairman: Dr P J Roberts, Southampton

4.15–4.40 **CT dosimetry: the joule in the crown of medical imaging**
Invited Review Mr B F Wall, NRPB, Didcot (*p. 150*)

4.40–4.48 **The radiation burden of patients undergoing percutaneous transluminal coronary angioplasty**
R J Chambers, Ottawa, Canada (*p. 150*)

4.48–4.52 **CTDI: confusion and clarification**
S Edyvean, London (*p. 150*)

4.52–4.56 **The use of lithium fluoride and lithium borate in CT dosimetry**
M A Lewis, London (*p. 151*)

4.56–5.00 **Increased accuracy of CT dose profile measurement by the use of film**
J F Carden, London (*p. 151*)

5.00–5.04 **Assessment of entrance doses received by patients undergoing lateral lumbar spine examinations**
D E Peach, Birmingham (*p. 151*)

Scientific Programme Abstracts

Monday 18 May

9.00 – 10.15

The Central Nervous System

Hall 9

Diffusional MRI of the brain

G. M. Bydder and J. V. Hajnal
NMR Unit, Department of Diagnostic Radiology, Royal Postgraduate Medical School, Hammersmith Hospital, DuCane Road, London W12 0HS, UK

By using strong gradient pulse sequences on either side of the 180° pulse of a spin-echo sequence it is possible to make Brownian motion of water the dominant form of contrast in magnetic resonance (MR) images of the brain and spinal cord. This can be done in any direction. Motion of water in the brain is restricted by the presence of membranes, macromolecules and myelin sheaths. By using gradients orientated in different directions it is possible to demonstrate that diffusion of water across myelinated fibres is much less than that along them. This enables white matter tracts to be demonstrated as a function of their direction. In disease, breakdown of membrane barriers and myelin sheaths usually increases the diffusion of water but in a surprisingly large proportion of cases the reverse happens. It is believed that in this situation water molecules may be trapped in myelin sheath layers. The technical developments necessary to implement diffusion imaging will be illustrated and applications in paediatric and adult diseases will be presented.

CT and MR in the diagnosis of intraventricular cerebral masses

N. S. McConachie, T. Jaspan, E. Cornford, M. Balsitis, R. Kerslake and B. S. Worthington
Departments of Neuroradiology and Pathology, University Hospital, Queen's Medical Centre, Nottingham NG7 2UH, UK

The computed tomography (CT) and magnetic resonance (MR) images were reviewed in all patients presenting with intraventricular cerebral masses at the University Hospital, Nottingham between 1985 and 1991. In an attempt to develop a logical approach to diagnosis, each site within the ventricular system was analysed for the relative frequency of each histological type. The radiological features were noted, in particular the number, extent and morphology of the masses, the presence or absence of calcification or cystic change, the presence and nature of any hydrocephalus, the CT attenuation before and after intravenous contrast enhancement and the MR signal characteristics. The appearances of the commonest masses are described for each site and the main differential diagnoses are discussed. Particular attention is drawn to intraventricular neurocytoma; a recently described tumour that may be mistaken histologically for intraventricular oligodendroglioma. A comparison is made of the value of CT and MR in the diagnosis of intraventricular masses.

Fast spin echo (FSE) techniques in cranial MR imaging

J. V. Byrne, P. Anslow, R. Gibson and A. J. Molyneux
Department of Neuroradiology, Radcliffe Infirmary, Oxford OX2 6HE, UK

Considerable savings in examination time are possible using newly available fast spin echo (FSE) sequences. These techniques are based on the principle that multiple phase encoding steps can be acquired in one excitation of the spin system. They provide images with tissue contrast similar, but not identical, to conventional spin echo (CSE) sequences. A prospective study of 50 patients referred for primary cranial magnetic resonance imaging (MRI) examination was undertaken on a 1.5 T imager. Spin density and T_2-weighted images were obtained using CSE and FSE sequences with identical parameters. The diagnostic yield, defined by the supervising radiologist and by two independent reviewers, was compared. A quantitative evaluation of all positive studies based on lesion counts was performed. The two techniques provided images of similar quality. There was complete concordance in the resulting diagnoses. In patients with clinically definite multiple sclerosis, quantitative assessment of scans showed lesions to be more conspicuous on the spin density weighted FSE sequence. The FSE sequence is therefore recommended for routine cranial MRI.

MRI of meningeal enhancement in malignant disease

R. Goy and D. MacVicar
Department of Diagnostic Radiology, The Royal Marsden Hospital, Downs Road, Sutton, Surrey SM2 5PT, UK

Gadolinium (Gd)-DTPA is essential for the diagnosis of metastatic meningeal disease on magnetic resonance imaging (MRI). Pathological enhancement of the cranial and spinal meninges may be difficult to differentiate from the normal and can have a range of appearances in patients with malignant disease. We have reviewed the MR appearances of 30 patients with abnormal meningeal enhancement. Scans were performed on a Siemens Magnetom operating at 1.5 T with a minimum of a T_1-weighted sequence before and after Gd-DTPA enhancement. If cerebrospinal fluid cytology was not obtained or was negative, the diagnosis of meningeal tumour was made by excluding other causes of abnormal meningeal enhancement and by longitudinal follow-up. The most common pattern of involvement of the cranial meninges was generalized dural enhancement. Diffuse leptomeningeal and focal linear and nodular enhancement were also seen, in one case simulating a parafalcine meningioma. Spinal meningeal involvement was either nodular or diffuse. In three cases meningeal involvement could only be identified on the enhanced scans and Gd-DTPA improved visualization in all cases. Meningeal involvement is well recognized in carcinoma of the breast and lung, melanoma, primitive neuroectodermal tumour and lymphoma, and in our series was also seen in metastatic cerebral glioma, teratoma and embryonal rhabdomyosarcoma.

Assessment of meningeal pathology by MRI and CT

C. E. Hutchinson, J. M. Hawnaur and I. Isherwood
Department of Diagnostic Radiology, University of Manchester, Manchester M13 9PT, UK

Diffuse meningeal disease may be difficult to identify on contrast-enhanced computed tomography (CT) due to partial volume effects and beam hardening, particularly at the skull base and vertex. Meningeal pathology may be obscured on unenhanced T_1- and T_2-weighted magnetic resonance imaging (MRI) sequences, by adjacent cerebrospinal fluid with similar relaxation times. We have reviewed nine patients with meningeal abnormalities where changes on enhanced CT and unenhanced MRI were difficult to detect. MRI with gadolinium-DTPA (Gd-DTPA) was diagnostic in all cases. Images were obtained on a 0.26 T Picker or 0.5 T GE Vectra MRI system using a head coil. T_1- and T_2-weighted spin echo sequences (time to repeat (TR)/time to echo (TE) 500–2000/20–90) were obtained pre-contrast. T_1-weighted sequences following 0.1 mmol/kg Gd-DTPA intravenously were repeated in three orthogonal planes. In four patients with diffuse meningeal pathology, CT and unenhanced MRI were normal or underestimated the full extent of disease, which was clearly demonstrated after Gd-DTPA. In five patients with focal meningeal lesions at the skull base or vault, CT either failed to demonstrate the lesion or provide conclusive diagnostic information. Meningiomas which were isointense with brain on both T_1- and T_2-weighted MRI sequences only became conspicuous after Gd-DTPA. Despite the high-contrast resolution, multiplanar facility and lack of bone artefact with MRI, meningeal lesions can still be difficult to detect. In patients with a suggestive clinical history and neurological signs, but inconclusive findings on CT and unenhanced MRI, administration of Gd-DTPA is mandatory to exclude meningeal disease.

The role of CT scanning in the investigation of low tension glaucoma

P. G. White, G. Larkin, M. D. Hourihan and C. M. Lane
Departments of Radiology and Ophthalmology, University Hospital of Wales, Heath Park, Cardiff CF4 4XW, UK

Low tension glaucoma (LTG) is the combination of glaucomatous optic nerve cupping and visual field defects with normal intraocular pressure. At this centre it is current practice to investigate such patients with computed tomography (CT) of the optic pathway. In this study 30 successive patients imaged for LTG were retrospectively reviewed. All patients underwent thin section contiguous contrast-enhanced coronal CT through the orbits and pituitary region. CT was normal in 18 cases, demonstrated an empty sella in 10 cases, a pituitary macroadenoma in one case and thyroid ophthalmopathy in another. In the latter two cases clinical re-examination was found to be consistent with the radiological diagnosis, rather than LTG. The results of this study suggest that careful clinical assessment should exclude the possibility of a pituitary or optic nerve lesion in LTG and CT should be reserved for patients with atypical features.

Ophthalmology referrals for brain CT — a retrospective audit

W. Kincaid, N. C. McMillan and G. Dutton
Departments of Radiology and Ophthalmology, Western Infirmary, Glasgow G11 6NT, UK

A retrospective study of patients referred for brain computer tomography (CT) by ophthalmologists was carried out to assess its effect on clinical management. 53

patients were included in the study. The most common presenting complaints were visual field defects, headaches, and glaucoma. 21 patients had plain skull X-rays before CT, seven (33%) were reported abnormal, five of which were false positives. In 38 patients the CT was normal and usually resulted in the patient's discharge. In the majority of the 15 patients who had an abnormal CT, this prompted discharge or neurosurgical referral. In the six patients who presented with a homonymous hemianopia, the CT was positive. Therefore we would recommend the following practice: (1) brain CT should be the first imaging examination in patients with a homonymous hemianopia; (2) brain CT should be considered early in the test sequence as this would reduce the number of additional investigations, and follow-up clinic appointments, with considerable cost savings; (3) plain skull X-rays have very little value in non-traumatic ophthalmic conditions and should not be performed; (4) in patients presenting with headaches, brain CT is not indicated in the absence of localizing signs and (5) brain CT is rarely helpful in glaucoma, except in some cases of low-tension glaucoma.

Computed tomography of the brain in psychiatric patients: an audit

D. J. Grier and A. Jones
Department of Clinical Radiology, Bristol Royal Infirmary, Bristol BS2 8HW, UK

Computed tomography of the brain (CT brain) is often requested in patients suspected of having dementia to exclude an underlying treatable cause. The indication for such scans in patients with psychiatric illness, particularly young patients and those not responding to standard treatment, is less clear. We reviewed the indications for and the results of CT brain scans performed at the request of the psychiatric department over a 4 year period. A total of 270 scans was performed on 256 patients (mean age 57.8 years). There were 118 normal examinations. 139 scans showed either cerebral atrophy, ischaemia or infarction (findings which do not require specific therapy). Significant abnormalities were found in nine patients (13 scans); when follow-up scans and those patients in whom the diagnosis was already known are excluded, the number of unexpected abnormal scans was six in six patients (2.2% of all scans). Indications for these scans included epilepsy, incontinence, neurofibromatosis, previous head injury and surgery. These findings are presented and discussed with suggested guidelines on the rational use of CT in these patients.

The outcome of fetal ventriculomegaly

P. Twining, T. Jaspan and J. Zuccollo
Departments of Radiology and Histopathology, University Hospital, Queen's Medical Centre, Nottingham NG7 2UH, UK

Over a 4 year period 34 cases of fetal ventriculomegaly were diagnosed at Queen's Medical Centre, Nottingham. All antenatal and post-natal scans were assessed, liveborn babies followed up from 1 month to 3 years and post-mortem examinations reviewed. There were 12 cases of spina bifida and all patients opted for a termination of pregnancy. There were 13 cases of isolated ventriculomegaly comprising five cases of aqueduct stenosis, four abnormalities of the corpus callosum, one cavum septum pellucidum cyst, one case of porencephaly and two cases of mild lateral ventricular dilatation. The fetuses in this group had a relatively good outcome with six normal babies, two with mild developmental delay, one stillbirth, two patients opted for a termination of pregnancy and two pregnancies are continuing. Associated abnormalities were seen in four cases and these carried a poor prognosis with one fetus stillborn, one neonatal death and two patients opted for a termination of pregnancy. The five remaining cases included three Dandy Walker syndrome, one brain tumour and one case of subdural haemorrhage. There were three terminations of pregnancy, one stillbirth and one baby with severe developmental delay. To conclude, isolated ventriculomegaly carries a relatively good prognosis, the presence of associated anomalies has a poor outcome.

9.00 – 10.15

Radiotherapy Treatment I

Hall 10a

Dose specification: is there a consensus?

H. J. Dobbs
South East London Radiotherapy Centre, King's College Hospital, London SE5 9RS, UK

The outcome of radiotherapy, as measured by local tumour control, can only be interpreted meaningfully if the distribution of radiation dose in space and time can be correlated accurately with the clinical and pathological extent of the disease. In order to compare and improve treatment results it is essential that there is a common language used for the definitions of basic criteria such as tumour volume, target volume and treatment volume. Studies are needed to provide anatomical and tumour data for improved definitions of "margins" around tumours for treatment planning. It is recommended by the International Commission on Radiation Units and Measurements (ICRU) that a common method of reporting radiation dose is used internationally in order to facilitate communication between institutions and allow meaningful comparison of treatment results. The ICRU reference point is selected at the centre of the target volume on or near the central axis of the beam as the most clinically relevant, unambiguous and representative point. The dose variation across the target volume is now a compulsory requirement for dose reporting according to new ICRU guidelines. These new ICRU recommendations for reporting external beam therapy will be discussed — do we at last have a consensus?

Radiobiological implications of physical dose inhomogeneity in radiotherapy treatment planning

A. E. Amin
CRC Beatson Laboratories, Radiation Oncology Department, Glasgow University, Glasgow G61 1BD, UK

Successful radiotherapy requires the delivery of a tumoricidal treatment while sparing as much normal tissue as possible in the irradiated volume. The aim of optimizing radiation treatment planning is to satisfy this requirement. However, expressing the treatment plan solely as a physical dose distribution might be misleading. In most centres, dose variation of 10% (±5%), or even more, is considered to be an acceptable range of inhomogeneity. Converting the physical dose distribution in the irradiated volume into a biological effect distribution (isoeffect lines), using the linear quadratic model, increases the inhomogeneity factor. The biological dose inhomogeneity factor depends on the fraction size as well as radiobiology of the irradiated tissue (*e.g.* α/β ratio). In this analysis the biological dose inhomogeneity factor resulting from a 10% physical dose inhomogeneity was calculated for isoeffective schedules with different fraction size (1–5). For late responding tissue with α/β 1–5, the biological inhomogeneity ranged from 12% (±6%) to 19% (±9.5%) depending on α/β and the fraction size. For tumours and for acute responding tissues with α/β in the range of 5–20, the biological dose inhomogeneity was between 11% (±5.5%) and 15% (±7.5%). For late-responding tissues an increase of 9.5% in the biological effective dose may give a significant increase in the complication probability. Also a reduction of the effective dose by 7.5% may give a substantial drop in the tumour curability. Therefore, it may be preferable to express the outcome of treatment planning in radiotherapy in terms of calculated biological effect distribution as well as distribution of physical dose.

Non-coplanar radiotherapy treatment planning

S. G. McNee
Department of Clinical Physics and Bioengineering and Beatson Oncology Centre, Glasgow G4 9LF, UK

Owing largely to limitations in methods of dose computation and target definition, external beam radiotherapy has traditionally operated under the constraint that the central axes of the beams be coplanar. The advent of a newer generation of planning computers, together with the use of computed tomography (CT) and magnetic resonance imaging (MRI), has removed this constraint. A number of examples, planned on the Helax TMS planning system, are presented to illustrate where non-coplanar treatments are valuable or even essential. These arise where it is necessary to ensure that beams do not exit through critical structures (such as eyes when treating tumours of the brain, ear or parotid) or enter through shoulders (when treating tumours in the neck/chest region) whilst maintaining good conformation of the beams to the target. Emphasis is given to the need to delineate the target as a three-dimensional (3D) object and the importance of its shape at the extremities and to facilities for 3D representation of the target, critical structures and the radiation beams.

Dose distributions for chest wall conformation therapy using 6 MV X-rays and cobalt beams

M. E. Oatey and T. J. Davy
Department of Medical Physics, Royal Free Hospital, Hampstead, London NW3 2QG, UK

Crescent-shaped isodose patterns have been generated in the patients transverse plane to irradiate the chest wall whilst sparing the adjacent lung. A technique using multiple glancing wedged fields combined with two arched fields has been devised for this purpose. The procedure has been applied clinically using the computer-controlled tracking cobalt unit and experimentally on a Philips SL18 linac using 6 MV X-rays. For comparative purposes, a tissue equivalent phantom with lung inserts was "treated" on both machines. Dose distributions were measured using thermoluminescence microrods and Ilford line film. The plan was devised on a Philips OSS treatment planning system. This single plane study demonstrates good control of the isodose pattern with effective sparing of the underlying lung tissue. As expected, the 6 MV X rays provide a more rapid fall-off of dose inside the chest than the cobalt beams. It is anticipated that this study will provide insights into the requirements for software for automatic therapy machine control, collimator design and treatment planning requirements.

Staging of head and neck cancer using magnetic resonance imaging

M. McCarty, M. Leslie, H. Baddeley, M. Saunders and S. Dische
Paul Strickland Scanner Centre and Department of Radiotherapy, Mount Vernon Hospital, Northwood, Middlesex HA6 2RN, UK

The magnetic resonance imaging (MRI) findings in 40 patients with head and neck cancer seen at Mount Vernon Hospital between March 1990 and October 1991 were reviewed. The patients were all clinically staged before the MRI scan. The MRI findings were compared with the clinical staging; at the time of review, the radiologists were not aware of the clinical findings. There were 14 cases of laryngeal carcinoma, two of post-cricoid tumour, five involved the pyriform fossa, six the tongue, five the mouth or oropharynx and two the epiglottis. In several cases, staging was altered as a result of the MRI scan, and radiotherapy planning fields were adjusted. Even when clinical staging agreed with MRI findings, the multiplanar images obtained gave a greater degree of accuracy in radiotherapy planning. We conclude that MRI is a useful imaging technique in head and neck cancer.

The clinician's expectations from treatment

T. Landberg
Department of Radiotherapy and Oncology, University Hospital, S-214 01 Malmö, Sweden

In radiotherapy, different decisions have to be made successively such as prescriptions of the aim of therapy, the tissue volumes to be treated to specified dose levels according to specified fractionation regimes, and the organs at risk to be spared. The results of treatment can be no better than the input data. A treatment technique that is acceptable and optimal for the particular patient has to be decided upon, and the treatment has to be given within the uncertainty limits that have been accepted for the particular situation. Recording of a sufficient number of data has to be done in order to allow for later analysis of the treatment and for communication with other centres. Increasing sophistication in radiotherapy technology should allow for a better definition of target volumes and better dose distributions, and should thus lead to higher cure rates and less complications. This requires, however, that all the different steps in the whole radiotherapy procedure are optimized.

9.00 – 10.15

Nuclear Medicine I

Hall 10b

Progress in the radionuclide therapy of cancer

K. E. Britton
Department of Nuclear Medicine, St Bartholomew's Hospital, London EC1A 7BE, UK

The treatment of thyroid cancer with iodine-131 radioiodine is dependent on the selective uptake of radioiodine due to a function of the differentiated thyroid cancer cells. This functional approach is applied in the use of ^{89}Sr and ^{153}Sm for irradiation of bone metastases of prostate and breast cancer. The new approaches to cancer therapy depend on tissue characterization, *i.e.* through the subtle differences between the surface of the cancer cell as compared with its normal counterpart and on the architectural disruption that is inherent in malignancy. ^{131}I metaiodobenzylguanidine (MIBG) has given benefit to patients with malignant paraganglioma and to children with neuroblastoma even when, as in the latter case, it is the last in the line of treatment after surgery and chemotherapy. For neuroblastoma there should be earlier application of ^{131}I MIBG therapy when the cellular active uptake mechanisms are better preserved. The surface glycoproteins of the cancer cell are antigenic and against these antigens murine antibodies, made monoclonal by the hybridoma technique, are developed. ^{111}In and ^{99}Tc^{m} radiolabelled monoclonal antibodies have now a routine place in the early detection of recurrent and metastatic cancer, but the treatment of cancer using monoclonal antibodies labelled with beta-emitting radionuclides to target the radiotherapy is much more complex. Since a typical tumour uptake is about 1% of the injected activity, strategies are essential to reduce the irradiation of critically sensitive normal tissues. These include intratumour, intracavity, intra-arterial administration and the use of a two or three stage approach to circumvent irradiation of normal tissues. A bifunctional, bispecific antibody is required, one part of which binds to the tumour cell surface and the other to the radiotherapy bearing ligand. This antibody is injected first and time is allowed for metabolism of the unbound antibody (which may be helped by a "chase", as in the antibody-biotin streptavidin chase, biotin-radionuclide system). Then the radiotherapy bearing ligand is given. This approach enables a long-lived beta emitter, such as ^{32}P, to be used. This also has a pro-drug effect, for when the ^{32}P-antibody is metabolized at the tumour surface, ^{32}P phosphate may diffuse into the cells and be incorporated in their DNA and RNA. These new approaches depend on the lessons learned from conventional radionuclide therapy and, with genetic enginering techniques providing the "designer" molecules, open the way for selective, cancer-specific targeted radiotherapy.

Dobutamine thallium tomography in the investigation of Syndrome X

P. J. Thorley, S. J. Outram, M. W. Baig, L. B. Tan and M. R. Rees
Radionuclide Department, Killingbeck Hospital, Leeds LS14 6UQ, UK

Syndrome X describes patients who have positive exercise tests, anginal symptoms but normal coronary angiograms. We studied a group of 13 Syndrome X patients using tomographic stress thallium scanning. Dobutamine, a β-1 stimulator which increases myocardial oxygen demand, was used as the stressing agent and infused in increasing stages of 5 μg/kg/min starting at 5 μg/kg/min, for 5 min. Blood pressure, ECG and symptoms were carefully noted at each stage. Dobutamine infusion was halted when significant ST depression or chest pain was noted, thallium being injected 2 min before the end of the infusion whenever possible. The stress was tolerated well in all patients with only minor side-effects such as tingling and shaking. Nine patients showed reversible perfusion defects on thallium scanning while four had essentially normal studies. All but two patients (one normal thallium) developed chest pain at 10–120 μg/kg/min Dobutamine infusion. The results show that a high proportion of Syndrome X patients have reversible thallium defects when using Dobutamine; which is a well tolerated and not patient limited method of stress. This suggests that a significant percentage of Syndrome X may be caused by some form of organic coronary artery disease, such as microvascular disease.

Study of left ventricular function in two families with Romano-Ward syndrome

S. J. Cross, J. Dean, H. S. Lee, M. Y. Norton,
F. W. Smith, K. Jennings and S. Walton
Departments of Cardiology, Genetics, Medical Physics and Nuclear Medicine, Aberdeen Royal Infirmary, Aberdeen AB9 2ZB, UK

Congenital long QT syndrome is thought to arise from an imbalance of the sympathetic innervation of the heart. There is a tendency to life-threatening ventricular arrhythmias. Post-mortem studies have found regions of myocarditis. Is it possible to detect areas of abnormal myocardium during life? We have studied regional wall motion of the left ventricle in eight subjects with one of these conditions. After labelling the blood pool with ^{99}Tc^{m}, tomographic radionuclide angiography was performed in young members of two families with Romano-Ward syndrome. Two sisters and their mother had significant infero-lateral wall motion abnormalities. The ejection fraction was substantially reduced in the two subjects who had arrhythmias (27% and 30%, normal $> 40\%$). The other family had completely normal left ventricular contraction and ejection fractions (five subjects, two of whom have had symptoms). These results suggest that Romano-Ward syndrome is a heterogeneous abnormality which, in some instances, is associated with abnormal left ventricular contraction. In the family with abnormal left ventricles, the degree of left ventricular impairment may affect the susceptibility to ventricular arrhythmias.

Detection of viable myocardium with gated F18 fluorodeoxyglucose (FDG) positron emission tomography (PET)

H. S. Lee, S. J. Cross, M. Y. Norton and S. Walton
Department of Cardiology, Aberdeen Royal Infirmary, Aberdeen AB9 2ZB, UK

Critical coronary artery stenosis may provide only sufficient perfusion for basal myocardial metabolism without achieving normal contractile function. We describe a novel approach to detect such regions of myocardium which are potentially viable after re-vascularization. This approach has the advantage of directly measuring cardiac motion simultaneously with regional fluorodeoxyglucose (FDG) uptake with only a single low dose of radiation. Gated positron emission tomography (PET) was performed for six transaxial slices 18 mm apart. Wall motion along 36 radii 10° apart was objectively measured for eight short axis slices. Bull's eye images were formed with segmental FDG uptake superimposed on the wall motion. We defined viable myocardium as a continuous region ($\geqslant 25\%$ of left ventricle) of good FDG uptake ($\geqslant$ normal myocardium uptake) and poor contraction (2 standard deviations below normal controls). We studied 32 glucose loaded patients consisting of eight normals and 24 patients (mean age = 61 years, 20 male patients) with angiographically proven coronary artery disease. Viable myocardium was detected in 15 patients: two in the anterior, four inferior, five septal, three apical and one in the lateral region. Study of a patient with dilated cardiomyopathy further validated the technique showing global good FDG uptake but reduced contraction. *Conclusion:* Gated FDG PET can simultaneously detect regions of metabolically active myocardium with poor contraction using a single low dose of radiation.

Regional left ventricular function following CABG: evidence for hibernating myocardium

M. J. Metcalfe, M. Y. Norton, S. Cross, K. Jennings and S. Walton
Cardiac Department, Aberdeen Royal Infirmary, Foresterhill, Aberdeen AB9 2ZB, UK

Tomographic radionuclide ventriculography, unlike conventional two-dimensional (2D) imaging techniques, is able to quantify changes in regional left ventricular function. It is, therefore, a useful method for studying the effects of coronary artery bypass surgery and the concept of hibernating myocardium. 20 patients (90% male, mean age 60) were investigated using this technique before and after coronary artery bypass surgery. All patients were imaged using the Aberdeen Section Scanner, which has acquisition and processing times of 25 and 30 min, respectively. Comparisons were made using polar map subtraction of regional ejection fraction and ventricular phase values. 13 patients had triple vessel and three double vessel coronary disease. Seven patients were known to have had at least one prior myocardial infarction pre-operatively and one patient was identified as sustaining a peri-operative infarction. The mean global ejection fraction, for all patients, was 42% pre-operatively and 45% post-operatively (ns). For regional ejection fraction, 26 out of the 80 total segments improved, 24 were unchanged and 30 showed signs of deterioration, post-operatively. With respect to regional phase values, 26 segments improved, 45 remained unchanged and nine showed evidence of deterioration. Thus, although the global ejection fraction changes little following surgery, there are nevertheless important physiological changes in regional function.

Autologous platelet survival in volunteer blood donors

V. S. Turner, R. J. Hawker, S. G. Mitchell,
*S. R. Hesslewood and *L. K. Harding
*West Midlands Regional Blood Transfusion Centre,
Vincent Drive, Edgbaston and *Department of Medical
Physics, Dudley Road Hospital, Birmingham, UK*

Healthy age-retired blood donors were invited to take part in research into the preparation and storage of platelets. 31% of donors approached gave their written consent to participate. Volunteers donated either 40 ml or 1 unit of whole blood from which platelets were prepared by standard BTS techniques. Platelets were either returned within 2 h to the donor ($n = 8$) or, in the case of a unit donation, stored agitated at 22°C for 4 ($n = 11$) or 5 ($n = 5$) days. Platelets were radiolabelled with indium-111 before returning an autologous aliquot to the donor. Samples were taken from each donor 1 h post-injection and daily for up to 8 days for determination of platelet recovery and survival. One in three volunteers underwent gamma camera imaging to determine platelet distribution. Four of the 24 volunteers involved in this particular project took part twice to estimate individual variation. The remaining stored platelets were assayed *in vitro* for platelet function and biochemistry. Whilst platelets radiolabelled and immediately returned demonstrated the best recovery (45.1%) ± 13.2) and survival (238.9 h ± 21.7), those stored for up to 5 days remain high (41.9% ± 8.8 and 185.2 h ± 11.8, respectively). Individuals taking part twice showed similar results on each occasion.

Technetium-HMPAO labelled leukocyte scanning in the initial diagnosis of inflammatory bowel disease

P. N. Malcolm, C. Bearcroft, D. Rampton, N. W. Garvie
and P. G. Pratt
*Radioisotope and Gastroenterology Departments, The
Royal London Hospital, Whitechapel, London E1 1BB, UK*

The use of technetium-HMPAO labelled leukocyte scanning (WCS) in assessing activity in inflammatory bowel disease (IBD) is well known. We have retrospectively evaluated its role in the diagnosis of possible IBD in 43 new patients attending gastroenterology out-patient clinics. In 31 patients (Group 1) the WCS was the initial imaging investigation. In 12 patients (Group 2), in whom IBD was more strongly suspected by the clinician, it was used in conjunction with other radiological and/or endoscopic techniques. The prevalence of confirmed IBD was significantly lower in Group 1 (two of 31, 6%) compared with Group 2 (five of 12, 42%) (Fisher's exact text $p < 0.05$). The WCS showed high sensitivity, specificity and accuracy in both groups (sensitivity, specificity and accuracy in Group 1 were 100%, 93% and 94%, respectively, and in Group 2 were 100%, 86% and 92%, respectively). There were two false positive scans in Group 1 and one in Group 2, but no false negative results. The data suggests that the WCS, when negative, is useful as an initial screening test by excluding IBD. The anatomical information it provides, when positive, helps direct further endoscopic or radiological investigations.

The use of HMPAO-labelled white cell scintigraphy in the assessment of recurrent Crohn's disease

R. P. McAvinchey, C. Bearcroft, P. N. Malcolm,
P. G. Pratt, D. Rampton and N. W. Garvie
*Radiosotope and Gastroenterology Departments, The Royal
London Hospital, Whitechapel, London E1 1BB, UK*

In Crohn's disease (CD), radiological assessment of disease activity is frequently complicated by the radiographic stigmata of previous disease or surgical intervention. This study evaluates the use of Tc-HMPAO white cell scintigraphy (WCS) in recurrent CD, and correlates the findings on scintigraphy with those obtained by barium follow through examinations (BaFT), in 18 patients presenting with symptoms suggestive of CD. The patient group included 11 subjects with previously documented CD, and the final evaluation of disease activity was established by independent clinical methods. The WCS, if positive, was graded for uptake intensity, number of positive sites and anatomical extent. Each BaFT was carefully inspected for ulceration as the indicator of active disease and other stigmata of previous CD, including strictures and mucosal distortion, were recorded. The findings demonstrated a good correlation between clinical and scintigraphic results in recurrent CD. The presence of ulcers in particular correlated with positive WCS, but a significant number of patients without radiographic evidence of ulceration were scintigraphically positive, and subsequently established by clinical asessment as having recurrent CD. The results demonstrated that WCS is a sensitive and specific tool for the assessment of recurrent disease activity, particularly when BaFT is hampered by established stigmata of earlier disease.

9.00 – 10.15

The Application of BS5750 to Radiology

Hall 11a

Management and audit — BS5750 in radiology

I. R. F. Hendra
Bureau Veritas Quality International Ltd, 70 Borough High Street, London SE1 1XF, UK

The BS5750 Series, otherwise known as ISO9000–9004, is a set of international standards which provides fundamental guidance on quality management systems, and includes specifications for the use of purchasers. The specifications cover the means by which a supplier of goods and services can establish its management systems to ensure that the purchaser's needs are continuously met. The purchaser may not be the customer in terms that are currently understood in National Health Service parlance. A set of purchaser and customer requirements will be described in the context of a quality management system based upon BS5750. Reference will be made to assessment work already undertaken by Bureau Veritas Quality International in two NHS departments, namely diagnostics and radiology.

Total quality management in a clinical radiology department

R. Warren
Department of Radiology, Princess Alexandra Hospital, Harlow, Essex CM20 1RB, UK

Total quality management is a concept playing an important part in the managerial culture of the best commercial firms at the present time. It is based upon the notion that the end product of a commercial organization is made up of the work of individuals at many levels in that organization, and that if the work of each individual is performed in a way that is the best work of that kind, then the whole will be enhanced in such a way as to serve the customer and gain new markets. This is a leadership challenge to senior managers and results in a well motivated and satisfied workforce. These principles are so relevant to the work of health service organizations, that their implementation is worthwhile. The West Essex Directorate of Radiology is implementing a programme of quality management. They are monitoring all aspects of the quality chain and developing computer programs with Kodak for recording and for planning corrective action when variation exceeds agreed parameters. One department, the Breast Screening Service, is applying for registration under BS5750 so that the quality system is accredited by outside auditors.

The value of BS5750 to any work or business activity — a company view

A. D. O'Neill
Director, Quality, Europe, Africa and Middle East Region, Eastman Kodak Company, London W6 8PL, UK

The registration of a work or business activity to one of the BS5750/ISO 9000 series of standards provides a number of important benefits. (1) It gives customers assurance of reliable quality of products and services. (2) It gives greater understanding and control of the business to the staff and managers. (3) It provides a robust framework for continuous improvement of business activities. (4) It pulls together different disciplines in a structured customer-focused way. (5) It is a standard of excellence that recognizes good business practice. This paper covers how registration to BS5750 can help many different work and business activities improve both business performance and customer satisfaction.

9.00 – 12.00

Workshop: How Does Radiology Prosper in the Trust Hospital?

Hall 11b

Chairman: H. Loose

Presentations by: H. Loose, *Freeman Hospital, Newcastle upon Tyne;* D. Perry, *District General Manager, Oxford;* P. Wright, *Deputy Medical Director, Freeman Hospital Trust, Newcastle upon Tyne;* A. Carty, *Medical Director, Royal Liverpool Hospital Trust;* P. Davies, *Clinical Director, City Hospital, Nottingham and* A. Saunders, *Clinical Director, Guy's Hospital Trust.*

This workshop is designed to provide a consensus decision on a subject that is taxing all those concerned. The introduction of the trust hospital has required many overburdened radiologists to adopt managerial and financial skills in addition to their diagnostic and therapeutic expertise. The department of radiology will prosper if it generates income, however, because a greater proportion of the work done is for the other clinical departments of the trust, the department of radiology may be seen as an internal provider? This forum will address the common problems encountered and a number of clinical directors who have wrestled with new philosophy will be prepared to present their solutions. It is hoped that the workshop will be led by discussion. The experts will give presentations on aspects of "trust status" that have caused particular concern. Departmental clinical directors and managers must maintain the profile of the X-ray department and ensure provision of good safe equipment and an efficient 24 h service to patients. It is a challenge which is familiar, but now the funding must also be generated, and the system must be correct to enable the X-ray departments to flourish under "trust status".

10.45 – 12.00

The Chest: Biopsy Techniques and High Technology Imaging

Hall 9

The use of a powered cutting needle (Biopty) for obtaining histopathological material in intrapulmonary lesions

J. A. A. Haddock, C. M. Allen, M. Sheppard and D. M. Hansell
Department of Radiology, Royal Brompton National Heart and Lung Hospital, London SW3 6NP, UK

The sensitivity, specificity and safety of percutaneous transthoracic needle biopsy of pulmonary lesions is well established. Aspiration samples allow an estimation of whether a lesion is benign or malignant but often do not provide an adequate specimen for a specific histological diagnosis. Manual and powered cutting needles provide a larger core in which the lung architecture is preserved, but experience has been limited to chest wall lesions because it has been suggested that there is a higher incidence of pneumothorax and haemorrhage with this type of needle. We present a series of 53 patients in whom intrapulmonary lesions have been biopsied using a powered cutting needle, (Biopty TM, Radioplast, Sweden). 28 lesions were entirely surrounded by lung and 25 had pulmonary lesions abutting a pleural surface. A definitive histological diagnosis was achieved in 44 cases; in nine patients a diagnosis was not established. A wide spectrum of benign and malignant diagnoses was made, including some which could not have been made with non-cutting needles, for example, bronchioalveolar carcinoma, lymphoma, cryptogenic organizing pneumonia and Wegeners' granulomatosis. In this small series only one patient suffered an acute pneumothorax, which required a chest drain. Percutaneous biopsy using the Biopty Gun is a simple and effective method of obtaining high quality samples which allow accurate histopathological diagnoses.

Radiologically guided mediastinal biopsy: a 10 year review

B. Morrissey, M. D. Crane, *A. R. Gibbs and H. Adams
*Departments of Radiology and *Pathology, Llandough Hospital, Penarth, South Glamorgan CF6 1XX, UK*

Between 1981 and 1991, 73 biopsies of presumed mediastinal masses were performed in 71 patients. In 34 patients the mass arose mainly from the anterior mediastinum, in 24 from the middle mediastinum and in 13 from the posterior mediastinum. Final diagnosis was based on surgical resection (25 patients), definitive Trucut specimen histology (21), clinicopathological correlation (20), demonstration of the cystic nature of the mass (three), and supportive scintigraphic features in two cases of mediastinal goitre. Fine needle techniques were used in 57 cases, cutting needles (Trucut) in 32 patients and 16 patients underwent both procedures. Since its introduction to our department 3 years ago, computed tomography has completely replaced fluoroscopy as the imaging modality for needle guidance. Sensitivity and specificity in relation to differentiating malignant from benign disease was 89% and 83%, respectively, for fine needle aspiration, and 96% and 86% for Trucut biopsy. Accuracy in terms of classification of the precise nature of the mass was 75% for fine needle aspiration and 94% for Trucut biopsy. There were no major complications. Radiologically guided mediastinal biopsy is a safe procedure which provides accurate diagnostic information in most cases.

Ultrasound guided biopsy of peripheral lung and pleural lesions

L. Robinson and A. J. S. Saunders
Department of Diagnostic Radiology, Guy's Hospital, London SE1 9RT, UK

Guided biopsy of lung and pleural lesions can prove difficult. Small lesions may be impossible to see at fluoroscopy, lesions can be obscured by pleural fluid: the use of computed tomography (CT) is limited and has its own problems of access and single plane imaging. Many small lung lesions lie against the pleura and so are visible on ultrasound. We have performed a study to see if ultrasound guided biopsy is an alternative method for the management of such lesions. 14 patients, (11 males, three females) (age range 48–77 years) have undergone ultrasound guided biopsy of peripheral lung or pleural lesions (from 1 cm to 4 cm in size) in the last 12 months. Solitary lesions were seen in 10 patients (associated with an effusion in four); one patient showed isolated pleural thickening and three had multiple bilateral lesions. A 20 G Temno needle was used in 13 cases and an 18 G Biopty Gun was used in one case. All patients underwent several passes. Tissue samples were obtained in 12 patients; in one patient failure occurred as the lesion disappeared on introduction of local anaesthetic, in the other the procedure was abandoned when a pneumothorax and surgical emphysema occurred. The only other complication was minor haemoptysis (two patients). The biopsy histologies include malignancy (eight cases) granuloma (one patient) and normal lung (two patients). One sample was inadequate for diagnosis. We believe that ultrasound guided biopsy of such lesions is a simple and safe procedure with a good diagnostic yield. The technique will be discussed.

Avoidance of pneumothorax during percutaneous biopsy of the chest: creating an extrapleural "window"

S. J. Golding
Regional CT Unit, Churchill Hospital, Headington, Oxford OX3 7LJ, UK

This paper reports a method of reducing the incidence of complications of percutaneous chest biopsy by improving extrapleural access. Pneumothorax is the most common complication of percutaneous chest biopsy when the needle crosses the pleural space. Although pneumothorax is not usually serious, the discomfort can be distressing to the patient and is preferably avoided. The parietal pleura is attached to the chest wall by loose areolar tissue, the endothoracic fascia, and can be easily displaced by injecting normal saline to create a track between the chest wall and the pleura, through which a needle can be passed. This technique can be used to approach lesions deep in the mediastinum by either an anterior or posterior approach. Injection alongside vertebral bodies produces some aching but this resolves quickly; local anaesthetic is not used to create the needle-track in view of the risk of entering an anomalous nerve root sheath and injecting into the theca. The injected saline clears rapidly, usually in a few minutes, and no serious sequelae have been observed.

CT assessment of the size of pulmonary nodules: an *in vitro* study

K. M. Harris, D. C. F. Lloyd and H. Adams
Department of Radiology, Llandough Hospital, Penarth, South Glamorgan CF6 1XX, UK

Categorization of the severity of coal worker's pneumoconiosis (CWP) is traditionally based on the plain radiographic features. The size and profusion of opacities is important, with the presence of nodules measuring 1 cm or more in diameter constituting complicated pneumoconiosis. There is currently considerable interest in the use of computed tomography (CT) for the assessment of CWP and we have undertaken an *in vitro* study to assess the accuracy of CT measurement of the size of pulmonary nodules. 45 rounded nodules of synthetic material of approximate soft tissue density (70 Hounsfield units) were supported in gauze (−950 H) to simulate pulmonary nodules. The true size was accurately measured using a micrometer screw gauge and ranged from 0.58 cm to 2.14 cm. Using 10 mm collimation CT sections, standard lung settings (window level −750 H, window width 850 H) and broad lung settings (WL −550 H, WW 1350 H) permitted highly accurate measurement. On mediastinal settings (WL 20 H, WW 400 H), CT failed to detect nodules under 0.85 cm diameter. Above this size, the degree of accuracy increased as nodule size increased due to decreasing partial volume effect. The use of narrower collimation sections was of no real advantage. Under these optimized conditions, the use of both standard and broad CT window settings permits accurate measurement of nodule size.

Computed tomography (CT) in the assessment of the opaque hemithorax in children

J. M. E. Kirk and C. Dicks Mireaux
Department of Diagnostic Radiology, Hospital for Sick Children, Great Ormond Street, London WC1N 3JH, UK

We examined 22 patients with a completely, or partially, opaque hemithorax to assess the value of computed tomography (CT) in the diagnosis. All features helping to distinguish between differing aetiologies were noted. Diagnoses were subsequently confirmed by histology, microbiology and angiography. All 10 patients with pleural fluid exhibited distinguishing features. All four with empyema showed marked pleural enhancement, two with lymphoma had mediastinal masses, one of which had enhancing pleural nodules. Of two patients with a soft tissue mass and pleural fluid, one mass, a haemangioma, was markedly enhancing, the other, a rhabdomyosarcoma, enhanced less. Rib abnormalities were seen in a patient with lymphangiomatosis and intrapulmonary nodules in an asthmatic patient with veno-occlusive disease. Infected cysts or abscesses were demonstrated in four patients and absence or hypoplasia of the lung in three patients. In one of these, a small trachea with possible obstruction of the normal bronchus by the pulmonary artery was shown. Of five solid masses there were no specific features in two, a fibrosarcoma and an embryonal rhabdomyosarcoma. Calcification and posterior rib splaying, characteristic of a neuroblastoma, were seen in one, and rib abnormalities in two patients with an Askin's tumour. We conclude that CT, with intravenous contrast, demonstrates many different diagnostic features in children with an opaque hemithorax.

A quantitative HRCT technique for the serial assessment of bronchiectasis

S. R. Desai, A. U. Wells, F. K. Cheah, P. J. Cole and
D. M. Hansell
Department of Radiology, Royal Brompton National Heart and Lung Hospital, London SW3 6NP, UK

The clinical management of bronchiectasis is hampered by the lack of a reproducible system for monitoring the disease. High resolution computed tomography (HRCT) has an established role in the diagnosis of bronchiectasis but its utility in identifying disease progression has not been studied. Measurements of bronchial wall thickness on computed tomography (CT) vary greatly with window setting and are thus unsuitable for serial assessment. We have evaluated interobserver and intra-observer variation in objective measurements of bronchial wall circumference, made by three observers. In addition, to assess how accurately a previously scored section could be re-imaged at follow-up, patients were scanned on two separate occasions. 12 patients were scanned on an Imatron Ultrafast CT scanner; circumferences of 61 bronchi were measured using the tracing facility on the scanner console. There was minimal intra-observer variation (standard deviations (SD) for the readings of three observers = 0.40 mm, 0.60 mm, 0.67 mm) and interobserver variation (SD = 0.71 mm); variance was increased in the presence of contiguous vessels. The SD for differences in bronchial circumference on re-scanning patients was 1.57 mm. The reproducibility of measurements of bronchial circumference in this study indicates that this quantitative system promises to be valuable in assessing disease progression.

High resolution CT appearances in pulmonary complications of rheumatoid disease

K. T. Tung, F. Cheah, *R. M. duBois and D. M. Hansell
*Departments of Diagnostic Radiology and *Thoracic Medicine, Royal Brompton National Heart and Lung Hospital, London SW3 6NP, UK*

The lung may show a wide variety of manifestations in association with rheumatoid disease. The more common complications include pleural effusions, fibrosing alveolitis and necrobiotic nodules. Less commonly recognized associations are obliterative bronchiolitis, lymphoid follicular bronchiolitis, chronic organizing pneumonia and bronchiectasis. The plain radiograph findings of these latter conditions are often non-specific. In addition, interstitial fibrosis secondary to immunosuppressive therapy such as methotrexate or gold salts may be difficult to distinguish from fibrosing alveolitis on chest radiography. This presentation illustrates the wide spectrum of pulmonary manifestations seen on high resolution computed tomography (HRCT) and its use in refining the differential diagnosis of pulmonary complications in patients with rheumatoid disease.

High resolution CT appearances of pulmonary haemosiderosis with pathological correlation

F. K. Cheah, M. Sheppherd and D. M. Hansell
Departments of Radiology and Histopathology, Royal Brompton National Heart and Lung Hospital, Sydney Street, London SW3 6NP, UK

Pulmonary haemosiderosis is an uncommon condition with non-specific plain radiographic features: disparate and sarcoidosis. The utility of high resolution computed tomography (HRCT) in patients with chronic interstitial lung disease is now well established, but there is no literature on the HRCT appearances of pulmonary haemosiderosis; recent research has been directed towards the immunological basis of pulmonary haemorrhage. We present the HRCT findings in six patients with pulmonary haemosiderosis with pathological correlation in two cases and suggest a pathological basis for these CT appearances. The HRCT findings were similar in all six patients and not reminiscent of other chronic interstitial lung disease. The dominant abnormality was a diffuse nodular pattern with no zonal predominance. The nodularity was uniform in any one patient but varied between patients (ranging from 1–3 mm). Patchy areas of increased attenuation of the lung parenchyma were present in five patients due to more recent haemorrhage. This finding was associated with masking of the background nodularity. In view of these findings it is suggested that the HRCT appearances in the appropriate clinical context are sufficiently diagnostic for the initiation of therapy.

The ATS nodal map — a CT demonstration

J. G. Murray and E. Breatnach
Department of Radiology, Mater Misericordiae Hospital, Eccles Street, Dublin 7, Ireland

The American Thoracic Society (ATS) has proposed the use of a mapping scheme when describing mediastinal lymph node metastases in bronchogenic carcinoma. The map references major anatomical landmarks which are identifiable at mediastinoscopy. Numerical coding is used to denote specific nodal groups. Importantly for radiologists, this scheme is ideally suited to modern cross-sectional imaging methods and in particular computerized tomography (CT) and magnetic resonance imaging. Benefits from the generalized acceptance include the avoidance of vague terminology, thus: (a) accurate correlation of normal/abnormal nodal size with site; (b) a more planned and uniform approach to decision making regarding biopsy route; (c) accurate comparison of multi-institutional data. This study utilizes calcified mediastinal lymph nodes seen on axial CT scans to demonstrate this classification and thereby act as a teaching aid to its wider acceptance.

Anterior mediastinal lymphoma

I. R. Brand, D. Wright and A. G. Chalmers
Department of Diagnostic Radiology and Haematology, Leeds General Infirmary, Leeds LS1 3EX, UK

21 patients with lymphoma, 11 male and 10 female with a mean age at diagnosis of 33 years were studied. Ages ranged from 18–70 years but only three were aged over 40. All patients had a histologically proven lymphoma with a predominantly anterior mediastinal disease distribution. Computed tomography (CT) demonstrated a soft tissue mass rather than individual lymphadenopathy in all but three patients. Associated findings included middle mediastinal involvement in 70% and chest wall invasion in 42%. Low density areas within the anterior mediastinal mass consistent with necrosis or cystic change were found in 25%. Hodgkin's disease accounted for 13 (62%) patients, and non-Hodgkin's lymphoma for eight (38%) patients, all high grade T or B cell. Despite the disease primarily involving the anterior mediastinum, less than 40% had symptoms related to the chest. Involvement of the lung parenchyma, great vessels and pleura were less commonly demonstrated. Despite often extensive thoracic involvement, disease beneath the diaphragm was infrequently found.

MRI of residual lymphoma masses

D. MacVicar, A. Roldan, T. Hickish, D. Cunningham, J. Mansi and J. Husband
Department of Radiology and Lymphoma Unit, The Royal Marsden Hospital, Sutton, Surrey SM2 5PT, UK

Following chemotherapy or radiotherapy, lymphoma masses frequently resolve to leave smaller residual soft tissue abnormalities. Evaluation of adequacy of treatment when these abnormalities remain is a frequent clinical problem. Some authors have claimed that magnetic resonance imaging (MRI) may discriminate between "active" and "sterilized" lymphoma, a low signal on T_2-weighted imaging indicating fibrosis and inactivity within the residual mass. In a prospective study of 34 patients, MR images were obtained of stable residual lymphoma masses identified by computed tomography (CT) scan after chemotherapy and/or radiotherapy. The ability of MRI to assess activity within the residual mass and thus to predict early relapse, was compared with high dose gallium scanning (HDGS) and erythrocyte sedimentation rate (ESR). 11 patients subsequently relapsed. MRI yielded a sensitivity of 44%, specificity of 91%, positive predictive value of 71% and negative predictive value of 78% for detection of residual active disease. These figures compared favourably with HDGS and ESR in our series and suggest a role for MRI in follow-up of lymphoma patients.

10.45 – 12.00

Radiotherapy Treatment II

Hall 10a

Shaping the treatment volume

P. C. Williams
North Western Medical Physics Department, Christie Hospital, Manchester M20 9BX, UK

Successful radiotherapy for localized tumours depends on the irradiation of a target volume including the tumour and an appropriate margin, to a high dose whilst shielding adjacent normal tissues. In many circumstances this can be achieved by projecting megavoltage beams of rectangular cross-section towards the tumour bearing tissues. However, in order to exploit the strong inverse relationship between dose and volume, and to be able to treat tumours near to particular radiosensitive normal tissues, it is necessary to use beams of irregular cross-section and to consider the resulting dose distribution in three dimensions. Simple methods of producing irregular beams have become well established and are widely available. More recently, the availability of detailed anatomical data for individual patients, computers with power to manipulate images and graphics in seconds rather than minutes and linear accelerators which can be operated under computer control have allowed the developments of some elegant solutions to the volume shaping problem. The simple methods will be reviewed and discussed in comparison with present developments in this important technical aspect of radiotherapy.

Optimizing dose with a multileaf collimator for conformal radiotherapy

S. Webb
Joint Department of Physics, Institute of Cancer Research and Royal Marsden Hospital, Sutton SM2 5PT, UK

The use of several, preferably non-coplanar, photon beams, geometrically shaped to the beam's-eye-view of the target volume using a multileaf collimator (MLC), can achieve the goal of conformal therapy. A high dose volume may be fitted around the target volume. This paper addresses the extra difficulties which arise when the target volume has one or more concavities in its outline with organs at risk in such depressions. In these circumstances it is not so easy to select beams "seeing" the target volume, which do not also "see" part or all of the organs at risk. The problem then arises of the optimum distribution of beamweights to apply to each MLC location. This problem has been studied extensively and several solutions have been identified. The simplest solution shown in the figure is to use two beamweights per field, one for the part seeing only target volume and one for the part seeing both target volume (TV) and organs at risk (OAR). The optimum distribution of such pairs of weights (for a group of fields) has been determined by simulated annealing for a number of model problems and results will be shown. A second potential solution is to vary the intensity of the radiation continously across the open shaped ports and it will be shown that this leads to even better solutions. In a typical model problem where the organs at risk were entirely surrounded by target volume, the maximum in the dose-volume-histogram of the organs at risk was reduced to some 50% of the maximum in the dose-volume-histogram of the target volume. All solutions are enormous improvements on using the same beamweight for each field.

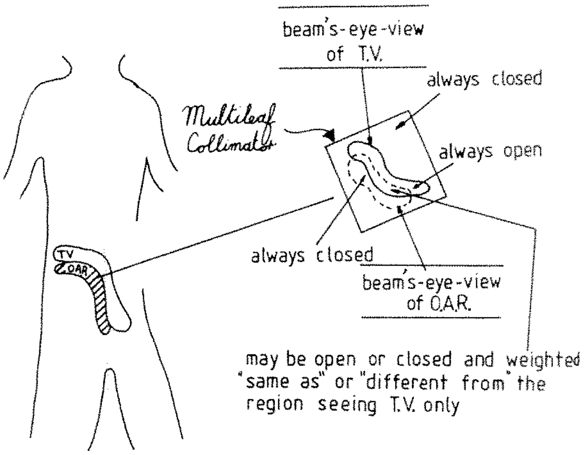
beam's-eye-view of T.V.
always closed
Multileaf Collimator
always open
TV
OAR
always closed
beam's-eye-view of O.A.R.
may be open or closed and weighted "same as" or "different from" the region seeing T.V. only

Potential advantages of 3D conformal planning in extremity soft tissue sarcoma

M. H. Robinson and A. M. Bidmead
Departments of Radiotherapy and Physics, The Royal Marsden Hospital, London SW3 6JJ, UK

The late complications and subsequent limb function, following treatment of sarcomas are related to radiation dose used and tissue volumes irradiated. The impact of conformal blocking on the radiotherapy planning of lower limb soft tissue sarcomas has been studied in 11 patients. Tumour, target and normal tissue volumes were reconstructed in 3D following a computed tomography (CT) planning scan. Dose calculations were performed for conventional and conformal plans using a block margin of 6 mm around the target volume. The volumes of tissue receiving 50%, 80% and 90% of the prescribed dose were compared using CVDDs. There was no compromise of target dosimetry with the use of conformal blocks. The treatment volume was reduced in all patients, and by > 20% in four of the five patients with thigh tumours. The mean volume of muscle outside the target volume which was irradiated to the 50% isodose was 4.2 l. The volume irradiated to > 90% was reduced by > 30% in five of the eight patients with thigh and lower leg tumours. The volumes of femur, tibia/fibula and ilium irradiated to > 90% were reduced by 38%, 18% and 14%, respectively, by conformal blocking. Considerable sparing was achieved in the volumes of pelvic contents irradiated, including gonads and rectum. This simple but time consuming technique can achieve major reductions in normal tissue irradiation and subsequent improvement in limb function. To realize this potential fully similar advances in patient immobilization and treatment verification are required.

Technical aspects of fractionated stereotactic radiotherapy

A. P. Warrington, R. W. Laing and M. Brada
Department of Physics, The Royal Marsden Hospital, London SW3 6JJ, UK

We have developed fractionated, stereotactic external beam radiotherapy for the treatment of malignant brain tumours. The technique utilizes the relocatable Gill–Thomas frame, which is reproducible to an accuracy of 1 mm. This precision depends on skill and expertise in the fitting process, and is monitored regularly. Computed tomographic (CT) scanning is carried out in the frame using a fiducial marker system. Tumour localization on the CT slices accounts for the largest uncertainty in the planning process. An additional error of 1 mm arises from image resolution on the treatment planning computer. The isocentre obtained from the treatment plan is often displaced from the geometrical centre of the target volume by up to 2 mm for larger, more eccentric lesions. The combined error in setting up this target isocentre to coincide with the mean radiation isocentre is 1 mm, and depends upon careful monitoring of the alignment lasers and machine parameters. The dose delivered by multiple arcs is potentially less accurate than with fixed fields. Regular comparison of phantom measurements with computer planning calculations are therefore required. Fractionated stereotactic radiotherapy can be carried out on a standard linear accelerator used for the routine workload of a department. However, it requires additional quality assurance with attention to detail. Even in ideal conditions, a 2–3 mm margin around the tumour is required for technical margins of error.

Fractionated stereotactic external beam radiotherapy for the treatment of recurrent gliomas and solitary brain metastases: a dose escalation study

R. W. Laing, J. D. Graham, A. P. Warrington and M. Brada
Neuro-oncology Unit, Institute of Cancer Research and Royal Marsden Hospital, Sutton SM2 5PT, UK

Fractionated stereotactic external beam radiotherapy (SRT) has been used to treat patients with recurrent gliomas and as a boost for patients with solitary metastases after whole brain radiotherapy. We report the acute toxicity and early survival results of the first 41 patients. A 5 MV linac and a relocatable stereotactic frame were used. Dose was prescribed to the 90% isodose which encompassed the ring enhancement on computed tomography. Accuracy of dose delivery was within 2 mm. 22 patients with recurrent gliomas have been treated. Two patients received 20 Gy in 4 fractions, two received 30 Gy in 6 fractions, four received 35 Gy in 7 fractions, eight received 40 Gy in 8 fractions, four received 45 Gy in 9 fractions and two received 50 Gy in 10 fractions. Previous radiotherapy varied between 45 Gy in 20 fractions and 60 Gy in 33 fractions. The median survival of this group from SRT was over 50 weeks. Follow-up ranged from 10 to 90 weeks. 19 patients with solitary metastases received SRT boost following whole brain radiotherapy. Doses ranged from 10 Gy in 2 fractions to 20 Gy in 2 fractions. The median survival of this group was 33 weeks and follow-up ranged from 10 to 80 weeks. Fractionated SRT is well tolerated and the initial survival results are encouraging. In recurrent gliomas the results are similar to interstitial radiotherapy.

A computer program for scheduling radiotherapy courses

E. Claridge and A. L. Bradshaw
Department of Medical Physics and Bioengineering, Queen Elizabeth Medical Centre, Edgbaston, Birmingham B15 2TH, UK

The program was developed to enable radiotherapy courses to be booked in advance for a number of consultants in a department with a waiting list for treatment. The allocations for individual consultants were subject to agreement but could easily be changed. A commercial 4GL database retains all of the administrative data for each patient and a linked suite of programs written in "C" keeps track of available start dates and schedules each course according to a specified pattern of treatment days each week. The suite allows for changing and deletion of courses and the use of the "spare slots" created by such activities. It is possible to weight allocations for the more time-consuming set ups. Calendar-related functions automatically provide current dates and allow for Bank Holidays and maintenance days. Mould room and simulator appointments are also dealt with and day lists are provided for all activities. Printed appointed letters are also generated. Over a period of 2 or 3 years data have been archived to provide information on waiting times, patient attendances and working practices, *e.g.* fractionation routines. With the addition of a post code/health district index data are produced for the quarterly returns to the purchasers.

Use of CT planning to improve mantle radiotherapy dosimetry

A. J. Rathmell, G. M. Workman, J. E. Clinkard,
R. E. Taylor and B. Carey
Departments of Radiotherapy, Radiology and Medical Physics, Cookridge Hospital, Leeds LS16 6QB, UK

Conventional dosimetry for mantle radiotherapy provides only a series of midplane doses at specified points within the target volume and accurate dose determination for specific lymph node groups and critical normal tissues is not possible. We have developed a method of integrating computed tomography (CT) planning and computerized dosimetry with conventional techniques in the planning of mantle radiotherapy in order to provide a more accurate and detailed dose distribution. Patients are first planned using conventional supine and prone simulation and lead blocks for shielding lung and spinal cord are cut as specified. Patients then undergo supine and prone CT planning and the individual target lymph node groups plus critical normal structures are indicated on the CT slices. A Theraplan dosimetry system is used to create accurate dose distributions throughout the target volume, taking account of the specified lead shielding, changing body contours, etc. In the first three patients planned in this way (for an 8 MV linear accelerator at 150 cm focus–skin distance) the doses received by specified lymph node groups were found to vary by a mean of −8% to +10% as compared with the midplane dose at the centre of the field. This gave a dose range of 32.2 Gy to 38.5 Gy for a prescribed dose of 35 Gy. The subcarinal/para-aortic nodes consistently received the lowest doses and the anterior cervical nodes the highest. The dose to the spinal cord with posterior shielding was, on average, 55% of the unshielded dose. The improvement in dosimetry achieved with this technique has important implications for mantle dose specification.

10.45 – 12.00

Nuclear Medicine II

Hall 10b

The influence of nuclear medicine in paediatric imaging

I. Gordon
Department of Radiology, Hospital for Sick Children, Great Ormond Street, London WC1N 3JH, UK

Advances in imaging techniques have affected paediatric radiology. The use of ultrasound, computed tomography (CT) and magnetic resonance imaging (MRI) has caused a reappraisal of the first line imaging. All these techniques are based on anatomy. Nuclear medicine is characterized by providing physiological data and functional images. Nuclear medicine examinations must be taken in conjunction with the anatomical information. *Renal tract:* In the renal tract vascular abnormalities may be better understood and clearly defined with the use of nuclear medicine, this includes renovascular disease as well as following renal transplantation. In urinary tract infection a dimercaptosuccinate (DMSA) is required to exclude a scar. Vesicoureteric reflux may be detected using indirect radionuclide cystography and thus avoiding the need for bladder catheterization and a marked reduction in radiation dose. In children with a pre-natal diagnosis of a urological abnormality, the ultrasound and dynamic renal scan go hand in hand in grouping these children for further management. *Skeleton:* In the skeleton radioisotopes have a role in suspected infection as well as in children with a limp. Disseminated malignancy is best excluded with bone scanning. *Brain:* ^{99}Tc^{m} HMPAO, a lipophilic agent, gives a map of regional cerebral perfusion and provides unique information on seriously ill children in intensive care. In epilepsy pre- and post-ictal HMPAO studies combined with MRI may yet provide new understanding of children with intractable epilepsy. *Respiratory:* In the respiratory tract the small or hypoplastic lung can be readily diagnosed with a chest radiograph and a ventilation/perfusion lung scan. The role to look at the long-term sequelae of children with a foreign body has also been well explored. *Conclusion:* Imaging in paediatrics should be based on the principle of using the least invasive technique and also the lowest radiation burden. Heavy sedation including general anaesthesia may be required for both magnetic resonance and also CT scanning. In general nuclear medicine procedures have a low radiation burden and rarely require sedation of the child. An integrated approach where the pathophysiology as demonstrated by nuclear medicine can be firmly attached to the anatomical diagnosis leads to appropriate use of resources and inflicts the least burden on the children investigated.

Multipurpose scintigraphy with ^{99}Tc^{m} pyrphotech in paediatric oncology

B. F. Sinyuta
Department of Radiology, Kiev Research Institute of Oncology, Kiev 252022, Ukraine

Children with tumours and tumour-like lesions of bones and retroperitoneal space were studied both in the dynamic and static modes of multipurpose scintigraphy using ^{99}Tc^{m} pyrphotech. In children with retroperitoneal tumours information obtained using multipurpose scintigraphy after single injection of ^{99}Tc^{m} pyrphotech is compared with that using four traditional radionuclide investigations, *i.e.* osteoscintigraphy, renography, nephroscintigraphy and positive tumour scintigraphy. Such related information enables isolation scintigraphic patterns of Wilms' tumour, neuroblastoma and abnormalities in kidney development (including combination with tumours) to be produced, which improve differential diagnosis of these retroperitoneal lesions. Multipurpose scintigraphy also reveals primary tumour, tumour metastasis into bones, renal dysfunction, urodynamics and deformation of urinary bladder in children with tumours of pelvic bones. Scintigraphy with ^{99}Tc^{m} pyrphotech in combination with roentgenography contributes to the differential diagnosis of osteogenic sarcoma and Ewing's sarcoma and affords exclusion of some benign bone lesions. Multipurpose scintigraphy is of particular value, when the findings from other modalities are difficult to interpret or require additional evaluation, *i.e.* a "dumb" kidney, bilateral Wilms' tumour, tumours with abnormalities in kidney development, difficult cases of differential diagnosis of osteogenic sarcoma and Ewing's sarcoma, and others.

The external radiation hazard from parents and infants undergoing nuclear medicine procedures

P. J. Mountford
Department of Medical Physics and Biomedical Engineering, Queen Elizabeth Hospital, Birmingham B15 2TH, UK

Regular close contact between a radioactive parent and a young infant, or a parent and a radioactive infant, represents the worst possible radiation hazard to a member of the public from either type of radioactive patient. The doses in these circumstances following diagnostic nuclear medicine procedures have been estimated from published external dose rate measurements and from effective exposure times which allow for the intermittency of close contact and for dose rate decay. These effective exposure times have been based on published observations of the greatest total time per day spent by an infant in close contact with a parent. It is concluded that for ^{99}Tc^{m} procedures, the dose equivalent to an infant from a radioactive adult, and to an adult from a radioactive infant, will be less than 1 mSv as long as in the former case, the activity administered to the adult patient does not exceed the ARSAC maximum value. For ^{111}In leukocytes, the activity administered to an adult should not exceed 8 MBq. It is also concluded that a nurse caring for one radioactive child or paediatric patient is unlikely to receive a dose equivalent of 60 μSv in a working day, unless the patient is classified as totally helpless.

An evaluation of the clinical usefulness of captopril renal scintigraphy

G. C. Ooi, D. Finlay and I. Belton
X-Ray Department, Leicester Royal Infirmary, Leicester LE1 5WW, UK

The primary objective of this study is to evaluate the clinical usefulness of captopril renal scintigraphy in the diagnosis of renal artery stenosis. 48 patients who underwent pre- and post-captopril ^{99}Tc^{m} DTPA renal scintigraphy in our hospital over the last 3 years were reviewed. A fall of > 5% in split renal uptake between pre- and post-captopril scans was considered positive. 35% were positive scans, almost all of whom had either follow-up renal arteriography or Doppler ultrasound. This confirmed renal artery stenosis in 60%, the remainder having normal renal vasculature. Angioplasty was performed in those with stenotic lesions and the outcome will be discussed. Of those with negative scans, three patients underwent arteriography which demonstrated single renal artery stenosis in one and bilateral disease in another. The remaining patients with negative scans have satisfactory hypertensive control on medication. We conclude that while captopril renal scintigraphy is an effective and useful diagnostic tool, it remains a measure of renal physiological response to captopril unlike arteriography which demonstrates anatomical lesions. There remains a high incidence of false positives. A review of diagnostic criteria for a positive scan will be discussed.

Diagnosis of pulmonary embolism: clinical practice and the use of diagnostic imaging

C. S. Romaniuk and P. J. Robinson
Diagnostic Imaging Department, St James's University Hospital, Beckett Street, Leeds LS9 7TF, UK

We retrospectively reviewed 166 episodes of illness diagnosed as pulmonary embolism in 155 patients to assess the accuracy of the diagnosis. In 125 episodes (75%) VQ or Q scans were performed. In 29 episodes (17.4%) the diagnosis was made, without VQ/Q scans, on clinical grounds; in 14 (8.4%) of these episodes this clinical diagnosis was made after death but without a post-mortem examination. In 12 episodes (7.2%) pulmonary embolism (PE) was diagnosed only on post-mortem examination. In those patients having VQ/Q scans, the diagnosis of PE was made with a high probability VQ/Q scan in 84 episodes (50.1%), intermediate probability VQ/Q scan in 17 (10.2%), low probability VQ/Q scan in 18 (11.4%) and a normal VQ/Q scan in six (3.6%). Pulmonary angiography was performed only in one episode (0.6%) and was positive in a patient with a high probability Q scan. PE was diagnosed without confirmatory angiography or positive venography in 22 episodes where the VQ/Q scan showed low probability or a normal study. PE was diagnosed antemortem in 15 episodes without VQ/Q scan. Clinical presentation and risk factors for PE were scored for each episode. There was no significant difference in score between different VQ/Q groups or those diagnosed without scans. The diagnosis of pulmonary embolism continues to be made on unreliable clinical grounds.

A comparison of SPECT and planar imaging in pulmonary embolus

S. Eustace, N. Phelan, A. Adams and J. T. Ennis
Department of Radiology, Mater Misericordiae Hospital, Eccles Street, Dublin 7, Ireland

In an attempt to evaluate single photon emission computed tomography (SPECT) imaging in pulmonary embolus we compared SPECT with conventional planar ventilation perfusion scans performed consecutively on 11 patients referred with suspected pulmonary embolus. V/Q mismatches with a "high probability" of being due to pulmonary embolus were noted in three patients by both SPECT and planar imaging. In one of these patients

SPECT enabled segmental localization of a defect to the posterior segment of left upper lobe. In one other patient SPECT enabled identification of multiple additional subsegmental defects. A matched V/Q defect was seen in one patient by both SPECT and planar imaging. This study suggests that SPECT and planar scanning are equally sensitive in the diagnosis of "high probability defects," however, the ability to localize defects segmentally and to identify further subsegmental defects are sufficient to recommend SPECT scanning as a favourable alternative to planar scanning in the diagnosis of suspected pulmonary embolus.

Closing the feedback loop of audit

J. Griffith, W. H. Thompson, A. Notghi, N. J. Tolley,
V. M. Harding and L. K. Harding
Department of Physics and Nuclear Medicine, Dudley Road Hospital, Birmingham B18 7QH, UK

In 1990, the level of satisfaction felt by patients attending our department was assessed by means of a direct interview (100 patients) and postal survey (190 questionnaires posted, 105 returned). The questionnaire used in both cases was identical and designed to cover all aspects of patients attending for a nuclear medicine investigation (*e.g.* directions to hospital, parking, reception, etc). More criticisms were received from the postal survey subgroup. These initial surveys established a baseline level of patient satisfaction and identified areas where there was room for improvement. Certain areas were then targeted for action. One year on, the postal survey was repeated (200 posted, 105 returned). The number of "dissatisfied patients" had fallen from 18% to 13%. This improvement occurred primarily in those areas which we had targeted (hospital directions, waiting facilities). In those areas where no action could be taken (*e.g.* car parking), no improvement was seen indicating that the methods of assessment were valid. Whilst the need to repeat such surveys following the implementation of change has been stressed, it is surprising how few times this had been reported. Repeating the survey allows the effect of any action to be assessed, thereby closing the audit "feedback" loop.

Notes

10.45 – 12.00

Musculoskeletal Imaging — Joint Disease

Hall 11a

Advanced imaging of the hindfoot

A. M. Davies
Department of Radiology, The Royal Orthopaedic Hospital, Birmingham B31 2AP, UK

The complex structure and function of the hindfoot is often poorly understood and difficulties in localizing symptoms can cause problems in differentiating hindfoot pain from ankle and foot pain. The radiograph remains the initial investigation of choice but errors in interpretation may occur because of overlapping structures, numerous accessory ossicles and normal variants. It is for these reasons that many of the newer imaging techniques have a role in the investigation of the ankle and foot including bone scintigraphy, computed tomography (CT), magnetic resonance imaging (MRI) and to a lesser extent ultrasound. The principal role of scintigraphy is in the detection of occult lesions, such as stress fractures, osteoid osteomata and symptomatic normal variants. Whereas ultrasound is valuable in the assessment of tendon pathology, notably of the achilles, CT can be performed in a number of different planes with the coronal plane the most useful. Trauma is arguably the commonest indication for CT of the ankle and hindfoot and is used primarily to clarify the full extent of injury, rather than to make the initial diagnosis. Amongst other conditions, CT is also useful in the assessment of suspected tarsal coalition. The role of MRI in the foot and ankle is evolving, particularly with the increasing sophistication of software. It will undoubtedly be the investigation of choice for soft tissue disorders, although CT remains superior when bony detail is required.

Magnetic resonance and CT arthrography of the shoulder

I. W. McCall, J. Rees and V. N. Cassar-Pullicino
Department of Diagnostic Imaging, The Robert Jones and Agnes Hunt Orthopaedic Hospital, Oswestry SY10 7AG, UK

Double contrast computed tomography (CT) arthrography of the shoulder has been used to assess the capsular mechanism and glenoid labrum in patients with pain or instability. Magnetic resonance imaging (MRI) has recently been shown to demonstrate both damage to the rotator cuff and the glenoid labrum. High levels of sensitivity and specificity have been reported for tendinitis and labral tears. Detailed comparative studies of CT arthrography and MR are required to assess the relative role of each investigation and a prospective study has therefore been undertaken. 40 patients (29 male and 11 female) with average age of 32 years were evaluated. All patients underwent CT arthrography within 6 weeks of the MR study which was performed on a 0.5 T GE Max system. All images were reviewed separately by two authors in the absence of any clinical information. 29 patients were referred with recurrent dislocation and 11 were suspected of an impingement syndrome, but some patients with dislocation demonstrated evidence of rotator cuff disease and others with rotator cuff symptoms had labral defects. There was a close correlation of findings between the two techniques with regard to labral lesions with only one case out of 31 seen on MR that was not evident on CT arthrography. However, the anatomy of the labral injury was more confidently and accurately assessed on CT arthrography. Capsular stripping was only diagnosed in one case on MR, but 18 cases were demonstrated on CT arthrography while capsular thickening was only seen on MR. Hill-Sachs lesions were demonstrated on both CT arthrography and MR in 16 cases but an additional four cases demonstrated bone bruising without a cortical defect on MR. Tendinitis and impingement were demonstrated in 10 cases on MR but in only one of these cases was a partial tear diagnosed on CT arthrography. Seven full thickness tears were demonstrated on both MR and CT arthrography while one was demonstrated only on CT arthrography. These results show that MR is the first investigation of choice for extra-articular pathology while intra-articular changes, in particular the labral tears, were more confidently assessed by CT arthrography.

Superior image quality of high field MR system in comparison with low field MR system in joint disease

A. Mundinger, E. Dinkel, G. Sigmund, U. Blum and B. Stoever
Department of Diagnostic Radiology, University Clinics, W-7800 Freiburg, Germany

The optimal field strength in magnetic resonance imaging (MRI) is still discussed controversially. The objective of this study was to assess the effect of field strength on diagnostic quality in traumatic and inflammatory diseases of the knee and ankle. MRI studies at 2 T (79 examinations) or 0.23 T (104 examinations) were performed in 56 patients with traumatic and 127 patients with inflammatory lesions of the knee and ankle. The quality of all images was assessed by the consensus of three radiologists on a scale of diagnostic (3+, 2+) and non-diagnostic (1+) image quality. More than 90% of images in both systems were diagnostic. However, the proportion of 3+ quality images was significantly higher ($p < 0.001$) at 2 T (2 T:64/79 = 81% *vs.* 0.23 T:51/104 = 49%). Motion artefacts were the main cause of reduced image quality. We conclude that high field imaging at 2 T provides better image quality than low field imaging at 0.23 T in patients with traumatic and inflammatory diseases of knee and ankle.

Magnetic resonance tomography of the shoulder: a comparative study with arthroscopy

C. Gückel, *W. Jockers, K. Laver and A. Rudin
*Departments of Radiology and *Orthopaedics, University Hospital of Basel, CH-4031 Basel, Petersgraben 4, Switzerland*

In order to evaluate the diagnostic efficacy of shoulder magnetic resonance tomography (MRT), a prospective study was conducted in which MRT results were compared with arthroscopic data. *Method:* 61 patients were examined with a 1.5 T superconductive magnet (Magnetom, Siemens); mean age 44.1 years; 36 males; 25 females; 31 right; 29 left and one bilateral. The examination protocol consisted of a paracoronal T_2-weighted spin-echo (SE) sequence (time to repeat (TR) 2400/time to echo (TE) 19–90/2 acquisitions), a parasagittal T_1-weighted SE sequence (600/19/1) and a transversal gradient-echo sequence (FLASH 450/10/1 a = 50°) with a slice thickness of 4 mm each. 22 patients had an arthroscopy and the data could be compared. *Results:* The diagnostic efficacy of shoulder MRT was assessed as follows: impingement of the rotator cuff: sensitivity 100%, specificity 75%, accuracy 90%. Rupture of the rotator cuff: 100%/82%/90%. Rupture of the biceps tendon: 66%/100%/95%. Labral lesion: 60%/83%/72%. Lesion of the joint capsule 50%/85%/81%. Hill–Sachs defect 100%/100%/100%. *Discussion:* MRT of the shoulder, conducted as a non-invasive tool without intra-articular application of contrast media, is a valuable method to assess the rotator cuff. The differentiation between degenerative changes and ruptures might be difficult in some cases. The results concerning the diagnosis of shoulder instability are far less reliable. Despite good soft tissue contrast an intra-articular injection of contrast media is necessary to judge the glenoid labrum and the joint capsule.

The contribution of variations of acromial morphology in rotator cuff disorder — MR imaging

J. Namasivayam, *W. P. Chan, *M. Valensieck and *H. K. Genant
*Departments of Radiology, Glasgow Royal Infirmary, UK and *University of California, San Francisco, USA*

We evaluated the relationship between the supraspinatus outlet and the severity of rotator cuff disorders by magnetic resonance (MR) imaging in 55 shoulders of patients with clinical impingement syndrome. All cases had spin-echo T_1-weighted and gradient-echo sequences performed on a 1.5 T system. The acromial shape was categorized into three types (flat, curved, and hooked). The anterior slope was measured in degrees on oblique sagittal planes at the level of the coracoid process. The lateral slope was assessed on oblique coronal images at the level of the acromioclavicular joint. Rotator cuff disorders were categorized into four groups (normal, tendinitis, partial- and full-thickness tears). Surgical confirmation was available in 16 shoulders. Results of statistical analysis showed that severity of rotator cuff disorders was closely related to the acromial shape, anterior slope, and patient's age. Osteophytes protruding from the undersurface of the clavicle appeared frequently in the acromioclavicular joint. However, the lateral acromial slope did not reach statistical significance among groups. We conclude that MR imaging is of significant value in evaluating supraspinatus outlet; and thus the extent of the subacromial decompression can be accurately assessed for surgical planning.

Comparison of contrast media in CT arthrography of the shoulder

R. Wellings, A. M. Davies, *C. P. Walker and *V. N. Cassar-Pullicino
*Department of Radiology, Royal Orthopaedic Hospital, Birmingham and *Robert Jones and Agnes Hunt Hospital, Oswestry, Shropshire SY10 7AG, UK*

Evaluation of the shoulder by computed tomography (CT) arthrography is well recognized. Logistical problems in transferring the patient from the screening room to the CT suite may occur, thereby prejudicing the quality of the scan. The purpose of this prospective study is to quantify the relative absorption/dilution of two contrast media in 78 patients undergoing CT arthrography of the shoulder. All patients received 3.5 ml 300 mg I_2/ml contrast medium and 10 ml air. Group A received iohexol, Group B iohexol and 0.1 ml of 1 in 1000 adrenaline and Group C iotrolan. A CT slice through the midglenoid was selected and the attenuation value of the contrast medium measured as was the time from the initial injection (approx. 20 min). A single CT slice through the same anatomical level was repeated 1 h after the injection and the attenuation value was measured again. The mean attenuation in Group A was considerably lower than in Groups B and C both at 20 min and 1 h. The mean attenuation in Group B was slightly lower than Group C at 20 min but higher at 1 h. Marked dilution of all the contrast media occurred in the presence of a complete rotator cuff tear. This study shows that the absorption/dilution rate of the dimeric contrast medium iotrolan is significantly less than that of iohexol alone. The synovial vasoconstriction from the addition of adrenaline to the iohexol results in superior contrast quality on the delayed scans. Further analysis and discussion of the data is presented.

Ultrasound evaluation of displacement in the ossified hip

L. H. Berman, A. Egan and *C. Verity
*Departments of Radiology and *Child Development,*
Addenbrooke's Hospital, Cambridge CB2 2QQ, UK

Clinical evaluation of children with abnormal muscle tone is unreliable. These children, at increased risk of late hip dislocation, undergo frequent pelvic radiographs for assessment and reassurance. Sonographic assessment of unossified neonatal hips is an established technique, but it has not been adopted in ossified hips because of an inability to demonstrate the acetabular floor. The authors compared sonography with pelvic radiography in 24 children aged 9 months to 12 years, most of whom had cerebral palsy. Sonograms were reported without knowledge of plain radiographic findings. 22 normal hips in 11 subjects were correctly identified sonographically. Displacement of 18 hips in 10 subjects correlated with plain films. In two cases radiographic displacement of the femoral heads was not detected sonographically. This discrepancy is due to the scans being obtained in hip flexion but the plain radiographs in extension. This has been observed to cause transient changes in displacement. In one case posterior displacement was identified on a sonogram but was impossible to detect on radiography. Transient femoral head migration during muscle spasms was clearly demonstrated sonographically. This would require prolonged fluoroscopy for radiographic evaluation. In the authors' institution sonography is considered to provide additional information and has replaced the plain radiograph for most assessments.

Demonstration of osteochondritis dissecans of the elbow by computed tomographic arthrography

P. Holland, A. M. Davies, *V. Cassar-Pullicino and
*I. W. McCall
X-ray Departments, Royal Orthopaedic Hospital,
*Birmingham and *Robert Jones and Agnes Hunt*
Orthopaedic Hospital, Oswestry, Shropshire SY10 7AG,
UK

Osteochondritis dissecans (OD) of the elbow is an uncommon condition usually affecting the capitellum in young males. Like OD elsewhere, its aetiology is unknown, though repeated trauma, vascular insufficiency, or both, have been implicated. Appropriate treatment depends on accurate delineation of the lesion, the integrity of the overlying cartilage, and the identification of loose bodies. 11 patients with OD of the elbow were assessed. From the plain radiographs, only 5 out of 10 visible lesions were confidently diagnosed as OD. Conventional arthrography contributed little to the diagnoses. In eight of the 11 patients plain computed tomography (CT) identified the site and extent accurately in all, and the presence of intra-articular loose bodies in four. Computed tomographic arthrography (CTA) was performed in all cases using a standard technique and confirmed the plain CT findings in all, with the exception that one osseous loose body was obliterated by contrast media. CTA was able to delineate precisely the state of the overlying cartilage in every case. In five of the 11 patients, the whole cartilage was intact, whilst in two cases fissuring and thinning of the cartilage was seen. Cartilage defects overlying the area of OD were identified in four of the 11 patients, three of which had associated loose bodies. OD affected the capitellum in nine patients, the capitellum and olecranon in one, and the trochlear in one. Examples of OD demonstrated by CTA will be shown.

Automated measurement of interbone distance on macroradiographs of osteoarthritic knees using the symmetric axis transformation

J. A. Lynch, J. C. Buckland-Wright and D. J. Hawkes
Division of Anatomy and Division of Radiological Sciences,
UMDS, Guy's Hospital, London SE1 9RT, UK

Radiographic changes in osteoarthritis include joint space narrowing, subchondral cortical thickening or changes in underlying cancellous bone and osteophytosis. Automated methods of quantifying the changes are being developed to aid understanding of the inter-relationship between disease features. A method of analysing digitized radiographs of knees has been developed to delineate bony margins of the joint space automatically and convert them, using the symmetric axis transform, into profiles of interbone distance across joints. Problems addressed include those arising from taking measurements from a two-dimensional projection of a three-dimensional object. Using ×5 macroradiographs of post-mortem knee joints, the accuracy and reproducibility of the technique has been analysed. It was found that interbone distance could be measured with a reproducibility of between ±0.20 mm and ±0.06 mm depending on the position in the joint. A rigid protocol for radiography of patients allowed accurate assessment of joint space narrowing in the knees of 39 osteoarthritic patients with medial tibiofemoral compartment involvement. Weight-bearing ×5 macroradiographs taken in both standing and tunnel views, allowed assessment of cartilage loss on the tibial plateau and both inferior and popliteal surfaces of the femoral condyle and showed that different patterns of cartilage loss could be found.

The patello-femoral joint — a comparison of geometry measured on the "skyline" view and axial computed tomography

C. P. Walker and V. Cassar-Pullicino
Department of Diagnostic Radiology, The Robert Jones and Agnes Hunt Hospital, Oswestry SY10 7AG, UK

In the quest for a treatable cause of anterior knee pain, 30°, 60° and 90° "skyline" views of the patella are obtained, primarily to assess the functional relationships of the patello-femoral joint. Patello-femoral malalignment predisposes to recurrent subluxation and dislocation, articular cartilage damage and premature degenerative change. The aim of this study is to evaluate critically, by comparative assessment, the information provided by skyline views and computed tomography (CT). *Methods:* We studied patello-femoral geometry on 50 symptomatic knees imaged by a "skyline" view (Marchant's view), and axial CT. Respective measurements of the patello-femoral angle (assesses patellar tilt), the congruence angle (assesses lateralization) and trochlear depth were obtained. The data from each technique were assessed independently to avoid the possibility of observer bias. *Results:* Significant numbers of false positives and false negatives are observed on the "skyline" views in all three measurements (*e.g.* 12% false positive and 24% false negative for lateralization). The results are presented in graphic form and visual examples will be shown to correlate with the statistical results. *Conclusion:* "Skyline" views are inaccurate and unsuitable primarily because they cannot be obtained in less than 30° of flexion. CT shows that all but the worst cases of misalignment have corrected at this degree of knee flexion. We suggest that "skyline" views have no role in screening for maltracking as florid examples will be missed, and would strongly urge that no surgery be performed on their basis alone as this would result in inappropriate operations. Although CT is the preferred mode of assessing patello-femoral geometry, difficulties are still encountered and the ways of circumventing them will be discussed.

Notes

12.15 – 1.15

Mackenzie Davidson Memorial Lecture

Hall 9

Molecular biology in common disease

D. J. Weatherall
Nuffield Professor of Clinical Medicine and Hon. Director, Institute of Molecular Medicine, University of Oxford, Oxford, UK

The "new" sciences of molecular and cellular biology have important implications for every aspect of clinical practice. The ability to isolate, sequence and express human genes is making it possible to define the molecular basis for monogenic disease and in the future should lead to a much better understanding of the pathogenesis of common polygenic diseases, conditions such as heart disease, stroke, autoimmune disease, the major psychoses and cancer. This field is already making a major impact on the pharmaceutical industry and biotechnology is starting to play a major role in diagnosis and therapy. To illustrate some aspects of the applications of molecular biology to clinical practice, current work on human gene action and how this appears to break down in common disorders such as cancer will be described. The likely practical applications of this new knowledge, particularly for diagnostic medicine, will be reviewed and an attempt will be made to anticipate the changes in clinical practice which may follow on from these new advances.

2.15 – 3.45

Ultrasound

Hall 9

Ultrasound exposure measurement for safety

F. A. Duck
Medical Physics Department, Royal United Hospital, Bath BA1 3NG, UK

Diagnostic ultrasound has an enviable and well-deserved reputation as a powerful investigative tool without apparent hazard. The question of safety has been kept under periodic review, and recent developments have caused further re-evaluation. By reviewing published surveys of measurements of ultrasonic output, steady increases have been demonstrated over two decades in both pressures and intensities. Exposure in some pulsed Doppler applications now differs little from that used in ultrasonic physiotherapy. It is now possible to make measurements of the pressure pulse with considerable accuracy using a PVDF hydrophone. The peak negative pressure, which may exceed 4 MPa, is relevant to the assessment of cavitation, and the degree of shock relates to the heating and streaming potential of the beam. Derived measurements of time-averaged intensity (I_{spta}) reach $5\,\text{W/cm}^2$ in some Doppler beams, and tissue absorption at these intensities causes temperature increases of a few degrees. However, total acoustic power, from a force balance measurement, may be a more useful indicator of heating potential; diagnostic powers reach 300 mW for some Doppler applications. Changes in US FDA regulations may throw a greater responsibility onto the user to make informed judgements regarding safety, using on-screen indices. The value and limitations of the models used in deriving these indices need to be understood.

Three-dimensional ultrasound of the fetus

I. M. G. Kelly, W. R. Lees and J. E. Gardener
Departments of Radiology and Medical Physics, Middlesex Hospital, Mortimer Street, London, W1N 8AA, UK

Objective: To investigate if three-dimensional (3D) ultrasound data sets of the fetus can be acquired in routine practice. Is transabdominal (TA) or transvaginal (TV) ultrasound the best means of acquiring 3D data sets in early pregnancy? To create 3D fetal reconstructions and to examine with high speed multiplanar reconstructions. To measure fetal volumes. *Methods and materials:* A 3.5 MHz sector probe and 5 MHz vaginal probe for the Acuson 128 were used in conjunction with an electromagnetic 3D position sensor (Polhemus) to acquire 3D data sets on more than 20 fetuses ranging in gestational age from 11 to 20 weeks. The 256 × 256 × 128 × 8 bit data set is processed and stored on a multiprocessor transputer workstation. 3D fetal image reconstructions were made and high speed multiplanar reprocessing (MPR) was performed. TA and TV data sets were compared. Fetal volumes were calculated after data set segmentation. *Results:* 3D reconstructions and high speed MPR reveal morphological information not possible with conventional scanning. Data set archiving and interactive multiplanar reformatting allows complete elective ultrasound re-examination of the fetus. TV ultrasound gives best results in early pregnancy. *Conclusion:* 3D fetal ultrasound is a completely new way of imaging the fetus which has great potential for diagnosis of fetal abnormalities.

Measurement of ultrasound exposure *in utero*

F. A. Duck, J. Aindow, N. Sharpe, H. C. Starritt and H. M. Tonge
Medical Physics Department and Obstetrics and Gynaecology Department, Royal United Hospital, Bath BA1 3NG, UK

The quantification of ultrasound exposure *in utero* is important for the assessment of ultrasound safety. Estimates from *in vitro* measurements involve substantial approximations. In this work we measured ultrasound exposure directly *in utero* using a miniature PVDF hydrophone introduced trans-cervically. All measurements were carried out immediately prior to termination of pregnancy typically at about 10 weeks gestation. The hydrophones were rectangular in area, mounted on the obliquely-cut tip of a steel rod. Absolute calibration was carried out against the NPL Ultrasound Beam Calibrator, and both frequency dependence and directional dependence were measured. Intra-uterine measurements were carried out in both imaging and pulsed Doppler fields. The pulse waveform was captured on a digital oscilloscope, at a digitization rate of 200 MHz, and downloaded to a microcomputer for subsequent analysis. Initial measurements using a 3 MHz phased array demonstrated peak negative pressures up to 0.9 MPa at a depth of about 6 cm, and clear evidence of non-linear harmonic generation in amniotic fluid. The method allows a direct evaluation of the "estimated *in situ* exposure" values required by the US FDA, and quoted by many manufacturers.

Comparison of antenatal ultrasonography and postmortem findings in abortuses for lethal renal disease

R. Rajah and J. McHugo
Department of Diagnostic Radiology, Queen Elizabeth Hospital, Birmingham B15 2TH, UK

Comparison was made between antenatal ultrasonography and postmortem findings on fetuses terminated for lethal renal disease. 29 postmortems were performed over 4 years (1987–1990). The distribution was as follows: outflow obstruction = 9 (31%); cystic disease = 7 (24%); developmental abnormalities = 11 (38%); miscellaneous group = 2 (6.8%). The ultrasonography sensitivity varied between 60% and 88%, and specificity was between 58% and 77%. We review reasons for the difference and discuss ways in which to improve the quality of antenatal renal scanning.

Correlation of antenatal ultrasound and pathological examination in 153 malformed fetuses

M. J. Weston, *H. Porter, *P. J. Berry and
H. S. Andrews
*Departments of Radiology and *Paediatric Pathology, Bristol Maternity Hospital, Bristol BS2 8EG, UK*

153 cases of fetal abnormality which came to pathological examination and had also undergone antenatal ultrasound were reviewed. The autopsy diagnosis was taken as correct and any ultrasound errors revealed were classified according to whether or not the missed abnormality would have affected management. This included any effect on genetic counselling for future pregnancies. The primary diagnoses in the 153 cases were: 67 nervous system anomalies, 19 gastrointestinal, 18 genitourinary, 13 chromosomal, 10 skeletal and 26 other abnormalities. 46% of the total number had multiple abnormalities. There were 67 cases (44%) where autopsy showed further anomalies (whether detectable ultrasonically or not) or altered the ultrasonic diagnosis. Of these 67 cases, 10 were due to false positive ultrasound diagnoses. However, only 36 (24% of the total) were findings which altered management. Errors in ultrasound diagnosis were associated with the presence of multiple anomalies and oligohydramnios. One third of those with spinal neural tube defects were shown to have renal anomalies. Pathological examination remains a valuable tool in the management of fetal anomaly. The presence of one abnormality on ultrasound examination must prompt the search for others.

Antenatal detection of congenital diaphragmatic hernias: the Northern Region experience

E. Dillon, E. Hey and M. Renwick
Department of Radiology, North Tees General Hospital, Stockton-on-Tees TS19 8PE, UK

Notifications of congenital diaphragmatic herniation to the Northern Regional Fetal Abnormality Survey were studied for the 7 year period 1985–1991. The NRFAS is a central register for this large but fairly well defined geographical area of 3 million people. Antenatal ultrasound made a specific diagnosis of diaphragmatic herniation in only 19 of 99 fetuses although this has improved to 40% in the last 2 years. In the majority the diagnosis was made by identifying cardiac displacement, usually with stomach alongside the heart in the thorax when the hernia was left sided. We have evidence that some congenital diaphragmatic hernias (CDH) are undiagnosed because of their dynamic nature. A further 12 structurally abnormal fetuses found to have CDH were identified by antenatal scans; the commoner associated defects were of the body wall (six), heart (six), neural tube defects (nine), renal agenesis (four) and ascites and/or pleural effusion (three). Differentiation from cystic adenomatoid malformation (CAM) of the lung was a problem in two fetuses; four CAMs and 1 thoracic enterogenous cyst occurred in these 7 years. The overall survival rate (36%) is poor. Termination may be offered if diagnosis is made early in pregnancy but in this study four fetuses diagnosed before 24 weeks gestation are alive.

Evaluation of "echo-shadow" complex in sonographic diagnosis of cholelithiasis in non-visualized gallbladders

B. Banerjee and S. H. Khan
Department of Radiodiagnosis and Imaging, Tameside General Hospital, Fountain Street, Ashton-under-Lyne, Lancashire OL6 9RW, UK

A prospective study was performed on 1470 patients referred for gallbladder ultrasound to determine the reliability of the "echo-shadow" complex for diagnosis of gall stones in non-visualized gallbladders. In 1294 patients, the gallbladders were clearly visible and they were either normal or contained unequivocal stones and were excluded from the study. In 176 patients, gallbladder lumen were not demonstrated but an "echo-shadow" complex was noted in the region of gallbladder fossa. Among them in 142 patients, (Group 1), although the gallbladder lumen were not visible, the anterior wall of the gallbladders were outlined with ultrasound, demonstrating the "double-arc-shadow" or "WES" sign. In the remaining 34 patients, (Group 2), the walls of the gallbladders could not be imaged with ultrasound. Following sonography, oral cholecystograms were carried out in all 176 patients belonging to the two groups. Cholecystograms of all Group 1 patients revealed either non-functioning gallbladders or contracted gallbladders with stones. However, in four patients belonging to Group 2, normal gallbladders were demonstrated with cholecystograms, although sonography failed to outline the gallbladders. Reasons for the failures will be analysed and the importance of demonstrating the gallbladder wall in such cases prior to diagnosis of gall stones will be highlighted.

Ultrasound monitoring of diabetic injection technique

A. Coulthard and J. C. Thow
Departments of Radiology and Medicine, Royal Victoria Infirmary, Newcastle upon Tyne NE1 4LP, UK

Do thin diabetics accidentally inject insulin into muscle? This is a theoretical risk if subcutaneous tissue (SCT) thickness is less than needle length (13 mm), given the current recommendation of full-depth needle insertion perpendicular to the skin. A novel technique was devised to determine depth of injection. The smallest saline bolus consistently identified in SCT by ultrasound was 0.8 ml. Addition of air (optimum volume 0.1 ml) allowed 0.2 ml saline (equivalent to 20 U insulin) to be detected. Ultrasound was used to measure SCT thickness in 50 insulin-treated diabetic patients. Men had significantly less SCT thickness compared with women. 30 patients had less than 10 mm of SCT at upper anterior thigh. These patients injected a simulated insulin bolus (0.2 ml saline + 0.1 ml air) into this site by the recommended technique. The depth of the bolus was determined by ultrasound. In 63%, the bolus was clearly in SCT; in 37%, the bolus was either in deeper SCT or within the fascial plane between SCT and muscle. No patients injected into muscle. Contrary to widespread belief, accidental injection into muscle does not appear to be common in thin diabetics who avoid this complication by modifying the recommended injection technique.

Endo-anal ultrasound is reliable in mapping anorectal sphincter defects

K. I. Deen, *D. Kumar and J. Olliff
*Departments of Radiology and *Surgery, Queen Elizabeth Hospital, Birmingham B15 2TH, UK*

Defects in the anorectal sphincter complex have been identified in the past by electromyography. This technique is painful and time consuming. We have compared endo-anal ultrasound (EUS) with operative findings to assess its value in identifying defects in the anorectal sphincter complex in a prospective analysis. A total of 37 patients was studied ($F = 33$; $M = 4$). Their ages ranged from 26 years to 80 years (median = 56). The reason for anorectal assessment was faecal incontinence ($n = 33$) and rectal prolapse ($n = 4$). The examination was performed with a Bruel and Kjaer ultrasound scanner type 1846 and endoprobe type 1850 using a 7 MHz rotary transducer. All patients were in the left lateral position. EUS identified all external anal sphincter defects ($n = 19$) and all but one internal anal sphincter defects accurately ($n = 20/21$), $p = < 0.001$. A deficient puborectalis was identified in two patients and combined defects were identified in 11 cases. 18/19 external sphincter defects were anterior. Of the internal sphincter defects, 12/20 were anterior, 5/20 posterior, 2/20 were seen on the right and 1/20 on the left. We conclude EUS is a quick and reliable method of mapping defects in the anorectal sphincter complex.

2.15 – 3.45

Radiotherapy Treatment III

Hall 10a

Quality assurance — what is possible?

S. Griffiths
Department of Radiotherapy, Cookridge Hospital, Leeds LS16 6QB, UK

The adequacy of technical methods used in treatment set-up may affect the value of the whole radiotherapy process. A quality assurance programme using portal films may be used to investigate the accuracy of the techniques used, and to establish the pattern of errors which arise, together with their causes. This provides information for improving or modifying methods, and establishes an achievable baseline or quality standard. Many studies have reported the achievable accuracy for various sites and methods, and stress the need to check portals on the treatment machine to detect and correct systematic errors early in the course. The availability of digital portal imaging devices is an important development which will allow dynamic intervention to correct a treatment set-up. To make effective corrections, it is necessary first to analyse the error trends with each technique and gain knowledge of the factors involved. Systematic errors are potentially correctable, random errors are not. Technique modifications can reduce random error and prevent most systematic errors. At this centre, sequential studies, analysis and practice modifications have increased accuracy so that a standard deviation of 1.5 mm can be achieved when treating the pelvis.

Imaging and portal verification

W. Swindell
Physics Department, Royal Marsden Hospital, Sutton SM2 5JA, UK

Megavoltage portal imaging is becoming a well established method for assisting in the accurate positioning of patients who are being set up for external beam radiotherapy. The major improvements over film-based methods are (1) instantaneous imaging, which facilitates pre-treatment changes to the patient set-up, (2) digital image processing and display, which improves image quality and utility, and (3) digital image handling, which permits, for example, rapid image retrieval and comparison. A variety of different hardware implementations is available although the method which is currently favoured by the manufacturers is based on a metal-phosphor fluorescent-screen detector which is viewed by a television camera. These methods will be reviewed and typical images will be shown. A system has been developed at the Royal Marsden Hospital/Institute of Cancer Research in which simulator images, CT images and treatment-time images are all available to verify and if necessary correct the patient position. It is VAX based with several different means for entering and comparing CT, simulator and megavoltage (portal) images. Patient images are held in a data base. An 18-month study of reproducibility of patient position for several common treatment sites has been concluded (as of December 1991). This has involved more than 140 patients and 2000 individual patient images.

Precision radiation therapy using on-line portal imaging

S. Shalev, S. Ryder, R. Strachan, K. McGee,
G. Gluhchev, S. El-Sayed and S. Larsson
Departments of Medical Physics and Radiation Oncology, Manitoba Cancer Treatment and Research Foundation, Winnipeg, Manitoba, Canada

An in-depth evaluation of on-line portal imaging has been carried out over the period 1989–1991, using a fluoroscopic imaging system with the capability of acquiring, processing and displaying static and dynamic ("movie") portal images. After alignment of anatomical features in matching portal and simulator images, field positioning errors are calculated by a rigid-body regression analysis. Parameters used to quantify treatment errors are target coverage, target under-dose area (TU), normal tissue over-dose area (NTO), field edge displacements, and field shifts. Action levels are defined for various treatment sites and field sizes, which indicate the need for correction of the beam location relative to the patient. Field positioning errors observed during a course of treatment are displayed either as a plot of cumulative dose coverage or as a parametric image of regret. Plots of TU *versus* NTO are used to define minimum margin widths for planning treatments of the head and neck, thorax and pelvis. On-going studies are evaluating the effect of patient immobilization on treatment accuracy.

The implementation of patient position correction using on-line radiography imaging

P. M. Evans, W. Swindell, J. Q. Gildersleve, E. J. Morton and Z. R. Xiao
Joint Department of Physics, Institute of Cancer Research and Royal Marsden Hospital, Sutton SM2 5PT, UK

Several groups have been involved in the development of digital image systems for the purpose of obtaining images during, or immediately prior to, the delivery of external beam radiotherapy. Such a facility enables direct, on-line verification of patient set-up if a suitable "gold standard" image is available with which to compare the images obtained. An integrated imaging system has been developed for verification of patient position. Digital treatment-time images are compared with digitized simulation images, obtained from film or from an X-ray image intensifier. All simulation images have any distortion removed and are scaled to the magnification of the treatment-time images before the comparison procedure. Various methods may be used to obtain the translation and rotation necessary to make the treatment-time image register with the simulation image. Should the treatment set-up be significantly in error, the treatment may be paused while the patient's position is corrected. The facility exists to carry out such a procedure for any combination of couch and gantry angles, within 2 min and to an accuracy of 3 mm or better. The implementation of the facilities discussed above will be described. Specifically, the various methods of comparing planar radiological images and the algorithms for registering simulation and treatment-time images and for evaluating the necessary adjustment to the patient position as a function of couch and gantry angle will be presented.

The use of an integrated megavoltage imaging system for studies of patient positioning reproducibility

J. Gildersleve, P. M. Evans, W. Swindell, C. Rawlings and D. P. Dearnaley
Royal Marsden Hospital, Downs Road, Sutton, Surrey, UK

A megavoltage imaging system designed and built at the Royal Marsden Hospital has been in clinical use for over 18 months. This comprises a scanning detector for portal imaging, facilities for incorporation of simulator images, and computerized image storage and display. Image comparison software is available to permit use of the system for studies of patient position reproducibility during routine radiotherapy. Results are presented of both random errors (those resulting from day-to-day variability in set-up) and systematic errors (those repeated on each occasion that the treatment is given), for radical treatments of the brain, head and neck, and pelvic regions. For in-cast treatment, both for brain and head and neck regions, random errors are small. 522 set-ups analysed from 26 patients show 95% of treatments to lie within ±3 mm from the mean daily position. Mean systematic errors for this patient group are small, although for individual fields, systematic errors of over 5 mm have been found. For radical pelvic irradiation, 269 set-ups from 24 patients have been analysed. Random errors are rather larger, with 95% of set-ups being within ±4.5 mm of the mean daily position. Mean systematic errors are again small, although for individual fields, errors of over 5 mm have been found.

Ovarian tumours: a prospective study to audit the role of CT scanning

J. Brailsford, B. M. Carey and D. V. Ash
*St James's Hospital, Leeds LS7 and *Cookridge Hospital, Leeds LS16 6QB, UK*

A prospective study was performed to audit the role of CT scanning in the current management of ovarian tumours in the Yorkshire Regional Oncology Centre. A total of 60 abdominal-pelvic scans was obtained on 44 patients over a 1 year period. Pre-scan questionnaires were completed by the referring clinicians in respect of their clinical impression of disease status, and their intended management. The data were subsequently correlated with information on patient follow-up over a 21 month period from initial CT scan. There was agreement between clinical and CT staging in 41 cases (68%); non-agreement occurred in 19 cases (32%) and in nine (47%) of those immediate management was changed. CT scanning was most likely to alter management in patients with stage III or more disease and in patients with epithelial tumours. Post-operative, pre-treatment scanning did not have a major effect on immediate management and the role of such base-line scanning is questioned.

An investigation into radiotherapy treatment couch sag

G. Quinn
Department of Radiotherapy, Cookridge Hospital, Leeds LS16 6QB, UK

Radiotherapy treatment techniques which involve posteriorly directed fields require certain sections of the couch to be radiotransparent whilst maintaining rigidity. Many designs are available, *e.g.* tennis racket-type, Perspex and Melinex sections. They may sag in the region of contact with the patient as increased radiotransparency is often at the cost of mechanical rigidity. In this investigation, four different couch panels were tested for sag, when patients were lying on them, by using a mechanical pointer. 125 measurements were taken for each panel. The results demonstrated that three out of four of the panels regularly sagged more than 0.5 cm during routine use. This amount of sag may constitute a systematic error for isocentric treatments and if not accounted for could potentially give a geographic miss to some of the target volume, *e.g.* from lateral fields. This issue of couch sag may need addressing further by manufacturers and radiotherapy staff.

A simple method of verifying dose distribution around a Selectron applicator

M. S. Tarakanath, F. R. Hudson and M. Jameel Ahmed
Departments of Medical Physics and Radiation Oncology, Kuwait Cancer Control Centre

This paper describes a simple method of verifying the dose rates at point of interest by measurement with TL dosimeters. These measurements have been compared with the calculated dose rates using a RT planning system at these points. The measurements agree closely with the calculated values. This makes the post-installation quality control of a new Selectron remote afterloading machine easy and fast.

Notes

2.15 – 5.15

Committed for Life: Purchasing Equipment Seminar (A seminar arranged by the National COR in conjunction with the BIR)

Hall 10b

Purchasing — art or science?

M. R. Eddy
National Centre of Responsibility (Diagnostic Imaging), South East Thames Regional Health Authority, Bexhill-on-Sea, TN39 3NQ, UK

Purchasing would appear on the surface a relatively simple task. The purpose of this paper is to show what should be taken into consideration when embarking on radiology equipment buying. How often are goods or services purchased that meet the needs of the customer, but do not give value for money! The paper will give an overview of the formalized tender procedure taking into account appraisal of suitable sources of supply, EEC regulations pertaining to equipment purchase and the application of charity monies. The legal framework required to safeguard authorities in this multimillion pound area of NHS expenditure will also be covered. All equipment purchased should be at the lowest possible cost commensurate with acceptable standards of quality and specification which meet the customer's needs. The role of negotiation is vital to establish true value for money, but it can only do this as an integral part of the whole procurement process.

Quality issues

E. Davis
Medical Devices Directorate, Department of Health, 14 Russell Square, London WC1B 5EP, UK

The following topics will be discussed: the Manufacturers' Registration Scheme (MRS), and the responsibility of manufacturers under the scheme; HEI 98 which refers to a management system for all equipment, and the importance of maintenance of equipment; the work of MDD, and its future role within Europe, the CE marking, and MDD's role to ensure that all medical devices meet the appropriate standards of safety, quality and effectiveness, and comply with the relevant EC Directives; evaluation and assessment of up-to-date equipment and the role of FAXIL and KCARE, in this process; the importance of publishing the findings; the Department's position with regard to the TRS document within the European market, and the importance of maintenance of equipment.

Department profiles

D. J. Manton
Frimley Park Hospital, Camberley, Surrey, UK

Planning is a problem. As with solving any problem, the first step is to define it — a statement of the obvious, but planning will require many statements of the obvious. The needs of the New Department have to be defined early so that resources are made available. Only when these are known can detailed planning start. There will be discussion of the complexity of determining the radiological needs of a district and of designing a department to meet those needs.

The outward tender

E. M. Pitcher
Department of Medical Physics and Bioengineering, Bristol General Hospital, Bristol BS1 6SY, UK

This paper discusses the production of a tender specification for diagnostic X-ray equipment. The process starts with the establishment of a clinical statement of need and continues with the translation of these requirements into a technical specification. The tender will be produced by a partnership of engineers, physicists, users and purchasing officers. The format of the specification will depend on whether any building work required will be organized "in-house" or will be a "turnkey" operation. The technical specification may be divided into sections specifying the general type of equipment required, the particular requirements of each site, the accessories and options available and the provision of training and maintenance. The specification should be designed with the knowledge of equipment available on the market but should clearly specify the users' requirements. The tender should ensure that all relevant safety standards and minimum performance requirements are met and allow information in a common format to be collected to allow a true comparison to be made during the option appraisal process. The criteria for the selection of equipment should be established at an early stage and may include such considerations as the reduction of patient dose. If an accurate tender specification is produced the equipment selected should satisfy the users' requirements whilst also being value for money.

Reply to the outward tender

R. W. Mark (with co-operation of the industry)
Association of X-Ray Equipment Manufacturers, London WC2H 7BN, UK

Receiving the outward tender is not always straightforward, as when published in the *European Journal* the entry can easily be missed owing to the vast number of items and headings that have to be read. As every tender is so different once the tender has been received you then have to endeavour to interpret what the user really requires. Modern X-ray, imaging and radiotherapy equipment is very complex, and adapting to meet the users' exact requirements is not always easy or indeed possible. Over-detailed tender specifications, which are usually compiled to suit individual requirements, increase the cost to the manufacturer and customer alike, as the manufacturer has to respond to each question separately, rather than return the tender together with his standard equipment specification. Turnkey projects can often involve the manufacturer in a great deal of expense, often amounting to many thousands of pounds for the production of drawings and costings to submit with the tender for a contract which in the end he may not get.

Maintenance

J. A. Garrett
United Bristol NHS Healthcare Trust, Horsfield Road, Bristol BS2 8ED, UK

However complex, radiological equipment is no exception to the rule that it is purchased for its capability to satisfy the user requirements in a reliable fashion. Capability and reliability, however, are specific design features available when the equipment is installed and operated under certain specified conditions. These conditions will include installation requirements and recommended maintenance specifications. Maintainability is a specific design feature; it determines how easily the maintenance specifications can be applied. Capability, reliability and maintainability with their associated maintenance specifications, are all outcomes of the quality of design, manufacture, installation and maintenance of the equipment. Systems for control of quality are essential in each facet. They merit detailed consideration when purchasing the product. When ownership transfers to the user, maintenance is a cost of use and as such a service to be purchased and managed with the same care and attention given to the selection and specification applied to the performance and quality of the equipment itself. In the same way that the equipment purchaser at the outset was able to consider alternative manufacturers who could satisfy his purchase specification, likewise it is possible to consider alternative service suppliers judged capable of meeting the equipment supplier's recommended maintenance specification. Capability and reliability of the maintenance function are quality features and therefore equally accessible to assessment by the purchaser as they too are a design feature of that service, whether implicit or explicit. While the purchase of the equipment and its subsequent service may be considered as two entirely separate purchase transactions not necessarily obtainable from a common source, clearly they must be considered together since they have a mutual influence on each other in the areas of documentation and training. These issues will be explored in the light of the principles embodied in reports published by the NCOR and Medical Devices Directorate of the Department of Health.

Alternative finance and leasing

E. H. W. Luxton
NHS Supplies Authority, 14 Russell Square, London WC1B 5EP, UK

Health authorities normally obtain their capital for major equipment and building purchases from allocations from public funds. The cost of such funds is significantly less than the cost of financing from alternative private and commercial sources. However, in certain circumstances use of private sector finance as an alternative to outright purchase from public funds may represent best value for money and facilitate cost-effective and quicker development of new and existing services. Guidance on the scope for use of private sector capital in the NHS was issued in October 1989 (EL(89)MB142) and updated in April 1991 (EL(91)53). The Treasury has also issued its own guidance on use of private sector finance. Despite the availability of such guidance many health authorities continue to make decisions relating to leasing or financing of equipment which represent poor value for money and which are based on inadequate option appraisal.

2.15 – 3.45

Nuclear Medicine III

Hall 11a

The metastatic survey revisited

M. V. Merrick
Departments of Radiology and Nuclear Medicine, Western General Hospital, Edinburgh EH4 2XU, UK

Although scintigraphy, of the whole skeleton or limited to the trunk, is still widely practised in patients with cancers which are known commonly to metastasize to bone, there is little evidence that this does or should affect current management. A Consensus Panel at Radiology 90 agreed that there is no tumour in which *routine* skeletal imaging can still be justified, although there remain many specific indications. Evidence which has continued to accumulate since then has largely reinforced this view. In carcinoma of the breast additional centres have confirmed that few of the patients presenting with stage 1 disease but who develop metastases within 3–4 years are detected at the initial screen, which itself carries a not insignificant false-positive rate. Some papers suggest that the detection rate is increased if SPECT is employed, but the effect of this on the false-positive rate has not yet been determined. Although the detection rate is higher in more advanced disease it affects management in only certain subgroups. In carcinoma of prostate evidence now suggests that bone scintigraphy is necessary only in patients with prostate-specific antigen levels over 20 ng/ml, to determine the extent of skeletal involvement. In other tumours indications have become more specific and complex.

The role of bone scan in trauma

I. Fogelman
Nuclear Medicine Department, Guy's Hospital, St Thomas Street, London SE1 9RT, UK

The isotope bone scan provides a convenient means of evaluating the whole skeleton and is exquisitely sensitive for lesion detection. It is particularly helpful in clarifying cases of bone trauma where a fracture is suspected *e.g.* a scaphoid injury with typical clinical features, yet negative X rays. The bone scan has been extensively used to assess sports injuries, *e.g.* to evaluate lower limb pain, and differentiate stress fractures from other causes of pain such as shin splints. An accurate diagnosis can greatly affect the management of these cases. The bone scan also has a role to play in the evaluation of non-accidental injury of childhood.

Clinical high resolution skeletal SPET in 8 min utilizing a multidetector gamma camera

J. R. Buscombe, C. E. Townsend, K. Kouris, G. Clarke, P. H. Jarritt, S. Mahmood and P. J. Ell
Institute of Nuclear Medicine, UCMSM, Middlesex Hospital, London W1N 8AA, UK

The purpose of this study was to assess the ability of a new whole body multidetector gamma camera system (Toshiba GCA 9300A) to produce clinical high resolution skeletal single photon emission tomography (SPET) with an 8 min acquisition. 23 patients in whom there were clinical indications for skeletal SPET were imaged with the Toshiba GCA 9300A system using high resolution parallel hole collimators and continuous rotation acquisition mode; projections were binned at 60 steps, matrix size was 128 × 128 corresponding to a 3.2 mm pixel size. In five patients three acquisitions were performed for 8, 16 and 32 min. Reconstruction was performed with Butterworth prefiltering and a Shepp and Logan backprojection filter. Images were displayed in transaxial, sagittal and coronal views. 8 min skeletal scintigraphy demonstrated good localization of both benign and malignant pathology. There was no clinical advantage in performing 16 or 32 min acquisitions though there was an improvement in image quality. A multidetector gamma camera produces high resolution skeletal SPET images within 8 min. This will enable precise information on the localization of pathology in the skeleton to be obtained with practical imaging times and no additional radiation burden to the patient.

The role of isotope bone scanning in patients with foot/ankle pathology

M. Bengoechea and W. W. Gibbon
Department of Radiology, Cardiff Royal Infirmary, Cardiff CF2 1SZ, UK

We present the findings of a retrospective study comparing radiography and bone scintigraphy in 96 consecutive patients undergoing isotope bone scanning for clinically suspected localized foot or ankle pathology. An experienced radiologist reviewed the relevant radiographs and made a prediction as to the expected bone scan findings "blind" as to clinical information and bone scan results. A second investigator correlated these predictions with reports produced by one of two radiologists experienced in bone scintigraphy and also with the clinical outcome. In the 58% of patients with an abnormality demonstrable on initial radiographs, bone scan predictions corresponded well with actual scan reports. In these circumstances the bone scan failed to provide additional clinical information. In the 42% of patients with normal initial radiographs 10% of bone scans revealed abnormalities of varying clinical significance. We discuss these radiographically occult abnormalities and the clinical relevance of our overall results.

Radiology in the clinical management of osteoid osteoma

C. E. Hutchinson, R. W. Whitehouse, J. E. Adams and J. M. Hawnaur
Department of Diagnostic Radiology, University of Manchester, Manchester M13 9PT, UK

19 patients with clinical symptoms and radiographic abnormalities suggestive of an osteoid osteoma were referred for CT and/or MRI. The diagnosis of osteoid osteoma was made in 11, and involved the lower limb (five), the spine (four) and the hand (one) and foot (one). In several patients there was considerable delay (3 months to 6 years) between presentation and confirmation of the diagnosis. All patients had plain radiographs; in six there was characteristic sclerosis but in three the lesion was not seen. Radionuclide bone scan ($n = 9$) showed increased uptake in eight. CT ($n = 11$) demonstrated the nidus in nine of 10 active lesions, with surrounding sclerosis in seven; there were linear cortical lucencies within the sclerosis in six. To demonstrate diagnostic features it was essential to perform thin section CT with appropriate targeting and bone algorithms. MRI ($n = 4$) did not demonstrate the cortical lucencies seen on CT, but marrow oedema and parosteal soft tissue changes were better seen on MR. The extent and distribution of soft tissue changes and bone sclerosis differentiated osteoid osteoma from other pathologies (stress fracture ($n = 4$) and osteomyelitis ($n = 4$)) confirmed in the remainder of the patients. *Conclusion:* In patients in whom a clinical diagnosis of osteoid osteoma is considered, a radionuclide bone scan is imperative, even if radiographs are normal, since this will localize the area of increased uptake. This can then be scanned using an appropriate high resolution CT technique which will confirm the diagnosis and localize the nidus pre-operatively. MRI should be reserved for patients in whom the differential diagnosis between osteoid osteoma, trauma and infection remains uncertain, and in whom the increased sensitivity of MRI to soft tissue changes may be helpful.

Metastatic disease and the equivocal bone scan: the value of magnetic resonance imaging

F. Aitchison, F. W. Poon, H. W. Gray, A. W. Forrester and D. Hadley
Department of Radiology, Glasgow Royal Infirmary, Glasgow G31 2ER, UK

We studied 45 consecutive patients referred to our department in a 6 month period with known primary malignancy and back pain in whom the isotope bone scan was reported as equivocal. All patients had abnormal isotope uptake localized to the spine. 12 patients (12/45) were shown to have bony metastases on plain X ray. In the remainder, X rays showed normal or benign appearance and magnetic resonance imaging of the spine was offered. 24 patients underwent MRI examination which showed vertebral metastases in 11 (11/24). MRI is a useful, non-invasive, complementary investigation for evaluation of patients known to have malignant disease and suspected of having vertebral metastases on bone scan.

A study of two anti-CEA monoclonal antibodies for immunoscintigraphy of small cell lung cancer

M. L. Wastie, C. H. Macmillan, A. C. Perkins and D. A. L. Morgan
Clinical Oncology, Nuclear Medicine and Radiology Departments, General and University Hospitals, Nottingham, UK

21 patients with histologically diagnosed small cell lung cancer underwent immunoscintigraphy with one of two radiolabelled anti-CEA monoclonal antibodies (Mab). 10 patients received Mab F6 labelled with indium 111 (Oris Industrie, France) while 11 patients received BW341/26 labelled with technetium 99m (Behringwerke, Germany). 38 sites of disease were identified by clinical examination, chest radiography or other relevant investigations. Serum CEA concentration was measured in 19 patients and was raised in three. Tumour was imaged in 13 patients corresponding to 18/38 known sites of disease. Seven out of the 10 patients imaged with ^{111}In antibody were positive (9/18 sites) and 6 of the 11 patients imaged with ^{99}Tc^{m} antibody were positive (9/20 sites). The ^{99}Tc^{m} antibody did not offer any clear advantage over the ^{111}In antibody. All three patients with raised serum CEA levels showed positive images as did eight of the 15 patients with normal CEA levels. Although routine use of anti-CEA antibody in patients with small cell lung cancer is not advocated, immunoscintigraphy warrants further study using more specific antibodies.

2.15 – 3.45

Cardiovascular Advances

Hall 11b

The current role of diagnostic and interventional bronchial angiography

D. M. Nichols
Department of Radiology, Raigmore Hospital, Inverness IV2 3UJ, UK

Selective angiography of the bronchial arteries in Man was first performed in 1964 by Viamonte, only 10 years before bronchial artery embolization for the treatment of massive haemoptysis was first described by Remy. Further experience since then has greatly increased our understanding of the pathophysiology of the pulmonary circulation. Diagnostic angiography of the systemic supply to the lungs is helpful: (a) in sequestration and scimitar syndrome; (b) in chronic pulmonary artery obstruction, congenital or acquired; (c) in arteriovenous malformations; (d) in the investigation and treatment of severe haemoptysis. Thus a thorough exploration may require seeking (where appropriate) a patent ductus arteriosus, anomalous aortopulmonary feeders, the bronchial arteries themselves, and transpleural feeders from interior phrenic, internal mammary, thyrocervical and axillary arteries. Massive haemoptysis usually arises from the enlarged systemic circulation in damaged lung as in tuberculosis or bronchiectasis. Where surgery is contraindicated because of bilateral disease or poor respiratory reserve, and where medical management has failed, embolization offers an 80% chance of stopping the bleeding. The complication rate is low but extreme care must be taken to avoid any spinal artery feeders. Embolization may also have a role in the management of recurrent non-life-threatening haemoptyses.

Preliminary experience with the Palmaz coronary artery stent

M. R. Rees, U. M. Sivananthan and S. P. Verma
Killingbeck Cardiac Research Unit, Killingbeck Hospital, Leeds LS14 6UQ, UK

14 patients were treated by the placement of Palmaz coronary stents in 15 vessels. Stent placement was carried out either because of acute re-occlusion following angioplasty or severe dissection, with the exception of two cases in which stents were placed electively because of recurrent re-stenosis following angioplasty. A total of 16 stents were placed (LAD 10, circumflex 1, RCA 5). Complications were experienced in one patient in which the stent and balloon could not be passed through the stenosis and the stent could not be withdrawn into the guiding catheter. In this case the stent was expanded proximally in the artery. Following stent placement all the patients were followed up by frequent clinic visits and re-angiography and thallium scanning at 3 months. All patients were placed on Warfarin for 3 months. One patient had acute re-occlusion of the stent despite being placed on Warfarin and this was successfully re-opened. Two patients had to undergo further angioplasty (for re-stenosis, 1, distal disease, 1). In the case of the patient with distal disease, a second stent had to be placed. Patient follow-up data and results of re-angiography are presented.

Observer variability of contrast echocardiography for the detection of patent foramen ovale

S. J. Cross, L. Thomson, S. Evans, H. S. Lee and K. P. Jennings
Cardiology and Hyperbaric Medicine Departments, Aberdeen Royal Infirmary, Aberdeen AB9 2ZB, UK

There is increased interest in the use of contrast echocardiography for the detection of patent foramen ovale, both in patients with unexplained stroke and divers with decompression sickness. The interpretation of individual scans is very subjective. We have assessed the inter- and intra-observer agreement on a consecutive series of contrast echocardiograms. 100 subjects were studied. Agitated saline contrast was injected rapidly into an antecubital vein during imaging of an apical four chamber view of the heart. All injections were recorded on video tape. Four observers subsequently reviewed the recordings independently, on two occasions each in a darkened room. Only the last injection for each subject was displayed. Repeated observation of an injection was allowed. The kappa statistic for intra-observer variability for each of the four observers was

0.95, 0.91, 0.90 and 0.88 (a value of 1 implies complete agreement betweeen an observer's two interpretations). The inter-observer variability (95% CI), using the proportion of agreement method, was 0.78 (0.72–0.84) and 0.91 (0.87–0.93) for the presence and absence of patent foramen ovale, respectively. We conclude that contrast echocardiography when used for the detection of patent foramen ovale is subject to clinically acceptable inter- and intra-observer variability.

Functional parameters for the right ventricle evaluated by magnetic resonance imaging in patients with single lung transplantation

C. S. Richter, R. H. Mohiaddin and D. B. Longmore
Magnetic Resonance Unit, Royal Brompton National Heart and Lung Hospital, London SW3 6NN, UK

Purpose: Qualitative and quantitative assessment of flow in the main pulmonary artery (MPA) and superior vena cava (SVC) in patients with chronic lung disease, before and after single lung transplantation. *Materials and methods:* Cine magnetic resonance imaging with velocity mapping was used to study 13 patients before and 16 patients after lung transplantation. Eight normal subjects with dobutamine induced tachycardia were studied for comparison. *Results:* Despite the slower heart rate in the post-transplant patients 91 ± 12/min compared with the pre-transplant group 101 ± 12/min ($p < 0.001$), MPA flow (mean ± SD) in the first group 3.09 ± 0.64 l/min/m^2 was significantly higher than in the second group 2.91 ± 0.41 l/min/m^2 ($p < 0.05$). SVC flow in the post-transplant patients 1.21 ± 0.32 l/min/m^2 was higher than in pre-transplant patients 1.02 ± 0.26 l/min/m^2 ($p < 0.001$). The SVC flow in all but three pre-transplant patients showed a forward systolic peak with absent or reverse flow during diastole. The three patients showed a biphasic curve with a dominated diastolic peak. In all post-transplant patients the flow curve showed a systolic and a diastolic forward peak and a ratio (1.41 ± 0.62) similar to that of controls (1.39 ± 0.33) matched for heart rate (96 ± 13/min). *Conclusion:* A significant improvement of MPA and SVC flow after lung transplantation was demonstrated with magnetic resonance imaging owing to a decreased vascular resistance which could be useful to monitor right ventricular performance after lung transplantation.

The value of coronary angioscopy in coronary angioplasty

M. R. Rees, U. M. Sivananthan and S. P. Verma
Killingbeck Cardiac Research Unit, Killingbeck Hospital, Leeds LS14 6UQ, UK

Coronary angioscopy was carried out in three patients using a new disposable angioscope, designed to be delivered to the coronary arteries via standard coronary angioplasty guiding catheters. The device is 4.5 french in diameter and can be passed over an 0.14 diameter coronary guide wire. A clear field is obtained by dilating a small latex balloon attached to the angioscope and flushing clear fluid through the scope at a rate of 30–600 ml/min. The fibre is moveable and can be passed down the artery even when the balloon is inflated. Angioscopy with this instrument appears to give cleaner and more reliable imaging than two other devices tested. Angioscopy was carried out in conjunction with coronary angioplasty in the three patients, documenting the disease before and after angioplasty. In all three cases a coronary stent was deployed and the angioscopic findings were used to determine the site of stent placement as well as confirming that satisfactory stent deployment had occurred. The angioscopic findings also contributed to the decision making process in deciding to place the stent.

Various manifestations of hypertrophic cardiomyopathy on ultrafast computed tomography

T. Sekiya and M. Karikomi
Department of Radiology, Kyoun-do Hospital, Tokyo 101, Japan

Ultrafast computed tomography (UFCT), which is a new type of computed tomography based upon electron beam technology, was performed in 28 patients with hypertrophic cardiomyopathy, using an Imatron C-100. Images were assessed on variability of left ventricular hypertrophy, the pattern of left ventricular contraction, right ventricular hypertrophy, dilatation of the left atrium and thickening of the mitral valve. The long-axis and short-axis views of the left ventricle were obtained by sluing the patient's table. 40 ml of non-ionic contrast material was administered intravenously, using a mechanical injector for each study, and typically three studies were required for one patient. 14 of 28 patients (50.0%) had asymmetric septal hypertrophy (ASH), five (17.9%) had diffuse hypertrophy, and nine (32.1%) had apical hypertrophy. In 10 patients with ASH and two with apical hypertrophy, non-hypertrophied segments in end-diastole showed vigorous contraction, 15 patients showed homogeneous left ventricular contraction, and one showed partial apical contraction. Right ventricular hypertrophy was noted in 12 patients (42.9%), dilatation of the left atrium in 13 patients (46.4%), and mitral valve thickening in three (10.7%). UFCT was useful in the evaluation of apical hypertrophy, right ventricular hypertrophy and left atrial dilatation, which could be difficult to obtain with echocardiography.

MR imaging of heart after correction of tetralogy of Fallot

U. M. Sivananthan, D. Waller, J. Ridgway, K. Bann,
D. Walker and M. R. Rees
Cardiac Radiology/MRI Unit, Killingbeck/St James's University Hospital, Leeds LS14 6UQ, UK

The purpose of this study was to assess the function and anatomy of right ventricle, outflow tract, and pulmonary arteries using MR imaging in patients who had correction of tetralogy of Fallot 10 years previously, in conjunction with echocardiography. 14 patients were studied (eight males and six females), with an age ranging from 13 to 19 years. There were two groups: the first group (eight patients) consisted of patients who had extensive right ventricular outflow tract/resection with Gortex patch, and the second group (six patients) consisted of resection with or without pulmonary valvotomy. Right ventricular dimensions were assessed using spin echo images and then systolic and diastolic volumes were assessed using contiguous gradient echo images. In all patients the right ventricle was enlarged and the average election fraction was 50%. The regurgitation fraction and gradient across the pulmonary valves were assessed using phase encoded flow mapping, and the results corresponded with echocardiography. There were four peripheral pulmonary artery stenoses which were not detected by echocardiography. There were two residual septal defects. There were three other associated cardiac anomalies. We found that MR imaging allowed quantitative and anatomic insight of the heart in patients who had correction of tetralogy of Fallot, thus supplementing the clinical and echocardiographic evaluation of the patient.

Feasibility of left ventricular aneurysm resection assessed using tomographic radionuclide ventriculography

M. J. Metcalfe, M. Y. Norton, S. Cross, K. Jennings and
S. Walton
Cardiac Department, Aberdeen Royal Infirmary, Foresterhill, Aberdeen AB9 2ZB, UK

It is now established that patients with dyskinetic aneurysms are much more likely to benefit from aneurysm resection than patients with akinetic aneurysms. We have, therefore, developed a new method of acquiring multigated, tomographic, radionuclide ventriculograms which are able to assess both the anatomy and the extent of the "backward" stroke volume into the aneurysm. From this latter measurement, a prediction of the improvement in overall stroke volume following resection can be made. Imaging using the Aberdeen Sector Scanner and processing using a dedicated small computer takes 20 min and 30 min respectively, allowing the technique to be used routinely. 20 consecutive patients with ventricular aneurysm and 10 controls were compared. The mean age of the patients was 57 (90% being male) and the mean age of the controls was 55 (70% being male). In eight patients, simulated resection improved the stroke volume by less than 10%, in eight patients by 10–20% and in four patients by > 20%. No control subject demonstrated any significant aneurysmal stroke volume. This technique shows great promise in assessing aneurysm formation and suitability for resection.

Radiology of the Churg–Strauss syndrome

Wai Lup Wong,* D. D'Cruz, A. B. Ayers and
J. Pemberton
*Departments of Clinical Radiology and *Rheumatology, St Thomas' Hospital, London SE1 7EH, UK*

The Churg–Strauss syndrome is a rare disorder characterized by hypereosinophilia and systematic vasculitis occurring in patients with asthma and allergic rhinitis. We reviewed the radiological features in nine patients (three men and six women), with this syndrome. All nine patients had chest radiographs, six had CT scans of their paranasal sinuses, three had routine paranasal sinus views, three had hand radiographs, two had radiographs of the feet, whilst one patient had an MR of the brain. A total of 27 chest radiographs, eight paranasal sinus radiographs, six CT scans of the paranasal sinuses, four pairs of hand radiographs, two pairs of feet radiographs and one MR scan of the brain were analysed. Radiological features present included thickened mucosa and soft tissue masses within the paranasal sinuses which in one case was associated with bony destruction, isolated antral polyps, cardiomegaly related to congestive cardiomyopathy owing to cardiac granulomas, pulmonary infiltrates and multiple small areas of white matter abnormalities in the brain on MRI.

Artefacts in the ascending aorta on computed tomography: yet another measure of aortic distensibility?

P. Set, D. Lomas, G. Maskell, C. D. R. Flower and A. K.
Dixon
Department of Diagnostic Radiology, Addenbrooke's Hospital and the University of Cambridge, Hills Road, Cambridge CB2 2QQ, UK

On modern CT systems capable of 1 s data acquisition times, the ascending aorta often appears to have a blurred outline. It has been suggested that this new artefact arises because of aortic wall motion during systole/diastole. Thus the artefact might provide an indication of aortic distensibility (as on ultrasound and magnetic resonance). The artefact was evident in 48 of 53 patients undergoing routine chest CT; its extent was subjectively and objectively assessed. The maximum and minimum cross-sectional aortic areas were assessed from the margins of the blur. The area of the blur, expressed as a fraction of the minimum aortic cross-sectional area, decreased with age ($p < 0.001$) and was significantly smaller in the 13 patients with known cardiovascular problems ($p < 0.05$). These findings were substantiated by the subjective gradings which showed less marked artefacts amongst elderly patients (although this observation did not reach statistical significance). Artefacts were less prominent in 16 patients with evidence of aortic wall calcification, both on subjective grading ($p < 0.05$) and formal area measurements ($p < 0.05$). These observations lead us to believe that this artefact is an indicator of aortic distensibility and thus, indirectly, of cardiovascular status.

Magnetic resonance flow mapping in the thoracic aorta of patients with aortic coarctation

R. H. Mohiaddin, P. J. Kilner, R. S. O. Rees and
D. B. Longmore
Magnetic Resonance Unit, Royal Brompton National Heart & Lung Hospital, Sydney Street, London SW3 6NP, UK

Magnetic resonance imaging with velocity mapping was used to characterize and to measure flow and its regional distribution in the thoracic aorta of 10 patients with coarctation of the aorta. 10 healthy volunteers were studied for comparison. Flow waveforms were studied in an oblique plane perpendicular to the ascending aorta (AA) at the level of pulmonary bifurcation and to the descending thoracic aorta (DA) 1 cm distal to the coarctation segment. Instantaneous flow was calculated from mean velocity and the cross-sectional area of the vessel. Peak forward flow (Q_f,l/min), time-averaged flow (Q_m,l/min) and DA/AA flow ratio were measured. In the controls, Q_f in the AA and DA (mean ± SD) was 28.3 ± 4.4 and 17.8 ± 2.7, respectively. Q_m in the AA was 5.6 ± 0.8 and in the DA was 3.5 ± 0.7, and the ratio of DA/AA flow (Q_m) was 0.62 ± 0.07. In patients with coarctation, AA Q_f 25.5 ± 4.8 and AA Q_m 5.8 ± 1.2 were similar to those of controls, while DA showed a lower Q_f 10.4 ± 3.4 ($p > 0.001$), a lower Q_m 2.6 ± 0.9 ($p < 0.05$) and a lower DA/AA ratio 0.47 ± 0.18 ($p < 0.05$) than controls. These differences are most likely related to the resistance imposed on flow by the coarctation and could be an additional index for monitoring patients with coarctation of the aorta.

Notes

4.15 – 5.30

Gastrointestinal imaging

Hall 11b

Videofluoroscopy in the assessment of dysphagia following neurological disease

R. C. V. Bhatt, A. S. Ahmed, D. Chand and *V. Quemby
*X-Ray Department and *Department of Speech and Language Therapy, Sandwell District General Hospital, West Bromwich B71 4HJ, UK*

A significant number of patients with stroke or other neurological disease present with difficulty in swallowing. We have examined over 55 such patients over a wide age range in the last 3 years, using videofluoroscopy. Patients are examined in presence of a speech therapist initially in the lateral and then, if necessary, in the AP projection, starting with 1, 3 and 5 ml aliquots of barium suspension, followed by barium paste and solid food mixed with barium paste. The average screening time is approximately 5 min. The diagnosis is often made on screening and subsequent management techniques can also be assessed. Videotape allows detailed analysis of the findings to be made later. Once identified, many of the problems are amenable to treatment by re-educating the patient using techniques employed by speech therapists. Our findings suggest that about half the patients are at risk of silent aspiration. 20 patients are now able to continue with oral feeding; two have had to go on to non-oral means; 11 patients are receiving on-going treatment; one has had surgery and eight have died. We suggest that videofluoroscopy has a valuable role in the assessing and planning of treatment of patients with dysphagia.

A swallow assessment clinic: why and how

F. R. Wright and N. Ervine
Departments of Radiodiagnosis and Photography, The Ulster Hospital, Dundonald, Belfast BT16 0RH, UK

This 15 min VHS video programme highlights the number of patients with a wide range of conditions in whom a dynamic videofluoroscopic assessment of the oral, pharyngeal and cervical oesophageal phases of swallowing is indicated. The need is probably greater than has been realized to date. It has been shown that at least 40% of stroke patients, in hospital or at home, will have a swallowing problem and almost half of these will be silently aspirating, having lost their cough reflex. This number could be 500 each year in Northern Ireland (population 1.5 million). There are also many patients with other neurological conditions, congenital and acquired or who have had major throat or neck surgery who will have similar swallowing difficulties. All these need assessing and some require training or therapy in order to reduce the risk of aspiration pneumonia and to help manage their nutrition and hydration. We illustrate how a swallow assessment clinic, operated by a radiologist, a speech therapist and a dietitian, can satisfy this need. Our videofluoroscopic technique, using a modified barium swallow, is demonstrated with a variety of cases from the 400+ patients we have examined since 1986. References are available with the video.

A new chair of radiology — a purpose-designed seat to assist fluoroscopy

D. F. Martin and R. Wyatt
Departments of Radiology and Speech Therapy, University Hospital of South Manchester, Manchester M20 8LR, UK

Fluoroscopic examination of the seated patient is occasionally necessary, particularly when evaluation of swallowing is required in the patient with neuromuscular or cerebrovascular disease, as well as for proctography in all patients. We have used a variety of methods, including sitting a patient on the table foot rest or on a narrow wheelchair, but no method has proved satisfactory. We have designed and built a simple chair of tubular steel, which has a padded seat and back support and a detachable foot rest. The arm rests of the seat can be swung behind the seat to allow access and proctography. The total cost of materials for the seat was under £100. The seat attaches to the foot rest of the fluoroscopy table by a single central lug, which fits a hole in the foot rest provided by manufacturers for the fixation of other devices. Single central fixation allows the seat to pivot about a vertical axis allowing lateral, frontal and oblique views during assessment of swallowing and lateral views during proctography. The patient can be secured within the seat by a seat belt attachment. One particular advantage of the seat is that the foot rest can be removed and the base and upright back of the seat positioned on a trolley, so that even the most immobile patient can be seated securely and examined. The use of this device allows safe and controllable examination of all patients with swallowing disorders and allows greater comfort for those undergoing proctography.

Patterns of colonic transit in severe intractable constipation using oral ^{111}In-DTPA scintigraphy

J. P. Roberts, M. S. Newell, J. J. Deeks, N. W. Garvie and N. S. Williams
Surgical Unit and Radioisotope Department, The Royal London Hospital, London E1 1BB, UK

A simple, clinically applicable method for assessing colonic transit in constipated patients has been developed. 3.7 MBq of ^{111}In-DTPA is taken in water on day 1. The following day at 18 h posterior and anterior abdominal scans are acquired and repeated twice daily until the 5th day. No bowel preparation is used and normal diet is maintained throughout. Six regions of interest (ROIs), from caecum and ascending colon (1), to rectosigmoid colon (6), are drawn on each colonic image. Counts from anterior and posterior ROIs are combined, and decay and background corrected. Percentage of ingested activity in each ROI, and faecal loss (ROI 7) is calculated, and used to calculate the geometric centre of gravity of the isotope (COG). A normal range of COG was obtained from 16 control subjects. 33 patients with constipation were investigated and showed three patterns of transit: (1) transit within normal range ($n = 5$); (2) proximal delay ($n = 26$), who showed early delay of progression of COG (< 3.6 at 48 h), with delayed right colonic emptying and accumulation of isotope in the transverse colon and splenic flexure; (3) left colonic delay ($n = 7$) where progression of COG was normal at 48 h but later showed accumulation of isotope occurring in the descending and rectosigmoid colons. The oral scintigraphic method enables differentiation of patterns of colonic transit in constipated patients which may influence treatment.

Validation of region of interest drawing in oral colonic transit scintigraphy

J. P. Roberts, M. S. Newell, C. Skinner, J. J. Deeks, N. W. Garvie and N. S. Williams
Surgical Unit and Radioisotope Department, The Royal London Hospital, London E1 1BB, UK

The changing morphology of the colon during prolonged studies of transit hinders the application of fixed regions of interest (ROIs) for analysis. Drawing ROIs individually on each image was adopted to overcome this problem but in turn may increase the subjective error in analysis. The validity of individual ROI drawing was therefore investigated. Inter- and intra-individual variation in analysis of seven colonic transit studies was assessed. Each scan was assessed on at least one occasion by three assessors at intervals of 6 weeks. Each anterior and posterior scan was divided individually into six ROIs. Corrected counts were used to calculate the percentage of ingested activity in each ROI and the centre of gravity of the isotope (COG). Results from each analysis were compared using repeated measures ANOVA. The major source of variation in analysis was the between patients component (variation estimate VE = 1.9), and the patient/time component (VE = 0.46). Although the assessor/patient component (*i.e.* variation between assessors' analysis of scans) was a significant source of variation (VE = 0.003), it was small compared with the other components and could be regarded as negligible. Individual ROI drawing in the analysis of oral colonic transit scintigraphy is a reliable and reproducible technique.

Oesophageal scintigraphy in the assessment of balloon dilatation of the oesophagus for achalasia

D. C. F. Lloyd and H. Adams
Department of Radiology, Llandough Hospital, Penarth, South Glamorgan CF6 1XX, UK

Balloon dilatation of the distal oesophageal sphincter is widely employed for the treatment of achalasia of the cardia. We have used oesophageal transit scintigraphy to assess the effectiveness of dilatation and for the long term follow-up of patients with achalasia. Taking the whole oesophagus as the region of interest, time-activity curves were generated following ingestion of a 10 ml bolus of a solution of ^{99}Tc^{m} sulphur colloid in the erect position. After 30 s, the isotope was followed by a bolus of 100 ml of water to produce "oesophageal washout". Parameters measured included the time taken for activity to fall below 50% of maximum (T50), and the percentages of retained activity at 30 s (B30) and at 100 s (B100). The normal transit curve was established by study of 22 healthy volunteers. Oesophageal transit studies were performed in 17 patients both before and after balloon dilatation. Mean T50 fell from 66 s pre-dilatation to 25 s post-dilatation, mean B30 fell from 76% pre-dilatation to 55% post-dilatation, and mean B100 fell from 43% pre-dilatation to 17% post-dilatation. Serial post-dilatation transit studies were also performed in a group of patients to assess the long term response to balloon dilatation. The results are fully presented and the usefulness and limitations of oesophageal transit scintigraphy in the assessment of achalasia are discussed.

Radiology of Crohn's disease in Asian immigrants of East Birmingham

K. Jeyapalan, M. Belhag, P. Asquith and J. R. Ferrando
Department of Diagnostic Radiology, Alistair Frazer and John Squire Metabolic Unit, East Birmingham Hospital, Birmingham, UK

Crohn's disease (CD) is thought to be uncommon amongst the Asian population. The aim of this study is to assess whether there is any difference in the pattern of disease in Asian immigrants. We report 20 cases of intestinal CD from Asian immigrants who presented to our Unit since 1970. We note no difference in the diagnostic radiological features. However, small bowel studies show that 30% of patients with active mid small bowel disease have a disease free terminal ileum. Barium enema studies show that 38% of patients with colonic CD have the disease confined to the distal colon and the mean age of such patients is 23.5 years (range 14–37). In white populations, disease free terminal ileum is reported to occur in 3% of patients with CD and localized proctocolitis is noted to be a common feature of CD of the elderly. We feel that the above features are atypical. Although distal colitis in Asians is commonly due to an infective cause or ulcerative colitis, the possibility of CD needs to be considered and investigated in unresolving cases.

Long linear ulceration in Crohn's Disease

P. Holland, M. Mantle and J. R. Lee
X-ray Department, Birmingham General Hospital, Steelhouse Lane, Birmingham, UK

There are many patterns of ulceration seen in Crohn's colitis, and some of these are felt to be specific when differentiating Crohn's from ulcerative colitis. We undertook a retrospective assessment of 106 patients (40 male, 66 female) who all had proven Crohn's colitis, and who had all had at least one double contrast barium enema (DCBE) in a period between 1977 and 1990. In particular, the sites and extent of ulceration were noted, as well as features such as strictures, fistulae, pseudopolyps and nodularity. These results will be demonstrated. A particular form or pattern of ulceration in the large bowel was noticed in seven patients. We have called this long linear ulceration, and it seems to be a separate, but probably related, form of ulceration from the usual fine, shorter linear ulcers occasionally identified in the small bowel of patients with Crohn's disease. We define them as being deep, long, linear ulcers 5 cm or more in length. All seven patients affected were young (20–30 years old) except for a woman of 45 years. Six were female and one was male. The transverse colon was the commonest site (five patients), and in every case there was associated extensive ulceration in the colon, with aphthous ulcers and deep ulceration between 1–3 mm. Three patients had repeat DCBE at a later date and in none was long linear ulceration seen again. Two of the three developed a stricture, but not at the site of the linear ulcers. The features of these ulcers will be demonstrated. Long linear ulceration may be another pattern which when seen will help differentiate Crohn's from ulcerative colitis.

Peritoneal slide: an observation to identify peritoneal adhesions

A. K. H. Hasan, A. S. McCulloch and D. J. Sinclair
Department of Clinical Radiology, Ninewells Hospital and Medical School, Dundee DD2 1UB, UK

Adhesion of bowel loops to the anterior abdominal wall is not an uncommon finding in patients who have had previous laparotomy. These adhesions are usually not confined to the region of the abdominal wall scar. Owing to the increased trend in laparoscopic procedures such as laparoscopic cholecystectomy, there is a need to identify the presence and location of such adhesions. This is because puncturing a fixed bowel loop by introducing a laparoscopic trochar into the abdomen may have grave consequences. Ultrasound is a well established investigation to look for peritoneal masses and free intraperitoneal fluid. Using a high frequency probe (7.5 MHz) one can clearly identify the movement between parietal and visceral peritoneum in a normal subject during all phases of respiration. Adhesion of a bowel loop to the anterior abdominal wall will certainly restrict such a slide. Therefore, by observing the peritoneal slide with real time ultrasound at the potential sites for the introduction of the laparoscopic trochar on the anterior abdominal wall, we believe that the presence and location of fixed bowel loops can be easily defined. A video tape of about 2–3 min demonstrating normal and abnormal peritoneal slide and how to locate the position of the fixed bowel loops will be presented.

Radiological evaluation of the ileoanal (Parke's) pouch: should we continue to do pouchograms?

M. T. Keogan, P. A. Set, E. P. Wraight and
A. N. Freeman
Department of Radiology and Nuclear Medicine, Addenbrooke's Hospital, Cambridge CB2 2QQ, UK

The radiological investigations of 68 patients who had a Parke's pouch (W type) were reviewed. Underlying diagnoses were ulcerative colitis (52 patients), familial polyposis coli (11 patients) and Crohn's disease (five patients). 50% of the patients had a loop ileostomy as part of a two stage procedure. 20 patients had documented post-operative complications. 45 pouchograms were performed, 35 of which were routine prior to closure of the ileostomy in a two stage procedure; one demonstrated an unsuspected leak. 10 were obtained in patients with documented post operative complications; in this group there were six true positive, one true negative and three false negative results. 21 indium labelled leukocyte scintigrams were performed in patients with symptoms of infection. 19 true positives and two true negatives were found. Three CT scans were obtained in patients where an abscess was indicated by scintigraphy and CT guided drainage was performed in two. We conclude that scintigraphy should be the first investigation in patients with a Parke's pouch and infective complications, followed by CT if an abscess is suspected. The role of the pouchogram is unclear from our series and further studies may be helpful.

Small bowel changes following the modified Scopinaro procedure for morbid obesity

M. Murray, G. Franks, J-C. Gazet and A. Grundy
Department of Diagnostic Radiology, St. George's Hospital, London SW17 0QT, UK

Scopinaro (1986) described partial gastrectomy with pancreatico-biliary by-pass for morbid obesity which combines the advantages of gastric reduction and small bowel by-pass without the detrimental metabolic effects of jejuno-ileal by-pass. Between 1987 and 1991 48 patients underwent a modified operation of truncal vagotomy, stapled transverse gastric partition and gastro-ileal anastomosis, and upper GI tract contrast studies have been performed on 24 patients. Mucosal fold thickness and luminal diameter were correlated with time following the procedure (range 1–50 months). There was a significant increase in mucosal fold thickness with log(time) ($p < 0.0005$), and a similar significant increase in lumen diameter with log(time) ($p < 0.0044$). Mucosal fold thickness and bowel lumen calibre changes reach a plateau at 20–30 months post-procedure. This is mirrored by the patients' weight loss which is rapid initially but also plateaus at around 30 months. Jejunalization of the ileum is a recognized feature following jejuno-ileal by-pass, but has not been described previously following gastric reduction surgery.

Magnetic resonance imaging following surgery for ano-rectal anomalies

D. J. Grier, A. W. Duncan and P. R. Goddard
Department of Clinical Radiology, Bristol Royal Infirmary, Bristol BS2 8HW, UK

The diagnosis of ano-rectal anomalies in the newborn is made by a combination of clinical and simple radiographic examination. The majority of children are satisfactorily treated on this basis. However, a small proportion of patients will have subsequent problems, in particular troublesome faecal incontinence. The assessment of these children for further management is often difficult. We investigated the potential role of magnetic resonance imaging in this situation. 11 patients (mean age 12 years) were studied using a Picker Vista HP2025 0.5 T scanner. T_1-weighted images were obtained in sagittal, coronal and axial planes. The images were assessed for pelvic musculature, the appearance of the lower bowel and spinal anomalies. These were correlated with the clinical findings and results of conventional radiological imaging. Abnormalities of the distal bowel and pelvic musculature were most common (in seven patients each). These included gross rectal dilatation and deficiency of pelvic floor muscles, particularly puborectalis. Spinal anomalies were found in four cases, including sacral agenesis, hemivertebrae and a sacral lipoma. These findings are illustrated and are discussed with reference to their effect on subsequent management.

Congenital duodenal obstruction: diagnostic features in 53 neonates

S. Eustace and N. Blake
Radiology Department, Our Lady's Hospital for Sick Children, Crumlin, Dublin 12, Ireland

This study reviews the radiographic features of 53 neonates presenting to a national Children's Hospital over a consecutive 4 year period with congenital duodenal obstruction. In each case correlation was made between radiographic features and subsequent findings at surgery. Of 53 children, 27 presented with intrinsic obstruction, owing to duodenal stenosis in nine cases, owing to duodenal duplication in two cases, owing to isolated annular pancreas in two cases and owing to the presence of a web in one case. 26 patients presented with extrinsic obstruction owing to malrotation; of those, 17 patients had a high caecum with associated volvulus and bands and nine patients presented with volvulus secondary to incomplete bowel rotation. These results suggest that intrinsic and extrinsic congenital duodenal obstruction occur with similar frequency. It highlights the role of prenatal ultrasound in the early diagnosis of duodenal atresia and the specificity of the "double bubble", "beak", "windsock", and "corkscrew" signs in accurate diagnosis.

Ultrasound in the investigation of the gastrointestinal tract

W. Kincaid, S. Ingram and R. Vallance
Radiology Departments, Gartnavel General Hospital and The Western Infirmary, Glasgow, UK

Barium radiology of the small and large bowel involves a substantial radiation dose to patients, many of whom are young, often with a low index of clinical suspicion, or requiring repeated examinations for inflammatory bowel disease (IBD). We prospectively examined the value of ultrasound (US) in patients undergoing small bowel barium studies and in patients having barium enema examinations for suspected IBD. Using an Acuson 128 5 MHz curved linear array probe US was performed by a radiologist unaware of the clinical history, immediately prior to the barium study. Another radiologist performed the barium examination unaware of the US findings. To date 37 patients have had 46 barium examinations (small bowel enema 18, follow-through 12, barium enema 16). 18 revealed an abnormality (IBD 15, tuberculosis one, diverticular abscess one, subacute obstruction one). US correctly detected 15 of the 18 radiological abnormalities. Of the three false negatives on US two examinations were difficult owing to the presence of multiple abdominal scars. There were two false positives on US both of which occurred at the beginning of the study. The preliminary results suggest that with experience US could be the first line investigation in patients with suspected small bowel pathology and in those with suspected large bowel IBD. This may enable more selective use of barium radiology.

Notes

Tuesday 19 May

9.00 – 10.15

MR Technology

Hall 9

The current status of MR angiography and flow measurement techniques

M. A. Smith
Academic Unit of Medical Physics, University of Leeds, Leeds General Infirmary, Leeds LS1 3EX, UK

Magnetic resonance (MR) flow techniques are available which give a quantitative measurement of velocity or flow. Velocity phase maps can be acquired in which the pixel value is linearly related to the velocity at that point within a vessel. Such techniques can be used to obtain measurements at various points in the cardiac cycle. In addition, flow in small cerebral vessels can be measured. Recently, pulse sequences have been developed to obtain a rapid display of the velocity profiles in vessels. MR angiography gives a qualitative assessment of flow in vessels, producing an image which mimics X-ray angiography. The three main categories of MR angiographic technique will be reviewed. The first is the phase contrast method which can produce images of either a thick section or a three-dimensional (3D) volume where stationary tissue appears black and flowing blood appears as a high signal. The second technique is known as the inflow or time-of flight method, this produces a 3D data set using either 2DFT or 3DFT. The angiogram can then be viewed from any angle after acquisition using computer reconstruction. The third technique utilizes fast imaging following an injection of MR contrast. The various techniques will be described and their relative merits and shortcomings will be discussed.

An evaluation of signal properties for MRI

J. P. Bean, K. Straughan and *J. A. Lunt
*Department of Electrical/Electronic Engineering, Imperial College, *Department of Health, London SW7 2BT, UK*

The evaluation of the performance of magnetic resonance (MR) systems can be divided into the following categories: signal properties, geometric properties, artefacts and MR specifics such as T_1, T_2 relaxation rates. MAGNET, the Magnetic Resonance National Evaluation Team, quantifies an extensive set of parameters which cover the wide range of the four groupings. The aim of the team is to assess these properties for a selection of coils and imaging sequences. The results of assessments are supplied to the National Health Service to assist purchasing decisions. This paper will address the first and most fundamental grouping, signal properties. These are characterized by the parameters; the signal-to-noise ratio (SNR), and uniformity, the distribution of signal throughout the image field. The range of techniques to evaluate SNR will be presented and reviewed for their efficacy, including spatial and Fourier domain analysis. An indication will be given of the appropriate method to use in the presence of non-uniformity and artefacts. The use of contour plots to characterize uniformity will be discussed in depth. Volumetric assessments for head coils and surface coils will be demonstrated. The results presented will compare a number of commercially available systems of varying field strength and coil type, identifying those with high SNR and uniformity values.

Radio frequency eddy current losses for an annular conductor in MRI

D. W. McRobbie
Department of Radiation Physics, Charing Cross Hospital, London W6 8RF, UK

The quantitative assessment of the signal-to-noise aspects of magnetic resonance (MR) imaging as a function of static field strength depends upon the provision of a means of simulating the r.f. interaction (loading) between the MR receiver and the patient. A popular practical solution is the use of a saline-filled test object of annular geometry within which standard MR test objects may be positioned. The present study provides a theoretical and experimental framework for this type of loading. A semi-infinite model is used to derive the induced electric field and equivalent resistance of an annular conductor located within an idealized saddle coil. Predictions made with this model agree well with both test object experiments and data for the human head over the frequency range 1–63 MHz.

Applications for machine design of the use of superconducting coils

A. S. Hall, R. Johnston and I. R. Young
GEC Marconi Ltd, Hirst Research Centre, Wembley, Middlesex HA9 7PP, UK

The dominant sources of noise in whole body magnetic resonance imaging are associated with the receiver coils and the body itself. Typically, the former is dominant at low fields (less than 0.3 T) and the latter at high. Therefore, it might be expected that the use of superconducting coils would be of greater value at low field rather than high. The availability of high temperature superconducting materials (HTSC) such as yttrium barium copper oxide, which have a critical temperature greater than that of liquid nitrogen liquidation, offers the possibility of practical systems. Extrapolation from high frequency results indicates that HTSC coils at megahertz operation frequencies should have a surface resistance, at 70 K, several orders of magnitude smaller than that of copper, which implies a substantial increase in the intrinsic Q of the coil. Consequently, receiver coil design must be reconsidered to attain the maximum signal-to-noise ratio and body noise dominance. Coil geometry can be optimized for r.f. performance, without regard for filling factor, in the conventional sense, which is no longer an issue.

3D MR imaging—manipulation and display on an independent console and independent workstation—a comparative study

C. E. Hutchinson, X. P. Zhu, J. M. Hawnaur and I. Isherwood
Department of Diagnostic Radiology, University of Manchester, Manchester M13 9PT, UK

The aims of this study were: (1) to compare an independent console (GE DCIII) with a workstation (Sun Sparcstation 2), and (2) to compare three commercially available software packages, "Sun vision" (Sun Microsystems Inc.), "Analyze" (Mayo Foundation) and "MR Console" (General Electric) with respect to their ability to display and manipulate three-dimensional (3D) data. Magnetic resonance (MR) imaging studies were obtained on an IGE Vectra 0.5 T MR system as 3D volume acquisitions from patients being investigated for underlying tumours. Particular attention was directed in these comparative studies to functionality and user friendliness and the capacity for further program development. Data from each tumour study were manipulated separately on each system. The time required to perform each of a series of functions was measured. A scoring system (0–4) was used to assess perceived image quality, tumour conspicuity and quality of viewing facilities for a variety of functions. A further assessment of user friendliness was obtained by counting the number of interactions required to perform each manipulation. The facilities for transferring images from MR scanner to DCIII and workstation were also compared with respect to ease, speed and quality of transfer. The DCIII has some advantages over the "Sun" station because of its integral relationship with the scanner. Post-processing on the DCIII, however, was frequently slower, required more interaction and had restrictions which did not apply on the "Sun" station. For routine image display and diagnosis the DCIII performs well but, for more sophisticated post-processing, an independent workstation is desirable.

Applications of a simple method of 3D MR image reconstruction from regular 2D images

L. Shapiro
Magnetic Resonance Center, Strong Memorial Hospital, University of Rochester Medical Center, Rochester, New York 14620, USA

Three-dimensional (3D) imaging has been shown to be useful in clarifying structures difficult to visualize with two dimensional images. Three-dimensional magnetic resonance (MR) imaging has a lot to offer due to MRI's remarkable ability to distinguish between soft tissues. Software has been developed that will transfer and reformat regular 2D MR images from a General Electric (GE) SIGNA Scanner in such a way as to enable them to be displayed in three dimensions on a Sun workstation. The equipment and software needed for a 3D imaging system is described. This 3D imaging system has been applied to MR angiography using GE's flow-sensitive sequences. This system has also been used to view cartilage of the patello-femoral articulation in the knee. Clinical examples are illustrated. Routine GE pulse sequences were used, although special parameters were used to obtain good contrast between the tissue of interest and other tissues. Limitations of 3D imaging have arisen from non-uniformity of the images and from the great sensitivity of MR to internal signal differences in individual tissues. Possible solutions to these problems and improvements in the techniques are discussed. This technique, when used to complement 2D images, helps the radiologist to visualize and, more importantly, to convey to other doctors, complex relationships of pathology and normal structures.

The phase-inverting harness; a new method of dual surface coil imaging

D. Dobson and N. R. Moore
MRI Centre, John Radcliffe Hospital, Headington, Oxford OX3 9DU, UK

Local receive-only surface coils are widely used in magnetic resonance to image the spine and many joints. The increase in the magnitude of signal received improves spatial resolution and reduces examination time. However, the signal intensity from planar coils is not uniform and diminishes rapidly beyond the radius of the coil. We have developed a system using the dual coil adaptor to link two r.f. matched and tuned coils. These can be placed anterior and posterior, or lateral to the area of interest. In order to overcome the 180° phase shift experienced by the opposed coils, which would otherwise lead to signal cancellation at the mid-point of the imaging volume, a length of cable, equal to half the wavelength at the resonant frequency, is added to the circuit. This results in even signal distribution across the imaging volume. We have used this system to image the shoulder, wrist and brachial plexus. Examples of these applications will be demonstrated, including the effect of removing the phase harness. This simple device expands the range and applications of existing surface coils with minimal cost implications.

APT—hard pulse trains for fat suppressed MRI at 0.5 T

T. W. Redpath and S. C. Wayte
Departments of Clinical Physics and Bioengineering, Walsgrave Hospital, Coventry CV2 2DX, UK

Fat suppression can be achieved by the use of frequency selective r.f. excitation applied at the fat frequency, which is shifted by about 3.5 ppm from the water resonance for proton magnetic resonance imaging (MRI), or about 74 Hz at 0.5 T. The effect can be achieved either by applying a single r.f. pulse, shaped to tailor its spectral content, or by applying a string of hard pulses. A number of groups have used binomial hard pulse trains (*e.g.* 121, 1331, 14 641) to saturate fat selectively, with limited success. Such pulse trains are probably of limited value in MRI, as the lower order trains do not have a flat null response around the water frequency, while the higher order trains have a very sharp response at the fat frequency. Thus the desired effect of the sequence is degraded by relatively small static field errors. Significantly better results can be achieved by hard pulse trains (APT, for Cockneys) specifically designed for a flat response at both the water and fat resonances. APT has some significant technical advantages over tailored single pulses. Good results have been achieved in imaging the orbit at 0.5 T. Unlike short tau inversion recovery, fat-suppressed T_1-weighted images unambiguously enhance signal from tissues which take up paramagnetic contrast agents.

Magnetization transfer imaging of the brain

C. J. Baudouin, J. V. Hajnal, A. Oatridge, J. M. Pennock and I. R. Young
NMR Unit, Department of Diagnostic Radiology, Royal Postgraduate Medical School, Hammersmith Hospital, DuCane Road, London W12 0HS, UK

Magnetization transfer (MT) imaging is a technique involving the application of off-resonance pulses to saturate the macromolecular pool of spins invisible on nuclear magnetic resonance imaging. The aim of this study was to assess the effects of such saturating pulses on the images obtained from volunteers and patients with intracranial lesions. *Methods:* Imaging was performed at 0.15 and 1.0 T. 23 patients with intracranial lesions (13 neoplasms, five infarcts, three haemorrhage, two other) were imaged. Off-resonance saturating pulses were incorporated into short and long time to repeat (TR) spin echo, and short and medium TI inversion recovery sequences. *Results:* The application of off-resonance pulses results in loss of signal from normal grey and white matter with reduction of both available magnetization and measured T_1. Pathological tissues show varying amounts of MT. Saturating pulses cause little signal loss in cystic tumour components and haemorrhage. Solid tumour, oedema and infarction are less affected than normal tissue. This results in increased conspicuity of lesions particularly with sequences such as the MT-single tau inversion recovery sequence which exploit T_1 changes as well as loss of available magnetization. *Conclusion:* Pathological tissues show varying amounts of magnetization transfer. Sequences can be designed to exploit these effects and can result in increased lesion conspicuity.

9.00 – 10.15

Combined Chemotherapy and Radiotherapy — Promises and Problems

Hall 10a

Combined chemotherapy and radiotherapy in non-small cell lung cancer

M. H. Cullen
Birmingham Oncology Centre, Queen Elizabeth Hospital, Birmingham B15 2TH, UK

The standard treatment for localized, inoperable non-small cell lung cancer in the UK, and most of the rest of Europe, is with radiotherapy. Fewer than 5% of cases achieve long-term survival with the vast majority of patients dying with distant metastases and local recurrence. The need for effective systemic treatment is clear. Until recently the activity of chemotherapeutic agents has been insufficient for serious consideration as potential adjuncts to radiotherapy. Furthermore the toxicity, in an elderly population, has been prohibitive. However, there are now a handful of drugs (cisplatin, vinblastine, ifosfamide, mitomycin C) which, having been tested in more than 100 cases, demonstrate objective responses in 20% of cases or more. Combinations of these seem reliably capable of producing partial and complete remissions in around 50% of patients. Improvements in anti-emetic therapy have significantly enhanced the potential use of drugs like cisplatin and ifosfamide in non-curative chemotherapy settings. Hence the current interest in combined modality therapy for non-small cell lung cancer. Two studies reporting survival benefit in randomized trials have recently appeared. In one case (CALGB trial), the trial was discontinued on the basis of a significant difference between the chemotherapy plus radiotherapy arm and the radiotherapy alone arm on group sequential analysis. No estimate of the degree of benefit can be made when trials are analysed in this way. In the other trial (from France) the original report was negative. Later analysis demonstrated a modest survival advantage for the combined arm. In both trials the response rate to chemotherapy was low and no mention is made of symptomatic improvement. There is an urgent need for more secure answers to this question and at least one UK trial (the MIC trial) is attempting to address it, and will be discussed.

Adjuvant and adjunctive chemotherapy in head and neck cancer: a meta-analysis

S. El-Sayed and N. Nelson
Radiation Oncology and Epidemiology and Biostatistics, Manitoba Cancer Treatment and Research Foundation, Winnipeg, Manitoba, R3E 0V9, Canada

Despite 43 prospective randomized studies published in the literature and 30 years of research, the value of adjuvant and adjunctive chemotherapy in head and neck cancer remains controversial. Many overviews of the published literature have been previously published and presented, but none of these have included all the published literature. Here we review the 43 prospective and randomized studies which have been published to date and address the question as to the value of chemotherapy. These studies have been very extensively reviewed to check whether their design complied with the criteria for a prospective randomized study. Before arriving at the final number of 43 prospective randomized studies, many studies were excluded owing to irregularity in the design and failure to comply with the criteria for meta-analysis. Mantel Haenszel summary analyses were used to obtain the relative risks of side-effects

Figure 1

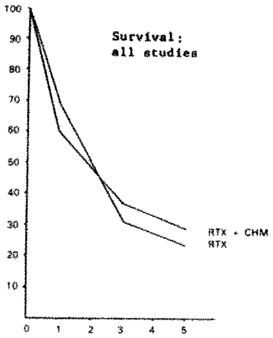

Figure 2

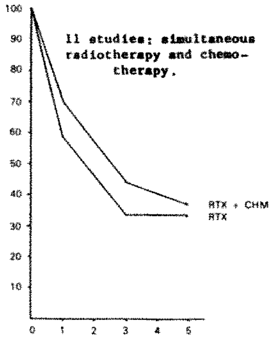

in the radiotherapy plus chemotherapy group from the 43 studies. It was fairly obvious that the addition of chemotherapy has indeed significantly increased the morbidity as well as the chance of tumour response to treatment and the local control of the tumour at 2 years. Surgery and a schedule of radiation did not seem to impact on the overall outcome from the treatment. Overall, the addition of chemotherapy did significantly improve the 5 year survival rate, but that improvement was found to be due to simultaneous chemotherapy alone rather than any other scheduling of chemotherapy (Figs 1 & 2). Further analyses will be presented.

Interrupted hyper-fractionated radiotherapy with concomitant chemotherapy for bulky, inoperable Ewing's sarcoma

D. Spooner, *A. Cassoni and †M. Sokal
*Queen Elizabeth Hospital, Birmingham 15, *Middlesex Hospital, London, WC1 and †Nottingham General Hospital, Nottingham, UK*

In an attempt to avoid a large interval between doses of cytotoxic drugs when conventional radiotherapy is given for Ewing's sarcoma, we have followed a regime piloted by the German CESS 86 protocol. Cytotoxic chemotherapy is given for the first 3 days, together with radiation therapy of 2240 cGy m.p.d. in 14 fractions (× 2 per day, separated by 6 h). This is repeated 3 weeks later and at 6 weeks 1600 cGy m.p.d. is given in 10 fractions over 5 days. 11 patients were treated and followed for a median follow-up period of 27 months; 10 patients had large inoperable pelvic primaries, and one had a large, inoperable skull tumour. The acute toxicity was minimal. *Late results:* one severe cutaneous fibrosis; one iliocaecal stenosis; one local recurrence (at 3 months) and three progressive distant disease. Our pilot study has demonstrated the feasibility of the above regime. Careful monitoring of late toxicity is required.

Acute toxicity study of synchronous chemotherapy and radiotherapy as adjuvant treatment after primary surgery in early breast cancer

I. N. Fernando, H. T. Ford, S. Ashley and T. J. Powles
Department of Radiotherapy/Breast Unit, Royal Marsden Hospital, Sutton SM2 5PT, UK

We are presently undertaking a randomized study of neoadjuvant *vs.* adjuvant therapy for early stage breast cancer. In both arms of the study patients received postoperative radiotherapy and synchronous full-dose chemotherapy with no dose modification, except for haematological toxicity. We now present the results of a prospective study comparing the acute toxicity profile of this group of patients (Group (A)) with a similar group treated with radiation alone (Group (B)). Our results have shown no significant difference in the acute skin toxicity with 46 of the 58 (79%) patients in Group (A) developing a mild/moderate skin reaction compared with 37 of the 50 (74%) patients in Group (B). 12 of the 58 patients (21%) in Group (A) developed a moderate/severe reaction compared with 13 of the 50 patients (26%) in Group (B). The main factors relating to the severity of the acute skin reaction have been examined and appear to be due to the radiotherapy technique and are discussed further. Out of 58 patients four (6%) developed symptomatic radiation pneumonitis in Group (A) but responded to a short course of steroids and had no permanent deficit. No patients have developed neutropenic septicaemia. We conclude that synchronous chemotherapy and radiotherapy has an acceptable acute toxicity profile.

Metastatectomy in patients with soft tissue sarcoma

M. H. Robinson, M. Shepherd and E. Moskovic
Department of Radiotherapy, The Royal Marsden Hospital, London SW3 6JJ, UK

Between 1970 and 1990, 220 patients with soft tissue sarcoma referred to the Royal Marsden Hospital Sarcoma Unit have developed lung metastases. Of these, 44 patients (median age 32 years) have been treated by metastatectomy. The commonest histologies were malignant fibrous histiocytoma (10) and synovial sarcoma (8) and extremity the commonest site. Mean time to lung metastasis was 934 days. The mean number of metastases found at surgery was two (range 1–15) and 22 patients had one. On nine occasions more lesions were present than were discovered preoperatively and on three occasions fewer. Surgical complications were minor apart from one pulmonary embolus and one post-operative death following tumour embolus into the middle cerebral artery. 14 patients received adjuvant chemotherapy and one patient received radiotherapy to unresected disease. Lung was the first site of relapse in 22 patients. All nine patients with bilateral resections relapsed in lung. Although the metastasis-free interval following primary treatment of both groups was the same overall, 5 year survival and survival from development of lung metastasis (50% *vs.* 20%) was better in those undergoing thoracotomy and was not related to the number of metastases resected or disease-free interval. On multivariate analysis of all 220 cases, the use of lung resection was the most important factor determining survival of those with lung metastases (RR 0.2) with age < 40 and extremity also important.

Measurements of platinum uptake in head and neck tumours using X-ray fluorescence

A. El-Sharkawi, †F. Al-Sadhan, *A. W. Seaby,
*C. J. Evans and *J. Dutton
*Department of Radiotherapy and *Medical Physics,*
Singleton Hospital, Swansea SA2 8QA, UK and
†Department of Physics, University College of Swansea,
Swansea, SA2 8PP, UK

Platinum is the basis of the first inorganic compound to be used widely in cancer chemotherapy. Quantification of the platinum concentration in tumours would be of value in evaluating the pharmaco-kinetic behaviour of the drug and achieving a better therapeutic ratio. Platinum can be measured *in vivo* by X-ray fluorescence using excitation sources of either ^{57}Co or, more recently, ^{99}Tc^{m}. Initially, the ^{57}Co source and a planar hyperpure germanium detector in a 90° scattering geometry were used. Whilst successful in measuring the platinum concentration in the kidneys, this scattering geometry was found in practice to be difficult to use for measurements about the head and neck. A new instrument was consequently developed in which an annular ^{99}Tc^{m} source was used in a 180° scattering geometry with the same planar detector. The results of an initial clinical study of patients with head and neck tumours indicate the benefit obtained in using this new arrangement.

MRI of osteosarcomas and Ewing's sarcomas: the potential of dynamic Gd-DTPA scanning for quantifying the chemotherapy response

R. Maas, M. Beese, M. Reuter, V. Nicolas, *U. Heise,
†K. Winkler and §G. Delling
*Department of Radiology, *Clinic of Orthopaedics, †Clinic of Paediatrics and §Institute of Bone-Pathology, University Hospital of Hamburg, 2000 Hamburg 20, Martinistreet 52, Germany*

Chemotherapy of osteosarcomas and Ewing's sarcomas has developed tremendously during recent years. After pre-operative chemotherapy the tumour may be resected locally. It remains a diagnostic challenge to answer the question as early as possible during pre-operative chemotherapy whether the tumour is responding or not, so that the treatment modalities can be intensified. During the last 5 years we examined 45 osteosarcomas and 22 Ewing's sarcomas with magnetic resonance imaging at 1.5 T. Of these, 16 osteosarcomas and six Ewing's sarcomas had a follow-up study for a 2–5 month period. They received a dynamic Gd scanning, which consists of one slice which is scanned repetitively in rapid succession using a T_1-weighted spin-echo sequence. Gadolinium-DTPA is given as a bolus immediately after the first scan. Quantification is done by means of an "irregular region of interest" (ROI). A phantom was introduced as a standard. The time-intensity diagram prior to treatment reflects the significant increase and high signal intensity level, indicating a hyperperfusion of a malignant tumour. During chemotherapy perfusion decreases and correspondingly the signal intensity declines. If the intensity decreases by more than 20% relatively to the baseline examination after 4 or 6 weeks, the pathologist will find less than 10% of residual tumour viability after completion of the chemotherapy. This indicates a response. The diagnostic accuracy lies between 85 and 90%. Therefore dynamic gadolinium-DTPA scanning seems to be an excellent tool for a reliable and non-invasive quantification of tumour response during pre-operative chemotherapy.

9.00 – 10.15

Radiological Audit

Hall 11a

The role of hysterosalpingography in the evaluation of infertility—a clinical audit

M. Callaghan and D. McQueen
Department of Radiology, and Department of Obstetrics and Gynaecology, Western Infirmary, Glasgow G11 6NT, UK

We have performed a retrospective study of 112 patients who presented for the investigation of infertility, over a 5 year period between 1986 and 1991. All patients had primary or secondary infertility for greater than 2 years. Ovulation and semen analysis had been shown to be satisfactory. In patients who also underwent laparoscopic hydrotubation these results were compared. Hysterosalpingography was performed without pre-medication, with up to 20 ml of non-ionic contrast using Leech–Wilkinson cannula, Foley or Harris catheter, under fluoroscopic control. Laparoscopic hydrotubation involved laparoscopy under general anaesthesia, with pneumoperitoneum and assessment of tubal anatomy. Patency was established by visual inspection of the tubes after trans-cervical injection of dye (methylene blue). The radiological and laparoscopic findings were compared and the cost of each type of investigation was also calculated. Results and implications for the rationalization of the management of the infertile patient will be discussed.

Observation of significant abnormalities on lumbar spine radiography

J. Fowler, P. Tyrell, J. S. Millar, J. F. Leahy, K. Patel, J. A. Hill and A. M. Davies
Department of Radiology, Birmingham General Hospital, Birmingham B4 6NH, UK

In the past some publications have advocated limiting the routine lumbar spine series to a single lateral film to reduce the departmental workload and radiation dose to the patient. Series have been quoted in support of this idea in which the prevalence of significant abnormalities was extremely small. The purpose of this study is to determine what proportion of significant abnormalities are detected on the antero-posterior (AP) and lateral films when viewed separately in a series of cases where the prevalence of abnormalities was artificially increased to an unknown level. Five radiologists of varying experience were required to report separately on the AP and lateral lumbar films of 300 cases in which randomly included were nine cases with a disc infection, 14 with a metastasis and seven cases with an inflammatory spondylitis. At a later date the radiologists repeated the exercise, reviewing all the films together. Analysis of the observations was performed. As might be expected in such a study the false positive rate was relatively high, particularly in the least experienced radiologists' responses. Nevertheless the overall results show that the majority of early inflammatory spondylitis cases will be missed on a solitary lateral film as will many of the metastases. Conversely fractionally more of the infections were observed on the lateral film than on the AP. Further analysis in terms of sensitivity, specificity, positive and negative predictive values are discussed. The authors conclude that it is preferable to reduce the overall number of lumbar spine examinations performed than to prejudice the detection rate of significant, albeit rare, abnormalities by restricting the number of films obtained.

Audit—the admission chest radiograph in a sickle cell crisis

Wai Lup Wong, P. D. Holder, A. B. Ayers and L. M. MacDonald
Department of Clinical Radiology, St Thomas' Hospital, London SE1 7EH, UK

A chest radiograph often forms part of the "diagnostic work-up" in a patient with a sickle cell crisis. This retrospective study assesses the diagnostic yield and suggests some guideline indications for chest radiography in this situation. We identified all patients admitted to St Thomas' Hospital with a sickle cell crisis who had a chest radiograph on admission, between 1 August 1989 and 31 July 1991. Of the 220 admissions, 30 (14%) were excluded because of incomplete records. The radiographs were divided into two groups. The first group were those with radiographic abnormalities which would have influenced the immediate clinical management. The other group consisted of normal chest radiographs and those with abnormalities associated with sickle cell disease which would have had no immediate influence on clinical management. The results of both groups were analysed with respect to the clinical signs, symptoms and age of the patients. Our study indicates a chest radiograph is not essential in all patients admitted with a sickle cell crisis. It is only required in those with specific clinical signs. The possible savings in terms of radiation and finance with more selective chest radiography in these patients is discussed. Sickle cell patients have numerous radiological investigations during their lifetime so it is vital to reduce their unnecessary exposure to radiation.

Chest radiography for general practitioners: effects of request review on referral patterns

A. R. Padhani, M. T. Keogan and C. D. R. Flower
Department of Diagnostic Radiology, Addenbrooke's Hospital, Cambridge CB2 2QQ, UK

In order to assess the value of chest radiography for general practitioners we prospectively reviewed 2017 chest radiographs over a 10 month period. A total of 1424 patients was referred to the chest clinic (requested unvetted) and 593 to the radiology department (formal consultative process). Referrals to the chest clinic were more likely to be inadequate with regard to history and physical examination (73% *vs.* 33%; $p < 0.005$) including smoking status. Patients referred to the chest clinic were more likely to have normal radiographs (66% *vs.* 53%; $p < 0.005$) and conversely were less likely to have clinically related abnormalities (21% *vs.* 26%; $p < 0.05$). Patients were more likely to be referred to the chest clinic for reassurance and for chronic airways disease and the radiology department was the more likely place of referral for rib fractures and for suspected primary or secondary cancer. Abnormalities were rare in the 10–29 year age group and when reassurance alone was sought. Patients presenting with haemoptysis or with symptoms of lower respiratory infection or of chronic airways disease often had abnormal examinations. Improved communications and the introduction of guidelines should promote the rational use of limited resources.

General practitioner access to radiology services

I. R. Brand and R. F. Bury
Department of Diagnostic Radiology and Nuclear Medicine, Leeds General Infirmary, Leeds LS1 3EX, UK

In 1981 a joint working party of the Royal College of General Practitioners and the Royal College of Radiologists agreed that direct access to radiology services was essential to GPs. A postal survey was performed a decade later to assess this ideal, involving both the local medical committees of the British Medical Association and local faculties of the Royal College of General Practitioners. Plain radiographs were found to be generally available (95%+), but access to contrast examinations, ultrasound and mammography was often limited or poor, 81% and 47%, respectively having access to barium meals and enema, 53% to obstetric ultrasound, 48% to non-obstetric ultrasound and 21% to mammography. More positively, a number of respondents noted that where there was a good relationship between GPs and the radiology department limited access was open, following direct communication, to all investigations available including computed tomography and nuclear medicine. Despite the often limited access, approximately 75% described the service as either good or excellent. This was often unrelated to the number of investigations available and was more likely to be related to the quality of service provided. This was echoed spontaneously by quoting either long waiting lists for investigations or unreasonable delays in obtaining reports.

General practitioners' opinions on the role of barium meals and endoscopy

L. A. Webb, M. E. Finlay, M. J. Keir, P. D. Clarke, L. R. Gordon and J. P. Owen
Department of Radiology, University of Newcastle upon Tyne, Newcastle upon Tyne NE1 4LP, UK

A total of 676 was surveyed and 325 (48%) completed questionnaires were returned. Difficulty in swallowing was the only clinical reason for preferring barium studies. Endoscopy was clearly preferred in patients aged over 20 years, for GP reassurance, prolonged symptoms, previous similar episodes and previous gastric surgery. There were no such preferences for barium studies. GPs had a good understanding of the diagnostic capabilities of the techniques but some areas of poor appreciation were identified. GPs also understood the significance of most phrases in radiological reports but specific areas of poor understanding were discovered. Treatment and specialist referral preferences in response to radiological phrases were identified and phrases poorly understood highlighted. Only 3% of respondents knew the radiation dose of a barium meal.

Diagnostic yield of barium enema in a district general hospital

T. Y. K. Chan, *S. Said, *D. Ellis, I. Mootoosamy, P. E. Thurley, N. G. Reading, J. W. Frank and C. P. Cooper
*Department of Radiology and *Medical Audit Unit, Whipps Cross Hospital, Leytonstone, London E11, UK*

The diagnostic yield of inpatient and outpatient referrals for barium enema over a 5 month period was assessed with reference to the specialities and presentations. There were 320 surgical (including 11 from urology and 10 gynaecology), 133 medical referrals and 47 from geriatrics. 28 cases had no diagnoses specified and were excluded from calculations. In those aged under 40 years, the overall positive yield was 31% (16/51). Only one cancer was detected. Of the remaining 15 positives, seven had inflammatory bowel disease. This contrasted greatly with the diagnostic pattern of the over 40s age groups in whom inflammatory bowel disease accounted for only five of the 266 positives. A large majority (208) had diverticular disease. There were 28 carcinomas and eight cases of polyps. The overall diagnostic yield for the over 40s was 63% (266/421). The diagnostic yield from surgical referrals was similar to that from medical ones, in both the outpatient and in-patient categories. Geriatric referrals had a higher yield mainly because of a proportionally higher detection of carcinomas. The proportion of diverticular disease was similar in all three referral groups. Change of bowel habits, diarrhoea, rectal bleeding and abdominal pain were the most frequent presenting complaints, although the presence of an abdominal mass gave the highest positive yield (carcinoma or diverticulitis). Clinical suspicion of diverticular disease was confirmed in 90% of cases but this was thought to be related to the high prevalence of the condition. Inpatients had higher diagnostic yield in all three referrals groups, reflecting the frequently more serious conditions warranting admission. This study shows that the diagnostic yield for hospital referrals was as high as 60% (282/472) of which a great majority were uncomplicated diverticular disease. Inflammatory bowel disease was diagnosed in 12 patients who tended to be younger and who might benefit from flexible sigmoidoscopy before proceeding to barium enema if warranted. The high overall positive yield was likely to be due to a secondary screening process whereby general practioners' referrals were further assessed by hospital specialists who had easier access to other investigative tools including sigmoidoscopy, radiography and ultrasound (for abdominal mass), as well as cross-specialty consultation.

Audit of outpatient barium services; user friendly or friendly abuse?

J. G. Houston and N. McMillan
Department of Radiology, Western Infirmary, Glasgow G11 6NT, UK

Over 3000 patients attend the X-ray department of two city hospitals annually for outpatient barium examinations, accounting for 15–30% of radiologists' work. With this size of service and the particular demands of these examinations on patients, an audit of the appointment system and patients' attitudes to the service was undertaken. 100 patients, 50 from each centre were asked to fill out questionnaires before and after their outpatient examination, and the delays in the appointment system were quantified. The average age was 51 years (range 18–83 years), 61 females, 49 males, equally referred by GPs and outpatient clinics. 40% of patients arrived late for their appointment; delays in public transport and insufficient parking were possible causes. 60% are taken within 15 min of their appointment. The level of information about examination that patients receive was thought too low. 60% were not told by the referring clinician what the procedure involved, 5% did not know what examination they had come for, 14% thought the preparation inadequately explained, 50% thought the examination better than expected, indicating unnecessary anxiety which might be allayed by further information while waiting for the procedure. 96% thought staff very helpful and 98% were overall satisfied with the service.

Audit on the management of patients for barium enema

T. Y. K. Chan, *S. Said, *D. Ellis, I. Mootoosamy, P. E. Thurley, N. G. Reading, J. W. Frank and C. P. Cooper
*Department of Radiology and *Medical Audit Unit, Whipps Cross Hospital, London E11, UK*

A 5 month prospective study of 500 consecutive hospital inpatients and outpatients referred for barium enema was analysed with respect to the preparation for, and the management at the time of, the investigation. All patients had colonic continuity (*i.e.* excluding colostomy enema). There were 320 surgical (299 general surgery, 11 urology, 10 gynaecology), 133 medical and 47 geriatric referrals. The female to male ratio was about 3 to 2. 60% in-patient requests were undertaken within 1 week. Some 16%, however, did not have the enema until more than 3 weeks after. Concomitant medical conditions that precluded necessary preparation, and early discharge with the enema being done as an outpatient procedure accounted for most of the delays. Only 11% outpatient appointments were performed within 1 week. 36% took 1–3 weeks and 53% longer than 3 weeks. The average delay from appointment time to the enema examination was less than 30 min in 62%. Two-thirds of those who had to wait longer suffered because of "departmental reasons". The screening and total examination times were both appreciably longer with the geriatric patients. This was probably due to their general frailty, which was subjectively but independently assessed by the radiologists and the nurses, the latter often having a lower score for these patients' fitness. Their frailty was also reflected in a high number of unsatisfactory preparation

(29%) and of incontinence (36%), leading to incomplete (35%) and undiagnostic (24%) examinations. Balloon catheters were used in 13% of all patients, but mainly in the elderly. 9% of all patients were distressed. 8% had defaulted previous enema appointments and 12% used ambulance transport, a large majority of these categories being over 70 years old (94% and 73%, respectively). The clinical relevance of the request, and the adequacy of clinical information given were deemed satisfactory in 85% and 79%, respectively. Only in 49% were the performance and/or findings of sigmoidoscopy specified. This study shows that better organization may be required, especially to reduce the delays in both the request–appointment and appointment–examination times, and that geriatric patients would need extra help to make barium enema a worthwhile diagnostic test.

Notes

9.00 – 10.15

Hepatobiliary and Pancreatic Imaging

Hall 11b

Imaging complications of liver transplantation

S. P. Olliff
Department of Diagnostic X-ray, Queen Elizabeth Hospital, Birmingham B15 2TL, UK

Orthotopic liver transplantation involves the creation of venacaval, portal venous, hepatic artery and biliary anastomoses. A wide variety of complications may arise in liver transplant patients. These include vascular, biliary and general complications as well as rejection or infections related to the necessary immunosuppression. Ultrasound with Doppler is the primary imaging method for the liver and associated structures. Angiography and venography may be required for direct visualization of the vasculature. Cholangiography may be performed via the T-tube or by PTC or ERCP. Computed tomography scanning is also helpful in some clinical situations. The role of magnetic resonance imaging has yet to be fully developed. The use of these imaging modalities in relation to the more common complications will be discussed.

Radiological evaluation of pancreatic allografts

S. Meecham Jones, C. Evans and K. Lyons
Department of Radiology, Cardiff Royal Infirmary, Cardiff CF2 1SZ, UK

Pancreatic transplantation is an acceptable treatment method for certain groups of diabetic patients, notably those who already require immunosuppression for renal allografts. In some centres, 70% of pancreas transplant patients are now insulin independent long term. As well as the well-recognized complications of immunosuppression, patients with pancreatic transplants have graft-related complications including rejection, exocrine leakage, vascular thrombosis, pancreatitis and sepsis. We have reviewed the role of radiology in the management of the last 12 pancreatic transplants. The value of contrast studies, angiography, ultrasound including Doppler, radioisotope scans, computed tomography and magnetic resonance imaging in the management of these patients is presented.

Scintigraphic differentiation of surgical jaundice from medical jaundice of viral/schistosomal origin

*†A. T. Khairy, *F. Kamel, *A. El-Feky, *K. Khairy, *A. El-Dorry and †J. J. Barrett
**Department of Diagnostic Radiology, Ain Shams University Specialized Hospital, El-Khalifa El-Maamoun Street, Abbassia, Cairo, Egypt, †Department of Nuclear Medicine, King's College Hospital, London, UK*

The hepatic index (HI) derived from $^{99}\text{Tc}^{\text{m}}$ IDA scanning and defined as the net liver to heart ratio, 2.5–10 min after injection, was evaluated in 33 cases with biopsy-proven hepatocellular disease and jaundice (G1), 14 patients with obstructive jaundice (G2), and 28 controls. The hepatocellular disease of G1 was due to hepatitis B infection and/or *Schistosomiasis mansoni*. The causes of biliary obstruction in G2 were biliary atresia, stone/stricture, carcinoma of pancreatic head or cholangiocarcinoma. They were verified by biopsy, on surgery or by ERCP. The 28 controls were divided into 18 matching the age and sex of 18 patients of G1 and 10 similarly matching 10 cases of G2. The HI was 3.16 ± 1.93 and 1.89 ± 1.45 (mean ±1 standard deviation (SD) in G1 and G2, respectively, with significant difference ($p < 0.05$)). Each of G1 and G2 also differed significantly from the corresponding controls ($p < 0.01$). None of the patients of G2 had shown a HI more than 5. It is concluded that the hepatic index is a simple and useful test in excluding biliary obstruction. However, owing to the overlap of ranges, it has only a potential value in differentiating obstructive from hepato-cellular jaundice.

Ultrasound assessment of the normal and obstructed Roux Loop following surgical biliary diversion

C. L. Holland, S. P. Olliff and J. F. C. Olliff
Department of Diagnostic Radiology, Queen Elizabeth Medical Centre, Edgbaston, Birmingham B15 2TH, West Midlands, UK

Curative and palliative surgical treatment of pancreatic and biliary tumours and other procedures including liver transplantation involve creation of a bile duct to small bowel Roux Loop anastomosis. Ultrasound is a well-established modality for the examination of the biliary tree. It is the first-line method for post-operative imaging of these patients. We describe the appearances in three cases of recurrent obstructive jaundice due to obstruction within the Roux Loop or more distally. The cause of the obstruction was demonstrated by ultrasound in all cases. This provided useful information for further management of the patients. For comparison purposes the ultrasound appearance of the unobstructed Roux Loop will also be demonstrated.

The role of pre-operative intravenous cholangiography in patients undergoing laparoscopic cholecystectomy

G. C. McInnes, J. C. Patel and G. Needham
Department of Radiology, Aberdeen Royal Infirmary, Aberdeen AB9 2ZB, UK

Laparoscopic cholecystectomy for gallstone disease is rapidly gaining in popularity amongst surgeons and patients. Its morbidity in experienced hands is almost as low as that of conventional cholecystectomy, and the small incisions required lead to fast recovery and improved cosmetic results. There has been much contention recently, however, as to which pre-operative investigations are required to exclude the presence of common bile duct calculi. In our hospital, the surgeons require routine intravenous cholangiography (IVC) on every patient considered for laparoscopic cholecystectomy, while in many other centres surgeons are content with a normal biliary tree ultrasound and liver function tests often combined with a peroperative cholangiogram. Our paper reviews 100 patients on whom IVCs were performed prior to laparoscopic cholecystectomy. We analyse liver function tests and ultrasound findings and review the IVCs evaluating the usefulness of this investigation. The IVC had previously become almost obsolete and its resurgence would have obvious implications. We therefore consider the implications of its routine use in terms of radiological practice, cost and patient morbidity and mortality, and discuss alternative pre-operative and peroperative assessment protocols.

Antegrade cholecystography following percutaneous cholecystostomy for acute cholecystitis

T. S. Creasy, S. Grønvall and J. G. Stage
Departments of Radiology and Surgery, Hvidovre Hospital, Copenhagen, Denmark

The diagnostic value of antegrade cholecystography in a consecutive series of 44 patients with scintigraphically confirmed acute cholecystitis, treated by percutaneous cholecystostomy, has been evaluated. Six patients did not have antegrade cholecystography due to either catheter migration or gangrenous gallbladder perforation. Antegrade cholecystography was performed in the remaining 38 patients in two separate clinical settings; firstly, in patients suspected on clinical grounds of having persisting cystic duct obstruction, and, secondly, in patients in whom return of bile drainage suggested spontaneous reopening of the cystic duct. In the clinically persisting cystic duct obstruction group, antegrade cholecystography showed the cause of obstruction to be impacted calculi in either the gallbladder neck or in the cystic duct, in all patients. In the clinically patent cystic duct group, antegrade cholecystography confirmed cystic duct patency in all patients, with good demonstration of the biliary tract in most patients. Nine patients from a total of 23 patients with acute calculous cholecystitis in this group had associated common duct calculi; in three patients with non-dilated common ducts. This latter finding suggests that small calculi may pass from the cystic duct into the extrahepatic bile ducts during an episode of acute calculous cholecystitis.

Gallstone recurrence following percutaneous cholecystolithotomy

J. J. Donald, A. R. Gillams, *S. Cheslyn-Curtis, *R. C. G. Russell and W. R. Lees
*Departments of Radiology and *Surgery, The Middlesex Hospital, London W1N 8AA, UK*

Using radiologic interventional techniques the gallbladder can be cleared of stones with a high success rate. As with any treatment option that leaves the gallbladder *in situ*, there is an accompanying risk of stone recurrence, which is currently unknown for the radiological method. A total of 98 patients was studied prospectively to determine the recurrence rate of stones and clinical outcome following successful percutaneous cholecystolithotomy (PCCL). Follow-up included clinical assessment and ultrasound examination at 3, 6 and 12 months followed by annual intervals. The overall recurrence rate was 27% at a mean follow-up of 17 months (range, 3–36 months). By actuarial life-table analysis, the cumulative proportion of gallstone recurrence was 10.3, 21.1, 32.0 and 29.1% at 6, 12, 24 and 36 months, respectively. Of the 27 patients with recurrent stones, 16 remain asymptomatic, four have experienced biliary colic, three abdominal pain, three non-specific upper gastrointestinal (GI) symptoms and one jaundice secondary to a common duct stone. Two patients have subsequently undergone cholecystectomy. 11 of the stone-free patients have remained symptomatic; seven with abdominal pain and four with non-specific upper GI symptoms. This data indicates that stone recurrence following successful PCCL occurs in the minority, and is usually asymptomatic. Despite the advent of laparoscopic cholecystectomy there remains a role for PCCL in selected patients.

CT assessment of gallstones; correlation with physicochemical properties

M. Blomley, D. A. Nicholson, *W. Man, G. Bartal, L. Banks, *S. Li, †A. Bradley and †M. Myers
*Departments of Radiology, *Biochemistry and †Medical Physics, Hammersmith Hospital, Du Cane Road, London W12 0HS, UK*

Computed tomography (CT) appears to be the modality with the best potential to classify gallstones. However, attempts to correlate CT with chemical composition have not always been successful. We have determined physical attributes (mass, weight and density) of 29 gallstones, which were then CT scanned. Morphology, mean attenuation and where appropriate, regional attenuation were determined. After fragmentation the stones were biochemically analysed for calcium, cholesterol and bilirubin content. All stones were visualized, at least in part with CT; none was completely isodense with saline. A mean CT density of < 0 Hounsfield units (HU) predicts the stone is morphologically rimmed ($p < 0.01 - \chi^2$). The majority of rimmed stones had a density < 1 g/cm^3. All non-rimmed stones had densities > 1 g/cm^3 and > 0 HU. Cross-correlation data with the biochemical analysis will be presented, along with the ease of fragmentation (performed in a standardized way using a holmium–YAG laser) of the different gallstones. It appears that physical, rather than chemical attributes, may be more important in determining the response to some of the newer non-surgical gallstone therapies.

Intravenous cholangiography — is there life after death?

P. N. M. Tyrrell and J. K. W. Li
Department of Radiology, The General Hospital, Birmingham B4 6NH, UK

The advent of laparoscopic cholecystectomy has seen the re-introduction of the intravenous cholangiogram as a method of imaging the extrahepatic biliary tree prior to surgery. We are in the process of reviewing the intravenous cholangiograms carried out on patients awaiting surgery for gallbladder disease (80 patients to date). The aims of the study are to assess the usefulness of the intravenous cholangiogram in detecting stones in the common bile duct, and hence assessing the radiographic and diagnostic quality of the examination. Comparisons with other imaging modalities of the biliary tree are made where available. Surgical management on the basis of the intravenous cholangiogram is discussed (including endoscopic retrograde cholangiography/sphincterotomy and laparoscopic cholecystectomy), along with outcome and follow-up over a period. Side-effects of the examination are also discussed.

Notes

10.45 – 12.00

Trauma

Hall 9

The advancement of trauma radiology

J. W. R. Young
Department of Diagnostic Radiology, University of Maryland Medical System, Baltimore, MD 21201, USA

Over the past decade, diagnostic imaging has become an increasingly important and integral part of the management of the traumatized and critically ill patients. In particular, the increasing application of cross-sectional imaging methods such as computed tomography and magnetic resonance has produced a revolution in the speed of the diagnostic process. Newer imaging procedures have naturally been compared with more traditional methods of physical diagnosis, which has spawned controversy about the safest, most accurate and most cost-effective diagnostic approaches to be used. This review examines the assessment of the critically injured patient both from the perspective of plain film analysis, as well as the more modern approaches using cross-sectional and even three-dimensional imaging techniques. The implications of the newer high-speed techniques will also be discussed.

Usefulness of three-dimensional computed tomography in cranio-facial traumatology

P. Pelotti, G. Pennesi, C. Malaguti, E. Rimondi and C. Monti
Servizio di Radiologia, Istituto Ortopedico Rizzoli, Via Pupilli, 1 Bologna, Italy

Imaging of cranio-facial traumatology has to define accurately the bone structures involved in the trauma and the associated soft tissue lesions, especially in the orbital cavity. Moreover, it has to offer all the details necessary to the surgeon to plan a reconstruction that is very often difficult for the complex anatomy of this region. 50 patients with cranio-facial fractures (10 cases of the nasofrontal-ethmoid region, 32 cases of the orbit-malar region, eight cases with complex lesions) were evaluated with conventional radiology, and two-dimensional (2D) and three-dimensional (3D) computed tomography (CT). The axial CT and the 2D reconstructions allowed us to define precisely lesions of the endocavitary orbita in seven cases not detected by conventional radiography. The 3D reconstructions modified the surgical plan in 20 cases. The axial CT and 2D and 3D reconstructions represent indispensable procedures in the evaluation of the major trauma in the cranio-facial region, often modifying both the diagnosis and the therapeutic approach when these were only evaluated on conventional radiology.

Instant MRI diagnosis and exclusion of occult femoral neck fractures

K. Lyons, C. Evans, *P. D. Evans, *J. A. Fairclough, L. A. Williams and *C. Wilson
*Departments of Radiology and *Orthopaedics, Cardiff Royal Infirmary, Newport Road, Cardiff, South Glamorgan, UK*

Whilst the majority of femoral neck fractures are readily diagnosed by clinical evaluation and plain radiography, a minority have normal radiographs but are unable to bear weight. ^{99m}Tc MDP bone scanning is recognized as a sensitive method of fracture detection, but it is time consuming and may be non-specific. In an attempt to facilitate early diagnosis of occult femoral neck fractures magnetic resonance imaging (MRI) (0.5 T) was utilized in 11 consecutive patients with normal radiographs and positive clinical findings. T_1-weighted spin-echo (SE) coronal images were obtained in all patients — a 5 min sequence. All patients subsequently had a radionuclide bone scan. Where MRI and bone scan showed no femoral neck fracture, the patient was mobilized and plain films obtained at 6 weeks. On MRI, five patients had femoral neck fractures. One patient had a normal MRI and bone scan. In addition, MRI differentiated a fracture of the greater trochanter from an intertrochanteric fracture when the bone scan was non-specific, demonstrated avascular necrosis where the bone scan showed non-specific uptake, demonstrated fractures of the sacrum and/or pubic rami in three patients all of which explained their symptoms and did not require surgical intervention. No patient with a normal femoral neck on MRI was subsequently shown to have a fracture. MRI where available can quickly and accurately diagnose and exclude occult femoral neck fractures and should be the investigation of choice when plain radiography is negative.

MR imaging in vertebra compression fractures

L. A. Mitchell, R. W. Kerslake and B. S. Worthington
Department of Academic Radiology, University of Nottingham, Nottingham NG7 2RD, UD

The present study assesses the ability of magnetic resonance (MR) imaging to identify the pathological basis of vertebral compression fractures correctly. The MR examinations of 65 patients with wedge compression fractures of the spine were reviewed. 35 were secondary to trauma or osteopenia, 20 to neoplasm and five to infection. In fractures of less than 3 weeks, a half showed increased signal in the vertebral body on T_2-weighted sequences and the short tau inversion recovery (STIR) sequence with a reduced signal on T_1-weighted sequences and these appearances presumably represent oedema/haemorrhage in the marrow cavity. A similar pattern is seen in neoplasm and it is frequently associated with multifocal disease, destruction of the posterior elements and extradural spread of tumour. In old fractures and osteopenia the signal returned from the vertebral body is the same as that from normal marrow on all pulse sequences. In pyogenic osteomyelitis a high signal in the whole of the disc space on T_2-weighted sequences and the STIR sequence and a low signal on T_1-weighted sequences accompanied similar signal intensities in the marrow space. Evidence of extension of pathological changes into the paravertebral soft tissues and extradural space were also seen. The appearances in tuberculosis, however, can closely mimic those of neoplasm. We conclude that the distinction by MR imaging between vertebral body compression fractures secondary to trauma, infection, osteopenia and neoplasm requires attention to detail and is not as straightforward as some authors have suggested.

Is unilateral facet dislocation of the cervical spine a stable injury?

V. N. Cassar-Pullicino, W. C. G. Peh and I. W. McCall
Department of Diagnostic Imaging, The Robert Jones & Agnes Hunt Orthopaedic Hospital, Oswestry SY10 7AG, UK

Unilateral facet dislocation (UFD) of the cervical spine following a flexion/rotation injury is reported and classified as a stable injury. A retrospective analysis of 28 patients with typical radiological criteria of UFD admitted to the Midlands Centre for Spinal Injuries over a 6 year period was undertaken to assses the natural history of this injury. The plain radiographs obtained on admission, during closed reduction with skull traction, and on follow-up were analysed. In addition, 23 patients also had computed tomography (CT) assessment while four patients had magnetic resonance imaging scans available. Criteria of instability were seen on the initial plain films with wide interspinous distance or facet joints (43%), anterior listhesis > 3.5 mm (40%), and a narrowed or widened intervertebral disc (48%). Subluxation of the contralateral facet joint was seen in 65%, and posterior neural arch fractures in 45% of cases. Radiographic assessment during traction/reduction in 23 patients revealed abnormal widening of the intervertebral disc, interlaminar and interspinous spaces at the injured level in 48%. Of these, follow-up radiographs showed that virtually all proved unstable after reduction, requiring surgical fusion. There was no deterioration in the neurological status following reduction or surgery. UFD should not be regarded a diagnostic entity, but a "radiographic status" of the post-traumatized spine with a high incidence of extensive soft tissue damage. Interlocking of the facets provides stability to the injured level which is removed during and following traction/reduction rendering the injured level unstable in 48% of instances.

Missed fractures in children from an accident service department

H. G. Thomas
Department of Radiology, John Radcliffe Hospital, Oxford OX3 9DU, UK

Fractures in children are often difficult to diagnose in view of the variable appearances of the development and fusion of the epiphyses. Many studies have looked at the incidence of missed injuries in accident service departments, but not specifically documented the fractures most commonly missed in children. A study was undertaken to identify the most commonly missed injuries in the accident service department over a 6 month period. From 25 798 attendances, 16 246 X-ray examinations were performed. There were 57 fractures missed and 18 suspected in children under the age of 16 years. The most common sites for missed fractures in children are the fingers (26%), elbow (21%), distal radius (12%) and metacarpals (11%). Of the 18 suspected fractures (*e.g.* owing to elbow effusions or opaque maxillary antra, where no definite fracture could be visualized), seven (39%) were in the elbow and five (28%) were of the skull or face. Improved training of the casualty officers on the distal arm is required with particular reference to the importance of fat pad signs and subtle angulation of the cortex. The metaphysis at the base of the proximal phalanges of the fingers warrants special attention.

Analysis of lateral cervical spine X ray in the assessment of 134 consecutive multiply injured trauma patients from the Helicopter Emergency Service

R. P. McAvinchey, K. Bhagat, C. Kirk, A. Wilson and W. Hately
Department of Radiology, The Royal London Hospital, Whitechapel, London E1 1BB, UK

During the first year of the Helicopter Emergency Service (HEMS) at The Royal London Hospital, 134 patients were admitted. All patients were clinically evaluated initially. Routine X rays of the lateral cervical spine, antero-posterior (AP) chest X ray, and AP pelvis were then performed. The quality of the cervical spine films was assessed for completeness of anatomical demonstration and the presence of bony and soft tissue abnormality. 12 patients (11%) required further assessment with computed tomographic cervical spine views. Other imaging modalities such as "swimmers" were monitored. A prospective study was commenced for patients where an initial lateral cervical spine view failed to demonstrate C7/T1. These patients were randomized to either a further attempt at a lateral or a swimmers view. Radiographic factors, time to obtain X rays and diagnostic information were assessed and results will be presented. The principal findings suggest that the lateral cervical spine alone is necessary in initial assessment and a guide to further imaging management.

The value of radiograph audit in an accident service department

H. G. Thomas, A. C. Mason, R. M. Smith and C. M. Fergusson
Departments of Radiology and Accident Service, John Radcliffe Hospital, Oxford OX3 9DU, UK

A study was undertaken to assess the numbers and outcome of patients whose initial trauma radiographs had been misinterpreted by the casualty officer when reported by a radiologist and establish the most common errors to improve performance and teaching. In our accident service department all trauma radiographs are reported acutely and those misinterpreted by the casualty officers presented at the daily clinico-radiological conference. Reviewing the 25 798 patients attending the accident service over a 6 month period, 16 246 radiographs were requested and reported. Of these 456 (2.8%) were considered to have been potentially misinterpreted. The errors included 167 (1%) missed fractures, 55 (0.3%) suspected fractures and 72 (0.45) false positive diagnoses of fracture. Subsequently 114 (0.7%) patients required recall for treatment or further imaging. Incorrect diagnoses were seen most frequently in the more commonly injured anatomical sites — the ankle, wrist, foot, elbow and hand. However, the incidence of misinterpretation was highest in examination of the fingers, especially in children. We believe these low figures are principally the result of involving orthopaedic surgeons and radiologists at the formal daily conference. We regard our system of audit as beneficial to patients' care and anticipate reduced litigation which may offset the increased cost of audit.

Computed tomography in blunt abdominal trauma: how helpful for management?

A. R. Padhani, C. J. E. Watson, R. Y. Calne and A. K. Dixon
Departments of Diagnostic Radiology and Surgery, Addenbrooke's Hospital and the University of Cambridge, Cambridge CB2 2QQ, UK

The computed tomography (CT) findings in 92 patients who had suffered blunt abdominal trauma have been correlated with the surgical findings and/or clinical follow-up. In 16 patients surgery followed CT within 24 h; in 10 there was good correlation between CT and operative findings. However, CT failed to detect significant injury in five patients and was falsely positive in another. 67 haemodynamically stable patients were initially managed conservatively in the light of the CT results. 52 of these patients had CT evidence of intraabdominal trauma: 46 were managed conservatively throughout; six underwent subsequent (> 24 h) surgery with good concordance with the CT findings (apart from one missed renal injury). There were three deaths amongst these 52 patients, including one where an injury missed by CT was contributory. The 15 patients with normal CT examinations were all successfully managed conservatively (apart from one late unrelated laparotomy). In nine patients the first CT study followed emergency surgery. CT provided a useful baseline for further management and assessed complications, even though CT failed to demonstrate two small hepatic lacerations seen at previous surgery. Active non-operative management of blunt abdominal trauma is now widely advocated; this report shows how CT can support this policy of surgical restraint.

10.45 – 12.00

Breast Oncology

Hall 10a

Planning radiotherapy treatment for breast cancer

J. R. Yarnold
Academic Radiotherapy Unit, The Royal Marsden Hospital, Sutton, Surrey SM2 5PT, UK

Most current techniques are based on fixed tangential fields to the breast using cobalt gamma rays or 4–6 MeV X rays. Despite the use of wedges as simple tissue compensators, 20% variation in minimum and maximum doses is common, arising to a large extent from longitudinal contour changes and lung attenuation. Systematic and random errors introduced during planning or radiotherapy, *e.g.* from patient movement, will add to this variation although the magnitude is likely to be less than 5%. 20% variation in dose per fraction is expected to have a detectable impact on cosmesis, although it is not clear how important this is relative to other factors such as genetic susceptibility and electron boost. Field placement errors will be reduced in future by on-line megavoltage imaging using beam's eye view devices. The multileaf collimator will also be introduced over the next few years. It can be used as a customized compensator, using the megavoltage imaging system as a source of data for calculating compensator thickness. If these improvements are to be introduced, it will be important to evaluate them in the context of randomized trials, with breast cosmesis as an endpoint. Finally, the matching of an anterior field to the axilla/supraclavicular fossa is best achieved with half-beam blocks. This uses the upper half-beam for the anterior field and the lower half-beam for tangential fields, with a single isocentre located on the field junction in the infraclavicular fossa.

Patterns of axillary lymph node metastasis in breast cancer

M. Van Lancker, C. Goor, R. Sacre, R. Lamote,
S. Van Belle, A. Roelstraete, C. Bourgain and G. Storme
Oncological Center, AZ VUB Laarbeeklaan 101, 1090 Brussels, Belgium

The patterns of axillary lymph node involvement are analysed in a review of 377 cases of T1–4 breast cancers. Clinical judgment of the axillary status proves wrong in approximately one-third of the cases. A strong correlation ($p < 0.01$) between the number of nodes involved, tumour size and blood vessel invasion is found. Other histological or clinical features of the primary (lymphatic invasion, degree of differentiation, presence of necrotic areas) are related to a lesser degree ($p < 0.05$), while others (age, site) are not at all significant. The more nodes resected, the more positives are seen. This is true as well concerning the simple distinction between negative and positive nodes ($p = 0.009$), and the number of nodes involved ($p = 0.003$). Skip metastases above level 1 and 2 are seen in 2% of the cases. A clear influence of the number of invaded nodes on survival can be demonstrated. Level of involvement (level 1 alone *vs.* all others involved except level 1) results in a 5 year survival of 86% *vs.* 76% and a 10 year survival of 84% *vs.* 19% ($p = 0.05$). These findings are discussed, especially concerning the technique, prognostic significance and therapeutic usefulness of axillary dissection.

Which imaging modality should be used in assessing response to treatment in breast cancer patients?

G. Needham, F. J. Gilbert, *J. Brittenden and *O. Eremin
Department of Radiology, Aberdeen Royal Infirmary, and
**Department of Surgery, University of Aberdeen, Aberdeen AB9 2ZB, UK*

The aim of this study was to assess the place of clinical examination, mammography and real-time ultrasound in the assessment of tumour size and to establish which technique could predict response to chemotherapy and final outcome at an early stage in the planned treatment. A cohort of women with T2–T4 breast cancer was given the tumour protein synthesis stimulator L-arginine prior to 4 cycles of CHOP chemotherapy followed by radiotherapy. We have undertaken detailed imaging using real-time ultrasound and mammography prior to each treatment cycle in an attempt to document tumour response. Correlation was made with clinical findings, fine-needle aspiration cytology and histological findings, all patients proceeding to either mastectomy or excision biopsy. 16 patients (18 tumours) with breast cancer have completed the regime. The overall clinical response rate was 39% complete response (CR) and 61% partial response (PR). This compares with a mammographic response of 33.3% CR and 27.8% PR and an ultrasound response of 27.8% CR and 44% PR. Ultrasound or mammography confirmed complete response where this was present clinically. Pathological correlation was made with the final ultrasound and mammographic appearances. An imaging protocol is discussed in patients undergoing extended treatment prior to surgery with the inherent pitfalls and drawbacks of the various imaging methods highlighted.

Imaging of local recurrence of breast carcinoma

T. J. Rissanen, H. P. Mäkäräinen and *M. Heikkinen
*Department of Diagnostic Radiology and *Department of Oncology, Oulu University Central Hospital, 90220 Oulu, Finland*

Because of the increasing incidence of breast carcinoma and the increasing proportion of early-state carcinomas with low mortality found by clinical or screening mammography, the prevalence of breast carcinoma in Finland is estimated to increase by more than 2.5-fold in 2006 compared with 1983. Breast-conserving operations have also increased as breast carcinoma is more often diagnosed at an early stage. A local recurrence after partial breast resection has a good prognosis. It has become a great challenge for both oncologists and radiologists to diagnose local recurrence at a curable stage. In order to evaluate the imaging methods in the diagnosis of the local recurrences of breast carcinoma, we studied all the operated carcinoma cases with the post-operative imaging follow-up sent from the Department of Oncology to the mammographic unit of the Department of Diagnostic Radiology during 1989–1991. This material consists of 89 patients (by the end of October 1991) with breast carcinoma treated with partial or total mastectomy, with or without radiotherapy. The breast operated or the scar after mastectomy and axilla were examined clinically and by imaging methods (mammography and/or ultrasound), and the findings were confirmed by fine-needle aspiration biopsy, histological examination, or clinical and radiological follow-up. The results of this study concerning the sensitivity and accuracy of each of these methods will be presented.

High dose-rate breast implants

C. G. Rowland
FORCE Cancer Centre, Exeter, UK

The dose-rate effect is low for tumour control but high for normal tissue. The critical organ in the breast is skin (rarely involved with tumour in the earlier presentation seen these days) and great effort must be made to reduce the dose as low as possible when working at high dose rate (HDR). The use of a rigid applicator/needle system allows reduction of the skin dose to about 10% of the tumour dose. Also the breast is compressed allowing treatment of a volume approximating a surgical quadrantectomy. In breast cancer, demolitive treatment of the primary complex appears to have little influence on survival and thus the issue is one of cosmesis and local control. Our aim should be to achieve minimal effective treatment and avoidance of overtreatment with its associated side-effects. The data presented suggests that HDR implants used as a boost or primary treatment allow excellent cosmesis with satisfactory local control. Breast conserving procedures have higher rates of local recurrence but approximately 50% of these can be salvaged by further surgery or radiation therapy (if only local treatment has been given) thus achieving results comparable with radical mastectomy. Many women, if fully and honestly informed, may opt for this more pragmatic approach.

Breast conservative therapy: preliminary report with HDR afterloading iridium–192 implants

Sun Shiliang, *Yang Jiaxiang, Li Jian Tang Xinshen, *Pen Yongmei and *Xiang Qian
*Departments of Radiotherapy and *Surgery, Chongqing Cancer Research Institute and Hospital, Chongqing, Sichuan 630030, PR China*

Conservative breast cancer therapy is a rapidly developing technique. It is as efficacious as mastectomy. In March 1990, we started using the high dose rate (HDR) afterloading technique for ^{192}Ir implants in combination with surgery and external beam radiation. 20 patients with T1–T3 tumour, after tumour excision and radical axillary dissection, received an external dose of 45–50 Gy to the whole breast using megavoltage X rays or ^{60}Co gamma ray in conventional fraction. An additional dose of 20 Gy to the tumour bed was delivered by interstitial irradiation with HDR ^{192}Ir afterloading unit according to the Paris system. Preliminary results are satisfactory. The patients feel well themselves. Puncture biopsies to tumour bed were performed 3 months after the therapy and no cancer cells could be found. The results will be discussed.

Breast cancer and thyroid dysfunction — risk and influence on the prognosis

V. Parvanova, L. Marinova and V. Milkov
Department of Radiotherapy, National Oncological Centre, Plopole Strasse 6, 1156 Sofia, Bulgaria

A group of women who have previously undergone surgery of the thyroid, and who subsequently present with breast cancer, are the subject of this study. These patients were treated with surgery, radiotherapy and tamoxifen in a multi-modality approach to their breast cancer. The study has documented the course of both the thyroid disease and the breast cancer and tried to analyse the effect of thyroid hormone status on outcome from breast cancer. A mechanism whereby deficiency, or excess, of thyroid hormones may alter the metabolism of sex steroids and prolactin has been proposed. The interaction of these pathways with tamoxifen is also addressed.

Notes

10.45 – 12.00

Developments of Products for Radiology

Hall 11a

Non-ionic contrast media — the golden idea that was hard to sell

T. Renaa
Nycomed (UK) Ltd, Birmingham B26 3EA, UK

It was the pain during peripheral angiographies that got the young Swedish radiologist Torsten Almén to think about ways to reduce contrast media osmolality and led to his proposal to develop non-ionic contrast media. The contrast medium companies were, however, not interested in this idea before he met Dr Hugo Holtermann from Nycomed. The first result was Amipaque* (metrizamide). Most of the pharmaceutical companies working with X ray contrast media are now supplying non-ionic contrast media. Today this group of products has taken over a major part of the use of contrast media because of their lower toxicity, improved safety and less discomfort than ionic contrast media. The different stages from the ideas of Dr Almén to the present situation will be presented and discussed.

Development of new X-ray films: experience and opportunity

G. Elsner
Department of Research and Development, Du Pont de Nemours (Deutschland) GmbH, Dornhofstrasse 10, 6078 Neu-Isenburg, Germany

The objective of this presentation is to gain radiologists' understanding and active support of the crucial role they have in new product development. The European Du Pont diagnostic imaging organization uses ISO 9001 methodology in product development and has received corresponding official certification from the German affiliate of ISO, the International Standards Organisation, in January 1991, as the first X-ray film manufacturer in the world. The Du Pont methodology includes a tool called Quality Function Deployment (QFD) for identifying and specifying radiologists' needs, converting their needs into product design requirements and following a disciplined path towards product robustness in manufacturing. Experiences gained in a recent development of a high-resolution blue-sensitive "full speed" screen film — Cronex* 4 Improved — are described to highlight both the strong benefits, as well as some limitations of QFD. It is concluded that successful product development requires a delicate balance of "widely" creative thinking supported by related scouting research, and of meticulously following a methodology with well-defined phases, the methodology itself being continuously improved based on experiences gained.

10.45 – 12.00

Radiobiology Day: Session I

In memory of Dr N. McNally

Hall 11b

Theoretical and experimental aspects of fractionation

M. C. Joiner
Cancer Research Campaign Gray Laboratory, P.O. Box 100, Mount Vernon Hospital, Northwood, Middlesex HA6 2JR, UK

The study of fractionation has developed from the need to understand the scientific basis of clinical radiotherapy. It is therefore a broad subject with a long history; however, the most important advances have taken place during the past 20 years as a result of the development of endpoints for normal tissue damage in laboratory studies. An emphasis on normal tissue as well as tumour radiobiology results directly from the concern of radiotherapists to treat cancer by the maximum dose possible that will not cause irreversible long-term damage to normal tissues in the radiation field. From this research it has emerged that the relationship between the total tissue-tolerance dose and the dose per fraction is different for tissues which react acutely after radiotherapy (*e.g.* skin, gut, mucosa and marrow), and the late-reacting tissues (*e.g.* lung, spinal cord and kidney). Tumours behave like acutely responding tissues. The conclusion is that use of lower doses per fraction (< 2 Gy) is therapeutically beneficial because it spares critical late normal tissue damage more than damage to tumours. However, this approach (hyperfractionation) is really only clinically viable if doses are given more than once per day. It is then important to know what interfraction interval should be used. Halftimes of repair of sublethal damage in tissues are generally between 0.5 and 2 h so that intervals of > 6 h should allow most repair to occur. Intervals less than 6 h should definitely not be used and clinical disasters have occurred in such trials, with excessive late tissue damage. However, in some tissues, notably the spinal cord, repair is more complicated with a "slow" component acting out to 24 h. In these cases extreme caution is needed when giving multiple doses per day and biological treatment planning based on the modern linear-quadratic and incomplete repair models should be used to check that tissue tolerance is not exceeded. Multiple doses per day are also given to reduce the overall treatment time. This approach (accelerated fractionation) has emerged from the study of tumour cell kinetics which has shown that significant cell proliferation during a treatment course can substantially offset the effect of radiotherapy. However, the extent of this proliferation varies between patients and so methods are being developed to assess tumour cell proliferation in each patient before therapy. The balancing of overall treatment time, number of fractions and interfraction interval to maximize the effect of therapy for each patient, is currently a challenge to both radiobiologists and radiotherapists.

Effects of repopulation of an HDR-, MDR- and LDR-radiotherapy on epidermoidal cervix carcinoma cells (Ca-Ski Cells) and primary human keratinocytes (HPK-cells)

R. Schulz-Wendtland, M. Bauer, T. Bauknecht and M. Dürst
Department of Gynaecological Radiology, Radiological Center, University of Freiburg, G-7800 Freiburg, Hugstetterst. 55, Germany

We carried out experiments on epidermoidal cervix carcinoma cells (Ca-Ski cells) and primary human keratinocytes (HPK-cells) obtained after transfection with human papillomavirus type 16 DNA, varying the dose rate (28–8000 cGy/h), the doses (1–100 Gy) and the fractioning (protracted, 3, 6 and 12 fractions) to verify the effects of repopulation. Overall, we made 50 000 measurements. Our conclusions are: (1) At dose rates of 75 cGy/h (Ca-Ski cells) and 110 cGy/h (HPK-cells) respectively, we found that the cells "fall asleep" at doses up to 100 Gy; the rate of cell mortality is insignificantly higher than the proliferation rate. (2) A first-time proof of an accumulation of repopulation effects (recovery from the sublethal radiation damage, progression of the cells during the partial cycle/proliferation and the acts of redistribution), if the radiation exposure reaches the median time of the cell cycle (HPK-cells, dose rate: 110 cGy/h, doses: 1–100 Gy). (3) At dose rates higher than 300 cGy/h (range of a percutaneous radiotherapy), we found that the survival rates of the cells could only be increased insignificantly in spite of a fractionated therapy (3, 6 or 12 fractions; doses: 1–100 Gy); the repopulation effects almost vanished. The results will be discussed with regard to the clinical relevance.

Tumour-dependent changes in the metabolic steady-state of CaNT tumours

D. Szeinfeld, N. de Villiers and S. Wynchank
Research Institute for Medical Biophysics, Medical Research Council, Tygerberg, 7505, South Africa

T_1 (spin lattice) and T_2 (spin spin) relaxation times were determined at 0.5 T for CaNT tumours in CBA mice. Tumours of different sizes were studied. The variation in the activities of hexokinase (HK), lactate dehydrogenase (LDH) and ATP concentration with tumour volume were also measured under normoxic conditions. The tumours were maintained by serial passage by the inoculation of 0.1 ml of a tumour cell suspension in McCoy's 5A medium and containing approximately 2×10^6 cells, subcutaneously into the sternal area of the mice. Tumours were assumed to be spherical and their volumes calculated by measurement in three perpendicular directions with a Vernier calipers. The T_1 and T_2 values, determined from regions of interest which excluded normal tissue, can reflect degrees of heterogeneity of tumour tissue and molecular levels of organization. A decreasing trend of both T_1 and T_2 values with tumour size was seen. Changes in the levels of the compounds with increasing tumour volume indicate energy deprivation associated with the degree of hypoxia in the tumour. Hypoxia, a typical solid tumour feature, is rare in normal tissue and arises from solid tumour blood vessels being more disorganized than those of normal tissue. Depletion of O_2 and other nutrients therefore occurs and in larger tumours circulation may cease in whole sections. Cells furthest from capillaries are hypoxic and anoxic. Hence averaged T_1 and T_2 can reflect the fraction of hypoxic and anoxic tissue. These values are also influenced by the tumour growth rate and ratio of free and bound water in the tissue. So this study may allow for better understanding of the degree of tumour hypoxia and hence radioresistance, with practical consequences for more effective radiotherapy.

Chemical protection of normal rodent tissue by exogenous ATP after neutron irradiation

D. Szeinfeld and N. de Villiers
Research Institute for Medical Biophysics, Medical Research Council, Tygerberg, 7505, South Africa

This work is concerned with the radioprotective role of ATP to reduce radiation damage to normal tissue. Male BALB/c mice aged from 6 to 8 weeks, were used for all the experiments. To obtain survival data after a lethal dose of neutron irradiation, they were divided into two groups. Group 1 received a dose of 6 Gy of neutrons only. Group 2 was treated with exogenous ATP prior to receiving the same dose of neutrons. The effect of exogenous ATP to protect the mice against neutron beam exposure was examined by using survival for 30 days post-irradiation as the end-point. The irradiation was carried out at the NAC cyclotron, Faure, using neutrons of the radiotherapy beam, produced by the reaction p(66 MeV)/Be. At selected times after 6 Gy neutron irradiation, the mice were killed for determination of the activities of acid phosphatase, hexokinase, glucose-6-phosphatase dehydrogenase (G6P-DH) and lactate dehydrogenase (LDH) in the testes. Exogenous ATP was administered by slow intraperitoneal injection of aqueous solution at 700 mg/kg body weight, 20 min before irradiation to study mice survival and the glycolytic enzymes post-irradiation. The dose modification factor in the activity of acid phosphatase as a feature of cell injury was determined by using the following ATP concentrations: 8, 25, 80, 250 and 700 mg/kg body weight. Survival of the mice, using 30 days post-irradiation as the end-point, was increased from 40% to 85% by action of the exogenous ATP. Furthermore, ATP's glucoregulatory effects, which modify basal physiological regulatory processes were studied in the testes and caused significant augmentation in the activities of the glycolytic enzymes HK, G6P-DH and LDH when compared with neutron radiation alone. Finally ATP reduced the activity of testicular acid phosphatase. The response of the activity of the enzyme acts as an indicator of lytic processes in the tissues damaged. These radioprotection actions in BALB/c mice reflect an adaptive defence mechanism to maintain homeostasis in response to the radiation injury.

The interaction of radiation and cisplatin in a transplantable hepatocarcinoma

M. J. Tomlinson and A. W. Preece
Department of Pathology, The University of Bristol, Bristol BS8 1TD, UK

The L10 hepatocarcinoma in the guinea pig is a slow growing tumour with a T_{pot} of 43 h, which was transplanted into the flank of the animal from an ascitic form. Tumour growth delay curves were produced for cisplatin alone and radiation alone. The interaction of radiation and cisplatin was investigated using a clinically relevant dose (3 Gy X rays). Radiation was administered to the tumour locally using 250 kVp X rays; cisplatin (2.5 mg/kg or 5 mg/kg) was injected intraperitoneally either immediately preceding or 6 h following the radiation. Tumour growth delay was assessed. All treatment was given 6 days after the inoculation of 10^6 tumour cells. An isobologram was constructed using the method described by Steel and Peckham, taking a growth delay of 10 days as the iso-effective dose. The dose of cisplatin, when injected 6 h after radiation, required to produce this degree of growth delay fell within the envelope of additivity. However a supra-additive response was observed when cisplatin was given immediately before the radiation. The clinical implication of this study is that when combining cisplatin with radiotherapy the two agents should be administered together. Frequently cisplatin is given after radiation because of its emetogenic potential, when additivity alone might be expected.

Effect of transfected EBV EBNA-1 on the radiation survival curve of BALB/C 3T3 cell line

Y.-S. Tyan, F.-D. Chen, Y.-S. Chang and S.-T. Liu
Molecular Genetics Laboratory, Department of Microbiology and Immunology, Chang-Gung Medical College, Kwei-Shan, Taoyuan, Taiwan

Epstein–Barr virus (EBV) is a human herpesvirus. This virus can infect both lymphoid and epithelial cells *in vitro* and can be found in many tumours such as Burkitt's lymphoma, lymphoma in immunocompromised patients, and in nasopharyngeal carcinoma (NPC). Although the direct evidence of EBV being the aetiological agent of NPC has yet to be established, biochemical and immunological evidence suggested that NPC is closely associated with EBV. For example, EBV-encoded nuclear antigen 1 (EBNA-1) was found in all the NPC tissues and latent membrane protein (LMP) was found in 65% of the NPC biopsies examined. If the radiosensitivity of NPC clinically is caused by the presence of EBV, this effect must be determined by one (or both) of these two proteins. This study used the cloned EBV EBNA-1 to co-transfect the mouse fibroblast cell line BALB/C3T3 with a G418-resistant plasmid pN2. The effect of EBNA-1 on the radiation survival curve of this cell line and its implications will be discussed.

In vivo study of rabbit irradiated skeletal muscle by NMR imaging

A. Francois-Joubert, J. L. Leviel, J. L. Lefaix and J. L. Lebail
Inserm U 318, Hôpital Albert Michallon, Pavillon B, BP 217 X, F 38043 Grenoble, France

Surgical treatment of an irradiated area needs an exact and sensitive imaging technique. We investigated the possible use of magnetic resonance imaging (MRI). Two groups of 16 rabbits were irradiated on the left iliospinalis muscle with an iridium-192 scaled source ($E_{\gamma} = 0.38$ MeV). The dose rate at 2 cm depth was 10 Gy for Group 1 and 20 Gy for Group 2. Proton imaging was performed regularly during 8 months for each rabbit in a 2.35 T imaging system with a special probe including a half saddle coil and a restraining system for the anaesthetized rabbit. Transverse images (2DFT 3000/34) were obtained before and after intravenous administration of Gd-DOTA (0.3 mmol/kg). In Group 1, five out of eight rabbits had a superficial muscular lesion without atrophy at the 22nd week. In Group 2, six out of eight had an extended muscular lesion with an important atrophy at the 18th week. (Two rabbits died after anaesthesia at the 13th and 17th weeks.) Histological findings obtained on another group of rabbits have shown some necrosis with fibrosis in the irradiated area from the 30th week for Group 1 and the 20th week for Group 2, and an inflammatory lesion from the 10th week in Group 1 and the 4th week in Group 2. An MRI lesion could probably be better explained by necrosis and the progressive fibrosis substitution than by inflammation.

12.15 – 1.15

Silvanus Thompson Memorial Lecture

Hall 9

The gene as a theme in the paradigm of cancer

E. J. Hall
Center for Radiological Research, Columbia University, New York, NY 10032, USA

An excess incidence of cancer and leukaemia was observed in the early radiation workers within a few years of the discovery of X rays. Thus, radiation was added to the bewildering array of physical, chemical and viral agents identified as able to cause cancer. The common mechanisms involved are only now becoming clear. There are four lines of research, rapidly converging, that illustrate how the function of specific genes can regulate cell behaviour — including transformation to a malignant state. (1) In the leukaemias and lymphomas, the activation of cellular oncogenes is important. The genes involved are present in all normal cells and are often associated with cell growth and regulation. When activated, they act in a dominant fashion to cause a cell to express the malignant phenotype. (2) In solid tumours, a more important mechanism may be the loss of a suppressor gene which acts in a recessive mode, *i.e.* both copies must be lost for a malignancy to be expressed. The classic example is retinoblastoma; the gene has been cloned and found to be associated with several other common cancers. It is likely to be one of a family of such genes. It may well be that the activation of one or more oncogenes, or the loss of one or more suppressor genes, or both is required for a tumour to progress from initiation through promotion to a metastasizing malignancy. (3) Recent studies indicate that heterozygotes of repair-deficient syndromes such as Ataxia Telangectasia are much more likely to develop cancer and may also be more sensitive to radiation induced malignancies. (4) The most recent candidate gene is the molecular checkpoint gene. This gene causes cells to stop in G_2 following exposure to DNA damaging agents, before proceeding with the complex task of mitosis. Mutants in which this gene is defective, missing or otherwise inoperative are exquisitely sensitive to killing by X rays or UV. To date these experiments are possible only in lower organisms, such as yeast, but homologues in mammalian cells are actively being sought. Defects in cell cycle regulating genes are likely to be the key to cancer induction.

2.15 – 3.45

Non-vascular Interventional Techniques

Hall 9

Non-vascular interventional radiology — biliary disease and stents

Ch. L. Zollikofer, F. Antonucci, G. Stuckmann,
P. Mattias and M. Heer
Institut für Radiologie, Kantonsspital Winterthur, 8401 Winterthur, Switzerland

Self expanding metallic stents with a diameter of 6–10 mm have been developed to improve long-term patency in benign and malignant biliary duct obstruction. We have treated 55 patients with the Wallstent-type endoprosthesis, 52 patients for malignant and three patients for benign disease. The stents were introduced percutaneously via a transhepatic approach in 44 patients and endoscopically in eight. Of the 52 patients with malignant disease, 44 died between 4 days and 19 months (mean survival 6 months). Eight patients are alive after 6 weeks to 14 months (mean 6 months). Stent obstructions occurred in 11 patients (21%). Nine of these patients were successfully treated with a secondary intervention. Treatment consisted of removing sludge or additional stent implantation. In three patients the obstruction was due to tumour overgrowth and in another three to tumour ingrowth through the mesh of the stent and in five patients due to sludge or food incrustations. Serious complications included cholangitis (six; 11.5%), and gallbladder hydrops (two; 3.8%). There was one procedure-related death due to cholangitis and bleeding (1.9%). The 30 day mortality was 15%. The three patients with benign disease were followed from 3 to 5 years. In two patients the stents occluded due to sludge and mucosal hyperplasia prompting a secondary percutaneous intervention. Use of the Wallstent is now our preferred method for palliation of malignant obstruction. The stent occlusion rate until death of 21% compares favourably with conventional plastic stents. For benign disease our experience is limited, however a conservative approach with stenting as the last non-surgical step seems advisable.

Fluoroscopically guided percutaneous gastrostomy

R. F. McLoughlin and R. G. Gibney
Department of Diagnostic Imaging, St Vincent's Hospital, Elm Park, Dublin 4, Ireland

We describe our experience with fluoroscopically guided percutaneous gastrostomy. A total of 16 patients was prospectively studied. The indication for gastrostomy was bulbar palsy in 12, head and neck carcinoma in three and duodeneo-enteric fistula in one patient. A COPE nephrostomy pigtail catheter (#10–#14 French in size) was inserted into the stomach under fluoroscopic guidance and local anaesthesia in all cases, and feeding via the tube commenced the following day. Two of the tubes (12%) became dislodged within a week of insertion, but with no complications. A further tube was removed due to patient dissatisfaction. In nine cases (56%), the tube remained patent until no longer needed, or is currently patent. Four tubes (25%) required changing because of wound site infection (2), tube blockage (1), or gastro-oesophageal reflux (1). Of these, one required a further tube change because of tube displacement and another required four further tube changes over several months because of tube blockage. All tube changes were performed along the mature tract of the original tube. Of the 25 tubes studied, the average patency rate is 9.2 weeks. We conclude that fluoroscopically guided percutaneous gastrostomy is a safe, successful method of enteral feeding.

The Holmium–YAG laser: safety in the biliary tract and elsewhere

M. Blomley, D. A. Nicholson, *C. Foster, †A. Bradley and †M. Myers
*Departments of Radiology, *Histopathology and †Medical Physics, Hammersmith Hospital, Du Cane Road, London W12 0HS, UK*

The Holmium laser has potential use in percutaneous cholecystectomy and gallstone lithotripsy. There is, however, a paucity of data regarding its effect on tissues and penetration in different media. We examined the effect of the laser on human gallbladder tissue at various energies with the laser fibre in direct contact with the tissue. Microscopic examination revealed zones of thermal damage with limited (< 1 mm) lateral extension from the ablation site. 20 shots at 130 mJ, caused near perforation of the gallbladder wall. Histological effects of tissue damage will be presented. We also examined penetration of the infrared beam through air, saline, bile, urine, blood, iohexol and diatrizoate solutions and admixtures. An exponential model of attenuation fitted the data very closely ($R^*2 > 0.99$ for all media). All media, except blood had a similar attenuation coefficient (range 2.1 to 2.8 mm^{-1}), blood had a coefficient of 4.6 mm^{-1}. We conclude that bile and other media strongly attenuate the laser's energy within a short distance, but when the fibre is in direct tissue contact, perforation is readily achieved. Therefore, clinical use of the Holmium laser in the biliary tract should be via a dual lumen catheter/basket system in order to prevent perforation. The results of the data will be discussed in relation to safety of the Holmium laser in different interventional radiological applications.

An assessment of the Holmium–YAG laser for fragmenting gallstones

D. A. Nicholson, M. Blomley, G. Bartal, *A. Bradley, *M. Myers, †W. Man, ‡C. Foster and L. Banks
*Departments of Radiology, *Medical Physics, †Biochemistry and ‡Histopathology, Hammersmith Hospital, Du Cane Road, London W12 0HS, UK*

The feasibility of using a Holmium laser to fragment large gallstones was examined *in vitro*. The energy from this 2.1 μm pulsed laser is transmitted through a flexible, 0.6 mm diameter fibre, which can be passed down an endoscope. The fibre was placed in close proximity to a gallstone, grasped in an endoscopy basket and immersed in a saline-filled beaker. A metal grid with 3 mm diameter holes was placed mid-way in the beaker. Fragmentation was complete when all fragments passed through the grid. To date, 29 large gallstones (mean mass 1.26 g) have been fragmented. A mean of 515 shots was required at a frequency of 5 Hz. The number of shots required increases approximately linearly with the stone mass. Fibretip degradation was investigated; a statistically significant ($p < 0.05$) fall-off in power output was demonstrated; technical aspects are discussed. All stones underwent physico-chemical and computer tomographic analysis. Cross-correlation with fragmentation data will be presented, showing the difference in energy required to fragment different stone types (rimmed, cholesterol, pigment). The Holmium laser can effectively fragment gallstones and therefore has potential uses in fragmenting retained common duct stones at ERCP and gallbladder stones prior to percutaneous cholecystectomy, adding to its already established uses in surgery and laser angioplasty.

Pelvi-ureteric junction obstruction — treatment by balloon dilatation in 21 patients

S. Garber, D. Rickards and J. Castro
Department of Radiology, The Middlesex Hospital, Mortimer Street, London W1N 8AA, UK

Pelvi-ureteric junction (PUJ) obstruction is surgically treated by open Anderson Hines or Culp pyeloplasty. Less invasive therapies have been developed including percutaneous endopyelotomy and balloon dilatation. A total of 21 patients (M:F 12:9; aged 23–78, mean 43 years) had radiological and renographic evidence of significant PUJ obstruction. Three patients were asymptomatic and 18 complained of intermittent loin pain. At cystoscopy, the ureteric orifice was catheterized with a guide wire and a 10 mm, 4 cm balloon passed over it into the PUJ. Dilatation was performed. Rupture of the PUJ, as evidenced by contrast extravasation, was seen in 16 cases. The ureter was stented for 6 weeks with a JJ stent. Technical success was achieved in all patients. Clinical improvement was seen in 17 patients at follow-up, supported by both renographic and radiological evidence. No improvement was seen in four and three of these went on to open pyeloplasty. Minor immediate post-operative complications were common. Major late complications occurred in one patient who developed a PUJ stricture that required open surgery. When compared with the success reported for percutaneous pyelolysis (80%) and Anderson Hines Pyeloplasty (85%), balloon dilatation compares well (76%). Complications are few and failure can be corrected by surgery or potentially a repeat dilatation. PUJ balloon dilatation is an effective, minimally invasive treatment for PUJ obstruction.

Renal biopsy in diffuse renal disease — experience with a 14 gauge biopsy gun

K. T. Tung, M. O. Downes and *P. J. O'Donnell
*Department of Diagnostic Radiology, Kent and Canterbury Hospital, Canterbury CT1 3NG, UK and *Department of Histopathology, King's College Hospital, London SE5 9RS, UK*

We retrospectively review our experience of percutaneous renal biopsy (PRB) in native kidneys with diffuse disease to assess the efficacy and safety of a 14 gauge biopsy needle in an automated gun (Biopty TM, Uppsala). 104 biopsies in 103 patients (64 male, 39 female; age range 14–78 years, mean 45.4 years) were performed by single radiologists (one consultant or one of a number of senior registrars) using a 14 gauge Biopty needle with continuous ultrasound guidance. 103 of 104 (99%) procedures resulted in sufficient tissue for light and electron microscopy and immunofluorescence allowing a definitive diagnosis. An average of 2.6 passes were made at each procedure with a mean of 13.4 glomeruli per tissue core. There were four (3.8%) minor complications of transient macroscopic haematuria. Three (2.9%) significant complications consisted of two symptomatic perirenal haematomas and one arterio-venous fistula which was successfully embolized. Our diagnostic and complication rate compare favourably with published rates using various techniques and different needles. The importance of sample size with regard to accurate diagnosis is discussed. We suggest that use of the 14 gauge Biopty gun guided by real-time ultrasound should currently be the method of choice for PRB in adults.

Mechanical and ultrasonic properties of urinary stones

N. P. Cohen, H. N. Whitfield, *J. C. Shelton and
*G. P. Evans
*Department of Urology, St Bartholomew's Hospital, West Smithfield, London EC1A 7BE and *Interdisciplinary Research Centre, Queen Mary and Westfield College, Mile End Road, London, UK*

Urinary stones are now treated by extracorporeal shockwave lithotripsy and/or percutaneous stone surgery. Some stones can prove remarkably resistant to these techniques. A study has been performed to examine the physicochemical and acoustical parameters of kidney stones with the aim of predicting the ease of fragmentation. 30 intact urinary stones were rehydrated. Parallel surfaces were machined. One of the two offcuts from each stone was analysed for composition and structure by infrared spectroscopy and scanning electron microscopy; the other embedded in a polyester resin, polished and microhardness tested with a Shimadzu microhardness tester. The speed of ultrasound through the stones was measured using a pulse transit time technique. Stones were placed in a water bath between two 1 MHz transducers of 11 mm diameter, connected to a generator/digital receiver and PC IBM-compatible computer. Density of the stones was measured using Archimedes' principle and a theoretical modulus of elasticity calculated from:

$$E = C^2\sigma$$

where E is the Young's modulus and σ is the density.
Compression testing with an Instron testing machine gave a direct measure of the modulus and compressive strength. Stone specimens were fragmented in the focus of the Dornier MPL 9000 lithotripter. Early results have shown an increase in the parameters for the series struvite to brushite as follows:

Stone type	Density (mg/mm^3)	Modulus	Velocity (m/s)	Microhardness (Vickers)
Struvite	1.6	7.2	2116	43
Uric acid	1.8	11.9	2602	68
Calcium oxalate	2.1	11.9	3004	108
Brushite	2.2	32.6	3808	142

The relationship between ultrasound velocity and the modulus characteristics of stones may be useful in predicting the resistance of stones to fragmentation *in vitro*. Presently there is no satisfactory method for determining the composition and structure of stones before treatment. Clinical methods for measuring the velocity of sound through stones in the clinical situation are being investigated.

Percutaneous balloon dilatation for transport ureteral stenosis

D. A. Nicholson, M. Sheikh, N. Chetty and G. Williams
Department of Radiology, Hammersmith Hospital, Du Cane Road, London W12 0HS, UK

We have reviewed 15 patients who have undergone percutaneous dilatation of distal ureteric strictures following renal transplant. Obstruction was clinically suspected in all patients by rising blood creatinine levels and comparison ultrasound scans. The time from transplantation ranged from 2 to 48 months (mean 13 months), with 11 out of the 15 patients having had temporary stenting (4–7 weeks) following transplantation. In all cases dilatation was performed with 8–10 mm (larger than in most previous series), high pressure balloon catheters passed over a rigid guide wire. 12 strictures were fully dilated, with seven patients requiring more than one dilatation. 10 out of 15 patients were successfully managed with nephrostomy drainage and balloon dilatation only, all showing progressive reduction in creatinine levels; follow-up has ranged from 3 to 12 months. One complication of frank haematuria was encountered following dilatation; this was managed non-operatively. The remaining five patients required other procedures after partial balloon dilatation, including stent insertion and endoscopic ureterotomy. The success of balloon dilatation was not related to time from transplantation, however it appears that the late occurring strictures are more difficult to dilate requiring several balloon dilatations. Antegrade dilatation is successful in treatment of transplant ureteral stenosis. Post-dilatation stenting as advocated by other authors is not needed in the majority.

Complication rate of combined endoscopic and percutaneous stent insertion

M. B. Sheridan and D. F. Martin
Department of Radiology, University Hospital of South Manchester, Manchester M20 8LR, UK

Endoscopic insertion of biliary stent has a success rate of 90% with a complication rate of approximately 10%. In those patients in whom endoscopic stenting fails, percutaneous transhepatic assistance (the combined procedure

(CP)) is used, although a high complication rate has been reported. We have reviewed our complication rate for CP in 40 consecutive patients. Following failure of endoscopic stent insertion, PTC with external drainage is performed within 72 h, followed by CP and stent insertion, again within 72 h. All procedures are performed under antibiotic cover and sedation using midazolam and nalbuphine. 39 patients had successful CP. The total procedure related complication rate was 32.5% with a 2.5% 30 day mortality. Cholangitis occurred in nine patients, haemobilia in one; one developed a right subphrenic collection and two developed severe right upper quadrant pain. All complications settled on conservative treatment. Our complication rate for ERCP, PTC and CP is higher than for endoscopic stenting alone, but complications were minor. We suggest that the complication rate for these procedures can be kept to a minimum by adherence to antibiotic and fluid regimes and by early recourse to staged CP.

Notes

Transuretheral ureteric stent retrieval using the Amplatz snare

I. Robertson, R. Edwards and A. Jardine
Department of Radiology, Western Infirmary, Glasgow G11 6NT, UK

Internal ureteric stents are widely used transiently to maintain ureteric patency and removal/replacement usually requires general anaesthesia. The Amplatz goose neck snare enables non-operative transuretheral stent retrieval and a technique using the snare introduced via a haemostatic sheath is described. Stent retrieval has been performed in 20 female patients using mild intravenous sedation and topical uretheral anaesthesia. The length and course of the male urethera make manipulation more difficult but this has been successfully negotiated using a steerable catheter system. Procedural times are less than 20 min with screening times of approximately 2–3 min. In addition, stent replacement has been performed in five patients. There have been no post-procedural complications and the procedure was well tolerated by all patients. This technique offers a simple, safe cost-effective technique for transuretheral stent retrieval/replacement which can be performed under local anaesthesia.

2.15 – 3.45

Radiological History

Hall 10a

1927 and after: the Annual Congress in retrospect

N. G. Trott
Cheam, Surrey SM1 2DR, UK

In Central Hall, Westminster, the amalgamation of the Röntgen Society and the then BIR to form the present Institute was celebrated on 17 and 18 November 1927 in our 1st Annual Congress, which included a Technical Exhibition by 20 firms. The story of those Congresses, the first 42 in London and subsequently on tour, can be traced in the *BJR* and BIR Annual Reports supplemented by personal recollections, especially since December 1952, the first post-war Congress. One reflects on the dinner in 1929, with the speeches reported in 5000 words in the *BJR:* notes a paper at that same Congress describing the overwhelming superiority of Germany over Britain in the quality and provision of radiological equipment; recalls that revolutionary presentation of 20 April 1972 by Ambrose and Hounsfield. Until recently, meetings at Congress consisted almost entirely of some 30–40 invited papers in pre-arranged Symposia. Manchester 1985 saw a transformation, a joint venture with other societies: 150 papers, many proffered, on the theme "Information Technology in Radiology" and, for the first time for many years, a large Technical Exhibition. But, all Congresses and their dinners come to an end: will Birmingham 1992 match the 1929 Burlesque, a Radiological Drama in One Act, "Blood and Whitewash"?

Encephalography, development and introduction into clinical (neuro-)radiology

Hans-Joachim Maurer and A. Wolfgang Pulst
Department of Radiology, Faculty of Medicine, University of Malaya, 59100 Kuala Lumpur, Malaysia

In 1919 Dandy reported on eight patients investigated by translumbar insufflated air into the ventricle system. With respect to possible complications, Dandy abandoned this procedure in favour of ventriculography: air insufflation through one or two holes in the dorsal parietal bone (1920) used before in children as transfontanellar access (1918). Wideroe tested the translumbar air filling of the ventricle system at about the same time but did not continue regarding the bad quality of contrast in some test cases. On the other hand, Bingel developed, independently of Dandy as well as Wideroe due to his own testimony (1921), the translumbar encephalography at the Medical Department, LKA Brunswick, Germany. Based on a trial of 30 patients as well as corpse tests he had done in 70 patients a translumbar encephalography without adverse reactions. The results have been published by Bingel (1921) mentioning references of Dandy's papers as well as Wideroe's paper. Based on this publication, 10 further papers, and some lectures, the translumbar encephalography was introduced into clinical routine (neuro-)radiology in Germany as well as Europe, probably all over the world. The abandonment by Dandy would have perhaps completely eradicated this procedure with respect to his reputation as leading neurosurgeon of the USA and probably the whole world at that time. Introductions of cerebral angiography (Moniz), later CT and last MRT as well as magnetic power measurement have displaced completely translumbar encephalography (Dandy, Bingel) as well as ventriculography (Dandy).

The birth and development of the X-ray motor car

J. M. Guy
Department of Radiology, Yeovil District Hospital, Higher Kingston, Yeovil, Somerset TA12 6NS, UK

Pioneer motor cars and early X-ray sets grew up together at the end of the nineteenth century. For the first 20 years of this century the development of both was linked to provide mobile radiography. At first, the car was merely the means of transport for the equipment. Later the engine provided the source of electrical power. A civilian radiologist in England described one of the earliest X-ray motor cars. British, French, German and American engineers designed X-ray vehicles with some degree of sophistication during the First World War, mainly for military use.

The Nuffield Institute for medical research, Oxford, and the radiology of the throat

S. J. Golding
Department of Radiology, University of Oxford, UK

This is a story of fortuitous combination of funding, facilities and talent. Lord Nuffield's benefaction to the University in 1936 and personal interest in the development of cineradiology provided conditions for the veteran pioneer radiologist from Manchester, Alfred Barclay, to establish the Institute as an important centre of cineradiological research, in particular of the fetal circulation. From this fertile ground grew the investigation of swallowing and the airway. In 1948 Dr Gordon Ardran arrived at the Institute to replace Barclay and formed a collaboration with Dr Fred Kemp, from Oxford's Radcliffe Infirmary. Both men were gifted with enquiring and scientific minds and almost immediately began a steady stream of fundamental observations on the functional anatomy of the throat. This continued for 30 years, despite Ardran's other major interest in radiological protection and quality control, and Kemp's increasing involvement in the development of the Radcliffe Infirmary as a teaching hospital. Today some of these publications are 40 years old, but they are still frequently cited in the literature and the accuracy of Ardran and Kemp's work has never been seriously disputed. This review describes their work and examines its significance to current practice in imaging the pharynx and larynx.

Dr John Hall Edwards: Birmingham's X-ray martyr and first radiologist

J. G. L. Cole
Formerly consultant radiologist, Dudley Road Hospital, Birmingham, UK

Dr John Hall Edwards, born in 1858, followed in the footsteps of his father and grandfather who had also practised in the city of Birmingham. Setting himself up in a practice in Moseley, he became very much involved with photography, and on the evening that the news of Roentgen's discoveries were leaked to the Vienna press he decided with his friend Dr Ratcliffe to assemble a unit and radiographed his hand. In February 1896 a needle was successfully removed from the hand of Mrs Berry, which Edwards had located. From this his work expanded and he moved to some rooms close to the Medical School and the General Hospital to which he was appointed surgeon radiographer, a post he held until 1919. Came the Boer War and after much persuasion the War Office allowed him to set up a unit in the 1st Yeomanry Hospital in Deelfontein. His articles to local papers both from South Africa and from home were much appreciated and he was awarded membership of the Press Council. He also continued with his photography. Alas he noticed that his hands were becoming affected by the rays and because of a cancerous skin lesion his hand was amputated. He continued to work, painted, wrote articles, edited the Archives of Roentgen Ray. During the First World War he supervised the X-ray facilities not only for Birmingham but also for southern command. After the War, he entered local politics as member from Rotton Park, but ill-health gradually rendered him less and less mobile so that near the end he was confined to a wheelchair. His name is inscribed on the memorial to the X-ray martyrs in Hamburg and his efforts to introduce radiation protection have been of immense value to following generations of radiation workers.

2.15 – 3.45

Musculoskeletal Imaging

Hall 10b

Ultrasound of the spine in infants with lumbosacral skin lesions

J. Vive and A. C. Lamont
X-ray Department, Leicester Royal Infirmary, Leicester LE1 5WW, UK

A total of 30 infants with lumbosacral skin lesions referred for neurospinal ultrasound over an 18 month period was studied retrospectively to assess which cutaneous markers were most often associated with closed spinal dysraphism. 20 infants with a simple low-lying dimple and one with a pilonidal sinus had normal scans. Two infants with sacral skin swelling had a subcutaneous abscess but no neurospinal abnormality. Three of four infants with hairy patches had anormal scans (one with multiple vertebral abnormalities, one with a conal cyst and one with a tethered cord). Capillary naevi were seen in one otherwise normal infant and in the infant with a hairy patch and vertebral abnormalities. A high-positioned dimple was present in a second infant with tethered cord syndrome. A case of lipoma of the filum terminale presented with a skin tag offset from the midline. In conclusion, ultrasound is a reliable and non-invasive technique for the early screening of lumbosacral skin lesions for closed spinal dysraphism with the prognosis varying from very good for low-lying simple dimples to relatively poor for most hairy patches. However, the early identification of closed spinal dysraphism has allowed more successful management of these patients.

Ankylosing spondylitis: a comparison of clinical and radiographic features in men and women

S. Eustace, R. J. Coughlan and C. McCarthy
Departments of Radiology and Rheumatology, Mater Misericordiae Hospital, Eccles Street, Dublin 7, Ireland

The clinical and radiographic features of ankylosing spondylitis in men and women are felt to differ. Reisnick concluded that women presented at an earlier age, with more peripheral and cervical spine arthritis and tended to have more benign disease. This study was undertaken to compare clinical presentation, radiographic features, course and complications in 83 patients conforming to the Rome criteria. There were 64 males and 19 females, mean ages at presentation of 23 years and 26 years, followed for a mean of 13 and 11 years. At presentation, females had more peripheral arthritis and asymptomatic sacroilitis ($p < 0.001$). Males had more symptomatic sacroilitis ($p < 0.001$). Initial views of sacro-iliac joints were scored grades 0–4 in 42 patients, eight patients had Grade 4 sacroilitis at presentation. 35 patients had lumbar spine changes and nine patients had cervical spine changes. No difference in the rate of lumbar and cervical spine involvement in men and women was identified. Five patients developed spinal fusion (four males, one female). One male patient developed upper lobe pulmonary fibrosis, one male patient developed the cauda equina syndrome, one male patient required joint replacements. However, no significant difference in the rate of complications occurring in men and women was demonstrated.

First metatarsal pronation in hallux valgus

S. Eustace, J. O'Byrne, J. Stack and M. M. Stephens
Departments of Radiology and Orthopaedics, Mater Misericordiae Hospital, Eccles Street, Dublin 7, Ireland

The aetiology of hallux valgus is unclear. Previous authors have correlated development of hallux valgus with convexity and width of the first metatarsal head, others have highlighted the importance of metatarsus prima varus. Pronation in the first metatarsal is to date unreported primarily because clear markers of rotation in that bone have not been identified. 20 metatarsals were dissected from cadavers and radiographed in degrees of rotation (0°, 10°, 20°, 30°, to 90°). The inferior tuberosity of the base moved laterally as the bone pronated, position correlating to degree of rotation. This model was applied to 40 controls with clinically normal feet and 40 patients with hallux valgus. 38 of 40 controls had less than 10° of first metatarsal pronation. 37 of 40 patients with hallux valgus had

20° or more first metatarsal pronation ($p < 0.001$). We have identified features that enable assessment of rotation in the first metatarsal. We have proved that patients with hallux valgus have first metatarsal pronation. Preliminary evaluation suggests that this rotation may be reversed by orthotic insoles. Incorporation of a derotational manoeuvre into standard oesteotomy may reduce the current 20% post-surgical recurrence rate.

The influence of clinical data on the interpretation of MRI scans of the lumbar spine in disc disease

B. S. Worthington, R. W. Kerslake, L. A. Mitchell,
T. Eichhorn and A. G. Gale
Department of Academic Radiology, University of Nottingham, Nottingham NG7 2RD, UK

A total of 100 patients with suspected lumbar disc disease was investigated by magnetic resonance imaging in the sagittal and transverse axial plane employing a variety of pulse sequences. The resulting scans were reported independently by three different radiologists firstly without any clinical data and again after an interval of several weeks with knowledge of the history and clinical findings. 50 of the patients have come to surgery and the degree of complete concordance between the radiological and operative findings in the initial reports was 67%, 63% and 64% respectively. The three observers gave a different report in over 10% of the cases when they had access to clinical findings. In most cases this was to give a positive interpretation to questionable features in the presence of corroborating clinical data. We conclude that whilst access to clinical data may reduce the number of false negative and equivocal scan reports this is at the expense of an increase in the number of false positives.

Cervical spondylosis: correlation of MR imaging and plain film findings

B. C. M. MacPherson and D. H. Hadley
Department of Neuroradiology, Institute of Neurological Sciences, Glasgow G51 4TF, UK

It has been stated that magnetic resonance imaging (MRI) is unreliable in the demonstration of osteophytic and other bony lesions, and that plain film changes correlate poorly with clinical features in cervical spondylosis. To assess the validity of these beliefs, balanced and T_2-weighted sagittal MRI was prospectively compared with cervical radiography in 45 patients (270 disc levels) presenting with spondylotic myelopathy. The commonest level affected by osteophyte and/or narrow disc was C5–6. Offsets occurred with equal frequency at C3–4, C4–5 and C5–6, with very few outwith these levels. 147 levels (54%) were normal on both examinations. Osteophyte occurred at 52 levels (19%) – of these, MRI was abnormal in 90%. Offset was present at 39 levels (14%) — MRI was abnormal in 64%. Narrow disc, 23 levels (9%) — MRI was abnormal at all but one (96%). 85% of osteophytes demonstrated on radiographs were seen on MRI. On MRI, an annular bulge was demonstrated at 33 levels (12%) — 13 (39%) having normal radiographs. Posterior extension touching the cord occurred at 32 levels (12%) — 10 (31%) having normal radiographs. Cord indentation was seen at 34 levels (13%), four (12%) with normal radiographs. Of 147 levels normal on radiography, MRI abnormality was demonstrated at 29 (20%), but in only four was cord indentation present. Thus, MRI demonstrated bony abnormalities such as osteophytes and changes related to narrow disc spaces. Radiographs reliably predicted normality as demonstrated on MRI, and can therefore be used to screen patients with clinical features suggesting cervical spondylotic myelopathy.

MRI of discitis/osteomyelitis

A. J. Tottle, A. M. M. Jones, A. Case, I. Watt,
P. Goddard, C. Johnson, B. Penry, J. R. Bradshaw and
A. Longstaff
Department of Radiodiagnosis, Bristol MRI Centre, Frenchay Hospital, Frenchay, Bristol BS16 1LE, UK

Magnetic resonance (MR) imaging is establishing an important role in the investigation of musculoskeletal abnormalities. Most interest has been in diagnosing and staging tumours. We have looked at its application in investigating osteomyelitis and discitis. Notes and MR scans of 35 consecutive patients with suspected osteomyelitis or discitis were examined. 23 studies were performed for back pain, seven post-surgical intervention. Each scan was re-interpreted looking specifically at vertebral body and disc signal, inflammatory mass effect, and any enhancement post-gadolinium when given. Each case was categorized as either inactive, active or infective discitis, or negative. Five were felt to be inactive; seven active; six infective; one sacral osteomyelitis; one poor quality image where a repeat was suggested; and three negative. The negative results showed degenerative disease (2) and metastases (1). All six infective cases were confirmed by blood culture, serological tests or biopsy. One of the inactive, and three of the active cases have been confirmed. 12 other cases have been investigated due to suspected osteomyelitis in the hip (3), lower limb (6), mandible (1), skull (1) and sternum (1). Results were positive for neoplasia in one, infection in three, equivocal in two, and negative in six. The use of MR in discitis/osteomyelitis is discussed. We feel that it is helpful in diagnosing and categorizing discitis, in assessing bony involvement in known osteomyelitis, and in the follow-up of the infective complications of surgery.

CT scanning of L3/4 in suspected disc prolapse: is it necessary?

P. de V. Meiring, M. Gandhi and R. A. Nakielny
Department of Radiology, Royal Hallamshire Hospital, Sheffield, UK

A retrospective study of all orthopaedic referrals for computed tomography (CT) scanning of suspected lumbar disc disease to the Hallamshire Hospital for a 2 year period from July 1989 to July 1991 was done to assess the necessity for scanning the L3/4 level. Of a total of 723 lumbar spine scans performed, 511 were from the orthopaedic services in the Hallamshire and Northern General Hospitals. 460 were for clinically suspected disc disease. There was clinical suspicion of L3/4 pathology in 29 cases (6.3%). Of these 29, CT abnormality was found in 18 (62%) but in only seven was an L3/4 abnormality found (24%), two of which were diagnosed as a prolapsed disc (7%). Four cases had abnormal CT scans at the L3/4 level with no related clinical findings (0.9%). In one of these a significant disc prolapsed was also found at L5/S1 which was thought to be the significant lesion while the other three findings were not thought to be significant and the symptoms resolved on conservative treatment. None of these four patients went to surgery and in none did the L3/4 CT abnormality affect management. These findings have changed the practice in the Hallamshire CT department and only the two lowest lumbar levels are now scanned unless a higher level is clinically suspected or other factors necessitate wider scanning, *e.g.* disordered segmentation. This results in reduced radiation dosage, scanning time and overall cost.

The influence of smoking on adverse effects following iohexol lumbar myelography

M. Greaves and J. Gholkar
Department of Radiology, Shotley Bridge General Hospital, Shotley Bridge, Consett DH8 0NB, UK

A prospective trial to evaluate the influence of smoking on the incidence of headache, nausea, vomiting and dizziness in 50 consecutive patients referred for lumbar myelography. All patients had suspected lumbar disc disease. The needle size was standardized at 22 G and 12–15 ml Iohexol (240 mg/ml) was injected intrathecally. Following the procedure, the patients were routinely ambulatory and were requested to complete a questionnaire the following day. The incidence of headaches graded as moderate or severe was significantly increased in smokers when compared to non-smokers. Smokers experienced more nausea, vomiting and dizziness than non-smokers (borderline significance). A statistically significant number of smokers did not feel well enough to be discharged on the day of the procedure. These results suggest that smokers have an increased tendency to suffer adverse effects, particularly moderate and severe headaches, following lumbar myelograms. This may have relevance when selecting patients for day case myelography.

Sonographic features of plantar fasciitis

W. W. Gibbon
Department of Radiology, Cardiff Royal Infirmary, Cardiff CF2 1SZ, UK

Plantar fasciitis is a common cause of heel pain either as an overuse phenomenon or related to an inflammatory arthropathy, particularly the seronegative arthropathies. We have examined 24 patients with clinical plantar fasciitis or unexplained heel pain using a 7.5 MHz linear array transducer. The investigator was "blind" as to side of symptomatic heel and relevant clinical history. The thickness of the plantar fascia at its point of crossing the anterior calcaneal border was 1.5 to 4.1 mm (mean 3.0 mm) for the asymptomatic and 2.9 to 6.7 mm (mean 4.7 mm) for the symptomatic heels, respectively. A thickness difference of 1.0 to 3.8 mm (mean 1.45 mm) was demonstrated when comparing opposite limbs of the same individual with a relative percentage difference of 32% to 100% (mean 64%). We also demonstrated qualitative changes either diffusely along the plantar fascia or locally at calcaneal insertion. These appearances correspond well with the recognized sonographic features of tendon disease. We discuss these sonographic features and their clinical relevance with reference to objective evidence of diagnosis and monitoring the natural history of this condition.

CT anatomy of the pelvis following hindquarter amputation

J. Fowler, A. M. Davies, *S. R. Carter and *R. J. Grimer
*Departments of Radiology and *Bone Tumour Treatment Centre, Royal Orthopaedic Hospital, Birmingham B31 2AP, UK*

The current management for the majority of musculoskeletal sarcomas is reconstructive surgery with or without chemotherapy. Pelvic lesions tend to present late and, in a minority of cases, surgery requires a hindquarter amputation (HQA). The role of cross-section imaging in the preoperative assessment of these cases is well established. Mutilating surgery deforms the normal symmetrical anatomical relationships in the pelvis. The purpose of this study is to review the computed tomography (CT) appearances of the pelvis following HQA. CT was performed in 14 cases; 12 primary bone and two soft tissue sarcomas. In the normal cases CT showed that, following removal of the normal skeletal support from one half of the pelvis, the bladder and small bowel "herniated" towards the side of surgery. The remaining ipsilateral musculature comprising the gluteal flap and pyriformis muscle, forming the lateral pelvic wall, and the psoas and erector spinae muscles posteriorly all show varying degrees of wasting. The surgical scar highlighted by surrounding fat is easily identified. In six cases recurrent tumour was identified arising at the resection margin. Recurrent tumour could be distinguished from scar tissue by the presence of a mass such that any focal enlargement of the muscles within the surgical field invariably denoted tumour. The attenuation value of recurrent tumour approximates to that of muscle apart from the chondrosarcomas which had a low attenuation which should not be mistaken for a cystic collection. Examples of the normal and abnormal anatomy of the pelvis after HQA are shown and the value of CT in this clinical context is discussed.

If it isn't a soft tissue sarcoma, what is it? A review of 1 year's referrals to the sarcoma unit — CT findings with pathological correlation

E. C. Moskovic, *J. Serpell, †C. Fisher, *J. M. Thomas and C. Parsons
*Departments of Diagnostic Radiology, *Surgery and †Histopathology, Sarcoma Unit, Royal Marsden Hospital, Fulham Road, London SW3 6JJ, UK*

Soft tissue sarcomas (STS) are rare; they comprise less than 1% of all malignant tumours with approximately 1000 new cases arising per year in the UK. Clinically, the commonest presentation is that of an enlarging mass, usually within a lower extremity but their rarity, diverse biological behaviour and heterogeneous histological appearances may give rise to considerable diagnostic difficulty. A review of all new patients referred for treatment to the sarcoma unit at the Royal Marsden Hospital with a clinical diagnosis of soft tissue sarcoma (STS) during the course of 1 year (1989–1990) was undertaken. Of 118 patients, 65 (55.1%) had primary STS, 26 (22.0%) had recurrent STS, 19 (16.1%) had benign soft tissue tumours and eight (6.8%) had malignant tumours other than STS involving and presenting as soft tissue tumours. All patients underwent computed tomography (CT) scanning which was used to assist diagnosis, assess operability and for radiotherapy planning where indicated. The CT findings in the non-sarcomatous tumours, both benign and malignant, are discussed and the key role of CT in aiding diagnosis in these clinically confusing cases is emphasized. Benign soft tissue tumours encountered included fibromatosis, myxoma, arteriovenous malformations, lipomas, myositis ossificans and a psoas abscess. The malignant tumours mimicking STS included lymphoma, osteogenic sarcoma and a soft-tissue metastasis from an undiagnosed bronchogenic primary carcinoma.

Bone cortical and periosteal changes as seen on MRI

G. B. Greenfield
*Department of Radiological and Diagnostic Imaging,
H. Lee Moffitt Cancer Center and Research Insitute, P.O. Box 280179, Tampa, Florida 33682-0179, USA*

Magnetic resonance imaging (MRI) is now widely accepted as a means of demonstrating bone marrow and soft tissue detail. Its ability to elucidate bony changes has been less well appreciated. The basic changes of cortical destruction with geographic or permeative destructive patterns, as well as erosion of the cortex can also be demonstrated. In some cases, cortical destruction can be better shown on MRI than on conventional films. The patterns of petriosteal reaction, including simple periosteal reaction, spiculated periosteal reaction, and laminated or "onion-skin" periosteal reaction can be well seen. The cortex is seen as a solid black line and interruptions of the cortex can be seen as high signal intensity on proton density and on T_2-weighted images. The various changes on MRI are illustrated and compared to conventional radiographs and computed tomography.

MRI of musculoskeletal tumours: a comparative study with X-ray and CT

V. Lozano, E. Gomez-Catalán, P. Aunión and A. Bernardo
Diagnóstico por Imágen, Hospital 'Ramón y Cajal', Crta. Colmenar Viejo Km. 9,100, 28 034, Madrid, Spain

We evaluated 64 musculoskeletal tumours, 11 benign lesions and 53 malignant lesions. In the results, conventional radiograph remained a technique with specific diagnostic information. Computed tomography (CT) was superior in evaluating lesion in flat bones in all cases and provided valuable information about cortical integrity and presence of calcification in seven and nine cases, respectively. Magnetic resonance imaging (MRI) offered a high "sensitivity" in depicting tumour extent (88%), with acceptable rates of "accuracy" in defining the intramedullary extent of tumour (92%) and in the relationship of the tumour to adjacent neurovascular bundle (82%). In summary, although CT is useful, MRI should be regarded as the examination of choice of "staging" musculoskeletal tumours.

Hall 10b

The accessory navicular — a cause of medial foot pain

C. A. J. Romanowski and N. A. Barrington
Department of Radiology, Royal Hallamshire Hospital, Sheffield, UK

Many different accessory ossicles occur around the foot. Occasionally these ossicles are the direct cause of a patient's symptoms. This is most commonly recognized in the os-trigonum syndrome. We present 10 cases of a seemingly less familiar, but equally important clinical scenario related to the accessory navicular. There are three types of accessory navicular, the most frequently occurring of which (type II) is united to the navicular by a synchondrosis. This is the type that causes pain due to a chronic stress reaction at the synchondrosis in physically active people. Over the last 18 months, 10 patients have been seen with a typical clinical history of chronic or acute on chronic pain over the medial aspect of the foot overlying the navicular. Seven of these were female and the mean age was 26.5 years (range 17–38 years). All the patients were physically active on their feet, either in leisure activities or as part of their occupation. All had Type II accessory naviculars on plain radiography and eight had localized increased uptake on ^{99}Tc^{m} MDP bone scan. Two patients had surgical excision of the accessory navicular with relief of their symptoms. In summary the diagnosis is made by finding a Type II accessory navicular in the context of a typical clinical history and can be confirmed by a positive bone scan.

Notes

2.15 – 5.30

Workshop: Greening the Radiology Department

Hall 11a

E. Ison
Centre for Greening the NHS, 1st Floor, Radcliffe Infirmary, Oxford OX2 6HE, UK

Over the last 3 years, there has been a significant drive to "green" the National Health Service; green groups are developing in many units throughout the UK, and the parliamentary under-secretary of state for health, Mr Stephen Dorrell, has addressed the issues of energy use and waste management in the NHS by setting targets and incorporating them into regional reviews. In this session, our objective is to determine what constitutes good practice in a radiology department when environmental impact is used as a quality criterion. In order to provide baseline information for the session, a questionnaire about current practice in relation to environmental considerations has been circulated to BIR members. The results of the questionnaire will be presented, and taken as a starting point for the discussion. Areas of practice that may be examined include administration and good-housekeeping practices, the disposal and recycling of processing chemicals, indoor air pollution, energy efficiency and age of equipment, use of resources, and compliance with legal and regulatory requirements with respect to radioactive substances and hazardous chemicals. Other areas for discussion may arise as a result of the responses to the questionnaire and the particular interests of the delegates attending this particular consensus session. It is envisaged that there will be an iterative process after the session in order to refine the outcomes of the debate for publication. We hope to produce guidelines for staff working in radiology departments that will reduce the overall impact of this discipline, not only on the environment, but also on those organisms, human or otherwise, who are dependent upon it.

2.15 – 3.45

Radiobiology Day: Session II

In memory of Dr N. McNally

Hall 11b

Clinical experience with CHART in the UK

M. I. Saunders and S. Dische
Marie Curie Research Wing for Oncology, Mount Vernon Hospital, Northwood, Middlesex HA6 2RN, UK

In 1984 continuous hyperfractionated accelerated radiotherapy (CHART) was devised utilizing the radiobiological data regarding normal tissues and tumours available at that time. The aim was to maximize cure and minimize normal tissue injury in patients with cancer. Pilot studies in squamous cell carcinoma of the head and neck and non-small cell carcinoma of the lung (NSCLC) were commenced in January 1985 and completed in April 1991, when multicentre randomized controlled trials were commenced. The probability of local tumour control at 3 years in T3 and T4 patients with head and neck tumours is 44% compared to 24% previously achieved. Likewise, in 76 patients with NSCLC the probability of local tumour control at 2 years is 22% compared with 4% previously. In 18–80 months of follow-up the normal tissue changes have been less than expected, except for spinal cord. New work is continuing whereby CHART is combined with radiotherapy and chemotherapy. Carbogen and nicotinamide are to be employed to overcome hypoxia which may be associated with such accelerated radiotherapy. Further quantitative measurements of normal tissues are proceeding.

Hyperfractionated accelerated radiotherapy for carcinoma of the oesophagus

J. Sule-Suso, A. M. Brunt and J. E. Scoble
North Staffordshire Royal Infirmary, Stoke-on-Trent ST4 7LN, UK

We report on 73 patients with carcinoma of the oesophagus treated by hyperfractionated accelerated radiotherapy as an update of an earlier report (Sule-Suso et al, 1991). The patients, aged 46–93 years, were considered suitable for radiotherapy on their performance status irrespective of the presence of metastases. The radiotherapy was given three times a day over 2 weeks with a minimum of 3 h between treatments. The treatment was well tolerated acutely and to date there have been no unacceptable long-term side-effects. Dysphagia was improved in 54 (74.0%) patients for a mean of 40 weeks (range 2–206). Product-limit survival for all 73 patients was 34.7%, 20.4%, 14.6% and 7.3% at 1, 2, 3 and 4 years, respectively. Product-limit survival for those without obvious metastasis was 46.4%, 31.2%, 22.2% and 16.7% at 1, 2, 3 and 4 years, respectively. We conclude that this regime is feasible within the normal working day, well tolerated, effective and the short overall treatment duration desirable.

Reference

Sule-Suso, J., Brunt, A. M., Lindup, R. & Scoble, J. E., 1991. Hyperfractionated accelerated radiotherapy for carcinoma of the oesophagus. *Clinical Oncology, 3,* 209–213.

Early changes in flow and pH of saliva when treating with radiotherapy

M. D. Leslie and S. Dische
Marie Curie Research Wing, The Mount Vernon Centre for Cancer Treatment, Northwood, Middlesex HA6 2RN, UK

The early changes in salivary gland function of 47 patients undergoing radical radiotherapy (37 continuous hyperfractionated accelerated radiotherapy (CHART) and 10 conventionally fractionated treatment) for head and neck cancer have been studied. Resting whole saliva and stimulated parotid saliva have been collected from these patients before, during and up to 12 weeks from the start of treatment. Marked falls in salivary flow can be detected within a week of the start of treatment and the fall is more marked for the stimulated parotid flow as opposed to the resting whole flow which is predominantly the product of the submandibular glands. The reduction in parotid flow is related to the proportion of the gland in the treatment volume and the dose it receives. Corresponding falls in salivary pH are found. The early effects of radiation on salivary gland function is as marked and is seen earlier in the patients receiving CHART compared with those treated by conventionally fractionated radiotherapy. We have previously demonstrated a greater preservation of late parotid function in patients treated by CHART as compared with conventionally fractionated radiotherapy. This cohort of patients is being assessed further in follow-up to determine any relationship between early and late changes in function.

Tumour cell kinetics in lung cancer

B. E. Lyn, M. I. Saunders, M. H. Bennett, G. D. Wilson and S. Dische
Marie Curie Research Wing, Mount Vernon Hospital, Northwood, Middlesex HA6 2RN, UK

In vivo tumour cell kinetics were performed in 28 patients with lung cancer. 200 mg bromodeoxyuridine (BUdR) were administered by intravenous injection 6 h prior to surgery. Resections were performed in 25 cases but in three biopsy only was possible. Immediately adjacent samples were taken for analysis by flow cytometry and for immunohistochemical staining for incorporated BUdR. Of 27 non-small cell lung cancer patients, only four were diploid. The median potential doubling time was 7 days, duration of S-phase (T_S) 15.3 h and labelling index (LI) 8.3%. In 17 patients multiple samples were taken from the resection specimens and showed the doubling times in the periphery of the tumours to be significantly faster than in the centre (median values 5.7 and 8.0 days). The LI was also significantly higher in the periphery (median values 9.6% and 7.7%). Light microscopic examination showed heterogeneity of tumour cell labelling. Manual cell counting gave average LIs (median 19%) higher than those obtained by flow cytometry. Maximum and average LIs combined with the T_S obtained by flow cytometry gave faster doubling times, median values 1.2 and 3.5 days, respectively. Studies with antibodies to Ki67 and PCNA were compared with the BUdR results and the kinetic indices were correlated with outcome.

Tumour proliferation assessed by combined histological and flow cytometric analysis: implications for therapy in squamous cell carcinoma in the head and neck

M. H. Bennett, *G. D. Wilson, †S. Dische, †M. I. Saunders, *C. A. Martindale, B. M. Robinson, A. E. O'Halloran, †M. D. Leslie and ‡J. H. E. Laing
*Histopathology Department, *CRC Gray Laboratory, †Marie Curie Research Wing, and ‡RAFT Department of Research in Plastic Surgery, Mount Vernon Hospital, Northwood, UK*

The two techniques of flow cytometry analysis (FCM) and immunohistochemical localization of bromodeoxyuridine (BrdUrd) incorporation after *in vivo* administration, were combined to study proliferation in squamous cell carcinoma of the head and neck region. Care was taken in this study to ensure that similar material was processed using both techniques such that comparisons could be made. FCM underestimated the labelling index (LI) in tumours classified as diploid compared with the histological evaluation of the tumour cells within those tumours (4.6% *vs.* 17.1%). However, in aneuploid tumours, the FCM LI (10.7%) was similar to that obtained from histology (13.5%). Indeed, proliferation assessed by the combination of histology LI and FCM duration of S-phase (T_S) indicated that diploid tumours had a shorter median potential doubling time (T_{pot}) of 2.1 days compared with aneuploid (2.8 days). Despite the heterogeneity of proliferation evident histologically within the specimens, there was not a wide variation in the results of FCM analysis when multiple samples from resections were studied. Using FCM data alone, 46% of the tumours showed a T_{pot} of less than 5 days. When the T_S from the FCM data was combined with the average histological LI, 84% were less than 5 days and with the maximum LI, 99% were within this time interval. Compared with previous estimates, the proportion of tumours possessing proliferative characteristics indicating the need for acceleration of treatment seems to be much larger.

TGFß$_1$, collagen I and III gene expression in human skin fibrosis induced by therapeutic irradiation

S. Delanian, *M. Martin and *J. L. Lefaix
*Service de radiothérapie de l'Hôpital Necker, 149 rue de Sèvres, 75015 Paris, and *D.P.T.E. (C.E.A.)/D.S.V., Laboratoire de Radiobiologie Appliquée, 91191 Gif sur Yvette, France*

The genetic aspects of radiation-induced fibrosis in humans have not been well characterized. We studied collagen Type I, III and transforming growth factor ß$_1$ gene expression in dermal skin samples from women with no evidence of local disease after prior irradiation therapy for breast cancer. The samples were obtained surgically 7 months to 4 years (irradiated dermis = ID) and 20 years (late fibrosis = LF) after treatment, and compared with unirradiated skin samples (control dermis). We used a modified "rapid" Chomczynski method to extract total RNA from powdered frozen tissue samples. Northern blot analysis and successive hybridizations were performed. (1) Total RNA was 2–3 times higher in irradiated tissues. In "early fibrosis" (ID), this corresponds with the increased cell proliferation. In (LF), however, since few cells are present, elevated RNA levels could correspond to increased cellular metabolism. (2) Collagen I and III genes are highly expressed (2–3 times) in both ID and LF, probably following increased transcription of the genes. (3) $TGFß_1$ is overexpressed in both ID and LF (2–3 times, respectively). We propose that in highly cellular ID, TGFß may be secreted by various inflammatory cells, while in LF fibroblasts, autocrine stimulation may play a predominant role.

Significance of carbohydrate metabolism control during pre-operative beam therapy of colorectal cancer on the background of short-term artificial hyperglycemia and synchronization of tumour cells on division cycle

S. K. Karamian and A. Z. Alexanian
Oncological Research Centre, Ministry of Health of Armenian Republic, Armenia

Growth of malignant tumours, morbidity of rectum and dissatisfaction with treatment results, especially of spread, forces elaboration of combined methods of treatment by using the most up-to-date achievements in radiobiology and experimental oncology. A new method of combined treatment of locally spread rectum cancer (T_{40-1} M_0) using effects of short-term artificial hyperglycaemia and synchronization of tumour cell division rhythm on division cycle with 5 FU was worked out in the Oncological Research Centre. The treatment programme foresees the following succession of events: (a) synchronization of tumour cells by division cycle; (b) pre-operative beam therapy in the regime of dose dynamic fractioning; (c) short-term artificial hyperglycaemia; and (d) operation. If necessary adjuvant chemotherapy is also used in the pre-operative period. Our experience proved the high effectiveness of the method. Realization of short-term artificial hyperglycaemia necessitates the definition of glucose tolerance in these patients. The need for carbohydrate metabolism control was confirmed by diabetes mellitus in 14% cases. Tolerance test revealed 32% of patients with latent diabetes mellitus. High frequency of diabetes in patients with rectum cancer prevents artificial hyperglycaemia in those patients who need special pre-operative treatment as well. Retrospective analysis of case histories of patients with rectum cancer with accompanying diabetes mellitus does not confirm the literature data about interconnection of diabetes and age in this group of patients and brings to mind a defensive mechanism of carbohydrate metabolism in patients with rectum cancer.

Functional state of antioxidant system under the influence of low doses of radiation

E. Kostyushov, I. Voltchek, L. Goncharova, I. Izyumtsev, V. Dyachek, A. Tyaptin and I. Popov
Department of Extreme Medicine, Leningrad Institute of Advanced Medical Studies, USSR

We have studied the state of the antioxidant system in liquidators of the consequences of Chernobyl AES crash 4–4.5 years ago and the effect of radiation influence in doses of 20–25 rem. The significant changes were observed in the thioldisulfide system which displayed by prevailing of reduced equivalents. The increasing of SH/SS ratio was revealed both in protein and non-protein fractions of whole blood. At the same time the functional state of ascorbic redox system was characterized by oxidated components in plasma. Increased activity of catalase and glutathionreductase and reduced activity of superoxidedismutase were established in most patients. The level of malonic dialdehyde in blood was significantly raised in all cases. Thus, the adaptational failure of the antioxidant system may be regarded as one of the leading links in pathogenesis of damage by low doses of radiation. It may lead to development of various organ's pathology. Changes in thioldisulfide system may facilitate proliferation, differentiation disorders and neoplastic processes. On the basis of achieved results we are able to propose a pathogenetically founded metabolic therapy for the consequences of low doses of radiation with the employment of antioxidants.

4.15 – 5.30

Advances in Imaging the Liver

Hall 9

Imaging of liver tumours: Japanese experience in detection and characterization

Y. Itai
Department of Radiology, Institute of Clinical Science, University of Tsukuba, Tsukuba 113, Japan

With advancement of non-invasive imaging modalities there has been a great progress in the detection and characterization of liver tumours. In Japan where hepatocellular carcinoma (HCC) is one of the most important cancers, non-invasive imaging diagnosis is positively applied to many patients especially at high risk of HCC to pick up tumours as small as possible. Ultrasound and/or incremental dynamic computed tomography (CT) actually detect many hepatic masses which need a correct diagnosis, if possible, with imaging alone. Thus single level dynamic CT, magnetic resonance (MR) imaging with or without Gd-DTPA, and colour Doppler have been used for this purpose. On the other hand, meticulous imaging techniques including a combination of non-invasive modality with angiography (lipiodol CT, CT during arterial portography, and ultrasound with CO_2) have also been developed for the detection of tiny lesions or for the characterization of liver tumours and non-cancerous hepatic lesions. In this lecture (1) detection of small liver cancer and (2) characterization of hepatic mass among HCC, cavernous hemangioma, metastatic tumour, cholangiocellular carcinoma and non-cancerous hepatic lesions will be discussed mainly based on the Japanese experience of CT, MR imaging and ultrasound.

Round flow defects in CT arterial portography — a potential pitfall in interpretation

M. E. Roddie, N. Jonker, *I. S. Benjamin, *N. Habib and *A. Adam
*Departments of Diagnostic Radiology and *Surgery, Hammersmith Hospital, Du Cane Road, London W12 0HS, UK*

Recent clinical studies have demonstrated improved survival after resection of primary and secondary liver tumours. In order to select appropriate patients for surgery, accurate pre-operative evaluation of the liver is essential. Computed tomography (CT) with arterial portography (CTAP) has been shown to be more sensitive than conventional contrast-enhanced CT, CT with iodized oil or CT arteriography for the detection of focal liver lesions. A high incidence of perfusion defects has been reported with CTAP. These can be peripheral and wedge-shaped, geographical or may involve the whole of the right or left lobes (the "straight line" sign). In a series of 22 patients undergoing CTAP in our hospital, 18 of whom went on to have surgery, CTAP detected 92% of liver tumours compared with conventional contrast-enhanced CT which detected only 69%. Flow artefacts were detected in 82% of cases. These consisted of 14 geographical defects, six wedge-shaped defects and four cases of the straight line sign. In four cases, however, round flow defects mimicking tumours were seen. Intraoperative ultrasound and histological examination were negative for malignancy in these cases. To our knowledge, round perfusion defects have not been reported with CTAP previously and represent a potential cause of false-positive results. We conclude that round perfusion defects do not necessarily represent tumour deposits and should be investigated further before a patient is denied potentially curative surgery.

Dynamic and delayed contrast-enhanced MR scanning of hepatic haemangioma

C. Allen, M. A. Hall-Craggs, M. Paley and I. Wilkinson
Magnetic Resonance Unit, Department of Radiology, The Middlesex Hospital, London W1N 8AA, UK

Liver haemangiomas, particularly large tumours with central necrosis and cystic change, still present a diagnostic challenge. Dynamic and delayed scanning after intravenous contrast enhancement has improved diagnostic specificity with computed tomography (CT). Similar techniques have not been applied to magnetic resonance (MR) because of long scan times. We report the use of a rapid acquisition spin-echo (RASE) sequence which obtains 3–5 slices in 20 s, thus enabling the acquisition of sequential breath-holding abdominal scans following injection of intravenous Gd-DTPA. Preliminary work was performed to optimize the flip angle. 27 patients with hepatic haemangiomas were studied by ultrasound (US), dynamically enhanced CT and by MR. T_1-weighted spin-echo (SE) with electrocardiogram triggering and T_2-weighted SE sequences were performed. Sequential breath-holding RASE scans were performed at 2 min intervals for 15 min after injection of Gd-DTPA. Measurements of tumour signal intensity were made during enhancement and the enhancement time curves are described. Tumour appearances and enhancement characteristics were compared with US and CT and the results are reported. Using this technique MR is as sensitive and specific as CT and more specific than US. MR showed segmental involvement of tumour in the liver more reliably than either CT or US and therefore may be the imaging modality of choice for pre-operative assessment.

The detection, localization and characterization of hepatic mass lesions with MRI at 1.5 T

M. W. Bourne, H. G. Lewis-Jones, M. Lipton and
G. H. Whitehouse
Department of Radiodiagnosis, University of Liverpool,
Liverpool L69 3BX, UK

Recent advances in computed tomography (CT) and magnetic resonance imaging (MRI) have greatly improved the detection and characterization of hepatic mass lesions. The subcentimetre lesion can now be regularly demonstrated and mass lesions can be characterized reliably. The role of pharmaceutical contrast agents both non-specific and targeted will play an increasingly important role in both lesion detection and characterization. Advances in surgical techniques now mean that patients with primary hepatoma and in certain cases, patients with metastatic liver disease are no longer considered as unsuitable for a potentially curative operation. For example, 5 year survival rates in operated patients with a suitable number and distribution of metastases from colorectal primaries, approach 30–40%. The precise radiological staging of hepatic neoplasms will become an increasingly routine request. This study addresses the following questions in relation to a series of 50% patients referred for radiological assessment of suspected hepatic mass lesions: (1) global detection of hepatic mass lesions; (2) individual lesion detection; (3) individual lesion characterization and (4) staging for possible surgical resection. The quantitative and qualitative results will be presented and discussed.

Differential diagnosis of space occupying lesions of the liver with MR imaging

L. Vlahos, A. Gouliamos, D. Matsaidonis, L. Kaïlidou
and A. Papadopoulos
Department of Radiology, University Areteion Hospital,
Athens 11528, Greece

In a retrospective study we reviewed the records of 112 patients who underwent magnetic resonance (MR) examination of the liver. In 84 of them with a definitive diagnosis we studied 152 lesions, *i.e.* 48 hemangiomas, 54 secondary deposits, 23 hepatomas, 17 hydatid cysts, eight simple cysts, one abscess and one focal fatty infiltration. Parameters evaluated were the margin, capsule, shape, internal architecture and signal intensity. The following are the results in the most important of them. Hemangiomas: had smooth margins in 97.5%, no capsule, round or oval shape in 90%, homogeneous architecture in 96%, low density on T_1-weighted in 87% and very high density on T_2-weighted in 94%. Secondary deposits: had smooth margins in 59%, no capsule, round or oval shape in 78%, homogeneous architecture in 61%, low density on T_1-weighted 94.5% and 80% high density on T_2-weighted. Hepatomas: had smooth margins in 52.3%, complete or incomplete capsule in 43.5%, round or oval shape in 56.5%, inhomogeneous architecture in 91%, low density in 61% on T_1-weighted and high density in 87% on T_2-weighted. In conclusion, MR imaging is a very helpful method in the differential diagnosis of space-occupying lesions of the liver.

CT-fluoroscopy (CTF) in the diagnostic and therapeutic approach to hepatic lesions

L. F. Frigerio, C. Spreafico, A. Marchianò, M. Milella,
F. Zucchi and B. Damascelli
Special Radiologic Procedures, Istituto Nazionale Tumori
1, Via G. Venezian, Milano – 20133, Italy

We have coupled a digital subtraction image intensifier to a computed tomography (CT) scanner. The patient is lying on the CT table and a usual Seldinger manoeuvre is performed for positioning the angiographic catheter into the superior mesenteric artery. Then a CT arterial portography is performed so that the liver is opacified from the portal system. After that a complete angiographic study is carried out; the X-ray unit is provided with a tape recorder and a multiformat camera for the documentation. If necessary, a pre-surgical or definitive chemoembolization can be carried out in the same session and CT provides an immediate control of the path of the emboli. This method has shown some advantages: (a) it allows the real-time fluoroscopic control of the angiographic manoeuvres; (b) it reduces the time requested for the two studies; (c) the entire procedure can be carried out in one room without moving the patient; and (d) it allows a smoother handling of patients at risk.

The liver surface in cirrhosis

R. C. V. Bhatt, C. L. Holland, D. Chand, A. Ahmed and *H. Bradby
*Departments of Radiology and *Gastroenterology, Sandwell District General Hospital, West Bromwich B71 4HJ, UK*

Ultrasound diagnosis of cirrhosis of liver is fraught with difficulty because many of the signs commonly described are observer dependent. We present results of a prospective study in which patients with cirrhotic livers were assessed by additional examination of the anterior surface of the liver by 7.5 and 10 MHz frequency. The normal liver surface presents as a bright line due to specular reflection. Established cirrhosis causes irregularity in the liver surface which scatters ultrasound and this is manifest as a "broken" bright line or an undulating line. We shall attempt to correlate the ultrasonic liver appearances with biopsy findings, where available. We feel that ultrasonic examination of the surface of the liver is a useful adjunct to the routine liver examination in cirrhotic patients.

Liver fat estimation using magnetic resonance imaging

N. R. Moore and S. Marks
Departments of Radiology and Medicine, University of Oxford and Radcliffe Infirmary, Oxford OX2 6HE, UK

We report early experience with a novel application of magnetic resonance imaging (MRI) to estimate the degree of liver fat infiltration. This technique is based on the 220 Hz difference in the resonant frequency of fat and water at 1.5 T. We have combined a chemical pre-saturation radiofrequency (RF) pulse centred on the resonant frequency of water with RF receive filters centred on the resonant frequency of fat to create an image comprising only the fat components of the body. 14 patients being investigated for biliary disease were studied. All patients had an MRI study within 48 h of a standard liver biopsy. The biopsy specimens were graded for the degree of fat infiltration (absent, mild, moderate, severe according to the number of fat vacuoles per high power field). The magnitude of the liver fat signal was measured using regions of interest (ROI) positioned peripherally over the right lobe, with background noise subtraction (an equivalent ROI positioned along the same phase encoding lines). At least 15 ROIs were measured and the mean value obtained. All patients with absent liver fat had signal intensity measurements of less than 25 units. There was a trend in which the more marked degrees of fat infiltration were mirrored by increasing signal intensity. This simple technique may provide a non-invasive method of liver fat estimation.

Sonography versus scintigraphy in chronic liver disease due to hepatitis B/schistosomiasis

*‡A. T. Khairy, †Y. Abdel-Ghaffar, *K. Khairy, *M. El-Masry, *A. El-Dorry and ‡J. J. Barrett
*Departments of *Diagnostic Radiology and †Internal Medicine, Ain Shams University Specialized Hospital, El-Khalifa El-Maamoun Street, Abbassia, Cairo, Egypt, and ‡Department of Nuclear Medicine, King's College Hospital, London, UK*

To compare ultrasonography with colloid scintigraphy in chronic liver disease (CLD) due to hepatitis B and/or *Schistosomiasis mansoni*, 412 patients were examined. All cases showed biochemical evidences of CLD, which was verified histologically in 234 patients. The aetiologic factors derived from liver biopsy, serology or sonography were virus B in 141, schistosomiasis only in nine, a mixture of both entities in 178 and were undetermined in 84 cases. Sonography provided specific features for schistosomiasis in 173 out of 370 patients with non-specific scintiscans (47%). However, it was less reliable in cirrhosis as it missed 69 out of 331 cases with characteristic scintiscans (21%). Scintigraphy was inferior to sonography in detection of ascites and missed 54 out of 96 cases with positive sonoscans (56%). There was no correlation between the portal vein diameter on sonoscans and the percentage portal venous flow estimated by dynamic colloid scintigraphy ($r = 0.09$, $p > 0.05$, $n = 122$). There was a significant association between extra-hepatic colloid shift on scintiscans and disease activity on liver biopsy ($p < 0.0001$) with scan sensitivity of 84%. In conclusion, both tests perfectly filled the diagnostic gaps of each other and are recommended for routine assessment of CLD due to hepatitis B/schistosomiasis.

Quantitative volumetric study of the liver

L. F. Frigerio, C. Spreafico, A. Marchianò, G. Colella, C. Segura, M. L. Tatonetti, F. Zucchi and B. Damascelli
Special Radiologic Procedures, Istituto Nazionale Tumori - 1, Via G. Venezian, Milano - 20133, Italy

All patients undergoing liver surgery are studied to assess the exact staging of the disease. All imaging techniques now available (ultrasound, computed tomography (CT), CT-LUF and CT-arterial portography (CT-AP)) are applied for determining the number, site, diameter and vascular relationship of the tumour and its satellite nodules. When performing CT-AP, we usually evaluated the hepatic volume of the whole liver and of the tumour nodules. This procedure is very important in liver transplantation, as it allows an optimization for using the donors' organ, and in hepatic surgery, as it is likely to correlate the percentage of resected non-neoplastic parenchyma to the pre-surgical functional tests to give a predictive index of the remaining liver function and the regenerative index. In all cases of liver transplantation we compared our measurements with the actual weight of the explanted liver which was provided by the pathologist.

Notes

4.15 – 5.30

Audit, Teaching and Management Approaches in Radiology

Hall 10a

A computer-assisted method for teaching basic radiology

A. R. Wright, P. B. N. Mtema, S. N. E. Marsden,
M. J. Keir and J. P. Owen
University Department of Radiology, Royal Victoria Infirmary, Newcastle upon Tyne NE1 4LP, UK

Computer-assisted instruction (CAI) has been enthusiastically received in a number of areas of medical teaching not least because it encourages the student to take an active part in his/her own education. The presentation of images for radiology teaching offers a difficult challenge to the CAI process which has been only partially overcome by digital techniques such as interactive video-disc. A novel system has been developed employing a back-illuminated X/Y digitizer interfaced to a microcomputer running commercially available authoring and graphical software. This allows the use of standard radiographs in which anatomical or pathological features can be identified by mapping co-ordinates in relation to a fixed reference point. The student follows the text of the CAI module on a computer screen and is asked to point to these features using a cursor. Two teaching modules have been devised so far; one on lobar pneumonia and one on basic CT anatomy of the mediastinum. It is proposed to design a "shell" programme to enable modules to be written by radiologists with no computer expertise. The potential of the system will be demonstrated and results of an evaluation presented.

Awareness of the POPUMET regulations at a teaching hospital and medical school

A. K. M. Taylor
Department of Radiodiagnosis, Western Infirmary, Glasgow G11 6NT, UK

The Ionizing Radiation (protection of persons undergoing medical examination and treatment (POPUMET) Regulations 1988 set out a core of knowledge in radiation protection which is designed to ensure that patient exposures to ionizing radiation conform to the ALARA (as low as reasonably achievable) principle. This study has assessed understanding of the core of knowledge published by the local health boards amongst clinicians at a group of teaching hospitals and students at their affiliated medical school, by means of an anonymous multiple choice questionnaire. The results are presented in relation to stage of training, "user category" and possession or otherwise of a POPUMET certificate, and the implications for effective training in this area are discussed.

Clinical audit — developing solutions for the unreported film

A. H. Troughton, D. F. Ettles, D. Presdee, W. Tucker
and E. R. Davies
Department of Radiology, Bristol Royal Infirmary, Bristol BS2 8HW, UK

While general agreement exists amongst radiologists that all radiological examinations should be reported, it is recognized that this ideal is rarely attained. Computerized patient data allows precise quantification of reporting practices. The extent to which this goal was achieved in our department was assessed by audit of reporting practices over a 1 month period. For each of 14 examination areas the time taken for reports to be issued and incidence of unreported examinations was recorded. Of 7262 examinations performed in June 1991, 2251 (31%) were recorded as unreported. 75% of these unreported examinations were mobile and outpatient chest radiographs, casualty examinations and coronary angiograms. The unreported rates for each of them were chest X-rays (43%), mobiles (92%), coronary angiograms (76%) and casualty examinations (30%). The average unreported rate for remaining areas was 5%. True failed reporting most commonly resulted from failure of film retrieval. Incorrect data entry was responsible for a high incidence of apparent failed reporting. Failed entry of reports by operating cardiologists accounted for almost all unreported coronary angiograms. Changes implemented in film retrieval and computer data entry have substantially reduced unreported rates. To simplify and increase efficiency of coronary angiogram reporting, a new computer program is being developed. We conclude that computer-assisted clinical audit is of value in improving reporting practice.

Systematic audit of radiology reports by computer link with a pathology computer

R. H. Sawyer
Department of Radiology, Wythenshawe Hospital, Manchester M23 9LT, UK

The White paper requires standards of quality as well as efficiency to be established by providers to allow purchasers a more rational choice than merely by cost. In a radiological report, quality is linked to the accuracy of the examination and its interpretation. A technique is described which provides systematic and independent verification of a radiological diagnosis if either surgery or a biopsy has been performed. Over a 3 month period in a district general hospital all the histology reports were transferred to a computerized X-ray reporting system and linked to the patients' radiology reports. The histology and radiology were then automatically displayed simultaneously on a computer screen for review by a radiologist. Cases of interest, disparity or confirmation were stored for later analysis. Of 1850 histology reports, 700 corresponding patients were found on the X-ray system. 96 cases of interest were identified of which 61 were helpful confirmation of a suggested diagnosis. A discrepancy was noted in 22 cases including four cases of appendicitis missed on ultrasound and five of mild colitis. Three cases showed up significant clinical management issues. Eight cases of negative histology despite a strong X-ray diagnosis were likely to result from an inadequate specimen. The ability to create a computer link as described depends on co-operation with software firms but need not be expensive with total costs of £900. Additional validation using ICD9 codes and potential further developments are also discussed.

The cost-effectiveness of duplex scanning in peripheral vascular disease

S. Morris, P. Murphy, A. H. Davies, S. E. A. Cole, M. Horrocks and R. N. Baird
Departments of Clinical Radiology and Vascular Studies, Bristol Royal Infirmary, Bristol BS2 8HW, UK

Duplex scanning is a non-invasive method of assessing the femoral and popliteal arteries with an accuracy of 98% and 96% for detecting SFA/popliteal occlusions and stenoses respectively in our institution. In patients with symptoms of claudication not severe enough to merit bypass graft, duplex scanning can satisfactorily identify lesions morphologically unsuitable for angioplasty and thus avoid unnecessary angiography. 502 patients who presented for their first arteriogram to Bristol Royal Infirmary between December 1990 and December 1991 were assessed. These included patients with both iliac and SFA/popliteal disease and with symptoms ranging from intermittent claudication to rest pain and gangrene. 348 of these arteriograms were claudicants with SFA and popliteal disease. 163 of these had a bypass graft, 123 had an angioplasty and 62 had no surgical or radiological intervention. 123 patients had Gruntzig dilatation and 62 had neither bypass graft or angioplasty. Scans would have needed to be performed on all these patients with a cost of £9250 (£50 per duplex scan). A transfemoral arteriogram costs £330. 62 patients would not require angioplasty (£20 460). The total cost saving is thus £11 210. We conclude that duplex scanning of the superficial femoral and popliteal arteries is cost-effective and approximately 20% of claudicants with SFA/popliteal disease would be saved unnecessary arteriography.

Audit of MRI for internal derangement of the knee

K. Lyons, C. Evans, *P. D. Evans, *J. A. Fairclough, *M. Patil and L. A. Williams
*Departments of Radiology and *Orthopaedics, Cardiff Royal Infirmary, Newport Road, Cardiff, South Glamorgan, UK*

Magnetic resonance imaging (MRI), when available, is generally accepted as the primary imaging modality in the investigation of internal derangement of the knee (IDK). It has a reported sensitivity ranging from 69% to 88% and a specificity ranging from 57% to 84% in different series. Reasons for this variability include differing observer experience and non-standard imaging protocols. In our centre, once we had identified a suitable imaging protocol, MRI (0.5 T) replaced arthrography as the primary investigation of IDK. We have audited 250 consecutive examinations using our standard protocol: sagittal T_2-weighted GE 3 mm slices with interleaving slices through the intercondylar notch, coronal T_2-weighted GE 5 mm slices and axial T_2-weighted GE 5 mm slices through the patella if the patient had anterior knee-pain and compared the MRI findings with the arthroscopic findings. All films were reported by two radiologists. The pitfalls, errors and discrepancies with arthroscopy will be discussed. The sensitivity and specificity in our unit will be presented.

A protocol for radiological investigation of the renal tract: 1 year on

U. L. Udeshi and T. Sowerby
Department of Radiology, Kidderminster General Hospital, Kidderminster DY11 6RJ, UK

Owing to constantly increasing demand for intravenous urography (IVU), and the necessity for radiation protection practice, we devised a protocol to help referring clinicians choose between IVU and ultrasound scan of the renal tract. Where appropriate, a plain radiograph of the abdomen was advised. The protocol was widely discussed with referring hospital clinicians and general practitioners prior to its introduction. The result of the introduction of the protocol was a 40% reduction in the number of IVU examinations performed during the following year. However, the number of requests then began to increase again and therefore we decided to audit the IVUs performed over a 6 month period to re-assess the effectiveness of the protocol. 189 IVU examinations were reviewed and the results are presented in the form of colour bar charts and pie graphs which illustrate the origin of the requests, main indications and findings. The indications were assessed for diagnostic yield and we concluded that the largest single group of IVUs with a low diagnostic yield were those performed for investigation of urinary tract infections and that we should enforce our protocol more vigorously as these would then be avoided.

The use of the CT scanner in ophthalmology

D. Kinsella, C. Williams, S. Cook and A. Jones
Department of Radiology and Ophthalmology, Bristol Royal Infirmary and Bristol Eye Hospital, Bristol BS2 8HW, UK

An audit of 113 computed tomography (CT) scans carried out over a 12 month period was performed. The clinical details, scan result and patient outcome were assessed. 54% of the scans were requested to exclude other pathology. These scans were expected to be negative. 88.5% of these were indeed normal and of the remainder only one showed significant pathology. 46% of the scans were expected to yield a positive result such as an intracranial lesion, thyroid ophthalmoplegia, foreign bodies and tumours. 89% of this patient group yielded abnormal scans. This study demonstrates a high correlation between clinical expectations and CT findings. It is an overused investigation when the clinical probability of a lesion is low. We propose a series of guidelines for optimal use of CT scanning in ophthalmology.

Audit of mesenteric angiography for gastrointestinal haemorrhage

M. E. Lipton, M. Bourne and P. C. Rowlands
Department of Radiodiagnosis, Royal Liverpool Hospital, Liverpool L7 8XP, UK

We reviewed our cases of mesenteric angiography for gastrointestinal haemorrhage over the last 18 months. All our patients presented with acute haemorrhage and half the patients were haemodynamically unstable. We had a detection rate for the cause of haemorrhage in 90%. One third of our patients died during their admission. Angiodysplasia was the commonest cause of haemorrhage with warfarin being an important related factor. There were two false negative reports attributed to inexperienced radiologists. There was little agreement between the findings at angiography, surgery and pathology. We conclude that this group of patients require early referral for angiography by an experienced radiologist.

A simplified approach to the antenatal diagnosis of skeletal dysplasias

P. Twining and J. Zuccollo
Departments of Radiology and Histopathology, University Hospital, Queen's Medical Centre, Nottingham, UK

In order to develop a systematic approach to the antenatal assessment of skeletal dysplasias we initially reviewed our experience at Queen's Medical Centre, Nottingham. Over a 4 year period 10 cases of skeletal dysplasias were encountered. The commonest was thanatophoric dysplasia — four cases, followed by one case each diastrophic dysplasia, camptomelic dysplasia, short rib polydactyly syndrome, achondroplasia, focal femoral dysplasia and the Jarcho Levin syndrome. An accurate diagnosis was made in nine out of 10 cases. We used this experience together with a literature review of the most frequent skeletal dysplasias to produce an algorithm for their assessment. The algorithm will be presented and involves a critical evaluation of the whole fetus. Emphasis is placed initially on the assessment of the distribution and degree of limb shortening together with the presence of bowing whether angulated, rounded or due to fractures. This is followed by an evaluation of the hands and feet looking for polydactyly, abduction of the thumb and talipes. In the face — facial clefting, micrognathia and frontal bossing. The fetal chest is scrutinized for reduction in chest size, the head for hydrocephalus and spine for demineralization and scoliosis. We present this algorithm as a logical and simplified assessment of skeletal dysplasias.

4.15 – 5.30

Teach-in: Thrombo-embolic Phenomena in Clinical Angiography — Role of Materials and Technique

Hall 10b

P. Dawson and A.-M. Belli
Department of Radiology, Hammersmith Hospital, Du Cane Road, London W12 0NN, UK

Thrombo-embolism represents one of the most important complications of clinical angiography and may be disastrous. New attention has been focused on the subject since the suggestion emanating from the USA that non-ionic contrast agents might be implicated in the aetiology. Indeed, in the USA, one of the greatest controversies in the history of radiology has raged over this question. In fact, the role of contrast agents of all kinds is essentially an inhibitory one whereas catheters and guidewires represent (variably) thrombogenic foreign bodies inserted into the bloodstream. The role of materials, including contrast agents, and technique in the aetiology of this important complication will be discussed in detail.

4.15 – 5.30

Radiobiology Day: Session III

In memory of Dr N. McNally

Hall 11b

EORTC fractionation trials in head and neck cancer

H. Bartelink (on behalf of the EORTC Radiotherapy Co-operative Group)
Department of Radiotherapy, The Netherlands Cancer Institute, Amsterdam, 1066 CX, The Netherlands

The EORTC Radiotherapy Group has performed a series of fractionation trials to explore the potential therapeutic gain of: (1) multiple fractions per day radiation in combination with high daily doses of an hypoxic cell sensitizer by reducing the number of treated weeks from seven to three with the same overall treatment time; (2) delivering higher radiation doses by reducing the dose per fraction from 2 to 1.15 Gy and increasing the number of fractions from 35 to 70; and (3) reduction of the overall treatment time from 7 to 5 weeks with multiple fractions per day. The hypoxic cell sensitizer misomidasol was tested in the three-arm trial comparing conventional fractionation alone with both multiple radiations per day and with multiple radiations per day in combination with misomidasol. This trial demonstrated that it was possible to give the treatment more concentrated with no increase in late toxicity and a similar local control, no gain has been seen from adding misomidasol to this treatment. The next hyperfractionation trial was carried out in patients with an oropharynx tumour. This trial demonstrated that an increased control can be achieved without an increase of late normal tissue toxicity. At present the accelerated fractionation trial is still going on. The preliminary results of this trial demonstrated that reduction of the overall treatment time is certainly possible without an increased late toxicity. An interesting aspect of this trial is the measurement of the potential tumour doubling time. Preliminary results are suggesting that selection of patients based upon the individual tumour growth rate for accelerated fractionation or hyperfractionation will increase the therapeutic efficacy of radiotherapy.

Hyperfractionated radiotherapy of head and neck cancers —preliminary results

M. Niewald, W. Berberich, K. Schnabel, *P. Federspil and †B. Hell
*Department of Radiotherapy, *ENT Clinic and †Department of Oromaxillofacial Surgery, University Hospital of Saarland, D-6650 Homburg/Saar, Germany*

In the period January 1988 to June 1991, a total of 107 patients was irradiated hyperfractionally for cancer of the head and neck region. The mean age at the beginning of therapy was 55.6 years, the mean Karnofsky performance status 7.4. 69% of the patients had been operated on before, the remaining 31% had no pre-treatment. The T-classification was: T1 19.63%, T2 31.78%, T3 20.56% and T4 28.04%. The N-classification was: N0 40.19%, N1 18.69%, N2 34.58%, N3 6.54%. There were no distant metastases found. 44.86% of the patients had a cancer of the cavity of the mouth, the remaining of the oropharynx. 97 patients received standardized hyperfractionated radiotherapy with single doses of 1.2 Gy twice daily up to a total dose of 82.8 Gy. In the others, radiotherapy was abandoned due to deterioration of general status or intolerable acute side-effects. We observed a complete remission in 58%, a partial remission in 13% and a primary progression in 25% of the patients. In the remaining ones the local tumour status was not achievable. Using the Kaplan–Meier estimate we observed an overall 2-year survival of 52.2% (cavity of mouth 68.1% oropharynx 40%; this difference was statistically significant). Prognostic factors were T- and N-classification, the UICC-stage, the duration of therapy and the delay between biopsy and start of radiotherapy. Compared with a similar collective of conventionally treated patients (single dose 2 Gy once a day, total dose 70 Gy), we saw no difference in survival at any stage or localization. There were some more acute reactions in the mucous membranes, but a sparing effect in late reactions in the skin or subcutaneous tissues.

Prognostic factors for acute and long-term side effects after radiotherapy of head and neck tumours

M. Niewald, W. Berberich, K. Schnabel, *P. Federspil and †M. Engel
*Department of Radiotherapy, *ENT-Clinic, †Department of Oromaxillofacial Surgery, University Hospital of Saarland, D-6650 Homburg/Saar, Germany*

In the period October 1983 to June 1991, a total of 308 patients was irradiated for cancer in the cavity of the mouth or in the oropharynx. 126 of them received a total dose of 60 Gy in 30 fractions, 88 a total dose of 70 Gy in 35 fractions once a day and the remaining 94 patients were treated hyperfractionally twice a day with 69 fractions making a total dose of 82.8 Gy. We recorded the acute reactions of the skin and the mucous membranes and the late reactions of skin, subcutaneous connective tissue and salivary glands during follow-up. Using non-parametric tests no correlation was found between acute skin reaction and single or total dose; a positive correlation, however, between acute reactions of the mucous membranes and the use of small single doses and the total dose. Late reactions of the skin and subcutaneous tissue correlated negatively with the total dose, those of the salivary glands, however, positively. Using hyperfractionation we observed some more acute reactions in the mucous membranes but had a reduction of the late reactions of the skin and subcutaneous tissues.

Logical presentation and mechanical analogies in the development of mucositis in the oral cavity

T. Ljubenov
Department of Radiotherapy, National Oncological Centre, Medical Academy, 1142 Sofia, Bulgaria

This is a way of depicting the function of interdiction on the geometrical model in the Boolean space (M). This is a distributive screen. If we indicate the erythema with "a", the oedema with "b", the epithelolysis with "c" etc., respectively in the presence Stage I of mucositis (p), in Stage II — (q) and in Stage III — with "r", each element of the space and each combination of the meaning of the characteristics of mucositis being represented by a separate cell. If $a = 1$, $b = 0$ and $c = 0$, we can write down this with a $a \wedge \bar{b} \wedge \bar{c}$ or else corresponds to the vector 1-0-0. This means that we have a Stage I mucositis and cannot have a Stage II or III. If $ab\bar{c}$ ($a \wedge b \wedge \bar{c}$), then $a = 1$, $c = 0$ and $b = 1$ and it is not possible to have a Stage III mucositis. The surface energy (E) of ionizing radiations appears as a universal function of speed (V) in the development of ulceration. In the development of ulceration, two kinds of fluctuations are observed: (1) mechanical (the epithelium area (A) a coefficient of friction, speed of growth of the epithelolysis (V), bending of the epithelium (c)); and (2) dose (energy-caused) fluctuations (resistance of the tissue (R), the force of energy transformed into an increase of the temperature (i), a magnitude contrary to the condensation capacity ($1/C_0$), induction for the formation of elastically folded edges of the ulceration (L). In figure can be seen the sequence of the graphical representation of the stages of the formation of ulceration. These useful analogies render practical guidelines for the inclusion of parenteral feeding.

Non-specific cellular resistance disorders induced by low doses of radiation

I. Voltchek, E. Kostyushov, L. Filyov, V. Dyachek, I. Izyumtsev, A. Tyaptin, I. Popov, Yu. Medvedev and L. Goncharova
Department of Extreme Medicine, Leningrad Institute of Advanced Medical Studies; All-Union Research Institute of Highly Pure Biopreparations, Leningrad, USSR

Some integral proofs of non-specific cellular resistance were studied in liquidators of the consequences of Chernobyl AES crash 4–4.5 years ago exposed to radiation influence of 20–25 rem. The share of blood mononuclears with viral inclusion bodies and degree of its viral effect, metabolic and phagocytic monocyte activity in the NBT-test were appraised. A lysosomal-cationic test was used to reveal the functional state of granulocytes. It was established that in all patients influenced by low doses of radiation there was increased evidence of viral effect of mononuclears in comparison with control group of healthy donors. At the same time most liquidators had functional defects of monocytes and granulocytes. Consequently, there may occur non-specific (antiviral) cellular resistance disorders under the influence of radiation low doses which in turn may lead to development, unfavourable course, chronization of infection diseases, forming of immunocomplex pathology, neoplastic processes. (Olifen, Interlock).

Measurement of normal cell radiosensitivity — a possible path to improve tumour cure?

N. G. Burnet, R. Wurm and J. H. Peacock
Radiotherapy Research Unit, The Royal Marsden Hospital and Institute of Cancer Research, Sutton, Surrey SM2 5NG, UK

Tumour control probability is related to the total dose delivered, but this dose is often limited by the tolerance of the surrounding normal tissues. More specifically, maximum doses are determined by a minority of patients who sustain significant, morbid normal tissue damage. Identification of this group of patients might allow dose increase in the majority, with potential increase in local control and cure, possibly by as much as 20%. In an attempt to utilize cellular radiosensitivity measures as a potential predictive assay of tissue response, fibroblast strains from seven patients have been irradiated at high dose-rate, and low dose-rate. Five of the strains showed similar relative recovery with low dose-rate. Two strains showed no recovery and these two were raised from patients who suffered severe normal tissue reactions to clinical radiotherapy. A further series of nine fibroblast strains from patients with a spectrum of well-defined radiation reactions is now being studied. Any relationship between normal tissue radioresponsiveness and relative cellular sensitivity in these patients may provide the basis for improved results from individualization of radiotherapy schedules.

Notes

Wednesday 20 May

9.00 – 10.15

Mammography — Quality Control and Screening

Hall 9

Excellence our only aim — total quality management in mammography

R. Warren
Breast Screening Service, St Margarets Hospital, Epping, Essex CM16 6TN, UK

The nature of breast cancer as an important and emotive cause of death and disease sharpens the motivation of those working in this field to raise standards of film quality and patient care to the very best levels that can be obtained. The variation in the results of trials indicate that there are aspects of quality that are critical to the implementation of a breast-screening programme, and may be the difference between effective mortality reduction and none at all. Quality principles must extend throughout the different professional disciplines involved so that there are no weak links in the quality chain. Pathology, surgery and radiotherapy are as much a part of this as the imaging disciplines. The quality culture must run through the service as a common belief so that clients, patients and their doctors perceive the high and caring standards of the organization. The Epping breast screening service has chosen to develop this culture by applying for registration under BS5750, a commercial quality standard. This is assessed by outside auditors, the British Standards Institute, who award the kite mark to registered companies.

National self-assessment of radiologists' film reading performance in breast screening

A. G. Gale, J. A. Towle *E. J. Roebuck and
*A. R. M. Wilson
*Department of Academic Radiology, University Hospital and *Breast Screening Training Centre, City Hospital, Nottingham, UK*

A national self-assessment programme of radiologists' film-reading performance has been established by the NHSBSP and the Royal College of Radiologists. This programme will enable each radiologist involved in screening to learn how they interpret sets of known cases. This paper presents the full results of a trial carried out in three regions. A set of screening mammograms which encompass a diverse range of screening appearances has been established from screening training centres and a gold standard of radiological intepretation obtained. Individually some 40 screening radiologists in the three regions have reviewed these cases and measures of their film-reading performance recorded. Performance indices monitored include the number of cases recalled for assessment; sensitivity and specificity; identification of key radiological features; and ROC measures of detection and classification ability. Furthermore the data analyses allow identification of areas where an individual has particular difficulty which then permits the suggestion of appropriate revision strategies. Results demonstrate overall good performance of the participant radiologist in classifying the cases as compared with the gold standard. This self-assessment programme is currently being extended nationally.

Breast cancer and screening Asian populations

S. Tucker, A. G. Gale and *E. J. Roebuck
*Department of Academic Radiology, University Hospital, and *Breast Screening Training Centre, City Hospital, Nottingham, UK*

Suggestive information from the national breast screening programme indicates that breast cancer is less prevalent amongst Asian than non-Asian women. This paper reports research which investigates whether this reflects a poorer attendance at screening centres or whether Asian women have a lower incidence of breast cancer. Data from two breast-screening centres over the past 2 years were reviewed. Information for some 17 500 women was examined and ethnic origin determined by a standardized name examination technique. Overall attendance rate was 69.1%. Non-Asian attendance rate was 71.3% and Asian 52%. Attendance rates at one centre were 67.4% overall; Asian 42% and non-Asian 69.9%. Overall attendance at the second centre was 71%; with Asian 56% and non-Asian 72%. Additionally marked variation was found for attendance rates dependent on GP practice (range 39.5–81%) for both Asians and non-Asians. This demonstrates the important role of the primary care team in facilitating breast screening. Of 549 Asian women invited, 286 were screened with no cancers detected. This suggests that the actual cancer incidence is less in Asian women, within the screening age, even though fewer Asian women attend for screening.

Changes in mammographic image quality due to film processor variation

J. G. Murray, D. J. Dowsett and J. T. Ennis
Radiology Department, Mater Misericordiae Hospital, Eccles Street, Dublin 7, Ireland

In contrast to the majority of mammographic breast-screening programmes, film processing at this centre occurs on site in both hospital and mobile trailer units. Initial (1989) daily step-wedge tests revealed a large variation in film-processor performance at the latter. To assess the clinical significance of these findings and determine acceptance limits of processor performance, 10 abnormal mammograms were copied using high-definition 35 mm film. A range of optical densities for each original image was obtained. Copy film was then matched with test film variation using a densitometer. All films were subsequently ranked for spatial and contrast resolution. Acceptance limits for processing time (3 min ±30 s) and temperature (34 ± 1°C) were obtained. Longer times and higher temperatures are most advantageous in terms of patient dose and thus a regime of 3.5 min and 35°C is suggested as optimal. The use of film copies as a means of monitoring processor performance is discussed. Careful quality assurance has ensured steady mobile unit processor performance which is now comparable to the hospital-based unit. The advantages of on-site film processing are outlined, and its more widespread acceptance is recommended.

Image quality in contact and magnification mammography

J. Czajka and A. P. Hufton
North Western Medical Physics Department, Christie Hospital, Manchester M20 9BX, UK

Magnification mammography is often used to improve visualization of fine detail, such as microcalcifications. Compared with contact mammography, the effective noise is reduced while resolution may be improved, as long as focal spot blurring does not dominate screen-film unsharpness. To investigate the interdependence of these factors affecting image quality, focal spot and screen-film modulation transfer functions (MTFs) and signal-to-noise ratios (SNRs) were measured under different magnification and scatter conditions on an IGE/CGR Senographe 600T. The MTFs were calculated from microdensitometer traces of slit images, while SNRs were determined from images of a specially designed test object containing details of varying size and contrast. Detailed results are presented which demonstrate, amongst other things, that the total MTFs for nominal magnifications of × 1.5 and × 1.85 are very similar, but better than in contact mammography. Image contrast is slightly better for × 1.85 magnification, compared with × 1.5, and is similar to that in contact mode, using a grid. However, × 1.85 magnification gives about a factor of two improvement in signal-to-noise ratio which, combined with the resolution data, gives optimum magnification performance for this particular type of X-ray set.

Patterns of breast calcification in patients on renal dialysis

A. J. Evans, M. E. L. Cohen and *G. F. Cohen
*Breast Screening Unit and *Renal Unit, City Hospital, Derby, UK*

Patients undergoing renal dialysis have disturbed calcium metabolism which often leads to metastatic calcification. The aim of this study was to evaluate patterns of breast calcification in patients on dialysis with particular reference to the presence of any calcification which could simulate malignancy. We analysed the mammograms of 16 women on renal dialysis and compared them with a control group of 32 women attending for routine mammographic screening. We found a significant increase in vascular and parenchymal calcification in women on renal dialysis. Ductal calcifications were no more prevalent in the patients on dialysis and in no case did the calcification simulate malignancy. There were no significant correlations between breast vascular calcification and either calcium/phosphate product, PTH, duration of dialysis treatment or vascular calcification present on skeletal surveys.

Breast screening: deciphering the structure of mammographic microcalcification

†B. Reeves, A. G. Gale, *E. J. Roebuck and *A. R. M. Wilson
*Department of Academic Radiology, University Hospital, and *Breast Screening Training Centre, City Hospital, Nottingham and †Visual Sciences Unit, Radcliffe Infirmary, Oxford, UK*

Differentiating between benign and malignant features of microcalcification in mammograms can be extremely difficult. This paper reports an investigation of the features of microcalcification which experts consider important for differential diagnosis and the relative importance of the features for differential diagnosis. Several mammograms, for which the clinical outcome was known, were selected to represent the wide diversity of appearance of microcalcification. Experts, interviewed individually, viewed the mammograms under normal breast-screening conditions. They were asked to identify as many features as possible which they believed to be important for differential diagnosis, and scored each mammogram on every feature. Feedback was then given by calculating intercorrelations between scores, allowing an expert to identify further features to describe any differences still perceived between mammograms scored in a similar way. Common structures across experts were identified by multivariate analysis of the data for individuals; using the known clinical outcome for the mammograms, discriminant analysis was also carried out to determine the relative importance of features for differential diagnosis and the weightings that should be attached to them. The discussion examines the extent to which the common structures extracted and the relative importance and weightings of features accord with clinical experience.

Image analysis of microcalcifications in X-ray microscopy of paraffin-embedded breast tissues

K.-H. Ng, †D. A. Bradley, *L.-M. Looi and *Y.-F. Lim
*Departments of Radiology and *Pathology, University of Malaya, 59100 Kuala Lumpur, Malaysia, and †Regional Radiation Physics and Protection Service, Queen Elizabeth Medical Centre, Birmingham B15 2TH, UK*

The mammographic appearance of clustered microcalcifications in breast tissue and its potential predictive value in carcinoma of the breast has long been a subject of interest. In the present investigation a retrospective study has been made of specimen blocks of paraffin-embedded breast tissues. Histological results are available. Contact X-ray microscopy of these paraffin-embedded breast tissue blocks has been performed using a low-kV X-ray unit operating at 5 kV. X-ray microscopy studies reveal clustered microcalcifications in a number of specimens in which malignancy is indicated, whilst for the specimens in which benign and non-neoplastic conditions have been observed lesser incidence of clustered microcalcifications have been noted. Digitization of radiographs has been carried out with an in-house developed image analysis system based on a PC/AT microcomputer and an 8-bit video digitizer. The image is digitized with a pixel resolution of 512 × 512 and 256 grey levels, processed and then converted into a binary image. A boundary-tracing algorithm is used to delineate the edges automatically of each calcification. Techniques are being developed to quantify individual calcification parameters such as size, perimeter and shape factor, and clustered parameters such as total number, number density and neighbour-to-neighbour distance.

Performance of mammography screening units in Finland

A. Servomaa, *M. Pamilo and T. Parviainen
*Finnish Centre for Radiation and Nuclear Safety, and *Mammography Screening Centre, Cancer Society of Finland, Helsinki, Finland*

Mammography screening of women aged 50–59 was initiated in Finland in 1987 and now encompasses all age groups. The first national results are available. They show quite good sensitivity and specificity. Most of the tumours are found in earlier stages. The performance of about 50 mammography screening units, including image receptors and film processing, was evaluated according to the Nordic recommendations for mammographic quality assurance. Image quality was studied with technical and clinical phantoms. Film processing was tested sensitometrically. Glandular dose was calculated from measured surface dose of 4.5 cm thick perspex phantom. Radiation risk from screening was estimated using the relative risk model of BEIR V. The main deficiencies in performance were the low power of the generators, inadequate performance of automatic exposure controls, large focal spot sizes and the use of stationary grids. These deficiencies are corrected in modern mammographic units. Optimized film processing was used in most of the screening centres. The main reasons for the wide dose range obtained were the use of slow image receptors, non-optimized film processing, high optical densities of the film and the use of an antiscatter grid.

9.00 – 10.15

Imaging and Investigation in Clinical Oncology

Hall 10a

Scrotal neoplasms — possibilities using real-time ultrasound

S. I. Mattila and H. P. Mäkäräinen
Department of Diagnostic Radiology, Oulu University Hospital, Kajaanintie 52A, 90220 Oulu, Finland

More than 95% of testicular neoplasms are malignant. Testicular malignancies are seen in all age groups, but they are most common (75%) in males of 20–49 years of age. Extratesticular neoplasms are rare and almost always benign. Testicular neoplasms can be visualized by real-time ultrasound (US), but the method has been thought to be non-specific. Few papers about US findings of extratesticular neoplasms are available. We wanted to study the US findings of scrotal neoplasms, testicular and extratesticular. We also wanted to study the possibility of visualizing the possible invasion of the neoplasm through the tunica albuginea and the significance of the thickness of the scrotal wall in the differential diagnostic. We also wanted to study whether there are any clues to lead us to suspect an extratesticular neoplasm. The US examinations were made using Toshiba 77 A or Aloka 650 real-time US equipment by the direct contact method using a 7.5 MHz linear probe. The men were examined at Oulu University Hospital in Finland during 1985–1991. There were 75 scrotal neoplasms, 65 testicular (63 malignomas) and 10 extratesticular (two malignomas) neoplasms. In the paper the results presented will include: age groups; histological groups; US findings of neoplasms and differential diagnostic possibilities.

Prognosis of cystic change in residual masses following chemotherapy for metastatic teratoma

D. J. Wilcock, P. J. McMillan and M. Sokal
Departments of Radiology and Radiotherapy, General Hospital, Nottingham, UK

Retroperitoneal lymph node dissection (RPLND) is often performed for the removal of residual masses after chemotherapy for metastatic teratoma. However, there is controversy regarding the indications for this operation. Morbidity from the operation is significant; most notable is retrograde ejaculation in these usually young patients. It would be advantageous to predict a subgroup in these patients in whom RPLND is unnecessary. Therefore, a retrospective review of the case notes of the patients on the Nottingham teratoma register was made. Of these, seven patients were identified who had residual masses which showed cystic change or decrease in attenuation on computered tomography in comparison with the pre-chemotherapy scan. All these patients are alive and well and none show any sign of active disease. Four of these patients had RPLND and no evidence of malignancy was found in the resected specimens. We advocate a more conservative approach to RPLND in patients with post-chemotherapy residual masses in which there is low attenuation and/or cystic changes.

Hepatoblastoma: CT findings pre- and post-therapy

S. J. King, P. S. Babyn and M. L. Greenberg
Department of Diagnostic Imaging, Hospital for Sick Children, 555 University Avenue, Toronto, Ontario M5G 1X8, Canada

Successful treatment of hepatoblastoma depends on complete surgical resection which is facilitated by preoperative chemotherapy. The changes on computed tomography (CT) after chemotherapy and surgery have not been described previously. A retrospective review was performed of CT of the chest and abdomen of 15 children with hepatoblastoma following pre-operative chemotherapy and surgery. 12 children had unresectable tumours on CT at diagnosis either because of bilobar tumour, metastatic disease or vascular involvement. Following chemotherapy, tumour volumes decreased by 20–98%. Tumours had increased areas of hypodensity and calcification and margins were better defined facilitating disease staging. However, staging of primary tumours was sometimes problematic and was overestimated in three children. Children with lung metastases improved after chemotherapy and the majority had normal chest CT pre-operatively. 14 of the 15 children survived surgery. All tumours had areas of necrosis on pathological examination but there was no correlation between the degree of hypodensity on CT and amount of tumour necrosis. Five children developed either low attenuation and calcification along liver resection margins or low attenuation areas in residual liver. None of these findings represented tumour recurrence. CT remains one of the most practical methods of documenting disease of the chest and abdomen post-therapy in hepatoblastoma.

Assessment of CT measurements of tumour volume as an indicator of response to chemotherapy in osteosarcoma

R. Wellings, A. M. Davies, P. Pynsent, *S. R. Carter and *R. J. Grimer
*Department of Radiology and *Bone Tumour Treatment Service, Royal Orthopaedic Hospital, Birmingham B31 2AP, UK*

Cross-sectional imaging is now an integral part of the pre-operative staging of bone sarcomas. In osteosarcoma most of the criteria for assessing tumour response to chemotherapy are qualitative. With Ewing's tumour, however, correlation between alterations in tumour size and response to chemotherapy are recognized. The purpose of this study is to review the CT data of a series of osteosarcomas to determine whether any quantitative measurement correlated with response to chemotherapy. The archived image data of 37 conventional osteosarcomas of the lower limb was reviewed and tumour length, cross-sectional areas and volumes both pre- and post-chemotherapy were measured. Tumour response to chemotherapy, expressed as % necrosis, was obtained from the histology of the excised specimen. Analysis of the results showed no correlation between all the CT measurements, including alterations in tumour volume, and % tumour necrosis. On CT qualitative observations (*e.g.* mineralization) remain a more accurate method of assessing tumour response to chemotherapy than absolute measurements.

MRI — as a predictor of tumour invasion of the mandible and oral region

J. Griffith, J. S. Brown, P. D. Phelps and R. M. Browne
Department of Radiology, Walsgrave Hospital, Coventry CV2 2DX, UK

At present there is no accepted protocol for the use of magnetic resonance imaging (MRI) in squamous cell carcinomas affecting the oral region. Many surgeons decide on the appropriate mandibular resection purely on clinical grounds and claim that pre-operative investigations are unreliable and therefore oncologically unsafe. This prospective study was designed to assess the predictability of MRI in detecting the presence and extent of tumour invasion of the mandible and the oral region. 15 consecutive patients with squamous cell carcinoma of the oral region were investigated pre-operatively by MRI using T_1-weighted axial sections before and after contrast. These scans were examined by four radiologists and the extent of tumour invasion recorded. This was compared with the actual tumour invasion after a detailed histological investigation involving division of the mandible into 4 mm sections. We found that MRI was not helpful for small (T1 or T2) carcinomas in which early mandibular invasion was suspected. It gave important additional information, however, for T3 and T4 tumour in relation to mandibular involvement and in assessing patients with tongue fixity and trismus. In the same way, extension of the disease into the nasopharynx and hypopharynx can be predicted by MRI.

5 FU modulation and metabolism in colonic cancer monitored by 19 F MRS

M. O. Leach, M. Findlay, J. Glaholm, J. Mansi, D. Collins, G. Payne, V. R. McCready and D. Cunningham
CRC Clinical Magnetic Resonance Research Group and Section of Medicine, Institute of Cancer Research and Royal Marsden Hospital, Downs Road, Sutton, Surrey SM2 5PT, UK

19 F magnetic resonance spectroscopy allows the metabolism of fluorinated drugs to be monitored directly in the patient. In this study, we have monitored the metabolism of 5 fluorouracil (5 FU) during low-dose continuous infusion, and have observed the effects on metabolism of modulation by alpha-interferon. We have performed serial studies in 25 patients with colonic cancer, monitoring metastatic disease in the liver with a 16 cm diameter surface coil. Despite the low rate of 5 FU infusion (300 mg/m^2/day) the spectra generally showed large peaks from fluoro-ureido-propionic acid (FUPA) and fluoro-beta-alanine (FBAL), the major catabolites. In addition: (1) during the initial phases of 5 FU infusion, both 5 FU and FUPA/FBAL were evident in some patients; (2) at maximum response, only catabolites were apparent; (3) with the addition of alpha-interferon, 5 FU and fluoronucleotides, from the anabolic pathway, were evident in some cases. Where 5 FU pooling was evident within the first 8 weeks, this correlated with response. Following addition of alpha-interferon, a decrease in catabolites and an increase in 5 FU and fluoronucleotide levels correlated with further response.

Interstitial laser hyperthermia: the importance of imaging in tumour therapy

J. J. Donald, *A. Masters, *R. Kant, *S. G. Bown and
W. R. Lees
*Department of Radiology, The Middlesex Hospital, London
W1N 8AA, and *The National Medical Laser Centre,
University College Hospital, London, UK*

Percutaneous interstitial laser hyperthermia (ILH) is emerging as an alternative approach in the palliation of inoperable liver and pancreatic tumours. We report our experience in 17 patients treated with the neodymium: yttrium-aluminium-garnet laser (Nd:YAG) and outline the importance of detailed imaging at all stages of the therapy. Pre-procedural assessment included ultrasound (US) and computed tomography (CT) to determine the number, site, size and morphology of the lesions. Under ultrasound-guidance 1–4 19 gauge needles, each bearing a 0.2 mm laser fibre, were percutaneously positioned within the tumour at a separation of 1.5 cm. An output power of 1.5–2.0 W was applied for 500 s. Continuous US monitoring showed progressively enlarging hyperechoic foci at the treatment sites, which within a few minutes produced a confluent hyperechoic area. Enhanced CT scans were performed at 24 h. 12 liver and five pancreatic tumours have undergone a total of 52 treatment sessions without complications. Necrosis was identified as areas of non-enhancement at the treatment site. ILH in conjunction with detailed imaging is a safe and precise method of inducing necrosis in tumours of the liver and pancreas.

Accuracy of MRI in staging of prostate carcinoma. Cost-effective analysis

V. Lozano, J. Azpeitia, L. Mazaira and
J. Marcos y Robles
*Departamento de Diagnóstico por Imágen, Hospital
'Ramón y Cajal', Crta. Colmenar Viejo Km 9, 100. 28.034
Madrid, Spain*

We have determined the "accuracy" of magnetic resonance imaging (MRI) in evaluating patients with prostate cancer. The role of MRI was assessed in 27 patients. All MRI examinations were performed on a Magnetom Siemens 1.5 T MRI system. We used T_1 (600/20) and T_2(2500/40/80) weighted in a spin-echo sequence, with images in the axial, sagittal and coronal planes. Sometimes, use of a prone position decreases respiratory motion artifacts. Information was obtained about the presence, size, and location of the tumours, as well as periprostatic fat infiltration (neurovascular bundle), seminal vesicle involvement, and adenopathy. We compared imaging results with information obtained at the time of surgery and on pathological results, and MRI correctly staged 78% of the cases. In summary MRI was accurate for 78% of the patients. It may be cost-effective to perform MRI for staging carcinoma of the prostate.

Diagnosing prostate cancer at normal PSA levels: importance of clinico-sonographic correlation

J. Spencer, A. Alexander, T. Helinek, *L. Gomella,
T. Matteucci, M. Rifkin and B. Goldberg
*Departments of Diagnostic Ultrasound and *Urology,
Thomas Jefferson University Hospital, Philadelphia, PA
19107, USA*

Prostate-specific antigen (PSA) levels increase in proportion to the stage of prostate cancer more accurately than prostate-specific acid phosphatase (PAP). PSA levels rise earlier than PAP and have proved extremely valuable in diagnosis of and screening for early stage disease. Our prospective study of the diagnostic efficacy of transrectal ultrasound (TRUS)-guided prostate biopsy in 460 men confirms this previously reported association between the level of PSA and the presence and stage of prostate cancer. They were referred for TRUS for a variety of indications including abnormal digital rectal examination (DRE). 86 of the 460 men (19%) who underwent guided biopsy had normal levels of PSA (< 4 ng/ml). Sonographic features suggestive of cancer in these men included focal hypoechoic lesions, areas of inhomogeneous echogenicity and focal areas of asymmetry. 23 of the 86 men (27%) had abnormal biopsy results: 16 (19%) cancer, three premalignant atypia and four prostatitis. 63 men had normal or other benign findings. There was overlap between the sonographic findings of men with normal and abnormal biopsy findings at normal PSA levels. Abnormalities corresponding to DRE findings correlated more strongly with the presence of cancer or atypia. Our findings are of major importance for the early diagnosis of prostate cancer, the second most common cause of cancer death among males.

Serum prostate-specific antigen: before, during and after radical radiotherapy in localized adenocarcinoma prostate

M. McLean, P. Warde, C. Catton, W. Duncan, R. Bisset,
H. Richmond and T. Panzarella
*Department of Radiation Oncology, Princess Margaret
Hospital, 500 Sherbourne Street, Toronto, Ontario
M4X 1K9, Canada*

Purpose: To study prospectively the effect of radical radiation therapy upon serum prostate specific antigen (PSA) levels during and after treatment of clinically localized carcinoma of the prostate. *Method:* A group of consecutive patients, entered over a period of 15 months from February 1989 to July 1990, had one or more pre-treatment PSA levels, PSA levels weekly through treatment and at each follow-up visit. 117 patients were eligible for analysis if clinically localized adenocarcinoma of prostate (T_1-T_4, N_0, M_0) and fully compliant with the treatment and follow-up requirements of the protocol. Analysis date was 1 June 1991. *Results:* Serum PSA levels were found to correlate with advancing T stage and Gleason score. The trend throughout radiation therapy was for the level to fall. The ultimate time to decay post-therapy was as function of the pre-treatment value of PSA. As a result of study of the decay patterns it is possible to identify three patient subgroups: a group characterized by high initial PSA levels and early relapse, a group with persistently elevated PSA levels without evidence of relapse who might benefit from earlier hormone manipulation, and a third group who may represent local cure.

Neoplasia induced renal vascular changes: sonographic evaluation of 48 hypernephromas

B. Banerjee, B. R. Choraria and A. Rennison
Departments of Radiodiagnosis and Imaging, Tameside General Hospital, Fountain Street, Ashton-Under-Lyne, Lancashire OL6 9RW, UK

Pre-operative detection of tumour invasion within renal veins and inferior vena cava is important for planning of treatment of hypernephroma patients. This type of tumour invasion has been reported in 21% to 55% of surgically excised tumours. The ability of ultrasound to image vascular changes non-invasively makes it ideally suited for pre-operative evaluation of hypernephromas. Over a period of 8 years sonographic evaluation of 48 hypernephromas which were subsequently confirmed at surgery were undertaken with a real-time sector scanner and duplex Doppler ultrasound equipment. Intraluminal thrombus in renal veins and inferior vena cava were noted in eight patients (17%). In three patients (6%) renal veins were enlarged without any tumour invasion and in three patients (6%) the renal arteries supplying the tumour-bearing kidneys were found to be enlarged while compared with arteries on the non-affected side. High-velocity blood flow was seen in these renal vessels with high diastolic component, indicative of marked decrease of vascular impedance. In this project, an attempt has been made to determine the incidence of neoplastic vascular invasion and detail other vascular changes exhibited at the initial presentation of hypernephromas.

Quantitative T_1 and T_2 measurements of lumbar vertebrae in multiple myeloma

V. Nicholson, J. Husband, T. Hickish, D. Cunningham, D. Collins, P. Gowland, M. Leach and V. Ayton
Department of Diagnostic Radiology, The Royal Marsden Hospital, Downs Road, Sutton, Surrey SM2 5PT, UK

A common clinical problem in the management of multiple myeloma is the failure of bone marrow sampling to provide an accurate reflection of disease as infiltration is frequently focal. This study evaluates quantitative T_1 and T_2 values in lumbar vertebral bodies as opposed to images alone. These magnetic resonance imaging values are compared with marrow histology and paraprotein levels. Quantitative T_2 values are helpful where low signal foci are studied and in individual patients parallel their clinical progess.

Notes

9.00 – 10.15

Genitourinary Imaging

Hall 10b

A modern imaging approach to pelvic malignancy

R. J. Johnson
Department of Diagnostic Radiology, Christie Hospital & Holt Radium Institute, Manchester M20 9BX, UK

Patients with cancer require the relevant investigations carried out as quickly and efficiently as possible. Different techniques are appropriate in initial assessment, staging, monitoring the response to treatment, and in the management of relapse. The new techniques like X-ray computed tomography, endo-luminal ultrasound and magnetic resonance imaging have usually been assessed by specialist groups and then introduced into general hospital practice on a patchy basis, and often with restricted patient access. Financial constraints are in part responsible for this, but the overall result is that patients are sometimes referred for oncological opinion without having had simple investigations on which major treatment decisions can be made. In other situations they may have been subjected to inappropriate investigations, incomplete studies which need to be repeated, or multiple unnecessary investigations. This creates extra work, wastes financial resources and may delay treatment. This talk will focus on the interrelationship between imaging techniques and the clinical status of the patient, and between the imaging techniques, with particular emphasis on carcinoma of the cervix and carcinoma of the bladder.

Clinical significance of prostate calcification. Transrectal ultrasound and plain film correlation

H. Roberts, D. Rickards, S. Garber and J. Noble
Department of Radiology, The Middlesex Hospital, Mortimer Street, London W1N 8AA, UK

Prostatic calcification is commonly seen on plain radiographs. Transrectal ultrasound (TRUS) precisely localizes the calcification to a specific prostatic zone, and combined with urodynamic, biopsy and clinical data, identifies five types of calcification. 100 patients (ages 22–89, mean 56 years) underwent clinical evaluation, bi-planar TRUS and a 30' caudal, pelvic radiograph. In 35, urodynamics were performed. Five types of calcification were identified. (1) Curvilinear, crossing the midline, symmetrical and positioned in corpora amylacea. This has no clinical significance and is seen on both plain films and TRUS. (2) Punctate and unilateral, localized to central and transitional zones, occurring in detrusor instability and patients with bladder neck dyssynergia. It is due to intraprostatic reflux and seen on both plain film and TRUS. (3) Block-like confined to transitional zones in benign prostatic hyperplasia and present on both plain films and TRUS. (4) Single calcific foci, unilateral, and confined to the ejaculatory ducts, representing duct calculi, more commonly seen on TRUS than plain films. (5) Small irregular foci associated with an echo poor area in the peripheral zone of the gland, seen only on TRUS and associated with carcinoma. TRUS specifically locates and identifies types of calcification. Plain films identify the type of calcification, but not location. Clinical conclusions may be derived from either technique.

MRI of solid renal mass lesions

J. Houston, *S. Fulford and C. I. Meanock
*Departments of Radiology and *Urology, Royal Berkshire Hospital, Reading RG1 5AN, UK*

Over a 9 month period, 28 patients with solid renal lesions were examined by magnetic resonance (MR) and computed tomography (CT) imaging to evaluate their relative merit regarding the nature and extent of pathology, and to compare different MR imaging sequences. Operative correlation was available in 22, the other six were Stage IV on presentation and therefore not operated upon. MR imaging sequences included: VE 2000/30 and 90 (27 subjects): T_1 600/25 (18 subjects): post gadolinium (Gd) DTPA 90° GE (18 subjects) and short tau inversion recovery (STIR) (13 subjects). All patients underwent CT (21 with contrast enhancement). In the 22 patients with operative correlation the histology included: renal cell carcinoma (18); oncocytoma (3); angiomyolipoma (1) and haemorrhagic cyst (1). Comparison with operative staging showed both CT and

MR imaging to be accurate in 19 of the 22 cases (86%) with no advantage of T_1 or STIR over the VE. The post-Gd images provided no additional information, and in terms of speculating upon the histological diagnosis MR imaging shows no advantage over CT. In three patients overstaged by CT, the coronal plane of imaging available with MR imaging clearly showed no local invasion. It is concluded that apart from avoiding ionizing radiation, MR imaging has no advantage over CT in the investigation of solid renal lesions.

Observer error in pelvimetry

A. J. Liddicoat, W. W. Gibbon and D. Griffiths
Department of Diagnostic Radiology, University Hospital of Wales, Cardiff CF4 4XN, UK

Computed tomography (CT) pelvimetry is widely accepted as a simple low radiation dose technique for assessment of maternal pelvic dimensions. We have assessed the interobserver and intraobserver error for our CT pelvimetry technique. Antero-posterior (AP) pelvic inlet and outlet diameters were measured from a lateral scanogram, transverse pelvic inlet diameter from a frontal scanogram and interspinous diameter from a single axial scan performed at the level of the foveae. We now present the results comparing measurements obtained on two separate occasions by three observers (two radiologists and one senior radiographer) for 17 women undergoing CT pelvimetry. The overall intraobserver error range was 0–42.8 mm with a mean of 2.9 mm. The interobserver error range was 0.1–35.1 mm with a mean of 7.2 mm. Both the intraobserver and interobserver errors were greatest for the AP outlet diameter and least for the transverse pelvic inlet diameter. We discuss possible causes and potential ways of minimizing these errors, and their clinical significance.

The age-dependency of the renal resistive index in healthy children

R. O. Bude, M. A. DiPietro, J. F. Platt and J. M. Rubin
Department of Radiology, University of Michigan Medical Center, 1500 E. Medical Center Drive, 2910TC, Ann Arbor, MI 48109-0326, USA

The renal resistive index (RI) is known to be age-dependent in normal children, but this relationship has been incompletely studied to date. We undertook to determine this relationship, as knowledge of it will be crucial for the application of the RI to the evaluation of paediatric diseases. The mean RIs in peripheral renal arteries were prospectively evaluated in 71 healthy children, from newborns through 11 years. We found the normal mean renal RI to be age-dependent. It is commonly elevated above the adult upper limit of normal (0.70) in the first year of life, and, in general, from individual to individual, decrease with age. From 4 years onward, the likelihood is low (2% probability) that it is > 0.70. We conclude that renal RI criteria developed for the evaluation of adult renal disease, whereby an RI > 0.70 indicates abnormality, do not apply to children younger than 1 year, and are not as yet applicable to children from 1 to 4 years. These criteria should be applicable to children 4 years and older.

Assessment of Gd-DTPA as a CT contrast agent within the renal tract

R. J. Gibson, C. I. Meanock, E. P. H. Torrie and T. Walker
Department of Radiology, Royal Berkshire Hospital, London Road, Reading RG1 5AN, UK

Gadolinium DTPA (Gd-DTPA) given intravenously in appropriate dosage is visible as a radiographic contrast agent on computed tomography (CT). Magnetic resonance imaging (MRI) installations are often in close proximity to a CT scanner. If a CT examination is performed soon after a Gd-DTPA enhanced MRI examination, confusing appearances may occur on CT because of enhancement within the renal tract. We present 12 cases of renal masses examined with both modalities. The amount of contrast enhancement is variable and not predictable. There was clear visualization of Gd-DTPA within the renal collecting systems on CT in four cases, vague visualization in four cases, and contrast was not apparent in four cases. There is no apparent relationship between contrast visualization and the time after injection (range 17–182 min), or to indices of renal function. Gd-DTPA in normal dosage may be visualized in the renal collecting systems on CT in 66% of cases.

Furosemide and fluid-load Doppler sonography in non-obstructive pyelocaliectasis

R. O. Bude, M. A. DiPietro, J. F. Platt and J. M. Rubin
Department of Radiology, University of Michigan Medical Center, 1500 E. Medical Center Drive, 2910TC, Ann Arbor, MI 48109-0326, USA

Recent published literature describes an increase in the renal resistive index (RI) after oral fluid load and furosemide administration in obstructive pyelocaliectasis, relative to normal kidneys, in children. We evaluated the renal RI in six normal and eight non-obstructed, pyelocaliectatic kidneys in nine children, aged 3–18 years, before and 1–2 h after intravenous (IV) fluid load and furosemide. We found the RI decreased from a mean of 0.63 to a mean of 0.56 ± 0.05 SD (decrease significant to $p < 0.005$) in the non-obstructed, pyelocaliectatic kidneys, while the RI decreased, but not statistically significantly, in the normal kidneys. Although the children in our study were studied under slightly different conditions than those described previously (IV *vs.* oral fluid, respectively, and different timing of furosemide administration and scanning), it is interesting to note that there is now evidence showing the RI goes up in obstructive pyelocaliectasis, and down in non-obstructive pyelocaliectasis, relative to normal kidneys, after fluid load and furosemide. It is hoped that these findings may lay the foundation for fluid-loaded furosemide challenge renal Doppler sonography for the evaluation of pediatric hydronephrosis, perhaps as an alternative to dynamic renal scintigraphy.

Ultrasound evaluation of the urethral sphincter in women with obstructed voiding dysfunction

J. G. Noble, *J. Dixon, †C. J. Fowler and D. Rickards
*Departments of Uro-Radiology, *Gynaecology and †Neurophysiology, The Middlesex Hospital, London W1N 8AA, UK*

Obstructed voiding in females has been shown to be associated with abnormal electromyographic (EMG) activity within the urethral sphincter. Muscle displaying this activity will increase in volume due to the effects of work hypertrophy. The aim of this study has been to quantify urethral sphincter volume utilizing transrectal sonography (TRUS) thus providing a simpler and less invasive method of evaluating these patients. 15 female patients (mean age 29 ± 3.2 years) with obstructed voiding underwent videocystometry (VCMG), urethral sphincter EMG and TRUS. EMG was carried out using a concentric needle electrode placed into the para-urethral tissue and in all patients abnormal EMG activity (decelerating bursts and complex repetitive discharges) was identified. TRUS was undertaken with the patient in the left lateral position using a 7 MHz Aloka linear array probe. The sonographic findings were compared with those obtained from 15 age-matched females with normal urodynamics. In each of the patients studied, VCMG revealed obstructed voiding at the level of the urethral sphincter with widespread, spontaneous, abnormal EMG activity. The urethral sphincter was clearly seen on TRUS as an oval, echo-poor structure distal to the bladder outlet. The volume of the sphincter in those patients with abnormal EMG activity (mean $2.9 \pm 0.14\ cm^3$) was significantly greater than in the control group (mean $1.26 \pm 0.75\ cm^3$) ($p < 0.001$). These results suggest that there is a significant increase in the volume of the urethral sphincter with obstructed voiding and abnormal sphincter EMG activity and that TRUS provides a useful means of evaluating these patients.

Diagnostic features of bladder neck dyssynergia on ultrasonography: a new radiological sign?

J. G. Noble and *D. Rickards
*Departments of Urology and *Radiology, The Middlesex Hospital, London W1N 8AA, UK*

Bladder neck dyssynergia (BND) has long been recognized as a cause of outflow obstruction in male patients but the pathophysiology of the condition is poorly understood. The diagnosis is conventionally obtained by the characteristic features of high pressure/low flow voiding, a failure of bladder neck opening and a positive "Whiteside Sign" at videocystometrography (VCMG). The aim of this study was to quantify the appearances of the bladder neck using transrectal ultrasonography (TRUS). 58 male patients aged 24–67 years (mean = 41 ± 4.4), with BND, underwent TRUS using a 7 MHz Aloka linear array probe. The findings have been compared with TRUS appearances in 170 male patients aged 21–85 years (mean = 54 ± 5.2); prostate obstruction, $n = 95$; normal, VCMG $n = 75$. In 24 of the 58 patients studied, "trucut" biopsies of the bladder neck were taken under ultrasound control and were analysed using histological and electron microscopic techniques. In all of the patients studied with BND, an ovoid, echo-poor area was seen in the bladder neck region which was absent in the other patient groups. The area was predominantly anterior to the urethra and had a mean diameter of 16.8 ± 1.1 mm. Light microscopy demonstrated smooth muscle fibres interlaced with connective tissue and electron microscopy suggested that the connective tissue was predominantly collagen and elastic tissue. This report details a well-defined, poorly echogenic area at the level of the bladder neck, which has not been described previously. Histological analysis of this area suggests that the configuration of the smooth muscle in this region may play a role in the mechanism of bladder outflow obstruction in BND.

Ultrasonic appearance of the epididymis and chronic post-vasectomy testicular pain

A. K. M. Taylor, *A. J. McMahon, *R. F. Deane and *D. Kirk
*Departments of Radiodiagnosis and *Urology, Western Infirmary, Glasgow G11 6NT, UK*

Several authors have described a "post-vasectomy syndrome" of chronic testicular pain, with symptoms putatively attributed to back pressure in the epididymis following ligation or division of the vas deferens. With local ethical committee approval, one of us performed scrotal ultrasound scans in 27 volunteers from a group of 172 respondents to a postal follow-up survey administered 4–4½ years after vasectomy. One-third of respondents reported chronic testicular discomfort dating from their vasectomy ("symptomatic"), although few had sought further medical attention. Ultrasound scanning ("Acuson" 128 scanner, 7.5 MHz linear array transducer) was performed in 14 symptomatic and 13 asymptomatic men: single or multiple epididymal cysts were seen in seven of the symptomatic group and four of the asymptomatic group. We conclude that epididymal cysts are commonly present in men who have undergone vasectomy, but we have shown no significant association with chronic testicular discomfort.

Evaluation of impotence by pharmaco-cavernosometrography

A. M. Parikh, S. J. Hampson and *D. R. Rickards
*Departments of Urology, and *Radiology, The Middlesex Hospital, London W1N 8AA, UK*

We report our experience with pharmaco-cavernosometrograms in 40 patients being investigated for impotence. The mean age of the group was 49 years and patients with obvious psychogenic or hormonal abnormalities were not studied. Papaverine was used as the vasoactive agent in all cases (range 30–80 mg). Two 23 G butterfly needles were inserted to the corpora cavernosa, one connected to the pressure transducer, the other being used for papaverine, saline or contrast infusion. Parameters documented were the pressure rise occurring in the 15 min following papaverine injection and the erectile grade obtained. After 15 min the corpora were perfused with saline at rates varying from 40–300 ml/min as necessary to produce erect corpora. The rate of decay of the erection and the maintenance rate of infusion were also documented. If venous leakage (VL) was implied by a poor response to papaverine and a maintenance rate > 50 ml/min the saline infusion was replaced with 50% urograffin. Spot films were taken to confirm leakage and to document the anatomy of the veins. Arterial insufficiency (AI) was implied by a poor response to papaverine in the absence of venous leakage. A normal response was obtained in 10 patients, AI was diagnosed in 10 and VL confirmed fluoroscopically in 18. Two patients were considered to have a picture of mixed disease. The high rate of venous leakage is consistent with patterns being reported elsewhere, if these patients are to have surgery more information about the arterial inflow must be obtained from colour Doppler imaging or from arteriography.

Notes

9.00 – 10.15

Angioplasty

Hall 11a

Current trends in PTA

W. Seyferth and R. Ertel
Radiological Department, General Hospital Ansbach, Ansbach W-8800, Germany

Angioplasty was introduced as a therapeutic procedure of vascular disease more than 25 years ago. The primary success rate, the risk of percutaneous transluminal angioplasty (PTA) and hopefully the long-term results have been changed by the technical progress of the X-ray equipment (digital subtraction angiography mobile C-arm units with subtraction facilities), the further development of guide wires, balloons, rotating systems, lasers and stents. The influence of the individual points will be discussed, validated and the question "who will and can perform PTA in the future?" will finish the presentation.

Monitoring platelet deposition following angioplasty using a platelet-specific monoclonal antibody

A. C. Perkins, R. J. Lonsdale, M. L. Wastie,
S. C. Whitaker, R. M. Marshall, M. Frier and R. Gregson
Departments of Medical Physics, Vascular Surgery and Radiology, University Hospital, Nottingham NG7 2UH, UK

Platelet activation at the site of angioplasty has been implicated as a cause of subsequent arterial re-stenosis. Current techniques for assessing platelet deposition rely on *in vitro* platelet labelling techniques. We have investigated the use of a platelet-specific monoclonal antibody for *in vitro* platelet labelling to monitor platelet deposition following angioplasty. 30 patients undergoing femoral and popliteal artery angioplasty received an intravenous injection of 100 μg (20 MBq) ^{111}In-P256 Fab′ antibody. Gamma camera images of both lower limbs were obtained at 2, 6 and 24 h following angioplasty and recorded by computer. Deposition was expressed as a ratio of the count rate over the uptake site to that over the contralateral site. In all patients accumulation of labelled platelets was seen at the puncture site demonstrating the functional viability of the radiolabelled platelets. In 12 patients no sites of uptake were visualized. Platelet deposition was seen at sites of angioplasty or distal emboli in 17 patients and in one patient with thrombophlebitis, not clinically apparent until 8 days later. Uptake ratios of the order of 2:1 were measured at the angioplasty site. This antibody has proven to be valuable for monitoring platelet deposition following angioplasty and should be useful in the assessment of adjuvant antiplatelet therapy.

Use of human tissue type plasminogen activator in the prevention of early rethrombosis following the treatment of femoral occlusions by percutaneous angioplasty

J. N. P. Higgins, J. M. Gibson and A. D. Platts
X-ray Department, Royal Free Hampstead NHS Trust, London NW3 2QG, UK

Prophylatic infusion of tissue plasminogen activator (rtPA) for the prevention of early rethrombosis after recanalization and angioplasty of femoral arterial occlusion. Patency rates for femoral artery occlusions treated by angioplasty are inferior to those for similarly treated stenoses. Thrombosis following angioplasty may occur within hours and is found more commonly following the recanalization of occlusions than following the dilatation of stenoses. Some success has been achieved in preventing this by infusion of rtPA into the dilated segment of artery, isolated from the circulation by two balloons. All patients with occluded superficial femoral arteries successfully recanalized by angioplasty receive perfusion of the angioplasty site with 0.5 mg per hour of rtPA for 24 h. Early results suggest this may be beneficial.

Thermal angioplasty using high-frequency ablator

D. A. Gould and T. A. Houghton
X-ray Department, Broadgreen Hospital, Liverpool, UK

Thermal angioplasty has been shown to be of some value in recanalization of arterial occlusions. Systems based on laser energy sources are expensive. High-frequency ablation (HAT) is inexpensive and has been previously used in His bundle ablation and more recently to produce thermal recanalization for percutaneous transluminal angioplasty (PTA). We have conducted a study to assess the value of HAT in PTA of occlusions in the superficial femoral artery, where angioplasty by conventional means (guidewire and catheter) had failed. Recanalization was attempted using a 0.035 in monopolar guidewire electrode passed through a 5 French catheter. Between 2.5 and 50 W could be delivered, generating tip temperatures which produce tissue vaporization. Of 60 occlusions in 60 patients, 39 (65%) were recanalized with technical and clinical evidence of a successful result; follow-up is available in 18 patients up to 17 months. Problems encountered include pain and subintimal and transmural passage of the electrode. No complication was of long-term significance. Recanalization using HAT could frequently be achieved in occlusions where conventional PTA techniques had failed.

Angioplasty of long femoral occlusions — can the success rates be improved?

M. R. E. Dean
Department of Radiology, Royal Shrewsbury Hospital South, Mytton Oak Road, Shrewsbury, Shropshire SY3 8XF, UK

Initial reports of the treatment of long femoral occlusions indicated that the primary success rate was only 59% and the 1 year patency was only 64%. The development of newer guidewires with hydrophilic coatings have improved the primary success rates but the 1 year patency rates remain unchanged. Over a 2 year period, 17 long femoral occlusions were treated by percutaneous transminimal angioplasty (PTA), and all were primarily successful. The lengths of the occlusions varied between 12 cm and 28 cm (mean length 18.7 cm). Three of the first eight occlusions reoccurred within 3 months. The subsequent nine cases have been carefully monitored at 1, 3, 6, 9 and 12 months following the angioplasty and their ankle–arm indices are recorded. Fine needle digital arteriograms are performed if there is a 15% reduction in the ankle–arm index and, where there are recurrent stenoses, they are treated by PTA. Two of the nine patients required repeat angioplasties and all nine patients show a maintained improvement in the ankle–arm index and are symptom-free. Careful follow-up, with repeat angioplasties at an early stage when indicated, appears to improve the patency rates of long femoral occlusions.

Changes in lower limb blood flow following angioplasty: assessment with duplex Doppler ultrasound

S. C. Whitaker, R. J. Lonsdale, R. Gregson, P. W. Wenham, G. S. Makin and B. R. Hopkinson
Departments of Radiology and Vascular Surgery, University Hospital, Nottingham NG7 2UH, UK

Complex local changes in blood flow occur following angioplasty which are assumed to be due to residual plaque, thrombus or intimal flaps. Recent work has shown that assessment of residual stenosis with duplex Doppler ultrasound is often misleading in comparison with the angiographic appearances and clinical measurements. We have examined the pattern of blood flow in the legs of 35 patients before angioplasty, at 24 h afterwards and, where possible, at 6 weeks. Maximum systolic velocity, average velocity, pulsatility and resistive indices were measured at various sites in the limb. Successful angioplasty in the iliac/common femoral segments was associated with an increase in all parameters when measured at the common femoral artery but changes at lower levels were often modified by more distal lesions. Successful angioplasty in the superficial femoral or popliteal arteries was associated with an increase in peak systolic velocity in the proximal superficial femoral and distal popliteal arteries, and with a decrease in the deep to superficial femoral peak systolic velocity ratio. Other parameters and velocity measurements at other sites showed inconsistent changes. Changes in the velocity gradient at the site of angioplasty were also assessed. A residual velocity increase was detected at the site of angioplasty in half the patients, but was significant (*i.e.* > 2) in only two. We conclude that duplex Doppler ultrasound is a useful method of quantifying the changes in regional blood flow following angioplasty.

Percutaneous transluminal angioplasty of crural arteries — results in 32 patients

U. M. Sivananthan, M. R. Rees, T. Browne and S. P. Verma
Department of Cardiac Radiology and Cardiac Research, Killingbeck Hospital, Leeds LS14 6UQ, UK

Percutaneous transluminal angioplasty (PTA) of the intra-popliteal arteries is an alternative to surgical treatment, and improves outflow when performed with proximal interventions. We present the results of 48 angioplasties in 32 patients (26 males and six females). 20 anterior tibial, eight posterior tibial, five tibio-peroneal, five peroneal and trifurcation lesions were dilated. 28 angioplasties were carried out in conjunction with proximal angioplasties to improve the outflow. There were six isolated interventions of the tibial vessels. In seven procedures associated thrombolysis was carried out and in two procedures thrombolysis was combined with a 5 French Trac system to re-open occluded arteries. Immediate complications included dissections with flow impairment in two cases, thrombosis in two cases and one case of spasm. There were five cases of late complications, two occlusions and three restenosis. In four cases the repeat angioplasties were successful. The overall technical success rate was 96%. Most of the patients fell into Fontaine classification Group 2b and 3 (18 and 13 cases, respectively) and one case in Group 4. Patients were followed-up with Doppler studies and isotope limb blood flow studies at 3 weeks, 3 months and 6 months after initial PTA and then at 6 monthly intervals. Maximum follow-up time was 3 years. We will present the results of our angioplasties and analyse some of the technical and anatomical factors that influenced the outcome.

Prospective randomized trial of PTA versus supervised exercise therapy for intermittent claudication

T. S. Creasy, E. W. L. Fletcher, J. Walton, J. Collin and P. Morris
Departments of Clinical Radiology and Surgery, John Radcliffe Hospital, Oxford OX3 9DU, UK

The purpose of this study was to compare percutaneous transluminal angioplasty (PTA) with supervised exercise therapy, as treatment modalities for patients with unilateral intermittent claudication who had lesions suitable for treatment by PTA. A total of 56 patients was recruited and randomized; 30 to PTA and 26 to supervised exercise therapy. Mean ankle brachial pressure indices (ABPI), mean treadmill claudicating and maximum walking distances were measured prior to treatment and at regular intervals up to 2 years. All PTAs were performed or supervised by a single specialist vascular radiologist. Graduated exercise therapy was supervised by a physiotherapist. In each treatment group there was a similar and significant increase in both mean treadmill claudicating and maximum walking distances at review, though this was achieved without an increase in mean ABPI in the exercise group. However, subdivision of patients according to the level of disease ("iliac" *vs.* "femoropopliteal") showed PTA to be more effective in patients with iliac disease and supervised exercise therapy to be better in patients with femoropopliteal disease.

Angioplasty above the arch

R. A. Morgan and I. P. Wells
Department of Radiology, Derriford Hospital, Plymouth, UK

Although the first report of percutaneous transluminal angioplasty (PTA) in the supra-aortic territory was as far back as 1980, the technique has not been widely used in the carotid or subclavian arteries because of the perceived risk of cerebral thrombo-embolism. Recent reports have suggested increasing enthusiasm for PTA in the vessels supplying the head and upper limb, particularly in Europe and the USA. These workers report a success rate of 95% and a major complication rate of 0.5%. We have performed PTA in seven supra-aortic stenoses including the treatment of one stenosis of a carotid artery by PTA in a patient with a developing stroke. All procedures were successful and without complication. Our results are presented with illustrative examples and description of the method used. The literature is reviewed, indications for PTA of the carotid and subclavian arteries discussed, and the important requirements of a comprehensive imaging work-up prior to angioplasty also stated.

9.00 – 10.15

Physics I — Body Composition

Hall 11b

Radiological assessment of body composition

S. Mattsson
Department of Radiation Physics Malmö, Lund University, Malmö General Hospital, S-21401 Malmö, Sweden

Depending on the high precision in the new type of measurements, which have been developed, there is a renewed interest in applying body composition methods to clinical medicine. The objective of this paper is to review the field and compare the techniques in terms of precision, accuracy, patient exposure, complexity, etc. Body protein can be directly measured by prompt gamma *in vivo* neutron activation analysis of nitrogen as can bone using various types of *in vivo* photon absorption techniques. Body water can be directly assessed by isotope dilution. This makes it possible to describe the body composition in terms of protein, bone, water and fat. As there is no established method of measuring fat directly it has to be estimated as the difference between body weight and the three other body component masses. Together with the above mentioned methods, a range of indirect methods (total body potassium, electrical impedance, anthropometry, etc.) are widely used. These methods are based on the fact that for "normal" adults, there are relationships between the different components in the body, for example, between total body potassium and lean body mass. These relations are however seldom applicable in sick people, in very thin or very obese, or very young or old persons. In limited groups of persons, computed tomography and magnetic resonance imaging have also been used for cross-sectional characterization of soft tissue distribution *in vivo*. The paper will also cover *in vivo* measurements of toxic trace elements like lead, cadmium, mercury and aluminium.

Energy-dispersive X-ray scattering for assessment of crystalline tissues

G. J. Royle and R. D. Speller
Department of Medical Physics and Bioengineering, University College, London WC1E 6JA, UK

A new technique has been developed for assessing the state of crystalline body tissues. The method can provide information on the state of trabecular bone during osteoporosis, which could be used for diagnosis, and on the identification of calculi. A collimated X-ray beam focused on the object causes interference effects between coherently scattered photons. In objects with a crystalline nature the interference causes peaks at certain momentum transfer values, making the scattered pattern unique for a particular material. Patterns are recorded with an energy-dispersive X-ray detector. Measurements of trabecular bone have shown two main peaks in the scattered spectrum: a peak at 0.0175 nm^{-1} caused by the crystalline calcium salt component within the bone network, the other is a broader spread (0.0203–0.0228 nm^{-1}) caused mainly by homogeneous scattering from the water content of the marrow. Quantitative analysis of the pattern can determine the ratio of bone to marrow and so indicate the presence of osteoporosis. Gallstone patterns show clear peaks at positions relating to the constituent components; results characterize the stones into the three main categories. Main advantages of this technique are its ability to focus on a small volume within the object and the capability of *in vivo* measurement.

Comparison between radionuclide and polarized X-ray sources for *in vivo* X-ray fluorescence

P. Tothill
Department of Medical Physics and Medical Engineering, Western General Hospital, Edinburgh EH4 2XU, UK

The use of polarized X rays (PXR) for *in vivo* X-ray fluorescence analysis of heavy metals in organs such as the kidney and liver has theoretical advantages in reducing the background due to scatter. To provide a more mobile apparatus, alternative radionuclide sources in different geometries were explored and compared with PXR, which were generated by scattering of 160 kVp X rays from aluminium. The radionuclide sources considered were ^{57}Co, ^{99}Tc^{m}, ^{153}Gd and ^{133}Xe used in 90° and backscatter (approximately 155°) geometries and ^{99}Tc^{m} as a kidney-seeking radiopharmaceutical. The minimum detectable concentration (MDC) of platinum, gold or lead at the depth of the kidney was limited by the counting-rate characteristics of the electronic equipment, rather than the radiation dose to the patient. The best radionuclide set-up used the 100 keV gamma rays from ^{153}Gd in a 90° geometry and the MDC was not greatly inferior to PXR.

The long-term retention of platinum in human tissues following cancer chemotherapy

P. Tothill, *H. S. Klys, L. M. Matheson and J. F. Smyth
*Imperial Cancer Research Fund Medical Oncology Unit and *Department of Pathology, Western General Hospital, Edinburgh EH4 2XU, UK*

The highly sensitive and specific technique of inductively coupled plasma source mass spectrometry has been used to extend studies of the distribution and retention of platinum in the tissues of patients following the administration of cisplatin or carboplatin. Measurements of blood platinum were made up to 2 years and renal excretion up to 5 years after treatment. The pattern of disappearance of platinum followed a power law, with a steeper slope for plasma and red cells than for urine. Autopsy samples were used to examine the distribution of platinum in various human organs up to 17 months after treatment. By far the highest concentrations were found in the liver. Although there was much scatter of results between patients, there seemed to be little loss of platinum with time after about 1 month. In comparison with our previous studies in experimental animals, we conclude that the pig is a better model of platinum retention and distribution for humans than the rat. The prolonged retention of platinum may be relevant to long-term toxicity.

X-ray fluorescence for the determination of gold *in vivo*

J. Shakeshaft and S. Lillicrap
Wessex Regional Medical Physics Department, Royal United Hospital, Bath BA1 3NG, UK

X-ray fluorescence is now a fairly well-established technique for the determination of heavy metals *in vivo*. The technique is now fairly extensively used for measuring metals in organs near the skin surface such as lead in tibia. Methods of determining the concentration in organs lying at a depth, such as platinum in kidneys, have also been described in the literature. These methods have described a number of excitation sources and geometries. Our interest has been in the determination of low levels of gold in the kidney following chrysotherapy. A description of our clinical work to date is presented, together with the results from computer-modelling studies, to determine sensitivity variation with kidney position. A summary of how gold distribution within the kidney might affect the results is also presented. The work described uses an excitation source of ^{153}Gd in a 90° geometry, with a 32 mm diameter germanium detector. The measurement time is between 20 and 30 min, and the patient receives an equivalent dose not exceeding 30 μSv with our current apparatus.

Determination of body fat by DEXA: a comparison with neutron activation

S. J. S. Ryde, *A. Laskey, W. D. Morgan and †J. Compston (Swansea *In Vivo* Analysis Research Group)
*Department of Medical Physics, Singleton Hospital, Swansea SA2 8AQ, and *Department of Nuclear Medicine and †Department of Medicine, Addenbrooke's Hospital, Hills Road, Cambridge CB2 2QQ, UK*

Recent developments of dual-energy X-ray absorptiometry (DEXA) instrumentation and software have enabled rapid measurements of body fat. The objective of this study was to compare body fat computed from DEXA (Lunar DPX, software V3.1) with that derived from *in vivo* neutron activation analysis (IVNAA). 11 female subjects (covering a wide range of BMI) were measured by both methods on two occasions approximately 11 weeks apart. During this time the subjects adhered to a very low calorie diet and had a mean weight reduction of 16.2 (± 2.4) kg. A total of 22 measurements was obtained. The mean (± SEM) total body fat evaluated from DEXA, 39.2 (±1.8)%, was not significantly different ($p = 0.28$) from that determined by IVNAA, 39.9 (±1.8)%. The results obtained by the two techniques were significantly correlated ($r = 0.94$, $p < 0.0001$). The bias (±2SD) of the DEXA measurement (*i.e.* IVNAA minus DEXA) was 0.7 (±5.9)% of fat. The agreement between the methods with increasing fat was evaluated by regression analysis relating the difference between measured values to the mean of the methods; the resulting slope (± SE) and correlation coefficient were 0.03 (± 0.08) and 0.07, respectively. From this study it is concluded that DEXA provides a measurement of total body fat comparable with that derived from IVNAA.

A comparison of techniques for the assessment of body fat

S. J. S. Ryde, D. W. Thomas, J. L. Birks, *C. J. Evans, W. D. Morgan and *N. H. Saunders (Swansea *In Vivo* Analysis Research Group
*Department of Medical Physics, Singleton Hospital, Swansea SA2 8QA, and *Department of Physics, University College of Swansea, Swansea SA2 8PP, UK*

A knowledge of body composition is a diagnostic aid in many medical specialties. The objective of this study was to compare the estimation of fat in normal and obese subjects using a variety of radiological and other techniques and to assess the usefulness of those more recently introduced. A total of 43 subjects was studied using eight techniques. The results showed significant ($p < 0.001$) differences between the estimates of fat in normal subjects by several methods, although highly significant ($p < 0.0001$) correlation coefficients were observed between all the methods used. Similar differences were noted in obese subjects but lower correlation coefficients were obtained between the site specific, and thereby localized, measurements using skinfold anthropometry and infrared interactance and those other measurements utilizing the whole or most of the body. This suggests that optimum results may not be obtained with some localized techniques in subjects who depart radically from normal composition and in whom the greatest clinical interest may be shown.

Approaches to the determination of total body protein

W. D. Morgan and *S. J. S. Ryde
*Department of Medical Physics, Queen Elizabeth Hospital, Birmingham B15 2TH, and *Department of Medical Physics, Singleton Hospital, Swansea SA2 8QA, UK*

Assessment of nutritional status is important in the management of a variety of chronic and acute conditions. Traditionally, a two-compartment model, comprising fat and non-fat, may be differentiated by measuring the total body density. However, the density of non-fat tissues is not constant, but depends on the relative amounts of protein, water and minerals which comprise the lean body mass. Measurements of total body nitrogen (TBN) by *in vivo* neutron activation analysis provide a direct measure of total body protein (TBP). Water (TBW) can be determined by radioisotope dilution, and minerals by neutron activation or X-ray absorptiometry. However, not all of these techniques are readily accessible. Recent work has shown that changes in TBP can be inferred from changes in total body density and TBW, assuming that any corresponding changes in mineral content are minimal or can be ignored. Current availability of dual energy X-ray absorptiometry (DEXA) instruments should enable this approach to be refined by providing measurements of total body bone mineral. Furthermore, the DEXA method also separates the non-bony tissues into fat and non-fat components. It is argued that this approach, allied to measurements of total body water can provide an indirect measure of TBP. Measurements on obese and non-obese volunteers are used to test this approach.

The effects of very low calorie diet on total body nitrogen

S. J. S. Ryde, J. L. Birks and D. W. Thomas (Swansea *In Vivo* Analysis Research Group)
Department of Medical Physics, Singleton Hospital, Swansea SA2 8QA and Department of Physics, University College of Swansea, Swansea SA2 8PP, UK

Recent developments in body composition research enable more direct measurements to be made of changes that occur during weight reduction programmes. The objective of this study was to evaluate the body composition change resulting from an 11 week period of adherence to a very low calorie (405 kcal) diet. The technique of *in vivo* neutron activation analysis was used to provide a non-invasive measurement of total body nitrogen, and hence protein, in a group of 11 female volunteers. Measurements were made immediately before and after the period of diet. During the diet, the mean weight loss was 16.2 (±2.4) kg, corresponding to a mean reduction in BMI from 32.1 to 26.2 kg/m^2. The mean loss of total body nitrogen was 125 (±57) g, equivalent to 781 (±356) g of protein. Assuming the nitrogen concentration of the fat-free mass to be 33 g/kg, the mean fat-free component of the weight loss was 23.7 (±3)%. Only four subjects recorded a fat-free loss of more than 25% and only one was greater than 32%. These results suggest that the use of a very low calorie diet as described above does not lead to a disproportionate loss of fat-free mass. The fat-free mass loss was not clearly related to BMI.

10.45 – 12.00

New Applications of MRI

Hall 9

New MRI techniques for musculoskeletal imaging

S. E. Harms and D. P. Flamig
Magnetic Resonance Imaging Section, Department of Radiology, Baylor University Medical Center, Dallas, Texas, USA

Methods have recently emerged that are expanding the capability of magnetic resonance imaging (MRI) in musculoskeletal diagnosis. These new techniques are reviewed with clinical examples. *Methods:* Images are acquired using a General Electric Signa 1.5 T imager with 4.6 level software. Image processing is provided by the General Electric Independent Console and the Sun 3/260 workstation. *Results:* New three-dimensional (3D) pulse sequences produce improved resolution and contrast. Joint imaging is optimized with a T_1-weighted sequence without spoiling so that fluid is hyperintense. Bone marrow disease is well visualized with new fat-suppressed 3D acquisitions. A variety of angiographic methods is used for extremity diagnosis depending upon the clinical needs. Patients with peripheral vascular disease and poor visualization of distal vasculature on conventional angiography can often benefit from two-dimensional time-of-flight imaging which is sensitive to slow flow. High-resolution vascular imaging can be achieved with a non-selective fat suppressed 3D acquisition. Phase contrast angiography is well suited for studying flow direction and velocity. Real-time image reformations and fast projection imaging are generated with dedicated viewing workstations. *Conclusions:* New acquisition and image procession techniques are used to improve diagnostic accuracy and clinical efficiency of musculoskeletal MRI.

MRI the evaluation of the thoracic outlet syndrome

R. J. Gibson, N. R. Moore, *P. Panegyres and *M. Donaghy
*Departments of Radiology and *Neurology, John Radcliffe Hospital, Oxford OX3 9DU, UK*

The thoracic outlet syndrome presents diagnostic and management difficulties, and imaging has not addressed these problems adequately. We used magnetic resonance imaging (MRI) to identify the anatomy of the brachial plexus and to display any deviation of the nerve roots or trunks. We used a 1.5 T machine and linked two surface coils anteriorly and posteriorly to improve the spatial resolution and the signal to noise ratio. We obtained short time to repeat (TR)/short time to echo (TE) (T_1-weighted), contiguous 3 mm coronal sections and a T_1-weighted spoiled gradient recalled acquisition in the steady state (SPGR) volume acquisition. This produces 60 1.5 mm thick sections, which can be reformatted in any plane. 18 patients were referred with clinical and electrophysiological evidence of the thoracic outlet syndrome. On a prospective basis, blinded to the clinical features, we identified the affected side using MRI in 17 out of 21 sides (sensitivity = 81%), and identified normality in 13 out of 15 sides (specificity = 87%). On the spin-echo sequence cervical ribs were seen more clearly, and the gradient-echo sequence showed root and trunk displacement better. We believe that MRI has a clear role in the evaluation of the thoracic outlet syndrome.

Magnetic resonance imaging in the assessment of peripheral arterio-venous malformations

D. Kinsella, A. Longstaff, P. Murphy and P. Goddard
Department of Radiology, Bristol Royal Infirmary and the Bristol MRI Centre, Frenchay Hospital, Bristol BS2 8HW, UK

Magnetic resonance (MR) scans were obtained in 11 patients with suspected peripheral arterio-venous malformations. T_1-weighted and short tau inversion recovery (STIR) sequences were performed in each case. In one patient no soft tissue or bony abnormality was demonstrated. Examples will be presented that show the value of MR in assessing the extent of the lesion and its relationship with surrounding structures. The STIR sequence acts to highlight the areas of vascular abnormality. MR scanning is the initial imaging method of choice if surgical excision of a peripheral venous malformation is being considered.

Initial experiences using fast spin echo

S. J. Golding (for the Oxford MRI Group)
MRI Centre, John Radcliffe Hospital, Headington, Oxford OX3 9DU, UK

This paper reports initial experience of a new sequence designed to improve patient throughput by reducing examination times, within the context of a high throughput service based on a 1.5 T Signa system. Fast spin echo (General Electric CGR) permits the collection of a range of phase-encoding values in a given time to repeat (TR) interval by producing multiple echoes. The effect in practice is to reduce the acquisition time for conventional T_2-weighted images to approximately a quarter. The images are similar to conventional spin-echo T_2-weighted images, although some difference in contrast exists. This sequence produces a small but significant increase in throughput. Other advantages of reducing acquisition time include reduced movement artefact and shortened-examination times in patients who have difficulty co-operating with the technique. The clinical applications where we have found this sequence of value are reviewed and areas of further development indicated.

Dynamic MRI of the pancreas — gadolinium enhancement in normal tissue

J. A. D. Brailsford, A. G. Chalmers, J. P. Ridgway,
J. Ward and P. J. Robinson
MRI Unit, St James's University Hospital, Leeds LS9 7TF, UK

The purpose of this work was to measure signal enhancement in the normal pancreas following gadolinium injection with the aim of improving recognition of perfusion abnormalities in acute pancreatitis. We studied 25 patients before and after the rapid bolus injection of gadolinium DTPA (Magnevist 0.2 ml per kg). Images were obtained on a 1.0 T Siemens Magnetom using a multislice TurboFLASH sequence (time to repeat (TR) = 100; time to echo (TE) = 4; flip angle = 80). The very short echo time allows 11 5 mm slices to be acquired simultaneously during a breath hold period of 19 s. A block was obtained pre-contrast followed by dynamic post-contrast acquisitions starting 12–15 s after the bolus injection. There was a 10 s interval between the post-contrast blocks. Signal intensity was measured for the pancreatic head and tail and also for the liver. These figures were then normalized to fat values for each scan to allow for scaling factor variations. Peak enhancement in normal pancreatic tissue occurred in the first and second post-gadolinium acquisitions and declined on subsequent scans. The pattern of enhancement and normal pancreatic anatomy in the coronal and axial planes is described.

A fast technique for demonstrating vascular anatomy and patency using contrast-enhanced TurboFLASH

J. P. Ridgway, J. Ward, K. Bann, J. Cullingworth and P. J. Robinson
MRI Department, St James's University Hospital, Leeds LS9 7TF, UK

Magnetic resonance angiography (MRA) performed without the use of contrast media has improved substantially over the past few years and both in-flow and phase contrast techniques give excellent results for certain applications. The acquisition times for MRA are still quite long, however, and variable results are common where the blood flow is poor or highly pulsatile. TurboFLASH imaging following bolus injection of gadolinium-DTPA (Gd-DTPA) offers a quick and easy method of demonstrating vascular anatomy and patency. The intrisically short echo time (4 ms) of TurboFLASH sequences, when used in simultaneous multislice acquisition mode, allows a relatively high number of slices to be acquired within an acceptable breath-hold period. Several such acquisitions are performed following bolus injection of Gd-DTPA allowing both the arterial and venous system to be imaged in just 2 min. Maximum intensity projection through the slices allows the full extent of all vessels included to be visualized on a single image. We have used a T_1-weighted TurboFLASH sequence (time to repeat = 100 ms; time to echo = 40 ms; flip angle = 80; 11 × 5 mm slices; acquisition time = 19 s) to image a range of vessels in the abdomen, thorax and pelvis. Details of the technique and resultant images are presented, and the advantages and limitations of the technique in comparison with MRA are discussed.

Fast MR angiography using TurboFLASH sequences in advanced aorto iliac disease

U. M. Sivananthan, M. R. Rees, J. Ridgway, S. P. Verma, K. Bann and J. Ward
Department of Cardiac Radiology, Killingbeck Hospital and MRI Unit, St James's University Hospital, Leeds LS14 6UQ, UK

We have employed two-dimensional TurboFLASH gradient echo sequences with gadolinium-DTPA enhancement to image advanced atherosclerotic aorto iliac disease in 20 patients. Three sets of 10, 4–5 mm thick slices were acquired simultaneously during breath holding, 10 s after an intravenous bolus of gadolinium. A 400 mm field of view with 160 × 256 acquisition matrix was used. Time to repeat (TR) of approximately 100 ms and a fixed time to echo (TE) of 4 ms were employed. The images were post-processed for using the maximum intensity projection algorithm to produce projection images. In all patients the magnetic resonance (MR) angiography was comparable with that of the conventional angiography. Four aortic occlusions and seven iliac occlusions were all diagnosed correctly, although the MR imaging overestimated the length of the occlusions in almost all cases. Haemodynamically significant stenoses (more than 50%) were seen in 25 segments of the conventional and in 31 in the MR angiography group. High-grade stenoses (more than 80%) were shown as signal void just distal to the area of stenosis in the maximum intensity projection images. We will discuss the technique, the methods of improving image quality and also some of the artefacts. We conclude MR angiography using TurboFLASH sequences and gadolinium enhancement promises to be another non-invasive technique to assess advanced aorto iliac disease.

Notes

Quantitative T_1 and T_2 measurements of CSF in patients with multiple myeloma

V. Nicolson, J. Husband, T. Hickish, D. Cunningham, D. Collins, P. Gowland, M. Leach and V. Ayton
Department of Diagnostic Radiology, The Royal Marsden Hospital, Downs Road, Sutton, Surrey SM2 5PT, UK

Involvement of the meninges in multiple myeloma is rare. However, an "M" band in the cerebrospinal fluid (CSF) of patients without other evidence of CSF or meningeal disease has been reported by Foronzo et al (1978). The T_2-weighted magnetic resonance signal is related to viscosity and hence quantitative T_2 measurements potentially provide a means for detecting CSF paraproteinaemia. We have measured the quantitative T_2 signal in the CSF of 30 patients with multiple myeloma. There is an inverse relationship between the serum paraprotein and CSF T_2 values. In five patients for whom serial measurements are available, a reduction in serum paraprotein due to treatment corresponded to a rising T_2 level.

Reference

Foronzo, R. A., Cooke, R., Wright, J., Humphrey, R. 1978. *Medicine*, *57*, 151.

10.45 – 12.00

Counselling and Quality of Care in Oncology

Hall 10a

Costs and benefits of counselling

E. J. Maher
Department of Radiotherapy, Mount Vernon Centre for Cancer Treatment, Northwood, Middlesex HA6 2RN, UK

Cancer patients have many unrecognized psychosocial problems. A variety of interventions has been suggested to improve the detection and management of these, including teaching professional staff communications and counselling skills; improved information, particularly in written form or employment of trained counsellors. All these interventions have resource implications. A study was conducted at Mount Vernon Centre for Cancer Treatment to investigate the impact of a radiographer counsellor and clarify the answer to four questions: (1) how many routine radiotherapy patients might benefit from counselling? (2) how should need be assessed? (3) how much does it cost? and (4) how should the benefits be evaluated?

Comparison of methods for obtaining quality of life assessments in oncology

J. Morris
Centre for Health Economics, University of York, York YO1 5DD, UK

There is an increasing awareness of the need to measure quality of life as an indicator of the success of a particular treatment as well as morbidity and mortality. Such information can be used to: (1) aid decision making where different modes of treatment result in similar clinical outcomes; (2) quantify the extent to which treatment affects adversely patients' quality of life and thus provide a focus for additional support; and (3) together with cost data provide more comprehensive information on the costs and effectiveness of different forms of treatment. The method of choice for collecting quality of life information will depend largely upon the resources available for a study and, more importantly, the rationale for collecting such data. This paper highlights the advantages and disadvantages of obtaining data from (i) interviews, and (ii) questionnaires, and also illustrates how quality of life questionnaires can be selected for use in cancer clinical trials.

Treatment of oesophageal carcinoma with combined external beam and intracavitary radiotherapy

R. K. Agrawal, *C. S. Robertson, P. J. D. K. Dawes, *S. M. Griffin and *M. B. Clague
*Departments of Radiotherapy and Oncology, and *Surgery, Newcastle General Hospital, Newcastle upon Tyne NE4 6BE, UK*

Prognosis for patients with inoperable oesophageal carcinoma remains poor and the optimal treatment remains to be defined. Between April 1987 and December 1990, 131 patients (72 male, 59 female, age range 36–91 years, median 70 years) with histologically proven (98 squamous, 30 adenocarcinoma, two adenosquamous, one malignant on cytology) advanced or metastatic oesophageal carcinoma unsuitable for surgery were referred for radiotherapy. Megavoltage external radiotherapy (20–50 Gy in 4–20 fractions, the majority receiving 30 Gy in 10 fractions) was followed by endoscopically inserted afterloading oesophageal applicator (10 Gy at 1 cm in 1.66 h) in 123 patients. In eight patients the intracavitary dose was modified, the procedure was abandoned in one patient and there was one procedure-related death. Swallowing (Grade II or better) was restored in 107 patients (82%) with 55 patients subsequently requiring dilatation. Median survival was 11 months (range 1–43 months); actuarial survival at 6, 12, 24 months being 71%, 36% and 16%, respectively. Combined external beam and intracavitary radiotherapy is well tolerated, associated with few complications, provides good palliation and may improve survival in this group of poor prognosis patients.

Radiological audit in oncology; improving the diagnostic algorithm for today's cancer patient

E. C. Moskovic, *E. Wiltshaw and C. Parsons
*Department of Radiology and *Medicine, Royal Marsden Hospital, Fulham Road, London SW3 6JJ, UK*

Imaging and monitoring response to therapy is becoming increasingly complex and expensive in all branches of medicine. New diagnostic modalities are introduced almost daily presenting both the clinician and radiologist with a bewildering array of tests, the merits of which may not be established. This dilemma is particularly acute in the cancer patient, for whom the price of an invasive investigation may be high in terms of morbidity and low in long-term gain. The aim of a modern oncological imaging department must be to provide its patients with a prompt, specific and highly accurate diagnostic service; completely tailored to individual disease categories thereby conserving valuable economic resources and sparing both unnecessary radiation and patient morbidity. Provision for continuing research must not be neglected. With these principles in mind, the following projects have been undertaken by this department and the results used to improve the quality of our service: (1) chest X ray in the follow-up of breast cancer, (2) the role of computed tomography (CT) scanning of the brachial plexus, (3) the monitoring of ovarian cancer: serum CA125 or CT scanning? (4) the current value of lymphography, (5) the provision of mammography outside the national screening cohort, and (6) the accuracy of X-ray request form data.

Percutaneous nephrostomy in malignant disease

A. F. Watkinson, E. Moskovic and D. M. King
Department of Radiology, Royal Marsden Hospital, Fulham Road, London SW3 6JJ, UK

Percutaneous nephrostomy has become a well established technique for rapid relief of ureteric obstruction and improvement of renal function. This procedure is both invasive and uncomfortable and its role in renal failure resulting from abdominopelvic malignancy is often controversial. There are currently no clear guidelines available for the prediction of which of these patients will gain real benefit from such intervention and an emergency decision in favour of drainage may not always be in the long-term interest of the subject. Quality of life with resumption of a normal lifestyle, at least in the short term, is paramount in such patients and a useful therapeutic option must be available after nephrostomy in order to justify its implementation. In an attempt to establish a protocol for selection of patients with malignant disease suitable for nephrostomy the medical records and radiographs of 74 consecutive nephrostomy patients at this institution were reviewed. The results will be presented and discussed with reference to the patient's age, histology, grade and stage of tumour both at presentation and at the time of nephrostomy and an analysis of the factors affecting outcome will be made.

The role of pulmonary computed tomography in the management of Wilms' tumour. 1: Clinical management

C. M. Owens, S. J. D. Burnett and C. Dicks-Mireaux
The Hospital for Sick Children, Great Ormond Street, London, UK

The staging and therapy of Wilms' tumour is based on data collected before the availability of computed tomography (CT). It is established in the adult population that chest CT may reveal metastatic lesions not apparent on chest radiographs; no such data has been published regarding childhood malignancies. 453 children with Wilms' tumour were entered into the United Kingdom Children's Cancer Study Group (UKCCSG), between June 1986 and October 1991. 359 had normal chest films at presentation of which 165 had pulmonary CT performed at that time. 36 of the 165 (22%) patients with normal chest radiographs had abnormal CT, and on review 16 (10%) had intrapulmonary nodules. Of these 16 patients, 10 relapsed, nine with pulmonary lesions, giving a pulmonary relapse rate of 56%. The current pulmonary relapse rate of all 453 patients is approximately 8%. Although this result may not achieve statistical significance in our data, it may demonstrate a subgroup that are at higher risk of pulmonary relapse. Whether this affects the final clinical outcome will be discussed.

The role of pulmonary computed tomography in the management of Wilms' tumour. 2: Cost–benefit analysis

S. J. D. Burnett, C. M. Owens and C. Dicks-Mireaux
The Hospital for Sick Children, Great Ormond Street, London, UK

The staging and therapy of Wilms' tumour is based on data collected before the availability of computed tomography (CT). The current use of imaging makes certain assumptions about the sensitivity of plain chest radiography. Review of the United Kingdom Children's Cancer Study Group (UKCCSG) data shows that of 453 patients entered between June 1986 and October 1991, 359 had normal chest films at presentation. We have examined the impact that routine chest CT has on staging. 165 had pulmonary CT performed at that time of which 22% had abnormal CT despite normal plain films, and of these 10% had pulmonary nodules. Of these latter patients, 10 relapsed, nine in the lungs, giving pulmonary relapse rate of 56%. The overall pulmonary relapse rate approximated 8%. Therefore the information obtained at CT may demonstrate a subgroup that is at higher risk of pulmonary relapse. However, this may not be reflected in the final clinical outcome; the data suggests that there may be no significant difference in the percentage of disease-free patients in each group. We discuss this data in the form of a cost–benefit analysis to explore the value of chest CT in Wilms' tumour.

10.45 – 12.00

Measurements of Bone Mineral

Hall 10b

Measurement of bone mineral

D. Felsenberg
Department of Radiology, University Clinic Steglitz, Freie Universität Berlin, 1000 Berlin 45, Germany

The necessity for osteodensitometric measurements can be explained by the inability to diagnose reliably a decrease of bone in various other ways. Clinical symptoms are unspecific and just as few typical serum parameters exist. Osteodensitometry is the only non-invasive procedure, until now, that is able to give reliable information about bone mineral density. The conventional X ray, for a long time the only instrument capable of diagnosing osteoporosis, no longer complies with today's technology. The aim of the modern diagnosis of osteoporosis is the early and precise measurement of bone mass deficiency. To meet these requirements there are two basic thoughts to keep in mind: a representative measuring area and a precise method. The methods in current use such as quantitative computed tomography of the spine and hip, peripheral quantitative computed tomography of the radius, dual-energy X-ray absorptiometry of the spine, the hip and the whole body, single photonabsorptiometry and ultrasound measurement of the heel will be introduced. The clinical validity, the boundaries, possibilities and errors of the above mentioned methods will be compared with one another.

Non-invasive vertebral texture analysis based on HRCT — a new diagnostic tool in osteoporosis

A. Mundinger, A. Beck, E. Dinkel, A. Helwig and A. Heinzel
Department of Diagnostic Radiology, University Clinics, W-7800 Freiburg, Germany

Osteoporosis is characterized by low bone mass and microarchitectural deterioration of bone tissue leading to enhanced bone fragility. Up to now changes of bone architecture could not be assessed non-invasively. The objective of our study was to introduce and apply clinically the new non-invasive technique of vertebral texture identification based on high resolution computed tomography (HRCT) and computer assisted imaging analysis of vertebral body texture. 189 women and 49 men were studied by one midvertebral HRCT scan through a non-fractured lumbar vertebra, and by osteodensitometry (SEQCT). Variations in the architecture were assessed by a computer assisted imaging analysis system, and statistically analysed. The total number and diameter of trabecular plates and intertrabecular spaces were the most relevant texture parameters and showed characteristic age and sex dependent changes ($p < 0.01$). Vertebral mineral content of patients with silent osteoporosis (without fractures) compared with patients suffering from manifest osteoporosis (with fractures) was similar. Both groups, however, showed a discriminating pattern of spongiosa texture changes ($p < 0.05$). We conclude that vertebral texture analysis can assess remodelling changes of the spongiosa architecture non-invasively, and in combination with osteodensitometry promises further prediction of individual risk for fractures and monitoring of treatment efficacy.

SPA, QCT and DXA reference range for British women and correlations between the techniques

*J. E. Adams, *R. W. Whitehouse, †A. Silman, ‡P. H. Adams and C. Kay
*Bone Disease Research Centre and Departments of *Diagnostic Radiology, †Epidemiology and ‡Medicine, The University of Manchester and Barlow Medical Centre, Manchester M13 9PT, UK*

Methods (single photon absorptiometry (SPA), quantitative computed tomography (QCT) and dual-energy X-ray absorptiometry (DXA)) for bone mineral density measurement (BMD) are now widely available; reference ranges for interpretation of results are generally provided with the equipment by the manufacturers. It is recognized that ethnic and national differences in bone mass may occur, and our study was undertaken to ascertain if these reference data were generally applicable to the local community. *Methods:* Over 6 months, 200 women (aged 45–75 years), drawn at random from a local medical practice, were invited to attend for BMD measurement. To date, 142 women of 200 invited (response rate 71%) have attended. SPA was performed in two sites of the forearm (proximal and ultra distal). Single and dual energy QCT was performed in the spine (T12–L3) and DXA measurements were made in the spine and both femoral necks. The data collected were compared with reference data provided. BMD measurements in the same patients by different techniques were compared. *Results:* SPA (distal) compared with reference data gave a significantly higher mean value (± 0.52 SD; $p < 0.001$). The proximal forearm measure was not significantly different from those of a European population (Brunner study). QCT results were not significantly different from published data (Block et al, 1989). DXA measurements in both the spine (± 0.294 SD; $p < 0.016$) and femoral neck (± 1.179 SD; $p < 0.001$) were significantly higher than American reference data provided. Correlations *(r)* between measuring techniques varied between 0.49 to 0.76. *Conclusion:* The results confirm significant differences in SPA and DXA reference data for forearm, hip and lumbar spine. Institutions providing BMD measurement should ensure that the reference BMD range which is used is appropriate to the local population and ethnic groups. Correlations confirmed that BMD measured by one technique could not be used to predict the BMD by another method in the same or different anatomical site.

Reference

Block, J. E., Smith, R., Glueer, C.-C., Steiger, P., Ettinger, B. & Genant, H. K., 1989. Models of spinal trabecular bone loss as determined by quantitative computed tomography. *Journal of Bone Mineral Research*, *4*, 249–257.

Methods of assessment of spinal deformity

G. L. Thomas, D. J. Green, A. Armstrong and
A. Wallace
Radiology Department, City Hospital, Hucknall Road,
Nottingham NG5 1PB, UK

This study compares and contrasts current methods for assessing the effects of osteoporosis on the spine by analysing the deformity produced by vertebral body collapse and fracture on lateral radiographs. The study compares subjective and objective digital methods to assess vertebral deformity and fracture indices. Two methods of assessing spinal deformity are examined; the Spinal Deformity Index and a system of comparing heights of neighbouring vertebral bodies to define fracture. 25 osteoporotic patients and 25 controls are compared using dual energy X-ray bone absorbtiometry and with questionnaire based assessments of the pain and disability. Results will be presented, assessed and discussed.

Assessment of axial osteopenia: plain radiography versus dual energy X-ray absorptiometry

M. J. Garton, *E. M. Robertson, *F. J. Gilbert and
D. M. Reid
Department of Rheumatology, City Hospital, Urquhart
*Road, Aberdeen AB9 8AU and *Department of Radiology,*
Royal Infirmary, Foresterhill, Aberdeen AB9 2ZE, UK

Osteopenia is frequently diagnosed on plain radiographs, although previous studies have suggested that this is a poor method of assessing bone mineral density (BMD). To study this further, standardized plain lateral radiographs of the thoraco-lumbar spine were compared with dual energy X-ray absorptiometry (DXA) scans of the antero-posterior (AP) lumbar spine in 99 (45 male) randomly selected subjects, aged 50–84 years. DXA measurements were made on a Norland XR26 bone densitometer; the precision of AP lumbar spine scans is good (c.v. 0.9%). Radiographs were reported blind by two independent senior radiologists, and given an "osteopenia score" based on the radiological criteria of demineralization or vertebral deformity (biconcavity, height loss or frank collapse). Patients with lumbar vertebra collapse (L2–4) were excluded from further analysis. About one-fifth of radiographs were reported as normal, and the interobserver correlation was moderate ($r = 0.63$, $p < 0.001$). The mean BMD of radiologically normal subjects was higher than that of osteopenic subjects ($1.20\ \mathrm{g/cm^2}$ *vs.* $0.94\ \mathrm{g/cm^2}$, $p = 0.002$). Using a fracture threshold of $0.75\ \mathrm{g/cm^2}$, the predictive value of a normal radiograph was 100%, but of an osteopenic X ray was only 20%. In conclusion, normal radiographs may usefully exclude severe osteopenia, but abnormal X rays are non-specific, reflecting the importance of factors other than BMD in determining fracture risk.

Spinal bone mass measurement: QCT or DXA?

A. Karantanas, R. W. Whitehouse and J. E. Adams
Diagnostic Radiology, University of Manchester,
Manchester M13 9PT, UK

Quantitative computed tomography (QCT) and dual energy X-ray absorptiometry (DXA) are both used to measure spinal bone mineral density (BMD). QCT measures trabecular bone whilst DXA measures integral (cortical and trabecular) bone, but will include spinal degenerative changes in the measurement. The study was performed to assess the influence of age, scoliosis, fractures, osteophytes, facet joint disease, disc space narrowing and aortic calcification on the relationship between QCT and DXA. *Methods:* QCT and DXA results in 335 females were compared. The CT scout projection radiograph was used to score each subject for the presence or absence of the features listed above. The data were analysed by stepwise multiple linear regression. *Results:* All the spinal features described became increasingly common with age, with osteophytes present in $> 50\%$ over 60 years. Where analysis was restricted to subjects without degenerative features, age remained a significant variable influencing the relationship between QCT and DXA. The presence of fractures in the lumbar spine caused considerable overestimation by DXA compared with QCT. Osteophytes, disc space narrowing and facet joint disease had smaller but significant effects. *Conclusions:* DXA is quick, precise, accurate and carries a negligible radiation burden but the results of spinal DXA may be misleading in older patients and those with spinal fractures and/or spinal degenerative disease. A conventional lumber radiograph may be necessary to assess these features but negates the low dose advantage of DXA.

Increased bone mineral density in the hip and spine by dual X-ray absorptiometry (DEXA)

E. F. J. Ring, D. M. Elvins, R. Woodward and
A. K. Bhalla
Department of Clinical Measurement, Royal National
Hospital for Rheumatic Diseases, Bath BA1 1RL, UK

The dual energy X-ray absorptiometry (DEXA) technique for measuring *in vivo* bone mineral density (BMD) is of particular interest for the assessment of osteoporosis. Most of the literature is concerned with decrease in BMD compared with normal population data. High BMD is also found in certain diseases, especially in long-term ankylosing spondylitis (*e.g.* 2.87 SD above aged matched control mean: Z score). The formation of syndesmophytes falsely elevates spinal BMD, while the true BMD in patients without syndesmophytes is lower than aged matched controls. We have also reported high values for BMD of the hip in cases of osteoarthritis, with values for the femoral neck being significantly higher than controls or the unaffected hip $p < 0.001$ — with a mean Z score of +1.5. In Paget's disease of bone, very high values for spine BMD have been obtained, *e.g.* a Z score of +8.24. Artifactual elevation of BMD can also occur, especially in the spine. Disturbance of soft tissue "background" may occur from isotope investigation, or long-term gold therapy. Localized increases have been found in vertebral haemangioma and calcified aorta. More commonly crush fractures of one or more vertebrae, degenerative changes and osteophyte growth will have the effect of higher BMD values, which if not excluded can mask true osteoporosis. In such cases simple comparison of the patients' BMD result with reference population data can be misleading. Further radiological investigation may be indicated.

Assessment of bone growth activity in leg lengthening procedures, using DEXA

M. J. Haddaway, *J. Richardson, C. V. Pullicino, *G. A.
Evans and I. W. McCall
*Department of Diagnostic Imaging, and *Children's Unit,*
Robert Jones and Agnes Hunt Orthopaedic Hospital,
Oswestry, Shropshire SY10 7AG, UK

The aim of this study is to determine the role of dual energy X-ray absorptiometry (DEXA) in monitoring the healing process to help determine the optimum timing of external fixation removal. Using a Hologic QDR-1000 absorptiometer, serial bone mineral densitometry (BMD) measurements in six patients were obtained through the entire process of leg lengthening from commencement of distraction through consolidation and removal of the external fixation device. Assessment of new bone formation during lengthening, compared with both ipsilateral and contralateral long bone shows a pattern of healing with identifiable characteristics to both the proliferative and consolidative stages. The BMD measurements were compared with the sonographic appearances particularly in the early stages of lengthening and with fracture stiffness measurement in the later stages of healing. The various methods of presenting this BMD data are described, together with their place in predicting rate of healing and fixation removal. The alternative and complementary methods of determining the characteristics of new bone formation are helpful in supporting the conclusions reached from the BMD data. We conclude that serial BMD estimation using DEXA promises to provide a reliable, safe and reproducible means of monitoring fracture healing providing an insight to the ideal timing of fixation removal.

10.45 – 12.00

Chest Radiology

Hall 11a

AIDS and the chest

M. McCarty
Department of Radiology, St Mary's Hospital, London W2, UK

Most patients with the acquired immune deficiency syndrome (AIDS) develop a pulmonary complication during the course of their disease. These complications include bacterial pneumonias, opportunistic infections and neoplasms such as Kaposi's sarcoma and lymphoma. The radiologist has an important role in the management of these patients, not only in the interpretation of radiographs but also in providing diagnostic tissue by means of guided biopsy where appropriate. Chest radiograph interpretation is a challenge; although certain patterns can suggest particular diagnoses, there is considerable overlap in radiographic appearances between conditions. The patient often has more than one pulmonary complication at any one time; this further complicates the picture. In this presentation, the typical patterns of chest radiograph abnormalities seen in AIDS are reviewed and some atypical cases are shown.

The terminology and radiology of cryptogenic organizing pneumonia (COP)

J. A. A. Haddock and D. M. Hansell
Department of Diagnostic Radiology, Royal Brompton National Heart and Lung Hospital, London SW3 6NP, UK

Cryptogenic organizing pneumonia is an increasingly recognized condition with a distinctive constellation of clinical features and radiographic abnormalities, such that the radiologist may be the first to suggest the diagnosis. The term cryptogenic organizing pneumonia (COP) was first coined in the early 1980s. Subsequently another series of patients with a similar clinico-pathological condition was reported and the term bronchiolitis obliterans organizing pneumonia (BOOP) was used. The relative merits of the two terms (BOOP *vs.* COP) are considered. The diagnosis of COP is one of exclusion and requires histological confirmation. It has been suggested that the radiology of COP is too variable to be helpful but we present a series with uniformity of many of the radiographic abnormalities. The clinical findings, radiographic features and method of biopsy confirmation of nine patients with a histologically confirmed diagnosis of COP are presented. All patients complained of shortness of breath, cough and malaise; none had responded to antibiotics. Chest radiographs showed bilateral multifocal consolidation with a lower zone (6/9) and peripheral predominance (5/9). Relapsing shadows (3/9) and new areas of consolidation (3/9) occurred during the course of the disease with or without treatment. The importance of establishing an accurate diagnosis lies in the extreme responsiveness of COP to steroid treatment.

Organizing pneumonia – "BOOP" or "COP" — a review

O. Constant and R. Robertson
King Edward VII Hospital, Midhurst, West Sussex and Killingbeck Hospital, Leeds, UK

In 1983, Epler and Colby described a clinico-pathological syndrome, called "bronchiolitis obliterans — organizing pneumonitis" (BOOP). It was characterized by cough, fever, malaise, raised erythrocyte sedimentation rate, patchy radiographic shadowing and a restrictive pattern on lung function testing. No response to antibiotics but a good response to steroids was seen. The same year, Davison et al described a similar clinical syndrome which they called "cryptogenic organizing pneumonitis" (COP). Histology in both series was similar, showing organizing pneumonitis without evidence of infection. An association has been described between organizing pneumonitis and rheumatoid disease, ulcerative colitis and human immunodeficiency virus infection, and drugs such as amiodarone, but in most cases there is no underlying cause. Since then, the condition has been the subject of many reports and of much confusion, particularly because of overlapping terminology between BOOP and bronchiolitis obliterans (an entirely different subject). Whichever terminology is used, histology from open lung biopsy is identical in both groups. The terminology has recently been the subject of three editorials in medical journals but the topic seldom appears in British radiology journals. We feel that it is underdiagnosed radiologically and present here a spectrum of radiological appearances in 20 patients in whom histological proof of organizing pneumonia without infection is available.

Lymphocytic interstitial pneumonitis in HIV-infected children

C. M. Owens, D. Gibb, C. Dicks-Mireaux and D. Shaw
Departments of Radiology and Infectious Diseases, The Hospital for Sick Children, London WC1N 3JH, UK

We describe the clinical presentation and radiological manifestations of human immunodeficiency virus (HIV) infected children with pulmonary lymphoid hyperplasia and lymphocytic interstitial pneumonitis (PLH-LIP) at the Hospital for Sick Children. All HIV infected children have a chest radiograph performed at first presentation, and if clinically indicated, the radiological abnormalities are pursued with more invasive investigations such as lung biopsy and broncheoalveolar lavage (BAL). 27 vertically HIV infected children are being followed in our unit, and nine (33%) had radiological ± clinical evidence of PLH-LIP at presentation (three of these patients in association with other respiratory infections). The diagnosis of PLH-LIP was made on lung biopsy in three symptomatic patients. The remaining six were diagnosed on clinical and radiological grounds. The spectrum of radiological features ranged from initial hyperinflation of the lungs, progressing to diffuse bilateral reticulonodular infiltrates, in a child without major respiratory symptoms. In conclusion, the clinical and radiological features, differential diagnoses and natural history of PLH-LIP will be discussed.

The role of computed tomography in stable cystic fibrosis

M. Logan, R. O'Laoide, D. Mulhern, S. O'Mahony,
M. X. Fitzgerald and J. Masterson
Department of Radiology, St Vincent's Hospital, Dublin 4, Ireland

Plain chest radiographs are the standard radiographic method of assessment in cystic fibrosis (CF) and quantitative assessment of the chest radiograph has been shown to correlate with pulmonary function and clinical examination. The aim of this study was to establish whether quantitative assessment of conventional and high resolution computed tomography (CT) give any added information over and above plain films, especially in those patients with haemoptysis or allergic broncho-pulmonary aspergillosis (ABPA). 30 stable adult CF patients participated. Each had, on the same day, full pulmonary function testing, clinical examination (scored using Shwachman's System) and radiological investigations — plain chest radiograph, conventional knowledge of patient identity using the Birmingham Scoring System. There was significant correlation ($p < 0.01$) between the scores for clinical examination, pulmonary function and all three radiographic modalities. We found no statistical difference in the radiographic scores of these patients with haemoptysis or ABPA over those who never had haemoptysis or were ABPA negative, respectively. We conclude that quantitative assessment of conventional CT and high-resolution CT correlate with pulmonary function and clinical examination. These correlations are similar, but no closer, to previously noted correlations using quantitative assessment of the chest radiograph. No added information results from CT in the subgroups of patients with haemoptysis or ABPA.

Ultrafast CT appearances of obliterative bronchiolitis and bronchomalacia in lung transplant recipients: early experience

C. M. Allen, M. Yacoub and D. M. Hansell
Department of Radiology and Department of Cardio-Thoracic Surgery, Royal Brompton National Heart and Lung Hospital, Fulham Road, London SW3 6NP, UK

Obliterative bronchiolitis (OB) is a frequent complication and a cause of serious morbidity in lung transplantation. Recently bronchiomalacia (BM) with large airway collapsability has been described in association with OB in some patients. This leads to further severe airflow obstruction and increasingly poor respiratory function. Spirometric testing cannot distinguish between patients with OB alone or OB and BM; it is also inadequate for assessing function in single lung transplants. In this study we describe the appearances of OB and BM using an Ultrafast computed tomography (CT) scanner (Imatron C-100, San Francisco, USA). Six patients with biopsy-proven OB were studied. Four had received single lung transplants and two heart-lung transplants. Dynamic scans were obtained at four levels (mid-trachea, carina, main bronchi, lung bases). At each level 15 50 ms axial scans were obtained over 5 s during normal respiration and forced expiration. The results will be displayed in real time as a video. Areas of OB were identified in all patients as patchy areas of air trapping. This could also be demonstrated graphically using time–density curves in selected regions of interest. In two patients, both single lung recipients, unsuspected large airway collapse consistent with BM was demonstrated. This is the first demonstration of OB and BM using ultrafast CT. This technique is useful in evaluating the extent and severity of OB and BM in patients after lung transplantation.

Chest magnetic resonance imaging in sarcoidosis

D. Kinsella, R. Uberoi and P. Goddard
Department of Radiology, Bristol Royal Infirmary, Bristol BS2 8HW, UK

The chest magnetic resonance imaging (MRI) findings of 15 patients with sarcoidosis are presented. Coronal T_1-weighted and short tau inversion recovery (STIR) sequences were used for imaging the chest. Mediastinal and hilar adenopathy is clearly demonstrated. Also, parenchymal disease (nodules and fibrosis) is apparent on these scans. The use of the STIR sequence in determining disease activity is discussed – comparison is made with gallium scans. Loss of parenchymal signal intensity on the STIR sequence following steroid therapy has been seen in two cases, indicating that this is an alternative method of demonstrating disease activity.

MRI of lung signal intensity and dimensions in patients with chronic lung disease before and after single lung transplantation

R. H. Mohiaddin, G. Notohamiprodjo, K. Schoser, D. B. Longmore and M. H. Yacoub
Magnetic Resonance Unit, Royal Brompton National Heart and Lung Hospital, Sydney Street, London SW3 6NP, UK

A retrospective analysis of lung signal intensity normalized for fat (SI) and lung cross-sectional area normalized for body surface area was obtained from cardiac-gated spin echo (time to echo (TE) 40 ms) images before and after single-lung transplantation in 12 patients with pulmonary air way disease (PAD) and 14 with interstitial lung disease (ILD). Nine healthy volunteers were studied for comparison. The main results (MRI findings) are tabulated below. Blood flow (l/min) to the transplanted lung (3.4 ± 1.1) was higher than that of the control (2.3 ± 0.74) and of the native diseased lung (1.9 ± 0.7). Arterial flow had little effect on signal intensity in the control and PAD groups while in the ILD, the lesser the blood flow the higher is the signal intensity. The cross-sectional area of the transplanted lung was comparable with that of the control. The transplanted lung has a similar SI to that of the control except when there was a rejection reaction (one patient) or infection (two patients). Distinctive features of lung SI and cross-sectional area were demonstrated in patients with PAD and ILD before lung transplantation. These measurements could be useful non-invasive indices for assessment of the transplanted lung and for follow-up of patients without exposure to ionizing radiation.

Disease	Signal intensity	Area
Pulmonary air way disease	Low – > normal	Large
Fibrosing lung disease	High	Small
Lymphangioleiomyomatosis	High	Large

High-resolution CT appearances of the lung in alpha-1-antitrypsin deficiency

P. M. Taylor and *P. V. Barber
*Departments of Diagnostic Radiology, University of Manchester M13 9PT, and *Department of Thoracic Medicine, Wythenshawe Hospital, Manchester, UK*

Alpha-1-antitrypsin (AAT) deficiency is an inherited disorder characterized by low levels of serum alpha-1-antitrypsin. Clinical manifestations include pulmonary emphysema. Previous pathological and radiological studies have shown this to be characteristically panlobular involving predominantly the lower lobes. We have studied seven patients with homozygous AAT deficiency. (M:F = 2:5; age range 43–61; mean 55). All patients were examined on an IGE 9800 scanner with 3 mm thick sections at 10 mm increments obtained throughout the lungs during maximum inspiration. Five patients demonstrated computer tomography appearances of emphysema, in four of these there was lower zone predominance of disease, in one all three pulmonary zones were affected. The remaining two patients had no emphysema although one showed scattered thin-walled cysts and the other had multiple thick-walled cysts within the mid zones and lower zones of the lung. These findings support the hypothesis that patients with documented AAT deficiency may not have radiological demonstrable emphysema. Three patients showed features of bronchiectasis with bronchial dilatation and bronchial wall thickening. Bronchiectasis is a feature of AAT deficiency, having been described previously on bronchographic studies.

10.45 – 12.00

Physics II — Image Assessment

Hall 11b

Human visual perception and ROC methodology in medical imaging

M. S. Chesters
Department of Medical Physics, The General Infirmary/
United Leeds Teaching Hospitals NHS Trust, Leeds
LS1 3EX, UK

Receiver operating characteristic (ROC) analysis is among the most reliable methods currently available for measuring diagnostic performance. Among several factors influencing diagnostic decisions are: (1) the inherent diagnostic capability of the combined imaging system and user, and (2) the decision criterion adopted by the user. Only ROC analysis is able to distinguish between these two facets of performance. Alternative methods implicitly rely on the user maintaining a constant decision criterion, an assumption that may not always be justified. Unfortunately, however, ROC analysis is relatively more time consuming than alternative methods. ROC analysis can also provide a measure of the absolute efficiencies of the imaging system and the human user. Human efficiency in performing certain discrimination tasks has been shown to approach the maximum attainable although in other tasks the human user can be very inefficient. In this paper, the concepts underlying ROC analysis and the techniques for carrying out the analysis are briefly described. The relative advantages of ROC and alternative methods of analysis are discussed. The implications for imaging processing and machine vision of human efficiency are considered.

"All the better to see you with" – the use of a minifying lens in radiology

B. S. Worthington and A. G. Gale
Department of Academic Radiology, University of
Nottingham, Nottingham NG27 2RD, UK

The spatial frequency model of vision provides useful insights into the physiological limits of the eye–brain system to perceive structures of different size and contrast in radiological images. Visual contrast sensitivity can be assessed using as a test object a grating pattern of alternating light and dark bars whose spatial frequency corresponds to the number of cycles subtended on one degree arc of retina. The eye–brain system has its maximum sensitivity to low contrast at three cycles to a degree but can detect up to 50 cycles per degree at high contrast. The presence of grain noise in radiographic images, which consists of relatively high spatial frequencies, causes randomization of density gradients with loss of boundary information. A minification lens can ensure the best match in the spatial frequency domain between low contrast detail of a given size and the performance capabilities of the visual system. Minification can improve visualization of edge detail since elements in the noise are effectively shifted below the threshold of visibility in the spatial frequency domain. The fact that a smaller image will require less fixations for full scrutiny is considered a less plausible rationalization for the use of a minifying lens.

The SDRD: a novel digital radiographic system

A. Martinez, R. D. Speller, J. A. Horrocks, D. J. Miller and L. I. Shekhtman
Medical Physics and Bioengineering, University College
London, 11–20 Capper Street, London WC1E 6JA, UK

The performance of the SDRD has been evaluated. It uses a multiwire proportional chamber detector in a configuration which gives good rejection of scattered photons. Standard test tools were exposed on the SDRD and the images were evaluated in comparison with screen-film images. Contrast-detail-dose diagrams were produced using thermoluminescent dosemeter (TLD) dosimetry, and showed comparable performance for all but the finest features of the test objects. Dose levels for clinical images with the SDRD were compared with a recently published UK survey. The two main advantages of the new system are: (a) that the wide dynamic range of the SDRD allows both soft tissue and bone to be imaged in one exposure, and (b) that some clinical examinations show significant dose savings with the SDRD.

Monte Carlo study of the design and performance of anti-scatter grids

*M. Sandborg, D. R. Dance, *G. Alm Carlsson and *J. Persliden
*Department of Physics, The Royal Marsden Hospital, London SW3 6JJ, UK and *Department of Radiation Physics, University Hospital, Linköping, Sweden*

A Monte Carlo computer program has been developed to study and optimize the design of anti-scatter grids used in diagnostic radiology. The program simulates the scatter from tissue slabs of various sizes and calculates image contrast and noise, energy imparted to the tissue slab and the conventional grid parameters, Bucky Factor and contrast improvement factor. Three examples are given of applications of the program. Firstly, the advantage of using low atomic number materials for the grid covers and interspace is quantified for four grid designs and four tube potentials. The dose reduction achievable varies between 10 to 50% depending upon operating parameters. Secondly, the results of a global optimization of grid design and tube potential are presented for a simulation of a paediatric examination. It is shown that grids with widely different line densities or grid ratios can have good performance provided that they have lead lamellae of appropriate thickness and are used with the correct tube potential. Lastly, the performances of various commercially available grids are compared for chest radiography. We are not aware of any other work which has made a detailed study of the influence of tube potential on grid performance.

Quantitative assessment of TV fluoroscopy

D. W. McRobbie, J. Nieto-Camero and R. G. Dale
Riverside District Department of Medical Physics, Charing Cross Hospital, London W6 8RF, UK

Although the widespread use of the Leeds test objects has been beneficial in the quality assurance of fluoroscopy systems a number of difficulties has led us to develop an alternative approach. The basic drawbacks of the Leeds Test objects are the subjective aspect, the lack of a definitive signal-to-noise test and proper transfer functional analysis. An alternative approach is to analyse the video signals using a Leeds E1 test object. A trial has been carried out using a 40 MHz digital oscilloscope plus a video line selector connected via GPIB interface to a Toshiba portable computer. Algorithms have been written to analyse the system and quantum signal to noise ratios, low frequency contrast loss, Wiener spectrum and modulation transfer function. Initial results are encouraging showing, where applicable, good correlation with subjective assessments, but providing much more detailed information. Moreover, the tests are very quick to perform requiring a single X-ray exposure. A prototype dedicated device is being built with development funding from the British Technology Group.

First experiences with a DSI digital image review workstation

A. R. Cowen and A. G. Davies
Medical Physics Unit, The General Infirmary, Leeds LS1 3EX, UK

Digital image workstations are becoming increasingly common in modern radiology departments. This increase is partly fuelled by the number of imaging modalities producing digital images, rather than (purely) film-based output, and partly by the possible advantages of an interactive review environment such as that provided by a workstation. Recently, Philips Medical Systems announced Easy-Vision, a clinical workstation designed specifically for the review of images produced by a digital spot imaging (DSI) modality. A prototype workstation was installed in the General Infirmary at Leeds during October 1991 initially in the Department of Medical Physics, to allow an initial trial before final installation in the Diagnostic X-Ray Department for evaluation by FAXIL as part of the Department of Health X-ray systems evaluation program. The results of a preliminary evaluation of the EasyVision workstation are presented, which include investigation in terms of its display quality, range of features, clinical relevance of these features, ergonomic acceptability and computational performance. The workstation is also assessed in terms of its aid to productivity in a clinical environment when coupled with the communication, storage and hardcopy products which form the family of products of which EasyVision is a part. *Acknowledgment:* Philip Medical Systems (Netherlands) and the Medical Devices Directorate of the UK Department of Health.

Density profile measurements for quality assurance in digital radiology

S. D. Tabakov, I. A. J. Fife and C. A. Lewis
Department of Medical Engineering and Physics, King's College Hospital, London SE5 9RS, UK

Digital systems are capable of displaying images with a variable window level and width. This flexibility makes the contrast and resolution of images operator dependent and hence subjective. To ensure optimal image quality of the processed image it is desirable to have an objective measure. Image quality is conventionally assessed using the modulation transfer function (MTF). The theoretical complexity of this parameter makes it unsuitable for use in routine assessment. A method, which is particularly suitable for digital systems (CT, DSA, etc.) and based on the concept of MTF, is described which measures the loss of modulation amplitude with increasing spatial frequency. The input signal is derived from imaging a resolution test object. The output signal is the density profile extracted from the processed image. In a similar manner to TV system assessment, the contrast modulation obtained from the density profiles is plotted against spatial frequency producing the contrast transfer function (CTF). Examples of the CTF are presented and discussed for high and low contrast test objects. Practically, CTF and MTF are closely comparable. CTF is a rapid, quantitative method for assessing image quality in digital systems. CTF can also be applied to other imaging modalities.

Development of a test object for evaluating image quality of photo-stimulable phosphor computed radiology systems in clinical service

A. R. Cowen, J. S. Price, A. Workman and S. McArdle
Department of Medical Physics, Leeds General Infirmary, Leeds LS1 3EX, UK

With the increasing availability of systems using photostimulable phosphor computed radiography (PPCR) technology, as opposed to conventional screen-film, there is an increasing need to set up quality assurance strategies for such systems. Aware of the different imaging requirements and unique properties of PPCR, we at FAXIL are designing and constructing a set of X-ray test objects for the purposes of facilitating computed radiography (CR) system set-up and routine quality assurance. The PPCR system can be split into several imaging components: the photostimulable phospor plates, the reading mechanism, the computer processing, the display and the hardcopy facilities, all requiring a new approach to image quality assessment. In this presentation we will describe progress so far with this project, illustrating various points with test images derived from CR systems in clinical use. Our ultimate aim will be to develop a generic package of test objects which can be used universally with all designs of CR system. This set will include tests to assess low contrast sensitivity, high contrast spatial resolution, exposure linearity and sensitivity, uniformity, dynamic range and a number of other PPCR specific parameters. *Acknowledgments:* This work is jointly supported by the Medical Devices Directorate of the UK Department of Health and Agfa-Gevaert NV, Belgium.

Variability of X-ray image intensifier — TV system performance

A. J. Shaw
North Western Medical Physics Department, Christie Hospital, Manchester M20 9BX, UK

The performance of all 178 fluoroscopy units in the North Western Region was measured over a 2 year period in order to determine the variability of factors affecting image quality and patient dose and to identify any trends with equipment design, manufacturer or age. Measurement protocols were based on HPA and Leeds procedures for safety and performance testing of image intensifer–TV systems. X-ray automatic dose rate control and automatic collimation performance were analysed to assess dose efficiency, while limiting resolution and perception of threshold contrast against detail size were used to indicate image quality. The results show, for example, that input dose rates vary by a factor of over 400, the variation increasing with age. 25% of units less than 1 year old did not meet the requirements for limiting resolution. However, only systems older than 10 years showed significant signs of deterioration in overall image quality. Further results are presented and the implications for quality assurance, maintenance and equipment replacement discussed.

Phosphor screens image characteristics

G. E. Giakoumakis
Physics Department, University of Ioannina, 451 10 Ioannina, Greece

We present the results of an experimental study concerning mainly the efficiency and the modulation transfer function (MTF) of granular X-ray phosphor screens. Measurements have been carried out on phosphor screens prepared by sedimentation of four different phosphor materials (YVO_4:Eu, La_2O_2S:Tb, $CdPO_3Cl$:Mn, ZnCdS:Au,Cu). The screens' densities ranged from 20 to 250 mg/cm^2 and the X-ray tube voltages from 50 to 250 kVp. In brief presentation the experimental results show considerable differences between the various screens both in efficiency and resolution, which in general are consistent with the Hamaker–Ludwig model predictions. Graphs of absolute values showing the dependence of these two quantities (efficiency and resolution) on various parameters (thickness, voltage, etc.) are presented for each one of the phosphor materials. All the experimental data are explained and discussed on the basis of appropriate theoretical models taking into account the granular structure of the screens as well as the beam quality and the optical properties of the phosphor material.

An approach to assessing the adequacy of fluoroscopy equipment to produce adequate images over a wide range of clinical conditions under automatic control

M. Holubinka
Radiation Physics Group, St Mary's Hospital, Portsmouth, UK

Image intensifier fluoroscopy equipment is expected to provide images of diagnostic quality over a very wide operating range, for example, locating fractures in the wrist

12.15 – 1.15

3M Mayneord Memorial Lecture

Hall 9

Targeted magnetic resonance imaging

W. Vennart
Department of Physics, University of Exeter, Exeter EX4 4QL, UK

Clinical magnetic resonance imaging (MRI) is characterized by the use of large whole-body magnets and expensive proprietary computer systems. Use of such systems for research purposes (*e.g.* for tissue characterizations in normal and diseased states) can be prohibitively expensive; in addition certain parts of the body (*e.g.* fingers and hands) are relatively difficult to image in whole-body machines. In this talk imagers developed for visualizing limited parts of the body, *e.g.* fingers, wrists, head and knee will be discussed highlighting the technology that has enabled these developments. Further, the use of such systems to make relatively high resolution measurements *in vivo* will be outlined with illustrations of the elucidation of normal and abnormal anatomy as demonstrated by MRI.

2.15 – 3.45

Angiography and Interventional Radiology

Hall 9

Digital *versus* conventional angiography: a comparative study

E. Jurriaans, I. P. Wells, J. M. Wilkie, J. C. A. Pearn and T. A. Pratt
*Department of Radiology, Derriford General Hospital, Plymouth PL6 8DH and *Department of Medical Physics, Freedom Fields Hospital, Plymouth PL4 7JJ, UK*

Recent advances enable digital angiography (DA) to be performed in either subtracted or non-subtracted form, and digital peripheral scanning ("bolus chasing") to be undertaken. This has influenced the use and application of DA appreciably. The conventional angiographic equipment (Philips Angiodiagnost 2 with Puck film changer) at Derriford General Hospital, Plymouth, was recently replaced by a new DA system (Philips Integris C2000). This permitted a comparison of conventional and digital angiography within the same clinical setting to be performed. Approximately 50 consecutive peripheral arteriograms, 15 femoral angioplasties and 15 percutaneous nephrolithotomies undertaken with conventional angiography were compared with a similar group of examinations performed with DA. The following parameters were assessed: (1) duration of examination, (2) radiation dose to patient and radiologist, (3) cost of consumables, (4) image quality (subjective), (5) other factors, *e.g.* access to patient, ease of use of equipment. The results of this study will be presented. The implications with regard to the use of and need for DA in a district general hospital will be discussed.

Enhancing the thrombogenicity of embolization coils

D. A. Nicholson, J. Cockburn, P. Dawson and A. Bradshaw
Department of Diagnostic Radiology, Hammersmith Hospital, Du Cane Road, London W12 0HS, UK

Steel embolization coils are well established as embolic agents for the treatment of many conditions. Ineffective thrombosis is occasionally seen in high blood flow situations and patients with abnormal clotting. Several authors have commented on the increased thrombogenicity of coils following soaking in thrombin solutions. However no study has quantified this effect. We have carried out an *in vitro* study, carefully measuring the effect on whole blood clotting time (WBCT), of soaking coils in thrombin solutions of different concentrations (100, 200, 400, 1000 U/ml). Untreated coils are shown to be very thrombogenic, reducing normal WBCT from 14.85 min to 5.53 min. Passing coils down a saline-filled catheter (simulating *in vivo* technique) slightly reduces their thrombogenicity, but not significantly ($p = 0.21$). Soaking coils in thrombin solutions over 100 U/ml has the effect of further reducing WBCT significantly (2.1–2.6 min). Although there is a trend of increasing thrombogenicity with increasing thrombin concentration from 200–1000 U/ml, a plateau in WBCT is seen, and the difference is not significant. We conclude soaking coils in thrombin has a very beneficial effect on reducing WBCT and that only a small quantity of thrombin is required to elicit prompt coagulation, limiting the thrombin's potential systemic effects. We suggest the use of such thrombinized coils in the treatment of various conditions, which will be discussed.

A comparison of pulse-generated run-off and arteriographic assessment of the pedal arch in the outcome of femoro-distal bypass grafting

D. Kinsella, E. Horrocks, J. Scott and M. Horrocks
Department of Radiology and Vascular Studies, Bristol Royal Infirmary, Bristol BS2 8HW, UK

The outcome of 100 non-reversed femoro-distal grafts, performed for critical ischaemia, were analysed. 16 grafts were to the above-knee popliteal artery, 36 to the distal popliteal artery, three to the tibio-peroneal trunk and 45 to a single calf vessel. The 1 year graft patency rates for grafts to a pulse-generated run-off derived complete, incomplete and occluded pedal arch were 88%, 75% and 9%, respectively ($p < 0.01$). Arteriographic scoring did not discriminate between successful and failed grafts. The reasons for this will be discussed. Pulse-generated run-off (PGR) derived pedal arch status does appear to be an excellent predictor of long-term graft function. In those patients with an occluded pedal arch on PGR, a primary amputation should be considered.

Calf vessel preservation in peripheral vascular disease — angiography *versus* pulse generated run-off

T. O'Brien, H. G. Thomas, A. Crow and P. Lamont
Oxford Regional Vascular Unit and Department of Radiology, John Radcliffe Hospital, Oxford OX3 9DU, UK

Previous angiographic and anatomical studies have suggested that the peroneal artery is the best preserved of the calf vessels in peripheral vascular disease and should be the site of preference for femoro-distal by-pass grafts. Calf vessel run-off assessed by pulse generated run-off (PGR) provides a more accurate prediction of graft success or failure than angiography and may therefore give a better functional picture of vessel patency than angiography. This study compares the presence of and degree of preservation of the three calf vessels in patients with severe peripheral vascular disease using both intra-arterial digital subtraction angiography (DSA) and PGR. 34 limbs in patients with either ischaemic rest pain, ulceration or gangrene were studied and the results were scored according to the extent and severity of disease in the peroneal, posterior tibial and anterior tibial arteries. The peroneal is present, and seen as the best preserved vessel, on DSA in significantly more cases than the other vessels. The three vessels are seen more often and are equally well preserved on PGR. This study shows that angiography may be misleading because the more functional PGR studies show no significant differences in patency or preservation between the three calf vessels.

Colour duplex, impedance analysis and DSA in femorodistal vein bypass graft surveillance

D. Glew, *A. H. Davies, R. Parry, *T. R. Magee, *M. Wyatt, P. Murphy, *R. N. Baird and *M. Horrocks
*Departments of Radiodiagnosis and *Vascular Studies, Bristol Royal Infirmary, Bristol BS2 8HW, UK*

Graft surveillance has improved rates of graft patency and limb salvage. A technique of impedance analysis has been described previously, but no comparison of colour duplex scanning, impedance analysis and digital subtraction arteriography (DSA) has been reported. 45 patients have been followed-up with non-invasive tests at 1 week, 3 months and 6 months after femorodistal bypass surgery, using intra-arterial DSA as the gold standard. An impedance score of > 0.45 was used to identify "at risk" grafts, and a doubling of peak velocity on duplex was used to define a stenosis. DSA identified nine "at risk" grafts. Eight of these were identified by impedance analysis and eight by colour duplex. Mean impedance scores (95% confidence limits) were 0.39 (0.36–0.42) for the grafts without problems and 0.48 (0.43–0.53) for the "at risk" grafts ($p = 0.003$, Mann-Whitney *U*-test). Colour duplex failed to recognize one graft "at risk" from poor run-off, impedance analysis failed to identify one graft with a retained valve cusp. Impedance analysis is non-invasive and rapid to perform. As it compares well with more invasive and time-consuming tests, we suggest it is the test of choice for graft surveillance.

Intra-arterial femoral studies in anticoagulated patients using 3 French catheters

C. N. Ludman and J. F. Reidy
Radiology Department, Guy's Hospital, London SE1 9RT, UK

Femoral arteriography is contraindicated in patients who are on anticoagulant therapy. Clotting profiles will therefore usually be normalized prior to the procedure. This sometimes results in complications or delay in the procedure, and may be hazardous for those patients in whom anticoagulation is vital. Intravenous digital angiography is a safer alternative procedure, however, the images are of inherently poorer quality and large doses of contrast media are required. As a result of using 3 F catheters in over 400 patients with peripheral vascular and renovascular disease, we aimed to study the safety of this technique without stopping anticoagulant therapy. 11 patients, (INR values of 1.7–3.4, mean 2.4) were studied using a standard 3 F catheter technique but prolonging post-procedure pressure haemostatis from the usual 5 min to 10 min. Studies were performed on both an in-patient and an outpatient basis without any complications. That is, there was no prolongation of hospital stay, no post-procedural bleeding, and only one very minor haematoma was reported. We conclude that 3 F catheterization would appear to be safe in patients who have been anticoagulated within the normal range, without the need to stop treatment first.

A comparative study of the effects of ionic and non-ionic contrast media on oxygen desaturation following intravenous intra-arterial administration

P. S. Sidhu, J. F. Cockburn, D. A. Nicholson, A. Kennedy and P. Dawson
Department of Diagnostic Radiology, Hammersmith Hospital, Du Cane Road, London W12 0HS, UK

Transient oxygen desaturation following conventional radiographic contrast medium administration has been shown to occur both with intravenous and intra-arterial studies. The effects, if any, of the newer non-ionic contrast agents on oxygen desaturation have not been evaluated. To determine if non-ionic contrast media administration either intravenously or intra-arterially results in oxygen desaturation, we prospectively studied 100 patients undergoing radiological investigations requiring the administration of contrast media. These patients were divided into two groups: one requiring ionic contrast; the other group non-ionic contrast. Arterial oxygen saturation was monitored for 3 min prior to, during and then for at least 20 min after the administration of contrast media. The results from the two groups will be compared with previous studies and the effects of the newer non-ionic contrast media on oxygen desaturation will be presented. The mechanisms of this phenomenon and its clinical relevance will be discussed.

Inoculation hazards during interventional radiological procedures

S. Eustace, J. O'Byrne and O. Legge
Radiology Department, Mater Misericordiae Hospital, Eccles St, Dublin 7, Ireland

An intact barrier between the operator's hands and the patient is important to prevent transmission of disease in either direction. Between 10% to 40% of surgical gloves develop punctures during general surgical cases. In this study, we determine if the incidence of glove perforation is higher during interventional radiological procedures and whether there is an indication for double gloving during specific procedures as recommended in other specialities (orthopaedics). 150 pairs of gloves were tested. The gloves tested were Ansell and Regent. The operator, first assistant, if present, and nurse completed questionnaires that specifically asked the nature of the operation (instrumentation or not), whether they were aware of a perforation and if so, how it happened. Gloves were tested for holes by inflating the glove with water and occluding the cuff. The total perforation rate was 8%, 3% of the gloves had unrecognized perforations. The operator was most at risk of perforations. Perforations were usually associated with guide wire studies. Double gloving should be undertaken during these studies on at-risk patients despite the minimal loss of manual dexterity.

Embolization of peri-pancreatic visceral artery pseudo-aneurysms

M. Blomley and J. E. Jackson
Department of Diagnostic Radiology, Hammersmith Hospital, Du Cane Road, London W12 0HS, UK

Visceral artery pseudo-aneurysms are uncommon but potentially fatal lesions which are associated with a mortality of up to 80% depending upon their location. They most commonly occur secondary to chronic pancreatitis but may also be associated with trauma, surgery, or infection. Surgical management of these lesions is associated with a high mortality particularly when situated around the pancreatic head. Over the past 6 years we have treated 12 patients with visceral artery pseudo-aneurysms by transcatheter embolization. The pseudo-aneurysm involved the gastroduodenal artery in eight patients and the splenic artery, an hepatic artery, the transverse pancreatic artery and the superior mesenteric artery in one patient each. The majority of patients presented with gastrointestinal bleeding. Transcatheter embolization was technically successful in all patients. Three patients died within a month of embolization, one following recurrent bleeding from a second pseudo-aneurysm which was not amenable to embolization, one from intercurrent cardiac failure and one from generalized bleeding due to a profound coagulopathy following massive transfusion requirements prior to embolization. The technique of embolization of visceral artery pseudo-aneurysms will be discussed.

Approaching and lysing the thrombosed prosthetic graft

P. Guest and T. Buckenham
Department of Diagnostic Radiology, St George's Hospital, London SW17 0QT, UK

Thrombosed prosthetic grafts continue to be both a clinical and radiological problem. Surgical management carries its own significant morbidity. The radiological approach has traditionally involved diagnostic studies and possibly thrombolysis with agents such as streptokinase. We treat all our thrombosed grafts aggressively with direct intrathrombus administration of tissue plasminogen activator (TPA). Direct puncture of the graft and pulsed administration of the drug facilitates and accelerates the procedure. Supplementary angioplasties are usually required to prevent rethrombosis. We present the radiological management and our own results in a series of all patients (23 patients, 30 procedures) presenting with occluded grafts over a period of 1 year to our hospital. We discuss the factors influencing a successful procedure, the problems encountered and possible ways of overcoming these.

TIPSS: The Edinburgh experience

N. Chalmers, D. N. Redhead and P. C. Hayes
Department of Radiology, The Royal Infirmary of Edinburgh, Edinburgh EH3 9YW, UK

Transjugular intrahepatic portosystemic shunt (TIPSS) is a recently described percutaneous technique for portosystemic shunting. We have undertaken the procedure in four patients to date, with success in three. These are patients with recurrent variceal bleeding not controllable by sclerotherapy. The technique involves creating a track through the liver parenchyma between hepatic and portal veins using a trans-septal needle via a jugular sheath. The track is dilated with an angioplasty balloon and one or more metallic stents inserted to maintain patency. We describe our experience of the technique, including various difficulties and some modifications. Hepatic vein wedge pressure measurement following TIPSS has shown a substantial reduction in portal pressure gradient. One patient, whose portal pressure gradient prior to TIPSS was 29 mmHg, re-bled 3 weeks after the procedure and was found to have a persistently elevated pressure gradient at 19 mmHg, indicating an inadequate shunt. The shunt was dilated from 8 to 11 mm diameter with a satisfactory result. To date no other patient has re-bled following successful TIPSS and none has developed encephalopathy. Widespread adoption of TIPSS will depend on the long-term effectiveness. The mortality and cost of TIPSS compare favourably with surgical shunting.

Utility of trans-jugular intrahepatic portosystemic shunting for treatment of portal hypertension

W. K. Chong, *C. Lind, A. C. Fleischer and M. Mazer
*Departments of Radiology and *Gastroenterology, Vanderbilt University Medical Center, Nashville TN 37232-2675, USA*

Aim: To determine the effectiveness of relieving portal hypertension by percutaneous transjugular portosystemic shunting with an expandable metal stent, and the role of sonography for shunt evaluation. 13 patients with portal hypertension and recurrent variceal bleeding were treated with transjugular intrahepatic portosystemic shunting (TIPS). A 16G Cooke transjugular liver biopsy needle was positioned in a hepatic vein and used to access the main or right portal vein. A 1 cm Schneider Wallstent was placed across the track. Pre- and post-procedure colour Doppler sonography and angiography were performed and portal pressure measured. Stents were successfully placed in all but one patient whose portal vein was thrombosed. Sonography correctly demonstrated shunt patency in 11/12 patients. In one patient stent thrombosis was correctly diagnosed. Mean peak shunt velocity was 90 cm/s (flow rate 21 ml/s) in eight patients. In two patients with portal or splenic vein stenosis MPV was 27.5 cm/s (flow rate 5 ml/s). Two patients died within 1 month: from variceal bleeding and from mediastinitis unrelated to the procedure. A fall in portal pressures and endoscopic evidence of variceal reduction were seen in the remainder. Their shunts have remained patent. Early results indicate transjugular portacaval shunting effectively relieves symptoms. Colour Doppler sonography is useful for establishing the integrity of the portal circulation and confirming shunt patency.

Notes

2.15 – 3.45

Teach-in: Imaging in Paediatric Oncology

Hall 10a

Orbital tumours in childhood and their differential diagnosis

S. Chapman
Department of Radiology, The Children's Hospital, Birmingham B16 8ET, UK

Primary malignant tumours of the eye and orbit are rare in childhood; benign and non-neoplastic swellings are more common and frequently mimic malignant disease. Clinical presentation is with disturbance of vision, proptosis, strabismus or buphthalmos. Classifications of diseases at this site may be based on clinical presentation, age at presentation or site of involvement. The paper discusses the radiological appearances of the most common primary malignant lesions — rhabdomyosarcoma, retinoblastoma and optic nerve glioma; the most common metastatic lesions — neuroblastoma and leukaemia; benign lesions — haemangioma and epidermoid, and non-neoplastic lesions — cellulitis, pseudotumour, arteriovenous malformations and bone dysplasias.

Neonatal tumours — antenatal and post-natal diagnosis

J. M. McHugo
Department of Ultrasound, Birmingham Maternity Hospital, Birmingham B15 2TG, UK

Tumours diagnosed within the first month of life are rare (incidence 1: 12 500–1: 17 300 total births). Less than half of these are malignant but the type and behaviour of these tumours are different from those encountered in later childhood. The increasing use of ultrasound during the latter part of pregnancy now means that an increasing number of these cases are being diagnosed antenatally. *Teratomas* are the most frequent neonatal tumours accounting for between 15–33% of all cases. They are essentially all benign but prognosis depends on the site. *Soft tissue tumours*, both benign and malignant, are common and together form the largest group. Fibrous tissue tumours predominate comprising the fibromatoses (infantile fibromatosis and myofibromatosis) and fibrosarcomas. *Neuroblastoma* is the commonest malignant tumour in this age group although, again, prognosis is unusually good. Most neonates with disseminated disease have Stage IVS disease but many show spontaneous regression. *Leukaemia*. Acute non-lymphoblastic leukaemia predominates neonatally. Prognosis is generally poor and leukaemia accounts for the majority of deaths from neonatal malignancy. Brain tumours both supra- and infra-territorial are rare tumours. Examples of cases and the experience gained at Birmingham Maternity Hospital and Birmingham Children's Hospital will be discussed.

The role of radiology in the management of neuroblastoma

C. Dicks-Mireaux
Department of Radiology, The Hospital for Sick Children, London WC1N 3JH, UK

Neuroblastoma is the most common solid malignant tumour in children and usually presents before 5 years of age. The tumour arises from the adrenal gland and the sympathetic nervous system. 65% of patients have an abdominal primary and present with an abdominal mass. The tumour may also rise in the chest and pelvis. The role of radiology is to diagnose the primary mass and to define the stage of disease by demonstrating the extent of the mass and the presence of metastases. This initial evaluation includes ultrasound, computerized tomography and magnetic resonance imaging. The relative merits of these techniques will be presented. Approximately 70% of children have metastases, usually to bone and bone marrow. The role of both ^{99}Tc^{m} MDP bone scanning and iodine-labelled metaiodobenzyl guanidine scanning will be discussed. The radiological features of more unusual cases of neuroblastoma, such as Stage 4S, the opsomyoclonus syndrome and the vasoactive intestinal peptide secreting form will be presented. The role of radiology in assessing response to treatment and recurrence will be discussed.

2.15 – 3.45

ENT Imaging

Hall 10b

The investigation of sinus disease and its intracranial complications

P. Anslow
Department of Neuroradiology, Radcliffe Infirmary, Oxford OX2 6HE, UK

Recent advances in endoscopic sinus surgery have called for an enormous increase in imaging requirements. Coronal CT scanning is now a mandatory, standard procedure providing the necessary anatomical and pathological information for successful surgery to be performed. This presentation will briefly present some of the common and important sinus pathologies demonstrated on CT and will relate these to known sinus physiology. It will then move on to cover those aspects of anatomy and pathology relevant to the intracranial complications of sinus disease. The illustrations will demonstrate the ways in which tumour and infection spread from the skull base into the intracranial compartments. Whilst CT is the most commonly used imaging modality, the role of MRI will be discussed.

Subtraction magnetic resonance imaging for tumours of the skull base and paranasal sinuses

G. A. Lloyd and P. G. Barker
X-ray Department, Royal National Throat, Nose and Ear Hospital, London WC1X 8DA, UK

The subtraction method Ziedses des Plantes has been applied to gadolinium-enhanced magnetic resonance imaging (GdMR). Using short acquisition times T_1-weighted spin echo sequences are made immediately before and after 10 cm^3 of intravenous gadolinium DTPA. To avoid moving the patient from the scanning tunnel between sequences the venipuncture is made into the dorsum of the foot. 40 patients with histologically verified naso-sinus or skull base tumours have been investigated by this technique and satisfactory studies obtained on all patients other than the claustrophobic. The densities recorded on the subtraction image are dependent upon the blood supply of the tissues concerned, thus producing a record of their vascularity: in effect a vasculogram. Improved demonstration of tumour extent was recorded in 85% of patients examined. Because of their infiltrative nature adenoid cystic carcinoma is particularly well shown by this technique, as are nasopharyngeal tumours, glomus tumours and recurrent naso-sinus tumours. In summary subtraction is most advantageous in situations where the anatomy is complex as in the skull base, or where normal structures have been distorted by previous surgery. It provides a more accurate record of tumour extent than that shown on unsubtracted GdMR scans.

MR appearances of skull base lesions

S. Amin and R. Guy
Diagnostic Radiology Department, The Royal Marsden Hospital, Downs Road, Sutton, Surrey SM2 5PT, UK

Lesions at the skull base are an important cause of morbidity and the extent of involvement of surrounding structures can be difficult to appreciate on computed tomography (CT). We have evaluated the role of magnetic resonance imaging (MRI) in 100 patients with suspected skull base lesions. Clinical presentations included headache, diplopia, facial pain and cranial nerve palsies. MR images were obtained at 1.5 T, T_2-weighted axial and T_1-weighted coronal and sagittal images before and after gadolinium (Gd)-DTPA enhancement were obtained, with short tau inversion recovery images in selected cases. The MR images were evaluated to determine the size, signal characteristics and involvement of surrounding structures. Comparison was made with CT where available. Lesions of the skull bases were demonstrated in 35 cases. The commonest lesions were metastases, particularly from breast, bronchogenic and prostatic carcinoma and lymphoma. Other lesions were myeloma, nasopharyngeal carcinoma, meningioma, chordoma and chondrosarcoma. The diagnosis was confirmed by biopsy or longitudinal follow-up. MR was of particular value in assessing vascular and cranial nerve involvement. Bone marrow involvement was well seen although bony destruction was less easily evaluated. Gadolinium enhanced images helped to demarcate tumour margins and, when they were viewed in conjunction with unenhanced images, separation from surrounding high signal fat was not a problem.

Extension of malignant neoplasms upwards through the skull base: role of enhanced MRI

D. J. Beale and P. D. Phelps
Department of Radiology, Walsgrave Hospital, Coventry CV2 2DX, UK

The foramen lacerum is bounded by the sphenoid, basiocciput and petrous temporal bones. The carotid canal opens into the postero-lateral side. Formerly bone erosion in the region of the foramen lacerum was often the only radiological sign of intracranial extension of a nasopharyngeal carcinoma. The onset of cranial nerve lesions will indicate this intracranial spread which upgrades the staging to T4 and alters the field for radiation therapy. Demonstration of this extension by imaging helps the assessment greatly. We studied the role of contrast enhanced magnetic resonance imaging (MRI) for showing extension of malignant neoplasms arising below the skull base and subsequently extending through the area of the foramen lacerum into the parasellar region. We identified this extension in 11 cases, comprising three nasopharyngeal carcinomas, one carcinoma of tonsil, three adenoid cystic carcinomas, one melanoma, one case of lymphoma and two sarcomas. Invasion of the cavernous sinus needs to be identified by careful comparison of pre- and post-contrast scans, if possible with subtraction. Narrowing of the engulfed carotid artery was shown in three cases. Pain in the face was a common symptom from involvement of the trigeminal nerve and we would suggest that such persistent and intractable pain warrants an enhanced MR assessment, particularly in the coronal plane.

Clinical evaluation of combined MRI, CT and MRA in skull-base surgery planning

S. E. M. Green, D. L. G. Hill, G. P. Robinson,
J. E. Crossman, T. C. S. Cox, D. J. Hawkes, A. J. Strong,
M. G. Graves, C. F. Ruff and M. J. Gleeson
Departments of Radiological Sciences, Surgery and Neurology, UMDS, Guy's Hospital, London SE1 9RT, UK

In our institution patients are routinely imaged using computed tomography (CT), conventional magnetic resonance imaging (MRI) and sometimes MR angiography in preparation for skull-base surgery. Recently we have been using an anatomical landmark based registration technique to produce three-dimensional (3D) combined multimodal datasets. We are undertaking a clinical evaluation to determine whether appropriate displays of these combined datasets provide the surgeon with useful additional information compared with conventional viewing. We present the results of two experiments. The first was a retrospective evaluation of two-dimensional slices incorporating MR and CT information. The surgeon who had performed the operation identified key questions which he had needed to answer from the images, such as extent of pathology and best surgical approach. Independent surgeons and a neuroradiologist were then asked to answer these questions from conventional viewing of the MR and CT films, then to view the combined images and document any change to, or increase in confidence in their answers. In the second experiment, pseudo 3D displays were generated from the combined datasets using volume rendering techniques. Surgeons were asked to assess whether these displays (which included MR, CT and MR angiograms) provided an improved means of visualizing the 3D relationship between anatomical structures compared with multislice displays.

Benign and malignant enlargement of the pterygomasseteric muscle complex

P. Set, J. M. Somers, P. D. Britton and C. E. L. Freer
Department of Diagnostic Radiology, Addenbrooke's Hospital, Hills Road, Cambridge CB2 2QQ, UK

The masseter and pterygoid muscles comprise the major muscles of mastication. Isolated enlargement of these muscles is rare and is most frequently caused by benign masseter hypertrophy (BMH). Less frequently enlargement may be due to neoplastic or inflammatory processes. We present seven cases of unilateral enlargement of the pterygoid and/or masseter muscles. Two cases are of haemangioma and two of rhabdomyosarcoma. One case of BMH is presented and two cases of leukaemic infiltration of the masseter, mimicking BMH. The latter entity has, to our knowledge, not been described previously. The use of computed tomography in the differential diagnosis is emphasized and other rare differential diagnoses are discussed.

The basal turn of the cochlea

P. D. Phelps and A. Duncan
Department of Radiology, Walsgrave Hospital, Coventry CV2 2DX, UK

The coils of the cochlea are now demonstrated readily by thin section high resolution computed tomography (CT) in the axial plane. This assessment has now become important in severely deaf patients who are candidates for cochlear implant surgery. The commonest abnormality shown in these cases is post-meningitic or tympanogenic labyrinthitis ossificans which can obstruct the passage of the electrode.

Severe otosclerosis can cause a similar problem. Congenital deformities of the labyrinth are rarely suitable for implantation, but the procedure may be indicated for the true Mondini deformity; implantation is contraindicated for severe dysplasia of the cochlea and for the recently described variety of X-linked deafness with deficient bone at the fundus of the internal auditory meatus. Recent studies in the USA have shown that thin section 3DFT magnetic resonance imaging (MRI) can give spatial resolution comparable with CT as well as showing some soft tissue detail especially after gadolinium enhancement. We have used these techniques to study the cochlea both in normal subjects and in patients with severe cochlear type deafness, including candidates for cochlear implant surgery. We found that although MRI can suggest inflammation of the nerves and membraneous labyrinth or fibrosis in the cochlear coils, it has little value for patient management at present.

The parotid node – a pitfall in diagnosis?

M. J. Bradley, S. Ward and P. G. McAndrew
Department of Medical Imaging and Medical Physics, Rotherham District General Hospital, Rotherham S60 2UD, UK

Ultrasound is being increasingly used in the detection and localization of the parotid gland tumour. In our experience it is a highly sensitive technique to demonstrate the tumour and may often show multiple lesions not detected with other imaging even in the contra-lateral asymptomatic gland. However, the parotid gland lymph nodes may appear ultrasonically similar to the tumour. It is important to identify these as lymph nodes if possible to avoid an overestimation of tumour extent and a false positive diagnosis for malignancy as these nodes are commonly seen in simple head and neck inflammatory conditions. This paper describes the usual sonographic characteristics and distribution of the parotid lymph nodes to aid the sonologist in the differentiation of the nodes from the parotid tumour and the aetiology of the abnormal nodes is discussed.

Salivary gland scintigraphy — a suitable substitute for sialography?

W. J. Pilbrow, S. M. Brownless, J. I. Cawood, A. Dynes, J. D. Hughes and H. R. Stockdale
Department of Radiology, Countess of Chester Hospital, Chester, Cheshire CH2 1BQ, UK

The paper describes the use of salivary gland scintigraphy to investigate patients presenting with a variety of salivary gland symptoms/signs. A total of 72 patients was examined over a 5 year period, the vast majority referred from an oral and maxillo-facial surgeon. The patients were split into the following groups. (a) *correlative sialography:* 32 patients who presented with ? sialadenitis ? duct blockage problem; a further eight patients were examined following unsuccessful sialography. (b) *? Sjogrens:* 15 patients had scintigraphy alone as part of the investigation of xerostomia and/or xerophthalmia. In this group a correlation is made with the clinical/biochemical findings. (c) *Scintigraphy alone:* seven patients had scintigraphy alone, *e.g.* following refusal to have sialography, duct trauma, etc. (d) *Normal scintigraphy and sialography:* 10 patients had both normal scintigraphy and sialography despite presenting with salivary gland symptomatology. The series does not describe the use of scintigraphy to investigate possible salivary gland tumours but discusses the contribution to the functional/secretory aspects in assessing salivary gland disease. The conclusion reached is that scintigraphy is an accurate study of the accumulation/secretory aspect of the four main glands and might be considered as a substitute for sialography as the initial study, *e.g.* if sialography is technically difficult or the functional aspect is considered the most important. Sialography is still essential to demonstrate the anatomical detail of the duct system.

CT in diagnosis of naso-pharyngeal carcinoma (NPC)

H.-J. Maurer and A. B. J. Jeet
Department of Radiology, University Hospital, Kuala Lumpur 59100, West Malaysia

Nasopharyngeal carcinoma (NPC) is frequently found in the South Chinese population and in Chinese living in South-East Asia and other parts of the world; men are more frequently affected than women (PRASAD). Therefore, all patients suffering "colds" or other symptoms of the naso-pharyngeal region for a long period, especially if they are resistant to therapy, or patients showing enlarged neck lymph nodes should be carefully investigated with respect to NPC. After clinical examination computed tomography (CT) should be the first imaging procedure used. In our experience this has been done using a bolus injection (50 ml i.c.m.) followed by a dynamic scan (50 ml i.c.m. 1–2 ml/s) Advanced cases do not cause problems as lymph node metastases of the neck are mostly palpable. The problem is that early NPC is at times difficult to separate from its surrounding area and this cannot be shown in a very early stage. CT is very important in controlling chemotherapy. In addition, in advanced stages an isotope bone scan is performed to exclude bone metastases. *Conclusion:* CT is a very useful imaging method for detecting NPC as well as looking for the effects of therapy on follow-up. Compared with ultrasound, bone invasion can be shown by CT. However, in the future MRI will probably replace CT.

Diagnostic — therapeutic possibilities of interventional sonography on pathologic processes of the neck

A. Nedeva, P. Nedev, A. Hilendarov and E. Simova
Department of Radiology, Medical University "I. P. Pavlov", Plovdic 4000, Bulgaria

The study reveals the current possibilities of interventional sonography concerning benign and malignant processes of the neck, divided into two groups: (1) engaging the thyroid gland, and (2) not engaging the thyroid gland. The authors present the results of 102 diagnostic fine-needle biopsies of solid formations and diagnostic-therapeutic fine-needle punctures of liquid collections, both made under ultrasound control. Improvements and modifications of the classic method are offered, including: (1) volumetric evaluation of the findings prior to, during and after the invasive manipulation; (2) automatic aspiration applied to liquid collections and very dense processes; (3) a modification of the ultrafine needle "Chiba" and (4) a device for the conventional linear transducer, used for narrowing the ultrasound (US) beam. The results received when using the above mentioned improvements and modifications are compared with those from the classic US method. The authors conclude that the new modified method increases the diagnostic possibilities and enriches the therapeutic effects.

The ultrasonic appearances of normal vocal cords

J. C. Hacking, M. L. Harries and J. Tudor
Departments of Radiology and Otolaryngology, Addenbrooke's Hospital, Cambridge CB2 2QQ, UK

There is much current research in laryngology with the appearance of voice clinics and the development of new phonosurgical techniques. Mirror examination with a protruded tongue and extended vocal cords does not give an accurate view of the cords in their normal position for voice production. New techniques such as endoscopic video straboscopy can achieve this but is expensive and not widely available. Little investigation has so far been performed on the ultrasonic appearances of the vocal cords. Using a 7.5 MHz linear array transducer, we examined the cords of adult males, adult females and pubertal boys. In all cases the cords were identified with clear delineation of both the membranous and cartilaginous components. Movement in respiration and vocalization can be observed and recorded for assessment and documentation. Measurements of the separate components can be obtained and these correspond to accepted anatomical values. This work demonstates that ultrasound can be applied to the evaluation of normal vocal cords. It is particularly useful in the demonstration of movement and previously undescribed changes with growth and development of the pubertal larynx. Further work on research into changes in the male larynx at puberty and on pathological conditions is envisaged.

2.15 – 3.45

Physics III — Radiation Protection and Risks after ICRP 60

Hall 11b

Reappraisal of risks to the patient in diagnostic radiology

P. J. Roberts
Medical Physics Department, Southampton General Hospital, Southampton, UK

Even before the Adrian Committee report was published in 1966 there was a consuming interest in radiation doses to patients. 25 years later, the questions being asked on patient dose and risk can be answered with slightly more confidence but almost as much uncertainty. Allowing for the variability in the human race, there are still orders-of-magnitude differences in the doses delivered within a hospital as well as between hospitals for the same radiological examination. Causes of differences and systems to reduce these can be audited, and action taken leading to a reduction in risk to the patient. In the light of the new recommendations from the International Commission for Radiological Protection (ICRP), the effective dose equivalent values received by diagnostic radiology patients have been reduced. However, the overall risk has increased as the risks of radiation have been re-evaluated upwards. The question of acceptability of risks should be considered by all referring clinicians and especially by those clinically directing radiation exposures. Patient groups particularly at risk are children and perhaps young adults in that the expression of a cancer is more likely in the potential life-years remaining.

The dilemma of leakage radiation — how much should we accept?

H. M. Morgan and S. S. Lillicrap
Wessex Regional Medical Physics Service, Royal United Hospital, Bath BA1 3NG, UK

The IEC working party is considering proposals to increase the allowable leakage radiation through beam limiting devices, particularly as the area shielded by beam limiting devices increases. The pressures for this arise from the need to contain equipment costs and to limit the weight of electron applicators. This paper examines the risks associated with radiation treatment, from megavoltage X rays and electrons, for tissue in the radiation beam but outside the treatment volume, and for tissue irradiated by leakage and scattered radiation only. Measurements have been made of the absorbed dose arising from both leakage and scattered radiation for different field geometries. The risk to tissue adjacent to the treatment volume has been calculated using ICRP Publication 60 (1990), which gives the best estimates to date of mortality risks associated with irradiation of different organs. This risk is compared with that due to leakage radiation alone. Except for one or two field geometries the risk from leakage radiation is small compared with the overall risk. The case for increasing the allowable leakage radiation is discussed.

Direct measurement of the radiation doses to relations of nuclear medicine outpatients

L. K. Harding, A. P. Mills, A. B. Mostafa, N. B. Smith, A. Notghi and W. H. Thomson
Department of Physics and Nuclear Medicine, Dudley Road Hospital, Birmingham B18 7QH, UK

We have made direct measurements of radiation dose to relatives of patients who have had bone scans (measured over 24 h), or have been treated with ^{131}I for thyrotoxicosis (measured 2–3 days). Pocket dosemeters were issued to family members of the patient, and so as not to cause concern the digital readout was masked. At night they were asked to place them under the pillow. The maximum recorded radiation dose in 24 h to the relative of a patient having a bone scan was 19 μSv ($n = 22$). From the area under the activity time curves, based on ICRP 53, the maximum dose to the relative of a ^{99}Tc^{m} patient is calculated as 5 times this figure (for RBC cardiac study). In the case of patients treated with radioiodine ($n = 5$) the measured figures ranged from 7 to 37 μSv over 2–3 days in four of the patients, with corresponding figures corrected using the time activity curve, of 31–127 μSv. One relative showed a figure approximately 10 times this and the case is being investigated in more detail. Radiation doses to relatives following ^{99}Tc^{m} radiopharmaceuticals are small, compared with the annual dose limits for the general public proposed by ICRP. For radioiodine, figures are an order of magnitude higher.

Practical application of ICRP Publication 60 dose quantities to personal monitoring of staff who wear protective aprons

J. R. Gill
Health and Safety Executive, Technology and Health Sciences Division, Magdalen House, Bootle, Merseyside L20 3QZ, UK

The problem of how to undertake personal dosimetry for staff who wear protective aprons in diagnostic X-ray departments has for many years caused considerable debate. When the 1977 recommendations of ICRP introduced the concept of effective dose equivalent, a simple formula was derived to estimate this quantity from measurements made on the body beneath the apron and on the collar or forehead. The issue of new recommendations by ICRP in Publication 60 has brought with it the new quantities equivalent dose and effective dose. If and when these recommendations are introduced into radiation protection practice in Great Britain, there will again be a need to estimate the dose quantities for staff who wear protective aprons. This paper will re-examine the earlier formula, taking into account the new tissue-weighting factors of ICRP Publication 60, and will recommend a simple approach to personal dosimetry when the new quantities are adopted.

Radiation beam alignment at the chest-wall in mammography

A. G. Brennan and C. H. Johnson
North Western Medical Physics Department, Christie Hospital, Manchester M20 9BX, UK

National and IPSM standards specify that the radiation beam alignment with the edge of the cassette at the chest-wall should be coincident to within 0 to +3 mm. Unfortunately, measurement methods and tolerances are not specified and, in our experience, many X-ray units have poor alignment due to design limitations and poor servicing. We have developed a test tool that can be used to measure alignment to an accuracy of ±0.5 mm and a measurement procedure that gives clear unequivocal highly reproducible results. Results will be presented that specify the extent of the alignment problem, that illustrate the design of the test tool, the measurement method and that also support our proposal that the present limiting value (0 to +3 mm) should be changed (to +2 to +5 mm).

Comparison of high and low kVp techniques for PA chest radiographs

K. E. Goldstone and J. P. Wade
Radiation Protection Service, Addenbrooke's Hospital, Hills Road, Cambridge CB2 2QQ, UK

As part of a patient dose measurement programme, running in the East Anglian Region since Autumn 1990, measurements on postero-anterior (PA) chest X rays were carried out. Results showed that, in general, entrance doses given during high kVp chest X rays were higher than those at low kVps; furthermore all those departments which exceeded the National Radiological Protection Board guidelines on entrance doses were using the high kVp technique. The implications for effective dose to the patient are addressed. Reasons for the increased skin dose were investigated and a study has been made into ways of reducing the doses. Priorities have been assessed for the various methods of dose reduction. The differences in image quality for the different techniques are briefly considered particularly bearing in mind dose differences.

Patient dose measurement and reduction — a collaborative experience in East Anglia

K. E. Goldstone and J. P. Wade
Radiation Protection Service, Addenbrooke's Hospital, Hills Road, Cambridge CB2 2QQ, UK

In Regulation 4 of the Ionizing Radiation (Protection of Persons undergoing Medical Examination or Treatment) Regulations 1988 there is a requirement to ensure that the dose of ionizing radiation to the patient is as low as reasonably practicable to achieve the required diagnostic purpose. Furthermore Health Authorities in collaboration with clinicians have been encouraged to formulate a strategy for dose reduction (HC(89)18). In order to achieve these objectives it is necessary for X-ray departments to be aware of the patient doses being given using the department's current techniques and equipment. Areas where dose reduction is required can then be identified, priorities assessed and action evaluated. In East Anglia a programme has been in operation for over 15 months to measure skin entrance doses to patients undergoing four common diagnostic investigations. Measurements have been made on over 1000 patients X rayed in over 30 departments (in the public and private sector). The success of the programme has been dependent on the close collaboration between the Regional Radiation Protection Service and the X-ray departments. Organization of the survey will be described and results presented. Changes made, as a result of unnecessarily high doses being detected, will be evaluated and their cost effectiveness discussed. Proposals will be made (including resource implications) for the running of the programme as an integral part of a department's quality assurance programme.

Validation of software designed to calculate patient entrance exposures in diagnostic radiology

C. L. Skinner, E. A. Mumcuoglu and S. C. Klevenhagen
Department of Medical Physics, The Royal London Hospital, Whitechapel, London E1 1BB, UK

In order to regulate patient doses in diagnostic radiology, it has been recommended that periodic measurements of patient entrance skin dose are made, so as to make comparisons with previous results and national norms. Regulations recommend that exposure factors are inserted in the patient's record following an examination. A number of software packages have been developed that calculate entrance exposures from these factors. We have acquired and evaluated one such package, RADCOMP. This software employs an analytic function which can be scaled to calculate free air entrance exposures for a particular X-ray set. Physical verification of the package was accomplished by performing exposure measurements using a research X-ray set and a secondary standard ionization chamber at a variety of kilovoltages and filtrations. These measurements were compared with those calculated using RADCOMP. Results showed that when using a single calibration point for scaling, 94% of RADCOMP readings fell within 3 SD of the measured readings, with 53% falling within one standard deviation. Comparisons were also made between RADCOMP data and patient thermoluminescent dosimetry measurements for several X-ray units. Problems were encountered in obtaining the information necessary for the software on machines where automatic exposure control was in regular use.

A portable system for measuring area kerma product during fluoroscopic examinations

U. Reynolds, A. Cotterill and M. Fitzgerald
Medical Physics Department, St George's Hospital, Blackshaw Road, Tooting, London SW17 0QL, UK

This portable system has been developed as part of a Department of Health funded project to install a BS5750 quality system within a diagnostic radiology department. The measurement system consists of a PTW — M2 Diamentor connected to a portable PC, all mounted onto a small trolley. A transmission ionization chamber is fitted onto the LBD of an X-ray tube, permanently or temporarily, then examinations may be monitored as required. The whole system can be operated easily and quickly by the radiographer present during the examination. The computer automatically logs the area kerma product (AKP) readings from the Diamentor and prompts for other input data such as examination, patient size/sex, radiologist, numbers and sizes of films and kVp set. Data are filed and later transferred to a database for analysis. Thus patient exposures may be monitored throughout the hospital without incurring the cost of permanent installations. All types of examinations may be sampled and, where possible, AKP and energy imparted measurements may be compared within the hospital and with respect to national guidelines. Graphical analysis of exposure/time data collected during the examination may also be helpful in the training of radiologists.

Radiation dose to the breast from screening mammography in the West Midlands

M. A. Whall and E. A. McNeil
Regional Radiation Physics and Protection Service, Queen Elizabeth Medical Centre, Edgbaston, Birmingham B15 2TH, UK

Following an assessment of dose to the breast in terms of mean glandular dose (MGD) for each mammography unit involved in the Breast Screening Programme, an evaluation of the average dose received by the screened population was made. It was found that the average compressed breast thickness for these women was 5.5 ± 1.3 cm and the corresponding MGD approximately 60–70% greater than the value obtained using the standard breast thickness of 4.5 cm at 28 kV. Additional measurements have been carried out to determine: (1) how the exposure values in milliamperes obtained under AEC conditions at 28 kV over the range of breast thicknesses compared with the milliampere values obtained for different thicknesses of perspex phantom and (2) the effect of varying the selected kilovoltage on the dose to the breast. Separate assessments of MGD were made at 30 kV and 26 kV, for systems where these are used routinely. Use of a palladium or rhodium filter has been considered for thicker breasts. Acceptable image quality (Pritchard standards) has been obtained using a 25 micron palladium filter with a molybdenum target, giving an MGD approximately 60% less than the molybdenum target/molybdenum filtration combination. Further assessments of image quality are to be carried out.

Patient doses received using digital subtraction angiography and Puck serial film changer

H. R. Steele and D. H. Temperton
Department of Medical Physics and Biomedical Engineering, Queen Elizabeth Medical Centre, Birmingham B15 2TH, UK

The use of digital subtraction angiography (DSA) and a Puck serial film changer as a diagnostic tool for the visualization of blood vessels throughout the body is now widely accepted. A typical examination involves both fluoroscopy and a large number of multiple images taken at different projections and over different regions of the body. The exposure factors used are selected automatically. The dose to different patients may vary enormously but the complexity of the procedure also makes dose measurement difficult. Patient doses received during such examinations were assessed in order to calculate the risk of developing fatal cancers. The effective dose equivalent (EDE) was estimated using both a Diamentor to record the area-exposure product and lithium borate thermoluminescent dosemeters to measure the entrance surface (skin) doses. Carotid, femoral, renal and hepatic angiograms were studied. EDEs ranged from 0.6 mSv (femoral) to 44 mSv (hepatic). With an associated risk factor of 5×10^{-2} Sv^{-1} for developing fatal cancer a dose of 44 mSv would carry a risk of 2.2×10^{-3}. Such examinations therefore need to be carefully justified.

Assessment of organ radiation dose and associated risk for digital femoral arteriography

*I. A. Castellano, J. G. McNeill, *N. C. Thorp,
*D. R. Dance and M. J. Raphael
Department of Vascular Radiology, The Royal Brompton, National Heart and Lung Hospital, London SW3 6NT, and
**Physics Department, The Royal Marsden Hospital, London SW3 6JJ, UK*

The RCR/NRPB Joint Working Party Report *Dose Reduction in Diagnostic Radiology* indicates the need to assess patient dose for investigations undertaken with ionizing radiation. At present no published data are available for the dose delivered during digital femoral arteriography, and as this investigation accounts for 85% of the annual workload of the department, it was deemed necessary to make an assessment of radiation dose. Bilateral femoral arteriography was undertaken on 20 patients, using a filmless 1024 matrix digital image acquisition system with a discrete stepping tubestand and 40 cm image intensifier. A protocol of manual patient/tubestand positioning under fluoroscopic control and automatic stepping digital acquisition was followed. Skin entry doses were measured with a diamentor for each stage of the procedure, and the total gonad dose was assessed with thermoluminescent dosemeters. Conventional methods are supplemented with Monte Carlo simulations to calculate organ doses from the diamentor results. Surface doses to the pelvis and legs are presented with assessments of gonad and red bone marrow dose. However, there are inherent problems associated with the calculations and these are discussed. Additionally, the associated risk is evaluated with respect to the potential hazards of peripheral vascular disease.

Radiation doses during cardiac catheterization

C. Reek, M. Dunn and R. Keal
Radiology Department, Groby Road Hospital, Leicester LE3 9QE, UK

In recent years there has been increasing concern about the use of ionizing radiation for diagnostic purposes. In particular, there is concern over those procedures which give a high radiation dose to the patient and which may be repeated on several occasions. Cardiac catheterization is one such procedure. Following the installation of a new catheter room in June 1990 complete with a Diamentor, we have been able to measure the radiation doses to patients undergoing cardiac catheterization and, in conjunction with thermoluminescent dosemeter measurements from the skin of some patients, we have calculated whole body dose equivalents for the different investigations performed during cardiac catheterization. We have also undertaken a review of operator techniques which were thought likely to relate to patient dose. We present the results of this audit and discuss its possible implications.

4.15 – 5.30

Advances in Doppler Ultrasound

Hall 9

Doppler ultrasound flow measurement in the assessment of arteriovenous access for haemodialysis

J. E. Stutley, *D. A. Christopher, *P. N. Burns,
*F. S. Foster, A. M. Arenson, †C. Saiphoo and
†M. Manuel
*Departments of Diagnostic Radiology, *Medical Biophysics and †Nephrology, University of Toronto and Sunnybrook Health Science Centre, Toronto, Ontario M4N 3N5, Canada*

Effective haemodialysis requires adequate blood flow rates in the access fistula. We describe a prospective study of 27 patients with forearm arteriovenous access in which we used two Doppler ultrasound techniques to measure volumetric flow rate. A new Doppler method in which colour M-mode is used to estimate velocity profiles was compared with the conventional duplex technique. Measurements of fistula flow rate were correlated with clinical measures of dialysis efficiency, including recirculation rates and urea kinetics. All measurements were made within 4 days of each other. 13 patients had Brescia-Cimino (B-C) fistulas, 12 loop saphenous vein grafts (SVG), and two straight SVGs. Graft age was 1–60 months. We find that volume flow rates by the colour M-mode technique correlate linearly with those of conventional pulsed Doppler. The latter show higher flow rates than colour M-mode, an error we attribute to partial insonation. Saphenous vein loop grafts have higher flow than either the B-C fistulas or straight SVGs. There is no correlation between dialysis venous pressure and fistula flow. The high volumetric flow rates of normally functioning fistulae are consistently associated with low recirculation rates. Technical factors in both Doppler methods have a critical effect on reproducibility. Sources of error in flow estimation in these vessels will be discussed. We conclude that with careful technique, it is possible to use this colour Doppler method to measure volumetric flow rate in access fistulae.

	Colour M-mode	Pulsed Doppler
Loop SVG	190–1200 ml/min	500–1840 ml/min
B-C, Straight SVG	60–325 ml/min	100–760 ml/min

Colour flow mapping: does variance correspond to turbulence?

G. M. Baxter and J. F. Polak
Department of Radiology, Brigham and Women's Hospital, Boston, Massachusetts 02115, USA

Turbulent flow is known to occur in association with high grade carotid stenosis and causes spectral broadening and fluttering in the Doppler spectral waveform distal to the stenosis. Variance mapping on the colour Doppler flow image has been proposed as a means of documenting its presence. We prospectively evaluated this hypothesis by studying 15 patients with high grade (> 50%) stenotic lesions in the internal carotid artery. In all 15 cases, the site of increased variance on the colour Doppler map corresponded to the point of maximum velocity. In 10 cases of greater than 75% stenosis, the point of aliasing on the traditional colour Doppler map corresponded to the site of maximal variance. In five patients with stenoses between 50–75% diameter narrowing, the PRF was purposely decreased to induce aliasing. This resulted in the development of an abnormal variance map at the site of aliasing. In all 15 stenoses, the site of maximum turbulence, defined as fluttering in the Doppler spectral waveform, was not apparent on the variance map. We conclude that the variance map reflects spectral broadening and is more likely to occur at the site of aliasing. It does not necessarily depict turbulent flow.

A simple device to demonstate heating patterns in pulsed Doppler ultrasound beams

H. C. Strarritt, F. A. Duck and S. Stoker
Medical Physics Department, Royal United Hospital, Bath BA1 3NG, UK

A simple and novel method of visualizing heating patterns generated in acoustic beams is presented. Heating was produced in a plastic layer, approximately 1.0 mm thick, placed in a beam at right angles to the direction of propagation. A thin liquid crystal layer was spray-painted onto the distal side of the plastic, which underwent temperature-dependent colour changes in the range 25.7°C to 42.3°C.

This technique was used to produce cross-sectional thermal images in the field of a pulsed Doppler beam at different depths and under different equipment set-up conditions. The effect of varying the location of the range gate on the thermal profile was investigated.

Transcutaneous Doppler ultrasound imaging of the internal mammary arteries

N. Pugh, S. Barnard and A. J. Bryan
Departments of Bioengineering and Cardiac Surgery, University Hospital of Wales, Cardiff CF4 4XW, UK

32 adult patients admitted for elective cardiac surgery (26 males, age range 43–72 years) underwent pre-operative transcutaneous imaging of left and right internal mammary arteries (IMA) using a 7.5 MHz colour flow duplex scanner. The left internal mammary artery was satisfactorily visualized in all patients (mean diameter 2.2 ± 0.3 mm, peak systolic velocity 76.4 ± 23.4 cm/s) with a calculated mean flow of 43 ± 16.7 ml/min (range 21–90 ml/min). The right internal mammary artery was visualized satisfactorily in 91% of subjects (mean diameter 2.4 ± 0.4 mm, peak systolic velocity 72.7 ± 23.1 cm/s) with a mean calculated flow of 41 ± 16.7 ml/min (range 20–80 ml/min). Doppler velocity profiles were similar to those seen in other peripheral arteries and there was no difference in measured variables between internal mammary arteries. Intraoperative free flow measurements were made in 13 patients with a measured mean flow of 69 ml/min (range 36–140 ml/min). Intraoperative flows correlated poorly with calculated pre-operative flows ($r = 0.1$). Post-operative imaging of IMA grafts was attempted in six patients and satisfactory Doppler signals were obtained in four patients. These showed reduced peak systolic frequency and increased peak diastolic frequency compared to pre-operative measurements indicating increased diastolic blood flow. Duplex scanning provides a method of evaluating the internal mammary artery pre-operatively. Pre-operative flow measurements did not correlate with intraoperative measurements. Changes in the Doppler waveforms after grafting indicates that flow patterns adapt to the coronary vascular bed supplied.

Colour Doppler studies of axillary nodes in patients with breast cancer

J. Walsh, *J. M. Dixon, †D. Paterson and *U. Chetty
*Department of Radiology and University Departments of *Surgery and †Pathology, Royal Infirmary of Edinburgh, Edinburgh EH3 9YW, UK*

As malignant tumours increase in size they characteristically stimulate growth of new blood vessels by secretion of angionesis factor. Colour Doppler maps blood flow over an area of an ultrasound image and allows assessment of blood flow in and around lower axillary nodes. In the present study a positive scan was recorded if any clear colour Doppler signals were seen in or adjacent to axillary nodes visualized on ultrasound. 51 patients with 52 breast cancers have undergone an axillary colour Doppler scan and axillary nodes have been assessed histologically in 48 of these axillae. The results are shown below. The sensitivity of colour Doppler for axillary node involvement is 75%, with a specificity of 96%, a positive predictive value of 94% and a negative predictive value of 84%. These results are significantly better than those obtained by other non-operative techniques of axillary staging. The high level of specificity of colour Doppler for axillary node involvement suggests that this technique merits further investigation.

	Histology	Total	Number with positive scan
Axillary Nodes	Involved	20	15[a]
	Not involved	28	1
	Not known	3	0

[a] Two of five with negative scans had primary tumours which were negative on colour Doppler.

Colour and duplex Doppler in the diagnosis of hepatic venous outflow obstruction

M. A. Collins, J. F. C. Olliff and S. P. Olliff
Department of Diagnostic X-ray, Queen Elizabeth Hospital, Birmingham B15 2TH, UK

We have assessed the role of duplex and colour flow Doppler in the diagnosis of hepatic venous outflow obstruction in nine patients with suspected Budd Chiari syndrome and four patients with hepatic vein thrombosis following liver transplantation. All nine patients with suspected Budd Chiari had hepatic venography. Colour flow appearance correlated well with venography in eight. In one patient severe stenosis at the hepatic vein/IVC junction was missed by colour flow although duplex Doppler was grossly abnormal. In another patient there was colour flow in all major hepatic veins but abnormal duplex Doppler. Hepatic venography was normal but the patient deteriorated. Colour flow signals remained normal though the duplex signals deteriorated. At post mortem small vessel veno-occlusive disease was diagnosed. In four children following liver transplantation there was no flow within the hepatic vein (cut down liver). This was confirmed in each case by surgery. In conclusion colour flow correlates well with venographic appearance but the duplex venous waveform and the junction of the hepatic veins with the IVC must be carefully assessed.

Colour Doppler ultrasound in suspected scaphoid fracture — the way forward

D. A. Nicholson, *D. W. Hodgkinson, P. Hughes and M. Sheridan
*Departments of Radiology and *Accident and Emergency, Hope Hospital, Eccles Old Road, Salford, Manchester M6 8HD, UK*

The common clinical problem of the correct management for patients with suspected scaphoid fracture in the presence of normal carpal radiography remains unclear. The radial artery lies in close proximity to the scaphoid bone and its displacement may be the result of soft tissue trauma or haemarthrosis/effusion due to fracture. Both the radial artery and carpal bone contours are visible using ultrasound but conspicuity of the artery is considerably improved with colour Doppler. We have been measuring the scaphoid-radial artery distance in all patients with suspected scaphoid fracture, using the normal wrist as a control. All patients had standard radiography and were followed up to resolution of clinical symptoms. To date 64 patients have been scanned. A large variation in the normal scaphoid-radial artery distance (range 1.0–4.9 mm, mean 2.6 mm) was seen. The results were therefore analysed as a ratio of the symptomatic to asymptomatic sides. 20 of the 64 patients had ratios > 0.33, 11 of these proved to have fractures. Of the 44 with a ratio < 0.33, none proved to have fractures. The use of this method is a very sensitive (100%) predictor of scaphoid fracture. Although the ratio may be increased in soft tissue injuries (specificity = 83%), no false negatives have been seen. The routine use of Doppler ultrasound would significantly reduce the number of patients inappropriately immobilized in plaster casts.

Doppler pressure $\frac{1}{2}$ time estimation of valve area following percutaneous mitral balloon valvotomy

R. L. Parry, *T. MacConnell and R. P. H. Wilde
*Departments of Radiology and *Cardiology, Bristol Royal Infirmary, Bristol BS2 8HW, UK*

Since its introduction into Doppler echocardiography the term mitral valve area = 220/pressure $\frac{1}{2}$ time has been widely used to determine the severity of mitral stenosis. We have used Doppler derived pressure $\frac{1}{2}$ time measurements to determine mitral valve areas before and after percutaneous mitral balloon valvotomy in 40 patients. Whilst almost all patients showed significant clinical improvement this improvement did not always correlate well with an increase in valve area measured by the pressure $\frac{1}{2}$ time. The concept basic to the acceptance of the $\frac{1}{2}$ time measurement has been that the flow through the mitral valve depends only on left atrial pressure and valve area. We feel the sudden alteration in the compliance ratios between the left atrium and left ventricle and the decompressive effect of the transatrial septal puncture may also affect transmitral flow. We call into question the accuracy of the pressure $\frac{1}{2}$ time measurement following percutaneous mitral balloon valvotomy.

Prediction of vesicoureteric reflux in children using colour Doppler imaging

S. Sukumar and B. Wilson
Department of Radiology, Royal Manchester Children's Hospital, Pendlebury M27 1HA, UK

This is a prospective study of 25 patients referred for micturating cystourethrography (MCUG) for various urinary tract symptoms. Children with known anatomical deformity were excluded from the study. Colour Doppler imaging was used to visualize the ureteric jets and to locate the ureteric orifice by defining the point of origin of the jets. The distance of the ureteric orifice from the midpoint of the posterior wall (MLOD) and from the lateral angle of the bladder wall on the same side (LWOD) could then be measured. The measurements were compared with the results of MCUG performed on the same day. We found the refluxing ureters had a smaller LWOD than non-refluxing ureters and the difference was statistically significant ($p < 0.001$). Refluxing ureters also had a higher MLOD and the difference was not statistically significant ($p = 0.09$). A distance of < 8 mm included all the refluxers and 36% of non-refluxers. We conclude that the more laterally positioned the ureteric orifice the more likely it is to reflux. The LWOD is a better reading and we discuss the superiority of this over MLOD. This method may be useful for predicting which children with a urinary tract infection would benefit from MCUG.

Ultrasound diagnosis of Peyronie's disease in impotence

U. Patel, Z. Amin, E. Friedman, *S. J. Hampson, †R. Kirby and W. R. Lees
*Departments of Radiology and Urology (*The Middlesex Hospital, †St Bartholomew's Hospital), The Middlesex Hospital, London W1N 8AA, UK*

A total of 281 patients (aged 28–74, mean 57 years) with erectile failure (EF) underwent colour Doppler and duplex ultrasound imaging (CDI), following intracorporeal papaverine. After achieving a Grade 2 or 3 erection visual inspection and palpation revealed plaques and/or constriction or deformity of the penis in 55 (20%) cases. 10 (4%) were known to have Peyronie's plaques prior to referral. Of these 55 patients, ultrasound showed focal echogenic plaques in 14 (25%) and diffuse thickening of the tunica albuginea or corpus spongiosum in 41 (75%). CDI diagnosed arteriogenic EF in 20 (36%) of these patients, venous leak in 10 (18%), arterial and venous in three (5%), and a normal response in 23 (41%). In 11 (20%) patients (seven with arteriogenic EF and four with venous leak) the plaque was seen to be affecting vessels. *Conclusion:* We believe that the diffuse thickening is a form of Peyronie's disease which is only recognized after pharmacological induction of penile erection. Patients with EF who also have Peyronie's disease commonly have a vasculogenic cause for their EF (59%).

Colour Doppler imaging and prostatic disease

I. M. G. Kelly, W. R. Lees and D. Rickards
Department of Radiology, Middlesex Hospital, Mortimer Street, London W1N 8AA, UK

Objective: To study colour Doppler imaging (CDI) in the normal and diseased prostate. To correlate with conventional sonographic appearances (TRUS) and biopsy proven pathology. *Methods and materials:* 318 patients were examined using prototype CDI software with a transverse axial transrectal probe for the Acuson 128. Focal and generalized increases in CDI intensity were graded on a scale of 0–3. 100 biopsies were taken. *Results:* 132 had normal TRUS and CDI. 71 out of 91 cases of BPH had normal and 3 out of 91 significantly increased CDI. 36 out of 40 cases of prostatitis had increased CDI, 12 confined to the central zone (CZ), nine to the peripheral zone (PZ) and 19 out of 40 had a diffuse distribution. 42 out of 55 biopsy-proven carcinomas had increased CDI of grade 2 or more. 11 cancers had normal CDI; five had had radiotherapy, two were microfoci from reference biopsy sites. Increased CDI was confined to the PZ in all but two where it was diffuse. One case of cancer was diagnosed by CDI alone. *Conclusion:* There is generally no increase in CDI in BPH. Increased CDI in prostatitis was generally less than that seen in cancer and had a CZ or diffuse distribution. Increased CDI in cancer is seen in the PZ. CDI helps discriminate benign from malignant nodules and improves the specificity of conventional TRUS appearances.

Colour Doppler imaging in the investigation of impotence

Z. Amin, U. Patel, E. Friedman, *S. J. Hampson, †R. Kirby and W. R. Lees
*Departments of Radiology and Urology (*The Middlesex Hospital, †St Bartholomew's Hospital), The Middlesex Hospital, London W1N 8AA, UK*

Colour Doppler and duplex ultrasound (CDI) was performed following intracorporeal papaverine on 220 patients (mean age 66 years) with erectile failure (EF). 154 (70%) patients were found to have an organic cause for their EF on CDI. Arteriogenic EF was diagnosed in 85 (39%) patients when the maximum systolic velocity, $V_{max} < 35\,cm/s$. Five patients had a $V_{max} > 35\,cm/s$ without a full erection, and seven patients with a $V_{max} < 35\,cm/s$ achieved a full erection, giving this criterion a sensitivity of 94% and specificity of 85%. All patients with a systolic rise time (delta T) $> 0.1\,s$ had arteriogenic EF, making this a very useful parameter indicating proximal stenosis. Venous leak was diagnosed in 69 (31%) patients, when the end diastolic velocity, $V_{min} > 7\,cm/s$ for at least 5 min and $V_{max} > 30\,cm/s$. Using cavernosometry and cavernosography as a gold standard in 48 patients, CDI had a sensitivity of 94% and specificity of 69%. Frequent measurements from both cavernosal arteries are required as the peak V_{max} occurred between 1 and 18 min (mean 7 min), and marked asymmetry of flow altered the diagnosis in 20 (9%) patients. *Conclusion:* Papaverine stimulated CDI is simple and provides helpful diagnostic information in the majority of patients with EF.

4.15 – 4.45

Body CT — Clinical and Technical Advances

Hall 10a

Spiral *versus* conventional dynamic CT: a randomized trial

J. C. Hacking and A. K. Dixon
Department of Radiology and the University Department of Radiology, Addenbrooke's Hospital, Cambridge CB2 2QQ, UK

Spiral volumetric computed tomography (SVCT) has been predicted to improve vascular and organ enhancement with little effect on image quality. To investigate this, we studied 100 patients referred for CT where we would normally have performed dynamic incremental computed tomography (DICT). Patients were randomly allocated to undergo either DICT or SVCT. The resulting images were analysed for overall diagnostic quality, degree of enhancement and extent of artefacts associated with the technique. No statistically significant difference in overall image quality between SVCT and DICT was found, except for hepatic studies where the quality was significantly worse on SVCT ($p < 0.05$) due to the low milliamperes permissible. Enhancement was better with SVCT, although only in the thorax ($p < 0.01$) and for the group as a whole ($p < 0.01$) did this improvement reach significance. There was no significant difference in the extent of artefacts observed. All examination acquisition times were shorter using SVCT. The benefits of SVCT include the absolute contiguity of the reconstructed images and the ability to obtain many images at peak contrast enhancement. We have confirmed the latter effect. We are now also satisfied that there is no appreciable loss of image quality except where large volumes of solid tissue are examined.

Congenital abnormalities of the interior vena cava: diagnosis by computed tomography

D. I. Boxer, J. Danin and A. Al-Kutoubi
Department of Diagnostic Radiology, St Mary's Hospital, Praed Street, London W2 1NY, UK

Congenital abnormalities of the inferior vena cava (IVC) and its tributaries are not uncommon. They may have important clinical consequences, complicating surgery and the interventional treatment of venous thrombo-embolic disease. These abnormalities may be simply diagnosed by computed tomography (CT) scanning of the abdomen, however, if their true nature is not appreciated they may provide a diagnostic pitfall by simulating para-aortic lymphadenopathy or other retroperitoneal disease. The commest abnormalities are double IVC, left-sided IVC, retrocaval ureter and retroaortic left renal vein. We demonstrate how these and other congenital abnormalities of the IVC may be diagnosed by CT scanning and illustrate how they may simulate pathology.

Computed tomography of the abdominal wall

R. FitzGerald and *R. H. Grace
*Departments of Radiology and *Surgery, New Cross Hospital, Wolverhampton WV10 1QP, UK*

Computed tomography (CT) demonstrates the abdominal wall very well. Examples are shown of neoplastic, inflammatory, infective, vascular haemorrhagic and traumatic conditions of the abdominal wall imaged with CT. Its role in patients with abdominal wall hernia and ileostomy is illustrated. Pitfalls in interpreting abdominal wall CT, *e.g.* post-operative changes, are dealt with. Its limitation as well as its advantages are also addressed.

Optimum dose of non-ionic contrast media in abdominal and pelvic CT

K. Choji, N. Fujita, M. Chen, G. Irie and S. J. Golding
Department of Radiology, Hokkaido University Hospital, Sapporo 060, Japan

In order to determine the optimal amount of non-ionic contrast media (NICM) in intravenously enhanced computed tomography (CECT) in adult and paediatric liver, para-aorta and pelvis, extent of enhancement was assessed and analysed in relation to amount of NICM (iohexol or iopamidol) administered and conditions of CECT including the amount of iodine contained in NICM administered per body weight (I-dose/BW). Numbers of CECTs analysed were from 48 to 56 in adults and 16 to 33 in paediatrics. Contrast between the landmarking vessels and adjacent tissues including tumours or swollen lymph nodes was evaluated and categorized as "good", "fair" and "poor". Discriminant analysis was applied to the results of the assessment, in which the criterion variable was the categorized contrast evaluation; the explanatory variables were age (8 months–80 years), body weight (2.9–75 kg), I-dose/BW (0.1–2.3 gI/kg) and time-lapse from the administration of NICM to the scanning of the examination site. A standard of the minimum I-dose/BW for 50% of cases or more to achieve "good" contrast by each site of examination ranging from 0.6 to 1.9 kgI/kg according to the body weight was established, of which detailed figures will be discussed.

Notes

4.45 – 5.30

The Breast — Clinical and Technical Advances

Hall 10a

Mammography in the assessment of response to treatment in patients with large primary breast cancer

E. C. Moskovic, *J. L. Mansi, C. Murch, F. K. Cheah, D. M. King and I. E. Smith
*Departments of Radiology and *Medical Oncology/Breast Unit, Royal Marsden Hospital, Fulham Road, London SW3 6JJ, UK*

Recently, treatment of large primary breast cancer has altered, with a trend toward initial management by chemotherapy or hormone therapy rather than immediate mastectomy. This allows tumour response to an individual therapy to be evaluated and if unsatisfactory, changed. Clinical examination to assess such response is essential, but the role of mammography in providing a more objective parameter for monitoring change is unclear. In order to determine the value of mammography in this group of patients, the sequential mammograms of 47 patients (age range 24–84 years) undergoing primary medical treatment for locally advanced breast cancer at this institution were reviewed and compared with the findings at clinical assessment. 26 patients underwent endocrine therapy and 21 chemotherapy. All had more than two mammograms which were reviewed blindly by two independent radiologists. Response to treatment was recorded using WHO definitions (NC, PR, CR, PD) by both evaluation modalities. Overall comparison of clinical examination with mammography showed agreement in 38 cases (81%) and disagreement in nine (19%). Agreement in type of response but not its degree was found in 21 cases (45%). The results suggest that whilst in the majority of cases mammography is a useful adjunct to clinical examination in monitoring response to treatment for locally advanced breast cancer, it does not provide a "gold standard" and the search for alternative modalities of assessment should continue.

Interval cancers in the breast screening programme

B. E. Nathan
Breast Screening Unit, Edgware General Hospital, Edgware, Middlesex HA8 0AD, UK

In the prevalent round of breast screening in the North-west Thames Region, some 60 000 women have been screened and 340 women with breast cancer diagnosed. These have included 12 women whose initial screening mammograms were passed as normal and who presented within 12 months of this negative screen with carcinoma of the breast. The clinical data of these women and their mammograms have been reviewed and the findings analysed. An attempt is made to assess which cancers were missed rather than true interval cancers and which might have been diagnosed had clinical examination been part of the original screening process. Two of the 12 mammograms were thought to be abnormal on review and three of the 12 malignancies might have been diagnosed had clinical examination been carried out at the time of the initial screen. The value of double reading the mammograms is discussed and quality assurance guidelines presented to ensure as many interval cancers as possible are reported back to the screening centres.

The indeterminate breast mass. Does gadolinium-enhanced MRI have a role?

P. F. Hickman, N. R. Moore and B. J. Shepstone
Department of Radiology, John Radcliffe Hospital, University of Oxford, Oxford OX2 6HE, UK

Difficulty in mammographic and clinical differentiation of scar tissue from carcinoma is an increasing problem, owing to more conservative breast surgery. We used magnetic resonance imaging (MRI) to examine 22 women who presented with a mass which was indeterminate on clinical and/or mammographic examination. MRI was performed prior to biopsy. Surface coil axial T_1- and sagittal T_2-weighted images were obtained initially. Dynamic enhancement following intravenous gadolinium DTPA (Magnevist) injection was then assessed at 20 s intervals for 8 min using a T_1-weighted gradient echo sequence. A post-contrast T_1-weighted sequence was performed. Fat suppression images were obtained in two patients and were more sensitive in lesion detection. The dynamic gradient echo sequence was the most useful sequence in predicting tissue character. All carcinomas enhanced significantly, defined as $> 100\%$ of the original mean signal intensity. Areas of scar showed either no enhancement or enhancement $< 32\%$. These initial results suggest that contrast-enhanced MRI has a role in the assessment of the indeterminate breast mass. Further assessment of fat suppression sequences is required.

Digital mammography: evaluation of digitizers

D. H. Davies
Department of Physics, The Royal Marsden Hospital, London SW3 6JJ, UK

At the present time the resolution achievable using computed radiography systems is insufficient, and to study the potential of the computer interpretation of digital mammograms, it is necessary to use digitized conventional films. In this paper we present a method to evaluate the technical performance of three film digitizers. These are being assessed as possible methods for obtaining digital mammograms for a national data-base. The digitizers investigated are a scanning microdensitometer, a laser scanning digitizer and a CCD camera. Each has a high resolution sampling pixel size (50 microns or less) and is capable of digitizing to a grey level of at least 8 bits over the complete range of diffuse optical densities (0–3) typically found in a mammogram. The digitizers have been compared by measuring the modulation transfer function, noise and linearity of each system. The results demonstrate the importance of considering all these aspects of performance when choosing a digitizer.

Computer detection of soft tissue masses in digital mammograms: automatic region segmentation

D. H. Davies and D. R. Dance
Department of Physics, The Royal Marsden Hospital, London SW3 6JJ, UK

The automatic location of suspicious areas in digital mammograms is difficult for a number of reasons. There is sometimes very little contrast between a tumour area and its background in the image. Tumours can have fuzzy edges, can be very small and are sometimes obscured by normal anatomical structure. A radiologist uses the anatomical symmetry of a pair of normal breasts as one of his many tests for locating suspicious areas in mammograms. In this paper we describe a method for unsupervised segmentation of equivalent regions in a pair of breasts. These regions can then be used to check for asymmetry between breasts. The first stage in the regional segmentation process is the development of a clustering procedure based on textural and spatial features sampled from a training set of pairs of mammograms. The resulting clusters are used by a weighted minimum distance classifier to partition any given pair of mammograms into regions with similar properties. Results for a test set of 50 patients are presented and it is shown that the algorithm is successful in separating the images into regions of axillary tail, regions radiographically very dense with structure and regions corresponding to adipose tissue. This is the initial step in the development of a system which will locate and classify soft tissue masses by comparing left and right breast images.

Ultrasound demonstration of small cancers detected by mammographic screening

A. J. Potterton and D. J. Peakman
Breast Screening and Assessment Centre, Queen Elizabeth Hospital, Gateshead, Tyne and Wear NE9 6SX, UK

Previous studies have found ultrasound unreliable in the demonstration of small breast cancers (lesions measuring 10 mm or less). As a result, ultrasound has not gained wide acceptance as a method for assessing small, screen-detected lesions. In this centre, ultrasound is considered to be a useful modality for imaging small cancers found at screening. The visualization of these lesions has often been aided by combined mammography and ultrasound — a recently described technique developed in our unit. The mammographic and ultrasound appearances of 80 small cancers have been retrospectively analysed. Ultrasound demonstrated the vast majority of small cancers which presented as a mass on mammography. Cases showing only microcalcification on the mammogram were much less frequently demonstrated. Detailed results are discussed. We believe that ultrasound has an important role in the assessment of small breast cancers.

Colour flow characteristics of benign and malignant breast lesions

M. McNicholas, J. Miller, E. McDermott, P. Mercer, N. O'Higgins and D. MacErlean
Departments of Radiology and Surgery, St Vincent's Hospital, Dublin 4, Ireland

Malignant tumours stimulate the growth of new vessels by a process known as neovascularization. The vessels have abnormal flow patterns and high velocity signals. These abnormal vessels are detectable using colour flow Doppler ultrasound. Early reports have indicated that malignant lesions of the breast may be distinguished from benign lesions by visualization of abnormal vessels in and around the lesions. Spectral pattern analysis of the vessels identified on colour ultrasound may show typical features in malignant lesions. We have studied 150 women of all ages with a variety of breast lesions, using colour flow Doppler. We have correlated the histological analysis of the breast lesions with the vascularity and flow characteristics seen on colour ultrasound. We have found that certain malignant lesions have typical "malignant" circulation. However, some carcinomas show no abnormal vessels, and large benign lesions may also show abnormal flow. Colour ultrasound is very useful in the analysis of certain breast lumps, but a normal study must be interpreted in the clinical context.

Notes

4.15 – 5.30

Physics IV — Radiation Protection and Risks

Hall 11b

CT dosimetry: the joule in the crown of medical imaging

B. F. Wall
Radiological Measurements Department, NRPB, Chilton, Didcot, Oxfordshire, UK

Computed tomography (CT) is the crowning triumph of medical imaging technology in the excellence of the images and the speed of their acquisition, but it still delivers radiation energy to patients in doses that are large in comparison to those from conventional X-ray examinations. The undoubted benefits of improved diagnostic capability are achieved at the cost of increased radiation risks. Not all referring clinicians or radiologists are aware of this or of the fact that CT examinations now contribute as much as 20% of the collective dose to the population from all medical and dental X-rays. To make sensible dose comparisons, CT exposures should be expressed in a form that can be related to the potential radiation risks for the patient. Dosimetry methods have been developed at NRPB which allow the derivation of doses to radiosensitive organs from a simple dose measurement on the axis of rotation of the CT scanner. These methods, based on computer simulation of CT examinations on a geometric anthropomorphic phantom, are outlined. Results of a national survey showing the magnitudes of, and variations in, effective doses delivered by different CT facilities are presented. The variations are appreciable, and with effective doses for routine body scans exceeding 20 mSv (0.02 J/kg) at some facilities, the need for regular dose monitoring and control is evident.

The radiation burden of patients undergoing percutaneous transluminal coronary angioplasty

R. J. Chambers, P. L. Pattee and P. C. Johns
Cardiac X-ray, Ottawa Heart Institute, Ottawa Civic Hospital, University of Ottawa, Ottawa, Ontario K1Y 4E9, Canada

The first large-scale estimate of radiation dose and associated stochastic risks surrounding the use of percutaneous transluminal coronary angioplasty (PTCA) was undertaken. Retrospectively, 2063 PTCA cases from 1987–1989 at the Ottawa Heart Institute were analysed. Skin entrance dose, individual and collective effective dose equivalent (EDE) were calculated. A subgroup of 311 patients who had multiple (3, 4 or 5) PTCAs was selected for a worst case analysis. Estimated skin doses are higher than in any other report and make PTCA the producer of the largest X-ray dose of any procedure in diagnostic or interventional radiology. Some skin doses are of an order considered to be near the skin erythema dose. We conclude that for the average patient this study justifies the current practice of PTCA. However, cumulative radiation burden should be monitored in patients under age 40 especially in young women where the risk of radiation-induced detriment to the breast or lung may be significant. We propose that a longitudinal epidemiological study be carried out on the cohort of women in this study.

CTDI: confusion and clarification

S. Edyvean, M. A. Lewis and J. F. Carden
Department of Health CT Assessment Group (ImPACT), Medical Physics and Bioengineering, St George's Hospital, London SW17 0QT, UK

The Department of Health Computerized Tomography Assessment group (ImPACT) perform dose measurements for type tests which are an adapted form of the computerized tomography dose index (CTDI). The CTDI is the most widely used dose parameter for X-ray CT specification, having its origins in early CT dosimetry papers. Since then, the definition has evolved in various forms, leading to confusion over its application. One particular adaptation of the CTDI has been adopted for use by the Food and Drugs Administration (FDA) in the USA, and as a consequence many CT manufacturers quote it in their technical literature. This paper describes the differences between the various definitions of the CTDI and examines different approaches to its measurement. Comparisons between the FDA and ImPACT versions of the CTDI are illustrated by means of data from a number of scanners. The practical application of CTDI measurements to acceptance testing and quality assurance is also discussed.

The use of lithium fluoride and lithium borate in CT dosimetry

M. A. Lewis, J. F. Carden and S. Edyvean
Department of Health CT Assessment Group (ImPACT), Medical Physics and Bioengineering, St George's Hospital, London SW17 0QT, UK

Lithium fluoride (LiF) and lithium borate ($Li_2B_4O_7$) are two thermoluminescent (TL) materials suitable for use in patient dosimetry. Until recently lithium fluoride was the material of choice as it was more readily available in a reliable form. Lithium borate however has an energy response which more closely corresponds to that of soft tissue and is therefore now sometimes favoured, particularly at diagnostic X-ray energy levels. In the energy range 30–100 keV there is a variation of 30% in the ratio of mass energy absorption coefficients of lithium fluoride to soft tissue, whereas for lithium borate this ratio remains close to unity. Because the effective X-ray energy of a CT scanner in the patient/phantom is usually not known, the use of lithium fluoride can lead to significant errors in absolute dose estimates. The disadvantage of lithium borate is that with most TL dosimetry readers it demonstrates a lower sensitivity than lithium fluoride. This paper presents measurements of the effective X-ray energies encountered in CT examinations and discusses the errors that can be introduced by the use of lithium fluoride. Comparisons are made with results obtained using lithium borate, indicating the optimum choice of dosimeter for this application.

Increased accuracy of CT dose profile measurement by the use of film

J. F. Carden, M. A. Lewis and S. Edyvean
Department of Health CT Assessment Group (ImPACT), Medical Physics and Bioengineering, St George's Hospital, London SW17 0QT, UK

In order to ensure the accuracy of the slice collimation of a CT scanner, it is important to be able to make accurate measurements of the dose distribution in the direction perpendicular to the scan plane. Thermoluminescent dosimetry (TLD) is currently used to measure dose profiles, but with many scanners now able to achieve slice widths down to 1 mm, this method is severely limited in terms of accuracy and spatial resolution. These problems can be considerably reduced by replacing the TLD with a sheet of envelope-wrapped film. An optical density profile is obtained using a scanning densitometer. Because of the non-linearity of the film's dose response, the width of the density profile differs slightly from the width of the corresponding dose profile. However, measurements carried out on a number of different scanners using a range of exposures and slice widths have shown that the full-width half-maximum (FWHM) of the dose profile may be derived directly from the FWHM of the density profile by the application of a simple numerical factor. Dose profiles accurate to within 0.2 mm may be achieved by this means, whereas TLD measurements are limited by the 0.9 mm thickness of each chip. Improvements in speed and convenience are also obtained.

Assessment of entrance doses received by patients undergoing lateral lumbar spine examinations

D. E. Peach and D. H. Temperton
Regional Radiation Physics and Protection Service, Department of Medical Physics, Queen Elizabeth Medical Centre, Birmingham B15 2TB, UK

Entrance surface doses to male patients were evaluated for lateral lumbar spine examinations in a sample of 11 hospitals within the West Midlands Region. Doses were evaluated using lithium borate thermoluminescent dosemeters placed on the patients' skin. The mean dose was 29.0 mGy (range 3.4–77.0 mGy, SD = 18 mGy, n = 43) for a mean patient weight of 70 kg (range 48–110 kg). This compares with the NRPB 1985 national survey: mean dose = 25.2 mGy (range 2.4–73.8 mGy, SD = 13.0 mGy, n = 185) for a mean patient weight of 73 kg (range 46–114 kg). For patient weights up to 30 kg, three hospitals gave doses exceeding the CEC guideline level of 30 mGy. Reasons for this included low film screen speed, filtration, kVp and small focus skin distance. Following the pilot study the procedure has been incorporated into the RRPPS routine survey of 67 hospitals and extended to cover thoracic spine, skull, pelvis and abdomen examinations. In addition to thermoluminescent dosimetry measurements, doses are calculated based on the exposure factors supplied by radiographic staff and technical data obtained during radiation surveys of the X-ray equipment.

Index to Authors

Abdel-Ghaffar, Y., 86
Adam, A., 84
Adams, A., 19
Adams, H., 11, 12, 41
Adams, J. E., 35, 117, 118
Adams, P. H., 117
Agrawal, R. K., 115
Ahmed, A. S., 40, 86
Aindow, J., 26
Aitchison, F., 35
Alexander, A., 100
Alexanian, A. Z., 83
Al-Kutoubi, A., 145
Allen, C., 84
Allen, C. M., 11, 121
Alm Carlsson, G., 124
Al-Sadhan, F., 50
Amin, A. E., 4
Amin, S., 133
Amin, Z., 143, 144
Andrews, H. S., 27
Anslow, P., 1, 133
Antonucci, F., 69
Arenson, A. M., 141
Armstrong, A., 118
Ash, D. V., 30
Ashley, S., 49
Asquith, P., 42
Aunión, P., 78
Ayers, A. B., 38, 51
Ayton, V., 101, 114
Azpeitia, J., 100

Babyn, P. S., 98
Baddeley, H., 5
Baig, M. W., 6
Baird, R. N., 89, 129
Balsitis, M., 1
Banerjee, B., 27, 101
Banks, L., 57, 70
Bann, K., 38, 113
Barber, P. V., 122
Barker, P. G., 133
Barnard, S., 142
Barrett, J. J., 55, 86
Barrington, N. A., 79
Bartal, G., 57, 70
Bartelink, H., 92
Baudouin, C. J., 47
Bauer, M., 65
Bauknecht, T., 65
Baxter, G. M., 141
Beale, D. J., 134
Bean, J. P., 45
Bearcroft, C., 8
Beck, A., 117
Beese, M., 50
Belhag, M., 42
Belli, A.-M., 91
Belton, I., 19
Bengoechea, M., 34
Benjamin, I. S., 84
Bennett, M. H., 82
Berberich, W., 92, 93
Berman, L. H., 23
Bernardo, A., 78
Berry, P. J., 27
Bhagat, K., 60
Bhalla, A. K., 119
Bhatt, R. C. V., 40 86
Bidmead, A. M., 16
Birks, J. L., 110, 111
Bisset, R., 100
Blake, N., 43
Blomley, M., 57, 69, 70, 130
Blum, U., 21
Bourgain, C., 61
Bourne, M. W., 85, 90
Bown, S. G., 100
Boxer, D. I., 145
Brada, M., 16
Bradby, H., 86
Bradley, A., 57, 69, 70
Bradley, D. A., 97
Bradley, M. J., 135
Bradshaw, A. L., 17
Bradshaw, A., 128
Bradshaw, J. R., 76
Brailsford, J. A. D., 30, 113
Brand, I. R., 14, 52
Breatnach, E., 13
Brennan, A. G., 138
Brittenden, J., 61
Britton, K. E., 6
Britton, P. D., 134
Brown, J. S., 99
Browne, R. M., 99
Browne, T., 107
Brownless, S. M., 135
Brunt, A. M., 81
Bryan, A. J., 142
Buckenham, T., 130
Buckland-Wright, J. C., 23
Bude, R. O., 103
Burnet, N. G., 93
Burnett, S. J. D., 116
Burns, P. N., 141
Bury, R. F., 52
Buscombe, J. R., 34
Bydder, G. M., 1
Byrne, J. V., 1

Callaghan, M., 51
Calne, R. Y., 60
Carden, J. F., 150, 151
Carey, B. M., 17, 30
Carter, S. R., 99
Carty, A., 10
Case, A., 76
Cassar-Pullicino, V. N., 21, 22, 23, 24, 59
Cassoni, A., 49
Castellano, I. A., 140
Castro, J., 70
Catton, C., 100
Cawood, J. I., 135
Chalmers, A. G., 14, 113
Chalmers, N., 130
Chambers, R. J., 150
Chan, T. Y. K., 52, 53
Chan, W. P., 22
Chand, D., 40, 86
Chang, Y.-S., 67
Chapman, S., 132
Cheah, F. K., 13, 147
Chen, F.-D., 67
Chen, M., 145
Cheslyn-Curtis, S., 56
Chesters, M. S., 123
Chetty, N., 71
Chetty, U., 142
Choji, K., 145
Chong, W. K., 131
Choraria, B. R., 101
Christopher, D. A., 141
Clague, M. B., 115
Claridge, E., 17
Clarke, G., 34
Clarke, P. D., 52
Clinkard, J. E., 17
Cockburn, J. F., 128, 129
Cohen, G. F., 96
Cohen, M. E. L., 96
Cohen, N. P., 71
Cole, J. G. L., 74
Cole, P. J., 13
Cole, S. E. A., 89
Colella, G., 86
Collin, J., 108
Collins, D., 99, 101, 114
Collins, M. A., 142
Compston, J., 110

Constant, O., 120
Cook, S., 90
Cooper, C. P., 52, 53
Cornford, E., 1
Cotterill, A., 139
Coughlan, R. J., 75
Coulthard, A., 28
Cowen, A. R., 124, 125
Cox, T. C. S., 134
Crane, M. D., 11
Creasy, T. S., 56, 108
Cross, S. J., 7, 36, 38
Crossman, J. E., 134
Crow, A., 129
Cullen, M. H., 48
Cullingworth, J., 113
Cunningham, D., 14, 99, 101, 114
Czaijka, J., 96

Dale, R. G., 124
Damascelli, B., 85, 86
Dance, D. R., 124, 140, 148
Danin, J., 145
Davies, P., 10
Davies, A. G., 124
Davies, A. H., 89, 129
Davies, A. M., 21, 22, 23, 51, 99
Davies, D. H., 148
Davies, E. R., 88
Davis, E., 32
Davy, T. J., 5
Dawes, P. J. D. K., 115
Dawson, P., 91, 128, 129
D'Cruz, D., 38
de Villiers, N., 66
Dean, J., 7
Dean, M. R. E., 107
Deane, R. F., 104
Dearnaley, D. P., 30
Deeks, J. J., 41
Deen, K. I., 28
Delanian, S., 82
Delling, G., 50
Desai, S. R., 13
Dicks Mireaux, C., 12, 116, 121, 132
Dillon, E., 27
Dinkel, E., 21, 117
DiPietro, M. A., 103
Dische, S., 5, 81, 82
Dixon, A. K., 38, 60, 145
Dixon, J., 104
Dixon, J. M., 142
Dobbs, H. J., 4
Dobson, D., 47
Donaghy, M., 112
Donald, J. J., 56, 100
Downes, M. O., 70
Dowsett, D. J., 96
duBois, R. M., 13
Duck, F. A., 26, 141
Dunan, A., 134
Duncan, A. W., 43
Duncan, W., 100
Dunn, M., 140
Dürst, M., 65
Dutton, G., 2
Dutton, J., 50
Dyachek, V., 83, 93
Dynes, A., 135

Eddy, M. R., 32
Edwards, R., 72
Edyvean, S., 150, 151
Egan, A., 23
Eichhorn, T., 76
El-Dorry, A., 55, 86
El-Feky, A., 55
Ell, P. J., 34
Ellis, D., 52, 53
El-Masry, M., 86
El-Sayed, S., 29, 48
El-Sharkawi, A., 50
Elsner, G., 64
Elvins, D. M., 119
Engel, M., 93
Ennis, J. T., 19, 96
Eremin, O., 61
Ertel, R., 106
Ervine, N., 40
Ettles, D. F., 88
Eustace, S., 19, 75, 130
Evans, A. J., 96
Evans, C., 55, 58, 89
Evans, C. J., 50, 110
Evans, G. A., 119
Evans, G. P., 71
Evans, P. D., 89
Evans, P. M., 30
Evans, S., 36

Fairclough, J. A., 58, 89
Federspil, P., 92, 93
Felsenberg, D., 117
Fergusson, C. M., 60
Fernando, I. N., 49
Ferrando, J. R., 42
Fife, I. A. J., 124
Filyov, L., 93
Findlay, M., 99
Finlay, D., 19
Finlay, M. E., 52
Fisher, C., 78
Fitzgerald, M., 139
Fitzgerald, M. X., 121
Fitzgerald, R., 145
Flamig, D. P., 112
Fleischer, A. C., 131
Fletcher, E. W. L., 108
Flower, C. D. R., 38, 52
Fogelman, I., 34
Ford, H. T., 49
Forrester, A. W., 35
Foster, C., 69, 70
Foster, F. S., 141
Fowler, C. J., 104
Fowler, J., 51
Francois-Joubert, A., 67
Frank, J. W., 52, 53
Franks, G., 43
Freeman, A. N., 42
Freer, C. E. L., 134
Friedman, E., 143, 144
Frier, M., 106
Frigerio, L. F., 85, 86
Fujita, N., 145
Fulford, S., 102

Gale, A. G., 76, 95, 96, 123
Gandhi, M., 77
Garber, S., 70, 102
Gardener, J. E., 26
Garrett, J. A., 33
Garton, M. J., 118
Garvie, N. W., 8, 41
Gazet, J.-C., 43
Genant, H. K., 22
Gholkar, J., 77
Giakoumakis, G. E., 125
Gibb, D., 121
Gibbon, W. W., 34, 77, 103
Gibbs, A. R., 11
Gibney, R. G., 69
Gibson, J. M., 106
Gibson, R., 1
Gibson, R. J., 103, 112
Gilbert, F. J., 61, 118
Gildersleve, J. Q., 30
Gill, J. R., 138
Gillams, A. R., 56
Glaholm, J., 99
Gleeson, M. J., 134
Glew, D., 129
Gluhchev, G., 29
Goddard, P. R., 43, 76, 112, 122
Goldberg, B., 100
Golding, S. J., 12, 74, 113, 145
Goldstone, K. E., 138
Gomella, L., 100
Gomez-Catalán, E., 78
Goncharova, L., 83, 93
Goor, C., 61
Gordon, I., 18
Gordon, L. R., 52
Gould, D. A., 106

Gouliamos, A., 85
Gowland, P., 114
Goy, R., 2
Grace, R. H., 145
Graham, J. D., 16
Graves, M. G., 134
Gray, H. W., 35
Greaves, M., 77
Green, D. J., 118
Green, S. E. M., 134
Greenberg, M. L., 98
Greenfield, G. B., 78
Gregson, R., 106, 107
Grier, D. J., 3, 43
Griffin, S. M., 115
Griffith, J., 20, 99
Griffiths, D., 103
Griffiths, S., 29
Grimer, R. J., 99
Grønvall, S., 56
Growland, P., 101
Grundy, A., 43
Gückel, C., 22
Guest, P., 130
Guy, J. M., 73
Guy, R., 133

Habib, N., 84
Hacking, J. C., 136, 145
Haddaway, M. J., 119
Haddock, J. A. A., 11, 120
Hadley, D. H., 35, 76
Hajnal, J. V., 1, 47
Hall, A. S., 46
Hall, E. J., 68
Hall-Craggs, M. A., 84
Hampson, S. J., 105, 143, 144
Hansell, D. M., 11, 13, 120, 121
Harding, L. K., 8, 20, 137
Harding, V. M., 20
Harms, S. E., 112
Harries, M. L., 136
Harris, K. M., 12
Hasan, A. K. H., 42
Hately, W., 60
Hawker, R. J., 8
Hawkes, D. J., 23, 134
Hawnaur, J. M., 2, 35, 46
Hayes, P. C., 130
Heer, M., 69
Heikkinen, M., 62
Heinzel, A., 117
Heise, U., 50
Helinek, T., 100
Hell, B., 92
Helwig, A., 117
Hendra, I. R. F., 9
Hesslewood, S. R., 8

Hey, E., 27
Hickish, T., 14, 101, 114
Hickman, P. F., 147
Higgins, J. N. P., 106
Hilendarov, A., 136
Hill, D. L. G., 134
Hill, J. A., 51
Hodgkinson, D. W., 143
Holder, P. D., 51
Holland, C. L., 55, 86
Holland, P., 23, 42
Holubinka, M., 125
Hopkinson, B. R., 107
Horrocks, E., 128
Horrocks, J. A., 123
Horrocks, M., 89, 128, 129
Houghton, T. A., 106
Hourihan, M. D., 2
Houston, J., 102
Houston, J. G., 53
Hudson, F. R., 31
Hufton, A. P., 96
Hughes, J. D., 135
Hughes, P., 143
Husband, J., 14, 101, 114
Hutchinson, C. E., 2, 35, 46

Ingram, S., 44
Irie, G., 145
Isherwood, I., 2, 46
Ison, E., 80
Itai, Y., 84
Izyumtsev, I., 83, 93

Jackson, J. E., 130
Jameel Ahmed, M., 31
Jardine, A., 72
Jarritt, P. H., 34
Jaspan, T., 1, 3
Jeet, A. B. J., 135
Jennings, K., 7, 36, 38
Jeyapalan, K., 42
Jiaxiang, Y., 62
Jockers, W., 22
Johns, P. C., 150
Johnson, C., 76
Johnson, C. H., 138
Johnson, R. J., 102
Johnston, R., 46
Joiner, M. C., 65
Jones, A., 3, 76, 90
Jonker, N., 84
Jurriaans, E., 128

Kaïlidou, L., 85
Kamel, F., 55
Kant, R., 100
Karamian, S. K., 83

Karantanas, A., 118
Karikomi, M., 37
Kay, C., 117
Keal, R., 140
Keir, M. J., 52, 88
Kelly, I. M. G., 26, 144
Kennedy, A., 129
Keogan, M. T., 42, 52
Kerslake, R., 1, 59, 76
Khairy, A. T., 55, 86
Khairy, K., 55, 86
Khan, S. H., 27
Kilner, P. J., 39
Kincaid, W., 2, 44
King, D. M., 116, 147
King, S. J., 98
Kinsella, D., 90, 112, 122, 128
Kirby, R., 143, 144
Kirk, C., 60
Kirk, D., 104
Kirk, J. M. E., 12
Klevenhagen, S. C., 139
Klys, H. S., 110
Kostyushov, E., 83, 93
Kouris, K., 34
Kumar, D., 28

Laing, J. H. E., 82
Laing, R. W., 16
Lamont, A. C., 75
Lamont, P., 129
Lamote, R., 61
Landberg, T., 5
Lane, C. M., 2
Larkin, G., 2
Larsson, S., 29
Laskey, A., 110
Laver, K., 22
Leach, M., 99, 101, 114
Leahy, J. F., 51
Lebail, J. L., 67
Lee, H. S., 7, 36
Lee, J. R., 42
Lees, W. R., 26, 56, 100, 143, 144
Lefaix, J. L., 67, 82
Legge, O., 130
Leslie, M. D., 5, 81, 82
Leviel, J. L., 67
Lewis, C. A., 124
Lewis, M. A., 150, 151
Lewis-Jones, H. G., 85
Li, J. K. W., 57
Li, S., 57
Liddicoat, W. W., 103
Lillicrap, S., 110, 137
Lim, Y.-F., 97
Lind, C., 131
Lipton, M. E., 85, 90

Liu, S.-T., 67
Ljubenov, T., 93
Lloyd, D. C. F., 12, 41
Lloyd, G. A., 133
Logan, M., 121
Lomas, D., 38
Longmore, D. B., 37, 39, 122
Longstaff, A., 76, 112
Lonsdale, R. J., 106, 107
Looi, L.-M., 97
Loose, H., 10
Lozano, V., 78, 100
Ludman, C. N., 129
Lunt, J.j A., 45
Luxton, E. H. W., 33
Lyn, B. E., 82
Lynch, J. A., 23
Lyons, K., 55, 58, 89

Maas, R., 50
MacConnell, T., 143
MacDonald, L. M., 51
MacErlean, D., 148
MacMillan, C. H., 35
MacPherson, B. C. M., 76
MacVicar, D., 2, 14
Magee, T. R., 129
Maher, E. J., 115
Mahmood, S., 34
Mäkäräinen, H. P., 62, 98
Makin, G. S., 107
Malaguti, C., 58
Malcolm, P. N., 8
Man, W., 57, 70
Mansi, J. L., 14, 99
Mantle, M., 42
Manton, D. J., 32
Manuel, M., 141
Marchiano, A., 85, 86
Marcos y Robles, J., 100
Marinova, L., 62
Mark, R. W., 33
Marks, S., 86
Marsden, S. N. E., 88
Marshall, R. M., 106
Martin, D. F., 40, 71
Martin, M., 82
Martindale, C. A., 82
Martinez, A., 123
Maskell, G., 38
Mason, A. C., 60
Masters, A., 100
Masterson, J., 121
Matheson, L. M., 110
Matsaidonis, D., 85
Matteucci, T., 100
Mattias, P., 69
Mattila, S. I., 98
Mattsson, S., 109
Maurer, H. J., 73, 135
Mazaira, L., 100
Mazer, M., 131
McAndrew, P. G., 135
McArdle, S., 125
McAvinchey, R. P., 8, 60
McCall, I. W., 21, 23, 59, 119
McCarthy, C., 75
McCarty, H., 5
McCarty, M., 120
McConachie, N. S., 1
McCready, V. R., 99
McCulloch, A. S., 42
McDermott, E., 148
McGee, K., 29
McHugo, J., 27, 132
McInnes, G. C., 56
McLean, M., 100
McLoughlin, R. F., 69
McMahon, A. J., 104
McMillan, N. C., 2, 53
McMillan, P. J., 98
McNee, S. G., 4
McNeil, E. A., 139
McNeill, J. G., 140
McNicholas, M., 148
McQueen, D., 51
McRobbie, D. W., 45, 124
Meanock, C. I., 102, 103
Medvedev, Yu., 93
Meecham Jones, S., 55
Meiring, P. , 77
Mercer, P., 148
Merrick, M. V., 34
Metcalfe, M. J., 7, 38
Milella, M., 85
Milkov, V., 62
Millar, J. S., 51
Miller, D. J., 123
Miller, J., 148
Mills, A. P., 137
Mitchell, S. G., 8
Mitchell, L. A., 59, 76
Mohiaddin, R. H., 37, 39, 122
Molyneux, A. J., 1
Monti, C., 58
Moore, N. R., 47, 86, 112, 147
Mootoosamy, I., 52, 53
Morgan, D. A. L., 35
Morgan, H. M., 137
Morgan, R. A., 108
Morgan, W. D., 110, 111
Morris, J., 115
Morris, P., 108
Morris, S., 89
Morrissey, B., 11
Morton, E. J., 30
Moskovic, E., 49, 78, 115, 116, 147
Mostafa, A. B., 137
Mountford, P. J., 19
Mtema, P. B. N., 88
Mulhern, D., 121
Mumcuoglu, E. A., 139
Mundinger, A., 21, 117
Murch, C., 147
Murphy, P., 89, 112, 129
Murray, J. G., 13, 96
Murray, M., 43
Myers. M., 57, 69, 70

Nakielny, R. A., 77
Namasivayam, J., 22
Nathan, B. E., 147
Nedev, P., 136
Nedeva, A., 136
Needham, G., 56, 61
Nelson, N., 48
Newell, M. S., 41
Ng, K.-H., 97
Nichols, D. M., 36
Nicholson, D. A., 57, 69, 70, 71, 128, 129, 143
Nicolas, V., 50
Nicolson, V., 101, 114
Nieto-Camero, J., 124
Niewald, M., 92, 93
Noble, J. G., 102, 104
Norton, M. Y., 7
Notghi, A., 20, 137
Notohamiprodjo, G., 122

Oatey, M. E., 5
Oatridge, A., 47
O'Brien, T., 129
O'Byrne, J., 75, 130
O'Donnell, P. J., 70
O'Halloran, A. E., 82
O'Higgins, N. 148
O'Laoide, R., 121
Olliff, J. F. C., 28, 55, 142
Olliff, S. P., 55, 142
O'Mahony, S., 121
O'Neill, A. D., 9
Ooi, G. C., 19
Outram, S. J., 6
Owen, J. P., 52, 88
Owens, C. M., 116, 121

Padhani, A. R., 52, 60
Paley, M., 84
Pamilo, M., 97
Panegyres, P., 112
Panzarella, T., 100
Papadopoulos, A., 85
Parikh, A. M., 105

Parry, R., 129, 143
Parsons, C., 78, 115
Parvanova, V., 62
Parviainen, T., 97
Patel, J. C., 56
Patel, K., 51
Patel, U., 143, 144
Paterson, D., 142
Patil, M., 89
Pattee, P. L., 150
Payne, G., 99
Peach, D. E., 151
Peacock, J. H., 93
Peakman, D. J., 148
Pearn, J. C. A., 128
Peh, W. C. G., 59
Pelotti, P., 58
Pemberton, J., 38
Pennesi, G., 58
Pennock, J. M., 47
Penry, B., 76
Perkins, A. C., 35, 106
Perry, D., 10
Persliden, J., 124
Phelan, N., 19
Phelps, P. D., 99, 134
Pilbrow, W. J., 135
Pitcher, E. M., 32
Platt, J. F., 103, 106
Polax, J. F., 141
Poon, F. W., 35
Popov, I., 83, 93
Porter, H., 27
Potterton, A. J., 148
Powles, T. J., 49
Pratt, P. G., 8
Pratt, T. A., 128
Preece, A. W., 66
Presdee, D., 88
Price, J. S., 125
Pugh, N., 142
Pullicino, C. V., 119
Pulst, A. W., 73
Pynsent, P., 99

Qian, X., 62
Quemby, V., 40
Quinn, G., 30

Rajah, R., 27
Rampton, D., 8
Raphael, M. J., 140
Rathmell, A. J., 17
Rawlings, C., 30
Reading, N. G., 52, 53
Redhead, D. N., 130
Redpath, T. W., 47
Reek, C., 140
Rees, J., 21
Rees, M. R., 6, 36, 37, 38, 107, 113
Rees, R. S. O., 39
Reeves, B., 96
Reid, D. M., 118
Reidy, J. F., 129
Renaa, T., 64
Rennison, A., 101
Renwick, M., 27
Reuter, M., 50
Reynolds, U., 139
Richardson, J., 119
Richmond, H., 100
Richter, C. S., 37
Rickards, D., 70, 102, 104, 105, 144
Ridgway, J., 38, 113
Rifkin, M., 100
Rimondi, E., 58
Ring, E. F. J., 119
Rissanen, T. J., 62
Roberts, H., 102
Roberts, J. P., 41
Roberts, P. J., 137
Robertson, C. S., 115
Robertson, E. M., 118
Robertson, I., 72
Robertson, R., 120
Robinson, B. M., 82
Robinson, G. P., 134
Robinson, L., 11
Robinson, M. H., 16, 49
Robinson, P. J., 19, 113
Roddie, M. E., 84
Roebuck, E. J., 95, 96
Roelstraete, A., 61
Roldan, A., 14
Romaniuk, C. S., 19
Romanowski, C. A. J., 79
Rowland, C. G., 62
Rowlands, P. C., 90
Royle, G. J., 109
Rubin, J. M., 103
Rudin, A., 22
Ruff, C. F., 134
Russell, R. C. G., 56
Ryde, S. J. S., 110, 111
Ryder, S., 29

Sacre, R., 61
Said, S., 52, 53
Saiphoo, C., 141
Sandborg, M., 124
Saunders, A. J. S., 10, 11
Saunders, M. I., 5, 81, 82
Saunders, N. H., 110
Sawyer, R. H., 89
Schnabel, K., 92, 93
Schoser, K., 122
Schulz-Wendtland, R., 65
Scoble, J. E., 81
Scott, J., 128
Seaby, A. W., 50
Segura, C., 86
Sekiya, T., 37
Serpell, J., 78
Servomaa, A., 97
Set, P., 38, 42, 134
Seyferth, W., 106
Shakeshaft, J., 110
Shalev, S., 29
Shapiro, L., 46
Sharpe, N., 26
Shaw, A. J., 125
Shaw, D., 121
Sheikh, M., 71
Shekhtman, L. I., 123
Shelton, J. C., 71
Shepherd, M., 49
Sheppard, M., 11, 13
Shepstone, B. J., 147
Sheridan, M. B., 71, 143
Shiliang, S., 62
Sidhu, P. S., 129
Sigmund, G., 21
Silman, A., 117
Simova, E., 136
Sinclair, D. J., 42
Sinyuta, B. F., 18
Sivananthan, U. M., 36, 37, 38, 107, 113
Skinner, C. L., 41, 139
Smith, F. W., 7
Smith, I. E., 147
Smith, M. A., 45
Smith, N. B., 137
Smith, R. M., 60
Smyth, J. F., 110
Sokal, M., 49, 98
Somers, J. M., 134
Sowerby, T., 89
Speller, R. D., 109, 123
Spencer, J., 100
Spooner, D., 49
Spreafico, C., 85, 86
Stack, J., 75
Stage, J. G., 56
Starritt, H. C., 26, 141
Steele, H. R., 139
Stephens, M. M., 75
Stockdale, H. R., 135
Stoever, B., 21
Stoker, S., 141
Storme, G., 61
Strachan, R., 29
Straughan, K., 45
Strong, A. J., 134

Stuckmann, G., 69
Stutley, J. E., 141
Sukumar, S., 143
Sule-Suso, J., 81
Swindell, W., 29, 30
Szeinfeld, D., 66

Tabakov, S. D., 124
Tan, L. B., 6
Tarakanath, M. S., 31
Tatonetti, M. L., 86
Taylor, A. K. M., 88, 104
Taylor, P. M., 122
Taylor, R. E., 17
Temperton, D. H., 139, 151
Thomas, D. W., 110, 111
Thomas, G. L., 118
Thomas, H. G., 59, 60, 129
Thomas, J. M., 78
Thomson, L., 36
Thomson, W. H., 20, 137
Thorley, P. J., 6
Thorp, N. C., 140
Thow, J. C., 28
Thurley, P.E., 52, 53
Tolley, N. J., 20
Tomlinson, M. J., 66
Tonge, H. M., 26
Torrie, E. P. H., 103
Tothill, P., 109, 110
Tottle, A. J., 76
Towle, J. A., 95
Townsend, C. E., 34
Trott, N. G., 73
Troughton, A. H., 88
Tucker, S., 95
Tucker, W., 88
Tudor, J., 136
Tung, K. T., 13, 70
Turner, V. S., 8
Twining, P., 3, 90
Tyan, Y.-S., 67
Tyaptin, A., 83, 93
Tyrell, P., 51, 57

Uberoi, R., 121
Udeshi, U. L., 89

Valensieck, M., 22
Vallance, R., 44
Van Lancker, M., 61
Van Belle, S., 61
Vennart, W., 127
Verity, C., 23
Verma, S. P., 36, 37, 107, 113
Vive, J., 75
Vlahos, L., 85
Voltchek, I., 83, 93

Wade, J. P., 138
Walker, C. P., 22, 24
Walker, D., 38
Walker, T., 103
Wall, B. F., 150
Wallace, A., 118
Waller, D., 38
Walsh, J. 142
Walton, J., 108
Walton, S., 7, 38
Ward, J., 113
Ward, S., 135
Warde, P., 100
Warren, R., 9, 95
Warrington, A. P., 16
Wastie, M. L., 35, 106
Watkinson, A. F., 116
Watson, C. J. E., 60
Watt, I., 76
Wayte, S. C., 47
Weatherall, D. J., 25
Webb, L. A., 52
Webb, S., 15
Wellings, R., 22, 99
Wells, A. U., 13
Wells, I. P., 108, 128
Wenham, P. W., 107
Weston, M. J., 27
Whall, M. A., 139
Whitaker, S. C., 106, 107
White, P. G., 2
Whitehouse, G. H., 85
Whitehouse, R. W., 35, 117, 118
Whitfield, H. N., 71
Wilcock, D. J., 98
Wilde, R. P. H., 143
Wilkie, J. M., 128
Wilkinson, I., 84
Williams, C., 90
Williams, G., 71
Williams, L. A., 58, 89
Williams, N. S., 41
Williams, P. C., 15
Wilson, A., 60
Wilson, A. R. M., 95, 96
Wilson, B., 143
Wilson, C., 58
Wilson, G. D., 82
Wiltshaw, E., 115
Winkler, K., 50
Wong, W. L., 38, 51
Woodward, R., 119
Workman, A., 125
Workman, G. M., 17
Worthington, B. S., 1, 59, 76, 123
Wraight, E. P., 42
Wright, A. R., 88
Wright, D., 141
Wright, F. R., 40
Wright, P., 10
Wurm, R., 93
Wyatt, M., 129
Wyatt, R., 40
Wynchank, S., 66

Xiao, Z. R., 30
Xinshen, L. J. T., 62

Yacoub, M., 121, 122
Yarnold, J. R., 61
Yongmei, P., 62
Young, I. R., 46, 47
Young, J. W. R., 58

Zhu, X. P., 46
Zollikofer, Ch. L., 69
Zucchi, F., 85, 86
Zuccollo, J., 3, 90

PUBLICATIONS OF THE BRITISH INSTITUTE OF RADIOLOGY

Please send me the following publications:

Latest Publications:

☐	**Medical Radiation Protection Practice within the EEC,** 1991, 56 pp, ISBN: 0 905749 26 X	£13.50
☐	**Report 22: The Future of Human Radiation Research,** 1991, 174 pp, ISBN: 0 905749 27 8	£27.50
☐	**The Safe Use of Diagnostic Ultrasound,** 1991, 48 pp, ISBN: 0 905749 28 6	£16.00

BJR Supplements:

☐	23. **Treatment Simulators,** 1989, 48 pp, ISBN: 0 905 74919 7	£10.00
☐	22. **Megavoltage Radiotherapy 1937-1987,** 1988, 158 pp, ISBN: 0 905 74916 2	£28.50
☐	21. **Radionuclides in Brachytherapy: Radium and After,** 1987, 54 pp, ISBN: 0 905 74915 4	£15.00
☐	20. **The Safety of Diagnostic Ultrasound,** 1987, 48 pp, ISBN: 0 905 74914 6	£12.00
☐	18. **Criteria and Methods for Quality Assurance in Medical X-ray Diagnosis,** 1985, 180 pp, ISBN: 0 905 74912 X	£27.50
☐	17. **Central Axis Depth Dose Data for use in Radiotherapy** This standard work replaces BJR Supplement 11 (1972), 1983, 148 pp, ISBN: 0 905 74911 1	£25.00

Other Publications:

☐	**Assurance of Quality in the Diagnostic X-ray Department,** 1988, 108 pp, ISBN: 0 905 74917 0	£20.00
☐	**Basic Clinical Ultrasound** Hylton B Meire and Pat Farrant, 1982 (BIR Teaching Series No 4) 170 pp, ISBN: 0 905 74910 3	£12.50
☐	**Special Report 17: High Dose Rate Afterloading in the Treatment of Cancer of the Uterus,** 1980, 200 pp, ISBN: 0 905 74907 3	£18.50
☐	**Report 18: Technical and Physical Parameters for Quality Assurance in Medical Diagnostic Radiology,** 1989, 166 pp, ISBN: 0 905 74918 9	£30.00
☐	**Report 19: The Scientific Basis of Modern Radiotherapy,** 1989, 142 pp, ISBN: 0 905 74920 0	£30.00
☐	**Report 20: Optimization of Image Quality and Patient Exposure in Diagnostic Radiology,** 1989, 288 pp, ISBN: 0 905 74921 9	£30.00
☐	**Report 21: Risks from Radium and Thorotrast,** 1989, 188 pp, ISBN: 0 905 74922 7	£40.00
☐	**Current Research in Osteoporosis and Bone Mineral Measurement,** 1990, 96 pp, ISBN: 0 905749 23 5	£22.00
☐	**Clinical Applications of Ultrasonic Fetal Measurements,** 1991,30 pp, ISBN: 0 905749 24 3	£13.50
☐	**Guidelines for the Evaluation of Radiological Technologies,** 1991, 28 pp, ISBN: 0 905 74925 1	£13.50

The British Institute of Radiology

36 Portland Place, London W1N 4AT Tel. 071-580 4189 Fax. 071-255 3209

25% discount to BIR Members if cheque received with order. Please quote membership number.

Please add £1 per book for postage/packing.

Overseas orders will be sent by surface post. For airmail add £2 per book.

I enclose payment to the sum of £ ☐ by cheque ☐ Barclaycard/Visa ☐

My card number is ☐ Access ☐

Signature .... Please send to this address: (BLOCK CAPITALS)

Name .... Membership No. ....

Address ....

....

Postcode .... Country ....

PUBLICATIONS OF THE BRITISH INSTITUTE OF RADIOLOGY

Please send me the following publications:

Latest Publications:

☐ **Current Research in Osteoporosis and Bone Mineral Measurement II: 1992** 120pp, ISBN 0 905749 29 4.	£28.00
☐ **Medical Radiation Protection Practice within the EEC,** 1991, 56 pp, ISBN: 0 905749 26 X	£13.50
☐ **Report 22: The Future of Human Radiation Research,** 1991, 174 pp, ISBN: 0 905749 27 8	£27.50
☐ **The Safe Use of Diagnostic Ultrasound,** 1991, 48 pp, ISBN: 0 905749 28 6	£16.00

BJR Supplements:

☐ **23. Treatment Simulators,** 1989, 48 pp, ISBN: 0 905 74919 7	£10.00
☐ **22. Megavoltage Radiotherapy 1937-1987,** 1988, 158 pp, ISBN: 0 905 74916 2	£28.50
☐ **21. Radionuclides in Brachytherapy: Radium and After,** 1987, 54 pp, ISBN: 0 905 74915 4	£15.00
☐ **20. The Safety of Diagnostic Ultrasound,** 1987, 48 pp, ISBN: 0 905 74914 6	£12.00
☐ **18. Criteria and Methods for Quality Assurance in Medical X-ray Diagnosis,** 1985, 180 pp, ISBN: 0 905 74912 X	£27.50
☐ **17. Central Axis Depth Dose Data for use in Radiotherapy** This standard work replaces BJR Supplement 11 (1972), 1983, 148 pp, ISBN: 0 905 74911 1	£25.00

Other Publications:

☐ **Assurance of Quality in the Diagnostic X-ray Department,** 1988, 108 pp, ISBN: 0 905 74917 0	£20.00
☐ **Basic Clinical Ultrasound** Hylton B Meire and Pat Farrant, 1982 (BIR Teaching Series No 4) 170 pp, ISBN: 0 905 74910 3	£12.50
☐ **Special Report 17: High Dose Rate Afterloading in the Treatment of Cancer of the Uterus,** 1980, 200 pp, ISBN: 0 905 74907 3	£18.50
☐ **Report 18: Technical and Physical Parameters for Quality Assurance in Medical Diagnostic Radiology,** 1989, 166 pp, ISBN: 0 905 74918 9	£30.00
☐ **Report 19: The Scientific Basis of Modern Radiotherapy,** 1989, 142 pp, ISBN: 0 905 74920 0	£30.00
☐ **Report 20: Optimization of Image Quality and Patient Exposure in Diagnostic Radiology,** 1989, 288 pp, ISBN: 0 905 74921 9	£30.00
☐ **Report 21: Risks from Radium and Thorotrast,** 1989, 188 pp, ISBN: 0 905 74922 7	£40.00
☐ **Current Research in Osteoporosis and Bone Mineral Measurement,** 1990, 96 pp, ISBN: 0 905749 23 5	£22.00
☐ **Clinical Applications of Ultrasonic Fetal Measurements,** 1991,30 pp, ISBN: 0 905749 24 3	£13.50
☐ **Guidelines for the Evaluation of Radiological Technologies,** 1991, 28 pp, ISBN: 0 905 74925 1	£13.50

The British Institute of Radiology

36 Portland Place, London W1N 4AT Tel. 071-580 4189 Fax. 071-255 3209

25% discount to BIR Members if cheque received with order. Please quote membership number.

Please add £1 per book for postage/packing.

Overseas orders will be sent by surface post. For airmail add £2 per book.

I enclose payment to the sum of £. ☐ by cheque ☐ Barclaycard/Visa ☐

My card number is ☐ Access ☐

Signature .... Please send to this address: (BLOCK CAPITALS)

Name .... Membership No. ....

Address ....

....

Postcode .... Country ....

The professional difference

The CadPlan 400

Take software:
Written by leading physicists in Europe, the planning software takes into account specific European needs.

Take hardware:
Hewlett Packard's reputation for excellency is fully manifested in the 9000 series of graphics workstations, ideally suited for treatment planning.

Take performance:
The modularity of the software and the wide range of hardware available allow the matching of performance to the needs of each user.

Varian International AG
Medical Equipment
Kollerstrasse 38, CH-6300 Zug, Switzerland
Phone (042) 44 88 44

Varian – the Predictable Future

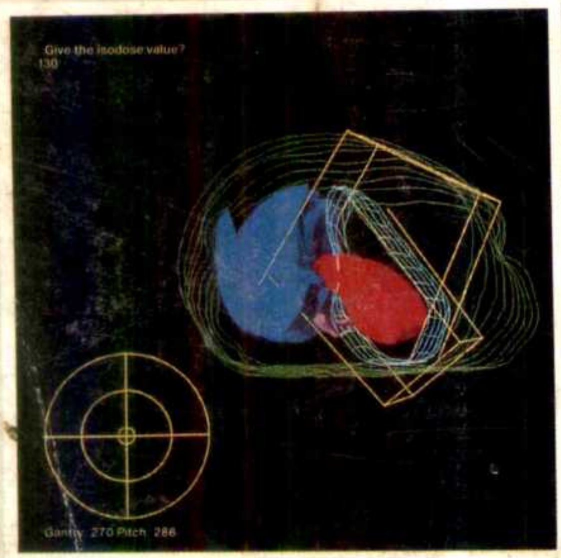
Give the isodose value?
130
Gantry 270 Pitch 288

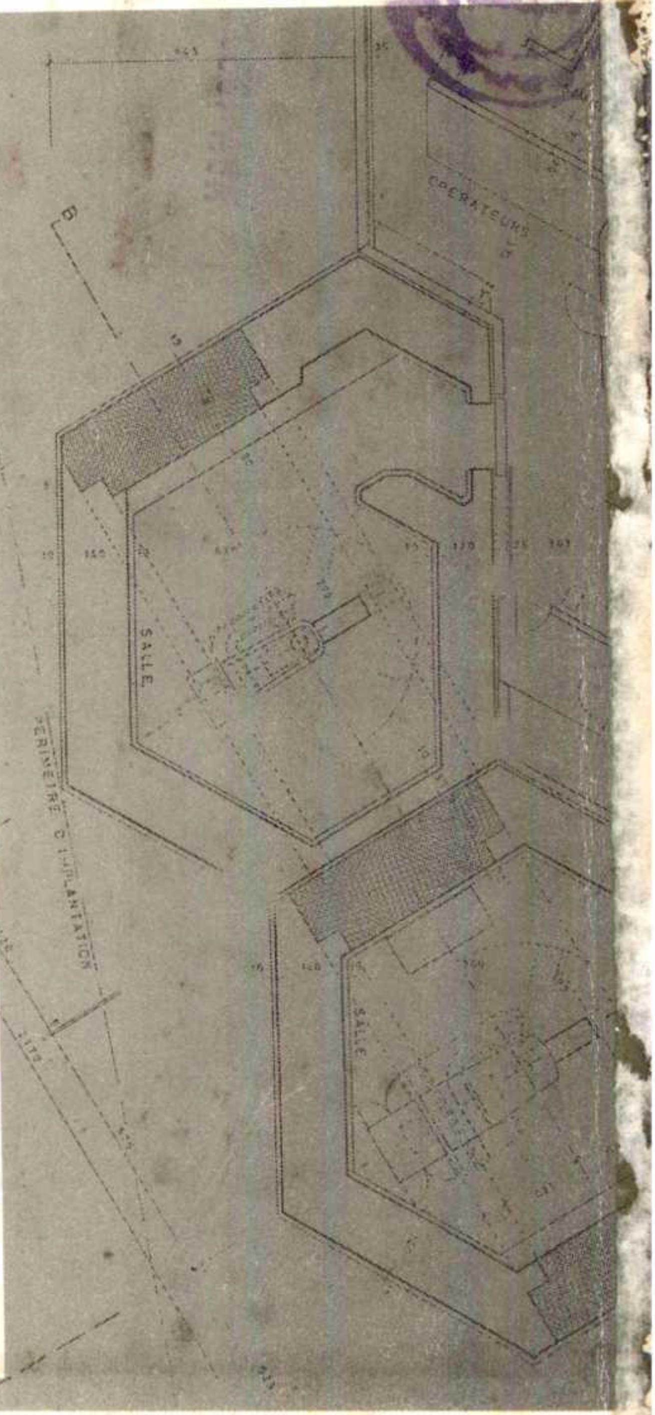
OPERATEURS
B
SALLE
PERIMETRE D'IMPLANTATION
SALLE

varian